



# *Bioelectromagnetics 2005*

A joint meeting of The Bioelectromagnetics Society and  
The European BioElectromagnetics Association

## *Abstract collection*

The following abstracts were reviewed by the Technical Program Committee, but the review should not be considered a full peer-review. Contributions here may not present completed work. Individuals wishing to reference or quote from these abstracts in whole or part should obtain permission directly from the author(s).

## Bioelectromagnetics 2005

### Governing Board

#### BEMS

**Stefan Engström**  
*Technical Program Co-Chair*  
Vanderbilt Univ Medical Ctr  
Neurology Dept  
Nashville, TN 37232-3375  
(615) 936-1522 Fax: (615) 936-0223  
stefan.engstrom@vanderbilt.edu

**Bruce McLeod**  
*BEMS President*  
Montana State Univ  
College of Graduate Studies  
Bozeman, MT 59717-2580  
(406) 994-5555 Fax: (406) 994-4733  
mcleod@montana.edu

**Robert Cleveland**  
*BEMS Treasurer*  
Federal Communications Commission  
Washington, DC 20554  
(202) 418-2422 Fax: (202) 418-1918  
robert.cleveland@fcc.gov

#### EBEA

**Kjell Hansson Mild**  
*Technical Program Co-Chair*  
Nat'l Inst for Working Life  
Umeå, Sweden  
+46 90 176 017  
Fax: +46 90 176 117  
mild@niwl.se

**René de Seze**  
*EBEA President*  
INERIS, DRC - Toxicologie  
Verneuil-en-Halatte, France  
+33 3 44 55 65 94 Fax: +33 3 44 55 66 05  
Rene.De-Seze@ineris.fr

**Alejandro Ubeda**  
*EBEA Treasurer*  
Hospital Ramon Y Cajal  
Dpto Investigacion-Bioelectromagnetismo  
Madrid, Spain  
+34 91 336 86 99 Fax: +34 91 336 81 71  
alejandro.ubeda@hrc.es

#### Conference Manager:

**Gloria Parsley**  
Association Services International, Inc.  
2412 Cobblestone Way  
Frederick, MD 21702  
(301) 663-4252 Fax: (301) 694-4948  
Bioem2005@aol.com



**Bioelectromagnetics 2005  
Technical Program Committee**

Co-chairs:  
Stefan Engström  
Kjell Hansson Mild

Lawrie Challis  
Robert Cleveland  
Yngve Hamnerius  
Sheila Johnston  
Isabelle Lagroye  
Marko Markov  
Michael McLean  
Bruce McLeod  
Junji Miyakoshi  
Gabi Nindl  
Arthur Pilla  
Frank Prato  
Maria Rosaria Scarfi  
Theodoros Samaras  
Tsukasa Shigemitsu  
Masao Taki  
György Thuróczy  
Shoogo Ueno  
Peter Valberg  
Marvin Ziskin



## Table of contents

Platform Presentations .....	7
Plenary I: EMF In Our Environment.....	7
Session 3: Role Of Electric Fields In Wound Healing And Nerve Regeneration (Continued).....	26
Session 4: Exposure Assessment.....	28
Session 5: Dosimetry I .....	42
Session 6: Dosimetry II .....	55
Session 7: In Vitro Elf I.....	61
Session 8: Dosimetry III.....	69
Session 10: Dosimetry IV.....	89
Session 11: Epidemiology.....	102
Alessandro Chiabrera Memorial Student Session.....	109
Alessandro Chiabrera Memorial Student Session (Continued).....	123
Plenary III: Animal magnetoreception .....	160
Session 14: Nanosecond Pulsed Electric Fields.....	161
Session 14: Nanosecond Pulsed Electric Fields (Continued).....	164
Session 15: In Vivo .....	169
Session 15: In Vivo (Continued).....	173
Session 16: European Programs .....	179
Session 18: Policy And Standards.....	197
Session 19: Mechanisms I .....	207
Plenary IV: The Low Field Effect On Free Radical Chemistry .....	222
Session 20: Electromagnetic Therapy .....	223
Session 20: Electromagnetic Therapy (Continued).....	225
Session 21: Mechanisms II.....	233
Posters.....	244
Poster Session A.....	244
Clinical Devices.....	244
Dosimetry.....	247
Epidemiology.....	282
High-throughput screening .....	286
Mechanisms of interaction – physical transduction.....	287
Human Studies.....	291
In vivo studies.....	292
In vitro – cellular.....	309
In vitro – sub-cellular.....	318
In-vitro – tissue and organ .....	319
Mechanisms of interaction – biological.....	320
Medical applications.....	328
Risk, safety standards and public policy.....	334
Theoretical and practical modeling.....	339
Late edits.....	348
Poster Session B.....	349
Clinical devices.....	349
Dosimetry.....	351
Epidemiology.....	374
Human studies.....	382

In vivo studies .....	396
In vitro - cellular .....	404
In vitro – sub cellular .....	420
In vitro – tissue and organ .....	423
Mechanisms of interaction - biological .....	426
Medical applications .....	433
Risk, safety standards and public policy .....	444
Theoretical and practical modelling .....	452
Late edits .....	458
Poster Session C .....	460
Clinical devices .....	460
Dosimetry .....	460
Epidemiology .....	493
High-throughput screening .....	498
Human studies .....	499
In vivo studies .....	504
In vitro – cellular .....	511
In vitro – tissue and organ .....	525
Mechanisms of interaction - biological .....	528
Mechanisms of interaction - physical .....	531
Medical applications .....	533
Risk, safety standards and public policy .....	537
Theoretical and practical modelling .....	548
Author Index .....	557

# Platform Presentations

## Plenary I: EMF In Our Environment

*Chair: Kjell Hansson Mild*  
8:45 - 9:30 am, O'Reilly Hall

**ELECTROMAGNETIC FIELDS IN OUR ENVIRONMENT - YESTERDAY, TODAY, AND TOMORROW.** Richard Tell. R.T. Associates, Las Vegas, NV.

Our living and working environment has always included the presence of electric, magnetic, and electromagnetic fields. Some of our electromagnetic background is from natural sources but much of it is produced by manmade systems used for communications, broadcasting, navigation, factory processes, etc. This presentation will provide an overview of many of these sources of electromagnetic fields in our environment, including older sources not much talked about today, present day systems, and newer technologies that have not have yet been fully exploited. Issues related to typical exposures and methods of assessing exposure from some of these systems will be discussed as well as the perceived significance of such exposures relative to hazards. Sources and systems included in this presentation will include natural fields, power lines, AM, FM, and TV broadcasting, shortwave broadcasting, cellular base stations, paging, satellite communications earth stations, radar, tropospheric communications, RF dielectric heat sealing and induction heating systems, WIFI systems, and others.

## **Session 1: Role Of Electric Fields In Wound Healing And Nerve Regeneration**

*Chairs: Richard Nuccitelli and Colin McCaig*  
**1:00 - 3:00 pm, Theatre L**

1-1

### **CONTROLLING CELL BEHAVIOR ELECTRICALLY: CURRENT VIEWS AND FUTURE POTENTIAL.** C. McCaig. School of Medical Sciences, Univ of Aberdeen, Scotland.

In virtually every system that has been tested, from microbe to man, endogenous electrical signals have been found. In vertebrates in particular, these coexist with major events in development and in regeneration and have long been thought to influence cell behaviours. The sources of these naturally occurring electrical signals, their effects on single cells, multicellular model systems and in whole animals and the prospects of mimicking this type of signal by using electric field stimulation in regenerative medicine will be discussed. Examples will include the central nervous system, epithelial wound healing in cornea, skin and lens and the control of vascular endothelium to form new blood vessels.

1-2

### **AN OSCILLATING ELECTRICAL FIELD AS A TREATMENT FOR HUMAN SPINAL CORD INJURY.** R. Borgens. Purdue Univ, IN.

It is well understood that an imposed gradient of voltage can initiate nerve fiber outgrowth and direct it. These neurotrophic and neurotropic effects occur in physiological conditions by single neurons that usually project fibers towards the cathode, while retracting from the anode. Similar results have been proven for axons of vertebrate spinal cords including identified fibers of Lamprey ammocoete larvae and adult guinea pigs and laboratory rats. These responses to applied electrical fields would have remained the provenance of the laboratory until a discovery was made that proved clinically useful. Nerve fibers initiate growth towards the negative pole soon after tips experience a cathodal field while retrograde degeneration occurs long after fibers experience an anodal field. This allowed the development of a clinical utility, which promoted growth then, in both directions in fiber tracts lying parallel to each other –but projecting in opposite directions. This clinical tool, called Oscillating Field Stimulation or OFS was first tested on cases of naturally occurring, and neurologically complete paraplegia in dogs and subsequently in human spinal cord injury. In neurologically complete spinal injured humans, OFS stimulators were implanted and electrodes routed to the vertebral column above and below the level of injury within the first 3 weeks of trauma. The units were removed 14 weeks later and patients were followed for 1 year post treatment. OFS proved to enhance a recovery of sensory (ascending function) in more than half of the patients, while motor recovery was less pronounced, though still clinically useful. These results were published in a clinical report in the Journal of Neurosurgery, January 2005, and were positive enough to prompt further testing in human paraplegia and quadriplegia under approval from the United States Food and Drug Administration.

**ELECTRICALLY DRIVEN WOUND HEALING – A MOLECULAR AND GENETIC PERSPECTIVE.** M. Zhao. School of Medical Sciences, Univ of Aberdeen, Scotland.

Naturally occurring direct current electrical fields (EFs) regulate directed cell migration, cell division and cell proliferation. These cell behaviours are coordinated during wound healing and may be orchestrated by the instantaneous EF generated at skin and corneal wounds. The molecular and genetic control over these events is beginning to be elucidated by using readily manipulated model systems. The soil amoeba *Dictyostelium discoideum* and genetically manipulated transgenic mouse tissues are two good examples. The mechanisms underpinning EF-directed cell behaviours will be outlined using these systems.

**A “SMART” BANDAGE: TISSUE REGENERATION FACTORS SELECTIVELY RELEASED FROM CELL-FREE EXTRACELLULAR MATRICES BY APPLIED SPECIFIC ELECTRICAL POTENTIAL.** S. J. Braunhut<sup>1</sup>, D. McIntosh<sup>1</sup>, E. Vorotnikova<sup>1</sup>, P. Tan<sup>2</sup>, R. Pande<sup>3</sup>, T. Zhou<sup>4</sup>, K. A. Marx<sup>4</sup>. <sup>1</sup>Dept of Biological Sciences, Univ of Massachusetts, Lowell, MA, <sup>2</sup>Saints Memorial Hospital, Lowell, MA, <sup>3</sup>Pierce Biotechnology Inc., Woburn, MA, <sup>4</sup>Dept of Chemistry, Univ of Massachusetts, Lowell, MA.

**INTRODUCTION.** The extracellular matrix (ECM) serves as a reservoir for different growth factors (GFs) active in wound healing including transforming growth factor beta (TGF- $\beta$ ), vascular endothelial cell growth factor (VEGF) and fibroblast growth factor (FGF). Storage of GFs within ECM eliminates the need for new synthesis and they are more stable. When GFs are released from ECM, they are more potent in combination with other ECM derived molecules. Recently it has been shown that fragments of matrix molecules released during degradation are bioactive and may be essential for the recruitment of progenitor cells during tissue regeneration and injury repair.

**OBJECTIVE:** The objective was to devise methods to control the selective release of factors from cell-free ECMs that would stimulate wound healing and tissue regeneration.

**METHODOLOGY.** Endothelial cells (ECs) were grown to confluency in ECIS Electrode Array devices (Applied BioPhysics, Inc.). The cells were removed non-proteolytically using EGTA in successive 2-hour washes. At various times the cell free ECMs were overlaid with PBS and subjected to either  $-0.3V$  or  $+0.3V$  (vs. Ag/AgCl) electrical potential for 1 hr. The electrical potential releasate was collected after 23 hrs. In parallel, sham-treated ECM were allowed to condition PBS for 24 hrs. Samples were then tested in standard cell proliferation and MTT assays in vitro, and when bioactivity was detected, were used to treat full thickness wounds in adult male C57BL/6J black mice in vivo. Changes in proliferation rates and in wound closure rates were determined and data analyzed statistically using student T-tests. After wounds were healed, animals were euthanized and wound sites excised and analyzed by histopathology.

**RESULTS.** Protein microarray analysis of intact EC cell free ECM revealed that the matrix contained 179.8 pg/ml bFGF, 11.9 pg/ml VEG-F, 4.6 pg/ml hepatocyte growth factor and 6.0 pg/ml keratinocyte growth factor, when totally solubilized. Exposure of intact EC cell-free ECM to  $-0.3 V$ , but not  $+0.3V$ , released a bioactive fraction that stimulated fibroblasts and ECs to proliferate in vitro. These factors

applied in a single treatment at time of wounding reduced the wound healing time in half compared to controls. These factors promoted healing statistically faster than animals that received pure FGF(3 ng/ml), (TGFb1 = 800 pg/ ml), or VEGF(6 ng/ml) in wounds in parallel. When all wounds were healed, histopathology revealed that -0.3 V releasates caused vascularity, re-epithelialization, hair follicle and muscle regeneration to a greater extent than the other GFs. Wounds receiving PBS or sham releasates healed as scar tissue with fibrosis and lack of hair growth

**CONCLUSION.** We have developed methods to produce cell-free ECMs. These ECMs can be stored for up to 3 months, and when needed, we can stimulate the selective release of factors by a brief exposure to specific applied electrical potential. The factors mobilized from matrix cause true tissue regeneration, including muscle re-formation, extensive re-epithelialization, vascularity and hair growth, when applied to wounds. This work should lead to a new "Smart" type of bandage that can be customized to treat different types of injury.

This study was supported by the United States Defense Advanced Research Projects Agency (DARPA).

## **Session 2: Human Studies**

*Chairs: Monica Sandström and Maila Hietanen*

**1:00 - 3:00 pm, Theatre M**

2-1

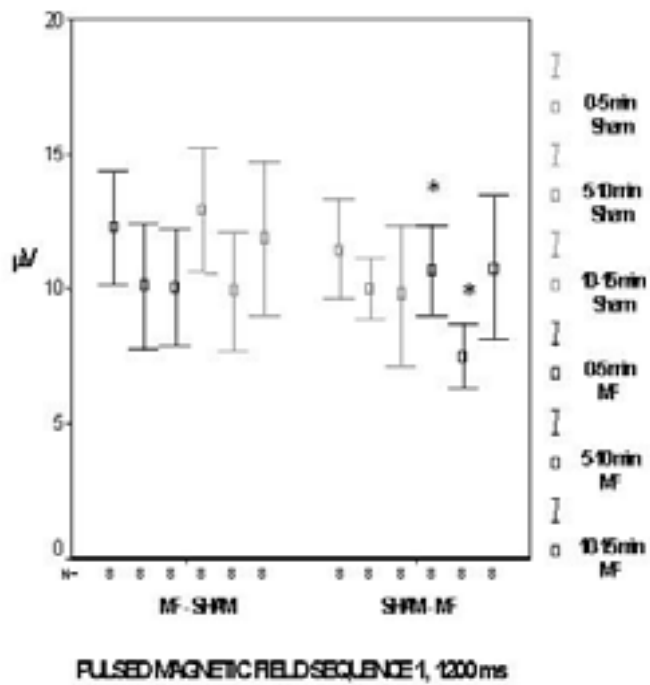
**CHANGES IN HUMAN EEG ALPHA ACTIVITY FOLLOWING EXPOSURE TO TWO DIFFERENT PULSED MAGNETIC FIELDS SEQUENCES.** C. M. Cook<sup>1,2,3</sup>, A. W. Thomas<sup>1,2,3</sup>, F. S. Prato<sup>1,2,3</sup>. <sup>1</sup>Lawson Health Research Institute, <sup>2</sup>St. Joseph's Health Centre, <sup>3</sup>Univ of Western Ontario.

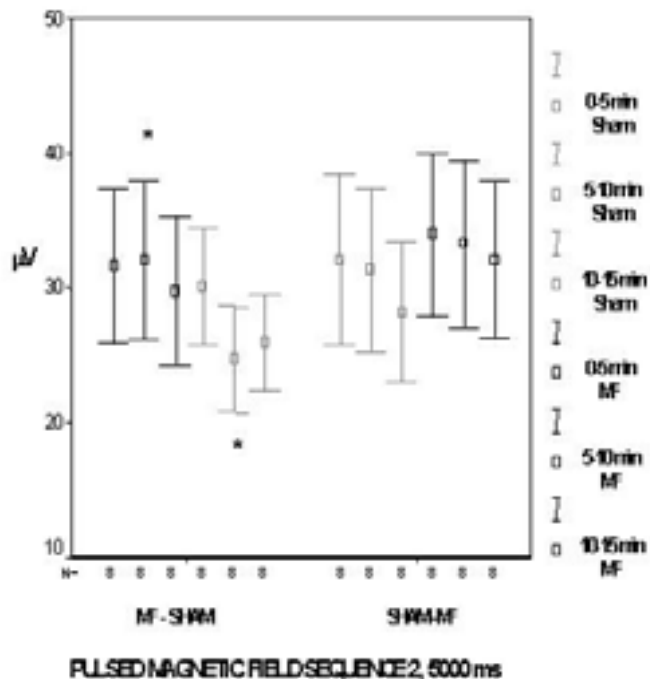
**Background:** We have determined that pulsed (200  $\mu$ T) extremely low frequency magnetic fields (ELF MF) affect the frequency content of the electroencephalogram (EEG), most notably the alpha frequency (8-13 Hz) [1,2]. However, differences in the length of the pulsed MFs 'refractory periods' (RP, 'no field' periods between magnetic field pulses) seemed to generate discrepancies between the results of our two experiments. The pulsed MF in the first experiment [1] contained a 1200 ms RP while the pulsed MF in the second experiment [2] contained a longer 5000 ms RP.

**Objective:** Assess the effects of two different pulsed MF sequences upon the frequency content of the EEG during 15 min exposure.

**Methodology:** 32 subjects were assigned to receive one of two pulsed MF sequences (1200 ms (n=16) and 5000 ms (n=16) refractory period) and a sham exposure in a counterbalanced design. Sessions were separated by 1 week. Subjects were placed within 3 orthogonal, nested square Helmholtz coils with the uniform magnetic field volume centred at the head level. In each 30 min session, subjects were exposed to either a 15 min sham or pulsed MF (< 500  $\mu$ T, 0-3 kHz). EEG was acquired with a commercial electrode cap (Quik-Cap, Neuroscan labs, Sterling, VA) from 14 scalp locations (F3, F4, Fz, FCz, C3, C4, Cz, CPz, P3, P4, Pz, O1, O2, Oz) using a 16 Channel Grass (Model 12, Astro-Med, Inc., West Warwick, RI) and processed using Scan 4.3 (Neuroscan labs, Sterling, VA). The sampling rate was the same for both sequences (1024 Hz), but two different EEG epoch lengths were used, based on the length of the pulsed MF refractory period (1023 ms epoch length for 1200 ms & 4095 ms for 5000 ms RP). The 15 min exposure was separated into three 5 min intervals during sham and MF exposure. EEG epochs were Fourier transformed to assess the frequency content of the EEG.

**Results:** Due to the difference in EEG epoch length (i.e. 1024 vs. 4096 data points), between group comparisons for the two pulsed MF sequences were not possible. Within group differences in occipital (O1, Oz, O2) alpha activity (8-13 Hz) were found for both sequences. Separate ANOVAs displayed 3 way interactions between exposure condition (sham/MF), exposure order (MF-sham or sham-MF) and time (0-5 min, 5-10 min, 10-15 min) for EEG alpha activity (8-13 Hz) in both sequences (Sequence 1, 1200ms: [ $F_{2,11}=3.134$ ,  $p < 0.10$ , partial  $\eta^2=0.363$ ] Sequence 2, 5000 ms: [ $F_{2,11}=5.917$ ,  $p < 0.05$ , partial  $\eta^2=0.518$ ]). Post-hoc t-tests determined that in Sequence 1, alpha activity decreased during the pulsed MF after 5 min in the sham-MF exposure order compared to the 0-5 min period of pulsed MF exposure ( $t_7=2.62$ ,  $p < 0.05$ )(Figure 1), while in Sequence 2, alpha activity was marginally increased during the pulsed MF after 5 min in the 'MF-sham' exposure order compared to the comparable sham period ( $t_7=2.048$ ,  $p=0.08$ )(Figure 2). EEG alpha activity was no longer significantly different from sham in the post-exposure period for both sequences.





**Conclusion:** Human brain electrical activity was found to be differentially affected by two different pulsed MF sequences. The two sequences were identical with the exception of their 'refractory' or 'no field' periods (1200 ms vs. 5000 ms). These results again indicate that ELF MF exposure can affect human EEG activity, particularly the occipital alpha activity (8-13 Hz). Furthermore, the effects were found to be dependent upon the order of exposure (MF-Sham vs. Sham-MF).

**References:**

- [1] Cook CM, Thomas AW, Prato FS. 2004 Bioelectromagnetics. 25(3):196-203.
- [2] Cook CM, Thomas, AW, Keenlside L, Prato FS. Bioelectromagnetics, (in revision).

**Acknowledgements:** This research was funded in part by the following: Canadian Foundation for Innovation (CFI), Ontario Research and Development Challenge Fund (ORDCF), Plunkett Foundation, Ontario Innovation Trust (OIT), Lawson Health Research Institute, an operating grant to Frank S. Prato from the Canadian Institutes of Health Research (CIHR) and a doctoral research award to Charles M. Cook from CIHR. Special thanks to J. Davis for technical and computer assistance

2-2 STUDENT

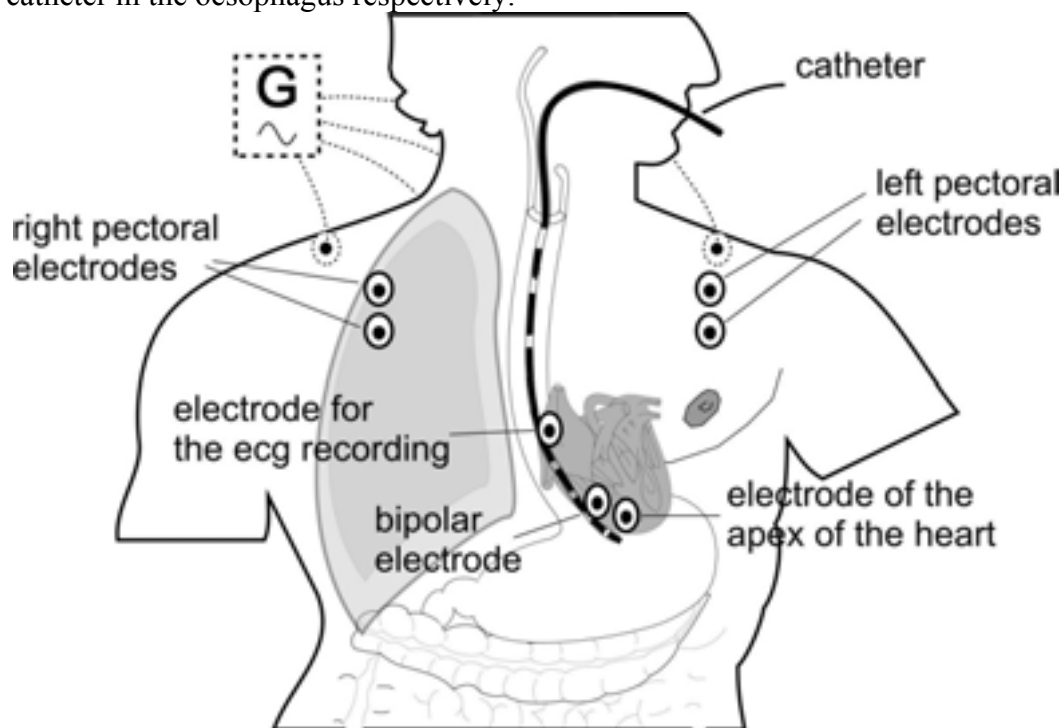
**THE INFLUENCE OF ANATOMICAL AND PHYSIOLOGICAL PARAMETERS ON THE INTERFERING VOLTAGE OF ELECTRONIC IMPLANTS IN LOW FREQUENCY ELECTRIC AND MAGNETIC FIELDS.** S. Joosten, K. Pammler, J. Silny. femu - Research Center for Bioelectromagnetic Interaction, Univ Hospital, Aachen Univ, Aachen, Germany.

**Objectives**

The aim of the study is to determine a possible influence of physiological and anatomical parameters on the electric fields in the human body generated in low frequency electric and magnetic fields and disturbing electronic implants. In this investigation the focus was to assess the worst-case conditions for the interference of implanted cardiac pacemakers and cardioverter defibrillators.

**Material and Methods**

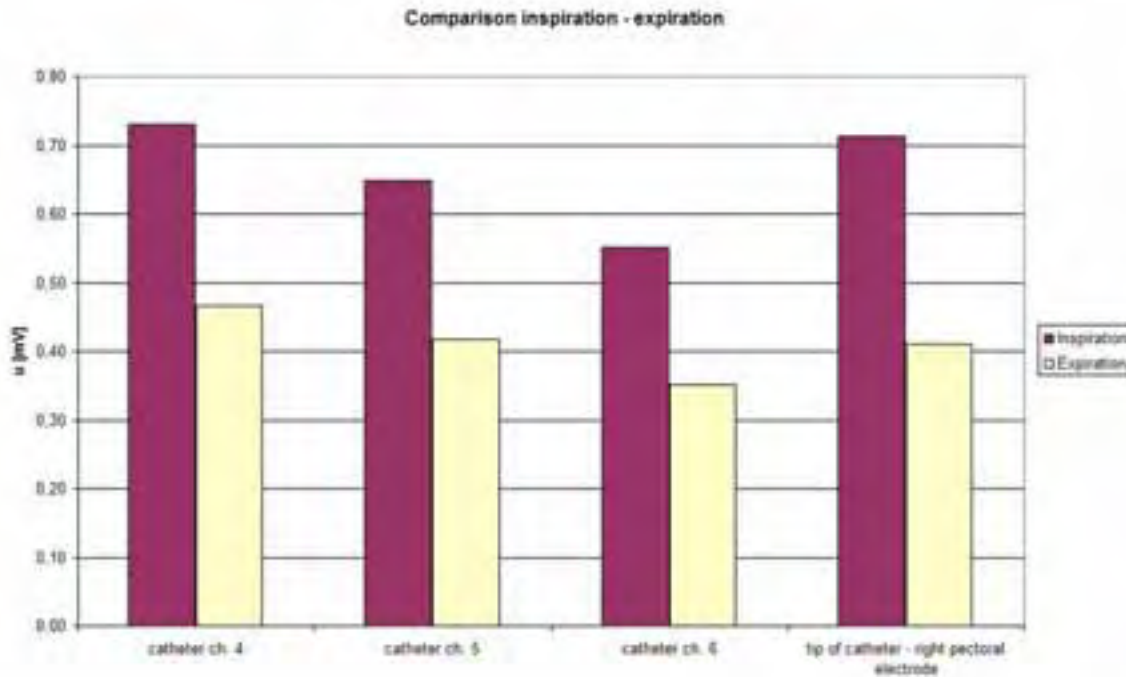
In the initial study fifteen volunteers took part. The volunteers with heights between 162 and 187 cm were aged from 23 to 61 years. To obtain reproducible results all volunteers were investigated under standardized conditions. Each volunteer was sitting between the two coils of a Helmholtz-arrangement. During the experiment sinusoidal continuous magnetic fields of 45  $\mu\text{T}$  or 90  $\mu\text{T}$  (RMS) with a frequency of 60 Hz were applied. To simulate the influence of an extra-corporal electric field sinusoidal continuous currents of 14 and 21  $\mu\text{A}$  (RMS, frequency of 60 Hz) respectively were injected by several electrodes on the surface of the body and feet. The test procedure took about 60 minutes per volunteer. Prior to the test procedure the body dimensions of each volunteer were measured. The test sequence itself was designed to check several physiological parameters which significantly change the volume conductor of the thorax, for example the state of respiration, systolic or diastolic conditions or stomach filling factors. Additionally, the contributions of the muscles to the electrical activity to the interfering voltage were recorded. The induced electric fields in the body are measured by self-adhesive electrodes and by a catheter in the oesophagus respectively.



With the help of seven electrodes which are positioned on the body surface different types of cardiac pacemaker sensing systems (bipolar / unipolar, left / right pectoral) were simulated (see figure 1). The field distribution measured on the body surface were verified by voltage recording from the catheter placed in the oesophagus. The positions of the electrodes on the catheter were especially chosen to represent different bipolar as well as unipolar pacemaker sensing systems (see figure 1). The tip of the catheter was positioned at the entry of the stomach with the help of two electrodes at the top. Thereby the first electrodes on the catheter are located close to the real position of a bipolar sensing system. During the exposure by electric or magnetic fields the voltages between all electrodes on the thorax and all electrodes on the catheter as well as between both systems are recorded. In this way the interference voltage at the input of a cardiac pacemaker can be established. The strength of the applied magnetic fields and electric current were controlled by a computer system. The same computer system carried out the recording of the signals.

## Results

The results show that a number of anatomical and physiological parameters have a significant influence on the interfering voltage at the pacemaker input. The state of respiration exerts the greatest influence: The difference between the inspiration and the expiration of the lung adds up to 40 % (see figure 2).



The values of this example were acquired by the application of a current sum of 14  $\mu$ A. In contrast the influence of other parameters like the filling of stomach or systolic or diastolic conditions are much smaller. Under the consideration of all physiological and anatomical factors as well as the dimension of the body the difference in the threshold can be up to 100%.

2-3

**COULD A 50 HZ, 1000  $\mu$ T MAGNETIC FIELD HAVE A TRANSIENT EFFECT ON HUMAN PHYSIOLOGICAL TREMOR?** A. Legros, P. Gaillot, D. Nguyen, D. Goulet, M. Plante, A. Beuter. Universite de Montpellier I, Hopital Gui de Chauliac, Montpellier, France.

### Introduction

Time varying extremely low frequency (ELF) magnetic fields (MF) effects on human physiology are still poorly known. Nevertheless information is needed for new limit exposure establishment. Several studies have examined their effect on electroencephalogram, evoked potentials, electrocardiogram, cognition or motor behavior but no consensus has been established yet (Cook et al., 2002, Legros and Beuter 2002). Moreover, measures are rarely made during exposure due to the "contamination" of data by the MF itself. However, Thomas et al. (2001) showed that normal human standing balance could be improved during the exposure to a specific 200  $\mu$ T pulsed MF centred at the level of the head. Another highly sensitive motor control parameter of the neurophysiological state is physiological tremor. It is an involuntary, irregular and continuous movement of the body's extremities (Beuter et al., 2003) and three mechanisms are known to contribute to its generation: (1) the mechanical resonance of the limb, (2) the stretch reflex feedback resonance and (3) the pacemaker action of the central nervous system. In this context, if MF had an effect on human neurophysiology, it should be instantaneously detected in physiological tremor.

## Objective

The main aim of this study was to determine if the transition of the MF could have a transient effect on human postural tremor by using a time-frequency analysis: the wavelet analysis.

## Methods

Twenty-four men between the ages of 20 and 50 years ( $37.8 \pm 8$ ) were recruited among the personnel of a French electricity company ("Electricite de France": EDF). The exposure device was developed by the "Institut de Recherche d'Hydro-Quebec" (Nguyen et al., 2004). It generated a continuous and homogenous sinusoidal 50 Hz MF of  $1000 \mu\text{T}$  centered at the level of the head and a laser recorded the dominant index vertical displacement (resolution =  $5 \mu\text{m}$ ) at 1000 Hz (Figure 1a and b). Subjects participated to one double blind session including two 14 minutes sequences of postural tremor recording (tremor occurring while subjects had to maintain a fixed position with their index finger): (1) postural tremor in real exposure condition and (2) postural tremor in sham exposure condition. Each sequence was composed of four 20 s recording periods centered on a MF transition (two "off/on" and two "on/off", Figure 2).

Tremor scalograms were computed on velocity time series between 2 and 20 Hz using the wavelet analysis (Torrence and Compo, 1998). An index we developed (mean significant power = MSP) was computed on the first and the last 10 s of recordings and was used for the statistical analysis.

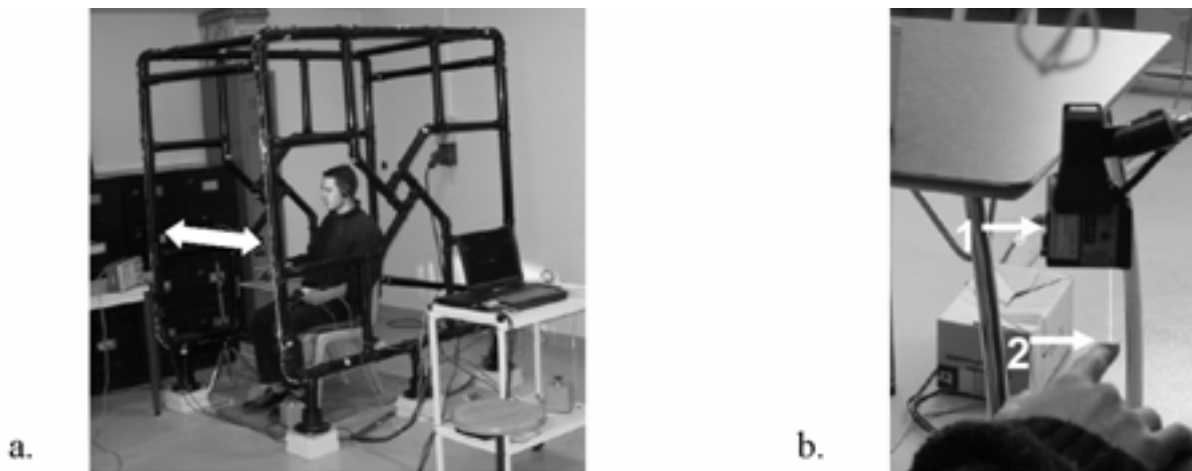


Figure 1: a. A subject in the experimental device. The white arrow shows the two coils. b. The beam of the laser (1) is pointing a white cardboard (

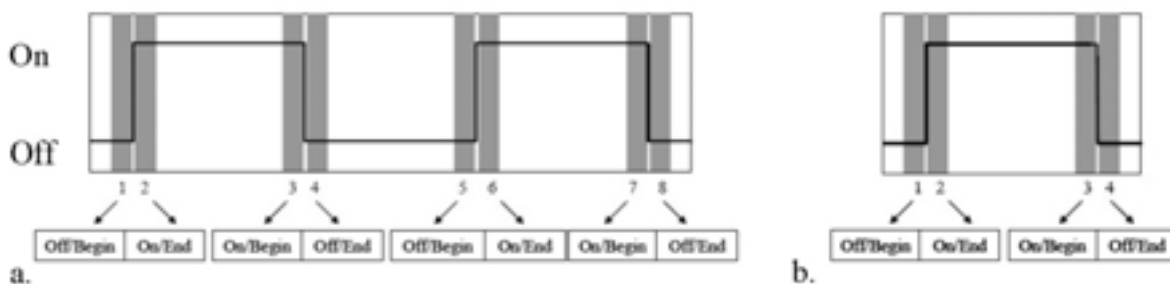


Figure 2: a. The 14 minutes of a sequence of test. Vertical grey bands represent the 20 s recording periods and full lines show MF status ("off" when the line is down and "on" when the line is up). b.

Recordings 1, 2, 3, 4 and 5, 6, 7, 8 are respectively equivalent: corresponding MSP were averaged for the statistical analysis.

### Results

Wavelet analysis allows a temporal localization of a transient change in amplitude or in frequency of tremor time series. Such observations linked with a MF transition were never seen in our spectrograms (Figure 3). A three way ANOVA with repeated measures realized on MSP investigated exposure condition effect (real or sham), MF effect (MF "on" or MF "off") and time effect (before or after MF transition). Results, showed a significant time effect: the MSP was higher before than after transitions ( $F=4.36$ ,  $p>.05$ ). Time effect was more pronounced under real exposure conditions ( $F=5.88$ ,  $p < .05$ , Figure 4).

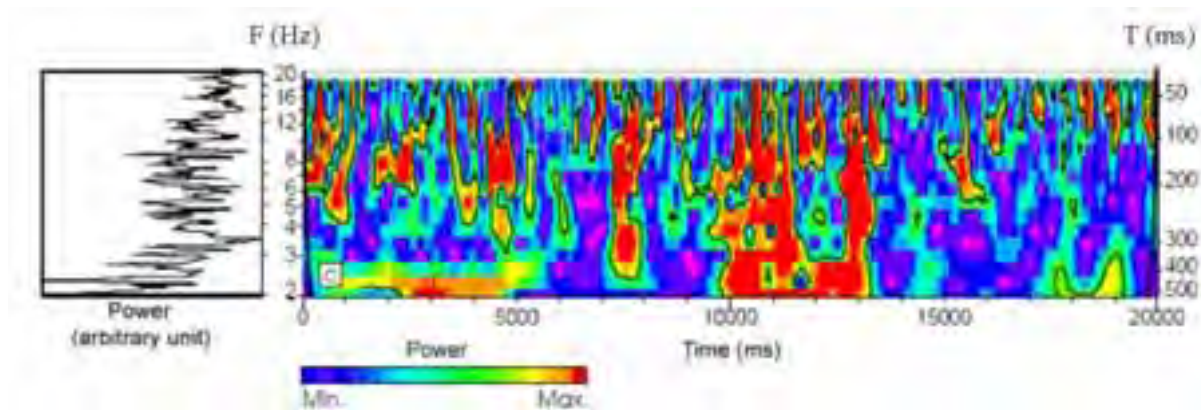


Figure 3: Classical normalized Fourier spectrum (left) and wavelet scalogram of velocity tremor time series for subject 25 ("off/on" transition). Right vertical axis represents the period in ms (T) and the left one to the corresponding frequencies in Hz (F). Areas inside the black lines are found significant using the statistical test developed by Torrence and Compo (1998).

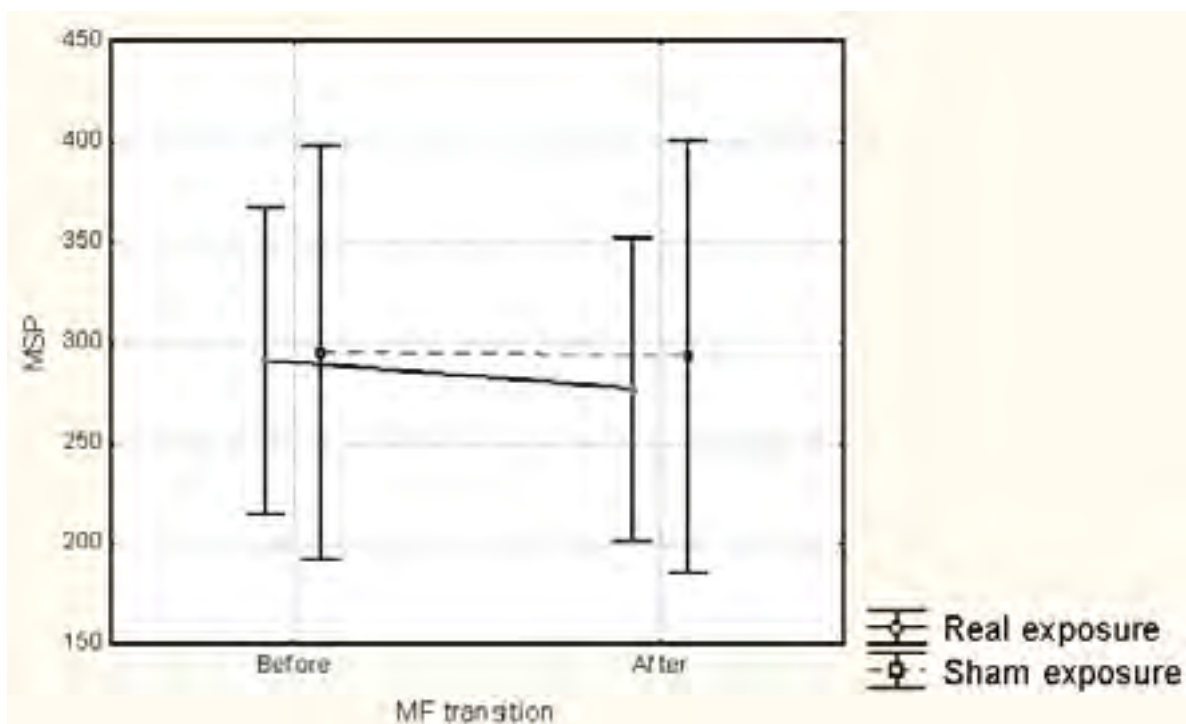


Figure 4: Interaction effect between time and exposure condition.

### Conclusions

A relaxing effect induced by the experimental procedure reduces tremor size between the beginning and the end of a recording and interestingly, this effect is more pronounced under real than under sham exposure. This could mean that the effect of the used MF could be comparable to the effect of relaxation. This study was pioneer and its main aim was rather detecting subtle changes in physiological tremor than explaining underlying mechanisms and it shows that exposure to a 50 Hz, 1000  $\mu$ T MF seems detectable in human physiological tremor. But further analyses are needed to confirm this result and to verify if they persist while there is no relaxation induced by the experimental procedure.

### References

- Beuter A, Glass L, Mackey MC, Titcombe MS. 2003. *Nonlinear Dynamics in Physiology and Medicine*. New York: Springer Verlag.
- Cook CM, Thomas AW, Prato FS. 2002. Human electrophysiological and cognitive effects of exposure to ELF magnetic and ELF modulated RF and microwave fields: a review of recent studies. *Bioelectromagnetics* 23(2):144-57.
- Legros A, Beuter A. Time-varying magnetic fields and neuromotor control: A review of selected literature; 2002; Poitiers, France. p 100.
- Nguyen DH, Richard D, Plante M. 2004. *Système de génération du champ magnétique et de commande des essais pour l'étude de l'effet des champs magnétiques sur le système nerveux central et périphérique par l'exploration des tremblements*. Montréal: Hydro-Québec.
- Thomas AW, Drost DJ, Prato FS. 2001. Human subjects exposed to a specific pulsed (200 microT) magnetic field: effects on normal standing balance. *Neurosci Lett* 297(2):121-4.
- Torrence C, Compo GP. 1998. A practical guide to wavelet analysis. *Bull Amer Meteor Soc* 79(1):61-78.

2-4

**EFFECTS OF CELLULAR PHONE USE ON EAR CANAL TEMPERATURE MEASURED BY NTC-THERMISTOR.** H. Lindholm<sup>1</sup>, K. Tahvanainen<sup>1</sup>, J. Nino<sup>1</sup>, P. Halonen<sup>2</sup>, T. Kuusela<sup>3</sup>, E. Lansimies<sup>4</sup>, M. Hietanen<sup>1</sup>. <sup>1</sup>Finnish Institute of Occupational Health, Helsinki, Finland, <sup>2</sup>Computing Center, Kuopio Univ, Kuopio, Finland, <sup>3</sup>Dept of Physics, Turku Univ, Turku, Finland, <sup>4</sup>Dept of Clinical Physiology, Kuopio Univ Hospital, Kuopio, Finland.

### INTRODUCTION

The widespread use of cellular phones has raised public and scientific concern about their possible adverse effects on health. The results of the clinical and epidemiological studies are discrepant and do not provide a clear pattern of possible health effects related to RF fields emitted by the cellular phones. While some studies have reported biological effects in the absence of heat, warming of tissues is the main established effect of exposure to RF fields. In the head phantom studies, the temperature in simulated brain tissue has found to increase 0.03 - 0.1 degree C during exposure to RF fields emitted by cellular phones. Recently, the skin temperature has been reported to elevate up to 2.3 degree C during similar exposure. The objective of this study was to measure the temperature changes in the ear canal during and after a 35 min exposure to RF fields emitted by two GSM phones. Evaluation of the ear canal temperature was chosen as the research target due to proximity of the ear canal to the brain tissues.

## STUDY DESIGN

Thirty-four healthy volunteers, 16 females and 18 males, average age of  $38.8 \pm 10.3$  years, were enrolled in this randomized, double-blinded and placebo-controlled cross-over study. The left ear of the subjects was exposed to GSM phones (900 MHz with the antenna power of 2 W and 1800 MHz with the antenna power of 1 W) during two different days, one week apart. The total duration of each session was 2 hours, including one 35 min RF exposure and one 35 min sham exposure. A similar, but inactive GSM phone was situated on the right ear of the subjects. Simultaneous recordings of temperature inside the left and right ear canals, electrocardiogram, and non-invasively measured arterial blood pressure signal from the finger (finger cuff method) were conducted. Also, pneumotachometrically measured respiration signal and the relative RF signal intensity produced by the cellular phone were recorded. Ear canal temperatures were measured using high precision miniature NTC thermistors (length 20 cm, diameter 0.3 mm) with a resistance of 3000 Ohms at 25 degreeC (BetaTHERM Corp., USA). For the statistical analysis, carry-over effect ( $p < 0.1$ ) and the period effect ( $p < 0.05$ ) were checked by using repeated measures analysis (general linear model). Student's t test for paired data was used in the comparisons between both interventions (RF exposure vs. sham exposure) for continuous outcome variables. Subgroup comparisons were carried out by independent t tests. Non-continuous variables were analyzed by using the McNemar test. Two-sided p-values were considered statistically significant at  $p < 0.05$ .

## RESULTS

### Exposed Ear

The differences in the ear canal temperatures between RF exposure and sham exposure were statistically significant, both for 900 and 1800 MHz phones. Also, there were statistically significant differences in the ear temperatures between post-exposure and post-sham conditions both with 900 and 1800 MHz phones. When subjects were exposed to 900 MHz fields, temperature was significantly higher during spontaneous breathing test, head-up tilt test and Valsalva manoeuvre compared to sham exposure intervention ( $p < 0.01$ ). The mean differences between the RF and sham interventions were  $0.4 \pm 0.9$  degreeC during spontaneous breathing test,  $0.6 \pm 0.7$  degreeC during head-up tilt test and  $0.7 \pm 0.5$  degreeC,  $0.7 \pm 0.5$  degreeC and  $0.7 \pm 0.5$  degreeC during the three analysis periods of Valsalva manoeuvres ( $p < 0.01$ ). The same pattern was observed with the 1800 MHz phone. No carry-over effects were observed either during the 900 MHz study or during the 1800 MHz study. A period effect was observed during the 900 MHz study as well as during the 1800 MHz study.

### Non-exposed Ear

There were no statistically significant differences in the ear canal temperature between the sham exposure and 1800 MHz RF exposure. During the 900 MHz study the temperature at the end of Valsalva manoeuvre was  $0.1 \pm 0.2$  degreeC higher during exposure compared to sham exposure ( $p < 0.05$ ). There were no statistically significant differences between post-exposure and post-sham exposure periods neither during 900 MHz nor during 1800 MHz studies. No carry-over effects were observed either during 900 MHz study or during 1800 MHz study.

## DISCUSSION

The results indicated that temperature in the canal of the ear increases during a 35 min exposure to RF fields emitted by 900 and 1800 MHz GSM phones. Although temperatures were significantly higher also during the post-exposure period, the maximal increases were found during the last three tests performed during the RF exposure period, reaching maximum increases of 1.2 degreeC (for the 900 MHz) and 1.3 degreeC (for the 1800 MHz). There were no increases in the ear canal temperature on the side of the head where the inactive phone was held, suggesting that the increases in the temperature exist only in the local area. The temperature started to decrease immediately after the RF exposure was

switched OFF. This study provides evidence that cellular phone use with maximal allowed antenna power results in statistically significant temperature elevation in the ear canal, when temperature is measured by NTC thermistors. It is, however, unclear whether this is caused by the RF fields emitted by cellular phones, or whether it is a result of the conducted/reflected heat between the skin and the battery of the cellular phone.

2-5

**IS THE SLEEP QUALITY OF HYPERSENSITIVE PERSONS ASSOCIATED WITH THEIR ELECTROSENSITIVITY?** J. Schroettner, N. Leitgeb, Roman Cech. Institute of Clinical Engineering, Graz Univ of Technology, Austria.

#### OBJECTIVES:

An increasing number of people associate their non-specific health symptoms with emissions of electromagnetic fields from transmitter stations, in particular with broadcasting antennas and telecommunication base stations. Above all, sleep disturbances are mentioned especially in the group of electromagnetic hypersensitive persons. Laboratory EMF sleep studies suffer from a number of limitations, therefore, a sleep study with a quite innovative new approach was designed. It is the goal of this investigation to study potential reactions to EMF reduction rather than to provocation in particular of electromagnetic hypersensitive people [1].

#### METHODS:

In the EPROS-study (Electrosensitives Protected Sleep), sleep is investigated on-site at home based on EEG-, EOG- and ECG- recordings and standardized questionnaires. Additionally, a continuous broadband frequency- selective EMF monitoring during the nights was chosen to monitor the actual EMF immission. Each evening and each morning the biological status of the volunteers is subjectively and objectively assessed via questionnaires and biological measurements such as electrosensitivity and reaction time. Electrosensitivity was characterized by the ability to perceive directly coupled electric currents [2]. To be able to measure even low perception thresholds, a stimulator with the applied part isolated from earth and extra low patient leakage currents of less than  $5\mu\text{A}$  was developed (medical device standards allow  $100\mu\text{A}$ ). Currents were applied via conventional adhesive ECG Ag/Ag Cl-electrodes at a standardized position at the lateral side of the forearms.

To allow the detection of placebo effects investigations are made using a verum-shield, a sham-shield and the unshielded control situation. It was possible to find a sham tissue that could not be distinguished from the verum tissue, neither visually nor tactually. Care was taken to completely shield the bedside including the bottom to avoid any unnecessary slits. Investigations were made double-blind. To allow this, the following arrangements were made:

- the volunteers were not informed about different shield condition
- the shields were mounted each evening and removed each morning to reduce the possibility for checks by the volunteers
- the sequence of the three conditions (verum- sham- and control) was selected by a random generator
- measurements on site and data analysis were performed by different teams
- the sequence of the test conditions was blinded for the evaluation team, uncovering was made after the finalized analysis.

#### RESULTS:

In a pilot study sleep was investigated during 86 nights at 9 volunteers. Since age- dependent normal

ranges are known for the used sleep questionnaire, the severity of the individual sleep problem could be assessed. The results of 7 volunteers showed a wide overlap of sleep quality with what is considered normal, in two cases the sleep quality was considerable worse.

The evaluation of the RF immission monitoring showed that mobile telecommunication radiation did not dominate. The overall limit- weighted sum of the RF immissions was well below 1% of the ICNIRP limit. Concerning a possible relationship between sleep quality and RF immissions no conclusion can be drawn at present time.

Although electrosensitivity had not been checked prior to the involvement of the study it is remarkable, that 89% of the volunteers showed considerably increased values compared with what is considered "normal". Compared with the general population 36% of the results derived from the electrosensitivity measurements lie in the sensitive and even 35% in the very sensitive range (Fig. 1). Further investigations are needed to clarify the role of increased electrosensitivity in regard to impaired sleep, and whether this indicates a causal role of EMF. There is some evidence that electrosensitivity could be a more general indicator for the status of the autonomous nervous system.

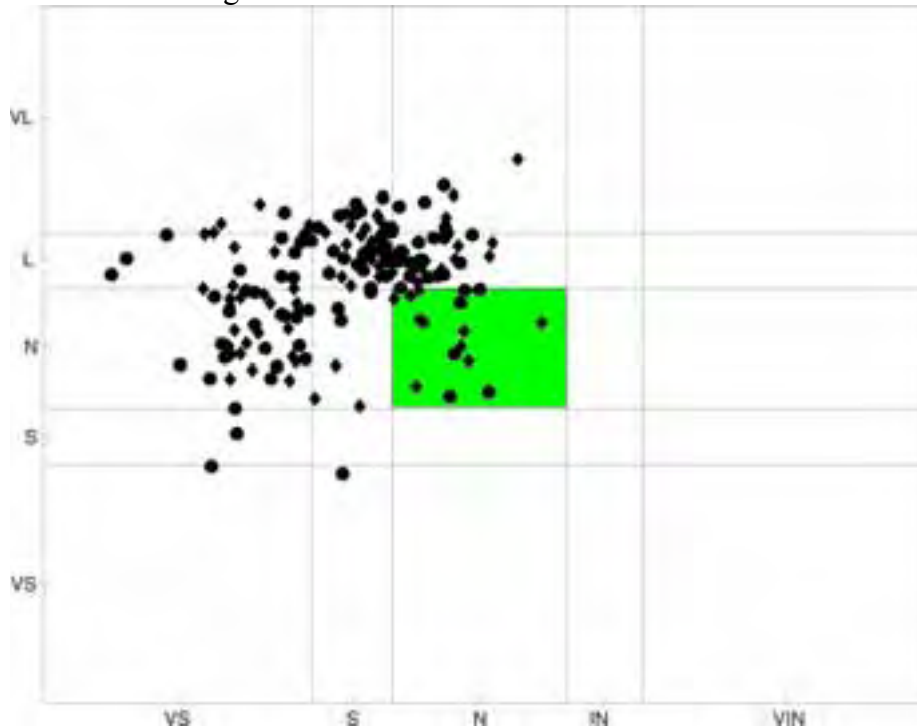


Figure 1: Electrosensitivity diagram [2] of all volunteers: electrosensitivity (VS...very sensitive, S...sensitive, N...normal, IN...insensitive, VIN...very insensitive) vs. variability coefficient (VS...very small, S...small, N...normal, L...large, VL...very large)

#### CONCLUSION:

The pilot study showed that the new approach is feasible, both in respect to the participation of volunteers in spite of the considerable discomfort and required engagement, and in respect to the on site data acquisition, RF monitoring and shielding. The preliminary results justify further investigations with the EPROS design.

#### ACKNOWLEDGMENT:

The pilot study was supported by the German Research Association for Telecommunication. The main study is supported by the Austrian ministry of life and the Austrian ministry of economics and labour.

## References:

1. Leitgeb, N., Schroettner, J., Cech, R., Kerbl, R.: Untersuchung von Schlafstoerungen um Hochfrequenz-Sendeanlagen, Investigation of Sleep Disorders in the Vicinity of RF Transmitters. *Biomed. Technik*, 49 (2004), 186-193
2. Leitgeb, N., Schroettner, J.: Electrosensibility and Electromagnetic Hypersensitivity, *Bioelectromagnetics* 24 (2003), 387-394

2-6

**EVALUATION OF AFFECTIVE RESPONSES TO 5  $\mu$ T MAGNETIC FIELDS MODULATED AT FREQUENCIES WITHIN EEG  $\alpha$ -RANGE.** P. Stevens. Koestler Parapsychology Unit, Univ of Edinburgh, Edinburgh, UK.

### **Method**

**Subjects:** 20 self-selected, right-handed subjects (13 male, 7 female) were recruited by poster and word of mouth. All subjects had given informed verbal consent to undergoing the magnetic field exposure and were paid a £10 participation fee.

**Apparatus:** Magnetic fields (MF) with maximum peak-peak amplitude of 5 microT were generated by 3 wire-wrapped coils via DC sinusoidally-modulated current from a arbitrary function generator (FGA2030, Tecstar Electronics, UK). Coils were embedded in the experimental room walls, with axes aligned North-South (subject faced North).

Skin conductance (SC) was monitored using two 8mm diameter sintered Ag/AgCl cup electrodes and pH-balanced aqueous gel, attached via adhesive washer to the second phalanx of the index and second fingers of the non-dominant hand. Data were sequentially sampled and saved to hard disk at 40 Hz via a 24-bit SC monitor [SC5-SA: PsyLab/Contact Precision Instruments, London, UK].

Electroencephalographic (EEG) activity was recorded using Ag/AgCl sintered electrodes [QuickCap and NuAmps model 7181 DC amplifier: Neuroscan, Texas USA] on twelve scalp positions (10-20 system: F3, F4, C3, C4, T3, T4, P3, P4, O1, O2, Fp1, Fp2) with linked ears reference. Data were sampled at 500Hz and band-pass filtered between 0.5 and 100 Hz.

All equipment used in the study was prechecked to ensure there was no direct detection or cuing as to the presence of the MFs.

Stimuli consisted of 60 second exposure periods to one of two MF types or no field (sham exposure). MF type 1 was sinusoidally modulated at a frequency corresponding to the peak frontal EEG frequency previously recorded for that subject during autobiographical recall of events associated with negative emotions. Likewise, MF type 2 used a peak frequency corresponding to positive emotions. Frequencies ranged from 8.3-12 Hz for type 1 and 8.4–12.2 Hz for type 2.

**Procedure:** Subjects were seated in a reclining chair in a sound-attenuated room. After a 5 minute relaxation period with music, they underwent a blind, pseudo-randomised schedule of 8 stimuli periods (2 MF type I, 2 MF type II, 4 Sham). Before each period, they were alerted by an audio tone and instructed on-screen to close their eyes until they heard a second tone. After each period, they were again alerted by an audio tone and asked to select via TFT touchscreen 4 words out of a possible 16 which best described their current emotional state. Half the words related to negative and half to positive emotions. This was followed by a 30 second rest period before the next stimulus period.

**Analysis:** EEG data were used to calculate z-normalised Global Field Power (GFP, defined as the standard deviation across multiple channels as a function of time within a sample interval).

Power spectra for each subject were constructed for electrodes F3 and F4 (75% overlapping 8.192s epochs, 10% cosine bell taper) and used to calculate frontal asymmetry (FA) in alpha (8-14 Hz) such that:

$$FA = \ln(\text{Right Frontal Power}_\alpha / \text{Left Frontal Power}_\alpha)$$

SC data were normalised for each subject by subtracting the session mean and dividing by the session standard deviation, and mean SC levels then calculated for each stimulus period. Subject's choice of emotion-related words were used to construct a Reported Emotional State (RES):

$$RES = [\# \text{ Positive Words} / (\# \text{ Positive Words} + \# \text{ Negative Words})] - 0.5.$$

### **Results**

For normalised mean SC, 57% of subjects showed a non-significant decrease in arousal for MF stimuli relative to control stimuli (Wilcoxon:  $V=98$ ,  $p=0.41$ , 1-tailed).

For GFP, 65% of subjects exhibited a significant decrease for MF stimuli relative to control stimuli (Wilcoxon:  $V=48$ ,  $p=0.03$ , 1-tailed). There was no significant differences between the two MF types or between GFP for left and right hemisphere.

The EEG-Emotion literature suggests that frontal alpha power in the F3 and F4 electrodes tends to be asymmetrical when a subject experiences an emotional state, with positive emotions showing decreased alpha (and therefore increased cortical activity) in the left frontal cortex and negative emotions showing decreased alpha/increased cortical activity in the right frontal cortex. It was therefore predicted that the MF stimuli would alter EEG frontal asymmetry (FA). Mean FA for MF stimuli was 0.04 and 0.05 for Sham stimuli. As higher FA values indicate a shift to positive emotion, the effect of the MFs was to slightly decrease the asymmetry associated with a positive emotional state (i.e., a decrease in left frontal cortical activity / increase in left frontal alpha). This difference was not statistically significant. Finally, it was predicted that subjects' Reported Emotional State (RES) would differ for MF versus Sham stimuli. The RES was 0.03 for MF stimuli and -0.27 for the Sham stimuli. A Wilcoxon test found this to be a statistically significant difference ( $V=189$ ,  $p=0.002$ , 2-tailed), suggesting a more positive reported emotional state associated with MF stimuli. There was no significant difference between the MF types.

A post-hoc analysis found no significant correlation between the RES and FA, nor between RES and GFP change

### **Conclusions**

MF stimuli were found to result in a significant decrease in cortical arousal, mirrored by a slight decrease in autonomic arousal (conceptually replicating an earlier paper by the author). Although subjects were not consciously aware of these changes and did not appear to directly experience an emotional state (based on EEG asymmetry measures), their choice of emotion-related words indicated a subsequent bias towards a positive emotional state. This novel finding could suggest that subjects interpreted the MF-induced change in arousal as an ambiguous emotional event, opting in the absence of any strong external cues for the default positive interpretation that the affect literature suggests is the human norm. Further research is underway to test this idea by attempting to influence subjects' interpretations through the manipulation of external cues.

This work was supported by the Fundação Bial, Porto, Portugal (Grant # 76/02).

Summary of Results				
	Mean SC ( $\sigma$ )	Mean GFP ( $\sigma$ )	Mean FA	Mean RES

MF	-0.65	16.17	0.04	0.03
Sham	0.55	17.31	0.05	-0.27

2-7

**OCCUPATIONAL 50 HZ MAGNETIC FIELD EXPOSURE MEASUREMENTS AMONG FEMALE SEWING MACHINE OPERATORS IN HUNGARY.** J. Szabó<sup>1</sup>, K. Mezei<sup>1</sup>, G. Thuróczy<sup>1</sup>, G. Mezei<sup>1,2</sup>. <sup>1</sup>National Institute for Radiobiology and Radiohygiene, Budapest, Hungary, <sup>2</sup>Electric Power Research Institute, Palo Alto, California 94304, USA.

#### Introduction

Occupational magnetic field exposure is less thoroughly characterized in occupations typically held by women. Our objective was to characterize occupational 50 Hz magnetic field personal exposure among female sewing machine operators.

#### Methods

We conducted full-shift measurements of occupational 50 Hz magnetic fields personal exposures among 51 female sewing machine operators in a garment factory producing swimming suits and lingerie in Hungary. During the measurements the women were working in two shifts (6h-14h and 14h-22h) according to their normal daily routine (8-hour continuous shifts with a few 15-minute breaks). Measurements were conducted using EMDEX PAL meters (Enertech, Campbell, California) in April and May 2004. Meters were worn in a pouch hanging on a lanyard at chest level. Recorded measurement data was transferred to a computer and analyzed by Microsoft Excel 97 and EPI Info 6.04.

#### Results

The average age of the women was 36 years (range 19-53). They had, on average, 12 years (range 1-31) of work experience in the garment industry. The average duration of the measurement periods was 449 minutes (range 420-470).

The average arithmetic mean magnetic field personal exposure for all women was 0.76  $\mu$ T (range 0.06-4.27). The average geometric mean was 0.56  $\mu$ T (range 0.06-2.78), and the average maximum value was 4.30  $\mu$ T (range 0.55-14.80). The average number of transients by certain ranges of the magnetic field (under 0.5  $\mu$ T, 0.5-1.0  $\mu$ T, and above 1.0  $\mu$ T) was 344, 418 and 65, respectively.

For women (n=10) who operated sewing machines produced in 1990 or earlier, the average arithmetic mean exposure was 2.09  $\mu$ T. For women (n=41) who operated sewing machines produced after 1990, the average arithmetic mean was 0.43  $\mu$ T. Other worker or sewing machine characteristics we examined did not significantly influence measured personal magnetic field exposure.

#### Conclusion

Based on our measurements we conclude that women working as sewing machine operators experience higher than average occupational magnetic field exposure compared to other working women (1). Most important determinant of the women's personal magnetic field exposure was the age of the sewing machine the women operated. Women working with older sewing machines experienced higher exposure than women working on newer sewing machines.

#### Reference

(1) Forssen et al. *Occup Environ Med* 2004.

**STUDIES ON HYPERSENSITIVITY TO NON-THERMAL RADIOFREQUENCY ELECTROMAGNETIC FIELD IN JAPAN.** Y. Ugawa<sup>1</sup>, Y. Terao<sup>1</sup>, M. Nishikawa<sup>2</sup>, T. Okano<sup>1</sup>, S. Shirasawa<sup>1</sup>, T. Furubayashi<sup>1</sup>, C. Ohkubo<sup>3</sup>, A. Ushiyama<sup>3</sup>, H. Msuda<sup>3</sup>, S. Soukejima<sup>4</sup>, M. Taki<sup>5</sup>, K. Wake<sup>6</sup>, S. Watanabe<sup>6</sup>. <sup>1</sup>Dept of Neurology, Univ of Tokyo, Tokyo, Japan, <sup>2</sup>Dept of Psychosomatic Medicine, Univ of Tokyo, Tokyo, Japan, <sup>3</sup>Dept of Environmental Health, National Institute of Public Health, Saitama, Japan, <sup>4</sup>Dept of Public Health Policy, National Institute of Public Health, Saitama, Japan, <sup>5</sup>Dept of Electronics and Information Engineering, Faculty of Engineering, Tokyo Metropolitan Univ, Tokyo, Japan, <sup>6</sup>National Institute of Information and Communications Technology, Tokyo, Japan.

#### MOTIVATION

Mobile telecommunications are becoming common technologies in everyday life. However, there are several reports of individuals having a variety of non-specific symptoms elicited by exposition to non-thermal level radiofrequency electromagnetic fields (RF-EMF). The exposed levels of RF-EMF at which these individuals show some symptoms are generally below the recommended limits of exposure determined to avoid adverse thermal effects. Various investigations have studied patients suffering from symptoms of Electromagnetic Hypersensitivity (EHS), under controlled laboratory conditions, although studies so far have failed to demonstrate empirical evidence linking EHS symptoms with RF-EMF except for the "TNO Report". To thoroughly determine any possible health effects resulting from mobile telephony radiofrequency radiation, further investigations employing proper scientific methodologies are essential.

#### OBJECTIVES

The aims of the present investigation are to give some answers to the following questions under the above backgrounds. 1 Does RF-EMF from base station or phone terminal have adverse effects on human health? 2 Are there differences in such effects between non-hypersensitive and hypersensitive subjects? 3 Is the hypersensitivity specific to EMF? 4 Do the native characters differ between hypersensitive and non-hypersensitive subjects? To answer these questions, in human subjects with or without subjective hypersensitive complaints, we will evaluate both cognitive and physiological functions before, during and after exposure of such level RF-EMF.

#### EXPERIMENTAL SCHEDULE

- 1 Pilot Study on Mobile Telephone Base Station (2004-2005)
  - 2 3G Cellular Phone Base Station Study (2005-2006) Intensity: 10 V/m
  - 3 3G Cellular Phone Base Station Study (2006-2007) Intensity: 1V/m
- Or 3G Cellular Phone Terminal Study

#### SUBJECTS

Twenty healthy volunteers without hypersensitive subjective complaints and 20 EHS subjects will be enrolled in this study.

#### RF EXPOSURE CONDITIONS

Each subject takes part in four different exposure conditions in random order. The orders of four conditions are counterbalanced among the subjects, and the subject, examiner and data analyzer are all blinded to the performed condition. 1. Continuous exposure. The RF-EMF is exposed continuously for 30 minutes. Its frequency is set at 2GHz band. E-field strength of the incident field (10 or 1 V/m) is lower than the guideline limit recommended by ICNIRP and Japanese Radio Law (61.4 V/m), RF-EMF from neighboring base stations is shut down in a shielded experimental laboratory. 2. Intermittent

exposure. The same RF-EMF is exposed intermittently: six periods (duration; 5 minutes) with and without exposure (3 with and 3 without) are randomly intermixed in thirty minutes. 3 Sham exposure. No RF-EMF is given in the same setting as the real exposure condition. 4. Noise exposure. Moderate noise is given without any RF-EMF in the same setting as the real exposure condition to see whether non specific stress has more effects on the EHS subjects than those without hypersensitivity.

#### PARAMETERS TO EVALUATE

Before exposure, to evaluate the personality of each subject, Mini International Neuropsychiatric Interview (MINI) and Big Five Personality Test (neuroticism, extraversion, openness, agreeableness, conscientiousness) are performed by one psychosomatic physician of our members. During any exposures, a few physiological parameters (skin temperature and pulse rate) are monitored. During exposure, the subjects are requested to subjectively differentiate the periods of exposure and non-exposure if possible.

Just before and after exposure, the well-being of the subject is evaluated with a questionnaire (Profile of Mood State (POMS)). This questionnaire will estimate Tension-Anxiety, Depression, Anger-Hostility, Vigour, Fatigue and Confusion state of the subject at a certain time. We also perform a pre-cued visuo-motor reaction time task previously reported by Terao et al (see reference) before and after the exposure. In this task, one should use two hints for the correct reaction task; one is the target the subject should reach, another is the hand (left or right) should be used for the task. This task is more difficult to perform as compared with a simple reaction time task and may be more susceptible to any kinds of embarrassment. Therefore, we consider it suitable for this experiment because small influence may be detected with this difficult task.

#### ANALYSIS

Statistical comparisons are done with multi-factorial ANOVA and appropriate post hoc analysis compensated for multiple comparisons.

1 Does RF-EMF from base station or phone terminal have adverse effects on human health? Changes in POMS scores before to after the exposure and physiological changes during exposure are compared between different exposure conditions.

2 Are there differences in such effects between non-hypersensitive and hypersensitive subjects? The above changes are compared between EHS subjects and non-hypersensitive subjects.

3 Is the hypersensitivity specific to EMF?

Comparisons between noise exposure and real exposure will show whether even noise does have some effects on the well-being. Comparisons of the noise effects between non-sensitive and sensitive subjects will reveal whether the EHS people are also sensitive to other kind of stress than EMF as compared with the non-sensitive group.

4 Do the native characters differ between hypersensitive and non-hypersensitive subjects? We will compare MINI and Big five scores between the two groups of subjects. Correlation of changes in POMS scores with MINI results may give us some information about the above question.

#### RESULTS and DISCUSSION

We will show the results of a pilot study of several volunteers at the meeting.

Terao Y et al, Interhemispheric transmission of visuomotor information for motor implementation. Cerebral Cortex (pressed in DOI on 2004/12/20)

## Session 3: Role Of Electric Fields In Wound Healing And Nerve Regeneration (Continued)

*Chairs: Richard Nuccitelli and Colin McCaig*  
3:30 - 4:30 pm, Theatre L

3-1

**THE BIOELECTRIC FIELD IMAGER: A NEW TOOL FOR MEASURING THE ELECTRIC FIELD AROUND SKIN WOUNDS AND LESIONS.** R. Nuccitelli<sup>1</sup>, P Nuccitelli<sup>1</sup>, R. Sanger<sup>2</sup>, P. J. S. Smith<sup>2</sup>. <sup>1</sup>RPN Research, Center for Bioelectrics, Norfolk, Virginia, USA, <sup>2</sup>BioCurrents Research Center, Marine Biological Laboratory, Woods Hole, Massachusetts, USA.

Introduction: We are studying the role of endogenous electric fields in mammalian skin wound healing. The epidermis generates a transepithelial potential (TEP) of 20-50 mV across itself, inside positive. Any wound or break in the epidermis creates a low resistance pathway and the TEP at the wound site is 0 mV. However the TEP of the intact epidermis around the wound is still present, resulting in a lateral voltage gradient or electric field along the skin surrounding the wound. We have evidence that this lateral electric field stimulates keratinocytes in the area to migrate towards the wound with the optimal response occurring at a field strength of 100 mV/mm. In order to determine the actual field strength present in mammalian wounds, we have developed a new instrument called the Bioelectric Field Imager (BFI). The BFI vibrates a small sensor perpendicular to the skin about 200  $\mu\text{m}$  above the surface and uses the oscillating capacitance signal to determine the surface potential of the epidermis just beneath the stratum corneum. By measuring this surface potential in many positions around the wound, we generate a spatial map of the surrounding electric field.

Experiments: We have measured the wound field near a 1 mm long, full thickness skin wound in mice. A field of 100-200 mV/mm is present just beneath the stratum corneum immediately following wounding and persists until wound healing is complete 3 to 5 days later. The polarity of this field has the positive pole at the wound site and the wound current is flowing away from this site. We infer from this that the electric field deeper in the epidermis is in the opposite direction, with current flowing towards the wound. The topical application of 1 mM of a blocker of Na<sup>+</sup> channels (amiloride) reduces this wound field by about 50%, supporting the hypothesis that one of the main driving forces for the wound current is the TEP. Preliminary measurements on human skin wounds detect lateral electric fields that are similar to those measured in mice.

We have also begun scanning melanomas induced in mice by injecting about 1 million melanoma cells under the skin and waiting four days. We can detect a local electric field associated with these lesions within one day after injection, even before a visible melanoma is present. The surface potential of the skin over the melanoma is more negative than the surrounding skin and preliminary measurements suggest that the magnitude of the electric field associated with melanoma is proportional to the growth rate of the melanoma.

Conclusions: The Bioelectric Field Imager is a useful technique for the non-invasive imaging of the electric field in mammalian skin. We measure fields of 100-200 mV/mm near skin wounds and melanomas in mice and are now developing a portable BFI to study human skin disease.

Acknowledgements: Supported by NIH R43 GM069194 to RPN and NIH NCRR P41 RR001395 to PJSS.

3-2

**A ROLE FOR BETA 4 INTEGRIN IN KERATINOCYTE GALVANOTAXIS.** C. E. Pullar<sup>1</sup>, P. Marinkovich<sup>2</sup>, R. Isseroff<sup>1</sup>. <sup>1</sup>Dept of Dermatology, Univ of California Davis School of Medicine, Davis, California, 95616 USA, <sup>2</sup>Program in Epithelial Biology, Stanford Univ School of Medicine, Stanford, California, 94305 USA.

Keratinocyte migration during wound repair requires growth factor induced migration and proliferation, but also depends on the expression of laminin-5, a ligand for alpha 6 beta 4 integrin. The electric field (EF), generated immediately upon wounding, could be one of the earliest signals that cells receive to initiate migration into the wound bed. Keratinocytes migrate directionally towards the cathode (cosine 0.5-1) in an applied DC EF of 100mv/mm, a process known as galvanotaxis. While we have established a role for the epidermal growth factor receptor (EGFR) in keratinocyte galvanotaxis (JCS 112, 1967-1978, 1999), the role of integrins is unknown. As laminin 5 is deposited over dermal collagen in the wound bed and as alpha 6 beta 4 integrin plays a role in regulating keratinocyte chemotaxis, directing migration towards a chemoattractant, (JCI 116, 3543-3556, 2003), we wondered if this integrin also plays a role in keratinocyte galvanotaxis.

Immortalized beta 4 negative keratinocytes, obtained from a patient with epidermolysis bullosa with pyloric atresia, were retrovirally transduced with a vector control (beta 4-) or vector containing the beta 4 gene (beta 4+) to generate beta 4- and beta 4+ cell lines. Cells were starved of growth factors overnight and experiments were performed in the absence and presence of epidermal growth factor (EGF) (2ng/ml).

In the absence of an applied electric field and added growth factors both cell lines migrate slowly and at about the same rate. The addition of EGF to both cell lines significantly increases the migration rate by 81% (beta 4-) and 57% (beta 4+), respectively, resulting in both cell lines migrating at about the same rate.

While the application of an EF had only a slight effect on migration rate, beta 4- cells in the absence of EGF were "blinded" to the electric field. Galvanotaxis was partially restored by either the addition of EGF to the beta 4- cells (cosine = 0.33 +/- 0.06) or transduction of beta 4 integrin in the absence of EGF (cosine = 0.32 +/- 0.07). Transduction of beta 4 integrin together with the addition of EGF further augmented the migration of the keratinocytes towards the cathode (cosine = 0.54 +/- 0.07), indicating an important novel role for beta 4 integrin and a possible synergistic cooperation between the EGFR and beta 4 integrin in keratinocyte galvanotaxis.

This work is supported by NIH grants AR 48827 (CEP) and AR 44518 (RRI).

3-3

**INTEGRINS MAY SERVE AS MECHANICAL TRANSUCERS FOR LOW-FREQUENCY ELECTRIC FIELDS OF PHYSIOLOGICAL STRENGTH.** F. X. Hart. The Dept of Physics, The Univ of the South, Sewanee, TN.

A hypothesis is presented that the transduction mechanism for low-frequency electric fields of  
*Bioelectromagnetics 2005, Dublin, Ireland*

physiological strength (apprx. 1 V/cm) is the same as that for sinusoidal fluid shear stresses of physiological strength (approx. 1 Pa) - the force exerted on an integrin. Simple calculations show that the forces exerted on a model integrin by transverse electric fields and fluid shears that produce cellular effects are comparable in magnitude, about 1 fN.

The electric force is provided by the interaction of the surface charges on the integrin,  $Z_e$ , with the tangential component of the applied field,  $E_o$ . Here  $Z$  is an integer and  $e$  is the electronic charge. Estimates for  $Z$  are based on literature values for the charge densities of surface IgER complexes, DNA, heparan sulphate and a GAG complex. A value of  $Z$  between 10 and 100 seems reasonable. The solution of Laplace's equation for the field at the surface of a spherical shell indicates that the maximum tangential field at the surface is  $1.5E_o$ .

The mechanical shear force is the transverse fluid drag force exerted on the cylindrical surface of the integrin. The shear stress at the cell surface is determined by the fluid flow rate and the dimensions of the flow channel. From the shear stress and the dimensions of the integrin the fluid speed at the middle of the integrin is determined to be on the order of 10  $\mu\text{m/s}$ . This value is used to obtain the transverse force on the integrin for laminar flow.

Either force, electrical or fluid shear stress, is coupled mechanically to the actin cortex within the cell. Application of the principles of translational and rotational equilibrium determine the force and torque exerted on the actin cortex by the integrin. The mechanical network of springs and dashpots, analogous to an electrical RC network, which exists within a cell and connects a cell to its surroundings would then be directly coupled to an applied electric field. The damping produced by the viscous loss in the network limits the frequency at which biological responses may be produced to below about 10 Hz. Such a diminution of response is observed for physiological strength electrical and fluid shear forces for frequencies above about 10 Hz. The fundamental transduction mechanism for some electric field effects may then be ultimately mechanical in nature.

## **Session 4: Exposure Assessment**

*Chairs: Greg Lotz and Ric Tell*

**3:30 - 5:45 pm, Theatre M**

4-1

**SARS FROM PORTABLE/MOBILE DEVICES MEASURED USING A HEAD PHANTOM, A FLAT TANK PHANTOM AND A REALISTIC TORSO PHANTOM.** P. Chadwick, H. Hall. MCL, 11 Kings Rd West, Newbury, Berkshire, UK.

Exposure of the body to SARs from mobile devices has been suggested as a possible health risk. There are few published data describing SARs from mobile devices in positions other than against the head. There is at present no standardised method for measuring body SARs from mobile phones and other portable devices.

There are standard assessment protocols in place which allow measurement of SAR in the head with the handset in two defined positions. This is the method by which the SAR values quoted by the manufacturers are measured. For the first time a realistic body phantom has been used to assess body SARs from mobile devices. This paper presents the first of these results and compares them to the SARs measured with the devices against a flat tank phantom and a head phantom, as used in standardised SAR

testing.

In this study SARs from mobile devices in the standard head measurement positions were compared with those measured against a flat phantom in various configurations. It is possible that geometry of a flat phantom may not be a worst case assessment, as the antenna may be closer to the surface in concave or convex areas of a realistic body shape body. For this reason an investigation into SARs with the handsets in different configurations and in various positions around the a realistic torso phantom was conducted. This torso phantom, based on the SAM dataset, is a new design with excellent provenance and its topography is defined in an associated CAD file which describes both its inner and outer surfaces, to enable computational modelling of SAR in addition to measurement.

The results are reported of a comparison of SARs measured with the devices against a SAM head phantom, a flat tank phantom and the new torso phantom.

It was found that body SARs, measured with the flat or realistic torso phantoms, can be quite different from head SARs and that there also can be profound differences between the body SARs measured with the two body phantoms. The orientation of the device is one of the most important drivers of SAR: head SAR measurements are made with the “front” of the device toward the head, whereas body exposures can result from a device with its front or back against the body. Many devices have very directional (eg patch type) antennas and the SARs from a device with its back to the body can be significantly higher than SARs measured with the front of the device towards the body.

4-2

**ASSESSMENT OF HUMAN EXPOSURE BY ELECTROMAGNETIC RADIATION FROM WIRELESS DEVICES IN HOME AND OFFICE ENVIRONMENT.** A. Kramer, S. Kuehn, U. Lott, N. Kuster. IT'IS Foundation, Swiss Federal Institute of Technology, Zurich, Switzerland.

**INTRODUCTION:** Short-range wireless RF devices are being used pervasively in home and office environments, although their contribution to the electromagnetic field exposure of the human has not yet been systematically assessed. Here we report on exposure measurements of several classes of wireless RF devices under worst-case and normal operating conditions.

**OBJECTIVE:** The aim of this study is to provide classifications of RF exposures from wireless devices other than mobile phones used in home and office environments.

**METHODS:** The most common wireless transmission technologies were selected for further investigation: DECT, Bluetooth, WLAN (IEEE802.11b and IEEE802.11g). In addition, information on devices whose transmission technology is not standardized was collected. From this and a survey of the availability and the degree of pervasiveness of these devices, five device classes were chosen for experimental exposure determination and measurement procedures for the specific transmission modes were designed. In the class of standardized technologies we assessed DECT telephones, WLAN access points and network interface cards as well as several Bluetooth devices. In the field of devices using proprietary communication standards we assessed wireless peripherals for personal computers (PC's) and baby surveillance devices. As displayed in Table 1, short-range wireless RF devices cover a broad frequency range with a large variation of peak output power levels.

The design of the experimental setup and measurement procedure for operating the devices under test (DUT) in the worst-case mode, i.e., in the highest time-average power mode, requires knowledge about

the underlying communication standard. If this mode cannot be maintained, the worst-case exposure can be determined by extrapolating the field values gained under a different operational condition. In the case of proprietary technologies the worst-case operational mode was determined experimentally due to lack of technical information.

We analyzed devices used normally or unintentionally in close proximity to the human body by measurement of the Specific Absorption Rate (SAR) using a DASY4 system (SPEAG, Switzerland). For DECT handsets a compliance test was conducted according to the standard IEEE 1528 (at the SAM phantom). Other devices were characterized using a flat phantom (wall thickness: 2mm) with the particular device positioned as close as possible to the phantom wall (worst-case position and orientation). During all SAR measurements the devices were operated at the highest applicable average output power. The results were compared with known SAR values, e.g., those from mobile phones.

For devices used at a greater distance we measured the E-field in the far field of the DUT in a shielded semi-anechoic chamber (using either a broadband antenna plus spectrum analyzer or Easy4 and E-field probes from SPEAG). The E-field was mapped over distance in the main beam direction of the DUT. The results were then compared to electromagnetic exposure caused by cellular base station exposure. Additionally, the determined exposure values were reviewed in relation to current guidelines on human exposure by electromagnetic fields.

**RESULTS:** Figure 1 gives an overview of the tested device classes and the results of the dosimetric and far-field exposure assessment. Only the maximum value of a certain device of each device class is shown. The E-field values are indicated for a distance of 1m.

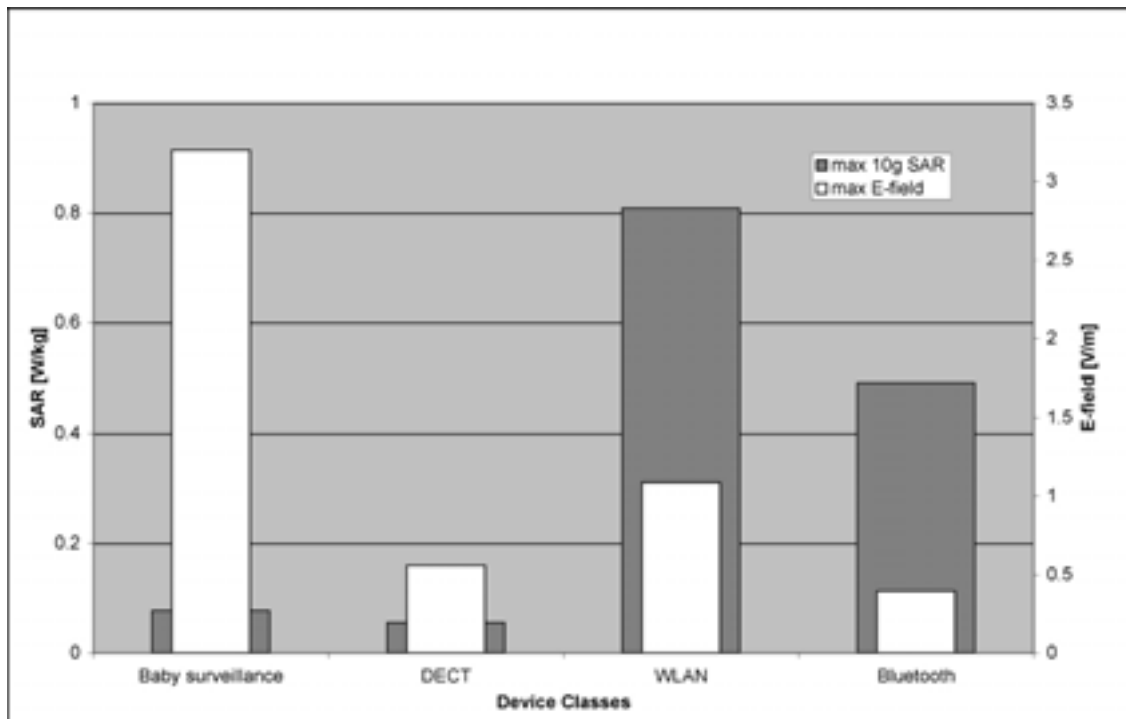


Figure 1: Maximum 10g-SAR and maximum E-field (at 1m distance) of several home and office wireless RF device classes.

**DISCUSSION:** In conclusion, all tested devices are compliant with currently existing exposure limits. The exposure levels are in the same range as exposures from base stations operated in the closer vicinity of an apartment/office. Typical values inside of buildings at distances between up to 100 m from GSM

base station sites are in the range of 0.1 - 1 V/m. High incident field values were also measured close to baby phones. In conclusion, in the very near future the background exposure in everyday life situations will exceed exposures from base stations and broadcast stations. This will considerably increase the complexity of epidemiological studies. The dominant source with respect to local and cumulative exposure will, however, be the cellular phone.

**ACKNOWLEDGMENTS:** The presented study was co-founded by the Swiss Federal Office of Public Health (BAG).

frequency (MHz)	type of device	peak output power (mW)	type of waveform
27	baby surveillance, PC peripherals	1-10	cw
40	baby surveillance, PC peripherals	10	cw
433	baby surveillance, PC peripherals	10	cw
446	baby surveillance	500	cw
863	baby surveillance, Private Mobile Radio	10	cw
1900	DECT	250	pulsed
2450	WLAN, Bluetooth, PC peripherals	1-100	pulsed / cw

Table 1: Operating frequency and peak output power of investigated wireless RF devices.

4-3

**EFFICIENT CALCULATION OF HUMAN EXPOSURE IN FRONT OF BASE STATION ANTENNAS.** A. Bitz, A. El Ouardi, J. Streckert, V. Hansen. Chair of Electromagnetic Theory, Univ of Wuppertal, Wuppertal, Germany.

For risk assessment of mobile communication systems, the determination of occupational and public exposure due to radiated fields of base station antennas is an application of increasing interest. Especially, since in Germany the employers' liability insurance association commits network providers to specify safe distances for their base station antennas [1,2] in order to keep the exposure of workers below the limits given by the guidelines [3].

Since it is necessary for the determination of human exposure to obtain results for the localized and whole body SAR the applied procedure has to be based on numerical calculations due to the lack of measurement techniques for whole body SAR. The underlying problem covers the analysis of antenna parameters, computation of near and far field distributions of base station antennas and the computation of the electromagnetic field distribution inside the human body. The procedure should allow for the use of an anatomical correct human body model as it is given by the 'visible human project' [4] in order to yield reliable results for the localized SAR. The most efficient numerical method for the field calculation

inside such high-resolution human body models is the Finite Difference Time Domain (FDTD) Method. Due to the character of the FDTD as a local numerical method, however, the FDTD is not suitable for problems with large dimensions. Therefore, in this work, a combination of the Hybrid<sup>(2)</sup>-Method and the FDTD-Method is performed. The Hybrid<sup>(2)</sup>-Method, introduced first in [5], is a very powerful method for solving complex electromagnetic problems consisting of arbitrarily shaped and inhomogeneous objects and electrically large structures. It is successfully applied to analyze base station antennas of mobile communication systems embedded in real environments. Both methods are combined by a discrete formulation of the equivalence principle inside the Yee-mesh of the FDTD-method. In the first step the current density on the metallic surface and the radiated fields of the antenna are calculated by use of Hybrid<sup>(2)</sup>-Method in absence of the FD volume. Afterwards equivalent sources on a closed surface inside the FD volume surrounding the human body model are derived from the antenna's fields. The equivalent sources are used as excitation for the field distribution inside the body by the FDTD-method. Because the FDTD-method is only used to compute the field distribution inside a relatively small solution space which encloses the human body model and since the integral equation method, applied inside the Hybrid<sup>(2)</sup>-method for the computation of the antenna currents, requires only the modeling of the metallic surfaces of the antenna, it is unnecessary to model the remaining space between antenna and body. Thus, the computational cost of the FDTD-method is independent of the distance between human body and antenna as well as of the complexity of the antenna model. From this it follows that the spatial resolution of the body model depends only on the available computer resources.

The above described procedure was applied to compute the electromagnetic field and SAR distribution inside human body models with various body masses of 110 kg and 42 kg in front of multi- and dual band base station antennas (Kathrein 742212, 742211, 739664, and 80010141). The 42 kg body model is considered according to the recommendation given in [6]. For the investigated antennas and the used body models the maximum whole body SAR was achieved for a centered position of the body model with respect to the main beam direction. It turns out that for distances larger than 50 cm the whole body SAR of the 42 kg body model is the limiting factor for the compliance distance. Compared to the whole body SAR of the 110 kg model the 42 kg model gives values which are at least higher by a factor of 2 for any considered configuration. For positions of the human body beside and behind the antenna the whole body SAR decreases drastically. However, the localized SAR depends strongly on the local material distribution and consequently on the spatial resolution of the body model. Furthermore, it was observed that the position of arms and hands in front of the trunk of the visible human model can have a significant effect on the localized SAR since field elevations can occur in the proximity of the arms and hands.

#### References:

- [1] BGR B11, BG-Regeln "Elektromagnetische Felder", Hauptverband der gewerblichen Berufsgenossenschaften, April 2001.
- [2] BGV B11, Unfallverhuetungsvorschrift "Elektromagnetische Felder", Hauptverband der gewerblichen Berufsgenossenschaften, March 2001.
- [3] ICNIRP, Guidelines for limiting exposure to time-varying electric, magnetic and electromagnetic fields (up to 300 GHz). Health Phys., vol. 74, pp. 494-522, 1998.
- [4] Brooks Air Force Base Laboratories: Visible Human Project, <http://www.brooks.af.mil/AFRL/HED/hedr/dosimetry.html>
- [5] Alaydrus, M., Hansen, V., The Hybrid<sup>(2)</sup>-Method: Combination of the FE/BE Hybrid Method with the UTD, IEEE Antennas and Prop. Symp., Orlando, Florida, 1999, pp. 1704-1707.
- [6] CENELEC: Basic Standard for the Calculation and Measurement of Electromagnetic Field Strength and SAR related to Human Exposure from Base Stations and Fixed Terminal Stations for Wireless Telecommunication Systems (110 MHz - 40 GHz). TC211, March 2001.

**MAGNETIC FIELD EXPOSURE OF NURSING STAFF PROVIDING TMS/RTMS TREATMENT.** E. Figueroa Karlström<sup>1</sup>, O. StenSSon<sup>1</sup>, R. Lundström<sup>2</sup>, K. Hansson Mild<sup>1,3</sup>. <sup>1</sup>National Institute for Working Life, Umeå, Sweden, <sup>2</sup>Occupational Medicine, Umeå Univ, Umeå, Sweden, <sup>3</sup>Dept of Natural Sciences, Örebro Univ, Örebro, Sweden.

Transcranial magnetic stimulation (TMS) is a non-invasive and focal stimulation tool for the study of connectivity of brain regions, localization of functions, pathophysiology of neuropsychiatric disorders, and a therapeutic intervention method in the treatment of chronic depression. A high intensity magnetic field produces a cortical stimulus through the induction of locally confined eddy currents, therefore tailored coils arrangement can be used to accomplish controlled local levels of stimulus. The TMS make use of current pulses accomplishing magnetic fields that can have intensities of up to 1 Tesla (T) with pulse durations in the range of ~0.05 to 0.2 ms. The resulting time derivative of the field can be of several tens of kT/s. This impulsive field transient is able to induce a rapid depolarisation of the nerve cells within a volume of about 5 mm<sup>3</sup> at the cortical level.

The method is known since the work of Penfield in 1954 [1] and it can be found thoroughly reviewed in the medical literature (se Baker et al [2]). Although TMS is aimed to expose patients, the nursing staff using this devices could also be exposed to magnetic pulses, eventually even to an extend surpassing the limits of occupational levels of exposure given in the new EU directive and ICNIRP guidelines. Motivated by concern among the nursing staff, measurements were performed at the equipment in current use at the Norrland Univ Hospital of Umeå to assess potential risks of overexposure (Medtronic Dantec MC-B70 Magnetic Transducer). Measurements were made at different distances from the coils of the transducer. The intensity of the field was found to decay proportionally to  $1/r^3$  (r: distance). The regulations set limits aimed to avoid excitation of the central nervous system, while TMS/rTMS is aimed just to accomplish high level of local exposure to produce cortical excitations in patients under controlled forms. For the pulse trains in use we found a period time of  $T \sim 0.3$  ms and about 72  $\mu$ s active pulse width, which gives an equivalent frequency of about 3.5 kHz. For this the limit value is about 1 T/s (see fig. 3 in [3], for recommended levels of exposure to pulsed waveforms).

We found that the limits for the magnetic field pulses are transgressed at distances of about 0.7 m from the surface of the transducer's coils under normal treatment conditions. In spite of this finding, further studies, especially of different designs of TMS devices, should be made to bring deeper insight in the issue of weather the settled limits in terms of current density also are transgressed. Until those studies are pursued it is suggested that nursing staff should not work in situations where their body or parts of it, are at distances closer to 0.7 m from the transducer to avoid risks of overexposure to magnetic pulses. The tested equipment has been designed with a coils holder, which should be used to avoid higher exposures while holding the transducer in the hand at treatment sessions.

Referenser:

1. Penfield W, Jasper H. Epilepsy and the functional anatomy of the human brain. Boston, Mass: Little, Brown & Co, 1954.
2. Barker A T, Jalinous R, Freeston I L. Non-invasive magnetic stimulation of human motor cortex, The Lancet. 1985, 1:1106-1107.
3. Guidance on determining compliance of exposure to pulsed and complex non-sinusoidal waveforms below 100 kHz with ICNIRP guidelines, Health Physics. 2003, 84(3): 383-387.

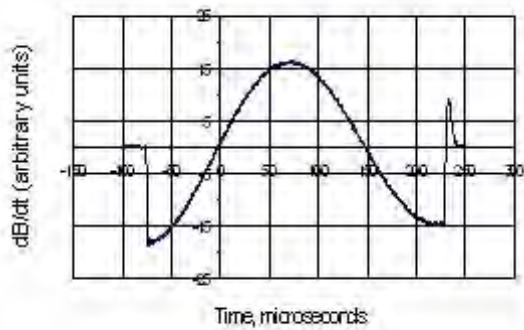


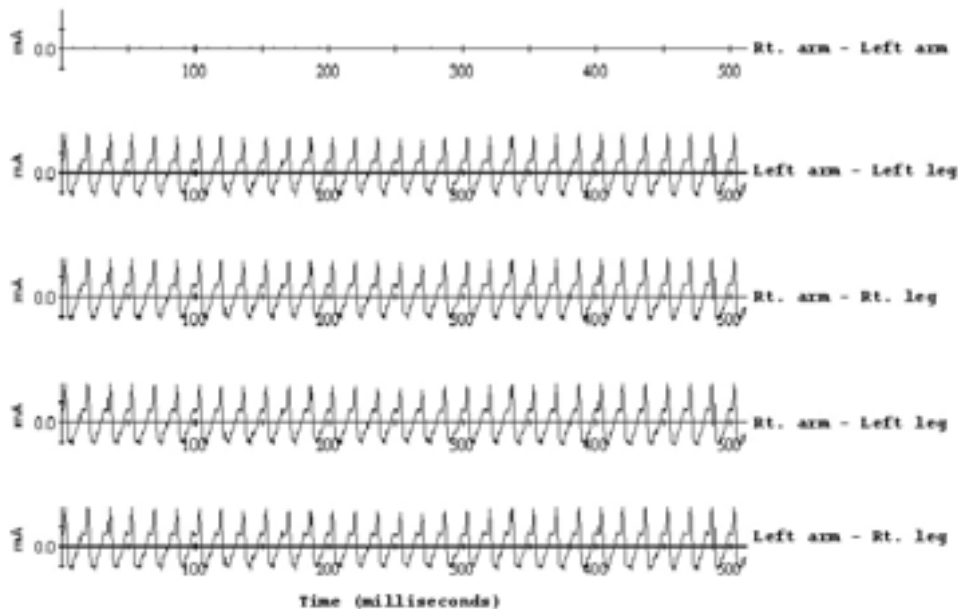
Fig. 1 Measured dB/dt at the axis of the 8-shaped transducer coils array, 10 cm from the surface of the transducer and away from the patient.

4-5

**PILOT MEASUREMENTS OF ELF CONTACT CURRENTS WITH ELECTRIC UTILITY WORKERS.** J. D. Bowman<sup>1</sup>, J. C. Niple<sup>2</sup>, R. Kavet<sup>3</sup>. <sup>1</sup>National Institute for Occupational Safety and Health, Cincinnati, Ohio, USA., <sup>2</sup>Enertech Consultants, Campbell, California, USA., <sup>3</sup>Electric Power Research Institute, Palo Alto, California.

A new contact current meter (CCM) was tested in a pilot study at Southern California Edison. This meter has medical electrodes on the arms and legs that measures voltage differences between the extremities.

When one of these voltages is above 0.5 mV, the meter captures the waveforms in a 24  $\mu$ V 220 Hz bandwidth for 512 ms (Figure).



These waveforms are stored in memory for later analysis of the 60 Hz currents that go through a person in touch with a voltage difference. To test this meter, 76 volunteers from eight occupations were

recruited to wear the CCM for a full-shift. They were exposed to an average of 283.8 contact current events above the meter's threshold, but most of these were electrostatic spark discharges. 14 employees experienced an average of 23.1 contact currents events whose primary frequency was 60 Hz. Using a circuit model of the human body, the average contact currents going from arm to arm was 9.8  $\mu\text{A}$  (maximum = 178.4  $\mu\text{A}$ ) and the average going down the torso was 25.5  $\mu\text{A}$ . Contact current waveforms between the extremities recorded simultaneously by the Contact Current Meter on an electrician working in the central office at Southern California Edison. (maximum = 661.8  $\mu\text{A}$ ). The maximum exposures were experienced by a technical support employee working in a substation. All measurements in this pilot study were below the 3,000  $\mu\text{A}$  Maximum Permissible Exposure for contact currents set by the Institute of Electrical and Electronic Engineers (IEEE). Combining these current measurements with the results of high-resolution dosimetry, the internal electric fields averaged an estimated 1.7 mV/m in the heart (maximum = 21.0 mV/m) and 1.9 mV/m in the hematopoietic bone marrow in the torso (maximum = 56.5 mV/m). These internal electric fields from contact currents are below the basic restriction of 2,100 mV/m in the IEEE exposure standards but are above 1 mV/m where biological effects have been often reported in laboratory studies. Safety concerns limited the measurements to low voltages (<600 volts) or de-energized equipment, so we did not obtain data on work in energized high-voltage environments, the most likely sources of high contact currents. This pilot study identified improvements to the contact current meter that would make it better able to measure exposures in future health studies.

4-6

**COMPARISON OF REALISTIC POWER-FREQUENCY ELECTRIC-FIELD EXPOSURES WITH GUIDELINE LIMITS.** T. D. Bracken<sup>1</sup>, R. S. Senior<sup>1</sup>, R. Kavet<sup>2</sup>. <sup>1</sup>T. Dan Bracken, Inc., Portland, Oregon, USA, <sup>2</sup>Environment Sector, EPRI, Palo Alto, California, USA.

Introduction: This paper describes a methodology for characterizing realistic electric-field exposures in occupational settings and suggests an approach for evaluating compliance with guideline limits in such settings. At most work locations the power-frequency electric fields are not uniform or vertical and the posture of the worker is not upright. In contrast, electric-field exposure guideline limits are typically based on empirical data on the responses of subjects standing upright in a uniform vertical electric field, the "guideline exposure scenario". The stimuli of most concern for electric-field exposures are spark discharges that might cause an inadvertent startle reaction. The levels of response to spark discharges of the severity experienced in electric fields appear to be dependent on the electric charge in the discharge. However, the electric field levels that result in annoying responses in the guideline exposure scenario have then been incorporated directly into guideline levels without allowance for the effects of field non-uniformity or body orientation and posture on the severity of potential spark discharges. Line workers climbing and working on high-voltage transmission lines represent exposure scenarios where even the highest occupational electric-field limits of 20 kV/m (IEEE Standard PC95.6-2002) and 25 kV/m (ACGIH Threshold Limit Values®) can be exceeded. For these activities the worker's posture, the uniformity of the field, and the field orientation differ significantly from the guideline scenario. These differences suggest need for care in comparing computed electric-field exposures in towers and their effects directly with the electric-field limits provided under guideline scenarios. Methods: An accurate estimate of the unperturbed non-uniform field in the space occupied by a line worker in a steel or aluminum lattice-type structure was computed using Monte Carlo methods that model surface and spatial electric fields on and near standard geometrical elements. To estimate a whole-body average as required by guidelines, fields were computed in a tower model that employed a cylindrical conducting element for each tower member. The unperturbed fields were computed at ten discrete points corresponding to segments of an articulated stick-figure model of a 1.78-m tall male

(Figure 1). The model was positioned in the tower to simulate location of the torso, head and extremities during a task. The whole-body average field was computed from fields at all the body points weighted by the fraction of body volume represented by the segment. In this way, electric-field exposures were expressed in terms of the unperturbed field averaged over the body as stipulated by guidelines. Computations were performed for climbing and work positions in seven towers with voltages ranging from 230 to 765 kV. Climbing and work locations were chosen at the points of maximum electric-field exposure to accommodate the ceiling-limit nature of guidelines. Besides the unperturbed electric field, we also estimated the space potential at the torso, the induced short-circuit current, induced open-circuit voltage, and the stored charge available for a discharge over a range of capacitances to ground. Results: The peak electric-field exposure during climbing ranged from 10 kV/m for a 230-kV tower to 31 kV/m for a 765-kV tower. Exposures at on-tower work positions were lower than the estimated peak exposures during climbing. For 500- and 765-kV towers, computed exposures while climbing and at some in-tower work positions exceeded the limit of 20 kV/m of IEEE Standard C95.6 2002 and, in some cases, the 25-kV/m Threshold Limit Value®. For lower voltage towers exposures did not exceed 20 kV/m. An increase in the height of the worker from 1.78 m (50th percentile 1985 US male) to 1.89 m (95th percentile US male) increased the electric-field exposure by about three percent. In-tower exposure parameters related to spark discharges and induced currents were estimated for each exposure scenario for comparison with those from the idealistic guideline exposure scenario. Even though the in-tower electric-field exposures exceeded the guideline field limits, the estimated charge available for a spark discharge and the estimated short-circuit current during in-tower exposures were less than the corresponding values associated with the electric-field limit of the guideline exposure scenario. An increase in the height of the worker from 1.78 m to 1.89 m increased the induced charge and current by about ten percent.

Conclusion: Occupational electric-field limits based on responses when standing erect in a uniform field can be exceeded in some realistic work scenarios. However, in the case of work in transmission-line towers, workers are not erect and are exposed to a non-uniform field resulting in lower induced charge and current than for equivalent exposures in a uniform vertical field. These latter parameters, as opposed to the average electric field, interact directly with the body and determine response. Therefore evaluation of electric-field exposures in terms of the induced charge or induced current provides a means of comparing any exposure scenario with the ideal guideline scenario in terms of an effects-related physical quantity. This approach is consistent with the exposure limit/basic restriction methodology that employs a basic restriction on a physical quantity as the ultimate determinant of compliance.

Supported by EPRI EP-P11573/C5739

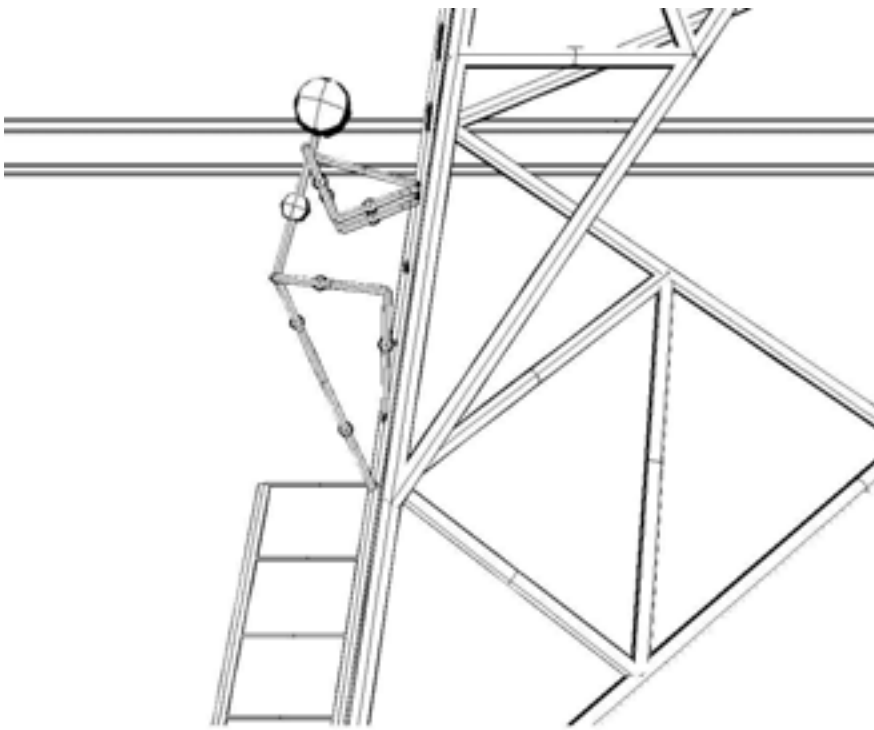


Figure 1: Articulated stick figure climbing 765-kV tower with field computation points shown for head, torso and extremities.

4-7

**RESIDENTIAL MAGNETIC FIELDS AND WATER-LINE-TO-EARTH VOLTAGES RESULTING FROM TRANSMISSION AND DISTRIBUTION LINES.** R. Kavet<sup>1</sup>, J. P. Daigle<sup>2</sup>, L. E. Zaffanella<sup>2</sup>. <sup>1</sup>EPRI, Palo Alto, California, USA, <sup>2</sup>Enertech Consultants, Lee, MA, USA.

Background and Study Description: We have developed and implemented software that computes average magnetic fields inside residences ( $B_{avg}$ ), as well as residential water-line-to-earth voltage ( $V_{W-E}$ ) in single-dwelling rectilinear neighborhoods typical of the United States. High voltage transmission lines may be located in proximity to such neighborhoods. This paper is concerned with the effect of a nearby transmission line carrying 500 amperes (A) per phase on  $B_{avg}$  and  $V_{W-E}$ , the line is roughly 55 m from the nearest and 300 m from the furthest residence. The study areas were 2-by-3 block neighborhoods with distribution lines either on the street-side of the residence or in the backyard. All water mains were conductive. All models consisted of 88 residences. The variable conditions selected for analysis include the phase angle of the transmission system relative to the distribution system, and the loading and balance of the primary feeder in the neighborhood. The phase angle was rotated in 60 degree increments. The feeders carried either 25 A per phase or 100 A per phase, each either balanced or with 25% unbalance.

Results: In the base case, i.e., without a transmission line present,  $B_{avg}$  and  $V_{W-E}$  were, not surprisingly, greater with 100 A-feeders than with 25-A feeders.  $V_{W-E}$  was uniformly greater in neighborhoods with unbalanced feeders compared to neighborhoods with balanced feeders, this effect, though apparent for 25-A neighborhoods, was pronounced for 100-A neighborhoods. Overall, the transmission line increased both  $B_{avg}$  and  $V_{W-E}$ , but the effect varied widely with transmission line phase. With respect to the median and 90th percentile  $V_{W-E}$  in the neighborhoods, balanced systems had greater transmission line effects than 25% unbalanced systems, and the transmission line had the least effect on 25% unbalanced 100-A

feeders; these results applied in both absolute and relative terms. The greatest amount of variability of transmission line effect on  $V_{W-E}$  across phases was also in the 100-A, 25% unbalanced group, also in both absolute and relative terms. The results for  $B_{avg}$  showed some similar trends, but did not follow a strict pattern. For backyard distribution fed with 25-A feeders, the fraction of residences with both  $B_{avg}$  and  $V_{W-E}$  increased above the base case varied between 48% and 88% depending on transmission line's phase, with marginal differences between 25% and 0% unbalance. For street-side distribution, the percent homes with both quantities increased varied from 63% to 97%, with marginal differences between 25% and 0% unbalance. For neighborhoods with 100-A feeders, the major observation was that for specific phase relations, the fraction of residences with both  $B_{avg}$  and  $V_{W-E}$  increased above the base case was far greater for balanced systems compared to unbalanced systems. For backyard distribution, the percent of residences with both  $B_{avg}$  and  $V_{W-E}$  increased above the base case varied from 25% to 66% for 25% unbalanced distribution and from 52% to 91% for balanced distribution. For street-side distribution, the corresponding values were 11% to 92% (unbalanced) and 61% to 86% (balanced). To simulate an extended geographical region in the US results from all 25% unbalanced cases were pooled. For the base case, the Spearman correlation between  $B_{avg}$  and  $V_{W-E}$  was 0.20 (N=352,  $p < 0.001$ ). With the transmission line operating in conjunction with all combinations of feeder loads and phases, the Spearman correlation was 0.08 (N=2,112;  $p < 0.001$ ). When the latter correlation was analyzed by transmission line phase, the result varied from -0.02 (N=352, not sig) to 0.25 (N=352,  $p < 0.0001$ ). Conclusion: The results indicate that the presence of a transmission line near a residential neighborhood may affect  $B_{avg}$  and  $V_{W-E}$  up to a distance of 300 m from the line but does not necessarily increase either or both of them owing to complex phase relationships among these quantities. The presence of transmission lines may dilute the correlation between  $B_{avg}$  and  $V_{W-E}$  that may have existed within and across neighborhoods proximal to the transmission right of ways. Finally, residential areas with lightly loaded, more balanced distribution systems may be more susceptible to dominant effects from nearby transmission lines, compared to areas with heavily loaded unbalanced distribution systems.

Supported by EPRI WO6929

4-8

**EM FIELD ASSESSMENT FOR OCCUPATIONAL EXPOSURE DUE TO A 30 KW DIGITAL TELEVISION TRANSMITTER PLACED ON A 380 KV POWER LINE LATTICE TOWER.** G. Remkes<sup>1</sup>, K. Koreman<sup>2</sup>. <sup>1</sup>Novec, Lopikerkapel, The Netherlands, <sup>2</sup>Tennet bv, Arnhem, The Netherlands.

#### OBJECTIVE

This research was done to determine the most reliable way to assess the electromagnetic field around a 380 kV power line steel lattice tower and its upper crossarm during occupational exposure situations, due to a 30 kW digital television transmitter (700 Mhz) located on top of the tower.

#### BACKGROUND

High power radio and television antennae are placed on overhead line supporting towers nowadays to satisfy the great need for broadcasting locations. The idea to do this was mainly inspired by the shortage of high objects. From the point of view of occupational expose it is not a desired situation: safe working conditions have to be created with respect to exposure to both 50 Hz and RF-fields. Both, electrical utilities and broadcasting companies are not eager to reduce power to create a safe working area. So accurate field assessment under normal operating conditions is relevant. RF-field measurement is complicated by the fact that 50 Hz EM-field rejection of traditional RF sensors amounts maximum 50 to

60 dB whereas strong 50 Hz electric fields are known to be present around the towers. On the other hand field numerical calculations require modeling of the antenna and the metal surrounding as well. Drastic simplifications of the real structure are required to be able to run the entire model on the computer. The basic question is: “what is the most reliable way to perform the field assessment in this case?”

## METHODS

Field assessment was done by both measurement and calculation.

First the 50 Hz interference of the RF-sensor was determined. Therefore, the RF-sensor was exposed to strong 50 Hz fields only (no RF-field present). The reading was recorded together with the magnitude of the 50 Hz electric field. The same was done for 50 Hz magnetic field interference. For the purpose of EM-field measurements around the tower first several ropes were attached to the metal structure on relevant locations, see figure 1. The RF-monitor was loosely connected to one of these ropes. Another rope was used to pull the sensor along the rope. EM- field data logging was done during the time that the sensor was moved along the rope. The 50 Hz electric field as well as the RF electric and the magnetic field were recorded and stored for further evaluation later. The 50 Hz field was minimized by grounding the electrical circuit one side of the tower.

Field strengths around the tower were calculated using super nec. This is a computer program using the method of moments similar to NEC2. For the modeling, the structure of the upper crossarm and the tower was drastically simplified. Sharp corners were round off and short elements were eliminated. These and other approximations were necessary to reduce the number of segments below the allowed maximum in order to be able to run the program.

## RESULTS

From 1 kV/m it was observed that the reading of the RF-sensor increases linearly with the applied 50 Hz-electric field. A similar result was not found for the 50 Hz magnetic field exposure. The results of RF-field measurements around the tower will be presented. An example is given by figure 2. The observed electric field strength is consistent with the observed magnetic field strength. Measurements yield mutually consistent results when measured along a different trails (different ropes). Results of measurement are consistent with the results of calculation in the free space region, see figure 3. Closer to the structure differences between the predictions and the measurement data are found.

## CONCLUSION

Field assessment for the purpose of creating safe working conditions on towers of overhead power lines with high power RF-transmitters present can be done by numerical calculations with acceptable accuracy. When the electrical circuit mounted on the side of the tower where the measurement is carried out is not grounded, results of RF measurement may be corrupted due to interference of the RF-sensor with the strong low frequency fields.

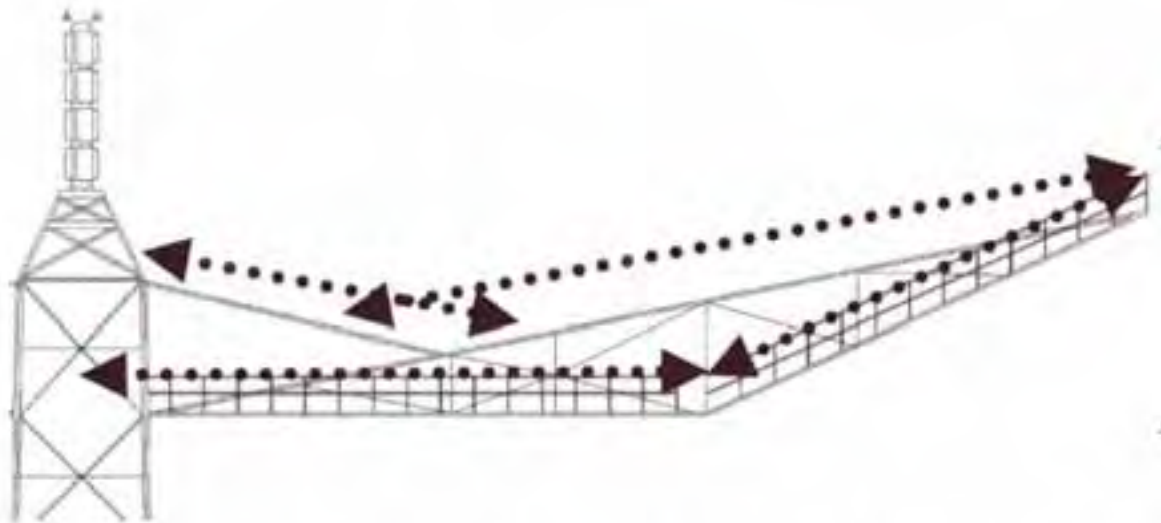


**Figure 1:** Schematic presentation of the power line tower and its upper crossarm. The dotted arrows mark the lines along which measurements were performed.

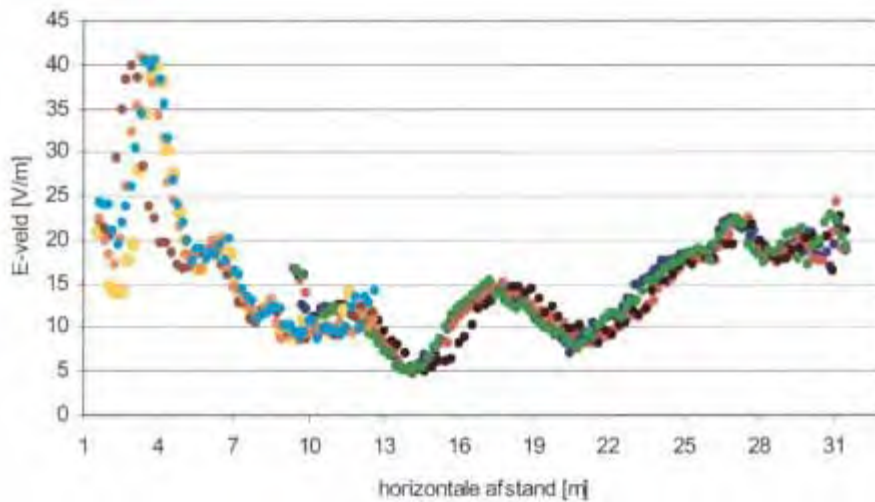


**Figure 2:** Combined results of electric field strength measurements along the upper two trails. The centre of the tower is at  $x = 0$  m and the ending of the upper crossarm at 31 m. All measurements have been repeated four times.

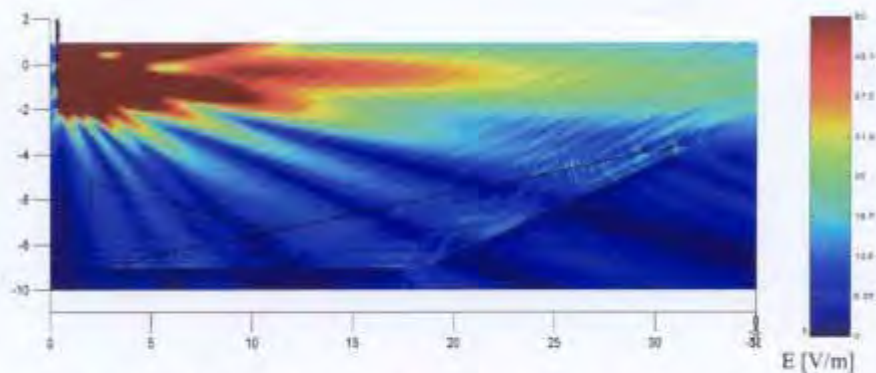


**Figure 3:** Result of electric field strength calculation in a vertical cross section through the middle of the tower and its upper crossarm.

**ELF (16.7 HZ) MAGNETIC FIELD EXPOSURE ASSESSMENT IN SWISS RAILWAY ENGINEERS.** M. Rössli<sup>1</sup>, M. Lörtscher<sup>2</sup>, D. Pfluger<sup>3</sup>, N. Schreier<sup>1</sup>. <sup>1</sup>Dept of Social and Preventive Medicine, Univ of Bern, <sup>2</sup>Federal Office of Transport, Bern, <sup>3</sup>datamatrix AG, Zürich.

**Objectives:** In the framework of an occupational cohort study on cause of deaths in Swiss railway employees, exposure to extremely low frequency (16.7Hz) magnetic fields will be estimated. The objective of this work is to determine the most relevant factors for exposure assessment based on data from three sets of measurement in a number of various engines.

**Methods:** The first set of measurement was carried out in 1993/94 using a commercial Bramur gaussmeter (Bramur, Lee, MA). The two other sets were completed in 2003 and 2004 using an EFA device from Wandel & Goltermann, now Narda Safety Test Solution (Germany). The measurement devices were fixed at the back of the driver's seat. In total 135 measurement runs have been performed under real service conditions. On average, one run lasted 1 to 2 hours. Data were analysed using multiple regression models in order to evaluate the effect of factors such as distance, profile or type of train on the measured magnetic flux density. A time-weighted average of the magnetic flux density was calculated for each engine type and measurement device. Subsequently, engines were classified into six exposure classes. Finally, the daily exposure of a railway engineer measured by means of a dosimeter (EFA carried in a backpack during the day) was compared with a calculation method based on the duration and the magnetic flux density from the different types of engines driven that particular day.

**Results:** Magnetic flux density varied considerably between different engine types (see Table). There was substantial variation between the measurements within the same engine type. The coefficient of variation (standard deviation divided by mean) varied between 0.5 and 1 in most cases. Generally, the 90th percentile value was a factor of 2.5 times higher than the mean value. Variation of measurements within the same engine type was due to a number of factors: e.g. i) the average magnetic flux density in passenger trains was 80% higher than in goods trains due to a more constant operational cycle in the latter; ii) driving downhill was associated with increased magnetic flux density compared to driving uphill or driving at the flat due to the regenerative breaking mode of the engine. From measurements in train wagons without field sources and from analysis of the three directions of the magnetic field in the engine was concluded that in the driver's cabin up to 10  $\mu\text{T}$  originates from the contact wire and not from the engine. The contribution from the contact wire was estimated to be 3  $\mu\text{T}$  on average for the whole Swiss railway system.

Dosimeter measurements of a typical engineer's work day resulted in an average magnetic flux density of 15.9  $\mu\text{T}$ . This value corresponds well to the calculated value of 14.5  $\mu\text{T}$  (9 percent differences).

**Conclusions:** The measured magnetic flux density in a railway engine depends on a number of factors associated with the operational cycle and the distance profile. Thus, exposure values of a specific engine derived from contemporary measurements do not necessarily equate to earlier values (e.g. 50 years ago). This is particularly so, if the field of application of that specific engine had been changed (e.g. from an express to a local train). For that reason exposure values for some old engines were measured and then used by a simulation software (FABEL), which allowed us to take the historical operational cycle into account. The simulation software has been validated by comparing today's measurement with today's operational cycle.

In addition, the measurement revealed that engineers in the alpine region ("Gotthard") were generally exposed to higher field strengths than the remaining drivers, due to the distance profile and the more

powerful engines. Taking this fact into account in the assessment of the driver's magnetic field exposure reduces exposure misclassification.

The study is supported by the Swiss Federal Office of Public Health and the Swiss Federal Office of Transport.

Exposure classification of the railway engines according to measured magnetic flux density at 16.7 Hz.				
Engine type	Exposure class	Number of engines at maximum	Time period with maximum inventory	Number of engines at present (2000)
Ce 6/8	60-100 $\mu$ T	51	1927-1965	1
Re 420	40-60 $\mu$ T	273	1985-2002	273
Re 620	20-40 $\mu$ T	88	1980-2002	88
Be 4/6	20-40 $\mu$ T	42	1923-1962	1
Re 460	10-20 $\mu$ T	119	1996-2002	119
Re 450	10-20 $\mu$ T	115	1997-2002	115
Re 4/4 I	10-20 $\mu$ T	50	1951-1992	4
Ae 4/7	10-20 $\mu$ T	127	1935-1974	2
RBe 540	5-10 $\mu$ T	81	1966-2000	79
RABDe 500	5-10 $\mu$ T	21	2000-2002	21
Ae 6/6	5-10 $\mu$ T	120	1966-2002	120
Ae 3/6	5-10 $\mu$ T	185	1929-1964	4
Ae 3/5	5-10 $\mu$ T	26	1925-1966	1
RABDe 560	$\leq 5$ $\mu$ T	126	1996-2002	126
RABDe 510	$\leq 5$ $\mu$ T	18	1967-2002	18

## Session 5: Dosimetry I

*Chairs: Camelia Gabriel and Soichi Watanabe*

**4:30 - 5:45 pm, Theatre L**

5-1

**DIELECTRIC PROPERTIES OF TWEEN BASED TISSUE-EQUIVALENT LIQUIDS.** K. Fukunaga<sup>1</sup>, H. Asou<sup>2</sup>, K. Sato<sup>2</sup>, L. Hamada<sup>1</sup>, S. Watanabe<sup>1</sup>. <sup>1</sup>National Institute of Information and Communications Technology, <sup>2</sup>NTT Advanced Technology Co.

**INTRODUCTION:** Mobile telecommunications equipment such as handsets are evaluated based on the specific absorption rate (SAR) value that is generally obtained by measuring the electrical field in a phantom made of a shell filled with a tissue-equivalent liquid. Various recipes for homogeneous tissue-

equivalent dielectric liquids have been introduced in international standards [1]. For higher frequencies, above 1 GHz, glycol type mixtures are recommended, and we previously reported that their dielectric properties are highly dependent on temperature [2]. For instance, the conductivity of a mixture of DGBE and water decreases 2% per one degree centigrade.

**OBJECTIVE:** We have developed odour-free, stable tissue-equivalent liquids for frequencies used in Japan, i.e., 50, 144, 430, 835 and 1200 MHz for walkie-talkies, and 900, 1450, 1950, and 2450 MHz for mobile phones. The head equivalent liquid is used in phantoms for mobile phones, while the 2/3-muscle-equivalent liquid is used for walkie-talkies.

**METHOD AND MATERIAL:** Based on the research of Bristol Univ [3], we have chosen Tween, de-ionised water and salt as ingredients. Dielectric properties of tissue-equivalent liquids were measured with a common coaxial probe (Agilent 85070 series) that is applicable to frequencies from 200 MHz to 20 GHz, and with a coaxial cell shown in Figure 1 (National Physical Laboratory, UK) for frequencies from 15 MHz to 1 GHz.

**RESULTS AND DISCUSSION:** Earlier, we reported that water evaporation changes dielectric properties, and that this evaporation is inevitable when using a mixture of water and glycol [2]. To compensate for this evaporation, we introduced a permittivity matrix that helps users adjust properties accordingly. The same phenomenon is observed in new tissue-equivalent liquids. For this reason, this paper provides a permittivity matrix for the recipes. Figures 2 (a) and (b) show examples of 50 MHz and of 1950-2450 MHz, respectively. Figure 3 compares the stability against the temperature between glycol type and Tween type for 2450 MHz. It is clear that Tween type is more stable, and if permittivity was adjusted at 21°C, the same mixture could be used from 18°C to 25°C in the case of Tween type. Although some preservatives would be needed for long time use, the new Tween type tissue-equivalent liquids must be useful for SAR measurements.

#### **REFERENCES:**

- [1] IEC 106/84/FDIS “Human exposure to radio frequency fields from hand-held and body-mounted wireless communication devices – Human models, instrumentation, and procedures – Part 1: Procedure to determine the Specific Absorption Rate (SAR) for hand-held devices used in close proximity of the ear (frequency range of 300 MHz to 3 GHz)”. Final Draft International Standard, Dec, 2004.
- [2] K, Fukunaga, S. Watanabe and Y. Yamanaka, “Dielectric properties of tissue-equivalent liquids and their effects on specific absorption rate”, IEEE Trans. EMC, Vol. 46, pp. 126-129, 2004.
- [3] S. Jenkins, T. E. Hodgetts, R. N. Clarke and A. W. Preece, “Dielectric measurements on reference liquids using automatic network analysers and calculable geometries”, IOP, Meas. Sci. Technol., Vol. 1, pp. 691-702, 1990.

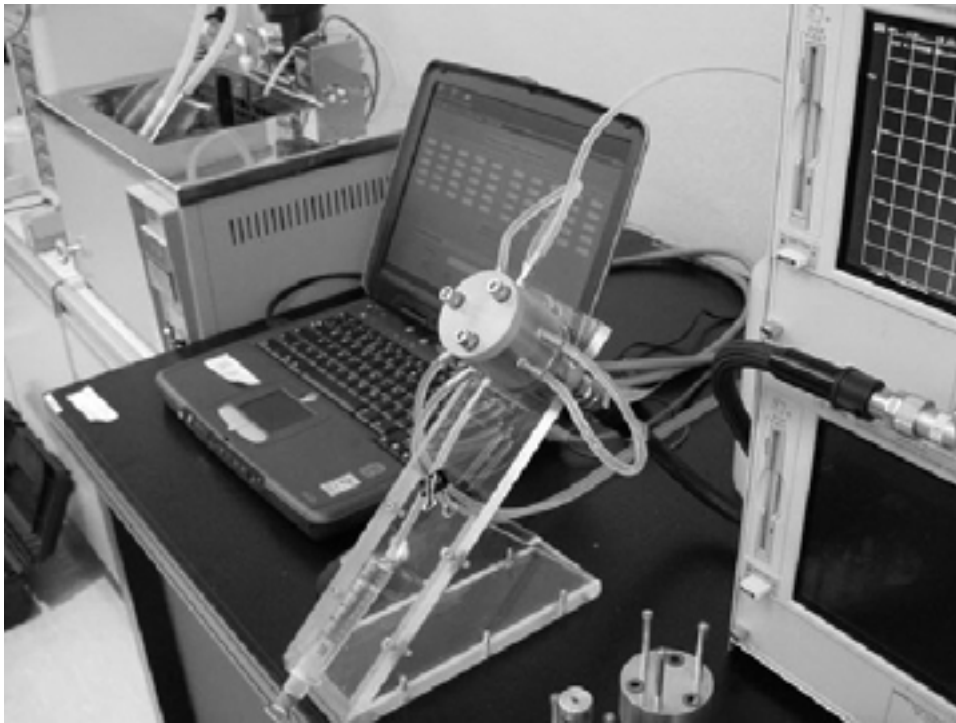


Figure 1: Dielectric measurement system (Coaxial cell for frequencies from 15 MHz to 1 GHz).

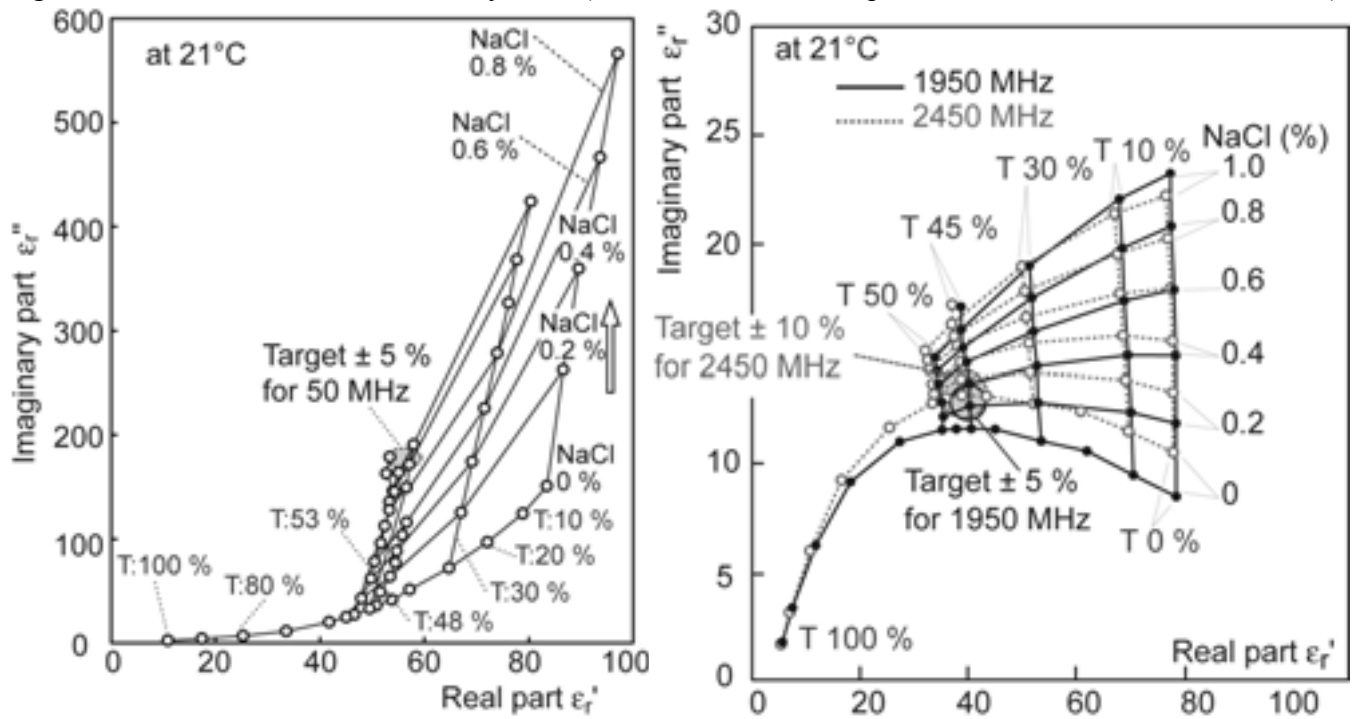


Figure 2: Permittivity matrix: (a) 50 MHz (2/3-muscle), (b) 1950 and 2450 MHz (brain).

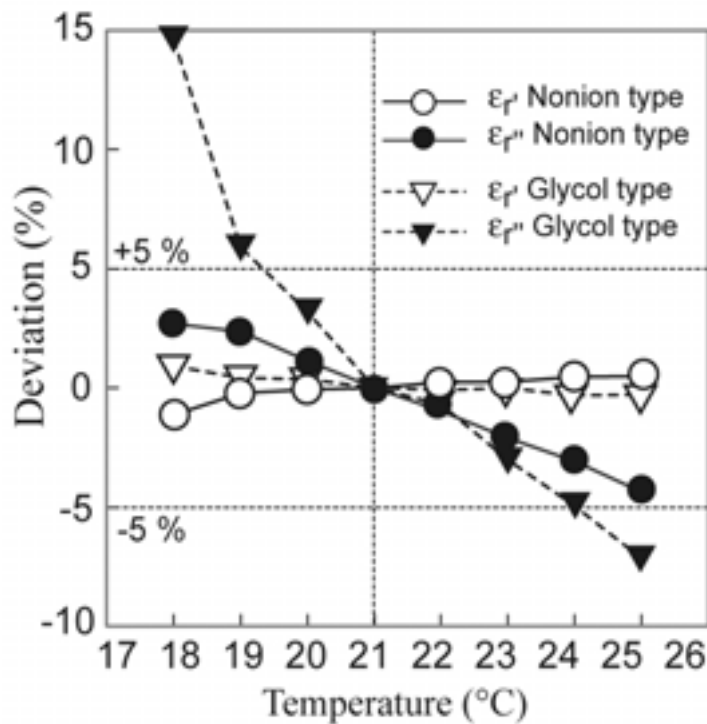


Figure 3: Temperature dependence of permittivities of Tween and glycol type tissue-equivalent liquids for 2450 MHz.

5-2

**NUMERICAL ANALYSIS OF THE LIQUID AND THE PHANTOM USED FOR MOBILE PHONE CERTIFICATION AT GSM, DCS AND UMTS FREQUENCIES.** V. Monebhurrin.

Supélec – L2S, Département de Recherche en Electromagnétisme, Plateau de Moulon, Gif-sur-Yvette Cedex, France.

Introduction

Limits of exposure to electromagnetic fields due to the use of mobile phones are defined in terms of the Specific Absorption Rate (SAR). Compliance tests of mobile phones are now routinely performed using a standard dosimetric facility wherein a phantom filled with tissue equivalent liquid is employed to measure the SAR. The European Committee for standardisation, CENELEC, has proposed a phantom (“SAM”) and appropriate values for the dielectric properties of the tissue-equivalent liquid at different frequencies. In a previous study [1], carried in the framework of the COMOBIO project, equivalent values were deduced at 900 MHz and 1800 MHz through numerical simulations by comparing the SAR induced in homogeneous and heterogeneous head models. The influence of the shape and the size of the phantom was also investigated at these two frequencies.

Objective

The analysis of the phantom and the tissue equivalent liquid is herein extended to the uplink UMTS frequency i.e. 1950 MHz in the framework of the ADONIS project. Numerical simulations are undertaken using the SAM phantom (Fig. 1) filled with the tissue-equivalent liquid proposed by the CENELEC standard (Table 1). Simple excitation sources are considered for different use positions recommended by the standard. For comparison with previous results, simulations are also undertaken at

900 MHz and 1800 MHz. In an aim to provide an answer to the question of child exposure, the influence of the morphology of the head is analysed. Furthermore, the suitability of the phantom and liquid for compliance testing of free handset kits is also assessed.



Figure 1. SAM phantom placed with a monopole antenna as left/check, right/check, left/tilt or right/tilt configuration.

Frequency [ MHz ]	Permittivity	Conductivity [ S/m ]
900 (GSM)	42	0.99
1750 (DCS)	40	1.38
1950 (UMTS)	40	1.38

Table 1. Dielectric properties of the tissue equivalent liquid used for the numerical simulations.

#### Method

Numerical approaches based on the FDTD (Finite Difference Time Domain) and the FITD (Finite Integral Time Domain) algorithms are used for the simulations. Indeed, time domain solvers prove appropriate when handling highly inhomogeneous media such as the human head. However, since these methods are based on a volumetric mesh, it becomes difficult to model the head in the presence of complex structures such as a real mobile phone. Instead, simple mobile phone models are employed such as dipoles, monopoles over a metallic box and pifa antennas in which case the modelling can be improved by including the battery, for example (Fig. 2). The free handset kit is modelled as a short wire placed near the phantom.



Figure 2. Excitation sources used for simulations: dipole, monopole over a metallic box and built-in antenna.

#### Results

Results show that, in the case of monopole antennas for example, the highest SAR value is obtained at 900 MHz for a given use position (Fig. 3). For comparable mobile phones and use positions, the SAM phantom is representative of the heterogeneous head model at the three frequencies. The comparison of the SAR in homogeneous and heterogeneous head models when used with free handset kit shows that the SAM phantom used with the recommended liquid provides a conservative overestimate.

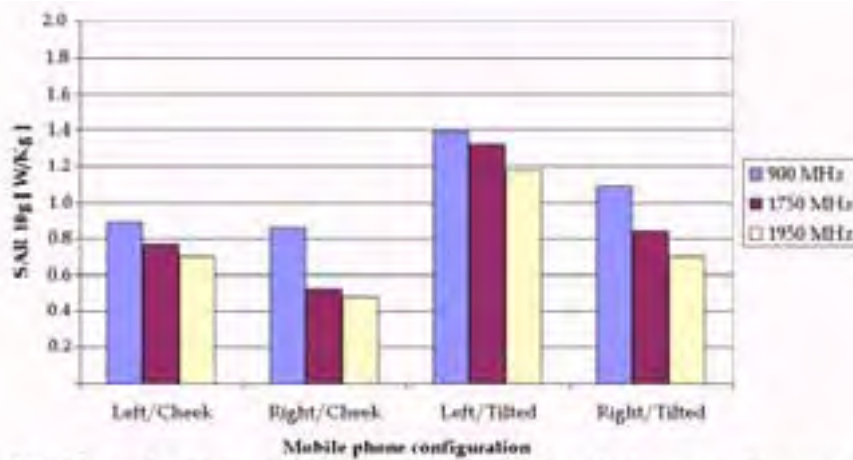


Figure 3 : SAR obtained with the SAM phantom for different phone positions and frequencies.

#### Acknowledgement

This research was sponsored by the French government in the framework of the ADONIS project (RNRT programme).

#### Reference

1. V. Monebhurrin et. al., "A numerical approach for the determination of the tissue equivalent liquid used during SAR assessments," IEEE Trans. Magnetics, 2002, 38, 2, 745-748.

5-3

**BIOLOGICAL TISSUE-EQUIVALENT AGAR-BASED SOLID PHANTOMS WITH WIDE BAND CHARACTERISTICS UP TO 10 GHZ.** T. Onishi<sup>1,2</sup>, T. Takimoto<sup>2</sup>, K. Saito<sup>2</sup>, S. Uebayashi<sup>1</sup>, M. Takahashi<sup>2</sup>, K. Ito<sup>2</sup>. <sup>1</sup>NTT DoCoMo, Inc. Kanagawa, Japan, <sup>2</sup>Chiba Univ, Chiba, Japan.

**BACKGROUND:** Wireless systems used at high frequency such as wireless LANs have recently become popular and the Ultra Wide Band (UWB) system was developed. In addition, the International Electrotechnical Commission (IEC) is now in progress of standardizing a measurement method for the Specific Absorption Rate (SAR). The IEC plans to expand the upper frequency limit from 3 GHz to 6 GHz [1]. From these points of view, it is expected that a tissue-equivalent phantom can be applied in a high frequency range and/or have broad-band characteristics.

**OBJECTIVE:** The objective of this study is to develop a biological tissue-equivalent solid phantom with the following characteristics: 1) only one phantom can be used over a broad band and 2) electrical constants of the phantom can be adjusted at each frequency over a broad band.

**METHODS:** An agar-based solid phantom is selected as the biological tissue-equivalent phantom. The solid phantom comprises agar, deionized water, polyethylene powder, sodium chloride, TX-151 and sodium dehydroacetate [2]. The phantom can maintain its shape by itself. Another feature of the phantom is that arbitrary shapes can be fabricated easily using a mold (Fig. 1). The electrical constants of this phantom can be adjusted mainly by using polyethylene powder and sodium chloride.

**RESULTS:** The electrical constants of the developed phantom were measured at frequencies from 0.9 to 10 GHz (Fig. 2). Error-bars indicate  $\pm 10\%$  of target values, which correspond to a 2/3-muscle model. The measured relative permittivity is within  $\pm 5\%$  of the target value except at 9 and 10 GHz. On the other hand, the measured conductivity is within  $\pm 5\%$  from 3 to 6 GHz. If  $\pm 10\%$  of the variation from the

target value is allowed, electrical constants are within this variation; therefore, the phantom can be used from 3 to 10 GHz. This means that it is not necessary to change the phantom for each frequency during the measurement process. Since, this time, we focused on a higher frequency range than that used for the present cellular systems such 2 GHz, the differences in the conductivity between the targeted and measured values are relatively large, but within  $\pm 50\%$ . We obtained the similar results with respect to an average brain model as well. It is also possible to adjust the electrical constants for a desired frequency by changing the amount of polyethylene powder and sodium chloride even though a lower frequency range is used.

**CONCLUSION:** A biological tissue-equivalent agar-based solid phantom is presented. It is confirmed that this phantom can be applied to a high frequency range and that it exhibits wide band characteristics up to 10 GHz.

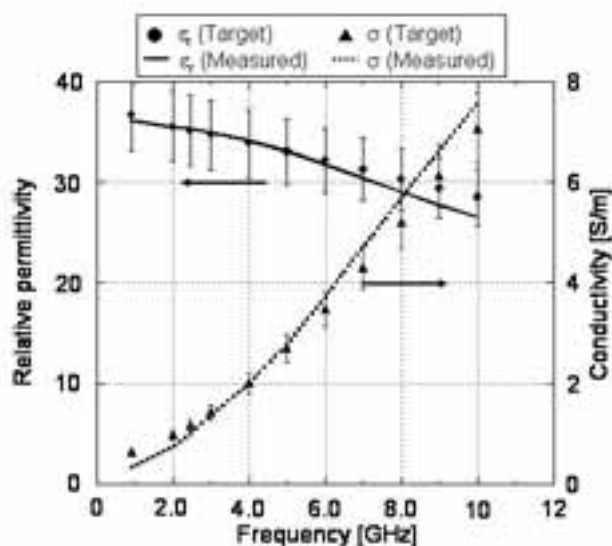
The authors are grateful to Dr. Hanazawa, Dr. Wake, and Dr. Watanabe of the National Institute of Information and Communications Technology (NICT), Japan, for their supports on the measurement.

References.

[1] IEC TC106 PT62209 Part2, 2004.

[2] R. Ishido, et al., EMC'04Sendai, 3B3-2, Sendai, Japan, Jun. 2004.





5-4

**DIELECTRIC PROPERTIES OF PORCINE BRAIN TISSUES AT MICROWAVE FREQUENCIES; IN-VIVO, IN-VITRO AND SYSTEMATIC VARIATION WITH AGE.** A. Peyman<sup>1</sup>, S. J. Holden<sup>2</sup>, S. Watts<sup>2</sup>, R. Perrott<sup>2</sup>, C. Gabriel<sup>1</sup>. <sup>1</sup>Microwave Consultant Ltd. Woodford Road, London E18 2EL, UK., <sup>2</sup>Defence Science and Technology Laboratory Biomedical Sciences, Porton Down, Salisbury, UK.

**INTRODUCTION:** Most of the dielectric data in the literature [1] and the extensive database published at 1996 [2] pertain to excised tissues. There is a general perception that data obtained in-vivo are more relevant to the assessment of the exposure of people, but is it? This paper will discuss the arguments and illustrate the points using data obtained from the recently completed dielectric measurement program carried out as part of the Mobile Telecommunication Health Research (MTHR) program.

**OBJECTIVE:** The main aim is to present dielectric data obtained for 5 different porcine brain tissues together with an assessment of the total uncertainty and an analysis comparing data obtained in-vivo and in-vitro in our lab and corresponding data recently published in the literature. Another aim is to re-examine the question of the variation of dielectric data with age for different brain tissues.

**METHODOLOGY:** The dielectric measurements of porcine brain tissues were made using an optimal size open-ended coaxial probe and computer controlled network analysers following a previously reported procedure [3]. The frequency range of the study was 50MHz-20GHz. Both in-vivo and in-vitro measurements have been carried out. Measurements were made on 5-10 pigs (depending on the tissue) of 50-70kg under general anesthesia for in-vivo condition. Similar measurements were carried out on tissue excised from 6-10 pigs of 50-70kg measured under in-vitro conditions. The totals of 6 tissues were identified in the brain (Dura matter, CSF, Arachnoid, Pia matter, Grey matter and White matter), and multiple measurements were made on each tissue. Statistical analysis was applied to the pooled data from all pigs and a total combined uncertainty assigned to the permittivity and conductivity of each tissue at different frequency regions of the spectrum. Finally, similar measurements were carried out on

pigs of 10kg and 250 kg under the in-vitro conditions to re-examine the issue of systematic variation of the dielectric data with age.

**RESULTS AND DISCUSSION:** Figures 1 and 2 show the comparison between dielectric properties of Grey matter measured in-vivo and in-vitro as well as data from recently available literature. For clarity, error bars were not added to the experimental data, however, the uncertainty budget will be discussed and presented in the final paper. Similar data and analysis will be provided for all other brain tissues. This exhaustive study also concludes that, at microwave frequencies, no significant differences were observed between data obtained in-vivo and in-vitro for grey matter. However, slight differences were observed in the case of white matter and spinal cord. Figures 3 and 4 show the variation in dielectric properties of Grey and white matter as a function of age. While no significant changes observed for grey matter, large variation detected in the measured dielectric data of white matter, spinal cord and dura when animal aged from ~10kg to ~250kg. These results will be compared and contrasted to previous finding of variation with age for rat brain tissue. **ACKNOWLEDGMENTS:** This work was undertaken by MCL in collaboration with DSTL, Porton Down. MCL received funding from the Mobile Telecommunication and Health Research Program. The views expressed in the publication are those of the authors and not necessarily those of the funders.

**REFERENCES:**

1. Gabriel C, Gabriel S. and Courthout E., 1996a Phys. Med. Biol. 41 (11), 2231-2250.
2. C Gabriel, 1997 Compilation of the Dielectric Properties of Body Tissues at RF and Microwave Frequencies: <http://www.brooks.af.mil/AL/OE/OER/Title/Title.html>
3. Gabriel, C., Chan, T. Y. A. and Grant, E. H., 1994, Phys. Med. Biol 39, 12, 2183-2200

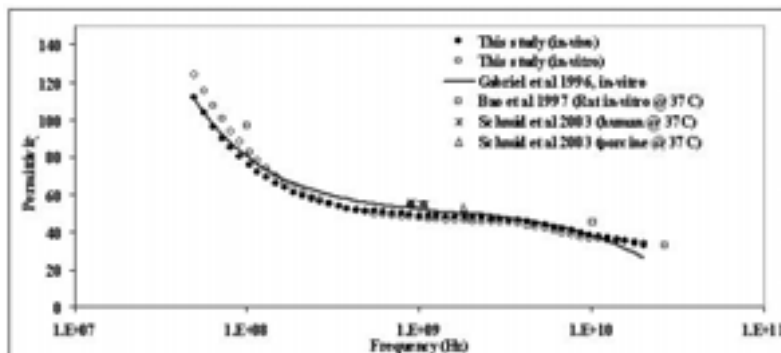


Figure 1. Comparison between the in-vivo and in-vitro Permittivity of porcine Grey matter

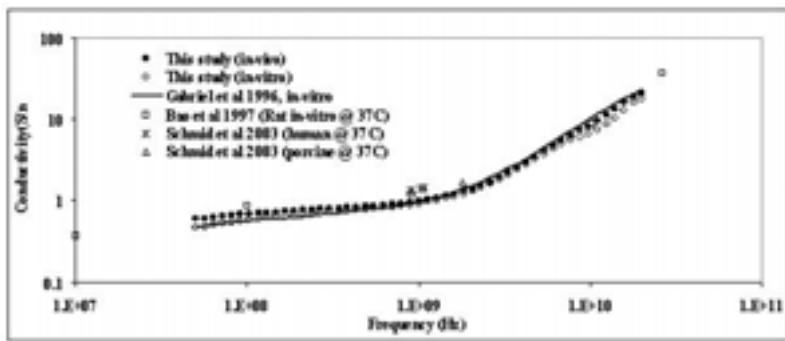


Figure 2. Comparison between the in-vivo and in-vitro Conductivity of porcine Grey matter

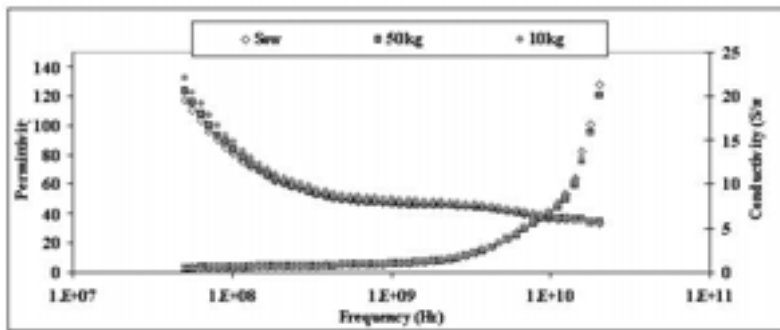


Figure 3. Dielectric properties of porcine Grey matter (in-vitro) of different ages

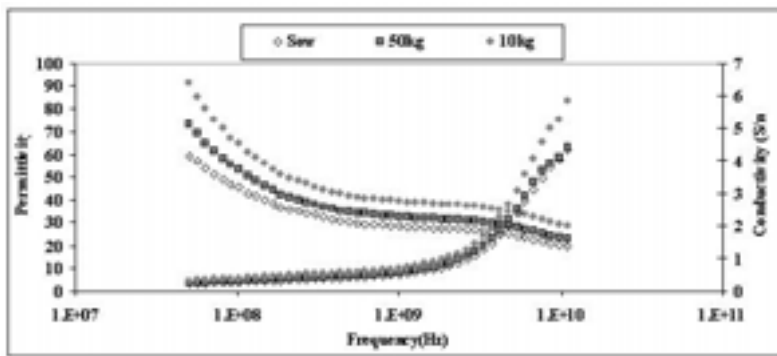


Figure 4. Dielectric properties of porcine White matter (in-vitro) of different ages

5-5

**AGE DEPENDENT DIELECTRIC PROPERTIES OF BOVINE BRAIN AND EYE TISSUES IN THE FREQUENCY RANGE FROM 400 MHZ TO 18 GHZ.** G. Schmid, R. Überbacher. ARCS Seibersdorf research GmbH, Seibersdorf, Austria.

**INTRODUCTION:** In recent years the question whether children are absorbing more electromagnetic energy during radio frequency (RF) or microwave (MW) exposure than adults is heavily discussed. Beside several other aspects a possible age dependence of the dielectric properties of body tissues might play an important role in this context. However, scientific data regarding this issue is scarce. Two early publications dealing with mice brain [1] and rabbit brain [2] as well as a more recent study [3] using rat tissues (brain, skull, skin, muscle, liver, spleen, tongue, kidney, tail, salivary gland) clearly indicated an age dependence of the dielectric properties of the investigated tissues. One of the major problems when using such small animals is the transferability of the data to human tissues, e.g., it is hardly possible to distinguish measurement data for grey and white matter on mice and rat brains.

**OBJECTIVE:** To provide statistically based data regarding age dependence of the dielectric properties of brain and eye tissues of mammals having tissue structures more similar to humans.

**MATERIALS AND METHODS:** In order to have access to a sufficient number of animals in a reasonable time frame all measurements took place in a slaughterhouse parallel to the slaughtering-process chain. Dielectric measurements in the frequency range 400 MHz to 18 GHz were carried out on freshly excised bovine brain and eye tissues of 52 animals which could be divided into two age groups: 42 adult animals (18-24 months) and 10 young animals (4-6 months old calves). The brain tissue was accessible for the measurements within 8 minutes after the animals death and the brain tissue temperature during the measurements was  $32 \pm 1$  degree C. The measurements on eye tissues took place within 15 minutes post mortem at tissue temperatures of  $25 \pm 1$  degree C. Measurements were carried out on the following types of tissues: brain grey matter, brain white matter, eye cornea, eye lens (cortical)

and the vitreous body of the eye. On each tissue sample the mean value of at least 3 consecutive measurements at slightly different positions was taken. As measurement system the commercially available dielectric probe kit HP85070B in combination with a vector network analyzer HP8722C (both devices from Technologies, Inc.) were used after air/short/water calibration. Calibration uncertainty was assessed by measurements on well known reference liquids (methanol and 0.9% NaCl solution) at the beginning and at the end of the measurements. Statistical analysis (comparison between data obtained on adult tissues vs. data from calf tissues) was performed using standard t-test in case of normally distributed data and homogeneity of variances (as found for all tissues except for the vitreous body). The measured data for vitreous body (not normally distributed) was analyzed by Mann-Whitney U-test. Type I error level alpha was generally set to 0.01.

**RESULTS:** Data analysis revealed no statistically significant difference in conductivity as well as in permittivity between the two age groups for brain grey matter and cornea. Brain white matter and eye lens showed significantly different dielectric parameters over the entire considered frequency range. In case of brain white matter the relative difference of mean values ranged between 15% and 22% for conductivity and 12% and 14% for permittivity over the considered frequency range. For eye lens this relative difference was found to be between 76% (at 400 MHz) and 42% (at 18 GHz) for conductivity and between 28% and 42% for permittivity. For both, white matter as well as eye lens, higher values of conductivity and permittivity were obtained on tissues from young animals. In case of the vitreous body conductivity showed a slight (5% - 13%) but statistically significant difference in the 400 MHz to 1 GHz range, but not at higher frequencies. of the vitreous body, on the contrary, showed a slight (5% - 10%) but statistically significant difference at frequencies above approximately 10 and no statistically significant difference at lower frequencies. In contrast to white matter and lens tissue the observed differences for the vitreous body showed lower values of conductivity and permittivity for the young animals.

**CONCLUSION:** The fact that only white matter and not grey matter showed lower permittivity and conductivity at higher age can be explained by the myelination process, taking place mainly in the white matter and reducing tissue water content and increasing tissue fat content. The observed age dependence of the dielectric parameters of lens tissue might be due to the complex development and aging processes in the lens which are continuing throughout life [4]. The observed behavior of vitreous body needs further discussion. The reported results provide additional evidence for the tissue specific age dependence of the dielectric properties in the RF and MW frequency range. Conclusions whether the observed extent of age dependence of the dielectric properties might have significant impact on the resulting power absorption in the head of children cannot be drawn before reliable data for all other relevant tissues are available. Furthermore the question of age-matching (correspondence between animal age and human age) has to be answered.

#### REFERENCES:

- [1] Thurai M, Goodridge VD, Sheppard RJ, Grant EH, 1984. Variation with age of the dielectric properties of mouse brain cerebrum, *Phys. Med. Biol.*, 29(9):1133-1146
- [2] Thurai M, Steel MC, Sheppard RJ, Grant EH, 1985. Dielectric Properties of the Developing Rabbit Brain, *Bioelectromagnetics* 6: 235-242 (1985)
- [3] Peyman A, Rezazadeh AA, Gabriel C, 2001. Changes of the dielectric properties of rat tissue as a function of age at microwave frequencies, *Phys. Med. Biol.* 46(2001):1617-1629
- [4] Bron AJ, GFJM, Kroetz J, Maraini G, Harding JJ, 2000. The Aging Lens; *Ophthalmologica* 2000; 214:86-104

## Plenary II: Cancer Overview Cell And Molecular Biology

*Chair: Kjell Hansson Mild*  
8:15 - 9:00 am, O'Reilly Hall

**HOW CAN A NORMAL CELL DEVELOP INTO TUMOR CELLS - ON THE ROLE OF EXOGENOUS AND ENDOGENOUS FACTORS.** Erik Lundgren. Dept of Molecular Biology, Umeå Universitet, Sweden.

There are two main driving forces for development of tumors. It is well known that tumours occur in tissues with a proliferative potential, either due to a stem cell population or due to continuous stimulation to growth. It is also established that tumors emerge as a result of multiple genetic changes, often as a result of defect control of the genetic integrity. Both forces can be reconciled in term of clonal expansion of cells with mutations of genes involved in growth regulation or cell survival. Electromagnetic fields and other physical factors are expected to contribute to genetic lesions in the first place and less by expansion of clones with mutated genes.

However, the fact that a chaotic genetic background seems to be a prerequisite for tumor disease illustrates that tumors are genetically heterogeneous. There is emerging evidence that even a distinct diagnostic entity might represent tumor cells with an array of mutations, not shared by all cells in a given population. This suggests that search for environmental factors might not always gain from looking on distinct diagnostic entities. There are two distinct forms of genetic heterogeneity in tumors involving either chromosomal rearrangements or point mutations. The genetic changes induced by low energy fields should be expected to fall into either of these categories. Thus, search for mechanisms for tumor initiation and development induced by physical forces could be either by defining their relative risks for chromosomal instability or for point mutations, as manifested by minisatellite instability.

## Session 6: Dosimetry II

*Chairs: C.K. Chou and Quirino Balzano*

11:30 - 12:30 pm, Theatre L

6-1

**UPPER BOUNDS OF SAR FOR DIPOLE ANTENNAS IN THE 300-3000 MHZ FREQUENCY RANGE.** M. Ali<sup>1</sup>, M. G. Douglas<sup>2</sup>, A. Faraone<sup>2</sup>, C-K. Chou<sup>2</sup>. <sup>1</sup>Dept of Electrical Engineering, Univ of South Carolina, Columbia, South Carolina, USA, <sup>2</sup>Motorola Florida Research Laboratories, Fort Lauderdale, Florida, USA.

**OBJECTIVES:** The specific absorption rate (SAR) of dipole antennas of different lengths and at various distances from a flat phantom is calculated in the 300 - 3000 MHz frequency range so as to determine the power threshold below which the SAR cannot exceed the compliance limit. **METHODS:** Since there are myriad mobile device geometries and antenna types, canonical dipole geometries were considered next to a flat phantom, in accordance with [1]. In the analysis, all antennas are made to be perfectly matched and have no conductor or dielectric losses. Thus the SAR values indicate the maximum that will be encountered considering a fixed amount of delivered power. The size of the antennas was chosen based on bandwidth considerations. Table 1 shows the fundamental limit on antenna Q and bandwidth from the McLean model [2]. Also shown are the bandwidths of a 3.6 mm diameter dipole antenna at 900 MHz, calculated in free space and at a 10 mm distance from a flat phantom using IE3D, a Method of Moments (MoM) solver. Since most portable wireless applications of interest have operating bandwidths of 2% to 15%, and antennas are designed to satisfy these bandwidth requirements within -10 dB or -6 dB return loss, it is unnecessary to investigate antennas of size  $\lambda/15$  or smaller. Using the FDTD method, SAR values of 3.6 mm diameter dipole antennas with lengths of  $L = \lambda/2$ ,  $\lambda/4$  and  $\lambda/8$  were computed at distances of  $d = 5, 10, 15$  and  $20$  mm between the dipole feed point and the phantom liquid. The dimensions and dielectric parameters of the phantom and phantom shell conform to [1]. The voxel size was less than  $\lambda/20$  in the medium and the distance of the dipole antenna to the PML absorbing boundaries was at least  $\lambda/4$ . From the SAR data, the power level at which the SAR equals the compliance limit is computed.

**RESULTS:** Figure 1 shows the output power of the dipole antennas resulting in a 1-gram averaged SAR of 1.6 W/kg. In the figure on the left, the data are plotted as a function of frequency for a  $d = 5$  mm. The 1-gram averaged SAR increases with frequency, due to higher liquid conductivity, lower liquid permittivity and higher current concentration on the shorter dipole antennas. A higher SAR results in a lower power threshold at which the SAR compliance limit is exceeded. In the figure on the right, the data are plotted as a function of distance  $d$  for  $f = 900$  MHz. As expected, the SAR decreases exponentially with increasing distance, resulting in an exponential increase in the power threshold. For example, at  $f = 900$  MHz and  $d = 5$  mm, the power thresholds for  $L = \lambda/2$ ,  $\lambda/4$  and  $\lambda/8$  are 95 mW, 50 mW and 32 mW, respectively. As a comparison, the power thresholds for 1344 SAR measurements from dozens of handset models held next to the ear and operating in the 800 - 900 MHz frequency range are plotted in Fig. 2. The dipole power thresholds are significantly lower than the power thresholds of the handsets. These data are useful in determining low-power SAR testing exclusions.

**CONCLUSIONS:** A method of determining power thresholds for SAR compliance is presented. The power thresholds have been shown to be conservative compared to existing handset data. (Supported by Motorola)

REFERENCES:

[1] IEEE, "IEEE Recommended Practice for Determining the Peak Spatial-Average Specific Absorption Rate (SAR) in the Human Head from Wireless Communications Devices: Measurement Techniques," IEEE Standard 1528, 2003.

[2] J. S. McLean, "A Re-Examination of the Fundamental Limits on the Radiation Q of Electrically Small Antennas," IEEE Trans. Antennas Propagat., vol. 44, no. 5, May 1996, pp. 672-676.

Table 1: Quality factors and bandwidths of electrically small antennas, using the McLean model [2], and bandwidths of dipole antennas in free space and 10mm from a flat phantom at 900 MHz. Values are shown as a function of maximum antenna dimension.

Maximum antenna dimension	McLean		3.6mm diameter dipole at 900 MHz		
	Model		Free space	10 mm from flat phantom	
	Q	-3 dB BW	-3 dB BW	-3 dB BW	-9.5 dB BW
$\lambda/15.7$	130	0.77%	0.53%	0.89%	0.33%
$\lambda/7.8$	18	5.55%	2.3%	4.6%	1.67%
$\lambda/5.2$	6.3	15.87%	6.3%	11.56	4.1%
$\lambda/3.9$	3.2	31.25%	13.1%	21.44%	7.44%
$\lambda/\pi$	2	50.0%	22.9%	33.11%	11.3%

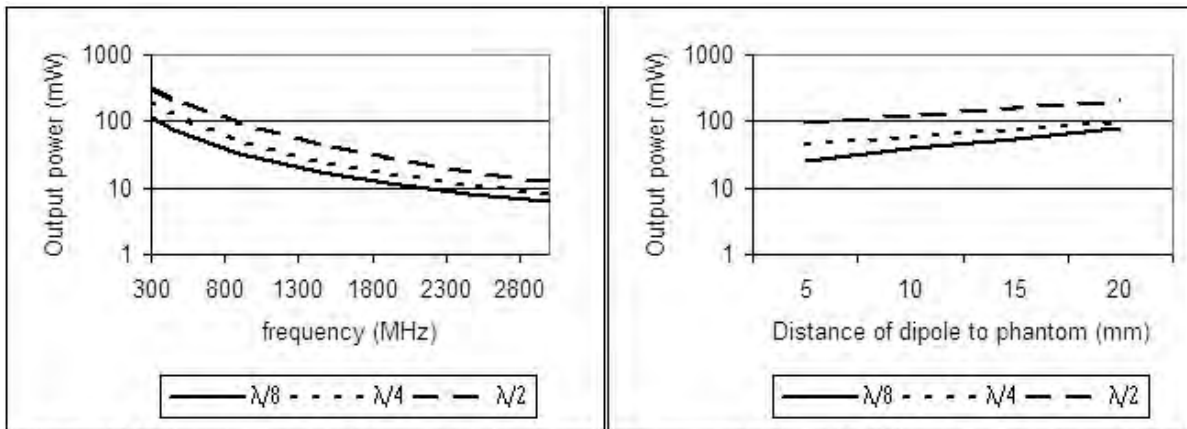


Figure 1: Dipole antenna output power resulting in a 1-gram averaged SAR of 1.6 W/kg. Data are shown for all frequencies and dipole lengths at a distance to the phantom of  $d = 5$  mm (left). Data are also shown for all distances and dipole lengths at a frequency of 900 MHz (right).

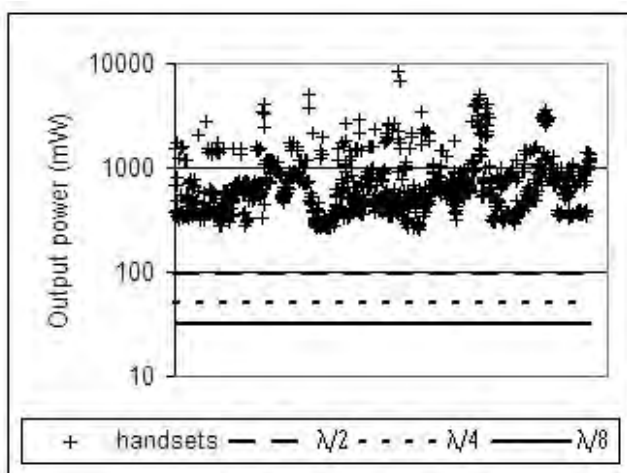


Figure 2: Power thresholds calculated from 1344 SAR measurement records of handset models held next to the ear and operating in the 800 – 900 MHz frequency range. The handset power thresholds are each marked by a '+' and are in random order. The handset power thresholds are compared with the dipole power thresholds at  $f = 900$  MHz and  $d = 5$  mm, which are 95 mW, 50 mW and 32 mW for  $L = \lambda/2$ ,  $\lambda/4$  and  $\lambda/8$ , respectively.

6-2

**THE INTERNATIONAL INTER-COMPARISON OF SPECIFIC ABSORPTION RATES IN A FLAT ABSORBING PHANTOM IN THE NEAR-FIELD OF DIPOLE ANTENNAS.** Q. Balzano, C. C. Davis. Dept of Electrical and Computer Engineering, Univ of Maryland, College Park, MD.

**INTRODUCTION:** This paper reports the results of an international intercomparison of the specific absorption rates (SARs) measured in a flat-bottomed container (flat phantom) filled with human head tissue simulant fluid, placed in the near-field of custom-built dipole antennas operating at 900 MHz and 1800 MHz, respectively.

**OBJECTIVE:** These tests of the reliability of experimental SAR measurements have been made as part of a verification of the ways in which wireless phones are tested and certified for compliance with safety standards.

**METHODS:** SAR measurements were made using small electric field probes placed in head simulant fluid in a flat phantom, and scanned in 3-dimensions to produce the spatial SAR distribution values in the phantom. Custom designed dipole antennas were used for exposure of the phantom. The intercomparison involved a standard flat phantom, antennas, some critical power meters, and RF components being circulated among 16 different laboratories, including governmental and industrial laboratories, and the Univ of Maryland. Each participating laboratory provided its own electric field probes, scanning system, and a simulant fluid prepared to a required prescription. Many of the specifications of the flat phantom system were guided by those given in the IEEE 1528 Standard [1], although it was not the intent of the intercomparison to replicate the IEEE 1528 procedures exactly. At the conclusion of each laboratory's measurements, its results were communicated to the coordinators including: spatial SAR scans at 900 MHz and 1800 MHz, and 1g and 10g spatial SAR averages for cubic volumes at 900 MHz and 1800 MHz. In this paper we will describe the detailed protocols involved in the intercomparison, and provide a detailed summary of all the results.

**RESULTS:** The overall results averaged over 15 participating laboratories in North America, Europe, and Asia are: at 900 MHz, 1g average  $7.85 \pm 0.76$ , 10g average  $5.16 \pm 0.45$ ; at 1800MHz, 1g average

18.44±10g average, 10g average 10.14±0.85, all measured in units of W/kg per watt of radiated power. **DISCUSSION:** The results of this intercomparison show that reliable SAR values for wireless phone certification were obtained by all the participating laboratories, with measurement uncertainties that were consistent with the expected difficulty of these measurements and the anticipated uncertainties of the various experimental steps involved.

#### REFERENCE

1. IEEE Standard 1528TM-2003. IEEE Recommended Practice for Determining the Peak Spatial-Average Specific Absorption Rate (SAR) in the Human Head from Wireless Communications Devices: Measurement Techniques.” IEEE SCC 34, IEEE, New York, 2003.

This work was supported by the Mobile Manufacturers Forum (MMF).

6-3

**ABSORPTION MECHANISM OF ELECTROMAGNETIC ENERGY FOR BODY-MOUNTED DEVICES OPERATING BETWEEN 30 MHZ TO 5800 MHZ.** A. Christ, A. Klingenböck, N. Kuster. IT'IS Foundation, Swiss Federal Institute of Technology, Zurich, Switzerland.

**INTRODUCTION:** In the past decade, substantial knowledge has been acquired on the absorption of electromagnetic (EM) near-field and compliance testing of wireless devices, whereby the research and standardization focus was on the exposure of the head posed by cellular phones. However, new cellular phone usage patterns (e.g. Bluetooth, modem or video functionalities, etc.) and novel body-worn wireless devices (e.g., laptop/palmtop computers with wireless network connection or emerging body-worn health support systems) require the coverage of a large variation of parameters. Compared to the relatively well defined location of cellular phones at the ear, the following additional parameters need to be considered:

- distances between 5 mm and 200 mm of the transmitter from almost any location of the body, i.e., different tissue compositions and different body curvatures are exposed,
- extended frequency range (30 MHz to 5800 MHz).

**OBJECTIVE:** The goal of this study is to analyze the impact of these additional parameters on the EM energy absorption and the impact on procedures/methodologies for compliance testing.

**METHODS:** The tissue composition at representative locations of the human body was analyzed with respect to worst-case energy absorption. Because of the large frequency range and distances between 5 mm and 200 mm, both near-field and far-field coupling effects were investigated using analytical and semi-analytical methods with generic body models and antenna types. Further, the findings of the generic models were confirmed by FDTD simulations (SEMCAD) using numerical models of real-world devices and anatomical high-resolution models of the human body. All results were compared to the spatial peak average SAR (1g and 10g) obtained with the dielectric parameters of head tissue simulating liquid.

**RESULTS:** A layer of tissue with low water content between two tissues with high water content (typically skin-fat-muscle) can have a significant impact on the energy absorption and the SAR. Under far-field conditions, standing wave effects in the layered tissue structure can lead to a significant increase of the SAR in the skin if compared to the SAR obtained using tissue simulating liquid. In the near field, reactive electrical field components can penetrate effectively in the presence of the low permittivity fat and therefore also lead to high SAR in the skin tissue. Whereas the far field effect depends on the frequency and fat layer thickness (approx.  $\lambda/4$ ), the increased coupling of the near field depends merely on the presence of a fat layer. It is dominant in the VHF range and below and further depends on the antenna type.

DISCUSSION: The coupling effects due to the tissue layering can lead to an SAR increase which cannot be modelled using a homogeneous structure such as a phantom filled with tissue simulating liquid. This may require the introduction of a multiplication factor to be applied for the measured spatial peak SAR values in order to obtain a conservative assessment of the worst-case exposure.

ACKNOWLEDGMENTS: Support from Mobile Manufacturers Forum (MMF), Belgium; Bundesamt für Strahlenschutz, Germany.

#### 6-4 STUDENT

**FREQUENCY CHARACTERISTICS OF POWER ABSORPTION AND OF TEMPERATURE ELEVATION FOR HUMAN EXPOSURE TO MILLIMETER WAVE.** T. Konno<sup>1,2</sup>, M. Hanazawa<sup>1</sup>, K. Wake<sup>1</sup>, S. Watanabe<sup>1</sup>, M. Taki<sup>3</sup>, H. Shirai<sup>2</sup>. <sup>1</sup>National Institute of Information and Communications Technology, Tokyo, Japan, <sup>2</sup>Chuo Univ, Tokyo, Japan, <sup>3</sup>Tokyo Metropolitan Univ, Tokyo, Japan.

INTRODUCTION: Recently, various applications of millimeter wave (MMW) gather momentum, and it is expected to increase the opportunity of the public exposure to MMW. MMW exposure produces superficial thermal effects. Those effects on eyes have been large concerns because of the possibility of high-strength radiation to the surface of the eyes and of the lack of blood flow in the eyes. For the surface of the skin, on the other hand, the warmth sensation is considered as the basis of the safety guidelines. The threshold of the incident power density, which causes the warmth sensation, has been studied [1, 2]. Ministry of Internal Affairs and Communications in Japan have set the safety guideline values of MMW exposure based on those studies. A few frequencies have been however investigated in the previous studies. Further studies on the threshold for the warmth sensation at other frequencies in MMW band are therefore needed.

OBJECTIVE: The purpose of this study is to investigate the frequency characteristics of MMW power absorption and of temperature elevation based on simple but very-high-resolution models.

METHOD: In this discussion, the structure below the human skin is modeled as the semi-infinite 3-plane models i.e. skin, fat, muscle. The thicknesses of the skin and of the fat are 1.2 mm and 11.85 mm. Specific absorption ratio (SAR) has been calculated for various incident angle of MMW by using analytical transmission line methods. Temperature elevation in each layer has been calculated based on the finite difference forms of the biological heat conduction equation with very high spatial resolution, i.e., 0.01 mm. Incident power density of MMW is 5 mW/cm<sup>2</sup> or the Japanese guideline under the controlled environment.

RESULTS AND DISCUSSION: SAR and temperature elevation distributions are shown in Figs. 1 and 2. These distributions are significantly dependent on frequency. SAR of MMW i.e. 30 GHz and 60 GHz almost exist in the skin layer, while SAR of microwave (MW) i.e. 2.45 GHz and 10 GHz is distributed in not only the skin layer but also the fat and muscle layers. Therefore the temperature elevations for MMW are about 2 ~ 3 times as high as those for MW at the surface of the body, while the temperature elevation for MMW become negligible below about 4 mm from the skin surface. The safety guideline for MMW in some countries is constant. But our preliminary study leaves room for possibility of improvement of MMW guidelines. The threshold temperature elevation of the warmth sensation including MMW has been reported as about 0.06 ~ 0.08 degree C on the surface of the body [3, 4]. Our study suggests that the MMW exposures with the guideline level (5 mW/cm<sup>2</sup>) can make the warmth sensation, while the MW exposures cannot. It is obvious that further studies to investigate detail of the

frequency characteristics are necessary. We should note the limitation of this study. Due to one-dimensional analysis, this study does not provide any knowledge about the exposure area, which is an important parameter for the warmth sensation. We are therefore developing the new model for evaluation of the effect of the exposure area.

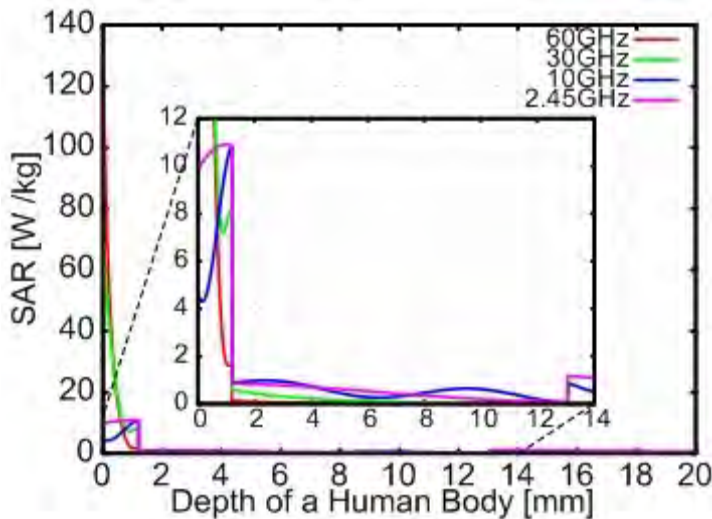


Figure 1: SAR distributions. The angle of the incident of the electromagnetic waves is normal.

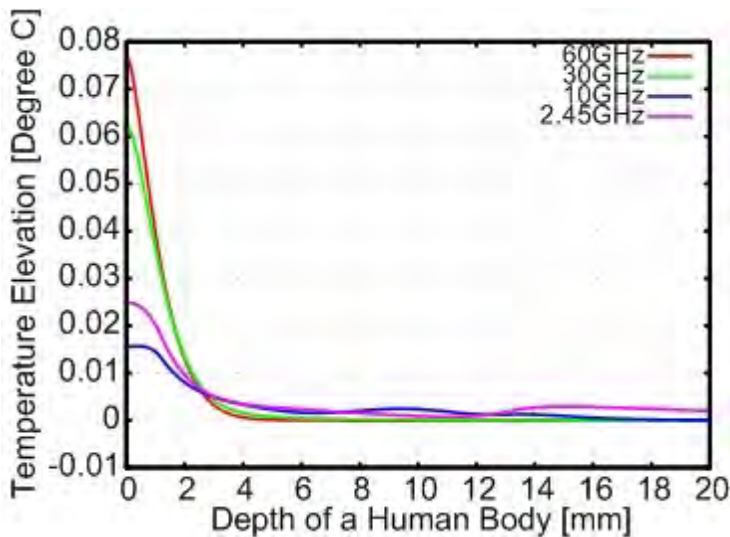


Figure 2: Temperature elevation distributions after 10-sec exposure. The angle of the electromagnetic waves is normal.

- [1] Gandhi O. P., Riaz A., "Absorption of millimeter waves by human beings and its biological implications";, IEEE Trans. Microwave Theory Tech. Vol.34, pp.228-235, 1986.
- [2] Elder J. A. and Cahill D. F. (eds.). "Biological Effects of Radio frequency Radiation", U. S. Environmental Protection Agency, Research Triangle Park. NC27711, Document EPA-600/8-83-026F
- [3] Dennis W. Blick, Eleanor R. Adair, William D. Hurt, Clifford J. Sherry, Thomas J. Walters, James, and H. Merritt, "Thresholds of microwave-evoked warmth sensations in human skin.", Bioelectromagnetics., Vol.18, pp.403-409, 1997.
- [4] Pere J. Riu, Kenneth R. Foster, Dennis W. Blick, and Eleanor R. Adair, "A Thermal Model for Human Thresholds of Microwave-Evoked Warmth Sensations.", Bioelectromagnetics., Vol.18, pp.578-583, 1997.

## Session 7: In Vitro Elf I

*Chairs: Mats-Olof Mattsson and Myrtill Simko*  
11:30 - 12:30 pm, Theatre M

7-1

**STATIC MAGNETIC FIELD EFFECTS ON PRIMARY CORTICAL NEURON CELLS. IN VITRO STUDY ON CELL STRESS, AND DIFFERENTIATION RESPONSES.** A. Prina-Mello<sup>1</sup>, E. Farrell<sup>2</sup>, P. J. Prendergast<sup>2</sup>, V. Campbell<sup>2</sup>, J. MD Coey<sup>1</sup>. <sup>1</sup>SFI Trinity Nanoscience Laboratory, Licoln Gate Place, Trinity College Dublin, Dublin, Ireland, <sup>2</sup>Centre for Bioengineering, Dept of Mechanical Engineering, Parsons Building, Trinity College Dublin, Dublin, Ireland.

The use of high uniform magnetic field intensity, such as that used in magnetic resonance imaging, is thought to exert little influence on cellular processes such as proliferation and differentiation, although the putative association between magnetic field and cancer onset [Koifman, 1993, Heende and Boteler, 1994] or neurodegenerative disease [Ahlbom, 2001] requires further investigation. Magnetic field has proven therapeutic value for bone disorders, such as bone fractures [Basset et al., 1982]. Also, magnetic field has been reported to induce apoptosis in human leukemic cells [Hisamitsu et al., 1997], and suppression of bacterial growth [Liu Y., 2005], suggesting several potential medical applications for magnetic field.

**OBJECTIVE:** In this work, we report on the modifications of the intracellular signalling cascades in rat cortical neurons cultured for one hour in magnetic fields of up to 5 tesla (T). The influence of magnetic field on activation of c-jun N terminal kinase (JNK), a stress-activated protein kinase involved in cell death, and extracellular-regulated protein kinase (ERK), and pro-survival enzyme, was assessed.

**METHODS:** Primary cortical neurons were prepared from 1-day old Wistar rats and cultured in neurobasal medium at 37°C / 5%CO<sub>2</sub> for up to 14 days before exposure to magnetic field. The cultured cortical neurons were exposed to static magnetic field strengt, (0.1, 0.5, 0.75, 1, 2, 5 T), for one hour at 37°C in CO<sub>2</sub>-independent culture medium. Cells were then fixed in 4% paraformaldehyde, permeabilised and washed with Tris-buffered saline prior to incubation overnight with the anti-phospho-specific JNK antibody or a polyclonal anti-phospho-specific ERK antibody. Immunoreactivity was detected using a horse-radish peroxidase secondary antibody and stable chromogen, diaminobenzamide. Cells were then viewed with a light microscope under x40 magnification for quantitative analysis. Intracellular Ca<sup>2+</sup> concentration in a dissociated neuronal cell preparation was measured using the Ca<sup>2+</sup>-sensitive indicator, Fura-2, in conjunction with spectrophotometric analysis. Experimental data was collected for each static magnetic field strength in terms of p-ERK and p-JNK responses over a normalised number of cells per slide ( $n_{\text{cell}}=400$ ). Ten series of neurons ( $n_{\text{batch}}=10$ ) were analysed and counted by independent observers. A following statistical analysis gave the mean and standard error of the mean, and Student's t-test was used to establish the significance of the data obtained.

### RESULTS:

The results demonstrate the maximal activation of ERK at 0.75 T (~10 %) (Fig 1) [Prina-Mello et al., 2004]. This ERK activation is similar to that activated by hormones and other agents associated with cell differentiation and proliferation (e.g., cAMP, cGMP, diacylglycerol, and Ca<sup>2+</sup>) [Cobb et al., 1995]. Since ERK is involved in cellular differentiation these results indicate a magnetic induction of the signalling

cascade events associated with cell differentiation (Fig. 2). In contrast, JNK was activated at the higher magnetic strength of 5T (Fig. 3), suggesting a cellular stress response similar to that induced by environmental stresses (e.g., radiation), pro-inflammatory cytokines (e.g., tumour necrosis factor- $\alpha$ ) and biosynthetic inhibitors [Chen et al., 2002].

Figure 4 demonstrates that static magnetic field (0.75T) increases resting intracellular  $\text{Ca}^{2+}$  concentration which may mediate a  $\text{Ca}^{2+}$ -dependent activation of ERK. The source of this increase in intracellular  $\text{Ca}^{2+}$  concentration was not determined in this study, but may involve the activation of voltage-dependent  $\text{Ca}^{2+}$  channels in the plasma membrane, since our previous data has demonstrated a microscale magnetohydrodynamic effect at a porous-membrane interface. Alternatively, the increase in  $\text{Ca}^{2+}$  concentration may arise from the release of  $\text{Ca}^{2+}$  from intracellular stores.

**CONCLUSIONS:** The responses of the JNK/ERK biochemical signalling pathways in primary cortical neurons were differentially modified by strong static magnetic field of order 1 tesla. This work is the first experimental evidence for any static magnetic field on intracellular signalling.

#### ACKNOWLEDGEMENTS

This study was supported by the Programme for Research in Third Level Institutions (PRTL) as part of the Trinity Centre for Bioengineering program and by Science Foundation Ireland as part of the CINSE program.

#### References:

- Ahlbom A. 2001. *Bioelectromag. Suppl.* 5:S132-S143.
- Basset CA, Mitchell SN, Gaston SR. 1982. *JAMA* 247(5):623-628.
- Chen, W., White, M.A., and Cobb, M.H. 2002. *J. Biol. Chem.* 277:49105-49110.
- Cobb, M.H., Goldsmith, E.J. 1995. *J. Biol. Chem.* 270:14843-14846.
- Heende WR, Boteler JC. 1994. *Health Phys.* 66:127-136.
- Hisamitsu T, Narita K, Kasahara T, et al. 1997. *Jpn. J. Physiol.* 47:307,V310.
- Koifman S. 1993. *Med. Hypothesis* 41:23-27.
- Liu Y., et al. 2005 *Chem. Commun.* (Published online).
- Prina-Mello A., Farrell E., Prendergast P.J., Campbell V., Coey J.M.D. 2005. *Physica Scripta* 71:1-3.

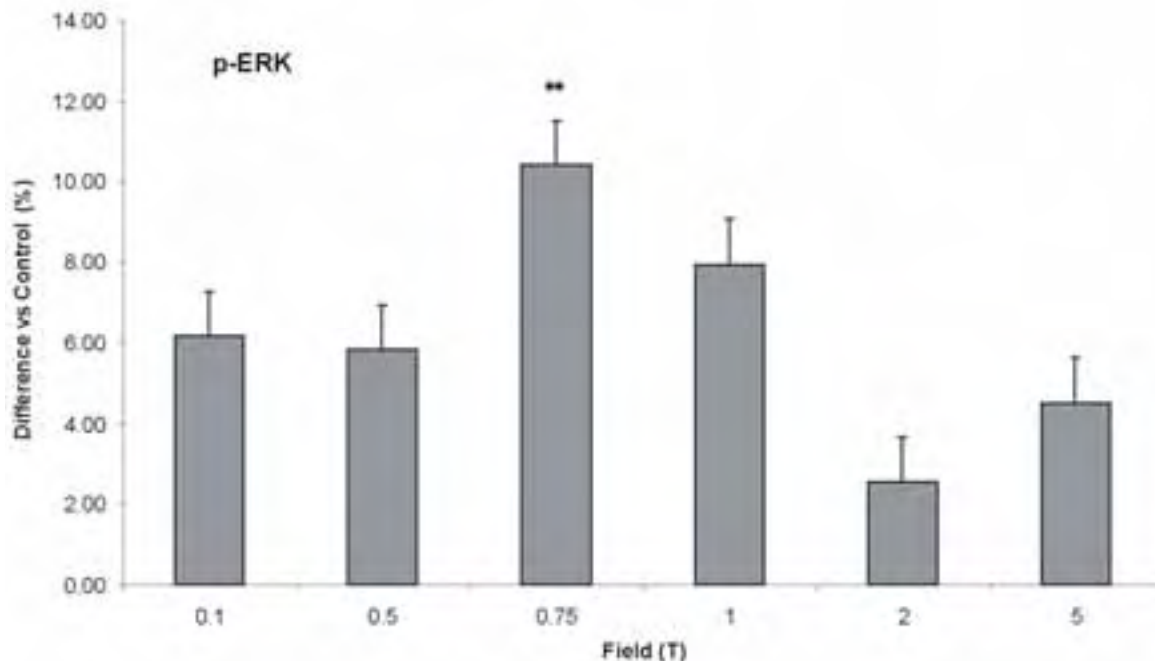


Figure 1. Change of positive activation of p-ERK in different magnetic fields (calculated over control/sham samples). Each histogram is based on 10 runs, each run is based on a standard sample size of 400 cells. Results are expressed as mean  $\pm$  SEM (\*\*  $p < 0.01$ , Student's t-test).

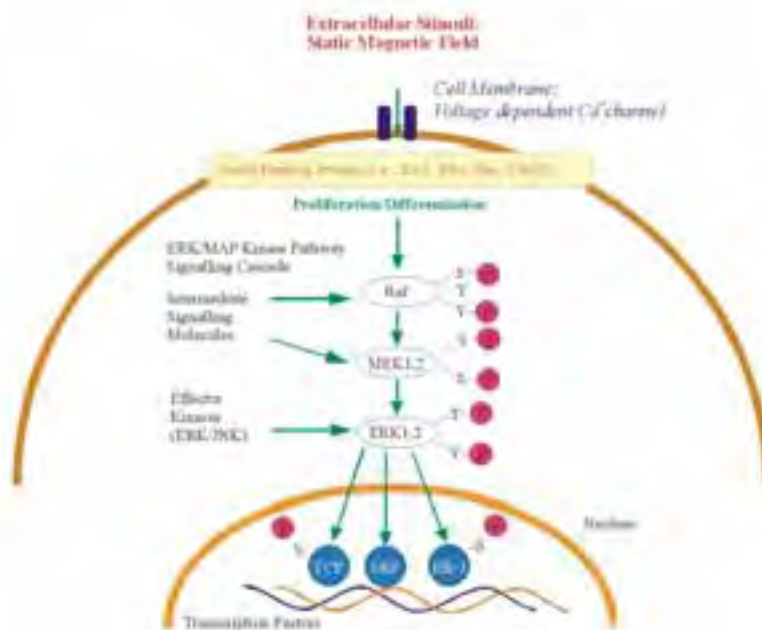


Figure 2. Extracellular regulated kinase pathway (ERK) triggered by static magnetic field as extracellular stimuli. This signalling cascade pathway is associated with cell proliferation and differentiation.

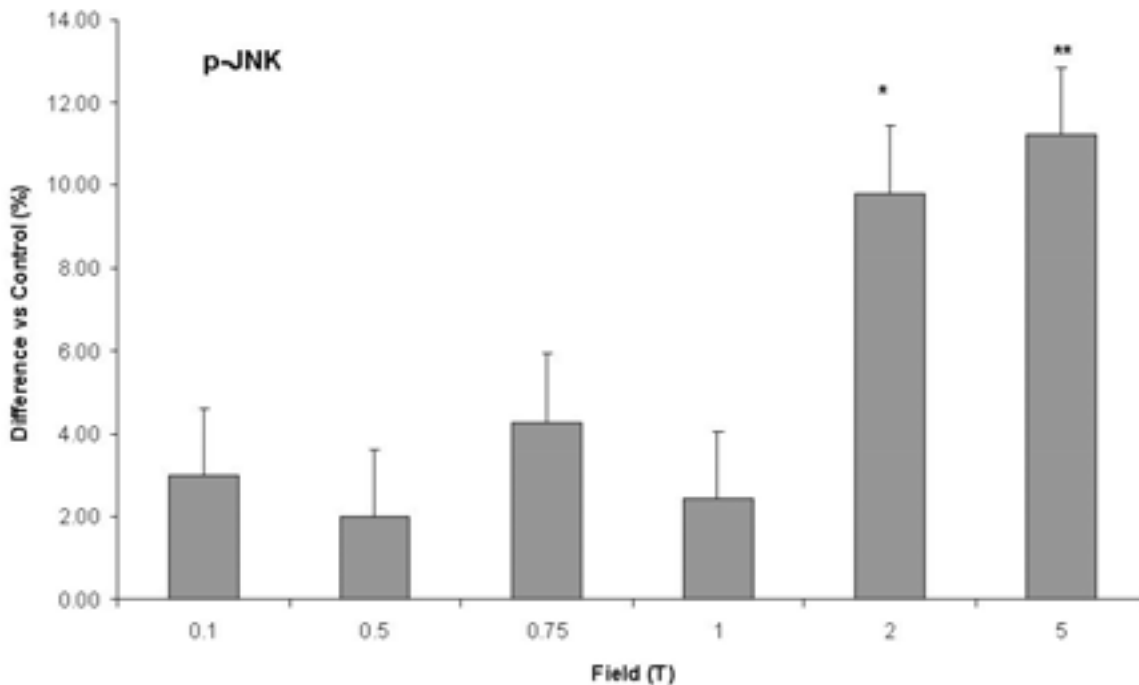


Figure 3. Change of positive activation of p-JNK in different magnetic fields (calculated over control/sham samples). Each histogram is based on 10 runs, each run is based on a standard sample size of 400 cells. Results are expressed as mean  $\pm$  SEM (\*  $p < 0.05$ , \*\*  $p < 0.01$ , Student's t-test).

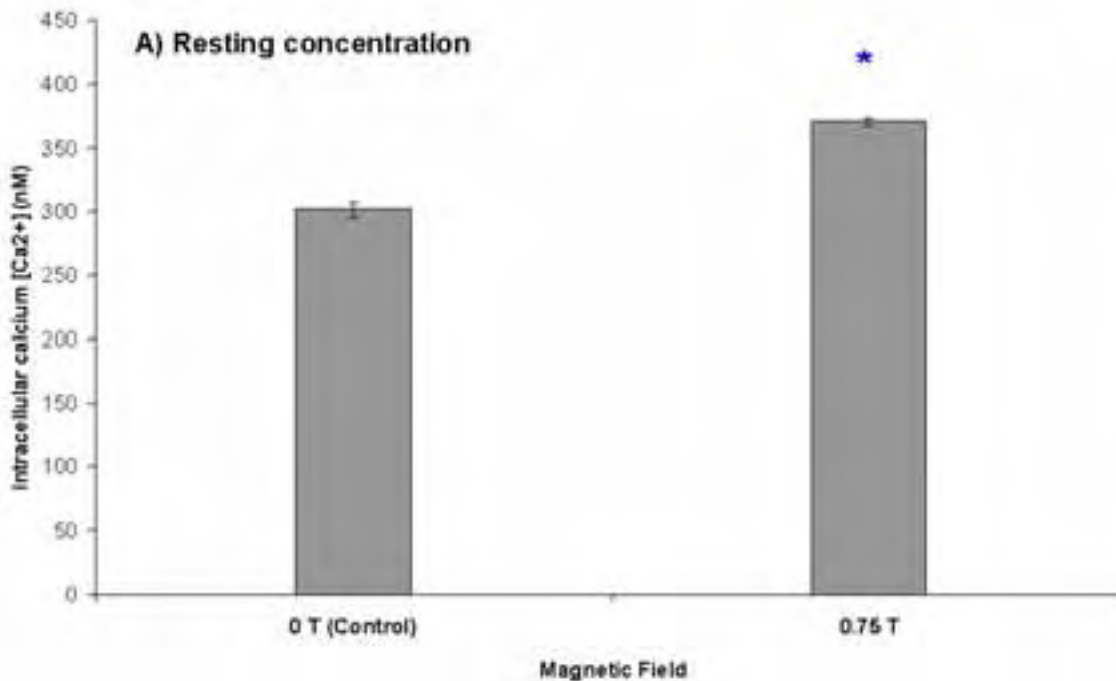


Figure 4. Resting intracellular calcium concentration ( $[Ca^{2+}]_i$ ) in control cells (sham sample) and cells exposed to magnetic field (0.75 T). Averages are of 10 independent experiments. Results are expressed as mean  $\pm$  SEM (\*  $p < 0.05$ , Student's t-test).

**MAGNETIC CONTROL OF NEURONS AND SCHWANN CELL ALIGNMENT AND GROWTH FOR APPLICATIONS TO NERVE REGENERATION.** S. Ueno, Y. Eguchi. Dept of Biomedical Engineering, Graduate School of Medicine, Univ of Tokyo, Japan.

**Objectives:** Most of living cells orient in the direction either in parallel or perpendicular to external magnetic fields when the cells are exposed to strong magnetic fields during cell division and proliferation. This study focused on magnetic control of living cell alignment and growth based on the phenomenon of magnetic orientation. The mixtures of collagen and living cells such as Schwann cells and dorsal root ganglia (DRGs) were exposed to 8 Tesla (T) static magnetic fields, and the axon elongation was observed. We also investigated the role of cytoskeletons such as stress fibers on magnetic orientation of Schwann cells to clarify the mechanism of magnetic orientation of adherent cells.

**Methods:** We used a horizontal-type superconducting magnet (bore: diameter=100mm, length=700mm, temperature=37 degrees Celsius), which produced 8 T at its center. Schwann cells were obtained from the dissected sciatic nerves of 2-day-old and cultured in Dulbecco's modified Eagle's medium (DMEM) containing 10% fetal bovine serum (FBS) and 1% antibiotics. Schwann cells were seeded in culture flask and exposed to 2-8 T magnetic field for 60 h. To investigate the role of cytoskeletons such as stress fibers on magnetic cell orientation, Y-27632, an inhibitor of ROCK/Rho associated kinase, was added to inhibit stress fibers before magnetic field exposure.

DRGs were obtained from 10-day-old chick embryos and cultured in Dulbecco's modified Eagle's medium (DMEM) containing 10% fetal bovine serum (FBS) and 1% antibiotics. DRGs and Schwann cells were cultured on Type-1 collagen gel after with or without magnetic field exposures for 2 h, and axonal elongation and orientation of Schwann cells were observed microscopically.

**Results and Discussion:** Schwann cells oriented parallel to the magnetic field after 60 h of more than 4-T magnetic field exposure. Schwann cell orientation was not observed by inhibit of stress fibers using Y-27632. These results indicate that actin fibers are needed to allow response to magnetic orientation of Schwann cells.

Schwann cells oriented in the direction parallel to the collagen fibers in the mixture of Schwann cells and collagen after 2 h of magnetic field exposure. In the culturing of the DRGs on collagen gel after 2 h of 8 T magnetic field, axons elongated parallel to the aligned collagen fibers. These results indicate that magnetically aligned collagen provided a scaffold for neurons and Schwann cells on which to grow and it directs the axon growth as a contact guidance.

**Conclusion:** Stress fiber formations are needed to respond to magnetic orientation of Schwann cells during strong magnetic field exposures, hypothesizing that the anisotropic diamagnetic susceptibility of cytoskeletons such as stress fibers is affected by magnetic torque, which gradually contributes to magnetic orientation of Schwann cells during cell division and proliferation. This observation provides a new aspect of the effect of static magnetic field on living cells. Magnetically aligned collagen provides a scaffold for neurons and Schwann cells on which to grow and it directs the axon growth as a contact guidance. Magnetically aligned collagen is useful in techniques in nerve regeneration in tissue engineering and regenerative medicine.

**THE EFFECT OF 120 HERTZ ELECTROMAGNETIC FIELDS ON LIGHT-DEPENDENT HYDROGEN PEROXIDE PRODUCTION OF JURKAT T CELLS AND T CELL MEMBRANES.** G. Nindl<sup>1</sup>, E. F. Hughes<sup>1</sup>, L. R. Waite<sup>2</sup>, W. X. Balcavage<sup>1</sup>. <sup>1</sup>Center for Medical Education, Indiana Univ School of Medicine, Terre Haute, Indiana, USA, <sup>2</sup>Applied Biology and Biomedical Engineering, Rose-Hulman Institute of Technology, Terre Haute, IN, USA.

**INTRODUCTION:** Our laboratory is interested in applying electromagnetic fields (EMFs) to regulate the activity of inflammatory T cells for human therapeutic needs. In earlier studies we showed that, *in vivo*, EMFs limit inflammation by down-regulating inflammatory T lymphocytes in a rat tendinitis model. Here we report a biological mechanism of action for our earlier *in vivo* studies by showing that in cultured T lymphocytes EMFs enhance interleukin-2 production and ultimately T cell apoptosis. These results suggest that in our system EMFs act by augmenting the normal activity of the T cell receptor (TCR), either directly at the TCR, and/or in signal transduction pathways downstream from the receptor. Our working hypothesis is that EMFs induce the same functional anti-inflammatory effects in T lymphocytes as chemokines, but in this case by regulating the lifetime and thus the concentration of reactive oxygen species. Hydrogen peroxide (H<sub>2</sub>O<sub>2</sub>) is one reactive oxygen species which mimics other TCR ligands by activating T cell signaling, leading to interleukin-2 production.

**OBJECTIVE:** The objective of this study is to investigate if EMFs interfere with T cells by changing their H<sub>2</sub>O<sub>2</sub> metabolism.

**METHODS:** The human T cell line Jurkat E6.1 (ATCC) was cultured in RPMI 1640 plus 10% FBS, 50 U/ml penicillin, 50 µg/ml streptomycin and 0.29 mg/ml L-glutamine, at 37 °C in a humidified 5% CO<sub>2</sub>/95% air atmosphere. Plasma membranes (PM) were purified from 10<sup>9</sup> Jurkat cells using a phase separation protocol. Protein concentration was determined using Coomassie Brilliant Blue G-250 (Pierce Inc.). Cells and PM were pre-treated with 1 mM NaN<sub>3</sub> for 5-10 minutes to inhibit catalase activity. H<sub>2</sub>O<sub>2</sub> was from Sigma (H-1005). For H<sub>2</sub>O<sub>2</sub> dismutation, 2.5 U of catalase (Sigma C-9322) were added per 50 µl of sample. H<sub>2</sub>O<sub>2</sub> was assayed electrochemically using our miniaturized H<sub>2</sub>O<sub>2</sub> electrode (Sathe et al., Biomed. Sci. Instrum., vol. 41, 2005), and these results were verified photometrically using the H<sub>2</sub>O<sub>2</sub> indicator Amplex Red. To study photochemical H<sub>2</sub>O<sub>2</sub> production in T cells and PM, we built a photochemical microreactor, in which multiple samples can be exposed to a uniform light flux (Nindl et al., Biomed. Sci. Instrum., vol. 41, 2005). Rat IgG (9 µM) was used as a positive control and produced H<sub>2</sub>O<sub>2</sub> in a light-dependent way. Sinusoidal 120 Hz EMFs were produced by a 16 gauge, enameled copper-wire coil (625 windings, 6" interior diameter) powered by Telulex Inc.(model SG-100/A) signal generator, coupled to a Crown amplifier (model Macro Tech 5000 VZ). Sham controls in a matched photoreactor were simultaneously exposed to the static geofield only (155 mG horizontal component).

**RESULTS:** With our real-time, electrochemical, H<sub>2</sub>O<sub>2</sub> monitor we found that 10<sup>7</sup> Jurkat cells pretreated with NaN<sub>3</sub> and suspended in 1 ml of phosphate buffered saline (PBS) produce about 60 nmol H<sub>2</sub>O<sub>2</sub>/min. when exposed to UVB light (1.5 W/cm<sup>2</sup>) at 37 °C. Electrode results were verified by Amplex Red analysis. In initial studies on the TCR as a source of H<sub>2</sub>O<sub>2</sub> we studied Jurkat PM employing our photochemical microreactor. Fifty µl of PM (1 mg/ml protein) were exposed to UVB light for a total of 8 hours producing an average of 46 ± 15 nmol H<sub>2</sub>O<sub>2</sub>/min. (n = 90). No H<sub>2</sub>O<sub>2</sub> was detected after catalase addition or in samples shielded from UVB. Likewise, UVB exposed controls (PBS or NaN<sub>3</sub> in PBS) did not produce H<sub>2</sub>O<sub>2</sub>. PM samples that were exposed to combined UVB and EMFs produced an average 33% less H<sub>2</sub>O<sub>2</sub> than identical non EMF exposed samples (n= 20, p < 0.05, Student's t-test). EMF exposure did not affect any of the controls or rat IgG samples which produced about 30 nM H<sub>2</sub>O<sub>2</sub>/min/mM protein after light activation.

**CONCLUSION:** Our results support the novel idea that activated T cells produce H<sub>2</sub>O<sub>2</sub> in a membrane-associated event, and that EMFs can regulate these events. The EMF effect is specific to T cells since the production of H<sub>2</sub>O<sub>2</sub> by activated antibodies was not altered by EMFs. These data provide important

insights into the role of H<sub>2</sub>O<sub>2</sub> in inflammatory T cells, to the mechanism of EMF interaction with T cells, and they have important therapeutic implications for inflammatory diseases.

7-4

**TRANSIENT CHANGES IN AMPLITUDE AND PHASE OF PEROXIDASE-OXIDASE OSCILLATIONS DURING STIMULATION WITH PULSED LIGHT.** K. Commerford<sup>1</sup>, F. S. Prato<sup>1,2</sup>, J. JL Carson<sup>1,2</sup>. <sup>1</sup>Lawson Health Research Institute, St. Joseph's Health Care, London, Ontario, Canada, <sup>2</sup>Dept of Medical Biophysics, Univ of Western Ontario, London, Ontario, Canada.

Background: The peroxidase-oxidase (PO) oscillator has a history of intense study by groups throughout the world and is considered the best characterized biochemical oscillator [1]. The PO reaction generates dynamical behaviour that is qualitatively similar to oscillatory processes found in biological systems [1]. Therefore, the PO oscillator is an excellent laboratory model for hypothesis generating studies on the interaction of biological systems with external stimuli. This theme has been investigated by several groups who have observed the PO oscillator response to modulation of the rate of reactant inflow [2], exposure to a magnetic field [3], or illumination [4]. The studies revealed that a periodically oscillating reaction suffers a small decrease in oscillation amplitude during exposure to a homogenous magnetic field and a large decrease in oscillation amplitude during illumination with red light. Slow modulation of the rate of reactant delivery was shown to affect the oscillation dynamics of the PO reaction. What is unknown is how the oscillator responds to periodic changes in magnetic field or red light.

Objective: The objective of the present study was to measure the effect of periodically modulated red light on the amplitude of PO oscillations. The stimulus was modulated at a frequency equal to the natural frequency of the PO oscillator and the phase relationship between the PO oscillator and the modulated stimulus waveform was controlled.

Method: Experiments were performed in a stirred (1270 RPM) quartz cuvette temperature-controlled to 28.0±0.1°C as described previously [4]. Briefly, three syringes were used to pump reactants into the reactor at a constant flow rate of 33.3 µl/min on each syringe. Syringe #1 contained 0.1 µM methylene blue, 100 µM DTPA, 20 µM 2,4-dichlorophenol and 0.1M phosphoric acid at a final pH of 6.30. Syringe # 2 contained a solution identical to #1, but supplemented with 10 µM horseradish peroxidase and 0.4 U/ml of glucose-6-phosphate dehydrogenase. Syringe #3 was similar to Syringe #1, except for the addition of 1.5 mM NAD<sup>+</sup> and 55 mM glucose-6-phosphate. The final volume of reactants in the cuvette was held steady at 2.2 ml by continuous removal by an overflow tube and peristaltic pump arrangement. The headspace above the reactants was gassed with 1% O<sub>2</sub>:N<sub>2</sub> at a flow rate of 50 ml/min. PO oscillations were recorded with an O<sub>2</sub>-electrode and absorbance spectroscopy in the spectral region of 390 and 440 nm. With this system we were able to observe stable oscillations for several hours as periodic variations in the concentration of dissolved oxygen, NADH, horseradish peroxidase and its oxidized forms such as Per<sup>6+</sup>. The reactor was illuminated with light from a current-controlled LED (656 nm, FWHM = 20 nm). Light was diffused evenly before reaching the reactor. The average irradiance was 450 µW/cm<sup>2</sup> as determined with a calibrated detector and meter. During each experiment (N ≥ 5 at each phase condition), illumination was steady (450 µW/cm<sup>2</sup>), then modulated ± 430 µW/cm<sup>2</sup> in intensity about the 450 µW/cm<sup>2</sup>. Experiments were terminated after a second period of steady illumination at 450 µW/cm<sup>2</sup>.

Results: Fig. 1 shows representative responses of a periodic PO oscillator during two individual experiments with steady and modulated red light. Oscillations in dissolved oxygen and Per<sup>6+</sup> were observed in the presence of both types of illumination. When the light was modulated at a frequency equal to the natural frequency of the oscillator, the amplitude of the dissolved oxygen decreased

transiently when the onset of exposure (or phase difference) was  $68^\circ$  (Fig. 1A) and increased when the phase difference was  $248^\circ$  (Fig. 1B). The phase was calculated as the difference between the point in time at which the last peak in  $\text{Per}^{6+}$  was observed and the time point at which the first upward lobe of the modulation waveform had occurred. The phase was converted to degrees by dividing this time difference by the average time interval between consecutive peaks in the  $\text{Per}^{6+}$  trace and multiplying by  $360^\circ$ . When the phase of exposure was  $158^\circ$  little to no response was observed (data not shown). The response to modulated light was transient lasting in most experiments only 3-5 oscillations. A transient shift in the phase of the  $\text{Per}^{6+}$  and dissolved oxygen waveforms occurred during the first four periods of light modulation followed by a stabilization of the phase difference thereafter.

**Discussion:** The results demonstrate that the PO reaction oscillates in the presence of either steady or modulated red light. The modulation of light at the resonance frequency did not lead to persistent changes in oscillator amplitude, but did cause rapid transients in both amplitude and phase that depended on the onset of modulation in relation to the intrinsic timing of the PO oscillations. Following each transient the phase difference between the oscillations and the modulated light stimulus remained constant. Therefore, modulated stimuli identical in every respect except for the timing of onset can elicit different (even opposite) responses from a biochemical oscillator. This finding could have implications for the design and interpretation of experiments with biological systems and modulated external stimuli.

**Acknowledgments:** This work was supported by the Lawson Health Research Institute Internal Research Fund.

#### References:

- [1]. Scheeline, A., D.L. Olson, E.P. Williksen, et al., Chemical Reviews (Washington, D. C.), 97, 739-756, (1997).
- [2]. Foerster, A., T. Hauck, and F.W. Schneider, Journal of Physical Chemistry, 98, 184-9, (1994).
- [3]. Moller, A.C. and L.F. Olsen, Journal of the American Chemical Society, 121, 6351-6354, (1999).
- [4]. Carson, J.J.L. and J. Walleczek, Journal of Physical Chemistry B, 107, 8637-8642, (2003).

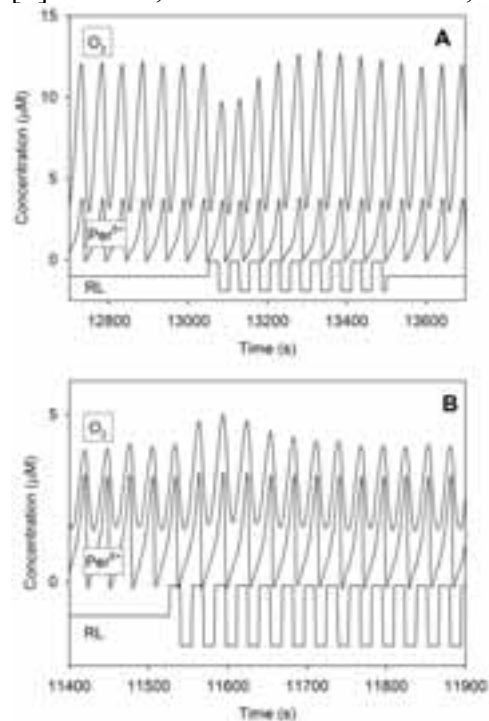


**Figure 1.** The dependence of periodic peroxidase-oxidase oscillations on steady and modulated red light (RL) from an LED at a time-averaged irradiance of  $450 \mu\text{W}/\text{cm}^2$ . In each plot, the bottom trace represents the illumination waveform (see methods, not to scale), the top trace represents dissolved oxygen ( $\text{O}_2$ , left scale) and the middle trace represents  $\text{Per}^{6+}$  (left scale), an oxidized form of horseradish

peroxidase. A, modulation began 68° after the first Per<sup>6+</sup> peak beyond 13000s (see Results). B, onset of modulation 248° after the first peak in Per<sup>6+</sup> beyond 11500s.

### Session 8: Dosimetry III

*Chairs: Niels Kuster and Christer Törnevik*

**2:00 - 3:30 pm, Theatre L**

8-1

**DOSIMETRY FOR RAT EXPOSURES IN A TEM CELL FOR 915 MHZ GSM MODULATED SIGNAL.** S. J. Allen<sup>1</sup>, K. S. Mylacraine<sup>1</sup>, J. McQuade<sup>2</sup>, P. A. Mason<sup>2</sup>. <sup>1</sup>General Dynamics, Advanced Information Engineering Services, Brooks City-Base TX, USA, <sup>2</sup>Air Force Research Laboratory, Human Effectiveness Directorate, Directed Energy Bioeffects Division, Brooks City-Base, TX, USA.

**OBJECTIVE:** Salford et al. (First World Congress for Electricity and Magnetism in Biology and Medicine, 1992), reported that very low-level microwave effects can affect the blood brain barrier (BBB). These investigators subsequently published several reports on low-level exposure effects on albumin penetration of the BBB (Persson et al., 1992; Salford et al., 1992b; Salford et al., 1993a; Salford et al., 1993b; Salford et al., 1994). Because of these concerns we have entered into an international collaborative research program to validate (or not) the results obtained by the Swedish research group. The objective of this portion of the effort is to analyze the expected specific absorption rate (SAR) by performing finite-difference time-domain (FDTD) analysis and to verify these results with empirical results. Using these results the exposure parameters are defined to determine 2.0, 0.2, 0.02, and 0.002 W/kg exposures. Whole body SAR is measured for each of the exposed animals.

**METHODS:** A TEM cell with the same dimensions as used by Salford et al. was used to expose rats (250 - 300 gm) to a GSM modulated signal. A plastic bottle with 300 gm of saline was used to measure the SAR by both thermometry and the differential power methods to assure accuracy of the differential power technique. A rat was euthanized and whole body SAR measured over 24 hours by differential power techniques to determine if any significant changes occurred due to degradation of tissue or temperature change in the tissue. FDTD calculations for the whole body and the brain were made for eight positions of the rat in the TEM cell. Whole body SAR and average SAR in the brain were determined using differential power and thermometry techniques for the same eight points as calculated by FDTD. These data were averaged and used to determine TEM input power required to expose rats to 2.0, 0.2, 0.02, and 0.002 W/kg whole body SAR. Input power and SAR were measured at one-second intervals throughout each 2-hour (7200 sec) rat exposure. The mean value of the input power and the whole body SAR as well as the % coefficient of variation was calculated for each exposure group.

**RESULTS:** Whole body SAR in the TEM cell as determined by thermometry was 1.38 W/kg/W and for the differential power technique 1.27 W/kg/W or a 9% difference. This is considered to be within the experimental limits. All subsequent whole body SARs were determined by the differential power method. Whole body SAR was measured in a rat (262 gm) within a few minutes of euthanization and continued at regular intervals for 24 hours. SAR remained within +/- 1% of the mean value over the entire 24-hour period. FDTD calculations predicted an average whole body SAR of 1.62 W/kg/W with a ratio of the maximum to minimum SAR of 3.1 over the eight positions. The average of the measured values over the same eight positions was 1.63 W/kg/W with a maximum to minimum value of 1.29. The

average SARs were within 1% with the empirical uniformity being considerably better than the FDTD prediction. Four holes were drilled in the skull of a euthanized rat and four Vitek probes were inserted to the base of the brain cavity. After approximately six hours the brain temperature reached equilibrium and either 3 or 6 W TEM input power, one-minute exposures were performed. Temperature change was converted to SAR by the equation  $SAR = 58.6 \text{ W/kg/}^\circ\text{C/min}$ . The same eight positions were investigated for both lower brain and mid-brain SAR and the results compared with FDTD predictions. FDTD predicted 2.8 W/kg/W average brain SAR with a maximum to minimum SAR ratio of 14.6. The empirical value was 1.29 W/kg/W average brain SAR with a maximum to minimum SAR ratio of 2.6. The results of three whole body SAR measurements were averaged to obtain the conversion factor of 1.63 W/kg/W and this value was used to determine the proper input power to achieve 2.0, 0.2, 0.02, and 0.002 W/kg exposures. Appropriate input powers of 1.23, 0.123, 0.0123, and 0.00123 W were determined. For the experimental rat exposures, the appropriate TEM input power was maintained and this value and the SAR for each exposure was measured at one-second intervals over the 7200-sec exposure. The summary of all exposures (24 exposures for each condition) is shown in the attached figure.

**CONCLUSIONS:** The exposure of rats in a small TEM cell violates the principal of proper TEM cell usage which requires that only the center third of the chamber be occupied. It would appear that the body of the rat loads the TEM cell preventing it from developing empty chamber fields. As a result, as the rat moves in the cell it experiences more uniform exposures than expected or predicted by FDTD particularly for the brain SAR. All SAR measurements were repeatable for rat sizes ranging from 250 to 300 gm. The average of 24 (1.23 W) exposures for the blood brain barrier experiment were within 0.1% of the target value with the average SAR with whole body SAR within 0.5%. Similarly the 0.123 and 0.0123 W exposures are within 0.1 % of the target with whole body SAR within 4%. The 0.00123 W exposures were more difficult to control even at this low power level; average exposure was within 2% and SAR within 6% of the target value. The dosimetry for this experiment provides the basis for a well-controlled experiment.

### Average of All Rat Exposure Data

Target	1.23	0.123	0.0123	0.00123	2	0.2	0.02	0.002
Mean	1.228	0.1230	0.01228	0.001256	1.989	0.1929	0.01926	0.002114
STDEV	0.005	0.0004	0.00005	0.000190	0.105	0.0128	0.00153	0.001355
COV	0.42	0.31	0.42	15.09	5.29	6.63	7.94	64.07
Exp./Target	0.999	1.000	0.999	1.021	0.995	0.964	0.963	1.057

8-2

**FDTD CALCULATION OF SAR LEVELS FOR TYPICAL 3G WCDMA BASE STATION ANTENNAS AT 2140 MHZ.** L. Hamberg<sup>1</sup>, E. Nordström<sup>2</sup>, C. Törnevik<sup>1</sup>. <sup>1</sup>Ericsson Research, Ericsson AB, Stockholm, Sweden, <sup>2</sup>Linköping Institute of Technology, Linköping, Sweden.

**INTRODUCTION:** The International Commission on Non-Ionizing Radiation Protection (ICNIRP) provides basic restrictions for radio frequency (RF) exposure in terms of the Specific Absorption Rate (SAR, W/kg), which are relevant for base stations in mobile telephony networks. Due to the complexity of SAR measurements and calculations also reference values in terms of electric and magnetic field strength are provided and generally RF exposure compliance distances for macro cell base station antennas are determined by assessments of the electromagnetic field strengths. Calculation of SAR with a detailed whole-body human model requires good computational resources and only in the past few years it has been possible to perform such calculations with an ordinary PC workstation. Previous work in this area has in general been focused on the feasibility of different calculation methods or investigated the exposure at lower frequencies than those investigated in this work.

**OBJECTIVE:** The objective of this work was to determine the RF exposure compliance distances for typical 3G WCDMA (Wideband Code Division Multiple Access) base station antennas by calculations of whole-body averaged and localized SAR in an anatomically realistic whole-body model.

**METHODS:** Numerical calculations at 2140 MHz were performed with the software SEMCAD 1.8 from SPEAG, which is based on the finite difference time domain (FDTD) method. Calculations both with and without a human model were performed in order to assess whole-body averaged and localized (10 g) SAR as well as free space electric and magnetic field strength levels. The human model, based on the male data set from the Visual Human Project®, comprised 113 different tissues, which were each assigned dielectric properties according to those suggested by Gabriel et al [1]. A grid step of 3 mm was used in the human model, except for the legs and the back side of the torso where the grid step was 10 mm and where the exposure levels at this setup were significantly lower than in other parts of the body. The weight of the model was 98 kg and the length was 1.86 m. Models of four different base station antennas with a directivity ranging from 9.8 dBi to 18.4 dBi were investigated. The antennas were collinear array antennas with a horizontal half power beam width of 65 degrees. They were composed of up to eight 45 degrees slanted dipoles in front of a metallic back plate and the length of the antennas ranged from 0.16 m to 1.1 m. The human model was positioned facing the front of the investigated antenna and with the center of the torso aligned with the center of the antenna, see Figure 1. The separation was varied in ten steps from 0.02 m to 2 m. The calculated exposure ratio, which is the estimated exposure (SAR,  $E^2$  and  $H^2$ ) divided by the relevant ICNIRP limit, was used for comparisons of the different results. The calculations were performed on a 3 GHz PC workstation with 4 GB RAM. Each calculation required up to six hours of processing time.

**RESULTS:** All calculated results showed that the reference levels can be used to conservatively show compliance with respect to the basic restrictions, also in the near-field of the antenna including the reactive near-field. However, usage of the reference levels significantly overestimates the compliance distances for low power levels, see Figure 2. At input power levels less than 1 W and 5 W, all antennas were unconditionally in compliance with the basic restrictions for general public exposure and occupational exposure, respectively. Based on whole-body and localized SAR calculations a simplified formula to estimate the compliance distance ( $R_{cd}$ ) in the direction of the main beam was proposed. The formula is expressed as  $R_{cd}=P/C$  where P is the antenna input power in watt and C is a constant equal to 25 W/m for general public exposure and 125 W/m for occupational exposure. At a typical maximum input power of 25 W for WCDMA antennas, the SAR based compliance distance is 1 m as compared to approximately 3 m using reference levels. The formula overestimates the compliance distance for all antennas of the type used in the calculations. At distances shorter than 0.5 m from the antennas, localized (10 g) SAR was the limiting basic restriction giving the highest exposure ratio. A post-evaluation of the results showed that the calculation uncertainty was less than  $\pm 20\%$ . However, SAR results in general and whole-body averaged results in particular were affected by the relatively heavy human model used. Usage of a model with the weight of the standard man (70 kg) might increase the whole-body averaged SAR results with up to 40 % in the near-field region of small antennas.

**CONCLUSIONS:** Compliance distances for four typical 2140 MHz 3G WCDMA base station antennas have been determined by calculations of whole-body averaged and localized (10 g) SAR and comparisons with the ICNIRP limits. For antenna input powers up to 25 W the general public compliance distance for all investigated antennas were less than one meter.

References:

[1] S. Gabriel, R.W. Lau and C. Gabriel, "The dielectric properties of biological tissues: III parametric models for the dielectric spectrum of tissues", *Physics in Medicine and Biology*, vol. 41, pp. 2271-2293, 1996.

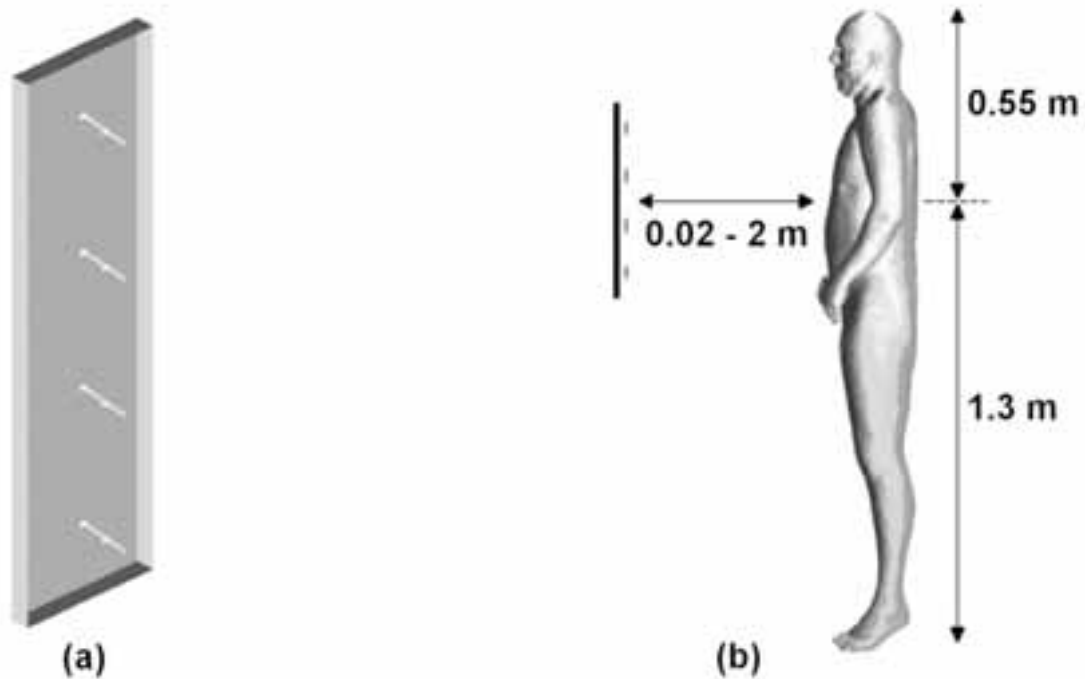


Figure 1. (a) Model of one of the antennas used in the calculations and (b) setup showing the positioning of the antenna in front of the human whole-body model.

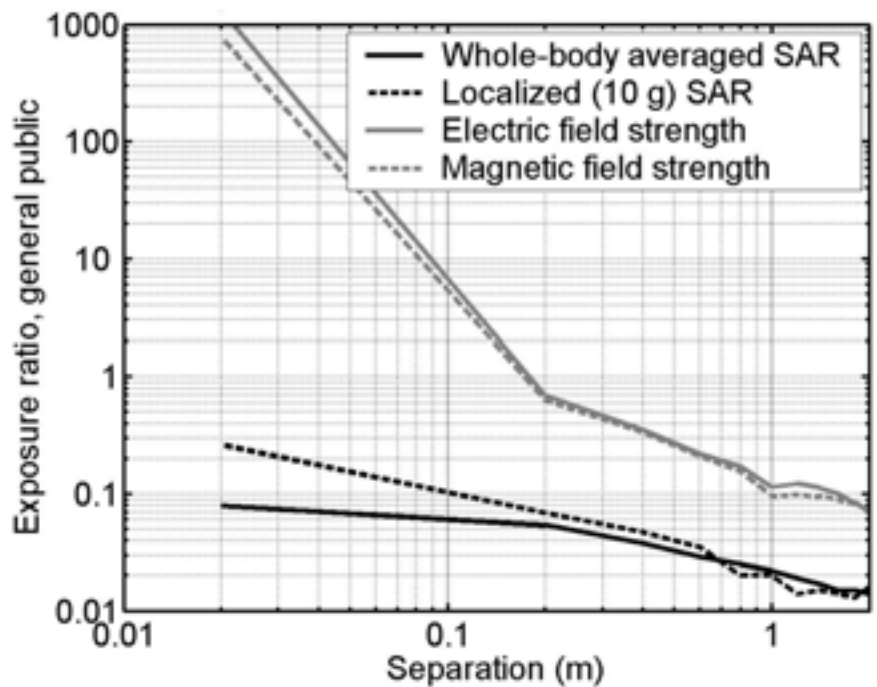


Figure 2. Exposure ratios for the 17.6 dBi antenna with 1 W antenna input power.

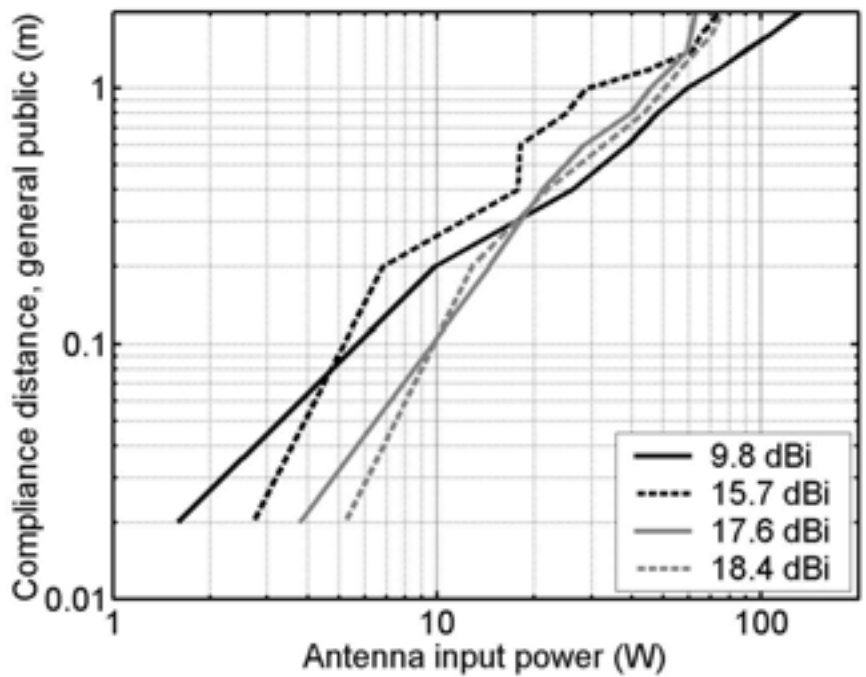


Figure 3. SAR based compliance distances for general public exposure from the four investigated antennas.

**SIMULATION OF WHOLE-BODY HUMAN EXPOSURE TO 2450 MHZ: MODEL RESULTS INCORPORATING THERMOREGULATORY FUNCTION.**

D. A. Nelson<sup>1</sup>, A. R. Curran<sup>2</sup>, E. A. Marttila<sup>2</sup>, J. M. Zirix<sup>3</sup>, P. A. Mason<sup>4</sup>, W. D. Hurt<sup>4</sup>. <sup>1</sup>Michigan Technological Univ, Houghton, MI, USA, <sup>2</sup>ThermoAnalytics, Inc., Calumet, MI, USA, <sup>3</sup>Naval Health Research Center Detachment, Brooks City-Base, TX, USA, <sup>4</sup>Air Force Research Laboratory, Directed Energy Bioeffects Division, Brooks City-Base, TX, USA.

**INTRODUCTION:** Exposure to radio frequency (RF) fields of sufficient power density can significantly increase tissue temperatures. The magnitude of temperature increase is a function of exposure time and the local specific absorption rate (SAR).

While short-term local temperature increases may be predicted by extrapolating from SAR values, long-duration exposures produce temperature increases which can be affected by the thermal properties of the exposed tissue and by physiological processes (metabolism, blood flow), environmental conditions and clothing. Sustained exposure to RF irradiation may produce thermophysiological responses, with the potential to profoundly alter the temperature response.

The use of human exposures have proven valuable in quantifying heating effects from RF exposure and the environmental and thermoregulatory impact on whole-body heating. The ability to simulate such exposures, using a whole-body heterogeneous model, allows the quantification of whole-body and local superficial heating effects, as well as prediction of deep-tissue temperature effects. The use of a model to predict tissue heating from RF exposure also makes it possible to evaluate effects of external variables and simulate exposures at power densities above those corresponding to published experiments. There are not yet any validated, whole-body models of RF heating which incorporate thermoregulatory feedback.

**OBJECTIVES:** This objectives of this work were (1) predict tissue temperatures in a seated adult human exposed to whole-body RF irradiation at a frequency of 2450 MHz, and (2) compare surface and deep-body temperatures for a 45-minute exposure with published experimental data obtained from human exposures.

**METHODS:** Simulations were performed using a seated, slightly modified version of the “Brooks Man” voxelized, whole-body heterogeneous model. An additional tissue type was added for the hypothalamus, to facilitate incorporating thermoregulatory feedback. Thermoregulatory feedback was implemented to describe vasodilatation and temperature-dependent changes in metabolic rate.

Localized SAR values were calculated using the finite-difference, time domain (FDTD) method. Temperature calculations were performed using “ThermoReg”, which is a parallelized, high resolution finite-difference code developed for this application. Tissue properties, including baseline rates for metabolism and blood flow, were determined from the literature. Whole-body exposure of an adult human to low-power RF irradiation (2450 MHz, continuous wave) was simulated at power densities of 35 mW•cm<sup>-2</sup>, 50 mW•cm<sup>-2</sup> and 70 mW•cm<sup>-2</sup> for exposure durations of up to 45 minutes, corresponding to the exposure protocol of Adair et al.

**RESULTS:** Preliminary results show temperature trends which are generally consistent with published experimental results. Core temperature, as well as surface temperatures obtained from the model, appear quite sensitive to the baseline metabolic rate.

**DISCUSSION:** Whole-body models potentially are a useful and important alternative to human exposures for determining the thermal effects from whole-body RF exposure. Validating these models requires detailed knowledge of human thermoregulation and localized metabolic rates.

**ACKNOWLEDGEMENT:** This work was supported by the Small Business Innovation Research (SBIR) Program and administered through the Office of Naval Research (ONR). The Program Officer was CDR

Stephen Ahlers of ONR and the Technical Monitor was John Ziriak of the Naval Health Research Center Detachment at Brooks City-Base.

This work was funded by the U.S. Air Force and U.S. Navy (Project Numbers: 0602236N/M04426.w6, 0601153N/M4023/60182). The views, opinions, and/or findings contained in this report are those of the authors and should not be construed as official Dept of the Air Force, Dept of the Navy, Dept of Defense, or U.S. government position, policy, or decision.

8-4

**IMPROVED NUMERICAL DOSIMETRY FOR THE WAVEGUIDE EXPOSURE CHAMBER USED FOR PROTEIN AND SPERM STUDIES AT 900 MHZ.** T. Toivo, L. Puranen, K. Jokela. STUK, Radiation and Nuclear Safety Authority, Helsinki, Finland.

## INTRODUCTION

To analyze biophysical mechanisms and replicate experiments for in vitro studies of RF bioeffects, strict control of SAR and temperature is needed (Schuderer et al, 2004; Schönborn et al. 2001). Distribution of SAR can only be computed in small cell cultures, but numerical data should always be checked with measurements at some reference point in the culture dish. New possibilities for numerical RF-dosimetry are provided by increased computation power of computers and improvements in software.

It has turned out difficult to achieve satisfactory agreement with numerical and measured SAR for the vertical waveguide exposure chamber (Toivo et al. 2001) used in protein studies of (Leszczynski et al 2002) and sperm studies of Falzone et al. (2005). In this study the problem was solved by using software (Speag SEMCAD) with non-uniform grid size, where the grid was denser (0,3 mm x 0,3 mm x 0,3 mm) in the culture medium. In the older software (Remcom XFDTD), only uniform grid (1 mm x 1 mm x 1 mm) was possible. We present results of computed SAR distribution and compare it with SAR previously measured with a thermistor probe (Vitek).

## MATERIALS AND METHODS

The exposure chamber is a waveguide resonator where two Petri dishes (diam. 55 mm) are placed above a water-cooling plate. In this set-up the electric field is parallel to the surface of the dish (k-polarization). The inner dimensions of the chamber are 248 mm x 175 mm x 420 mm (width x length x height) and the simulation grid consisted of over 24 million cells. The simulation time step was  $1.9 \times 10^{-13}$  s and 350000 time steps was counted. Simulations were carried out with flat liquid surface and curved (meniscus) surface. Sharp meniscus is problematic because it attracts electric field lines causing intense hot spot. Overview of the simulation setup and coordinate system is shown in Figure 1.

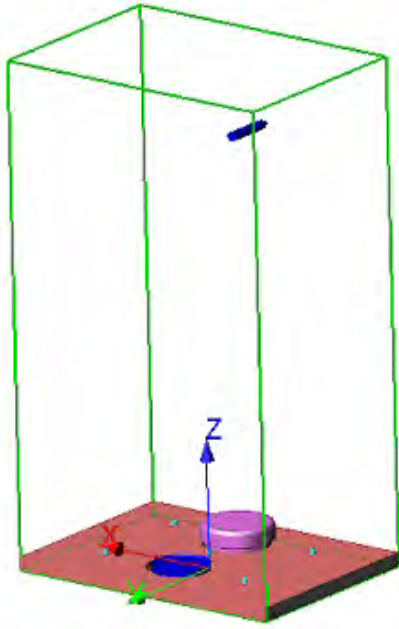


Figure 1. Simulation setup and coordinate system. The power feeding monopole is seen on the upper part and the two Petri dishes (front one removed) are above the water-cooling plate.

## RESULTS AND DISCUSSION

The distribution of computed SAR in front Petri dish is shown in Figure 2 and Table 1 presents computed data on SAR with and without the meniscus. The amount of liquid of Petri dishes (diam. 55 mm) is 5 ml.

Simulated SAR, at the bottom layer of medium, in the centre of front dish was 7.1 W/kg for 1 W input power. Corresponding measured value was 30% lower (5.0 W/kg). The values presented in this paper are scaled to 1 W input power and in the article (Leszczynski et al. 2002) the feeding power was 0.47 W, which must be taken into account when comparing the SAR values.

Vertical distribution in Figure 2 shows that SAR is quite homogeneous in the vertical direction. This is in contrast to the very non-homogeneous vertical distribution reported by Schönborn et al. (2001) for the waveguide chamber where the dishes are placed perpendicular to the E-field (E-polarization). Uniform vertical distribution enables accurate thermal measurement of SAR without great problems caused by heat diffusion in non-uniform SAR distribution.

The maximum SAR (42 W/kg) in the whole medium with the meniscus was almost two times higher than without the meniscus (25 W/kg). The maximum SAR at the lowest grid layer (0.3 mm height) was 15 W/kg and without the meniscus 17 W/kg. So the meniscus increases significantly SAR on the top level of the culture medium but not on the bottom layer. Meniscus is not problem in the present set-up in contrast to the set-up presented in Schönborn et al. (2001).

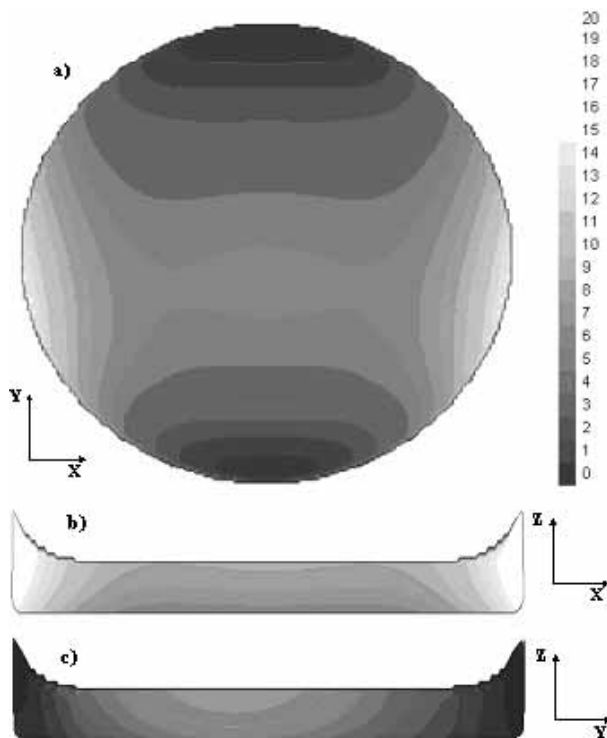


Figure 2. The SAR distribution in the front Petri dish. The distribution in the other dish is almost identical. The scale is in W/kg scaled to 1 W input power and the coordinates are same as in figure 1. a) lowest grid layer of the culture medium. b) Sideview along the longer side of chamber, maximum SAR found from the meniscus. c) Sideview along the shorter side of chamber.

## CONCLUSIONS

The simulations verified the SAR value (2.45 W/kg) measured for the exposure chamber used in protein and sperm studies.

## REFERENCES

- J. Schuderer, D. Spät, T. Samaras, W. Oesch and N. Kuster, "In Vitro Exposure Systems for RF Exposures at 900 MHz", *IEEE Trans. on Microwave Theory and Techniques*, Vol. 52, pp. 2067-2075, 2004.
- F. Schönborn, K. Pokovic, M. Burkhardt and N. Kuster, "Basis for optimization of in vitro exposure apparatus for health hazard evaluations of mobile communications", *Bioelectromagnetics*, Vol. 22, pp. 547-559, 2001.
- T. Toivo, A.-P. Sihvonen, L. Puranen and K. Keskinen, "Water cooled waveguide chambers for exposure of cells in vitro at 900 MHz", in *5th Int. Congr. Eur. Bioelectromagnetics Association*, Helsinki, Finland, 2001, pp. 62-63.
- D. Leszczynski, S. Joenväärä, J. Reivinen, R. Kuokka, "Non-thermal Activation of the hsp27p38MAPK Stress Pathway by Mobile Phone Radiation in Human Endothelial Cells: Molecular Mechanism for Cancer- and Blood-Brain Barrier-Related Effects", *Differentiation*, Vol. 70, pp. 120-129, 2002.

N. Falzone, C. Huyser, F. le R. Fourie, D. Franken and D. Leszczynski, "Pilot study: Effects of 900 MHz radiation on human sperm function", BEMS 2005, 2005.

Table 1. SAR data from the simulations (0.3 mm x 0.3 mm x 0.3 mm grid). The values are scaled to 1 W input power.

Medium	point SAR at center of dish (W/kg)	Average SAR (W/kg)	Maximum SAR (W/kg)	Volume within $\pm 3$ dB (%)
Meniscus, whole medium		7.6	42	78
Meniscus, bottom layer <sup>2)</sup>	7.1	6.8	25	83
No meniscus, whole medium		7.6	29	85
No meniscus, bottom layer <sup>2)</sup>	7.1	6.7	25	86
1) Variation of SAR within $\pm 3$ dB 2) 1 mm layer thickness				

8-5

**ON FDTD-CALCULATED WHOLE-BODY AVERAGE SAR AT RESONANCE FREQUENCY.**  
 J. Wang<sup>1</sup>, O. Fujiwara<sup>1</sup>, S. Koder<sup>1</sup>, S. Watanabe<sup>2</sup>. <sup>1</sup>Graduate School of Engineering, Nagoya Institute of Technology, Nagoya, Japan, <sup>2</sup>National Institute of Information and Communications Technology, Tokyo, Japan.

**OBJECTIVE:** It is known that the whole-body average specific absorption rate (SAR) reaches the maximum at a resonance frequency when the human height is approximately 0.4 wavelength in free space. For the safety assessment of electromagnetic radio-wave exposure, a free-space electric field or power density is being used as a reference level, which should never yield a larger whole-body average SAR than the basic limit, e.g. 0.4 W/kg for occupational exposure. The relationship between the reference level and the SAR, however, is derived from large-scaled numerical calculations, while few attentions have been paid to the accuracy analysis in conjunction with human modeling and numerical codes including their calculation domains. In this study, based on a detailed error analysis for the finite difference time domain (FDTD) numerical code, we show critical effect of perfectly matched layer (PML) on the whole-body average SAR. We then clarify to what extent the whole-body average SAR may reach at the resonance frequency using an anatomical whole-body human model.

**PML PERFORMANCE AND FDTD ACCURACY ANALYSIS:** The FDTD code used here incorporates a uniaxial PML boundary condition for absorbing outgoing scattered waves. The PML performance is usually evaluated in free space, while it should be degraded by the existence of human model due to the multiple and scattered near-field incidence. We therefore first investigated the reflection coefficients of 12 PML layers in free space and the relative error of average SARs for a homogeneous 2/3-muscle sphere. A Huygens surface was implemented in the FDTD code to allow the description of an incident field to separate the scattered fields for PML, and also to connect the PML layers to the total field region in the calculation domain. In comparison with the average SARs derived from Mie theory, we found that the PML performance deteriorates actually 40dB compared to the case

in free space and is the worst at the resonance frequency where the relative error of the average SAR may reach 10 %. We also found that the relative error actually varies with both the frequency and the distance from the PML layers. Careful attention should be paid in choosing an appropriate calculation domain for obtaining a high-accuracy SAR result.

**WHOLE-BODY AVERAGE SAR:** After determining the required FDTD calculation domain from the above error analysis, we further employed in the SAR calculations an anatomically based high-resolution human model - the Japanese whole-body model[1], which has a high-resolution of 2 mm and consists of 51 tissue types. With the human model, we calculated the whole-body averaged SAR in the resonance frequency band under the reference level for occupational exposure. As a result, we reconfirmed the resonance frequency of 70 MHz at about 0.4 wavelength of the human height of 173 cm, while we found a somewhat higher average SAR level than the previously reported ones by other researchers at the resonance frequency. Furthermore, it was found that the whole-body average SAR may exceed the basic SAR limit of 0.4 W/kg even if the reference level is under the safety guideline. This finding raises a critical issue in the FDTD calculation accuracy for the whole-body average SAR at the resonance frequency.

**CONCLUSION:** Based on a detailed error analysis for the FDTD code, the whole-body average SAR characteristics in the resonance frequency band have been derived for the Japanese whole-body model. We have shown a possibility that the whole-body averaged SAR may exceed the basic SAR limit under the reference level, although its further validation is necessary.

**REFERENCE:** [1] T. Nagaoka, S. Watanabe, K. Sakurai, E. Kunieda, S. Watanabe, M. Taki and Y. Yamanaka, *Phys. Med. Biol.*, vol.49, pp.1-15, 2004.

8-6

**STATISTICAL ANALYSIS OF THE INFLUENCES OF TECHNOLOGY, ANTENNA, MOBILE PHONE SHAPE AND POSITION ON SAR MEASUREMENTS FROM FCC COMPLIANCE TESTING DATA.** M. Weingart<sup>1</sup>, M. A. Kelsh<sup>1</sup>, M. Shum<sup>1</sup>, A. R. Sheppard<sup>2</sup>, N. Kuster<sup>3</sup>. <sup>1</sup>Exponent, Inc., Menlo Park, CA, USA, <sup>2</sup>Asher Sheppard Consulting, Redlands, CA USA, <sup>3</sup>IT'IS, Zurich, Switzerland.

**INTRODUCTION:** Improvement in exposure assessment of radiofrequency (RF) energy from mobile phone use is expected upon consideration of factors in addition to estimates of cumulative exposure and years of use (factors evaluated in most epidemiologic studies to date). Four additional candidate exposure factors are communication technology (digital--GSM, TDMA, CDMA, and analog--AMPS), phone shape ("candy bar" or "folding phone", antenna type and position (fixed, extendable-in, or extendable-out), and the position of the phone relative to the face (simplified as either "tilt" or "cheek" position). FCC staff assembled a database from SAR data in compliance testing reports. An evaluation of these data was presented recently (Cleveland et al BEMS 2003 Abstracts). Based on an analysis of approximately 500 records, the FCC researchers observed little correlation between various factors such as amplifier power, radiated power, and the spatial peak of time-averaged SAR at maximum output power--hereafter "SAR"--as measured for regulatory compliance. They also noted that test data for AMPS and CDMA exhibited somewhat higher SARs, although these differences were not quantified.

**OBJECTIVE:** To quantitatively evaluate the effects on SAR of communication technology, phone shape, presence and position of an antenna, and phone position using an updated and enlarged FCC database.

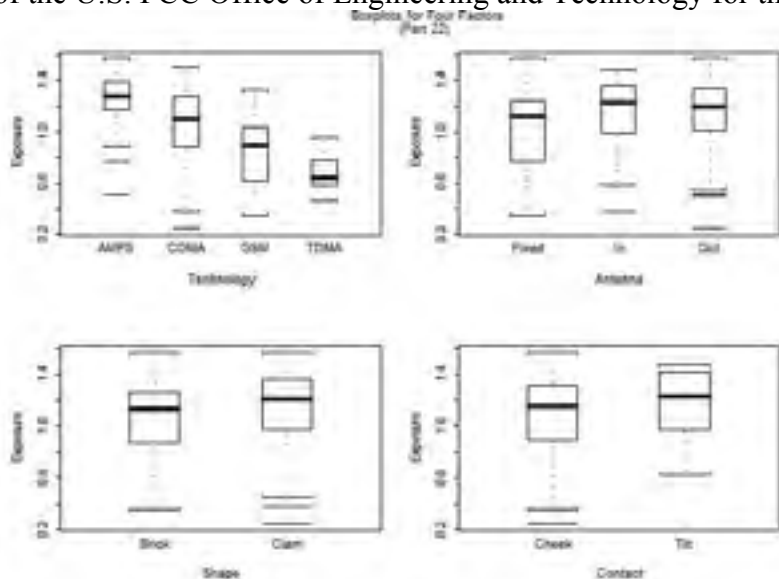
**METHODS:** FCC staff provided us with a database (derived from manufacturer-supplied compliance

reports) that included phone model, operational frequency, and the above four factors mentioned in the objective. Although the database included wireless devices regulated under both Part 22 (800 MHz band only) and "Part 24" (800 MHz band and PCS band at 1900 MHz), only "Part 22" data, which were very similar to those for Part 24 devices, are presented here. To assess sources of variability related to the above four factors, we used an unbalanced fixed effects analysis of variance (ANOVA) model. In addition, standard statistical summaries: mean, median, and standard deviation were calculated for the SAR values by each factor and combinations of factors.

**RESULTS:** The FCC database included 975 records evenly divided across technologies (244 each for AMPS, CDMA, and TDMA, and 243 records for GSM). A majority of phones, 487 (50%), were candy bar shaped; 360 (37%) were flip phone shaped; and for 128 (13%) phone shape was not available in the database. Mean and median SAR values (W/kg) were similar across antenna position (fixed, in, out), phone shape, and position. Technology had the most influence, with AMPS having the highest median SAR, followed by CDMA, GSM, and TDMA. The range of values for TDMA was lower than for the others while CDMA had the widest range of SAR values.

**DISCUSSION:** Our analyses of a larger and more recent set of SAR compliance data confirm the earlier findings of the FCC study, namely that AMPS and CDMA technologies generally had SARs 20-40% greater than GSM and TDMA and that SARs across the other factors (antenna, phone shape and position) did not exhibit significant differences. These findings suggest the need to consider service technology information as part of RF exposure assessment for epidemiologic studies. However, the poor correlation between SAR and handset power output found in the FCC (2003) analysis and the fact that the compliance data only include the maximum SAR, which may not indicate how a handset performs under network power reduction control, suggest that better exposure assessment may require direct determination of SAR under actual usage conditions.

**ACKNOWLEDGEMENTS:** Technical Oversight: Radiation Biology Branch, Center for Devices and Radiological Health, U.S. Food & Drug Administration (FDA). Research Funding: Cellular Telephone and Internet Association (CTIA). Data: We thank Dr. Robert F. Cleveland, Jr. and Mr. Tim Harrington of the U.S. FCC Office of Engineering and Technology for their assistance.



Notes: "Box-Whisker" Plot. The box shows the 25<sup>th</sup> to 75<sup>th</sup> percentiles with the median as a thick line; curved brackets show the last data point within 1.5 times the inter-quartile range. Lines beyond brackets are data points beyond that range. "Exposure" is SAR in W/kg, and "clam" identifies folding phones and "brick" identifies candy bar phones.

## Session 9: In Vitro Elf II

*Chairs: Mats-Olof Mattsson and Myrtil Simko*  
2:00 - 3:30 pm, Theatre M

9-1

**THE POTENTIAL OF 50 HZ ELECTROMAGNETIC FIELDS TO INDUCE EXTRACELLULAR MATRIX REMODELING IN HUMAN PRIMARY FIBROBLASTS.** C. Maercker<sup>1</sup>, D. Remondini<sup>2</sup>, S. Ivancsits<sup>3</sup>, H. W. Rudiger<sup>3</sup>, F. Bersani<sup>2</sup>. <sup>1</sup>RZPD German Resource Center for Genome Research, Heidelberg, Germany, <sup>2</sup>Univ of Bologna, Dept of Physics, Bologna, Italy, <sup>3</sup>Univ of Vienna, Division of Occupational Medicine, Vienna, Austria.

Primary fibroblasts (ES-1) were exposed to 50 Hz, 1 mT in 5min on/10 min off cycles (exposure setup by Niels Kuster and Jürgen Schuderer, IT'IS Zürich, Switzerland). In independent experiments, total RNA from exposed and sham-exposed cells was isolated after 15 h and after 24 h, respectively, and used for gene expression analysis on whole-genome human cDNA arrays (Human Unigene RZPD-2, 75,000 clones, spotted in duplicates).

Original expression profiling data were normalized and the background was removed. For each experiment at least two hybridizations were performed (4 data points per gene). In a first preprocessing, signals were removed giving a zero or an infinite ratio that could lead to a reduction of the available measurements for some genes. Data were processed in order to evaluate and reduce possible artifacts due to the array reading procedure. To increase the robustness of our selection, following the bootstrapping procedure as shown recently (Tusher et al. (2001) Proc. Natl. Acad. Sci. USA 98, 5116-5121), new datasets were generated as permutations of the original ones, and the same analysis was performed over these datasets, ranking the from larger to smaller. The outlier genes selected for each experiment were chosen from the intersection between the initial outliers and those from the bootstrapping procedure. The genes extracted by bio-statistics were linked to a gene ontology database. With the help of a text query tool regulated genes belonging to certain gene families of interest could be extracted manually. Additional information about the genes was found by text mining and by the help of the GeneCards database. We especially extracted gene families potentially relevant for a cellular answer to electromagnetic fields: signal transduction (GTP associated proteins, small G proteins, signaling via Jak, Rab, Ras and wnt pathway, phosphatases, protein kinases, phospholipases (phosphatidyl-inositol second messenger pathway), calcium, calmodulin (Ca<sup>2+</sup> binding protein), ion/electron transport (channels, voltage-gated transport, electron transport, ion transport), metabolism of energy/proteins (metabolism in general, ATP (energy), mitochondrial genes, RNA processing, ribosomal genes, translation, transcription), cell proliferation/apoptosis/differentiation, immune answer, inflammation, stress answer (stress in general, peroxidase, heat shock, DNA repair, oxide reductase), extracellular matrix, cytoskeleton (with actin), and adhesion (junction). The genes were listed according to function (adhesion, biosynthesis, cell proliferation, differentiation, energy metabolism, signaling, stress response, transcription, RNA processing, translation, transport).

Gene families with the highest number of up- or down-regulated genes were adhesion (12 genes up-regulated in EMF vs. sham, 5 genes down-regulated in EMF vs. sham), biosynthesis (10 up, 2 down), differentiation (10 up, 9 down), signaling (12 up, 2 down), stress response (8 up, 2 down), RNA processing and translation (24 up, 8 down), and transport (8 up, 1 down). 11 of those genes are directly or indirectly linked to calcium signaling. The two most prominent groups of proteins are collagens (4 genes up-regulated) and ribosomal proteins (20 up, 6 down).

Our results indicate that obviously the cellular turnover is up-regulated after ELF-EMF exposure. Regulated genes involved in RNA processing and translation, eg. eukaryotic translation elongation factor, point into this direction. In addition, we find some regulated genes, which are involved in energy metabolism (ATP synthase, cytochrome oxidase).

It is very likely that the contact of the fibroblasts with the ECM is intensified. This again might contribute to the interaction between fibroblasts and keratinocytes in skin tissue. Collagen turnover obviously is changed in psoriatic skin during disease and after treatment. After EMF exposure, we found an increase of COLA1 (collagen type I, alpha 1), COL3A1, COL8A1 and COL15A1. Other ECM components which appeared to be increased after 50 Hz treatment were proteoglycan 2 and decorin, another proteoglycan. SPARC (Secreted protein acidic and rich in cysteine, up-regulated after EMF exposure) modulates cellular interaction with the extracellular matrix (ECM) by its binding to collagen and vitronectin, and by its abrogation of focal adhesions. Consistently, we find both integrin alpha V and integrin beta 1 up-regulated in our experiments. These receptors interact with important components of the extracellular matrix, like vitronectin, fibronectin, and collagens. Another interaction partner is actin. Therefore, it was interesting to see that quite a number of genes encoding actin interacting proteins were regulated in our experiments, among them calponin 3 (CNN3), capping protein CAPZA1, coactosin-like protein CLP, coronin (CORO1C), destrin, and villin, all involved in the actin cytoskeleton. Quite a number of identified genes are directly or indirectly related to calcium signaling. This is true for the adhesion related genes EFEMP1, FSTL1, SPARC, and THBS2, as well as for the signaling related genes AMBP, CGI-67, REPS1 and RCN2. A molecule possibly involved in signaling is caveolin 1 (CAV1), which showed up-regulation in both independent experiments. This protein is a membrane protein, which again interacts with G-proteins and also is involved in actin-integrin-mediated interaction with the ECM. The increase of cellular activity related to RNA processing and translation, as well as the potential modulation of cell adhesion together with actin and interacting proteins might even be a possible explanation for the improvement of psoriasis in patients treated with ELF-EMF (Philipp A et al. (2000) Eur J Dermatol 10(3),195-198.).

Our work was funded by the EU (REFLEX project).

9-2

**EFFECTS OF EXTREMELY LOW FREQUENCY MAGNETIC FIELDS ON CYTOSOLIC FREE CALCIUM IN SYNCHRONIZED JURKAT E6.1 CELLS.** C. R. McCreary<sup>1</sup>, S. J. Dixon<sup>2</sup>, L. J. Fraher<sup>2</sup>, F. S. Prato<sup>1</sup>. <sup>1</sup>Lawson Health Research Institute and Dept of Diagnostic Radiology, St. Joseph's Health Care, London, ON, Canada, <sup>2</sup>Faculty of Medicine and Dentistry, Univ of Western Ontario, London, ON, Canada.

**INTRODUCTION:** Extremely low frequency magnetic fields (ELF MF) have been reported to alter a number of cell signaling events including pathways involved in proliferation, differentiation, and apoptosis. Cytosolic calcium ( $[Ca^{2+}]_c$ ) is a ubiquitous second messenger that is involved in the regulation of many of these physiological functions and may be involved in the detection of ELF MF at the cellular level. The detection and replication of ELF MF effects have been difficult because subtle differences in cell state have not been entirely defined or adequately controlled. Previous results (1) have demonstrated that Jurkat cells with G2-M enrichment exposed to combined static and 60 Hz magnetic fields had an increase in  $[Ca^{2+}]_c$  after anti-CD3 stimulation.

**OBJECTIVE:** To determine which magnetic fields are needed to elicit an effect on  $[Ca^{2+}]_c$  by comparing four exposure conditions on  $[Ca^{2+}]_c$  signalling, This will provide insight into possibly biophysical coupling mechanisms

**METHODS:** To understand the biological conditions under which ELF MF exposure alters cytosolic calcium, we compared calcium responses in synchronized Jurkat E6.1 cells exposed to a null ambient magnetic field (Null), a parallel combination of 60 Hz, 100  $\mu$ T<sub>peak</sub> sinusoidal and 78.1  $\mu$ T static magnetic fields (AC+DC), the AC field alone or the DC field alone. Cells were synchronized using 18 h treatment with aphidicolin (200 ng/mL). From a growth curve and from flow cytometry data, it was determined that G0/G1, S, and G2-M phases were maximally enriched 14-18 h, 1-4 h, and 6-8 h after aphidicolin treatment, respectively. Exposure measurements were made for these three distributions of cells within the cell cycle. The concentration of cytosolic free calcium was determined using ratiometric fluorescence techniques. Fluorescence was monitored for 15 min to establish basal levels then cells were stimulated with 0.67  $\mu$ g/mL anti-CD3 and fluorescence was followed for another 20 min. Parameters describing the fluorescence tracings were compared using analysis of variance.

**RESULTS:** Unlike the previous experiments (figure 1), no significant differences in  $[Ca^{2+}]_c$  were detected between exposure conditions. When these two studies were compared, several differences in the fluorescence tracings were detecting, including the response to anti-CD3 stimulation. In both studies, the  $[Ca^{2+}]_c$  response was biphasic with a rapid increase followed by an elevated steady state level. However, in the present study, recovery after stimulation was monotonic, while in the previous study there was a transient undershoot prior to the new steady state level (figure 2).

**SUMMARY:** The difference in the shape of the response to anti-CD3, which has not been reported previously for G2-M-enriched population, may be important in the sensitivity of nonlinear biological systems to ELF MF. These results suggest that if ELF MF effects on  $[Ca^{2+}]_c$  are present, they depend on the metabolic state of the cell, which may include phase of the cell cycle.

**REFERENCES:**

1. C.R McCreary and F.S. Prato. (2003) BEMS 25th Annual Meeting, Wailea, Hawaii, USA p.323.
2. C. Eichwald. and F. Kaiser. (1993) Biophys. J. 65:2047-2058.
3. W. Grundler, F. Kaiser, F. Keilmann, and J. Walleczek. (1992). Naturwissenschaften 79:551-559.

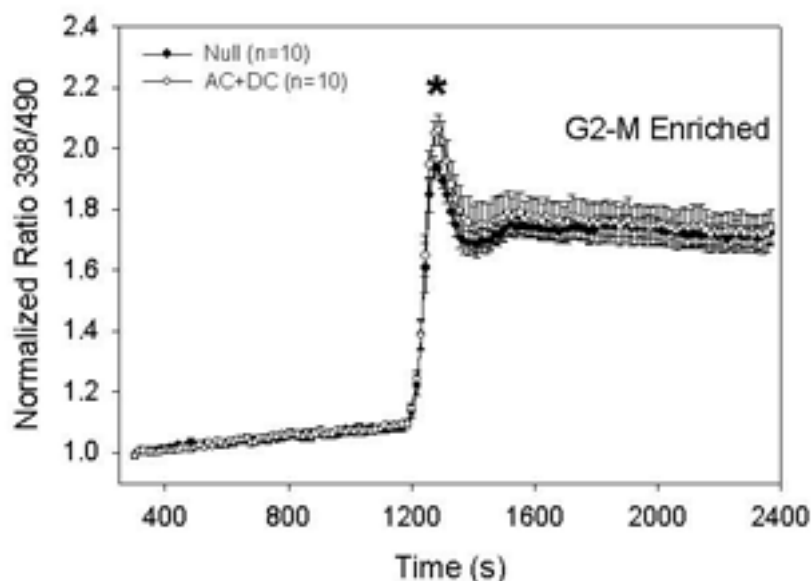


FIGURE 1. Comparison of normalized fluorescence ratio tracings between Null and AC+DC for samples with G2-M enrichment. The group means and standard error of the normalized fluorescence intensity ratios of Null and AC+DC exposed groups are shown for aphidicolin treated cells. The asterisk

indicates significant increase of 7% in the maximum fluorescence ratio after the introduction of anti-CD3 in Jurkat cells exposed to AC+DC magnetic fields.

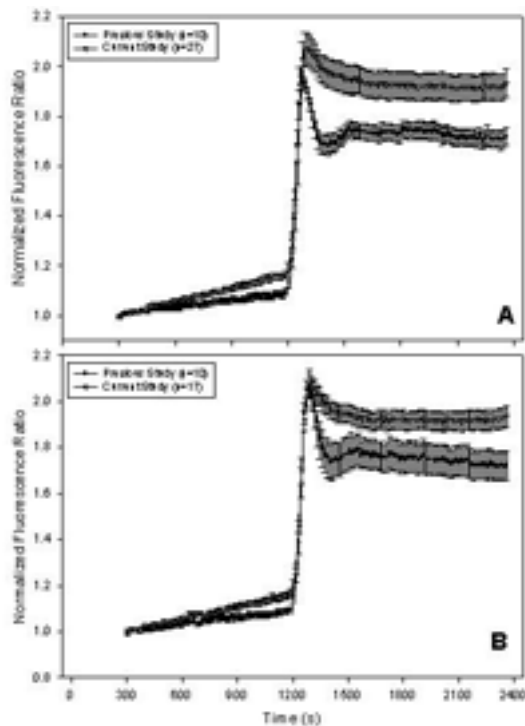


FIGURE 2. Comparison of the mean normalized fluorescence tracings between the previous and current studies showing differences in the shape of the response. The mean and standard error of normalized fluorescence tracings over time from samples with G2-M enrichment are shown. Samples exposed to Null static magnetic fields are shown in panel A and samples exposed to AC +DC magnetic fields are shown in panel B.

9-3

**DECREASE IN GLUCOSE-STIMULATED INSULIN SECRETION BY EXPOSURE TO EXTREMELY LOW FREQUENCY MAGNETIC FIELDS.** T. Sakurai<sup>1</sup>, S. Koyama<sup>1,2</sup>, Y. Komatsubara<sup>1,3</sup>, J. Wang<sup>1</sup>, J. Miyakoshi<sup>1</sup>. <sup>1</sup>Dept of Radiological Technology, School of Health Sciences, Faculty of Medicine, Hirosaki Univ, Hirosaki, Japan, <sup>2</sup>Dept of Interdisciplinary Environment, Graduate School of Human and Environmental Studies, Kyoto Univ, Kyoto, Japan, <sup>3</sup>Applied Biology Division, Kashima Laboratory, Mitsubishi Chemical Safety Institute Ltd., Kashima, Japan.

**INTRODUCTION:** Recently, studies applying electromagnetic fields to clinical use have increased markedly. Extremely low frequency magnetic fields (ELFMFs) have also been applied to the treatment of osteoporosis, bone diseases, Parkinson's disease, etc. Most recently, we have demonstrated that exposure to ELFMF decreased KCl-stimulated insulin secretion from RIN-m cells. In type 2 diabetic patients, excessive insulin secretion is thought to cause serious metabolic disorders, and prior to the decline in patients  $\beta$  cell function,  $\beta$  cells are believed to secrete insulin excessively. Therefore, the benefits of inhibitors of insulin secretion in the treatment or prevention of diabetes have been reported clinically. On this basis, we hypothesize that ELFMF could be used to attenuate insulin secretion in the treatment or prevention of type 2 diabetes.

**OBJECTIVE:** The objective of this study was to confirm whether exposure to ELFMF decreases glucose-stimulated insulin secretion to evaluate the potential for treatment or prevention of type 2 diabetes.

**METHODS:** We stimulated HIT-T15, glucose responsible insulin secreting cell line, to secrete insulin under exposure to ELFMF or sham conditions, using our established system for the exposure of cultured cells to the ELFMF (a sinusoidal vertical magnetic field at a frequency of 60 Hz and a magnetic density of 0.4-5 mT). The effects of ELFMF were assessed by the amount of insulin secretion, alterations of membrane potentials, cytosolic free calcium ion concentration ( $[Ca^{2+}]_i$ ), and metabolic activity.

**RESULTS:** Exposure to ELFMF at 5 mT decreased glucose-stimulated insulin secretion (Figure 1) by preventing the depolarization and the increase of  $[Ca^{2+}]_i$ . Glucose metabolic activity was not affected by exposure to ELFMF.

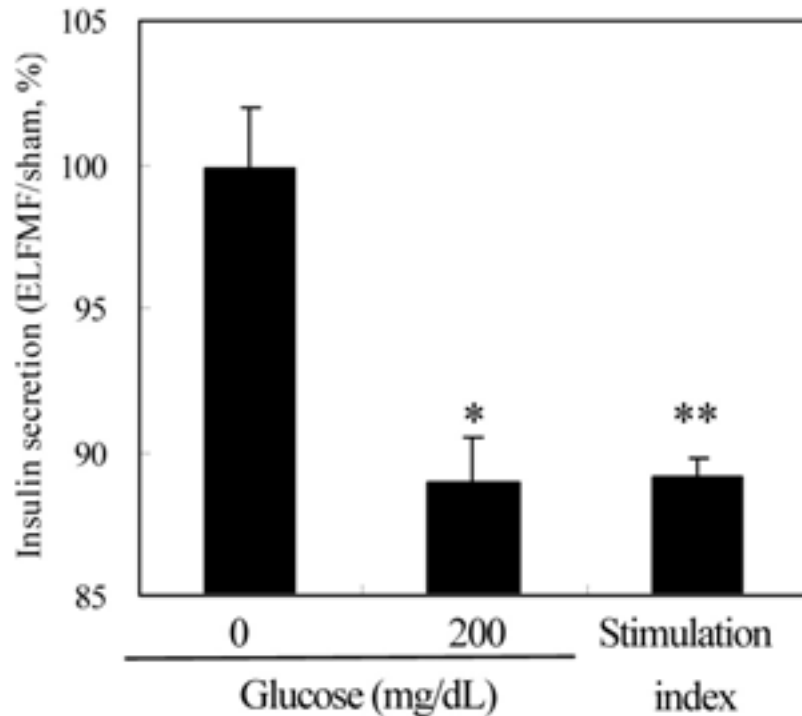


Figure 1. The effects of ELFMF on insulin secretion from HIT-T15 cells were evaluated in the presence of 0 or 200 mg/dL glucose. The ratio of insulin secretion under ELFMF to under sham exposure is shown. The stimulation index was calculated by dividing the level of insulin secretion under stimulation conditions (200 mg/dL glucose) by the level of insulin secretion without glucose-stimulation. \*  $p < 0.05$ , \*\*  $p < 0.01$ , by Student's *t*-test.

**CONCLUSION:** These findings demonstrate the high potential of exposure to ELFMF at strong magnetic flux density, as an inhibitor of insulin secretion in order to induce  $\beta$  cell arrest and to improve  $\beta$  cell function and viability in type 2 diabetes with excessive insulin secretion.

9-4

### **EFFECTS OF ELECTRIC AND MAGNETIC FIELDS ON HUMAN LEUKOCYTES IN VITRO.**

A. Aly, K. Rathnabharathi, E. Zhou, M. Cheema, F. Barnes. Univ of Colorado at Boulder.

**INTRODUCTION:** Leukocytes(white blood cells) play an essential rolls in our human immune system as part of the bodies defense against invading bacteria, viruses, fungi, and parasites. Leukocytes attack the invading organisms (pathogens), by identifying them, attaching, destroying them, and taking them out of the blood, and by continuously produce antibodies against that organism for the rest of the bodies life.

**OBJECTIVE:.** The focus of this study has been to improve our understanding of how electric and

magnetic fields may modify the ability of these cells to find invading organisms and the threshold field strengths at which these fields become significant.

**METHODS:** Blood was drawn from a number of healthy students, centrifuged to concentrate the leukocytes and placed on a microscope slide in a concentration gradient of cyclic-AMP. The ability of leukocytes to track the cyclic-Amp concentration gradient has been observed as a function of frequency, and field strength.

**RESULTS:** Our experimental results to date show significant change in leukocytes behavior, including more rapid changes in shape, changes in direction, and more rapid movement. For RF exposures at field strengths of 100 V/m and magnetic fields of 0.26 iT increases of velocity of approximately 50% have been shown over that which could be achieved at the same temperature as well as changes in the direction of motion upon the application of the fields. For DC electric fields the direction of motion could be reversed with the reversal of the direction of the field. The velocity of the cells both increased and decreased as a function of the field strength in the range of 200 V/m to 1.5 KV/m. with respect to it velocity in the presence of the C-AMP gradient alone. Above about 1 KV/m the velocity decreases. DC magnetic fields in the range of 20 to 100 iT increased the velocity of the leukocytes. For 60 Hz AC magnetic fields in the range from 11 to 20 iT the velocities decreased below those in the presence of the C-AMP alone.

**CONCLUSIONS:** It is likely that more than one physical mechanism is affecting the ability of these cells to track concentration gradients. DC external electric fields are expected to modify the flow of ion currents around the cells and shift the voltages across the membranes by a few millivolts. The voltage shift in turn may modify the ion flow through the membranes and thus chemical reaction rates inside the cell. The DC magnetic fields are more likely to modify free radical reaction rates and lifetimes than current flows. The mechanism by which AC and RF electric field may modify the leukocyte behavior is not understood but could be by means of the field gradients or by modifying the transition times between closely placed energy states. Farther work is needed illuminate how eternally applied fields modify chemical reaction rates in cells and the cells sensory systems.

9-5

**EFFECTS OF LOW AND HIGH STATIC MAGNETIC FIELDS ON CELL DEATH KINETICS OF HUMAN LIVER CANCER CELL LINE HEPG2.** Y. Haik<sup>1,2</sup>, H. Yuan<sup>1</sup>, S. G. Schneiderman<sup>1</sup>, C-J Chen<sup>1</sup>. <sup>1</sup>Center for Nanomagnetism and Biotechnology, Florida State Univ, Tallahassee, FL, <sup>2</sup>Dept of Mechanical Engineering, United Arab Emirates Univ, UAE.

**INTRODUCTION:** There are a few studies investigating the effects of magnetic field on cell death of mammalian cells in vitro. Dye exclusion, DNA stain, flow cytometry and morphological analysis were used to evaluate cell death (apoptosis and necrosis) after magnetic exposure. However the results are not conclusive. Also those data only showed apoptosis or necrosis cells at certain time points after exposure. They didn't tell any information about magnetic effect on the whole cell death process (cell death kinetics). In this study, we exposed human liver cancer cell line HepG2 to 0.5 T and 12 T static magnetic fields for 4 hour and 4 days. 125IudR release assay was used to investigate the kinetics of cell death by continuous monitoring the release of 125IudR from cells in which DNA was labeled with 125IudR before exposure.

**OBJECTIVE:** The objective of this study was to investigate cell death kinetics of human cancer cell line due to static magnetic exposure. Under different magnetic flux density and exposure time, comparisons were made between treated cells and control cells by 125IudR release assay.

**METHODS:** A human hepatocellular carcinoma cell line HepG2 were purchased from ATCC (Manassas, VA). HepG2 was grown in minimum essential medium (Eagle) supplemented with 2 mM L-glutamine, 10% FBS, 0.01 mg/ml Gentamicin. Cells were grown a 37 °C in a humidified 5% CO<sub>2</sub>/95% air atmosphere, tissue culture incubator. Cells were re-cultured from the frozen vials in the cell bank after two months' culture. Low and high static magnetic field were applied in the experiments. Neodymium Iron Boron magnets provide up to 0.5 T magnetic field. High resolution NMR magnet system provides homogeneous 12 T magnetic field at the center of the magnet. Temperature, humidity and pH were controlled to keep the same as controlled group during the exposure. Cells were incubated and labeled by the incorporation of radioactive Iodine-125-IudR into DNA. Then the dying cells were monitored continuously by counting total radioactivity of total cell using gamma ray counter every 12 hours. 125IUdR release assay provides a time profile of percentage of dead cells.

**RESULTS:** Preliminary results on effects of low and high magnetic fields are reported here. Statistical significance was calculated with the t test for control and magnetic treated samples. There are no significant effects of 0.5 T static magnetic fields on HepG2 cell death kinetics for both 4 hours and 4 days exposure (see figure 1, 3 and table 1). The 4 hours exposure of 12 T static magnetic fields slowed down cell death process (see figure 1, 2 and table 1). There was maximum delay after 50 hours of exposure. Then the cell death of control and magnet treated groups became close after four days. These results indicate that 1. High intensity magnetic field has a bigger impact on cell death than low intensity field. 2. The influence of static magnetic field on cell death decrease after a certain time. 3. The overall effect of High static magnetic field on cell death of HepG2 is not significant although the difference between control and magnet treated is statistically significant. Additional results on DNA synthesis and growth inhibition will be reported at the conference.

This study is supported by Florida State Univ Research Foundation.

P value of comparison between control and magnet treated groups						
TIME (HOURS)	12	27	39	52	74	86
P VALUE LOW MAG	0.85	0.86	0.056	0.66	0.05	0.13
P VALUE HIGH MAG	0.095	0.063	0.019 *	0.016 *	0.02 *	0.049 *

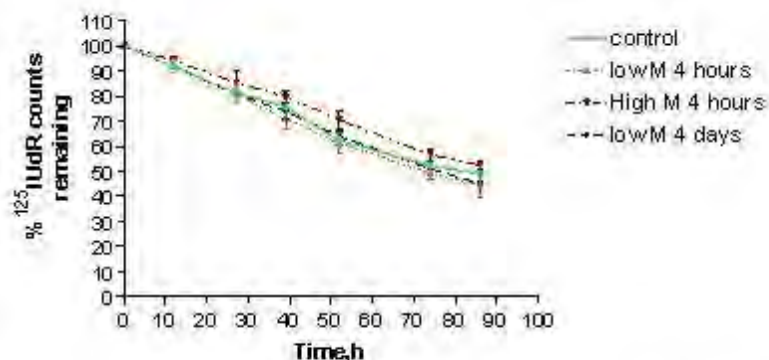


Figure 1 Effect of Magnetic Field on HepG2 Cell Death. Low M: 0.5 T; High M: 12 T.

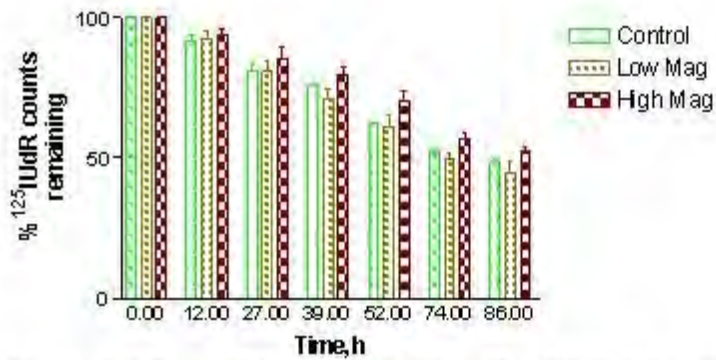


Figure 2 Effect of Magnetic Field on HepG2 Cell Death (15 T vs 0.5 T)

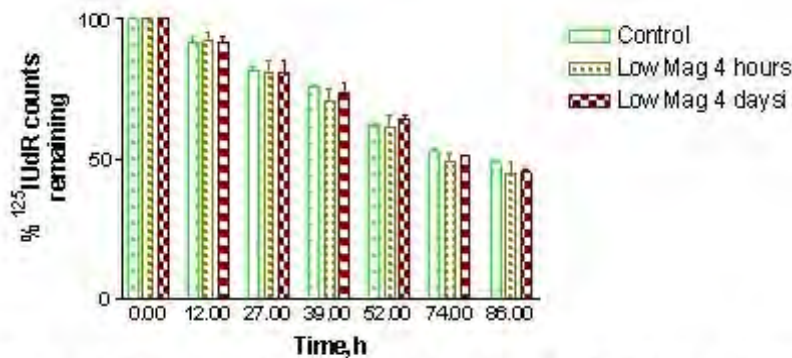


Figure 3 Effect of Magnetic Field on HepG2 Cell Death (0.5 T short vs long exposure)

9-6

**EFFECT OF LOW-FREQUENCY ELECTROMAGNETIC FIELD STIMULATION ON PLURIPOTENT HUMAN STEM CELLS DIFFERENTIATION.** A. Lisi<sup>1</sup>, M. Ledda<sup>1</sup>, A. Patti<sup>2</sup>, A. Vulcano<sup>2</sup>, L. Giuliani<sup>3</sup>, E. Rosola<sup>1</sup>, S. Grimaldi<sup>1</sup>. <sup>1</sup>Istituto di Neurobiologia e Medicina Molecolare C.N.R. Rome Italy, <sup>2</sup>Dipartimento di Scienze di Sanità Pubblica G. Sanarelli Università, <sup>3</sup>ISPESL Venezia.

**Introduction:** In literature is well described that mesenchymal cells are able to differentiate to osteoblast following treatment with chemical agents such as dexamethasone. Regulation of osteoblast differentiation its an important phenomena that must occur to maintain the continuous supply of mature osteoblast needed for bone growth, remodeling, and in particular for bone repair.

**Objective:** In this study we evaluate whether applying extremely low frequency electromagnetic field (ELF-MF 50Hz 1mT) may influence differentiation on mesenchymal human cells of bone marrow.

**Methods:** Culture and differentiation of mesenchymal stem cells: Height- ten ml of bone marrow, obtained from iliac crest, was mixed with one volume of phosphate-buffered saline and nucleated cell fraction was enriched for mesenchymal stem cells by density-gradient centrifugation over Lympholyte-H cushion. The cells at the medium-Lympholyte-H interface were collected, washed three times with culture

medium and seeded into culture flask. Confluent monolayers of adherent cells were obtained about one week after the start of cell division. To promote osteogenic differentiation cells were stimulated during

sub passages by cultivation in standard medium supplemented with 100nM dexamethasone or by exposure to extremely low frequency electromagnetic field (50Hz 1mT) under controlled condition. The constant electro-magnetic field of 1mT at 50 Hz was generated in a solenoid.

Results: This study showed that 5 days ELF-MF 50Hz 1mT exposed resulted in a change in plasma membrane morphology, this modification were also accompanied by a rearrangement in actin filaments as showed by confocal microscopy analysis after cells labeling with FITC-phalloidin. Mesenchymal cells exposed to the field showed the same intra cytoplasmic organization found in the cells after treatment with the chemical differentiating agent dexamethasone. Chronic exposure to low frequency electromagnetic field resulted in an impairment of cell growth (up to 30%) as showed by BrdU labeled cells compared to non exposed mesenchymal cells. By real-time RT-PCR we have studied the expression of osteoblast-specific markers differentiation factors such as alkaline phosphatase and osteopontin. The expression of genes encoding for both markers, was up regulated by exposure to ELF-MF. Moreover a synergistic effect of low frequency electromagnetic field with dexamethasone potentiate the expression of both markers.

Conclusions: These findings suggest that exposure to ELF-MF can act as a differentiating agent on mesenchymal human cells and outline the importance of low frequency electro-magnetic field as a therapeutic agent suggesting a possible use of to low frequency electromagnetic field as support in medicine for different pathologies therapy.

### **Session 10: Dosimetry IV**

*Chairs: Phillip Chadwick and Theodoros Samaras*

**4:00 - 5:30 pm, Theatre L**

10-1

#### **ASSESSMENT OF SAR FROM IN-VEHICLE RADIO DEVICES USING A NOVEL MEASUREMENT SYSTEM.** H. Hall, P. Chadwick. MCL, West, Newbury, Berkshire, UK.

There are standardised and established methods for assessing head SARs from mobile telecommunications devices. Work is underway to extend these methods to SARs from body-mounted devices. However, the existing and proposed SAR measurement systems are laboratory-based and cannot easily be used in many of the situations where people are exposed to radiofrequency electromagnetic fields from fixed and portable systems. Particular concern has been expressed about exposures to fields from radios on and inside vehicles – including emergency services and military vehicles. This paper reports the development and first results of assessments made using a novel in-vehicle SAR assessment system.

The system is based, as is the case with current SAR measurement systems, on a shell phantom filled with fluid, the SAR being measured with a robot-mounted positioner. The novel feature of the new MCL system is that the robot positioner is mounted inside a whole-body phantom. For the first time, SAR distributions in the body can be measured and mapped while in a real exposure environment and SAR can be measured anywhere within the head and torso. The phantom used has excellent provenance: it is based on the 95th percentile of the anthropomorphic data collected by the US Army, (the same dataset used to define the SAM phantom head)

The phantom is sectional, with removable arms and legs and has been built in two configurations: seated

and standing. The seated version, shown in Figure 1, is intended specifically for measurements inside vehicles. CAD files describing the inner and outer surfaces of the phantom have been developed to facilitate computational modelling of exposure situations in parallel to physical measurement.

The results of measurements of radios operating at frequencies around 400 MHz are reported.

This work was supported by the UK Home Office



10-2

**EXPOSURE SYSTEM FOR SIMULATING GSM AND WCDMA MOBILE PHONE USAGE.** A. Bahr<sup>1</sup>, H. Dorn<sup>2</sup>, T. Bolz<sup>1</sup>. <sup>1</sup>IMST, Kamp-Lintfort, Germany, <sup>2</sup>Charité - Universitätsmedizin, Berlin, Germany.

**INTRODUCTION:** For health risk assessment of mobile phone exposure different setups are in use in human volunteer studies. This includes near field exposure setups with commercially available mobile phones and cable fed antennas which are placed in the near field or the quasi-far-field with respect to the human body.

For sleep studies or long exposure times (up to 8 hours) only quasi-far-field setups with distances of >10 cm between the antenna and the human body are used at the moment. The objective of this study was the design of a new near field exposure setup with enhanced carrying properties for simulating GSM and WCDMA mobile phone usage. The setup is used in a project entitled 'Investigation of volunteers exposed to electromagnetic fields of mobile phones' [1].

**EXPOSURE SYSTEM:** In Fig. 1a the exposure setup is depicted [2]. It consists of a GSM and a WCDMA signal generator. The GSM signal consists of a 900 MHz pulse modulated carrier with a pulse length of 553 ms with a repetition rate of 217 Hz. The WCDMA signal is generated according to [3]. In addition the system includes an RF switch, a power amplifier covering the frequency range from 900 MHz up to 2000 MHz, a directional power meter and a dual band antenna. The antenna is connected to the power meter via 5 m coaxial cable in order to guarantee a sufficient freedom of movement.

The whole setup is computer controlled. Double-blind scenarios are realized by the RF switch which enables GSM, WCDMA and sham exposure. The output of the power meter is permanently recorded by the PC. If the forward or reflected power are out of range the PC generates an alarm and the exposure system is switched off.

Fig. 1b shows the design of the dual band antenna with a mass of 14 g and in Fig. 1c the position of the antenna at the human head is depicted. The antenna consists of a PCB with typical mobile phone dimensions (110 mm x 40 mm) and a radiating element which is similar to common PIFA radiators of modern mobile phones. In order to account for good carrying properties the design is completely planar with a total thickness of 1 mm. The metal parts are covered with foam and a washable textile cover. The foam towards the human head has a thickness of 2 mm, the foam away from the human head has a thickness of 1 mm. Carrying properties are further enhanced by a slot inside the PCB. This enables an exposure position where the antenna is placed at the head surface and the pinna is put through the slot of the antenna.

**METHOS:** The numerical dosimetry was carried out using the Finite-Difference Time-Domain (FDTD) simulation tool EMPIRE from IMST [4]. For the numerical dosimetric assessment the male head model based on the Visible Human Project is applied. In addition the numerical simulations are validated by SAR measurements with a DASY 4 measurement system from SPEAG.

**RESULTS:** Table 1 shows the localised SAR inside the human head model for both frequencies under investigation and an antenna input power of 1 W. The SAR values are comparable to the SAR values of commercially available GSM and WCDMA phones, when scaling to the corresponding output powers. For the SAR evaluation the compressed pinna of the human head model is not considered.

**CONCLUSION:** In this study a new exposure setup for simulating GSM and WCDMA mobile phone usage was investigated. It can be shown, that concerning SAR the antenna shows characteristics which are comparable to mobile phones.

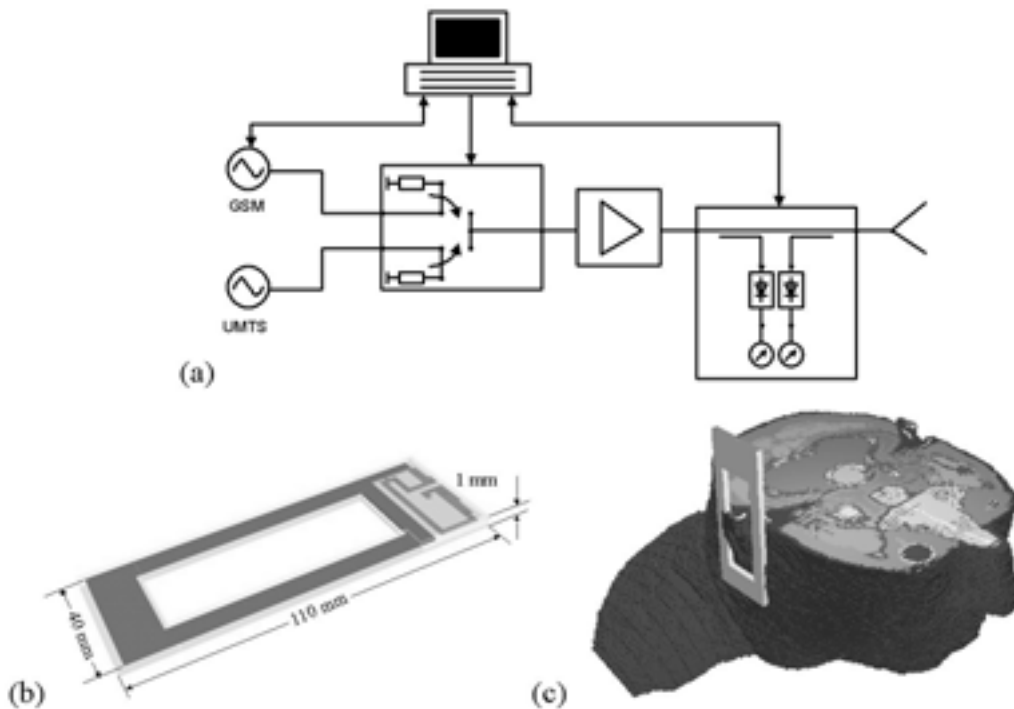
#### REFERENCES:

- [1] Danker-Hopfe, H, Dorn, H. 2004. Untersuchungen an Probanden unter Exposition mit hochfrequenten elektromagnetischen Feldern von Mobiltelefonen - Literaturübersicht. Berlin (Germany). <http://www.emf-forschungsprogramm.de>.
- [2] Bahr A, Dorn H, Bolz T. 2004. Dosimetric assessment of an exposure system for simulating GSM and WCDMA mobile phone usage. Submitted to Bioelectromagnetics.
- [3] Ndoumbè Mbonjo Mbonjo H, Streckert J, Bitz A, Hansen, V, Glasmachers A, Gencol S, Rozic D. 2004. A generic UMTS test signal for RF bio-electromagnetic studies. Bioelectromagnetics, vol. 21, no. 6, 415-425.
- [4] IMST. 2004. EMPIRE Version 4.1. User and Reference Manual: IMST GmbH.

This work is carried out in a project that is funded by the Federal Office for Radiation Protection (BfS) within the German mobile telecommunication research program.

1 g and 10 g averaged SAR inside the heterogeneous human head model at 900 MHz and 1966 MHz for an antenna input power of 1 W.

f [MHz]	SAR_1g [W/kg]	SAR_10g [W/kg]
900	14.61	6.27
1966	25.69	13.09



### 10-3 STUDENT

**AN FDTD STUDY OF THE INTERACTION BETWEEN BODY-WORN BIOMEDICAL-MONITOR WIRES AND A COUPLED 435 MHz DIPOLE RADIATOR.** A. D. Ball<sup>1</sup>, N. E. Evans<sup>1</sup>, S. E. Troulis<sup>1</sup>, W. G. Scanlon<sup>2</sup>. <sup>1</sup>Centre for Communications Engineering, School of Electrical & Mechanical Engineering Univ of Ulster, Shore Road, Newtownabbey, Co Antrim, N. Ireland, UK, <sup>2</sup>School of Electrical & Electronic Engineering, Queen's Univ of Belfast, N. Ireland, UK.

#### Introduction

With the public's awareness of safety hazards in the workplace, there is a growing concern with regard to personnel such as fire-fighters deployed in hostile situations. This has created a demand for continuous, remote biomedical monitoring by radio. Typically, the subject wears appropriate instrumentation interfaced to their medium-power personal radio (PR), or a separate and dedicated biomedical telemeter. This poses a number of constraints on the instrumentation, whereby it must remain interference-free. Interference can originate in unwanted coupling between transmitting PR antennas and any proximate circuitry such as ECG lead sets and PCBs carrying sensitive amplifiers. Coupled wires can also affect SAR distribution [1].

The effects of coupling between short vertical and tilted wires laid over a muscle tissue slab (to mimic human ECG radio telemetric monitoring) and a nearby 435 MHz  $\lambda/2$  dipole were investigated using a custom FDTD simulator written in 'C' (COCA: Code for Coupled Antennas).

The frequency selected lies in the lower UHF band, widely used for PR deployment in the Emergency Service sector. This topic is novel as it represents a practical biomedical monitor exposed to a potential RFI source, modelled in this instance as an illuminating dipole. It is also challenging to model in FDTD, as the introduction of tilted or curved conductors can lead to a number of inaccuracies due to stepping.

**Methodology and Results**

The undesirable effects of analysing tilted elements in the Yee algorithm were overcome by applying Dey-Mitra special update equations. To date, research using this method has primarily focussed on cylindrical and spherical cavities, circular/square microstrip patch antennas, and horns [2]. Here, the technique has been extended to investigate thick dipole and wire elements.

The approach was initially validated by comparing the input impedances and resonant frequencies of isolated dipoles oriented vertically and at 45° in the modelling space. The resonant-frequency shift was zero and the input resistance changed by only 1.72% when applying the Dey-Mitra technique: see Figure 1 and Table 1.

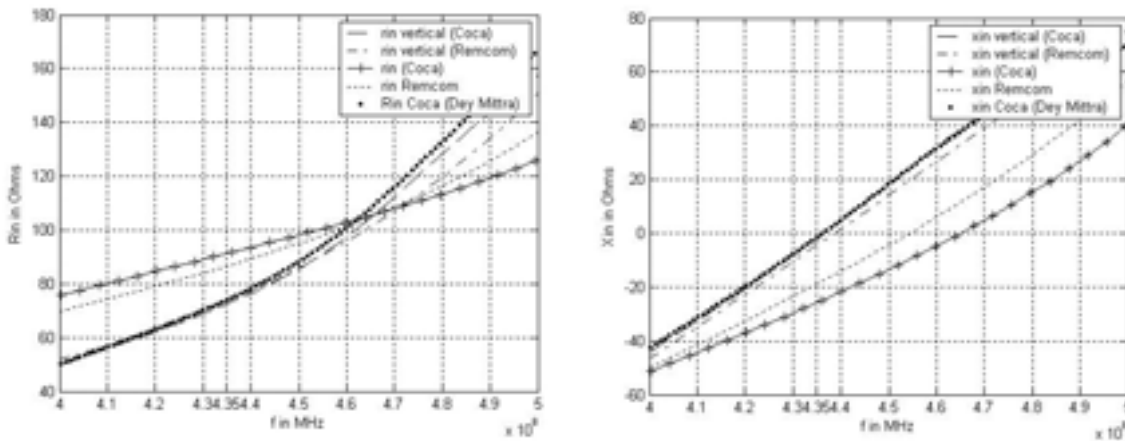


Figure 1: Comparing techniques for calculating (a) feed resistances and (b) feed reactances for a vertical dipole and a dipole tilted 45°.

We then introduced human tissue close to the test dipole. To ease computing requirements, an adult body torso was represented by a homogeneous muscle slab (Table 2) 70cm x 30cm x 15cm, in a 2.5mm Yee lattice. The effects of near-tissue-surface vertical (Figure 2a) and tilted wires (Figure 2b) on the dipole's input impedance (Figure 3) and current distribution were investigated by varying the horizontal separation between the dipole and wire from 10-100mm. The wire length was 188mm, representative of that used in ECG radio-monitoring practice.

Conductivity 0.805 S/m

Relative permittivity 56.86

Loss tangent 0.59

**Table 2:** Muscle dielectric properties at 435 MHz.

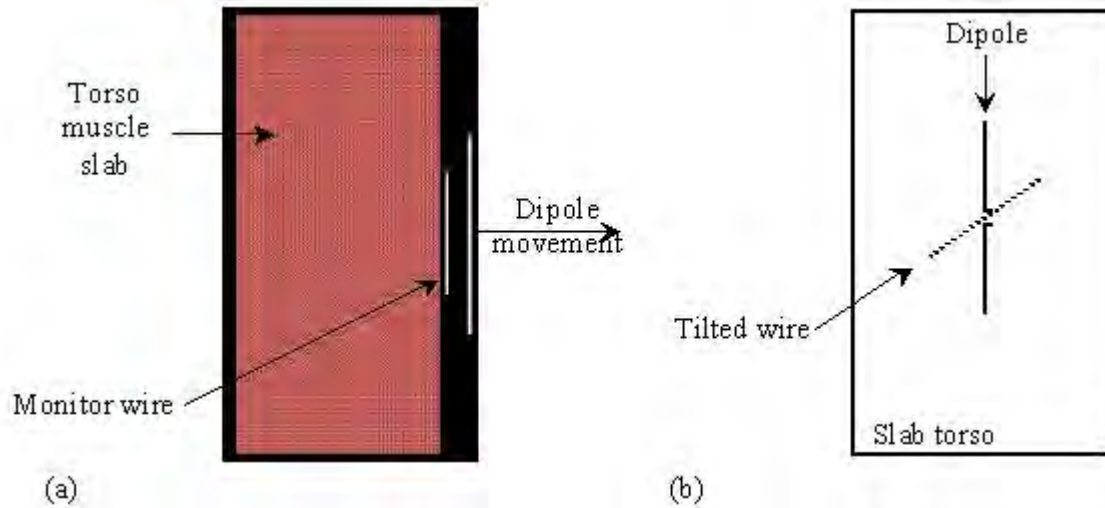


Figure 2: (a) Centre-section through the FDTD model of a vertical ECG monitor wire illuminated by a vertical  $\lambda/2$  dipole, the wire is 10mm from the slab's surface. (b) Anterior view of the dipole, tilted monitor wire and muscle slab.

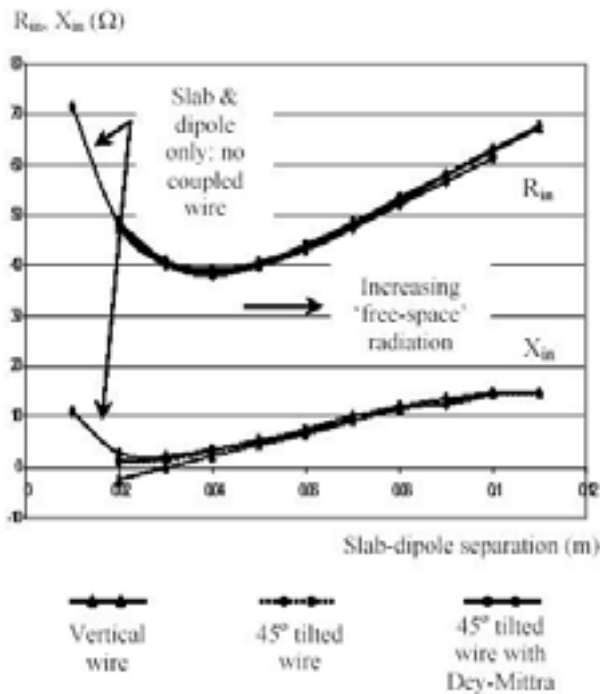


Figure 3: Input resistance and reactance for a vertical dipole adjacent to a dielectric slab and following the introduction of vertical and tilted wires close to the slab surface, versus dipole separation.

For the dipole and body only, minimum separation results in significant detuning, with an inductive input reactance and high body loss. Reactance falls with increasing separation, as does the feed resistance initially as absorptive loss reduces, minima being reached at 25 and 40mm, respectively. Thereafter, the feed reactance remains inductive and the input resistance begins to rise towards the free-space value at about 120mm spacing. Introducing the wire de-emphasises direct body coupling: close-in feed reactance is virtually unchanged from the isolated dipole case and direct absorption reduced, as evidenced by the smoother, vertically shifted (by about  $6\Omega$ ) resistance plots. Note that the feed resistance profiles of the dipole adjacent to both wires are almost identical. The difference between the reactance plots is low, less than  $0.5\Omega$  at separations greater than 40mm.

The peak current induced in the monitor wire was calculated for a dipole feed-point drive normalised to 100mA. During the initial drop of  $R_{in}$  with separation distance, the induced current in the vertical wire reaches its maximum of 22mA (Figure 4). It then decays with separation as the feed resistance grows, settling to 2.3mA at 11cm. For the tilted wire, the close-in induced current has a maximum of 7mA and then drops to a minimum, corresponding to the dipole's feed resistance beginning its rise. As  $R_{in}$  increases further, this current also reaches levels of around 2mA, at 11cm separation. In both instances the coupled current magnitudes are well within the RFI detection threshold of nearby circuitry, whether by unintentional envelope demodulation or by amplifier saturation.

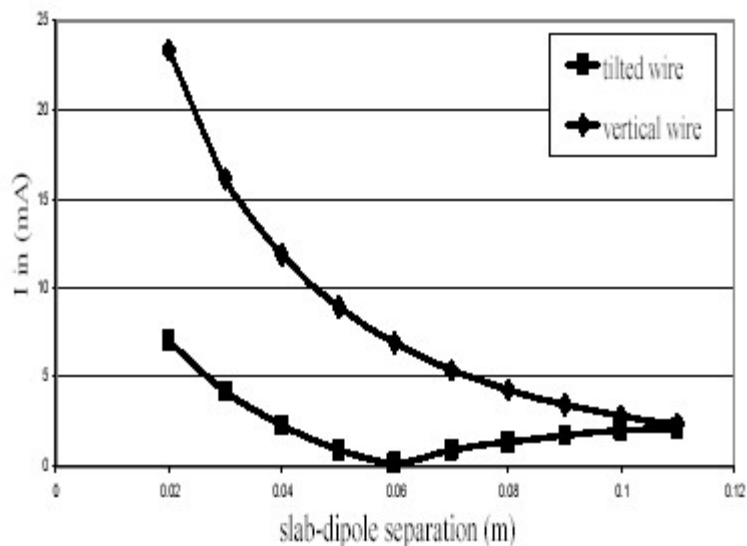


Figure 4: Variation of the maximum induced monitor-wire current versus separation distance, for a dipole feed of 100mA.

### Summary

Dey-Mitra special update equations have been applied to increase the modelling accuracy of tilted conductors in an FDTD environment, and applied to the realistic problem of a biomedical monitor wire laid close to human tissue, the whole structure under illumination from a UHF dipole. The work quantifies the RFI potential of personal radios operating in close proximity to susceptible conductors. The Conference presentation will include current distributions found along the wire length and the effect of close coupling on PR antenna polar patterns and body SAR.

for a waist-mounted 1.8 GHz cellular telephone handset," *Phys. Med. & Biol.*, 48, pp1675-1684, June 2003.

2. Schneider J.B. and Shlager K.L. "FDTD simulations of TEM horns and the implications for staircased representations," *IEEE Trans. Ant. & Prop* </U>, 45, 12, pp1830-1838, Dec 1997.

Table 1: Comparing feed characteristics of similar 435 MHz half-wave dipoles (a) mounted vertically (b) tilted at 45°.							
Resonant frequency (MHz)	Input impedance ( $\Omega$ )			Software used			
		Remcom XFDTD	COCA	COCA (+Dey-Mitra)			
Vertical dipole		438.85	73.41-j4.34	436.29	72.88-j0.77	-	
45° dipole		454.29	77.58+j2.98	465	76.43+j2.29	436.29	74.13-j1.56
Shift from 'vertical' resonant frequency (%)		+3.52		+6.58		0	
Shift in $R_{in}$ (%)		+5.68		+4.87		+1.72	

10-4 STUDENT

**DOSIMETRY AND UNCERTAINTY ASSESSMENT OF PERFORM A EXPOSURE SYSTEMS.**  
 V. J. Berdiñas Torres, S. Ebert, A. Klingenboeck, J. Froehlich, N. Kuster. Foundation for Research on Information Technologies in Society, Zurich, Switzerland.

**INTRODUCTION:** The exposure phases of the studies on effects associated with chronic exposure to cell phone RF radiation performed within the PERFORM A project of the European Union have been completed. Two types of exposure setups for mice and two types for rats were developed for a large toxicological/carcinogenic study to be performed in the context of the health risk assessment of low-level exposure to the RF of mobile phones. A detailed dosimetric evaluation of the exposure is a basic precondition to enable high quality discussions and interpretations of the results of the histopathology.

**OBJECTIVE:** The goal of this study is to provide the dosimetric results of the whole-body spatial peak and averaged exposure levels as well as the organ-specific SAR values. The data shall include the uncertainty of the assessment, the instant variations, the variations of the averaged exposure during an entire exposure session as well as of the entire lifetime.

**METHODS:** Three mouse and four rat high-resolution anatomical models were developed based on microtom slices, considering different mouse and rat strains, genders and weights, with more than 100 parts of the body discriminated. Those models were scaled and/or stuffed in order to cover a wide range of weights and positions in the wheel. The dosimetry, the uncertainties and variations were determined as a function of size, age, anatomy, posture. The interactions between the animals and asymmetries due to the setup and higher-modes were evaluated experimentally. The FDTD simulation platform SEMCAD (SPEAG, Switzerland), was used to conduct the numerical evaluations. DASY4 and EASY4, equipped with the latest electric, magnetic, dosimetric and temperature probes, were used to perform the experimental analysis.

RESULTS AND DISCUSSION: Various parameters and their interactions with respect to the animal models and exposure setup (Figure 1) have been considered to assess the SAR variations and uncertainties for whole-body and single organs:

- animal weight: 7 mouse and 6 rat models (original size and scaled) for lifetime
- posture: restrained animal versus non-restrained
- position: animal displacement, front and back, in the restrainer tube
- sector position: 4 different positions of the sector in the wheel
- stopper contact: from full contact to no contact
- anatomy: different models scaled to the same weight (different strain and gender)
- dielectric parameters: variations of  $\pm 10\%$  in epsilon and sigma of all tissues/organs
- spatial and anatomical resolutions
- sweating

All setups, at both 902 MHz and 1747 MHz, were analyzed considering the same variations. SAR evaluation included whole-body averaged SAR, organ-specific averaged SAR and spatial peaks over different masses for the whole-body and organs, 5 and 0.5 mg for mice and 50 and 5 mg for rats. Measurements and simulations using animal phantoms were performed in order to validate the simulations with anatomical models.

ACKNOWLEDGMENT: This study was supported by the 5th Framework Program of the European Union, the Swiss Government, the Mobile Manufacturers Forum and the GSM Association.

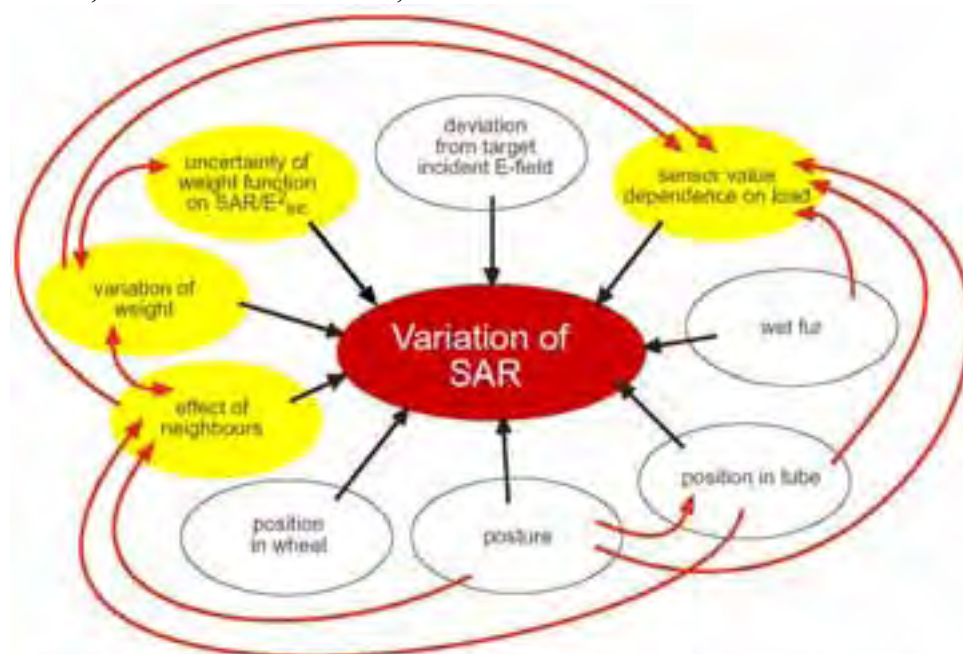


Diagram of parameters and their interactions considered to assess the SAR variations for whole-body and single organs

10-5

**A STUDY ON TEMPERATURE INCREASES IN RABBIT EYES DUE TO 2.45-GHZ ELECTROMAGNETIC WAVE EXPOSURES.** A. Hirata<sup>1</sup>, S. Watanabe<sup>2</sup>, M. Taki<sup>3</sup>, M. Kojima<sup>4</sup>, I. Hata<sup>4</sup>, K. Wake<sup>2</sup>, K. Sasaki<sup>4</sup>, T. Shiozawa<sup>5</sup>. <sup>1</sup>Osaka Univ, <sup>2</sup>National Institute of Information and Communications Technology, <sup>3</sup>Tokyo Metropolitan Univ, <sup>4</sup>Kanazawa Medical Univ, <sup>5</sup>Chubu Univ.

**Objectives:** This paper presents SAR and temperature increases in rabbit eyes due to 2.45-GHz electromagnetic exposures. The rationale for this is that the eye seems one of the organs, which is sensitive to microwave heating. The temperature increase in eyes has been investigated widely (reviewed in [1]). However, microwave sources used in these papers are different (e.g., [2-4]). In order to bridge this gap, we conduct computational studies using the model validated in our previous paper [5].

**Methods:** A numerical rabbit phantom with the resolution of 1 mm is used in our work. For calculating the SAR distribution in the rabbit, the FDTD method is used. Then, the temperature increase in the eye is calculated by solving the bio-heat equation with the substitution of the SAR as the heat source. An active blood flow model, which is varied with local and global temperatures in the rabbit, is used.

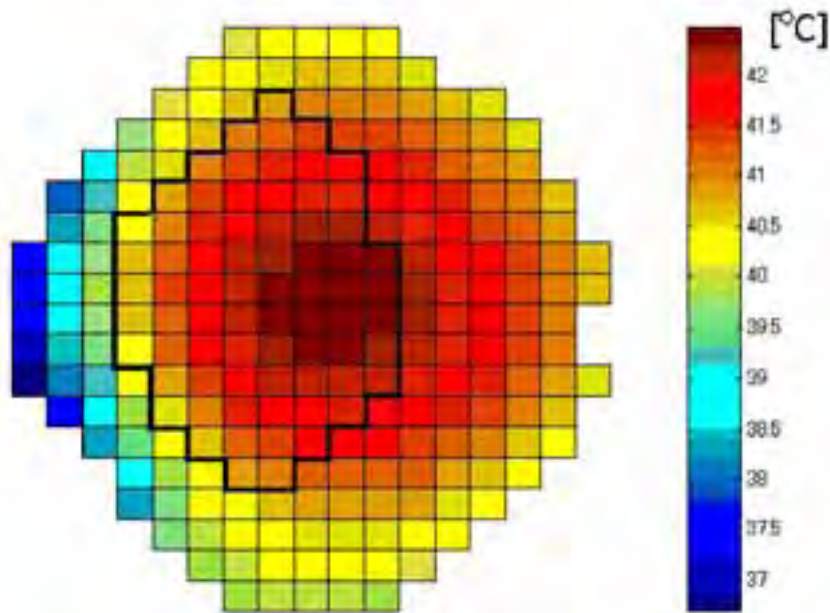
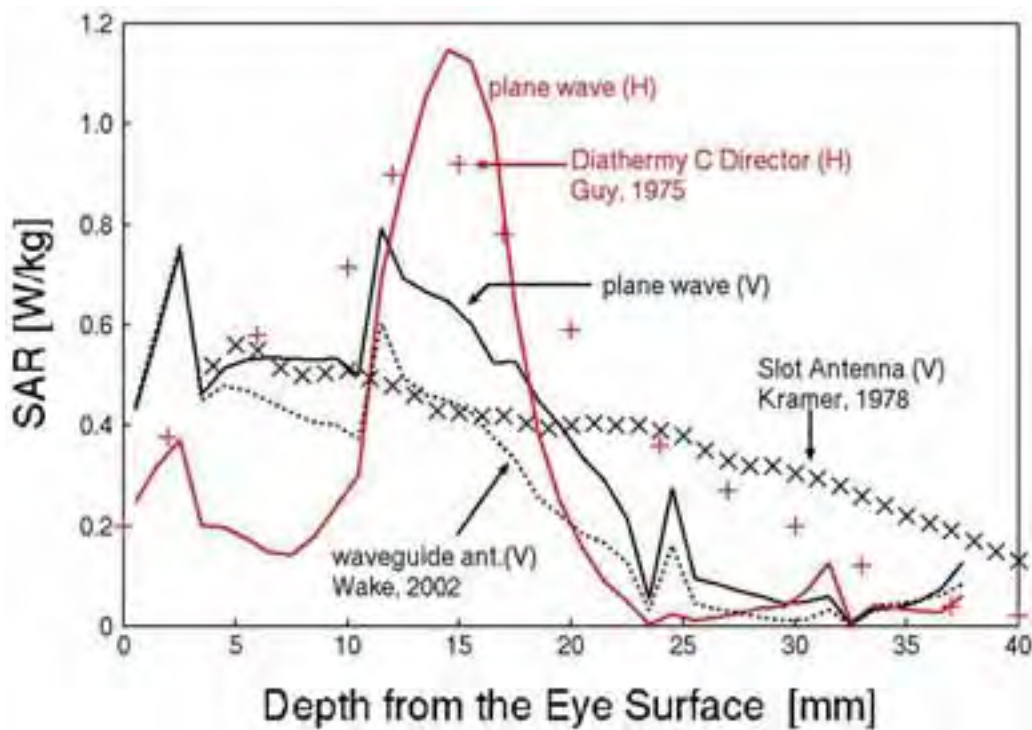
**Results:** Figure 1 illustrates the SAR distribution along the center axis of the eye for near-field microwave sources. For comparison, the results for the plane waves are also drawn. The notations of (V) and (H) in this figure represent the vertical and horizontal polarizations. From this figure, the polarization of the incident waves is found to be the most dominant factor to characterize the SAR distribution in the eye. It is noteworthy that the SAR distributions of the waveguide antenna and plane wave both with the vertical polarization are comparable around the eye surface. With penetrating into the eye, the SAR value for the former source becomes smaller than the later. This is because of diffraction of EM waves due to a finite dimension of the antenna aperture.

The temperatures in the eye with 40-min. EM wave exposures are presented in Fig. 2. The power density of the EM wave is 300 mW/cm<sup>2</sup>. As a wave source, the waveguide antenna with the vertical polarization is chosen in this paper. As seen from this figure, the maximum temperature appears around the posterior of the lens. This is consistent with the result in [2]. This distribution is attributed to the following two factors. One is the thermally steady-state temperature distribution in the eye without EM exposure, or the initial condition. Due to lower temperature in air than in rabbit eyes, the temperature around the eye surface is the lowest in the eye. The other factor is that the SAR becomes large in the aqueous and vitreous due to their large conductivity. Note that the temperature increase is largely affected by the SAR distribution. For other sources, the positions where the maximum temperature appears are almost the same. The temperature distributions for other sources are presented at the conference.

#### Conclusions:

There are two points to be stressed in this paper. Firstly, the most dominant factor to characterize the SAR distribution in the eye is the polarization of incident EM waves. The second point is that the maximum temperatures in the eye for microwave exposures at this frequency band appear around the posterior of the lens.

- 1.J. Elder, *Bioelectromagnetics Suppl.*, vol.6, pp.S148-S161, 2003.
- 2.A. W. Guy et al., *IEEE Trans. Microwave Theory & Tech.*, vol.23, no.6, pp.492-498, 1975.
- 3.P. O. Kramer et al., *Annals. NY Acad. Sci.*, pp.155-165, 1978.
- 4.K. Wake et al, *Proc. of URSI GA*, 2002.
- 5.A. Hirata et al, *ICNIRP Workshop*, May 2004 (Seville, Spain).
- 6.J. J. Lagendijk, *Phys. Med. Biol.*, vol.27, no.11, pp.1301-1311, 1982.



10-6

**SIMULATION OF SAR-PROBE CALIBRATION USING ANTENNAS IN THE LIQUID.** N. Ishii<sup>1</sup>, K. Sato<sup>2</sup>, L. Hamada<sup>3</sup>, T. Iwasaki<sup>3</sup>, S. Watanabe<sup>4</sup>. <sup>1</sup>Niigata Univ, Niigata, Japan, <sup>2</sup>NTT Advanced Technology, Tokyo, Japan, <sup>3</sup>The Univ of Electro-Communications, Tokyo, Japan, <sup>4</sup>National Institute of Information and Communication Technology, Japan.

**INTRODUCTION:** The most popular method for SAR-probe calibration uses waveguides with a  $\lambda/4$ -matching dielectric slab. At higher frequency, however, the SAR probe can affect the E-field distribution in the waveguide because the tip size of the probe is comparable with the cross section of the waveguide. It can deteriorate the accuracy of the calibration significantly. In this view point, a calibration procedure with analytical fields determined by the Friis transmission formula in the liquid has promise as one candidate of the SAR probe calibration above 3GHz.

**OBJECTIVE:** As a preliminary study on the new calibration, the absolute gain of the half-wavelength dipole in the liquid, which can be used for evaluation of the standard E-field in the new calibration procedure, is simulated with the method of moment (MoM).

**METHOD:** The electromagnetic wave suffers more attenuation at the higher frequency in the liquid so that the accuracy of the positioning of the probe would be required. To improve the precision of the calibration, the conventional two antenna method is used to determine the absolute gain of the reference antenna. This method is based on curve fitting technique of  $S_{21}$  between two antennas as a function of the distance.

**SUMMARY OF THE RESULTS:** The new calibration should be performed in the far-field. The far-field region should be identified in consideration of the attenuation in the liquid. Figure 1 shows the ratio of the magnitude of the far field to that of the rigorous field as a function of the distance R. The ratio is almost unity if  $R > 60, 40,$  and  $20\text{mm}$  at  $900, 1450,$  and  $5400\text{MHz}$ , respectively. The wavelength is about  $25.2, 16.0,$  and  $4.5\text{mm}$  at  $900, 1450,$  and  $5400\text{MHz}$ , respectively. Therefore, it has been estimated that the far field in the liquid ranges further than one-half wavelength from the antennas. Figure 2 shows the absolute gain as a function of the distance which indicates the center of the range of the curve fitting. At each distance in the figure 2, the measured  $S_{21}$  at the distance from  $-10\text{mm}$  to  $+10\text{mm}$  were used for the curve fitting. In the figure, dashed lines are the values of the absolute gains evaluated in ideal far-field region by the MoM code. If the fitting is appropriately performed, the dashed lines agree with marked solid lines. For the higher frequencies, good agreements are observed even if the distance between the antennas is a few centimeters. This fact means that the new calibration is applicable for the higher frequencies.

**CONCLUSION:** A new SAR-probe calibration method based on the S-parameters of the antenna network as a function of the distance between the antennas is proposed. We have investigated the method using the two small antennas as the reference antennas in the liquid and determined the distance between the antennas which is required for accurate calibration.

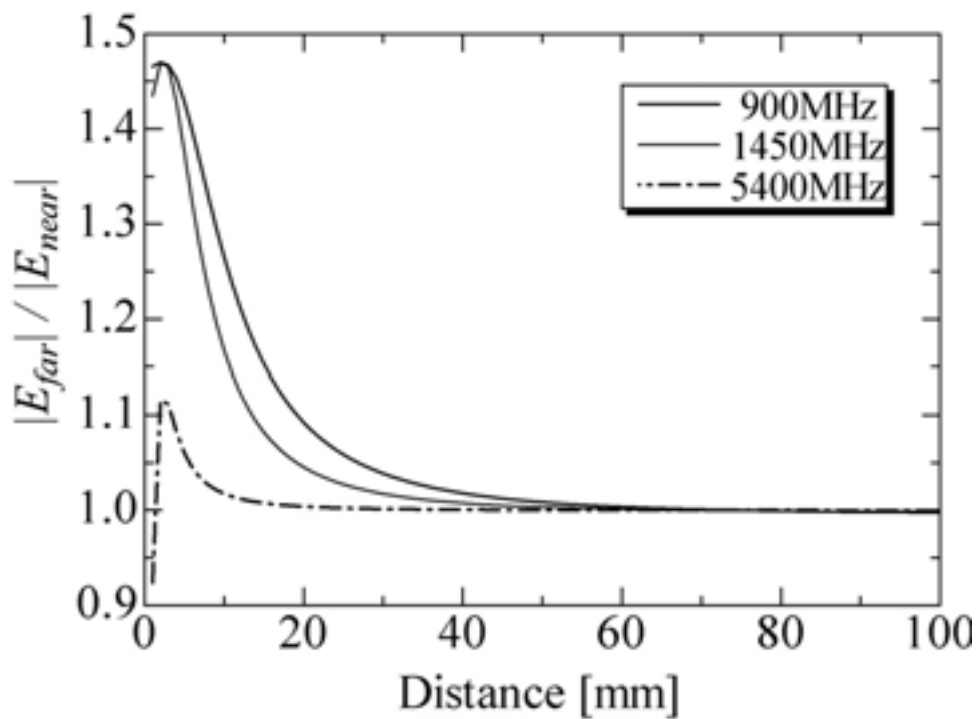


Figure 1: Ratio of the magnitude of the far field to that of the rigorous field of the half-wavelength dipole in the liquid.

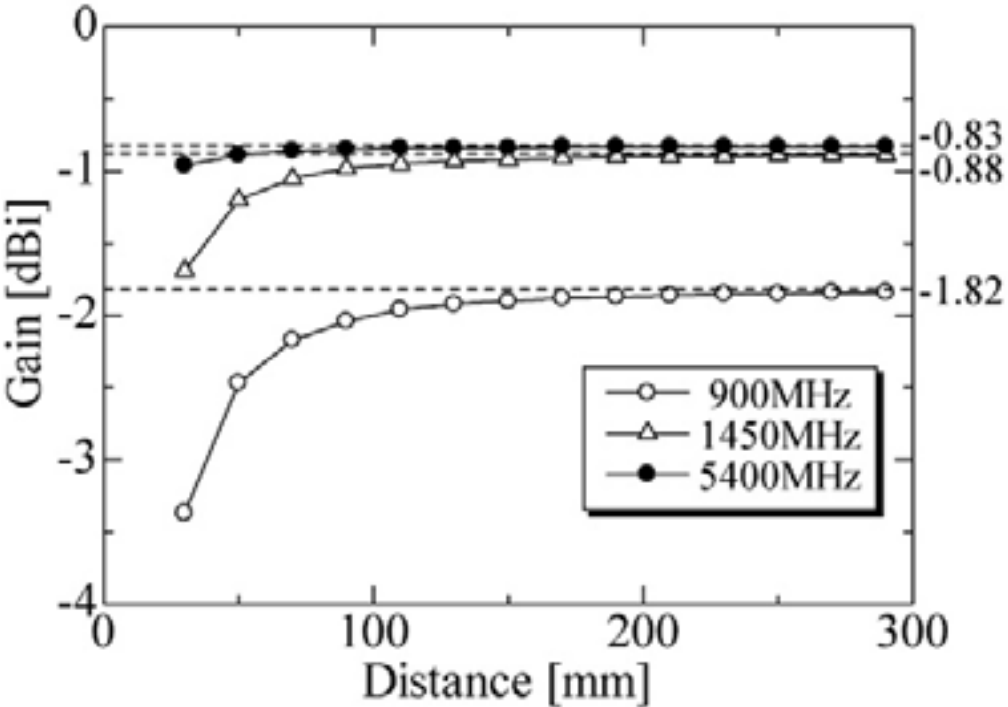


Figure 2: Distance between two half-wavelength dipoles v.s. absolute gain.

**Session 11: Epidemiology**  
**Chairs: Elizabeth Cardis and Maria Feychting**  
**4:00 - 5:30 pm, Theatre M**

11-1

**FEASIBILITY OF FUTURE EPIDEMIOLOGICAL STUDIES ON POSSIBLE HEALTH EFFECTS OF MOBILE PHONE BASE STATIONS.** G. Neubauer<sup>1</sup>, M. Röösl<sup>2</sup>, M. Feychting<sup>3</sup>, Y. Hamnerius<sup>4</sup>, L. Kheifets<sup>5</sup>, N. Kuster<sup>6</sup>, I. Ruiz<sup>1</sup>, J. Schüz<sup>7</sup>, J. Wiart<sup>8</sup>. <sup>1</sup>Seibersdorf research, Austria, <sup>2</sup>Univ Bern, Switzerland, <sup>3</sup>Karolinska Institutet, Sweden, <sup>4</sup>Chalmers Univ, Sweden, <sup>5</sup>UCLA, USA, <sup>6</sup>ITIS, Switzerland, <sup>7</sup>Univ of Mainz, Germany, <sup>8</sup>France Telecom research center, France.

**INTRODUCTION:** The increasing use of mobile phones in the last decade triggered an important deployment of mobile telephone base stations worldwide and in particular in Europe. Base stations are already ubiquitous, e.g. around 18,000 base stations are operated in Austria. Concerns have been raised by both the general public and decision makers about potential health effects of emissions from base stations. There is therefore a need for the society to have information on exposure and the effects of exposure, leading to the demand on epidemiological studies on potential health effects. **OBJECTIVE:** This research project brings together in a collaborative effort leading international scientists in RF-engineering/dosimetry and epidemiology to jointly assess the feasibility of epidemiological studies on health impacts of RF-exposure from mobile phone base stations. The feasibility of epidemiological studies on possible health effects of mobile phone base stations depends on finding solutions to scientific problems, e.g. reliable estimates of exposure, control for bias and confounding, selection of health outcomes, therefore these aspects were analysed. Because studies using inadequate design could lead to wrong conclusions and/or increasing concerns in the population, we include recommendations and quality criteria for such studies.

**METHODS:** Based on the evaluation of existing knowledge in that field epidemiological study designs for the investigation of potential health effects of RF exposure were developed. Types of health outcome to be investigated, basic principles of exposure assessment, definition of metrics, and the relevance of other RF sources, proxies and exposure blinding were considered. The relevance of control for bias and confounding was discussed. Suggested methods are given for immediate, short term and long term effects. Because exposure assessment is crucial requirements on future assessments are given. Calculations, spot measurements, monitoring of exposure and the use of dosimeters are discussed.

**RESULTS:** Possible dosimetric approaches are summarized below:

- One approach might be the use of monitoring systems to assess variations in time of different contributions, in particular in studies where people are expected to stay at the same location
- Another approach might be the use of dosimeters to assess individuals exposure where people are expected to change their location
- Numerical and/or analytical tools could be used to provide crude estimates (for stratification) of exposures from specific fixed transmitting installations

Given paucity of data, selection of the outcome may be based on anecdotal reports and/or on analogy from ELF research. Physiological measures can be objectively measured and are useful to evaluate hypothesized biological mechanisms. On the other hand, soft outcomes, e.g. sleep, headache, well-being are more difficult to assess. Soft outcome measurements are primarily based on questionnaires and are only occasionally complemented by objective methods. Dealing with different types of outcomes we have to be aware that Nocebo effects are in general very relevant in the context of base station exposure. The Nocebo effect is the inverse of the Placebo effect and means that adverse symptoms are expressed by expectations (due to concerns). The Nocebo effect has to be addressed when designing studies. It is recommended that methods are used which are as objective as possible, e.g. actigraphs for sleep, validated questionnaires for assessing well-being. Note that the use of questionnaires is always very problematic if study participants are aware of exposure status.

For “electromagnetic hypersensitivity” there are currently no diagnostic criteria, objective signs, or measurement instruments available. The concept “electromagnetic hypersensitivity” is in itself problematic as the exposure is included in the definition of the condition. The concept relies solely on the subject's own attribution of his/her symptoms to electromagnetic fields. Chronic diseases can be objectively diagnosed, however need long term follow up and often a retrospective exposure assessment.

It is not generally recommended to neglect a priori the contributions from other RF sources than mobile phone base stations. Knowledge about biologically critical exposure circumstances and knowledge about exposure contribution from base stations compared to other RF sources in the general population is still limited. Exposure from base station might be relevant if one is interested in total exposure time above a very low threshold, e.g.  $> 0.5$  V/m, it may be relevant for 24 hours whole body exposure, or if an effect is extremely frequency and/or signal specific. In contrast, base station exposure seems not to be relevant for momentary exposure levels at a specific body site.

This project is sponsored by the Swiss Research Foundation on Mobile Communication, the Swiss Agency for the Environment, Forests and Landscape and the Swiss Federal Office of Public Health

11-2

**DO MOBILE PHONES CAUSE BRAIN TUMOURS – REPORT FROM THE DANISH PART OF THE INTERPHONE STUDY.** C. Johansen<sup>1</sup>, H. C. Christensen<sup>1</sup>, J. Schuz<sup>2</sup>, M. Kosteljanetz<sup>3</sup>, H. S. Poulsen<sup>4</sup>, J. D. Boice, Jr<sup>5</sup>, J. K. McLaughlin<sup>5</sup>. <sup>1</sup>Institute of Cancer Epidemiology, The Danish Cancer Society, Copenhagen, Denmark, <sup>2</sup>Institute for Medical Biostatistics, Epidemiology and Informatics, Univ of Mainz, Germany, <sup>3</sup>Neurosurgical Dept, Univ Hospital of Copenhagen, Denmark, <sup>4</sup>Oncological Dept, Univ Hospital of Copenhagen, Denmark, <sup>5</sup>International Epidemiology Institute, Rockville, MD, USA.

A nationwide population-based case-control study of incident cases of meningioma and glioma was conducted to evaluate a possible association with use of cellular telephones. We ascertained all incident cases of glioma and meningioma diagnosed in Denmark between 1 September 2000 and 31 August 2002. We enrolled 252 persons with glioma and 175 persons with meningioma aged 20–69. We also enrolled 822 randomly sampled, population-based controls matched

on age and sex. Information was obtained from personal interviews, medical records containing diagnoses and the results of radiological examinations. For a small number of cases and controls, we obtained the numbers of incoming and outgoing calls. We evaluated the memory of the respondent's with the Mini Mental State Examination and obtained data on socio-economic factors from Statistics Denmark.

There were no material socioeconomic differences between cases and controls or participants and non-participants. Use of cellular telephone was associated with a low risk for high-grade glioma (odds ratio, 0.58, 95% confidence interval, 0.37–0.90). The risk estimates were closer to unity for low-grade glioma (1.08, 0.58–2.00) and meningioma (1.00, 0.54–1.28).

Our results do not support an association between use of cellular telephones and risk for glioma or meningioma.

The study was funded by the European Union Fifth Framework Program, the Danish Cancer Society, and the International Union against Cancer (UICC). The UICC received funds for this purpose from the Mobile Manufacturers' Forum and GSM Association. Provision of funds to the INTERPHONE study investigators via the UICC was governed by agreements that guaranteed INTERPHONE's complete scientific independence. These agreements are publicly available at <http://www.iarc.fr/pageroot/UNITS/RCA4.html>

**LONG-TERM MOBILE PHONE USE AND THE RISK OF BRAIN TUMORS – RESULTS FROM THE SWEDISH PART OF THE INTERPHONE STUDY.** S. Lonn<sup>1</sup>, A. Ahlbom<sup>1</sup>, P. Hall<sup>2</sup>, M. Feychting<sup>1</sup>. <sup>1</sup>Institute of Environmental Medicine, Karolinska Institutet, Stockholm, Sweden, <sup>2</sup>Dept of Medical Epidemiology and Biostatistics, Karolinska Institutet, Stockholm, Sweden.

#### INTRODUCTION AND OBJECTIVE

The level of human exposure to radiofrequency radiation has increased during recent years due to the widespread use of mobile phones. If radiofrequency radiation has a carcinogenic effect the exposure poses an important public health problem, and intracranial tumors would be of primary interest. A study based on the Swedish population will have a relatively large proportion of long-term mobile phone users. We performed a case-control study of mobile phone use and the occurrence of brain tumors as part of the INTERPHONE study.

#### METHODS

The study population included approximately 3.7 million people and was restricted to all residents aged 20 to 69 years in the geographical areas covered by the regional cancer registries in Umeå, Stockholm, Göteborg, and Lund. The study period was from 1 September 2000 to 31 August 2002. Eligible cases were all individuals diagnosed during the study period with intracranial glioma or meningioma. Controls were randomly selected from the study population stratified on age, gender, and residential area. Information about mobile phone use and other possible risk factors was collected through personal interviews. Associations between indicators of mobile phone use and the tumors were estimated as relative risks, approximated by odds ratios, using unconditional logistic regression models, with 95 percent confidence intervals (CI). Adjustment for the stratification variables and education were made in all analyses.

#### RESULTS

Detailed information about mobile phone use was collected from 371 glioma and 273 meningioma cases, and 674 controls. For regular mobile phone use the relative risk was estimated to 0.8 (95% CI: 0.6, 1.0) for glioma and 0.7 (95% CI: 0.5, 0.9) for meningioma. Similar results were found for more than 10 years duration of mobile phone use. No risk increase was found for ipsilateral phone use for tumors located in the temporal and parietal lobes. Furthermore, the relative risk did not increase, regardless of tumor histology, type of phone, or amount of use.

#### CONCLUSION

This study includes a large number of long-term mobile phone users, and we conclude that the results do not support the hypothesis that mobile phone use increases the risk of glioma or meningioma.

The study was funded by the European Union Fifth Framework Program, the Swedish Research Council, and the International Union against Cancer (UICC). The UICC received funds for this purpose from the Mobile Manufacturers' Forum and GSM Association. Provision of funds to the INTERPHONE study investigators via the UICC was governed by agreements that guaranteed INTERPHONE's complete scientific independence. These agreements are publicly available at <http://www.iarc.fr/pageroot/UNITS/RCA4.html>

**CASE-CONTROL STUDY IN PATIENTS DIAGNOSED 2000-2003 WITH ACOUSTIC NEUROMA OR MENINGIOMA AND USE OF CELLULAR AND CORDLESS TELEPHONES.**

L. Hardell<sup>1,2</sup>, K. Hansson Mild<sup>2,3</sup>. <sup>1</sup> Dept of Oncology, Univ Hospital, Örebro, Sweden, <sup>2</sup> Dept of Natural Sciences, Örebro Univ, Örebro, Sweden, <sup>3</sup>National Institute for Working Life, Umeå, Sweden.

We performed a case-control study on the use of cellular and cordless telephones and the risk for brain tumors. Cases diagnosed with acoustic neuroma or meningioma were recruited during the time period July 1, 2000 until December 31, 2003. Both men and women aged 20-80 years at the time of diagnosis were included. They were inhabitants in the Uppsala/Örebro and Linköping medical regions in Sweden. All had a histopathological diagnosis that had been reported to the regional cancer registries. One control from the national population registry was identified to each finally included case. They were matched on age and selected at random in 5-year age groups according to the number of cases in the different age groups and lived in the same geographical area as the cases. We report the results for benign brain tumours with data from 413 cases (89 % response rate), 305 with meningioma, 84 with acoustic neuroma and 24 with other types, and 692 controls (84 % response rate). Analogue phones yielded for meningioma odds ratio (OR) = 1.72, 95 % confidence interval (CI) = 0.98-3.01 increasing to OR = 2.46, 95 % CI = 1.21-5.00 with >10 years latency period. Also digital cellular phones and cordless phones increased the risk. For acoustic neuroma analogue phones gave OR = 4.24, 95 % CI = 1.78-10.1. With >15 years latency period OR increased to OR = 9.22, 95 % CI = 1.79-47.5, but based on low numbers. Digital phones gave OR = 1.97, 95 % CI = 1.04-3.70. In the multivariate analysis analogue phones were a significant risk factor for acoustic neuroma.

**EFFECT OF SHORT-WAVE MAGNETIC FIELDS ON SLEEP QUALITY AND MELATONIN CYCLE IN HUMANS: THE SCHWARZENBURG SHUT-DOWN STUDY.** M. Rösli, E. Altpeter,

T. Abelin. Dept of Social and Preventive Medicine, Univ of Bern.

**Objectives:** This paper describes the results of a unique 'natural experiment' of the operation and cessation of a broadcast transmitter with its short-wave electromagnetic fields on sleep quality and melatonin cycle in a general human population sample.

**Methods:** In 1998, 54 volunteers (21 men, 33 women) were followed for one week each before and after shut-down of the short-wave radio transmitter at Schwarzenburg (Switzerland). Salivary melatonin was sampled 5 times a day and total daily excretion and peak time of the acrophase were estimated using complex cosinor analysis. Sleep quality was recorded daily using a bipolar visual analogue scale (VAS) to rate freshness (100) and tiredness (0) in the morning. Only workday measurements have been analysed in order to ensure comparability. Chronic effects of short wave radiation were investigated by comparing outcome measurements during the baseline period (before shut-down) in association with the magnetic field exposure (cross-sectional). Acute effects from shut-down were studied in a within subject analysis where every subject served as his/her own control. For this analysis, we fitted the outcome measurements after shut-down using a random effects model taking into account the respective baseline value. All models were adjusted for age and sex. Melatonin excretion levels were log transformed due to skewed data distribution. A robust coefficient estimation method was used (median regression). In

addition stratified analyses in good and poor sleepers were carried out separately, using median sleep quality as division criteria.

Results: Before shut down of the transmitter H-field exposure of the study population was in the range of 0.2 to 6.7 mA/m (mean 1.5 mA/m, median 0.92 mA/m). After shut down there were no emission sources left in this frequency range. Before shut down self rated sleep quality was increased by 3.9 units (95% CI: 1.7 to 6.0) per mA/m decrease in magnetic field exposure indicating a chronic effect (see Table). The corresponding increase in melatonin excretion was 11 percent (95% CI: -17 to 47 percent). With respect to acute effect, sleep quality improved by 1.7 units (95% CI: 0.1 to 3.4) per mA/m decrease in magnetic field exposure after shutdown. Melatonin excretion increased by 15 percent (95% CI: -3 to 36 percent) compared to baseline values suggesting a rebound effect. Peak time of the melatonin cycle was neither chronically nor acutely associated with EMF exposure. Stratified analyses showed an acute exposure effect on sleep quality and melatonin excretion in poor sleepers but not in good sleepers (see Table).

Conclusions: We found evidence, though limited, of an effect of short-wave EMF on sleep quality and melatonin excretion in poor but not good sleepers. Blinding of exposure was not possible in this observational study and this may have affected the outcome measurements in a direct or indirect (psychological) way.

The study was supported by the Swiss National Science Foundation and SWISSCOM corporation.

Chronic and acute effects of EMF on morning tiredness, AUC and Peak time. Coefficients refers to a change in outcome parameter per unit decrease in EMF exposure [mA/m].

Outcome	type of effect	of sleep quality	Coefficient	Lower 95%-CI	Upper 95%-CI	p-value
Sleep quality [VAS]	chronic	all	3.9	1.7	6.0	0.001
Melatonin excretion [ratio]*	chronic	all	1.11	0.83	1.47	0.476
Peak time [min]	chronic	all	4.4	-16.6	25.4	0.675
Sleep quality [VAS]	acute	poor	3.5	1.7	5.4	0.00
	acute	good	-1.3	-3.9	1.3	0.33
Melatonin excretion [ratio]*	acute	poor	1.26	1.08	1.47	0.00
	acute	good	1.01	0.73	1.39	0.96
Peak time [min]	acute	poor	5.6	-8.2	19.3	0.43
	acute	good	0.8	-16.4	18.0	0.93

\* For AUC the coefficients refer to a change in the ratio due to the logarithm transformation.

## **A COMPARISON OF RECALL OF MOBILE PHONE USE WITH BILLING RECORD DATA.**

M. Shum<sup>1</sup>, M. A. Kelsh<sup>1</sup>, K. Zhao<sup>1</sup>, L. S. Erdreich<sup>2</sup>. <sup>1</sup>Exponent, Inc., Menlo Park, CA, <sup>2</sup>Exponent, Inc., New York, NY, USA.

**INTRODUCTION:** In many epidemiologic studies of potential health effects of radiofrequency (RF) exposure from mobile phones, duration of phone use is often used as the only surrogate of exposure. Oftentimes, billing records are not available and exposure is estimated from participants' recall of their mobile phone use, ascertained from questionnaires or interviews. In several previous validation studies of user recall of mobile phone use, either the period of recall was very short (e.g. past week or past month) or the number of study participants was relatively small. The availability of a centralized data set of billing information that spanned several years allowed us to examine the accuracy of self-reported usage over a longer recall period.

**OBJECTIVE:** To evaluate the accuracy of recall data from questionnaire surveys compared to billing records in a population of scientific and engineering consultants.

**METHODS:** Volunteer participants from a subset of employees who had been issued company cellular phones, were asked to complete a web-based questionnaire that included questions about cell phone usage including 1) number of daily calls, 2) duration of usage in daily, weekly, or monthly intervals, 3) usage during weekends and weekdays, 4) time of day of most frequent use, as well as other questions. Participants were asked to recall not only recent usage, but to recall usage up to three years in the past. Questionnaire results were compared with billing records data, and agreement and the precision of self-reported data were assessed.

**RESULTS:** Data are summarized for 61 volunteers who participated in this study and for whom data were available. Of these 61 volunteers, 43 (70%) could be matched with billing records going back three years, 15 (24.6%) could be matched with records going back 2 years, and 3 (5%) had only records for the past year. The average number of minutes per call based on billing records was 2.8. The average number of minutes used per day based on questionnaire responses was 15.2 compared to 18.3 from the billing record data. The average number of minutes on weekdays based on questionnaire responses was 15.2 compared to 20.4 from the billing record data. The average number of minutes of weekend days based on questionnaire responses was 6.4 compared to 10.5 from the billing record data. A large proportion of participants could not estimate their duration of usage to within 50% of the billing record data (42%, 39%, and 68% for daily, weekday, and weekend questions, respectively) (Table 1). Additional results by calendar period, demographics, and other factors are also discussed.

**DISCUSSION:** Few studies have evaluated the accuracy of historical mobile phone usage recall. Our research is unique in that we evaluate recall of cellular phone use going back three years. In general, participants underestimated their duration of cellular phone usage when compared to billing record data. A majority of participants were not able to report their duration of use to within +/- 25% of the minutes ascertained from billing record data. One possible explanation for recall bias is that these individuals use company phones and may not review their company-paid bills. In addition, most participants in this study, consistent with current market trends for mobile phone service, were under "flat-rate" monthly-plans, making them less likely to be aware of the actual duration of phone use. We note, however, that the study population consisted of mainly engineers and scientists and may not be representative of the general public. Although based on a relatively small sample, our study suggests that relying solely on recall of cellular phone usage as a surrogate for RF exposure may result in considerable misclassification in epidemiologic studies.

**ACKNOWLEDGEMENTS:** Technical Oversight: Radiation Biology Branch, Center for Devices and Radiological Health, U.S. Food & Drug Administration (FDA). This research was reviewed and approved by an Institutional review board (WIRB). Research Funding: Cellular Telephone and Internet Association (CTIA)

Table 1: Frequency Distribution of Percentage Difference Between Questionnaire Data and Billing Record Data

% Difference	# of Participants	% of Participants
Daily		
+/- 25%	19	30.7
+/- 50%	16	25.8
>+/-50%	26	41.9
Weekdays*		
+/- 25%	15	24.2
+/- 50%	17	27.4
>+/-50%	24	38.7
Weekends*		
+/- 25%	9	14.5
+/- 50%	7	11.3
>+/-50%	42	67.7

\*Totals do not add up to 61, because not all participants answered these questions in the questionnaire.

## Alessandro Chiabrera Memorial Student Session

*Chairs: Marko Markov and Gabi Nindl*

**8:00 - 10:00 am, O'Reilly Hall**

ST-1

**NUMERICAL SIMULATION OF WHOLE-BODY SAR IN HIGH-RESOLUTION VOXEL HUMAN MODELS STANDING ON THE GROUND PLANE.** K. Arai<sup>1,2</sup>, T. Nagaoka<sup>2</sup>, S. Watanabe<sup>2</sup>, J. Wang<sup>3</sup>, O. Fujiwara<sup>3</sup>, M. Taki<sup>4</sup>, T. Uno<sup>1</sup>. <sup>1</sup>Tokyo Univ of Agriculture and Technology, <sup>2</sup>National Institute of Information and Communications Technology, <sup>3</sup>Nagoya Institute of Technology, <sup>4</sup>Tokyo Metropolitan Univ.

Introduction: Numerical human models with 2mm-resolution voxels have been developed based on anatomical images from MRI and X-ray CT [1-3]. These voxel models have been used for SAR calculation with FDTD method. It is however difficult to apply these models to whole-body SAR calculation in VHF band because required time steps and space between the human models and the absorbing boundaries often become unpractical. Most previous studies have reluctantly transformed from the voxel models with fine mesh (1-2 mm) to those with coarse mesh (5-10mm)[1-2]. Objectives: With using a super computer, we have tried very large-scale numerical simulation for whole-body SAR calculation in VHF band. In order to validate and optimize such large-scale calculations, at first, we investigate required time steps and spaces between the human models and

absorbing boundaries. After establishment of the calculation conditions, we calculate the whole-body SAR calculation of the human body standing on the ground plane in VHF band, in which the whole-body resonance can occur.

Preliminary results and discussion: In order to establish required conditions for FDTD calculation in VHF band, we calculated whole-body averaged SARs in a homogeneous sphere with 1.7-m diameter and compared with analytical solutions of Mie theory. Liao's absorbing boundary conditions were used. Two cell sizes (5 mm and 10 mm) were assumed. The comparison between the FDTD calculation with 10-mm cells and the Mie theory are shown in Fig. 1. At higher frequencies (100MHz~), the error of the FDTD calculation increases. The comparison in the case of 5-mm FDTD cells is shown in Fig. 2. In this case, opposite trend appears that the errors of the FDTD calculation increase at lower frequencies (~100 MHz) while good agreement is shown at higher frequencies. Enlarging the space between the sphere and the boundaries, especially, the space in the direction of the incident E-field, reduces the error at the lower frequencies. We will present the detail of our investigation on the requirement for FDTD calculation in VHF band and various characteristics of the whole-body SAR with very high spatial resolution.

Reference:

- [1] P J Dimbylow "Fine resolution calculations of SAR in the human body for frequencies up to 3 GHz", Phys. Med. Biol. 47, pp.2835-2846, 2002
- [2] Mason P A, et al. "Recent advancements in dosimetry measurements and modeling Radio Frequency Radiation Dosimetry" ed B J Klauenberg and D Miklavcic (Dordrecht: Kluwer) pp.141-55, 2000
- [3] Tomoaki Nagaoka, et al. "Development of Realistic High-Resolution Whole-Body Voxel Models of Japanese Adult Male and Female of Average Height and Weight, and Application of Models to Radio-Frequency Electromagnetic-Field Dosimetry" Physics in Medicine and Biology, Vol.49, pp.1-15, 2004.

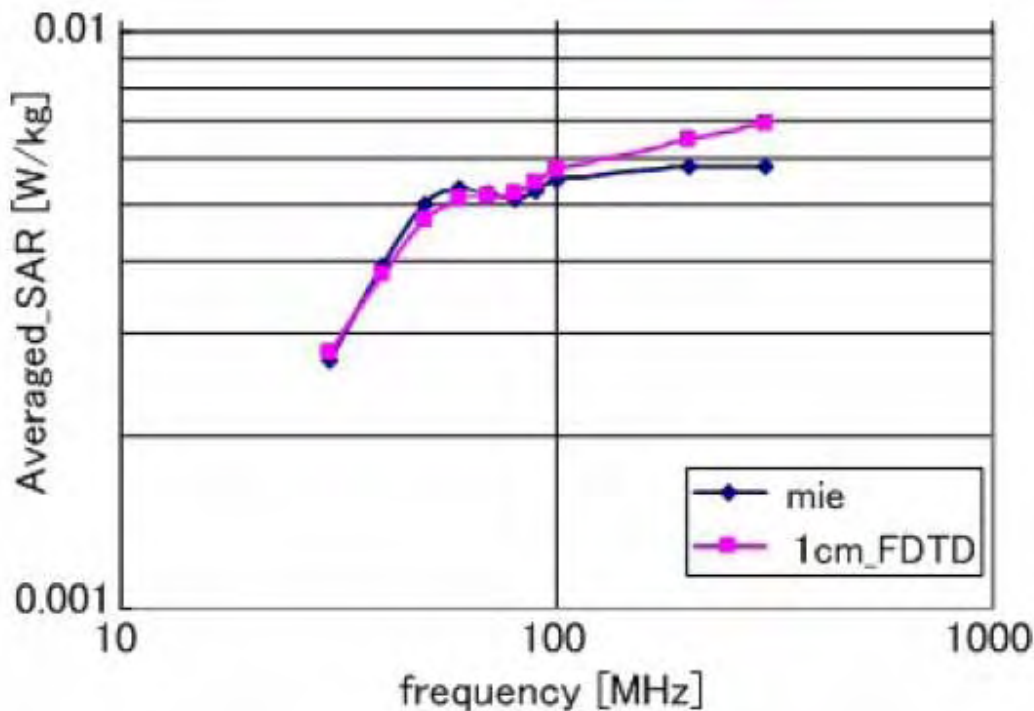


Figure 1: Frequency characteristics of whole-body averaged SARs of the homogeneous sphere evaluated from FDTD calculation with 10-mm cell sand from analytical solutions of Mie theory.

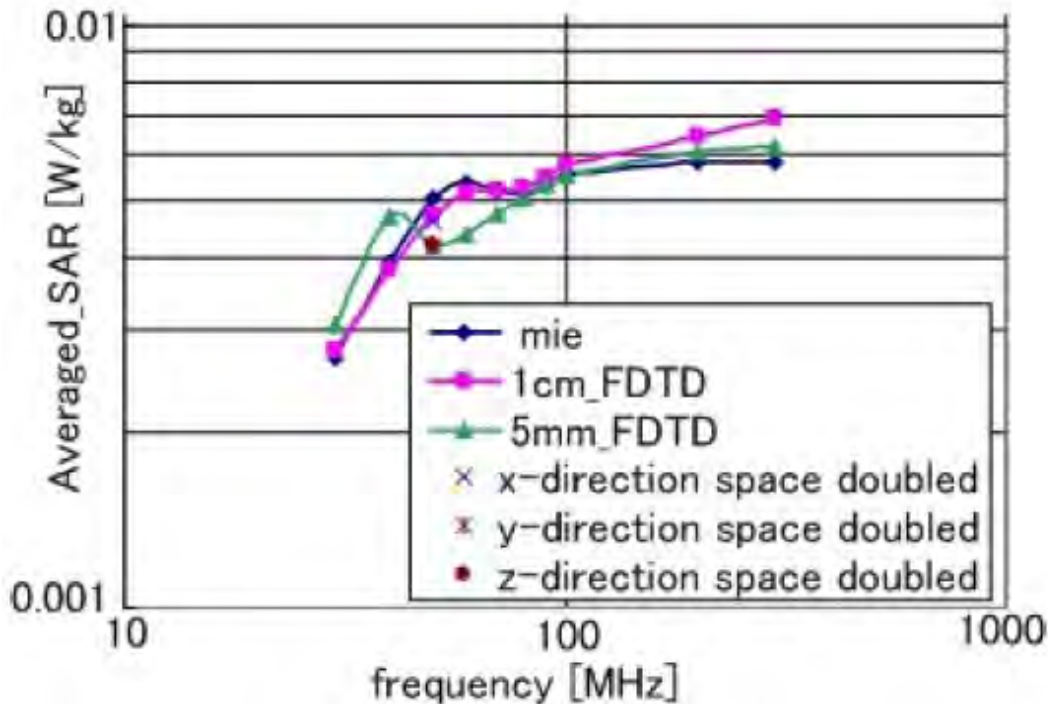


Figure 2: Frequency characteristics of whole-body averaged SARs of the homogeneous sphere evaluated from FDTD calculation with 5-mm cells and from analytical solutions of Mie theory. "x-axis double" means analytic region is expanded in the direction of the incident E-field.

ST-2

**EFFECTS OF 900 MHZ MOBILE PHONE RADIATIONS ON NEURONAL ACTIVITY OF RAT.** E. Brillaud<sup>1</sup>, A. Piotrowski<sup>1</sup>, P. Romanini<sup>2</sup>, R. de Seze<sup>1</sup>. <sup>1</sup>INERIS, Parc technologique ALATA, Verneuil-en-Halatte, France, <sup>2</sup>Institute of Human Physiology, Univ of Bologna, Italy.

Objectives:

Electromagnetic fields (EMF) are suspected to have biological effects. In the framework of RAMP 2001 project, we try to evaluate possible effects of GSM exposure on the central nervous system and to determine the Specific Absorption Rate (SAR) limit that produces them. Precedents results of B. Bontempi (COMOBIO project, presented at SFRP meeting, April 2004, Pessac; article in progress) show a modification of the cerebral cartography of rats, using the c-fos activity marker, after a 120 min exposure to a standard GSM signal 900MHz (exposure head only, loop antenna set up). These data show a window effect. In comparison to control sham animals, activity is mainly modified after a 2 hours exposure to a SAR of 1.5 W/kg, but not at all for lower or higher doses (SAR of 0.75, 3 and 6 W/kg). Moreover, non superficial cerebral structures, not directly exposed to the emitted signal (except frontal cortex and prefrontal median), also seem to have a modified activity. It could indicate that a cascade of reactions intervenes upstream the activation of FOS gene. The goal of this study was to reproduce and to supplement the study of project COMOBIO, in order to check the c-fos activity following an exposure at a 900MHz signal. Moreover, we chose to study in parallel an earlier marker, the phosphorylation of the CREB protein (pCREB), being able to involve a c-fos activation.

Methods:

Rats were exposed using a head only set up (loop antenna) to a GSM 900 MHz signal to various SAR and duration:

- 120 min with DAS of 0.75, 3 and 6W /kg
- - 15, 30, 45 or 120 min with a DAS of 0 and 1.5W/kg
- Animals were then sacrificed (15 min afterwards for the 120 min exposures; 90 min afterwards for the other duration) and the brains recovered to be analysed by immunohistochemical methods, in order to identify by coloured staining the proteins c-fos and pCREB. Number of stained proteins was counted (number of points/mm<sup>2</sup>) using an imaging analysis software (Visilog®, company NOESIS) in 24 cerebral areas (on the basis of work of Bontempi) including cortical zones (frontal, prefrontal and temporal), septal and the hippocampus.
- 
- Results and conclusions:
  - After statistical analyses (one way ANOVA), first results show an agreement with the COMOBIO project results at a SAR of 1.5 W/kg during 120min, and a differential effect according to the exposure time ( $p < 0.05$ ). For this same first exposure, an effect is also observed concerning the pCREB protein, in comparison of control sham group, showing a reduction in phosphorylation in structures implied in the Papez circuit ( $p < 0.05$  to 0.001), and an increase of phosphorylation in temporal cortex ( $p < 0.05$ ). Before being able to correlate these various results, analysis of all groups is necessary and final conclusions will be exposed during the presentation.

Support: European project RAMP (CE) contract n°QLK4-CT-2001-00463, Ministry of Ecology and Durable Development and Research Ministry BCRDn°12-02

ST-3

**RF INDUCED THERMOELASTIC PRESSURE WAVES IN DIFFERENT SIZE HUMAN HEAD MODELS IN MRI BIRDCAGE COILS.** Z. Wang<sup>1</sup>, J. C. Lin<sup>1,2</sup>. <sup>1</sup>Dept of Bioengineering, Univ of Illinois – Chicago, Chicago, Illinois, USA, <sup>2</sup>Dept of Electrical and Computer Engineering, Univ of Illinois – Chicago, Chicago, Illinois, USA.

#### Introduction

The usefulness of magnetic resonance imaging (MRI) in medicine has elevated the demand for increased resolution from MRI instruments, and has prompted the use of higher magnetic fields. These requirements have stipulated the use of higher levels of radio frequencies and powers. There have been increasing concern about the safety and potential health hazards, which may be present in the high-field strength and ultra-fast MRI instruments. Aside from the well-known acoustic noises from the switching currents and gradient magnetic fields associated with MRI instrument operations, microwave auditory effect has been widely reported as a biological response evoked when the head a human subject is irradiated with pulsed microwave energy [1-2]. The mechanism of interaction for the auditory effect is understood to be a microwave pulse induced thermoelastic expansion, due to the small but rapid temperature rise in soft tissues, which generates an acoustic wave of pressure inside the head. This paper investigates the pressure and power spectra of thermoelastic pressure waves generated by RF pulses absorbed by subjects inside a birdcage MRI coil.

#### Methods and Materials

Two spherical models: a 9-cm radius (adult head size) and a 5-cm radius (child head size), filled with human-brain material in a high-pass birdcages MRI coil operating at 64 MHz (1.5T) and 300 MHz

(7.0T) are studied in the paper. The computation of RF induced thermoelastic waves was conducted using the FDTD technique both for the electromagnetic and thermoelastic waves. We began by first computing the SAR and temperature distributions, and then followed by calculation of the elastic waves generated by the thermal stress, using the elastic-wave equation for a lossless medium [3].

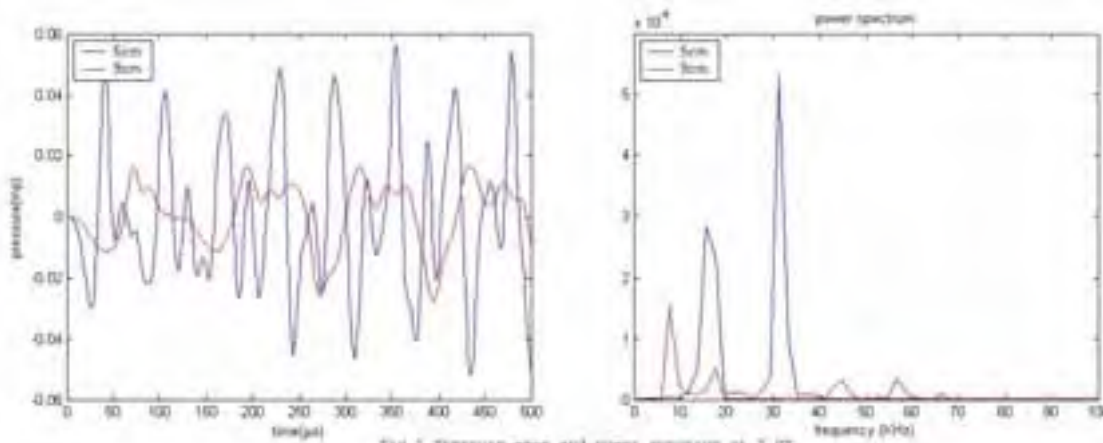
The high-pass birdcage MRI coil (14-cm radius; 22-cm length) was consisted of 16 rungs with a 1-cm rung width. The radius and length of the shield were 18 cm and 28 cm, respectively. Current sources were placed at the midpoint of each end-ring element. Each current source had a sinusoidal waveform with a 22.5-degree phase-shift between elements. The FDTD cell dimensions were set to at 5 mm to shorten the time required to complete the simulation. The brain-equivalent material in the sphere had the following properties: dielectric constants of 82.8 and 52, and conductivities of 0.4 and 0.55 S/m at 64 MHz (1.5T) and 300 MHz (7.0T), respectively. Rectangular excitation pulses were applied, singly, with a pulse width of 200  $\mu$ s, which was modulated by an error function in order to reduce higher frequency components that cannot be efficiently computed by the FDTD method. A stress-free boundary condition was imposed at the surface of the spherical head model.

### Results and Discussions

Representative results of computed RF induced thermoelastic pressure waves in the center of the brain spheres and the corresponding power spectra for 64 MHz and 300 MHz are shown in Figs. 1 and 2, respectively. Since we normalized the absorbed power to 10 W, the peak pressure amplitudes at 64 MHz and 300 MHz are almost the same for either the smaller and larger brain spheres. Note that in each case the pressure begins at zero, then grows to a peak value, and is followed by oscillations, which rise to even higher peaks as a function of time, and immediately after cessation of the first pulse. The pressure waves also oscillate in a similar pattern for the two RF frequencies. But there are obvious differences due to the sphere size - the amplitude and frequency of thermoelastic pressure waves are higher for the smaller brain sphere, at both RF frequencies. The power spectra for the pressure waves showed that the dominant induced frequency components are about 8 kHz for the larger (9 cm) sphere and 31 kHz for the smaller (5 cm) one. While the spectral power at 7.0T is much higher than that at 1.5T, their similarity indicates that the spectral power peaks correspond to the resonant frequency of pressure waves in the sphere model. Clearly, RF-induced thermoelastic pressure wave depends on model size, pulse width and SAR or absorbed power, which varies as a function of tissue property.

### References

1. J.C. Lin, *Microwave Auditory Effects and Applications*, Thomas, Springfield, IL USA (1978)
2. J.C. Lin, "Further Studies on the Microwave auditory Effect", *IEEE MTT* 25:938-943 (1977)
- . Y. Watanabe et al, "FDTD analysis of Microwave Hearing Effect", *IEEE MTT* 48:2126-2132 (2000)



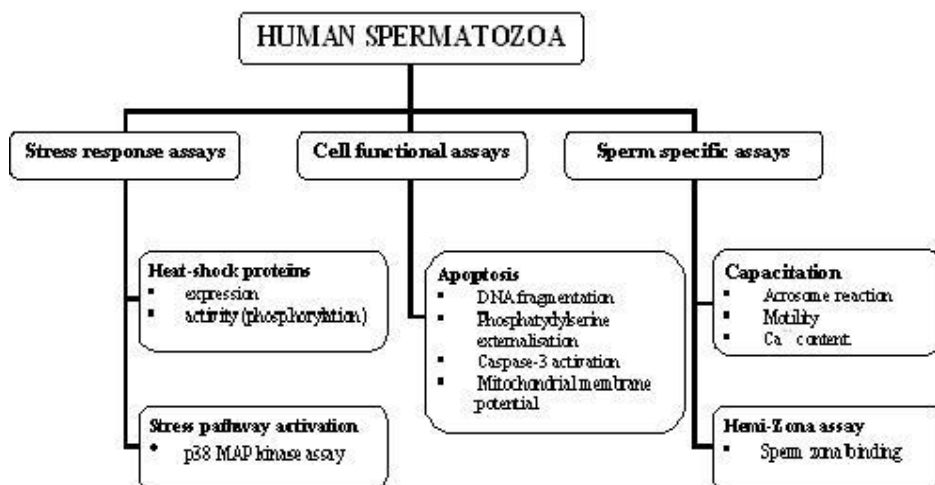
## PILOT STUDY: EFFECTS OF 900 MHZ GSM RADIATION ON HUMAN SPERM FUNCTION.

N. Falzone<sup>1</sup>, C. Huyser<sup>2</sup>, F. le R. Fourie<sup>3</sup>, D. Franken<sup>4</sup>, D. Leszczynski<sup>5</sup>. <sup>1</sup>Dept of Biomedical Science, Tshwane Univ of Technology, Pretoria, South Africa, <sup>2</sup>Reproductive Biology Laboratory, Dept of Obstetrics and Gynaecology, Univ of Pretoria, Pretoria, South Africa, <sup>3</sup>Dept of Research and Development, Standards South Africa, Pretoria, South Africa, <sup>4</sup>Tygerberg Hospital, Dept of Obstetrics and Gynaecology, Stellenbosch Univ, South Africa, <sup>5</sup>Functional Proteomics Group, Radiation Biology Laboratory, STUK-Radiation and Safety Authority, Helsinki, Finland.

**INTRODUCTION:** Recently Fejes and co-workers (2004) reported that mobile phone radiation affects human semen quality. Although the study was broadly criticized (EC FP6 Coordination Action, 2004), it focused attention on the possible effects that mobile phone radiation could have on male fertility. We have launched a new research project with the objective to examine the effects of 900 MHz GSM radiation on human sperm function. The study design focuses on three areas pertinent to the functionality of human spermatozoa (see diagram below):

- 1) stress response,
- 2) 2) apoptosis and viability,
- 3) 3) sperm specific functions.
- 4)

### BACKGROUND AND STUDY DESIGN:



In some studies mobile phone radiation has been noted to induce a cellular stress response, by changing the expression of heat-shock proteins (Hsp19 - analog of human Hsp27 - De Pomerai *et al.*, 2000; Hsp27 - Leszczynski *et al.*, 2002 and Hsp70 - Czyz *et al.*, 2004) and activating p38 MAP kinase stress response pathway (Leszczynski *et al.*, 2002). Miller *et al.*(1992) found that human male gametes contain a complex repertoire of Hsp's, which may include sperm-specific variants, however, the roles of most of these proteins remain to be defined (Eddy, 1999 and Neuer *et al.*, 2000). Hsp70 function in fertilization is still speculative, though it has been associated with a decline in sperm quality (Huang *et al.*, 2000a), linked to mechanisms that inhibit apoptosis (Dix *et al.*, 1996 and Neuer, *et al.*, 2000). Huang and co-workers (2000b) reported that Hsp90 could play a crucial role in regulating sperm motility. It has been hypothesized that mobile phone radiation might be an anti-apoptotic factor (Leszczynski *et al.*, 2002). It

has also been shown that the exposure of cells to mobile phone radiation causes a decline in the expression of genes encoding proteins in the FAS/TNF $\alpha$  apoptotic pathway (Leszczynski *et al.*, 2004). Therefore, the effect of mobile phone radiation exposure on sperm apoptosis will be studied. Finally, we will examine several physiological properties, including elements of sperm movement, zona recognition, signal transduction, exocytosis and cell fusion necessary to achieve the ultimate goal of oocyte fertilization. With this paper we report on the preliminary findings of the investigation on sperm apoptotic parameters and mitochondrial membrane potential.

## MATERIAL AND METHODS:

**Human sperm:** Semen samples were obtained from normospermic donors ( $n = 7$ ) and processed by density gradient centrifugation. Motile sperm were seeded in 55 mm glass Petri dishes ( $20 \times 10^6$  sperm/3 ml Hams F10 containing 5% BSA). Duplicate sham and RF exposed dishes were prepared simultaneously and exposed for periods of 1 h inside the RF-EMF chamber (RF exposed samples) and next to the chamber (sham exposed samples) inside a humidified CO<sub>2</sub> incubator maintained at 37°C and 5% CO<sub>2</sub>. Directly after the sham/RF exposure, spermatozoa ( $5 \times 10^6$ ) were prepared for flow-cytometric analysis using a Beckman Coulter ALTRA Flow Cytometer (Beckman Coulter, Miami, FL, USA) equipped with an Enterprise II water-cooled laser and data was analysed using EXPO 32 software (Beckman Coulter, Miami, FL, USA). For each test a minimum of 10 000 spermatozoa were examined.

**RF-EMF exposure system and exposure protocol:** The RF-EMF exposure system simulating a 900 MHz GSM signal previously described by Leszczynski *et al.* (2002) was used in this study. A pulse repetition frequency of 217 Hz was used and the average SAR level was 2 W/kg. Temperature during exposures remained constant at  $37 \pm 0.3^\circ\text{C}$ .

**Apoptosis:** Staining with Annexin V and PI (propidium iodide) were done according to the manufacturers staining protocol (Annexin V-FITC apoptosis detection kit II, BD Bioscience, USA) before flow cytometric analysis.

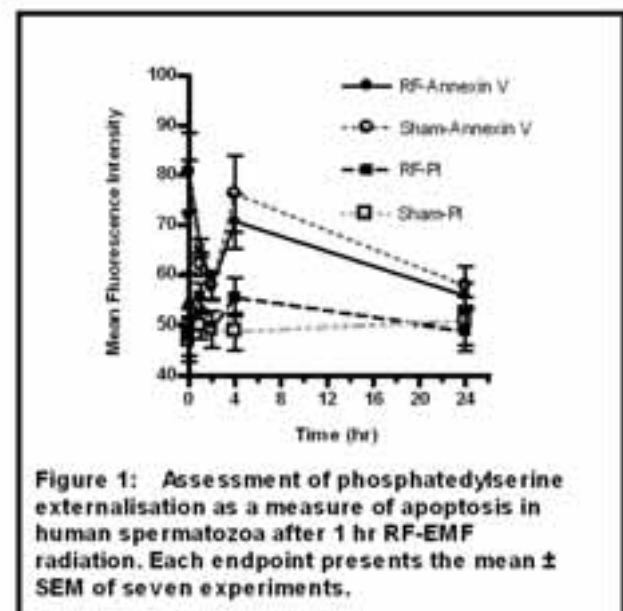
**Mitochondrial membrane potential:** After RF and sham exposure, MitoTracker Red® CMXRos (250 nM) (Molecular Probes, Eugene, USA) was added to sperm according to manufacturers specification before being analyzed by flow cytometry.

**Statistical analysis:** Results were analyzed using GraphPadPrism version 3.00 software (GraphPadSoftware, San Diego, CA, USA). For comparison between RF and sham exposed spermatozoa a nonparametric two-tailed t-test was performed.

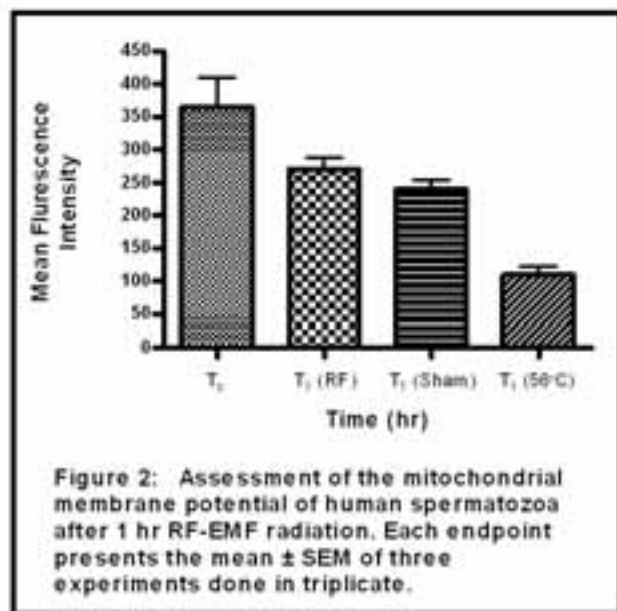
## PRELIMINARY RESULTS AND DISCUSSION:

Pilot experiments of RF exposed sperm appeared to show less phosphatidylserine externalization than control sperm, although the difference is not statistically significant ( $p=0.604$ ) (Figure 1). Mitochondrial membrane potential (mmp) after 1 hr RF-EMF irradiation appeared to decrease, but this was not statistically significant ( $p=0.1886$ ) (Figure 2). As a positive control (T<sub>1</sub> 56°C), sperm were exposed for 1 hr at 56°C to

*Bioelectromagnetics 2005, Dublin, Ireland*



establish an acute loss of mmp. Because of the possible variability between sperm from different donors more experiments are needed to determine statistical and physiological significance of these pilot observations.



**CONCLUSION:** Current evidence on RF radiation and male fertility is extremely limited. Concerns have been raised that mobile phone exposure might impair sperm function. Our pilot data suggest a possibility of RF-induced decrease in PS externalization compared to sham exposed sperm and a decline in mmp - both events associated with apoptosis. Donor variability requires, however, that more experiments must be performed before reaching any valid conclusions.

#### ACKNOWLEDGEMENTS:

This Research was funded by the National Research Foundation, Pretoria, South Africa (Grant No: 2054206) and by internal funds of STUK. Dosimetry support was provided by K. Jokela, T. Toivo & A-P Sihvonen, NIR Laboratory, STUK, Helsinki, Finland.

#### REFERENCES:

- Czyz *et al.* (2004). *Bioelectromagnetics*. 25(4): 296-307.  
 De Pomerai *et al.* (2000). 405:417-418.  
 Dix *et al.* (1996). *Proceedings of the National Academy of Sciences of the USA*. 93: 3264-3268.  
 EC FP6 Coordination Action. (2004). European fast response team on EMF and Health. Short notes on the influence of cellular phones on human fertility.  
 Eddy (1999). *Reviews of Reproduction*. 4:23-30  
 Fejes *et al.* (2004). Presented at the European Society for Human Reproduction and Embryology Annual Meeting, ESHRE, Berlin.  
 Huang *et al.* (2000a). *Animal Reproduction Science*. 63:231-240.  
 Huang *et al.* (2000b). *Theriogenology*. 53:1177-1184.  
 Leszczynski *et al.* (2002). *Differentiation*. 70:120-129.  
 Leszczynski *et al.* (2004). *Proteomics*. 4(2): 426-31.  
 Miller *et al.* (1992). *Human Reproduction*. 7: 645-637.  
 Neuer *et al.* (2000). *Human Reproduction Update*. 6(2): 149-159.

ST-5

**THE SENSITIVITY OF HUMAN EVENT-RELATED POTENTIALS AND PERFORMANCE TO MOBILE PHONE EMITTED EMFS.** D. L. Hamblin<sup>1,2</sup>, R. J. Croft<sup>2,3</sup>, A. W. Wood<sup>4,2</sup>, J. Spong<sup>1</sup>, C. Stough<sup>1</sup>. <sup>1</sup>Faculty of Life and Social Sciences, Swinburne Univ of Technology, Hawthorn, Victoria, Australia, <sup>2</sup>Australian Centre for RF Bioeffects Research, RMIT, Melbourne, Victoria, Australia, <sup>3</sup>Brain

Sciences Institute, Swinburne Univ of Technology, Hawthorn, Victoria, Australia, <sup>4</sup>Bioelectromagnetics Laboratory, Swinburne Univ of Technology, Hawthorn, Victoria, Australia.

There is growing interest in whether mobile phone (MP) emitted EMFs affect human neurophysiology. Some consistency has been found in relation to GSM900 exposure on auditory processing. This includes various reports of event related spectral power modulation in response to auditory tasks requiring discrimination [1,2]. A recent pilot study used a similar task to investigate any effect of exposure on auditory Event-Related Potentials (ERPs) and found the amplitude and latency of a sensory component N100 to decrease and the latency of a later cognitive component (P300) to increase [3]. Similar findings have since been reported in relation to modulation of the early sensory component [4]. Several previous studies dismiss the claim of MP-related effects but have often suffered methodological limitations [5]. Frequently, exposure durations were brief and the source was an unmodified MP undergoing adaptive power control, discontinuous transmission (DTX) and therefore minimal power output. Additional contributors to null findings may included small, unrepresentative samples and the lack of double-blinding.

The current study was designed to account for such limitations. Specific hypotheses were derived to test the results of a previous pilot study [3], namely that the N100 amplitude and latency would decrease and that the P300 latency and reaction time would increase under active exposure during the auditory task. Any effects on the visual P100, P300 and RT would also be explored.

The sample comprised 120 volunteers who were required to attend two sessions one week apart. In double-blind, counterbalanced conditions half underwent active exposure in the first session, the other half in the second. In both sessions, once the participant had been fitted with EEG recording apparatus, a phone set to sham exposure was mounted over the temporal region. Subjects then performed an auditory oddball task and a visual oddball task. The second administration of both tasks was then given with the handset set to active/sham exposure (duration 30 minutes). The MP was set via laptop and manufacturer software to continuously transmit an 895 MHz signal at a mean power output of 250 mW, thus avoiding DTX and adaptive power control. This signal was pulse modulated (217 Hz) with a duty cycle of 12.5% and a pulse width of 576  $\mu$ s. SAR measurements were conducted using a precision robot RF Dosimetric Assessment System. The average SAR measured over 10g of tissue in-line with the phone's antenna was 0.110 W/kg. EEG was recorded using Neuroscan Synamps amplifiers and data acquisition software. Average waveforms were calculated using Neuroscan Edit software.

Statistical analysis has been completed and will be presented.

The present research represents the largest and most rigorous test of MP-related effects on human neurophysiological function, and as such will provide the strongest evidence to date for or against any such effects.

(NHMRC Grant: 154905)

- [1] Eulitz et al. 1998. Neuroreport 9:3229-3232.
- [2] Croft et al. 2002. Clin Neuro 113:1623-1632
- [3] Hamblin et al. 2004. Clin Neuro 115:171-178.
- [4] Maby et al. 2004. Med Biol Eng Comput 42:562-568.
- [5] Hamblin & Wood. 2002. Int J Radiat Biol 78:659-669.

**ASSESSMENT OF SAFETY DISTANCES OF GSM BASE STATION ANTENNAS OPERATING AT 900 AND 1800 MHZ FOR OCCUPATIONAL EXPOSURE.** W. Joseph, L. Martens. Dept of Information Technology, Ghent Univ, Ghent, Belgium.

**Objective:** The safety distances of base station antennas can be obtained either by assessment of the electromagnetic fields and comparison with the reference levels or by assessment of the Specific Absorption Rate (SAR) and comparison with the basic restrictions [1]. The objective of this paper is to determine and to compare the safety distances based on the electromagnetic fields for two different types of GSM base station antennas operating in a different frequency band. Furthermore, we will make a comparison of the safety distances based on the electromagnetic fields and based on the SAR using simulations and measurements for one type of antenna.

**Methods:** We investigate GSM base station antennas of the type Kathrein 736863 at 947.5 MHz and K739495 at 1862.5 MHz, respectively. At these frequencies, the antennas radiate maximally. We determine the safety distances based on the electromagnetic fields in front of the antennas, noted as  $D^X$  ( $X = E$  or  $H$ ) because they will be most restrictive in this case. The measurements are performed with a network analyzer (Rohde & Schwarz ZVR) and are compared with FDTD simulations. We use a robot to position the measurement probes. The measurements are performed with a spatial grid of 2 cm, smaller than  $\lambda/10$  at 947.5 and 1862.5 MHz. We determine the safety distances for the fields in three ways: by determination of the maximum field (worst-case situation) values  $X^{\max}$  ( $X = E$  or  $H$ ) in  $xy$ -planes in front of the antenna, by determination of  $X^{\text{plane}}$ , the field value averaged in  $xy$ -planes with dimensions  $70 \times 40 \text{ cm}^2$ , and by determination of  $X^{\text{vol}}$  ( $X = E$  or  $H$ ), the field value averaged in a volume of  $70 \times 40 \times 20 \text{ cm}^3$ . Next, we determine the safety distances based on the SAR for the K736863 antenna, noted as  $D^{\text{SAR}}$ . For the SAR assessment we use a rectangular box phantom (dimensions  $80 \times 50 \times 20 \text{ cm}^3$ ) [2]. We position the rectangular box phantom at distances 1 mm to 20 cm from the K736863 antenna. We use a SAR probe of the type ESD3DV1, delivered and calibrated for the DASY3 system of Schmid & Partner Engineering AG. Finally, we determine the difference of the safety distances based on the electric field and based on the SAR i.e.,  $\Delta = D^X - D^{\text{SAR}}$  [ $m$ ] ( $X = E$  or  $H$ ). Using  $\Delta$  we can determine the input power from which on the electromagnetic fields will deliver the largest safety distances.

**Results:** Fig. 1 and 2 show that the electric field values of the K739495 antenna at 1862.5 MHz are higher than those of the 947.5 MHz K736863 base station antenna for the investigated positions. This was expected because the gain of 1800 MHz base station antennas (around 18 dBi) is generally higher than the gain of 900 MHz base station antennas (around 15 dBi). The gain of the K736863 antenna is 15.5 dBi, while the gain of the K739495 antenna is 18 dBi. On the other hand the reference levels are higher at 1862.5 MHz than at 947.5 MHz [1] (129.47 V/m and 0.35 A/m at 1862.5 MHz against 92.34 V/m and 0.25 A/m at 947.5 MHz for occupational exposure). There is a very good agreement between measurements and simulations (Fig. 1 and Fig. 2). Table 1 compares the safety distances for the electric and magnetic field of both antennas. The safety distances of the K739495 antenna at 1862.5 MHz are of the same order as those of the K736863 antenna at 947.5 MHz. For averaging in a plane and volume, the safety distances of the 1862.5 MHz antenna are lower than those of the 947.5 MHz antenna due to the considerably higher reference levels at 1862.5 MHz.

The safety distances of the K736863 antenna (at 947.5 MHz) based on the electric field averaged in a volume are compared with the safety distances based on the localized SAR. This will lead to the most restrictive condition to determine the input power from which on the field values deliver the largest distances for occupational exposure. Fig. 3 shows that  $\Delta$  equals zero at 10.2 W (simulations) and at 10.8 W (measurements). From this power on the safety distances based on the electric field are larger than the

safety distances based on the localized SAR ( $\Delta > 0$ ). This results in a safety distance of 1.9 cm (simulations) and 2.2 cm (measurements). It is then not necessary to determine the SAR for input powers larger than about 11 W to obtain the most restrictive safety distance. **Conclusions:** We compared the safety distances based on the electromagnetic fields for two types of GSM base station antennas. For a typical input power of 20 W the maximum safety distances of the K736863 and K739495 antenna are approximately 30 cm. For the K736863 antenna, the safety distances based on the electric field averaged in a volume will be higher than those based on the SAR from input powers of about 11 W on.

### References.

1. International Commission on Non-ionizing Radiation Protection, "Guidelines for limiting exposure to time-varying electric, magnetic, and electromagnetic fields (up 300 GHz)," Health Physics, Vol. 74, No. 4, pp. 494-522, 1998.
2. CENELEC EN50383, "Basic standard for the calculation and measurement of electromagnetic field strength and SAR related to human exposure from radio base stations and fixed terminal stations for wireless telecommunication systems (110 MHz - 40 GHz)", Sept. 2002.

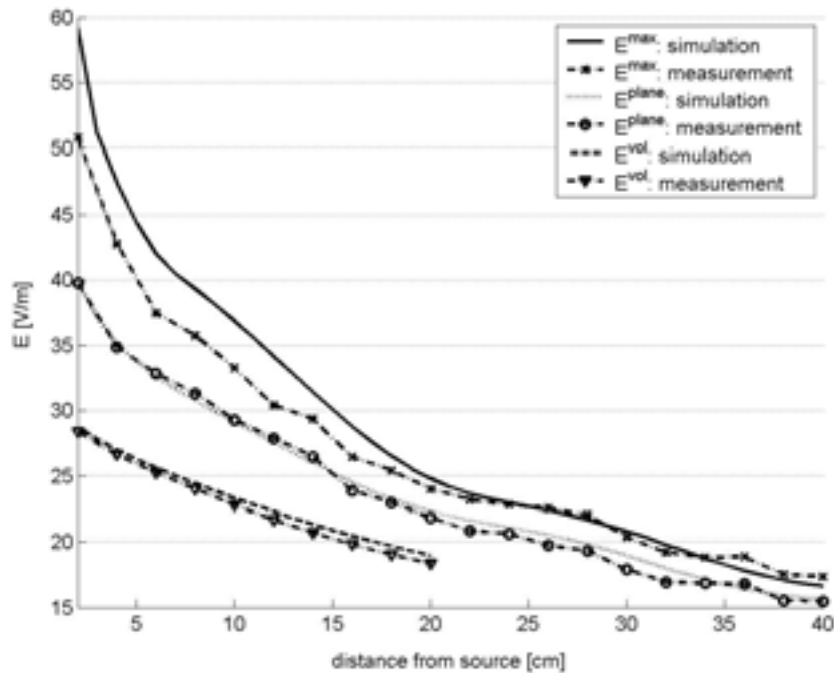


Figure 1: Comparison of measurements and simulations of  $E^{\max}$ ,  $E^{\text{plane}}$  and  $E^{\text{vol}}$  for the K736863 antenna at 1 W input power at 947.5 MHz.

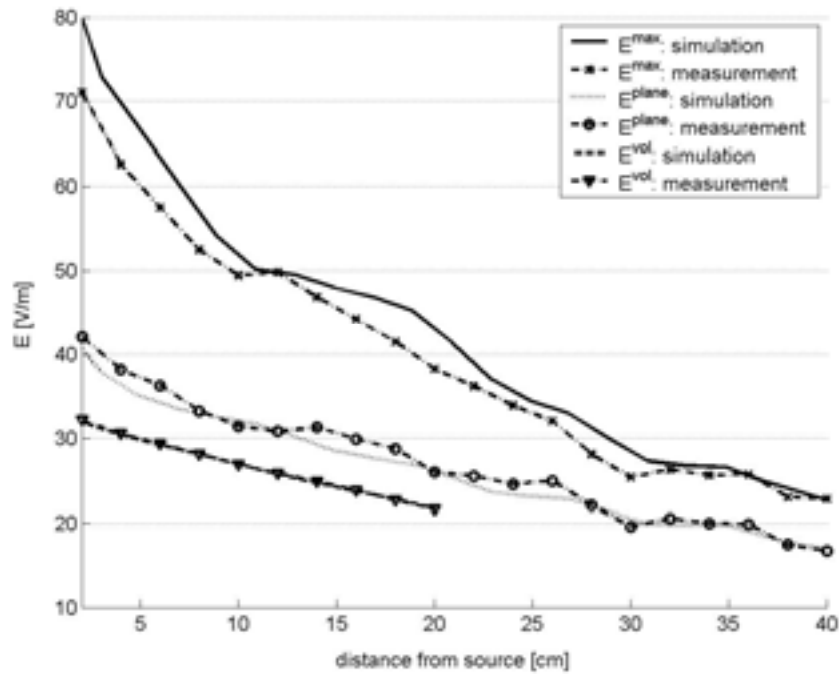


Figure 2: Comparison of measurements and simulations of  $E^{\max}$ ,  $E^{\text{plane}}$  and  $E^{\text{vol}}$  for the K739495 antenna at 1 W input power at 1862.5 MHz.

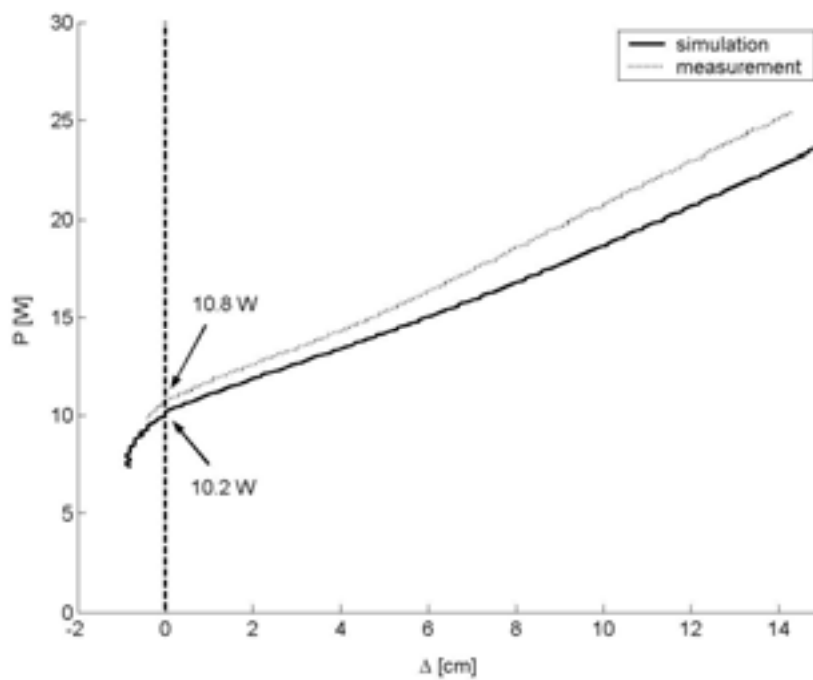


Figure 3: Input power as function of  $\Delta$ .

Table 1: Comparison of simulations and measurements of safety distances for the electric and magnetic field at 10 and 20 W for the K736863 (at 947.5 MHz) and K739495 (at 1862.5 MHz) antenna.

		K736863	K736863	K739495	K739495
--	--	---------	---------	---------	---------

	input power	D <sup>E</sup> [cm]		D <sup>H</sup> [cm]		D <sup>E</sup> [cm]		D <sup>H</sup> [cm]	
	[W]	simulate	measure	simulate	measure	simulate	measure	simulate	measure
max	10	15.7	14.1	13.5	16.0	21.1	18.3	23.3	21.3
	20	30.4	29.6	28.9	30.8	29.3	27.6	31.1	33.0
plane	10	10.0	10.0	8.8	8.7	1.8	2.3	1.6	2.5
	20	25.6	23.9	25.2	24.4	14.3	17.8	17.3	18.5
vol	10	1.8	2.0	1.3	<2	<0.1	<2	<0.1	<2
	20	15.6	8.2	14.7	13.3	6.4	6.6	9.1	9.3

ST-7

**THE EFFECTS OF ELECTROMAGNETIC FIELDS EMITTED BY GSM MOBILE PHONES ON HUMAN SLEEP.** S. P. Loughran<sup>1,2</sup>, A. W. Wood<sup>2</sup>, J. J. Barton<sup>1</sup>, R. J. Croft<sup>3</sup>, B. Thompson<sup>4</sup>, C. Stough<sup>1</sup>. <sup>1</sup>Centre For Neuropsychology, Swinburne Univ of Technology, Hawthorn, Victoria, Australia, <sup>2</sup>Bioelectromagnetics Laboratory, Swinburne Univ of Technology, Hawthorn, Victoria, Australia, <sup>3</sup>Brain Sciences Institute, Swinburne Univ of Technology, Hawthorn, Victoria, Australia, <sup>4</sup>Dept of Respiratory Medicine, The Alfred Hospital, Melbourne, Victoria, Australia.

**INTRODUCTION:** Previous research has shown that exposure to RF exhibits effects on conventional sleep parameters such as sleep latency, REM sleep, and waking after sleep onset [1, 2, 3, 4]. Additionally, increased spectral power in the alpha frequency range has been shown following RF exposure both prior to and during sleep [1, 2, 5, 6, 7].

**OBJECTIVE:** To examine whether aspects of sleep architecture show sensitivity to the electromagnetic fields emitted by GSM mobile phone handsets placed in the normal position next to the ear of human volunteers.

**METHODS:** Fifty participants attended four overnight sessions at a sleep laboratory, over two successive weekends. The Saturday nights acted as adaptation nights. On the following Sunday night a GSM mobile phone, either transmitting (0.25 W, 217 Hz modulated, 895 MHz output) or off, was positioned next to the right hemisphere for a period of 30 minutes prior to sleep. The on/off order was balanced, and the experiment was carried out double blind with regard to phone status. During sleep, EEG, ECG, EOG, EMG, SaO<sub>2</sub> and respiratory measures were monitored using the Compumedics™ E-series polysomnography system. Sleep was staged and scored according to standard criteria [8] by an experienced sleep technician blind to the experimental condition. EEG channel data was further analyzed to provide power spectral density estimates for each 20 second epoch (FFT routine, Hanning window, averages of five 4-second epochs) for the first 30 minutes of NREM sleep.

**RESULTS:** The preliminary results showed a significant difference in REM sleep latency between the two conditions,  $F(1,48)=5.797$ ,  $p < .05$ . Other sleep parameters showed no evidence of alteration. EEG spectral changes are in the process of analysis and will be completed early 2005.

**CONCLUSIONS:** The preliminary results suggest that exposure to the electromagnetic fields emitted by mobile phones may have an effect on REM sleep latency when used prior to sleep.

Study supported by the National Health and Medical Research Council of Australia (Grant: 154905)

- [1]Mann K, Roschke J. 1996. Effects of pulsed high-frequency electromagnetic fields on human sleep. *Neuropsychobiol* 33:41-47.
- [2]Borbely AA, et al. 1999. Pulsed high-frequency electromagnetic field affects human sleep and sleep electroencephalogram. *Neurosci Lett* 275:207-210.
- [3]Wagner P, Roschke J, Mann K, Hiller W, Frank C. 1998. Human sleep under the influence of pulsed radiofrequency electromagnetic fields: A polysomnographic study using standardized conditions. *Bioelectromagnetics* 19:199-202.
- [4]Mann K, et al. 1998. Effects of pulsed high-frequency electromagnetic fields on the neuroendocrine system. *Neuroendocrinol* 67:139-144.
- [5]Huber R, et al. 2002. Electromagnetic fields, such as those from mobile phones, alter regional cerebral blood flow and sleep and waking EEG. *J Sleep Res* 11:289-295.
- [6]Huber R, et al. 2000. Exposure to pulsed high-frequency electromagnetic field during waking affects human sleep EEG. *NeuroReport* 11:3321-3325.
- [7]Huber R, et al. 2003. Radio frequency electromagnetic field exposure in humans: Estimation of SAR distribution in the brain, effects on sleep and heart rate. *Bioelectromagnetics* 24:262-276.
- [8]Rechtschaffen A, Kales A. 1968. A manual of standardized terminology, techniques, and scoring system for sleep stages of human subjects. Washington DC: Public Health Service, U.S. Government Printing Office.

ST-8

**TISSUE EQUIVALENT SOLID PHANTOM AND MOBILE PHONE EMF DOSIMETRY.** E. B. Elabbassi, R. de Seze. UMR INERIS: EA 3901 DMAG – TOXI, Institut National de l'Environnement Industriel et des Risques, Verneuil-en-Halatte, France.

**INTRODUCTION:** The thermal effect due to the absorption of the electromagnetic field (EMF) emitted by the mobile phone (MP) on the user's head is very small. Air insulation and thermal conduction due to the MP in contact with the user's head contribute more to heating [1]. The thermal effect of the MP EMF emission could also be masked by activation of the thermoregulation mechanisms permitting control and stabilization of the body temperature.

**OBJECTIVE:** To improve the sensitivity of the measure, we chose to measure the temperature increase produced by a higher-power EMF than that of a MP: the MP antenna was fed by a RF generator through an amplifier and applied to structures representing a biological tissue equivalent. A solid phantom of a simple human head model has been used (truncated sphere). This phantom is constituted of an envelope filled of a gel of which the dielectric permittivity reproduced the biological tissue. The absorbed power (SAR: Specific Absorption Rate) has then been calculated.

**METHODS:** The phantom has been exposed to EMF of 900 MHz frequency, in continuous wave (CW), to different powers of 2, 4, 8 and 10 Watts emitted by a patch antenna. The temperature of the gel phantom has been measured at 3 levels, using a Luxtron 790 fiberoptic thermometer: at the surface, at 1 cm and 2 cm of this surface. The temperature courses were modelled by the theoretical heating curves:  $T = T_i + (T_f - T_i) (1 - \exp(-Kt))$  where  $T_i$  and  $T_f$  are respectively the initial and final temperatures (degreeC);  $t$ : the time (min) and  $K$ : the heating constant ( $\text{min}^{-1}$ ). Once the heating coefficient is known,

it is possible to estimate the apparent mean SAR:  $SAR = c \cdot \Delta T / \Delta t = c \cdot K \cdot \Delta T$  with  $\Delta T / \Delta t$ : initial slope and  $c$ : specific heat of the biological tissue ( $J \cdot kg^{-1} \cdot degree C^{-1}$ ).

RESULTS: The values of calculated SAR at the surface are of 1.6 – 2.5 – 5.4 and 6.9  $W \cdot kg^{-1}$  for the exposure powers of 2 - 4 - 8 and 10 W, respectively. The absorption of the EMF power is maximal at the surface and decreases while penetrating deeper in the phantom gel. The values of calculated SAR decreased at 1 cm and 2 cm of the surface.

CONCLUSIONS: The biological tissue equivalent solid phantom presented in this study permits to make EMF exposition at more important powers than the one of the MP, in order to assure a detectable measure of the temperature variation. The combination of the experimental dosimetry data with the physiological and the numerical modelling data provides the complete picture required to assess the thermal effects of EMF exposure on human subjects.

References:

[1] Elabbassi E.B. & de Seze R. "Mobile Phone Use and Temporal Skin Heat Sensation" Proceeding of the 3rd International Workshop on Biological Effects of Electromagnetic Fields 4-8 October, 2004, Kos, Greece. Volume I, pp 543 – 548.

This work was financially supported by the Regional Council of Picardy (France) and the French Ministry of Ecology and Sustainable Development (BCRD 2003, DRC 02-03)

## **Alessandro Chiabrera Memorial Student Session (Continued)**

*Chairs: Marko Markov and Gabi Nindl*

**10:30 - 12:00 pm, O'Reilly Hall**

ST-9

**DIFFERENTIAL EFFECTS OF NANOSECOND PULSED ELECTRIC FIELDS ON COLON CARCINOMA CELLS IN S-PHASE.** E. H. Hall<sup>1,2</sup>, K. H. Schoenbach<sup>2</sup>, S. J. Beebe<sup>1,2</sup>. <sup>1</sup>Center for Pediatric Research, Eastern Virginia Medical School, Children's Hospital of the King's Daughters, Norfolk, VA, USA, <sup>2</sup>Center for Bioelectrics, Old Dominion Univ, Eastern Virginia Medical School, Norfolk, VA, USA.

Nanosecond pulsed electric fields (nsPEFs) are non-thermal (mJ/cc), ultra-short pulses with high electric fields (kV/cm) and high power (megawatts). Previous studies demonstrated nsPEF-selective effects on intracellular structures and functions. However, roles for the cell cycle in response to nsPEFs have not been established. The objective of this study was to determine effects of nsPEFs on cells during the cell cycle S-phase (DNA synthesis). HCT116 colon carcinoma cells were synchronized to S-phase and exposed to nsPEF at 60kV/cm with either 60ns or 300ns durations. Cells were analyzed for apoptosis markers defining effects at the plasma membrane, cytoskeletal structure, caspase activation, nuclear/DNA integrity, and cell survival. S-phase cells pulsed in the presence of ethidium homodimer-1 exhibited significantly less fluorescence indicating greater membrane integrity as compared to un-synchronized cells. Annexin V-FITC binding, another membrane marker, was not significantly different between S-phase and un-synchronized cells, indicating similar levels of phosphatidylserine externalization regardless of cell cycle phase. Phalloidin fluorescence exhibited a uniform staining pattern of the cytoskeletal structure in S-phase and non-pulsed cells, but presented a more random, altered staining pattern in un-synchronized cells under the 60ns conditions. Caspase activation in S-

phase cells was significantly higher than in un-synchronized cells. However, regardless of cell cycle phase the nuclei were enlarged and presented an abnormal DNA histogram twenty-four hours post pulse. Both S-phase cells and un-synchronized cells survived exposure to nsPEF, but cells did not proliferate as the pulse duration was increased regardless of the cell cycle phase. The results indicate that S-phase cells exposed to nsPEFs exhibit more robust membrane integrity, cytoskeletal structure, and caspase activation. These studies provide the first demonstration of differential effects of S-phase cells during exposure to nsPEFs

ST-10

**ROLE OF THE MAGNETIC FIELD IN DECREASE OF THE 5-HT<sub>1B</sub> SEROTONERGIC RECEPTOR AFFINITY UNDER EXPOSURE TO POWER FREQUENCY FIELDS.** J. M. Espinosa<sup>1</sup>, I. Lagroye<sup>1</sup>, G. Ruffie<sup>1</sup>, Jp. Gernez<sup>2</sup>, B. Veyret<sup>1</sup>. <sup>1</sup>PIOM/Bioelectromagnetics laboratory, CNRS UMR5501, ENSCPB, Univ of Bordeaux, Pessac Cedex, France, <sup>2</sup>EDF R&D, Laboratory of electrical material, Moret sur Loing, France.

#### OBJECTIVES:

Massot et al. (2000) have shown that a specific and reversible desensitization of the 5-HT<sub>1B</sub> receptor of rat brain membrane preparations was caused by exposure to 50-Hz magnetic fields. The authors demonstrated that the effect was maximum after 60 min, at 2000  $\mu$ T with a threshold at ca. 600  $\mu$ T. We undertook a confirmation study of the work of Massot et al. using the same exposure system. These data may be of importance since physiological functions or pathologies such as sleep quality, anxiety, or depression are closely controlled by the serotonergic central system. 5-HT<sub>1B</sub> receptors are presynaptic receptors located on serotonergic as well as on other axon terminals, where they regulate the release of the corresponding neurotransmitter. They are part of the G-protein coupled receptors family (GPCR) and are negatively coupled with the adenylate cyclase.

#### METHODS:

Three types of signals were tested: 1) 50-Hz magnetic field at 100, 500 and 1100  $\mu$ T, 2) static magnetic field at 1100  $\mu$ T, and 3) 400-Hz magnetic field at 675  $\mu$ T. The exposure setup was similar to that used by Massot et al. Briefly, it consists in two sets of Merritt coils which produce a uniform magnetic field (MF) varying from 0 to 1100  $\mu$ T<sub>rms</sub> at a frequency of 50 Hz. Power supplies were adapted to the setup for experiments at 0 and 400 Hz. Rat-brain membranes were placed in temperature-regulated boxes located inside each set of coils, which could be independently activated (sham and exposed samples). Temperature and intensity were monitored in real time. Exposures were carried out at 25°C.

Membranes were isolated from Wistar rat brains according to standardized procedure and 80  $\mu$ g of proteins were incubated in a binding buffer containing increasing concentrations (2.5-40 nM) of [<sup>3</sup>H]5-HT in 96-well filtration plates (MAFB NOB, Millipore, 6.5-mm diameter wells). Immediately afterward, exposure started and lasted 60 min at 25°C.

Non-specific binding was determined using 10  $\mu$ M of 5-HT. Specific 5-HT<sub>1B</sub> binding was calculated as the difference between 5-HT<sub>1B/1E/1F</sub> and 5-HT<sub>1E/1F</sub> binding. At the end of the incubation period, the 96-well filtration plates were filtered under vacuum and each filter was washed twice with ice-cold incubation buffer. The radioactivity retained on coded filters was then measured using a Beckman counter. In saturation experiments on 5-HT<sub>1B</sub> receptor, K<sub>d</sub> (inversely proportional to the ligand affinity) and B<sub>max</sub> (reflecting the total number of receptors) were determined. Part of the data is still preliminary.

#### RESULTS AND DISCUSSION:

The data are summarized in the table below.

We confirmed the decrease in affinity of the 5-HT<sub>1B</sub> receptor for the radiolabelled neuromediator as evidenced by the significant increase in K<sub>d</sub> after exposure to 50-Hz magnetic fields at 1100 μT. An increase in B<sub>max</sub> was also shown. At lower flux densities, there was no significant effect of exposure. GTP is known to uncouple the 5-HT<sub>1B</sub> receptors from the G-protein, and indeed GTP treatment decreased the affinity of the receptor to the same level as exposure to the field, thereby suggesting that both GTP and field induced the uncoupling of the G protein from the receptor. However, GTP treatment did not affect B<sub>max</sub>. When we tested the effect of a static magnetic field, K<sub>d</sub> value increased significantly, whereas B<sub>max</sub> was unchanged. We therefore performed experiments at 400 Hz and 675 μT, which was the maximum field strength that could be obtained with the generator. No significant changes were noted for both K<sub>d</sub> and B<sub>max</sub>. Taken together these results suggest that the magnetic field plays a major role in eliciting the decrease of the affinity induced by 50 Hz magnetic fields.

Acknowledgement:

We thank EDF R&D, CEM-EDF and RTE for financial support.

Exposure	Sham		Exposed or treated		n
	K <sub>d</sub> (nM)	B <sub>max</sub> (CPM)	K <sub>d</sub> (nM)	B <sub>max</sub> (CPM)	
50 Hz (1100 μT)	2.10 ± 0.42	1919 ± 277	5.90 ± 1.25 *	3066 ± 565 *	6
50 Hz (500 μT)	2.04 ± 0.46	1736 ± 214	1.25 ± 0.34	1658 ± 186	6
50 Hz (100 μT)	2.37 ± 0.48	1756 ± 256	2.31 ± 0.65	1723 ± 269	4
0 Hz (1100 μT)	2.00 ± 0.19	1698 ± 107	2.90 ± 0.32 *	1895 ± 96	13
400 Hz (675 μT)	1.57 ± 0.24	1300 ± 236	2.65 ± 0.88	1529 ± 290	6
GTP (1mM)	1.41 ± 0.09	1798 ± 151	6.94 ± 0.8 *	2052 ± 230	6

ST-11

**ASSESSMENT OF ELF MAGNETIC FIELDS FROM FIVE MOBILE HANDSETS.** M. Tuor, S. Ebert, J. Schuderer, N. Kuster. IT'IS Foundation, Swiss Federal Institute of Technology (ETH), Zurich, Zurich, Switzerland.

**INTRODUCTION:** Mobile phones not only expose the user to radiofrequency (RF) electromagnetic fields (EMF) but also to extremely low frequency (ELF) EMF. Hence, some agencies have called for combined RF and ELF health risk experiments. Such experiments require good knowledge of the strength and spectral power content of the ELF signal. ELF fields are caused by high supply currents inside the phone. The circuit with the highest power consumption is the front-end amplifier which is only active during transmission, i.e., the resulting ELF EMF signal has similar lower frequency components than the demodulated RF signal.

**OBJECTIVE:** This study examines the magnetic field strength and waveform of five mobile phones: Sony Ericsson T610, Siemens A50, Motorola TP, Sony Ericsson T68, and Nokia 3310. Additionally, a worst-case signal with respect to maximum B-field and maximal frequency components is proposed.

**METHODS:** The ELF magnetic fields of the five phones were examined by surface scans of the front

and the back sides of the phones. They were conducted with the DASY4 near-field scanner equipped with a hall probe (F.W. Bell Gaussmeter 7000,

RESULTS: The maximum ELF magnetic field strength at 5mm measurement distance was detected on the back side of the phones with up to 34 $\mu$ T and on the front side with up to 15 $\mu$ T; applying the extrapolation to the surface of the phone leads to B-field strength on the back side of up to 75 $\mu$ T. The waveform of the magnetic field represents the structure of the GSM pulse. Each phone showed a characteristic pulse shape in the time domain. Table 1 summarizes the results. The resulting data enable the definition of a worst-case exposure signal including ELF components, which can be used for risk assessment exposure setups.

ELF magnetic field and pulse form characteristics of the five mobile phones.					
B-Field	Phones				
	Motorola Timeport	Siemens A50	Nokia 3310	Sony Ericsson T68	Sony Ericsson T610
Pulse Height on Front Side 5mm from Surface [ $\mu$ T]	4.7	7.5	14.6	6.1	4.9
Pulse Height on Back Side 5mm from Surface [ $\mu$ T]	29.5	31.9	33.7	29.5	28.1
Pulse Height on Front Side Extrapolated to 0mm [ $\mu$ T]	8.3	12.4	19.3	8.3	11.7
Pulse Height on Back Side extrapolated to 0mm [ $\mu$ T]	52.8	35.1	66.1	74.8	56.3
Pulse Half Rise Time [ns]	24	68	49	39	88
Pulse Full Width Half Maximum [ms]	0.59	0.58	0.58	0.58	0.59

ST-12

**FREE RADICAL PRODUCTION, HSP70 EXPRESSION AND PROTEIN PROFILING AFTER 1800 MHZ RF EXPOSURE IN DIFFERENT IMMUNE RELEVANT CELLS.** M. Lantow<sup>1</sup>, C. Hartwig<sup>1</sup>, C. Maercker<sup>2</sup>, M. Simko<sup>1</sup>. <sup>1</sup>Univ of Rostock, Institute of Cell Biology and Biosystems Technology, Division of Environmental Physiology, Rostock, Germany, <sup>2</sup>Resource Center for Genome Research (RZPD), Heidelberg, Germany.

OBJECTIVES AND INTRODUCTION: The goal of our study is to investigate the cell activating capacity of radiofrequency (RF) radiation (1800 MHz) using different cell systems, and various exposure and co-exposure conditions.

**METHODS:** Human umbilical cord blood-derived monocytes, Mono Mac 6, and K562 cells were used to examine free radical release after exposure to RF-EMF, 1  $\mu$ M TPA, 1  $\mu$ g/ml LPS or to co-exposure conditions. Cells were exposed to 1800 MHz RF-EMF (IT'IS, Zurich, Switzerland) or to chemicals in parallel to sham and incubator conditions, as well as to heat (40°C) for 45 min. For RF-EMF exposure different signals (continuous wave, GSM Basic, DTX Only, and GSM Talk) and SAR values (0.5, 1.0, 1.5, 2.0 W/Kg) were applied. Super oxide radical anion release (colorimetry), ROS production (flow cytometry), and heat shock protein 70 (Hsp70) expression (flow cytometry) was determined after RF-EMF exposure. Data were compared to sham and/or to control values and the statistical analysis was performed by the student's t-test ( $p < 0.05$ ). Protein profiling using 512 different antibodies (BD-array) in a total protein lysate of human umbilical cord blood-derived monocytes was performed after exposure to GSM-DTX Signal to 2 W/kg SAR-value.

**RESULT AND CONCLUSION:** Heat (40°C) and TPA treatment induced a significant increase in super oxide anion radicals and in ROS production in all investigated cells when data were compared to sham or to incubator conditions. After RF-EMF exposure a significant increase of super oxide radical anions and ROS production (1.4 fold) were detected when data were compared to sham, but this difference disappeared if data were compared to the incubator control. The same results were detected using Mono Mac 6 cells. Investigations of the Hsp70 expression level after exposure to GSM-DTX signal (2 W/kg) for 0, 1, and 2 hours did not reveal any differences from control conditions using human Mono Mac 6 and K562 cell. On the other hand, a significant increase of Hsp70 expression could be detected 2 hours post exposure to heat (42°C) for 45 min. The protein profiling showed a dys-regulation in more than 150 proteins after exposure to GSM-DTX, 2W/kg RF-EMF. After evaluation of data we hope to get more details and indications to elucidate the underlying mechanisms and to detect the effected pathways which were influenced by RF-EMF.

This work is supported by the Federal Office for Radiation Protection, Salzgitter, Germany.

ST-13

**IMPORTANT ASPECTS OF ELECTROMAGNETIC MODELING IN HYPERTHERMIA TREATMENT PLANNING.** E. Z. Neufeld<sup>1</sup>, T. Samaras<sup>2</sup>, N. Chavannes<sup>1</sup>, N. Kuster<sup>1</sup>. <sup>1</sup>Foundation for Research on Information Technologies in Society (IT'IS), Zurich, Switzerland, <sup>2</sup>Dept of Physics, Aristotle Univ of Thessaloniki, Thessaloniki, Greece.

**OBJECTIVES:** This study addresses issues pertaining to the realistic modeling of applicators commonly used in clinical practice and aims at clarifying some difficulties and parameters involved in the electromagnetic simulations.

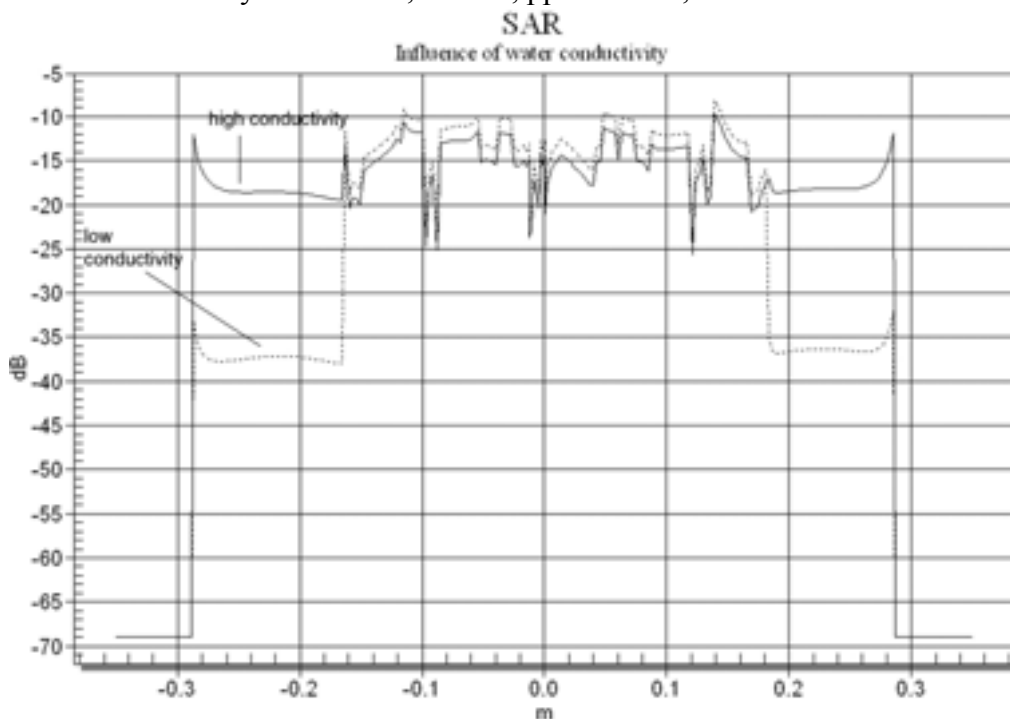
**METHOD:** The study is part of ongoing work toward the development of a treatment planning tool for deep regional hyperthermia. The results presented here concern the modeling of the antennas, the effect of the water bolus conductivity and the voxel size, in an effort to achieve specific absorption rate (SAR) distributions of acceptable accuracy with reasonable computational resources. The electric field and SAR distributions have been calculated with SEMCAD, which is being used as the basis for the development of the treatment planning tool. The Sigma-60 applicator (BSD Medical Corp., Salt Lake City, Utah) operating at 80MHz has been modeled incorporating a water bolus. The conductivity of the water has been varied (Fig. 1), in order to examine its influence on the convergence of the simulations. Visual Human Project data has been used to create a model of the patient's body trunk. The arms and hands of the model have been removed, to better fit into the applicator (Fig. 2). Nonuniform meshes are used to reduce computation time. The mesh size ranged from 8.5 to 20 million voxels. Different

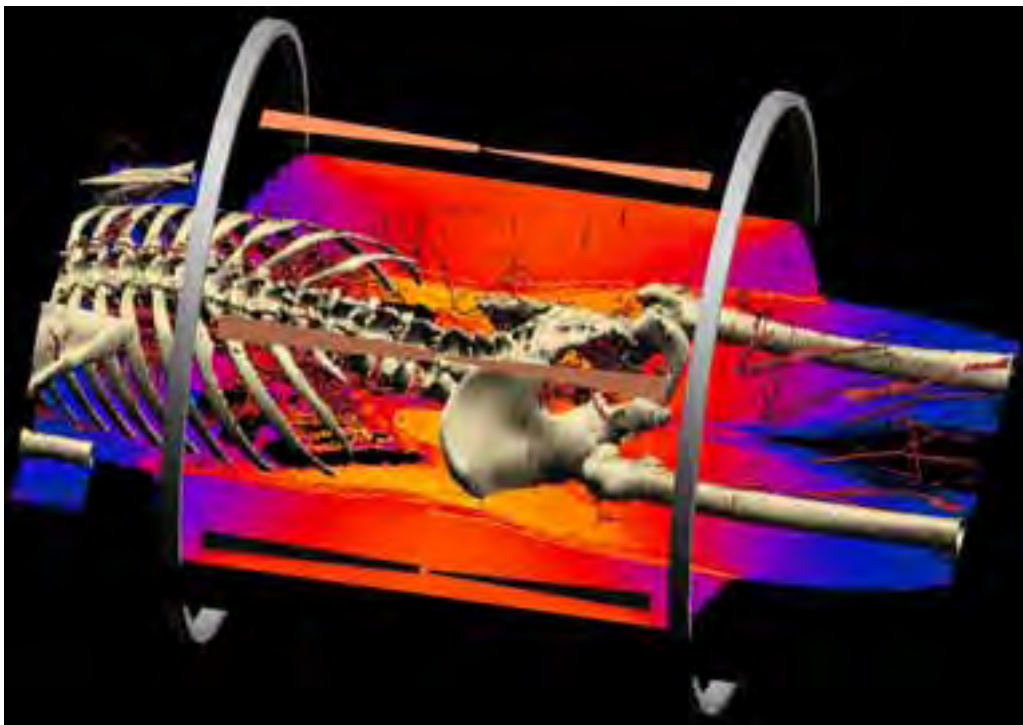
boundary conditions have been applied and minimal requirements established. The antennas have been modeled as flat bow-tie and cylindrical dipoles and their differences assessed (Fig. 3). The antennas have been modeled in contact with the water bolus and separated by a small gap from it.

**RESULTS:** The results have shown that the bow-tie dipoles are more broadband compared to cylindrical dipoles. When placed together in an array, they form a high-Q resonant system which must be loaded with a lossy phantom or a water bolus of high conductivity, in order for the FDTD simulations to reach steady state within a reasonable time period [1]. Therefore, the behavior of the two antenna types with dielectrics in their near field has been investigated separately. Moreover, the simulations reveal that modeling of the gap between the flat antennas and the water bolus is a crucial issue. Flat antennas are also problematic when not aligned to the rectilinear FDTD grid. Nevertheless, the results for the realistic patient model are encouraging and show little variation in SAR distribution when downsizing the mesh size or using cylindrical instead of flat dipoles.

**CONCLUSIONS:** The results until now support the feasibility of creating a treatment planning tool for deep regional hyperthermia on a patient basis, using numerical models of unprecedented detailedness. This becomes possible by applying nonuniform FDTD technique. It still remains to determine a semi-automatic segmentation process for the creation of such models and to investigate in detail the important modeling aspects with FDTD.

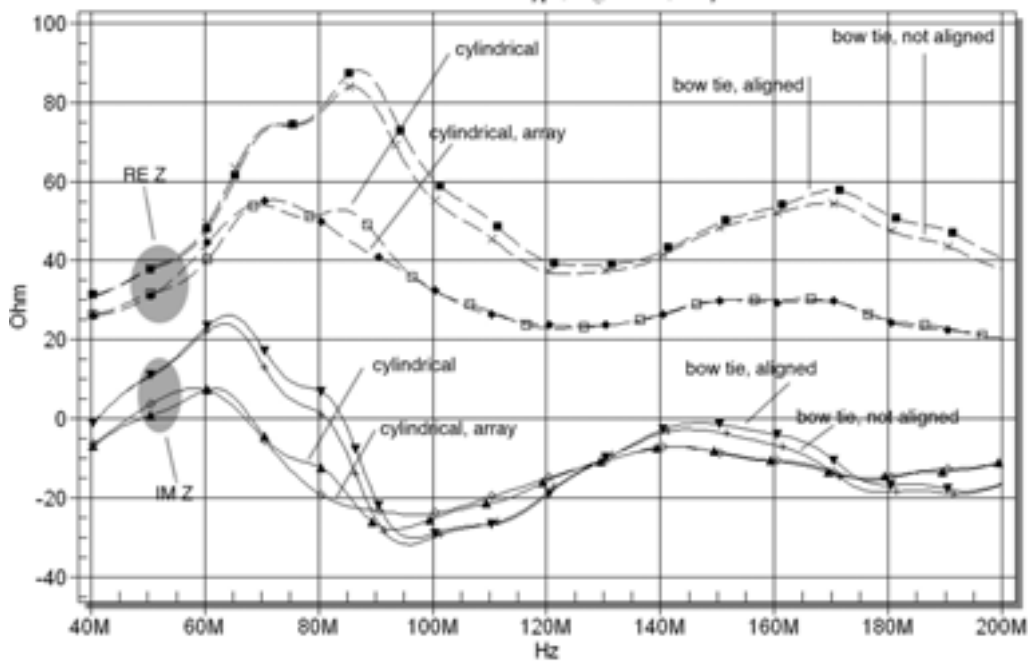
[1] C.E. Reuter, A. Taflove, V. Sathiaselan, M. Picket-May, B.B. Mittal, "Unexpected physical phenomena indicated by FDTD modeling of the Sigma-60 deep hyperthermia applicator", IEEE Trans. Microwave Theory and Techn., vol. 46, pp. 313-319, 1998





### Impedance Z (RE/IM)

influence of antenna-type, alignment, array



ST-14

**EFFECTS ON THE CYTOKINE PRODUCTION AFTER EXPOSURE TO THE REPETITIVE MAGNETIC STIMULATION.** S. Yamaguchi, M. Ogiue-Ikeda, M. Sekino, S. Ueno. Dept of Biomedical Engineering, Graduate School of Medicine, Univ of Tokyo, Bunkyo-ku, Tokyo, Japan.

**OBJECTIVES:** Biomagnetic stimulation is a method for stimulating tissues non-invasively. The basis

of magnetic stimulation is to induce eddy currents in a target by using a time-varying pulsed magnetic field [1]. However, the effects of magnetic stimulation on immune systems were poorly understood. In this study, we carried out *in vivo* and *in vitro* experiments to clarify the effects on immune systems. **METHODS:** Magnetic stimulations were performed with a magnetic stimulator (Nihon Kohden), which delivered biphasic cosine current pulses for 238  $\mu$ s. A circular coil (inner diameter = 15 mm, outer diameter = 75 mm) was used in the experiments. Based on our previous study [2], [3], stimulus conditions were determined as follows: peak magnetic field = 0.25 T (at the center of the coil, 50% of the motor threshold), frequency = 25 pulses/sec, and 1000 pulses/sample/day. Magnetically induced eddy currents were estimated as follows: 0.79 – 1.54 A/m<sup>2</sup> (in mice) or 2.36 – 2.90 A/m<sup>2</sup> (at the bottom of the culture dish). C57BL/6J mice (6-8 w, female) were exposed to the magnetic stimulation for 3, and 7 times. 24 hours after the final stimulation, IL-2 and TNF- $\alpha$  were measured by ELISA method (Immunoassay Kit: BIOSOURCE). In the cellular study, spleen cells were isolated and pre-treated by lipopolysaccharide (LPS: 10  $\mu$ g/mL) for 2 hours. 24 hours after the exposure, proliferative activity and TNF- $\alpha$  production were measured. For statistical analysis, Mann-Whitney U-test was performed. Probability (p) values

**RESULTS AND DISCUSSION:** Fig. 1-A shows the cytokine production of each mouse group. TNF- $\alpha$  production was significantly increased in the stimulated group compared with the shams (3-day group: p < 0.05, and 7-day group: p < 0.05). The increase of TNF- $\alpha$  production in the stimulated group showed dose dependency. Although IL-2 production in both of the stimulated group showed the up-regulation compared with the shams, statistically significance was not detected. In the cellular study, the proliferative activity was not changed after the magnetic stimulation exposure. However, TNF- $\alpha$  production in the exposed group was activated (141.1%) compared with controls. Fig. 1-B shows the cytokine production of each group.

The present study indicated evidence for functional changes in the immune system might be caused by magnetic stimulation for 3 or 7-times. In the cellular study, results of the present study showed the direct effects of magnetic stimulation on lymphocytes.

**CONCLUSION:** We have demonstrated that the functional changes in immune system might be caused by magnetic stimulation *in vivo* and *in vitro*.

**ACKNOWLEDGMENT:** We thank Dr. Izumi Nisimura, Central Research Institute of Electric Power Industry, for providing technical guidance.

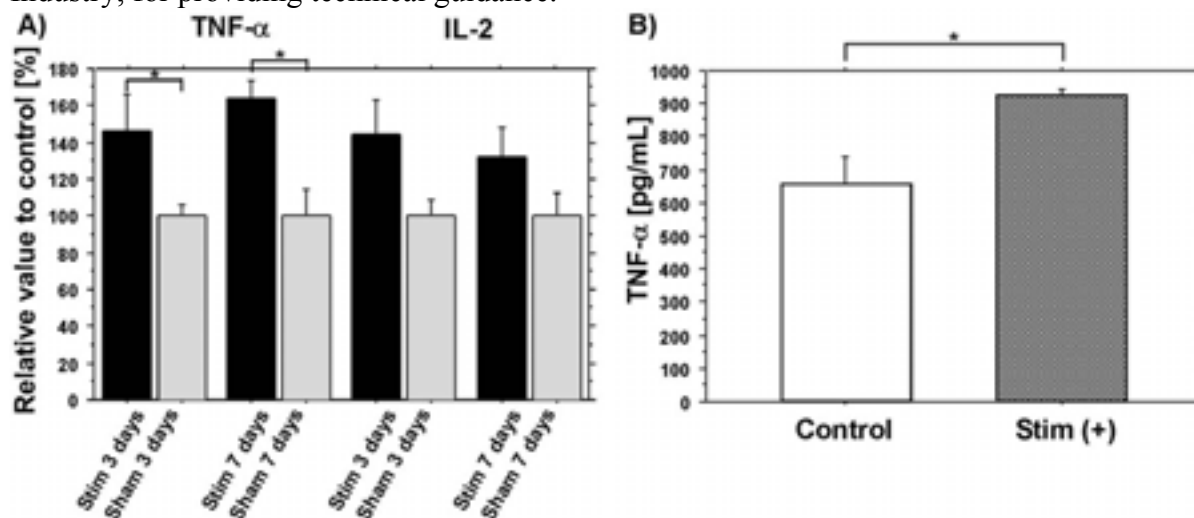


Fig. 1 Effects on the cytokine production after exposure to the repetitive magnetic stimulation. A) TNF- $\alpha$  and IL-2 production in mice spleens. B) TNF- $\alpha$  production in spleen cells.

**REFERENCES:**

[1] S. Ueno, T. Tashiro, and K. Harada, Journal of Applied Physics, vol. 64, pp. 5862-5864, 1988.

[2] M. Ogiue-Ikeda et al, Brain Research, vol. 993, pp. 222-226, 2003.

[3] S. Yamaguchi et al, IEEE Transactions on Magnetics, vol. 40, pp. 3021-3023, 2004.

## Session 12: Dosimetry V

*Chairs: James Lin and Wolfgang Kainz*

**4:00 - 6:00 pm, Theatre L**

12-1

**SAR DISTRIBUTION PRODUCED BY CELLULAR PHONES RADIATING CLOSE TO THE HUMAN BODY.** P. Bernardi<sup>1</sup>, M. Cavagnaro<sup>1</sup>, S. Pisa<sup>1</sup>, E. Piuzzi<sup>1</sup>, J. C. Lin<sup>2</sup>. <sup>1</sup>Dept of Electronic Engineering, 'La Sapienza' Univ of Rome, Rome, Italy, <sup>2</sup>Dept of Bioengineering and Dept of Electrical and Computer Engineering, Univ of Illinois at Chicago, Chicago, IL, USA.

**INTRODUCTION:** Cellular phones commonly are used in contact with the ear. However, when they are used with a headset, they can be positioned at different body locations. Moreover, unintentional exposures also might occur for a subject standing close to someone using a cellular phone, for example, in a crowded environment. For localized exposures, international standards limit the maximum SAR to 1.6 W/kg as averaged over 1 g [1] or to 2 W/kg as averaged over 10 g [2]. These limits often are used for compliance assessment of cellular phones when positioned in contact with the ear. However, for studies on biological effects of the electromagnetic field, SAR distributions in the various body tissues and organs are of similar significance.

**OBJECTIVES:** The aim of this investigation is to study human exposure to cellular phones placed at various positions close to the human body. In particular, eleven different locations have been considered, in front of: the right and left ear, the nose, eye, heart, lung, shoulder, stomach, hip, lower back, and groin, as shown in Fig. 1. The exposure due to a dipole model of the cell phone will be compared by computing the maximum SAR as averaged over 1 g ( $SAR_1$ ) and 10 g ( $SAR_{10}$ ) in the body, and the maximum  $SAR_1$  in the principal organs or tissues exposed to the field radiated by the phone.

**METHODS AND MODELS:** The FDTD technique is used by considering a time-harmonic excitation and by applying a uniaxial perfectly matched layer for the truncation of the computational domain. The phone model consists of a simple half-wavelength dipole operating at 900 MHz. The model for the exposed subject is derived from a 3-mm resolution tissue-classified version of the "Visible Human" data set. Since local SAR values are strongly dependent on the averaging procedure, it is important to accurately define this procedure. In this paper, we have followed that suggested in [3].

**RESULTS:** The results obtained for 1 W of radiated power and with the closest point of the dipole arms placed at a distance of 9 mm (3 FDTD cells) from the human body, are given in Table I. It can be seen that, in all cases, more than 60% of the radiated power was absorbed inside the human body. The maximum values of  $SAR_1$  and  $SAR_{10}$  are obtained when the phone is close to the ear (items 1 and 2 in Fig. 1). The  $SAR_{1fat}$  and  $SAR_{1muscle}$  have their highest values when the phone was placed in front of the lung (item 6 in Fig. 1), while the  $SAR_{1brain}$  and the  $SAR_{1eye}$  are the highest when the dipole was in front of the eye (item 4 in Fig. 1).

**CONCLUSIONS:** The SAR distributions produced by a cellular phone placed at various body locations have been investigated. The phone model was a simple dipole and it was used for comparing the SAR under various exposure conditions. More realistic phone models may produce different SARs, but similar behavior with source position is expected.

**References.**

- [1] IEEE Standard for Safety Levels With Respect to Human Exposure to Radio Frequency Electromagnetic Fields, 3 kHz to 300 GHz, IEEE Standard C95.1, 1999.
- [2] ICNIRP, "Guidelines for limiting exposure to time-varying electric, magnetic, and electromagnetic fields (up to 300 GHz)," Health Phys., vol. 74, no. 4, pp. 494-522, Apr. 1998.
- [3] K. Caputa, M. Okoniewski, and M.A. Stuchly, "An algorithm for computation of the power deposition in human tissue," IEEE Antennas Propagat. Magazine, vol. 41, no. 4, August 1999.

	P < SUB>ABS	SAR <sub>1</sub>	SAR <sub>10</sub>	SAR <sub>1fat</sub>	SAR <sub>1muscle</sub>	SAR <sub>1brain</sub>	SAR <sub>1eye</sub>
1	0.84	13.84	6.22	0.69	0.97	0.82	0.028
2	0.84	15.02	7.05	0.10	2.70	0.77	0.024
3	0.60	9.47	4.08	0.08	0.91	0.20	0.589
4	0.81	9.09	5.78	0.18	2.13	1.23	7.988
						SAR <sub>1lung</sub>	SAR <sub>1heart</sub>
5	0.69	3.22	1.99	1.12	2.45	1.54	0.294
6	0.72	4.43	2.73	2.99	3.56	2.41	0.020
7	0.83	6.61	3.67	2.08	3.40	1.79	0.002
						SAR <sub>1testicle</sub>	SAR <sub>1bladder</sub>
8	0.83	3.77	1.72	1.96	1.81	0.001	0.003
9	0.88	9.09	5.78	0.18	2.13	< 0.001	< 0.001
10	0.89	3.89	2.35	2.11	1.18	< 0.001	0.002
11	0.80	8.00	3.40	0.45	0.39	3.28	0.01

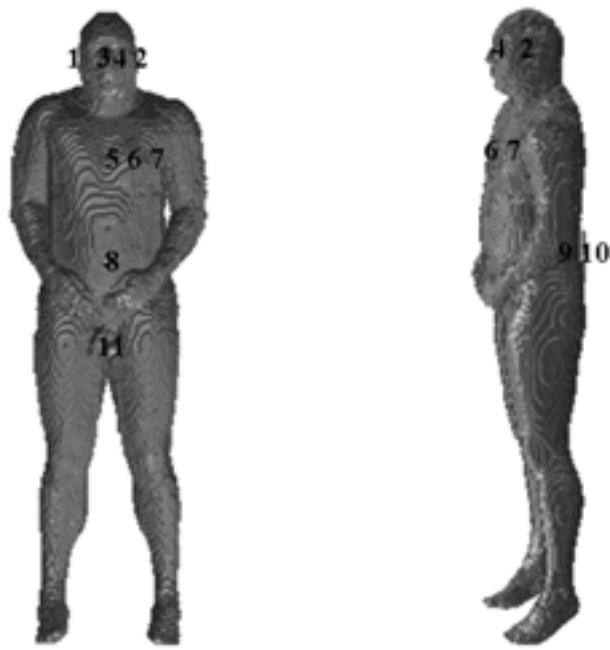


Fig. 1. Phone positions with respect to the "Visible Human" model

12-2

**EVALUATION OF THE LOCAL SAR IN A SIMPLE ABDOMEN MODEL OF PREGNANT WOMEN AT 150 MHZ.** K. Ito<sup>1</sup>, H. Kawai<sup>2</sup>, M. Takahashi<sup>1</sup>, K. Saito<sup>1</sup>, T. Ueda<sup>3</sup>, M. Saito<sup>3</sup>, H. Ito<sup>3</sup>, H. Osada<sup>4</sup>, Y. Koyanagi<sup>5</sup>, K. Ogawa<sup>6</sup>. <sup>1</sup>Research Center for Frontier Medical Engineering, Chiba Univ, Japan, <sup>2</sup>Graduate School of Science and Technology, Chiba Univ, Japan, <sup>3</sup>Radiation Oncology, Graduate School of Medicine, Chiba Univ, Japan, <sup>4</sup>Chiba Univ Hospital, Japan, <sup>5</sup>R & D Center, Panasonic Mobile Communications Co., Ltd., Japan, <sup>6</sup>Communication Devices Development Center, Matsushita Electric Industrial Co., Ltd., Japan.

**OBJECTIVE:** Recently, RF (radiofrequency) devices, which are usually placed in the vicinity of the human body, are widely used in various situations. Pregnant women and their fetuses may be exposed to the EM (electromagnetic) waves radiated from the devices, e.g., portable radio terminals for business, IH (induction heating) cookers, hand-held metal detectors, etc. It is therefore necessary to evaluate the EM waves' exposure to the fetus inside the pregnant women. However, in the previous studies [1], [2], the structure inside the pregnant women was inaccurate because it is difficult to obtain the MR (magnetic resonance) images. In addition, little is known about the dielectric constants of the amniotic fluid and those of the fetus because the measurement of such values is quite difficult. Therefore, an abdomen model, which has accurate structure, and actual dielectric constants of the fetus are indispensable to evaluate the precision EM waves' exposure in the fetus. This paper presents the simple modeling of the abdomen of the Japanese pregnant women and the evaluation of the SAR (specific absorption rate [W/kg]) in the proposed model close to the portable radio terminals at 150 MHz. **METHODS:** First, the dielectric constants of the amniotic fluid and fetus of rabbits, which are easier to obtain those of the human, are measured because the electrical properties of mammals are almost equal to those of the human [3]. Next, a simple abdomen model, which is composed of three different types of tissues, of pregnant women based on measurements of MR images is introduced, as shown in Fig. 1 (left). Finally, the SAR inside the abdomen model close to a  $0.11\lambda$  NHA (normal mode helical antenna)

is calculated using the FDTD (finite-difference time-domain) method at 150 MHz, which is commonly used in the portable radio terminals for business, e.g., police, broadcasting industry, fire fighting, etc. Here, the NHA is placed in front of the proposed model to evaluate the worst-case exposure, when the distance between the antenna and model is 40 mm to realize the actual situation, as given by Fig. 1 (right).

**RESULTS:** Figures 2 and 3 show the measured dielectric constants of the amniotic fluid and those of the fetus of rabbits at 23 °C. Here, the amniotic fluid of the human has been received from a Japanese healthy volunteer. As shown in Fig. 2, the dielectric constants of the amniotic fluid of the rabbit fit those of the human. From Figs. 2 and 3, the conductivity of the tissues is 1.8 or 1.3 times larger than that of the human muscle of adults [3] at 150 MHz. Literature [4] proposed almost the same result for the measured dielectric constants of rats. From these results, it is appropriate to use the dielectric constants of the fetus of the rabbits instead of those of the human. Therefore, the simple abdomen model of pregnant women, which uses the measured dielectric constants of the amniotic fluid and those of the fetus of rabbit, is proposed and applied to calculate the SAR in the model close to the NHA at 150 MHz. Figure 4 illustrates the SAR distribution inside the abdomen model ( $x$ - $y$  plane,  $z = 0$ ) [see Fig. 1], when the antenna input power is 1.0 W. Here, the output power is corrected by use of the efficiency of the NHA in free space. As a result, the high SAR distribution in the amniotic fluid is obtained. In addition, the peak SAR in the fetus is less than 38% of that in the mother's body. Moreover, the SAR distribution is asymmetrical on the  $y$  axis because of the structure of the NHA. Furthermore, we have also confirmed that the 10-g average SAR in the fetus is less than 1.50 W/kg, when the output power of the NHA is 5 W, which is the maximum output of the portable radio terminals in Japan. Here, the input impedance of NHA is perfectly matched close to the abdomen model. In actual situation, it is assumed that the SAR is strongly reduced by the mismatch loss, which is caused by the vicinity of the human body, e.g., -10 dB in the same position [5].

**CONCLUSIONS:** This paper presented the simple abdomen model of pregnant women and its application to the SAR estimation. From these investigations, the abdomen model including the amniotic fluid is necessary to evaluate the accurate SAR in the fetus. In addition, we have confirmed that the 10-g average SAR in the fetus is sufficiently less than 2 W/kg in the worst-case exposure.

#### REFERENCES:

1. A. H. J. Fleming and K. H. Joyner, Estimates of absorption of radiofrequency radiation by the embryo and fetus during pregnancy, *Health phys.* 1992, 63, 2, pp. 149-159.
2. W. Kainz, D. D. Chan, J. P. Casamento, and H. I. Bassen, Calculation of induced current densities and specific absorption rates for pregnant women exposed to hand-held metal detectors, *Phys. Med. Biol.* 2003, 48, pp. 2551-2560.
3. C. Gabriel, Compilation of the dielectric properties of body tissues at RF and microwave frequencies, *Brooks Air Force Technical Report* 1996, AL/OE-TR-1996-0037.
4. A. Peyman, A. A. Rezazadeh, and C. Gabriel, Changes in the dielectric properties of rat tissue as a function of age at microwave frequencies, *Phys. Med. Biol.* 2001, 46, pp. 1617-1629.
5. K. Ogawa, Y. Koyanagi, and K. Ito, An analysis of the effective radiation efficiency of the normal mode helical antenna close to the human abdomen at 150 MHz and consideration of efficiency improvement, *Electronics and Communications in Japan, Part I*, 2002, 85, pp. 23-33.

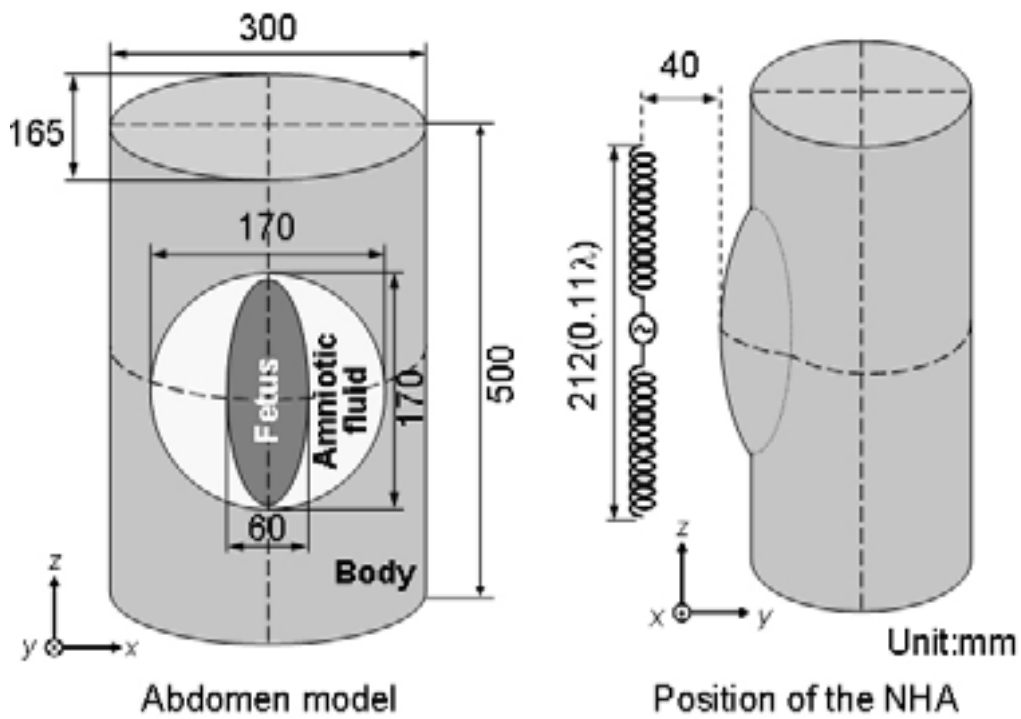


Figure 1: Calculation model.

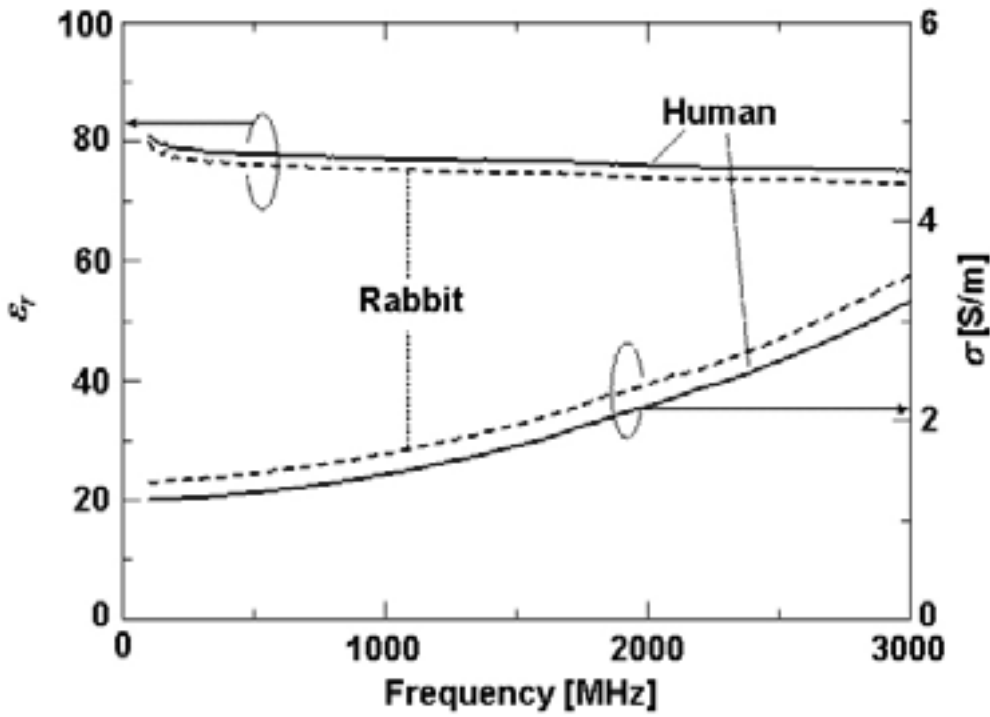


Figure 2: Measured dielectric constants of the amniotic fluid.

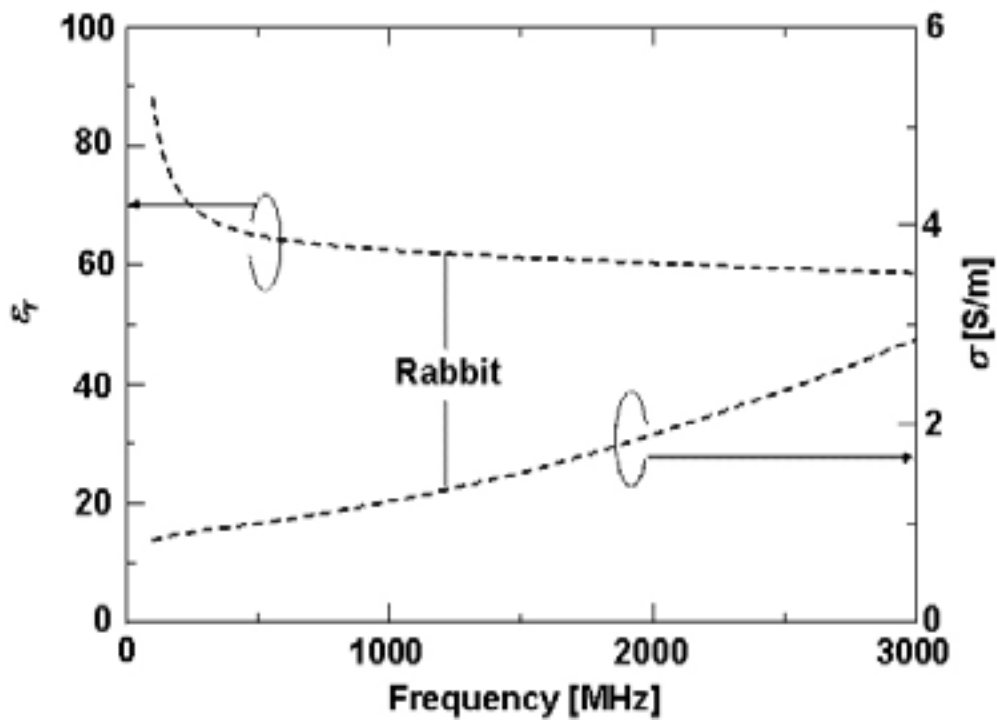


Figure 3: Measured dielectric constants of the fetus of rabbits.

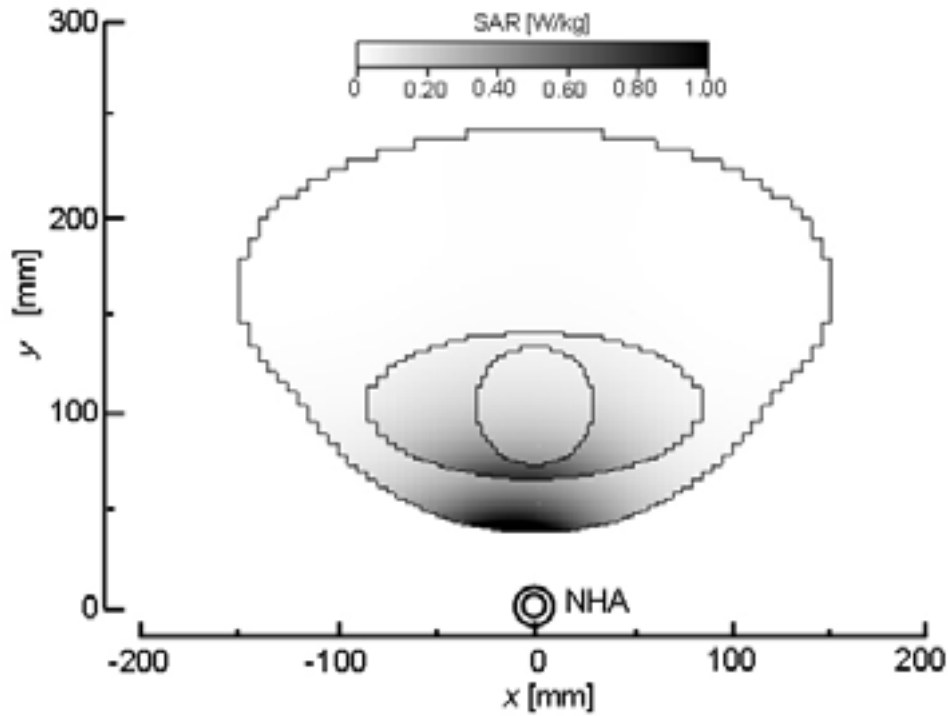


Figure 4: SAR distribution inside the abdomen model ( $x$ - $y$  plane,  $z = 0$ ).

**DEVELOPMENT OF PREGNANT WOMAN MODELS FOR NINE GESTATIONAL AGES AND CALCULATION OF FETUS HEATING DURING MAGNETIC RESONANCE IMAGING (MRI).** W. Kainz<sup>1</sup>, T. R. Kellom<sup>1</sup>, R. Qiang<sup>2</sup>, J. Chen<sup>2</sup>. <sup>1</sup>U.S. Food and Drug Administration (FDA), Center for Devices and Radiological Health (CDRH), Maryland, <sup>2</sup>The Univ of Houston, Dept of Electrical and Computer Engineering, Texas, USA.

We developed nine pregnant woman models, one for each month of pregnancy. For the model corresponding to a pregnancy in the eighth month we calculated the spatial deposition of RF energy during a magnetic resonance imaging (MRI) scan. In addition to calculating the specific absorption rate (SAR) distribution, we calculated the temperature rise inside the pregnant woman and the fetus by solving the bio-heat equation for the three-dimensional model.

Over the past decade, MRI has proven useful in diagnosing certain uncommon cardiovascular problems such as cardiac tumors or congenital heart disease. MRI is also a valuable research tool for studying more common cardiac disorders such as ischemia and cardiomyopathy. Thus, it is not surprising that the question of whether or not a patient should undergo an MRI procedure during pregnancy will often arise. Today, pregnant woman are clearly disadvantaged if they are in need of MRI. Because of the lack of appropriate numerical models of a pregnant woman and the fetus, the SAR absorption and the temperature distribution inside the mother and the fetus are still unclear.

Data that describe the shape of the body surface of a pregnant woman in the 34<sup>th</sup> gestational week (body 1) were obtained. This data was provided by FarField Technology Limited, Christchurch, New Zealand. A second CAD (Computer Aided Design) model, a body surface of a non-pregnant woman (body 2), was obtained from 21<sup>st</sup> Century Solutions Ltd. Fetus, bladder, uterus, placenta and bones are based on MRI data of a woman in the 35<sup>th</sup> gestational week. The MRI data has a resolution of 5 mm and was provided by Prof. LeRoy Heinrichs from the Stanford Univ. We converted the data sets to STL (Stereolithography) format and combined them into one CAD object. To make the CAD data useable for meshing it is important to have watertight objects. We used Rhino 3 to manipulate and scale the objects and a special plug-in for Rhino 3 (Meshworks from Floating Point Solutions) to make the objects watertight. For the models month-1 to month-4 we used body 2, and for the models month-5 to month-9 we used body 1. Assuming the belly of a pregnant woman begins noticeable growing between the third and fourth month, we scaled the belly from body 1 for the pregnant woman models month-5 to month-7. Body 2, used for the models month-1 to month-4, remained unchanged. Uterus, placenta and fetus were scaled according to the different sizes for the different gestational age.

In addition to the nine pregnant woman models, we developed a computer model of a 3 T MRI coil with 16 legs operating at 128 MHz. Both the month-8 pregnant woman model and the MRI coil were imported in SEMCAD and meshed in a graded mesh with a resolution between 4 mm and 5 mm. The SEMCAD v1.8 electromagnetics solver and thermal solver were used to calculate the SAR and temperature distribution inside the model. The calculation took 24 h on a 3 GHz workstation and used about 1 GB of memory.

The SAR and the temperature values for the month-8 model are given in table 1. All values are scaled to

a whole body average SAR of 2 W/kg. Uterus and placenta have organ SAR averages above the whole body average SAR. The highest temperature increase occurring in the body was 0.9 °C. The highest local temperature increase in the fetus is 0.3 °C. The data for the month-8 model shows that the fetus exposure and the fetus temperature increase is less than those for the mother. The fetus seems to be protected from heating by relatively high blood flow in the placenta and the uterus. The second highest temperature increase, 0.5 °C, was located in the amniotic liquid.

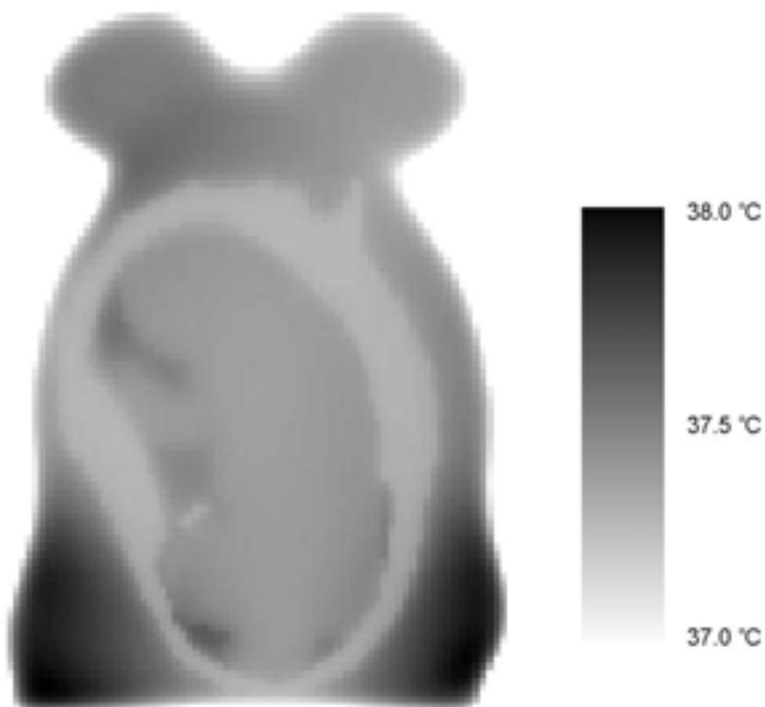


Figure 1. Temperature distribution inside the pregnant woman model for a whole body SAR of 2 W/kg.

This is the first time that anatomical CAD models of pregnant women for different gestational ages were developed and used for MRI dosimetry and heating calculations. Although scaling a fetus from the eighth month to the first month is not anatomically correct, we used this method as a first approach to estimate the fetal SAR dose and the fetal heating. Future calculations will include all nine models exposed to a 1.5 T MRI coil operating at 64 MHz and a 3 T MRI coil operating at 128 MHz and a comparison to a real MRI data set of a pregnant woman in the 7<sup>th</sup> month of pregnancy. The pregnant woman CAD models and the dosimetry calculations will help to define SAR safety limits for MRI procedures for pregnant woman and fetus heating.

The opinions and conclusions stated in this paper are those of the authors and do not represent the official position of the Dept of Health and Human Services. The mention of commercial products, their sources, or their use in connection with material reported herein is not to be construed as either an actual or implied endorsement of such products by the Dept of Health and Human Services.

Tissue	SAR <sub>organ average</sub>	SAR <sub>local peak</sub>	$\Delta T_{\max}$
	W/kg	W/kg	°C
All Tissue	2.0	24.8	0.9

Body	2.0	24.8	0.9
Fetus	0.6	5.0	0.3
Uterus	2.4	14.8	0.2
Bladder	0.9	3.3	0.2
Bone	0.4	2.5	0.1
Liquid	1.0	9.2	0.5
Placenta	3.1	10.1	0.2
Table 1. SAR (average and local peak value) and maximum temperature rise for each tissue.			

12-4

**EVALUATION OF MOBILE PHONE HANDSET EXPOSURES USING SOFTWARE MODIFIED PHONES AND FIELD PHANTOM SYSTEMS.** M. A. Kelsh<sup>1</sup>, C. Sulser<sup>2</sup>, M. Shum<sup>1</sup>, M. McNeely<sup>1</sup>, N. Kuster<sup>3</sup>, J. Froehlich<sup>3</sup>, A. Sheppard<sup>4</sup>. <sup>1</sup>Exponent, Inc., Menlo Park, CA, <sup>2</sup>Schmid & Partner Engineering AG, Zurich, Switzerland, <sup>3</sup>Foundation of Research on Information Technologies in Society (ITIS) Zurich, Switzerland, <sup>4</sup>Asher Sheppard Consulting, Redlands, California, USA.

**INTRODUCTION:** Information in epidemiologic studies on mobile phone exposure is derived from estimation of cumulative duration of use or the total/average number of calls, with relatively little attention to date on the actual radiofrequency (RF) energy or SAR values involved. Recently limited information on the potential intensity and variability of RF exposure has been examined through the use of software modified dose phones (SMPs) and through evaluation of FCC compliance testing data. Mobile phone compliance data measure the maximum averaged spatial peak SAR, but these data do not necessarily determine SAR levels that can occur during actual use. The development of a mobile phantom SAR measurement system that allows real time estimates of energy output, which is then linked to device specific SAR distributional data, allows for more precise exposure evaluation.

**OBJECTIVES:** To observe inherent differences between handsets of various technologies, manufacturers, and handset styles under different environmental conditions in the San Francisco Bay area.

**METHODS:** Three phantom heads, each containing two dipole field probes placed near each ear canal were used to simultaneously evaluate radiated power absorbed in the dielectric medium (i.e., SAR). The heads had 10, 14, or 30 mm dipoles, as required for the sensitivity and dynamic range needs of each technology. Each handset position was adjusted on the head surface to obtain the greatest signal level. The data recording and analysis system (SYNEHA) could simultaneously measure radiated power from four mobile phones, (two each on two phantom heads) while the third phantom was used with two software-modified phones capable of recording PWC independently of SYNEHA. The two software-modified phones (SMP) (Motorola Timeport P7389) measured PWC at 2.5 s intervals and stored the data in onboard memory before being downloaded to a PC. The phantom field system was installed in a van to conduct tests while driving, which permitted evaluation of the effects of changing distances to base stations and different environments. Three routes were used: 1) freeway, major thoroughfare, and surface streets in the San Francisco Bay area; 2) densely urban downtown San Francisco streets; and

3) a rural route outside the Bay Area. Stationary measurements were also collected at predetermined locations for each route.

The SYNEHA system specifications are:

- sampling rate: > 3000 samples/s
- dynamic range (SAR): < 1mW/kg to 2W/kg
- linearity: < 0.2dB deviation
- noise: < 1mW/kg
- operating conditions: 10-40°C (<< 1dB deviation); 0 - 90% humidity
- relative position accuracy (head/phone/probe): < 1mm
- power: 12V DC (internal battery and external DC power)

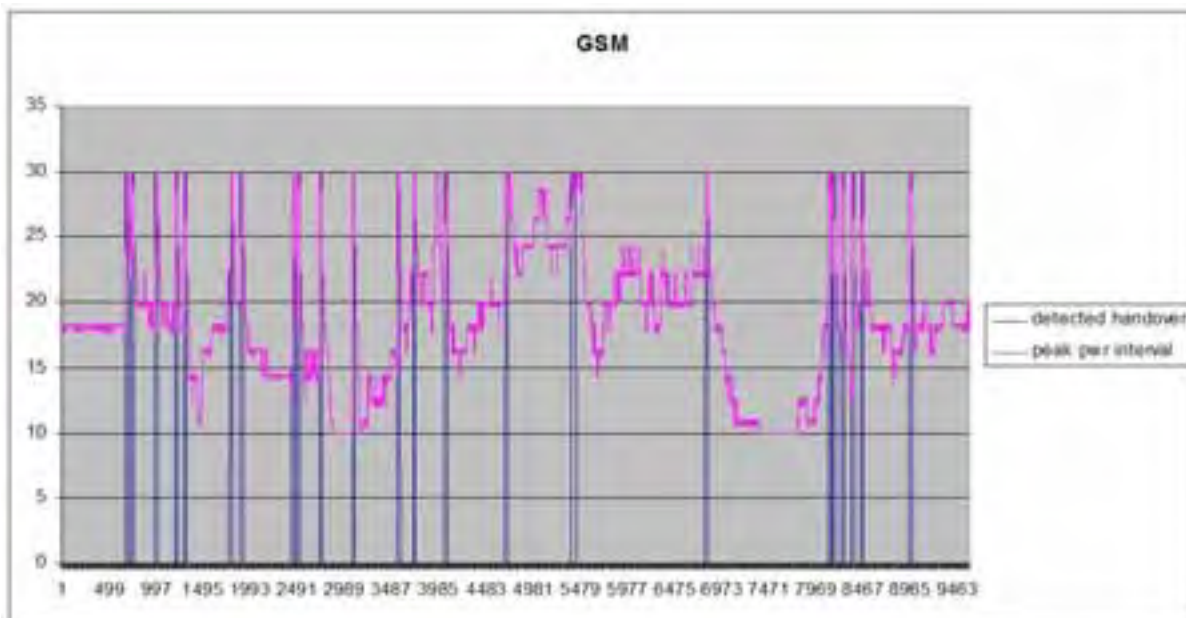
A GPS receiver synchronously records location during the measurement period. Data evaluation is performed in three major steps: 1) probe signals are fed to an EASY4 measurement server that processes these into electromagnetic field data for transfer to a PC running the SYNEHA software; 2) the data are further processed into power values and saved to a file with the GPS data; and 3) post processing reduces the data by calculating various summary statistics of range of power values, average power, and average maximum power over an interval. Finally, these post-processing power values are converted to SAR estimates using laboratory distributional data and using calibration data of maximum power levels.

**RESULTS:** Our results indicated that GSM data were dominated by handovers as evidenced by peaks in the time series data, whereas TDMA, CDMA, and AMPS were not. Handsets using the CDMA technology produced the lowest peak power levels of all four technologies (Figure 1).

**DISCUSSION:** Handset output power and SAR levels will be controlled over a wide dynamic range by the base station in a manner that differs greatly among technologies (analog, GSM, CDMA, TDMA) and may be a major factor in estimating exposure to individuals. The SYNEHA system was successfully tested for use with the above mobile phone technologies that operate in the United States. Preliminary results were not consistent with trends noted from an evaluation of FCC compliance testing data, where CDMA was higher than TDMA and GSM technologies. This indicates the need for further field data evaluation in order to help to identify factors that influence potential SAR levels among mobile phone users.

**ACKNOWLEDGEMENT:** The study was supported by the Cellular Telephone and Internet Association (CTIA) with technical oversight by the U.S. FDA.

Figure 1: Power control data from a GSM handset during freeway/highway/surface street route (Average Peak Power (dBm) v. time)



12-5

**ANALYSIS OF SAR AND TEMPERATURE IN A CANONICAL HEAD MODEL EXPOSED TO DIFFERENT SOURCE CONFIGURATIONS AND FREQUENCIES.** J. C. Lin<sup>1,2</sup>, Z. Wang<sup>2</sup>. <sup>1</sup>Dept of Electrical and Computer Engineering, Univ of Illinois – Chicago, Chicago, IL, <sup>2</sup>Dept of Bioengineering, Univ of Illinois – Chicago, Chicago, IL, USA.

### Introduction

Computer simulation of biological models exposed to radio frequency (RF) and microwave radiation have provided useful information on electromagnetic energy absorption and/or temperature change. The computation generally has been conducted using homogeneous and heterogeneous bodies of revolution, or by using anatomically accurate human models, especially for the head, under a variety of exposure conditions. However, results have been inconsistent, and often been controversial because of the large variety of exposure situations and/or biological models examined. Results based on canonical formulations would serve as a reference for comparison. In this paper, we present a numerical comparison of the SAR and temperature in a canonical model of the human head - homogeneous, different sized, spherical models under typical exposure situations represented by a plane wave and a dipole for wireless communication, and by a high-pass birdcage coil for magnetic resonance imaging (MRI). The frequencies range from 64 MHz to 900 MHz.

### Methods and Materials

A finite-difference-time-domain (FDTD) method was used to analyze the interaction between the spherical head models and the plane-wave, dipole, and high-pass birdcage coil sources of electromagnetic fields. An 8-layered, Berenger's PML was implemented as the absorption boundary. The computational domain consisted of a 120x120x120 grid of 4x4x4 mm cells. The dipole length was in parallel with the Z-axis. The models adopted are two spheres: an 18-cm diameter for an adult-size head and a 10-cm diameter child-size head. The dielectric properties were equivalent to the average brain material, which was obtained by a four parameter Cole-Cole extrapolation. A high-pass birdcage MRI coil (15-cm radius; 16-cm length) with 16 rungs was employed in this study. Each of rungs was 1-cm wide. The radius and length of the shield were 19 cm and 24 cm, respectively. Ideal current sources

were placed at the midpoint of each end-ring element of the MRI coil. The computational analysis was performed at 64, 128, 300 and 400 MHz, which correspond to 1.5, 3.0, 7.0, and 9.4 T, for all sources. In addition, computation was included for the 900 MHz band used by some cellular telephone systems. In order to validate the algorithm used for SAR and temperature calculations, we had replicated the experiment where a muscle cylinder was exposed to a plane wave.

#### Results and Discussions

As expected, the computed SAR and temperature distributions were different for the plane wave, dipole and birdcage coil, in all cases. In addition to serving as a set of references for comparison, the results showed SAR and temperature distributions vary with the size of the sphere model, source type and frequency, as well as the distance of separation between the source and model. At low frequencies, the SAR has the characteristic of monotonic exponential decay from the surface to the center of the models. With increasing frequency, a standing wave like behavior becomes prominent as revealed by the corresponding oscillatory wave patterns.

In homogeneous spheres, the induced temperature distributions were closely related to SAR distributions since the spheres contained the same tissue with identical thermal properties. The situation would be different in an anatomically accurate human brain model. It is interesting to note that in all cases, the temperature elevations were slightly lower at the edges - because of the convective effect.

12-6

#### **NUMERICAL DOSIMETRY IN A MODEL OF THE HUMAN INNER HEARING SYSTEM EXPOSED TO 900 MHz.** M. Parazzini, G. Tognola, F. Grandori, P. Ravazzani. Istituto di Ingegneria Biomedica CNR, Milano, Italy.

**INTRODUCTION:** This paper presents the methodology and some preliminary results obtained in the evaluation of the RF EMF and absorbed power distribution produced by mobile phones at frequency of 900 MHz in a numerical model of human inner hearing system. The numerical method used in this work is the Finite Integration Technique (FIT), implemented by the software package Microwave 5 by CST GmbH.

**MATERIAL AND METHODS:** In this study an anatomical head model including the peripheral hearing (cochlea) and vestibular systems, generated from MRI image segmentation was used. Two different sets of MRI images were taken. From the first MRI data set (160 images, 256x256 pixels; 0.93x0.93x1mm) a 4 tissues numerical voxel-head model was obtained. This model was integrated using a second set of MRI images (60 images, 256x256 pixels; 1.01x1.01x0.8 mm) of the same subject, scanned using a specific acquisition protocol to enhance the signal coming from both inner ear and adjacent structures, from which a realistic representation of the cochlea and of semicircular canals of the vestibular system was obtained (in the following, the term vestibulus will be referred to both the cochlea and the vestibular system).

The radiation source was modelled as a  $\frac{1}{4}$  monopole on a conducting box at the working frequency of 900 MHz and a total radiated power of 1 W. The antenna was centred on the metal box. The metal box was covered with a dielectric insulator of 2 mm of thickness and  $\epsilon_r = 2$ . The numerical simulations were performed with the phone placed so that its longitudinal axis followed an imaginary line from the entrance to the ear canal to the corner of the mouth, with the antenna feedpoint directly behind the opening of the auditory canal. The handset and the external layer of the head were in contact, therefore the distance between the monopole and the closest head surface, the pinna of the ear, was 1.5 cm. The interaction between the RF EMF and the vestibulus has been studied evaluating the spatial-peak distribution of the E, H and absorbed power in the target anatomical structure (vestibulus) and along a

series of lines passing through it (particularly one line going from the vestibular to the cochlear region, called Vestibular-to-Cochlea line and one line inside the cochlea from the apex to the base, called Apex-to-Base line) and along a straight line from one ear to the other on the medial plane of the head.

**RESULTS:** First of all, the influence of the presence of the vestibulus inside the head model on the EMF and SAR distributions has been evaluated comparing the results obtained with two models whose only difference was the presence or the absence of the vestibulus model. The absence of the vestibular model produces an underestimate in the SAR distribution. However, the differences in the SAR distribution are localized only in the ear region: the influence of the vestibulus model is therefore only local. As expected, the peak values in the contralateral ear are much more reduced compared to the one in the ear near the source.

The trend of E and H field distributions along the lines inside the vestibulus show an exponential decay along the Vestibular-to-Cochlea line and a quadratic trend along the Apex-to-Base line in the ear near the source, while the E and H field distribution in the contralateral ear is characterized by a quadratic trend along all the considered lines inside the vestibulus. As for the SAR distribution, the trend is an exponential decay along the Vestibular-to-Cochlea lines and a quadratic trend along the Apex-to-Base in both ears. Preliminary results relative to the effects of anatomical variability and changes in EMF characterization of the tissues should be also presented.

**CONCLUSIONS:** The results of this study clearly demonstrate that the dosimetry of radiofrequency fields in the hearing system, must be performed including a model of the hearing system itself.

As to the distribution of the fields inside the peripheral hearing system, the exponential decay trend of EMF and SAR suggests an higher EMF interaction in the vestibular region compared to the auditory region of the vestibulus, while the quadratic trend suggests an higher interaction in the basal and apical region of the cochlea compared to the middle one.

**ACKNOWLEDGEMENTS:** This work is partially supported by the European Project GUARD *°Potential adverse effects of GSM cellular phones on hearing*± (FP5, QLK4-CT-2001-00150, 2002-2004), the European Project EMFNear *°Exposure at UMTS Electromagnetic Fields: Study on Potential Adverse Effects on Hearing*± (DG Health & Consumer Protection±, Agreement Number: 2004127, 2004`C2007), the national project ALERT *°Studio degli effetti delle microonde a 900 e 1800 MHz sulla funzionalit`± del sistema uditivo nell`uomo e nell`animale*±(the Italian Consortium ELETTRA 2000) The authors thanks Dr. F. Baruzzi of Ospedale di Circolo di Varese for the MRI images and kind assistance.

12-7

**AN OPTIMIZATION PROCEDURE TO DEVELOP SIMPLE NUMERICAL MODELS OF CELLULAR PHONES FOR AN ACCURATE EVALUATION OF SAR DISTRIBUTION IN THE HUMAN HEAD.** S. Pisa<sup>1</sup>, M. Cavagnaro<sup>1</sup>, V. Lopresto<sup>2</sup>, E. Piuzzi<sup>1</sup>, P. Bernardi<sup>1</sup>. <sup>1</sup>Dept of Electronic Engineering, 'La Sapienza' Univ of Rome, Rome, Italy, <sup>2</sup>Section of Toxicology and Biomedical Sciences, ENEA Casaccia Research Center, Rome, Italy.

**INTRODUCTION:** The consolidated approach for compliance testing of mobile phones is based on experimental measurements, carried out using real phones and head phantoms. These phantoms are simplified models of the human head and they are not suitable to perform an accurate analysis of the SAR distribution in the various tissues and organs of the head. For this kind of analysis, a study based on numerical simulations, exploiting the availability of anatomically-based numerical models of the human head, is particularly useful. However, a numerical approach for studying the interaction between mobile phones and exposed subjects requires an accurate and realistic model of the mobile phone, which is rather difficult to be obtained. The use of FDTD codes with graded mesh or with subgridding makes

the simulation of both helical and planar antennas, present in last generation phones, possible [1], [2]. Yet, an accurate modeling of the phone case remains a difficult task, even though CAD files have been recently used to accurately model the internal structure (PCB, battery, keypad and buttons, etc.) of the phone [3].

**OBJECTIVES:** In this work the possibility to use simple numerical models of the phone for an accurate evaluation of the field and of the SAR inside an exposed head is investigated. In particular, a computationally-efficient approach for the realization of such models is presented. This approach consists in starting from an accurate model of the antenna and a simplified model of the phone case, which includes only the main parts (keyboard, internal box, plastic coating, etc.) with "realistic" dimensions and electric constants. Then, these "realistic" case parameters are tuned by using an appropriate optimization procedure [4].

**METHODS AND MODELS:** The adopted optimization procedure is based on the minimization of a cost function depending on the differences between near field and SAR data obtained through simulation of the phone model and measurements performed on the real phone. In particular, the comparison considers the free-space electric and magnetic field over planes parallel to the phone front face and the SAR inside a homogeneous cubic phantom along lines parallel to the antenna axis, with the phone front face in contact with one side of the phantom. The optimization procedure has been applied to a commercial GSM cellular phone, equipped with a helical antenna. The helix geometry has been exactly determined by removing the antenna cover. In order to reveal the inner structure of the phone, both visual inspection, by disassembling the phone, and radiographic investigations have been used. In this way, a preliminary model of the phone has been built, consisting of an inner box, a plastic coating, a keyboard, and the antenna (see Fig. 1). The external dimensions of the model have been chosen according to the real phone dimensions, whereas the thickness (CT) and the permittivity of the coating, the thickness (KT), height (KH) and permittivity of the keyboard, and the box conductivity have been optimized in order to match the computed near fields and SAR distributions with the corresponding experimental measurements.

**RESULTS:** A fine optimization of the phone model has been performed, by using a graded-mesh FDTD code [5], by applying small variations on both geometrical and dielectric parameters, and testing the obtained results by means of the above mentioned cost function. The numerical results obtained with the optimized model of the commercial phone, operating at 900 MHz, have shown a good agreement with measured near fields and SAR values. As an example, Fig. 2 shows a comparison between simulated and measured free-space E-field distributions along a line parallel to the antenna axis, at a distance of 3 mm from the phone front face. The discrepancies remain within measurement uncertainty.

**CONCLUSIONS:** In this paper, an optimization procedure to obtain accurate and realistic numerical models of cellular phones has been developed. The procedure is suitable to be applied with many custom or commercial codes, based either on the FDTD technique or on the finite element method. In fact, the proposed phone optimization procedure requires only the modeling of the phone and of a cubic homogeneous phantom. The main advantage of this procedure, as compared to the use of finer phone models, including all the internal details, is that it leads to a phone model which can be easily implemented and used for fast and accurate SAR computations in the various tissues of anatomically-accurate human head models. This kind of numerically performed analysis may be employed as a support for compliance tests, to provide SAR values to be used for in vivo and in vitro experimental studies devoted to the evaluation of the effects of radiofrequency/microwave radiation on the human being, as well as to evaluate possible dose-effect relations in conjunction with epidemiological studies.

## References.

1. P. Bernardi, M. Cavagnaro, S. Pisa, and E. Piuzzi, "Power absorption and temperature elevations induced in the human head by a dual-band monopole-helix antenna phone," *IEEE Trans. Microwave Theory Tech.*, vol. 49, no. 12, pp. 2539-2546, Dec. 2001.

2. J. T. Rowley and R. B. Waterhouse, "Performance of shorted patch antennas for mobile communication handsets at 1800 MHz," *IEEE Trans. Microwave Theory Tech.*, vol. 47, no. 5, pp. 815-822, May 1999.
3. N. Chavannes, R. Tay, N. Nikoloski, and N. Kuster, "Suitability of FDTD-based TCAD tools for RF design of mobile phones," *IEEE Antennas Propagat. Magazine*, vol. 45, no. 6, pp. 52-66, Dec. 2003.
4. S. Pisa, M. Cavagnaro, V. Lopresto, E. Piuze, G. A. Lovisolo, and P. Bernardi, "A procedure to develop realistic numerical models of cellular phones for an accurate evaluation of SAR distribution in the human head," *IEEE Trans. Microwave Theory Tech.*, vol. 53, no. 4, Apr. 2005.
5. P. Bernardi, M. Cavagnaro, S. Pisa, and E. Piuze, "A graded-mesh FDTD code for the study of human exposure to cellular phones equipped with helical antennas," *Appl. Comput. Electromag. Soc. J.*, vol. 16, pp. 90-96, July 2001.

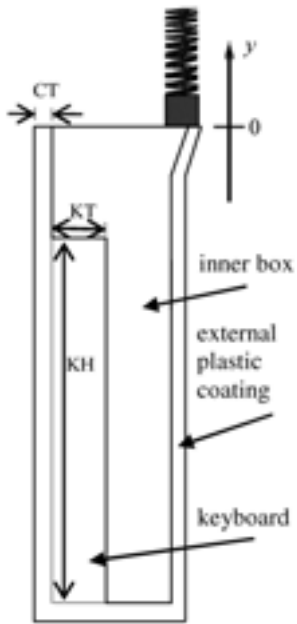


Fig. 1. Side view of the phone numerical model

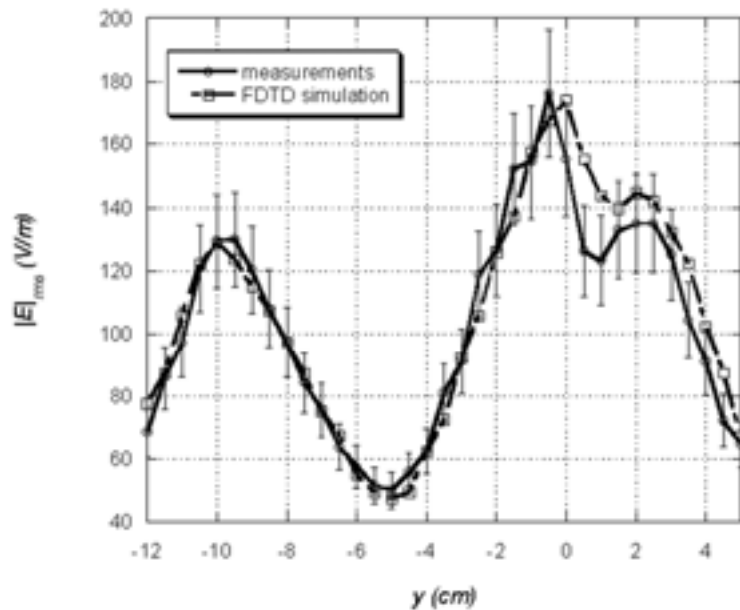


Fig. 2. Free-space E-field distribution produced by the GSM phone along a line parallel to the antenna axis 3 mm from the front face

12-8

**CHILDREN HEAD RF EXPOSURE ANALYSIS.** J. Wiart<sup>1</sup>, A. Hadjem<sup>1</sup>, N. Gadi<sup>2</sup>, I. Bloch<sup>2</sup>, M. F. Wong<sup>1</sup>, A. Pradier<sup>1</sup>, V. Fouad Hanna<sup>3</sup>, D. Lautru<sup>3</sup>, R. de Seze<sup>4</sup>. <sup>1</sup>France Telecom RD, <sup>2</sup>ENST Paris, <sup>3</sup>Universite Paris VI, <sup>4</sup>Ineris.

#### Introduction:

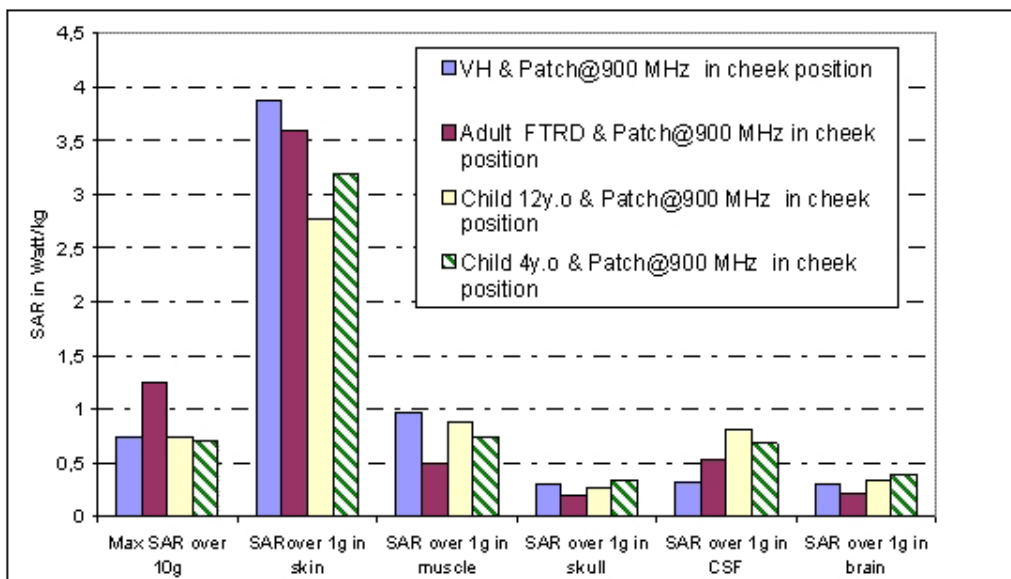
With the increase number of children using a handset there is a public concern about their specific sensitivity to Radio Frequency (RF) exposure. In the dosimetry area recent workshop organized in Istanbul by World Health Organization has recommended to improve the analysis of the power deposited in children head. The French project ADONIS under the umbrella of RNRT analyzes the influence of the morphology on the power absorbed by children head and organ

#### Methods

First using image coming from MRI, different children head models (at different ages 5, 6, 9, 12 years...;) have been built using a segmentation process. These numerical head models are after that used with different handset model in an electromagnetic solver (FDTD) to analyze the power deposited in different organs.

#### Results:

Comparisons (such as those presented in figure below) are carried out between the power absorbed by children head and the power absorbed by different adult head and with SAM .



## Session 13: Clinical Devices - Medical Applications

*Chairs: Michael McLean and Alex Thomas*

4:00 - 6:00 pm, Theatre M

13-1

**COMPARATING ANALGESIC EFFICACY OF A LOW FREQUENCY SPECIFIC PULSED MAGNETIC FIELD (CNP) TO PRESCRIPTION ORAL OPIOID ANALGESIA.** S. Chari<sup>1</sup>, A. W. Thomas<sup>2</sup>. <sup>1</sup>Fralex Therapeutics Inc., <sup>2</sup>Dept of Medical Biophysics, Univ of Western Ontario Lawson Health Research Institute and Dept of Diagnostic Imaging, St. Joseph's Health Care (London), London, Ontario, Canada.

**INTRODUCTION:** Relatively weak (100 $\mu$ T to 400 $\mu$ T) low frequency (< 1000 Hz) specific pulsed magnetic fields (Cnp) have been shown to have an antinociceptive (analgesic) effect in the land snail [1], mice [2], and in healthy human volunteers [3] measuring thermal sensory and pain thresholds. We now attempt to quantify the analgesic effect of Cnp in patients with chronic pain from musculoskeletal causes and compare said analgesic effect to that achieved in randomized controlled trials involving common prescription opioid analgesics. The demonstration of comparable analgesic efficacy may lead the way to the use of Cnp as a non-drug modality for the alleviation of chronic pain.

**OBJECTIVE:** To quantitatively compare the analgesic efficacy of Cnp to prescription opioid analgesia.

**METHOD:** We quantitatively compare the analgesic efficacy of a ( $\pm$ 400 $\mu$ T head surface to  $\pm$ 140 $\mu$ T deep brain) low frequency specific pulsed magnetic field (Cnp) to that achieved by common prescription opioid analgesics on similar patient populations. Data from randomized clinical trials involving

morphine formulations [4], CR Codeine [5] and CR Oxycodone [6] were used. All three studies included patients with chronic pain from osteoarthritis. Data on analgesia achieved by Cnp was gathered through St. Joseph's Health Care (London) Outpatient Pain Clinic in a double-blinded randomized placebo-controlled trial of patients with chronic musculoskeletal pain. In this study, subjects were loaned a Cnp unit (either active or placebo) for 7 days, to be used at least twice per day for 40 minutes (compliance was monitored through a hidden data logger). Pain diaries were completed after each treatment, and during each day of a washout week following the trial (after the patients returned the Cnp unit). In all studies, pain was measured before and after treatment using a visual analog scale (VAS) with higher numbers indicating greater pain. The analgesic effect of treatment and placebo was calculated as  $(VAS \text{ baseline} - VAS \text{ post intervention}) / VAS \text{ baseline} \times 100\%$ . The difference in analgesic effect between treatment and placebo is the net analgesic effect (NAE) for each modality and represents the amount of pain relief affected over and above placebo. For each opioid analgesic, the dosage used in the study was converted into an equivalent oral morphine dose using standard conversion ratios.

RESULTS: See Table 1.

DISCUSSION: The results of Cnp are presented within the bottom two lines of Table 1. The first includes all patients who completed the study and the second includes only those patients who were compliant to the treatment regimen and fell strictly into the inclusion criteria (intake VAS baseline > 5 of 10). Using the data obtained on all patients (NAE=20%, N=34), Cnp compares favorably with moderate to high dose opioid analgesia as studied in the two groups of patients given CR Oxycodone. The data for the selected Cnp patients (NAE=38%, N=15) is superior to the net analgesic effect obtained in the highest opioid dose study (CR Codeine). Interestingly, the data also shows a growing cumulative effect of pain relief over the treatment week, and a significant retained effect more than 1 day after entering the 'washout' phase (the patients had turned in their Cnp units) [data not shown]. Further studies involving larger groups of patients and longer study length are required to make a meta-analysis between Cnp and opioid analgesia.

#### REFERENCES

1. Thomas, Kavaliers, Prato and Ossenkopp. Antinociceptive effects of a pulsed magnetic field. *Neuroscience Letters* (1997) 222:107-110.
2. Shupak, Hensel, Cross-Mellor, Kavaliers, Prato, Thomas. Analgesic and behavioral effects of a 100  $\mu$ T specific pulsed extremely low frequency magnetic field on control and morphine treated CF-1 mice. *Neurosci Letts* (2004) 354(1) 30-33.
3. Shupak, Prato and Thomas. Human exposure to a specific pulsed magnetic field: effects on thermal sensory and pain thresholds. *Neurosci Letts* (2004) 363 157-162.
4. Caldwell et al. Efficacy and Safety of Once-Daily Morphine Formulation in Chronic, Moderate to Severe Osteoarthritis Pain: Results from a Randomized, Placebo-controlled Double-Blind Trial and an Open-Label Extension Trial. *J Pain Symptom Manage* (2002) 23:278-291.
5. Peloso et al. Double Blind Randomized Placebo Control Trial of Controlled Release Codeine in the Treatment of Osteoarthritis of the Hip or Knee. *J Rheumatology* (2000) 27:764-71.
6. Roth et al. Around-the-Clock Controlled Release Oxycodone Therapy for Osteoarthritis Related Pain. *Arch Intern Med.* (2000) 160:853-860.

Comparison of Cnp and prescription opioid analgesia in humans						
	Dosage	Morphine daily equivalent dose	NAE	NP/Rx	NP/PL	Followup
Avinza	30 mg qam	30	12%	46	50	28 d

Avinza	30 mg qpm	30	8%	40	50	28 d
MS Contin	15 mg bid	30	8%	48	50	28 d
CR Codeine	159 mg bid	95	34%	31	35	28 d
CR Oxycodone	10 mg bid	40	16%	20	18	14 d
CR Oxycodone	20 mg bid	80	23%	25	18	14 d
Cnp (all)	40 min bid	NA	20%	17	17	7 d
Cnp (VAS >5/10)	40 min bid	NA	38%	7	8	7 d
NAE=Net Analgesic Effect, NP=Number of Patients, Rx=Active treatment, PL=Placebo.						

13-2

**CHRONIC TREATMENT WITH LOW-FREQUENCY REPETITIVE TRANSCRANIAL MAGNETIC STIMULATION INHIBITS SEIZURE INDUCTION BY PENTYLENETETRAZOLE IN RATS.** X. Huo<sup>1</sup>, X. Bao<sup>1</sup>, Y. Shi<sup>1</sup>, W. Yang<sup>1</sup>, Z. Shen<sup>1</sup>, T. Song<sup>1</sup>. <sup>1</sup> Bioelectromagnetic Lab, Institute of Electrical Engineering, Chinese Academy of Sciences, Beijing, China, <sup>2</sup> Bioelectromagnetic Lab, Institute of Electrical Engineering, Chinese Academy of Sciences, Beijing, China, <sup>3</sup> Bioelectromagnetic Lab, Institute of Electrical Engineering, Chinese Academy of Sciences, Beijing, China, <sup>4</sup> Bioelectromagnetic Lab, Institute of Electrical Engineering, Chinese Academy of Sciences, Beijing, China, <sup>5</sup> Bioelectromagnetic Lab, Institute of Electrical Engineering, Chinese Academy of Sciences, Beijing, China, <sup>6</sup> Bioelectromagnetic Lab, Institute of Electrical Engineering, Chinese Academy of Sciences, Beijing, China.

**INTRODUCTION:** Transcranial magnetic stimulation (TMS) is a non-invasive technique that uses the principle of electromagnetic induction to generate currents in the brain via pulsed magnetic fields. At present, repetitive transcranial magnetic stimulation (rTMS) has been used in the evaluation of higher cognitive functions and modulation of neuroplasticity[1]. But the most exciting potential use for rTMS is in the treatment of seizures. It has been recently demonstrated that rTMS may have a therapeutic utility in drug-resistant epilepsy [2,3]. Some findings indicate that acute low-frequency rTMS has suppressive effects on seizure susceptibility in rats [4], but it is unclear whether chronic low-frequency rTMS will have similar effects.

**OBJECTIVE:** The objective of this study was to test the effects of chronic low-frequency rTMS on seizure susceptibility and the neurochemical changes in the central nervous system in rats.

**METHODS:** Male Sprague-Dawley rats (200±10 g, n=16) were used. During the whole experiments, the animals were housed under controlled ambient conditions, a 12:12 h light-dark cycle and free-access to food and water. The magnetic stimulations were performed on 8 rats with a magnetic stimulator (BEMS-1, IEE, CAS, China) using monophasic pulses. The stimulation was given with a figure-of-eight coil with the frequency of 0.5 Hz. The coil had seven turns in each loop with the inner radius of 3.5cm and the outer radius of 5cm. The stimulation was done once daily on 15 consecutive days. A stimulation train was consisted of 500 pulses. Stimulation intensity was adjusted to 250 V/m at the plane of 0.5cm distance from the coil, which was above the threshold for evoking motor responses in the hindlimb muscles. The rats were placed in the holder made of epoxy. The coil was held tangentially to the parietal

bones 0.5cm above the skull and the coil handle was parallel to the midline of the head. The sham stimulation rats were also placed in the holder away from the coil about 20 cm, which prevented effective stimulation of the brain. Immediately after the last stimulation, pentylenetetrazol (PTZ) was injected intraperitoneally at a dose of 35 mg/kg. The behavior of the rats were observed for 30 min and classified in accordance to Racine groups. Then the rats were decapitated to determine the levels of 5-HT of hippocampus and brainstem. The concentration of 5-HT was determined using F-4500 fluorescence spectrophotometer (Hitachi, Japan). The assay was performed as described by Curzon et al. RESULTS: No any seizures developed and behavioral changes during the stimulation sessions in any of the rats. 50% of the rats that received rTMS had no responses after PTZ i.p. There was a significant inhibition effects on the seizure development according to the stage groups of Table 1 (Pearson Chi-Square test,  $p < 0.05$ ). The concentration of 5-HT of hippocampus and brainstem was assayed (Figure 1). The concentration of 5-HT of hippocampus increased significantly after chronic low-frequency rTMS (t test,  $p < 0.01$ ).

CONCLUSIONS: In this study we have shown that chronic low-frequency rTMS had suppressive effects on seizure susceptibility in rats. The rTMS caused a selective alteration of 5-HT in hippocampus and brainstem, despite the fact that probably the entire rat brain was stimulated. Experimental data in animals have shown that 5-HT receptor are predominantly located in limbic areas and suggest that serotonin, via these receptors, mediates an antiepileptic and anticonvulsant effect. Results of this study imply that the regulation of 5-HT in hippocampus plays an important role in the inhibition effects of seizures in rats after chronic low-frequency rTMS.

#### References

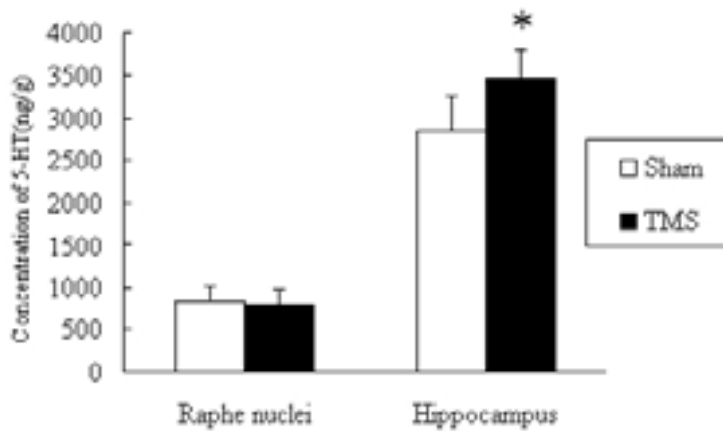
- [1]A. Pascual-Leone, F. Tarazona, J. Keenan, J.M. Tormos, R. Hamilton,M.D. Catala, Transcranial magnetic stimulation and neuroplasticity, *Neuropsychologia* 37 (1999) 207–217.
- [2]F. Tergau, U. Naumann, W. Paulus, B.J. Steinhoff, Low-frequency repetitive transcranial magnetic stimulation improves intractable epilepsy, *Lancet* 353 (1999) 2209.
- [3] W.H. Theodore, M.D. Hunter, R. Chen, F. Vega-Bermudez, B.Boroojerdi, P. Reeves-Tyer, K. Werhahn, K.R. Kelley, L. Cohen, Transcranial magnetic stimulation for the treatment of seizures, *Neurology* 59 (2002) 560–562.
- [4] N. Akamatsu, Y. Fueta, Y. Endo, K. Matsunaga, T. Uozumi, S. Tsuji. Decreased susceptibility to pentylenetetrazole-induced seizures after low frequency transcranial magnetic stimulation in the rat. *Neurosci Lett* 310 (2001) 153-156.

This research was supported by National Natural Science Foundation of China (No.50307013) and a grant from Chinese Academy of Sciences (No. KJCX1-09).

Table 1 Behavior changes after chronic low-frequency rTMS (Pearson Chi-Square test,  $p < 0.05, n=8$ )

Figure 1 The concentration of 5-HT of hippocampus and brainstem. The concentration of 5-HT of hippocampus increased significantly after chronic low-frequency rTMS (t test,  $p < 0.01, n=8$ )

Table 1 Behavior changes after chronic low-frequency rTMS (Pearson Chi-Square test, $p < 0.05$ )			
	No response	1~3 stage	4~5 stage
rTMS	4	3	1
Sham	1	1	6



13-3

**'DARK EYES' ANTENNA FOR MICROWAVE BREAST CANCER DETECTION: EFFECT OF SIZE REDUCTION AND FEED DESIGN ON THE TUMOR RESPONSE.** M. Popovic, H. Kanj. McGill Univ, Dept of Electrical and Computer Engineering, Montreal, Quebec, Canada.

**OBJECTIVES:** In this work, we present numerical assessment of the broadband 'Dark Eyes' antenna intended for use in microwave breast cancer detection; in particular, we model and observe the effect of miniaturization and the complete feed design on the simulated tumor-response level.

**METHODS:** The antenna simulations were performed with SEMCAD (three-dimensional finite-difference time-domain (FDTD) solver) and HFSS (three-dimensional finite-element (FEM) solver) for verification. For the SEMCAD simulations, a non-uniform mesh was used with a minimum and maximum cell size of 0.035 mm and 1mm, respectively. The modeled antennas were fed with a 1-V resistive source and their resistive portions were loaded with a surface resistivity of 100 Ohm/square. An eight-cell perfectly matched layer (PML) was used as the absorbing boundary condition. For the HFSS simulations and for comparison with the SEMCAD simulations, the antenna was considered to be 0.070 mm thick. Finally, the return loss for each antenna was computed assuming a 50-Ohm feed impedance and plotted over the frequency range 1–11 GHz. Next, the preliminary 'Dark Eyes' antenna (8 cm in total length) and the miniaturized antenna (2 cm) with the complete feeding structure are both numerically tested to assess tumor response level detectable by each antenna design. Each antenna is modeled adjacent to a 1-mm skin layer, beneath which is a fat layer containing a 5-mm tumor, centered 30mm from the skin-air interface. A 100-ns Gaussian pulse modulated by a 6-GHz continuous waveform is launched from each antenna under investigation. The reflection off the tumor is observed in time domain and compared, magnitude-wise, to the incident pulse to obtain the tumor response level in decibels.

**SUMMARY OF RESULTS:** First, we introduce the complete miniaturized geometry with the designed  
*Bioelectromagnetics 2005, Dublin, Ireland*

microstrip feed printed on a high permittivity substrate. This design was obtained by a number of trials and tuning of the individual geometric parameters of the metallic and the resistive portion of the antenna. Figure 1 shows the outline of the initial design (8cm total length) and the miniaturized antenna (2cm total length, 2cm total width including the microstrip feed), both sketched to scale for comparison. Simulated return loss (S11 parameter) for the miniaturized design is shown in Figure 2, demonstrating wideband behavior within the microwave range of interest. The tumor response for both antennas is comparable and lies in the -80 dB range. However, one of the important results of this study is the following. The reduction of the size and the inclusion of the microstrip feed in the model resulted in a significant change of the radiation pattern of the antenna. For best results, the plane of the miniaturized design must be turned to stand perpendicularly to the air-skin interface in order for potentially embedded tumor to be within the main radiation beam of the newly designed antenna structure.

**CONCLUSIONS:** Further work is presented on the broadband 'Dark Eyes' antenna, designed for microwave detection of breast tumors. We conclude that the successful miniaturization of the antenna and inclusion of the microstrip feed in the design implies a change in the radiation pattern. In order to obtain sufficient response from the underlying tumor, this effect must be taken into account for proper placement of the antenna-element with respect to the plane of the air-skin interface.

**ACKNOWLEDGMENT:** This work was supported by Natural Sciences and Engineering Research Council of Canada through an Individual Research Grant.

13-4

**RETROSPECTIVE STUDIES OF THE EFFECT OF BIOELECTROMAGNETIC DEVICES ON PAIN.** M. A. Richardson<sup>1</sup>, J. Li<sup>2</sup>, C. C. Lin<sup>3</sup>, N. Marquina<sup>4</sup>, J. Kiernan<sup>5</sup>, T. Procyshen<sup>6</sup>. <sup>1</sup>National Foundation for Alternative Medicine, <sup>2</sup>Univ of Maryland, <sup>3</sup>George Mason Univ, <sup>4</sup>Clinical Technologies Research/Virginia State Univ, <sup>5</sup>Kiernan Chiropractic and Sports Injury Center, <sup>6</sup>Bio-Medical Pain Center, USA.

**Objectives:** Pain is one of the most common symptoms and the primary cause of one third of all first consultations. Treatment remains a challenge, particularly with an unidentified etiology, and includes non-steroidal anti-inflammatory drugs, steroids, ultrasound, physical therapy, moist heat, massage, transcutaneous electrical nerve stimulation. The objectives of this study were to extract data from patient records and evaluate the clinical outcomes of two electromagnetic treatments for pain. One device (PAPIMI) delivers a pulsed electromagnetic field (PEMF) of a high intensity and short duration whereas the other, Electro Pressure Regeneration Therapy (EPRT) delivers a bipolar balanced waveform.

**Methods:** The PAPIMI is a noncontact electromagnetic device induces an alternating electrical field of high peak (instant) electric current of high bio-energy and limited heat. Frequency = 0.3 to - 0.5 MHz, amplitude =125 Gauss; repetition rate = 1 to 3.5 Hz; with a square wave shape. The magnetic field penetrates and induces micro-currents up to 6 inches into the body tissues. The therapeutic effects are attributed to the high amplitude electromagnetic pulses of rapid rise time (nanoseconds) and short duration (microseconds), which are produced by a patented plasma resonance chamber. The applicator probe of the device is a low impedance 15cm diameter loop that is held flat against the clothing or skin over the affected area of the body for ten to fifteen minutes. The EPRT device is a long-term alternating, bipolar balance waveform, battery operated, investigational device that delivers a direct current

(maximum of 3 milliamperes) of one polarity for 11.5 minutes and the opposite polarity for another 11.5 minutes. This device can be considered a long-term bipolar balanced waveform device. Frequency = 0.000732 Hz; square wave shape; repetition rate = 11.5; amplitude = 1mill-amp to 1000 nanoamps. Medical records were reviewed for patients who were treated for pain between September 2003 and September 15, 2004 with the PAPIMI at the Bio-Medical Pain Center, Calgary Canada and with the EPRT at the Kiernan Chiropractic and Sports Injuries Center in Rockaway Park, New York. Data extracted included demographics (age, sex, ethnicity), clinical (date of diagnosis, level of pain, use of medication) and treatment related (treatment duration and frequency, concomitant therapies). Change in the pain rating score, as measured by the verbal Numerical Rating Scale (NRS), was the primary endpoint. Data was reported as frequencies and cross tabulations; statistical techniques (chi-square tests, general linear models, ANOVAS) were used to evaluate changes in pain scores over time.

Summary: A total of 127 patients were treated with the PAPIMI primarily for knee and shoulder pain (54.5%) and on average, with 6.87 treatments (SD 4.35; range 1-22). Patients were 55 years of age (SD 14.02), 55.9% women, and 100% Caucasian. Of those with pre and post pain scores (n=56), initial pain scores were 6.41(SD 2.14) and post treatment pain scores were 2.08 (SD 1.92), indicating a significant reduction in pain (mean=4.33, SD 2.48, range 2.67-4.99,  $t(55)=13.07$ ,  $p < .0001$ ). Possible confounders did not modify the effect of PAPIMI on pain: age ( $p < .335$ ), gender ( $p < .532$ ), or number of treatments ( $p < .938$ ). A total of 20 patients were treated with the EPRT primarily for shoulder (35%), low back (25%), and knee pain (15%) and on average, with 7 treatments (SD 6.19; 75%  $\leq 7$  treatments). Patients were 57.2 years of age (SD 14.9), 55% men, and 65% Caucasian. Initial pain scores were 7.85 (SD 0.99) whereas post treatment pain scores were 2.0 (SD 2.62), indicating a significant reduction in pain (mean=5.85, SD 2.48, range 1-9,  $t(19)=10.50$ ,  $p < .0001$ ). Possible confounders did not modify the effect of EPRT on pain: number of treatments ( $p < .80$ ), gender ( $p < .45$ ), other medications ( $p < .56$ ), home treatment ( $p < .334$ ), gender ( $p < .45$ ), age ( $p < .96$ ).

Conclusions: Based on these retrospective studies, the data collected within the clinical practice settings indicate that these bio-electromagnetic treatment devices provided significant reductions in patients' perception of pain. Moreover, the number of treatments, pain medication and other treatments, age, or gender did not modify these effects. The findings are the first systematic assessments of the benefits of these devices and merit further examination in more rigorous prospective, sham-controlled, outcomes studies.

13-5

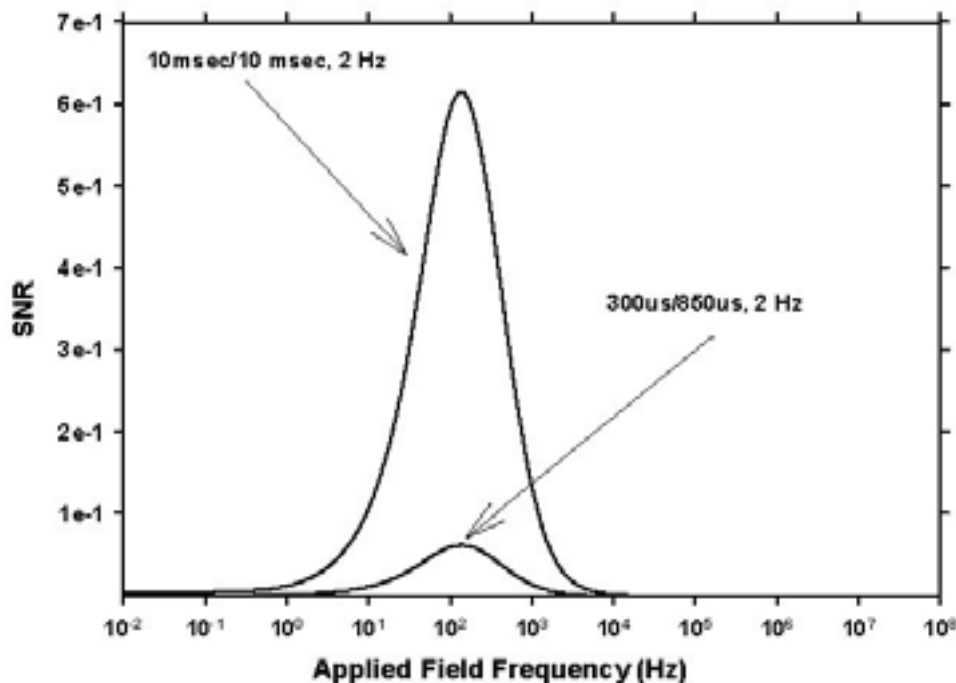
**SCIATIC NERVE REGENERATION IN A RAT MODEL DEPENDS UPON PEMF SIGNAL CONFIGURATION.** B. F. Sissen<sup>1,2</sup>, J. L. Walker<sup>3,4</sup>, D. J. Muehsam<sup>5</sup>, A. A. Pilla<sup>5</sup>. <sup>1</sup>Center for Biomedical Engineering, Univ of Kentucky, Lexington, KY, <sup>2</sup>Dept. of Anatomy and Neurobiology, Univ of Kentucky, Lexington, KY, <sup>3</sup>Division of Orthopedic Surgery, Univ of Kentucky, Lexington, KY, <sup>4</sup>Shriners Hospitals for Children, Univ of Kentucky, Lexington, KY, <sup>5</sup>Dept of Biomedical Engineering, Columbia Univ, New York, NY, USA.

INTRODUCTION: Several studies show EMF of various configurations can accelerate sciatic nerve regeneration in a rat model. However, the array of EMF signals employed ranges from sinusoidal to rectangular pulses with varied results. The study will attempt to provide a rationale for these varied

results by establishing the parameters which any signal must meet to be effective using SNR and power analyses in a Ca/CaM pathway.

EXPERIMENTAL SIGNALS: Sprague Dawley rats with standard crush injuries to the sciatic nerve have been treated with the following EMF signals: i) 50 Hz, 0.1mT, no effect; ii) 50 Hz 0.4mT, effect; iii) 1000 Hz, 0.1mT, effect; 2000 Hz, 0.1 mT, no effect; Interrupted 50 Hz, 1.4s on, 0.8s off, 0.5mT, effect; Single repetitive bipolar pulse, 1ms/0.3ms, 2Hz, 1.8mV/cm, no effect; Single repetitive bipolar pulse, 10ms/10ms (1 ms dwell), 2 Hz 1mV/cm, effect.

SIGNAL ANALYSIS: EMF signals configured to match the kinetics of a proposed target pathway have been shown to produce physiologically significant bioeffects. A strong candidate for EMF effects in this system is the Ca<sup>2+</sup>/CaM pathway which is known to modulate the release of growth factors and other cytokines the inflammatory and subsequent stages of repair.



The potential physiological effectiveness of a given EMF signal may be determined by an estimation of its detectability at the Ca<sup>2+</sup> binding site vs baseline thermal fluctuations (Signal to Thermal Noise Ratio = SNR), Pilla et al 1999. This was performed for all of the signals listed above. Sample results are shown for both bipolar pulse signals in the Figure. Here it may be seen the relatively narrow asymmetrical signal, 300/850  $\mu$ sec repeating at 2 Hz, produces substantially less amplitude at Ca<sup>2+</sup> binding frequencies vs that produced by the 10/10 ms signal at 2 Hz. Peak SNR indeed occurs for both signals at the relatively low frequency which corresponds to Ca/CaM binding kinetics. SNR values for all of the other sinusoidal signals exhibit the identical behavior. It has been shown that a PEMF signal which produces SNR < 0.1 in the target pathway typically has no physiologically significant effect.

CONCLUSIONS: The analysis presented here accurately tracks the reported results suggesting the Ca/CaM pathway is an important modulator of repair in this model. A signal is effective if it produces enough voltage increase at the binding site (vs thermal noise) within the frequency range of Ca/CaM binding kinetics. The same voltage induced outside the time constant frequency range is not effective. This explains why 1000 Hz only requires 0.1mT, whereas 50 Hz required 0.4mT. Similar reasoning applies to the 2000 Hz sinusoidal signal at 0.1mT and to the 300/850  $\mu$ sec pulse signal, both of which

were ineffective. This clarifies the apparent contradictory results for the variety of EMF signals utilized in this nerve regeneration model and could provide a method to optimize EMF signals for nerve regeneration.

13-6

**THE DEVELOPMENT OF ENDOSCOPIC ATTACHABLE ELECTRODE ARRAYS FOR THE TREATMENT OF INTRALUMINAL TUMOUR TISSUE.** D. M. Soden<sup>1</sup>, J. Larkin<sup>1</sup>, J. Piggott<sup>2</sup>, A. Morrissey<sup>2</sup>, G. C. O'Sullivan<sup>1</sup>. <sup>1</sup>Cork Cancer Research Centre, Mercy Univ Hospital and BioSciences Institute, Univ College, Cork, <sup>2</sup>National Microelectronics Research Centre, Univ College, Lee Maltings, Prospect Row, Cork, Ireland.

#### I Abstract Introduction:

Therapeutic “electroporation” involves application of electric fields to target cells/tissues, thereby rendering their cell membranes transiently porous, thus making feasible the cellular uptake and efficacy of previously impermeant and ineffective therapeutic agents. The objectives of this research are a) the development of flexible electrode arrays for incorporation into microsystem endoscopic devices, and b) the assessment of their efficacy in delivering selected genetic and pharmaceutical anti-cancer therapies. Gold electrodes were fabricated on flexible polyimide substrates following predictive modeling and simulation of electric fields using FEMLAB software. Subsequent assessment of electroporation efficiency in-vitro involved 1) enumeration of viable tumour cells after delivery of electric pulses and exposure to low concentrations of bleomycin, otherwise known as electrochemotherapy 2) Efficacy of gene delivery by detection of emitted green fluorescence by cells after electroporation with the pEGFP plasmid and 3) In-vivo efficacy of electrochemotherapy in a variety of human solid tumour masses in nude mouse models (xenografts). The flexible electrode system was found to be successful for electrical delivery of plasmids and drugs in-vitro and in-vivo. We found in-vivo complete regression of prostate, colon, oesophageal, and renal cancers with reduced growth rates for fibrosarcoma and breast cell lines. These flexible electrodes are suitable for electrochemotherapy or gene therapy to solid tumours masses and may be fabricated for application to the treatment of some cancers in humans by transcutaneous or endoscopic delivery systems.

#### II. Methodology

##### Fabrication:

Gold electrodes were fabricated on flexible polyimide. The polymer was roughened using Argon plasma etching. This provided an excellent surface for the adhesion of chromium (20 nm) and gold (200 nm) layers that were evaporated through patterned stainless steel stencils (Alfa-Fry Technologies, Ireland). Electrode arrays were packaged in a format suitable for in vitro and in-vivo studies of electroporation efficacy (figure 1).

##### Tumour induction and monitoring:

We used athymic nude mice for induction of human tumours. Tumours were induced by injecting subcutaneously into the flank of female mice. When the tumours reached approximately 100 mm<sup>3</sup> in volume, mice were randomly divided into experimental groups and subjected to specific experimental protocols (n=6).

Tumours were measured every 48 hours using a digital calliper.

#### Electrochemotherapy Protocol:

Mice were anaesthetised during all procedures using a mixture of halothane and O<sub>2</sub>. For the ECT, 0.25U bleomycin (Blenoxane, Sigma Chemical Co.) in PBS was injected intratumourally. The tumour was grasped percutaneously at the opposite margins of the tumour using two parallel flexible electrodes (6mm diameter) and their distance apart measured using a digital callipers. Good contact between the electrodes and the skin was assured by means of ultrasound gel (Rich Mar, USA). Electric pulses were generated by an electropulsator ECM 2001 (BTX Inc., San Diego, CA, USA) and incorporated four electric pulses (100microseconds, 1300 v/cm). In the electrochemotherapy protocol, mice were treated with electric pulses immediately after bleomycin injection. All treatments were well tolerated by the animals.

### III. Results

Finite element modeling using FEMLAB software was used to simulate the electric fields generated by the flexible electrodes as each of a range of pulse waveforms were applied. The electroporation parameters required optimization prior to experimental use. The variables analysed included the applied voltage, pulse shape, pulse duration, frequency, the total number of pulses applied and the pulse type (i.e., monopolar versus bipolar). This optimization minimised the number of electrode array design options produced as only those most likely to yield successful results were fabricated (Figure 1).

Initially the efficacy of the electrodes were assessed in-vitro by electroporation enhancement of the chemotherapeutic agent bleomycin. The effect of increasing the electrical field and bleomycin concentrations on a human prostate cell line are shown below. Cell viability was assessed 24 hours relative to control studies (Figure 2). Lower voltages are ineffective irrespective of bleomycin concentration suggesting requirement of electroporation for optimal drug efficacy. Similar results were obtained from experiments conducted on oesophageal, renal, colon, fibrosarcoma, and breast cell lines. Additional experiments were performed to optimise the electric pulses delivered in terms of pulse length and frequency. We found four pulses at 1400v/cm with greater than 100nanograms of bleomycin to effectively kill nearly 90% of tumour cells. Additionally, the in-situ cell detection kit (Roche, MA, USA) was used to assess apoptosis in cells after electrochemotherapy. In all cases greater than 90% of the treated cells were apoptotic within six hours of the electrochemotherapy.

In-vivo treatment of the tumours was performed in nude mice with the flexible electrodes attached to a biopsy jaw in order to demonstrate its suitability for future clinical use. Full regression of OE19 tumour xenographs was observed in four out of six electrochemotherapy treated oesophageal (Figure 3)

The remaining two nodules were subsequently eliminated by repeating the procedure after three weeks. Similar results were obtained for the prostate, renal, and colon tumours. The fibrosarcoma and breast cell lines had very aggressive growth rates which were stabilised following electrochemotherapy. Although the tumours were not eliminated their growth rates did not change in the three weeks after therapy. Tumour growth rates were only affected in all cases in those treated with electrochemotherapy.

### IV. Conclusion

Flexible electrodes may be fabricated for electroporation enhanced delivery of genes and drugs to cells and tissues. Successful deployment of these electrodes in endoscopic biopsy forceps, suggest that they may be used in minimally invasive surgical or endoscopic therapy systems. Most solid tumours are responsive to electrochemotherapy.

V. Acknowledgements.

We would like to acknowledge the generous support of Enterprise Ireland whose funding made this work possible.

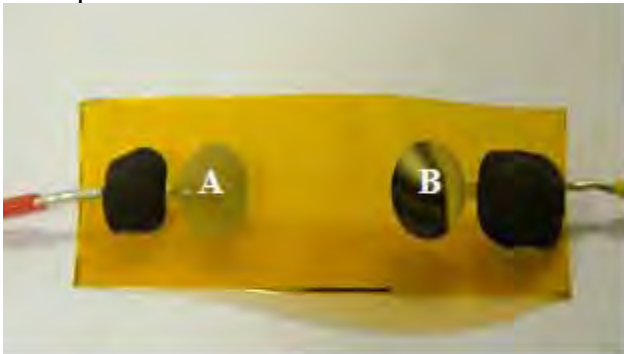


Figure 1. Flexible gold electrodes used in the course of the electrochemotherapy experiments. Picture shown here demonstrates gold electrodes (A and B) adherent to a polyimide as produced prior to mounting on a biopsy jaw.

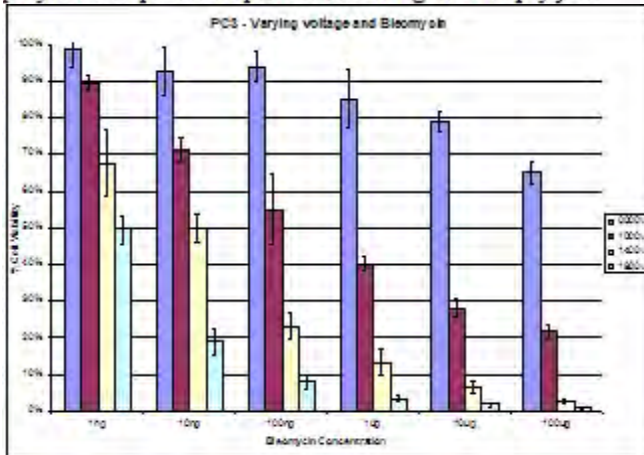


Figure 2. Cells of PC3 – human prostate carcinoma were subjected to increasing electric field strengths and increasing concentrations of bleomycin. Cell viability after 24 hours was assessed using the Cyquant assay. Note: Higher voltages above 800 v/cm are necessary for efficacy of bleomycin indicating the requirement for electroporation.



Figure 1. Flourescein-activated d-micrograph in an athletic male mouse model - days 0, 2 and 23 after electrochemotherapy. Note complete resolution of the lesion at 23 days.

13-7

**CHANGES IN CIRCULATING LYMPHOCYTES AS OBJECTIVE EVIDENCE FOR THE SUCCESS OF EMF THERAPY OF REFLEX SYMPATHETIC DISORDER.** C. F. Hazlewood<sup>1</sup>, A. D. Ericsson<sup>2</sup>, M. S. Markov<sup>3</sup>, F. Crawford<sup>4</sup>. <sup>1</sup>Research Consultant International, The Woodlands TX, USA, <sup>2</sup>Institute of Biological Research, Houston TX, USA, <sup>3</sup>Research International Williamsville NY, USA, <sup>4</sup>SpectroCell Labs, Texas USA.

A new approach of using electromagnetic fields (EMF) for therapeutic purposes has been developed, which is linked to its potential systemic effect. In order to prove the efficacy of this approach an objective measure of the efficiency of EMF therapy was deemed necessary. In the present study, ten patients (10) with RSD were clinically evaluated, and circulating isolated lymphocytes were cultured before and after therapy with EMF. The metabolic uptake for specific biochemical energy and nuclear turnover compounds were determined in the cultured cells that were taken before and after exposure of the uninvolved limb to an electromagnetic device (THERAMAG). A conventional visual analogue scale (VAS) technique was used to evaluate the intensity and level of pain before and after EMF exposure as well as the degree of contracture and swelling of the affected extremity. This approach allowed a comparison between objective and subjective measures. According to the medically evaluated VAS scores, exposure to the EMF resulted in an overall pain reduction, reduction in edema and dramatic relaxation of the extremity. Utilizing the objective method of thymidine tagged, protein-free media, cultured and stressed lymphocyte cultures were found to have significantly elevated fructose, serine, glycine, and calcium cellular metabolic uptake ( $p < 0.01$ ) following exposure to EMF. These findings are in concert with the new hypothesis that, with relief of pain, lymphocytes are predominately altered in their cycle from M phase to S phases associated with increased structuring of intracellular water. It is postulated that these changes also reflect a fundamental shift in production of Th1 T lymphocytes to Th 2 T lymphocytes, by means of the effect on gating of tRNA mechanisms. A consideration of the basic

understanding of the role lymphocytes may be inferred from this preliminary study. A review of the literature on the theoretical and therapeutic use of magnetic fields in humans is provided in an attempt to understand the relevance of biomagnetic therapy in specific pain syndromes.

13-8

**THE USE OF CERAMIC PERMANENT MAGNETS FOR TREATMENT OF SCAPHOID NONUNIONS.** R. A. Roachefsky<sup>1</sup>, M. S Markov<sup>2</sup>. <sup>1</sup>Dept Orthopedics, SUNY, Stony Brook, NY, <sup>2</sup>Research International, Williamsville NY USA.

**OBJECTIVES:** Scaphoid fractures have a high incidence of nonunion due to the fact that the majority of the surface is cartilage and that the blood supply to the bone is tenuous and easily disrupted during fracture. As a result these fractures can be very challenging and difficult to treat. Poor healing in a cast is common and surgical fixation and bone grafting is frequently necessary. Permanent magnetic fields have been shown to stimulate osteosarcoma cell proliferation and to increase the level of IGF-2 production, the major bone stimulating growth factor.(1) Others have shown that in an animal model magnetic fields accelerate fracture healing.(2) Also, Melone et al showed that pulsed electromagnetic fields accelerate scaphoid nonunion healing post operatively with surgical treatment(3).

This study was therefore designed to investigate the potential benefit of applying static magnetic fields for treatment of scaphoid fracture.

**METHODS:** This study is a retrospective review of 19 cases of scaphoid fractures that went on to nonunions. They were treated with open reduction and internal fixation and bone grafting. Seven of the cases in the control group were treated post operatively in a cast until healing, and twelve cases reviewed in the experimental group were treated with a cast and a 1000 gauss surface strength ceramic magnet placed over the fracture site externally at the wrist and incorporated into the cast. Each patient was treated in a cast until the fracture was determined to be healed by plain x rays and clinically by demonstrating no tenderness at the wrist to palpation. Once the cast was removed the patient was placed into a removable splint and started in a course of therapy. The charts were retrospectively reviewed to assess time from injury to surgery, type of fixation and bone grafting, healing time, follow-up time, and pre-op and post operative range of motion

**RESULTS:** In the group treated with the cast only the mean time from injury to surgery was 10 months (range 4-24). The mean age of the patients was 22 years (range 16-32) and all the patients were male. The types of fixation used were small AO cannulated compression screws, Herbert screws or Accutrak screws. Cancellous bone graft was used in five patients and tricortical and cancellous in two. The average time to healing was eight weeks (range 6-12). The mean follow-up time was six months (range 3-10) and the mean follow-up flexion and extension arc of motion was 107 degrees (range 95- 120) with an average improvement from the preoperative motion of 18 degrees. The group that had the cast and the magnet had a time from injury to surgery an average of 10 months (range 2-12). The mean age of the patients was 29 years (range 17-55) and all the patients were male. Fixation used were AO small cannulated compression screws, Herbert screws or Accutrak screws. Cancellous bone graft was used in eleven cases and tricortical and cancellous in one patient. The mean time to healing was five weeks

(range 4-8). The mean follow-up time was six months (range 2-7) and the average flexion and extension arc of motion was 107 degrees (range 80-120) with an improvement from preoperative of 33 degrees.

**CONCLUSION:** The data obtained during this study demonstrated in a series of patients that permanent magnets are effective for accelerating healing of scaphoid nonunion. A significant acceleration in the healing time of scaphoid non unions by approximately 3 weeks (38%) by the magnetic field as compared to control group was clearly shown. The most likely mechanisms involve not only the stimulation of metabolic activity of the osteoblast but the increased in blood flow to the fracture region.

**REFERENCES:** 1. Fitzsimmons RJ, Ryaby JT, Subburaman M, Magee FP, Baylink DL: Combine magnetic fields increase insulin- like growth factor-II in TE-85 human osteosarcoma bone cell cultures. *Endocrinology*, 136: 3100- 3106, 1995. 2. Darendeliler MA, Darendeliler A, Sinclair PM: Effects of static magnetic and pulsed electromagnetic fields on bone healing. *Int J Adult Orthodon Orthognath Surg*, 12: 43-53, 1997. 3. Melone CP, Pess GM: Treatment of Scaphoid Pseudoarthrosis with Bone Graft and Pulsed electromagnetic fields. AAOS Handout.

### **Plenary III: Animal magnetoreception**

*Chair: Stefan Engström*

**8:45 - 9:30 am, O'Reilly Hall**

**ANIMAL MAGNETORECEPTION: FUTURE DIRECTIONS.** John B. Phillips. Dept. of Biological Sciences, Virginia Tech., Blacksburg, VA, USA.

Over the last several decades the role of the geomagnetic field in spatial orientation has been documented in a wide variety of animals. These findings have helped to establish the existence of specialized sensory mechanisms that mediate interactions of the static magnetic field with biological systems. Recent studies of one such mechanism, the light-dependent magnetic compass, have also provided evidence for sensitivity to low-level radio frequency fields (~1-10 MHz). After briefly summarizing recent findings, I will focus on the question of what are future studies of animal magnetoreception systems are likely to contribute to the larger field of bioelectromagnetism? I will argue that the next 5-10 years will see rapid progress in: (1) establishing the lower limits of sensitivity to static magnetic, ELF, and RF fields in biological systems, (2) localizing specialized receptors responsible for sensing the geomagnetic field, (3) characterizing the underlying molecular and biophysical mechanisms, (4) identifying regions of the brain involved in processing magnetic stimuli, and (5) understanding how animals' perception of the magnetic field constrains its use to determine compass direction and spatial position. The key to progress in all five areas, however, will be interdisciplinary collaborations among investigators working in a number of different fields.

Our living and working environment has always included the presence of electric, magnetic, and electromagnetic fields. Some of our electromagnetic background is from natural sources but much of it is produced by manmade systems used for communications, broadcasting, navigation, factory processes, etc. This presentation will provide an overview of many of these sources of electromagnetic fields in our environment, including older sources not much talked about today, present day systems, and newer technologies that have not have yet been fully exploited. Issues related to typical exposures and methods of assessing exposure from some of these systems will be discussed as well as the perceived significance

of such exposures relative to hazards. Sources and systems included in this presentation will include natural fields, power lines, AM, FM, and TV broadcasting, shortwave broadcasting, cellular base stations, paging, satellite communications earth stations, radar, tropospheric communications, RF dielectric heat sealing and induction heating systems, WIFI systems, and others.

## **Session 14: Nanosecond Pulsed Electric Fields**

*Chairs: Martin Meltz and Stephen Beebe*

**9:00 - 10:00 am, Theatre L**

14-1

**RESEARCH EFFORTS IN THE MULTIDISCIPLINARY UNIV RESEARCH INITIATIVE ON SUBCELLULAR EFFECTS ON NARROWBAND AND WIDEBAND RADIOFREQUENCY RADIATION.** K. H. Schoenbach<sup>1</sup>, S. J. Beebe<sup>2</sup>. <sup>1</sup>Center for Bioelectrics, Old Dominion Univ, VA, <sup>2</sup>Eastern Virginia Medical School, USA.

The interest in subcellular effects of high intensity, radiofrequency radiation on biological cells and tissue has led to the establishment of an AFOSR/DOD funded Multidisciplinary Univ Research Initiative (MURI) with scientists from six academic institutions (Old Dominion Univ, Eastern Virginia Medical School, Massachusetts Institute of Technology, Washington Univ, Univ of Wisconsin and Univ of Texas Health Science Center) participating. The Old Dominion Univ-led MURI works closely with its sister MURI, led by Purdue Calumet Univ. Because of the interest in the new field of ultrashort (nanosecond) electrical pulse effects on cells, the members of the two consortia have decided to focus their research on these wideband radiofrequency radiation effects. The researchers in the two MURIs are using standardized pulsed electric field sources (10 ns duration, maximum voltage 40 kV at maximum currents of 4000 A) to explore the effect of ultrashort pulses on cell morphology and functions, with particular emphasis on ultrashort pulse-induced apoptosis. Other studies deal with intracellular effects on the nucleus, mitochondria, and endoplasmic reticulum, the ultrashort pulse-induced alterations in intracellular calcium levels, and field-induced changes in genes and proteins. In the past year we have also made progress in developing a novel imaging technique for the study of ultrashort pulse effects with a temporal resolution of 5 ns, which allows us to record changes in the membrane potential in real-time. The experimental studies are supported by modeling efforts (macro- and micro-dosimetry). In addition to the basic studies, there is an increasing effort to explore therapeutic applications of the ultrashort pulse technology, such as tumor treatment.

14-2

**GENOMIC RESPONSES TO RF FIELDS: CURRENT RESEARCH OF AFOSR PURDUE MURI CONSORTIUM.** C. C. Tseng<sup>1</sup>, M. A. Gealt<sup>1</sup>, S. M. Wang<sup>2</sup>. <sup>1</sup>Purdue Univ Calumet, Hammond, IN, USA, <sup>2</sup>ENH Research Institute, Northwestern Univ, Evanston, IL, USA.

Introduction: This report summarizes an overall view of selected research projects on genomic responses to RF fields. The studies were based on different exposure systems such as the 837 MHz RTL system, the 2.45 GHz waveguide system, and nanosecond pulsed electric field systems. Microarrays and SAGE

(Serial Analysis of Gene Expression) were used for genomic analysis of RF effects on human cultured cells.

Objectives: 1) To determine the effects of RF fields on human gene expression at the genomic level, 2) To classify the affected genes based on their function, 3) To identify the early and late RF response genes, and 4) To identify potential novel RF response genes.

Materials and Methods: Four RF sources were used: 837 MHz (5 W/kg), 2.45 GHz (10 W/kg), 60 nsPEF (15 kV/cm), and 10 nsPEF (280 kV/cm). Two human cell lines (HL-60 and Jurkat) were used for genomic analysis. Microarrays used included the plastic microarray with 12k gene probes (Clontech), the CodeLink microarray with 20k gene probes (Amersham), and the CodeLink whole genome microarray with 55k gene probes (Amersham). Basic preparations for microarrays included RNA isolation, cDNA synthesis, in vitro transcription and biotin-labeling of cRNA, fragmentation of cRNA, hybridization of cRNA with probes on the microarray, staining with fluorophore, scanning, and data analysis. The SAGE process involves isolation of RNA, cDNA synthesis, NlaIII digestion of cDNA, 3' cDNA collection, release of tags from 3'| cDNA, di-tag formation, di-tag concatenation, cloning, DNA sequencing, tag sequence collection, and bioinformatics/statistical analysis.

Results: 1) Microarrays: After exposing HL-60 cells to 837 MHz for 2 h, 93 genes (2/3 up regulated and 1/3 down regulated) were affected. They included genes for cell cycle and metal ion binding. No cell viability was affected. After exposing HL-60 cells to 3 pulses of 60 nsPEF (15kV/cm) followed by incubation for 6 h, 53 genes were affected with more up regulated than down regulated genes. They included genes for cell adhesion, cell defense, immune inflammatory and stress, transcription control, DNA binding, and phosphorylation. Again, no cell viability was affected. In the Jurkat cells, which were exposed to 2 pulses of 10 nsPEF (280 kV/cm) followed by incubation for 1 h and 6 h, several groups of affected genes (500 genes at 1 h and 300 genes at 6 h of post incubation) were identified using cluster analysis. In general, genes for transporter activities were up regulated at 1 h and 6 h of post incubation periods, genes for stress response, cell cycle, and chromosome organization were up at 1 h (early response genes), and a different set of genes for cell cycle was down regulated initially at 1 h but the expression level increased at 6 h. Genes for plasma membrane synthesis were highly induced at 6 h of post incubation. The expression levels of apoptosis genes were lowered at both post incubation periods. 2) SAGE: HL-60 cells were exposed to 2.45 GHz for 2 h and 6 h. After 2 h of exposure, 206 genes (including 23 potential novel transcripts) were affected, whereas after 6 h of exposure, 746 genes (including 118 potential novel transcripts) were affected. The up regulated genes included carbohydrate metabolism, RNA process, and apoptosis, and the down regulate genes included those for transport, ATP synthesis, and cell cycle. A slight decrease in cell viability was observed in the 6 h exposed cells.

Conclusions: 1) Although cell viability is not affected by the exposing to 837 MHz RF fields or 60 nsPEF at 15 kV/cm, subcellular changes do occur, as indicated by differential expressions of many genes. The changes in gene expression are probably for physiological adjustment, as part of the recovery process. 2) The 10 nsPEF (280 kV/cm) induced Jurkat cell genes at 1 h of post incubation are early response genes, several of which are similar to those sensitive to chemicals. They are related to cell cycle and chromosome organization. The increased expression of the DD13 gene suggests that the cells are responding to the high electric field induced DNA damage. A set of plasma membrane genes is up regulated in 6 h, indicating that they may be involved in membrane repair. The increased expression of transporter genes may signify a process for maintaining the homeostasis of ions. There is no sign of activation of apoptosis genes, although the cell viability is reduced to about 1/2 at 30 min after exposure. This suggests that nsPEF may affect cells at different levels. The immediate effect is at the biochemical level, which may account for the initial death of half of the cells in the population. The genomic

responses are slower, and the currently identified genes belong to those cells that survive the initial stress. The response genes are therefore mainly for repairing process. 3) The SAGE study on the RF (2.45 GHz) effect on HL-60 cells shows that more genes are differentially expressed at 6 h than 2 h of exposure. Most significantly induced genes are apoptosis genes, although only a small portion of the cells are dead after 6 h of exposure. The reason is not clear at this time. It is possible that the initial induction of apoptosis genes may not result in cell death because the actually process may be blocked by anti-apoptosis mechanisms at the protein level. 4) It has been a concern of the thermal effect by the RF (e.g. waveguide) system. To assure nonthermal effect, the temperature of the waveguide system is tightly regulated and monitored so that the temperature range is within  $37 \pm 0.03^\circ\text{C}$ . The lack of heat shock gene changes provides a biological evidence that cells respond to RF fields through a non-thermal mechanism.

14-3

**MODELING AND THEORY FOR CELLULAR RESPONSES TO NANOSCALE AND SCALE VERY LARGE ELECTRIC FIELDS.** J. C. Weaver<sup>1</sup>, R. P. Joshi<sup>2</sup>. <sup>1</sup>Harvard-MIT Division of Health Sciences and Technology, Massachusetts Institute of Technology, Cambridge, MA, <sup>2</sup>Dept of Electrical & Computer Engineering, Old Dominion Univ, Norfolk Virginia, USA..

**Introduction.** Over the past few years there have numerous reports of intracellular effects caused by pulses with durations of 10 to 300 ns and corresponding field magnitudes of order 300 to 30 kV/cm. Key findings are (1) initial cell survival followed in about 0.5 h by programmed cell death (apoptosis), and (2) prompt, extensive translocation of phosphatidylserine (PS) at the cell's outer, plasma membrane (PM). Strikingly, the temperature rise associated with these observations is of order 1 K, so a nonthermal interaction mechanism is strongly suggested. Traditionally, electric field interactions with cell have focused on the PM, which tends to concentrate the field at the membrane to cause large transmembrane voltage changes. Several of the published reports suggest that the PM is not electroporated, while membranes of organelles are significantly perturbed, including the possibility of electroporation. The challenge to modeling and theory is to explain these dramatic effects, and also to make predictions of phenomena not yet observed.

**Methods.** The modeling and theory efforts reported here focus on the membranes of a cell (PM and organelle membranes) as well as the aqueous electrolytes external and internal to the cell.

Molecular dynamics simulations. At the membrane level molecular dynamics (MD) simulations examine the spontaneous molecular rearrangements that occur in the presence of a strong electric field across a phospholipid bilayer membrane. A time dependent membrane field typical of a cell's response is used. A well accepted hypothesis is that electroporation involves the rapid formation of transient aqueous pores. MD analysis can look for the occurrence of membrane rearrangements that lead to water-filaments or large water-filled structures.

Spatially distributed local electroporation models. At the organelle and cell level another method is to create a space-filling model with assignment of passive conduction and dielectric properties to the aqueous electrolytes, but a passive capacitance and highly nonlinear and hysteretic active model for pore creation assigned to local membrane areas. In this case the local membrane model assumes a pore creation rate constant governed by a Boltzmann factor and a nonlinear conductance of the created pores. The resulting system model involves interactions between all the passive and active local models, such that solutions describe the spatially distributed evolution of potentials and fields near and within the cell

model. This approach is also extended to a larger spatial scale by constructing a model of fifty irregular, closely spaced cells in order to approximate a solid tissue.

**Results.** Both types of membrane-based analysis yield results relevant to experimental observations.

Molecular dynamics simulations. MD simulations show that pores appear on a time scale of 5 ns for very large electric fields, somewhat larger than expected for experimentally applied fields. More specifically, the simulations show a fluctuating entry of water into a phospholipid membrane and a subsequent appearance of a fluctuating toroidal shaped pore. Translocation of PS is observed.

Spatially distributed local electroporation models. Cell system models show that poration occurs at the PM and also organelle membranes. However, the pores are predicted to be very small (radius  $\cong$  0.8 nm), which predominantly transport small, monovalent ions that are responsible for electrical behavior. Transport of indicator dyes and large molecules is predicted to be minimal, in qualitative agreement with experiments. Candidate mechanisms for initiating apoptosis have been identified.

**Acknowledgments.** Supported by a AFOSR/DOD MURI grant on Subcellular Responses to Narrowband and Wideband Radio Frequency Radiation, administered through Old Dominion Univ, and by NIH grant RO1-GM63857.

## Session 14: Nanosecond Pulsed Electric Fields (Continued)

*Chairs: Martin Meltz and Stephen Beebe*

**10:30 - 12:00 pm, Theatre L**

14-4

**CELL AND TISSUE RESPONSES TO NANOSECOND PULSED ELECTRIC FIELDS: DYNAMIC EFFECTS AND APPLICATIONS.** S. J. Beebe<sup>1,2</sup>, P. F. Blackmore<sup>2</sup>, E. H. Hall<sup>1,3</sup>, J. A. White<sup>1,3</sup>, L. K. Willis<sup>1</sup>, L. I. Fautleroy<sup>3</sup>, J. F. Kolb<sup>3</sup>, C. Bickens<sup>3</sup>, S. Xiao<sup>3</sup>, K. H. Schoenbach<sup>3</sup>. <sup>1</sup>Center for Pediatric Research, Eastern Virginia Medical School, Norfolk Virginia, <sup>2</sup>Dept of Physiological Sciences, Eastern Virginia Medical School, Norfolk Virginia, <sup>3</sup>Center for Bioelectrics, Old Dominion Univ, Norfolk Virginia, USA.

Nanosecond, high intensity pulsed electric fields [nsPEFs] that are below the plasma membrane [PM] charging time constant have decreasing effects on the PM and increasing effects on intracellular structures and functions as the pulse duration decreases. Objectives of the studies reported here were to determine effects of nsPEF on cells and tissues using conditions that were above and below the threshold for apoptosis induction and to determine the role of the cell cycle in responses to nsPEFs.

Methods include analysis of markers for membrane responses using ethidium homodimer-1, propidium iodide and Annexin-V binding; apoptosis markers including caspase activation, cytochrome c release into the cytoplasm, and DNA fragmentation using TUNEL; calcium mobilization using Fura-2; and effects on gene expression using green fluorescent protein.

Summary: When human cell suspensions were exposed to nsPEFs where the electric fields were sufficiently intense [10-300ns,

To determine the role of the cell cycle nsPEF-treated cells, colon carcinoma cells were tested unsynchronized and synchronized in S-phase by double thymidine block. In contrast to unsynchronized cells, nsPEF-treated in the S-phase exhibited lower ethidium homodimer-1 and Annexin-V-FITC fluorescence as measures of plasma membrane effects and less F-actin rearrangement as measured by rhodamine phalloidin staining. Furthermore, S-phase cell exhibited higher caspase activity than unsynchronized cells.

When nsPEF conditions were below thresholds for apoptosis and classical PM electroporation, non-apoptotic responses were observed similar to those initiated through plasma membrane purinergic receptors in HL-60 cells, CD-3 in Jurkat cells, and thrombin in human platelets. These included Ca<sup>2+</sup> mobilization from intracellular stores [endoplasmic reticulum] and subsequently through store-operated Ca<sup>2+</sup> channels in the PM. In addition, nsPEFs increased intracellular calcium and induced platelet activation measured as aggregation responses in human platelets.

Finally, when nsPEF conditions followed classical electroporation-mediated transfection, the expression intensity and number of GFP-expressing cells were enhanced above cells exposed to electroporation conditions alone.

Conclusions: These studies demonstrate that application of nsPEFs to cells or tissues can modulate cell-signaling mechanisms with possible applications as a new basic science tool, cancer treatment, wound healing, and gene therapy.

These studies were supported by a Multi-Univ Research Initiative from the Dept of Defense through the Air Force Office of Scientific Research administered by Old Dominion Univ, The American Cancer Society, The Eastern Virginia Medical School, and Old Dominion Univ.

14-5

**ESCHERICHIA COLI RESPONDS TO NSPEP WITH INDUCTION OF DNA REPAIR FUNCTIONS.** M. A. Gealt<sup>1</sup>, S. M. Wang<sup>2</sup>, C. C. Tseng<sup>1</sup>. <sup>1</sup>Purdue Univ Calumet, Hammond, IN, <sup>2</sup>ENH Research Institute, Northwestern Univ, Evanston, IL, USA.

Introduction: Bacteria offer several advantages for the study of responses to environmental stimuli: smaller genomes than eukaryotes, short time lag between stimulus and mRNA synthesis, and, generally, a response characterized by a large number of mRNA molecules synthesized. Escherichia coli was used as a model system to determine if bacteria respond to RF in a manner similar to what has been observed in eukaryotic systems.

Materials & Methods: E. coli grown to mid-log phase at 37 degreeC in Luria broth grown to a density of OD<sub>600</sub> of 0.6, or approximately 10<sup>9</sup> cells/ml in 30 ml were resuspended in Hank's balanced salt solution before being treated with 25 10 ns pulses at 270 kV/cm. Following this treatment the cells were incubated for an additional 10 minutes at 37°C to allow gene expression, i.e., RNA synthesis. Following this incubation, cellular RNA was extracted and RT-PCR was used to create cDNA with incorporated cyanine-3-dCTP or cyanine-5-dCTP. Hybridization of the labeled cDNA to oligonucleotide probes specific for the E. coli genes was performed with the MWG® DNA Array for E. coli K12-V2. The hybridization was performed directly on the MWG microarray slide. Following washing of the

hybridized nucleic acids, the microarray was scanned in a GenePix® 4000B Microarray Scanner. The results were analyzed with Genepix® Pro 5.0 software and Microsoft Excel.

Results & Discussion: Viability counts showed that no cell death was caused the 25 pulses. Several genes associated with cellular response to DNA damage were induced (up-regulated) by this treatment: yebG (induced by DNA damage; part of the SOS regulon), ruvA (Holliday junction helicase; associated with DNA repair), sulA (inhibits cell division upon DNA damage/inhibition), and yglF (specific for G/U mismatches in DNA). The response of these genes suggests that RF alters DNA structure analogous to the affects of other radiation (non-ionic/ionic). Concurrent with repair of DNA there is a repression (down-regulation) of approximately 20 genes. There does not appear to be any general pattern to the repressed gene activities, although a few are associated with transport across the cell membrane. Several conserved gene sequences of unknown function were down-regulated. The response to RF by *E. coli* appears to be consistent with the general stress response that is commonly observed in eukaryotic cells. This suggests a common physiological affect of RF on cells across all kingdoms.

14-6

**INTEGRATED APPROACH TO EXAMINING THE BIOEFFECTS OF HIGH PEAK POWER 10 NSPEFS AND UWB TEMFS: CELL RECOVERY, VIABILITY, PROLIFERATION, GENOMICS AND PROTEOMICS.** M. L. Meltz<sup>1</sup>, B. K. Nayak<sup>1</sup>, C. Galindo<sup>1</sup>, K. Hakala<sup>2</sup>, M. Natarajan<sup>1</sup>, S. Weintraub<sup>2</sup>, K. Schoenbach<sup>3</sup>. <sup>1</sup>Dept of Radiation Oncology, Univ of Texas Health Science Center at San Antonio, TX, <sup>2</sup>Dept of Biochemistry, Univ of Texas Health Science Center at San Antonio, TX, <sup>3</sup>Center for Bioelectrics, Old Dominion Univ, Norfolk, VA, USA.

Our Radiobiology Group is addressing the possible effects of two different UWB signals, 10 ns pulsed electric fields with an extremely high peak power of up to 30 MV/m, and pulse numbers of 1 – 50 delivered in a matter of seconds in a cuvette in the ODU pulser device, and UWB transmitted electric fields with a pulse with a smaller pulse width (780 ps), a lower (but high) peak power of 100 kV/m, a pulse repetition frequency of 250 pps with exposures lasting a total of 90 min (intermittent 30 min on and 30 min off). The studies have initially focused on the 244B lymphoblastoid cell line, since it is presumptive normal, a human cell line, and grows in suspension. We have observed changes in the former in recovery, viability, and cell cycle alterations which suggest a possible mechanism shift between apoptosis and anti-apoptosis, as reflected by the cell density changes, viability changes (by dye exclusion), and induction of an anti-apoptotic gene and a decrease in p53 protein in remaining viable cells. We are performing genomic assessment first with analysis of 12,000 human genes, but are changing systems to be able to analyze 22,000 human genes. With respect to the UWB TEMF exposures, where we observed no changes in cell cycle distributions after exposure, we were surprised to see increases and decreases in specific genes by microarray assay. The number of genes that can be examined for changes by microarray assessment far exceeds the number of proteins that can be examined, using 2D gels and MALDI analysis; we are in the position of being able to do a comparative assessment, and look for overlaps to determine when changes in transcription which are necessary for protein synthesis may not be sufficient for causing protein synthesis. In the region of overlap, we will use hypothesis driven studies, which are far less costly, to examine the impact variation of both physical and biological variables. The former include peak power, numbers of pulses, pulse width, etc; the latter include cell type, time post exposure, cell stage at the time of exposure, etc.

**NANOSECOND PULSED ELECTRIC FIELD-INDUCED MCL-1 GENE EXPRESSION IS REGULATED BY THE AP-1 TRANSCRIPTION FACTORS.** B. K. Nayak<sup>1</sup>, M. L. Meltz<sup>1</sup>, C. A. Galindo<sup>1</sup>, M. Natarajan<sup>1</sup>, S. T. Weintraub<sup>2</sup>, K. H. Schoenbach<sup>3</sup>. <sup>1</sup>Department of Radiation Oncology, Univ of Texas Health Science Center at San Antonio, Texas, <sup>2</sup>Dept of Biochemistry, Univ of Texas Health Science Center at San Antonio, Texas, <sup>3</sup>Center for Bioelectrics, Old Dominion Univ, Norfolk, Virginia, USA.

**OBJECTIVE:** The anti-apoptotic Mcl-1 gene has a role in cell survival, differentiation, and apoptosis. Studies from our laboratory have shown the simultaneous induction of Mcl-1 and fos/jun transcription factors after nanosecond pulsed electric field (ns PEF) exposures. The objective of the present study was to determine the regulation of induction of the Mcl-1 gene expression by AP-1 transcription factors in response to ns PEF exposures.

**METHODS:** The 244B human lymphoblastoid cell line was used in the present study. Cells were exposed to a series of 1, 3, 10, 25, or 50 pulses at average peak field intensities of 50 to 300 kV/cm using the 10 ns Pulse Device. The pulses had an average rise time of <2 ns, with a frequency range of D.C. to 60 MHz. In the experiments involving inhibitors, the cells were treated with the AP-1 inhibitors curcumin (50  $\mu$ M) or nordihydroguaiaretic acid (NDGA-100  $\mu$ M) for one hour before pulsing. The expression of the Mcl-1 and fos/Jun (AP-1) factors was analyzed at 3, 6, 10, and 24 hour post-exposure, using the RNase protection assay (RPA) and western blotting. The binding of AP-1 complex to the native Mcl-1 gene promoter was examined at 2 hour post-exposure, using the electrophoretic mobility shift assay. Cell viability and apoptosis were examined using trypan blue dye exclusion and mitochondrial membrane potential.

**RESULTS:** Early induction of the anti-apoptotic gene Mcl-1 and members of the fos and jun families of genes were observed, occurring within 6 hours after the nanosecond PEF exposures. The level of expression of these genes returned to a basal level after 6 hours post-exposure. The induction of the Mcl-1, fos and jun transcription factors was proportional to the number of pulses, and also to the average peak field intensity (i.e. two dose-dependent responses were observed). Functional studies using electrophoretic mobility shift assay have shown an increased binding of AP-1 transcription factor to the native Mcl-1 gene promoter in response to ns PEF pulses. Further, it has been shown that the binding of the AP-1 complex to the Mcl-1 promoter, and the Mcl-1 gene expression, were inhibited in the presence of the AP-1 inhibitors curcumin and NDGA. Upon inhibiting the Mcl-1 expression using AP-1 inhibitors, the apoptotic response by ns PEF was enhanced.

**CONCLUSION:** These studies show that there is transient and rapid induction of the anti-apoptotic gene Mcl-1 and the fos/jun (AP-1) families of transcription factors after ns PEF exposures. The AP-1 inhibitors reduced the nsPEF-induced binding of AP-1 complex to the Mcl-1 promoter, and inhibited the Mcl-1 gene expression. Upon inhibiting the Mcl-1 expression by AP-1 inhibitors, the apoptotic response by nsPEF exposure is enhanced. These studies therefore indicate that the ns PEF-induced Mcl-1 expression is regulated by the AP-1 transcription factors, and that the apoptotic response can be modulated in combination with the AP-1 inhibitors. The ns PEF pulses might be used to modulate the differentiation and apoptosis programs in specific therapeutic regimens.

This work was supported by AFOSR MURI Grant No. F49620-02-10320, by AFOSR Grant No. F49620-01-1-0349, by San Antonio Area Foundation Grant No. 119264, and by the Dept of Radiation Oncology (UTHSCSA).

**OXYGEN EFFECT ON CELL VITALITY AFTER EXPOSURE TO HIGH-INTENSITY, 10-NS ELECTRICAL PULSES.** A. Pakhomov<sup>1</sup>, K. Walker III<sup>2</sup>, J. Kolb<sup>3</sup>, K. Schoenbach<sup>3</sup>, B. Stuck<sup>2</sup>, M. Murphy<sup>4</sup>. <sup>1</sup>Dept of Physiology, Univ of Texas Health Science Center, San Antonio, TX, <sup>2</sup>US Army Medical Research Detachment, Brooks City-Base, San Antonio, TX, <sup>3</sup>Center for Bioelectrics, Old Dominion Univ., Norfolk, VA, <sup>4</sup>Directed Energy Bioeffects Division, Human Effectiveness Directorate, Air Force Research Laboratory, Brooks City Base, San Antonio, TX, USA.

**OBJECTIVES:** In our previous studies, we have analyzed how the cytotoxic effect of high-voltage, 10-ns electrical pulses (EP) depends on such parameters of exposure as the E-field amplitude, pulse repetition rate, and the number of pulses applied. For a wide range of EP treatment parameters, the cell survival was found to be a function of the absorbed dose. In two studied mammalian cell lines (Jurkat and U937), the cell survival curve started with a plateau at low doses, followed by an exponential decline. This type of the dose response is typical for some other known cytotoxic factors, such as low-LET ionizing radiations (x-rays and electrons), which kill cells primarily by generation of free radicals that damage DNA. A “signature” characteristic of this mechanism is its potentiation by oxygen, a classic radiomodifier, whereas hypoxic conditions are protective. One can speculate that extreme EP voltages tested in our studies (up to 300 kV/cm) could cause water ionization and/or dissociation, leading to free radical formation and cell death. If this is the case, then the EP effect should be modified by oxygen in the same manner as the effect of low-LET ionizing radiations. The present work was aimed to test this hypothesis.

**METHODS:** Experiments were performed in two cell lines, U937 (human histiocytic lymphoma) and Jurkat (human T-cell leukemia). Cells were grown at 37 oC with 5% CO<sub>2</sub> in air in ATCC-modified RPMI 1640 medium with 10% fetal bovine serum. Prior to exposure, cell cultures (0.2 x 10<sup>6</sup> cells/ml) were bubbled with either air (21% oxygen), or pure oxygen, or pure nitrogen. The bubbling continued for a few minutes, until the oxygen content in the medium reached within 2-3% of the targeted level, as measured with a miniature Clark oxygen electrode. The samples were exposed in capped and sealed 2-mm gap gene transfer cuvettes (BIORAD) using a Blumlein line pulser manufactured at the Old Dominion Univ. Pulse shape and amplitude were monitored with a 500-MHz TDS3052B Tektronix digital oscilloscope using a custom-made high-voltage probe. All exposures were performed at a room temperature of 24-25 oC. Live and dead cell densities were determined by hemocytometer cell counts after Trypan blue staining, at intervals when the post-exposure cell survival reached its minimum (4 hr for Jurkat and 24 hr for U937). In experiments with hypoxia, we used EP doses that normally decreased cell survival to 10-20% (400 pulses at 80-90 kV/cm for Jurkat and 300 pulses at 120-130 kV/cm for U937, both at 2 Hz), so that any increase in survival would be readily detectable. In experiments with oxygen saturation, when the expected effect was a decrease in survival, the EP dose was decreased to produce about 60% survival in air-bubbled controls (Jurkat only, 200 pulses at 80-90 kV/cm).

**RESULTS:** Bubbling nitrogen prior to EP exposure caused a profound and statistically significant protective effect in both tested cell lines; it increased cell survival about 2-fold compared with exposed samples that were bubbled with room air. In contrast, saturating the medium with pure oxygen prior to EP exposure decreased cell survival 1.5 times ( $p < 0.01$ , Jurkat). In unexposed parallel control samples, bubbling of either nitrogen or oxygen had no effect on cell culture growth or cell survival.

**SUMMARY:** The experiments established that oxygen depletion increased cell survival after EP treatment, whereas oxygen saturation had the opposite effect. This modifying action was exactly the same as known for low-LET ionizing radiations, thereby indicating that the mechanism of cell killing by high-voltage, 10-ns EP may indeed involve free radical formation and DNA damage.

The study was performed when A.G.P. and K.W. were with McKesson BioServices Corporation. The

work was supported by the U.S. Army Medical Research and Materiel Command and the U.S. Air Force Research Laboratory under U.S. Army contract DAMD17-94-C-4069 awarded to McKesson BioServices Corporation, and by an AFOSR/DOD MURI grant on Subcellular Responses to Narrowband and Wideband Radiofrequency Radiation, administered through Old Dominion Univ.

### **Session 15: In Vivo**

*Chairs: Masao Taki and Alexander Lerchl*

**9:00 - 10:00 am, Theatre M**

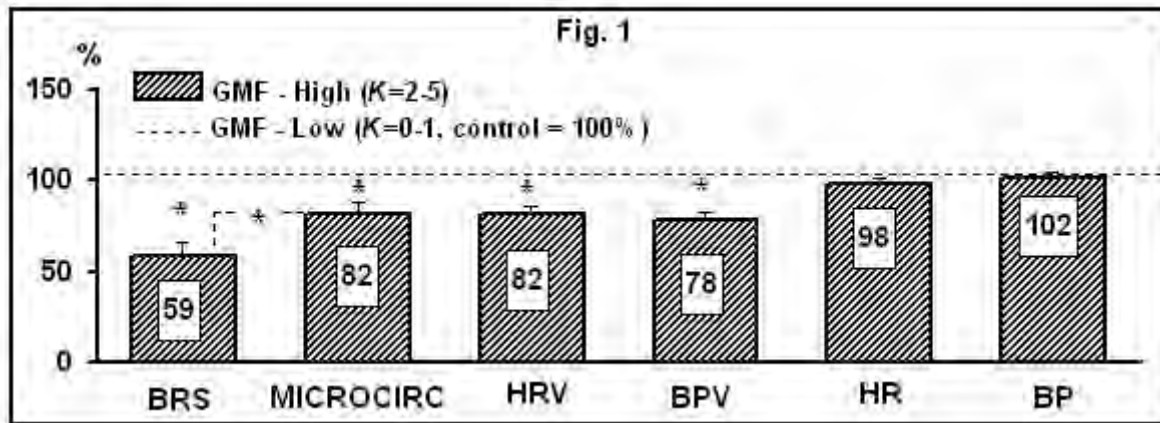
15-1

**GEOMAGNETIC FIELD EFFECT ON CARDIOVASCULAR REGULATION AND ON MICROCIRCULATION.** J. Gmitrov<sup>1,2</sup>. <sup>1</sup>National Institute of Public Health, Tokyo, Japan, <sup>2</sup>Internal Specialist Polyclinic, Presov, Slovak Republic.

**OBJECTIVE:** Increasing evidence suggests that geomagnetic storms are associated with severe clinical events including cerebral strokes and myocardial infarctions [1]. The objective was to explain the physiological mechanism for the influence of the geomagnetic field (GMF) disturbance (estimated by the K-index) on cardiovascular regulation by analyzing the arterial baroreflex mechanism. Extensive evidence exists about important role of the arterial baroreflex on blood pressure, and on microcirculatory regulation and its malfunction can have serious clinical consequences. Patients with low baroreflex sensitivity (BRS) have a reduced capacity to antagonize sympathetic activation, which is sufficient to initiate arterial hypertension and to increase cardiovascular morbidity and mortality [2].

**MATERIALS AND METHODS:** One hundred forty-three experimental runs (one daily) comprising 50-min hemodynamic monitoring sequences were carried out in rabbits sedated by pentobarbital infusion (5 mg/kg/h). We examined the arterial baroreflex effects on the short-term heart rate (HRV) and blood pressure variability (BPV) reflected by the standard deviation of the average values of the mean femoral arterial BP and the heart rate (HR). Simultaneously with general hemodynamic, the skin microcirculation in the capillary network of the ear lobe was measured using microphotoelectric plethysmogram. Baroreflex sensitivity (BRS) was estimated from BP/HR response to intravenous (i.v.) bolus injections of vasoconstrictor (phenylephrine) and vasodilator (nitroprusside) drugs. The values of GMF disturbance as reflected by K-index were kindly supplied by the nearby Kakioka Magnetic Observatory.

**RESULTS:** We found a significant negative correlation of increasing GMF disturbance (K) with BRS ( $p=0.027$ ), HRV ( $p=0.021$ ) and BPV ( $p=0.007$ ), signifying the involvement of the arterial baroreflex mechanism. A significant negative correlation was also found between GMF disturbance and microcirculation ( $p=0.04$ ).



Microcirculatory blood flow, similarly with BRS, HRV and BPV, significantly decreased on days with intense geomagnetic activity ( $K = 2-5$ ) compared with quiet days ( $K = 0-1$ ), Fig 1. The decrease was significantly larger for BRS then for MPPG suggesting that GMF primary attenuated arterial baroreflex vascular control mechanism followed by decrease in microcirculation. The reduction of the microcirculatory blood flow did not accompanies with changes in BP supporting GMF direct baroreflex-mediated microcirculatory response then systemic BP - microcirculatory blood flow relationship.

**CONCLUSIONS:** Most likely, GMF affects central hypothalamic and brain stem baroreflex regulatory centers [3] enhancing the effector limb of sympathetic response, leading to increase in vascular tone and to reduction of microcirculatory blood flow in target organs. We recommend in days with intense geomagnetic activity, and especially during geomagnetic storms, intensify the therapy of ischaemic cerebral and heart diseases to improve microcirculation in brain tissue and in myocardium. Verapamil, a  $Ca^{2+}$  channel blocking agent should be especially effective, due to its favorable effect on BP, HR, microcirculatory blood flow and for its potential specific magneto-protective properties [4].

#### References

- [1] E. Stoupelet et al. (2002) *J Clin Basic Cardiol* 5:225–227
- [2] M.T. La Rovere et al. (1998) *Lancet* 351:478–484
- [3] J. Gmitrov and A. Gmitrova (2004) *Bioelectromagnetics*, 25:92-101
- [4] J. Gmitrov and C. Ohkubo (2002) *Bioelectromagnetics* 23:531-541

15-2

**REAL-TIME MEASUREMENT OF BRAIN MICROCIRCULATION DURING RF-EMF EXPOSURE USING AN “8”-SHAPED LOOP ANTENNA.** H. Masuda<sup>1</sup>, A. Ushiyama<sup>1</sup>, S. Hirota<sup>1</sup>, H. Watanabe<sup>2</sup>, K. Wake<sup>2</sup>, S. Watanabe<sup>2</sup>, Y. Yamanaka<sup>2</sup>, M. Taki<sup>3</sup>, C. Ohkubo<sup>1</sup>. <sup>1</sup>Dept of Environmental Health, National Institute of Public Health, Saitama, Japan., <sup>2</sup>Biomedical EMC Group, EMC Center, Wireless Communications Dept, National Institute of Information and Communications Technology, Tokyo, Japan., <sup>3</sup>Dept of Electrical Engineering, Graduate School of Engineering, Tokyo Metropolitan Univ, Tokyo, Japan.

**OBJECTIVE:** Few studies have directly observed brain microcirculation during exposure to radio frequency electromagnetic fields (RF-EMF). Our previous study showed no effects of RF-EMF

exposure on blood-brain barrier (BBB), plasma velocity or vessel diameter, as microcirculatory parameters in rat brain using a cranial window method. However, the changes in these parameters were measured just after RF-EMF exposure, but not during exposure. To simultaneously perform measurements of rat brain microcirculation and RF-EMF exposure to a local cerebral region just under the cranial window, we developed a new type of antenna, "8"-shaped loop antenna. Aim of the present study was to investigate whether RF-EMF exposure induces reversible effects on brain microcirculation observable only during RF-EMF radiation.

**METHODS:** Twenty male Sprague-Dawley rats ( $456 \pm 7$  g) were used. The rats were divided into two groups: RF group was exposed to RF-EMF and Sham group was not exposed to any RF-EMF. All rats were subjected to cranial window implantation and intravital-microscopic observation under pentobarbital anesthesia with a cocktail of ketamine and xylazine. The pial microcirculation within cranial windows were observed using a fluorescent microscope equipped with an ICCD camera. In order to measure the microcirculatory parameters, several types of fluorescent dyes were administered via the tail vein. Rat heads were locally exposed to 1,439MHz electromagnetic near-field TDMA (time division multiple access) signal for PDC (Personal Digital Cellular, Japanese cellular telephone standard) systems by an "8"-shaped loop antenna placed 4 mm over the cranial window. RF-EMF exposure was maintained at a brain averaged SAR (2.0W/kg). During 80 min experimental period including 50 min RF-EMF exposure, three microcirculatory parameters (BBB-function, plasma velocity and vessel diameter) in pial venules were measured every 10 min, and the results were compared between RF and Sham group.

**RESULTS:** We were able to direct observe pial microcirculation through the cranial windows during RF-EMF exposure to rat brain. But no changes in any of the three microcirculatory parameters were elicited by RF-EMF exposure. No extravasation of fluorescence dye, FITC-Dx (MW: 70000) from the pial venule was detected in the two groups. Although plasma velocity increased during the experimental period, there were no differences between the two groups. Furthermore, vessel diameter showed no changes throughout experimental period.

**CONCLUSION:** These results reveal no effects of RF-EMF exposure, at least not on BBB-function, plasma velocity or vessel diameter in rat brain microcirculation, under these conditions.

*This study was financially supported by The Committee to Promote Research on the Possible Biological Effects of Electromagnetic Fields, Ministry of Internal Affairs and Communications, Japan.*

15-3

**EFFECTS OF 915 MHZ EXPOSURE ON THE INTEGRITY OF THE BLOOD- BRAIN BARRIER.** J. S. McQuade<sup>1</sup>, J. H. Merritt<sup>2</sup>, O. Rahimi<sup>3</sup>, S. A. Miller<sup>2</sup>, T. Scholin<sup>2</sup>, A. L. Salazar<sup>1</sup>, M. C. Cook<sup>1</sup>, P. A. Mason<sup>2</sup>. <sup>1</sup>General Dynamics, Advanced Information Engineering Services, Brooks City-Base, TX, <sup>2</sup>Air Force Research Laboratory, Human Effectiveness Directorate, Directed Energy Bioeffects Division, Brooks City-Base, TX, <sup>3</sup>Univ of Texas at San Antonio, San Antonio, TX.

**OBJECTIVE:** To determine whether exposure to 915 MHz alters the integrity of the blood brain barrier (BBB).

**METHODS:** Transverse Electromagnetic (TEM) cells made by Dr. Lars Malmgren that had the same dimensions as the TEM cells used by Salford et al. (1992) were used to expose freely moving Fisher male rats (250-300 gm) for 30 minutes to 915 MHz (continuous wave) at whole-body specific absorption rate (SAR) values of 20, 2, 0.2, 0.02, and 0.002 W/kg. Other animals were exposed to a 915

MHz signal modulated at 16 (~0.2, 0.02, 0.002 W/kg) or 217 (2.5, 0.25, 0.025, 0.0025 W/kg) MHz. Sham controls were identical to the exposures with the exception that the TEM cell was not activated. Home cage control animals, which were not removed from their cages, were also included in the study. Following removal of the exposed or sham-exposed animals from the TEM cells, the number of excreted fecal pellets was recorded, as indirect indicators of stress. Rats were anesthetized post-exposure and perfused intracardially by a gravity-fed drip of heparinized saline followed by 4% paraformaldehyde in 0.1M phosphate buffer. The brains were paraffin embedded and sectioned at 4  $\mu$ m. Endogenous albumin was visualized by reaction with IgG fraction of rabbit anti-rat albumin as described in Salford et al. (1994). To verify that the albumin antibody was working as designed, brain sections from positive control animals that had urea (10 M) injected into the right internal carotid were included in each staining run. Each brain was sectioned into seven blocks, but only sections from the three medial blocks (~0, 2.5, 4.5 mm posterior to bregma) were evaluated in a blind manner by two neuroscientists working independently of one another. Intracellular and extracellular albumin leakage was rated independently on a scale ranging from 0 to 5, similar to that scale used by Salford et al.

**RESULTS:** Animals placed in the TEM cells generally demonstrate docile behavior. Due to their size in relation to the interior dimensions of the TEM cells, the animals would lie in diagonal/bent positions. The animals exposed to 20 W/kg demonstrated more splayed behavior, presumably due to the increase in core temperature. Upon removal from the intracranial cavity, the brains showed no gross pathological changes. The urea positive-control rats showed unilateral albumin leakage. In all animals, albumin leakage was observed in the circumventricular regions. The scores for intracellular and extracellular albumin staining will be presented.

**CONCLUSIONS:** The results will present a dilemma that will need to be resolved. If the results are consistent to those found by Salford et al., the question will remain as to why relatively low whole-body SAR values alter the integrity of the BBB. If the results are inconsistent to those found by Salford et al, the question will be raised as to why two laboratories that used similar exposure chambers, SAR values, and the same strain of animals were unable to find similar results.

#### REFERENCES:

- Salford LG, Brun A, Stuesson K, Eberhart JL, Persson BRR. 1997. Permeability of the blood-brain barrier induced by 915 MHz electromagnetic radiation; continuous wave and pulse modulated at 8, 16, 50, and 200 Hz. *Microscopy Res Tech*: 535-542.
- Salford L, Brun A, Eberhardt J, Malmgren L, Persson B. 1992. Electromagnetic field-induced permeability of the blood-brain barrier shown by immunohistochemical methods. In: Norden B, Ramel C, editors. *Resonance Phenomena in Biology*. Oxford Univ Press. p 87-91.

**LACK OF EFFECTS OF 1439 MHZ ELECTROMAGNETIC NEAR FIELD EXPOSURE ON THE BLOOD-BRAIN BARRIER IN IMMATURE AND YOUNG RATS.** T. Shirai<sup>1</sup>, M. Kuribayashi<sup>1</sup>, J. Wang<sup>2</sup>, O. Fujiwara<sup>2</sup>, Y. Doi<sup>3</sup>, K. Nabae<sup>3</sup>, S. Tamano<sup>3</sup>, T. Ogiso<sup>1</sup>, M. Asamoto<sup>1</sup>. <sup>1</sup>Dept of Experimental Pathol and Tumor Biol. Nagoya City Univ Graduate Sch of Medical Sciences, Nagoya Japan, <sup>2</sup>Dept of Electrical and Computer Engineering, Nagoya Institute Technol, Nagoya Japan, <sup>3</sup>DIMS Medical Science, Ichinomiya Japan.

Possible effects of 1.5 GHz electromagnetic near field (EMF) exposure on the blood-brain barrier (BBB) were investigated using immature (4-weeks-old) and young (10-weeks-old) rats, equivalent in age to the time when the BBB development is completed and the young adult, respectively. Alteration of BBB-related genes, such as those encoding p-glycoprotein, aquaporin-4 and claudin-5, was assessed in the brain after local exposure of the head to EMF at 0, 2 and 6 W/kg specific energy absorption rates (SARs) for 90 min/day for 1 or 2 weeks. Although expression of the 3 genes was clearly decreased after administration of 1, 3-dinitrobenzene (DNB) as a positive control, when compared with the control values, there were no biologically meaningful differences with the EMF at any exposure levels at either age. Vascular permeability, monitored with reference to transfer of FITC-dextran, FD20, was not affected by EMF exposure. Thus, these findings suggest that local exposure of the head to 1.5 GHz EMF exerts no adverse effects on the BBB in immature and young rats.

### **Session 15: In Vivo (Continued)**

*Chairs: Masao Taki and Alexander Lerchl*

**10:30 - 12:00 pm, Theatre M**

**THERMAL RESPONSE AND THRESHOLD MEASUREMENTS IN MICE EXPOSED TO 905MHZ.** S. Ebert<sup>1</sup>, C. Dasenbrock<sup>2</sup>, T. Tillmann<sup>2</sup>, N. Kuster<sup>1</sup>. <sup>1</sup>IT'IS Foundation, Swiss Federal Institute of Technology (ETH), Zurich, Zurich, Switzerland, <sup>2</sup>Fraunhofer Institute Toxicology and Experimental Medicine, Hannover, Germany.

**INTRODUCTION:** The exposure strength of risk assessment studies focusing on the potential hazards of radiofrequency (RF) electromagnetic fields (EMF) needs to be carefully chosen. The exposure level cannot be arbitrarily increased, since significant body heating would mask possible nonthermal or athermal effects. Consequently, studies investigating the possible nonthermal or athermal effects of RF EMF should choose an exposure strength just below the threshold in order to be most relevant for extrapolation to lower doses.

This study presents an evaluation of the thermal regulatory and breakdown thresholds for multiple mouse models together with a detailed dosimetry including an uncertainty estimation for the applied exposure strength.

An optimized exposure setup was applied which provides a uniform exposure distribution for the mice and minimized exposure variability. However, the mice are mechanically restrained during exposure in plastic tubes. This might lead to a decreased heat transfer and a higher stress level as compared to free

running animals. Nevertheless, various in vivo risk assessment studies are performed with restrained mice in order to guarantee well defined exposure. Therefore, the results are especially useful for such studies. Additionally, the derived threshold values for restrained mice are also valid for non-restrained animals, since their threshold is expected to be equal or larger.

**OBJECTIVE:** The objective of this study was the determination of the thermal regulatory and the thermal breakdown thresholds for restrained B6C3F1 and NMRI mice exposed to radiofrequency electromagnetic fields at 905 MHz.

**METHOD:** Different levels of the whole-body averaged specific absorption rate (SAR = 0, 2, 5, 7.2, 10, 12.6 and 20W/Kg) have been applied to the mice, and their body temperature was rectally measured prior, during and after the 2h exposure session in a parallel plate waveguide setup [1]. For B6C3F1 mice, the thermal response was examined for three different weight groups (20 g, 24 g, 29 g), both genders and for pregnant mice. Additionally, NMRI mice with a weight of 36 g were investigated to compare different strains. All experiments were conducted in standard laboratory environments (22±2 °C) and have been approved by the responsible ethical commission.

**RESULTS:** The thresholds show a clear dependence upon the metabolic rate and weight. For example, the NMRI mice showed significantly greater anxiety when restrained than the B6C3F1 and responded at lower SAR values with thermal regulation and breakdown. The thermal regulatory threshold of tube restrained mice was found at SAR levels between 2 W/kg and 5 W/Kg, whereas the breakdown of regulation was determined to be 10.1±4.0 W/kg (K=2) for B6C3F1 mice and 7.7±1.6 W/kg (K=2) for NMRI mice. In other words, the presented data suggest that the thermal breakdown for restrained mice may occur at SAR levels as low as 6 W/kg at standard environmental laboratory conditions.

**ACKNOWLEDGEMENTS:**

This study was supported by the Mobile Manufactures Forum (Belgium).

**REFERENCE:**

[1] Eom SJ, et. al. 2003, "An Exposure System for Behavioral Studies with a Small Number of Mice at 905 MHz", Proceedings 25th Annual Meeting of the Bioelectromagnetics Society, p. 17, Wailea, Maui, Hawaii.

15-6

**EFFECTS OF MAGNETIC FIELD EXPOSURE IN THE DMBA MODEL OF BREAST CANCER IN FEMALE FISCHER 344 RATS.** M. Fedrowitz, W. Löscher. Dept of Pharmacology, Toxicology, and Pharmacy, Univ of Veterinary Medicine, Hannover, Germany.

**INTRODUCTION:** Last year at the 26th Meeting of the Bioelectromagnetics Society (Washington D.C. 2004), we reported that among several different rat strains only the Fischer 344 (F344) rats showed a significantly increased cell proliferation in breast tissue after two weeks of magnetic field (MF) exposure (50 Hz, 100 µT), indicating striking strain differences in MF-sensitivity. This cell-proliferation-enhancing effect in the mammary gland of F344 rats after MF exposure was comparable to the effect that we previously observed in MF-sensitive Sprague-Dawley (SD) rats (Fedrowitz et al., Cancer Res. 62, 1356-1363, 2002). One disadvantage of SD rats as an outbred rat strain is the occurrence of different substrains of SD rats that might respond in different ways to the same experimental design. This was already considered to be an explanation for differing results of studies on

tumor-promoting MF effects in SD rats from different countries (Anderson et al., Environ. Health Perspect. 108, 797-802, 2000). Recently, we described differences in the sensitivity of neoplastic response to the carcinogen 7,12-dimethylbenz[a]anthracene (DMBA) between two different MF-exposed SD substrains from the same breeder (Fedrowitz et al., Cancer Res. 64, 243-251, 2004). The MF-sensitive SD substrain we used over years in our MF experiments with reproducible results was obviously a fortunate exception for studies of cell-proliferation-enhancing and tumor-promoting MF effects among several other strains and substrains of rats. The inbred rat F344 might be another MF-sensitive rat strain because of the cell-proliferation-enhancing effect in F344 breast tissue after MF exposure which we reported recently.

**OBJECTIVES:** In the present study, we investigate the tumor-promoting effects of prolonged MF exposure in the DMBA breast cancer model in female F344 rats in order to examine whether MF exposure is not only able to enhance cell proliferation in breast tissue of this inbred strain but also has the ability to promote tumor incidence after administration of the carcinogen DMBA.

**METHODS:** For this study, we obtained 216 female F344 rats from Charles River, Sulzfeld, Germany (108 rats per group). Rats were allowed to acclimatize to the environmental conditions for at least one week. In September 2004, all rats received a single dose of the carcinogen DMBA when the animals were at an age of about 50-54 days. After 10 mg DMBA per rat were administered intragastrically, the MF or sham exposure started (50 Hz, 100  $\mu$ T). The dosage of DMBA (10 mg/ rat) corresponds to about 90 mg/ kg body weight. Over the period of MF exposure, rats are palpated once weekly to assess the development of mammary tumors. After 26 weeks of exposure (March 2005), rats were killed for necropsy and histopathological analysis of all grossly recorded tumors of the mammary gland. The study was done in a blind fashion, so that the persons involved in the study were not aware whether the animals were MF- or sham-exposed.

**RESULTS:** MF exposure significantly increased tumor development and growth in female Fischer 344 rats in the DMBA breast cancer model. The tumor incidence (proportion of rats with tumor detected by palpation and dissected during necropsy) was significantly higher in MF-exposed Fischer 344 rats. These data substantiate and extend results from previous experiments on mammary cell proliferation, indicating that the mammary tissue of Fischer 344 rats is particularly sensitive to MF exposure.

**CONCLUSIONS:** An inbred rat strain like the F344 rat would be an appropriate tool to study the role of the genetic background for MF-sensitivity and the mechanisms underlying MF effects. Fischer rats appear to exhibit an intermediate sensitivity to the carcinogen DMBA and carry neither of the known mammary cancer suppressor genes nor susceptibility genes that could be found in other rat strains (Gould and Zhang, Environ. Health Perspect. 93, 161-167, 1991). Thus, other mechanisms or genes might be responsible for the MF effects in breast tissue of F344 rats.

This work is funded by a grant (Lo 274/6-2) from the Deutsche Forschungsgemeinschaft (Bonn, Germany).

15-7

**EFFECTS OF GSM-MODULATED 900 MHZ ON IN VIVO ANTIBODY RESPONSE.** F. Nasta, M. Grazia Prisco, R. Pinto, L. Ardoino, G. A. Lovisolo, C. Marino, C. Pioli. Section of Toxicology and Biomedicine, Italian Agency for New Technologies, Environment and Energy.

**INTRODUCTION:** Studies on lymphocytes exposed in vitro to RF radiation describe effects ranging from inhibition of cell proliferation to lack of effects whereas few data are available on the effects of in vivo exposure on the immune system. Our previous in vivo study [1] showed that GSM-modulated RF does not affect spleen cell counts, T and B cells frequencies and phenotype.

**OBJECTIVES:** In order to verify whether RF can affect in vivo functional responses, in the present study we investigated the effects of GSM-modulated 900 MHz EMF on antibody response in vivo.

**MATERIALS AND METHODS:** We performed two sets of experiments. In the first series we evaluated the effects on B cell compartment in non immunised animals; in the second one we used antigen-primed mice. For both sets of experiments C57Bl/6 female mice (8/group) were exposed in a TEM cell to GSM basic signals, 2 W/kg (whole body average), 2h/day, for 4 consecutive weeks. Dosimetric analyses have been performed through experimental evaluation of the SAR in phantoms and in vivo as previously described [1]. Sham-exposed mice were treated as SAR-exposed mice with the exception that the signal was off. A control group was maintained in the animal facility with minimal handling. A blinded procedure was used for exposure, and laboratory staff did not know the exposure levels for the specimens during processing.

**RESULTS:** Results on not-immunised mice show that the frequencies of B cells and of the B cell sub-populations characterised by different levels of IgM/IgD and CD21/CD23 expression (namely Marginal Zone, Transitional and Mature B cells) are not affected by the exposure. Serum immunoglobulin (Ig, antibodies) levels were also analysed. Data show that total IgM and IgG levels in sera are not statistically different in EMF-exposed vs. sham-exposed mice. Moreover, when B cells from these mice are stimulated in vitro with LPS they produce comparable levels of IgM and IgG.

For the second set of experiments, C57Bl/6 female mice were immunised twice with ovalbumin emulsified in adjuvant and exposed as described above. At the end of the exposure period, sera from these mice were analysed for the presence of OVA-specific antibodies. Results show that EMF exposure does not affect the levels of OVA-specific total Ig. Moreover, the OVA-specific IgM and IgG classes of antibodies are also not affected.

**CONCLUSIONS:** Altogether our data show that exposure to 900 MHz GSM-modulated EMF does not affect the frequency of B cells and B cell sub-populations as well as antibody serum levels. Moreover, in immunised mice EMF exposure does not affect antigen-specific antibody response. In conclusion, under the experimental conditions used so far, there is no evidence for an effect on B cell compartment by GSM-modulated signals.

1. Gatta L., R. Pinto, V. Ubaldi, L. Pace, P. Galloni, G.A. Lovisolo, C. Marino and C. Pioli. Effects of in vivo exposure to GSM- modulated 900 MHz on mouse peripheral lymphocytes. *Radiat Res.* 160: 600-605, 2003.

This study was partially supported by the project “Human and environmental protection from electromagnetic emissions” from MIUR (Italian Ministry for Research).

15-8

**IN VIVO STUDIES OF THE EFFECTS OF GSM MICROWAVE EXPOSURE ON HEAT SHOCK PROTEIN EXPRESSION.** F. Poullétier de Gannes<sup>1</sup>, S. Sanchez<sup>1</sup>, H. Masuda<sup>2</sup>, I. Lagroye<sup>1</sup>, E. Haro<sup>1</sup>, M. Taxile<sup>1</sup>, G. Ruffié<sup>1</sup>, B. Billaudel<sup>1</sup>, B. Veyret<sup>1</sup>. <sup>1</sup>PIOM/Bioelectromagnetics Laboratory, ENSCPB/EPHE, Pessac, France, <sup>2</sup>Dept of Environmental Health, National Institute of Public Health, Saitama, Japan.

**INTRODUCTION:** Conflicting results have been published on the expression of heat shock protein (HSP) in different models in response to RFR exposure.

**OBJECTIVES:** Our study focuses on the in-vivo expression of HSP in the two main targets of mobile phone exposure, which are the skin and the brain.

**METHODS:** Hairless and Wistar rats were used for studies on skin and brain, respectively. Rats were progressively trained to the exposure setup (rockets) over two weeks. Thereafter, the animals were exposed or sham-exposed locally to GSM-900 and GSM-1800 microwaves using a loop antenna located at a selected location at the head or at the right rats' backside. For each group, five animals (brain) or eight animals (skin) were used. Acute exposures of rat brains were performed for one hour at 2 W/kg and local exposures of rat skin lasted two hours at 4 W/kg. Semi-chronic exposures consisted in exposing the animal brains one hour/day, 5 days per week for four weeks at 2 W/kg or exposing the animal skins 2 hours/day, 5 days per week for 12 weeks at 2 and 4 W/kg. At the end of the experiment, the animals were sacrificed and skin samples or brains were removed and treated for immunohistochemistry. The 25 and 70 kDa HSP families were tested. Expression levels of heat shock proteins were estimated by image analysis using the Aphelion® software.

Positive controls for heat shock protein induction were performed using kainic acid injection (brain) or UV irradiation (skin). Brain and skin samples were coded and the analysis were performed in a blind manner.

**RESULTS:** After acute exposure (4 W/kg) of rat skins, a statistically significant decrease (-23%,  $p = 0,013$ ) in Hsp25 expression was observed with GSM-1800 while no effect was seen with GSM-900.

No such alteration of the expression of heat shock proteins in the skin was seen after sub-chronic exposure to either GSM signal at the two SAR levels tested.

Immunohistochemical analysis of brain tissues is in progress.

**DISCUSSION AND CONCLUSION:** Our data show that significant effects were observed on the 25 kDa Hsp family in the rat skin after a 2-hour exposure to GSM-1800 microwaves at 4 W/kg. However, a 12-week exposure to either signal at 2 and 4 W/kg did not alter heat shock proteins expression. This may suggest an adaptation of skin tissues to the RFR exposure. Results on the brain will be presented at the meeting.

This work was supported by France Telecom R&D, the European Union (Reflex Project of the 5th frame Work Programme), the Aquitaine Council for Research and the CNRS.

15-9 STUDENT
--------------

**UMTS-MODULATED ELECTROMAGNETIC FIELDS DO NOT INFLUENCE THE DEVELOPMENT OF LYMPHOMA IN FEMALE AKR/J MICE.** A. M. Sommer<sup>1</sup>, A. Lerchl<sup>1</sup>, A. Bitz<sup>2</sup>, J. Streckert<sup>2</sup>, V. Hansen<sup>2</sup>. <sup>1</sup>School of Engineering and Science, International Univ Bremen, Germany, <sup>2</sup>Chair of Electromagnetic Theory, Univ of Wuppertal, Germany.

**BACKGROUND:** Although electromagnetic fields are not genotoxic by themselves, some studies indicated that GSM-modulated electromagnetic radiation, such as from mobile phones and base stations, may promote cancer development. While there is still a scientific discussion about the relevance of such findings, a new telecommunication technique is being introduced in Europe. The field characteristics of the UMTS-standard (Universal Mobile Telecommunication System) differ significantly from the GSM-standard (Global System for Mobile Communications). Therefore, it was investigated experimentally whether electromagnetic fields characteristic for UMTS affect lymphoma development in a mouse strain, which is viremic from birth and spontaneously develops thymic lymphoblastic lymphoma within one year.

**OBJECTIVE:** Experimental investigation to determine whether chronic electromagnetic field exposure

according to the UMTS-standard influences lymphoma development in a mouse strain that is genetically predisposed to this disease.

Methods: 48 groups of 6-7 unrestrained female AKR/J mice were sham-exposed or exposed (n = 160 animals per group) to a generic UMTS test signal [Ndoumbè Mbonjo Mbonjo et al. 2004] for 24 hours per day, 7 days per week by using a radial waveguide setup [Bitz et al. 2004]. Average whole body SAR was 0.4 W/kg. Animals were visually checked daily for signs of a developing disease and were weighed and palpated weekly to detect swollen lymph nodes. Starting at the age of 6 months, blood samples were taken every 2 weeks from the tail to perform differential leucocyte counts. Animals with signs of disease or with an age of about 43 weeks were sacrificed and a gross necropsy was performed. The study was performed in a blinded way, so that the persons actually involved in the experiment did not know which is the exposed and which the sham-exposed group. The code was broken only at the end of the study.

RESULTS: There was no effect of electromagnetic field exposure on body weight gain or survival rate, and lymphoma incidences did not differ significantly between exposed and sham-exposed animals.

CONCLUSION: These data support earlier findings at 900 MHz (GSM) and do not support the hypothesis that exposure to electromagnetic fields used by mobile telecommunication systems is a significant risk factor for developing lymphoma in a genetically predisposed mouse species.

This study was part of a project supported by the Bundesamt für Strahlenschutz, St. Sch 4399: "In vivo-Experimente unter Exposition mit hochfrequenten elektromagnetischen Feldern der Mobilfunkkommunikation. B Kanzerogenese".

#### References:

Bitz, A. K., Streckert, J., Sommer, A. M., Lerchl, A., Hansen, V. W.: 2 GHz-exposure of non-restrained AKR/J mice in a slightly over-moded radial waveguide. 26th BEMS Annual Meeting, Washington, DC, June 2004, 139.

Ndoumbè Mbonjo Mbonjo, H., Streckert, J., Bitz, A., Hansen, V., Glasmachers, A., Gencol, S., Rozic, D. (2004) Generic UMTS test signal for RF bioelectromagnetic studies. *Bioelectromagnetics* 25(6):415-425.

#### 15-10 STUDENT

**SHORT-TERM EXPOSURE TO 1439-MHZ TDMA SIGNAL DOES NOT HAVE THE ESTROGEN-LIKE ACTIVITY IN RATS.** H. Yamashita<sup>1,2</sup>, K. Hata<sup>1</sup>, H. Yamaguchi<sup>1</sup>, T. Giichirou<sup>1</sup>, K. Wake<sup>3</sup>, S. Watanabe<sup>3</sup>, M. Taki<sup>4</sup>, S. Ueno<sup>2</sup>, H. Nagawa<sup>1</sup>. <sup>1</sup>Dept of Surgical Oncology, The Univ of Tokyo, Tokyo, Japan., <sup>2</sup>Dept of Biomedical Engineering, Graduate School of Medicine, The Univ of Tokyo, Tokyo, Japan., <sup>3</sup>National Institute of Information and Communications Technology, Tokyo, Japan., <sup>4</sup>Dept of Electrical Engineering, Graduate School of Engineering, Tokyo Metropolitan Univ, Tokyo, Japan.

INTRODUCTION: Exposure to electromagnetic fields (EMF) has been suggested to increase the risk of hormone-dependent cancers such as breast and endometrial. One suggested pathway is that deficient melatonin function might have anti-estrogenic properties. Postmenopausal women have a decreased melatonin level, and are known to have a higher risk of endometrial cancer. Recently, we have shown that melatonin synthesis is not affected by short-term and long-term exposure to 1439-MHz pulsed EMF used for Japanese Personal Digital Cellular (PDC) system with time division multiple access (TDMA) signal, in rats [1, 2]. Thus, it seems unlikely that such a pulsed EMF decreases melatonin function and

subsequently allows estrogen level to rise. However, its direct effects on hormonal mechanisms are not fully understood. The aim of this study was to clarify whether the exposure to the 1439-MHz TDMA signal results in estrogen-like activity in the target organ .

**METHODS:** A total of 32 ovariectomized female Sprague-Dawley (SD) rats were used in this study. They were divided into four groups; the electromagnetic field (EM), the sham, the cage control, and 17 beta-estradiol injected groups (as a positive control). The EM group was exposed to the 1439-MHz TDMA signal by a carousel type exposure system for 4 hours on three consecutive days, the sham group was placed in the exposure system without feeding TDMA signal to the antenna, and the cage control group was not placed in the exposure system. The average specific absorption rate in the brain was estimated as 7.5 W/kg. One day after treatment, under sufficient anesthesia, the uterine was removed, and then stripped of fat and connective tissue in order to determine uterine wet weight. Concurrently, blood was collected and the serum estradiol level was measured by radioimmunoassay.

**RESULTS AND DISCUSSION:** Neither uterine wet weight nor serum estradiol level was altered with short-term TDMA exposure. Further investigation for long-term TDMA exposure is warranted. We thank the members of the Committee to Promote Research on the Possible Biological Effects of Electromagnetic Fields in Ministry of Internal Affairs and Communications in Japan.

#### REFERENCES

1. K. Hata, H. Yamaguchi, G. Tsurita, S. Watanabe, K. Wake, M. Taki, S. Ueno, H. Nagawa, Short term exposure to 1439 MHz pulsed TDMA field does not alter melatonin synthesis in rats, *Bioelectromagnetics*. 26 (2004) 49-53.
2. K. Hata, S. Ueno, H. Yamaguchi, G. Tsurita, S. Watanabe, K. Wake, M. Taki, H. Nagawa (2004). Long-term effects on melatonin synthesis in male rats after exposure to a 1439 MHz TDMA electromagnetic field. In "Bioelectromagnetics Society Annual Meeting".

## Session 16: European Programs

*Chairs: Paolo Ravazzoni and Bernard Veyret*

**1:00 - 2:45 pm, Theatre L**

16-1

**POTENTIAL EFFECTS OF CELLULAR PHONES ON HEARING. EUROPEAN PROJECT GUARD, 2002-2004: ANIMAL STUDIES.** J. M. Aran<sup>3</sup>, A. Brazzale<sup>1</sup>, N. Carrere<sup>3</sup>, P. Galloni<sup>2</sup>, C. Marino<sup>2</sup>, Y. Hondarrague<sup>3</sup>, M. Parazzini<sup>1</sup>, R. R. Pinto<sup>2</sup>, M. Piscitelli<sup>2</sup>, P. Ravazzani<sup>1</sup>. <sup>1</sup>Biomedical Engineering Institute, Italian National Research Council, Milan, Italy, <sup>2</sup>Italian National Agency for New technologies, Energy and the Environment - Section of Toxicology and Biomedical Sciences, Rome, Italy, <sup>3</sup>Inserm and Univ Bordeaux-2 Cellular & Molecular Biology of Hearing, Pellegrin Hospital, Bordeaux, France.

Introduction: during the last decade, the use of cellular phones has dramatically increased; hence, concerns have been raised that exposure to their emissions may represent a potential hazard for humans and environment. In January 2002 the three-years long GUARD Project (FP5,QLK4-CT-2001-00150, 2002-2004) had started: its final aims were to define general guidelines for producers of mobile phones, support health and environmental authorities and public information (in correlation with National and

International Societies and Organizations), provide industry and policy-makers with adequate tools for assessing and managing the potential risks for hearing.

The project planning included the study of the effects of phones emissions on the hearing system and functions of animals and humans. In particular, two out of nine partners involved in the project, ENEA in Rome, Italy (in collaboration with ISIB-CNR of Milan), and INSERM in Bordeaux, France, had performed a number of experiments utilizing physiological (DPOAEs and ABR) and structural (Organ of Corti's morphology) endpoints in the evaluation of possible effects of both 900 and 1800 MHz electromagnetic fields on the auditory system of rodents (Sprague-Dawley rats and Guinea Pigs, GP). The Inserm group particularly focused on the potential effects of microwave exposure on the ototoxicity of other well documented agents such as the aminoglycosidic antibiotic Gentamicin (GM).

#### Materials and Methods:

ENEA - The ENEA experiments included various schedules as well: Sprague-Dawley rats were exposed (or sham exposed) to 900 or 1800 MHz EMF, GSM-modulated or CW, 2 or 4 W/kg, for 2 hours/day, 5 days/week, 4 weeks, treated or not with GM. DPOAEs recordings were performed before the exposure, during the exposure (i.e. at the end of each week of exposure) and after (the day after and one week after the end of exposure).

Regarding the "in vivo" exposures, both laboratories utilized loop antennas as source of "localized" exposure, close to the animal's ear, resembling the use of a cellular phone

INSERM - In a first experimental series, eight pigmented GPs were treated with daily intramuscular injections of the well known ototoxic aminoglycoside antibiotic GM at 60 mg/kg (a dose close to ototoxic level) one hour prior exposure of the left ear to 900 MHz GSM microwaves at SAR of 2W/kg for 2 hours. They were so treated 5 days/week for 4 weeks. Eight other GPs were submitted to the same GM treatment but sham-exposed to the GSM microwaves. For all GPs, both ears were tested before, at the end and one month after the end of the treatment for DPOAE and for ABR thresholds from 1 to 24 kHz.

A second experimental series consisted in 24 albino GPs (more prone to develop ototoxic damage) treated with a higher daily dose of GM (75 mg/kg/day), 5 days/week during 2 weeks. Twelve of these had their left ear simultaneously exposed to the GSM microwaves at SAR of 4 W/kg (thus 2 hours/day, 5 days/week for 2 weeks). The other 12 GPs were sham-exposed. DPOAEs and ABR thresholds were measured for each ear before, at the end and 1 month after the end of the treatment/exposure period.

#### Results:

ENEA - Experiments were performed varying SAR levels (2 or 4 W/kg), exposure time (1-4 weeks), RF modulations (GSM or CW) and frequency (900 or 1800 MHz). Comparing data recorded from exposed and sham animals, no statistically significant differences in the level of DPOAEs recorded before and after exposure were evidenced, throughout all the acoustic frequencies' spectrum analyzed. The ototoxic effect of gentamicin was not modified by co-exposure to RF electromagnetic field

INSERM - A DPOAE amplitude decrease limited to the highest frequencies was observed in all GPs in experiment 2. ABR threshold elevations, only on the highest frequencies tested, were observed in both experiments at the end of the treatment/exposure periods, with partial recovery one month later. These differences were more pronounced in the second experimental series. There was, however, in both experiments, no difference between exposed and sham-exposed groups, as well as between ears, at any time. The changes at high frequencies observed in both ears, independent of the exposure conditions, are typical of aminoglycoside antibiotic damage.

Conclusion: according to planned schedules, effects of cell phones related electromagnetic fields exposure on rat's cochlea function were investigated. Regarding to the "in vivo" protocols, no effects of both 900 and 1800 MHz exposure were evidenced in rats' OHC function.

Moreover the INSERM two experimental series tend to confirm the lack of toxic effects of chronic exposure of the GP's ears to GSM microwaves, in normal ears as well as in ears exposed to another well recognized pathological agent such aminoglycoside antibiotic ototoxicity.

Acknowledgements: this study was funded by: (1) the European Project GUARD "Potential adverse effects of GSM cellular phones on hearing" (FP5,QLK4-CT-2001-00150, 2002-2004); (2) the national research project "Protection of humans and environment from electromagnetic emissions"; (3) ELETTRA 2000 Consortium; (4) Inserm and Bordeaux-2 Univ

16-2

**PERFORM-B ORNITHINE DECARBOXYLASE SUB-PROGRAMME: INVESTIGATION ON THE IN VITRO EFFECTS OF MOBILE PHONE SIGNALS EXPOSURE ON ORNITHINE DECARBOXYLASE ACTIVITY.** B. Billaudel<sup>1</sup>, J.C. Groebli<sup>3</sup>, A. Hoyto<sup>2</sup>, N. Kuster<sup>3</sup>, I. Lagroye<sup>1</sup>, J. Luukkonen<sup>2</sup>, J. Naarala<sup>2</sup>, N. Nikoloski<sup>3</sup>, G. Ruffie<sup>1</sup>, J. Schuderer<sup>3</sup>, M. Sokura<sup>2</sup>, D. Spaet<sup>3</sup>, M. Taxile<sup>1</sup>, B. Veyret<sup>1</sup>. <sup>1</sup>Bioelectromagnetics Laboratory, EPHE /PIOM-ENSCP, Pessac, France, <sup>2</sup>Univ of Kuopio, Dept of Environmental Sciences, Kuopio, Finland., <sup>3</sup>IT'IS Laboratories, Zurich, Switzerland.

**OBJECTIVES:** The ornithine decarboxylase (ODC) enzyme plays a pivotal role in the synthesis of polyamines that are essential for cell growth. The Litovitz group(1) had reported a temporary increase in ODC activity in L929 fibroblasts after exposure to microwaves emitted by mobile phones (50 Hz modulated DAMPS-835 MHz): only did modulated RF have an effect on the ODC enzyme, in contrast to continuous wave (CW) signals. Such an increase in ODC activity might indicate that RF acts as a non-genotoxic carcinogen. The Perform-B investigation on ODC activity was realised in five phases, which extended Litovitz initial experiments to other exposure systems, signals, cells types and studied biological end-points.

**METHODS:** Phase 1 was intended to replicate the experiments of the Litovitz group by using an identical exposure system, i.e., Crawford cells. The Crawford cells were characterised and provided by IT'IS for exposure to RFR under the conditions published by Litovitz et al. However, dosimetric data(2) showed that when fans were turned off as reported in earlier studies, measured SAR and temperature increase were higher than those reported in the initial Penafiel's work(1). Therefore, additional experiments were performed at 2.5 (PIOM) and 6 W/kg (UKU) with fans turned off to investigate the effect of the temperature increase on ODC activity (as probably experienced by Litovitz and co-workers), i.e. 0.33°C at 2.5 W/kg and 0.78 °C at 6 W/kg. In phase 2, the same procedure was followed using other exposure systems with a well-defined dosimetry (UKU: STUK resonator and PIOM: IT'IS waveguide sXc-900). The aim of phase 3 was to test the influence of CW or 217 Hz modulated GSM using 872, 900 and 1800 MHz signals on ODC activity using phase 2 exposure systems. Besides the UKU chamber and the IT'IS waveguide (PIOM), additional experiments were performed using the wire-patch cell for the exposure of L929 cells to a GSM/217Hz/900 MHz signal (PIOM). Phase 4 was intended to investigate tissue specificity. Therefore, human and rat nerve cell lines have been tested for their response to RFR using the well-characterised exposure setups. Since no effect was observed on ODC activity in L929 cells after 8 hours of exposure to RFR, cellular transformation was not investigated. However, the intention of phase 5 was for UKU to investigate further the effects of one exposure level to RFR - GSM/872 MHz or CW/872 MHz at a SAR of 5 W/kg- on different parameters linked to cancer (ODC activity, apoptosis, proliferation, lipid peroxidation). Statistical analysis was done using the Wilcoxon test for paired values.

RESULTS-CONCLUSIONS: In the different phases, all results failed to support the previously reported effect of the low-level RFR on the activity of the ODC enzyme. The strict replication data of phase 1 was in good agreement with those recently reported by Owen and co-workers at FDA(3). The replication of the former work of the group of Litovitz, using 835 MHz/DAMPS and CW signals and murine L929 fibroblasts was thereafter extended to various RFR signals experimental cases, but no significant effect of RFR exposure was observed to affect ODC activity or other tested endpoints. With the provision that at least a ten-fold increase in ODC activity is necessary to induce deleterious effect on cellular functioning, these results give no support for the possibility of neoplastic transformation via an effect of ODC activity induced by RFR.

REFERENCES:

(1) Penafiel et al., 1997, *Bioelectromagnetics*, 18, 132-141.

(2) Nikoloski et al., 25th Annual Meeting of the Bioelectromagnetics Society, June, 2003, Maui, USA, p. 52.

(3) Desta et al., 2003, *Radiation Research*, 160, 488-491.

Acknowledgements: This work is supported by the MMF, the GSM Association, TEKES, the Aquitaine Council for Research, and the CNRS.

Sponsor coordination: Univ of Helsinki.

16-3

**WHOLE-BODY EXPOSURE TO 2.45 GHZ ELECTROMAGNETIC FIELDS DOES NOT ALTER SPATIAL WORKING MEMORY, ANXIETY RESPONSES AND BLOOD-BRAIN BARRIER PERMEABILITY IN RATS.** B. Cosquer<sup>1</sup>, R. Galani<sup>1</sup>, A. P. de Vasconcel<sup>1</sup>, J. Fröhlich<sup>2</sup>, N. Kuster<sup>2</sup>, J-C. Cassel<sup>1</sup>. <sup>1</sup>LN2C Univ Louis Pasteur-CNRS Strasbourg, France, <sup>2</sup>IT'IS Foundation ETH Zürich, Switzerland.

Mobile communication is based on utilization of electromagnetic fields (EMFs) in the microwave range (0.3-300 GHz). Some human and animal studies suggest that EMFs in the 0.1 MHz-300GHz range might interfere with cognitive processes. In 1994, a report by Lai and colleagues (*Bioelectromagnetics* 15, 95-104) showed that, in rats, whole-body exposure to pulsed 2.45 GHz microwaves (500 pps, 2 µsec pulse duration, repetition rate of 500 Hz, specific energy absorption rate [SAR] 0.6 W/kg) for 45 min resulted in altered spatial working memory performance assessed in a 12-arm radial-maze task. Using naïve (no experience of exposure device), sham-exposed (experience of the exposure device without microwaves) and microwave-exposed rats, we have tried to replicate this experiment, but could not confirm the results reported by Lai et al. (*Behavioural Brain Research* 155, 2004, 37-43). As the arms and the platform used by Lai et al. (1994) were bordered by 20-cm high opaque walls, rats had limited access to spatial cues, which in turn might have influenced performance and could explain our replication failure. To address this possibility, we ran another experiment according to exactly the same conditions as in our replication attempt, except that 30-cm high opaque walls were placed all around the arms and the central platform in order to reduce access to spatial cues. We found that the performance of exposed rats was comparable to that observed in sham-exposed or in naïve rats. These results extend our previous study and further support our initial conclusion that the microwave-induced behavioural alterations measured by Lai et al. might be due to factors liable to yet unexplained performance bias, rather than to alteration of either spatial working memory per se or non-spatial strategies compensating for the reduced access to spatial cues. In search of such factors, we first considered possible effects of EMFs on anxiety. Indeed, EMFs exposure was previously found to increase the number of benzodiazepine receptors in the rat cortex (Lai et al., *Bioelectromagnetics* 1992;13(1):57-66) and it is well known that anxiety might influence cognitive performance. Rats were exposed to 2.45 GHz EMFs

for 45 min (2  $\mu$ s pulse width, 500 pps, whole-body and time averaged of SAR 0.6 W/kg +/-2dB, brain-averaged SAR of 0.9 W/kg +/-3dB) and subsequently tested in an elevated-plus maze under an ambient light intensity of either 2.5 lux or 30 lux. The low intensity level set the behavioural baseline for the detection of anxiogenic effects, while the higher one corresponded to the detection of anxiolytic effects. Whatever light intensity was used, EMF exposure failed to induce any significant effect on anxiety responses in the elevated plus-maze. The present experiment demonstrates that exposure to EMFs did not alter anxiety responses assessed in the elevated plus maze (Behavioural Brain Research 156, 2005, 65-74). Secondly, we considered possible effects of EMFs on blood-brain barrier (BBB) permeability. Indeed, data in the literature suggest that, under some conditions, EMFs may alter BBB permeability, whereby molecules that normally do not penetrate into the brain can do so and might interact with normal information processing. Thus, we first verified that our 12-arm radial maze test enabled demonstration of a memory deficit in rats treated with the peripherally and centrally active muscarinic antagonist scopolamine hydrobromide (0.5 mg/kg, i.p.). In two subsequent experiments, we investigated whether a systemically-injected quaternary-ammonium derivate of this antagonist (scopolamine methylbromide; MBR), which poorly crosses the blood-brain barrier (BBB), altered radial-maze performance after a 45-min exposure to 2.45 GHz electromagnetic field (EMF; 2  $\mu$ s pulse width, 500 pps, whole-body SAR of 2.0 W/kg +/-2dB and brain averaged SAR of 3.0 W/kg +/-3dB). Such an alteration would reflect changes in BBB permeability. In one of these experiments the drug was injected before exposure, in the other one right afterwards. Whether scopolamine MBR was injected before or after exposure, the exposed rats did not perform differently from their naïve or sham-exposed counterparts. As the EMFs used in the present experiment did not allow scopolamine MBR to penetrate the brain in a sufficient amount to induce alterations of cognitive functions, these EMFs most probably failed to disrupt the BBB. In a complementary experiment, we studied possible alterations of the BBB permeability by an additional approach : rats were subjected to i.v. injections of Evans blue, a dye binding serum albumin (serum albumin does not cross the BBB), before or after EMF exposure. The absence of Evans blue extravasation into the brain parenchyma of our exposed rats, whether the dye was injected before or after the exposure, confirmed an absence of BBB disruption during EMFs exposure in our conditions.

Altogether, the present series of data suggest that whole-body exposure to 2.45 GHz EMFs i) at a SAR of 0.6 W/kg, does not alter spatial working memory in a radial-maze task, and has neither anxiolytic nor anxiogenic effects assessed in an elevated plus-maze, and, ii) at a SAR of 2.0 W/kg, does not alter the permeability of the blood-brain barrier.

Within the Perform-B programme, this work was funded by MMF and GSM A.

16-4

**EFFECTS OF CELL-PHONES RELATED EMISSIONS ON SPRAGUE-DAWLEY RATS' AUDITORY SYSTEM: DPOAE'S MEASUREMENTS AND COCHLEAR CELL'S MORPHOLOGY.** P. Galloni<sup>1</sup>, A. Brazzale<sup>2</sup>, M. Parazzini<sup>2</sup>, R. Pinto<sup>1</sup>, M. Piscitelli<sup>1</sup>, P. Ravazzani<sup>2</sup>, C. Marino<sup>1</sup>. <sup>1</sup>Toxicology and Biomedical Sciences Unit, Enea Casaccia, Rome, Italy, <sup>2</sup>Biomedical Engineering Institute, CNR, Milan, Italy.

Introduction: the ear and its function could be the first biological target of cell phone's electromagnetic emissions. The aim of this study was the evaluation of possible changes in cochlear physiology and morphology in rats exposed to EMF at the typical frequencies of mobile phones. The cochlear functionality was investigated by Distortion Product Otoacoustic Emissions (DPOAE) measurements,

known as indicator of the cochlea status. They are in particular associated to outer hair cells (OHC) function; any significant reduction in their level can therefore be a signal of mild to severe impairment on this sensorial epithelium.

**Materials and Methods:** on account of the results obtained in our previous studies, performed in the framework of GUARD project (see below), the experimental procedures were carried out as follows: animals (male Sprague-Dawley rats, weight of 250 gr.) were subjected to a localized exposure (right ear), simulating the use of a cellular phone, by 3 different sets of 4 loop antennas, one for sham and two for exposed animals. Animals were exposed 2 hours/day, 5 days/week, for 4 weeks, 4 W/kg of SAR, Continuous Wave mode; during the exposure rats were kept in plastic restrainers. Gentamicin-treated (GM, dose of 150 mg/kg) animals were also included as positive control, so 4 groups of rats were eventually scheduled: a RF-exposed group, a RF-exposed + GM group, a sham-exposed group, a GM only group. DPOAE tests were carried out before exposure, during exposure (i.e. at the end of each week) and after (the day after and one week after); the measurement sessions were performed keeping animals under general gas anesthesia (isoflurane in O<sub>2</sub>, 1.5-2 %).

**Results:** the experiments and the statistical evaluation were performed in blind mode with respect to the exposure conditions (sham or exposed). No statistically significant differences were found in the DPOAE level between exposed and sham group, and no influences of RF exposure on GM ototoxicity were evidenced.

**Conclusions:** no effects of 900 MHz, 4 w/kg RF exposure were evidenced on OHC's function in this experimental conditions.

**Acknowledgements:** this study was founded by: (1) the European Project GUARD "Potential adverse effects of GSM cellular phones on hearing" (FP5,QLK4-CT-2001-00150, 2002-2004); (2) the national research project "Protection of humans and environment from electromagnetic emissions"; (3) ELETTRA 2000 Consortium.

16-5

**PERFORM B: BEHAVIOURAL STUDIES WITH MICE.** N. Jones<sup>1</sup>, A. Bottomley<sup>1</sup>, R. Haylock<sup>1</sup>, R. Saunders<sup>1</sup>, N. Kuster<sup>2</sup>, Z. Sienkiewicz<sup>1</sup>. <sup>1</sup>National Radiological Protection Board, Chilton, Didcot, Oxfordshire, UK, <sup>2</sup>IT'IS, Zurich, Switzerland.

Perform B was an international research programme aimed at replicating key in vitro and in vivo studies recommended by the WHO agenda of 1999. The programme included studies investigating the effects of radiofrequency (RF) fields on the behaviour of rats and mice performing spatial memory tasks in radial arm mazes. The studies using mice are reported here.

Adult male C57BL/6J mice were exposed to 900 MHz GSM (talk) signals for 1 h before behavioural testing. Some animals were exposed using a mini-wheel system to produce whole-body exposure (at SARs of 0.1, 0.6 or 3 W/kg), whereas others were exposed using a waveguide system to produce head-mainly exposure (at local SARs in the head of 0.1, 0.4 or 2.2 W/kg). Additional animals were sham-exposed. All animals were given one trial in an 8 arm radial maze each day for 15 days. The trial was finished only when the animal had located all food rewards (8 x 45 mg Noyes pellets). A confinement procedure was used to stop the animals using non-spatial strategies to solve the maze.

For each trial, the total numbers of errors (assessed as a re-entry into an arm), the number of arms visited before the first error, and the numbers of errors in the first eight arm visits were recorded. All tasks and assessments were conducted without knowledge of the exposure status of the animals.

These data were analysed by estimating the probability that an animal will not re-enter any given arm of the maze, and then using these probabilities as the measure of performance of the task. Different models were fitted, using maximum likelihood techniques, to the performance scores to determine whether there

were any differences between the groups. The models were compared by referring changes in the deviance divided by the associated changes in the degrees of freedom to the chi-squared distribution. These techniques may be considered equivalent to a two way ANOVA but using a binomial distribution for the underlying random variability.

For both whole-body and head-mainly exposure, no significant field-dependent effects were observed on maze performance at any SAR used ( $p < 0.05$ , in all cases). Small, but significant differences were noted between groups in the rate of increase in performance following whole-body exposure but these were not attributable to the exposure status of the animals.

It is concluded that acute, repeated exposure to 900 MHz GSM signals under the conditions of these experiments did not engender any significant behavioural effects. These results are consistent with similar studies performed within the Perform B programme using rats exposed to pulsed 2.45 GHz fields, and with other studies using the fields associated with mobile phones.

All procedures involving animals were carried out the approval of the local ethical review committee and in accordance with the Animals (Scientific Procedures) Act 1986.

This work was funded in part by the MMF and GSMA

16-6

## **FINNISH NATIONAL RESEARCH PROGRAM ON HEALTH RISKS OF MOBILE TELEPHONY.** J. Juutilainen. Dept of Environmental Sciences, Univ of Kuopio, Finland.

**BACKGROUND:** The increasing use of mobile phones has radically increased human exposure to radiofrequency (RF) electromagnetic fields. At present, more than 80% of the Finnish population have a mobile phone. Although the exposure levels are low, the high number of users and some provocative but inconclusive scientific results have raised concerns about possible adverse health effects of RF electro-magnetic field exposure from mobile communication systems.

During the years 1994-2003, Finnish universities and research institutes have carried out three national research programs to address the public concerns and to support the ongoing international efforts to assess possible health effects of RF electromagnetic fields. The Finnish research programs have been funded by the governmental TEKES (National Technology Agency; about 70% of the funding) and by the industry (about 30%). The present research program "Health Risk Assessment of Mobile Communications (HERMO)", will continue this unique series of national research programs. The three-year HERMO project was started in June 2004.

While the previous Finnish research programs and other recent studies have produced a lot of useful data for risk assessment of RF electromagnetic fields from mobile phone systems, there are still many open questions. The HERMO research programme was planned based on the research needs listed in the WHO Research Agenda (2003 Research Agenda for Radio Frequency Fields of the World Health Organisation) and review of recent literature.

**AIMS:** The aims of the HERMO research program are:

1. to study the biological relevance of amplitude modulation
2. to study acute and chronic effects of RF fields on the nervous system and sensory organs
3. to investigate the effects of RF fields on children
4. to study the sources of error in an epidemiological study on mobile phone use and cancer
5. to improve dosimetry and to provide dosimetric support for biological studies of this project
6. to study the dosimetry of RF fields near metallic implants

7. to provide materials for risk communication on RF fields

PROJECTS: The following projects are at present included in the HERMO research program:

1. The effects of radiofrequency electromagnetic fields on inner-ear sensitivity
2. Long- and short-term effects of GSM electromagnetic fields on preattentive auditory discrimination in the human brain
3. Thermophysiological and cardiovascular responses of human subjects exposed to RF fields from mobile phones
4. Effects of radiofrequency electromagnetic fields on developing nervous system – a study relevant to children's use of mobile phones
5. The effects of radiofrequency radiation from mobile phone systems on brain functions
6. Cellular phones and brain tumour risk: assessment of sources of error
7. Development of radio-frequency dosimetry
8. Computational dosimetry of RF exposure cases
9. In-vivo estimation of tissue permittivity
10. Interaction of mobile phones with superficial implants

PARTICIPANTS: The HERMO research program is conducted by 7 universities and research institutes: Univ of Kuopio, Univ of Turku, Univ of Helsinki, Tampere Univ of Technology, STUK - The Radiation and Nuclear Safety Authority, Finnish Institute of Occupational Health, and VTT Information Technology.

16-7

**THE EUROPEAN PROJECT GUARD: EFFECT OF GSM CELLULAR PHONES ON HUMAN HEARING.** P. Ravazzani<sup>1</sup>, L. Collet<sup>2</sup>, M. Lutman<sup>3</sup>, G. Tavartkiladze<sup>4</sup>, G. Thuroczy<sup>5</sup>, M. Tsalighopoulos<sup>6</sup>, V. Uloza<sup>7</sup>, I. Uloziene<sup>8</sup>, A. Brazzale<sup>1</sup>, S. Bell<sup>3</sup>, A. Moulin<sup>2</sup>, M. Parazzini<sup>1</sup>, N. Thomas<sup>3</sup>, G. Tognola<sup>1</sup>. <sup>1</sup>Istituto di Ingegneria Biomedica CNR, Milano, Italy, <sup>2</sup>Laboratoire Neurosciences et Systèmes Sensoriels Université Claude Bernard Lyon 1 and CNRS, Lyon, France, <sup>3</sup>Institute of Sound and Vibration Research, Univ of Southampton, Hi, Southampton, UK, <sup>4</sup>National Research Centre for Audiology and Hearing Rehabilitation, Moscow, Russia, <sup>5</sup>National Research Institute for Radiobiology and Radiohygiene, Dept. of Non-Ionising Radiation, Budapest, Anna u.5, Hungary, <sup>6</sup>AHEPA District General Hospital of Thessaloniki, Greece, <sup>7</sup>Kaunas Univ of Medicine, Kaunas, Lithuania, <sup>8</sup>Kaunas Univ of Medicine, Institute of Biomedical Research, Kaunas, Lithuania.

INTRODUCTION: The multicenter project funded by the European Commission named GUARD involved nine centers and aimed to assess potential changes in auditory function as a consequence of exposure to low-intensity electromagnetic fields (EMF) produced by GSM cellular phones both on laboratory animals and on humans. The purpose of this paper is to present the final results of the project for what concerns human experimentation.

MATERIALS AND METHODS: Two experimental paradigms were used in the human study. The within-subject paradigm entails measurements before and after genuine or sham exposure to EMF in a repeated double-blind design. The between-subject paradigm uses two groups: heavy users and light users of cellular phones, where high users are defined as typically speaking for at least 30 minutes per day and low users are defined as typically speaking for less than 5 minutes per day. Participants are healthy young adults (18-30 years old) without any evidence of hearing or ear disorder. Tests for assessment of auditory function were: transient otoacoustic emissions (TEOAE), distortion product otoacoustic emissions (DPOAE), effects of contralateral acoustic stimulation (CAS) on TEOAE and

auditory brainstem response (ABR). For the within-subject study, the recordings were performed immediately before and after exposure to EMF and only the exposed ear was tested. For the between-subject study, the recordings were performed only once on both ears. For the within-subject study only, the exposure consisted of speech at a typical conversational level delivered via an earphone to one ear, plus genuine or sham EMF exposure, where EMF exposure utilized the output of a consumer cellular phone (NOKIA 6310) at full power for 10 minutes. Half of the participants received GSM exposure at 900 MHz (full power = 2W) and the other half receive GSM exposure at 1800 MHz (full power = 1W). The sham or genuine exposure was performed using a “load” or a “dummy load” and were on separate days (at least 24 hours apart). A system of phone positioning that allows participants to freely move their head without affecting exposure was designed. During the exposure the phone was placed so that its longitudinal axis follows an imaginary line from the entrance to the ear canal to the corner of the mouth. All mobile phones included in the project passed validation tests before use. During the tests the power, the frequency and the spatial distribution of the radio frequency exposure was processed.

**RESULTS:** A total of about 500 subjects in six laboratories were involved across both studies. The variations in the audiological measures before and after exposure or between the two groups of mobile phone user were no statistically significant. Moreover, individual variability was within the limits at which the effect should be notified to the ethics committee. Details on the final statistical analysis of the GUARD pooled data will be presented and discussed.

**CONCLUSIONS:** These findings show no significant effects of GSM electromagnetic fields on the main measures of the status of the human auditory system.

**ACKNOWLEDGEMENTS:** This work was financed by the Project GUARD “Potential adverse effects of GSM cellular phones on hearing” (European Commission, 5th Framework Programme, QLK4-CT-2001-00150, 2002-2004).

## Session 17: In Vitro RF

*Chairs: Myrtil Simko and Isabelle Lagroye*

**1:00 - 2:45 pm, Theatre M**

17-1

**CLASTOGENIC EFFECTS OF UMTS RADIOFREQUENCY SIGNAL IN HUMAN LYMPHOCYTES.** M. L. Calabrese<sup>1</sup>, G. d'Ambrosio<sup>1</sup>, G. Gialanella<sup>2</sup>, G. Grossi<sup>2</sup>, L. Manti<sup>2</sup>, R. Massa<sup>1</sup>, M. Pugliese<sup>2</sup>, A. Rienzo<sup>2</sup>, P. Scampoli<sup>2</sup>. <sup>1</sup>Univ of Naples Federico II - DIET, Naples, Italy., <sup>2</sup>Univ of Naples Federico II - DSF, Naples, Italy.

**OBJECTIVE:** In the framework of the research programs on Information and Communication Technologies funded by the Campania Region (Italy), four different research groups joined a three-year project, for evaluating cancer-risk related endpoints in mammalian cells following in vitro exposures to UMTS radiofrequency signal. Here we present some preliminary results of one of these activities: the genotoxic effects of an UMTS modulated signal, and cooperative effects with ionising radiation, in human peripheral blood lymphocytes.

**METHODS:** Cells were seeded into 35 mm Petri dishes (2x10<sup>6</sup> cells / 3 ml complete RPMI medium without mitogen). Radiofrequency/sham exposure was carried out in a waveguide inside a commercial CO<sub>2</sub> incubator. The exposure set-up consisted in a short-circuited waveguide: under horizontal E field polarization, high efficiency (up to 80 %) and limited SAR non-uniformity (less than 30 %) were obtained. Temperature and dose were carefully controlled during the exposure. Cells were exposed for 30 min or 24 hours at 0.8 and 1.6 W/kg SAR levels. The signal source was an Agilent E4432B, ESG-D series, signal generator. The carrier frequency of the UMTS signal was 1950 MHz (centre of the up-link frequency range), and a WCDMA modulation, according to the 3GPP 3.5 2001-03 specifications, was used. For each separate experiment, we prepared four samples: (a) non-irradiated sample, used as negative control, (b) sample exposed to ionizing radiation only (4 Gy of 250 kVp X-rays), used as positive control, (c) sample exposed to microwaves only, d) sample exposed to X-rays first, and then exposed to microwaves in the same conditions as for the (c) sample. Immediately after exposure, all samples were stimulated to grow in RPMI medium supplemented with 1% phytohaemagglutinin. Following 48 and 72 hours in culture at 37 degreeC, mitotic cells were accumulated with 2 hours incubation in 0.2 µg/ml colcemid, and metaphases were harvested following standard procedure. Finally, chromosomes were hybridized in situ with whole-chromosome DNA probes specific for human chromosomes 1 and 2. All kinds of visible structural chromosomal aberrations (dicentric, translocations, complex-type exchanges, rings, acentric fragments) were scored at a fluorescent microscope (Zeiss) using an automatic metaphase finder and image analysis system (MetaSystems).

**RESULTS AND CONCLUSIONS:** Preliminary results indicate no direct clastogenic effect of the microwave field. In fact, the frequency of chromosomal aberrations in samples exposed to microwave alone (sample c above) is not statistically different from the negative controls. Experiments are under way to determine the influence of the non-ionizing radiation field on the repair of ionizing radiation-induced DNA breaks.

Research done within the framework of the "Wireless Technology Health Risks (WITHER) Project" (Calabrese et al, The BEMS 2004 Annual Meeting), supported by the "Centre of Competence on Information and Communication Technologies" of the Regione Campania, Italy.

**KILLING OF BIOLOGICAL AGENTS WITH HIGH PEAK E-FIELD MICROWAVE RADIATION.** J. L. Kiel<sup>1</sup>, P. A. Mason<sup>1</sup>, M. A. Sloan<sup>2</sup>, A. J. Tijerina<sup>2</sup>. <sup>1</sup>Human Effectiveness Directorate, US Air Force Research Laboratory, <sup>2</sup>Conceptual MindWorks, Inc.

**INTRODUCTION:** Prohofsky has explained recently (Prohofsky EW. 2004. RF absorption involving biological macromolecules. *Bioelectromagnetics* 25:441-51) that there are two primary ways in which a molecule can absorb energy: (1) vibrational modes that consist of in-phase, intermolecular motion over large segments of bulk matter and (2) opposing displacements between adjacent atoms within the molecule. The first results in rapid thermalization of the absorbed energy. The second, involving these intramolecular vibrations, takes place at higher frequencies. Prohofsky states that in many biological molecules, physical displacement of atoms from one conformation to another is intimately connected to their biological function. Prohofsky's calculations indicate that "absorption below several hundred GHz would not be resonantly absorbed into an intramolecular mode" for any biological molecule. Any absorption should be into bulk modes of the material in which the molecule is embedded. Thermalization of the RF energy would be primarily in this bulk material, rather than to a single molecule. He states that for an athermal effect to occur there would have to be an energy transfer to one mode in excess of the energy in all other modes, which is extremely unlikely. Here we show how effects on the biosynthetic organic semi-conductor diazoluminmelanin (DALM) must be based on quantum effects not considered by Prohofsky.

**OBJECTIVES:** The specific goal of this study was to determine how the organic semi-conductor DALM sensitizes spores to microwave radiation killing.

**METHODS:** We have previously reported the killing of anthrax bacillus spores using pulsed microwave radiation (Kiel et al. 2002. *IEEE Trans. Plasma Sci.* 30: 1482-1488). In these previous experiments, 1.25-GHz microwaves at a 10-Hz repetition rate of 6 ms pulses and a peak forward power of 2 MW were used for 15 min. The spores were sensitized to microwave radiation by treatment with DALM, luminol, sodium bicarbonate, and dilute hydrogen peroxide. The kill was in the order of 4-5 logs reduction in colony forming units. Here we report killing of *Bacillus thuringiensis* spores with 2.45 GHz, 50% duty cycle, 15kV/m peak, 1 kW average power; and 1.25 GHz, 2MW peak, 100 Hz repetition rate of 5-ms pulses, 140 kV/m peak, 1 kW average. In another exposure system, the samples were treated for 1 to 20 min. The microwave source was operated at 2.7-2.9 GHz and a pulse repetition rate of 390 Hz with a 2.5-ms pulse width and 180 kW (1.1 kV/cm – 2.3 kV/cm) peak power for the treatments.

**RESULTS:** For the 2.45-GHz CW exposure, about 4 logs of kill was achieved in 10 minutes and for the 1.25 GHz PW exposure, at the same average power, the same level of kill was achieved in 5 minutes. For the 2.7-2.9-GHz system, the result was a kill of 5-7 logs (the detectable limit was 2 logs, below which the colony forming units dropped in 2 minutes). The mechanism of kill appears to be related to the coupled electric field rather than the average power.

**CONCLUSION:** We have shown how effects on the biosynthetic organic semi-conductor diazoluminmelanin (DALM) must be based on bulk field effects on quantum states (partition into different types or states, the ratio determining whether the molecules release energy or absorb it and the E field shifting the balance). Although Prohofsky's classical mechanism may apply to much lower E fields than those generated by the devices that cause the large bioeffects discussed here, Prohofsky appears to have made no such distinction in his classical mechanism and did not consider the quantum effects. Without them, the DALM results cannot be explained by the classical explanation of Prohofsky,

with the quantum explanation, the bulk and quantum effects not only co-exist they complement each other. The mechanism of kill appears to be related to the coupled electric field rather than the average power based on a quantum mechanical mechanism. This work was supported in part by the USAF Office of Scientific Research

17-3

**EFFECT OF MILLIMETER WAVES ON CYCLOPHOSPHAMIDE INDUCED NF-KB.** M. K. Logani<sup>1</sup>, M. Natarajan<sup>2</sup>, V. R. Makar<sup>1</sup>, A. Bhanushali<sup>1</sup>, M. C. Ziskin<sup>1</sup>. <sup>1</sup>Richard J. Fox Center for Biomedical Physics, Temple Univ School of Medicine, Philadelphia, Pennsylvania, USA, <sup>2</sup>Dept of Radiation Oncology, Univ of Texas Health Care Center at San Antonio, San Antonio, Texas, USA.

**BACKGROUND:** Millimeter waves (MWs) are widely used for the treatment of many diseases in Russia and former Soviet Union countries. Three common frequencies employed in these treatments are 42.2, 53.6, and 61.2 GHz. MWs can be used as a mono-therapy or in combination with other treatment methods. As an adjunct to chemotherapy, it has been reported to protect the immune functions from the adverse effect of chemotherapy (Makar et al, 2003, 2005). However the mechanisms involved in this protection are not known. Several immune functions are regulated by nuclear factor kappa B(NF-kB), an inducible transcriptional regulator. Many chemotherapeutic agents have been reported to induce this factor. Once activated, it binds specifically to the promoter-enhancer region of its target genes and transactivates their expression. The present study was undertaken to determine whether MWs can modulate activation of NF-kB induced by cyclophosphamide, an anticancer drug.

**METHODS:** MWs were produced with a Russian-made YAV-I generator. The device produced 42.2±0.2 GHz modulated wave irradiation through a 10 x 20 mm rectangular output horn. The animals, BALB/C male mice, were irradiated on the nasal area. Peak SAR and incident power density were measured as 730±99 W/kg and 36.5±5 mW/cm<sup>2</sup>, respectively. The maximum skin surface temperature elevation, measured at the end of 30 minutes, was 1.50C. For measurement of NF-kB activity, the animals were irradiated for 3 consecutive days, 30 minutes each day. CPA (15 mg/kg body weight) was given intraperitoneally on day 2 and the animals were sacrificed 2 days after CPA injection. NF-kB DNA- binding activity in spleen cells was analyzed by the Electrophoretic Mobility Shift Assay (EMSA). Quantitation of specific binding activity was performed by densitometric scanning of the autoradiogram and analyzed using Multiimage software package (BIORad Inc., Hercules, CA). Fold increase of NF-kB p50/p65 was calculated taking control as 1 fold

**RESULTS:** CPA caused a marked increase (5.8 fold) in NF-kB DNA-binding activity as compared to the control group. Combined treatment with CPA and MWs resulted in a significantly less enhancement of NF-kB activity (1.75 fold). On the other hand, MW irradiation without CPA treatment did not show any effect on NF-kB activity (Fig. 1).

**CONCLUSION:** MW therapy significantly inhibited CPA induced activation of NF-kB.

The work was supported by the National Center for Complementary and Alternative medicine; Contract Grant Number: A TO0492

**REFERENCES:** Makar VR, Logani MK, Bhanushali A, Kataoka M, and Ziskin MC: Effect of millimeter waves on natural killer cell activation, *Bioelectromagnetics* 26:10-19, 2005

Makar VR, Logani MK, Szabo I, and Ziskin MC: Effect of millimeter waves on cyclophosphamide induced suppression of T cell functions, *Bioelectromagnetics*, 24: 356-365, 2003

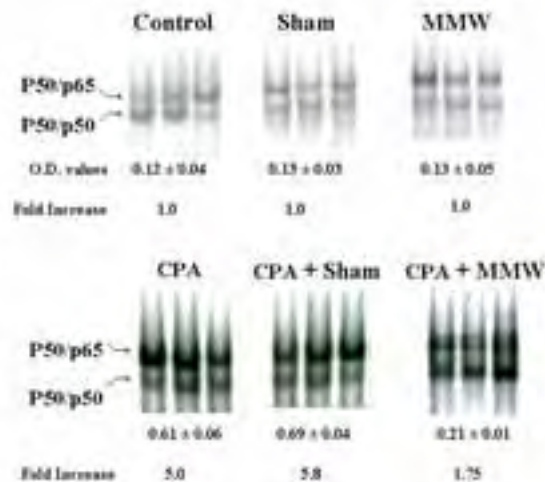


**Figure 1:** Autoradiograms showing the  $^{125}\text{I}$ -32P-DNA-binding activity in spleen cells of three animals from each group. Five microgram of each sample was analyzed by EMSA, as described in Methods. Complexes indicating the specific binding of  $^{125}\text{I}$ -32P are indicated by the arrow. Quantitation of specific binding activity was performed by densitometric scanning of the autoradiogram and analyzed using Multi-Image software package (BioRad Inc., Hercules, CA). Fold increase of  $^{125}\text{I}$ -32P/p50/p65 was calculated by taking control as 1 fold.

17-4

## ADVERSE EFFECTS OF MICROWAVES FROM GSM/UMTS MOBILE PHONES DEPEND ON CARRIER FREQUENCY AND TYPE OF SIGNAL.

E. Markova<sup>1,2</sup>, L. Hillert<sup>3,4</sup>, R. Sarimov<sup>2,5</sup>, L. Malmgren<sup>6</sup>, B. Persson<sup>6</sup>, I. Belyaev<sup>2,5</sup>. <sup>1</sup>Molecular Genetics, Cancer Research Institute, Bratislava, Slovak Republic, <sup>2</sup>Genetics, Microbiology and Toxicology, Stockholm Univ, Stockholm, Sweden, <sup>3</sup>Occupational and Environmental Health, Stockholm County Council, Stockholm, Sweden, <sup>4</sup>Public Health Sciences, Occupational Medicine, Karolinska Institutet, Stockholm, Sweden, <sup>5</sup>Radiobiology, General Physics Institute, Russian Academy of Science, Moscow, Russia, <sup>6</sup>Radiation Physics, Lund Univ Hospital, Lund, Sweden.

**INTRODUCTION:** Biological effects of non-thermal microwaves (MWs) occur dependent on several physical parameters including carrier frequency and modulation [1]. **OBJECTIVE:** Contrary to monochromatic GSM (Global System for Mobile Communication) signal, mobile phones of the 3rd generation irradiate UMTS (Universal Global Telecommunications System) wide-band signal. MWs representing wide-band signal may result in higher biological effects because of eventual effective frequency windows. GSM and UMTS have also different modulations. Here, we investigated whether non-thermal MWs from a GSM and UMTS mobile phone induce stress response or double strand breaks (DSBs) of DNA in lymphocytes of healthy and hypersensitive persons. **MATERIALS AND METHODS:** Lymphocytes were obtained from periphery blood of 26 healthy persons and 17 persons who reported hypersensitivity to electromagnetic fields. Exposure to MWs was performed during 10 min - 2 h in two identical transverse electromagnetic transmission line cells (TEM-cells). Lymphocytes were exposed to GSM MWs at frequencies in-between 895 - 915 MHz and UMTS MWs (1947.4 MHz, middle channel), all standard modulations included, output power being the same, 0.25 W, using GSM and UMTS test-mobile phones [2]. Changes in chromatin conformation, which are indicative of stress response and DNA damage, were measured by the method of anomalous viscosity time dependencies [3]. 53BP1 and  $\gamma$ -H2AX proteins that co-localize with double strand breaks (DSBs) of DNA in distinct

foci were analyzed by immunofluorescence confocal laser microscopy [3]. The effects were compared by non-parametric tests. Heat shock, camptothecin and  $\gamma$ -rays were used as positive controls. RESULTS: Frequency-dependent effects of GSM MWs on chromatin conformation were observed. These effects depended on duration of exposure, saturated at 30-60 min, and were similar to stress induced by heat shock. Exposure at 915 MHz induced statistically significant decrease in 53BP1 and  $\gamma$ -H2AX foci in cells from all tested donors. In contrast, exposure to 905 MHz induced either decrease or increase in 53BP1 and  $\gamma$ -H2AX foci suggesting induction of either stress response or DSBs, respectively, dependent on donor. The effects of MWs at 905 and 915 MHz on foci were statistically significantly different. UMTS MWs affected human lymphocytes stronger or in the same manner as GSM MWs. Remarkably, the effects of UMTS and GSM MWs on 53BP1/ $\gamma$ -H2AX foci persisted up to 72 h following exposure of cells indicating severe stress response. No significant differences in effects between groups of healthy and hypersensitive subjects were observed. CONCLUSIONS: GSM microwaves from UMTS and GSM mobile phones affect DSB-co-localizing 53BP1 and  $\gamma$ -H2AX foci and chromatin conformation in human lymphocytes. These persistent effects suggest severe stress response and/or DNA damage. Adverse effects of non-thermal MWs from GSM/UMTS mobile phones depend on carrier frequency and type of signal. This dependence should be taken into account in setting safety standards and in planning in vivo and epidemiological studies. Our data encourage identification of those frequency channels/bands for mobile communication, which do not affect human cells. ACKNOWLEDGEMENTS: We thank Dr. T. Halazonetis (The Wistar Institute, Univ of Pennsylvania, USA) for donation of antibodies to 53BP1; Dr. S. Lang and Mr. P. Sinisalo (Nokia Research Center, Helsinki, Finland) for help with the UMTS exposure installation; Mr. W. D. Hurt and Dr. P. Mason, Air Force Research Laboratory, Human Effectiveness Directorate, Directed Energy Bioeffects Division for using the finite difference time domain (FDTD)-method to predict the specific absorption rate in the test tube during exposure in the TEM-cell. The Swedish Council for Working Life and Social Research, the Swedish Authority for Radiation Protection supported these studies.

#### References

- [1] I. Y. Belyaev, V. S. Shcheglov, E. D. Alipov, and V. L. Ushakov, "Non-thermal effects of extremely high frequency microwaves on chromatin conformation in cells in vitro: dependence on physical, physiological and genetic factors," *IEEE Transactions on Microwave Theory and Techniques*, vol. 48, pp. 2172-2179, 2000.
- [2] R. Sarimov, L. O. G. Malmgren, E. Markova, B. R. R. Persson, and I. Y. Belyaev, "Non-thermal GSM microwaves affect chromatin conformation in human lymphocytes similar to heat shock," *IEEE Transactions on Plasma Science*, vol. 32, pp. 1600-1608, 2004.
- [3] I. Y. Belyaev, L. Hillert, M. Protopopova, C. Tamm, L. Malmgren, B. Persson, G. Selivanova, and M. Harms-Ringdahl, "915 MHz microwaves and 50 Hz magnetic field affect chromatin conformation and 53BP1 foci in human lymphocytes from hypersensitive and healthy persons," *Bioelectromagnetics*, in press, 2005.

#### 17-5 STUDENT

**GSM-1800 FRAME SIGNAL: EFFECTS ON HUMAN SKIN CELLS.** S. Sanchez, F. Poullietier de Gannes, E. Haro, G. Ruffié, I. Lagroye, B. Billaudel, B. Veyret. PIOM laboratory, ENSCP/CNRS, Univ of Bordeaux, Pessac Cedex, France.

#### BACKGROUND:

The GSM-1800 signal has been in use for several years and questions have been raised about its potential biological effects in view of the fact that increase in frequency (with respect to GSM-900) induces a more superficial absorption in the tissues. Consequently, the skin becomes even more the main

target of the RFR. The skin can be considered as an organ, constituted by two main tissues: the epidermis, composed mainly of keratinocytes and the dermis, composed mainly of fibroblasts. The keratinocytes play an important role in the skin protection: associated with the melanocytes, they protect the skin against solar injury. Moreover, they can act as immune cells when needed. The role of the fibroblasts is mainly to maintain the integrity of the skin by keeping its elasticity but these cells have also a protective role in inflammatory processes and promote epidermalization.

**OBJECTIVES:**

Normal human primary keratinocytes and fibroblasts were chosen to study the in vitro effect of GSM-1800 frame signal on the skin by focusing on a potential induced cellular stress. Apoptosis induction and expression of heat shock proteins were the two studied parameters.

**MATERIALS:**

Normal human primary keratinocytes and fibroblasts were purchased from Cambrex and cultured in KGM and FBM respectively. They were cultured and exposed to the GSM signal until the fourth passage. The exposure system was a double waveguide (SXC1800, IT'IS, Zurich), placed in a temperature control incubator (37°C, 5% CO2). Exposure was done under blind conditions the duration of exposure was 48 hours at a specific absorption rate (SAR) of 2 W/kg and the radiofrequency signal was GSM 1800 MHz frame.

The analysis of the cellular apoptosis was done using flow cytometry and double fluorescent labeling (Annexin V/ Propidium Iodide) on cell suspensions.

The analysis of the expression of heat shock proteins was performed using immunofluorescent labeling of fixed cells. Hsp expression was measured as the fluorescent intensity using Aphelion™ image analysis software.

**RESULTS:**

The results showed that exposure to GSM-1800 did not induce cellular stress in either of the cell type studied.

As shown in table 1, the percentage of apoptotic human keratinocytes detected by AnnexinV/PI labeling was  $6.9 \pm 1.8\%$  in exposed cells against  $7.4 \pm 2.5\%$  in the sham condition (8 independent experiments). No difference between GSM- and sham- exposure could be detected regarding the amount of viable and necrotic epidermal cells. Similar data were observed in dermal cells where there was no difference between GSM- and sham exposure ( $3.2 \pm 0.7\%$  versus  $3.2 \pm 0.8\%$ , respectively, 6 independent experiments). On the other hand, GSM-1800 exposure at 2 W/kg did not affect heat shock proteins expression in normal human epidermal and dermal cells.

We thus conclude that a 48-hour exposure to GSM-1800 frame microwaves, at 2 W/kg does not induce cellular stress in human primary skin cells.

**Acknowledgments:** This work was supported by France Telecom R&D, Bouygues Telecom, and the CNRS

Apoptosis detection in normal human primary keratinocytes and fibroblasts after a 48-hour GSM-1800 exposure at 2W/kg.

Cell type	Exposure	viable cells	Apoptotic cells	Necrotic cells	Sham/GSM	Sham/Inc	GSM/Inc
Keratinocytes	Sham	79.0 (4.4)	7.4 (2.5)	13.6 (3.3)	p= 0.7	p= 0.6	P= 0.6
	GSM 1800	79.9 (4.1)	6.9 (1.8)	13.1 (3.2)			
	Inc	81.0 (3.4)	10.4 (1.2)	8.6 (2.3)			

Fibroblasts	Sham	90.6 (1.6)	3.2 (0.8)	6.2 (1.5)	p= 0.6	p= 0.9	p=0.9
	GSM 1800	92.0 (0.0)	3.2 (0.7)	4.7 (0.5)			
	Inc	90.9 (0.5)	4.1 (0.9)	5.0 (0.5)			

The percentage of cells represents the average± SEM of 8 independent experiments for the keratinocytes or 6 independent experiments for the fibroblasts. The statistical analysis was the Wilcoxon non-parametric paired test.

17-6

**GENOTOXIC EFFECTS OF 1800 MHZ RADIOFREQUENCY ELECTROMAGNETIC FIELDS IN HUMAN PROMYELOCYTIC HL-60 CELLS ARE ACCOMPAGNIED BY INCREASED INTRACELLULAR GENERATION OF REACTIVE OXYGEN SPECIES (ROS) DURING RF.** K. Schlatterer, R. Gminski, R. G. Fitzner. Dept. Clinical Chemistry and Pathobiochemistry, Charité - Universitätsmedizin Berlin, Campus Benjamin Franklin, Berlin, Germany.

**OBJECTIVES:** Radiofrequency electromagnetic fields (RF-EMF, 1800 MHz, continuous wave, SAR 1.3 W/kg, 24 h exposure) cause DNA damage in human promyelocytic HL-60 cells as determined by single-cell gel electrophoresis (SCGE) assay and cytokinesis-block micronucleus (MN) assay, without affecting cell viability, cell death or cellular growth behavior. Aim of this study was to investigate the induction of oxidative stress by RF-EMF as one possible underlying mechanism for disruption of genomic integrity and to localize the production of free radicals. Oxidant levels and oxidative damage were the two characteristics, which were focused on. The ability of free radical scavengers like ascorbic acid to prevent RF-EMF associated DNA damage was also investigated.

**METHODS:** Human HL-60 cells (ATCC, Rockville, MD, USA) were cultured in RPMI 1640 medium supplemented with 10% fetal bovine serum, penicillin G (50 IU/ml) and streptomycin (50 µg/ml). Cells were maintained in logarithmic growth phase at 37°C / 5% CO<sub>2</sub>. Exposure or sham-exposure respectively was performed within waveguides of a highly standardized RF exposure setup (N. Kuster, ITIS, ETH Zurich, Switzerland).

For measuring intracellular ROS levels, cells were incubated in growth medium containing 5 µmol/L dihydrorhodamine 123 (DHR123). The fluorescence intensity of rhodamine123 (Rh123), the product of cellular oxidation of DHR123, was detected flow cytometrically (Becton Dickinson FACSCalibur, Heidelberg, Germany). Extracellular production of reactive oxygen species during RF-EMF exposure was excluded by performing the DHR123 assay in pure cell culture medium without cells.

Beside verification of the intracellular generation of reactive oxygen species, the oxidative damage of DNA was proven by detection of 8-oxoguanine as the major oxidative DNA product (fluorometric OxyDNA Assay, Calbiochem-Novabiochem GmbH, Bad Soden, Germany). Augmentation of the FL-1 fluorescence intensity in RF-EMF-exposed cells was compared to sham-exposed cells.

Prevention of RF-EMF induced HL-60 cell DNA damage by co-administration of ascorbic acid (10 µmol/l) as free radical scavenger was investigated by performance of the alkaline single cell gel electrophoresis assay.

Cellular growth was monitored by determination of the cellular doubling time. Cell viability was determined by the MTT assay. Apoptosis was excluded by the Annexin V and TUNEL assay respectively.

**RESULTS:** Cellular production of ROS was shown by measuring the rhodamine fluorescence of HL-60 cells. In RF-field exposed cells the fluorescence intensity showed an increase of about 20 % in comparison to sham-exposed cells. The treatment of cells in an incubator with 100  $\mu\text{mol/l}$   $\text{H}_2\text{O}_2$ , as a positive control, resulted in an increase of fluorescence intensity of about 30 % in comparison to sham-exposed cells. These enhanced fluorescence intensities reflect an elevated production of intracellular ROS as an effect of RF-field exposure and  $\text{H}_2\text{O}_2$  treatment of HL-60 cells, respectively.

Figure 1 shows fluorescence histograms for RF-field exposed (1800 MHz, continuous wave, SAR 1.3 W/kg, 24 h) and sham-exposed HL-60 cells simultaneous treated with 5  $\mu\text{mol/L}$  dihydrorhodamine 123 (DHR123). The blue line (1) represents sham-exposed, the green (2) RF-field exposed cells and red line (3)  $\text{H}_2\text{O}_2$ -treated positive control cells (100  $\mu\text{mol/l}$ , 1 h). DHR123 reacts with intracellular ROS to form fluorescent Rh123, which is then retained by the mitochondria, enabling a flow cytometric assessment of cellular oxidant production.

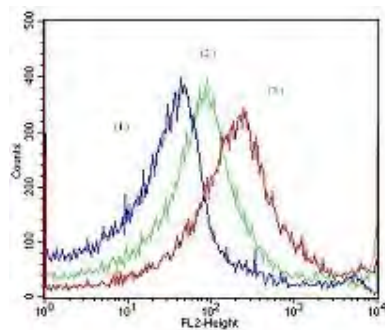


Figure 1

The possibility of extracellular generation of reactive oxygen species and consecutive cell-membrane permeation of free radicals with the consequence of DNA adduction and breakage of chemical bonds within DNA molecules was ruled out by exclusion of Rh123 fluorescence in RF-exposed aqueous cell culture media.

The presence of oxidized DNA (8-oxoguanine) was indicated for the RF-exposed cells by an augmentation of the FL-1 fluorescence intensity in comparison to sham-exposed cells. RF-field exposure of HL-60 cells induced an increase of oxidative DNA damage of about 20 % compared to sham-exposed cells.

RF-EMF-induced DNA damage could be prevented by co-administration of the free-radical scavenger ascorbic acid (10  $\mu\text{mol/l}$ ).

Neither cellular growth nor cellular viability were affected by RF-EMF exposure (1800 MHz, continuous wave, 1.3 W/kg, 24 h). Additionally no induction of apoptosis was detected in HL-60 cells under these

conditions.

**CONCLUSIONS:** Genotoxic effects of RF-EMFs in HL-60 cells (1800 MHz, continuous wave, SAR 1.3 W/kg, 24 h) are closely associated with an elevated intracellular generation of reactive oxygen species and the consecutive presence of oxidized DNA. This oxidation together with the consecutive DNA fragmentation can be prevented by co-administration of the free-radical scavenger ascorbic acid. RF-EMF mediated disruption of genomic integrity in HL-60 cells has no influence on cellular growth behavior, cell viability or cell death, this gives important mechanistic hints for the action of RF-EMF in certain cell types. First, cellular repair capacities seem to be efficient enough to cope with RF-EMF induced damages. Second, induction of oxidative stress as a prevalent answer to multiple kinds of environmental, nutritional, pharmacological, infectious agents- or injury-associated influences under circumstances of imbalanced cellular self-regulation by scavenging of free radicals can lead to disturbed physical conditions with the effects of development of disease states.

17-7

**NO EVIDENCE FOR IN VITRO GENOTOXIC EFFECTS INDUCED ON HUMAN BLOOD CELLS BY RF EXPOSURE AS ASSAYED BY CYTOGENETICS.** L. Stronati<sup>1</sup>, A. Testa<sup>1</sup>, M. Appolloni<sup>1</sup>, A. M. Freseghna<sup>1</sup>, E. Cordelli<sup>1</sup>, P. Villani<sup>1</sup>, C. Marino<sup>1</sup>, D. Lloyd<sup>2</sup>, J. Moquet<sup>2</sup>, A. Edwards<sup>2</sup>. <sup>1</sup>Italian National Agency for New Technologies, Energy and the Environment, Section of Toxicology and Biomedical Sciences, Rome, Italy, <sup>2</sup>National Radiological Protection Board, Chilton, UK.

In view of the widespread use of mobile phones, concern has been expressed about the possibility of adverse health effects related to mobile telephony.

Despite the majority of studies having concluded that RF per se, in the absence of significant heating, is not genotoxic, a minority of reports suggest that they might be operating on genetic material in a more subtle manner. One hypothesis has been raised that RF may potentiate the effect of other undisputed mutagens, possibly by compromising the fidelity of repair of initial DNA damage.

This presentation is the result of a series of integrated experiments undertaken jointly by ENEA (Italy) and NRPB (UK) laboratories aimed at investigating the possible genotoxic effects of microwaves exposure alone and in combination with a well known physical genotoxic agent (X-rays) by using different cytogenetic end points (chromosome aberrations, micronuclei, sister chromatid exchanges, proliferation indices and alkaline comet assay).

The effect of 24 hours exposure to a GSM basic signal operating at 935 MHz, at 1 and 2 W/kg SAR or 1800 MHz at 1 W/kg SAR on human blood cells alone or in combination with 1 Gy X-rays is reported. Blood samples from 14 donors were used for the 935 MHz exposure (10 in ENEA Lab. and 4 in NRPB Lab) and 4 for the 1800 MHz exposure. The RF apparatus comprised a pair of identical shielded waveguide exposure chambers installed in a standard cell culture incubator. After blind-coded irradiations, blood cells were processed following standard methods for each cytogenetic assay.

Results show no significant differences between radiofrequency exposed and sham samples for all tests. Similarly, the combined exposures failed to indicate the presence of any synergistic effect between radiofrequency and X-rays.

This study was partially supported by the Mobile Manufacturers Forum, GSM association, ELETTRA 2000 and the exposure systems were built by Information Technologies in Society IT'IS, Zurich, a partner in the project

**Session 18: Policy And Standards**  
*Chairs: Lawrie Challis and Michael Murphy*  
**3:15 - 5:00 pm, Theatre L**

18-1

**A DANISH RESEARCH PROGRAM ON THE POSSIBLE HEALTH ASPECTS OF MOBILE COMMUNICATIONS.** J. Bach Andersen<sup>1</sup>, J. B. Nielsen<sup>2</sup>, I. Sonbo Kristiansen<sup>2</sup>, S. Kjaergaard<sup>3</sup>, G. F. Pedersen<sup>1</sup>, A. Moeller<sup>4</sup>, A. Gjedde<sup>4</sup>, J. Boiden Pedersen<sup>5</sup>, C. Johansen<sup>6</sup>, J. H. Olsen<sup>6</sup>. <sup>1</sup>Dept of Communication Technology, Aalborg Univ, Aalborg, Denmark, <sup>2</sup>Institute of Public Health, Univ of Southern Denmark, Odense, Denmark, <sup>3</sup>Dept of Environmental and Occupational Medicine, Aarhus Univ, Denmark, <sup>4</sup>Center for Functionally Integrative Neuroscience, Aarhus Univ, Denmark, <sup>5</sup>Physics Dept, Univ of Southern Denmark, Odense, Denmark, <sup>6</sup>Institute of Cancer Epidemiology, Danish Cancer Society, Copenhagen, Denmark.

A major Danish government funded research effort has been initiated in 2004 motivated by the public concern related to the use of mobile phones, especially by children, and the public anxiety concerning 3G base stations. The following five projects are in an initial phase and progress will be reported.

1. Risk perception in relation to mobile phones (2) There is ample evidence that some people are very concerned about potential harm from 3G mobile phone systems. The perception of risk may be just as important as the 'objective' risk because people may distrust the information they receive about 3G systems and act on the basis of perceived rather than objective risk. The Danish risk perception study aims to describe the concerns people have, to analyse determinants of such concerns, and to explore how information best can be provided to lay-persons. On basis of the interviews, a questionnaire will be developed and used in a large survey of a representative sample of the Danish population.

2. Experimental study of mobile phone related radio-frequency electromagnetic radiation in healthy adults and adolescents (3,1)

This study focuses on replication of an experimental study of a UMTS signal at TNO in the Netherlands. In addition we will test two other signals related to third generation (3G) base stations to get a better understanding of the specific parts of the signal leading to symptoms or cognitive effects. In addition we want to expand the study with adolescents, and to look for susceptibility factors. The hypothesis concerns increased symptoms and decreased function, and that adolescents are more susceptible than adults. A controlled experimental study using cross-over type design with repeated observations is performed. 40 adults and 40 adolescents will be exposed for 45 minutes to 4 different types of exposures: Sham exposure, UMTS, continuous wave, and a modulated spread spectrum signal, (all 2140 MHz). Effect measurements include questionnaires using visual analogue scales for assessment of symptoms. Symptoms will be measured pre- and post-exposure.

3. PET Study of the Cerebrometabolic Effects on Non-ionizing Radiation from Mobile Phones (4,1) Healthy right-handed non-smoking subjects aged 18-40 years will be included for this study. A modified commercial GSM-telephone will be placed on the right ear. In randomized order the mobile phone will either transmit 900 MHz GSM signal or a null-signal Scan 1: A dynamic emission recording lasting three minutes will be made after bolus inhalation of [<sup>15</sup>O]-oxygen (1000 MBq), with continuous

sampling of arterial blood for measurement of hemoglobin, oxygen saturation and gamma-radioactivity. Scan 2: After an interval of 15 minutes to allow for complete decay of residual radioactivity, a dynamic emission recording lasting three minutes will be made after intravenous bolus injection of [<sup>15</sup>O]-water (800 MBq). Scan 3: After an interval of 15 minutes, a dynamic emission recording lasting 90 minutes will be made after bolus injection of [<sup>18</sup>F]-FDG (200 MBq) with continuous sampling of arterial blood for measurement of gamma-radioactivity and plasma glucose.

4. Examination of the effects of low static magnetic fields and rf-exposure on biochemical reactions by the radical pair mechanism (5) Examination of the effects of rf-exposure on biochemical reactions in the weak static magnetic field of the earth. The only well established mechanism by which weak radiofrequency magnetic fields can influence the rates and yields of chemical reactions is the Radical Pair Mechanism. This mechanism has been well established in strong magnetic fields ( $\geq 0.1$  T) but is largely unknown in low magnetic fields due to difficulties in obtaining useful solutions to the accepted theoretical description. The project intends to study the effect under well defined conditions by performing a series of accurate calculations; the aim is to produce a catalogue of the effect under varying situations which might serve as a guideline for possible health hazards.

5 Epidemiological studies (6) Three epidemiological studies in the Danish Research Program. The first study utilizes the large Danish cohort of mobile telephone subscribers (n=420.000). We have added some socio-economic information to the cohort information. The follow-up for cancer will be extended to 2002 and further we plan to link the cohort with a nationwide registry of multiple sclerosis to investigate the risk for this disease compared to the population. In a third study we will take the advantage of the National Patient Register, which has been in operation since 1978 and contains information of all hospital discharges and surgical procedures performed. We are interested in the risk for a number of rare CNS diseases. The other component include a Nordic case-control study including all incident cases of brain tumours in the age group 7 to 19 years of age as well as all prevalent cases two years in retrospective. The third component constitutes participation in an international prospective cohort study. We intend to begin data collection in the two last mentioned studies during fall 2005.

18-2

**STATUS OF IEEE C95.1 RF SAFETY STANDARD REVISION.** C-K Chou, J. A. D'Andrea, R. A. Tell, J. P. Reilly, E. R. Adair, M. L. Swicord, S. Lang, J. J. DeFrank, R. C. Petersen. Institute of Electrical and Electronics Engineers, Piscataway, New Jersey, USA.

The current IEEE C95.1 standard "IEEE Standard for Safety Levels with Respect to Human Exposure to Radio Frequency Electromagnetic Fields, 3 kHz to 300 GHz," was published in 1991 and modified in 1999 with essentially no changes to the basic restrictions (BR) and maximum permissible exposures (MPE), and without updating or reevaluating the supporting scientific literature.

Objective: To evaluate the extant scientific literature and update the C95.1 standard.

Methods: The current revision of IEEE C95.1 is based on the literature published through 2003 and is listed in a database containing more than 1300 references on biological effects. New insights, gained from a better understanding of the effects of acute and chronic exposures of animals and humans to RF electromagnetic fields, improved experimental methods, and the associated dosimetry and theoretical analyses, are included. The resulting recommendations, which are intended to prevent confirmed adverse health effects from RF exposures, are based on a comprehensive and critical review of the

scientific data. An important aspect of this revision process is that the standard should be harmonized with other international standards to the extent scientifically defensible.

Results: This standard presents two separate sets of limits for human exposure to electric fields, magnetic fields, and induced and contact currents to avoid all confirmed adverse health effects associated with exposure to such fields and currents. Specifically, in the frequency range of 3 kHz to 5 MHz, the rules protect against adverse effects associated with electrostimulation; in the frequency range of 100 kHz to 300 GHz, the rules protect against adverse health effects associated with heating. In the transition region of 0.1 to 5 MHz, each of the two sets of limits must be applied. These limits are expressed in terms of practical measures of external fields and induced and contact current (MPEs), or internal fields, SAR, and current density (BRs). The MPEs and BRs incorporate safety factors that account for uncertainties and that provide a margin of safety for all. As in the 1991 standard, there are two sets of values for the BRs and MPEs (an upper tier and a lower tier). The upper tier is science-based and is considered safe for all. A lower tier, however, with a greater margin of safety has been administratively set over the frequency range where effects associated with tissue heating predominate. This lower tier is a value judgment taking into account potential measurement uncertainties, sensitivity to public concerns, and an interest in harmonization with other standards. The lower tier could be used as the MPE and BR for the general public and as an action level set to implement an RF safety program (IEEE Std C95.7) to ensure avoiding exposures that exceed the upper tier. The upper tier of the revision of C95.1 retains the same BRs, i.e., whole-body-average SAR, incident power density (above 3 GHz), and MPEs as the 1991 standard. However, new peak spatial-average SAR limits are harmonized with those of ICNIRP, although these limits now apply to some different parts of the body. MPEs for the lower tier are harmonized with the ICNIRP general public exposure guidelines for frequencies between 300 MHz and 100 GHz. The revision is undergoing final sponsor (ICES) ballot, which is being conducted by the IEEE Standards Association.

Conclusion: Based on the weight of scientific evidence of literature through 2003, the C95.1 revision retains the whole body average SAR limit, and harmonizes the peak spatial average SAR and general public exposure MPE with the ICNIRP guidelines. Differences between the revised standard and earlier versions of C95.1 as well as with the ICNIRP guidelines will be highlighted. (The revision process established by the IEEE International Committee on Electromagnetic Safety is a continuing process that enables the opportunity for input from all stakeholders, including a rigorous and open scientific process that is transparent at all levels.)

18-3

**US NAVY'S ELF EMF BIOEFFECTS LIBRARY AND LITERATURE ASSESSMENT PROJECT.** R. B. Goldberg, W. A. Creasey, M. N. Collier, B. H. Kleinstein. Information Ventures, Inc., Philadelphia, PA, USA.

Introduction: The US Navy's ELF Communications System, which transmitted from 70 miles of overhead antennas in northern Wisconsin and Upper Michigan, was designed to communicate with submarines located anywhere in the world using an extremely low frequency (ELF) signal that was shifted between 72 and 80 Hz to produce binary coded messages. Controversy and opposition to the ELF Communications System continued at some level throughout its planning and operation. The Navy chose to address electromagnetic field (EMF) bioeffect concerns with two efforts: a substantial program of directed ecologic and laboratory research using the specific ELF Communications System signal, initiated in 1982 and costing \$7.4 million, and a more generalized systematic ongoing review and assessment of the international peer-reviewed scientific literature on EMF health and environmental

effects, initiated in 1985 and continued until the transmitter was shut down in September 2004. This presentation discusses the literature assessment activity as part of a successful policy for managing public concern about undetermined risks of EMF exposure.

**Objective:** To provide effective, comprehensive, and independent scientific literature monitoring services for assessing the potential of the Navy's ELF communication signal to produce adverse health or ecologic consequences, and to provide Navy staff with an objective analysis of any reported potential adverse effects.

**Methods:** The relatively remote location of the antenna lines made direct monitoring of health effects on the local population (e.g., epidemiological studies) impractical. Experimental studies involving the specific ELF communications signal were limited to those few directly supported by the Navy. Therefore, we gave highest priority to the following kinds of ELF EMF literature: (1) epidemiological studies concerning exposure of the public to power frequency fields from electric utility transmission and distribution, considered the only similar exposure likely to involve substantial numbers of exposed human subjects; (2) occupational epidemiological studies, generally involving exposure to more intense ELF fields from power transmission, electrified rail transport, and specialized workplace facilities; (3) physiological studies involving human subjects; (4) animal toxicology studies; and (5) field and laboratory studies of plants and animals, usually exposed to powerline fields, considered relevant to environmental impact (ecologic) issues. In addition, our staff reviewed and selectively reported on basic research concerning the biological and physical mechanisms of ELF EMF bioeffects: (1) hormonal effects, including effects on melatonin levels and circadian patterns, corticosteroids, and other stress hormones; (2) cellular studies, including effects on calcium ion flux, cell growth and differentiation, cell migration patterns, gene expression, and mutagenesis or co-mutagenesis (enhancing effects of mutagenic agents); (3) immune system effects; (4) behavioral and neurological effects, including mechanisms of electric and magnetic field detection and sensitivity, magnetic navigation, and impaired task performance and depression; (5) therapeutic effects, to the extent that they validate bioeffects involving unexplored mechanisms of interaction; (6) selected studies concerning radiofrequency and static fields (i.e., EMF exposures well outside the more relevant ELF range) when they reveal fundamental mechanisms of interaction or are likely to have a strong impact on the public's perception of EMF health risks; (7) technical papers on EMF measurement, personal dosimetry, exposure assessment, and epidemiologic methods and their limitations, considered important because of their relevance to interpreting epidemiologic studies of primary interest; and (8) reports and policy papers evaluating EMF research, establishing human exposure guidelines in occupational or residential settings, or proposing precautionary policies regarding EMF exposure, because of their potential impact on Navy Communications System staff and public perception of health risks. Detailed quarterly and annual written reports were prepared, along with brief annual oral presentations to Navy staff and the public summarizing research highlights during the previous year. Project staff maintained a computerized database and reprint collection of the reviewed documents (totaling 6,738 by program end), and responded to telephone and e-mail questions from Navy staff, the public, and legislators. Independent evaluations were prepared of 5-10 studies of particular importance each year to provide added detail on their strengths and weaknesses. Project staff attended and reported on major research meetings each year in which ELF EMF research was featured, and monitored press coverage of EMF issues to help identify research trends and new findings before they appeared in peer-reviewed publications. This provided increased awareness of EMF issues that might appear in press reports, and limitations of study results before they appeared as published papers.

**Results and Conclusion:** Few organizations maintain a research literature evaluation program that is as comprehensive and systematic as the ELF EMF Bioeffects Library program established by the Navy.

While the cost of this literature review program was a relatively small part of the overall ELF Communications System budget, it provided Navy staff with a valuable resource for dealing with questions about possible adverse effects from operation of their facility. The level of involvement and concern evidenced by this ongoing EMF research monitoring effort may also have helped the Navy maintain a positive relationship with the majority of the public living near the transmitter sites, and may be partly responsible for the Navy's ability to keep the transmitter operating for over 20 years in spite of activist opposition and protests.

18-4

**RISK MANAGEMENT OF MEDICAL DEVICES AND METALLIC IMPLANTS IN EMF WORKERS.** B. Hocking<sup>1</sup>, K. Hansson Mild<sup>2</sup>. <sup>1</sup>Specialist in Occupational Medicine, Vic, Australia, <sup>2</sup>National Institute for Working Life, Umea, Sweden.

**Introduction.** Medical devices and metallic implants are effective treatments for diverse conditions and are found in increasing numbers of workers. Industrial applications requiring intense electromagnetic fields (EMF, 0-300GHz) are growing and the potential risk of injurious interactions arising from fields affecting devices or implants needs to be managed. Injurious interactions may include electromagnetic interference, displacement, and electro-stimulation or heating of adjacent tissue, depending on the device or implant and the frequency of the fields.

**Guideline.** A guidance note is being developed within the EMF-NET project for use in the European Union to assist occupational physicians and scientists in the management of workers with medical devices and metallic implants who work in electromagnetic fields above the public exposure limits and within occupational limits. The guidance note is designed to help employers meet their several legal obligations to workers including duty of care for occupational health and safety, avoidance of disability discrimination, and privacy regarding medical data.

The guidance note uses a risk management framework to give generic advice:

- \* Risk identification. Procedures need to be implemented to ensure identification of workers who have devices and implants, and characterisation of the electromagnetic field exposures within an industry;
- \* Risk assessment. A physician and scientist should work together to assess an individual who has devices or implants in relation to their job exposures and the possible effects that interactions with the device could have for the health of the worker. This may require obtaining knowledge of the characteristics of devices, the accurate anatomical localisation of implants, use of occupational hygiene data regarding fields, application of basic physics principles regarding interactions, gathering information from manufacturers, and possible use of computer models;
- \* Risk control. Appropriately worded advice should be given to the worker regarding their safety and any necessary changes to work practices. The employer should be advised of any needed changes to work practices whilst being respectful of the workers right to medical privacy.

**Conclusion.** The guidance note is intended to provide a generic risk management framework for physicians and scientists to use when assessing the risks for workers with electronic devices and medical implants when working in intense electromagnetic fields, whilst being consistent with diverse legal requirements.

Paper was prepared in connection with the realisation of the EC FP6 project EMF-NET.

## **THE INTERNATIONAL COMMITTEE ON ELECTROMAGNETIC SAFETY (ICES): SAFETY STANDARDS FOR ELECTROMAGNETIC ENERGY.** M. R. Murphy<sup>1,2</sup>, R. C. Petersen<sup>2</sup>.

<sup>1</sup>Directed Energy Bioeffects Division, Human Effectiveness Directorate, Air Force Research Laboratory, Brooks City-Base, San Antonio, Texas, USA, <sup>2</sup>IEEE ICES, Piscataway, New Jersey, USA.

### What is ICES?

The International Committee on Electromagnetic Safety (ICES) develops standards for the safe use of electromagnetic energy in the range of 0 Hz to 300 GHz relative to the potential hazards of exposure to humans, volatile materials, and explosive devices, which includes methods for the assessment of human exposure to such fields, and standards for products that emit electromagnetic energy. ICES is sponsored by the Institute of Electrical and Electronics Engineers (IEEE) Standards Association Standards Board (SASB) and operates under its rules and oversight. ICES follows an open consensus process, with a balanced representation from the medical, scientific, engineering, industrial, government, and military communities. Present membership of the ICES parent committee is 119, including 43 members from outside the US, representing 23 different countries. ICES strives to achieve consensus among all the stakeholders in the safe use of electromagnetic energy, thereby producing practical standards that are readily accepted and applied. IEEE standards are “Living” documents that continue to be refined through the worldwide volunteer efforts of stakeholders in the safe use of electromagnetic energy.

### ICES Background

With roots dating back to 1884, the IEEE is today the world's largest technical professional society, with almost 360,000 members, approximately one third of whom are from outside the US, representing 175 countries. The development of internationally recognized voluntary standards, through an open consensus process, has long been a major effort of the IEEE. In 1960, IEEE (then IRE) and the U.S. Navy co-sponsored the first US radio frequency (RF) safety standard project (C95), which led to the first US national standard (C95.1-1966). Later, C95.1-1982 was the first US national standard in which field limits were derived from the frequency-dependant dosimetric quantity, specific absorption rate (SAR). Dosimetry and a threshold SAR of 4 W/kg are now the bases for most of the world's RF safety standards and guidelines, including those of the ICNIRP, NATO, NRPB, and the US DoD. In 1989 the C95 committee became IEEE Standards Coordination Committee (SCC28) under the sponsorship of the IEEE SASB. In 1995, the IEEE SASB approved a new committee (SCC34) to develop standards for products using or producing electromagnetic energy. In March 2005, the IEEE approved combining SCC-28 and SCC-34 into a single entity – ICES.

### Day-to-day activities of ICES are conducted by an Executive Committee:

Chair: Ronald C. Petersen, r.c.petersen@ieee.org

Past Chairman/Executive Secretary: Dr. Eleanor R. Adair, eadair@comcast.net

Chairman Emeritus: Dr. John M. Osepchuk, j.m.osepchuk@ieee.org

Vice Chairman: Dr. Ralf Bodemann, ralf.bodemann@siemens.com

Treasurer: Arthur G. Varanelli, a.g.varanelli@ieee.org

Membership: Dr. Tom McManus, mcmanustom@eircom.net

International Liaison: Dr. Michael R. Murphy, michael.murphy@brooks.af.mil

IEEE Staff: William Ash, w.ash@ieee.org

### ICES is further organized into the following Five Subcommittees:

SC1: Techniques, Procedures, and Instrumentation, Howard I. Bassen, hib@cdrh.fda.gov  
SC2: Terminology, Units of Measurements, and Hazard Communication Richard A. Tell, rtell@radhaz.com  
SC3: Safety Levels with Respect to Human Exposure, 0-3 kHz, Philip Chadwick, phil.Chadwick@mcluk.org, and Thanh Dovan, tdovan@spipowernet.com.au  
SC4: Safety Levels with Respect to Human Exposure, 3 kHz-300 GHz, Dr. C. K. Chou, ck.chou@motorola.com and Dr. John A. D'Andrea, john.dandrea@navy.brooks.af.mil  
SC5: Safety Levels with Respect to Electro-Explosive Devices, John DeFrank, john.defrank@amedd.army.mil and G. Drew Koban, gkoban@relay.nswc.navy.mil

#### IEEE/ICES Exposure Standard for Extremely Low Frequency EMF (C95.6)

In 2002 ICES published C95.6-2002 “IEEE Standards for Safety Levels with Respect to Human Exposure to Electromagnetic Fields, 0 to 3 kHz,” developed by SC3. The maximum permissible exposures (MPEs) and Basic Restrictions recommended by C95.6-2002 are scientifically derived to avoid: (1) aversive or painful stimulation of sensory neurons; (2) muscle excitation that might lead to injuries while performing potentially hazardous activities; (3) excitation of neurons or direct alteration of synaptic activity within the brain; (4) cardiac excitation (heart contraction that might lead to fibrillation); and (5) magneto-hydrodynamic effects.

#### IEEE/ICES Exposure Standard for the RF Range (C95.1)

C95.1, “IEEE Standard for Safety Levels with Respect to Human Exposure to Radio Frequency Electromagnetic Fields, 3 kHz to 300 GHz,” was updated in 1999 and a complete revision is currently undergoing sponsor ballot. More than 1300 relevant scientific papers were reviewed for this revision. In 2002, the Air Force Workshop, held just before the annual meeting of the Bioelectromagnetics Society, was a review of the RFR bioeffects literature pertaining to the revision of ICES SC4. The authors of these review presentations also submitted manuscripts for peer review and publication in the journal *Bioelectromagnetics* (Supplement 6, S1-S213, 2003). For an update on the progress of C95.1, see Chou, et al., “Status of IEEE C95.1 RF Safety Standard Revision,” BEMS Abstracts, 2005. A new standard (C95.7, “IEEE Recommended Practice for Radio Frequency Safety Programs,” is currently undergoing sponsor ballot.

#### Recently published IEEE/ICES standards include:

C95.1(b)-2004, “IEEE Standard for Safety Levels with Respect to Human Exposure to Radio Frequency Electromagnetic Fields, 3 kHz to 300 GHz. Amendment 2: Specific Absorption Rate (SAR) Limits for the Pinna”

C95.4-2002, “IEEE Recommended Practice for Determining Safe Distances from Radio Frequency Transmitting Antennas when Using Electric Blasting Caps”

C95.3-2002, “IEEE Recommended Practice for Measurements & Computations of Radio Frequency Electromagnetic Fields with Respect to Human Exposure to such fields, 100 kHz to 300 GHz”

C95.2-1999, “IEEE Standard for Radio Frequency Energy and Current-Flow Symbols” (now undergoing reaffirmation)

## How to Participate in ICES

All are welcome to participate in the meetings of ICES and to vote on the Subcommittees. To apply for voting membership on the ICES parent committee, send a letter and resume to:

Dr. Tom McManus  
ICES Membership Chair  
Dept of Communications, Marine and Natural Resources  
44 Kildare Street, Dublin 2, Ireland; or mcmanustom@eircom.net

## Join ICES in Ireland

ICES will meet in Dublin, Ireland, 24-26 June, immediately following BioEM2005. A schedule can be obtained from anyone named in this abstract or at: <http://grouper.ieee.org/groups/scc28/>

18-6

### **RISK PERCEPTION IN RELATION TO MOBILE PHONES – A QUALITATIVE APPROACH.**

J. B. Nielsen<sup>1</sup>, H. B. Frederiksen<sup>1</sup>, C. Johansen<sup>2</sup>, J. H. Olsen<sup>2</sup>, I. S. Kristiansen<sup>1</sup>. <sup>1</sup>Institute of Public Health, Univ of Southern Denmark, Odense, Denmark, <sup>2</sup>Institute of Cancer Epidemiology, Danish Cancer Society, Copenhagen, Denmark.

Non-ionising radiation from electric power lines, radio transmitters and, more lately, third generation (3G) mobile telephone systems has raised concern about health effects. The evidence here is conflicting, but policy decisions on such technologies will be taken by political bodies who act upon biological evidence as well as perception of risk. The perception of risk associated with radiation may be just as important as the “objective” risk because people act on the basis of perceived rather than objective risk and may distrust the information they receive. This creates a need for more insight into people's risk perception related to non-ionising radiation from mobile phones. Policy makers need information on what aspects of the radiation and its consequences that may cause concern, and they need know the best way to communicate risks such that the information is understood and trusted. This need is likely to increase as increased research into the biological effects may well create conflicting results.

#### Theory and previous research

Risk assessment of environmental exposures requires a description of the potential hazards (adverse outcomes), quantification of exposure, knowledge of dose-response relationships and the probability of adverse outcomes given the level of exposure. This requires insight into biology, biostatistics and epidemiology. Understanding people's perception of probabilities and valuation of outcomes (risk perception), however, calls on theories related to anthropology and psychology. A considerable proportion of lay people do not discriminate between the adverse outcome and the probability (risk) of the adverse outcome. In this case, the rational way to react is to aim for zero exposure. Perception of risk is always subjective, partly because people misinterpret probabilities, and partly because valuation of the adverse outcomes is a subjective matter. Thus, more factual knowledge will not necessarily change the perception of risk, but decreasing the relative importance of other factors related to risk perception may increase agreement between “objective” and “perceived” risk. It is therefore of considerable interest to know the major determinants of risk perception. Insight into people's worries and considerations in

relation to non-ionising radiation requires interviews and qualitative research while information on how widespread concerns are will call for a quantitative approach.

#### Study objectives

The study addresses the specific concerns in relation to mobile phones, the relative strengths of these concerns and how widespread they are in the population. Moreover, the study focus on people's understanding of and trust in information on risks associated with radiation from mobile phones and base stations and how it is influenced by the information format and source. Subsequently, the interviews will also reveal the role of mobile phones in everyday life of families, which is expected to be important in relation to risk management in relation to use of mobile phones and siting of base stations.

#### Study design

This presentation is based on semi-structured qualitative interviews with 20 families. These families represent four different situations. One group is living in a geographic area with no mobile phone base station implemented or presently planned, one group living in an area with a base station, one group living in an area with a base station placed on top of their children's institution (school, etc.) but without any measurement of radiation, and one group of families with children visiting a school with a base station on the roof and with intense discussions and measurement of radiation available to the parents. The inclusion criterion for the families was presence of at least one child aged 12-14 years and one child below the age of eight. This criterion assured that the interviews would cover adults (users/non-users), adolescents who are about to get or have recently got a mobile phone, and smaller children, where the main focus in relation to a potential risk would be the base stations. All interviews were tape recorded, transcribed, and analysed according to theories from anthropology.

#### Preliminary conclusions

1. Mobile phones have grown into an integrated platform for communication within the families, and removal of this communication form is not in question for the families.
2. The families do not ignore the risk from radiation, but they feel in control because they are able to decide how to use the mobile phones in the family.
3. Health risks associated with the use of mobile phones or an adjacent base station is not an important issue for these families. They are more worried about risks to their children related to unhealthy food, traffic and child molesters.
4. Perceived disadvantages related to mobile phones are primarily related to cost and the nuisance from people talking in public places and at meetings
5. Credible and unambiguous data on health risks may, however, reduce the use or increase the use of head sets.
6. The families make judgements about the trustworthiness of experts, and they have confidence only in information about risk assessment from impartial organizations or information given from The National Health Service
7. Several parents express their unhappiness with the placement of base stations on top of schools and kindergartens, but seem to accept their presence after a limited time period, mainly because they do not know what to do about it, and because the only way to cope with a risk you cannot get away from is to accept it or believe in experts who claim that the base stations do not pose any risk to people living in their proximity.
8. The present study is based on a limited number of families and further conclusions must await interviews of a wider stratum of the population. These interviews will be based on questionnaires developed on the basis of the present qualitative data.

**UPDATE ON PROGRESS OF THE AUSTRALIAN ELF STANDARD.** A. W. Wood<sup>1</sup>, C. Roy<sup>2</sup>.  
<sup>1</sup>Swinburne Univ of Technology, Hawthorn Vic, Australia, <sup>2</sup>Australian Radiation Protection and Nuclear Safety Agency, Yallambie Vic, Australia.

In Australia, the production of radiation protection standards is the responsibility of the Australian Radiation Protection and Nuclear Safety Agency (ARPANSA). In 2002, a standard was published covering the RF range 3 kHz –; 300 GHz (RPS3). The task of drafting a standard for the ELF range 0 –; 3 kHz was initiated in July 2002 by the establishment of an 11-person Working Group (WG). This group has expertise covering biophysics, cell biology, epidemiology, dosimetry, public interest and regulatory matters. The WG was given the task to draft a limits-based ELF standard for workers and the public based on established adverse health effects. A 16-person stakeholder Consultative Group (CG), to provide a wider pool for information gathering and a forum for discussion on specific issues was also appointed at the same time. The WG took the ARPANSA RF standard (RPS3) as its base document, but the initial focus was on determining appropriate limits for known adverse physiological effects. It noted that although the IEEE(ICES)[1] and ICNIRP [2] give as a rationale for basic (magnetic field) restrictions the prevention of synaptic effects in the retina, both sets of limits differ quite markedly. In resolving this difference, the WG was assisted by the appointment of a 3-person panel of specific experts in neurophysiology to further review key material and to examine the assumptions made in reaching these respective limits. The WG was further assisted by visits from international experts in clarifying the differences between the IEEE and ICNIRP (or NRPB) approaches. The WG has also taken into consideration the conclusions of recent reviews (for example [3-5]) but has also conducted an extensive literature search of recent (post 2000) research reports, particularly in relation to epidemiology and to reports of bioeffects occurring below ICNIRP/IEEE levels. Since the range encompasses 0 Hz, static field phenomena were also included.

At the time of writing, comment has been received on a draft circulated to the CG and other ARPANSA committees. This will be incorporated into a draft for public comment, to be made available, with a regulatory impact statement, via the ARPANSA website ([www.arpansa.gov.au/for\\_comm.htm](http://www.arpansa.gov.au/for_comm.htm)). Although details may change in the light of comment received, the draft ELF standard has the following features:

- Values for Basic Restrictions and Reference Levels are given in section 2 of the draft. These are derived from considerations of avoiding magnetophosphenes, neural stimulation, unpleasant spark discharges or contact currents. In the case of magnetic fields below 0.1 Hz, in view of paucity of bio-effects data, only Guidance Levels are given.
  - In the case of electric fields, these have a more extensive rationale than given by ICNIRP.
  - - For magnetic fields (above 0.1 Hz) the Basic Restriction metric is induced electric fields (which is similar to the IEEE approach, but departs from ICNIRP).
  - - Magnetic fields Reference Levels are derived in a manner similar to the Health Council of the Netherlands approach [6] (which uses data from small voxel size models of the human body to estimate external fields which would cause the Basic restrictions to be exceeded). This yields similar values to ICNIRP at 50/60 Hz and to the ARPANSA RPS3 values at 3 kHz. At frequencies below 50/60 Hz the values are more conservative than ICNIRP and between 50/60 Hz and 3 kHz less conservative.
  - - IARC classification of ELF magnetic fields as a 'possible carcinogen' is discussed in a number of places, including in the annex reviewing recent epidemiological findings.
  - - Precaution is extended to Occupational exposure in addition to General Public exposure. Precaution is discussed in relation to the WHO Framework document on Precautionary Measures

[7].

- Recent ICNIRP review for MRI safety [8] has provided useful references both on bio-effects at high static fields and electrostimulation effects.

-

It is anticipated that at the time of the conference, the public comment draft will have been released and that comment will have been received. It should therefore be possible to indicate the final form of the limit values in the light of this comment.

-

[1] IEEE (2002): "IEEE Standard for safety levels with respect to human exposure to electromagnetic fields, 0-3 kHz," New York C95.6.

- [2] International Commission on Non-Ionizing Radiation Protection (ICNIRP) (1998): Guidelines for limiting exposure to time-varying electric, magnetic, and electromagnetic fields (up to 300 GHz), Health Phys, vol. 74, pp. 494-522.

- [3] ICNIRP/WHO (2003): Proceedings International Workshop Weak electric Fields in the Body (MHRepacholi & AFMcKinlay eds). Radiat Prot Dosim 106(4).

- [4] NRPB (2004a): Advice on Limiting Exposure to Electromagnetic Fields (0 - 300 GHz). Available [http://www.nrpb.org/publications/documents\\_of\\_nrpb/pdfs/doc\\_15\\_2.pdf](http://www.nrpb.org/publications/documents_of_nrpb/pdfs/doc_15_2.pdf)

- [5] NRPB (2004b): Review of the Scientific Evidence for Limiting Exposure to Electromagnetic Fields (0 - 300 GHz). Available [http://www.nrpb.org/publications/documents\\_of\\_nrpb/pdfs/doc\\_15\\_3.pdf](http://www.nrpb.org/publications/documents_of_nrpb/pdfs/doc_15_3.pdf)

[6] Health Council of the Netherlands (2000): ELF Electromagnetic Fields Committee. Exposure to electromagnetic fields (0 Hz - 10 MHz). Publication No. 2000/06E.

- [7] WHO (2004): Framework to develop precautionary measures in areas of scientific uncertainty. Available <http://www.who.int/peh-emf>

- [8] ICNIRP (2004): Statement on Medical Magnetic Resonance (MR) Procedures: Protection Of Patients. Health Phys, Vol. 87, No 2, 2004

## Session 19: Mechanisms I

*Chairs: Guglielmo d'Inzeo and Mays Swicord*

**3:15 - 5:00 pm, Theatre M**

19-1

**BIOPHYSICAL MECHANISMS FOR EFFECTS OF RF ENERGY; REPORT OF A MULTI-INVESTIGATOR REVIEW. II - NONTHERMAL INTERACTIONS.** A.R. Sheppard<sup>1</sup>, M.L. Swicord<sup>2</sup>, R.D. Astumian<sup>3</sup>, Q. Balzano<sup>4</sup>, F.S. Barnes<sup>5</sup>, K.R. Foster<sup>6</sup>, R. Glaser<sup>7</sup>, E.W. Prohofsky<sup>8</sup>, J.C. Weaver<sup>9</sup>. <sup>1</sup>A. Sheppard Consulting, Redlands, CA, USA, <sup>2</sup>Motorola Laboratories, Ft. Lauderdale, FL, USA, <sup>3</sup>U. Maine, Orono, ME, USA, <sup>4</sup>U. Maryland, College Park, MD, USA, <sup>5</sup>U. Colorado, Boulder, CO, USA, <sup>6</sup>U. Pennsylvania, Philadelphia, PA, USA, <sup>7</sup>Humboldt-Universität of Berlin, Berlin, Germany, <sup>8</sup>Purdue U., W. Lafayette, IN, USA, <sup>9</sup>MIT, Cambridge, MA, USA.

**Introduction:** Our research aimed at setting numerical limits for the applicability of all identified mechanisms for radiofrequency (RF) interactions with biological systems. Many mechanisms depend explicitly on measurable physical properties: amplitude, frequency, polarization, modulation characteristics of the incident field, and system temperature. Others (stochastic processes that underlie genetic mutation, atomic-level details of chemical reactions, and the motion of ions) can be quantified

probabilistically. Still others are presently too poorly defined for such quantification and do not contribute to a science-based analysis of RF biological effects. This report focuses on interactions where temperature is not an essential variable.

**Methods:** Overall, approximately forty candidate mechanisms were analyzed at five international workshops attended by the present authors and more than 30 other scientists in various physical and biological disciplines.

**Results:** Quantitative information was obtained on the following major topics.

*Nonlinearity* - If modulation-dependent effects exist, biological cells and tissue must exhibit nonlinear interactions with RF fields, but present theories and biophysical experiments do not show nonlinear behavior above ~10 MHz in the absence of heating, which is proportional to  $E^2$  (E is the electric field strength), and therefore inherently nonlinear. More sensitive experimental devices (Q-factors of ~10,000 and amplification by 120-140 dB) could be used to look for the unique frequency signatures that mark nonlinear responses. If nonlinearities are too weak to be observed by these exceptionally sensitive techniques, the biophysical significance of athermal amplitude modulation would be questionable.

*Energy Absorption in Macromolecules* - Theory and observations show that resonant absorption in compact protein structures generally does not occur below ~720 GHz, or below ~182 GHz for shear waves in linear molecules of similar size. An exceptionally low-lying resonance at ~150 GHz found for the heme group in myoglobin emphasizes that even unusually weakly-bound molecular substructures absorb resonantly only above 100 GHz. A detailed analysis of energy absorption by macromolecules showed that chemically significant molecular changes cannot be made by direct interactions of RF energy with macromolecules.

*Error rates in multistep processes* - Error rates in processes such as DNA transcription and proofreading can be cumulative with no definite lower threshold for effects. A simple model shows that for an underlying error rate of 0.1% in the reading of DNA at 50 base pairs per second, perturbation by a 100 V/m RF electric field, would increase the error rate from  $0.05 \text{ s}^{-1}$  to  $0.0500075 \text{ s}^{-1}$ . On a statistical basis, approximately 1.5 days of RF exposure would produce one additional error among the approximately 6700 errors ordinarily expected. Proofreading and repair mechanisms sharply reduce the likelihood of meaningful errors and consequent biological effects. The very low rate of extra errors (0.015%) introduced by RF energy in the model suggest any cumulative effects would not be measurable.

*Microstepped Molecular Transducers, Ion-motive Proteins, and Signal-to-Noise Ratio (S/N)* - In principle, RF energy could affect molecular processes (e.g., chemical binding at ion-motive channels, receptor sites, and other proteins) through an accumulation of small molecular or dynamical changes. However, S/N sets a practical limit of the order of 0.1 RT ( $0.2 \text{ kJmol}^{-1}$  for scaling to chemical reactions) i.e., thermal energy density sets an effective limit for the lowest effective RF electric field strength. A field strength of  $\sim 10^9 \text{ V/m}$ --ordinarily unachievable--is required to create an electric field energy density equivalent to the thermal energy density. Unlike chemical processes that depend on thermal energy, the practical limits for ion transport are set by shot noise, averaging time, and ion transit rate. The upper bound for dynamical effects on ionic transport through a transmembrane channel protein is ~10 MHz, reflecting the underlying rate for ion movement through the protein. In general, sensitivity can be enhanced by frequency selective mechanisms, including resonance and dispersion-based phenomena, but these enhancements also are constrained by noise.

*Plasma Membrane Surface Gradients* - In principle, sufficiently large RF field gradients could alter

molecular and ion distributions near the plasma membrane by attractive or repulsive forces on molecular dipole moments. Observable ion dynamical effects over reasonable time periods appear to require average RF fields  $> \sim 10^3$  V/m<sub>rms</sub>. Such strong fields are likely to heat tissues, obscuring any possible direct effects on ion motions in a biological or biochemical experiment.

**General Conclusion:** Although nonthermal mechanisms of interaction with biological systems exist between 10 and 100 GHz, observable effects are predictable only for very strong fields. For exposures at typical environmental levels, only thermal mechanisms are plausible candidates for producing observable biological effects.

Research support: MMF, FGF, Motorola.

19-2

**BIOPHYSICAL MECHANISMS FOR EFFECTS OF RF ENERGY; REPORT OF A MULTI-INVESTIGATOR REVIEW. I - FIELDS AND ENERGY ABSORPTION AT TISSUE, CELLULAR, AND MOLECULAR LEVELS.** M.L. Swicord<sup>1</sup>, A.R. Sheppard<sup>2</sup>, R.D. Astumian<sup>3</sup>, Q. Balzano<sup>4</sup>, F.S. Barnes<sup>5</sup>, K.R. Foster<sup>6</sup>, R. Glaser<sup>7</sup>, E.W. Prohofskey<sup>8</sup>, J.C. Weaver<sup>9</sup>. <sup>1</sup>Motorola Laboratories, Ft. Lauderdale, FL, USA, <sup>2</sup>A. Sheppard Consulting, Redlands, CA, USA, <sup>3</sup>U. Maine, Orono, ME, USA, <sup>4</sup>U. Maryland, College Park, MD, USA, <sup>5</sup>U. Colorado, Boulder, CO, USA, <sup>6</sup>U. Pennsylvania, Philadelphia, PA, USA, <sup>7</sup>Humboldt-Universität of Berlin, Berlin, Germany, <sup>8</sup>Purdue U., W. Lafayette, IN, USA, <sup>9</sup>MIT, Cambridge, MA, USA.

**Introduction:** Our research aimed at setting numerical limits for the applicability of all identified mechanisms for radiofrequency (RF) interactions with biological systems. Many mechanisms depend explicitly on measurable physical properties: amplitude, frequency, polarization, modulation characteristics of the incident field, and system temperature. Others (stochastic processes that underlie genetic mutation, atomic-level details of chemical reactions, and the motion of ions) can be quantified probabilistically. Still others are presently too poorly defined for such quantification and do not contribute to a science-based analysis of RF biological effects. This report concerns energy absorption and field distribution for RF-exposed tissues, cells, subcellular fractions, and molecules.

**Methods:** Overall, approximately forty candidate mechanisms were analyzed at five international workshops attended by the present authors and more than 30 other scientists in various physical and biological disciplines.

**Results:** Quantitative information was obtained on these major topics.

*Temperature* - RF energy absorbed in tissue through Joule heating and dipolar loss appears as collisional, rotational, vibrational, and torsional energy, thereby increasing temperature. Diffusion of heat is so effective over small distances that it is impossible to increase the temperature by more than  $10^{-6}$  K in a sphere of radius  $\sim 10^{-5}$  m (comparable to a biological cell) absorbing RF energy at a rate of 10 W/kg. It follows that even smaller cellular entities (e.g., plasma membrane, organelles, individual molecules) cannot be selectively heated to any meaningful extent. During a very intense ( $SAR_{peak} = 1.8$  MW/kg) 1 ms-long pulse, temperature can increase by 0.4K, but such extreme exposures do not occur in the environment. Certain biological molecules and specialized organs (e.g., in vipers and bats) respond to temperature changes of  $< 10^{-2}$  K. This indicates that heat-related biological sensitivity thresholds are

>100 times below limits based on physiological changes such as thermoregulation by an organism or cell death, for which there are known hazards.

*Microdosimetry* - A simulated tissue model to quantify microanatomical effects for frequencies in the range 0.1 to 10 GHz, showed that the nonuniformity in transmembrane electric field strength does not exceed a factor of 10 over a variety of cellular locations and observation points, including those influenced by missing cells and invaginations filled with extracellular medium. Graphical data suggest that at 1 GHz SAR varied by less than a factor of 3 over all parts of the tissue model. Because the enhanced SAR in tissue is on the microscopic scale where diffusion strongly limits the occurrence of localized hot spots, temperature would not be affected significantly.

**General Conclusion:** For exposures at typical environmental levels, thermal mechanisms are possible candidates for producing some biological effects, but any temperature changes that could occur for selective heating of cells and subcellular structures are orders of magnitude smaller than other causes of temperature fluctuation and therefore would not contribute to observable biological or biochemical changes.

Research support: MMF, FGF, Motorola.

19-3

**MOLECULAR SIMULATIONS IN BIOELECTROMAGNETIC RESEARCH: BINDING REACTION IN THE HEME SYSTEM.** F. Apollonio, L. Dominici, S. Donatiello, G. d'Inzeo. ICeMB @ Dept of Electronic Engineering, "La Sapienza" Univ of Rome, Italy.

**OBJECTIVES:** In order to gain insight into the function of proteins, information about their dynamic behaviour, for example on intermediates along the chemical reaction pathway, are necessary. In this context the electromagnetic (EM) field represents a physical agent which perturbs the environment of the protein, hence a molecular dynamic approach should be the final goal in order to really understand the mechanism of bioelectromagnetic interaction. Unfortunately realizing a rigorous molecular dynamics based on quantum-mechanical considerations, taking into account electronic distribution, requires a strong computational effort even for molecular domains of few atoms: it is therefore necessary to reduce the problem [1]. When considering for example a protein reaction involving the binding of an atom or a molecule to a specific receptor site, identified as a portion of the entire molecule, a scaling of the problem complexity is obtained. Therefore a quantum calculation can be done for this restricted environment (ligand-receptor), considering the ligand moving on an identified direction at different distances from the receptor site. This is the first step toward a real molecular dynamics.

**MODELS AND METHODS:** Classical molecular dynamics simulations of myoglobin in water (similar to hemoglobin from a molecular point of view, but assigned to oxygen transport in muscle tissue) [2], suggested that a good candidate for the binding site is the imidazole-iron-porphyrin complex, indicated as FeP(Im), showed in Fig. 1. The ligand chosen in this analysis are the molecule of carbon monoxide CO and the molecule of oxygen O<sub>2</sub>. From a theoretical point of view it is well known that a quantum problem has to deal necessarily with the Schrodinger equation whose solution gives, through the electronic waveforms, information on the possible energetic levels of the system. Neglecting the simple case of hydrogen atom, a closed form for the solution of Schrodinger equation does not exist, therefore it is necessary to use numerical approximations. The method used here is the Perturbed Matrix Method

(PMM), based on perturbation theory in which the perturbing element is an electric field constant and locally homogeneous [3]. In particular the problem is first solved considering the system in an unperturbed situation: by means of a quantistic ab initio method, the Density Functional Theory (DFT), the minimal energy of the molecule is calculated. Then the perturbation, in this case the presence of the electric field, is taken into account considering an additive term, which is generally represented by the product of the electric field and the dipole moment of the molecule, summed to the unperturbed hamiltonian operator. The problem is solved with a matrix notation, diagonalizing the hamiltonian perturbed matrix on the basis of the unperturbed eigenfunctions.

RESULTS: A preliminary result has been the analysis of possible variation in the geometry of the structure due to the electric field. Structural modifications (the molecule loses its planarity becoming dome-shaped) have been observed for local electric field values of  $10^9$  V/m (Fig. 2). Therefore values of applied field of one order of magnitude lower have been considered in order to neglect geometry deformation and to evaluate the possible action of the electric field on electronic configuration and hence on binding process. The electric field has been applied along the three principal directions (x,y,z) but most evident effects have been found along the z axis. Attention has been focused on the trajectory of chemical reaction: binding of CO or O<sub>2</sub> to iron atom. The molecular system has been studied for all its spin multiplicities, the fundamental one (spin=1) and two other ones (spin=3 and spin=5) due to the important role that they have for the structure and the vibration of the molecule. Results relative to the potential energy profiles, in the fundamental multiplicity, for different values of the applied electric field are reported in Fig. 3 and 4 respectively for CO and O<sub>2</sub>, varying the distance of the ligand molecule from the plane of the porphyrin ring and considering fixed dFe, (the distance between the iron atom and the porphyrin plane) less significant for energetic variations. It is possible to note that positive electric fields applied in the same direction of the molecular dipolar moment decrease potential energy with respect to that of the unperturbed case, otherwise negative electric fields, that is to say fields applied in the opposite direction to the electric dipole increase total energy. Quantitatively the effect is significant for field intensities starting from 0.001 u.a. ( $\cong 5 \cdot 10^8$  V/m).

CONCLUSIONS: A rigorous study on the effect of the EM field on the hemoglobin metal-ligand bond strength has been proposed based on a quantistic approach. For both ligands the shape of the potential energy curves are not altered by the applied field and hence the energetic barrier for the binding process of CO or O<sub>2</sub> is not modified by the field. Such results on the ligand-receptor environment, are the bases for a dynamical analysis including side chain structures.

#### References

- [1] L. Dominici et al., XXV Annual Meeting of the Bioelectromagnetic Society (2003) 64-65.
- [2] M. Aschi et al., J. Comput. Chem. 25 (2004) 974-984.
- [3] M. Aschi et al. Phys. Lett. 344 (2001) 374-380.

This work was supported by European Union, V framework under the RAMP2001 Project.

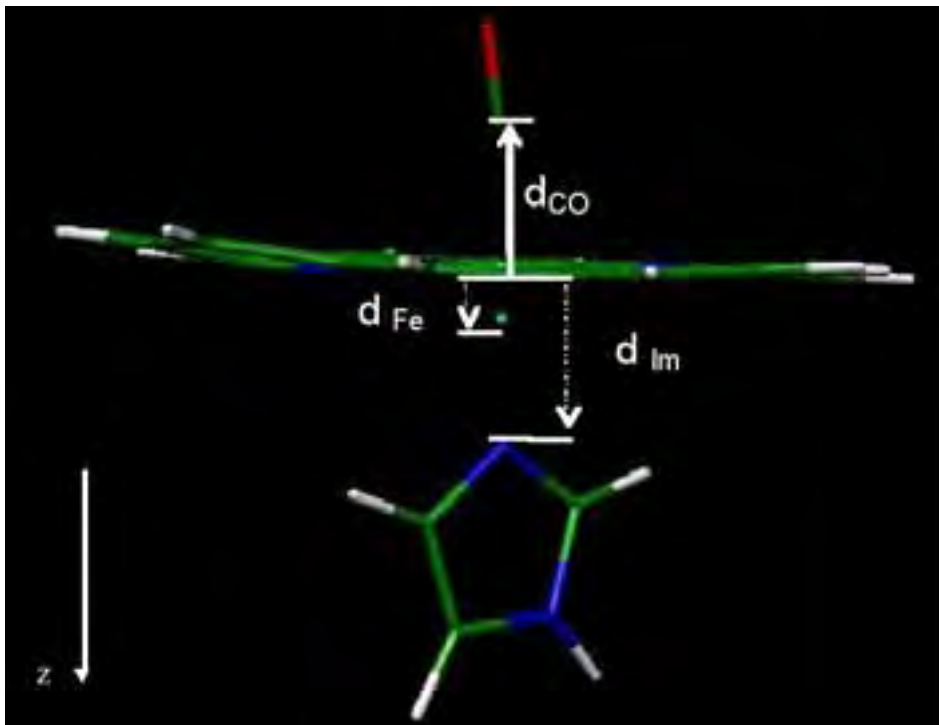


Figure 1. Molecular representation of the system used in the calculation: porphyrin ring at center (plane xy) with Fe atom evidenced, imidazole below and the binding ligand (CO or O2) above

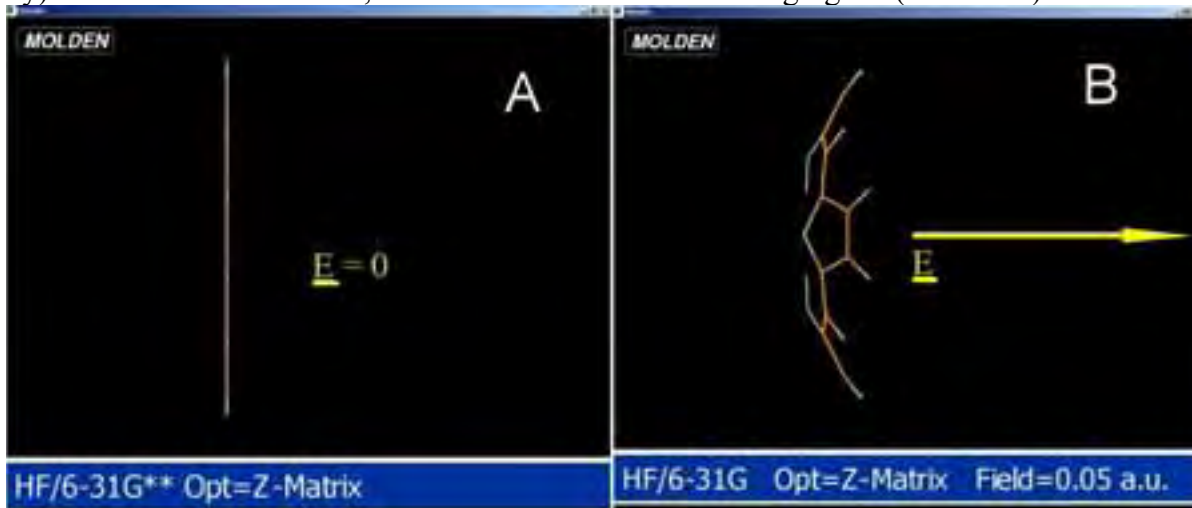


Figure 2. View of the molecule geometry in the plane  $z=0$ . (a) absence of E field (b)  $E \sim 5 \cdot 10^9$  V/m

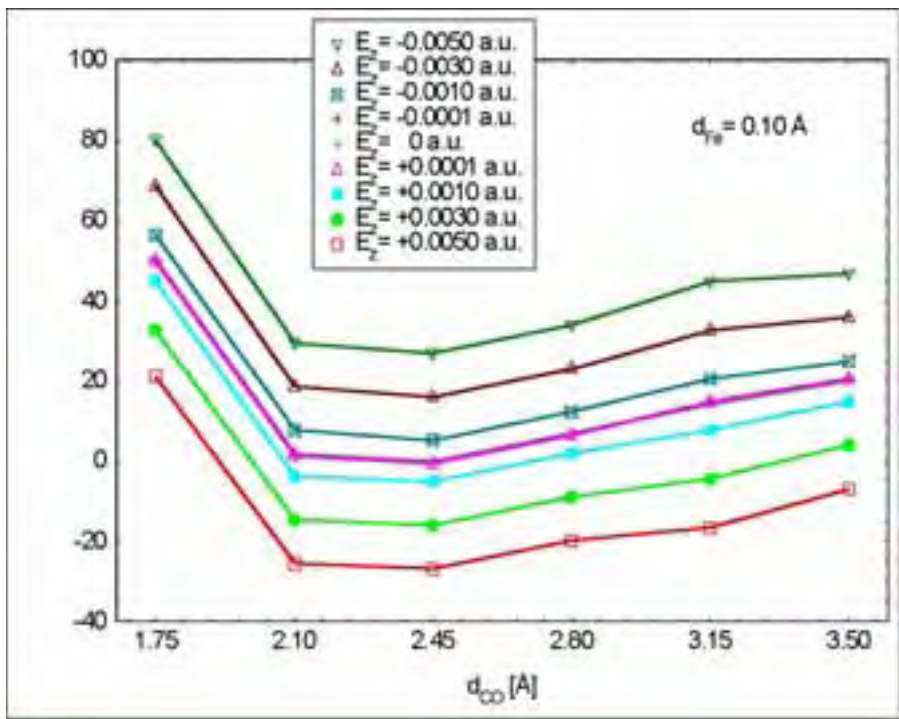


Figure 3. Potential energy vs  $d_{CO}$ , distance between the binding ligand CO and the plane of the porphin ring, for different values of electric field applied ( $5-25 \cdot 10^8$  V/m), positive and negative.  $1 \text{ a.u.} = 5.14 \cdot 10^{11}$  V/m

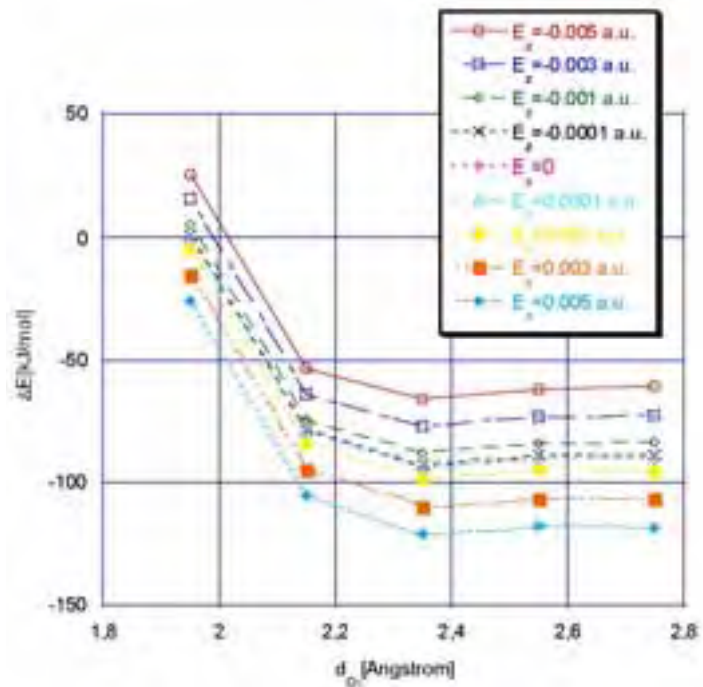


Figure 4. Potential energy vs  $d_{O_2}$ , distance between the binding ligand O2 and the plane of the porphin ring, for different values of electric field applied ( $5-25 \cdot 10^8$  V/m), positive and negative.

**THE POWER SPECTRAL DENSITY OF IONIC CURRENTS THROUGH CELL MEMBRANE: A THEORETICAL-EXPERIMENTAL COMPARISON.** A. Paffi<sup>1</sup>, G. Cotignola<sup>1</sup>, M. Liberti<sup>1</sup>, F. Apollonio<sup>1</sup>, G. d'Inzeo<sup>1</sup>, M. Mazzanti<sup>2</sup>. <sup>1</sup>ICeMB @ Dept of Electronic Engineering, "La Sapienza", Univ of Rome, Italy., <sup>2</sup>Dipartimento di Biologia Cellulare e dello Sviluppo, "La Sapienza", Univ of Rome Italy.

**OBJECTIVES:** At microscopic level, cell membrane and its sub-structures have been identified as the primary target of specific effects of electromagnetic (EM) fields on biological systems. Therefore, it is of crucial importance to dispose of suitable techniques for analyzing currents flowing through ionic channels embedded in the cell membrane, in order to evaluate possible effects, even of weak intensity, induced by the EM field. For this purpose, the analysis by means of the power spectral density (PSD), generally used in electrophysiological investigations, seems to be particularly powerful, since it enables us to detect weak current oscillations, not otherwise detectable by first order statistical moments, thus evidencing distinct contributions of different kind of applied EM signals. The aim of this work is to propose analytical expressions for the PSD of currents generated by suitable models of ionic channels. The possibility of obtaining such spectra directly from the parameters of the model enables us to overcome limitations due to long times of simulation necessary for obtaining a good spectral estimate. Moreover, such theoretical results, obtained independently from the particular model implementation, may be considered as a reference solution and used to synthesize channel models from spectral estimates of electrophysiological recordings.

**MODELS AND METHODS:** Experimental evidence shows that the ion channel behavior is well represented by a finite-state, continuous-time Markov process, whose parameters depend on physical quantities, such as the membrane voltage [1]. An exogenous EM field has been assumed to act on the cell as a perturbing component of the physiological transmembrane voltage [2]. In the stationary case, i.e. in physiological unexposed conditions, techniques used in Random Pulse Width Modulation (RPWM) [3] have been used for deriving an analytical expression for the PSD of the single channel current. In non-stationary conditions, like those obtained when an external EM field is applied, the membrane patch has been considered as a bipole described by its non-linear conductance. The membrane voltage across and the ionic current through represent, respectively, the input and the output of the system [4] that, for small input signals, has been linearized using the Volterra series theory [4].

**RESULTS:** In the stationary case, an analytical expression for the PSD of both mean value and random fluctuations of ionic currents generated by Markov models has been derived and experimentally validated. Fig.1 shows a good agreement between the spectrum analytically evaluated from the Calcium L-type model [5] and the spectral estimate of a single channel trace recorded through the patch-clamp technique [1]. In non-stationary case, the obtained expressions for the PSD of the mean Potassium and Sodium currents have been numerically validated, when sinusoidal signals (1 mV of amplitude, correspondent to a non linearity error of 5 %) were applied to the models. Fig.2 shows the perfect agreement between the estimated spectra of Potassium (panel a) and Sodium (panel b) currents, for input signals at different frequencies, and the theoretical envelopes. Fig.2 also evidences a low-pass behavior for both Potassium and Sodium channels, with a resonance peak in Sodium frequency response, strongly dependent on the resting voltage membrane value [6].

**CONCLUSIONS:** In this work, theoretical bases have been laid for the detection of possible effects induced by different kinds of EM signals on ionic currents, identifying a possible selective mechanism depending on the signal characteristics. Moreover, the analytical expressions derived for the PSDs of ionic currents represent a theoretical reference for the design of experimental activities suitable for the

extraction of the whole relevant spectral information from a specified channel current and for the successive synthesis of Markov models from electrophysiological recordings.

#### References

- [1] Single-Channel Recording, edited by B. Sakmann and E. Neher, Plenum Press New York and London, 1995.
- [2] C. Polk and E. Postow (eds.), CRC Handbook of biological effects of electromagnetic fields: CRC Press Boca Raton, 1986.
- [3] A. M. Stankovic', G. C. Verghese, and D. J. Perrault, "Randomized Modulation of Power Converters via Markov Chains," IEEE Transactions on Control Systems Technology, vol. 5, pp. 61-73, 1997.
- [4] R. S. Eisenberg, M. Frank, and C. F. Stevens, Membranes, Channels, and Noise. New York: Plenum Press, 1984.
- [5] L. Sun, J.-S. Fan, J.W. Clark, and P. T. Palade, "A Model of the L-Type  $\text{Ca}^{2+}$  Channel in rat ventricular myocytes: ion selectivity and inactivation mechanism," Journal of Physiology, vol. 529, pp. 139-158, 2000.
- [6] A. Paffi, G. Cotignola, M. Liberti, F. Apollonio, and G. D'Inzeo, "Spectral Analysis of Simulated Currents for the Study of the Interaction between Electromagnetic Fields and Cellular Ionic Channels," accepted to Electromagnetic Compatibility Symposium, Zurich, 2005.

This work was supported by the European Union, V framework under the RAMP2001 Project.

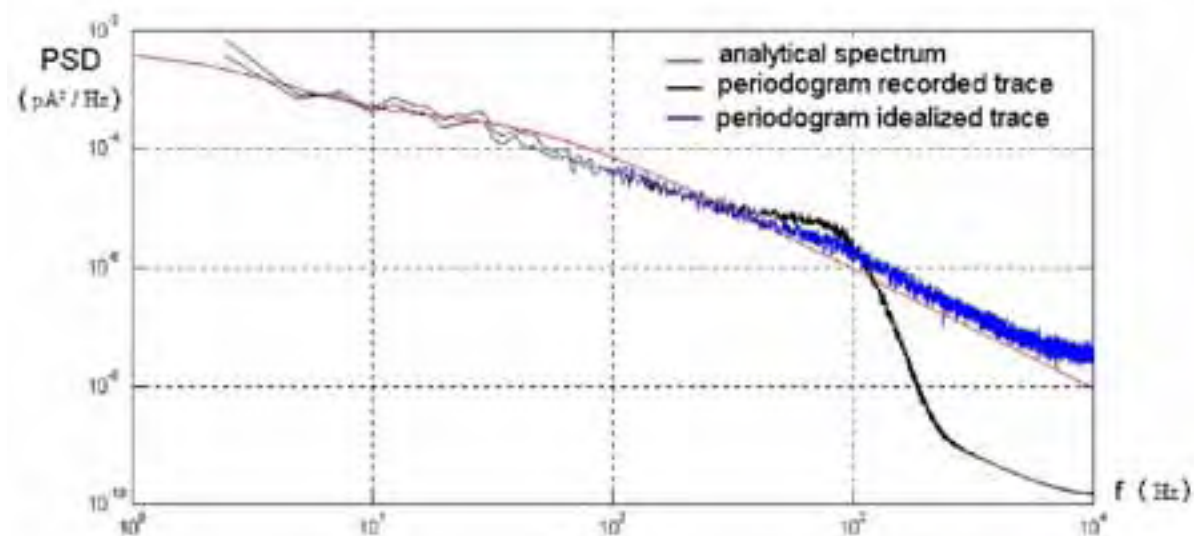
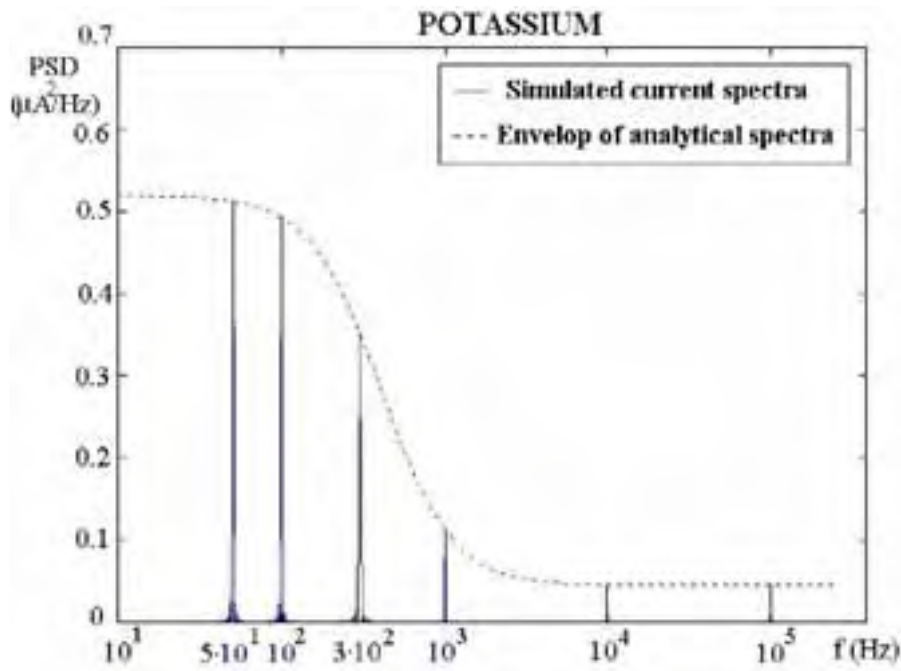
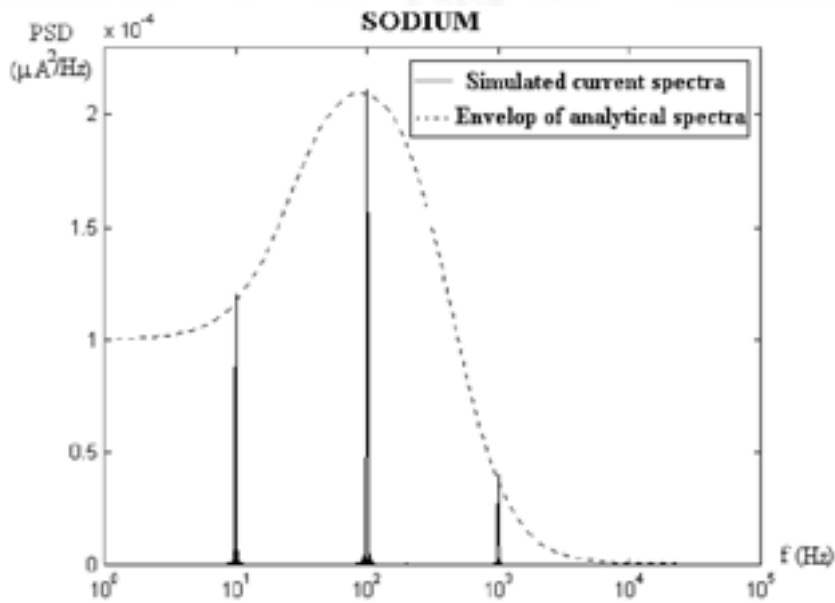


Fig. 1: Comparison between the spectrum calculated analytically for the Ca L-type model (red), the estimated spectrum of a Ca L-type recorded current (black), and the estimated spectrum of the same Ca L-type recorded current, after removing the effect of the data acquisition filter ( $f_c=1$  kHz).



(a)



(b)

Fig. 2: (a) Comparison between the envelope of the power spectral densities, calculated analytically, and the spectral estimates of Potassium simulated currents, when a sinusoidal voltage of amplitude 1 mV and variable frequency is superimposed to the membrane voltage ( $V_m = -50$  mV). (b) Same as panel (a), for Sodium channel.

**E-FIELD EFFECTS OF THZ RADIATION ON CARBONIC ANHYDRASE LOADED LIPOSOMES.** A. Ramundo-Orlando<sup>1</sup>, A. Doria<sup>2</sup>, G. Piero Gallerano<sup>2</sup>, E. Giovenale<sup>2</sup>, G. Messina<sup>2</sup>, I. Spasovsky<sup>2</sup>. <sup>1</sup>INMM-CNR, Rome, Italy. <sup>2</sup>ENEA C.R.-Frascati, Frascati, Italy.

**INTRODUCTION:** Rapidly increasing applications of radiation in the terahertz (THz) spectral range necessitate preventive rather than reactive research. At present very little is known of the effects of THz irradiation in biological systems. Recently data on the exposure of membranes, cells, and DNA to THz radiation in the frequency range of 100 GHz to 20 THz have been investigated in the THz-BRIDGE project, funded in the Key Action 4 of the "Quality of Life" European programme of FP5 [1]. In this context, effects of 130 GHz irradiation at different pulse repetition rates on the permeability of CA-loaded liposomes have been reported [2].

**OBJECTIVE:** The aim of this study is correlate the effects on liposome permeability induced by THz radiation at 130 GHz with possible primary physical parameters influenced by the field.

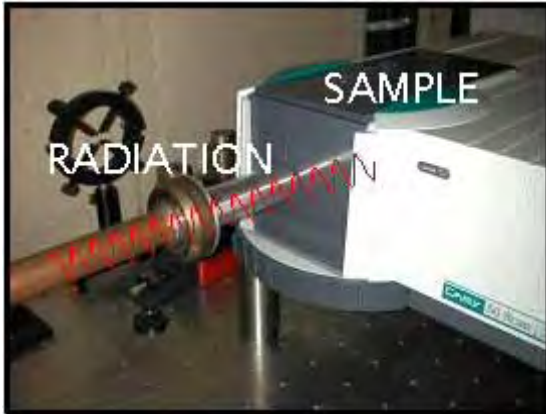
**METHODOLOGY:** Cationic liposomes consisting of dipalmitoylphosphatidylcholine, cholesterol and positive charged stearylamine (SA) at 5:3:2 molar ratio, entrapping Carbonic Anhydrase (CA) were used. The THz irradiation was performed by using the Compact Free Electron Laser at ENEA-Frascati. This source delivers 4 micros macropulses of 130 GHz radiation with a pulse repetition rate that can be varied between 1 and 10 Hz. Each macropulse is composed of a train of short (50 ps) pulses spaced at 330 ps intervals. A dedicated exposure set up was designed (Fig. 1). The cell compartment of the spectrophotometer (Fig.1 on the right) was modified to deliver the THz beam onto the cuvette containing the liposomes in a final volume of 3 ml. An electroformed copper horn is used to match the circular cross section of the THz beam to the rectangular cross section of the cuvette. The influx of the p-nitrophenyl acetate (p-PNA) across intact liposome bilayer was followed by means of spectrophotometric measurement of CA enzymatic activity. Any alteration of the lipid bilayer permeability induced by THz radiation may be evaluated by the ability of the substrate to diffuse across the lipid bilayer. The hydrolysis rate of p-PNA, expressed as the absorbance change at 400 nm ( $\Delta A/\text{min}$ ), was computed on the slope of the linear fitting of the recorded curve. The exposure of CA-loaded liposomes was performed at three different values of the pulse repetition rate for two mean values of the peak incident electric field ( $2.17 \pm 0.04$  and  $2.8 \pm 0.13$  kV/cm).

**RESULTS and DISCUSSION:** In Fig. 2 the effect of exposures is reported as the percentage increase of enzymatic activity in comparison to the total CA activity, determined after rupture of liposomes by detergent, and taken as 100%. We have confirmed previous results of 130 GHz irradiation at 7 Hz where the highest increase of CA activity from  $23 \pm 8$  to  $50 \pm 25$  ( $p = 3,5e10^{-6}$ ) was observed. Resonance effects on these cationic liposomes entrapping carbonic anhydrase have already been observed in the ELF (Extremely Low Frequencies) region at 7 Hz [3,4]. Interestingly, a significant increase of CA activity resulted also at the other frequencies tested by increasing the E-field value (from 2.1 to 2.8 kV/cm). A description of the possible mechanism of interaction will be discussed.

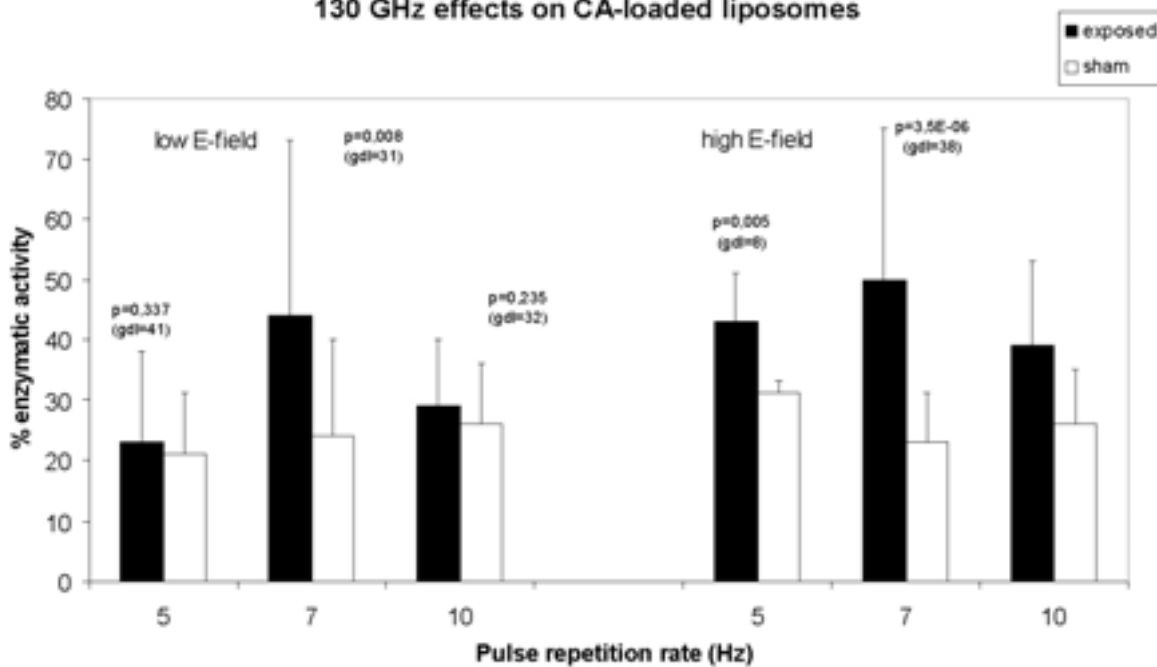
**References:**

- [1] Gallerano G.P. et al., THz-BRIDGE: A European project for the study of the interaction of THz radiation with biological systems, 26th BEMS Annual Meeting, Washington D.C., June 20-24, 2004. [2] L. De Gregori M. D'Arienzo, A. Doria, G.P. Gallerano, E. Giovenale, G. Messina, A. Ramundo-Orlando. Effects of THz radiation on carbonic anhydrase loaded liposomes, 26th BEMS Annual Meeting, Washington D.C., June 20-24, 2004 [3] Ramundo-Orlando A., Morbiducci U., Mossa G., d'Inzeo, G. Effect of low-frequency, low-amplitude magnetic fields on the permeability of cationic liposomes entrapping carbonic anhydrase.I. Evidence for charged lipid involvement *Bioelectromagnetics* 21: 491-498 (2000). [4] Ramundo-Orlando A., Mattia F., Palombo A., d'Inzeo G. Effect of low-frequency, low-amplitude magnetic fields on the permeability of cationic liposomes

entrapping carbonic anhydrase.II. No evidence for surface enzyme involvement *Bioelectromagnetics* 21:499-507 (2000).



130 GHz effects on CA-loaded liposomes



19-6 STUDENT

**SIMULATION OF BIOIMPEDANCE SPECTROSCOPY USING THE FINITE INTEGRATION TECHNIQUE AND HIGH-RESOLUTION HUMAN-BODY MODELS.** A. Barchanski, S. Wittorf, T. Weiland. Technische Universitaet Darmstadt, Institut fuer Theorie Elektromagnetischer Felder (TEMF), Darmstadt, Germany.

We have numerically estimated the whole-body as well as segmental bioimpedance values of the human body by numerically solving Maxwell's equations in a high-resolution human body model. Bioimpedance spectroscopy labels the measurement of the complex resistance of biological tissue at various frequencies. It is used as a low-cost, easy to use, and non-invasive approach to estimate various body parameters. Because of the capacitive properties of the cell and other body membranes the measured body impedance is higher at lower frequencies. By measuring the impedance at various

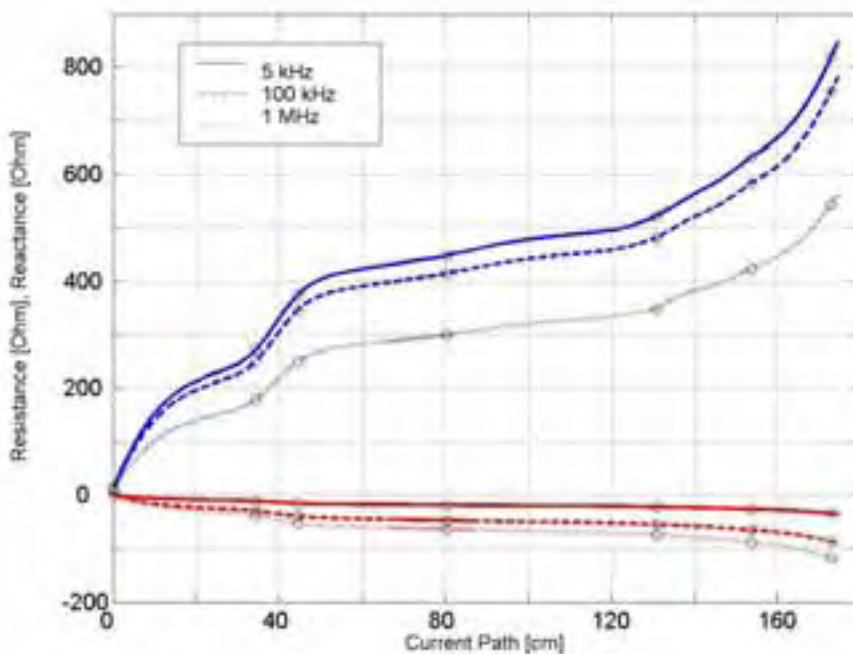
selected frequencies it is possible to estimate the balance between intracellular and extracellular fluids. In addition, fat tissue exhibits a lower admittivity than muscles allowing to estimate the muscle and fat masses of the measured person. Most equations used for these estimations have been derived from empirical data.

In this work the HUGO model, which has been constructed from the Visible Human Dataset, was used. This model offers a variable resolution ranging from  $8 \times 8 \times 8 \text{ mm}^3$  to  $1 \times 1 \times 1 \text{ mm}^3$ . Each voxel is assigned one tissue type, with a total of 31 various tissue types. In the finest resolution, the model consists of approximately 380 million voxels, representing a 38 years old, male person of 187 cm height and an approximate weight of 114 kg.

The dielectric properties of the biological tissue are extracted from the multiple Cole-Cole dispersion equation. In this parametric model proposed by Gabriel et. al. the complex permittivity is approximated by 14 parameters in four dispersion regions.

The Finite Integration Technique is a geometrical discretization of the Maxwell equations. Along with the constitutive material relations, the Maxwell equations are mapped onto a staggered, dual, orthogonal grid pair. Instead of field quantities defined at points, also integral state variables assigned to the elementary edges, facets and volumes of the grid are used to formulate the problem. For bioimpedance computation the electroquasistatic approximation can be used, resulting in a complex-valued scalar-potential formulation. After assembling and solving the algebraic system of equations, the bioimpedance of the body and the current density distribution everywhere inside the body can be derived in a post-processing step.

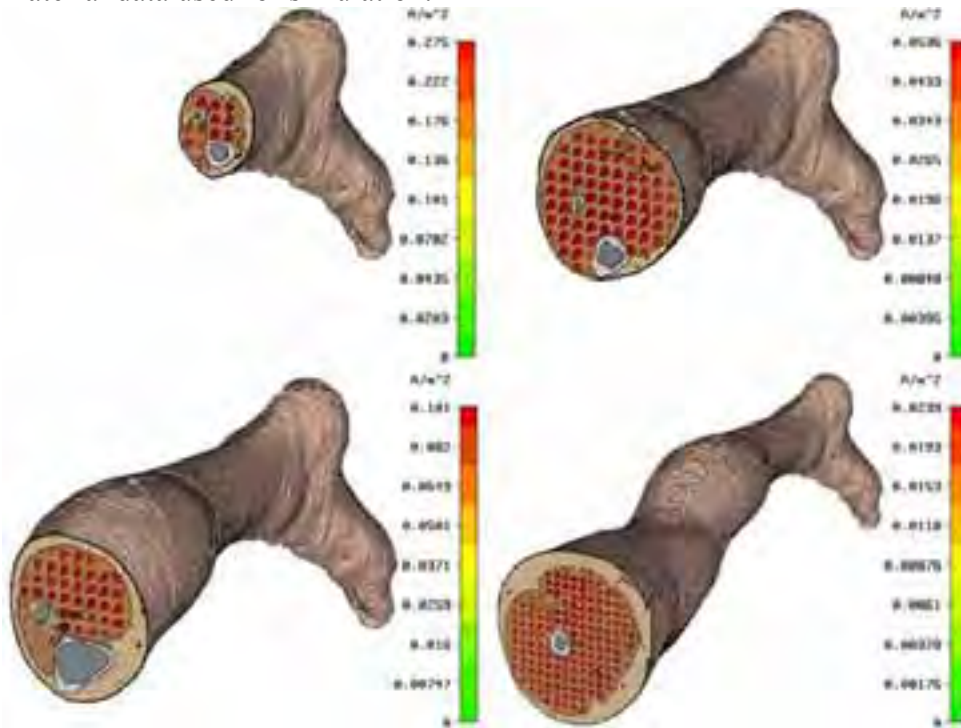
We have simulated the typical four pole measurement using electrodes at one ankle and at the opposite wrist. Figure 1 depicts the resistance (blue lines) and reactance (red lines) values along the path taken by the current inside the body at three typical frequencies.



The abscissa of the plot corresponds to a path through the body from ankle to wrist, where the electrodes are positioned. Changes of the slope of the plotted curve illustrate differences of the impedances of the individual body parts. In the vicinity of the knee (40 cm) the resistance rises significantly, indicating the narrower cross-section experienced by the current flow. The torso region is positioned between 50 cm

and 120 cm and exhibits a lower overall impedance because of the broader cross-section compared to the limbs. The slope rises again at 130 cm, when the current enters the arm of the model.

The numerically estimated impedance values allow a direct comparison with measured data. We compared the numerical results to measurements performed at our institute. The comparison showed a good qualitative agreement of the curve shapes but also showed quite different magnitudes. This is attributed to the inexact match of the test bodies to the HUGO body and to uncertainties in the dielectric material data used for simulation.



The numerical simulations of bioimpedance measurements, however, are valuable since they enable a qualitative assessment of the spatial distribution of the current through the different body parts. Extensive comparison between measured and simulated results for different test persons, would allow to derive more accurate material parameters for the different tissues in the human body.

## 19-7 STUDENT

**A METHOD BASED ON RECIPROcity THEOREM TO OBTAIN THE LEAD FIELD OF MEG.** H. Zhu<sup>1</sup>, G. Lindenblatt<sup>1</sup>, S. He<sup>1,2</sup>. <sup>1</sup>Centre for Optical and Electromagnetic Research, Zhejiang Univ, Hangzhou, China, <sup>2</sup>Division of Electromagnetic Theory, Alfvén Laboratory, Royal Institute of Technology, Stockholm, Sweden.

### OBJECTIVE:

The lead field approach is widely used in EEG and MEG when using the sphere model. But if using the brain-shape ("realistic") model, the lead field calculation is difficult and time consuming. We try to find a new method to calculate the lead field of MEG with a realistic head model.

### METHODS:

A measurement sensor is considered as a source when defining the differential equations and boundary conditions.

We calculate the lead field of each sensor instead of the positions of the trial dipoles inside the brain. Since the number of the sensors is usually far smaller than that of the possible dipole positions, this will greatly reduce the calculation time.

To obtain the lead field description, we first simplify the reciprocity theorem in a static limit, and insert this result in the Maxwell equations to be met by the MEG problem.

The equations are solved by Green's theorem and implemented numerically using the boundary element method (BEM). Through numerical simulation, we compare the storage, speed and accuracy of our approach with that of the standard approach.

We use a sphere model and calculate the results using the standard BEM and our presented method which are compared to the well-known analytical solution.

## RESULTS:

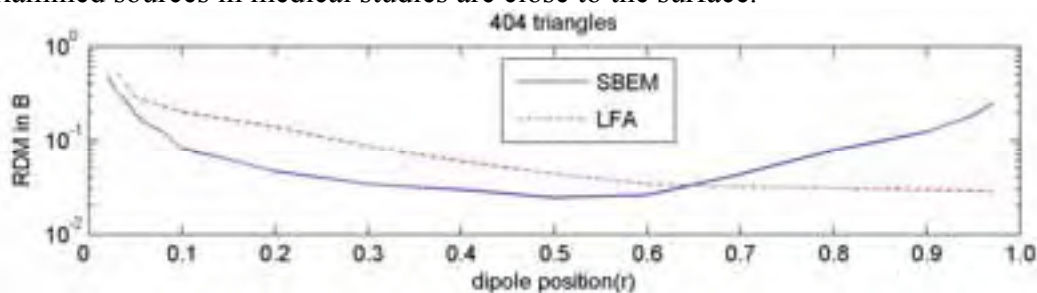
Comparing with the standard approach to obtain the lead field, the reciprocal formulation yields faster computation and less storage requirement.

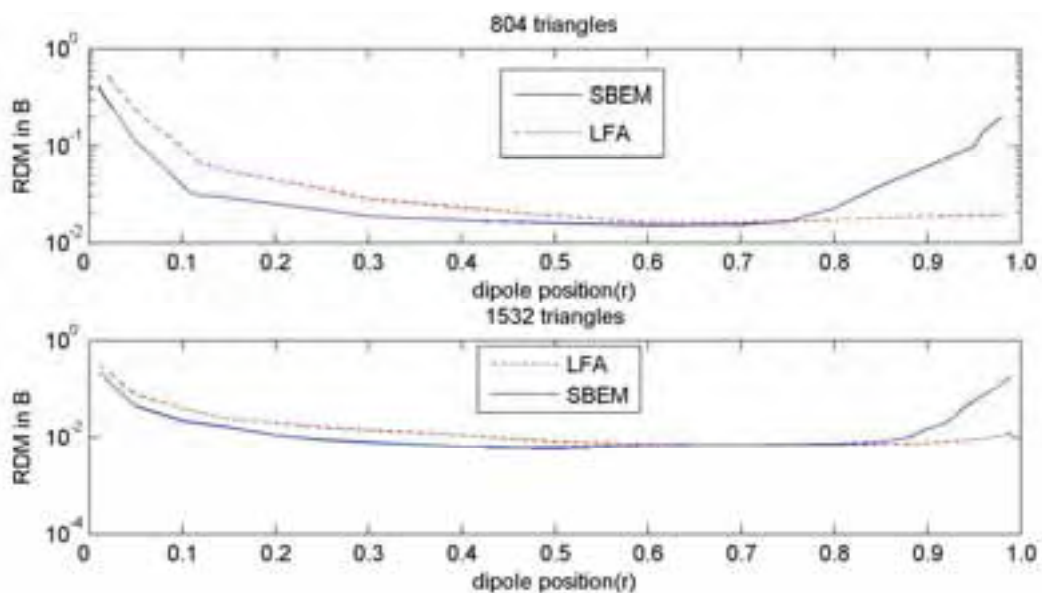
The memory requirements are reduced by the factor  $2(S+3)/(N+S+1)$ , where  $N$  denotes total number of the triangles of the brain (here: sphere) surface and  $S$  is the number of the sensors.

The computation time spend in our LFA has a linear relation with triangles number  $N$ , but that in standard BEM is quadratic in  $N$ . This is due to the fact that using BEM, the lead field calculation involves back substitution in the  $L$  and  $U$  matrices, which is an  $N^2$ -process, and calculation of a representation formula, which is a linear process in  $N$ .

When using LFA one only has to calculate the representation formula, which is only a linear process in  $N$ . In addition, for dipoles close to the brain surface, our formulation can obtain a better numerical accuracy, thus avoiding the time consuming local refinement of the mesh.

To describe the accuracy, we define the Relative Difference Measure (RDM), which has been used in EEG for the scalar electric potential on the surface. The following figure shows this error measurand for different numbers of triangles in a normalized coordinate system. We find that only for deep-source dipoles the standard BEM results a somewhat better accuracy, which is no advantage in practice, since the examined sources in medical studies are close to the surface.





## Plenary IV: The Low Field Effect On Free Radical Chemistry

*Chairs: Stefan Engström*

8:00 - 8:45 am, Theatre L

### THE EFFECTS OF WEAK MAGNETIC FIELDS ON RADICAL RECOMBINATION REACTIONS. C. R. Timmel. Physical and Theoretical Chemistry Laboratory, Univ of Oxford, UK.

There has been a lot of interest recently in the effects of weak magnetic fields on chemical and biological systems. The lecture will discuss the only known mechanism by which weak magnetic fields can affect chemical reactions, namely the Radical Pair Mechanism [1].

When a chemical bond is broken, radicals are formed, a process which occurs under conservation of total spin angular momentum so that a singlet molecular precursor results in the formation of a singlet radical pair in which the spins of the two radicals are aligned antiparallel. Certain interactions within the radical pair (such as the interaction of the electron spins with nearby nuclear spins) can cause the initial singlet radical pair, over time, to evolve into a triplet radical pair (with aligned electron spins) and vice versa, a process known as singlet-triplet interconversion.

If singlet and triplet radical pairs have, upon reencounter, different fates (eg, the singlet pairs might recombine whilst the reencounter of the triplet radical pairs is unreactive and leads to the formation of free radicals), any magnetic field that is applied and changes the efficiency of this singlet-triplet mixing will therefore lead to a change in the yield of singlet recombination products with respect to triplet products.

Even very weak magnetic fields ("weak" here symbolizes magnetic fields that are weaker than the average electron-nuclear spin interaction in the radical pair) can influence such radical recombination reactions quite considerably [2-11] (singlet recombination yields might fall by up to 40% in long-lived radical pairs, [3]). Chemical systems in which magnetic field effects have been studied will be discussed and a variety of experimental apparatus (facilitating the study of static and/or time dependent magnetic fields) introduced. Theoretical methods and data will be presented to accompany the experimental data.

- [1] U. Steiner, T. Ulrich, Chem. Rev. 89 (1989) 51.  
 [2] B. Brocklehurst, K. A. McLauchlan, Int. J. Radiat. Biol. 69 (1996) 3.  
 [3] C. R. Timmel, U. Till, B. Brocklehurst, K. A. McLauchlan, P. J. Hore, Molec. Phys. 95 (1998) 71.  
 [4] J. R. Woodward, C. R. Timmel, K. A. McLauchlan, P. J. Hore. Phys. Rev. Lett. 87 (2001) 077602.  
 [5] R. W. Eveson, C. R. Timmel, B. Brocklehurst, P. J. Hore, K. A. McLauchlan, Int. J. Radiat. Biol. 76 (2000) 1509-1522.  
 [6] J. R. Woodward, C. R. Timmel, P. J. Hore, K. A. McLauchlan, Molec. Phys. 100 (2002) 1181-1186.  
 [7] U. Till, C. R. Timmel, B. Brocklehurst, P. J. Hore, Chem. Phys. Lett. 298 (1998) 7.  
 [8] C. R. Timmel, P. J. Hore, Chem. Phys. Lett. 257 (1996) 401.  
 [9] J. R. Woodward, R. J. Jackson, C. R. Timmel, P. J. Hore, K. A. McLauchlan, Chem. Phys. Lett. 272 (1997) 376.  
 [10] D. V. Stass, J. R. Woodward, C. R. Timmel, P. J. Hore, K. A. McLauchlan, Chem. Phys. Lett. 329 (2000) 15.  
 [11] C. R. Timmel, J. R. Woodward, P. J. Hore, K. A. McLauchlan, D. V. Stass, Measurement Sci. Technol. 12 (2001) 635.

## **Session 20: Electromagnetic Therapy**

*Chairs: Arthur Pilla and Ruggero Cadossi*

**9:00 - 9:45 am, Theatre L**

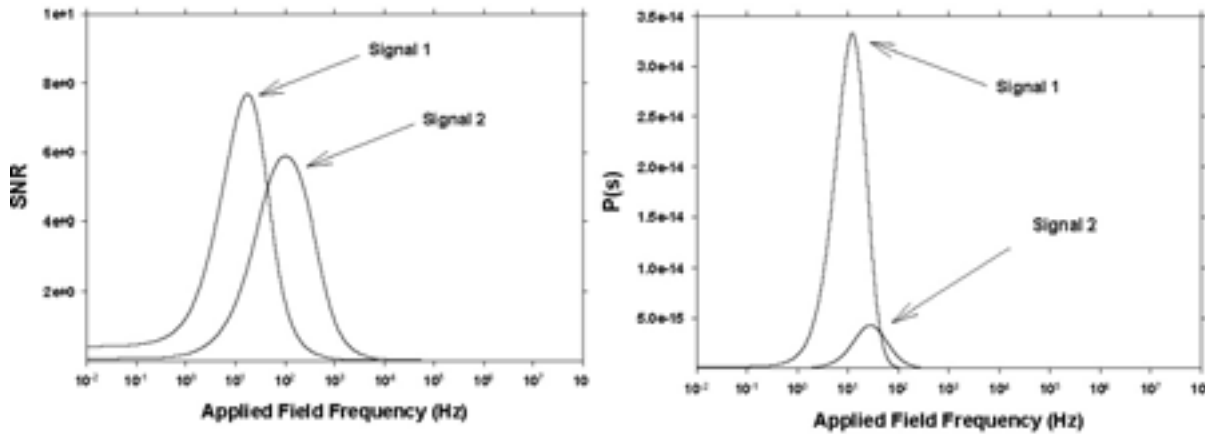
20-1

**WHAT MAKES AN ELECTROMAGNETIC FIELD THERAPEUTICALLY USEFUL?** A. A. Pilla<sup>1,2</sup>, D. J. Muehsam<sup>1,2</sup>. <sup>1</sup>Dept of Biomedical Engineering, Columbia Univ, New York, NY, <sup>2</sup>Dept of Orthopaedics, Mount Sinai School of Medicine, New York, NY, USA.

**INTRODUCTION:** There is an abundance of in vivo and clinical evidence that time-varying magnetic fields of various configurations can produce physiologically beneficial effects for conditions as varied as chronic pain, chronic wounds and recalcitrant fractures. It often seems the EMF signal was configured by some magical means. Certainly, dosimetry is not well understood. We have previously described evaluation of signal to thermal noise ratio (SNR) to guide the selection of signal parameters. This has proven to be a necessary, but not necessarily a sufficient, condition to configure EMF signals likely to produce physiologically meaningful effects. This work extends the SNR model by adding evaluation of power in the proposed target pathway. Ca/CaM is used as a sample EMF-sensitive target.

**EFFECTIVE WAVEFORM CONFIGURATION:** Analysis of binding kinetics equations yields resistance/capacitance electrical equivalent circuit analogs. This, along with knowledge of actual binding time constants, allows a given EMF signal to be assessed in the frequency domain with respect to its ability to produce a detectable (i.e. SNR<sub>11</sub>) voltage in the target. An example is shown in the left figure, wherein SNR for two PEMF signals is shown. Apparently both signals would be predicted effective, however only one produces a physiologically meaningful effect. The explanation is SNR does not go far enough and the reason is simple. An EMF effect on, e.g., Ca<sup>2+</sup> binding should affect the number of Ca<sup>2+</sup> ions bound, as well as produce sufficient voltage (above background noise) for a change in binding to occur. Evaluation of power produced in the target would provide this additional information since actual current flow in the binding pathway is directly proportional to the number of

bound ions. This is shown in the right figure wherein it becomes obvious that Signal 1 should be significantly more effective than Signal 2, despite their similar SNR values. It is.



**CONCLUSIONS:** This analysis further refines the SNR model by considering power across the binding pathway. Thus, while SNR provides a measure of the detectability of the applied EMF, the rate of energy delivery to the cell membrane or ion binding site can provide a means of assessing the magnitude of affects, and thus therapeutic efficacy. The mystery of why certain signals are effective whereas others are not is thus further unraveled, perhaps even providing an explanation for the sometimes elusive EMF bioeffects often reported. The approach presented in this study is a general one applicable to any signal configuration or target pathway. Its accuracy will depend upon how well we know the kinetics of the electrosensitive rate determining step.

20-2

**BIOPHYSICAL STIMULATION OF SKELETAL TISSUE REPAIR.** R. Cadossi. Laboratory of Clinical Biophysics, Igea srl, Carpi, (Modena), Italy.

The therapeutic possibilities at the physician's disposal foresee the use of both chemical and physical energy. Whereas the use of chemicals (drugs) and ionising electromagnetic energy for disease treatment has been well defined in the different branches of medicine and surgery, it has not been the same for non-ionising electromagnetic energies. The "clinical biophysics" is that branch of medical science that studies the action process and the effects of non-ionising electromagnetic fields utilised for therapeutic purposes. The principles on which the clinical biophysics is based are represented by the recognizability and by the specificity of the electromagnetic energy applied on the skeletal tissue.

Bone and cartilage cells exist in a complex biomechanical environment defined in large part by considerations of mechanical strain relative to the nature of the extracellular matrix. Electrokinetic events occur as the consequence of the flow of charged ions past stationary charges, e.g., streaming potentials. Biophysical signals can transfer information to cells and thus regulate their metabolism. Information is embedded in the signal characteristics in the form of amplitude, frequency, duration, coherence, and on-off cycle. Biophysical stimuli exert regulatory influences on gene expression and the synthesis of structural proteins including those comprising the extracellular matrix, and signaling and regulatory proteins including growth factors, and therefore has an overall influence on morphogenesis, particularly chondrogenesis. Studies have shown that biophysical stimulation can be used to prevent articular cartilage degeneration and favour healing.

New therapeutic opportunities exist in the use of biophysical regulation of articular cartilage function.

**THE USE OF PULSED ELECTRICAL STIMULATION TO DEFER TOTAL KNEE ARTHROPLASTY IN PATIENTS WITH OSTEOARTHRITIS OF THE KNEE.** M. A. Mont<sup>1</sup>, D. S. Hungerford<sup>2</sup>, J. R. Caldwell<sup>3</sup>, P. S. Ragland<sup>1</sup>, K. C. Hoffman<sup>4</sup>, Y. D. He<sup>5</sup>, L. C. Jones<sup>2</sup>, T. M. Zizic<sup>5</sup>. <sup>1</sup>Sinai Hospital of Baltimore, Center for Joint Preservation and Reconstruction, Baltimore, MD, <sup>2</sup>The Johns Hopkins Univ School of Medicine, Baltimore, MD, <sup>3</sup>Univ of Florida College of Medicine, Gainesville, FL, <sup>4</sup>Analytic Solutions Group, Inc., North Potomac, MD, <sup>5</sup>Bionicare Medical Technologies, Inc., Sparks, MD, USA.

**Introduction:** The limited capacity of articular cartilage to heal has stimulated a number of approaches to try to effectuate cartilage repair. Animal and clinical studies have suggested that pulsed electrical stimulation may have salutary effects on articular cartilage healing. The purpose of the present study was to evaluate the safety and effectiveness of pulsed electrical fields delivered to patients who had moderate/severe knee osteoarthritis and were total knee arthroplasty candidates.

**Methods:** One hundred and fifty-seven patients with osteoarthritis of the knee were treated with pulsed electrical stimulation to their knee for three months. These patients were compared to a matching group of 101 patients with osteoarthritis of the knee. Both groups were followed yearly till 4 years.

**Results:** Among electrically-stimulated patients by year of follow-up from one to four, 83%, 75%, 65% and 60% avoided a total knee arthroplasty. In contrast, the matched group had 67%, 51%, 46% and 35% of patients avoiding a total knee arthroplasty. Electrically stimulated patients were 50% less likely to have a total knee arthroplasty ( $p=0.0004$ ) and study patients who avoided a total knee arthroplasty had significant improvement in evaluations of pain scores (mean 40%), function (mean 38%), and physician global evaluation (mean 38%).

**Discussion:** This study demonstrated that pulsed electrical stimulation is a safe and effective method for avoiding total knee arthroplasty as well as relieving clinical signs and symptoms of osteoarthritis of the knee.

This study was partially supported by a grant from Murray Electronics, Hunt Valley, Maryland.

## **Session 20: Electromagnetic Therapy (Continued)**

*Chairs: Arthur Pilla and Ruggero Cadossi*

**10:15 - 11:45 am, Theatre L**

**EFFECT OF PEMF SIGNAL CONFIGURATION ON MINERALIZATION AND MORPHOLOGY IN A PRIMARY OSTEOBLAST CULTURE.** T. M. Ganey<sup>1,2</sup>, J. W. Kronberg<sup>4</sup>, E. B. Hunziker<sup>3</sup>, J. A. Naftel<sup>4</sup>, S. L. Gordon<sup>4</sup>. <sup>1</sup>Atlanta Medical Center, Atlanta, GA, <sup>2</sup>Univ of South Florida, Dept of Surgery, Tampa, FL, <sup>3</sup>ITI Research Institute for Dental and Skeletal Biology, Bern, SZ, <sup>4</sup>Healthonics, Aiken, SC, USA.

**INTRODUCTION:** PEMF has been successfully employed to treat skeletal injuries. Clinical outcomes  
*Bioelectromagnetics 2005, Dublin, Ireland*

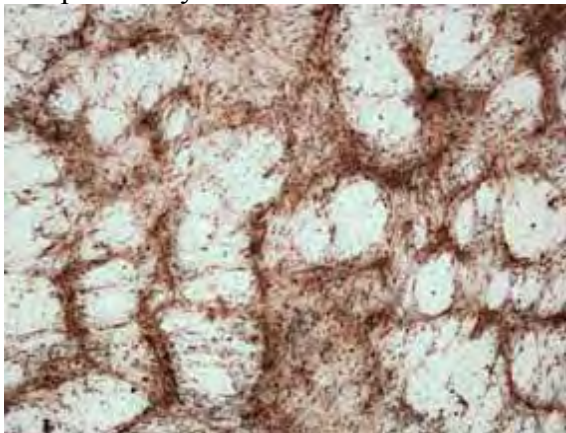
have demonstrated an enhanced capacity for accelerating the natural healing processes involved in fracture repair. One aspect of fracture repair particularly responsive to PEMF applications is the stress fracture. As an adjunct to surgery in spine fusion, or for treatment of recalcitrant non-unions in long bones, PEMF has proven effective as a non-surgical therapeutic.

**OBJECTIVE:** The goal of this study was to compare two PEMF waveform configurations delivered with capacitive coupling by evaluating biochemical and morphologic variations in a primary bone cell culture.

**METHODOLOGY:** Human osteoblast cells were established in 10 cm<sup>2</sup> individual culture chambers. Signals were applied to several chambers simultaneously by connecting them in serial via niobium wires which acted as a coupling capacitance. The stimulus was either a 9 msec burst of 200/30  $\mu$ sec bipolar rectangular pulses repeating at 15/sec, delivering 9mV/cm (similar to the standard clinical bone healing signal), designated signal B, or a 48 msec burst of 28/59  $\mu$ sec essentially unipolar pulses delivering 4 mV/cm, designated signal A. Cultures received either a 30-minute or a 2-hour stimulus twice a day. Samples were taken from the media and analyzed at 7-, 14-, and 21-day time points for alkaline phosphatase, osteocalcin, matrix calcium, and histology. Mineralization accompanying morphology was confirmed with Von Kossa stain. All biochemical analyses were performed by conventional assay techniques.

**RESULTS:** There was no significant difference in any outcome parameter for 30 min or 2 hr exposures. Alkaline phosphatase, which rose to a peak near the 10-14 day level and then gradually subsided, was increased in the supernatant stimulated by signal B. Osteocalcin deposition, measured subsequent to quenching the cultures and determined from the matrix component, was more pronounced following the B stimulus only and increased to its highest point at 21 days. Matrix calcium measured in mg/dl, and matrix calcium as a function of the area of the tissue culture plate were greatest with the B stimulus only. Mineral distribution as noted by histology and Von Kossa staining validated the biochemical data from the assays. The B stimulus conferred a greater amount of mineral, and moreover suggested a reticulated 2-dimensional pattern that may offer analogous tension dynamics as would be expected in a 3-D trabecular array (Figure 1). Cell proliferation appeared qualitatively higher with the A signal vs controls, whereas significantly increased mineralization and pattern was apparent at 21 days with signal B.

**CONCLUSION:** That the two signal configuration produced very different effects is readily explainable by a SNR analysis which showed the detectability of signal B was 10X higher than signal A, assuming a Ca/CaM target. This study demonstrates for the first time that PEMF has the potential to effect structural changes resonant with tissue morphology. The geometric pattern, apparent at 21-days of culture, mirrored the trabecular reticulation consonant with cancellous bone and starkly contrasted the random orientation of the cells in both the control and the cultures exposed to signal A at all time points evaluated. Such outcomes suggest that preferred signal configurations can effect structural hierarchies that previously were confined to tissue-level observations.



**SPECIFIC EMF WAVEFORMS ACCELERATE CUTANEOUS WOUND REPAIR IN A RAT MODEL.** B. Strauch<sup>1</sup>, M. Patel<sup>1</sup>, M. Berdichevsky<sup>1</sup>, A. Navarro<sup>1</sup>, A. A. Pilla<sup>2</sup>. <sup>1</sup>Dept of Plastic and Reconstructive Surgery, Albert Einstein College of Medicine and Montefiore Medical Center, Bronx, NY, <sup>2</sup>Dept of Biomedical Engineering, Columbia Univ, NY, USA.

**INTRODUCTION:** Chronic wounds such as arterial and venous ischemic ulcers, pressure ulcers and diabetic related ulcers are typically recalcitrant to standard care and costly to the health care system. There are few reported studies showing the beneficial effect of pulsed magnetic fields (PMF) on cutaneous wound healing and none which examine the effect of PMF regimen. Specifically, we were interested in characterizing the histological and mechanical changes that occur when cutaneous wounds are exposed to specifically configured radio frequency PMF signals as a step in establishing optimal PMF dosimetry for wound healing.

**METHODS:** A well established wound model consisting of an 8 cm linear skin incision on the dorsum of Sprague Dawley male rats was utilized in this study. Animals were treated in groups of ten to either a standard clinical signal consisting of a 65  $\mu$ s burst of 27.12 MHz sinusoidal waves at 1G, repeating at 600/sec, or signals, reconfigured via SNR analyses using Ca/CaM as the EMF-sensitive target, having 2-4 msec burst durations at 0.02-0.05G repeating at 1/sec (SofPulse™, Ivivi Technologies, Inc., Northvale, NJ). Both control and experimental groups were treated twice daily for 30 minutes in specially constructed plastic cages designed to treat 5 animals simultaneously. There were 10 animals in each group. After 21 days, two strips 1 cm in width were excised perpendicular to the incision and subjected to controlled strain to failure at a rate of 25mm/minute on a standard laboratory tensiometer. An additional specimen was sent to pathology for analysis of collagen content and vascularity.

**RESULTS:** Mean percent increase in tensile strength vs controls for the group treated with the 65  $\mu$ s burst duration signal was 48% ( $p < 0.01$ ) and for the groups treated with the set of signals having 2-4 msec burst durations ranged from 37-49% ( $p < 0.01$ ). Histologic studies revealed an apparent increase in collagen thickness and neovascularization in the PMF treated group.

**CONCLUSIONS:** One goal of this study was to determine if a radiofrequency PMF signal in current clinical use for wound repair could be reconfigured to be effective at significantly less power induced in the wound target. This would also allow miniaturization of the delivery device allowing its use over a broader clinical spectrum. Signals were reconfigured by matching frequency content to that of Ca<sup>2+</sup> binding kinetics to CaM which can modulate relevant growth factor cascades (e.g. TGF- $\beta$ ). This required longer burst widths, but allowed a significant (20-50X) decrease in induced amplitude and several hundred-fold decrease in power. The results suggest a trend toward more advanced biomechanical healing for longer burst durations at equivalent low amplitude, but this is not yet significant. Another goal of this study was to determine if PMF signals could accelerate wound repair to a physiologically significant degree. The results clearly show exposure of a linear cutaneous wound for 30 min 2X daily for 21 days in the rat significantly increased tensile strength. Specific signal parameters such as burst duration, amplitude and repetition rate proved to be extremely important in achieving clinical responses. These findings not only demonstrate the clinical effectiveness of PMF treatment in early wound healing in a rat but suggest a significant application to human wound repair. A human clinical trial using the reconfigured signals on recalcitrant wounds will follow.

**TURNING ON STEM CELL CARIOGENESIS WITH EXTREMELY LOW FREQUENCY MAGNETIC FIELDS.** F. Bersani<sup>1</sup>, C. Ventura<sup>2</sup>. <sup>1</sup>Dept of Physics, Univ of Bologna., <sup>2</sup>Laboratory of Molecular Biology and Stem Cell Engineering, National Institute of Biostructures and Biosystems, Univ of Bologna, Italy.

Objectives We used murine embryonic stem (ES) cells as an in vitro model of cardiac differentiation and assessed whether ELF magnetic field (MF) may be involved in the activation of a gene program of cardiac lineage commitment.

Methods MF were applied to GTR1 ES cells, a derivative of R1 ES cells bearing the puromycin resistance gene driven by the cardiac specific MHC promoter (GTR1 cells were kindly provided by Dr. William L. Stanford, Univ of Toronto and Centre for Modeling Human Disease, Canada). ES cells were maintained in the undifferentiated state by culturing in KNOCKOUT D-MEM containing 15% FBS, supplemented with 1000 U/ml LIF (Leukemia Inhibitory Factor). To induce cardiac differentiation, cells were plated onto specialty plates (Costar ultra low attachment clusters), containing KNOCKOUT D-MEM, lacking supplemental LIF. After 2 days, the resulting embryoid bodies (EBs) were plated onto tissue culture dishes. When spontaneous contractile activity was noticed, puromycin (2<sup>3</sup>/<sub>4</sub>g/ml) was added to eliminate non-myocardial cells. After 2 days, puromycin selected cells were transferred to new tissue culture dishes. EBs, collected at several stages after plating, as well as puromycin-selected cells were processed for gene expression analysis. Following LIF removal and throughout puromycin selection, GTR1 cells were also exposed to MF (50 Hz, 0.8 mTrms). The analysis of mRNA expression was performed by RT-PCR technique.

#### Conclusions

- 1.The development of a model of in vitro cardiogenesis based on “;gene trapping”; selection of cardiomyocytes from pluripotent GTR1 cells provided a homogeneous and reproducible approach to assess the effect of MF on developmental decisions in ES cells.
- 2.In this model of cardiogenesis, MF elicited the expression of a gene program of cardiogenesis, along with the induction of cardiac-specific transcripts.
- 3.MF failed to activate skeletal myogenesis but slightly enhanced the expression of a vertebrate neural determination gene.

**PULSED RADIO FREQUENCY EMF SIGNALS INCREASE ANGIOGENIC POTENTIAL IN EMBRYONIC NEURAL TRANSPLANTS.** D. Casper<sup>1</sup>, A. Pidel<sup>1</sup>, S. Singer<sup>1</sup>, M. K. Patel<sup>2</sup>, M. R. Bertichevsky<sup>2</sup>, B. Strauch<sup>2</sup>. <sup>1</sup>Dept of Neurosurgery, The Abert Einstein College of Medicine and Montefiore Medical Center, Bronx, New York, <sup>2</sup>Dept of Plastic and Reconstructive Surgery, The Albert Einstein College of Medicine and Montefiore Medical Center, Bronx, New York.

**INTRODUCTION:** Neural transplantation may be a promising therapeutic strategy for Parkinson's disease, but the failure to maintain the viability of transplanted neurons is still a major obstacle. Because neurons depend on the vasculature to survive, we hypothesized that neurons within donor tissue would benefit from an increased rate of vascularization from the host to the transplant. Pulsed magnetic fields (PMF) have been reported to increase angiogenesis in models of arterial transplants and bone repair. The goal of our study was to determine whether radiofrequency PMF, configured by matching frequency content to that of calcium/calmodulin (Ca/CaM) binding kinetics, could enhance mediators of angiogenesis in transplants of embryonic dopaminergic neurons.

**METHODS:** Adult Sprague Dawley rats received bilateral transplants of dissociated embryonic day-15 rat mesencephalon into the striatum. Control and experimental groups were exposed twice daily for 30 minutes with PMF signals configured via SNR analyses using Ca/CaM as the EMF-sensitive target, having 2-4 msec burst durations at 0.02-0.05G repeating at 1/sec (SofPulse™, Ivivi Technologies, Inc., Northvale, NJ), or with no signal. Animals were treated in specially constructed plastic cages designed to treat 5 animals simultaneously. After 1, 2, and 3 weeks, rats from each group were sacrificed and brains removed. Each brain was bisected at the mid-sagittal plane; the rostral half of one hemisphere was fresh-frozen and processed for determination of angiogenic factor levels by ELISA.

**RESULTS:** Vascular endothelial growth factor (VEGF) and basic fibroblast growth factor (bFGF), two angiogenic factors in brain, were induced by transplantation alone, most likely caused by the insertion of the needle delivering cells to the host. However, no significant effects of PMF treatment were found on VEGF or bFGF expression between 1 and 3 weeks after transplantation. In contrast, levels of tissue inhibitor of metalloproteinase-1 (TIMP-1), an inhibitor of angiogenesis, were significantly attenuated in the PMF group, with differences in expression relative to total protein of 20-25% after 2-3 weeks of PMF treatment.

**CONCLUSIONS:** The signal employed in this study was configured assuming a Ca/CaM transduction pathway because many reports demonstrate it is a frequent EMF target. This triggers a pathway leading to the modulation of growth factors, as well as anti-inflammatory cascades. The results reported here show this PMF signal significantly regulated the expression of the anti-angiogenic factor TIMP-1. TIMP-1 is normally expressed in brain, and may hold vascularization in check in the adult. Decreased levels of TIMP-1, an inhibitor of matrix metalloproteinases that break down the extracellular matrix to allow vascular sprouting, a prelude to the formation of new vessels, may set the stage for increased in-growth of vessels into avascular donor brain tissue. Future experiments will determine whether there is a concomitant increase in the survival of dopaminergic neurons.

20-8

**A CLINICAL TRIAL IN CHRONIC MUSCULOSKELETAL PAIN: DOUBLE-BLINDED PLACEBO-CONTROLLED DAILY REPEATED TREATMENT WITH A SPECIFIC LOW FREQUENCY PULSED MAGNETIC FIELD.** A. W. Thomas<sup>1,2,3</sup>, K. Graham<sup>2</sup>, L. Keenlside<sup>2</sup>, F. S. Prato<sup>1,2,3</sup>, R. A. MacKenzie<sup>1</sup>, D. Moulin<sup>4</sup>, P. M. Forster<sup>5</sup>. <sup>1</sup>Dept of Nuclear Medicine, St. Joseph's Health Care (London), Ontario, Canada, <sup>2</sup>Bioelectromagnetics, Imaging Program, Lawson Health Research Institute, Grosvenor Campus, London, Ontario, Canada, <sup>3</sup>Dept of Medical Biophysics, Faculty of Medicine and Dentistry, Univ of Western Ontario, London, Ontario, Canada, <sup>4</sup>Dept of Neurology, St.

Joseph's Health Care, London, Ontario, Canada, <sup>5</sup>Dept of Anesthesiology, St. Joseph's Health Care, London, Ontario, Canada.

## INTRODUCTION

Exposures to specific pulsed magnetic field designs (CNP) have been shown to have analgesic effects in humans [Shupak et al, 2004a], mice [Shupak et al., 2004b] and snails [Thomas et al., 1997]. Furthermore, using an opiate, such as morphine, in conjunction with CNPs, the side effects of the opiate are reduced. Extremely low frequency (ELF) magnetic fields have been shown to have both analgesic effects as well as no effects or even negative effects (increased nociception), depending on how the field is delivered [Prato et al, 2000]. Analgesic affects of exposure to CNPs has been previously shown to be present in human patients with chronic pain, specifically rheumatoid arthritis and fibromyalgia patients, when using a single thirty minute session [Shupak et al., 2005].

## OBJECTIVE

In a randomized, double-blinded, placebo-controlled clinical trial, assess the effectiveness and compliance to a portable magnetic field generator delivering a specific pulsed magnetic field design to the head of volunteer chronic pain patients.

## METHOD

Fifty patients were recruited from the Outpatient Pain Clinic (St. Joseph's Health Care) and screened for entry criteria (physical exam and visual analog scale pain rating). Patients were then randomized into 'active' and 'placebo' groups, each receiving a portable CNP generator and head-coils. Patients were instructed to use the unit for 40 minutes twice per day (with at least 4 hours between sessions). Patients were also negatively biased through verbal instructions to reduce a possible placebo effect: "You have a 50/50 chance of receiving an 'active' CNP generator, in fact, we're not sure if this treatment even works at all." This 2-arm 2-week long protocol allowed us to determine the lasting effects of the analgesia from the CNP exposure. A Visual Analogue Scale was used to record pain ratings before and after each treatment, while a McGill Pain Questionnaire was given to assess subjective measures daily, and before and after the treatment week as well as the washout week. Weekly verbal analog scale measures were called in weekly for 3 weeks post-study. The CNP generator consisted of two small head coils and a small portable battery-operated unit (see poster by Keenlside et al for details).

## RESULTS

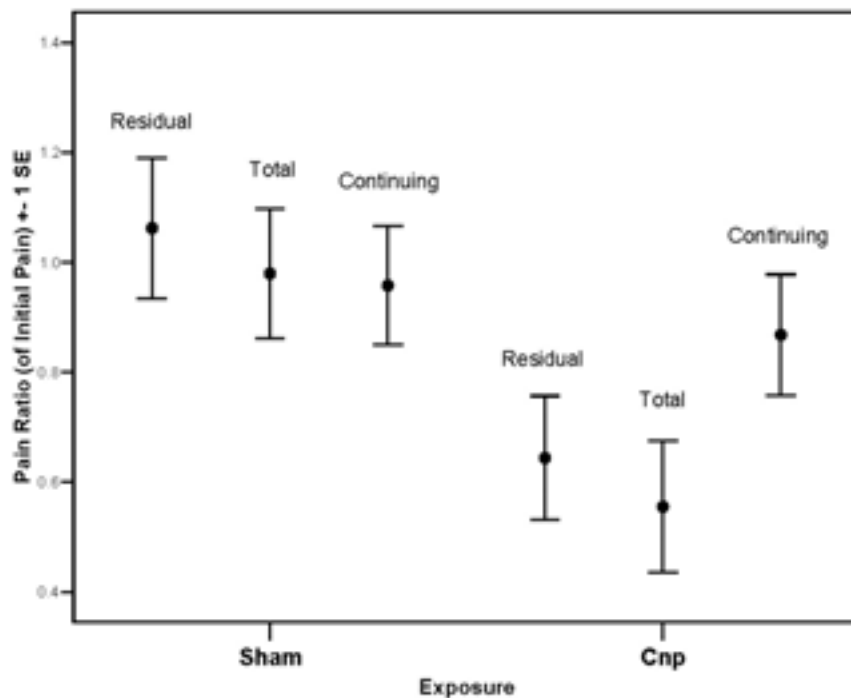


Figure 1: A 'pain ratio' was devised from dividing the last day pre-exposure VAS value by the first day pre-exposure VAS value (Residual), the last day post-exposure VAS value by the first day pre-exposure VAS value (Total, and the first washout day VAS value by the first day pre-exposure VAS value (Continuing). Note: patients did not have a unit on during the washout. A ratio of 1 represents no improvement in the patient's pain level, whereas decreasing values represent a respective decrease in pain. Error bars represent the standard error of the mean.

## DISCUSSION

Acute exposure to specific CNP designs has shown to be very effective in pain reduction, and it would appear that repeated daily exposure builds towards a cumulative effect, at least over a week of twice daily repeated 40 minute exposures. As may be noted in figure 1, the 'residual' effects of CNP treatment are evident prior to the second treatment of the last study day. The 'total' pain reduction includes the last treatment. The 'continuing' effect shows a return to near initial pain levels one day after the CNP generators were returned (washout period). There were no significant effects within the 'Sham' (placebo) group. Details of effects recorded during the protocol will be presented.

## REFERENCES

- Prato FS, Kavaliers M, Thomas AW: *Bioelectromagnetics* 4: 287-301, 2000.  
 Shupak N, Hensel J, Prato FS, Thomas AW. *Neurosci Lett* 363(2):157-62, 2004a.  
 Shupak NM, Hansel JM, Cross-Mellor SK, Kavaleirs M, Prato FS, Thomas AW. *Neurosci Lett* 354: 362-366, 2004b.  
 Shupak NM, Nielson WR, Prato FS, Rollman GB, Thomas AW. 2005 (submitted)  
 Thomas AW, Drost DJ, Prato FS. *Neurosci Lett* 297: 121-124, 2001.  
 Thomas, Kavaliers, Prato and Ossenkopp *Neurosci Lett*. 222:107-110, 1997.

**WEAK STATIC MAGNETIC FIELDS REDUCE NEUROPATHIC PAIN DEPENDENT UPON FIELD STRENGTH AND PENETRATION: A DISCUSSION OF TWO RANDOMIZED PLACEBO CONTROLLED TRIALS.** M. I. Weintraub. Dept Neurology & Internal Medicine, New York Medical College, Valhalla, NY.

**INTRODUCTION:** Static magnetic fields (SMF) ranging from 23-3,000G can alter electrical properties of solutions and influence cellular function producing significant biological effects. Several clinical studies using SMF for pain reduction ranging from osteoarthritic knees to fibromyalgia have been reported. The optimum dosimetry at the target area and exposure time have yet to be established, however it appears that 5G (10X the earth's magnetic field) is the threshold for physiologically meaningful bioeffects.

**OBJECTIVE:** The effect of magnetic field amplitude on clinical outcome is reviewed. Two specific randomized placebo controlled trials to reduce neuropathic pain (NP) in a homogeneous Diabetic and heterogeneous failed back population are compared.

**SPECIFICS:** Study 1: Nationwide randomized placebo controlled trial utilizing multipolar shoe insoles with a maximum surface field of 450 G worn constantly over a 4 month period in a population of moderate-severe diabetic peripheral neuropathy. 375 patients were enrolled in 48 centers to determine if baseline VAS pain scores, quality of life parameters and electrodiagnostic studies could be influenced. Statistically significant pain reduction (numbness, tingling, burning pains) was noted by the third and fourth months. It was concluded that the specific SMF had a useful penetration of 1 cm and appeared to target the ectopic firing nociceptors (unmyelinated and myelinated c-fibers) in the epidermis and dermis. Analgesic benefits were achieved over time (4 months). The magnetic shoe insole is reinforced and flexible magnetic rubber compound pressed with strontium ferrite powder and magnetized with a specific triangular multipolar configuration. The maximum surface strength of the magnetic field was 450 G measured with a conventional Lakeshore 420 gaussmeter on the surface of the insoles at the center of the triangular pole. The field decayed from the surface such that: at 1mm=249G; at 2mm=150G; at 3mm=90G; at 10mm=5G. Thus there appeared to be sufficient magnetic field level at the nociceptor targets to achieve a significant clinical outcome.

Study 2: Performed at two sites, utilized simultaneous and constant exposure of weak permanent magnets to feet and back in 17 randomized patients with failed back syndrome over two months. The shoe insole had a maximum surface field of 450 G and in the back corset the maximum surface field was 350 G. There was no statistical pain reduction or quality of life benefit produced by the magnetic fields in this heterogeneous population. Examination of the field decay from the back corset revealed it had decayed to background at approximately 1.5 cm. Thus the field at the deep tissue target in the lower back was no different than ambient and it is not surprising there was no significant clinical benefit.

**CONCLUSION:** Antinociceptive effect was significantly pronounced in Study 1 during the third and fourth month indicating that a tonic and chronic exposure must be present to inhibit and influence sensitized afferent pain fibers. We speculate there is either direct or indirect suppression of the afferent signal traffic of the c-fiber firing pattern of the distal part of the surviving axons thereby producing an antinociceptive effect. Clearly the amplitude of the magnetic field was sufficient for this target which was not deep below the skin. In contrast, a similar magnetic field configuration utilized for lower back pain failed to deliver any magnetic field to this deep tissue target. Clinical use of SMF must, therefore, be approached with an awareness of the field decay from the surface of the magnet. Unfortunately this information is rarely supplied by the vendors of such devices.

## Session 21: Mechanisms II

*Chairs: Martin Blank and Werner Sontag*

9:00 - 11:45 am, Theatre M

21-1

**A MECHANISM FOR SEPARATION OF DNA BASE PAIRS INDUCED BY EM FIELDS.** M. Blank<sup>1</sup>, R. Goodman<sup>2</sup>. <sup>1</sup>Dept of Physiology, Columbia Univ, New York, NY, <sup>2</sup>Dept of Pathology, Columbia Univ, New York, NY.

Low frequency electromagnetic (EM) field stimulation of stress protein synthesis shows that EM fields cause DNA to initiate gene expression. Since more energetic RF fields stimulate the same biosynthetic response and use the same biochemical pathway, it is clear that the rate of energy input (SAR) does not determine biological response and therefore, is not a sound basis for a safety standard (Blank and Goodman, 2004). The similar effects of ELF and RF probably arise because an increase in frequency increases the energy of a wave but simultaneously decreases the duration. Therefore, the (energy x duration) product is independent of frequency. **It is the energy/cycle, not the energy/time (SAR) that appears to be important.** A plausible mechanism is suggested by the finding that EM fields accelerate electron transfer reactions (Blank and Soo, 2001; Blank and Goodman, 2004). If EM fields induce a movement of electrons in DNA, the charging of a small segment by repeated signals could destabilize the H-bonds holding the two chains together. This consequence of charge transfer is in line with the well-established effect that increases in charge lead to the disaggregation of protein oligomers (Blank and Soo, 1987; Blank, 1989). Applying the same energetic principles to a DNA model shows that transfer of electrons in EM fields could contribute to separation of base pairs, and that EM fields would be most effective for small segments of base pairs with low initial charge. The CTCT bases associated with the response to EM fields have properties that increase the likelihood of separation of base pairs. This mechanism explains the need for repeated waves, the wide range of EM frequencies that can activate DNA, and predicts a frequency maximum.

References:

Blank M (1989) Surface Forces in Aggregation of Membrane Proteins. *Coll Surf* 42:355-364.

Blank M, Goodman R (2004) A Biological Guide for Electromagnetic Safety: The Stress Response Electromagnetic initiation of transcription at specific DNA sites. *Bioelectromagnetics* 25:642-646.

Blank M, Goodman R (2004) Initial Interactions in Electromagnetic Field-Induced Biosynthesis. *J Cellular Physiol* 199:359-363.

Blank M, Soo L (1987) Surface Free Energy as the Potential in Oligomeric Equilibria: Prediction of Hemoglobin Disaggregation Constant. *Bioelectrochem Bioenerg* 17:349-360.

Blank M, Soo L (2001) Electromagnetic Acceleration of Electron Transfer Reactions. *J Cell Biochem* 81:278-283.

21-2

**SEARCH FOR PROTEINS WITH AN ION BINDING SITE THAT HAS THE SYMMETRY NECESSARY FOR ION PARAMETRIC RESONANCE.** J. D. Bowman, C. K. Miller. National Institute for Occupational Safety and Health, Cincinnati, Ohio, USA.

**Objective:** To search the online Protein Data Bank (PDB) for proteins binding  $\text{Ca}^{+2}$ ,  $\text{Mg}^{+2}$  or  $\text{Zn}^{+2}$  in sites that have the symmetry theoretically necessary for ion parametric resonance (IPR).

**Background:** Engstrom and Bowman [1] recently proposed a quantum model for magnetic resonance of an ion bound to a protein, that might account for the experimental observations of ion parametric resonance (IPR) [2 and references therein]. In order to have an IPR response to magnetic fields, the model's requirements include: 1) the ion has zero spin and 2) the ligand atoms which make up the ion's binding site form a symmetric bipyramid. The goals of this study were to determine whether such symmetries exist in naturally-occurring human proteins and if so, to identify plausible targets for theoretical and experimental tests of the IPR mechanism.

**Methods:** A C++ program was written to search the PDB for proteins that have  $\text{Ca}^{+2}$ ,  $\text{Mg}^{+2}$  or  $\text{Zn}^{+2}$  (the biologically interesting ions with abundant isotopes that have zero electronic and nuclear spin) bound to ligand atoms that are all oxygens (the most likely scenario for the desired symmetry in proteins). When the program finds a protein meeting these search criteria, it extracts the coordinates for the ion and its oxygen ligands, plus the resolution of the X-ray diffraction (XRD) structure. From these data, a second C++ program determines the best fit between the ligand and a symmetric bipyramid centered on the ion, as measured by each ligand's root-squared deviation from perfect symmetry ( $d$ ). From the resolution, the experimental standard deviation ( $esd$ ) in each atom's position can be determined [3]. When  $d < esd$ , the binding site may be symmetric, as far as the XRD data can determine. The list of symmetric candidates is further reduced by discarding proteins that are synthesized, mutants or from non-human species. The Swiss PDB graphic viewer [4] was then used to identify ions loosely attached to the protein's periphery by water molecules since these are less likely to display IPR than those bound within a cage of amino acids.

**Results:** After searching the 27,000 molecular structures stored in the PDB, 773 of these structures had one or more of the target ions surrounded by oxygen ligand atoms, but 10 did not report the resolution for the structure determination. When symmetric bipyramids were fit to the ligand coordinates, the rms deviation from ideal ranged from 0.006–0.417 Angstroms per ligand. When compared to the experimental standard deviations for a ligand's position (0.029–1.837 Å), 467 of these structures (64%) had deviations from symmetry less than experimental error. Of these, 30 were naturally-occurring human proteins or protein complexes, although the symmetric binding sites in one protein were simply waters of hydration. The Figure shows a plausible site for IPR – a  $\text{Ca}^{+2}$  ion bound in calmodulin complex with a peptide from myosin light chain kinase ( $d = 0.180$  Å). According to theory [1], resonant combinations of static and oscillating magnetic field could focus the oscillations of the  $\text{Ca}^{+2}$  ion towards a gap in its binding site, altering its rate of dissociation from the calmodulin complex and the resulting biological response. The Table gives all protein substrates that meet our criteria.

**Discussion:** These results suggest that proteins with the bipyramidal symmetry needed for ion parametric resonance might occur in nature, but more evidence is needed to confirm IPR existence in human biology. First, the XRD data in the PDB is far too imprecise to determine the symmetry needed for IPR, which is 1 part in  $10^{11}$  according to theory [5]. In contrast, the experimental standard deviations in the Table are 4.6–22.3% of the typical 2.5 Å bond length. Furthermore, theory requires that the binding site's potential energy is symmetric, not just the atom's positions. Oxygen ligands belonging to different amino acids probably do not make a symmetric potential, but quantum mechanical calculations are needed to be sure. Whether IPR can change the ion-protein dissociation rate (or some other “detection” mechanism) also needs investigation with the compounds in the Table. A last shortcoming of this study is its restriction to ions with zero spin. Because ions with the hyperfine energy levels from nuclear spin can also have an IPR-like response [2], a similar PDB search for other ions should turn up additional symmetric candidates. Lastly, we note that IPR was observed with the  $\text{Ca}^{+2}$ -calmodulin-dependent phosphorylation of the myosin light chain [6], which is the complex with a symmetric calcium binding site (Figure and Table). None of the 36 other calmodulin-containing structures in the PDB has a symmetric binding site.

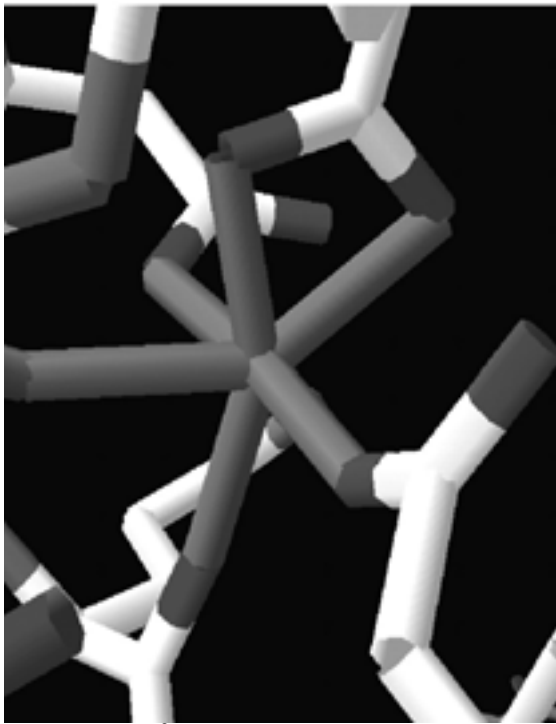


Figure:  $\text{Ca}^{+2}$  in a pentagonal bipyramid binding site (with one amino acid not shown by the PDB viewer). This is part of a calmodulin complex with a peptide in myosin light chain kinase.

**Conclusions:** A comprehensive search of the Protein Data Bank found 29 proteins and protein-complexes with ion binding sites that appear to have the bipyramidal symmetry necessary for ion parametric resonance. More experimental and theoretical work will be needed to confirm that these compounds are capable of IPR from exposure to magnetic fields.

**References:**

[1] Engstrom S, Bowman JD. Magnetic resonances of ions in biological systems. *Bioelectromagnetics*, 2004;25:620-30.  
 [2] Binhi VN. *Magnetobiology: Underlying Physical Problems*. San Diego: Academic Press, 2002.  
 [3] Tickle IJ, Laskowski RA, Moss DS. Error estimates of protein structure coordinates and deviations from standard geometry by full-matrix refinement of  $\gamma\text{B}$ - and  $\beta\text{B2}$ -Crystallin. *Acta Cryst.* 1998;D54:243-252.  
 [4] Guex N, Peitsch M, Schwede T, Diemand A. Deep View/Swiss-PdbViewer. GlaxoSmithKline. <http://www.expasy.org/spdbv/>.  
 [5] Adair RK. A physical analysis of the ion parametric resonance model. *Bioelectromagnetics*. 1998;19:181-91.  
 [6] Shuvalova LA, Ostrovskaja MV, Sosunov EA, Lednev VV. [The effect of a weak magnetic field in the paramagnetic resonance mode on the rate of the calmodulin-dependent phosphorylation of myosin in solution], article in Russian. *Dokl Akad Nauk SSSR*. 1991;317:227-30.

Naturally-occurring human proteins and protein-complexes with potentially symmetric ion binding sites from the Protein Data Bank.				
Substrate	Ion	# ligands	d (Å)	esd (Å)

Mitochondrial Ferretin	Mg	6*	0.009	0.159
Golgi Autoantigen Subfamily Member 4	Mg	6	0.030	0.159
Beta2-Adaptin	Mg	6	0.039	0.159
Adenosine Kinase	Mg	6	0.040	0.116
Stromelysin-1	Ca	6	0.045	0.304
Psoriasis (S100A7) Bound Form	Mg	6	0.068	0.159
Rho a. GDP. Mgf3-In complex with Rhogap	Mg	5	0.073	0.184
Hgprtase with Transition State Inhibitor	Mg	6	0.102	0.240
ADP-Ribosylation Factor 6	Mg	6	0.104	0.558
Nucleoside Diphosphae Kinase	Mg	6	0.105	0.240
Collagenase-3 (Mmp-13) complex	Ca	6	0.109	0.379
Mmp9-Inhibitor complex	Ca	6	0.120	0.340
Calcineurin heterodimer	Ca	7	0.143	0.271
Riboflavin Kinase with product complex	Mg	6	0.149	0.387
Aurora-A 122-403, phosphorylated and bound to Tpx2 1-43	Mg	6	0.165	0.420
Calgranuline C	Ca	7	0.180	0.301

(S100A12) – Copper complex				
Calmodulin complexed with a calmodulin binding peptide from smooth muscle myosin light chain kinase	Ca	7	0.180	0.304
Alpha-Psoriasin (S100A7)	Ca	7	0.185	0.255
Serum Paraoxonase	Ca	7	0.187	0.304
Calgranulin (S100A12)	Ca	7	0.203	0.509
Growth-Arrest- Specific Protein (Gas6)	Ca	7	0.204	0.304
Human Glyoxalase I with inhibitor	Zn	5	0.208	0.304
Annexin V	Ca	5	0.254	0.420
Fibrillin-1	Ca	8	0.266	0.322
Phospholipase A2 complexed with an acylamino- phospholipid analog	Ca	6	0.293	0.450
Alpha-Factor inhibiting Hif-1	Zn	5	0.302	0.420
Myeloperoxidase	Ca	5	0.320	0.322
Fibrinogen	Ca	5	0.358	0.420
Gelsolin G4- G6/Actin Complex	Ca	5	0.383	0.663
Cyclin A2 in complex with cell division protein kinase 2	Mg	5	0.417	0.509
*All 6 ligands are waters of hydration.				

**A COMPREHENSIVE MODEL FOR THE AVIAN MAGNETIC COMPASS.** K. A. Jenrow<sup>1</sup>, A. R. Liboff<sup>2</sup>. <sup>1</sup>Henry Ford Health Sciences Center, Detroit, MI 48202, <sup>2</sup>Center for Molecular Biology and Biotechnology, Florida Atlantic Univ, Boca Raton, FL.

In previous work (BEMS 21:555) it was shown that the avian optic tectum (TeO) is very likely capable of interacting with the horizontal component of the earth's magnetic field (GMF) and therefore serving as the site of the avian magnetic compass (AMC). This model has now been generalized to show that the TeO is organized to utilize the complete 3-dimensional GMF. The TeO consists of a series of lamina with a nearly hemispheric geometry. Radially-aligned neurons in the superficial lamina, which receive the primary retinal projection, exhibit gamma oscillations in response to visual stimuli, producing an oscillating (20-50 Hz) electric field  $E_r$  everywhere normal to the tectal surface. Transduction of the GMF within the TeO is hypothesized to involve electric field ion cyclotron resonance coupling between the GMF and  $E_r$ . It is further hypothesized that this resonance specifically involves the calcium ion, the only physiologically relevant ion for which resonance can occur over the entire GMF range. It is shown that such coupling results in symmetrical excitation regions, communicating both the inclination angle of the total field and the orientation of the head in relation to the field. These excitation regions are superposed upon the tectal map of visual and auditory space, presumably to be interpreted along with these other sensory data for navigational purposes. This is the first model to fully account for Wiltschko's evidence that the AMC functions as an inclination compass. It also explains other key factors observed in AMC studies: the failure of the AMC in the absence of a vertical field component, the dependence of the AMC on visual processing, and the relatively slow adaptation of AMC responsiveness to abrupt changes of GMF intensity.

**DYNAMICAL ENTRAINMENT OF THE NA/K PUMP MOLECULES BY SYNCHRONIZATION MODULATION ELECTRIC FIELD.** W. Chen. Univ of South Florida.

Large amounts of ATP molecules are expended by various pump molecules in the cell membrane to maintain ionic concentration gradients between intra- and extra-cellular fluids. The resultant electrochemical potential across the cell membrane is critical for many cell functions, including generating electrical signals, controlling cell volumes and providing energy to other transporters. Because many of these pump molecules are sensitive to the membrane potential, a pertinent question would be whether we can activate these pump molecules or control their functions using an electric field.

We studied the possibility of entrainment of the Na/K pump molecules by using an asymmetric 6-state model based on experimental results. The resulting voltage-dependence of the pump functions at physiologic conditions is consistent with experimental results. A synchronization modulation theory is developed to dynamically train the pump molecules and to activate their functions. Like training a group of soldiers, the first step to train the pump molecules is to synchronize them to work at the same pace by an oscillating electric field with a frequency close to the physiological turn-over rate. Then, a gradually increased field frequency can accelerate the pump rate in a step-wise pattern. The underlying mechanism is similar to that involved in electron synchronization accelerator. Our results showed that by this synchronized modulation, that pump functions can be activated exponentially as a function of the membrane potential. This study indicates that we should be able to train the pump molecules and to activate their functions by a well-designed oscillating electric field.

**INDUCTION OF CELL ACTIVATION PROCESSES BY LOW FREQUENCY ELECTROMAGNETIC FIELDS.** M. Simkó<sup>1</sup>, M. Olof Mattsson<sup>2</sup>. <sup>1</sup>Univ of Rostock, Institute of Cell Biology and Biosystems Technology, Division of Environmental Physiology, Albert-Einstein-Str. 3, D-18059 Rostock, Germany, <sup>2</sup>Cell Biology Laboratory, Dept of Natural Sciences, Örebro Univ, SE-701 82 Örebro, Sweden.

The aim of this paper is to present a hypothesis of a possible initial cellular event affected by exposure to ELF EMF, an event that is compatible with the multitude of effects observed after exposure. Based on an extensive literature review, we suggest that ELF EMF exposure is able to perform such activation by means of increasing levels of free radicals. Such a general activation is compatible with the diverse nature of observed effects. Free radicals are intermediates in natural processes like mitochondrial metabolism and are also a key feature of phagocytosis. Free radical release is inducible by ionizing radiation or phorbol ester treatment, both leading to genomic instability. EMF might be a stimulus to induce an "activated state" of the cell such as phagocytosis, which then enhances the release of free radicals, in turn leading to genotoxic events.

We envisage that EMF exposure can cause both acute and chronic effects that are mediated by increased free radical levels: 1. Direct activation of eg. macrophages (or other cells) by short-term exposure to EMF leads to phagocytosis (or other cell specific responses) and consequently, free radical production. This pathway may be utilized to positively influence certain aspects of the immune response, and could be useful for specific therapeutic applications. 2. EMF-induced macrophage (cell) activation includes direct stimulation of free radical production. 3. An increase in the lifetime of free radicals by EMF leads to persistently elevated free radical concentrations. In general, reactions in which radicals are involved become more frequent, increasing the possibility of DNA damage. 4. Long-term EMF exposure leads to a chronically increased level of free radicals, subsequently causing an inhibition of the effects of the pineal gland hormone melatonin.

Taken together, these EMF induced reactions could lead to a higher incidence of DNA damage and therefore, to an increased risk of tumour development. While the effects on melatonin and the extension of the lifetime of radicals can explain the link between EMF exposure and the incidence of for example leukaemia, the two additional mechanisms described here specifically for mouse macrophages, can explain the possible correlation between immune cell system stimulation and EMF exposure.

**ELECTROMAGNETIC FIELDS PROMOTE REGENERATION IN PLANARIA AND INDUCE BINDING OF INJURY-SPECIFIC FACTORS IN THE MAPKINASE CASCADE.** M. S. Geddis<sup>1</sup>, R. T. Ambron<sup>1</sup>, M. Blank<sup>2</sup>, R. Goodman<sup>1</sup>. <sup>1</sup>Dept of Pathology, Columbia Univ, New York, NY 10032, <sup>2</sup>Dept of Physiology, Columbia Univ, New York, NY 10032.

**Background.** The molecular mechanisms that govern the regeneration process in flatworms are just beginning to be identified, although the flatworm has been studied for more than 200 years. Planaria utilize a reservoir of embryonic stem cells that comprise up to 30% of all the total cells in the adult worm. These totipotent cells are scattered throughout the worm's body and are capable of giving rise to any other cell type. The regeneration of peripheral nerves following crush injury of sciatic nerve has been shown to be accelerated by application of electromagnetic (EM) fields. [Activation of injury-specific MAPKinase factors has been reported in *Aplysia* and mouse following peripheral nerve transection.]

**Objective.** We used this regenerative capability to determine whether, following injury, EM field exposures accelerate the process, elevating levels of the cytoprotective stress protein hsp70, activate ERKMAPK and phosphorylation of Elk1 and increasing serum response element binding (SRE).

**Methods. *Experimental and exposure protocol.*** Planaria (*Dugesia dorotocethala* Carolina Biological Supply Company) were bisected transversely. The length of the head and tail portion, from each Planaria was measured to the nearest half-millimeter and placed in numbered plastic 30mm Petri dishes with 10 ml of pond water. Individual head and tail samples (n=30) were sham exposed or EM field-exposed for 12 days to a 60 Hz sinusoidal signal at a field strength of 80 milligauss for one hour twice a day with a four hour interval between exposures. Growth was measured at time zero and at days 3,6,9 and 12. We defined  $\Delta$  as the growth, to the nearest half-millimeter, at each measured time point for each head or tail portion. Bar graphs plotted mean  $\Delta$  versus time for exposed and control portions for both heads and tails. For analytic comparison, we used contingency-table  $X^2$  tests to compare exposed and control portions. Protein, isolated from the head and tail samples at 0, 3, 6, 9 and 12 days, EM field-exposed and sham-exposed, was analyzed for hsp70 levels, activation of ERKMAPK and phosphorylation of Elk1 and binding of the serum response element. ***Electromagnetic field exposure system.*** Two exposure units maintained at 20-21oC provided simultaneous sham and experimental exposures using calibrated Helmholtz coils energized by a function generator. A digital ammeter measured the field intensity. Field parameters were monitored with a Hitachi V-1065 100MHz oscilloscope and a calibrated inductive search coil. Sham and active coils were each enclosed within Mu metal containers ~ 9 feet apart to minimize stray fields during EM field exposures. ***Antibodies and probes:*** the antibody to phosphorylated Elk1: Ab91 from New England Biolabs; the antibody to Elk1 and the serum response factor, the blocking phosphopeptide for Ab91 and the oligonucleotide containing the serum response element sequence from the c-fos promoter (nCCATATn) from Santa Cruz Biotechnology Inc.; anti- hsp70 from StressGen Inc. ***Temperature, Protein lysates, Protein kinase assays, Electrophoretic mobility shift assays, Western blots.*** As previously described in Lin et al. [J Cell Biochem (2001) 81:143)].

**Summary.** Short exposures to an 80 milligauss 60Hz sinusoidal EM field induced accelerated regeneration in Planaria that correlated with increased hsp70 levels. Furthermore, the injury-specific factors in the MAPKinase cascade were activated as indicated by phosphorylation of MAPKpp and ELK1 and increased binding of serum response element.

**Conclusion.** The regenerative ability of Planaria is accelerated by electromagnetic field exposure through activation of the MAPKinase pathway and increased hsp70 levels. These experiments suggest potential benefits in clinical application of electromagnetic fields for repair of peripheral nerves.

*{Acknowledgment: Supported by the Robert I. Goodman Fund.}*

**A NEURAL NETWORK MODEL TO EVALUATE RF EXPOSURE LEVEL FROM CDMA CELLULAR PHONE.** D. Won Kim<sup>1</sup>, S. Chan Kim<sup>2</sup>, K. Chang Nam<sup>1</sup>, C. Gyu Song<sup>3</sup>. <sup>1</sup>Dept. of Medical Engineering, Yonsei Univ College of Medicine, Seoul, <sup>2</sup>Graduate School of Biology & Information Technology, Hankyung Nat'l Univ, Ansong, <sup>3</sup>School of Electronics & Information Eng., Chonbuk Nat'l Univ, Chonjoo, Korea.

**OBJECTIVE:** To develop a neural network model to estimate RF exposure level from cellular phone and thus the individual risk of exposure by utilizing the available informations.

**METHODS:** The following factors were considered for the proposed model such as usage time a day, total years of usage, hands-free usage, antenna extraction or not, SAR of phone, and flip or folder. The weight of each factor was given from 0.1 to 1.0 for the neural network training. The proposed neural network model presents of RF exposure level from 0 to 10. Because the exposure level can be calculated by multiplying each factor's weight for a training purpose, the supervised method was used. The exposure level was obtained using a equation below.  $Exposure\ level = f(W \times p) + b$  W: weights obtained from neural network training p: factors influencing SAR b: input bias Considering every possible case for each factor, there are 800 cases (5x5x2x2x4x2)possible. For the neural network, six factors were used as input layers and Sigmoid function was used for decision function. Linear decision function was chosen to express the output layer of exposure level from 0 to 10. **RESULTS:** Implementation of the neural network was accomplished by Levenberg-Marquardt algorithm, which has the fastest training speed using MATLAB 6.5. Convergence of error into 0 was confirmed after 75th training. The time required for the 75th training using Pentium 4 (2.0 GHz, 512Mb) was 104 sec. Table 1 shows the various exposure levels determined by the neural network. The exposure levels in Table 1 were easily obtained by inputting each appropriate factor in the developed window. The final exposure levels were multiplied by 10. **CONCLUSION:** This proposed model would be quite helpful in providing quantitative exposure levels for cellular phone epidemiological studies regarding brain tumors.

Usage/day [hr]	Usage period [yr]	Hands-free	Antenna	SAR [W/kg]	Type	Exp. level
2.0	10	x	x	2.0	flip	9.9
2.0	6	x	x	2.0	flip	9.4
1.6	6	x	x	2.0	flip	8.7
1.6	6	x	x	1.3	flip	7.4
1.6	6	x	x	1.3	folder	4.4
0.8	4	x	x	1.3	folder	3.2
0.8	4	x	o	1.3	folder	1.6
0.1	0.5	o	o	1.0	folder	0.2

## ELECTROMAGNETIC FIELDS DO NOT INFLUENCE OSCILLATION FREQUENCIES OF THE BELOUSOV-ZHABOTINSKY REACTION. W. Sontag. no.

**Objective:** Physiological rhythms and oscillations are central to life. These rhythms (neuronal activity, beating of the hearts, glycolysis, NAD(P)H oscillations, cell cycle, circadian rhythms) arise from stochastic, nonlinear biological mechanisms interacting with a fluctuating environment (1). Disease is often accompanied by alterations of rhythms and it would be of great interest to influence such rhythms from outside of the body. As most of them are too complex and too difficult to measure continuously we have chosen a simpler model system. One of the simplest chemical oscillators is the so-called Belousov-Zhabotinsky (ZB) reaction. It was discovered in 1951 by Belousov and modified to the classic reaction by Zhabotinsky (2). It has been reported, that weak low frequency electromagnetic (EM) fields can affect the ZB reaction (3,4). **Methods:** The classical ZB reaction components - malonic acid, NaBr, NaBrO<sub>3</sub> and ferroin in a H<sub>2</sub>SO<sub>4</sub> solution – were used. The reaction was studied in a 5 ml glass tube placed in the centre of Helmholtz coils (90 mm diameter with 45 mm spacing). The applied EM fields were generated using a function generator (model 33120A, Hewlett-Packard). After addition of ferroin the oscillation started by changing the colour from red to blue and back. This colour change was recorded by measuring the transmission characteristic of a blue light-beam in the solution. The light was emitted by a blue diode and received with a photometer, which converted the light intensity into a proportional electrical signal. The digitised electrical signal was stored in a computer. The oscillation curves were analysed with a self-developed computer program and oscillation frequency calculated.

**Results and Discussion:** Several magnetic field applications have been used. a) The solution was exposed to 10, 20, 30, 40, 50 and 60 Hz at 1 mT. b) The solution was exposed to 50 Hz and different field strengths and wave forms. c) The solution was exposed to 60 Hz and field strengths from 0 to 500  $\mu$ T. d) The solution was exposed to 5  $\mu$ T in the frequency range of 0 to 1000 Hz, and e) The solution was exposed to 250 Hz and field strengths from 0 to 150  $\mu$ T. In no case any influence of the magnetic field application on the oscillation frequency of the Belousov-Zhabotinsky (ZB) reaction could be detected.

### References:

- (1) Glass, L. (2001) *Nature*, 410, 277.
- (2) Zhabotinsky, A.M. (1964) *Proc.Acad.Sci., USSR*, 157, 392.
- (3) Blank, M. and Soo, L. (2001) *J.Cell.Biochem*, 81, 278.
- (4) Blank, M. and Soo, L. (2001) *Bioelectrochemistry*, 61, 93.

## DRUDE-LORENTZ TREATMENT OF ION CYCLOTRON RESONANCE (ICR) PHENOMENA. C. Vincze<sup>1</sup>, A. Szasz<sup>1</sup>, A. R. Liboff<sup>2</sup>. <sup>1</sup>Biotechnics Dept, Szent Istvan Univ, Budapest, Hungary, <sup>2</sup>Center for Molecular Biology, Florida Atlantic Univ, Boca Raton, FL, USA.

The ionic resonance phenomena occurring in weak, non-stationary magnetic fields using Drude-Lorentz theory under the assumption of vanishing damping is examined in some detail. It is shown that ionic motion consists of both steady and periodic components. The steady ionic velocity contains a resonance-free Hall effect term while the other component includes resonance-dependent terms, one occurring at the cyclotron resonance frequency ( $\Omega$ ) and the other at subharmonics of  $\Omega$ . One interesting consequence of this formalism is that it subsumes the Bessel function solutions previously obtained by Lednev and by Blanchard, providing, however, an additional dependence on the applied frequency  $\omega$ , thereby enlarging

the possibilities for experimental verification beyond those connected merely to the functional dependence on magnetic field AC-DC ratios when  $\omega = \Omega$ . One additional conclusion resulting from this work is that in order to fully explain ion cyclotron resonance observations in biological systems it does not appear to be necessary to invoke resonance transitions between binding states in calcium-binding proteins or metallo-enzymes. The present treatment shows that ICR phenomena in biological systems are dependent on the AC magnetic intensity but not necessarily on high-frequency parametric transitions, thereby allowing one to explore a wider variety of underlying molecular explanations.

# Posters

## Poster Session A

9:45 - 11:45 am, O'Reilly Hall

Highlights by Ben Greenebaum, 9:30 – 9:45

**BIOELECTROMAGNETICS: JOURNAL UPDATE.** B. Greenebaum. Univ of Wisconsin-Parkside, Kenosha, Wisconsin 53141-2000, USA.

Comparative statistics for 2004 and prior years concerning manuscripts received and accepted, geographical and subject matter distribution, and review times will be presented at the meeting. Preliminary indications are that an all-time record number of 192 manuscripts were received in 2004, including 23 for a special issue containing presentations from the WHO-sponsored meeting in Istanbul on effects of fields on children. The 169 manuscripts that were not part of the special issue is also a record high. Preliminary figures show that submissions from outside North America (mostly from Europe and Asia, but including all continents but Antarctica) were about 76% of the total, up from 64% in 2003; North American submissions accounted for only 24%. For the first time, RF papers (47%) dominated, with ELF ones second (26%); DC and pulsed fields were each about 10%. At the meeting abstract deadline, excess pages bought by the Society had reduced the backlog at the publisher, but hard numbers on this and on changes in the typical length of the review cycle were not available at the abstract deadline. These will be presented at the meeting.

## Clinical Devices

P-A-1

**PRELIMINARY REPORT ON A RADIOFREQUENCY CONTROLLED DNA BIOSENSOR.** E. M. Bucci<sup>1</sup>, O. M. Bucci<sup>2</sup>, M. L. Calabrese<sup>2</sup>, G. d'Ambrosio<sup>2</sup>, R. Massa<sup>2</sup>, A. Messere<sup>3</sup>, G. Milano<sup>3</sup>, D. Musumeci<sup>1</sup>, G. Petraglia<sup>2</sup>, G. Roviello<sup>1</sup>. <sup>1</sup>CNR- Institute of Biostructures and Bioimaging, Naples, Italy, <sup>2</sup>Univ of Naples Federico II - DIET, Naples, Italy, <sup>3</sup>SUN– Environmental Sciences Dept, Caserta, Italy.

**OBJECTIVE:** The present work deals with the design, set up and preliminary testing of a new kind of biosensor remotely controlled by electromagnetic fields, able to identify selectively a target DNA sequence.

**METHODS:** The bio-sensor is made by a DNA duplex, complementary to a defined DNA target, which brings a metallic nanocrystal attached to one of the component strands. Upon radiofrequency excitation, the biosensor is switched to its active state and is able to bind to a potential DNA target; when the radiofrequency excitation is stopped, the biosensor goes back to its original state if the potential target is not fully complementary to the sensor, or is trapped in a different state if the target perfectly matches the biosensor coded sequence. The state of the sensor can be revealed by simple spectroscopic techniques. To incorporate a metallic nanocrystal into the DNA biosensor, a specially modified Thymine residue was used, which, upon conjugation to the nanocrystal, gave the modified thymine T\*. The biosensor,

consisting in two DNA strands of sequence T12 (strand A) and AT\*A12 (strand B\*) respectively was formed in solution as a duplex DNA (A/B\*).

A sample of A/B\* dissolved in bidistilled water was prepared in a quartz cuvette (HellMa, 0.1 cm) and supplemented with the strand B. An optically coupled cuvette was filled of bidistilled water. The cuvettes were inserted in a thermostated rectangular waveguide cavity (72 mm \* 33.8 mm \* 340 mm), coupled to the coax-adapter waveguide by means an inductive diaphragm, and excited by a pulsed 2.47 GHz radiation (15s on -15s off). Sample size (35 mm \* 10 mm \* 1 mm) and position (in contact with the short circuit) ensure a minimum interaction with the electric field and a satisfactory homogeneity of the magnetic field. The field distribution was evaluated numerically by using a commercial code (CST-Microwave Studio 3) and the coefficient of variation of the magnetic field resulted to be 0.27. The mean magnetic field intensity into the sample was deduced experimentally by measuring the Q factor of the loaded cavity by means a vector network analyzer. The temperature of the sample was measured during the exposures by means of a fiber optic thermometer. The DNA sample was examined by Circular Dichroism (CD) before and after the RF exposition, to detect conformational changes induced on the DNA by the RF.

**RESULTS:** Preliminary CD data evaluation indicates that the biosensor, albeit at low efficiency, may work. In particular, the CD spectra are different after the RF exposition, which can indicate at least a partial binding to the target DNA B by the sensor, which would be only possible if the RF are able to switch the sensor in its active state.

**CONCLUSIONS:** The experiments reported here are a first evidence that the designed biosensor might work. However, several aspects are currently being improved, concerning both the chemistry of the sensor (by changing the metallic nanocrystal from gold to magnetite) and the excitation apparatus (by increasing the RF power and by integrating directly into the apparatus an optical detector).

P-A-4

**STRAY RADIO-FREQUENCY RADIATION EMITTED FROM ELECTROSURGICAL DEVICES.** M. De Marco, S. Maggi. Dept of Medical Physics, Umberto I Hospital of Ancona, Ancona 60020, Italy.

**OBJECTIVES:**

Electro-surgery has worldwide been demonstrated to be simple to perform and beneficial for conventional surgical interventions. On the other side electro-surgical procedures are accompanied by a general increase of Electromagnetic field in operating room that may expose to relatively high levels of radio-frequency radiation (RF) both patients and personnel. Moreover it may also interfere with implanted cardiac stimulator (pacemakers) or any other life-support devices (such as monitors or ventilators).

This study is intended to evaluate the stray Electromagnetic radiation in an operating room due to therapeutic application of RF energy.

**METHODS:**

Electro-surgical generators are able to produce a variety of electrical waveforms; as they change, so will the corresponding tissue effects. Depending on frequency and wave modulation, peak-to-peak voltage and current delivered by the unit, the surgeon is able to obtain the desiderated effect.

In this study we have taken in count the RF radiation emitted from two different mono-polar electro-surgical devices (pure sinusoidal waves, nominal frequency of 330kHz for generator labeled #1 and of 390kHz for the other one). Measurements were recorded by the use of a broadband radiation meter with an isotropic B-field probe (cross-sectional area about 100 cm<sup>2</sup>). It were assessed Magnetic Field's (MF) peak value (in Amperes per meter) delivered by active electrode, and strayed from units and all other electro-surgical accessories (patient return plate, cables and forceps).

## RESULTS:

The next two tables present the data obtained; the first one refers to *Cutting Mode* while the other one to *Coagulation mode*. Data have been collected gradually increasing the power released by generators. Test has been than repeated after have increased peak-to-peak voltage. All data refer to MF's peak value.

Analyzing the data is easy to state that MF strength depends on generators' output characteristics: intensity changes slightly in proportion to theirs power output and it increases much more rapidly in proportion to theirs peak-to-peak voltage. This is particular evident comparing the data obtained at the same power output in Cutting mode (about 2300V) and Coagulation mode (more than 7000V).

The data also show that electro-surgical accessories much more than power units, present the highest values of MF strength; this is particularly evident near the return plate (worst case: 4 A/m) and near cables (1.8 A/m). These findings are consistent with the fact that disposable accessories generally have lower insulation level. Moreover we have demonstrated that overlapping them around the metal clip, as personnel usually do to reduce their length, enhances MF strength about 20%.

## CONCLUSIONS:

This study demonstrates that stray radiation emitted by the electro-surgical handle and active electrode never exceed ICNIRP's exposure guidelines; in the worst case surgeon's hands are exposed to a continuous and pulsed RF wave which MF strength is 0.6 A/m. However significant variations depend on the output characteristics of a generator that the surgeon sets to obtain the desired tissue effect. On the other side we have demonstrated that relatively high levels of exposure to RFs can occur to patient due to the return plate: it's mandatory to choose a location for its positioning that is close enough to the operative site and at the same time, farther away from any ECG electrodes or implanted devices. This study also demonstrates that every electro-surgical accessories, both power unit and cables, as a part of electric circuit become an RF source: to avoid possible interference and direct coupling with other electro-medical devices particular care must be spent in their positioning in operating room.

<b>Cutting mode</b>								
# 1	(1350 V)	Power (W)	Handle	Return plate	Power unit	@ 0.50 m		
		<b>80</b>	0.25	1.41	0.55	0.25		
		<b>120</b>	0.36	1.68	0.6	0.35		
		<b>180</b>	0.42	1.77	0.62	0.25		
	(2300 V)	<b>80</b>	0.46	2.75	0.8	0.5		
		<b>120</b>	0.55	3.05	0.9	0.5		
		<b>180</b>	0.6	3.21	1.1	0.8		
		Power (W)	Handle	Return plate	Power unit	@ 0.50 m	Cable	Loop </B>
# 2	(2000 V)	<b>100</b>	0.13	0.62	0.41	0.1	0.89	1
		<b>150</b>	0.17	0.65	0.39	0.1	1	1.2

		<b>200</b>	0.22	0.76	0.49	0.1	1.37	1.8
		<b>250</b>	0.23	0.9	0.5	0.15	1.4	1.9
	(2600 V)	<b>100</b>	0.18	1.11	0.6	0.21	1.39	1.65
		<b>150</b>	0.2	1.15	0.6	0.22	1.59	1.9
		<b>200</b>	0.25	1.3	0.67	0.22	1.75	2.2
		<b>250</b>	0.31	1.45	0.79	0.26	1.8	2.4

Table 1. MF strength released from generator #1 and #2 respectively. All data are expressed in Amperes per meter (A/m).

<b>Coagulation mode</b>						
		<b>Power (W)</b>	<b>Handle</b>	<b>Return plate</b>	<b>Power unit</b>	<b>@ 0.5 m</b>
# 1	(6900V)	<b>80</b>	0.45	4.5	0.5	0.45
		<b>120</b>	0.65	5.8	0.58	0.55
# 2	(7000V)	<b>80</b>	0.28	1.9	0.39	--
		<b>100</b>	0.22	2.22	0.44	0.2
	(7200V)	<b>80</b>	0.31	3.2	0.38	--
		<b>100</b>	0.29	3.8	0.4	0.2

Table 2. MF strength released from generator #1 and #2 respectively. All data are expressed in Amperes per meter (A/m).

## Dosimetry

P-A-7

**A NEW MULTICHANNEL HIGH RESOLUTION THERMOMETER FOR RADIOFREQUENCY DOSIMETRY.** L. Ardoino, V. Lopresto, G. Lovisolo, S. Mancini, R. Pinto. Bio-Tec Unit, CR ENEA Casaccia, Rome, Italy.

### Introduction

Radio-frequency and Microwave exposure produces heating of tissues which is, in general, proportional to the intensity of radiation. It leads that, in the research activities concerning the study of biological effects of radio-frequency, temperature measurements are an important and critical aspect at the same time.

The temperature measurement is important for two different aspects: measure of the temperature gradient for the experimental evaluation of SAR and the temperature monitoring during biological experiments to identify possible thermal effects.

These different targets lead different probes characteristics and requirements such as the high resolution for measuring SAR with good accuracy and the high thermal stability to monitor temperature during

experiments.

Therefore, an optimized probe for radio-frequency dosimetry, should satisfied the following requirements: very small size (1 or 2 mm section), very high temperature resolution, be unperturbed by RF/MW radiation and able to cause negligible field distortion, fast response, minimum thermal drift, and not easy to damage.

Not so many thermometer for RF dosimetry are commercially available: they, usually, have limited resolution and are almost expensive.

The aim of this work was the realization of an easy and low cost multichannel thermometer employing imperturbable probes with very high resolution.

## Materials and Methods

The complete system is constituted by four probes (but they can be much more), a specific circuit as interface, a DAQ card to transfer data to the computer and a dedicated software in Labview environment.

High impedance Vitek TP100 thermistors have been chosen for their suitable characteristics: they are, in fact, almost imperturbable, extremely flexible, showing a very good spatial and temperature resolution, good accuracy and stability. They are commercially available without any readout device.

First step of the job has been the thermistors characterization to know, for each probe, the impedance values in the temperature range of interest (15 C to 45 C). After that, a readout circuit has been designed: to avoid problems in stability and an over-heating of the probe which can determine a thermal drift, the thermistor is used as a simple, two-wire resistor variable with temperature, and the readout signal (voltage) is kept on a resistor in series with it. Of course, only highly stable components have been used. In this configuration, the device resolution depends on the voltage range determined by the excursion current produced by the thermistor and the resistor values (250 K $\Omega$ ): for our purposes, a resolution of 0,02 C has been accepted, but it can be improved increasing the output resistor value or adding an amplifier to the output signal.

A commercial DAQ card with high analog and digital resolution, is used as AD converter and for communicating with a computer. Setting, acquisition and post-processing are performed through a specific software. It includes the calibration section and two measurements sections, one for SAR measurements and the other for the experimental long monitoring.

The device has been calibrated with the aid of an high precision reference thermistor (Hart Scientific 1521) and a thermostatic water bath (Thermo Haake K10).

Due to the small fluctuation of the bath, the accuracy of the device resulted in 0,04 C, which is enough for our purposes.

Calibration has been performed with a 0,5 C step in the interval 15 - 45 C and a best polynomial fit is used to realize the calibration curve.

## Conclusions

A new easy and low cost temperature device has been designed and realized. In the present configuration, the device covers the range from 15 to 45 C with resolution and accuracy better than 0,1 C. It doesn't show any sensible thermal drift for several days, at any temperature value.

All commercially available components have been used, but they can be easily substituted by similar ones except for the probes.

Validation of acquired data and results has been performed comparing data with the theoretical model and with data obtained with a commercial thermometer (Luxtron), shown in Fig. 1.

## References

R.R. Bowman, A probe for measuring temperature in radio-frequency heated material. IEEE Trans on Microwave Theory and Technique 24: 43-45, 1976.

R.G.Olsen, R.R. Bowman, Simple nonperturbing temperature probe for microwave/ radiofrequency dosimetry. *Bioelectromagnetics* 10: 209-213, 1989.

A.A.C. De Leeuw, J. Crezee e J.J.W. Lagendijk, Temperature and SAR measurements in deep-body hyperthermia with thermocouple thermometry"; *Int. J. Hyperthermia* Vol.9 N.5: 685-697, 1993.

Figure2 - Picture of the complete system.

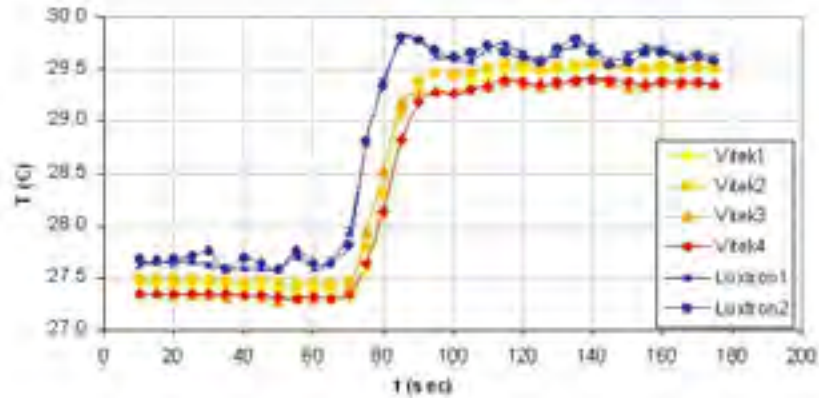
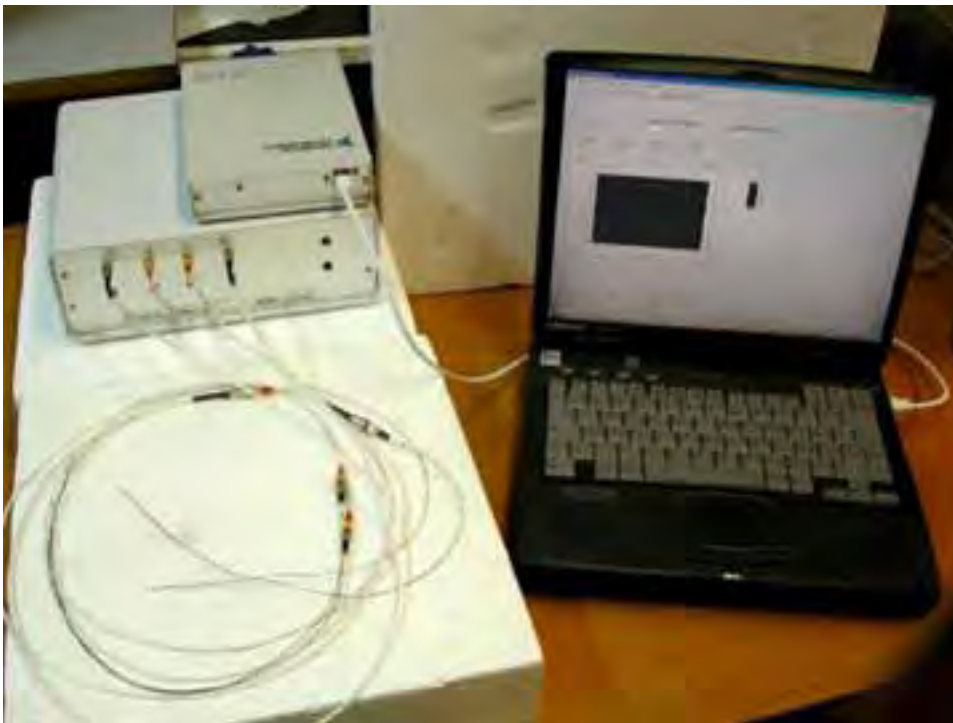


Figure1 - Comparison of data acquired with the new thermometer and a Luxtron dual-channel.



**THREE DIMENSIONAL VISUALIZATION OF THE TEMPERATURE DISTRIBUTION IN A PHANTOM FOR THE ASSESSMENT OF LOCALIZED EXPOSURE TO MICROWAVES.** M. Baba<sup>1</sup>, Y. Suzuki<sup>1</sup>, M. Taki<sup>1</sup>, K. Fukunaga<sup>2</sup>, S. Watanabe<sup>2</sup>. <sup>1</sup>Tokyo Metropolitan Univ, Tokyo, Japan, <sup>2</sup>National Institute of Information and Communications Technology, Tokyo, Japan.

**OBJECTIVE:** We have proposed a new method of specific absorption rate (SAR) measurement based on the visualization of three-dimensional (3D) temperature distribution by means of micro-capsulated thermo-chromic liquid crystal (MTLC) [1][2]. The objective of this paper is to report further developments of this method and to discuss application of this method to the assessment of local exposure especially of the microwaves and millimeter waves.

**METHODS:** Micro-capsulated thermo-chromic liquid crystal (MTLC) is used as a temperature sensor. The diameter of the capsule is about 20 to 30 micrometers and specific gravity is about 1.01g/cm<sup>3</sup>. When light is incident on MTLC, the wavelength of scattered light corresponds to the temperature of MTLC[3]. Therefore temperature of MTLC is visualized as the color of the scattered light. MTLC is suspended uniformly in the substance, such as liquid, gel, or solid. The substance needs to be transparent in order to allow observation of the scattered light. In our study we use  $\kappa$ -carrageenan $\pm$ , which forms gel and has high transparency. Complex permittivity of the carrageenan-based gel containing MTLC is adjusted to that of muscle at 1.45 GHz by mixing propylene glycol to use as a phantom. The visualized color is detected by a digital video camera. The camera which outputs uncompressed image data is used so that color of the image should be calibrated to a particular temperature. Color processing method adopted in this study utilizes H (Hue)-S (Saturation)-L (Lightness) color space that is transformed from RGB color space. The hue value basically represents the wavelength of the color and it is used as a calibration variable. We should note that the observed color or scattered wavelength and its intensity depend on the angle of measuring location

**RESULTS:** We have constructed correlation curves of hue versus temperature with its operating temperature range of 2, 5, and 10 degrees. The hue values are processed by a median filter with 6 x 6 pixels (0.9mm x 0.9mm). These curves show that hue and temperature have one-to-one correspondence.

**CONCLUSION:** We obtained calibration curves to relate the hue to the temperature. It enables quantitative measurements of temperature distribution. An improved temperature resolution is achieved by using MTLC with 2-degree temperature range and an uncompressed image camera. This method allows 3D measurement of temperature distributions with sufficient spatial resolution.

**DISCUSSION:** This method is applicable to the experimental studies to relate tissue temperature elevation with SAR and with incident power density in the microwave and millimeter wave region. Further studies are necessary to develop transparent phantom material with tissue equivalent electrical constants, and to analyze thermal properties of the phantom in comparison with those of human body.

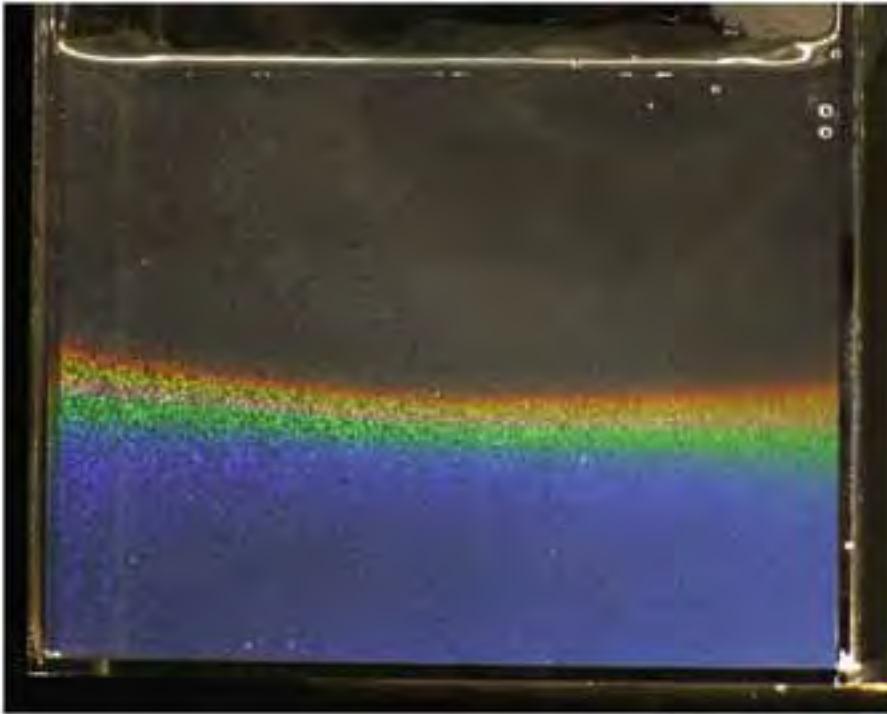


Fig.1 Temperature distribution is visualized when the phantom containing MTLC is heated from the bottom

#### References.

- [1] Y. Suzuki, et al. "Development of a transparency high molecular gel phantom for three-dimensional visualization of radio frequency electromagnetic power absorption with capsule thermo-chromic liquid crystal", 26th Bioelectromagnetic Society Annual Meeting, (2004)
- [2] M. Baba, et al.: "Visualization of Three-Dimensional Electromagnetic Power Absorption Using Gel Containing Capsule Liquid Crystal", 2004 International Symposium on Electromagnetic Compatibility (EMC '04 Sendai), (2004)
- [3] J. L. Fergason: "Liquid Crystals in Nondestructive Testing", Appl. Opt., vol. 7, pp. 1729-C1737 (1968)

P-A-13

**COMPUTATIONAL COMPARISON OF THE SAM PHANTOM TO ANATOMICALLY CORRECT MODELS OF THE HUMAN HEAD.** G. Bit-Babik, A. Faraone, C.K. Chou, M. Swicord. Motorola Florida Research Laboratories, Fort Lauderdale, FL. 33322. USA.

**INTRODUCTION:** The present compliance testing of mobile phones with respect to human RF exposure standards (IEEE C95.1-1999 *Standard for Safety Levels with Respect to Human Exposure to Radio Frequency Electromagnetic Fields from 3 kHz to 300 GHz* and *International Commission on Non-Ionizing Radiation Protection (ICNIRP) 1998 Guidelines for Limiting Electrical, Magnetic, and Electromagnetic Fields (Up to 300 GHz)*) relies on Specific Absorption Rate (SAR) measurements in the Specific Anthropomorphic Mannequin (SAM) exposed to the RF energy from handset under the test in predefined positions. The SAM phantom, as defined in the current measurement standards (*IEEE Std 1528-2003 and IEC 62209 Part 1-2005*), was developed to provide substantially conservative SAR

estimates. At the same time it is designed to be practical to simplify complex SAR measurement procedures. Recently, there have been concerns regarding conservative nature of the SAM phantom, in that measurements with SAM phantom could possibly underestimate the peak 1-g and 10-g average SAR values produced by the mobile handsets in the adult and child heads.

**OBJECTIVES:** The goal of this work was to compute SAR produced by the handset held next to the adult and child head models and compare it to the SAR values produced in the SAM phantom and thus determining conservativeness of the results obtained from current compliance measurement procedures. This work was also part of a broader study performed by 14 groups of researchers around the world to compare simulation results which also helped to check the robustness of the computational methodology employed.

**METHODS:** Computer simulations using the FDTD methodology were performed with two different head models. One head model was from the National Library of Medicine's visible man model which was further modified by the Air Force Research Laboratory (Brooks AFB, TX), another model was provided by Nagoya Institute of Technology (NIT), Nagoya, Japan. The Japanese head model was scaled down with non uniform scaling factors for different parts of the head to obtain the child head with representative anatomical properties. Exposure of those head models together with the SAM phantom model was simulated at 835 MHz and 1900 MHz using two different handset positions ("touch" and "tilt" compliance test positions). The SAR values produced in SAM phantom were compared to those produced in the head only tissues excluding the pinna, since pinna is subject to a different exposure limit (IEEE C95.1b-2004)

**RESULTS:** 1-g and 10-g peak average SAR values computed in SAM are higher than the corresponding peak values found in head only tissues of the adult and child head models at all frequencies and positions simulated in this study. The results further show that compliance with 1-g average SAR limit in SAM ensures compliance with 10-g average value in pinna (4 W/kg for 10-g average) for both adult and child head models used in this study.

**CONCLUSIONS:** SAR simulations of adult and child head models exposed to a handset at 835 MHz and 1900 MHz were performed. Comparison of those results with SAR values obtained for the SAM phantom have shown that SAM phantom is indeed a conservative model and is adequate for the compliance testing of mobile handsets with respect to RF exposure.

#### References:

- 1) Recommended Practice for Determining the Peak Spatial-Average Specific Absorption Rate (SAR) in the Human Body Due to Wireless Communications Devices: Experimental Techniques. IEEE Standard 1528-2003, IEEE, New York, 2003.
- 2) International Electrotechnical Commission (Iec), 62209/Fdis, Specific Absorption Rate (SAR) In The Frequency Range of 300 MHz TO 3 GHz – Procedure of Measurement
- 3) IEEE C95.1b-2004, Standard for Safety Levels with Respect to Human Exposure to Radio Frequency Electromagnetic Fields from to 3 kHz to 300 GHz. Amendment 2 Specific Absorption Rate (SAR) Limits for the Pinna.

P-A-16

**THE BROADBAND PIFA WITH MULTI-BAND FOR SAR REDUCTION.** D.-G. Choi<sup>1</sup>, N. Kim<sup>1</sup>, H.-S. Shin<sup>2</sup>. <sup>1</sup>Engineering of Information and Communication, Chungbuk National Univ, <sup>2</sup>Engineering of Electronics and Informaion, Gunsan National Univ.

OBJECTIVE: The broadband PIFA(Planar Inverted-F Antenna) mounted with the folder-type mobile

phone was designed to reduce SAR on the human head. The objective of this paper was to get the improvement of the bandwidth of PIFA and reduce the size of antenna and SAR. This paper proposed a novel broadband PIFA for IMT-2000/WLAN/DMB terminal.

**METHODS:** Two branch lines for meander line were utilized in order to improve the characteristics of PIFA which usually has a narrow band(as shown in Fig.1(a)). The shorting strip between the ground plane and meander-type radiation elements was used in order to minimize the size of the antenna. In order to design the PIFA and the phone, CST and SEMCAD(based on FDTD) were used. The simulated and measured values of 1 g and 10 g averaged peak SAR on human head were analyzed and discussed on the triple band PIFA mounted with folder-type handsets.

**RESULTS:** The measured -10 dB return loss bandwidth of a realized antenna was 38.2 % (1.84 GHz; 2.71 GHz), which contains the broadband bandwidth with triple band. (as shown in Fig. 1(b)). For the normalized input power to 1 W(conduction power at the feeding point), the 1 g peak averaged SAR caused by the simulated antenna was 1.09 [W/kg] and measured antenna was 0.61 [W/kg](as shown in Fig. 2).

**CONCLUSIONS:** In this study, the PIFA mounted on the folder-type mobile phone was deformed to the two branch lines for meander line antenna. The SAR distribution and other antenna characteristics are so variable as the change of the parameters for simulation. And we obtained the broadband property and the SAR reduction by this designed PIFA, respectively. As a result, the measured 1 g and 10 g averaged peak SAR values of PIFA were similar with the simulated values and were lower than the 1.6 W/kg and 2 W/kg of 1 g and 10 g averaged peak SAR limits.

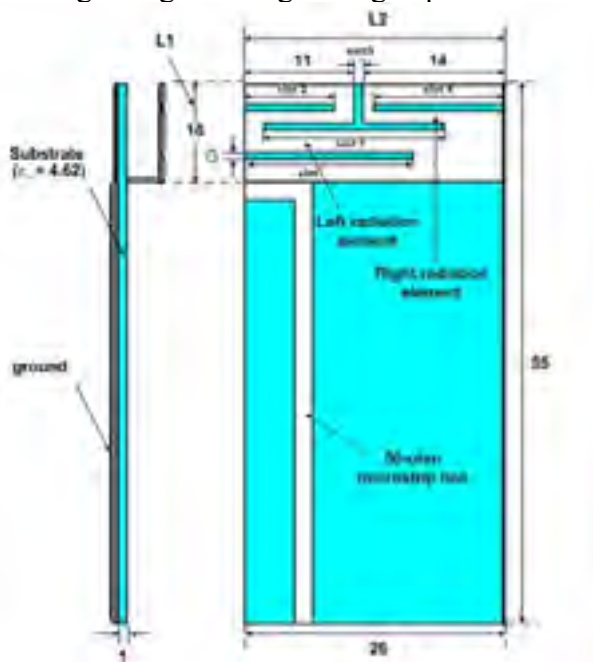


Fig. 1. (a) The structure of designed antenna.

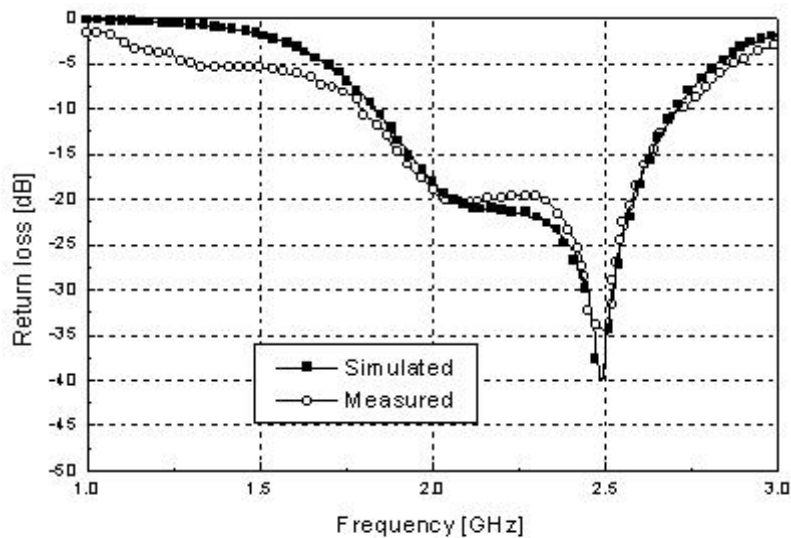


Fig. 1. (b) The return loss of designed antenna.

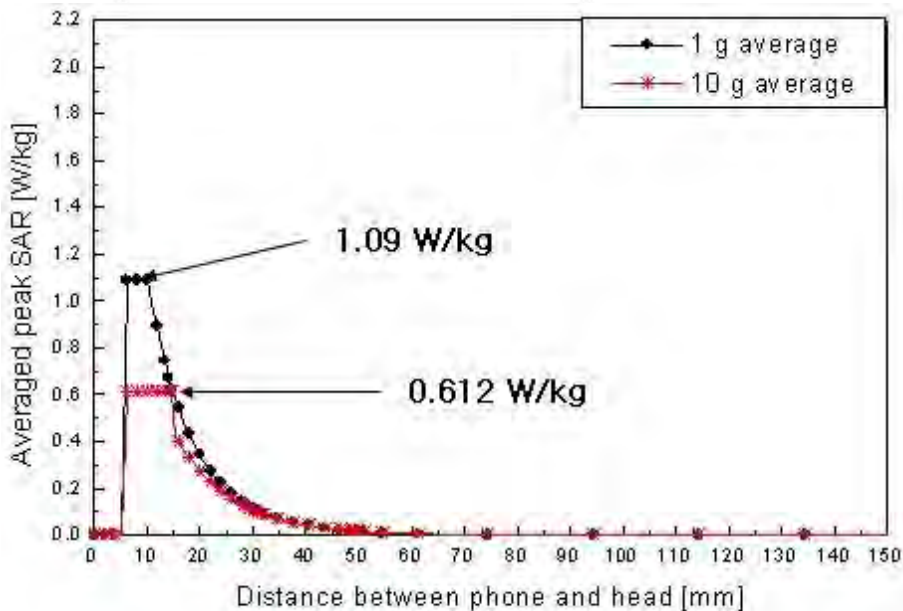


Fig. 2. Variation of peak SAR according to the depth of human.

P-A-19 STUDENT

**THE STATISTICAL TECHNIQUE FOR DOSIMETRIC POOLED ANALYSIS AT IN-VIVO AND IN-VITRO RESEARCH PAPERS ABOUT BIOEFFECTS OF RF ELECTROMAGNETIC FIELD.** S. ho Choi<sup>1</sup>, Y. Shin Kim<sup>1</sup>, S. Cheol Hong<sup>2</sup>, Nam Kim<sup>3</sup>. <sup>1</sup>Institute of Environmental and Industrial Medicine, College of Medicine, Hanyang Univ, Seoul, Korea, <sup>2</sup>Dept. of Occupational Health & Safety Engineering, College of Biomedical Science & Engineering, Inje Univ, Korea, <sup>3</sup>Dept. of Computer & Communication Engineering, Chungbuk National Univ.

Objectives: The objective of this study was to propose the estimating method of electromagnetic

dosimetric reliability at in-vivo and in-vitro experiments based on research papers related to bioeffects of RF electromagnetic field

Methods: For more accurate consequences of these researches, we have tried to find out any correlations among output power, power density and specific absorption rate(SAR) with the results of in-vivo, in-vitro research papers and SAR reports of cellular phone and PDA. We used 105 papers which was published from 1997 to 2003, submitted to WHO for EMF project and obtained 17 test reports from 14 SAR compliance test laboratory.

Results: In the case of in-vivo tests, the power density has close statistical correlations with SAR value and in the event of in-vitro tests, the output power has considerable statistical correlations with SAR containing duty factor. We analysed coefficients of determination to estimate the dosimetric uncertainty. The coefficient of determination at human tests was 45.5 %. This value was lower than 99.7 %, 89.9 %, coefficients of determination of in-vitro and in-vivo tests. The correlation and regression methods were used for statistical analysis.

Conclusions: Based on these results, we could estimate that the character of SAR measurement at human phantom has a high dosimetric diversity. If we use this method before evaluating techniques of measurement and analysis at both in-vivo and in-vitro experiments, we will conduct more accurate reliability test.

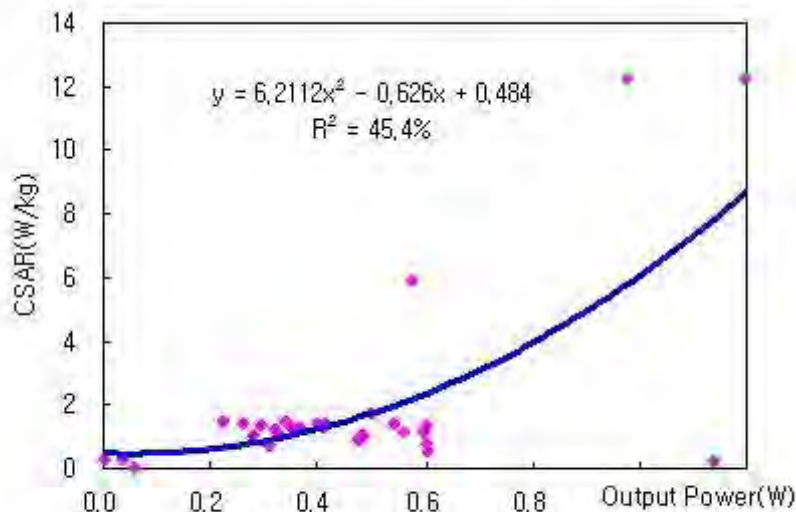


Fig 1. Fitted regression line for in vitro experiment between output power and CSAR.

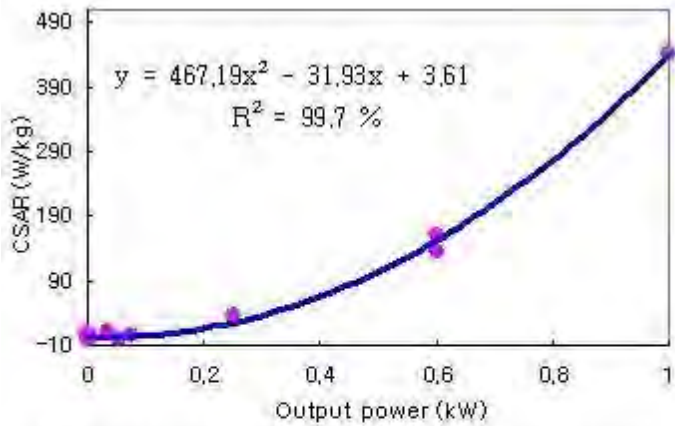


Fig 2. Fitted regression line for in vivo experiment between power density and SAR.

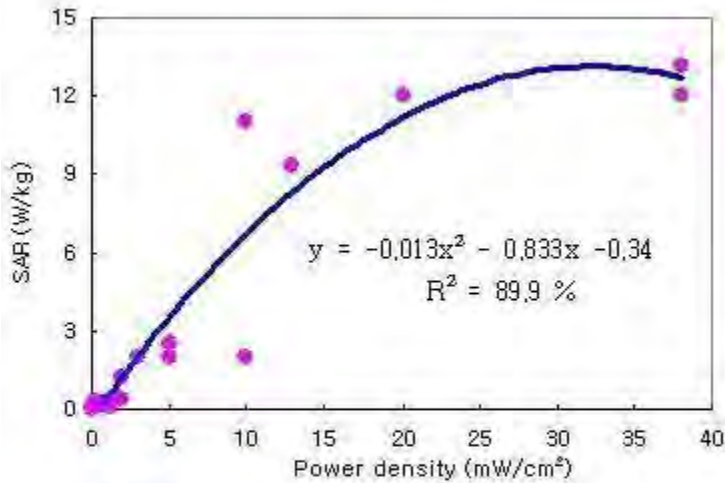


Fig 3. Fitted regression line for in vivo experiment between power density and SAR.

P-A-22

**SAR DISTRIBUTION IN CYLINDRICAL MOUSE MODELS IN A RADIAL CAVITY EXPOSURE SYSTEM.** C. J. East<sup>1</sup>, R. J. McKenzie<sup>1</sup>, R. L. McIntosh<sup>1</sup>, S. Iskra<sup>1</sup>, T. Kuchel<sup>2</sup>. <sup>1</sup>Telstra Research Laboratories, Clayton, Victoria, Australia, <sup>2</sup>Institute of Medical and Veterinary Science, Adelaide, South Australia, Australia.

**OBJECTIVES:** This study, using computational methods, seeks to investigate the distribution of SAR through differently sized mice (small pups, adults, and adults with fetuses) from 900 MHz GSM-type radio-frequency (RF) exposure in a 900 MHz radial cavity exposure system.

**BACKGROUND:** Previous studies [1] that have employed a radial cavity exposure system to consider the effects of RF exposure on mice, have used whole-body averaged SAR to describe the exposure [2, 3]. An in vivo study on wild-type mice at the Institute of Medical and Veterinary Science (IMVS) in Adelaide, Australia, is being performed to investigate neurobiological effects on the fetus, neonates and juvenile pups up to 10 weeks of age. The need to accurately describe the exposure in a small region of the mouse, the fetus, leads us to question the applicability of whole-body average SAR as the appropriate metric and to consider the distribution of SAR throughout the mouse. In particular, in [3] the thermographic results show that SAR is concentrated in the head, neck and shoulder, and abdomen, the latter being significant for foetal exposure. However, these variations are not quantified in the paper. Also, the so called "Ferris wheel" exposure system, designed by Motorola for IMVS, consists of parallel circular plates (480 mm in radius), joined on the perimeter by shorting posts, and centrally fed by a 50 ohm signal generator. The resultant cylindrical TEM wave aims to provide uniform plane-wave-type exposure to 40 adult mice all placed evenly in the system at a distance of 440 mm from the centre. The impact on the performance of this system when sparsely loaded with only neo-nates and young pups will also need to be considered.

**METHODS:** The computational modeling package XFDTD, from Remcom Inc., was used in this study. The exposure system, as discussed in [2, 3] was used as a basis for the model (the main difference being that the shorting posts were implemented in our model rather than approximated with a continuous sheet boundary). Forty homogenous cylinders, representing the mice, were placed evenly in the enclosure at a radius of 440 mm. Two separate mouse models have been used, one containing cylinders of 18 mm diameter and 30 mm length, and the other using cylinders of 36 mm diameter and 60 mm length, to simulate young pups and adult animals respectively. The mouse phantoms were given the dielectric values of  $\epsilon_r = 40$ , and  $\epsilon_{im} = 0.7$ . The cell size was uniform throughout the model with each cell side of length 1.5 mm. The system was excited using a 900 MHz sinusoidal source.

**RESULTS:** The field distributions for a single cylinder (36 mm by 60 mm) can be seen in Figure 1. It can be seen that the SAR varies by 6-8 dB across the cylinder, both length-wise and across. For the two cylinder dimensions used, very different field distributions have resulted. In Figure 2a (mouse pup) we see that the bulk of SAR is experienced on the leading edge of the cylinder, trailing off further in. However, for the case of the larger cylinder (adult) in Figure 2b, the trailing edge also receives considerable energy, with a null approximately 9 dB below maximum in the centre. Both cylinders see variations over a range of approximately 12 dB. Impact of the sparsely loaded chamber on performance of the system will be discussed following further assessment.

**CONCLUSION:** The results clearly indicate the non-uniform distribution of SAR in the adult mouse warrants more detailed investigation for the case of the exposed fetus. To progress this investigation it is proposed to use a scaled version of the complex tissue rat model available from Brooks US Air Force research facility.

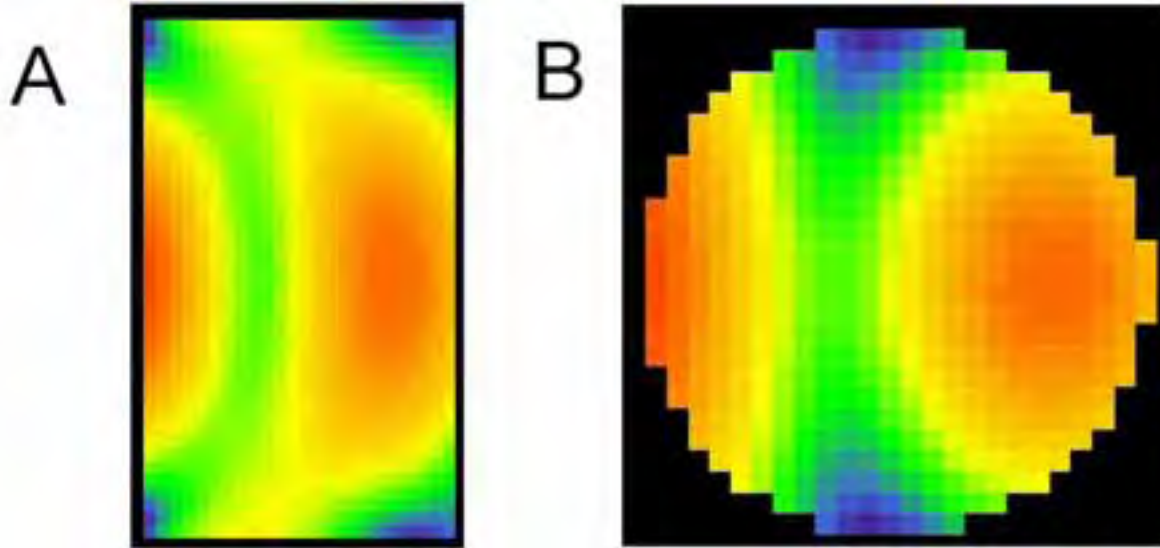


Figure 1. SAR distributions in central cross-sections of a 36mm x 60mm cylinder. (a) length-wise (b) across

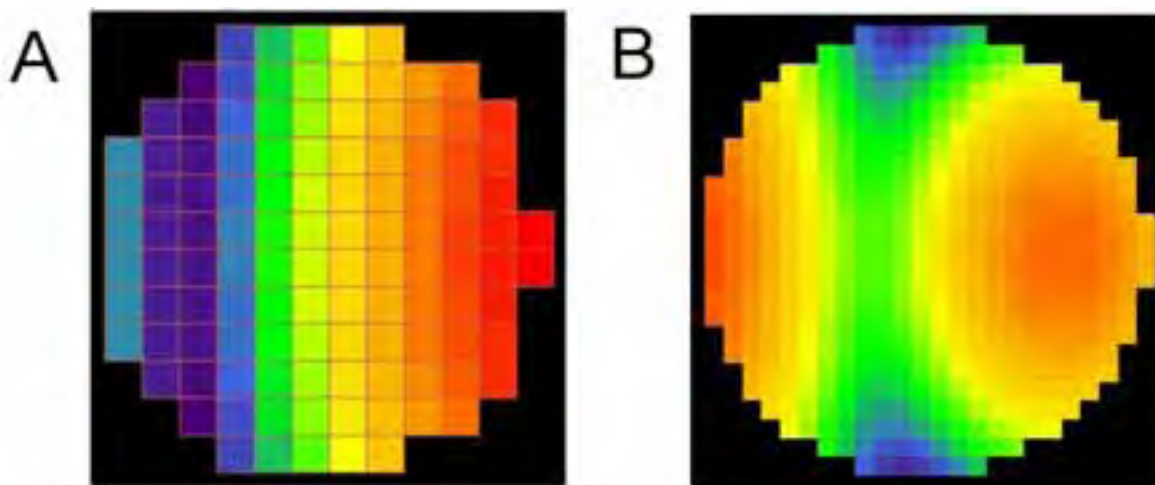


Figure 2. SAR distributions in different sized mice in the central plane. (a) mouse pup (b) adult



Figure 3. In all figures 0 db = 4 W/kg; dB. Figures not on same dimensional scale.

P-A-25

**DIELECTRIC MEASUREMENT OF SOLID LOSSY DIELECTRIC MATERIAL USING OPEN-ENDED WAVEGUIDE WITH IMPEDANCE MATCHING LAYER.** H. Ebara<sup>1</sup>, K. Tani<sup>2</sup>, D. Miki<sup>2</sup>, T. Onishi<sup>1</sup>, S. Uebayashi<sup>1</sup>, O. Hashimoto<sup>2</sup>. <sup>1</sup>NTT DoCoMo, Inc., 3-5 Hikari-no-oka, Yokosuka-shi, Kanagawa, 239-8536, Japan, <sup>2</sup>Aoyama Gakuin Univ, 5-10-1 Fuchinobe, Sagamihara-shi, Kanagawa, 229-8558, Japan.

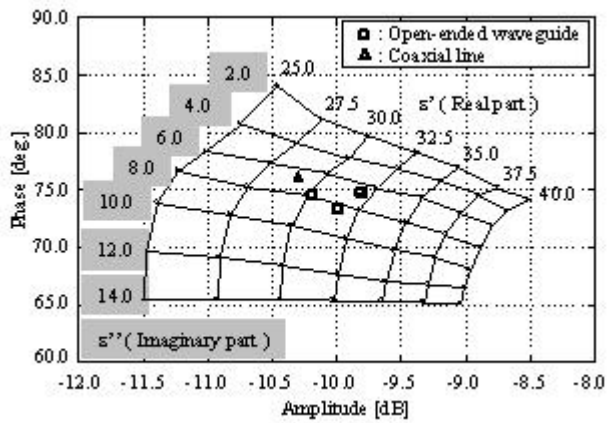
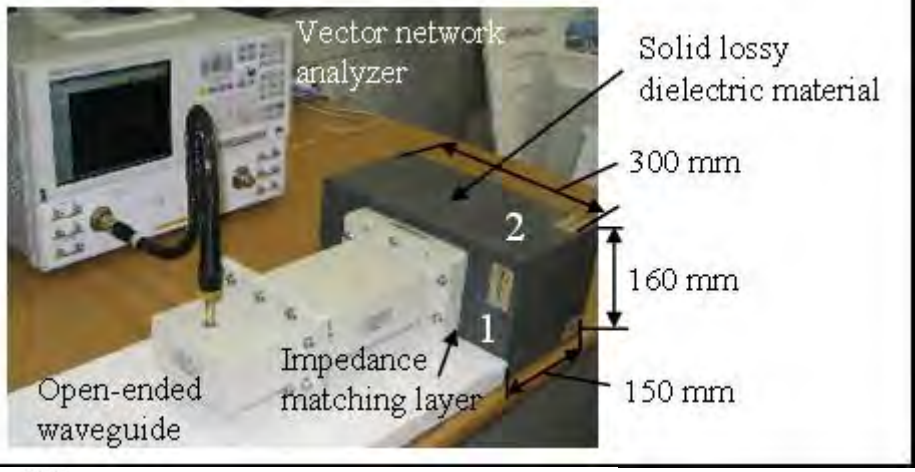
**INTRODUCTION:** The electric properties of a phantom, which is used in the Specific Absorption Rate (SAR) measurement related to mobile phones, are important. Liquid phantoms are adapted to the present standards and the complex permittivity is generally measured using the coaxial probe method. A SAR measurement method using a solid phantom is proposed in order to simplify the measurement [1]. It is also important to measure the complex permittivity of the solid phantom while retaining its configuration. Although a nondestructive dielectric measurement method for a solid phantom is required for that purpose, a method has not yet been established.

**OBJECTIVE:** The aim of this study is to establish a nondestructive dielectric measurement method for a solid lossy dielectric material, i.e., solid phantom. In this paper, a method using an open-ended waveguide with an impedance matching layer is proposed to measure the complex permittivity of the solid lossy dielectric material.

**MATERIALS AND METHODS:** The solid lossy dielectric material and the measurement configuration are shown in Fig. 1. When only an open-ended waveguide is attached to the surface of the lossy material with a high dielectric constant, the measured complex reflection coefficient changes little according to the variation of the complex permittivity of the material. Therefore, estimation on the complex permittivity of the material is difficult because measurement errors significantly affect the estimation accuracy. In order to overcome this problem, a low-loss dielectric material is placed between the end of the waveguide and the solid lossy dielectric material for impedance matching. The measured complex reflection coefficient drastically changes using this method because the condition of the impedance matching varies according to the variation of the complex permittivity of the material. The thickness of the low-loss dielectric material is determined so that the impedance matching is obtained using the transmission line theory. The permittivity charts representing the relationship between the complex reflection coefficient and the complex permittivity of a dielectric material are calculated using the FD-TD method according to the measurement configuration shown in Fig. 1. The complex permittivity of the solid lossy dielectric material is estimated by plotting the measured complex reflection coefficient at 2 GHz. In this study, the complex reflection coefficient is measured at each surface, for example, surfaces 1 and 2.

**RESULTS:** The permittivity chart using the impedance matching layer (thickness: 20 mm, complex permittivity:  $3.0 - j 0.1$ ) at 2 GHz is shown in Fig. 2. The calculated complex reflection coefficient exhibits significant change according to the variation in the complex permittivity. The averaged measurement results represented as squares are shown in the permittivity chart. The estimated complex permittivity is similar to the measurement results using the coaxial line method ( $29.1 - j 6.8$ ) represented by the triangle. The effectiveness of the proposed method is confirmed by these results. Further improvement of the measurement accuracy is the focus of future study.

**Reference** [1] Iyama et al., Mass-Averaged SAR Measurement in the SAR Estimation System Using Flat-Plane Solid Phantom, IEEE AP-S, June 2004.



**DEVICE FOR EXPOSURE OF INNER EAR HAIR CELLS TO RF SIGNALS.** A. El Ouardi<sup>1</sup>, T. Reinhardt<sup>1</sup>, J. Streckert<sup>1</sup>, A. Bitz<sup>1</sup>, V. Hansen<sup>1</sup>, J. Engel<sup>2</sup>, S. Münkner<sup>2</sup>. <sup>1</sup>Chair of Electromagnetic Theory, Univ of Wuppertal, <sup>2</sup>Institute of Physiology II, Univ Hospital Tübingen.

#### INTRODUCTION

This contribution reports about a new exposure set-up allowing the application of GSM and UMTS fields to biological cells stemming from the inner ear of mice in order to investigate possible influences of mobile communication signals on the auditory system. As an indicator for the performance of the inner hair cell system  $\text{Ca}^{2+}$ -ion flux through the cell membrane is measured with help of the patch clamp technique. Therefore, organ of corti from mice are prepared and kept in vitro in a dish with extracellular medium. Then a thin glass electrode filled with electrolyte is contacted to a single inner hair cell and the current due to Ca ions between the inner cell region and environment is measured.

#### REQUIREMENTS

The development of a suitable exposure equipments is a challenging task because some strongly contrary requirements have to be fulfilled: The distance between the microscope objective for the observation of cells and patch clamp electrode and the condensor lens for illumination is only some millimeters. Therefore a field with a vertical extension is in this range or even smaller is required. On the other hand a homogeneous field distribution over a sufficiently large area is necessary. The structure must be open for the patch clamp electrode and two tubes for perfusion, for the microscope objective from above and for the condensor lens from underneath. For all these components rather large openings must be foreseen. However, no radiation and no uncontrolled coupling to the metallic objects of the physiological equipment close to the exposure area shall occur. Altogether, the exposure field must be well-defined, stable and determinable with and without the biological target and it must be possible to perform a reliable calibration.

#### RESULTS

Our concept for this device is based on the creation of a concentrated field in the area of cells. This can be achieved for example with an extremely flat rectangular waveguide, or with a fin-line which is in principle a rectangular waveguide with two metal fins attached to the side walls. Both solutions are considered and a comparison of the essential characteristic and of the practical aspects for implementation like dimensions, field and SAR distributions, excitation, shielding effectiveness, insertion of samples etc. is performed in order to know which one is the more promising concept for matching the above discussed requirements.

Also a description of the total implemented system and details about the exposure signals will be given in the poster.

This study is part of a project supported by the Bundesamt für Strahlenschutz, StSch 4427: "Einfluss hochfrequenter elektromagnetischer Felder der Mobilfunkkommunikation auf Sinnesorgane A. Das Hörsystem".

**RF EXPOSURE ASSESSMENT USING A PERSONNEL DOSIMETER.** A. Gati, W. Man Fai, W. Joe. France Telecom RD.

Introduction: The extraordinary expansion of telecommunication networks to hold the growing demand on new mobile services induces a massive implantation of base stations antennas in urban areas. However, this development raises also public concerns about the potential health impact of the radio base stations and RF exposure in generally. For these reasons, recommendations have been outputted to limit the human exposure and to regulate the networks implantation.

Many programs are now conducted by local authorities as well as by the scientific community in different countries to inform people about their real exposure and to assess the EMF over a given period. These epidemiological studies need to perform several measurements over few hours in various situations to estimate the real exposure and the correlation between EM field strength and people behavior.

Large efforts have been done to assess the EMF exposure in accordance with measurement protocols which are under harmonization (cost 281, CENELEC, CEPT, IEEE .). The use of standard devices comprising spectrum analyzers and isotropic probes is not adapted for such studies. Therefore, personal and individual dosimeter devices that are easy to use are required to carry out this kind of measurements.

Objectives : In this paper, we present our personal dosimeter (PDM). This device was fabricated following the major requirements for epidemiological study in accordance with the measurements protocols. The PDM is a black box with a unique push button to perform frequency selective measurements comprising the most important broadcast bands. A tri axial probe is integrated to perform isotropic measurements. It is able to record thousands of measurement samples that can be loaded to perform statistical analysis.

The first step was the calibration regarding the measurement precision and the rejection between the bands. The results show a 1dB uncertainty at 66% confidence and a rejection bellow 40dB between the bands.

A first campaign was organized to compare the performances of the PDM compared with a classical in-situ measurements system. The results show a good agreement between the two traces. An average relative error of 30 % is observed in the worst case comprising the fast fading variations.

A second campaign is being performed to study the body influence depending on the operating frequency and the arriving direction of the waves. In fact, the tri orthogonal axes of the probe are oriented outside the body of the operator in the case of a holding situation. The first results show that the received signal is more variable but follow the same behaviour as those without a person near the device. The results have then to be statistically treated to draw out the significant values. To avoid these problems, a reverberation chamber is used to generate an all direction in a controlled environment. A phantom filled with an adequate equivalent liquid is then used to study the body influence on the PDM measurements. As a conclusion, the first results are very show a good agreement and will be presented.

**INFLUENCE OF THE EAR'S MORPHOLOGY ON SPECIFIC ABSORPTION RATE (SAR) INDUCED IN A CHILD HEAD USING TWO SOURCE MODELS.** A. Hadjem<sup>1</sup>, D. Lautru<sup>2</sup>, M. Fai Wong<sup>1</sup>, V. F. Hanna<sup>2</sup>, J. Wiart<sup>1</sup>. <sup>1</sup>France Telecom RD Issy les Moulineaux, <sup>2</sup>Universite de Paris VI.

**Introduction:**

Nowadays the wireless communications operators use more and more systems based on the transmission and reception of electromagnetic waves. On the other hand, the increases of children number using a mobile phone develop a many questions about the nature and degree of absorption of electromagnetic waves by this public class as a function of their age and their morphology. Objectives and methods:

This paper presents a study of the influence of the child ear morphology on the obtained SAR (Specific Absorption Rate) values. For this purpose, a comparison is performed between the different ear dimensions for the same head of a 12 years old child concerning the SAR and the power budget. The model that we employed is a real heterogeneous 12 years child head obtained from a 3D magnetic resonance image (MRI). This image is segmented to identify the various biological tissues, which form the human head. Once these tissues are identified, they are labeled in order to associate each tissue to its corresponding dielectric characteristics. The child head bounding box has a size of 175x205x241 mm<sup>3</sup> and the ear is contained in a parallelepiped of volume 18x39x59 mm<sup>3</sup>. The ear's dimensions are given in Table I. It worths mentioning that some differences can be observed between the ear dimensions in the 12 years age class. These differences have been studied and statistical characteristics (mean and standard deviation) have been published (Tab. I).

The different ear dimensions used in this study are given in Table II. Case 1 corresponds to an extreme compression of the ear while in case 5 no compression is applied (the normal ear of the child head). For the two operating frequencies of 900 MHz and 1800 MHz, the dielectric characteristics of human living tissues are not the same, but the tissue permittivities and conductivities are the same as those for the adult head. In each case, the head is exposed firstly to a dual band mobile phone having a patch antenna and secondly to a reference dipole. The results are obtained using an electromagnetic field solver employing the Finite difference Time Domain (FDTD) method. The source model is positioned close to the ear of the head. For each case of exposure, the absorbed power is calculated.

**Results:** It is found that the power absorption in the brain of the child head depends on the ear's morphology (auricle's dimensions and ear's width) and on the used source, while it remains at a weak level of exposure. No important differences are noted in the SAR over 1g in brain, in the case of a dipole at 900 MHz, between the different ear's dimensions, but when using a handset, the SAR values over 10g or 1g depend on the ear's morphology, and the positioning of the mobile with respect to the head.

It is important to put these results into their context and note that they are valid only for specific cases (specific model of source and child head with different ear's dimensions) and that the different models for the studied ears are built by deformation of a real ear of a 12 years old child.

EAR DIMENSIONS OF 12 YEARS OLD CHILD HEAD AND STATISTICS FOR THIS AGE CLASS			
Ear	Length of	Width of	Depth of
	the auricle (mm)	the auricle (mm)	the ear (mm)
12 y. old Child	59	33	10
head			
12 years	59,6 ± 3,6	35,3 ± 2,3	6 ± 4

age class			

P-A-40

**UNCERTAINTIES OF SAR-PROBE CALIBRATION AND OF SAR MEASUREMENT FOR COMPLIANCE TESTS OF CELLULAR PHONES (PART II).** L. Hamada<sup>1</sup>, Y. Miyota<sup>2</sup>, H.i Asou<sup>2</sup>, H. Kurokawa<sup>2</sup>, K. Satoh<sup>2</sup>, A. Suzuki<sup>3</sup>, T. Sugiyama<sup>3</sup>, S. Watanabe<sup>3</sup>, Yukio Yamanaka<sup>3</sup>, T. Shinozuka<sup>3</sup>, T. Iwasaki<sup>1</sup>. <sup>1</sup>Univ of Electro-Communications, Tokyo, 182-8585 Japan, <sup>2</sup>NTT Advanced Technology Corporation, Tokyo, 180-0012 Japan, <sup>3</sup>National Institute of Information and Communications Technology, Tokyo, 184-8795 Japan.

**INTRODUCTION:** In standard procedures for compliance tests of cellular phones, it is required to evaluate the uncertainties of specific absorption rate (SAR) measurement. Many uncertainty factors exist in the SAR measurement systems. Errors due to SAR-probe calibration are particularly significant because they directly affect the measured SAR values.

**OBJECTIVE:** In this study, some of the most important uncertainty factors were investigated, and evaluated uncertainties were compared with typical values described in international standard documents. The calibration factors of the different SAR-probes were compared, and uncertainties of the calibration factors due to deviations in the dielectric properties of the phantom liquid were evaluated. Frequency characteristics of the calibration factors were also investigated. Furthermore, uncertainties of SAR measurements for actual cellular phones due to the position of the devices under test and the frequency characteristics of the SAR measurements were investigated.

**METHODS:** To calibrate SAR probes, a well-known E-field must be attained in the phantom liquid. The SAR-probe calibration system consists of open-ended waveguides and a probe-scanning machine, as shown in Fig. 1. The waveguide is partitioned with a  $\lambda/4$ -matching slab, and the upper region is filled with the phantom liquid. The SAR probe to be calibrated is scanned along the center axis of the waveguide. Details of the calibration procedure are described in the standard procedures. The electrical properties of the phantom liquid were measured with an open-ended probe measurement system. The measured values of the electrical properties were maintained within  $\pm 1.0\%$  from the target values, while the standard procedures allow larger tolerance ( $\pm 5\%$ ). We investigated the effects of the electrical properties of the phantom liquid on the calibration factors with various electrical properties ranging from  $-10$  to  $10\%$  of the target values. Frequency characteristics of the calibration factors of a probe were also investigated. The calibration factors were evaluated at various frequencies up to  $\pm 10\%$  from the original calibration frequency. The electrical properties of the phantom liquid were adjusted to the target values at each frequency, which was determined by interpolation between the reference values. In order to investigate the dependence of the maximum local SARs, averaged over any 10-gram region of the head phantom, on the position of cellular phones under test, several types of cellular phones were tested, including different communication systems such as PDC and CDMA. Each cellular phone was set at the standard position, defined as the "cheek position". The phone was then slightly moved to the direction along the Front- Neck (FN) or Back-Mouth (BM) line, as shown in Fig. 2. The angle of the phone to the

head phantom was also slightly changed, as Fig. 2 shows. The maximum local SARs averaged over any 10-gram region were measured between the lowest and highest frequencies to be operated in actual services.

**RESULTS:** Various SAR probes were calibrated with the waveguide systems. Some of the SAR probes had significantly large variation (over 1 dB) in the calibration factors between the three sensors. It was also shown that the dependences of the calibration factors on the electrical properties and on frequency are relatively small (less than 0.2 dB typically). In the standard procedure, the typical uncertainty of the SAR-probe calibration is estimated to be 4.8%(0.2 dB). Our results suggest that the uncertainty of the SAR-probe calibration could be higher than the typical value in the worst cases. Further investigations are therefore necessary to establish the SAR-probe uncertainty.

In addition, it was shown that the deviation in the maximum local SARs due to the slight shift of the position and of the angle of the phones under test could be over 1 dB. The deviation was smaller along the FN line than along the BM line. This is because the curvature along the FN line was larger than that along the BM line. Consequently, shifting the cellular phones along the FN line resulted in less change in the distance between the cellular phones and the surface of the head phantom. This value of the deviation was significantly larger than the typical value, 6%or 0.25 dB, described in the standard procedures as "Test Sample Positioning". Because the typical value has been evaluated using statistical procedures as a TYPE-A uncertainty, it is necessary to increase the number of tested devices. It was furthermore shown that the maximum local SARs can vary by more than 1 dB within the operating frequency bands.

**CONCLUSIONS:** The results obtained in this study support the recommendation described in the standard procedures: the lowest and highest frequencies as well as the center frequency should also be tested when measuring SARs. Many uncertainty factors are included in SAR measurement and the effect of these is very complex. Our results suggest that the dependence of the uncertainty factors can be categorized with some key characteristics, e.g. the position of the maximum local SAR and the operating frequency bands. Although it is not easy to establish the uncertainty of SAR measurement, radio-frequency safety authorities urgently require it. International cooperation is therefore effective, and should be encouraged.

#### References

- [1] IEEE, Std 1528-2003: IEEE Recommended Practice for Determining the Peak Spatial-Average Specific Absorption Rate (SAR) in the Human Head from Wireless Communications Devices: Measurement Techniques, Dec. 2003.
- [2] Association of Radio Industries and Businesses (ARIB) in Japan, STD-T56 Ver2.0: Specific Absorption Rate (SAR) Estimation for Cellular Phone, Jan. 2002.
- [3] IEC, 106/61/CDV: Procedure to measure the Specific Absorption Rate (SAR) in the frequency range of 300 MHz to 3 GHz. Part 1: hand-held mobile wireless communication devices, Aug. 2003.

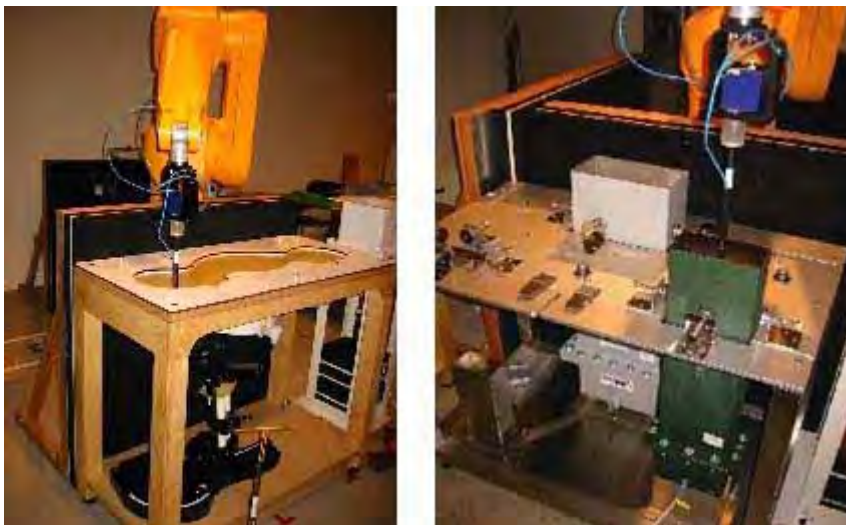


Figure 1: SAR measurement system for cellular-phone compliance tests (left) and SAR-probe calibration system (right).

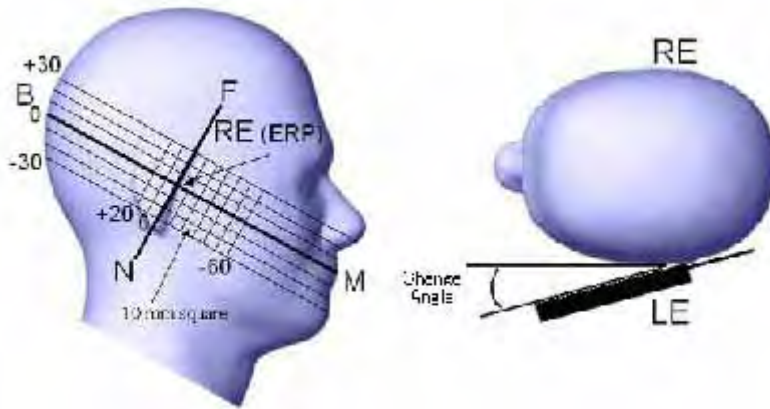


Figure 2: FN and BM lines on the head phantom (left) and angle of the cellular phone to the head phantom (right).

P-A-43

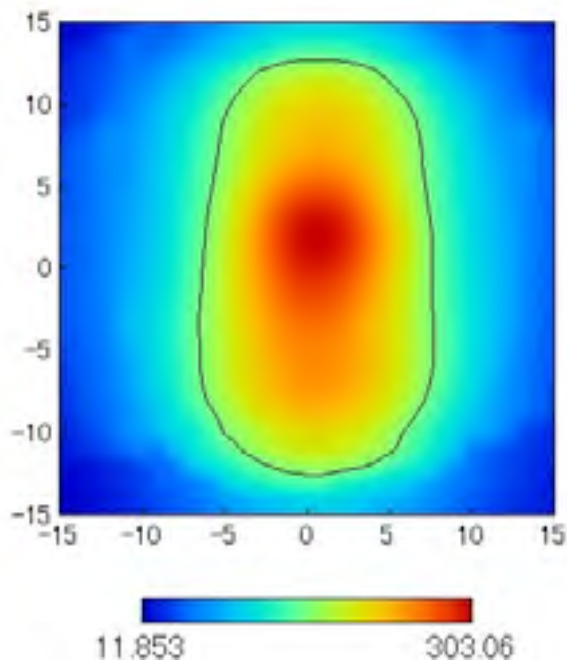
**ANTENNA MEASUREMENT FOR MILLIMETER-WAVE EXPOSURE SETUP.** M. Hanazawa<sup>1</sup>, T. Konno<sup>1,2</sup>, R. Kumahara<sup>1,2</sup>, K. Wake<sup>1</sup>, S. Watanabe<sup>1</sup>, M. Taki<sup>3</sup>, H. Shirai<sup>2</sup>. <sup>1</sup>National Institute of Information and Communications Technology, <sup>2</sup>Chuo Univ, <sup>3</sup>Tokyo Metropolitan Univ.

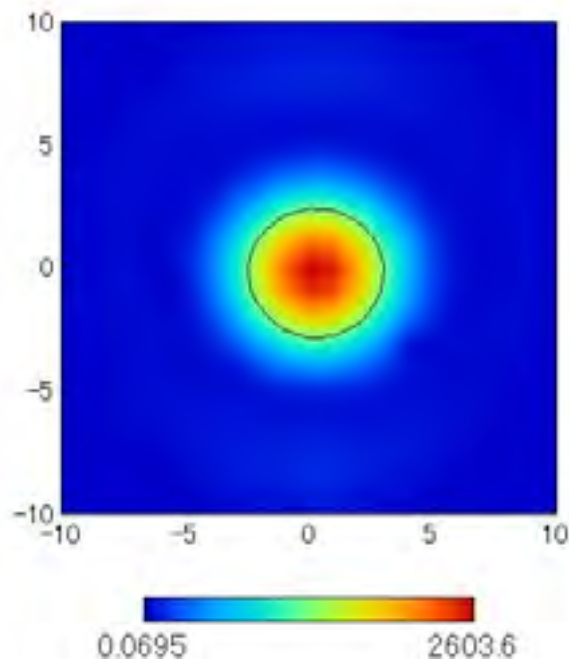
**INTRODUCTION:** Recently, millimeter-waves are being utilized for commercially available systems such as a wireless LAN (Local Area Network), automobile radar and the other applications. It is necessary to increase our biological knowledge for effects of millimeter-wave exposure. The object of this study was the development of exposure setup for rabbit eyes at 60 GHz band.

**OBJECTIVE:** We measured characteristics of a conical horn antenna and a lens antenna, and compared power distributions between those antennas to clarify their characteristics in practice use.

**MEASUREMENT METHOD:** Millimeter-wave generators are based on IMPATT (Impact-Avalanche and Transit-Time) oscillator. The millimeter-wave signal is delivered from the generator to an antenna under test (AUT) through a wave-guide circuit. A directional coupler and a dual-channel power meter monitor the forward power and received power of an open-end wave-guide as a probe. The probe mounted on a three-axis mechanical stage and move to each axis. Additionally, frequency and forward power were set to 60 GHz and 1W respectively.

**RESULTS AND DISCUSSION:** Figures 1 and 2 show measurement results of power distribution of a conical horn antenna at 2 cm from the aperture and of the lens antenna at the focus point (15cm form the aperture). In these figures, black line indicated  $-3$ dB down width of max power. As a results, the  $-3$  dB down width of the lens antenna at focus point was almost same size of rabbit eyes and power distribution of the lens antenna at focus point was about eight times that of the horn antenna at 2 cm from the aperture. We found that the lens antenna could be localized to rabbit eyes with high power distribution.





P-A-49

**INFLUENCE OF SAR AVERAGING SCHEMES ON CORRELATIONS BETWEEN MAXIMUM TEMPERATURE INCREASES AND PEAK SARs.** A. Hirata<sup>1</sup>, M. Fujimoto<sup>1</sup>, J. Wang<sup>2</sup>, O. Fujiwara<sup>2</sup>, T. Shiozawa<sup>3</sup>. <sup>1</sup>Osaka Univ, <sup>2</sup>Nagoya Institute of Technology, <sup>3</sup>Chubu Univ.

In recent years, there has been an increasing public concern about the health implications of electromagnetic (EM) wave exposure with the use of mobile telephones. Therefore, various public organizations throughout the world have established safety guidelines for EM wave absorption. For RF near field exposure, these standards are based on the spatial peak SAR (specific absorption rate) for any 1 or 10g of body tissue. Incidentally, note that a different averaging scheme is used for each guideline. However, physiological effects and damage to humans by EM wave exposures are induced by temperature increases. A temperature increase of 4.5 oC in the brain has been noted to be an allowable limit which does not lead to any physiological damage (for exposures of more than 30 minutes). Additionally, the threshold temperature of the pricking pain in skin is 45 oC, corresponding to the temperature increase of 10-15 oC. In view of these circumstances, the temperature increase in the anatomically-based human head model for exposure to EM waves from handset antennas has been calculated in several works. In [1], we have revealed that maximum temperature increases in the head and brain are reasonably proportional to peak SARs in these regions. The shape of volume for calculating peak SAR used in [1] was cube. Note that peak SAR is averaged over 10g of contiguous tissue in the ICNIRP guideline or tissues in the shape of a cube with a detailed regulation in the IEEE guideline.

This paper investigates statistically the maximum temperature increases in the head and brain for the SAR averaging schemes prescribed in the ICNIRP and IEEE guidelines. It should be noted that there are two major differences between two averaging schemes. One is the number of tissues taken into account. The other difference is the shape of averaging volume. In order to clarify these effects on the correlation,

a new averaging scheme is introduced. The maximum temperature increases in the head and brain are quantified and compared for the three averaging schemes.

#### Reference

[1]A. Hirata and T. Shiozawa, "Correlation of maximum temperature increase and peak SAR in the human head due to handset antennas," IEEE Trans., vol.MTT-51, pp.1834-1841, 2003.

P-A-52

**THE SPECIFIC ANTHROPOMORPHIC MANNEQUIN (SAM) COMPARED TO 14 ANATOMICAL HEAD MODELS USING A NOVEL DEFINITION FOR THE MOBILE PHONE POSITIONING.** W. Kainz<sup>1</sup>, A. Christ<sup>2</sup>, T. Kellom<sup>1</sup>, S. Seidman<sup>1</sup>, N. Nikoloski<sup>2</sup>, B. Beard<sup>1</sup>, N. Kuster<sup>2</sup>. <sup>1</sup>U.S. Food and Drug Administration (FDA), Center for Devices and Radiological Health (CDRH), Maryland 20906, USA, <sup>2</sup>IT'IS - The Foundation for Research on Information Technologies in Society, 8004 Zurich, Switzerland.

This paper presents new phone positioning definitions to obtain reproducible results in numerical mobile phone dosimetry and a new type of simple, but realistic, mobile phone model. Numerous numerical dosimetric studies have been published about the exposure of mobile phone users with conflicting conclusions. Many of these studies lack reproducibility due to shortcomings in the description of the mobile phone positioning.

By specifying three points on the anatomical model, EECL (entrance to ear canal left), EECL (entrance to ear canal right), and M (Mouth Point) it is possible to find an unambiguous definition for the phone position. With this definition it is possible to reconstruct the mobile phone positioning on the anatomical head. Using only anatomical landmarks on the head the phone position is independent of the original orientation of the head relative to the computation grid. It is not necessary to align the head with the computation grid before defining the phone position. The phone positioning definition is applicable to all shapes and sizes of pinna on anatomical models.

For most of the published studies, comparing SAM to anatomically correct head models, a metal box with monopole or helix antenna was used as the mobile phone model. Such a model is not an accurate model for modern mobile phones. Chavannes (2003) modeled a real world mobile phone using the original Computer Aided Design (CAD) files and obtained excellent agreement with measurements. Based on Chavannes' work we modeled the mobile phone as a flat metallic plate, representing the printed circuit board (PCB), inside a plastic box and a monopole antenna. This mobile phone model was discussed with members of the MMF (Mobile Manufacturers Forum) and found to be a more realistic and better approach for a mobile phone model than the outdated metal box phone model.

We used the new mobile phone positioning definition and the new mobile phone model to compare the specific absorption rate (SAR) for SAM to the SAR for 14 different anatomically correct head models at 835 MHz and 1900 MHz in 2 different phone positions, cheek and tilted. We used 2 different software packages, XFDTD and SEMCAD, and 2 of the 14 anatomical head models were calculated in both packages. The results of the peak spatial 1g and 10g average SAR obtained for SAM show less than 0.5 dB difference between the results independently assessed with XFDTD and SEMCAD. We also built a physical model of the mobile phone used for the computational study and measured the SAR in the SAM phantom. The agreement between computational results and with the measurements is better than 1dB. This is acceptable in view of the difficulties in obtaining a good experimental representation of the

numerical phone model. As expected the deviations are larger for the anatomical phantoms. This is due to the high sensitivities of slightly different positioning of the phone in such close proximity of the head. In general the differences are around 1 dB with a maximum of 1.2 dB. Without an unambiguous definition of the mobile phone position the differences would be much larger between XFDTD and SEMCAD.

The pinna peak spatial SAR for two anatomical correct head models of children's heads was found up to 2.1 times the current safety limit. Relaxing the SAR limit for the pinna as proposed in the latest draft for C95.1 will diminish this situation. A clear relation between the head size and the SAR can not be established because too many other factors (e.g. pinna size, pinna shape, head shape) have influence on the peak spatial SAR. The 14 head models used in this study do not represent all possible head shapes, pinna shapes, pinna sizes, anatomical differences of the head, pinna compression due to the mobile phone, etc. for all possible mobile phone users; but they give an overview on how these different head models compare to SAM. Considering the uncertainty of the measurement and the computations, SAM can be seen as conservative for head only tissue, excluding the pinna, for the 14 different head models used in this study.

For near-field electromagnetic radiations, a small change in the mobile phone positioning can lead to dramatic change in the calculated SAR. Therefore, the novel phone positioning definition will help researchers to compare their mobile phone positioning accurately. The use of the three anatomical landmarks (EERC, EECL, M) to unambiguously define the phone positioning have only been applied for the cheek and the tilted position. However, the same definitions can be applied to describe any position of the phone next to head, such that the results can be fully reproduced. Since the SAR estimation using SAM will not change soon and it is unclear if ICNIRP will also relax the pinna exposure limit, the future will reveal if the pinna relaxation of the new C95.1 standard can resolve the ongoing conflict about conservative SAR estimation using SAM.

The opinions and conclusions stated in this paper are those of the authors and do not represent the official position of the Dept of Health and Human Services. The mention of commercial products, their sources, or their use in connection with material reported herein is not to be construed as either an actual or implied endorsement of such products by the Dept of Health and Human Services.

Chavannes N, Tay R, Nikoloski N and Kuster N 2003 Suitability of FDTD based TCAD tools for RF design of mobile phones IEEE Antennas and Propagation Magazine 45 52-66

P-A-55

**THE FUTURE OF ANATOMICAL MODELS - ANATOMICAL CAD MODELS FOR NUMERICAL DOSIMETRY AND IMPLANT EVALUATIONS.** W. Kainz<sup>1</sup>, S. Seidman<sup>1</sup>, R. Qiang<sup>2</sup>, J. Chen<sup>2</sup>. <sup>1</sup>U.S. Food and Drug Administration (FDA), Center for Devices and Radiological Health (CDRH), Maryland 20906, USA, <sup>2</sup>The Univ of Houston, Dept of Electrical and Computer Engineering, Texas 77204, USA.

This paper discusses problems associated with existing voxel-based anatomical models for 3D electromagnetic (EM) computational dosimetry. As a solution, we propose replacing them with anatomical Computer Aided Design (CAD) models and present working examples.

Currently, a variety of anatomical models are available for numerical dosimetric analysis for EM. Up to now all available anatomical models are voxel-based. The body, or parts of the body, is represented by small cuboids, usually cubes, varying in size from 0.5 mm to 10 mm. The most common basis for anatomical models is the image data set from the Visible Human Project of the National Library of Medicine, USA. Several groups used this data set to develop an anatomical voxel model. Other groups developed similar voxel models based on their own Magnetic Resonance Imaging (MRI) or Computer Tomography (CT) data. All commercially available models are based on the visible human data set. Voxel-based models have several disadvantages: 1. decreasing the voxel size does not increase the anatomical resolution, 2. re-meshing is necessary to use graded meshes, 3. the data format is not standardized, which makes it difficult to import the datasets in different EM simulation software, 4. different organs are not defined by smooth surfaces, which is important for thermal and blood flow simulations, 5. scaling the whole anatomical model or individual organs is difficult, and 6. changing the posture or shape of the model, or an individual model part, is very difficult.

A proposed solution is to use CAD-based anatomical models. Instead of representing anatomical structures as a composition of voxels, CAD objects can define individual organs. All modern simulation software imports CAD data in different standardized formats (e.g. SAT, STEP, IGES, STL, etc). The main advantages of anatomical CAD models are: 1. every organ or the whole model can easily be scaled, 2. boundaries of the organs are well defined by a smooth surface for thermal and blood flow simulations, 3. the model can be meshed in any resolution as needed, 4. because the model will be meshed for each EM simulation graded meshes need no re-meshing, 5. tissue with the same electrical properties can be combined in groups, 6. data formats are standardized and can be translated into other formats, and 7. the posture of the model can be changed using existing CAD software. For the meshing process it is important that the surfaces have no holes or gaps (which is called "watertight"), representing solid objects, otherwise the meshing procedure will usually fail.

We developed several CAD models based on commercially available CAD data, laser scanned humans and MRI images of humans. Our first generation of anatomical CAD models is based on models commercially available from 3DSpecial ([www.3dspecial.com](http://www.3dspecial.com)). 3DSpecial based the development of their anatomical CAD models on anatomical pictures. Each organ is defined by an individual CAD object. Because the commercially available models were developed for visualization purposes, the surfaces were not watertight and, therefore, can not be used directly for meshing. In order to make the objects mesh-able we had to generate watertight surfaces by filling all holes in the objects. The final mesh-able data sets, developed in STL and SAT formats, were imported and tested in two different EM simulation packages: XFDTD and SEMCAD. Models for a child, an adult female and an adult male each represented by 58 CAD objects are available. These models will be provided with the new IEEE Standard C95.3a "IEEE Recommended Practice for Measurements and Computation of Electric, Magnetic and Electromagnetic Fields with Respect to Human Exposure to Such Fields, 0 - 100 kHz." Meanwhile 3DSpecial improved its models by developing CAD objects for each individual muscle. Also organs were improved and new organs were added. We purchased these models and generated mesh-able models for a female and a male. These two new models consist of 320 CAD objects. Meshing of these new models was tested for SEMCAD and XFDTD.

For a different project we developed a CAD model based on the laser scan of a woman in her 34th week of pregnancy (see figure 1). We used laser scanned data provided by FarField Technology Limited, New Zealand. Fetus, bladder, uterus, placenta and bones are based on MRI data of a woman in the 35th gestational week. These MRI data have a resolution of 5 mm and were provided by Prof. LeRoy Heinrichs from Stanford Univ, USA. The two data sets, body and internal organs, were combined into one model. For anatomical correctness we scaled the internal organs and aligned them inside the body

with the help of an obstetrics and gynecology physician. The CAD models were imported and meshing was tested in SEMCAD and XFDTD. Finally we scaled the uterus, placenta and fetus to generate models of pregnant women to represent all nine months of pregnancy. The easy scaling and realignment of internal parts was only possible because of CAD-based anatomical data. All nine models will also be used to calculate the RF induced heating that fetuses are experience when exposed to MRI fields and to calculate the induced currents when pregnant women are exposed to metal detectors.

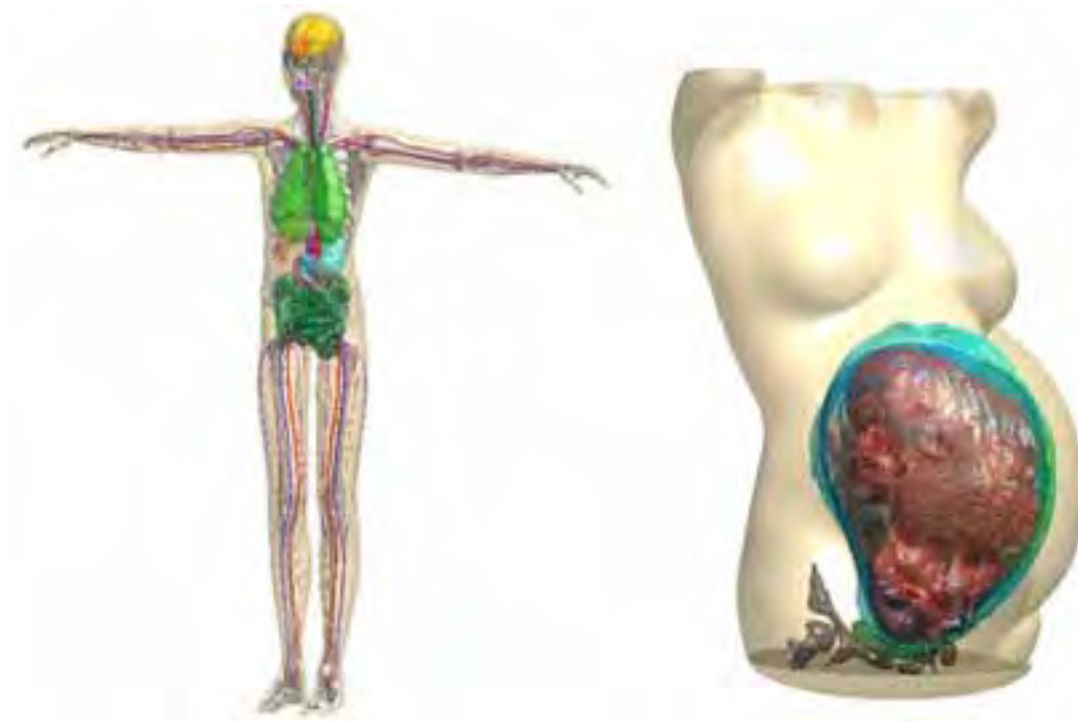


Figure 1. Left: Anatomical CAD model in XFDTD, right: pregnant woman CAD model near 35th week of pregnancy in SEMCAD.

The opinions and conclusions stated in this paper are those of the authors and do not represent the official position of the Dept of Health and Human Services. The mention of commercial products, their sources, or their use in connection with material reported herein is not to be construed as either an actual or implied endorsement of such products by the Dept of Health and Human Services.

P-A-58

**ROUTINE SAR EVALUATION USING THE EFFECTIVE MASS CONCEPT.** V. Monebhurrun<sup>1</sup>, J. C. Bolomey<sup>1</sup>, L. Duchesne<sup>2</sup>, M. Legoff<sup>2</sup>, P. Garreau<sup>2</sup>. <sup>1</sup>Supélec-L2S, Département de Recherche en Electromagnétisme, 3, rue Joliot-Curie, Plateau de Moulon, 91192 Gif-sur-Yvette Cedex, France, <sup>2</sup>Satimo, 22 avenue de la Baltique, ZA de Courtaboeuf 91953 Courtaboeuf, France.

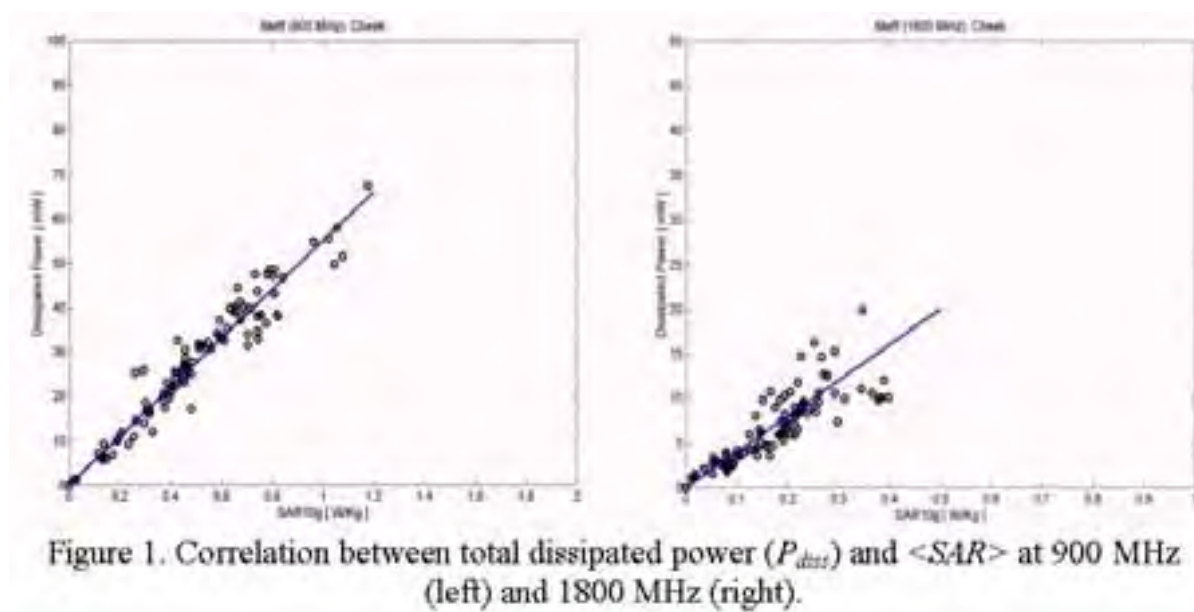
Introduction

The effective mass concept was previously introduced to estimate the (Specific Absorption Rate averaged over 10g of tissue) of mobile phones from radiated power measurements [1-2]. The power radiated by a mobile phone is measured with and without the phantom and the total power dissipated in

the phantom ( $P_{diss}$ ) is deduced. Statistical analysis of SAR data of a few hundred measurements performed using a standard dosimetric facility with either a spherical truncated phantom or the SAM phantom have shown that, by introducing an effective mass ( $M_{eff}$ ), the total dissipated power can be expressed as  $P_{diss} = M_{eff} \cdot \langle SAR \rangle$ . The correlation between total dissipated power and  $\langle SAR \rangle$  can be applied to rapidly estimate the using antenna test facilities such as anechoic and reverberating chambers. The standard procedure for measuring the is time-consuming and therefore inappropriate for mass measurements of mobile phones. For example, deviations are often observed among mobile phones of a given type. For such purposes, the effective mass concept proves appropriate to rapidly assess possible deviations. Thereafter standard dosimetric facilities can be used to obtain more rigorous results to confirm the deviations. The concept is also tailored for antenna designers who often require numerous preliminary measurements during the design stage of the mobile phone.

## Objective

The investigation of the effective mass concept is herein pursued by including recent standard dosimetric measurements. The statistical analysis of measurements performed with the spherical truncated phantom shows that the correlation between the total dissipated power and the is independent of mobile phone design. However, in the case of the SAM phantom which is nowadays used for compliance tests, a categorization of the mobile phones according to the antenna design (flip-flop or clamshell, built-in and external antennas) seems to be necessary to observe a good correlation between  $P_{diss}$  and  $\langle SAR \rangle$ . At both 900 MHz and 1800 MHz, mobile phones with built-in antennas provide the best correlation (Fig. 1). The correlation appears less pronounced in the case of flip-flop type mobile phones. This could be incurred either to insufficient data to carry meaningful statistical analysis or to the particular design of some mobile phones which adds some complexity to the application of the effective mass concept. Indeed, the electromagnetic coupling between the mobile phone and the phantom is considered to be negligible. But some mobile phone designs can produce a considerable mismatch in the presence of the phantom thereby yielding an overestimate of the total dissipated power. Clearly, a quantification of the electromagnetic coupling between the mobile phone and the phantom is needed.



## Method and Results

Both numerical simulations and experiments were carried out to support the effective mass concept. Simple generic mobile phone mock-ups (monopole over a metallic box and a commercial mobile phone with a built-in antenna) were employed to study the S11 parameter with and without the SAM phantom (Fig. 2). Clearly, for such mobile phone models the coupling can be safely neglected and, as expected, the maximum coupling is observed when objects are found in the close vicinity of the antenna (such as the presence of the hand, for example).

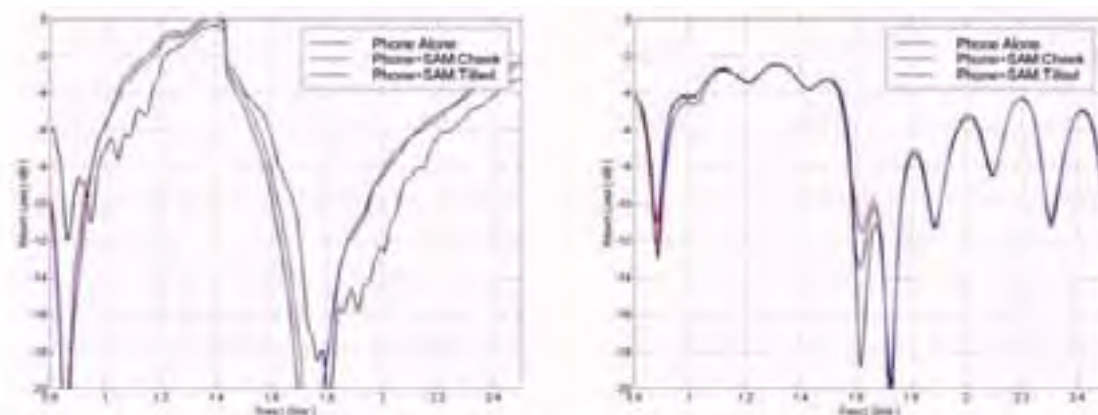


Figure 2. Return loss of generic mobile phones with and without phantom in the case of a monopole over a box (left) and a commercial built-in antenna phone design (right).

#### References

1. L. Duchesne et al., "Non-invasive statistical SAR assessment from rapid near-field measurements in a spherical antenna test range," in Proc. IEEE Wireless and Radio Conf., RAWCON'2002, Boston, Aug. 2002, pp. 129-132.
2. V. Monebhurrun et al., "Statistical analysis of SAR data: the effective mass concept," in Proc. EBEA Conference., EBEA'2003, Budapest, Nov. 2003.

P-A-61

**IMPACTS OF METEOROLOGICAL CONDITIONS ON THE FIELD PROPAGATION IN THE FREQUENCY RANGE FROM 0.8 TO 3 GHz.** M. Olsson<sup>1</sup>, W. Giczi<sup>1</sup>, H. Haider<sup>1</sup>, Y. Hamnerius<sup>2</sup>, G. Neubauer<sup>1</sup>. <sup>1</sup>Seibersdorf research, Austria, <sup>2</sup>Chalmers Univ of Technology, Sweden.

**INTRODUCTION:** Public concern about potential health effects of human exposure to the electromagnetic fields from mobile communications base stations has grown in the recent years. Needs due to legal requirements, e.g. the R&TTE directive from the European Commission and the mentioned public concerns made it necessary to develop reliable procedures for exposure assessment for in situ conditions. Several physical aspects make in situ exposure assessment a very challenging task, variations of the electromagnetic field levels in time and space have to be considered. Research about the impact of meteorological conditions on electromagnetic wave propagation has been carried out for a long time for radar applications and higher frequencies, but very little is known about the meteorological conditions on mobile communication.

**OBJECTIVES:** The objective of these investigations was to determine the impact of different meteorological conditions, e.g. rain and snow in the air as well as different conditions on the ground (dry, wet, snow etc.) on the field propagation of the electromagnetic fields from base stations.

**METHODS:** Two main experiments have been carried out: the first one was a study on field propagation in air while the humidity and the temperature was changed and the second one was a study on reflection of electromagnetic fields from the ground with changing meteorological conditions, e.g. snow on the ground. The first experiment was carried out in a climatic wind tunnel where the air temperature and humidity were controlled (see figure 1). Two antennas were mounted on tripods in the climatic wind tunnel and the power transmitted between them was recorded. The distances between the antennas were 2.5, 5 and 7.5m, and the temperature ranged from -25°C to 32°C, the relative humidity was between 30 and 90 %. For the experiments with different ground conditions two antennas were directed towards the ground, with an inclination angle of the main beam of about 30°. The transmitted power was measured for different ground materials (grass, asphalt, concrete, gravel and sand) and meteorological conditions, e.g. dry, wet, snow. A metal plate was used as reference reflector, experiments were performed in the frequency range from 0.8 to 3 GHz.

**RESULTS:** The results obtained indicate that the impact of humidity and temperature on direct field propagation in the investigated frequency range can be neglected. However, humidity on the radom of antennas and changes of antenna factors due to varying temperature might not be neglectable. The reflection coefficient on the ground varies considerably in the investigated frequency range depending on the respective ground conditions. So far only simple scenarios were investigated; the impact of changing ground conditions on complex multipath propagations scenarios might be considerable and requires further investigations.



Figure 1: Measurements in the climatic wind tunnel

These investigations are part of the EUREKA project BASEXPO. The authors would like to thank Rail Tec Arsenal and Bombardier for making it possible to perform the measurements in the climatic wind tunnel.

**ASSESSMENT OF UNCERTAINTY IN THE MEASUREMENT OF THE DIELECTRIC PROPERTIES OF BIOLOGICAL TISSUES AT MICROWAVE FREQUENCIES.** A. Peyman, C. Gabriel. Microwave Consultant Ltd. Woodford Road, London E18 2EL, UK.

**INTRODUCTION:** The measurement of the dielectric properties of tissues has been and remains an active area of research. As well as a large literature, established over nearly half a century, new data become available year after year. At microwave frequencies, observed differences in the reported data are often ascribed, to the natural inhomogeneity of the tissues, leaving out the contributions to the uncertainty of the measurement procedure and instrumentation, including the all important sample handling. Another area of scientific activity in the last 15-20 years revolved around the formulation of standard procedures for the experimental assessment of human exposure from electromagnetic sources, mostly telecommunication radio transceivers and their accessories. This created the need to formulate, measure and assess the measurement uncertainty in the dielectric properties of tissue equivalent material. There is a diversity of measurement procedures and no agreed method for the assessment of uncertainty. This paper will present a procedure developed to enable realistic bounds to be placed on measured dielectric data.

**OBJECTIVE:** This paper will deal with the fundamental issues that need to be established if dielectric measurement is to become a routine but accurate laboratory procedure. It applies those principles to the assessment of uncertainty of some tissues. It will illustrate the argument with data from a recently completed program of dielectric properties measurements of tissue in vivo.

**METHODOLOGY:** Statistical analysis has been carried out on dielectric data from tissues of different animals at microwave frequencies. The variation of both permittivity and conductivity data at selected spot frequencies were studied. Different sources of errors, which affect the dielectric measurements of biological tissues, have been identified including random and systematic errors. The random errors have been evaluated by statistical tools, while the errors associated with the methodology of the measurements have been evaluated by repeated dielectric measurements on selected standard liquids. Each type of error has been assigned with an uncertainty level and at the end the total combined uncertainty is calculated for different tissues at different frequency regions. The methodology is fairly general and applicable to the measurement of liquid tissue equivalent.

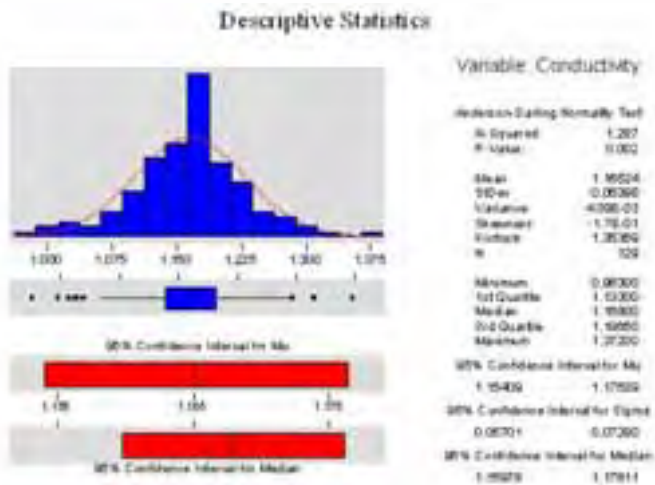
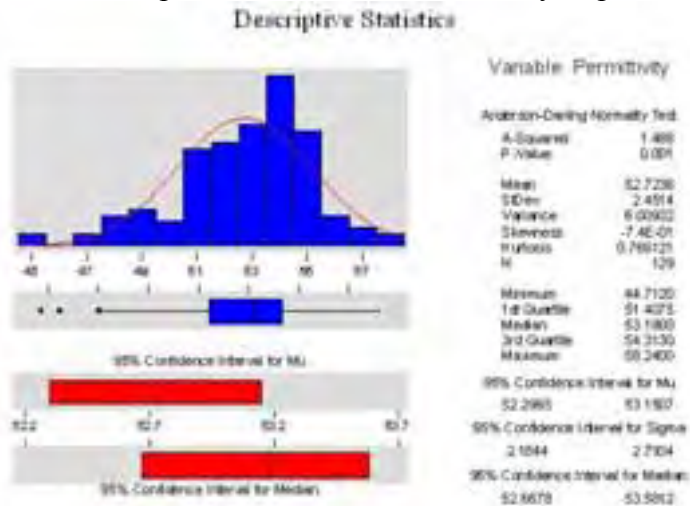
**RESULTS AND DISCUSSION:**

The outcome of the statistical analysis on the dielectric data of biological tissues suggested that the distribution of dielectric data is usually normal (Gaussian). Therefore the average (mean) value of a set of dielectric measurements approaches the true value in the limit as  $n$  (number of data) becomes infinitely large. As an example, Figure 1 shows the descriptive statistic for measured dielectric properties of porcine Cornea (in-vivo) at around 1GHz. This data set contains large number of measurements (129) on more than 20 animals and shows a typical Gaussian distribution with the mean value as the best representative of the data set. The standard deviation accounts for the repeatability of the measured data, however the best estimate of the variation of the mean value is given by standard deviation of the mean. Another observation was that clear outliers, if present, might spoil a set of measured dielectric data, it is therefore important to establish criteria for the definition of outliers. The procedure used to assess both random and systematic will be reported and applied to data for hard and soft tissue and to liquid tissue equivalent. Not surprisingly, we found that the individual errors are frequency dependent and so is the total combined uncertainty. In summary the main conclusion of this study is that, in the case of the dielectric properties of both soft and hard tissues, the statistical variability is the major contribution to the total uncertainty, far in excess of the contribution from procedural errors. In the case of liquid tissue equivalent, the two sources of uncertainty are of similar order of magnitude.

**ACKNOWLEDGMENT:** This work was undertaken by MCL. Some of the dielectric data discussed in this paper were obtained in collaboration with DSTL, Porton Down as part of the Mobile

Telecommunication and Health Research Program. The views expressed in the publication are those of the authors and not necessarily those of the funders.

Figure 1. Descriptive statistics for permittivity of porcine Cornea (in-vivo) at 1GHz  
 Figure 2. Descriptive statistics for conductivity of porcine Cornea (in-vivo) at 1GHz



**DIELECTRIC PROPERTIES OF SKELETAL TISSUES: BONE, BONE MARROW, PERIOSTIUM AND CARTILAGE.** A. Peyman<sup>1</sup>, S. Holden<sup>2</sup>, S.Watts<sup>2</sup>, R. Perrott<sup>2</sup>, C. Gabriel<sup>1</sup>. <sup>1</sup>MCL, Woodford Road, London E18 2EL, UK, <sup>2</sup>Defence Science and Technology Laboratory Biomedical Sciences, Porton Down, Salisbury, SP4 0JQ, UK.

**INTRODUCTION:** Skeletal tissues spread all over the body, good knowledge of their dielectric properties are important in computer simulation of the human head and body and for the development of appropriate tissue equivalent materials. Bone consists of a hard, open-structure matrix impregnated with organic matter and salts in an aqueous medium. It is classified as a hard tissue with relatively low water content and consequently low permittivity and conductivity compared to soft tissues. Hard tissues such as bone are difficult to sample which accounts for the scarcity of good dielectric data. This paper deals with the determination of the dielectric properties of porcine bone, bone marrow tissue, periosteum and cartilage measured both in- vivo and in-vitro in the frequency range of 50 MHz to 20 GHz. Measurements were also made on piglets and mature sows to re-visit the issue of variation of the dielectric properties with age [1].

**OBJECTIVE:** This paper has three objectives: 1- To present recently measured dielectric data of different bone and marrow tissues and the assessment of their associated uncertainty. 2- To carry out a comparative analysis of dielectric data obtained in-vivo and in-vitro from this study as well as recently available literature. 3- To report variation in dielectric properties of bone and bone marrow as a function of animal age.

**METHODOLOGY:** The dielectric measurements carried out on long bone, skull, periosteum, cartilage, inter-vertebral disc, red and yellow bone marrow using an optimal size open-ended coaxial probe and computer controlled network analysers following a previously reported procedure [2]. Measurements were made on 12-21 pigs of 50-70kg under general anesthesia for in-vivo condition. Similar measurements were carried out on 6 pigs of 50-70kg under the in-vitro condition. Statistical analysis was applied to the pooled data from all pigs and a total combined uncertainty assigned to the permittivity and conductivity of each tissue in different frequency regions. Finally, similar measurements carried out on pigs of 10kg and 250 kg under the in-vitro condition for the purpose of the age study.

**RESULTS AND DISCUSSION:** Figures 1 shows the measured dielectric properties of different porcine bone and marrow in-vivo. For clarity, error bars were not added to the experimental data, however, the uncertainty budget will be discussed and presented in the final paper. The differences observed in dielectric properties of bone tissues as a function of age will be presented and discussed in details in the final paper. In summary, the main conclusion from the age study was that significant differences were observed between the dielectric values of bone and marrow tissues of 10kg and 250kg animals (Figures 3 and 4).

**ACKNOWLEDGMENTS:** This work was undertaken by MCL in collaboration with DSTL, Porton Down. MCL received funding from the Mobile Telecommunication and Health Research Program. The views expressed in the publication are those of the authors and not necessarily those of the funders.

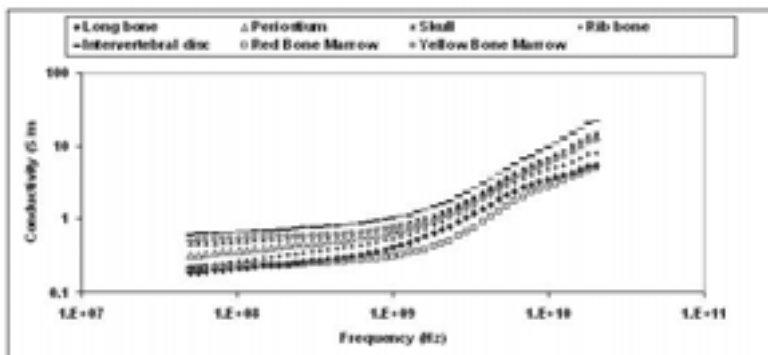
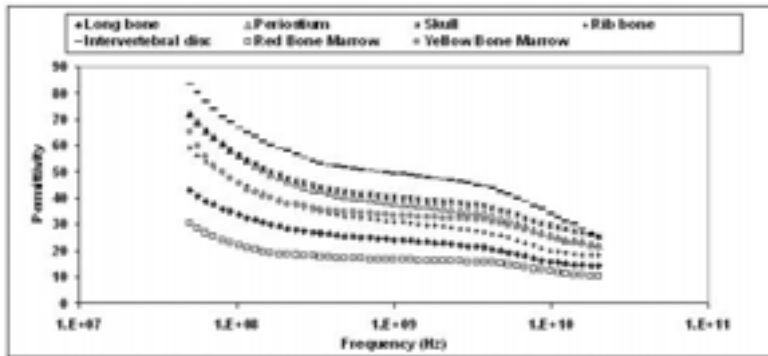
#### REFERENCES:

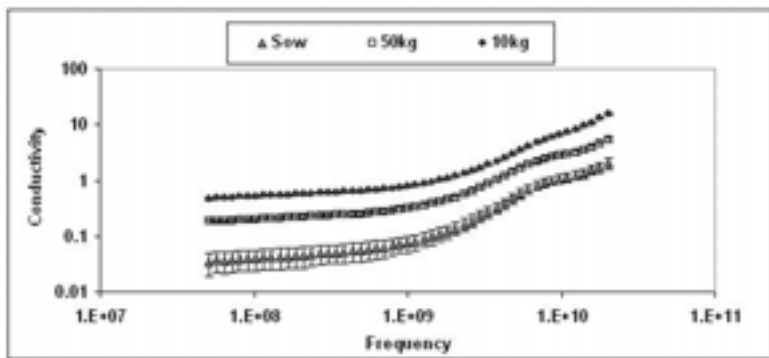
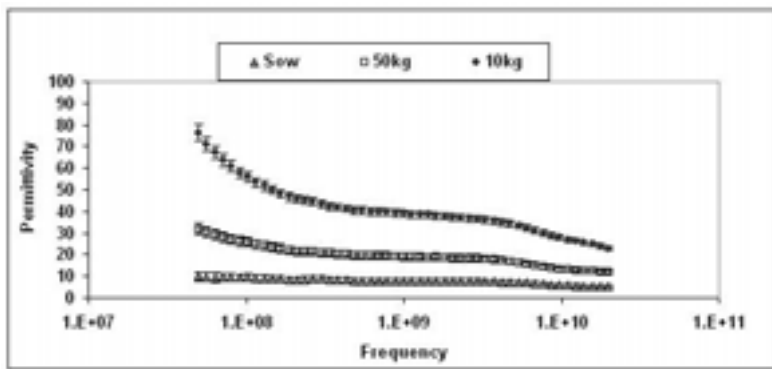
1. Peyman A, Rezazadeh A A and Gabriel C, 2001, "Changes in the dielectric properties of rat tissue as a function of age at microwave frequencies" *Phys. Med. Biol.* 46 No 6 1617-1629
2. Gabriel, C., Chan, T. Y. A. and Grant, E. H., 1994, Admittance models for open ended coaxial probes and their place in dielectric spectroscopy, *Phys. Med. Biol* 39, 12, 2183-2200

Figure 1. Permittivity of different porcine bone and marrow tissues

Figure 2. Conductivity of different porcine bone and marrow tissues

Figure 3. Permittivity of porcine yellow bone marrow as a function of age  
 Figure 4. Conductivity of porcine yellow bone marrow as a function of age





**P-A-70**

**VOLUMETRIC MANIPULATION FOR DOSIMETRY SIMULATIONS.** D. Silver<sup>1</sup>, K. Yaws<sup>2</sup>, C. Correa<sup>1</sup>, W. Hurt<sup>2</sup>, P. Mason<sup>2</sup>, J. Ziriak<sup>3</sup>. <sup>1</sup>Dept of Electrical and Computer Engr., Rutgers, The State Univ of New Jersey, PO Box 909, Piscataway, NJ 08855-0909 USA, <sup>2</sup>Directed Energy Bioeffects Division, Human Effectiveness Directorate, Air Force Research Laboratory, Brooks City-Base, Texas,

## ABSTRACT

Finite difference time domain (FDTD) simulations are used for dosimetry computations. As input, these simulations require segmented three-dimensional (3D) anatomical datasets. Many diverse datasets can now be acquired from imaging devices such as magnetic resonance imaging (MRI), CT or even cryogenic slicing. However, these datasets are static, i.e., they can not be reposed in a more natural or realistic position. For example, since MRIs are generally taken in a supine position, the resulting dataset will be in a supine position. Unfortunately, this is not generally the position needed for a simulation under real-world conditions. Computer graphics and CAD tools are currently unable to reposition voxelized data since these tools operate on polygons. In this presentation, we demonstrate our new voxel manipulation techniques which are able to repose volumetric datasets. The methodology is ubiquitous and can operate on any 3D dataset. An example is shown below in Figure 1. Figure 1(a) displays the original MRI of a rat. Using our voxel manipulation software, we were able to reposition the rat into a more natural “nosing” position within a TEM cell. In this presentation, we will show various examples of our manipulation software, and discuss its uses for bio-effects research in FDTD simulations.

This work was funded by the U.S. Air Force ((Project Numbers: 0602236N/M04426.w6, 0601153N/M4023/60182). The views, opinions, and/or findings contained in this report are those of the authors and should not be construed as official Dept of the Air Force, Dept of the Navy, Dept of Defense, or U.S. government position, policy, or decision unless so designated by other documentation. Trade names of materials and/or products of commercial or nongovernment organizations are cited as needed for precision. These citations do not constitute official endorsement or approval of the use of such commercial materials and/or products. Approved for public release; distribution unlimited.

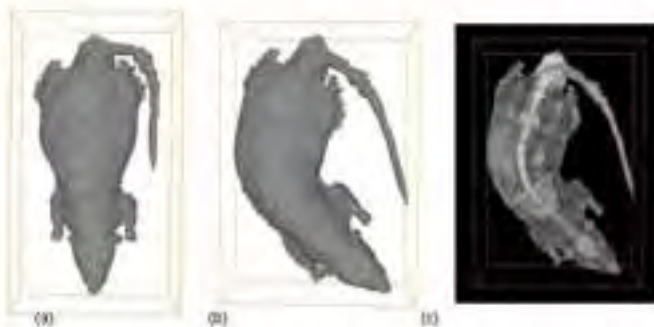


**Figure 1: Voxel Manipulation Example:**

*(a) MRI of rat with a resolution of 310x160x610. Original position.*

*(b) Reposed rat model (3D) in "nosing" position with new resolution of 458x143x379*

*(c) Internal view of reposed rat.*

**AN EVALUATION OF POTENTIAL BIASES IN EPIDEMIOLOGICAL STUDIES ON CHILDHOOD LEUKEMIA AND EXPOSURE TO EXTREMELY LOW-FREQUENCY MAGNETIC FIELDS.** J. Schüz<sup>1</sup>, M. Feychting<sup>2</sup>. <sup>1</sup>Institute for Medical Biostatistics, Epidemiology and Informatics, Univ of Mainz, Mainz, Germany, <sup>2</sup>Institute of Environmental Medicine, Karolinska Institute, Stockholm, Sweden.

**Objectives.** In 2001, extremely low-frequency magnetic fields (ELF-MF) have been rated as a possible carcinogen (1). This classification was based on epidemiological studies in which an association between exposure to ELF-MF and childhood leukemia has been observed (2). While the statistical association was quite consistent across studies, bias and confounding could not be ruled out with reasonable confidence. In this presentation, we want to address the potential impact of selection bias in studies based on ELF-MF measurements and of bias from exposure misclassification in studies based on ELF-MF calculations.

**Methods.** We used the data of a German study and a Swedish study to explore the potential impact of bias (3, 4). These studies were two among the few well-conducted studies showing statistically significant associations.

**Results.** In the German study, average ELF-MF were higher in apartment buildings compared to single-family homes (5). As more families of lower social status lived in apartment buildings and nonparticipation in measurement-based studies was particularly high among control families of lower social status, average ELF-MF could be higher for families of children with leukemia than among control families due to this selection bias. A simulation study in which ELF-MF for nonparticipants were simulated taking into account characteristics of their residence, revealed a decrease in the formerly 2.8-fold elevated risk estimate down to 1.6. In the Swedish study, selection bias is not a problem, however, since no contact with the study subjects were made, only ELF-MF from powerlines were captured, neglecting all ELF-MF contributions from other sources. The resulting exposure misclassification, however, is similar for cases and controls and therefore likely to underestimate the observed association. We have calculated that this underestimation is only marginal, because, while the sensitivity of the exposure measure is low, its specificity is extremely high. For apartments, however, the specificity is likely to be lower than for single family homes because the exact location of the residence within the apartment building was not always known, and the difference in distance to the power line between the apartment closest to the line and the apartment furthest away might be substantial.

**Discussion.** The method of ELF-MF calculations is unlikely to have contributed to a possible inflation of the observed risk estimates. In the opposite, it rather leads to a loss of statistical power of a study to detect an association. Selection bias in studies using ELF-MF measurements, on the other hand, might have lead to an overestimation of the strength of the association (4, 6). However, it is unlikely that the observed association can be completely explained by selection bias, especially since the association is observed in the majority of studies regardless of the potential for selection bias.

**Source of support.** Univ of Mainz and Karolinska Institute.

1. International Agency for Research on Cancer (IARC). IARC Monographs on the Evaluation of carcinogenic Risks to Humans: Volume 80. Non-Ionizing Radiation, Part 1: Static and extremely low-frequency (ELF) electric and magnetic fields. IARC Press, Lyon, 2002

2. Ahlbom A, Day N, Feychting M, Roman E, Skinner J, Dockerty J, Linet M, McBride M, Michaelis J,

- Olsen JH, Tynes T, Verkasalo PK. A pooled analysis of magnetic fields and childhood leukaemia. *Br J Cancer* 2000; 83: 692-8
3. Feychting M, Ahlbom A. Magnetic fields and cancer in people residing near Swedish high-voltage power lines. *Am J Epidemiol* 1993; 138: 467-81
4. Schüz J, Grigat JP, Brinkmann K, Michaelis J. Residential magnetic fields as a risk factor for childhood acute leukaemia: results from a German population-based case-control study. *Int J Cancer* 2001; 91: 728-35
5. Schüz J, Grigat JP, Störmer B, Rippin G, Brinkmann K, Michaelis J. Extremely low frequency magnetic fields in residences in Germany. Distribution of measurements, comparison of two methods for assessing exposure, and predictors for the occurrence of magnetic fields above background level. *Radiat Environ Biophys* 2000; 39: 233-40
6. Hatch EE, Kleinerman RA, Linet MS, Tarone RE, Kaune WT, Auvinen A, Baris D, Robison LL, Wacholder S. Do confounding or selection factors of residential wiring codes and magnetic fields distort findings of electromagnetic fields studies? *Epidemiology* 2000; 11: 189-98

P-A-76

### **SUNBED USER'S MOTIVATIONS, KNOWLEDGE AND HABITS IN BUDAPEST, HUNGARY.**

J. Bakos, J. Szabo, G. Thuroczy. *Natl. Res. Inst. for Radiobiology and Radiohygiene, Anna 5., Budapest, Hungary, H-1221.*

#### Objective

The aim of this study was: to recognize the main motivations of sunbed use of the Hungarian public, the user's knowledge of health effects and their habits related to tanning in sunbed and/or by sunlight. Being in possession of this knowledge it will be possible to establish better education programs for the public in order to be able to reduce the potential health consequences of excess artificial UV exposure.

#### Methods

The study was performed in five sunbed salons in Budapest. Sunbed users were asked to complete a questionnaire containing 59 questions, covering the following main topics: personal data(age, gender, profession, education), data of skin(skin type, number of moles, allergy), habits in sunbed use(age at first use, seasonal frequency, use of cosmetics and goggles, frequency of erythema), motivations of sunbed use, opinion about health effects of sunbed use and UV radiation, habits related to exposure to natural sun radiation, health awareness(body weight, sport activity, smoking, drinking), information sources about health effects of sunbed use.

The data will be stored on computer and statistically analyzed by EPI INFO 6.04 software intended to epidemiological use.

#### Results

443 of 500 questionnaires (88,6 %) were completed by customers of five sunbed salons in the Hungarian capital between 24/03/2004 and 31/05/2004.

The results of statistical evaluation of the 442 completed questionnaires are the following: 87 % of users were regular sunbed user, 64.7 % of users were women.

The average age was similar in both gender: 27.1 and 27.8 years in case of men(M) and women(W), respectively.

The average age of first sunbed use was 20.0/20.6 years M/W, respectively.

Most participants finished secondary school (66 %) and college(26 %).

52 % of participants (56 %/50 % M/W) classified their skin as "tan well" (Fitzpatrick skin Type 3). Although, only 1,1 %(5 W) classified her skin into Type 1 (most sensitive) 53 % of individuals reported rarely occurring "sun"burn due to sunbed use (15 % once, 16 % never) and 7 %(18 women and 10 men) frequent burning.

25 % of men and 30 % of women are suffering from some kind of allergic disease.

#### Conclusions

Most participants are younger than 30 years old and fairly educated. Although, almost everybody is aware of the cosmetic risks (ageing and burning of the skin), their knowledge of the health hazards is inconsistent.

Two-thirds are women, who have generally better knowledge about the risks of sunbed use. Contradictorily, although men consider it more harmful, they use sunbed more frequently and are exposed to more sunlight, also.

Sunbed users are keen on getting a sun tan because of the perceived beneficial effects and devalue the smouldering harmful effects.

As the main information source about the health risks was found to be the electronic media (while the school is the last), public relations campaigns must be undertaken, and children's awareness of the health risks of natural and artificial UV radiation is needed to be raised at schools.

P-A-79

**USE OF MOBILE PHONES, CANCER AND RARE CNS DISEASES – AN UPDATE OF A DANISH COHORT STUDY.** R. Jacobsen<sup>1</sup>, C. Johansen<sup>1</sup>, J. H. Olsen<sup>1</sup>, J. B. Nielsen<sup>2</sup>, I. S. Kristiansen<sup>2</sup>.  
<sup>1</sup>Institute of Cancer Epidemiology, The Danish Cancer Society, Copenhagen, Denmark, <sup>2</sup>of Public Health, Univ of Southern Copenhagen, Odense, Denmark.

**Background:** Use of mobile telephones is increasing exponentially and has become part of everyday life. Concerns about possible carcinogenic effects of radiofrequency signals have been raised, although based on limited scientific evidence. This study is an update of a previous study, including an extended follow up for cancer and adding information on risk for diseases in the central nervous system.

**Methods:** A retrospective cohort cancer incidence study was conducted in Denmark of all users of cellular telephones between 1982 and 1995. Subscriber lists from two operating companies identified 420,095 cellular telephone users. Cancer incidence was determined by linkage with the Danish Cancer Registry. In the present update we add a further seven years of cancer incidence. In addition we will follow-up for rare CNS diseases in the Danish Hospital Discharge Register and estimate the risk of multiple sclerosis based on data from the Danish Multiple Sclerosis Registry

**Results:** In the previous study a decreased risk for all cancers was observed. This was attributed primarily to deficits of smoking- and alcohol-related cancers and stomach cancer. No increased risk was observed for cancers a priori hypothesized to be associated with the exposure under study. In this presentation we will include the possible effect of socioeconomic status for the new cancer results.

**Conclusions:** Our large-scale study will bring further insight to the understanding of the risk for cancer and CNS diseases in adults hypothesized to be associated with the use of mobile phones.

**Funding source:** The National Strategic Research Council in Denmark and The Danish Cancer Society

**HIGH FREQUENCY TRANSIENTS ON ELECTRICAL WIRING: BLOOD GLUCOSE CHANGES AND ASTHMA EFFECTS ON HUMAN SUBJECTS.** L. Morgan<sup>1</sup>, D. Stetzer<sup>2</sup>, M. Hudes<sup>3</sup>. <sup>1</sup>Retired electronic engineer, Berkeley, CA, USA, <sup>2</sup>Industrial electrical consultant, Stetzer-Electric, Inc., Blair, WI, USA, <sup>3</sup>Sr. Statistician, Nutritional Science and Toxicology, Univ of California, Berkeley, CA, USA.

**INTRODUCTION:** Studies of the health effects of exposure to power frequency EMFs have almost entirely ignored the full spectrum of frequencies actually existing on electrical power wiring. These same studies have almost always examined ELF magnetic fields with little attention paid to the electric fields. The electrical wiring in buildings carries not only the 60 Hz or 50 Hz sinusoidal voltage and their associated harmonics, but also non-harmonic high frequency transients created by the intermittent use of electricity by electrical equipment. Beginning in the late 1970s, an enormous increase of high frequency transients on the electrical wiring has occurred. This increase is the direct result of the way solid-state electronic devices use electricity. Coincident with this increase in high frequency transients has been an as yet not fully understood dramatic increase in the incidence of diabetes and asthma. **OBJECTIVES:** 1) To show that health effects from electrical power EMFs are the result of exposure to high frequency transient electric fields and not from the ELF magnetic fields. 2) To investigate the biological effects from exposure to high frequency electric field transients on a human subject's blood glucose levels. 3) To investigate the effects of high frequency electric field transients on asthma in school children.

**METHODS:** An oscilloscope was used to observe the high frequency transients using a 10 kHz high-pass filter connected to the electrical outlet. The high-pass filter is used to remove the 60 (or 50 Hz) from the high frequency transients. Figure 1, shows an oscilloscope observation. Peak-to-peak voltage measurements were made using a low cost DVM (Digital Voltmeter) connected to an electrical outlet through a 10kHz high-pass filter followed by a peak detector circuit. Another low cost meter was used to measure the average rate of change of the high frequency transient voltage. Blood glucose measurements were made with a blood glucose meter commonly used by diabetics. Low-pass filters connected to the electrical wiring were used to filter the high frequency transients from the electrical wiring. Figure 2, shows the same oscilloscope observation after low-pass filter installation. **RESULTS:** 1) Exposure of a single subject, using peak-to-peak voltage measurements of the high frequency transients, was found to strongly correlate (RMS values showed no correlation) with high blood glucose levels even after adjusting for time of day (partial  $R^2=0.61$ ,  $p < 0.001$ ). 2) Filtering the high frequency transients from a rural elementary school, resulted in 92% (34/37) of the children with asthma, no longer having asthma. 4) 3) The low pass filters connected to the electrical wiring increase the ELF magnetic field by about 10%. A low-pass filter reduces the peak voltage of the high frequency transients by a factor of 100 and reduces the frequency by a factor of 10 (the capacitive energy coupled to human beings by the high frequency electric field is proportional to voltage AND frequency, implying a 1000 fold electric field decrease).

**CONCLUSIONS:** Changes in the peak-to-peak voltage of high frequency transients from electrical wiring correlates to blood glucose changes in one subject. Filtering of high frequency transients is associated with a reduction in asthma incidence at a rural elementary school. This suggests that high frequency transients may be associated with changes in blood glucose and the incidence of asthma. Removal of the high frequency transients slightly increases the ELF magnetic field and greatly reduces the high frequency electric field. This suggests that the biologically active agent may be the high frequency electric field.

Support: Personal funds

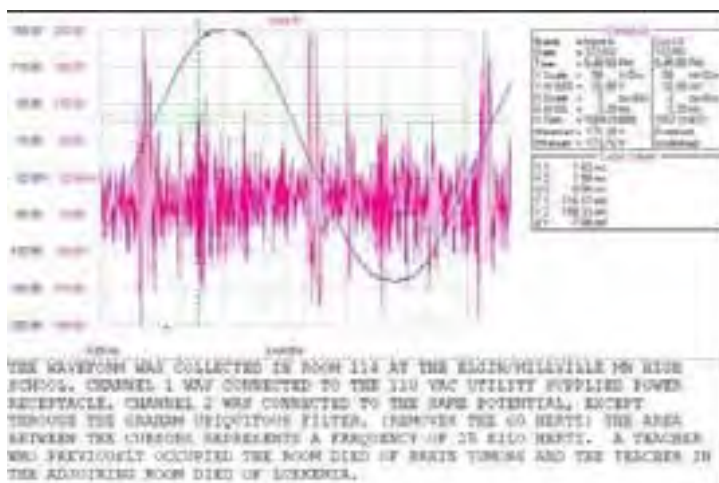


FIGURE 1

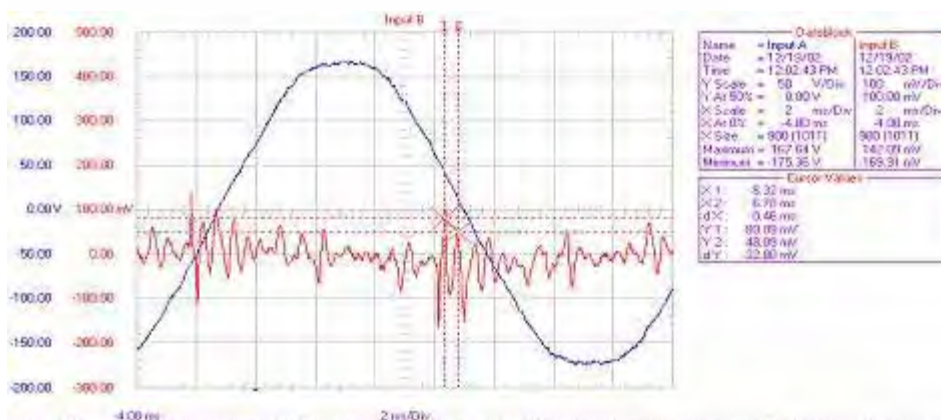


FIGURE 2

## High-throughput screening

P-A-85

ANALYSIS OF GENE EXPRESSION IN MICE EXPOSED TO RADIOFREQUENCY ELECTROMAGNETIC FIELDS USING MICROARRAY. J.-S. Lee<sup>1,2</sup>, T.-Q. Huang<sup>1</sup>, T.-H. Kim<sup>1</sup>, J.-K. Park<sup>3</sup>, J.-S. Seo<sup>1</sup>. <sup>1</sup>ILCHUN Molecular Medicine Institute MRC, and Dept of Biochemistry and Molecular Biology, Seoul National Univ College of Medicine, Seoul, Korea, <sup>2</sup>BK21 Human Life

Science, Seoul National Univ College of Medicine, Seoul, Korea, <sup>3</sup>Dept of Radio Sciences & Engineering, Chungnam National Univ, Daejeon, Korea.

In spite of increasing number of studies, the issue whether radiofrequency electromagnetic fields (RF EMFs) have adverse effect on public health is still controversial. Microarray technique is one of the most powerful tools to examine change of gene expression pattern by various stimuli. In this study, oligonucleotide microarrays were employed to investigate changes of gene expression in mice exposed to RF EMFs. Eight-week old male C57BL/6 mice were exposed to either whole body average SAR 12 W/Kg of 1,763 MHz RF-EMFs with whole body exposure system or brain average SAR 12 W/Kg with head-mainly exposure system. Spleen and brain were isolated immediately after exposure from the whole body exposed and the head-mainly exposed mice, respectively. Synthesized cDNAs from the isolated total RNAs were hybridized to a MAGIC Oligo-Mouse 11K chip (Macrogen Inc., Seoul, Korea). At least 2-fold change in more than five A (Signal Intensity) were seen for 23 genes in spleen and 34 genes in brain. Some of genes that altered their expression were confirmed using RT-PCR analysis.

## Mechanisms of interaction – physical transduction

P-A-88

**METHOD FOR MEASURING CHARGE ON AEROSOL PARTICLES NEAR AC TRANSMISSION LINES.** W. H. Bailey<sup>1</sup>, G. Johnson<sup>2</sup>, T. D. Bracken<sup>3</sup>. <sup>1</sup>Exponentô, New York, New York, 10170 USA, <sup>2</sup>Exponentô, Chicago, Illinois 60191 USA, <sup>3</sup>T.Dan Bracken, Inc., Portland, Oregon 97282.

**BACKGROUND:** The earth's atmospheric static electric field at ground level is produced by overhead space charge. The sources of space charge include both natural sources (e.g., cosmic rays, radon, waterfalls, blowing snow) and man-made sources (combustion sources such as motor vehicles, coal/waste burning, gas appliances, burning candles, electrostatic air cleaners, and corona activity). The ability of these sources to affect the space charge density by the generation of small air ions and, with the passage of time, the transfer of charge to aerosol particles is well known (Chalmers, 1967). Fews et al (1999) and Fews et al (2002) have hypothesized that fluctuating elevations in the static electric field averaging 120 V/m and 280 V/m in a 15-minute sampling period they measured downwind of 132-kV and 400-kV alternating current (ac) transmission lines are indicative of increased concentrations of air ions and charged aerosols at or near ground level. Fews and his colleagues have also predicted that downwind concentrations of air ions at ground level would be in excess of 3000 ions/cm<sup>3</sup> and 6000 ions/cm<sup>3</sup> for 132-kV and 400-kV lines, respectively. Empirical data upon which to base such hypotheses are quite limited. Until recently, only one investigator had measured ion concentrations downwind of an ac transmission line (Harris & Albertson, 1984). Bracken et al (2005) reported changes in electric fields and ion concentrations downwind of 230-kV and 345-kV transmission lines in a small percentage of observations, but the frequency and magnitude of the changes were not enough to elevate measures of a person's long-term exposure. To our knowledge, no measurements of charged aerosols per se, which are at the heart of the Fews et al hypothesis, have yet been made near ac transmission lines.

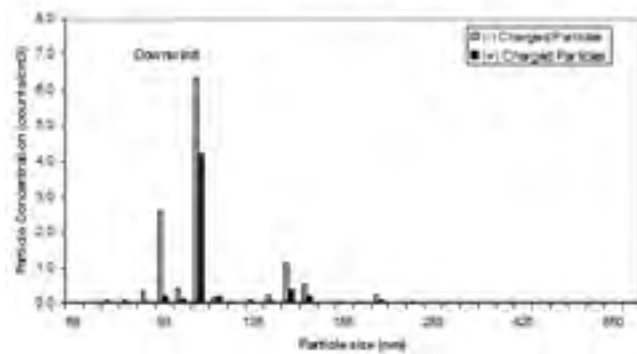
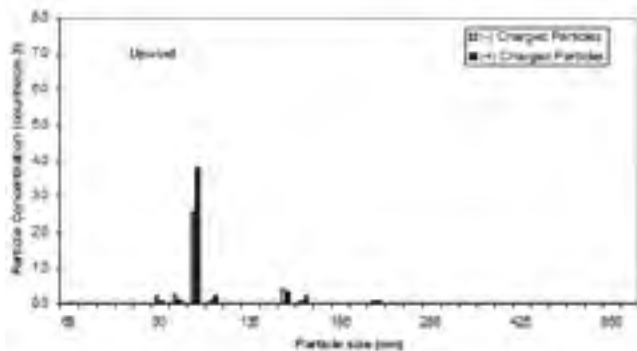
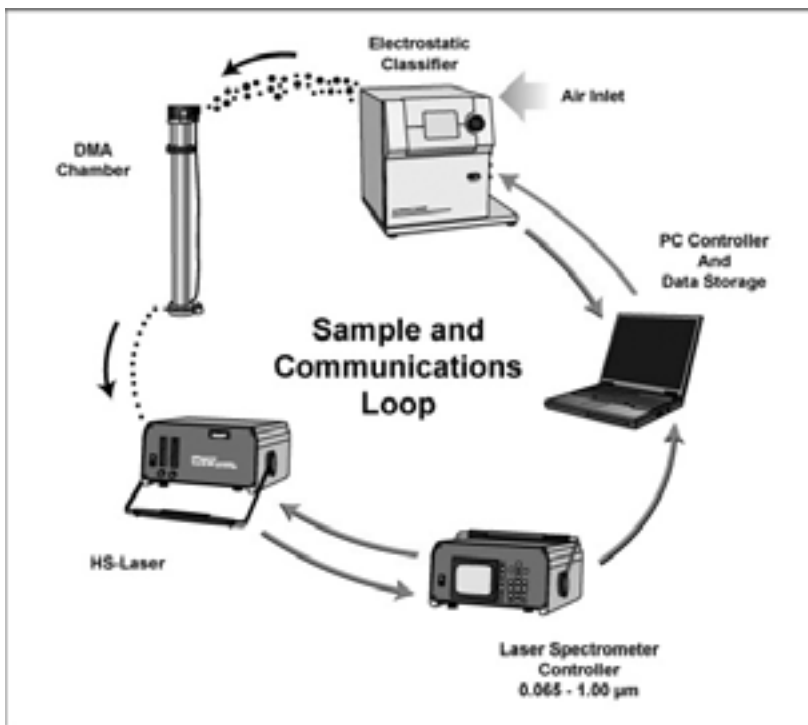
**OBJECTIVE:** The National Radiological Protection Board of Great Britain has recently recommended that experimental studies be conducted of the charge and size of aerosols upwind and downwind of

power lines (NRPB, 2004). To fill this data gap, we report our methodology for making measurements of charged aerosols near two 115-kV and two 345-kV transmission lines located on a common corridor, and the results of preliminary analyses.

**METHODS:** The instruments used to characterize the mobility and size of charged aerosols and their interconnected operation are depicted in Figure 1. Particles with a specified electrical mobility were obtained by drawing the sample air stream through an Electrostatic Classifier from which the Kr-85 particle-charging source had been removed. A differential mobility analyzer (DMA) controlled by the Classifier was used to select charged aerosols for counting. Particles exiting from the DMA were sized by a laser aerosol spectrometer over a size range of 0.065 to 1.00 micron. At 9 electrical mobility cut-points selected for analysis, the particles were counted and sized during a two-minute sampling period. Measurements of static electric fields, ion concentrations, wind speed/direction, temperature and humidity were made as well.

**RESULTS:** Measurements were taken 100 m from the twin conductor bundle of the nearest 345-kV line on two days, a day apart. These days were selected a priori for analysis because of differences in wind direction (upwind and downwind of transmission lines) and the similarity of weather conditions. The electric fields and ion concentrations were not elevated on either day. The highest concentrations of aerosols with single and multiple charges were measured at an electrical mobility of  $2.01 \times 10^{-4} \text{ cm}^2 / \text{V} \cdot \text{sec}$ . The size distributions of (+) charged aerosols on the two days were similar (Figure 2). A slightly higher concentration of (-) charged aerosols was observed on the day the wind was blowing predominately from the transmission lines.

**CONCLUSIONS:** A method for measuring the electrical mobility of ultrafine particles and their size distribution in the range of 0.065 –1.00  $\mu\text{m}$  has been demonstrated near operating ac transmission lines. The air ion concentrations reported here are 5-10 times lower and electric fields 10-times lower than values measured (electric fields) or modeled (air ions) by Fews et al downwind of transmission lines. Small differences between the distribution of (-) charges on aerosols but not (+) charged aerosols on day 1 and day 2 were observed. Whether this difference was replicable and attributable to a specific source, including the transmission lines or more distance sources of charged aerosols in the vicinity was not determined.



P-A-91 STUDENT

**IS A RECTIFYING JUNCTION ESSENTIAL FOR DEMODULATION OF MODULATED WAVEFORMS IN TISSUE?** I. Ahmed, P. S. Excell, R. A. Abd-Alhameed. Mobile and Satellite Communications Research Centre, Bradford Univ, Bradford BD7 1DP, UK.

The question of demodulation of modulated waveforms in tissue has been much discussed in connection

with evaluation of putative effects of radiated waves from mobile phones on the human biosystem. It has been argued by some that demodulation "must occur in some way" and that hence, to cite the most pertinent example, the severely amplitude modulated waveform of GSM signals could be converted into low-frequency signals at 217Hz (and possibly lower frequencies). Such low frequencies will be more likely to interact in a non-thermal fashion with the functioning of the human biosystem than is currently believed possible with the carrier frequencies of the GSM system (~800 to 1900 MHz).

It is easily shown that, in a neutral medium, it is necessary to have rectifying (or "square-law") behaviour at some presumed junction carrying the induced radio frequency currents, in order to demodulate the waveform. While such behaviour is well known in electronic devices, a plausible physical explanation of ways that it might be created in biological tissue has been very hard to identify: ideas that have been advanced include the use of the principle of quantum dots, but the existence of such exotic phenomena in tissue seems little less implausible than that of rectifying junctions.

On the other hand, it is much easier to envisage the existence of symmetrical voltage-limiting (saturating) regions in human tissue, such as are encountered, for instance, in metal-oxide voltage limiters. However, it is easily shown that such symmetrical junctions are not able to effect demodulation, although they will certainly generate high-order harmonics. A simple mathematically-tractable treatment of such a phenomenon can be created by presuming the device behaviour to approximate to a cube-law relationship between applied voltage and induced current. More realistic curves can be obtained by using higher-order odd powers of the voltage, but the principle is the same, and hence it is convenient to discuss the issue by using a cube law relationship as a simple exemplar:

(eqn 1: see Fig 2a)

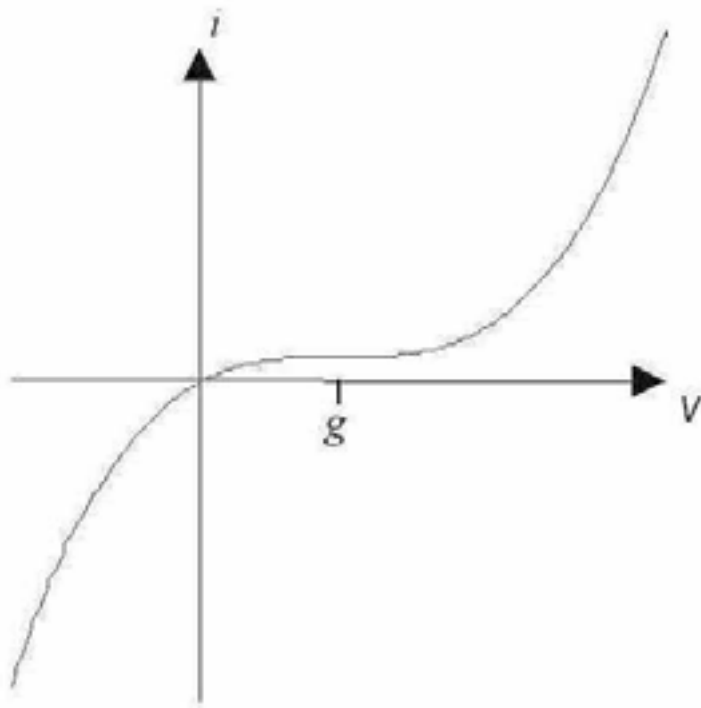
Physical consideration of the behaviour of a cube-law device suggested intuitively that, if it were biased to offset its central point from the origin of co-ordinates (zero applied voltage) then its shape, at least under low excitation, would appear to approximate to the shape of a square-law device, and hence it might be capable of effecting demodulation (Fig. 1).

Fig. 1. Cube-law characteristic with origin offset. It can be shown that the result of applying a modulated RF waveform to such a device is, discarding high frequency components: (eqn 2: see Fig 2b) where  $g$  is the offset (bias, as in Fig. 1),  $V_c$  is the carrier amplitude,  $x$  is the depth of modulation and  $m(t)$  is the information signal.

This shows that the biased cube-law device can indeed cause demodulation, to an extent that increases monotonically with the amount of bias (and is zero at zero bias, as expected). This then raises the question of whether such a biased symmetrical limiting device could occur in biological tissue. As discussed above, the symmetrical limiting device appears to be physically more plausible than a rectifying device and, since it is accepted that bias voltages occur at many points in the cellular structure (e.g. as implemented in the Hodgkin-Huxley approximate model [1]) this appears to give a mechanism that could indeed permit a degree of demodulation to occur, without the need for exotic mechanisms. Whether such demodulation would be significant is left for further work, as is the discussion of the probability of occurrence of the symmetrical limiting junction.

[1] A.L.Hodgkin and A.F.Huxley, "A quantitative description of membrane current and its application to conduction and excitation in nerve", *J.Physiol.*, vol. 117, 1952, pp.500-544.

This work is supported by the UK Dept of Health.



$$i = K_a v^3(t) \quad (1)$$

$$i = K_a \left[ -\frac{3gV_c^2}{2} - \frac{5gV_c^2}{2} x m(t) - gV_c^2 x^2 m^2(t) \right] \quad (2)$$

## Human Studies

P-A-94

**BIOELECTRICAL IMPEDANCE ANALYSE (BIA) OF PEOPLE EXPOSED TO RADIOFREQUENCY RADIATION BY ANTENNA OF 1062 KHZ MEDIUM WAVE RADIOBROADCASTING STATION.** S. Dasdag, M. Z. Akdag, M. Salih Celik. Biophysics Dept of Dicle Univ Medical Faculty, Diyarbakir 2120, Turkey.

The affects of radiofrequency (RF) and microwave radiation on people have been a subject of continuing investigations. Since one of the major exposed people is that who have been working radio broadcasting and TV transmitter stations and living in houses provided to employees of these stations, the present study intended to investigate whether radiofrequency affects bioimpedance of people exposed to RF by means of antenna of 1062 kHz medium wave radiobroadcasting station. The sudy was carried out on 31 adult people (20 male, 11 female, age:27-46) and 30 voluntary children (Boy:15, Girl:13, age: 5-15) working in radiobroadcasting station and living in houses provided to workers of radiobroadcasting station mentioned above because of their parent's job.

17 parameter such as resistance (R), reactance (X), phase angle (á), body capacitance (C), fatt-free

mass(FFM), body cell mass (BCM), extra cellular mass (ECM), fatt mass (FM), ECM/BCM, body mass index (BMI), basal metabolic rate (BMR), total body water (TBW), intra cellular water (ICW), extra cellular water (ECW), TBW/Fat-free mass, TBW/Total Weight (TW) were measured in people under investigation.

Phase angle, body capacitance and reactance values of experimental girl subjects were found lower than the control girl subjects ( $p < 0.001$ ,  $p < 0.01$ ,  $p < 0.01$  respectively). However, extra cellular mass/body cell mass ratio increased in experimental group of girl subjects ( $p < 0.01$ ).

Distance between the antennas of the radio broadcasting stations to the employees' workplace was approximately 250 meters. The distance of the antennas to the employee residential houses was between 300 and 350 meters. Exposure level of RF in the room where the control desk was placed was measured as 4.87 V/m in maximum and 4.04 V/m in average (Max Power Density: 0.0063 mW/cm<sup>2</sup>, Average Power Density: 0.0042 mW/cm<sup>2</sup>). Exposure level around the buildings in which the control desk and other equipment were placed was measured as 36.23 V/m in maximum and 31.88 V/m in average (Max Power Density: 0.3482 mW/cm<sup>2</sup>, Average Power Density: 0.2717 mW/cm<sup>2</sup>). E field and power density inside houses provided to employees measured between 0.48 V/m-2.86 V/m and 0.0001 mW/cm<sup>2</sup> - 0.0023 mW/cm<sup>2</sup>, respectively, depending on the distance from the antenna. However, average E field and power density in children's playgrounds were measured as 12.75 V/m and 0.0436 mW/cm<sup>2</sup>, respectively. Average E field and power density outside the playgrounds and employee residential houses were measured as 18.64 V/m and 0.0971 mW/cm<sup>2</sup>. E field and power density inside and around these houses where the subjects in the control group normally work and reside were measured as between 0.74 V/m - 2.00 V/m and 0.0000 mW/cm<sup>2</sup> - 0.0011 mW/cm<sup>2</sup>, respectively. In addition, the average noise level in the participating radio broadcasting stations was about 70 dB.

\*This study was supported by Research Foundation of Dicle Univ (DUAPK-02-TF-03)

## In vivo studies

P-A-97

### **EFFECTS OF EXPOSURE TO RF FIELDS ON SPATIAL LEARNING PROCESSES IN MICE.**

A. Bottomley<sup>1</sup>, N. Jones<sup>1</sup>, R. Haylock<sup>1</sup>, R. Saunders<sup>1</sup>, N. Kuster<sup>2</sup>, Z. Sienkiewicz<sup>1</sup>. <sup>1</sup>National Radiological Protection Board, Chilton, Didcot, Oxfordshire, OX11 0RQ, UK, <sup>2</sup>IT'IS, Zeughausstrasse 43, CH-8004 Zurich, Switzerland.

Lai and colleagues (1-3) have produced evidence that exposure of rats to low level pulsed radiofrequency (RF) fields may significantly impair the performance of spatial learning tasks. However other laboratories (4-7) have been unable to replicate or confirm these findings. The reasons for the differences in outcome have yet to be fully resolved.

The present experiments were undertaken using adult, male C57BL/6J mice to explore further the effects of the fields used in mobile telephones on spatial maze behaviour in mice. In the first series of studies, animals were exposed to 900 MHz GSM (talk) signals each day for 1 h over 15 days and their behaviour assessed using a food-reinforced, radial arm maze task. Animals were exposed using a mini-wheel system (whole body exposure) or using a waveguide system (exposure confined mainly to the

head). These exposure systems were designed and produced by IT'IS. In the second series, animals were exposed to either 400, 900 or 2200 MHz signals using a loop antenna system to irradiate the head for 1 h. Spatial learning was assessed using a Morris water maze task. The effects of single and repeated exposures were investigated, as were pulsed modulated and continuous wave fields. In addition, the effects of exposure on the baseline performance of a 5-choice serial reaction time (attentional) task were explored. The exposure system was designed and built by NRPB.

All tasks and assessments were conducted without knowledge of the exposure status of the animals. Results between groups were compared using standard model fitting techniques. In both series of studies, no measures of performance of any task were significantly impaired by exposure status, although small changes in behaviour were sometimes noted between groups.

It is concluded that, under the conditions of these experiments, none of the exposures had any significant field-dependent effects on learned behaviour. These results are consistent with similar studies with rats exposed to low level RF fields associated with mobile phones.

All procedures involving animals were carried out the approval of the local ethical review committee and in accordance with the Animals (Scientific Procedures) Act 1986.

The first series of studies was funded in part by the MMF and GSMA through the Perform B programme; the second series was funded by the UK Link MTHR Programme.

(1) Lai et al (1994) *Bioelectromagnetics*, 15, 95-104. (2) Wang and Lai (2000) *Bioelectromagnetics*, 21, 52-56. (3) Lai (2004) *Physiol Behav*, 82, 785-789. (4) Sienkiewicz et al (2000) *Bioelectromagnetics*, 21, 151-158. (5) Dubreuil et al (2003) *Behav Brain Res*, 145, 203-210. (6) Cobb et al (2004) *Bioelectromagnetics*, 25, 49-57. (7) Cassel et al (2004) *Behav Brain Res*, 155, 37-43.

P-A-100 STUDENT
-----------------

**EFFECT OF GSM EXPOSURE ON GLIA.** E. Brillaud, A. Piotrowski, R. de Seze. INERIS, Parc technologique Alata, BP 2, 60550 Verneuil en Halatte, FRANCE.

Introduction:

Electromagnetic fields (EMF) are suspected to have biological effects. In the framework of RAMP 2001 project, we try to evaluate possible effects of GSM exposure on the central nervous system and to determine the Specific Absorption Rate (SAR) and the duration limits that produce them. A recent paper (AL Mausset and al, december 2004) shows an increase of a specific marker of glial cells, the GFAP (Glial Fibrillary Acidic Protein), in striatum, hippocampus and cortex, 72 hours later a 15 min exposure to GSM-type radiation at a local SAR of 6 W/kg (head).

The aim of our experiment was to determine if that effect could be reproducible, and if it is persistent (sign of a potential gliosis) or temporary (sign of an inflammation).

Materials and methods:

Exposure system:

Animals were placed in Plexiglas rockets with an individual loop antenna placed above the rat's head. Four animals were exposed at the same time. Loops antenna were connected to a generator and emitted a

GSM signal (900 MHz, pulsed at 217 Hz, 1/8 duty factor) at a 6 W/kg-SAR.

Experimental group:

Sprague-Dawley male rats (weighting 200-250g on the experimental day) were randomly assigned to different groups:

- 36 animals exposed 15 min to a 6W/kg local SAR
- 9 sacrificed 2 days later
- 9 sacrificed 3 days later
- 9 sacrificed 6 days later
- 9 sacrificed 10 days later
- 12 animals exposed 15 min to a 0W/kg local SAR (sham animals)
- 6 sacrificed 3 days later
- 6 sacrificed 10 days later

To have an idea of physiological and pathological expression of GFAP, 6 animals were added:

- 3 without any treatment and manipulation (control cage)
- 3 treated with a Lipo Poly Saccharide (LPS) solution at 2,5 mg/kg (1ml/kg, i.v.)

LPS was used as positive control. It is known to provoke a corporal temperature increase, inducing brain inflammation and consequently an increase of the GFAP protein expression.

Immunohistochemical studies:

Animals were sacrificed by Para formaldehyde 4% intra-cardiac perfusion, and then brains were recovered and cut in 50 µm sagittal sections. Slices were then processed as free-floating sections for GFAP immunodetection.

Percentage of staining was determined in different areas: prefrontal cortex (Pfcx), cortex of cerebellum (CCx), dentate gyrus of hippocampus (DG), and lateral globus pallidus of striatum (LGP).

Results and discussion:

After statistical analyses (one way ANOVA test), results show a large increase of staining in Pfcx, more important at day 2 than day 3, statistically significant comparing to sham or control cages animals ( $p < 0.001$ ). In CCx, an increase was only observed at day 3 ( $p < 0.001$ ). In GD and LGP, no significant differences were observed. Increase seems to be due to a hypertrophy of glial cells, real visible at day 2 in hippocampus.

Our results show a temporary inflammation in external areas (cortex). Fact that effect was present at day 2 on frontal zone and day 3 on the other side of the brain, the cerebellum, could indicate a propagation of effect which could be the consequence of a dura mater and blood brain barrier impairments.

These results are not in accordance with A.L. Mausset results. Indeed, she found the maximal effect at 3 days in the striatum ( $p < 0.001$ ), and an effect in hippocampus ( $p < 0.001$ ) and cortex ( $p < 0.05$ ).

Support: European project RAMP (CE) contract n°QLK4-CT-2001-00463, Ministry of Ecology and Durable Development and Research Ministry BCRDn°12-02

P-A-103

**EFFECT ON NEURONAL BRAIN ACTIVATION IN MICE FROM A COMBINATION OF PULSED EXTREMELY LOW FREQUENCY MAGNETIC FIELDS AND IMMOBILIZATION.**

Y. Bureau<sup>1</sup>, D. Dunlop<sup>3</sup>, A. W. Thomas<sup>1,2</sup>, F. S. Prato<sup>1,2</sup>. <sup>1</sup>Lawson Health Research Institute and Dept of Nuclear Medicine, St. Joseph's Health Care (London), 268 Grosvenor St., London, Ontario, Canada, N6A 4V2, <sup>2</sup>Univ of Western Ontario, London, Ontario, Canada, <sup>3</sup>McMaster Univ, Hamilton, Ontario, Canada.

Background: Pulsed extremely low frequency magnetic fields (PELFMF) have been shown to increase analgesia to hotplate nociception in land snails [1,2] and more recently in mice [4] and to electrical shock and thermode heat in humans [3,5]. However, it has been suggested that the observed antinociception in mice is due to stress induced by the PELFMF. This is a phenomenon more commonly known as stressed induced analgesia or SIA.

Objective: This work has been carried out firstly to investigate whether or not neuronal activity is induced by PELFMF and secondly, if this activity is modulated in regions of the mouse brain associated with stress during a restraint stress procedure. We do not expect that neuronal activity will be greatly induced in mice exposed to PELFMF alone. However, if the observed antinociception seen in our previous publications is due to SIA, we expect to see greater activity in regions of the brain associated with stress in mice exposed to restraint and PELFMF compared to restraint alone.

Methodology: In brief, CD-1 mice were exposed to either; 1) PELFMF ( $\pm 200 \mu\text{TPK}$ ,  $< 500 \text{ Hz}$ ), 2) discontinuous 60Hz sinusoidal with a refractory period identical to that incorporated in the PELFMF ( $\pm 200 \mu\text{TPK}$ ), or 3) ambient MF sham for 60 minutes prior to 30 minutes of restraint plus field exposure in a 50cm centrifuge tube with air holes or sham restraint, followed by an additional 30 minutes of field exposure. All mice were euthanized 120 minutes following restraint termination and brains removed and processed for regional c-Fos immunoreactivity. C-Fos positive cells were then quantified by computer-automated software (Northern Eclipse).

Results: No effects were observed for magnetic field exposure. As expected, stress related regions of the brain such as the locus coeruleus, septal nuclei, periaqueductal grey and paraventricular nucleus of the hypothalamus showed significant increases in c-Fos positive neurons in the restraint groups.

Conclusions: PELFMF were ineffective in inducing or altering neuronal activity in this study. It is unlikely that PELFMF produce antinociception by SIA.

References:

- [1] Thomas, A.W., Kavaliers, M., Prato, F.S., and Ossenkopp, K.-P. (1997). *Peptides*, 18(5), 703-709.
- [2] Thomas, A.W., Kavaliers, M., Prato, F.S., and Ossenkopp, K.-P. (1997). *Neuroscience Letters*, 222, 107-110.
- [3] Rollman, G., Misener, T., Thomas, A., Prato, F. 24th Annual Bioelectromagnetics Society Meeting, Quebec, Canada, June 23-27th, 2002.
- [4] Shupak et al 2004, *Neuroscience Letters*, 354 (1), 30-33.
- [5] Shupak et al 2004, *Neuroscience Letters*, 363 (2), 157-162.

Acknowledgements: This study was funded by FrAlex Therapeutics Inc.; St. Joseph's Health Care (London) Foundation; the Lawson Health Research Institute; the Dept of Nuclear Medicine at SJHC; Natural Sciences and Engineering Research Council of Canada (NSERC); Canadian Institutes of Health Research (CIHR); National Research Council (NRC); the Ontario Research and Development Challenge Fund (ORDCF), Canada Foundation for Innovation (CFI); and the Ontario Innovation Trust (OIT).

P-A-106

**THE EFFECT OF PULSED EXTREMELY LOW FREQUENCY MAGNETIC FIELDS ON HOTPLATE NOCICEPTION AND NEURONAL ACTIVATION IN MICE.** Y. Bureau<sup>1</sup>, E. Adams<sup>2</sup>, A. W. Thomas<sup>1,2</sup>, F. S. Prato<sup>1,2</sup>. <sup>1</sup>Lawson Health Research Institute and Dept of Nuclear Medicine, St. Joseph's Health Care (London), 268 Grosvenor St., London, Ontario, Canada, N6A 4V2, <sup>2</sup>Univ of Western Ontario, London, Ontario, Canada.

Background: Pulsed extremely low frequency magnetic fields (PELFMF) have been shown to increase

analgesia to hotplate nociception in land snails [1,2] and more recently in mice [4] and to electrical shock and thermode heat in humans [3,5]. It is thought that PELFMF may influence neuronal activity in brains of mice, especially in regions of the brain associated with pain reduction. This may be a possible reason for the observed antinociception as shown by the hotplate test.

**Objective:** We wished to investigate the influence of PELFMF on hotplate nociception and neuronal activity in mice. Specifically, we hypothesized that areas of the brain associated with pain reduction would be activated in those mice with reduced nociceptive (pain) behaviour in the hotplate test.

**Methodology:** In brief, 30 CD-1 mice were tested for nociceptive behavior before and immediately following 120 minutes of exposure to; 1) PELFMF ( $\pm 200 \mu\text{TPK}$ ,  $< 500 \text{ Hz}$ ), 2) discontinuous 60Hz sinusoidal with a refractory period identical to that incorporated in the PELFMF ( $\pm 200 \mu\text{TPK}$ ), or 3) ambient MF. Nociception was defined as the time necessary for mice to display heat sensitive behaviours from being placed on a heated plate ( $50^\circ\text{C}$ ). All mice were euthanized 120 minutes following the last hotplate test and the brains removed and processed for regional c-Fos immunoreactivity. C-Fos positive cells were then quantified by computer-automated software (Northern Eclipse).

**Results:** Mice exposed to the PELFMF demonstrated significantly less nociception compared to all other conditions. However, there were no significant findings with respect to c-Fos quantification.

**Conclusions:** The robust antinociceptive effect of PELFMF repeatedly seen in this laboratory was not associated with c-Fos positivity.

**References:**

- [1] Thomas, A.W., Kavaliers, M., Prato, F.S., and Ossenkopp, K.-P. (1997). *Peptides*, 18(5), 703-709.
- [2] Thomas, A.W., Kavaliers, M., Prato, F.S., and Ossenkopp, K.-P. (1997). *Neuroscience Letters*, 222, 107-110.
- [3] Rollman, G., Misener, T., Thomas, A., Prato, F. 24th Annual Bioelectromagnetics Society Meeting, Quebec, Canada, June 23-27th, 2002.
- [4] Shupak et al 2004, *Neuroscience Letters*, 354 (1), 30-33.
- [5] Shupak et al 2004, *Neuroscience Letters*, 363 (2), 157-162.

**Acknowledgements:** This study was funded by FrAlex Therapeutics Inc.; St. Joseph's Health Care (London) Foundation; the Lawson Health Research Institute; the Dept of Nuclear Medicine at SJHC; Natural Sciences and Engineering Research Council of Canada (NSERC); Canadian Institutes of Health Research (CIHR); National Research Council (NRC); the Ontario Research and Development Challenge Fund (ORDCF), Canada Foundation for Innovation (CFI); and the Ontario Innovation Trust (OIT).

P-A-109

**IN VIVO EVALUATION OF THE POTENTIAL GENOTOXICITY OF A RTMS SIGNAL IN THE RAT BRAIN.** R. C. de Sauvage, I. Lagroye, B. Billaudel, B. Veyret. Bioelectromagnetics Laboratory, UMR 5501, EPHE /PIOM ENSCPB, 33607 Pessac, France.

**INTRODUCTION:** Repetitive Transcranial Magnetic Stimulation (rTMS) is widely used in clinical practice. It seems particularly useful in neuropsychiatry for applications such as the potential treatment of drug-resistant depression, either in clinical trials or in routine therapy (Canada, Israel). However, few biological studies have been performed, particularly on possible toxicological effects of rTMS signals.

**OBJECTIVES:** Our first objective was to evaluate the toxicity of rTMS signals used in clinical trials.

**METHODOLOGY:** In order to stimulate the cortex, rTMS signals commonly consist of pulsed magnetic fields with duration between 0.1 and 1 ms, with a repetition rate between 1 and several dozens of hertz (often 10 Hz), and with a maximum magnetic induction of about 2 teslas. We have thus built an

experimental magnetic stimulator with a repetition rate close to 20 pps and with water cooling. This apparatus allows for a multi-parametric research on biological effects of rTMS. With this apparatus, we stimulated a series of rats with a unique exposure sequence consisting in 20 trains at 10 Hz for 10 s with 50 s-intervals. Rats were exposed to rTMS signals produced by a coil placed on the top of the skull but not touching the head, with the coil parallel to the skull and the coil axis passing through the bregma point, as defined in the atlas of Paxinos and Watson (1986). Magnetic pulses induced by one-sine currents (duration 340  $\mu$ s), and with an amplitude reaching 80% of the hind-limb motor threshold were used (peak field around 1 T). These values are within the safety limits published by Wassermann (1998) and are close to the protocol followed by Pr Auriacombe at the Charles Perrens hospital (Bordeaux, France) in a clinical trial. A total of 2000 pulses were delivered to the animals. The starting direction of rTMS signals in the brain was clockwise. Mapping of the induced electric field, hence of the induced current density, was established for the flat 6.3 cm diameter coil used in this experiment. Eddy currents induced in the rat brain were calculated using a rat head model derived from the Brooks model constructed from MRI images in the rat. Tissue conductivities were estimated from low-frequency literature data. A software designed in the MatLab environment, based on the resolution of node and mesh equations, was used and validated. Peak current densities in the brain were estimated at around 10 A/m<sup>2</sup>.

**RESULTS:** Rats exposed to rTMS or sham exposed were restrained during exposure, which necessitated a period of habituation. Different groups of four animals were evaluated: (i) animals exposed to the rTMS signal, (ii) control animals for assessing the effects of contention and noise produced by the magnetic stimulator, (iii) cage controls with free movements and unexposed to noise, and (iv) positive controls. After exposing animals in vivo, the protocol was blinded (coded animals), and the evaluation of DNA damages in isolated brain cells done using the alkaline comet assay. The analysis of the experiment is in progress.

**CONCLUSION AND PERSPECTIVES:** The results on the ability of a single daily sequence of rTMS signals to induce DNA damages will be presented. These are part of a set of experiments dealing with cellular toxicity of signals with a high dB/dt. The next set of experiments will assess the effects, in the rat, of a clinical paradigm (20 min/day, 5 days/week, 2 to 4 weeks). Further studies will use in vitro exposure to rTMS signals for the evaluation of the induction of micronuclei and apoptosis in nerve cells.

**ACKNOWLEDGMENTS:** Support to this work was given by INSERM.

P-A-112

**INFLUENCE OF CHRONIC EXPOSURE TO WEAK VARIABLE MAGNETIC FIELD ON SERUM LIPIDS IN RATS.** G. Cieslar<sup>1</sup>, J. Zalejska-Fiolka<sup>2</sup>, E. Birkner<sup>2</sup>, S. Kasperczyk<sup>2</sup>, A. Sieron<sup>1</sup>.  
<sup>1</sup>Chair and Clinic of Internal Diseases, Angiology and Physical Medicine, Silesian Medical Univ, PL-41902 Bytom, Poland, <sup>2</sup>Chair and Dept of Biochemistry, Silesian Medical Univ, PL-41808 Zabrze, Poland.

**Objectives.** The aim of the study was to estimate the influence of chronic exposure to weak variable magnetic field used in magneto-stimulation on serum concentration of cholesterol and triglycerides in rats. **Methods:** Experimental material consisted of 48 male Wistar rats weighting 180-200 g. Weak variable magnetic field of saw-like shape of impulse, at a frequency of basic impulse 180-195 Hz and induction 120 $\mu$ T generated by device for magneto-stimulation VIOFOR JPS (Poland) basing on ion cyclotron resonance phenomenon was used. All animals were randomly divided into 2 groups. In first group (40 animals) whole body exposure to magnetic field lasting 36 minutes daily for 14 consecutive days was made. In this group at 24 hours after first exposure, then at 7th and 14th day of repeated

exposures and at 7th and 14th day after the end of a cycle of exposures every time a part of animals (8 rats) was exsanguinated in ether narcosis. The last 8 animals made up a control group. They were exsanguinated in ether narcosis without any exposure to obtain reference values of particular lipid parameters. In obtained blood samples concentration of total cholesterol ( $\alpha$ -diagnostics, Poland), HDL-cholesterol ( $\alpha$ -diagnostics, Poland) and triglycerides ( $\alpha$ -diagnostics, Poland) was determined. The concentration of LDL-cholesterol was calculated as difference between total cholesterol and HDL-cholesterol concentration. In the statistical evaluation ANOVA analysis with subsequent post-hoc Mann-Whitney's U test were used. Summary of results: The concentrations of particular serum lipids in consecutive days of exposure cycle are presented in table 1. A significant increase of total cholesterol serum concentration during exposure cycle with subsequent significant decrease at 7th day after the end of exposure cycle and normalization at 14th day after the end of exposure cycle was observed as compared to control values. Similar changes of LDL cholesterol serum concentration were also observed. On the other hand a significant decrease in HDL cholesterol serum concentration in last phase of exposure cycle and at 7th day after the end of exposure cycle with subsequent normalization at 14th day after the end of exposure cycle was obtained. Triglycerides serum concentration was significantly higher as compared to control values only at 7th day of exposure cycle. In other days no significant changes of this parameter were observed. Conclusion: Chronic exposure to weak variable magnetic field used in magneto-stimulation basing on ion cyclotron resonance phenomenon causes only transient changes of serum lipids concentration during exposure cycle.

Table 1 Serum concentration of cholesterol fractions and triglycerides in magnetic field-exposed rats and control group in particular days of exposure cycle with statistical evaluation to control values before exposure

Day of exposure cycle	Total cholesterol [mg%]	HDL cholesterol [mg%]	LDL-cholesterol [mg%]	Triglycerides [mg%]
	Mean value $\pm$ SEM	Mean value $\pm$ SEM	Mean value $\pm$ SEM	Mean value $\pm$ SEM
Before exposure	70,9 $\pm$ 1,5	30,4 $\pm$ 1,2	40,5 $\pm$ 1,3	41,5 $\pm$ 4,5
1 day of exposure	80,8 $\pm$ 3,7*	31,0 $\pm$ 2,4	49,8 $\pm$ 3,0	45,0 $\pm$ 9,2
7 day of exposure	75,3 $\pm$ 4,3	25,4 $\pm$ 1,1*	49,9 $\pm$ 2,7*	79,7 $\pm$ 7,1**
14 day of exposure	78,8 $\pm$ 3,9**	27,6 $\pm$ 2,4	51,2 $\pm$ 3,2*	29,3 $\pm$ 4,5
7 day after the end of exposure	54,8 $\pm$ 3,7***	26,1 $\pm$ 1,6*	28,7 $\pm$ 2,6*	26,1 $\pm$ 1,6
14 day after the end of exposure	69,9 $\pm$ 5,2	28,1 $\pm$ 2,7	41,8 $\pm$ 3,9	28,1 $\pm$ 2,7
*p less 0,05, **p less 0,01, ***p less 0,001				

**INFLUENCE OF CHRONIC EXPOSURE TO WEAK VARIABLE MAGNETIC FIELD ON ANTIOXIDANT ACTIVITY IN RATS WITH EXPERIMENTAL INFLAMMATION.** G. Cieslar<sup>1</sup>, J. Mrowiec<sup>1</sup>, J. Zalejska-Fiolka<sup>2</sup>, E. Birkner<sup>2</sup>, S. Kasperczyk<sup>2</sup>, A. Sieron<sup>1</sup>. <sup>1</sup>Chair and Clinic of Internal Diseases, Angiology and Physical Medicine, Silesian Medical Univ, PL-41902 Bytom, Poland, <sup>2</sup>Chair and Dept of Biochemistry, Silesian Medical Univ, PL-41808 Zabrze, Poland.

**Objectives** The aim of the study was to estimate the influence of chronic exposure to weak variable magnetic field used in magneto-stimulation on activity of some antioxidant enzymes in rats with experimental inflammation. **Methods:** Experimental material consisted of 128 male Wistar rats weighting 180-200 g. Weak variable magnetic field of saw-like shape of impulse, at a frequency of basic impulse 180-195 Hz and induction of 60  $\mu$ T generated by device for magneto-stimulation Viofor JPS (Poland) basing on ion cyclotron resonance phenomenon was used. All animals were randomly divided into 4 groups (32 animals each). In first group whole body exposure to magnetic field lasting 36 minutes daily for 14 consecutive days was made. In second - control group sham-exposure without generating magnetic field inside of applicator lasting 36 minutes daily for 14 consecutive days was made. Rats in third group were injected with 50  $\mu$ l of 5% solution of formaldehyde in region of right hip and after 24 hours were subjected to the same exposure cycle as in first group. The animals in fourth - control group were also injected with 50  $\mu$ l of 5% solution of formaldehyde in region of right hip and then after 24 hours were subjected to the same sham-exposure cycle as in second group. In all groups at 7th and 14th day of repeated exposures or sham-exposures and at 7th and 14th day after the end of a cycle of exposures every time a part of animals (8 rats from each group) was exsanguinated in ether narcosis. In obtained blood and hemolysates of erythrocytes samples contents of some antioxidant activity indicators: activity of catalase (CAT), glutathione peroxidase (GPX) and superoxide dismutase (SOD) in erythrocytes, activity of isoenzymes of superoxide dismutase (Mn-SOD and ZnCu-SOD)) in serum as well as serum concentration of malondialdehyde (MDA) was determined by means of spectrophotometric and kinetic methods. In the statistical evaluation ANOVA analysis with subsequent post-hoc Mann-Whitney's U test were used. **Summary of results:** The activities of antioxidant enzymes as well as serum malondialdehyde concentration in particular groups of rats are presented in table 1. In magnetic field-exposed group a significant decrease in activity of most of analyzed antioxidant enzymes both in erythrocytes and serum during exposure cycle was observed as compared to a group of rats with experimental inflammation, in which these activities were significantly increased comparing to control group. Besides in both magnetic field-exposed groups a significant decrease in malondialdehyde serum concentration during exposure cycle was obtained. **Conclusion:** Chronic exposure to weak variable magnetic field used in magnetostimulation basing on magnetic resonance phenomenon causes a beneficial effect antioxidant reactions in course of experimental inflammation in living organisms.

Table 1 The activity of some antioxidant enzymes in serum and erythrocytes and serum concentration of malondialdehyde in all groups of rats in particular days of exposure cycle with statistical evaluation to control group

Parameter	Group	Day of exposure or sham-exposure			
		7 day of exposure cycle	14 day of exposure cycle	7 day after the end of exposure cycle	14 day after the end of exposure cycle
Activity of CAT in erythrocytes					

[IU/mgHb]	Control	197,3	168,9	152,0	158,4
	Inflammation	142,4**	117,8**	211,1	102,9**
	Magnetic field	178,8	112,3**	105,5*	88,0**
	Magnetic field + inflammation	177,9	118,5**	115,3**	97,6**
Activity of GPX in erythrocytes [IU/gHb]	Control	139,7	79,6	118,2	60,2
	Inflammation	271,2**	164,4**	138,3	73,2
	Magnetic field	141,3	107,0*	103,1	118,7**
	Magnetic field + inflammation	102,6	117,6**	118,2	138,2**
Activity of SOD in erythrocytes					
[NU/gHB]	Control	135,7	132,5	122,0	285,6
	Inflammation	117,3	99,6	185,9	141,4**
	Magnetic field	97,1	169,9	220,7*	172,5**
	Magnetic field + inflammation	55,9	168,6	220,9*	152,1**
Activity of Mn-SOD in serum [NU/ml]	Control	8,2	12,0	13,2	7,7
	Inflammation	5,8*	9,3	3,2**	4,4
	Magnetic field	5,4*	8,6	3,6**	4,9
	Magnetic field + inflammation	3,4*	5,7**	3,0**	4,4
Activity of ZnCu-SOD in serum [NU/ml]	Control	19,2	15,4	18,4	21,7
	Inflammation	24,3*	20,4	24,7*	22,5
	Magnetic field	21,9	21,9	26,1*	26,1*
	Magnetic field + inflammation	20,0	22,0	27,5*	28,6*
Concentration of MDA [ $\mu$ mol/l]	Control	6,3	6,2	4,1	5,0
	Inflammation	4,9	4,3	3,7	3,4*
	Magnetic field	3,0**	2,9**	3,3	4,6
	Magnetic field + inflammation	3,9**	2,9**	3,5	4,6

\*p less 0,05, \*\*p less 0,01, \*\*\*p less 0,001

P-A-118

**ANALGESIC EFFECT OF CHRONIC, SIMULTANEOUS EXPOSURE TO WEAK VARIABLE MAGNETIC FIELD AND RED LIGHT IN RATS.** G. Cieslar<sup>1</sup>, J. Mrowiec<sup>1</sup>, K. Sieron-Stoltny<sup>1</sup>, A. Plech<sup>2</sup>, S. Kasperczyk<sup>3</sup>, A. Sieron<sup>1</sup>. <sup>1</sup>Chair and Clinic of Internal Diseases, Angiology and Physical Medicine, Silesian Medical Univ, PL-41902 Bytom, Poland, <sup>2</sup>Chair and Dept of Pharmacology, Silesian Medical Univ, PL-41808 Zabrze, Poland, <sup>3</sup>Chair and Dept of Biochemistry, Silesian Medical Univ, PL-41808 Zabrze, Poland.

**Objectives.** The aim of the study was to estimate the influence of chronic whole body simultaneous exposure to weak variable magnetic field used in magneto-stimulation and red light radiation on pain reaction in rats as well as the involvement of endogenous opioid system in the mechanism of this effect. **Methods:** Experimental material consisted of 32 male Wistar rats weighting 180-200 g. Weak variable magnetic field of saw-like shape of impulse, at a frequency of basic impulse 180-195 Hz and induction of 336-672  $\mu$ T (depending on the position of magnetic field induction measuring points) and light radiation (wavelength - 630 nm, mean power - 0,35 W, energy density - 0,48 J/cm<sup>2</sup>) generated by magnetic-light applicator of device for magneto-stimulation Viofor JPS (Poland) were used. All animals were randomly divided into 4 groups (8 animals each). In first group whole body simultaneous exposure to magnetic field and light radiation lasting 12 minutes daily for 2 periods of 5 consecutive days with 2 days-lasting break between them, was made. In second, control group sham-exposure without generating magnetic field and light radiation inside of applicator was made. In order to estimate the involvement of endogenous opioid system in the mechanism of magnetic field and light radiation-induced analgesic reaction, in next 2 groups after prior (30 minutes before exposure) i.p. injection of Naloxone hydrochloride (1mg/1kg of body mass) antagonist of opiates - following 12 minutes lasting exposure to magnetic field and light radiation or sham-exposure respectively was made. During whole-body exposure animals were placed individually in a specially designed plastic chamber with cover made up by square magnetic-light applicator. The pain perception was determined by latency of foot-licking or jumping from the surface of a 56°C hot plate. The measurements were made at 5th, 15th, 30th, 60th, 90th and 120th minute after the end of a single exposure. Next the estimation of pain reaction was made at 24 hours after a single exposure, at 5th and 12th day of exposure cycle and at 7th and 14th day after the end of a cycle of exposures. On the basis of obtained measurements of pain reaction latency time an analgesic index was calculated according to special formula. In the statistical evaluation ANOVA analysis with subsequent post-hoc Mann-Whitney's U test were used. **Summary of results:** The mean values of analgesic index in all groups in particular time intervals after a single exposure and in particular days of exposure cycle are presented in table 1. As a result of repeated exposures both to weak variable magnetic field and red light irradiation a significant increase of pain reaction latency index persisting also after the end of a cycle of exposures as compared to sham-exposed group was observed. This magnetic field and light radiation-induced analgesic effect was inhibited by prior injection of opioid antagonist - Naloxone. **Conclusion:** Chronic simultaneous exposure of rats to weak variable magnetic field and red light radiation evokes strong, persistent analgesic effect in rats. In the mechanism of this effect is involved endogenous opioid system.

Table 1 Mean values of analgesic index [%] in all groups of animals in particular time intervals after a single exposure and in consecutive days of exposure cycle with statistical evaluation to control sham-exposed group

Time interval	Control sham-exposure mean $\pm$ SEM	Magnetic field and red light mean $\pm$ SEM	Magnetic field and red light and Naloxone mean $\pm$ SEM	Sham-exposure and Naloxone mean $\pm$ SEM
Before exposure	-0,2 $\pm$ 0,9	-0,2 $\pm$ 0,6	-0,9 $\pm$ 0,3	-0,4 $\pm$ 0,3
5 min.	-0,9 $\pm$ 0,5	9,7 $\pm$ 1,2***	1,1 $\pm$ 0,9	-0,4 $\pm$ 0,3
15 min.	-0,2 $\pm$ 0,9	9,1 $\pm$ 0,8***	-0,2 $\pm$ 0,6	0,2 $\pm$ 0,8
30 min.	0,4 $\pm$ 0,8	9,7 $\pm$ 1,0*	0,4 $\pm$ 0,9	-0,4 $\pm$ 0,3
45 min.	-0,2 $\pm$ 0,7	9,7 $\pm$ 1,3*	1,1 $\pm$ 0,9	-0,4 $\pm$ 0,3
60 min.	-0,2 $\pm$ 0,7	11,1 $\pm$ 0,7***	-0,2 $\pm$ 0,6	0,2 $\pm$ 0,5
90 min.	-0,9 $\pm$ 0,5	9,7 $\pm$ 0,9***	-0,9 $\pm$ 0,3	-0,4 $\pm$ 0,3
120 min.	-0,9 $\pm$ 0,5	10,4 $\pm$ 1,0*	-0,9 $\pm$ 0,3	-0,4 $\pm$ 0,3
2 day of exposure cycle	1,1 $\pm$ 2,0	6,8 $\pm$ 0,8*	-	-
5 day of exposure cycle	0,5 $\pm$ 1,0	9,5 $\pm$ 0,7***	-	-
12 day of exposure cycle	-1,6 $\pm$ 0,9	8,1 $\pm$ 1,4***	-	-
7 day after the end of exposure cycle	-2,3 $\pm$ 0,8	6,1 $\pm$ 1,2***	-	-
14 day after the end of exposure cycle	-3,7 $\pm$ 1,1	5,4 $\pm$ 1,1**	-	-
1 day of exposure cycle	1,1 $\pm$ 2,0	6,8 $\pm$ 0,8*	-	-
*p less 0,05, **p less 0,01, ***p less 0,001				

P-A-121

**REVIEW OF 30 STUDIES INVESTIGATING CANCER IN LABORATORY ANIMALS EXPOSED TO RADIOFREQUENCY ENERGY.** J. A. Elder. Motorola Florida Research Labs, 8000 W. Sunrise Blvd., Ft. Lauderdale, FL 33322.

Objective: To review long-term exposure studies examining whether radiofrequency (RF) energy

causes/promotes cancer or affects survival and general health of laboratory animals. Methods: In three tables, this report summarizes 30 studies of cancer in laboratory animals exposed to RF energy published from 1962-2005. The first table indicates whether or not a statistically significant increase was observed in cancer incidence as well as effects on survival and body mass, if reported. For each of the 30 studies, information is provided on animal species, frequency (and modulation), dose rate (specific absorption rate, SAR), exposure conditions, cancer model, number of animals per group and reference. A second table presents the 15 studies in which animals were exposed for 12-25 months. Thus, 50% of the studies employed long-term exposures of one year or longer in duration; 13 of the 15 studies exposed the animals for 18-25 months. A third table lists the studies by cancer model (spontaneous tumors, genetically-modified animals, chemically-induced tumors, ionizing radiation-induced tumors and models employing injected tumor cells).

Results: Two studies (Preskorn et al., *J Surg Oncol* 10:483, 1978; Adey et al., *Rad Res* 152:293, 1999) reported that RF exposure had a "protective" effect on cancer development but such results are not supported by the overall evidence. Likewise, three reports (Szmigielski et al., *Bioelectromagnetics* 3: 179, 1982; Chou et al., *Bioelectromagnetics* 13:469, 1992; Rephacholi et al., *Rad Res* 147:631, 1997) of carcinogenic effects in RF-exposed animals are not supported by the weight of evidence from 30 studies. A follow-up investigation of the experiment by Rephacholi et al. (*Rad Res* 147:631, 1997) by Utteridge et al. (*Rad Res* 158:357, 2002) used eight times as many animals and four exposure levels (0.25, 1, 2 and 4 W/kg) and did not confirm an increase in tumors. Two studies reported changes that could not be replicated in the same laboratory (Bartsch et al., *Rad Res* 157:183, 2002; Anane et al., *Rad Res* 160:492, 2003). It is noted that all 21 cancer studies published since 1998 found no adverse effect of RF exposure.

Conclusion: The scientific weight of evidence in 30 cancer studies shows that there is no adverse effect of RF exposure up to two years in duration at dose rates up to 4 W/kg on 1) survival, 2) body mass, an indicator of general health status, and 3) carcinogenic processes (initiation, promotion and co-promotion). (Supported by Motorola)

P-A-124

**CHANGES IN BLOOD FLOW DYNAMICS RELATED TO INCREASED THERMAL EFFECTS OF RF-EMF IRRADIATION ON RABBIT EAR SKIN.** J. Fu<sup>1</sup>, G.F. Lawlor<sup>2</sup>, A. Ushiyama<sup>1</sup>, H. Masuda<sup>1</sup>, C. Ohkubo<sup>1</sup>. <sup>1</sup>Dept of Environmental Health, <sup>2</sup>Dept of Public Health Administration and Policy, National Institute of Public Health, 2-3-6 Minami, Wako-shi, Saitama 351-0197, Japan.

**OBJECTIVE:** Most of the known influences caused by radio-frequency electromagnetic field (RF-EMF) exposure to humans and laboratory animals have been ascribed to thermal effects. Previously we have reported that 20 minutes exposure to 1,500MHz RF-EMF (local SAR 2W/kg, 10W/kg and 30W/kg) could induce significant temperature increases in blood flow occluded rabbit ears, but these thermal elevations were reduced under normal physiological conditions in the rabbit ear. In this study we investigate the correlation between changes in blood flow dynamics and elevations in rabbit ear skin temperature induced by RF-EMF exposure, in order to elucidate the mechanism(s) of blood circulation in regulating RF-EMF induced thermal effects.

**METHODS:** Adult male Japanese white rabbits were used in experiments. For observing cutaneous microvasculature, rabbit ear chambers (REC) were surgically implanted into the ears of rabbits 6 weeks prior to starting the experiments. REC installed rabbit ears were set on a microscope stage and exposed to 1,500MHz RF-EMF emitted from a loop dipole antenna for 20 minutes. The intensities of exposures applied were effectively calculated as local SAR 0W/kg (sham), 36W/kg and 50W/kg. All rabbits were

anesthetized with an intramuscular injection of a cocktail of ketamine hydrochloride 63mg/kg and xylazine hydrochloride 7mg/kg, in order to maintain animals in a constant, stabilized position for REC observation and monitoring. Continuous intravenous injection of acetylcholine chloride (Ach) in saline (10 $\mu$ g/kg/hr), nor-adrenalin (NA) in saline (1.5 $\mu$ g/kg/hr), or only normal saline solution (NS) was administered to the unexposed ear to produce different blood flow conditions. Erythrocyte flow in venules (diameter 10-40 $\mu$ m) within REC was recorded with a high-speed video camera (FASTCAM-NEO 32K, Photron K.K., Tokyo) fixed to a microscope, image capture and analysis was performed for a series of selected times throughout the experimental period, i.e., before, during and after RF-EMF irradiation. Velocities of blood flow were evaluated using erythrocyte flow images with flow measurement software (Flow-Vec32, Library Co., Ltd., Tokyo). Time series changes in rabbit ear skin temperature proximal to the REC and rectal temperature were also recorded throughout the period of erythrocyte flow observation.

**RESULTS:** RF-EMF irradiation at both local SAR 36W/kg and 50W/kg induced statistically significant elevations in rabbit ear skin temperature compared with sham exposure, while temperatures of ear skin surfaces continued to decline due to anesthesia as expected when no RF-EMF irradiation was applied. However, the continual intravenous injection of NS, NA or Ach induced no significant changes in skin temperature after RF-EMF irradiation. Falling rectal temperatures due to anesthesia confirmed that, under all conditions of RF-EMF irradiation or continual intravenous injection, core body temperature was unaffected by any local thermal changes. Analysis of erythrocyte velocity, blood flow volume and any correlation to elevated skin temperature after RF-EMF irradiation is currently in progress.

**ACKNOWLEDGMENTS:** This study is financially supported by NTT DoCoMo Inc., Japan. The authors express their appreciation to Dr. Uebayashi and his colleagues for their generous suggestions and cooperation.

P-A-127

**ANTI-INFLAMMATORY EFFECTS OF LOW-INTENSITY MILLIMETER WAVES IN THE MODEL OF MOUSE FOOTPAD EDEMA.** A. B. Gapeyev, Konstantin V. Lushnikov, J.V. Shumilina, N. K. Chemeris. Institute of Cell Biophysics of Russian Academy of Sciences.

**INTRODUCTION:** In spite of widespread medical application of extremely high-frequency electromagnetic radiation or millimeter waves (MW) of non-thermal intensities [1-3], the specific mechanisms of realisation of the therapeutic effects of MW remained in many respects unclear. From the analysis of data in the literature and our own results, we supposed that the effects of MW at the level of whole organism could be realized with the immediate involvement of regulatory systems maintaining homeostasis, in particular, the immune system [4]. Earlier, we showed that short-term (20 min) whole-body exposure of mice to MW (42.0 GHz, 0.1 mW/cm<sup>2</sup>) resulted in a reduction of intensity of non-specific and immune inflammation [5, 6].

**OBJECTIVE:** The objective of the present study was the investigation of the mechanisms of anti-inflammatory effects of low-intensity MW in comparison with effects of well-known anti-inflammatory drug sodium diclofenac and antihistamine clemastine.

**METHODS:** A non-specific inflammatory response was induced by injection of 25  $\mu$ l of zymosan suspension (5 mg/ml) into the hind paw of NMRI mice. Diclofenac (2-20 mg/kg) or clemastine (0.02-0.6 mg/kg) were i.p. administered in 30 min after zymosan injection. In 1 h after zymosan injection, the mice were whole-body exposed to MW (42.0 GHz, 0.1 mW/cm<sup>2</sup>, 20 min) in the far-field zone of pyramidal horn antenna with an aperture of 32x32 mm<sup>2</sup>. The mice were exposed from the top in plastic containers with a size of 100x100x130 mm where animals free moved. Specific absorption rate on the

surface of mouse skin was about 1.5 mW/g. Animals of the control group were subjected to injection of physiological saline and/or sham-exposed. The footpad edema (relative increase in the paw thickness) and local hyperthermia were measured before initiation and during 3-8 h of development of the inflammation response.

**RESULTS:** Diclofenac caused a dose-dependent anti-inflammatory effect. Doses of 5-20 mg/kg reduced the footpad edema on the average by 26% ( $p < 0.01$  by the Student's t-test) as compared to the control. Hyperthermia decreased with increasing in a dose of diclofenac, and at a dose of 20 mg/kg decreased by 60% ( $p < 0.02$ ) in comparison with the control. We revealed that MW exposure decreased both the footpad edema and hyperthermia by about 20% ( $p < 0.02$ ) that was comparable with the effect of single therapeutic dose of diclofenac (3-5 mg/kg). Combined action of diclofenac and MW exposure produced a partial additive effect. Clemastine in doses of 0.02-0.4 mg/kg did not significantly change the exudative edema, but in a dose of 0.6 mg/kg reduced edema by 14-22% ( $p < 0.05$ ) in 5-8 h after zymosan injection. Combined action of clemastine and MW exposure resulted in a dose-dependent abolishment of the anti-inflammatory effect of MW.

**CONCLUSION:** On the basis of the results obtained we suggest that inhibition of non-specific inflammation caused by the exposure to low-intensity MW can be connected with the decrease in functional activity of phagocytes, which play a key role in the development of inflammatory response [5, 6]. The comparative pharmacological analysis showed that anti-inflammatory effects of MW are realized with involvement of both histamine and arachidonic acid metabolites. Thereby, our experimental results indicate that some therapeutic effects of low-intensity MW can be determined by inhibition of inflammatory processes at the level of phagocytic cells.

The work was supported by the grant from Russian Foundation for Basic Research (03-04-49210).

References.

- [1] Devyatkov ND, Golant MB, Betskii OV. Millimeter Waves and Their Role in Vital Activity. Moscow: Radio i Svyas', 1991 (in Russian).
- [2] Rojavin MA, Ziskin MC. Medical application of millimetre waves. Q J Med 1998; 91: 57-66.
- [3] Pakhomov AG, Akyel Y, Pakhomova ON, Stuck BE, Murphy R. Current state and implications of research on biological effects of millimeter waves: a review of the literature. Bioelectromagnetics 1998; 19: 393-413.
- [4] Lushnikov KV, Gapeyev AB, Chemeris NK. Effects of extremely high-frequency electromagnetic radiation on the immune system and system regulation of the homeostasis. Radiation biology. Radioecology 2002; 5: 533-545 (in Russian).
- [5] Lushnikov KV, Gapeyev AB, Shumilina YuV, Shibaev NV, Sadovnikov VB, Chemeris NK. Suppression of cell-mediated immune response and nonspecific inflammation on exposure to extremely high frequency electromagnetic radiation. Biophysics 2003; 48(5): 856-863.
- [6] Lushnikov KV, Shumilina YuV, Yakushina VS, Gapeyev AB, Sadovnikov VB, Chemeris NK. Effects of low-intensity extremely high frequency electromagnetic radiation on inflammatory processes. Bull Exp Biol Med 2004; 137(4): 364-366.

P-A-130

**THERMAL IMAGING AND MODELLING OF MICROELECTRODES IN A RADIOFREQUENCY FIELD.** A. Chris Green<sup>1</sup>, B. Truscott<sup>1</sup>, N. C.D. Mifsud<sup>1</sup>, Y. Alfadhl<sup>2</sup>, X. Chen<sup>2</sup>, J. E.H. Tattersall<sup>1</sup>. <sup>1</sup>Biomedical Sciences Dept, Dstl Porton Down, Salisbury, Wiltshire SP4 0JQ, UK, <sup>2</sup>Dept of Electronic Engineering, Queen Mary, Univ of London, Mile End Road, London E1 4NS.

**OBJECTIVE:** Previous studies have suggested that *in vitro* exposure to 700MHz radiofrequency (RF)

fields at SARs up to  $5\text{mW.kg}^{-1}$  can affect both evoked and spontaneous electrical activity in rat hippocampal slices (Tattersall et al, 2001). Recent experiments in our laboratory have found that 380MHz RF fields at a much higher SAR of  $400\text{mW.kg}^{-1}$  can rapidly and irreversibly abolish electrical activity in slices. We have investigated whether this unexpected effect at these higher powers could be due to artifacts produced by interaction of the RF field with the stimulating or recording electrodes used in the experiments.

**METHODS:** Hippocampal slices were exposed to 380 and 700 MHz RF fields in a parallel plate transmission line (Tattersall et al., 2001), to produce tissue SARs of up to  $800\text{mW.kg}^{-1}$ . An infrared camera (Cedip Infrared Systems Jade) was used to image the brain slice and the electrodes. This had a theoretical thermal resolution of  $0.025^\circ\text{C}$  and each pixel on the sensor corresponded to approximately  $200\mu\text{m}$  at the brain slice target. The acquisition rate was 3 frames/s. The measurements from the camera were validated using a Luxtron fluoro-optic probe placed in the same slice next to the tip of the stimulating electrode. Numerical modelling of the system was performed using a time domain simulation package based on the finite integral technique (FIT) algorithm in CST Microwave Studio™. The metal stimulating electrode was accurately represented by utilising thin sheet technology™ (TST), which allows smaller structures to be modelled within a larger FDTD cell.

**RESULTS:** Exposures of brain slices to continuous wave 380MHz fields at  $400\text{mW.kg}^{-1}$  did not produce any measurable temperature rise when the recording and stimulating electrodes were absent. When the metallic stimulating electrode was placed into the slice, however, heating was clearly visible in the area of the slice around the electrode tip. This was proportional to field intensity but was variable between experiments: the temperature rise immediately adjacent to the tip was approximately  $7\text{-}10^\circ\text{C}$  for a tissue SAR of  $400\text{mW.kg}^{-1}$ , rising to  $15\text{-}20^\circ\text{C}$  for a tissue SAR of  $800\text{mW.kg}^{-1}$ . No heating was observed in areas of the slice away from the electrode tip. For 700MHz exposures at the power levels used by Tattersall et al. (2001), the temperature rise immediately next to the electrode tip was approximately  $0.3^\circ\text{C}$ . Temperature rises also occurred in the recording electrode (a glass micropipette filled with 2M NaCl) during exposure to RF fields. These were much lower when the angle of the electrode was changed from approximately parallel to the electric field to be approximately normal to the E field.

Numerical modelling (at 900MHz) showed that the presence of the stimulating electrode had no significant effect on SAR when the electrode was normal to the E field, but the SAR values increased significantly as the angle moved parallel to the E-field. The enhancement of SAR was also affected by the proximity of the electrode to the plates of the transmission line.

**DISCUSSION:** The temperature rises produced near the electrodes at a tissue SAR of  $400\text{mW.kg}^{-1}$  appear to be sufficient to abolish electrical activity in the brain slice. At the field intensity used by Tattersall et al (2001), the temperature rise was much lower and the physiological significance, if any, of this small, localised increase in temperature is not yet clear. Future experiments using a new exposure system (Grose et al, Bioelectromagnetics Society Abstracts 2005) should help to resolve this question.

The work was supported by the Home Office (Police Information and Technology Organisation contract number CS 652). ©Crown Copyright 2005, Dstl.

## REFERENCES

Tattersall J. E. H., Scott I. R., Wood S. J., Nettell J. J., Bevir M. K., Wang Z., Somasiri N. P., and Chen X. Effects of low intensity radiofrequency electromagnetic fields on electrical activity in rat hippocampal slices. *Brain Res.* 904: 43-53, 2001.

**EFFECTS ON BRAINS OF FISHER 344 RATS EXPOSED TO GSM-900 SIGNALS: A CONFIRMATION OF THE SALFORD STUDY.** E. Haro<sup>1</sup>, I. Lagroye<sup>1</sup>, P. Leveque<sup>2</sup>, B. Billaudel<sup>1</sup>, G. Ruffie<sup>1</sup>, M. Laclau<sup>1</sup>, F. Poullietier De Gannes<sup>1</sup>, M. Taxile<sup>1</sup>, B. Veyret<sup>1</sup>. <sup>1</sup>PIOM/Bioelectromagnetics laboratory, ENSCPB/EPHE, Univ of Bordeaux, 33607 PESSAC Cedex, FRANCE, <sup>2</sup>IRCOM, CNRS UMR 6615, 87100 LIMOGES, FRANCE.

**INTRODUCTION:** In a paper recently published in *Environmental Health Perspectives*, the Swedish group of Leif Salford reported the occurrence of brain damage (presence of dark neurons) 50 days after a single 2-hour exposure of rats to a GSM-900 signal(1). In that investigation, exposed animals were mixed in terms of age (12- to 26-week old) and gender, while those differences were not taken into account in the analysis.

Our group undertook a confirmation of that study within a collaborative programme and attempted an improvement by adding a more specific staining method for dark neurons and the detection of apoptosis. Our study includes the detection of dark neurons, permeability of the blood-brain barrier 14 and 50 days after GSM-900 exposure and apoptosis 14 days after exposure.

**METHODS:** The exposure setup was the loop antenna(2) that allows for head-only exposure. The dosimetry of the TEM cell used in the Salford's experiments was performed using FDTD calculations. For 1 W incident, the mean whole-body SAR (4 positions of the rat in the TEM cell) was  $2.14 \pm 0.23$  W/kg while the brain average SAR (BASAR) was  $2.59 \pm 1.56$  W/kg. The BASAR/whole body SAR ratio was thus 0.83. The highest level of damage was detected by Salford at 0.2 W/kg whole-body. Therefore a local SAR of 0.14 W/kg as well as the ICNIRP limit value for the public local exposure (2 W/kg) were tested.

Five groups of 16 Fisher 344 rats (14-week old) were exposed to the GSM-900 signal during 2 hours at various SAR levels (0, 0.14 and 2.0 W/kg), or were used as cage controls or positive controls. Positive controls were obtained by submitted the rat head to a localized cold injury (dry ice during 5 minutes).

After exposure, rats were kept alive during 14 or 50 days to study brain damages. Then, they were anesthetized with urethane (i.p. 1.5 mg/kg), perfused with PBS and fixed with paraformaldehyde 4% (PAF 4%). Brains were extracted and put in cold PAF 4% during the following night, then placed in cold sucrose 20% during 2-3 days, frozen in isopentane and placed at  $-80^{\circ}\text{C}$ . Brains were coded before storage.

Frozen brains were cut in 3 different areas (frontal, median and posterior). Slides were stained with cresyl violet and FluoroJade B(3) to detect the presence of dark neurons. Apoptosis was investigated using the TUNEL method and endogenous albumin visualized using immuno-histochemical labeling as a marker of leakage of the blood-brain barrier. These analyses are ongoing.

**RESULTS AND DISCUSSION:** FDTD simulation showed that exposure in the TEM cell is highly nonuniform and that the BASAR is higher than expected for a given whole-body SAR level. Head-only exposure allows for an improved control of the exposure. The biological data will be presented at the meeting. These data, together with those of collaborative groups, should help to assess the effects of GSM-900 signal in the rat brain.

- (1) L.G. Salford et al. *Environmental Health Perspectives*, 111:881-883 (2003).
- (2) P Leveque et al. *IEEE Transactions on microwave theory and techniques*, 52(8): 2076-2083 (2004).
- (3) L. Schmued and K. Hopkins, *Brain Res.*, 874:123-130 (2000).

**TWO STUDIES OF EFFECTS OF STATIC MAGNETIC FIELDS ON NMDA-INDUCED SEIZURES IN MICE.** M. J. McLean, S. Engstrom, M. Zhang. Dept of Neurology, Vanderbilt Univ, Nashville, TN.

**RATIONALE:** Seizures produced in mice by intracerebroventricular (icv) injection of N-methyl-d-aspartate (NMDA) are characterized by sequential stages including wild running, loss of righting, clonus, tonic-hindlimb extension and death. This model is used to screen for and characterize potential antiepileptic drugs. In the first study, the incidence of clonic (CLO) seizures induced by icv injection of NMDA was reduced by pretreatment with certain static magnetic fields (SMF). However, tonic hindlimb extension (THE) and death (DEA) were frequent in controls and the incidence was higher in the group pretreated with the SMF. In the second study, we observed a low incidence of THE and DEA overall and a highly significant reduction of CLO. In an effort to explain the differences, data from both studies are compared here.

**METHODS:** ICR/CD-1 male mice (26-32 days old; Charles River Laboratories, Wilmington, MA) were handled in accordance with standards of the National Institutes of Health and the Vanderbilt Univ Institutional Animal Care and Use Committee. We used a water-cooled, static magnetic field (SMF) exposure device built with commercially available coils around four ferromagnetic cores in a square array with alternating polarity. A steel jacket surrounded each core assembly. A constant current power supply powered the coils. Field strength over the poles was monitored with a teslameter. All mice were kept in perforated tubes prior to experiments. Different groups of mice were pretreated with sham or SMF exposure before icv injection of NMDA (200-400 nM). After injection mice were observed in a plastic box. Seizures The mice were videotaped after icv injection of NMDA and seizure stages were recorded. Untreated seizures evolved from wild running (WR; 1), to loss of righting (LOR; 2), clonic jerks (CLO; 3), tonic hindlimb extension (THE; 4) and death (DEA; 5) and lasted about about 1 minute. Seizure severity was scored on the basis of the most severe stage observed.

**RESULTS:** In study #1, injections were near the midline. Incidence of THE ranged up to 88% and DEA up to 70% in the control group. The seizure severity was significantly different from control in mice pretreated with SMF with flux densities of 60 and 120 mT (pole strength;  $p < 0.05$  vs. control) for 15-90 minutes ( $p < 0.01$  vs. control). In study #2, icv injections were posterolateral and incidence of THE and death was  $< 0.01$ ). The reduction of severity of seizures after SMF exposure was inversely related to the NMDA dose.

**CONCLUSIONS:** Time- and flux density-dependent reduction of clonic seizures was highly significant after pretreatment with static magnetic fields. The incidence of THE and death in the first study limits conclusions about therapeutic efficacy. The relative absence of these seizure stages in the second study provides a clearer picture of therapeutic potential.

**SYSTEM OF HUMAN EXPOSURE TO RADIO-FREQUENCY FIELDS OF CELLULAR BASE-STATION FOR STUDIES ON ELECTROMAGNETIC HYPERSENSITIVITY IN JAPAN.** K. Wake<sup>1</sup>, P. Pongpaibool<sup>1</sup>, S. Watanabe<sup>1</sup>, M. Taki<sup>2</sup>, Y. Ugawa<sup>3</sup>, Y. Terao<sup>3</sup>, M. Nishikawa<sup>3</sup>, T. Okano<sup>3</sup>, S. Shirasawa<sup>3</sup>, T. Furubayashi<sup>3</sup>, C. Ohkubo<sup>4</sup>, A. Ushiyama<sup>4</sup>, H. Masuda<sup>4</sup>, S. Soukejima<sup>4</sup>.

<sup>1</sup>National Institute of Information and Communications Technology, Tokyo, Japan, <sup>2</sup>Graduate School of Engineering, Tokyo Metropolitan Univ, Tokyo, Japan, <sup>3</sup>Univ of Tokyo, Tokyo, Japan, <sup>4</sup>National Institute of Public Health, Saitama, Japan.

**OBJECTIVE:** The concerns about possible health effects by electromagnetic field of cellular telecommunications are growing among general public. There are several reports that investigate the relation between subjective symptoms of electromagnetic hypersensitivity (EHS) and radio frequency electromagnetic field (RF-EMF) exposure of non-thermal level. The purpose of this study is to develop the exposure system in order to put into practice the study on EHS in Japan.

**EXPOSURE SYSTEM:** Subjects are exposed to EMF of W-CDMA signal at 2 GHz region. Each subject is experienced continuous, intermittent, sham and noise exposures. The period of each exposure is 30 minutes. The orders of these 4 exposures are randomized. The W-CDMA signal generated by signal generator is amplified and applied to a horn antenna in a special shielded chamber. The antenna input power is controlled and monitored by a personal computer. The subjects are exposed at the distance of 2-3 m from the aperture of the horn antenna with the electric field of 1 or 10.0 V/m. We also monitor the level of electric field inside the chamber. Exposures can be stopped automatically when the electric field value exceed a limit for safety. We will show the results of numerical analysis of the specific absorption rate (SAR) inside the human exposed with this system at the meeting.

## **In vitro – cellular**

See also P-A-229

P-A-142 STUDENT
-----------------

**EFFECTS OF 2450 MHZ ELECTROMAGNETIC FIELDS ON METHYLCHOLANTHRENE-INDUCED TRANSFORMATION IN C3H10T1/2 CELLS.** J. Wang<sup>1,2</sup>, T. Sakurai<sup>1</sup>, S. Koyama<sup>1,3</sup>, Y. Komatsubara<sup>1</sup>, Y. Suzuki<sup>4</sup>, M. Taki<sup>4</sup>, J. Miyakoshi<sup>1</sup>. <sup>1</sup>Dept of Radiological Technology, School of Health Sciences, Faculty of Medicine, Hirosaki Univ, Hirosaki, 036-8564, Japan., <sup>2</sup>Dept of Radiation Medicine, Fourth Military Medical Univ, xi'an, 710082, China., <sup>3</sup>Graduate School of Human and Environmental Studies, Kyoto Univ, Kyoto, 606-8501, Japan., <sup>4</sup>Dept of Electrical Engineering, Graduate School of Engineering, Tokyo Metropolitan Univ, Tokyo, 192-0397, Japan.

**INTRODUCTION:** In recent years, there has been a rapid increase in the use of devices and systems employing electromagnetic energy. People are concerned about the association between environmental electromagnetic fields and cancer. The possible mechanisms of the induced effects remain unclear, although a number of theoretical models have been proposed. Tumor formation is considered to be a multi-step process including initiation (mutation), promotion and progression. Whatsoever, if EMF could contribute to the carcinogenic progress, it would affect one or more steps in the neoplastic transformation process.

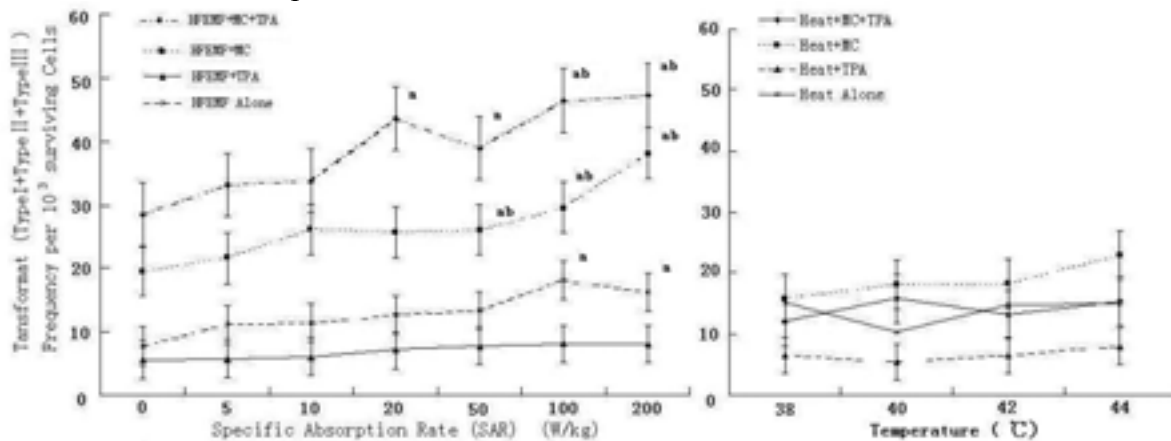
**OBJECTIVE:** The aim of this study was to investigate the possible effects and mechanism(s) of 2450 MHz continuous wave (CW) high frequency electromagnetic fields (HFEMFs) at different specific absorption rates (SARs) on MC induced transformation in C3H10T1/2 cells.

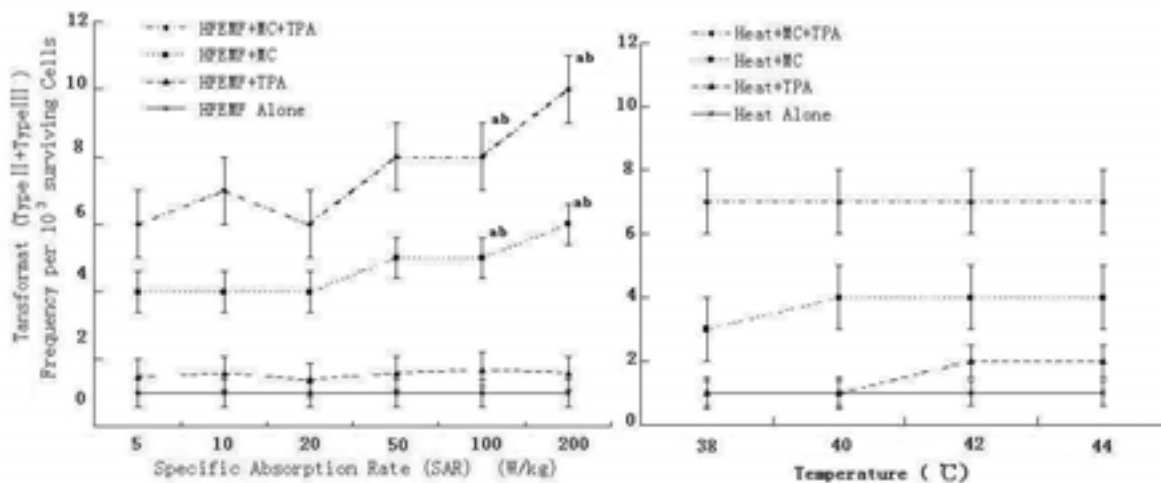
**METHODS:** Clone 8 of mouse C3H10T1/2 cells supplemented with 10% fetal bovine serum and 10 ml of 200mM L-Glutamine at 37°C with 95% air and 5% CO<sub>2</sub>. The cells were exposed to 2450 MHz HFEMF alone at SARs of 5, 10, 20, 50, 100 and 200 W/kg for 2 h. 2450MHz HFEMF at SARs: 50-200W/kg can induce temperature increases in culture medium. Therefore, we designed the appropriate temperature controls. Cellular transformation was used to assess the potential of an agent to cause cancer-like change in cells after different treatments. 20-Methylcholanthrene (MC) was used as an initiator of neoplastic transformation and 12-O-tetra-decanoylphorbol-13- acetate (TPA) was used as a positive control of tumor promoters. To determine whether HFEMF can initiate malignant transformation or synergistic transformation, we assessed the frequency of neoplastic transformation foci (Type I, Type II and Type III). Experiments were performed four times. Data were compared by analysis of variance followed by the one-way ANOVA (P < 0.01).

**RESULTS:** No significant differences were observed in the transformation frequency between sham-exposed control and the HFEMF exposure alone from 5 to 200 W/kg. The transformation frequency for MC plus HFEMF increased compared with MC alone at SAR > 100 W/kg. When cells were co-incubated with TPA throughout the experiment, the transformation frequency by MC alone was further increased. In the combined treatment with MC followed by HFEMF with TPA, the transformation frequency increased significantly at 100 to 200 W/kg. The results indicate that a statistically significant difference in transformation frequency (Types I+ II+III or Types II+III) of C3H 10T1/2 cells was not induced by 2450MHz HFEMF (CW, SARs 5, 10, 20, 50, 100, 200W/kg, 2h) alone or in combination with TPA (0.5ng/ml).(Fig 1-2)

**CONCLUSIONS:** This study demonstrated that exposure to 2450MHz HFEMF alone in combination with TPA at SARs from 5 to 200W/kg did not induce neoplastic transformation. However, 2450MHz HFEMF at high SARs combined with MC or MC and TPA can increase the transformation frequency. This result suggests that HFEMF is not a "carcinogen", but could act as a "co-carcinogens" at the SAR > 100 W/kg.

This work was supported in part by the committee to Promote Research on the Possible Biological Effects of Electromagnetic Fields, Ministry of Public Management, Home Affairs, Posts and Telecommunication, Japan.





P-A-145

**EVALUATION OF CYTOTOXIC AND GENOTOXIC EFFECTS IN HUMAN PERIPHERAL BLOOD LEUKOCYTES FOLLOWING EXPOSURE TO UMTS MODULATED SIGNAL.** A. Sannino<sup>1</sup>, P. Mita<sup>1</sup>, G. d'Ambrosio<sup>2</sup>, R. Massa<sup>2</sup>, M. Calabrese<sup>2</sup>, M. Sarti<sup>1</sup>, M. Rosaria Scarfi<sup>1</sup>. <sup>1</sup>CNR-Institute for Electromagnetic Sensing of Environment (IREA), via Diocleziano, 328, 80124, Naples, Italy, <sup>2</sup>Univ of Naples Federico II - DIET - Via Claudio, 80125 Naples, Italy.

**OBJECTIVE:** Aim of this study is to evaluate the cytotoxic and genotoxic effects induced in human peripheral blood leukocytes following 24h exposure to UMTS modulated signal (1950 MHz) at two Specific Absorption Rates (SAR): 0.8 and 1.6 W/kg.

Cytotoxicity was determined by trypan blue exclusion method, while DNA damage was evaluated by applying the alkaline single cell gel electrophoresis (SCGE)/comet assay.

**METHODS:** Human peripheral blood leukocytes were separated by buffy coats of 3 healthy donors selected for age (20-30 years), and smoking habits. Subjects on drug therapy were excluded.

Cells were seeded into 35mm Petri dishes ( $2 \times 10^6$  cells / 3 ml complete RPMI without mitogen) and radiofrequency exposure/sham exposure was carried out in a waveguide hosted in a commercial CO<sub>2</sub> incubator. The exposure set-up consisted in a shorted waveguide: under horizontal E field polarization, high efficiency (up to 80 %) and limited SAR non-uniformity (less than 30 %) were obtained. Temperature and dosimetry were rigorously controlled during the exposure. Cells were exposed for 24h at 0.8 and 1.6 W/kg SAR levels. The signal source was an Agilent E4432B, ESG-D series, signal generator. The carrier frequency of the UMTS signal was 1950 MHz (the centre of the up-link frequency range), and a WCDMA modulation, according to the 3GPP 3.5 2001-03 specifications, was used. Five power-controlled user data channels (960 kbit/s) + 1 control channel (15 kbit/s) were synchronously transmitted.

For each donor, 10 samples were set up: four of them were RF exposed (0.8 and 1.6 W/kg), four were sham exposed and two served as positive controls (hydrogen peroxide 50 mM for 30 minutes).

At the end of treatments cytotoxicity was estimated by trypan blue exclusion method and 50.000 cells were processed for the alkaline comet assay. For each treatment 250 cells (125 on two separate slides) per sample were examined. Since each sample was set up in duplicate, the results were obtained on 500 cells / treatment by a computerized Image Analysis System (Delta Sistemi, Rome, Italy) and the results were expressed as mean  $\pm$  SE of DNA % in the tail, comet moment and tail moment.

**RESULTS:** At both SAR values investigated neither cytotoxic nor genotoxic effects were detected. The two tailed paired Student's t test gave a p value higher than 0.05 in all cases. On the contrary, when positive controls were compared to their sham exposed samples, a statistically significant decrease in cell viability together with a significant increase in DNA damage was found.

**CONCLUSIONS:** From the preliminary results here reported, 24h RF exposure, to the above UMTS modulated signal, does not influence neither cell viability nor DNA integrity of human leukocytes at both SAR values investigated. Further experiments are planned to draw conclusions on a larger number of individuals.

Research done within the framework of the “Wireless Technology Health Risks (WITHER) Project” (Calabrese et al, The BEMS 2004 Annual Meeting), supported by the “Centre of Competence on Information and Communication Technologies” of the Regione Campania, Italy.

P-A-148

**ELEMENTAL NEURON NETWORKS DYNAMICS UNDER APPLIED SINUSOIDAL MAGNETIC FIELDS.** M. J. Azanza<sup>1</sup>, A. C. Calvo<sup>1</sup>, R. N. Perez-Bruzon<sup>1</sup>, A. del Moral<sup>2</sup>. <sup>1</sup>Laboratorio de Magnetobiología, Departamento de Anatomía e Histología Humanas, Facultad de Medicina, Universidad de Zaragoza, Spain, <sup>2</sup>Laboratorio de Magnetismo de Sólidos, Departamento de Física de Materia Condensada & ICMA, Facultad de Ciencias, Universidad de Zaragoza-CSIC, Spain.

**INTRODUCTION:** We have observed elsewhere that molluscan pacemaker neurones show oscillatory and recruitment activity when they are exposed to extremely low frequency (ELF) sinusoidal low magnetic fields (AMF) (1, 3). Such an activity induces a synchronizing effect in pairs of studied neurones (2) which needs a more detailed study.

**OBJECTIVES:** The objectives of this work were: 1) to make intracellular recordings from pairs of neurones in order to study their behaviour under applied ELF-AMF; 2) to study the responses of the neurone pairs to applied neurotransmitters, their agonists and antagonists; 3) to characterize the synchronizing activity induced under applied ELF-AMF in these elemental neurone networks of two neurones.

**MATERIALS AND METHODS:** The experiments were performed by simultaneously recording the activity from two different neurones randomly chosen from the brain ganglia of *Helix aspersa*. The intracellular recordings have been performed from single neurone units in real time. The dissected ganglia were immersed in mollusc Ringer solution (NaCl 80 mM, KCl 4mM, CaCl<sub>2</sub> 7mM, MgCl<sub>2</sub> 5mM, tampon TRIS-HCl 5mM, pH = 8) enriched with 10mM pyruvic acid. They were placed between a pair of Helmholtz coils. Alternating (A) MF of 50 Hz of peak intensity, ranging between 1 and 15 mT, was applied at time intervals of 1 min. The following chemicals were tested: acetylcholine, glutamate, kainate, quisqualate and N-metil-D-aspartate (Sigma). The experiments were performed at room temperature. Intracellular recordings were made using glass micro-electrodes, tip diameter less than 1 mm, filled with 1 M potassium acetate, and tip resistance of 2-20 MW. The electrophysiological recordings were made by testing natural neurone activity before (control), during, and after the AMF exposure.

**RESULTS.** In Figs. 1-3 A, B and C are shown the results from two different experiments made by simultaneously recording the activity of neurones V6 and V16. Both experiments were made from the

same kind on neurons, from different snail samples, in different days. Experiment A was made by applying AMF of well stabilized peak intensity, ranging between  $B = 1$  and  $15$  mT. The AMF intensity steps were made at intervals of  $0.05$  mT,  $15$  s. at each step, and each field intensity was tested during  $1$  min. In experiment B an AMF of constant intensity of  $4$  mT was applied during  $55$  min. In Fig C are enclosed the recordings of experiment A. In this figure it is shown the evolution of the bioelectric activity from neurons. The recordings a, b, c, d, e and f, match with the quoted times,  $t$ , in graph A. It is worthwhile to observe that the behaviour of the neurons and the evolution of the bioelectric activity under applied AMF is similar in both experiments A and B. In case A at a certain AMF a synchronization appears; in case B after some time of field application almost synchronization develops. There are two interesting differences which could be related with the applied field intensity. The modified bioelectric activity is faster as the intensity of the field is higher ( $B(t)$  is shown by the dashed lines). In both experiments we observe a biphasic response, but as the field intensity is higher (Fig. A) the decrease of frequency is faster, finally being the neurons activity almost completely inhibited.

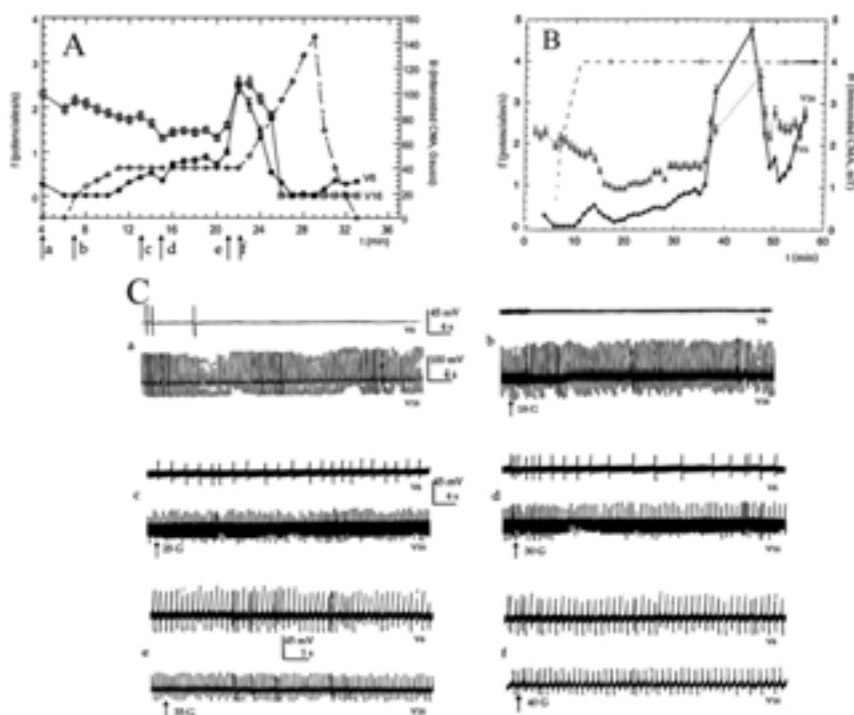


Figure 1.

**DISCUSSION.** Neuron synchronization under  $50$  Hz-AMF demonstrates the existence of frequency-dependent specific effects since firing frequency values change for both studied neurons after some time under exposure to AMF. The oscillation dynamics defines biological rhythmic behavior of essential importance in intercellular signal transmission. The existence of such oscillatory processes in neural networks poses a series of questions. How can oscillators

fire and are maintained so with a certain degree of stability? How are they linked to magnetic field stimuli? Are the studied neurons synaptically interconnected or it is the applied AMF able by itself to induce such a synchronizing activity? (separation between neurons was of  $325 \mu\text{m} \pm 10 \mu\text{m}$ ). If neurons were synaptically interconnected, a synaptic delay would be expected. Such a delay has not been observed (recordings C). We have shown that there is not a transmission of bioelectric potentials between neurons in the tested pairs through voltage/current paths across the extracellular medium. We have developed a physical model which explain the observed dependence of the firing frequency  $f$  with

the energy density of the applied magnetic field (i.e., ). Research is in progress to reveal if there exists the possibility of an added interneuron interaction through electrical synapsis, i.e. if the existence of gap junctions can be ruled out or not.

#### REFERENCES

- 1.- MJ Azanza, A del Moral. ELF-magnetic field induced effects on the bioelectric activity of single neurone cells. J.Magn.Magn.Mat. 177-181:1451-1452, 1998.
- 2.- M.J Azanza, AC Calvo, A.del Moral. Evidence of synchronization of neuronal activity of molluscan brain ganglio induced by alternating 50 Hz applied magnetic field. Electromagn. Biol.Med. 209-220, 2002.
- 3.- RN Pérez Bruzón, MJ Azanza, A.C.Calvo, A del Moral. Neurona bioelectric activity under magnetic fields of variable frequency in the range of 0.1-80 Hz. J. Magn.Magn.Mat. 272-276, 2424-2425,2004.

#### ACKNOWLEDGEMENTS

The authors are indebted to the PROFIT Project FIT 070000-2003-658 (Spanish Ministry of Science & Tecnology Spain), Project B-17-DGA (Diputación General de Aragón, Spain) and to the Project of the "Fundacion Humanismo y Ciencia" (Madrid, Spain)

P-A-151

**MICROWAVE (2.45 GHZ) EXPOSURE OF *SACCHAROMYCES CEREVISIAE*: EFFECTS ON GROWTH AND THERMAL STRESS TOLERANCE.** B. Bisceglia, S.J., M. Carmela Bruno, F. Chiadini, R. Paolo Croce, G. Donsi, G. Ferrari, V. Fiumara, A. Scaglione, A. Roscigno. Competency Regional Research Center on Agroindustrial Production, Univ of Salerno, 84084 Fisciano (SA), Italy.

#### Introduction

*Saccharomyces cerevisiae* is the common yeast used in **baking** (baker's yeast) and **brewing** (brewer's yeast). It is a popular *model* organism in the laboratory because it can be cultured easily and it grows rapidly.

*Saccharomyces cerevisiae*, by virtue of its rapidly fluctuating environment, has developed effective stress sensing and response mechanisms. Recent studies take care of mutagenicity of static and time-varying magnetic fields highlighting that the existence of possible non-thermal biological effect of MW is still matter of concern.

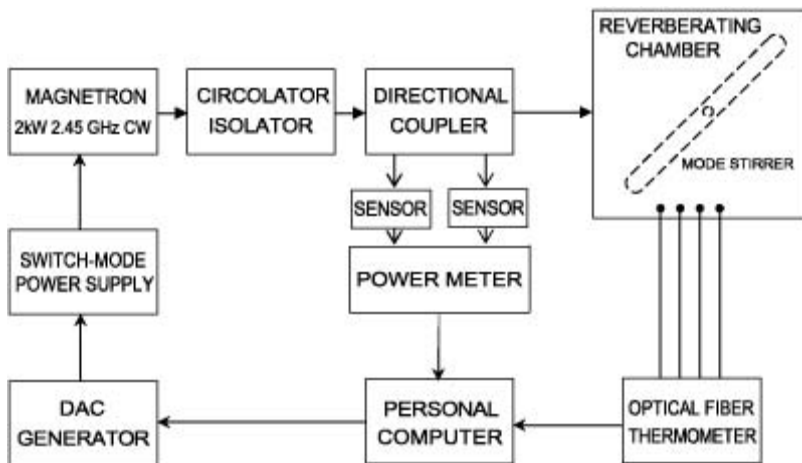
We will show some preliminary results about response of *Saccharomyces cerevisiae* culture to MW exposure.

#### Materials and Methods: biological samples

A sample of 50 ml of yeast (*saccharomyces cerevisiae*) culture in MRS (Man, Rogosa and Sharpe) broth was grown under 2.45 GHz microwave exposure for 24 h. The temperature of the sample was continuously monitored during the exposure by using a Fiso Technology UMI-4 fiber optic thermometer and FOT-L-TFL-03 temperature probe. The exposed sample was kept at temperature of  $32 \pm 0.5$  °C by properly modulating the power of the microwave source. A reference sample, completely similar to the exposed one, was also grown at 32 °C for 24 h in a conventional incubator. After the treatment, the evaluation of the yeast concentration of both samples was carried out. Successively, samples of 5 ml from both yeast cultures were treated, either by microwave exposure or by conventional heating in water bath, for 5 min at temperatures of 55 °C and 65 °C. Finally, the yeast concentration of all treated samples was evaluated by plate incubation at 32 °C for 48 h.

## Materials and Methods: Microwave exposure system

The figure shows a schematic of the microwave exposure system. Isotropic exposure of the sample was carried out in an aluminium made cubic (120 cm side long) reverberating enclosure equipped with two rectangular (90x20 cm) mode stirrers rotating at different velocities (0.4 and 1.1 rps respectively). A 2.45 GHz, 2 kW CW magnetron, powered by a switch-mode power supply, was used to provide microwave energy. The launching waveguide (WR340) circuit was composed by a waveguide isolator and a double directional coupler for the measurement of the power incident on and reflected from the enclosure. The power supply, and then the magnetron power output, was controlled by an external DC voltage signal (0-10 V) from a DAC generator. Consequently, the temperature of the exposed sample was properly controlled and kept at the desired value. All instrumentation necessary for the magnetron operation, the power measurements and the temperature regulation was interfaced to a PC for remote controlling. Long time treatments at 32 °C were performed by varying the power incident on the enclosure up to a maximum value of 9 W. For short time treatments at high temperatures, the power maximum value was 15.8 W.



## Results

Preliminary results show that the yeast concentration of samples grown at 32 °C for 24 h under microwave exposure did not show significant differences with respect to the ones grown in the incubator. Analysis of the samples treated at 55 °C highlights that yeast cultures grown under MW exposure exhibit ability to tolerate thermal stress greater than the unexposed ones. Such a difference is more pronounced in the case of the samples treated at 55°C using MW exposure (about 20%) with respect to the samples treated at 55°C using conventional heating. Further experiments are in progress to validate these results and more precisely evaluate the observed behaviour. Samples treated at 65 °C do not show a similar behaviour, the temperature being lethal in both cases.

## References

- N.S. BAGHDASARYAN, S.N. AYRAPETYAN, *The effect of extremely high power pulses- treated wort on growth and development of yeasts*, BEMS XXVIth Annual Meeting, Washington, June 20-24, 2004.
- M. IKEHATA, T. NAGAI, Y. SUZUKI, M. TAKI and T. KOANA, *Evaluation of mutagenicity of complex magnetic fields with static and time-varying components*, BEMS XXVIth Annual Meeting, Washington, June 20-24, 2004.
- I. SAFARIK, L. PTACKOVA, and M. SAFARIKOVA, *Adsorption of dyes on magnetically labeled baker's yeast cells*, *Eur. Cells Mater.*, vol. 3, 2002.

**POWER FREQUENCY MAGNETIC FIELDS BLOCK MELATONIN-INDUCED CHANGES IN ALPHA-FETOPROTEIN AND ALBUMIN IN HUMAN HEPATOCARCINOMA CELLS.** M. Antonia Cid<sup>1</sup>, A. Ubeda<sup>1</sup>, M. L. Hernandez-Bule<sup>1</sup>, M. Antonia Martinez<sup>1</sup>, M.a Diaz-Enriquez<sup>2</sup>, J. Leal<sup>1</sup>, M. Angeles Trillo<sup>1</sup>. <sup>1</sup>Serv. Investigacion-BEM, Hosp. Ramon y Cajal 28034, Madrid., <sup>2</sup>Dpto. Bioquimica, Hosp. Ramon y Cajal 28034, Madrid.

**INTRODUCTION:** There is growing evidence that extremely low frequency magnetic fields (ELF MF) and the hormone melatonin (MEL) can exert antagonistic effects. We have previously reported that ELF fields can antagonise MEL-induced cell differentiation (protein per cell, protein/DNA ratio and cellular morphology) *in vitro*. However, the mechanisms and the nature of such antagonistic interactions remain unknown.

**OBJECTIVE:** The aim of the present work is to study the potential differentiating effects of a physiological dose of MEL on the human hepatocarcinoma line HepG2, and to determine whether the induced cellular response is affected by the exposure to a 50-Hz, 10  $\mu$ T MF. The differentiating effects of MEL were estimated through analysis of alpha-Fetoprotein (AFP) expression and of albumin (ALB) release. AFP, a protein genetically close to albumin, is typically synthesized by foetal or poorly differentiated cells and has been currently used as a tumor-marker in the prognosis of different cancer types, including hepatocarcinoma. As for Albumin, it expresses in normal hepatocytes and is actively synthesised by well-differentiated cells.

**METHODS:** HepG2 cells were exposed to a 50-Hz, 10- $\mu$ T magnetic flux density, linearly polarised magnetic field. In each experimental replicate (N= 11) a total of 12 petri dishes (3 dishes per treatment) were exposed to one of the following treatment combinations: untreated controls, MEL alone (10 nM), MF alone, MEL + MF. The MEL treatment was applied at t = 4 h postplating. At t = 72 hours postplating the samples were either exposed to the MF in 3h On/3h Off cycles for two days or sham-exposed inside unenergized pairs of Helmholtz coils placed in a co-netic metal chamber, in a 5% CO<sub>2</sub>, 37 °C and 100% atmosphere. The effects of the treatments on cell viability and cell growth were determined through Trypan blue exclusion and hemocytometer counting. The content of albumin in the media was determined through Nephelometric analysis. In a second, parallel set of experiments the cellular expression of AFP in treated and control samples was Western-blot quantified. Additionally, in a third set of experiments, the cellular morphology and the AFP expression pattern were analyzed through standard cytological techniques, immunocytochemistry and image analysis.

**RESULTS:** As shown in Fig. 1, MEL significantly increases the levels of ALB released by the cells ( $p < 0.05$ ). In contrast, the exposure to the 10  $\mu$ T MF alone had no influence on the release of this protein. However, when applied on MEL-treated samples, the field inhibits the hormone-induced release of ALB down to levels equivalent to those in control samples.

Data in Fig. 2 show that the presence of 10 nM MEL significantly decreases AFP expression with respect to untreated controls ( $p < 0.01$ ). Again, the exposure to 10  $\mu$ T alone did not influence significantly the cellular expression of this protein. However, in the combined treatment, the exposure to the field antagonises the MEL-induced decrease in AFP expression, which reaches levels equivalent to those of controls and significantly above those in samples treated with MEL alone ( $p < 0.05$ ). The above changes induced by MEL in the protein release or expression were accompanied with significant changes in the cellular phenotype (increased cell size) and with decreased cell growth. The results of the combined treatment with MEL and MF indicate that MF also blocks these, melatonin-induced effects.

**CONCLUSIONS:** The present results confirm previously reported indications that a physiological dose of MEL exerts a potentially differentiating effect on HepG2 human hepatocarcinoma cells, inducing a significant increase in the ALB release that is accompanied with a significant decrease in AFP expression. The mechanism of such differentiating effects has not been elucidated yet. These MEL-

induced effects were blocked by a 42 h-exposure to 50-Hz, 10  $\mu$ T MF, suggesting that the exposure to ELF MF has a potential reversing effect on MEL-induced actions on differentiation processes. As a whole, the present results support previous observation that MEL and MF elicit antagonistic responses in HepG2 cells.

Fig 1

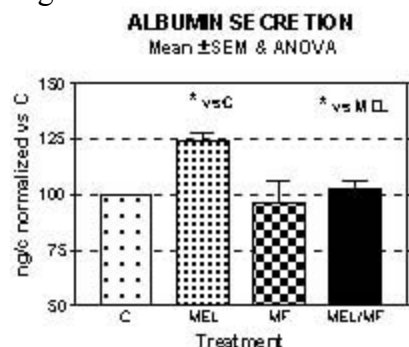
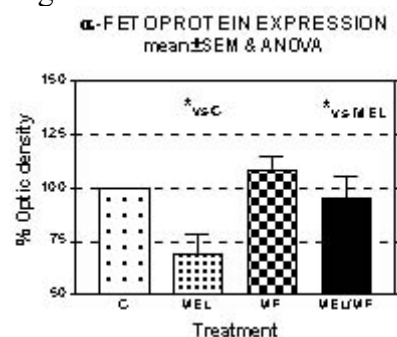


Fig 2



P-A-157

### USE OF CULTURED ADRENAL CHROMAFFIN CELLS AS AN IN VITRO MODEL SYSTEM TO STUDY NON-THERMAL EFFECTS OF RF RADIATION ON EXOCYTOSIS.

G. L. Craviso<sup>1</sup>, D. Brouse<sup>1</sup>, T. Hagan<sup>2</sup>, D. McPherson<sup>2</sup>, I. Chatterjee<sup>2</sup>. <sup>1</sup>Dept of Pharmacology, Univ of Nevada School of Medicine, Reno, Nevada 89557, USA, <sup>2</sup>Dept of Electrical Engineering, Univ of Nevada, Reno, Nevada, 89557, USA.

**OBJECTIVE:** One of the goals of our studies is to identify RF parameters in the 0.75 to 1 GHz frequency range that can induce non-thermal effects on catecholamine release from cultured bovine adrenal medullary chromaffin cells. To this end we have designed, characterized and fabricated a waveguide-based exposure system that permits on-line monitoring of catecholamine release during RF exposure. The system not only allows flexibility in choosing different frequencies and exposure paradigms but also provides for dynamic temperature control.

**METHODS:** Chromaffin cells are loaded onto a glass fiber filter fitted within a plastic Millipore filter holder (cell perfusion apparatus) and continuously superfused with a temperature-controlled (36.5°C)

balanced salt solution. The cell perfusion apparatus is placed inside a standard WR-975 rectangular waveguide and the perfusate reaches an electrochemical detector that monitors in the amperometric mode both basal and stimulated catecholamine release. The RF signal is amplified and fed to either a shorted waveguide, where cells are positioned in the electric field or magnetic field maximum of a standing wave at specific frequencies, or a matched waveguide, where cells are exposed to traveling waves. Temperature of the balanced salt solution immediately entering and exiting the plastic filter holder is monitored continuously by fluoroptic temperature probes and a temperature feedback system maintains superfusion of the cells at a constant temperature during exposure of the cells to RF fields.

**RESULTS:** Data obtained from a number of experiments show an increase in the secretory response of the cells to nicotinic receptor stimulation when cells are exposed to several different exposure paradigms in the frequency range of 750 to 850 MHz. There was no detectable temperature rise when increases in nicotinic receptor stimulation were observed. In addition, when a temperature rise was deliberately induced, either by increasing the temperature of the balanced salt solution superfusing the cells or by delivering RF field intensities that produce overt heating, nicotinic receptor stimulated catecholamine release underwent a decrease, rather than an increase.

**CONCLUSIONS:** The effects of RF exposure on catecholamine release that have been observed to date cannot be explained by an increase in temperature. We are currently investigating possible mechanisms to explain the non-thermal RF effects on catecholamine release.

Supported by the Air Force Office of Scientific Research, grants F49620-02-1-0360 and F49620-03-1-0262

P-A-163 STUDENT WITHDRAWN

### **In vitro – sub-cellular**

P-A-166 STUDENT WITHDRAWN

P-A-169

**IN VITRO EXPOSURE OF HUMAN T LYMPHOCYTES TO RADIOFREQUENCY RADIATION (900 MHZ, GSM SIGNAL) AND GENE EXPRESSION ANALYSIS BY MICROARRAY TECHNOLOGY.** M, Capri<sup>1,2</sup>, S, Pasi<sup>1,2</sup>, D. Remondini<sup>1,3</sup>, E. Bianchi<sup>2</sup>, A. Perrone<sup>2</sup>, P. Mesirca<sup>1,3</sup>, D. Forigo<sup>4</sup>, M. Deplano<sup>4</sup>, A. Schiavoni<sup>4</sup>, A. Leon<sup>5</sup>, A. Darrigo<sup>5</sup>, D. Luise<sup>5</sup>, C. Franceschi<sup>1,2,6</sup>, F. Bersani<sup>1,3</sup>. <sup>1</sup>CIG-InterDeptal Center L.Galvani, Univ of Bologna, 40126 Bologna, Italy, <sup>2</sup>Dept of Experimental Pathology, Section of Immunology, Univ of Bologna, 40126 Bologna, Italy, <sup>3</sup>Dept of Physics, Univ of Bologna, 40127 Bologna, Italy, <sup>4</sup>TILab, Telecom Italia Laboratories, 10148 Torino, Italy, <sup>5</sup>Research & Innovation, 35136 Padova, Italy, <sup>6</sup>INRCA, Italian National Research Center on Ageing, 60100 Ancona, Italy.

**Objective:** 900 MHz (GSM signal) radiofrequency (RF) provokes a slight decrease of human peripheral blood mononuclear cells (PBMCs) when stimulated with low dose of phytohemagglutinin (PHA) and exposed for three hours (1 hour per day) during 72 h of culture (Capri et al., Radiat Res, 162: 211,

2004). Aim of this work is the evaluation of a possible gene expression alteration responsible for the decreased proliferation, previously observed.

**Methods:** PBMCs from 4 human healthy young donors were exposed to RF (900 MHz, GSM signal, SAR 76 mW/kg) for three hours (1 h/day, where the first h of exposure was performed immediately after cell seeding and PHA-treatment) and cultured up to 1 h and 23 h after the last time of exposure, i.e until 50 h and 72 h of culture, respectively. The exposure system was provided by TILab (Telecom Italia Laboratories, Torino, Italy) and consisted of a TEM cell, connected to a generator, an amplifier and a personal computer. TEM cell and sham system were placed in a thermostatic chamber at constant temperature of 37 °C. Dosimetry was calculated and temperature was monitored. After cell culture, T lymphocytes were separated by Magnetic Cell Sorting (MACS, Miltenyi Biotec, De), extraction of total RNA was performed by TRIzol reagent (Invitrogen, Life Technologies, USA) and gene expression analysis was done using commercial-glass microarrays. Atlas<sup>TM</sup> Glass Human 1.0 (BD Bioscience, Clontech, Ca, USA) was used for the analysis of 1081 genes (genes correlated to cell cycle, proliferation, inflammation, cytokines and their receptor etc.) after 23 h of recovery from the last time of exposure, while the microarray from Research & Innovation (Pa, Italy) with 6144 genes was used to analyze gene expression after 1 h of the recovery.

**Results:** Gene expression resulted unchanged after 23 h of recovery from the last time of exposure. This result was obtained with the analysis of three microarrays performed in double (six on the whole) by means of dye swap control. On the contrary, gene expression resulted modified after 1 h of recovery from the last time exposure. Some genes appeared up and down-regulated. In particular CDC2, a Ser/Thr protein Kinase able to regulate different cyclines during cell cycle, appeared down regulated in cells exposed to RF. This result is preliminary but, if confirmed, could be fundamental for explaining previous functional observations (Capri et., Radiat Res, 162: 211, 2004). Further analysis are in progress to confirm this transient effect.

**Acknowledgments:** This study was fully supported by TILab (Telecom Italia Laboratories, To, Italy).

## **In-vitro – tissue and organ**

P-A-172

**A NEW TRANSMISSION LINE SYSTEM FOR EXPOSURE OF BRAIN SLICES TO RF FIELDS.** R. I. Grose<sup>1</sup>, R. G. Montague<sup>2</sup>, A. C. Green<sup>1</sup>, N. C.D. Mifsud<sup>1</sup>, Y. Alfadh<sup>3</sup>, X. Chen<sup>3</sup>, J. E.H. Tattersall<sup>1</sup>. <sup>1</sup>Biomedical Sciences Dept, Dstl Porton Down, Salisbury, Wiltshire SP4 0JQ, UK, <sup>2</sup>Poynting High Voltage, Harrier Park, Hawksworth, Didcot, Oxfordshire OX11 7EL, UK, <sup>3</sup>Dept of Electronic Engineering, Queen Mary, Univ of London, Mile End Road, London E1 4NS.

**OBJECTIVE:** Previous studies have suggested that *in vitro* exposure to 700MHz radiofrequency (RF) fields can affect both evoked and spontaneous electrical activity in rat hippocampal slices (Tattersall et al, 2001). The exposures were made in a parallel plate transmission line, in which the electric field was normal to the plane of the tissue slice. This resulted in poor coupling of the RF field to the tissue, as well as the potential for artifacts induced by coupling of the field into the electrodes used to stimulate and record from the brain slice. We have now developed a novel transmission line system to minimise these limitations.

**METHODS:** In the new transmission line, the plates oppose in the horizontal plane rather than in the

vertical plane. This gives easier access to the sample area (without the need for apertures in the plates) and maximises coupling of the RF fields to the brain slice, which is now aligned parallel to the electric field. At the same time, this configuration minimises coupling of the RF to the electrodes. The volume between the plates is filled with a solid dielectric material, polyethylene, which has a consistent dielectric constant ( $\epsilon_r = 2.25$ ) across the frequency spectrum. This value of  $\epsilon_r$  contributes to a reduction in the impedance of the transmission line from 75 to 50 $\Omega$ . Finally, a double dielectric lens system has been incorporated to reduce wave distortion in the tapered sections of the transmission line, based on a mathematical treatment of equal time of traverse.

The input voltage standing wave ratio (VSWR) of the new line was measured using a HP8720D network analyser, with a 50 $\Omega$  termination. Numerical modelling was performed using a time domain simulation package based on the finite integral technique (FIT) algorithm in CST Microwave Studio™. A variable meshing scheme was used to define higher cell density at the vital locations within the structure. Complex geometry was accurately presented by utilising partial cell filling techniques such as the perfect boundary approximation™ (PBA) and thin sheet technology™ (TST).

**RESULTS:** The VSWR values were comparable with those of the previous exposure system, but the insertion loss was lower, less than 2 dB across the frequency range 200MHz to 3GHz. Numerical modelling confirmed that the new line had better transmission and field profiles than the old system at 400, 700, 900, 1800, and 2450MHz. There was some periodicity of both the measured and modelled VSWR values with frequency, which was expected given that all the sources of distortion and reflection have not been entirely eliminated. The maximum VSWR measured was 1.6:1 at 2.85GHz.

**DISCUSSION:** Because of the enhanced coupling of RF fields to the brain slice, this new transmission line will require lower input power than the previous system to achieve a given SAR in the tissue; this is currently being modelled. At the same time, the coupling to the electrodes will be much lower because these are now normal to the electric field vector, resulting in a greatly reduced potential for electrode artifacts. Furthermore, the dielectric lenses and the absence of apertures should reduce the distortion of fast pulses.

This work was funded by the Electronics Systems Domain of the UK Ministry of Defence Scientific Research Programme. © Crown Copyright 2005, Dstl.

## REFERENCE

Tattersall J. E. H., Scott I. R., Wood S. J., Nettell J. J., Bevir M. K., Wang Z., Somasiri N. P., and Chen X. Effects of low intensity radiofrequency electromagnetic fields on electrical activity in rat hippocampal slices. *Brain Res.* 904: 43-53, 2001.

## Mechanisms of interaction – biological

P-A-175

### **A POSSIBLE INVOLVEMENT OF BETA-ENDORPHIN, SUBSTANCE P AND SEROTONIN IN RAT ANALGESIA INDUCED BY EXTREMELY LOW FREQUENCY MAGNETIC FIELD.**

X. Bao<sup>1</sup>, Y. Shi<sup>1</sup>, X. Huo<sup>1</sup>, T. Song<sup>1</sup>. <sup>1</sup>Bioelectromagnetic Lab, Institute of Electrical Engineering Chinese Academy of Sciences, Beijing 100080, China., <sup>2</sup>Bioelectromagnetic Lab, Institute of Electrical Engineering Chinese Academy of Sciences, Beijing 100080, China., <sup>3</sup>Bioelectromagnetic Lab, Institute

of Electrical Engineering Chinese Academy of Sciences, Beijing 100080,China., <sup>4</sup>Bioelectromagnetic Lab, Institute of Electrical Engineering Chinese Academy of Sciences, Beijing 100080,China.

**OBJECTIVES:** The aim of the present study was to determine the effect of extremely low frequency (ELF) magnetic field on rats in inducing antinociception and central beta-Endorphin, substance P and serotonin (5-HT), which are responsible for nociception.

**METHODS:** A self-made ELF magnetic exposure apparatus was used, which consisted of a special electrical source and a solenoid coil as described by Misakian et al. The exposure apparatus can generate a triangular magnetic field of 55.6 Hz, 8.1 mT in the solenoid. The length and diameter of the solenoid are 42cm and 19cm, respectively. Male Sprague-Dawley rats weighing 200±10 g were used. In experiment 1, rats were repeatedly exposed to ELF magnetic field for 14 consecutive days, and the tail flick latencies (TFLs) were measured. In experiment 2 the rats were repeatedly exposed to ELF for 4 days. In experiment 3, the rats were repeatedly exposed to ELF for 4 days, afterwards they were removed from the magnetic field. In all of the experiments, the magnetic exposures were carried out for 6 hours each day. Tail flick latency (TFL) was assessed using a tail-flick apparatus 6 hours after the rats were exposed to the magnetic field. After the last TFLs measurement, the rats were decapitated to determine the levels of hypothalamus beta-Endorphin, substance P and brainstem 5-HT. The levels of hypothalamus beta-Endorphin and substance P were estimated using RIA kits for rats. And the concentration of 5-HT was determined using F-4500 fluorescence spectrophotometer (Hitachi, Japan). The assay was performed as described by Curzon et al.

**RESULTS:** During the 14-day of repeated exposure, the value of TFLs increased significantly compared with those of sham groups on day 3 and day 4, ( $P < 0.05$ ). From day 5, TFLs values began to decrease, and on day 14 TFLs values decreased to the same level as that of the sham group (Fig. 1). The levels of hypothalamus beta-Endorphin, substance P and brainstem 5-HT did not change after the 14-day repeated exposure when the TFLs values of sham and exposure group were at the same level. The result of nociception in Experiment 2 is coincident with experiment 1 during the first 4 days. TFLs values increased significantly on day 3 ( $P < 0.01$ ) and day 4 ( $P < 0.01$ ) compared with the sham groups (Fig. 2). RIA assay showed that experimental group had significant increases of beta-Endorphin (sham=31.5434±9.39134, exposure=47.5196±16.2726,  $P < 0.01$ ), substance P (sham=48.6776±14.3450, exposure=63.7450±15.7703,  $P < 0.05$ ), 5-HT (sham=845.827±96.472, exposure=964.972±116.082,  $P < 0.05$ ) levels compared with those of sham groups (Tab. 2). The increase of TFLs in Experiment 3 occurred on day 4. When the rats were removed from magnetic field after 4 days exposure, their TFLs values dropped to the levels sham group within 1 day only (Fig. 3). Tab. 3 shows that when the TFLs values of exposed rats dropped to the sham rats level, the levels of beta-Endorphin, substance P and 5-HT did not show any significant changes.

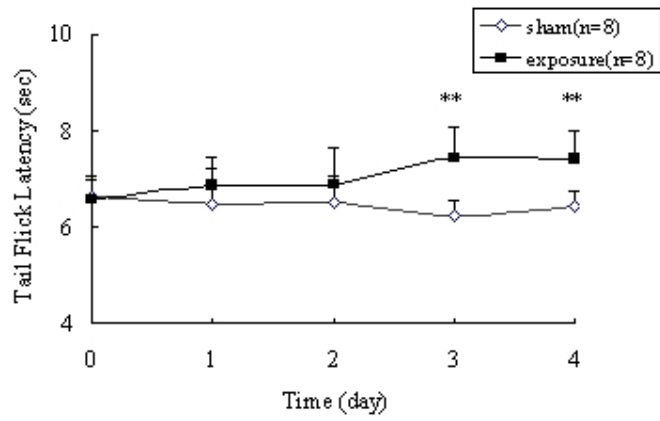
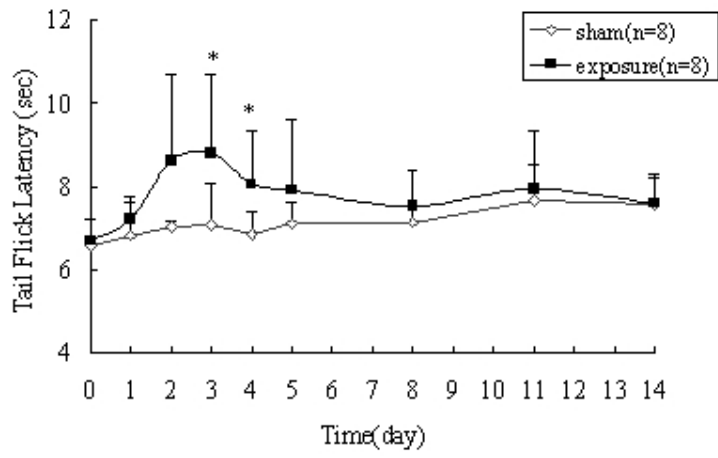
**CONCLUSION:** These results suggest that repeated magnetic exposure to rats had analgesic effects, and magnetic exposure might be valuable for possibly applied magnetic treatment of clinical pain.

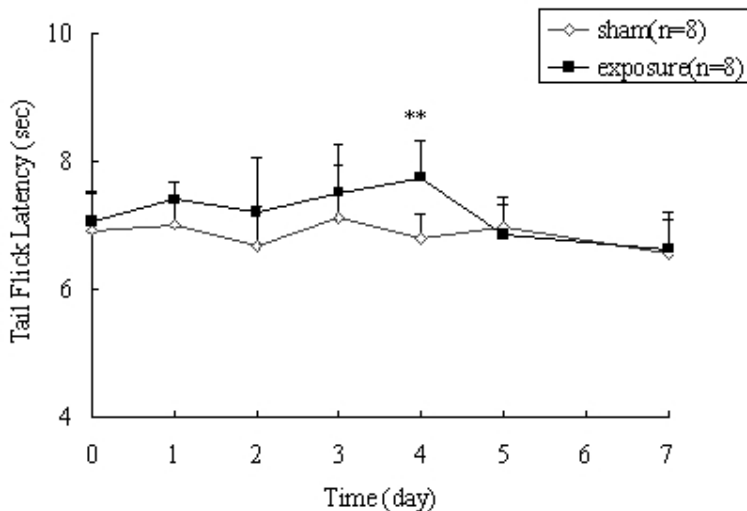
**SUPPORT:** The study was supported by a grant from Chinese Academy of Sciences (No. KJCX1-09).

Fig.1 Effects of ELF on TFLs of rats which were repeatedly exposed to magnetic field for 14 days, 6 hours each day.

Fig.2 Effects of ELF on TFLs of rats which were repeatedly exposed to magnetic field for 4 days, 6 hours each day.

Fig.3 Effects of ELF on TFLs of rats which were repeatedly exposed to magnetic field for 4 days, and then they were removed from it.





P-A-178

**VARIOUS EFFECTS IN ESCHERICHIA COLI CELLS DUE TWO DIFFERENT ELF-MF SIGNALS.** B. Del Re<sup>1</sup>, F. Bersani<sup>2</sup>, C. Agostini<sup>2</sup>, P. Mesirca<sup>2</sup>, G. Giorgi<sup>1</sup>. <sup>1</sup>Dept of Evolutionary Experimental Biology, Univ of Bologna, Bologna, Italy, <sup>2</sup>Dept of Physics, Univ of Bologna, Bologna, Italy.

**OBJECTIVE:** The aim of this study was to verify whether the exposure to different Extremely Low Frequency Magnetic Field (ELF-MF) signals could induce different biological effects. To this purpose experiments involving sinusoidal magnetic field (SMF) and pulsed-square wave magnetic field (PMF) were carried out.

**METHODS:** The exposure system consisted of two pair of Helmholtz coils, which was double-wrapped in order to obtain wound (active coil) or counter-wound (sham) configuration. We used two magnetic field signals: 50 Hz SMF and PMF (50% duty cycle, 50 Hz repetition frequency), both at the intensity of 1 mT (root mean square). The error in the magnetic flux density values was of the order of 2%.

Both the active and the sham coils were maintained in a thermostatic room at a constant temperature of 30° C. The bacterial cells were cultured in tubes and placed in the center of the coil system for 40 minutes.

**RESULTS:** In previous works we found that in Escherichia coli cells SMF reduced the Tn-10 transposition activity and enhanced cell viability (1) while PMF stimulated the transposition mobility and reduced the cell viability (2). In this work we have investigated the Heat Shock Proteins (HSPs) expression by western-blotting and we have found that bacteria exposed to SMF showed higher HSPs expression levels compared to sham-exposed bacteria and the bacteria exposed to PMF showed lower HSPs expression levels compared to sham-exposed bacteria.

**CONCLUSION:** These results show that the biological effects of ELF-MFs may critically depend on the physical characteristics of the magnetic signal, in particular the wave shape. Works are in progress in our laboratory to elucidate the possible molecular targets that might be involved in the observed phenomena.

**REFERENCES:**

- 1) - Del Re B., Garoia F., Mesirca P., Agostini C., Bersani F., Giorgi G. 2003. Extremely low frequency magnetic fields affect transposition activity in *Escherichia coli*. *Radiation and Environmental Biophysics.* 42, 2: 113-118
- 2) - Del Re B., F. Bersani, C. Agostini, P. Mesirca, G. Giorgi, 2004. Various effects on transposition activity and survival in *Escherichia coli* due to different ELF-MF signals. *Radiation Environmental Biophysics.* 43, 4: 265-273

P-A-181

**THE EFFECTS OF ACUTE REPETITIVE TRANSCRANIAL MAGNETIC STIMULATION IN THE NEUROCHEMICAL LESION RAT.** H. Funamizu<sup>1</sup>, S. Kawato<sup>2</sup>, S. Ueno<sup>1</sup>. <sup>1</sup> Dept of Biomedical Engineering, Graduate School of Medicine, Univ of Tokyo, <sup>2</sup>Dept of Biophysics and Life Sciences, Graduate School of Arts and Sciences, Univ of Tokyo.

Repetitive transcranial magnetic stimulation (rTMS) offers potential benefit as a therapeutic treatment for neurological and psychiatric disorders. Recently, a neuroprotective effect of rTMS could be demonstrated. However, the mechanism underlying the therapeutic effects of rTMS is still unknown and very little information is available concerning the acute neurochemical effects of rTMS. In this study, we investigated the rescue effects of rTMS and the reactive effects of rTMS in the lesioned rats by administering the neurotoxin MPTP (1-methyl-4-phenyl-1, 2,3,6-tetrahydropyridine). The rats then received rTMS (10 trains of 25 pulses/s for 8 s) 48 hours after MPTP injection, affecting tyrosine hydroxylase (TH) expression in the substantia nigra. The FOB-hunched posture score for the MPTP-rTMS group was significantly lower and the number of rearing events was higher compared with the MPTP-sham group, these behavioral parameters recovered to almost at the control levels. These results suggest that rTMS treatment modulates the brain dopaminergic system in MPTP-induced injured rats.

P-A-184 STUDENT

**CHANNEL NOISE IN A HODGKIN-HUXLEY NEURON MODEL: STOCHASTIC RESONANCE IN THE DETECTION OF ELECTROMAGNETIC FIELDS.** M. Gianni, A. Paffi, M. Liberti, F. Apollonio, G. D'Inzeo. ICEmB @ Dept of Electronic Engineering, "La Sapienza" Univ of Rome, Rome, Italy.

**INTRODUCTION:** Channel noise has been shown to play a significant role in neuronal processing, being at the basis of some well-known behaviors like response unreliability, missing spikes during firing, or spontaneous action potentials in resting state. Recently, a functional role has been proposed concerning ion channels clustering for preferred input processing, according to a phenomenon known as stochastic resonance [1]. This phenomenon has been previously observed in the detection of electromagnetic (EM) fields in the case of an additive white Gaussian input, roughly approximating the

ensemble of noise sources [2]. Here, an Hodgkin-Huxley (HH) like neuronal model is implemented and accurate channels stochastic models are adopted to investigate possible noise-induced enhancements in the detection of EM fields.

**MODELS AND METHODS:** Moving from the HH neuron model [3], in order to take into account the channel noise, Markov state machines were used for modeling both Potassium and Sodium currents and implemented by means of *channel state tracking* algorithms [4]. Once relative densities of Potassium and Sodium channels in a patch of neuronal excitable membrane have been fixed [5], channel noise level can be changed by varying the number of channels in the model, which means varying the membrane patch area. Channel noise level, for each kind of ionic currents, is quantified by the coefficient of variation (CV), indicating the current fluctuation amplitude, relative to the mean value [1]. The used stochastic neuron model has been shown to describe typical neuron behaviors, such as noisy baseline, spontaneous isolated spikes (Fig. 1a), missing spikes (Fig. 1b), and unreliable response to repetitive stimulation [6].

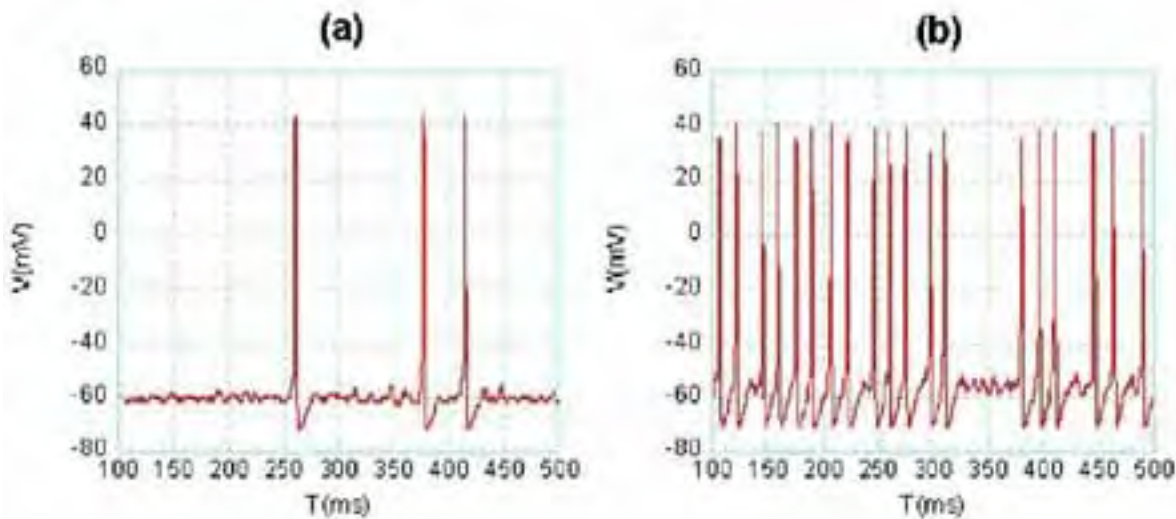


**Fig. 1: Examples of typical neuronal behaviors: isolated spikes in resting state (a) and missing spikes during firing (b).**

Such phenomena are strongly dependent on the relative amount of channel fluctuations which occasionally bridge the small distance in the phase space between the two stable states of the dynamic system (Fig. 2): the firing state (wide close trajectory) and the resting one (bold point). Due to its realistic behavior, the stochastic neuron model is the best candidate to simulate the neuronal encoding of an exogenous EM signal. For this purpose, ELF sinusoidal signals were applied to the model as a perturbation of the transmembrane voltage. The output signal to noise ratio (SNR) was considered as a quantitative measure of the encoding of the signal in the spike train, for different channel noise levels. The power of the signal was the value of the power spectral density (PSD) of the spike train at the EM frequency ( $f_{EM}$ ), in the presence of the input signal, whereas the power of the noise was calculated as the mean value of the PSD in a range of 10 Hz around  $f_{EM}$ , when no signal had been applied to the system [2].

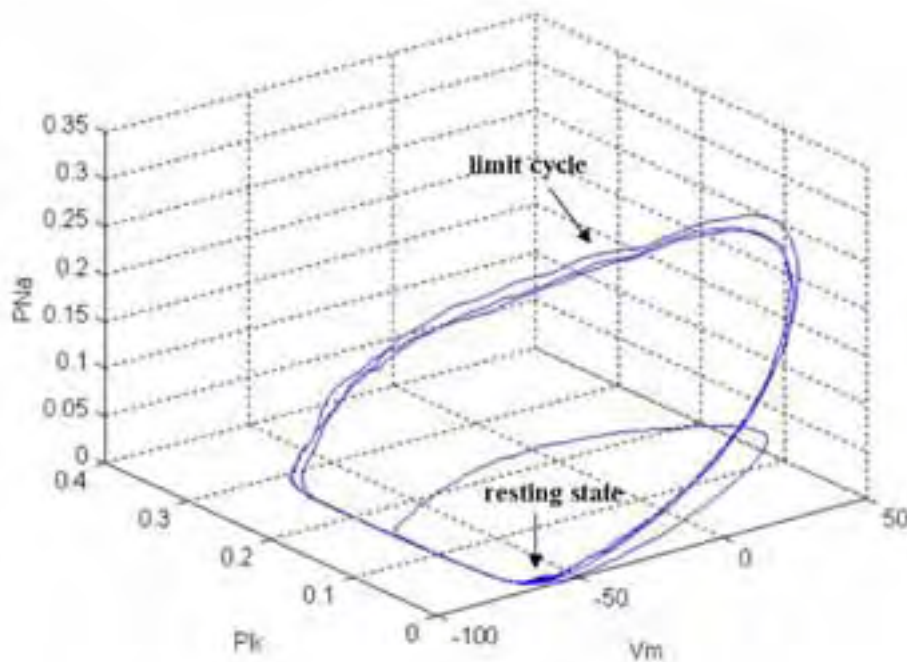


Fig. 2: Phase space diagram of the stochastic neuron model for a membrane patch area of  $200 \mu\text{m}^2$  and in the absence of external stimulation. The orthogonal axes in the plot represent the membrane voltage ( $V_m$ ) and the open probabilities for  $\text{Na}^+$  ( $P_{Na}$ ) and  $\text{K}^+$  ( $P_K$ ) channels.

**RESULTS:** In order to evaluate the possibility for the model to detect weak sinusoidal input signals, with respect to the intrinsic noise level, a subthreshold stimulation current was considered ( $I=4 \mu\text{A}/\text{cm}^2$ ) and a weak sinusoidal voltage signal, with amplitude equal to  $500 \mu\text{V}$  at  $f_{EM}=50 \text{ Hz}$ , was applied to the model. Nine different levels of noise were considered, corresponding to a number of Potassium channels from 90 up to 10800. It should be noticed that, as the number of channels (or the patch area) increases, the relative noise level decreases, since the CV expression is inversely proportional to the square root of the number of channels [1]. Fig. 3, reporting the SNR versus the number of Potassium channels in the model, shows a typical bell-shaped curve, with a maximum in correspondence of a well defined internal noise level.

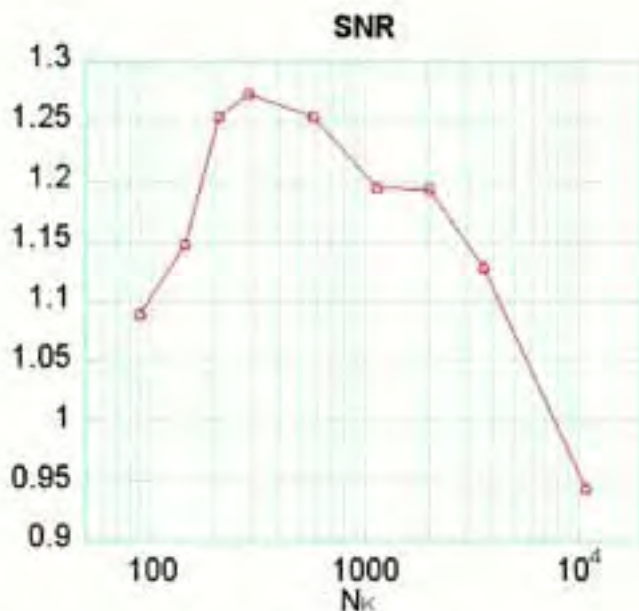


Fig. 3: Signal to noise ratio (SNR) versus the number of Potassium channels ( $N_K=90, 144, 210, 288, 576, 1152, 2000, 3600, 10800$ ) in the model. The signal is an exogenous sinusoidal EM field with frequency 50 Hz and amplitude 500  $\mu\text{V}$ .

This phenomenon, already evidenced in a neuron when an external Gaussian noise was applied [2], is known as stochastic resonance, and consists in the optimization of the response of a system to a subthreshold external stimulus, in correspondence of a particular amount of noise [1].

**CONCLUSIONS:** Although a resonant behavior for stochastic neuron model was plausible, its detection was a challenging goal. In fact, in this case, noise is not an external input, but arises from the intrinsic properties of the neuron, such as typology and number of channels in the membrane. A change in the number of channels does not only produce a different channel noise level, but also modifies other features of the system, such as the mean current through the families of ionic channels and the intrinsic firing frequency. The detection of stochastic resonance in the neuron behavior is therefore a remarkable result, and suggests that noise arising from ionic channels may play a role in the encoding of the inputs, including an exogenous EM field, which results to be optimized for a particular amount of noise [1]. Channel noise may therefore modulate field-induced effects on neuronal activity, and has hence to be accurately considered in models for bioelectromagnetic studies.

#### References

- [1] G. Schmid, I. Goychuk, P. Hanggi, S. Zeng, P. Jung, *Fluctuation and Noise Letters*, vol. 4, pp. L33-L42, 2004.
- [2] M. Gianni, F. Apollonio, M. Liberti, and G. D'Inzeo, XXVI BEMS Annual Meeting, Washington DC, 2004.
- [3] A. L. Hodgkin and A. F. Huxley, *Journal of Physiology*, vol. 117, pp. 500-344, 1952.
- [4] H. Mino and W.M. Grill, *IEEE Trans. Biomed. Eng.*, vol. 49, pp. 527-32, 2002.
- [5] E. Schneidman, B. Freedmann, I. Segev, *Neural Computation*, vol. 10, pp. 1679-1703, 1998.
- [6] Z. F. Mainen and T. J. Sejnowski, *Science*, vol. 268, pp. 1503-6, 1995.

This work was supported by the European Union, V framework under the RAMP2001 Project.

## Medical applications

P-A-187

### **MONITORING INTRACRANIAL HYPERCAPNEA-PROVOKED CHANGES IN THE RAT WITH PERMITTIVITY-BASED MEASUREMENTS (0.1 GHZ TO 3.0 GHZ): A PILOT STUDY.**

G. Jerome Beers<sup>1,2,3</sup>, Y. Iris Chen<sup>1,2</sup>, Kenneth K. Kwong<sup>1,2</sup>, G. Bonmassar<sup>1,2</sup>, J. L. Ackerman<sup>1,2</sup>. <sup>1</sup>Athinoula A. Martinos Center for Biomedical Imaging, <sup>2</sup>Dept of Radiology, Massachusetts General Hospital, <sup>3</sup>Dept of Radiology, Brigham and Women's Hospital.

#### INTRODUCTION:

Previous authors have reported permittivity changes at microwave frequencies, measured with in situ coaxial probes, that coincided with physiological changes in canine brain(1,2), kidney(2), and heart(3). We are performing similar studies in rats in order to confirm the possibility of monitoring intracranial physiological changes with permittivity-based measurements, with the ultimate goal of imaging physiological changes in animals and humans.

#### METHODS:

**Animal preparation:** 8 rats were anesthetized with ~1% halothane or isoflurane (in 1:1 O<sub>2</sub>:N<sub>2</sub>O) ventilation or alpha-chloralose (30mg/kg/hr) intravenous infusion. Adjustments in dosage were made as needed in response to changes in level of anesthesia. The calvarium was surgically exposed. A hole was drilled into the calvarium that penetrated to or just through the inner table.

**Hypercapnea:** Hypercapnea was induced via 33% CO<sub>2</sub> in the ventilation gas mixture for variable (1.98 – 4.85 minute) intervals between the hypercapnic episodes. Arterial blood samples were obtained through an arterial femoral catheter during the baseline and hypercapnic states to access the blood pCO<sub>2</sub> level. Each rat was sacrificed with KCl while measurements were continued until ~10–30 minutes after death.

**Probe and data recording:** A coaxial probe made from 3.6 mm (0.141 in) outer diameter semirigid coaxial cable, with a ~0.6 mm protruding inner conductor, was placed on the calvarium. The outer conductor terminated in a ground plate in contact with the outer table of the skull, and the inner conductor (diameter = 0.9 mm) fit into the drilled hole. Both the ground plate and the exposed center conductor were gold plated. S11 1-port calibration of the reflection coefficient was performed before probe placement. After probe placement the contact site was irrigated with saline during the experiment. The probe was connected to an HP/Agilent 4191A network analyzer, from which the complex reflection coefficient at 51 frequencies from 100 MHz to 3000 MHz was obtained every ~2.4 seconds. The linear magnitude of the reflection coefficient was analyzed at the following selected frequencies: 100, 506, 1028, 1492, 2014, 2420, and 3000 MHz. Since baseline drift in the data was common, analysis included baseline correction using data from 4 minutes before until immediately before the start of 33% CO<sub>2</sub> delivery and from 1 minute until 4 minutes after cessation of 33% CO<sub>2</sub> delivery.

#### RESULTS:

The first rat in the series was exposed to three episodes of 6% hypercapnea, which did not provoke a clear-cut change in arterial pCO<sub>2</sub> (pCO<sub>2</sub> was raised from baseline 53.0 ±4.79 only to 69.3 ±5.23), and then one episode of 33% hypercapnea, which was associated with a pronounced elevation in arterial pCO<sub>2</sub> (to 142). With the other rats variable numbers of episodes of 33% hypercapnea were employed, all of which provoked obvious changes in arterial pCO<sub>2</sub> (pCO<sub>2</sub> raised from 48.5 ±7.91 to 133.8 ±23.16).

The linear magnitude of the reflection coefficient typically showed obvious changes when exposure to 33% CO<sub>2</sub> was started and stopped, especially at lower frequencies (see Figure 1, which shows change in baseline-corrected reflection coefficient from a rat for three hypercapnic episodes [3.83 minutes, 4.35 minutes, and 4.85 minutes long, respectively]). The reflection coefficient also showed changes, pronounced in most cases, following administration of KCl. A clear deflection from the baseline was evident in some rats less than 10 seconds after the KCl infusion began. With both the hypercapnea data and the KCl data, in some cases changes were more readily apparent, or apparent earlier, with the real or imaginary reflection coefficient data than with the linear magnitude data.

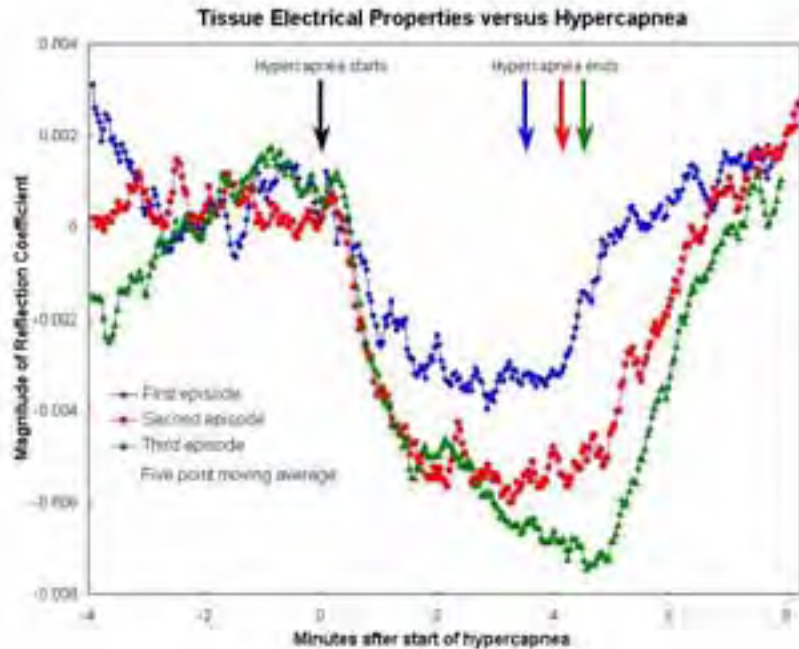
#### DISCUSSION AND CONCLUSION:

Our data are in keeping with prior evidence that physiological changes—in the case of our work, intracranial physiological changes arising from hypercapnea, or infusion of KCl—may cause changes in permittivity that occur with or shortly after the physiological changes. Limitations of our work at present include the following:

1. The volume of interrogated tissue at a given frequency has not been determined.
2. The potential effects of multiple variables, such as the identity and concentration of the anesthetic, have not been systematically investigated.
3. It is unproven that the changes represent brain physiology to any degree—they might only reflect changes in the meninges.
4. We have not calculated permittivity or conductivity values.
5. The cause or causes of the changes in reflection coefficient is unknown. Changes in water content associated with physiological changes in blood volume are presumed to be a major determinant. However other major influences could include compression of vessels with brain swelling, or movement of tissue in and out of the interrogated volume as the brain swells or shrinks. Nevertheless, the results so far do suggest that in vivo permittivity measurements potentially could have a role in highly temporally-resolved physiological monitoring of the brain, or, more remotely, even in physiological imaging.

#### REFERENCES:

1. Burdette EC, Friederich PG, Seaman RL, Larsen LE. In situ permittivity of canine brain: regional variations and postmortem changes. *IEEE Trans Microwave Theor Tech MTT-34* 1(1986): 38-49.
2. Burdette EC, Cain FL, Seals J. In-situ tissue permittivity at microwave frequencies: perspective, techniques, results. In: *Medical applications of microwave imaging*, Larsen LE, Jacobi JH, eds. IEEE Press, 1986: 18-40.
3. Semenov SY, Svenson RH, Posukh VG, Nazarov AG, Sizov YE, Bulyshev AE, Souvorov AE, Chen W, Kasell J, Tatsis GP. Dielectrical spectroscopy of canine myocardium during acute ischemia and hypoxia at frequency spectrum from 100 kHz to 6 GHz. *IEEE Trans Med Imaging* 2002 Jun; 21(6):703-7.



P-A-190

**EVALUATION OF ELECTRIC FIELD IN CAPACITIVE COUPLING SYSTEM.** B. Bianco<sup>1</sup>, B. Bisceglia,<sup>2</sup> R. Cadossi<sup>3</sup>, S. Setti<sup>3</sup>. <sup>1</sup>Facolta di Ingegneria, Università di Genova, Italy, <sup>2</sup>Dipartimento di Ingegneria dell'Informazione e di Ingegneria Elettrica, Università degli Studi di Salerno, Fisciano (SA), Italy, <sup>3</sup>IGEA, Carpi (MO), Italy.

### Introduction

This paper reports the analysis of a numeric model based upon a simple potential formulation to calculate the evolution of the electric field in bone materials.

The algorithm arises for biological tissues of centimeter-to-meter scale exposed to 60 kHz Capacitively Coupled Electric Fields (CCEF).

### Bone tissues

There is growing evidence that electric and magnetic fields can influence biological functions. Alternatives such as CCEF were then put forth to resolve some bone related disorders as an alternative procedure to conventional intervention of orthopedic surgery.

Bone is a complex material, with a multiphase, heterogeneous and anisotropic microstructure. The processes of fracture and healing can only be understood in terms of the underlying bone structure and its mechanical role.

An important aspect of bone behavior is its self-adaptive capacity, modifying its microstructure and properties according to the specific mechanical environment. Bone is not like inert engineering materials. It undergoes substantial changes in structure, shape and composition according to the mechanical and physiological environment, an adaptive process known as bone remodeling. Bone tissue has very interesting structural properties. This is essentially due to the composite structure of bone, composed of inorganic and organic material, and water. Inorganic components are mainly

responsible for the compression strength, while organic components provide the corresponding tension properties. This composition varies with species, age, sex, the specific bone and whether or not the bone is affected by a disease

From a macroscopic (physical) point of view, bone tissue is non-homogeneous, porous and anisotropic.

Mathematical model (numeric)

For the mathematical simulation of fracture healing a finite element model was developed. The algorithm should be useful in calculating the response of biological materials subject to excitation including modeling and electrical stimulation.

The electrical properties of dielectric materials inevitably vary with frequency. However, few if any published computational simulations of tissue interactions with low-frequency electric fields.

This holds for a variety of electrical signals within the body, for example those due to muscle action potentials, heart and brain activity, and functional electrical stimulation

In fact, it has even the availability of computational methods capable of straightforward modeling of electrical signals propagating within inhomogeneous, frequency dispersive biological tissues. For frequencies above about 1 MHz, the Finite Difference Time Domain (FDTD) method is a popular approach for such modeling. FDTD has not yet been extended fully to the low-frequency range that is of interest here for biological tissue structures having arbitrary inhomogeneities and subject to arbitrary excitations. At frequencies well below 1 MHz (appropriate for studies of the body's own electrical signaling network and many diagnostic and therapeutic procedures), we believe that the FDTD technique is currently one of the best computational approaches that permits the required level of realistic modeling of general time-dependent phenomena and arbitrary structures.

The CCEF generated by Osteobit has the following characteristics:

Burst frequency:  $\gamma = 60$  kHz

Repetition rate:  $\nu = 12.5$  Hz

Electrodes: 10 x 5 cm

V<sub>pp</sub>: 40 mV

The electric field in the osteobit environment is ELF.

The potential V in cylindrical coordinates

$$\frac{1}{r} \frac{\partial}{\partial r} \left( r \frac{\partial V}{\partial r} \right) + \frac{1}{r^2} \frac{\partial^2 V}{\partial \varphi^2} + \frac{\partial^2 V}{\partial z^2} = 0$$

that is

$$\frac{\partial^2 V}{\partial r^2} + \frac{1}{r} \frac{\partial V}{\partial r} + \frac{\partial^2 V}{\partial z^2} + \frac{1}{r^2} \frac{\partial^2 V}{\partial \varphi^2} = 0$$

We implement the above algorithms in a MATLAB code.

The model geometry and the finite-element mesh are generated with the software package FEMLAB.

Conclusions

From an electromagnetic point of view the evaluation of the electric field in bone tissues correlates the

therapeutic effect to the local characteristics of the field.

## References

- J. BLACK, Electrical Stimulation. Its role in growth, repair and remodeling of the musculoskeletal system, New York 1987.
- C. T. BRIGHTON, W. WANG, R. SELDES, G. ZHANG, and S R. POLLACK, Signal transduction in electrically stimulated bone cells, *The Journal of Bone and Joint Surgery* 2001.
- P. DUCHEYNE, L. Y. ELLIS, S. R. POLLACK, D. PIENKOWSKI and M. CREKLER, Field distributions in the rat tibia with and without a porous implant during electrical stimulation: a parametric modeling, *IEEE Transactions on Biomedical Engineering*, Vol. 39, N. 11, November 1992.

P-A-193 STUDENT

**CITOSTATIC RESPONSE OF HEPG2 HUMAN HEPATOCARCINOMA CELLS EXPOSED TO 0.6-MHZ ELECTRIC CURRENTS.** M.-L. Hernandez-Bule, M.-A. Trillo, J. Leal, A. Ubeda. Serv. Investigacion-BEM Hospital Ramon y Cajal, MADRID.

**OBJECTIVE:** Capacitive Electric Transfer (CET) therapies using 0.6-MHz currents have been successfully applied to thermal treatment of skin, muscle and tendon lesions. CET therapy has been described to be more efficient than other thermal therapies in healing injured tissues and relieving the associated pain. Although the specific mechanisms of response to CET remain unidentified, different authors have proposed that the electric stimulus and the electrically induced thermal increase could act in synergy. We have previously reported that short-term, in vitro exposure to 0.6-MHz currents at subthermal levels could exert cytostatic effects on HepG2, human hepatocarcinoma cells. The present study was aimed to investigate the cell growth response at different times after exposure and to identify differentiating processes potentially involved in the reported cytostatic effects.

**METHODOLOGY:** HepG2 cells were seeded in petri dishes and grown in a 37°C, 5% CO<sub>2</sub> atmosphere until 75% confluence. At that point (t = 0) pairs of sterile electrodes were inserted in the dishes. In the experimental dishes the electrodes were energized with 5-minute pulses of 0.6 MHz, 50  $\mu$ A/mm<sup>2</sup> currents for a 24-h period. This treatment has been reported not to affect the culture medium by increasing the temperature, inducing net displacement of charged molecules or releasing metal ions from the electrodes. During the exposure period the control samples were sham-exposed in petri dishes with non-energized electrode pairs, kept inside a CO<sub>2</sub> incubator identical to that used for exposed samples. At the end of the exposure lapse the cells were either processed for analysis or kept in culture for an additional period. Cell proliferation during and after exposure was estimated through Trypan blue dye exclusion. The potential effects of the electric stimulation on apoptosis at the end of the treatment and/or 24 hours after were estimated by TUNEL assay. Potential effects on cell differentiation were estimated through quantification of alpha-fetoprotein by immunoblotting and immunofluorescence, during the treatment (t = 12h) and at the end of the treatment (t = 24h). Alpha-fetoprotein being an efficient indicator of cell differentiation is currently used as a tumoral marker in human hepatocarcinoma.

**RESULTS AND DISCUSSION:** The dye exclusion analysis confirmed previously reported data that a 24-h exposure to 5-minute pulses of 50  $\mu$ A/mm<sup>2</sup> currents at 0.6 MHz can reduce cell growth in HepG2. The effect was particularly noticeable after 18 or 24 additional hours of incubation in the absence of the electric stimulus (t = 42h or 48h, respectively, Fig. 1). The TUNEL assay showed a statistically

significant increase in the percent of apoptotic cells at 18 h after the end of the exposure period (Fig. 2). However, this increase in the death rate, corresponding to less than 1% of the total number of cells, does not justify by itself the decrease in cell growth described in Fig. 1 (about 15% of the total number of cells). More plausibly, such a decrease could be connected to a potential, electrically-induced effect on cell differentiation. In fact, the immunoblot analysis showed that the electric treatment induced a significant decrease (30 - 70% of that in controls) in alpha-fetoprotein levels during the exposure period, which is indicative that the 0.6-MHz current can induce differentiation in HepG2 cells. Such a differentiating effect could result in a decelerated proliferation rate, leading to the reduction in the cell growth observed after the treatment.

**CONCLUSIONS:** the present results indicate that the herein-described apoptotic response of HepG2 cells would have only a minor incidence on the reported cytostatic effects induced by non-thermal, 0.6-MHz currents. Such cytostatic effects could rather be attributable to a potential deceleration of the cell growth rate linked to the observed differentiating response induced by the electric treatment. These data provide additional support to the hypothesis that in CET therapy the cellular response to the electric stimulus could act in synergy with the tissue's response to the electrically induced thermal increase. Further research is needed in order to determine whether the observed cellular effects can be used to optimize or extend the applications of CET therapy.

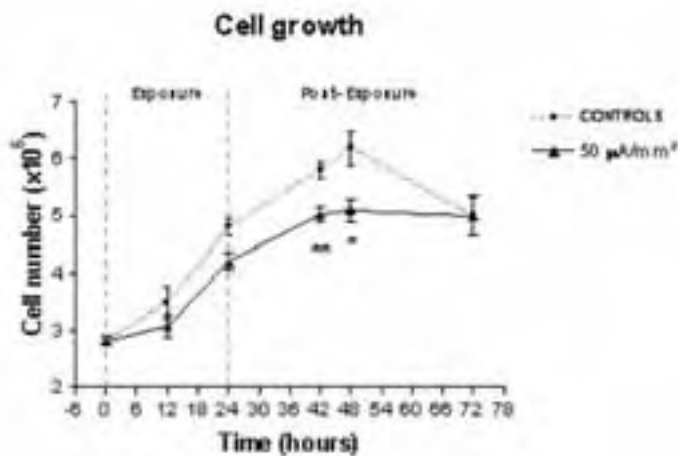


Figure 1: Cytostatic effect induced by a 0.6-MHz, 50- $\mu\text{A}/\text{mm}^2$  electric current. Total number of cells (mean  $\pm$  SEM) per dish, 3+ experimental repeats per point, 3+ dishes per experimental repeat. \*:  $0.01 \leq p < 0.05$ , \*\*:  $p < 0.01$  (Student's t-test.) A general decrease can be observed in the cell number during exposure (t = 12 h and 24h) which becomes statistically significant after exposure (t = 42 h and 48 h.) The convergence in the cell number at t = 72 h is attributable to growth saturation due to depletion of nutrients in the medium.

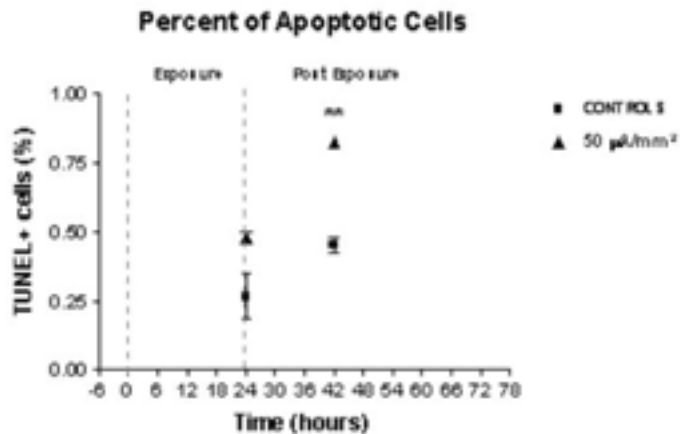


Figure 2: A significant increase in the rate of apoptosis was observed at  $t = 42$  h: 18 hours after the end of the exposure period. Two experimental repeats per point, two samples per experimental condition and experimental repeat. Same notations as in Fig. 1.

## Risk, safety standards and public policy

P-A-196

**EFFECT OF EXTREMELY LOW FREQUENCY MAGNETIC FIELD (ELF) ON UTERUS AND OVARIES OF RATS (ELECTRON MICROSCOPICALLY EVALUATION).** F. Aksen<sup>1</sup>, A. Ketani<sup>2</sup>, B. Yokus<sup>2</sup>, Z. Akdag<sup>1</sup>, A. Kaya<sup>1</sup>, S. Dasdag<sup>1</sup>. <sup>1</sup>Biophysics Dept of Dicle Univ Medical Faculty, Diyarbakir, Turkey, <sup>2</sup>Veterinary Faculty of Dicle Univ, Diyarbakir, Turkey.

The purpose of this study is to investigate the effect of the extremely low frequency (ELF) magnetic fields on the uterus, ovary and vagina of rats. Forty-eight female Wistar albino rats were divided into two groups. one for 50 days and the other for 100 days. Then they were also divided into two groups. one was the control group (n=12) which sham application done and the other was the experimental group (n=12).

Experimental rats were put into Plexiglas cages in order to exposure, at the 50 Hz frequency with 1mT intensity of magnetic field for three hours per day. The same experiment was applied to the sham group without applying magnetic field for three hours.

At the end of each ELF exposure process the rats sacrificed and the ovaries, uterus and vagina of rats

were taken for electron microscopically examination. Additionally, malondialdehyde concentration (MDA) was measured in the uterus and ovaries.

Electron microscopically examination shown that ELF magnetic field under investigation affected the uterus, ovaries and vagina after 50 and 100 days of exposure process.

Electron microscopically evaluation of 50 days ELF exposure caused following alteration in ovaries. Ultra structural dissolution, decrease in cell organelles, heterochromative view and typical structural losing of nucleus were observed in ovaries germinal epithel cells. A few number of lipid vacuoles which is determined in sham rats was not observed in experimental group. However, compact structure of tunica albuginea was disappeared and cavities occurred in cells of experimental group.

Electron microscopically evaluation of 100 days ELF exposure caused following alteration in ovaries. Ultra structural alterations were observed in germinal ephitel and tunica albuginea of ovaries. Irregular structure of nucleus was observed in cells under investigation. However, irregularity in nucleus and nucleolus, an increase in lipid vacuoles of cell cytoplasm and reduce in organelles were clearly observed in this exposure group. In addition, dissolution in connection units between germinal ephitel cells and irregular views in tunica albuginea were also observed in ovaries.

However, some of alterations were observed in uterus and vagina similarly.

In conclusion, the results of the study shown that 50 and 100 days exposure of 1mT ELF magnetic field can cause some alterations on cellular level in terms of rat fertility.

P-A-199

**FURTHER ANALYSIS FROM THE U.S. FEDERAL COMMUNICATIONS COMMISSION DATABASE: EXPOSURE FROM WIRELESS DEVICES AND COMPARISON OF SAR AVERAGING MASS.** R. F. Cleveland, Jr, M. L. Perrine, E. D. Mantiply. Office of Engineering and Technology, Federal Communications Commission, Washington, District of Columbia, USA.

**OBJECTIVE:** Exposure from wireless devices, such as mobile telephones held against the head or body, is evaluated in terms of the localized specific absorption rate (SAR) resulting from radio frequency (RF) emissions from the device. In the United States, the Federal Communications Commission (FCC) requires that wireless consumer devices comply with an SAR limit of 1.6 watts/kg averaged over one gram of tissue in the shape of a cube. Compliance is normally demonstrated through laboratory measurement procedures that have been developed by standards organizations such as the Institute of Electrical and Electronics Engineers (IEEE) and the International Electrotechnical Commission (IEC). Documentation of compliance with exposure limits must be submitted to the FCC for certain wireless devices and is included in an FCC database. The database is on-line and includes reports on SAR for various types and models of wireless devices, such as mobile and cordless telephones and WLAN devices. We previously reported the results of our analysis of SAR data for exposure to the head from mobile telephones. The objective of the present study is to analyze SAR data relating to: (1) exposure from mobile telephones when held against parts of the body other than the head, (2) exposure reported for wireless devices other than cellular telephones, and (3) how the mass over which SAR is spatially averaged affects reported values for SAR.

**METHODS:** Information used in this study was obtained directly from the database developed by the FCC for processing authorizations of various types of regulated transmitters. Data were downloaded into spreadsheets for analysis and plots were constructed related to the objectives of the study. Primary parameters of interest were operating power, SAR, device type and design, and measurement procedure.

**RESULTS/CONCLUSIONS:** Preliminary results of our analysis indicate that, as we reported previously for head exposure from mobile telephones, maximum SAR levels reported for body-worn phones and devices are not consistently related to device characteristics. Our analysis of SAR values reported for newer so-called cordless telephones (used for short distance communication but which use higher power than older models) shows that exposure levels are generally lower than those for cellular telephones but can potentially be a significant percentage of the exposure limit. Exposure values for other wireless devices, such as those used in notebook computers are generally relatively low, but can vary greatly depending on operating power and on where the transmitter is located in the host device. Comparison of SAR data for 1 gram versus 10 gram spatial averaging for specific devices shows that 10 gram averaging typically results in lower reported values for maximum average SAR. This reduction can be 40% or more for both head and body SAR. This is a significant issue for organizations developing recommendations for evaluating SAR due to mobile telephone exposure. A detailed summary of our findings will be presented.

*Note: Views expressed in this abstract are those of the authors. They do not necessarily reflect the views of the Federal Communications Commission.*

P-A-202

**OCCUPATIONAL EMF EXPOSURES: RESULTS OF CASE STUDIES.** P. Chadwick, H. Hall. MCL, Newbury, Berkshire, UK.

In 2004 a new European Directive limiting occupational exposure to EM fields in every workplace in the EU was published. This paper describes its likely impact on industry, based on analysis of a significant measurements database and two case studies, one addressing induction heating and the other addressing electrical welding.

This paper indicates that the following technologies will almost certainly require detailed investigation, and that there will be situations of non-compliance:

- Welding
- Induction heating
- Dielectric heating
- Electrochemical processes, or any other process requiring high DC currents.

These technologies are likely to require assessment but there should be few cases of non-compliance:

- Plasma discharge equipment
- Magnetisers and demagnetisers, including tape erasers
- Large arc furnaces
- High current crack detection equipment

- High current bus bars and conductors
- High current transformers
- VHF/UHF radios

These technologies should not require any assessment under the Directive:

- RFID/EAS
- VDUs
- Mobile phone base stations
- Wireless local area networks (WLANs)
- Cordless phones
- Bluetooth devices and hands-free kits

The overall conclusions regarding the impact of the Directive are:

- There will be an on-going requirement to provide authoritative health and risk information to employees.
- There may be requirements for further assessments if employees with implanted medical devices (including pacemakers) have access to the areas around the induction heaters and welders
- The impact on access and working practices in many situations will be minimal, and no more than good practice would in any case call for.
- There will be a requirement for access control close to some equipment, including some induction heaters operating at kHz frequencies. This requirement will persist whether or not the Directive is fully implemented.

This work was supported by the UK Engineering Employers Federation.

P-A-205
---------

**REPRESENTATION OF THE LITERATURE ON THE EFFECTS OF ELECTRO-MAGNETIC FIELDS.** S. Driessen, M. Meyer, R. Wienert, J. Silny. Research Center for Bioelectromagnetic Interaction, Univ Hospital, Aachen, Germany.

### **Background**

Due to the large number of already existing publications and constantly new published studies the appropriate representation of the contents of scientific literature is a growing concern today. The appropriate representation of difficult and complex publications is important especially when informing policy makers and interested citizens who are participants in such controversial discussions as the electro-magnetic interactions with biological systems or organisms. The knowledge-based literature database on the effects of electro-magnetic fields on the organism relies on relevant data and contents originating from peer-reviewed publications.

### **Aim**

The aim of the present work is to determine an appropriately brief but at the same time sufficiently

detailed summary representation applicable for the majority of publications on the effects of electromagnetic fields. Utilizing one common consistent structure, even complex contents of scientific publications should be reducible to an essential and comprehensible level.

## **Methods**

A representation structure was created that allows the registration of different publications in one consistent form. There is a basic version in which all main data are recorded and an extended version which considers additional details. Currently, the available scientific articles in the research area of electromagnetic interactions with biological and medical systems are extracted and summarized. In one consistent structure the following data are covered: aim of study, endpoints, exposure parameters, certain aspects of the exposed and investigated material or system, and main outcome (cf. figure). For selected articles, additional details such as the quantities of exposed and investigated animals or samples, as well as on ambient conditions can be included in the extended version.

Scientific publications are read and prepared in-house by two groups of experts: the technicians extract all essential data concerning the field exposure; the biologists summarize biological and medical contents such as aim of the study, investigated endpoints, methods and main results. The experts are to phrase their summaries in the style of the original authors. On the basis of one example, both versions (basic as well as extended) are presented, their structures are explained and individual advantages are pointed out.

## **Results**

An adequate representation of scientific publications and an appropriate platform for information on the effects of electro-magnetic fields are provided. Experience has shown that two versions of representation are needed to fulfil the requirements of the identified user groups: one basic version adequate for the needs of laymen, and an extended one for experts' demands. These structures complement each other without redundancy. Thus, EMF experts, scientists from other disciplines or decision makers as well as laymen are supplied with a rapid overview over the extracted publications. Up-to-date knowledge is reflected, so that users are given an idea of the scope and status of EMF research and are enabled to form their own view on the topic. The representation is laid out multi-lingually: English and German are currently supported; other languages can be added if desired.

So far, more than 900 extracted articles, mainly in the radiofrequency range, are available in the database. The presentation of the extracts is embedded in the context of the "EMF-Portal" (cf. Wienert et al. 2005).

Future objective of this work is the provision of popular extracts, summaries and evaluations of the bigger part of the published scientific corpus on the effects of electro-magnetic fields. Moreover, based on the available extractions of all articles and on the general descriptors extracted, general conclusions should be made possible.

## General Data for the article

"Lymphomas in Ep-Pin1 transgenic mice exposed to pulsed 900 MHz electromagnetic fields."

by Dipakshi Mishra, Debraj K. Ghosh, V. Thomas D. Paine J, Hans AW. published in *Health Res* 1997; 147 (3): 833 - 840

### Aims of study (according to author)

To determine whether long-term exposure to pulse-modulated radiofrequency fields similar to those used in digital mobile telecommunication would increase the incidence of lymphomas in Ep-Pin1 transgenic mice (expressing an activated Pin1) compared to their (control) cells.

### Endpoints (and methods)

- cancer (lymphofibrosarcoma and non-lymphofibrosarcoma lymphomas (lymphoma occurrence and time-to-onset), distribution of the cell lineage, see below)
- morphological/histopathological changes, histopathological tumor classification
- other vital measures, body weight

### Field characteristics

900 MHz, 100% pulsed (PRF)  
exposure duration: daily 30 min at 7h, 10 min each 30 min at 17h, 10 min, up to 15 months

### Parameters

power flux density: 0.26  $\mu\text{W}/\text{cm}^2$  @ min value  
power flux density: 0.41  $\mu\text{W}/\text{cm}^2$  @ mean value (output)  
power flux density: 1.1  $\mu\text{W}/\text{cm}^2$  @ max value (2.8 - 1.1  $\text{W}/\text{m}^2$ )  
SAR: 4  $\mu\text{W}/\text{kg}$  @ peak value  
SAR: 490  $\mu\text{W}/\text{kg}$  @ mean value  
SAR: 1.09  $\text{W}/\text{kg}$  @ mean value (1.49, 0.92, 1.09  $\text{W}/\text{kg}$ )  
SAR: 4.2  $\text{W}/\text{kg}$  @ peak value (1.09-4.2  $\text{W}/\text{kg}$ )  
power: 0.1  $\text{W}$  @ mean value  
power: 70  $\text{W}$  @ peak value

### Exposed system

mouse (genetically altered Ep-Pin1 transgenic (pp244) and nontransgenic, C57BL/6NTac)  
-whole body exposure

### Investigated system

investigation on: brain exposure  
organ system(s): immune system, tissues, lymph nodes, spleen, liver, lung, kidneys, adrenal, thyroid, parathyroid system, ovary, heart  
investigated material: tissue slices (in vitro), isolated organs (in vitro), single cell exposures  
investigation: during and after exposure

### Main outcome of study (according to author)

Lymphoma risk was found to be significantly higher in the exposed mice than in the controls.

(Study character: medical/biological study; experimental study; laboratory study)

## Theoretical and practical modeling

P-A-208

**A MODIFIED EQUIVALENT SURFACE BOUNDARY APPLIED TO FEM-FDTD HYBRID ELECTROMAGNETIC MODELS.** R. Alias, R. A. Abd-Alhameed, P. S. Excell. Mobile and Satellite Communications Research Centre, Bradford Univ, Bradford, UK.

The finite element method (FEM) is widely used in computation of unbounded static and quasi-static electric and magnetic fields at DC and low frequencies, and for enclosed systems (cavities etc) at high frequencies. However, its use for high-frequency open-field (radiation and scattering) has been limited due to the relatively large size of the computational tasks that result. The finite-difference time-domain (FDTD) scheme is very popular for electromagnetic modelling because of its simplicity and efficiency, but a drawback is the 'staircase' approximation of oblique and curved boundaries, which often gives poor accuracy: this problem is particularly troublesome with bioelectromagnetic modelling. The finite-element method (FEM) allows good approximations of complex boundaries and with edge elements it performs well for Maxwell's equations [1]. An obvious compromise is a hybrid that applies FDTD in large volumes, combined with FEM around regions with complex structure: the FEM may be applied in the frequency domain to achieve efficient solutions. Previously attempted hybrids of this type have only used time-domain FEM [2] and some have shown late-time instabilities [3,4].

The coupling between the hybridised methods is computed by using the equivalence-principle (EP) theorem. The objects in the different domains are not physically connected but need only be separated by a small distance, sufficient to permit the surface on which the equivalence principle is enforced to be located between them.

A modified EP inhomogeneous surface in which one or more faces are replaced by a conducting surface was investigated (see Fig. 1), although media other than conductors are possible. In this modification, the conducting surface can be extended beyond the size of the EP surface, for example a handset box for a mobile phone, where only the antenna part is within the EP surface. An Inverted F-Antenna (IFA) was chosen for evaluation purposes since it is a common mobile phone design. The antenna, including a finite ground plane, was modelled by using a standard FEM software package [5]. The EP surface boundary was chosen to reach to the edges of the finite ground plane representing the adjacent surface of the phone body (see Fig. 1) and then the size of the EP surface was reduced and the antenna performance was again predicted. Outside the FEM domain, the rest of the problem space was inserted in an FDTD region. The operating frequency was chosen as 1800 MHz: the antenna was excited by a magnetic frill. The FDTD cell size and the time step were 2.5mm and 3.375ps respectively. The FDTD PML (perfectly matched layer) was 6 cells wide.

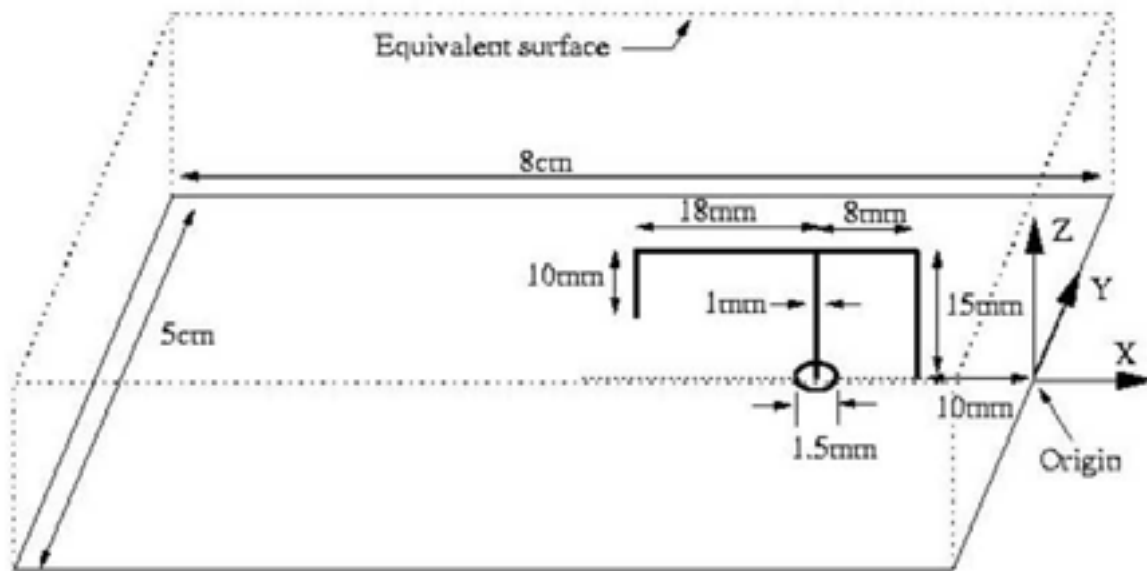


Fig. 1. Antenna structure with EP surfaces

The total field (for 1 watt input power) as seen 1cm underneath the centre of the ground plane, on a line parallel to the x-axis, was examined. A comparison with pure MoM [6] is shown in Fig. 2. The FDTD problem space dimension was 54 x 54 x 38 cells. The results show good agreement for all proposed equivalent surfaces.

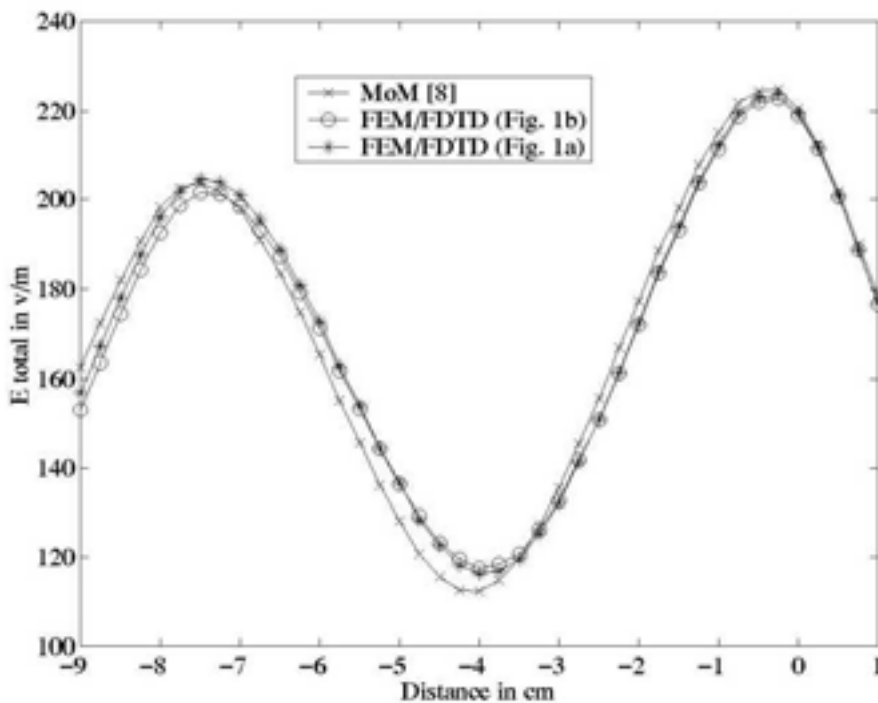


Fig. 2. The total field 1cm underneath the longitudinal centreline of the groundplane, using the hybrid method and a standard Method of Moments package for comparison. 'Figs 1a and 1b' refer to different sizes of the EP surface.

The method was validated with several canonical examples. In a bioelectromagnetic usage example, a simulated handset was placed close to a human head (Fig. 3). In this case, the handset was modelled with FEM and the head with FDTD, although the reverse is in principle possible, or a partial intersection of the EP surface with tissue could be arranged.

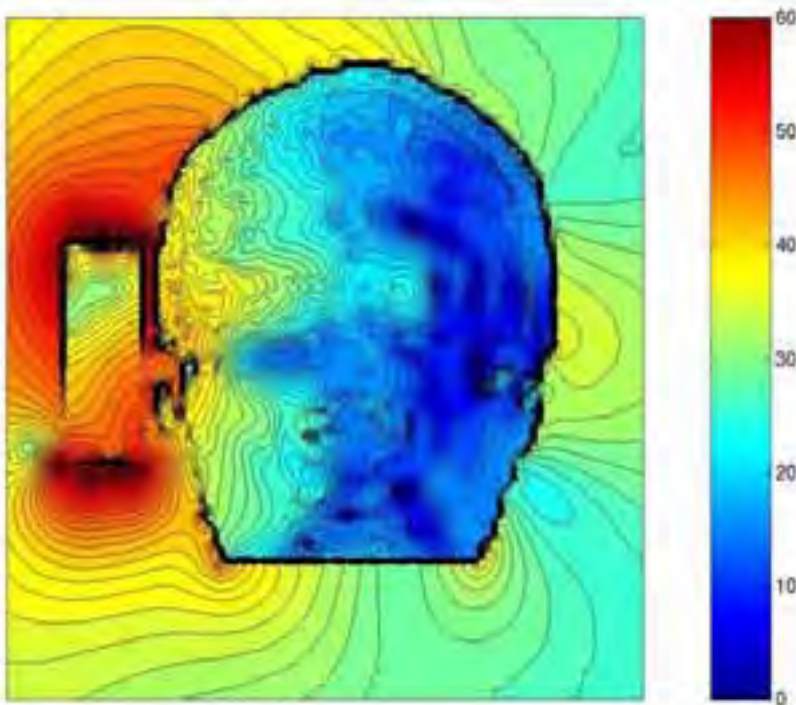


Fig. 3. SAR distribution over x-z plane for balanced antenna with dielectric substrate.

**CONCLUSIONS:** A hybridisation technique between the FEM and FDTD methods has been presented. An equivalence-principle surface, including a partially inhomogeneous surface, was successfully implemented through the boundary that coupled the two methods. A reduced-size EP surface has been presented and was found sufficient to predict the antenna performance with and without the presence of a nearby scatterer. This saved approximately 70% of the required memory locations of the field points between the two domains and also accelerated the updating boundary equations inside the FDTD method. The results are stable and show good agreement between the different techniques: the method gives increased flexibility for modelling of complex structures.

**REFERENCES:**

1. J. Jin, 'The Finite Element Method in Electromagnetics', New York: John Wiley & Sons Inc, 1993.
2. T. Rylander and A. Bondeson: 'Application of Stable FEM-FDTD Hybrid to Scattering Problems', IEEE Transactions on Antennas and Propagation, Vol. 50, No. 2, Feb. 2002, pp. 141-144.
3. R.B. Wu and T. Itoh, 'Hybrid finite-difference time-domain modeling of curved surfaces using tetrahedral edge elements', IEEE Trans. Antennas Propagat., vol. 45, pp. 1302–1309, Aug. 1997.
4. A. Monorchio and R. Mittra, 'A hybrid finite-element finite-difference time-domain (FE/FDTD) technique for solving complex electromagnetic problems', IEEE Microwave Guided Wave Lett., vol. 8, pp. 93–95, Feb. 1998.
5. Comsol AB, FEMLAB, Electromagnetic Software Version 3.0, Comsol Ltd., Jan. 2004.
6. Mangoud, M.A., Abd-Alhameed, R.A. and Excell, P.S.: 'Simulation of human interaction with mobile telephones using hybrid techniques over coupled domains', IEEE Trans. on Microwave Theory and Techniques, vol. 48, No. 11, Nov. 2000, pp. 2014-2021.

This work is supported by a studentship from the Government of Malaysia.

P-A-211

**EFFECTS OF POSTURE ON ENERGY ABSORPTION IN NORMAN, A HUMAN VOXEL MODEL.** R. P. Findlay, P. J. Dimbylow. NRPB, Chilton, Didcot, Oxfordshire, UK.

The purpose of this work is to investigate how a change in posture can affect the way the human body absorbs energy under isolated and grounded conditions when exposed to horizontally and vertically polarized electric fields. The finite difference time domain method was used to solve the coupled, time dependent Maxwell equations and calculate specific absorption rates (SARs) in the NRPB anatomically realistic voxel model of the human body, NORMAN (NORMALised MAN) in postures other than the standard, upright with arms by the side position. NORMAN is an anatomically realistic model comprising of approximately 9 million ~2mm voxels. This resolution allows us to determine the SAR value at a precise location within the model for a particular posture. Calculations were performed using plane wave irradiation at frequencies in the range of 10 MHz to 300 MHz, the results being presented in terms of whole body and local SAR values.

The magnitude of the whole body SAR resonant peak can be increased by up to 35% when the posture is changed from the standard position. Intensity plots of the power absorbed in each voxel gave a very accurate picture of the different regions in which energy is absorbed for a particular posture, frequency and electric field polarization.

**FAST LOCALIZATION OF CURRENT DIPOLES IN MEG USING A COMBINED SPHERE AND BRAIN-SHAPE MODEL AND AN ACCELERATED BOUNDARY ELEMENT METHOD.**

G. Lindenblatt<sup>1</sup>, H. Zhu<sup>1</sup>, S. He<sup>1,2</sup>. <sup>1</sup>Centre for Optical and Electromagnetic Research, Zhejiang Univ, Hangzhou, China, <sup>2</sup>Division of Electromagnetic Theory, Alfvén Laboratory, Royal Institute of Technology, Stockholm, Sweden.

**OBJECTIVE:**

In magnetoencephalography (MEG), the sphere model is known for its high computation speed, while the brain-shape model (or "realistic model") is used to gain high accurate results in inverse computations. We try to combine both advantages.

**PROCEDURE:**

The difference in the magnetic fields derived from the sphere model and a (single-layer) brain-shape model is calculated for many test positions of the dipole. We thus obtain a geometrical description of the relative difference between these two models. According to this description, we divide the brain into small difference areas (SDAs) where the relative difference is less than an acceptable threshold, and the large difference areas (LDAs) where the relative difference is larger than the threshold. If the trial dipole is inside a LDA, we choose the boundary element method (BEM) as the numerical optimisation method using the brain-shape model. The BEM is accelerated by using the potentials derived from the dipole located at the center of the LDA in an iterative algorithm. The faster sphere model is used if the dipole is inside a SDA.

**RESULTS:**

The subdivision into SDA and LDA can be simplified and assigned to anatomical structures, so that it can be transferred to any brain shape. The differences between the calculated positions of the dipoles using our combined model and the true dipole positions are comparable to those using the brain-shape model: both deliver high-accurate results. On the average, our new model is six times faster than the brain-shape model, gaining a speed close to that of the sphere model.

**IN SILICO BIOELECTROMAGNETICS.** J. C. Weaver, T. R. Gowrishankar, D. A. Stewart, A.T. Esser, Z. Vasilkoski, K. C. Smith. Harvard-MIT Division of Health Sciences and Technology, Massachusetts Institute of Technology, Cambridge, MA, USA.

**Introduction.** Quantitative models are equivalent to statements of hypotheses.<sup>1</sup> Our group has developed an initial capability for creating and solving biological system models that involve interactions with nonionizing electromagnetic fields and estimates of biochemical change. Interactions can range from environmental exposures at power line frequencies to telecommunication waveforms to conventional and supra-electroporation with potential medical applications. **Methods.** Our approach involves interactions on multiple spatial scales (e.g. molecules and membranes, cellular organelles, single cells, multiple irregular cells in close proximity, tissue level and whole body) and temporal scales of ns to hours.<sup>2-6</sup> The biological system models consist of a large number of interconnected local models. The purpose is estimating field-induced biochemical change, using local models that contain candidate

biophysical mechanisms that couple the field to ongoing biochemical processes. *In silico* (computer-based) assessments can provide rapid, approximate information for large numbers of exposures with different magnitudes and waveforms, a capability partly analogous to high throughput screening in biotechnology. **Results.** We have achieved an initial modeling/screening capability that is applicable at the tissue, multicellular, cellular and subcellular levels. Solutions to a biological system model: (1) describe the microscopic field redistribution due to the applied field (microdosimetry), and (2) estimate the biochemical change due to biophysical mechanisms assigned within the system model. This *in silico* approach can aid the design and interpretation of experiments involving biological effects of nonionizing electromagnetic fields ranging from dc to microwave frequencies, and can also provide preliminary exposure assessment for many different waveforms. The estimated biochemical change due to a particular electromagnetic field exposure is based on known biophysical mechanisms (presently heating, voltage-gated channels and electroporation; others can be added). This allows competing influences to also be considered quantitatively, thereby providing initial testing of a hypothesis that a particular biophysical mechanism might cause a biological effect.<sup>7</sup> **Acknowledgments.** Supported by NIH grant RO1-GM63857, a AFOSR/DOD MURI grant on Subcellular Responses to Narrowband and Wideband Radio Frequency Radiation, and an AFOSR subcontract from Trinity Univ.

- [1] B. M. Slepchenko, J. C. Schaff, I. Macara, and L. M. Loew. Quantitative cell biology with the Virtual Cell. *Trends Cell Biol.*, 13:570-576, 2003.
- [2] T. R. Gowrishankar and J. C. Weaver. An approach to electrical modeling of single and multiple cells. *Proc. Nat. Acad. Sci.*, 100:3203-3208, 2003.
- [3] D. A. Stewart, T. R. Gowrishankar, and J. C. Weaver. Transport lattice approach to describing cell electroporation: use of a local asymptotic model. *IEEE Transactions on Plasma Science*, 32:1696-1708, 2004.
- [4] T. R. Gowrishankar, C. Stewart, and J. C. Weaver. Electroporation of a multicellular system: asymptotic model analysis. In *Proceedings of the 26th Annual International Conference of the IEEE EMBS 2004*, pages 5444-5446, San Francisco, 2004.
- [5] T. R. Gowrishankar, Donald A. Stewart, Gregory T. Martin, and James C. Weaver. Transport lattice models of heat transport in skin with spatially heterogeneous, temperature-dependent perfusion. *Biomed. Eng. Online*, 3:42, 2004.
- [6] D. A. Stewart, T. R. Gowrishankar, G. T. Martin, and J. C. Weaver. Skin heating and damage by millimeter waves: Theory based on a skin model coupled to a whole body model. (in preparation).
- [7] T. E. Vaughan and J. C. Weaver. Molecular change signal-to-noise criteria for interpreting experiments involving exposure of biological systems to weakly interacting electromagnetic fields. *Bioelectromagnetics* (in press).

**DIELECTRIC MODELS OF BIOLOGICAL CELLS AND QUASI-STATIC EM ANALYSIS AT RADIO AND MICROWAVE FREQUENCIES: A MICRODOSIMETRIC STUDY.** C. Merla, M. Liberti, G. d'Inzeo. ICEmB @ Dept of Electronic Engineering, "La Sapienza" Univ of Rome, Italy.

**OBJECTIVE:** In the recent past the authors [1] have stressed the key role played by microdosimetric studies in order to properly relate the specific electromagnetic (EM) exposure to the possible biological effects. Recently the same item has been emphasized in the 2003 WHO Research Agenda for Radio Frequency Field [2]. To achieve such knowledge it is necessary first to identify dielectric models of microscopic substructures constituting tissues and cells and then to properly solve the EM problem. In this paper the dielectric cell model set up by the authors [3] will be used for the EM field solution. A suitable method to face the EM problem on a single cell as well as for an assemble of them is proposed by a quasi-static approach solving the Laplace equation on the structures. This approach has been previously characterized and its limit of applicability and accuracy has been tested [4].

**METHODS:** The estimation of dielectric parameters of cell microscopic substructures like membrane and bound water layers has been obtained by previous dielectric constant measurements on liposomes and reverse micelles solution [4]. This measure, conducted in frequency domain, is realized with a vector network analyzer (VNA) connected to a modified coaxial cable. The experimental procedure includes an effective calibration with three different standard liquids to de-embed the cable mismatch due to the connectors and parasitic effects [5]. The model parameter estimation is performed by an inverse application of the Effective Medium Theory (EMT). This is a general theory based on Laplace equation applicable in a quasi-static condition [6]. To obtain the EM field distribution on a single cell we use the dielectric parameters obtained by the mentioned procedure [3]. The EM problem to solve is characterized by the assumption  $\lambda \gg d$  where  $\lambda$  is the EM field wavelength and  $d$  the mean cell dimension ( $\mu\text{m}$ ), the previous assumption is verified for a maximum frequency of 100 GHz. Until this value quasi-static conditions are guaranteed: the EM waves present a constant phase in all points of the cell with an error of about 5% respect to a complete EM field solution implemented by Mie Scattering Theory [4].

**RESULTS** The shape of the cell is chosen as a five layered sphere (Figure 1), and its geometrical parameters are reported in Table 1. In Table 2 we briefly report the estimated parameters for the membrane and the bound water layers obtained with the previously outlined methodology. We calculated the EM field distribution on such single cell model at 2.450 GHz. We compared our results (Figure 2) with the EM field distribution achieved in [7] by means of Mie Theory at the same frequency. We have already shown in [4] the good accordance between Mie theory and Laplace equation results; therefore the strongly different electric field values of Figure 2 are due to the differences in the dielectric cell model adopted. A comparison between the two models at the operating frequency (2.450 GHz) is summarized in Table 3. Our dielectric parameters (Table 2) take into account the membrane relaxation phenomena, as suggested in [8] and the bound water relaxation with a Cole&Cole behaviour [9]. Moreover the EM values proposed (Figure 2) are in accordance with the ones obtained by Munoz et al. [10] with a numerical FE method for different cell shapes; these results stress the reliability of Laplace quasi-static solution on a simple spherical geometry.

**CONCLUSIONS:** An EM field distribution on a single cell is proposed solving the Laplace quasi-static equation. We showed the fundamental role played by an accurate dielectric model on the EM field characterization. The accuracy of the EM field distributions on a single cell depends not as much on the kind of the EM field solution and the morphological choice adopted (i.e. spherical, cylindrical, elliptical), suggesting that numerical methods could be effective only if more realistic structures like membrane proteins or cytoplasmatic organelles are considered.

## References

- [1] F. Apollonio, M. Liberti, G. d'Inzeo, L. Tarricone, IEEE Trans. Microwave Theory and Techniques, vol. 48, pp. 2082-2093, 2000
- [2] WHO Research Agenda for Radio Frequency Fields: Dosimetry [www.who.int/peh-emf/research/rf03/en/index5.html](http://www.who.int/peh-emf/research/rf03/en/index5.html), on line.
- [3] C. Merla, M. Liberti, A. Ramundo Orlando, F. Apollonio, G. D'Inzeo, 16th International Zurich Symposium on electromagnetic compatibility, Topical meeting on biomedical EMC Abstract Book, 2005
- [4] M. Rogante, M. Liberti, M. Cavagnaro, G. D'Inzeo, BEMS 25th Annual Meeting Abstract Book 2003, Wailea Maui Hawaii.
- [5] D. Fioretto, G. Onori, J. Chem. Phys., vol. 99, pp. 8115-8119, 1993
- [6] W.M. Merrill et al. IEEE Trans. Antennas Propagation, vol. 47, pp. 142-148, 1999
- [7] L. Liu, S. F. Cleary Bioelectromagnetics, vol. 16, pp. 160-171, 1995
- [8] T. Kotnik et al. Bioelectromagnetics, vol. 21, pp. 385, 2000
- [9] M. Freda, G. Onori, A. Paciaroni, A. Santucci, J. of Non-Crystalline Solids, vol. 307, pp 874-877, 2002
- [10] S. Munoz et al. Physics in Medicine and Biology, vol. 48, pp. 1649-1659, 2003

This work has been supported by the European Union, V Framework Program under the RAMP2001 Project.

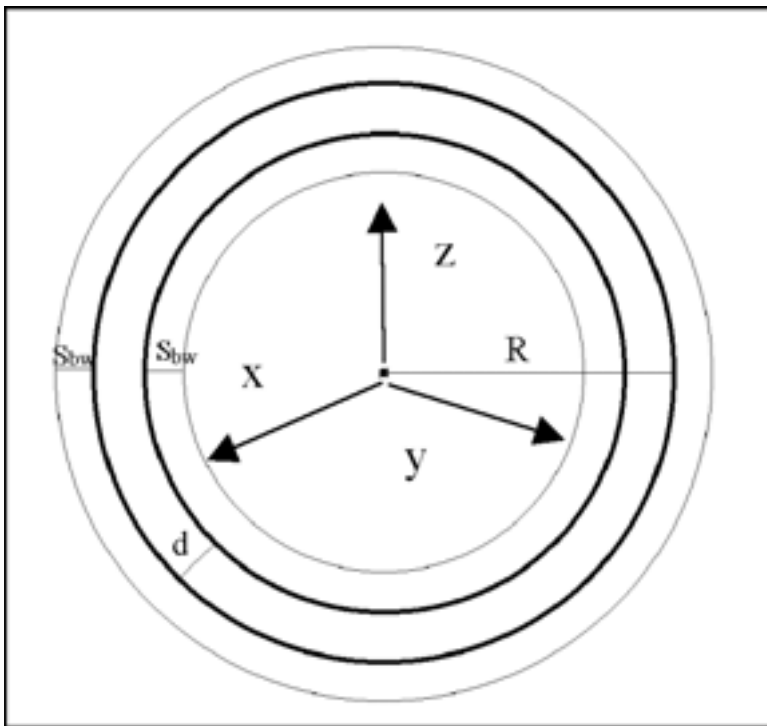


Figure 1: The cell model: a five layered sphere composed by internal and external bound water, cytoplasmic membrane, cytoplasm and extracellular medium

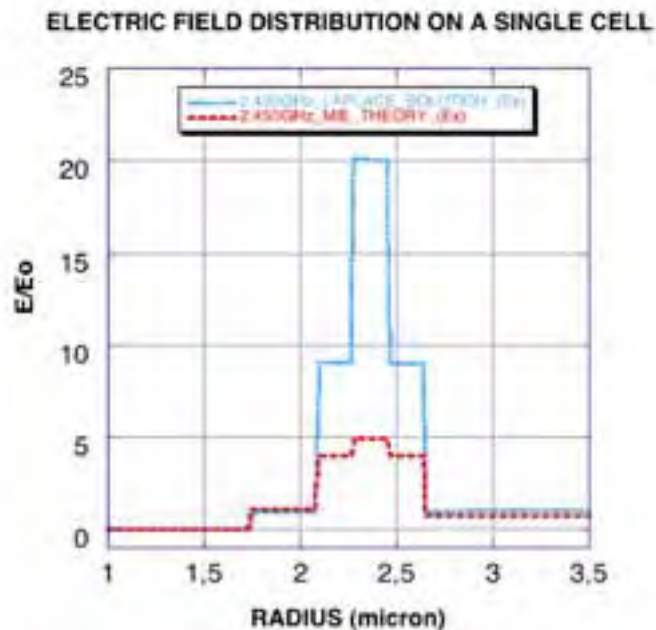


Figure 2: Electric field distribution on a single cell at 2,450 GHz, comparison between Laplace equation and Mie Scattering Theory

P-A-226

**ASSESSMENT OF EVERY DAY EXTREMELY LOW FREQUENCY (ELF) ELECTROMAGNETICS FIELDS (50-60HZ) EXPOSURE° : WHICH METRICS ?** A. Verrier<sup>1</sup>, I. Magne<sup>2</sup>, M. Souques<sup>3</sup>, J. Lambroz<sup>3</sup>. <sup>1</sup>EDF SGM, PARIS FRANCE, <sup>2</sup>RTE département des matieres electriques, <sup>3</sup>EDF SEM, PARIS FRANCE.

Because electricity is encountered at every moment of the day, at home with household appliances, or in every type of transportation, people are most of the time exposed to extremely low frequency (ELF) electromagnetic fields (50-60 Hz) in a various way. Due to a lack of knowledge about the biological mechanisms of 50 Hz magnetic fields, studies seeking to identify health effects of exposure use central tendency metrics. The objective of our study is to provide better information about these exposure measurements from three categories of metrics.

We calculated metrics of exposure measurements from data series (79 every day exposed subjects), made up approximately 20,000 recordings of magnetic fields, measured every 30 seconds for 7 days with an EDMEX II dosimeter. These indicators were divided into three categories : central tendency metrics, dispersion metrics and variability metrics.

We use Principal Component Analysis, a multidimensional technique to examine the relations between different exposure metrics for a group of subjects.

PCA enabled us to identify from the foreground 71.7% of the variance. The first component (42.7%) was characterized by central tendency; the second (29.0%) was composed of dispersion characteristics. The third component (17.2%) was composed of variability characteristics.

This study confirm the need to improve exposure measurements by using at least two dimensions intensity and dispersion.

**EFFECTS OF ELF MAGNETIC FIELDS ON SIGNAL TRANSDUCTION FOR THE DIFFERENTIATION OF OSTEOLAST-LIKE CELLS.** H. Yamaguchi<sup>1</sup>, K. Hosokawa<sup>2</sup>, H. Shichijo<sup>3</sup>, M. Kitamura<sup>2</sup>, A. Soda<sup>2</sup>, T. Ikehara<sup>2</sup>, Y. Kinouchi<sup>3</sup>, K. Yoshizaki<sup>2</sup>, H. Miyamoto<sup>2</sup>, K. Aizawa<sup>4</sup>, <sup>1</sup>Dept of Environmental Physiology, Faculty of Human Life Sciences, Tokushima Bunri Univ, Tokushima, Japan, <sup>2</sup>Dept of Molecular & Cellular Physiology, School of Medicine, <sup>3</sup>Dept of Electrical & Electronic Engineering, Faculty of Engineering, The Univ of Tokushima, Japan, <sup>4</sup>Dept of Physiology, Tokyo Medical College, Tokyo, Japan.

**OBJECTIVE:** The objective of this study is to examine the physiological effects of exposure to ELF magnetic fields on regulation of differentiation in cultured osteoblast-like cells(MC3T3-E1). We have obtained a few preliminary results that the treatment with some regulators of differentiation and the exposure to ELF magnetic fields for these resulted in same effects on the acceleration of differentiation. In this study, we tried a variety of approaches to reveal more about the effects of exposure to the magnetic fields.

**MATERIALS AND METHODS:** Osteoblast-like cells(MC3T3-E1) were cultured with alpha-modified minimum essential medium (H. Miyamoto et al. 1976) supplemented by 10% fetal bovine serum in plastic culture dish of 35mm diameter. The culture dishes were placed in two special incubators to keep the temperature of the cultures constant (37.0C). Sinusoidal(60Hz) magnetic fields were produced by two coils and their rms values were about 3.0 mT. Induced current density in the medium about 10 mA/m<sup>2</sup> in average. Duration of exposing to magnetic fields was 72 hours for 3 days cultures, respectively. Cultures were maintained to grow with or without 10 mM beta-glycerophosphate and Vitamin C of 50 ug/ml as inducer of of the differentiation. And then, IGF(20 ng/ml) and NGF(2 ng/ml) were add to fairly differentiated cells. Intracellular alkaline phosphatase(ALP) activities as the indicator of the differentiation of these osteoblasts in vitro were measured by calorimetric assay kit(WAKO Ltd, Japan). Collagen and non-collagen protein contents in the culture were measured microscopically by multispectral imaging method.

**RESULTS AND DISCUSSION:** In exposure to ELF magnetic fields for 3 days, both collagen and non – collagen protein content increased with exposure time in the cells peripheral regions of culture of culture dish than that at central regions of same dish. The exposure increased in collagen contents at the peripheral cells for 11 days. And also, the additive effects of the exposure and IGF treatment were observed. By the time in which magnetic fields and several inhibitors of MAP kinase as LY294002 or PD worked in the cell, the result of respectively differing was obtained.

**Poster Session B**  
**9:15 - 11:15 am, O'Reilly Hall**  
**9:00 – 9:15, Highlights by Ferdinando Bersani**

**Clinical devices**

P-B-2 STUDENT

**MORPHOMETRIC RESPONSE OF CARASSIUS AURATUS ON WEAK ELF MAGNETIC FIELD.** V. V. Alexandrov, L. V. Dubovoy, V. A. Efremov, O. Bogodist. Saint Petersburg State Polytechnic Univ, Russia.

**INTRODUCTION**

The present work has been realized with two scientific workgroups of Saint-Petersburg Polytechnical Univ: prof.V.V.Alexandrov's group from Dept of "Ecological Bases of Nature Management" & prof L.V.Dubovoy's group from Dept of "Physical Electronics".

A strong biological effect of ELF magnetic field action are well-known. The most arduous task at all magnetobiological investigations is the selection of optimal field parameters for maximal response of biological system. It was detected by scientific workgroup of professor Dubovoy approximately 10 years ago that magnetic fields with some parameters closed to natural geomagnetic is highly effective for therapy of wide spectrum of human diseases. Videlicet the amplitude of magnetic induction ranged between 30 microTesla and 100 microTesla; frequencies were in discrete row of values corresponding to set of geomagnetic micropulsations and set of "Ionosphere-Earth" resonator modes. Furthermore magnetic field was spatially homogeneous with index of heterogeneity approximately equal to 4%.

**MATERIALS AND METHODS**

In present work we used just foregoing approach to salvation of problem of optimal parameters selection. We chose Carassius Auratus as an object for magnetobiological action. Group of fishes was homogenous by sizes and ages (3 years old). A double-blind method was used. Conditions of maintenance and feeding were the same in control and test groups. Background natural magnetic field was about 37 microTesla; aeration was extremely hard in both groups, i.e. fishes suffered hypomagnetic environment and anoxia.

We put test fishes group into artificial magnetic field. Parameters of dipole spatially homogeneous sinusoidal uninterrupted magnetic field were following: 70 microTesla, 8Hz. Frequency equal to 8Hz corresponds to first mode of "Ionosphere-Earth" resonator. All action continued 2 weeks and consisted of 10 experiments at 13p.m. local time every day for 5 days at week. Duration of each experiment was 15 minutes. Thus we put test fishes under action of 3 strong stress factors of environment: anoxia hypomagnetic environment and artificial magnetic field. At the same time control fishes suffered just 2 factors: anoxia and hypomagnetic environment.

**RESULTS & DISCUSSIONS**

Two indexes of morphometric changes were observed during all time of experiment.

1. Fulton K-index of control group was stable for 7 experiments but decreased noticeably after eighth one. In our opinion most probable cause of such dynamics is anoxia-induced emaciation. At the same

time K-index of test group were stable during all time of experiment. It is possible that magnetic field with parameters closed to natural supports homeostasis, i.e. it compensates the anoxia.

2. So-called Kh-index (ratio of body length to body width) monotonically increased at control group but also monotonically decreased at the same time at test group. Hence Kh-index may be considered as some numerical parameter characterized changes of quality of fish life under magnetic field action.

## CONCLUSION

So we can conclude that findings indicate presence of some effect of magnetobiological action of field with parameters based on natural geomagnetics. However the task of selection of optimal field parameters remains open as it requires consideration of whole values spectrum.

P-B-5

**VERSION 5 PORTABLE CNP GENERATOR.** L. D. Keenlside, A. W. Thomas, F. S. Prato. Bioelectromagnetics, Imaging Program, Lawson Health Research Institute, Dept. of Nuclear Medicine, St. Joseph's Health Care, London, Ontario, Canada.

**Introduction:** It has been demonstrated that a specific pulsed magnetic field, having a number of variable design features, can affect a number of physiological/behavioural end points as diverse as nociception and standing balance [1,2]. However, these results have been achieved using large and expensive whole body exposure systems requiring significant system components including programmable computers, digital to analogue converters and large audio amplifiers to generate the pulse waveform. For this technology to have an impact in medical treatment of such conditions as pain or depression the exposure system must be both affordable and sufficiently portable so it can be used as people go about their lives.

**Objectives:** To continue development of a portable and programmable waveform generator which can deliver an arbitrarily pulsed magnetic field with the following criteria: a) simple enough for a patient to operate and ability to monitor patient compliance; b) dependent only on battery or AC adapter; c) capable of reproducing a sophisticated waveform such as the complex neuroelectrical pulse (Cnp) detailed in US Patent #6,234,953 [1]; d) contained within a compact case including a liquid crystal display; e) that multiple waveforms can be updated by patients with little or no technical skill using a standard laptop or desktop computer; f) have sufficient power output to deliver, without appreciable waveform degradation, a minimum of 200  $\mu$ T (peak) magnetic field to any part of the brain using two 3 cm diameter coils and a minimum of 400  $\mu$ T (peak) magnetic field 1cm from a single 3 cm diameter coil for relatively shallow tissue targets. A clinical pilot trial has been completed (see presentation by Thomas et al).

**Methods:** The objectives were achieved by incorporating into a single 290g box 1.2" x 3.6" x 7", the following microprocessor (MPU) controlled components: a) flash memory (internal to MPU) containing main program; b) EEPROM (electrically erasable programmable read-only memory) (internal to MPU) containing preset values and patient log data during power down so that no resetting is required to begin device use; c) dual EEPROMs which contain two pattern data sets; d) a Real Time Clock to date and time stamp patient compliance logs, e) a 12-bit analogue to digital converter (ADC); and f) 2x16 character LCD. The unit is powered by four 'AA' alkaline batteries or AC adapter and incorporates switching regulators for efficient battery operation, providing 15 hours of use per set of batteries.

The unit operates by converting the digitally stored waveform to bipolar voltage signals as data is transferred directly from the EEPROM to the ADC. This reduces processing time and provides signals which faithfully represent the waveform characteristics within a frequency band of 7 kHz. The output circuit is a dual channel bipolar driver with a phase switch to drive a variety of coils. A communication interface permits connection to a computer for verification log uploads, waveform downloads, schedule download, adjustment to specific waveform parameters such as those associated with our Cnp, and choice of active or sham patterns.

#### References:

1. Shupak N., Hensel J., Prato F.S., Thomas A.W.(2004) Effects of exposure to a specific pulsed magnetic field on thermal sensory thresholds in humans. *Neurosci Letts* 363(2):157-62.
2. Thomas A.W., Drost D.J., and Prato F.S. (2001). Human subjects exposed to a specific pulsed (200  $\mu$ T) magnetic field: Effects on normal standing balance. *Neuroscience Letters*, 297, 121-124.

**Acknowledgements:** This study was funded by St. Joseph's Health Care (SJHC - London) Foundation; Natural Sciences and Engineering Research Council of Canada (NSERC); Canadian Institutes of Health Research (CIHR); Canada Foundation for Innovation (CFI); and the Ontario Innovation Trust (OIT).

#### Dosimetry

P-B-8 STUDENT
---------------

**DOSIMETRIC ANALYSIS OF 1800-MHZ AND 2.45-GHZ IN VIVO AND IN VITRO EXPOSURE SETUP.** A. Collin A<sup>1</sup>, P. Leveque<sup>1</sup>, A. Perrin<sup>2</sup>, G. Testilier<sup>2</sup>. <sup>1</sup>Institut de Recherche en Communications Optiques et Micro-ondes, Limoges, France, <sup>2</sup>Centre de Recherche du Service de Santé des Armées, La Tronche, France.

**INTRODUCTION:** This paper describes a dosimetric analysis of specific in vivo and in vitro exposure setup. The in vivo one is used to expose animals like rats or mice, in the whole body, at 1800-MHz, and 2.45-GHz. The animal can move easily in the incubator (so no stress can interfere with the analysis of the brain by biologists). The in vitro exposure setup is to irradiate cells in petri dishes located on a very special incubator in rotation to homogenize the electric field. Both setups are exposed to a antenna horn, and the emission can be considered in plane wave, as the animal or the petri dishes are in a far field.

**OBJECTIVE:** The aim of our work is to study the dosimetry of an in vivo exposure setup and a thermostated in vitro exposure setup.

**METHODS:** The in vivo exposure setup consists of a box made of plexiglas ( $\epsilon_r = 2.6$ ) whose dimensions are 30\*30\*45 cm, the thickness of the walls is 1 cm. The rat is on bars, located at 3 cm from the bottom of the box. This box has been modelled using the FDTD method, in order to know electromagnetic field levels and distribution in the box, with a plane wave exposition. To simulate the rat, we have used a digital rat model made by the Brooks Air Force Base. The model has been placed in different location in order to model the fact that the rat can move in this box. The FDTD method was also used to calculate the SAR distribution in the rat body. The SAR was

obtained from the electric-field value using the formula  $SAR = \sigma |E|^2 / (2\rho)$  en W/kg, where  $\sigma$  is the conductivity in S/m,  $E$  is the electric field in V/m and  $\rho$  the density in kg/m<sup>3</sup>. The in vitro exposure setup is mostly composed of plexiglas. However, this system is more complicated to model because of the rotation system under the incubator, and above all, the system is composed of PVC blades ( $\epsilon_r = 5$ ), plexiglas ( $\epsilon_r = 2.6$ ), glass balls ( $\epsilon_r = 5$ ), water pipe (water :  $\epsilon_r = 75$ ), and the whole system is covered by a plexiglas blade.

The thermostated system is also modelled with the FDTD method, and the SAR distribution in the petri dishes is calculated with the same method as for that rat.

**RESULTS:** We have simulated the box to compare E-fields with the experimental measures of E fields into the box, and know the E-fields levels in the rat location. With the model of the box, we can study the SAR distribution in the modelled rat. In the case shown figure 1, we can calculate a mean SAR equivalent to 0.043 W/kg (for  $P_{inc} = 1 \text{ W/m}^2$ ) in the whole body. We also have considered the influence of the animal position in the box to obtain a mean SAR in the whole body and in the head, whatever the rat position. We will also be careful with the metallic probe which is located in the brain of the rat.

The incubator for in vitro experiments is much more complicated to simulate. The multi-blade structure, with several materials and characteristics favours a lot of interactions. We can use them to get a better coupling, and obtain high SAR levels with not too much source power. Instead of simulating the horn antenna with a plane wave, we will have more precise results (E field levels and SAR distribution), using a model of the horn antenna to simulate the exposure setup. We have to study these exposure setup at the frequency of 2.45 GHz

**CONCLUSION:** These results in the in vivo case indicate the mean SAR, in the whole rat's body and in its head in its modelled box. In the in vitro experiment, we can also calculate the mean SAR in the petri dishes, and the best location for the dishes to have a maximum mean SAR.

P-B-11

**SPECIFIC ABSORPTION RATES IN A FLAT ABSORBING PHANTOM IN THE NEAR-FIELD OF DIPOLE ANTENNAS.** Q. Balzano<sup>1</sup>, M. Kanda<sup>2</sup>, C. C. Davis<sup>1</sup>. <sup>1</sup>Dept of Electrical and Computer Engineering, Univ of Maryland, College Park, MD, <sup>2</sup>Motorola Inc. Corporate Research Laboratory, Plantation, FL.

**INTRODUCTION:** National and international regulatory bodies require compliance testing procedures for hand-held wireless telephones. The IEEE has promulgated a compliance verification procedure (IEEE 1528) [1] to be followed in verifying whether a wireless phone is compliant with international standards. Manufacturers are required to assess the maximum near-field exposures that phones might produce in the head of a user. A recent intercomparison of the testing procedure has involved the cooperation of 15 government and industrial laboratories. These laboratories measured the 1cm<sup>3</sup> and 10cm<sup>3</sup> cubic volume averaged specific absorption rates (SARs) in a flat phantom filled with a standardized lossy dielectric fluid. The phantom absorber was placed in the near field of a custom dipole antenna.

**OBJECTIVE:** To support this research we have carried out a detailed analysis of the SAR distributions produced in the flat phantom by the antennas used in the international inter-comparison. The relatively

simple geometry allows an analytical description of the fields, and permits a precise comparison between experimental and theoretical field and SAR spatial distributions. Most other computations of this kind for absorbing objects in the near field of wireless phones or their models have been carried out by finite difference time domain techniques (FDTD). Our analytical approach allows the parametric variation of field and SAR to be examined in a straightforward way.

**METHODS:** The analytical method consists in expressing the fields emanating from the dipole as a superposition of a continuous spectrum of traveling and evanescent plane waves [2]. The plane waves are evanescent or propagating away from the antenna in the free half space, the waves are attenuating in the tissue-simulating liquid and stationary in the thin, lossless phantom shell and in the space between it and the dipole. The current on the antenna is represented by a discrete spectrum of orthogonal sinusoidal harmonics, matching the requirement of zero current at the tips of the antenna. Enforcing the boundary conditions of continuity of the tangential electric and magnetic fields at various dielectric interfaces, and the zeroing of the tangential E-field on the antenna yields the amplitude of the continuous spectrum of plane waves and of the discrete current harmonics.

**RESULTS:** We have computed the  $1\text{cm}^3$  and  $10\text{cm}^3$  volume-averaged SARs for cubic and maximum SAR volumes at 900MHz and 1800MHz, and corresponding SAR spatial patterns. Our theoretical calculations are in very good agreement with experimental results. The  $1\text{cm}^3$  and  $10\text{cm}^3$  average SARs in shapes giving maximum SARs are about 35% larger, and 50% larger, respectively, compared to cubic volumes.

**DISCUSSION:** Our results show that for a simple geometry of antenna and nearby absorbing phantom, theoretical SAR values and profiles are in close agreement with experiment. This agreement verifies that experimental and theoretical SAR determinations can be consistent, and provides further assurance of the reliability of SAR wireless phone certification procedures.

#### REFERENCE

1. IEEE Standard 1528<sup>TM</sup>-2003. IEEE Recommended Practice for Determining the Peak Spatial-Average Specific Absorption Rate (SAR) in the Human Head from Wireless Communications Devices: Measurement Techniques. IEEE SCC 34, IEEE, New York, 2003.
2. LB Felsen, N Marcuvitz . Radiation and Scattering of Waves, Prentice-Hall, Inc, Englewood Cliffs, NJ, 1969, Section 5.1-5.9, pp 442-629.

This work was supported by the Mobile Manufacturers Forum (MMF).

P-B-14

**NEW CONCEPT FOR LOCAL BRAIN 2-GHZ EXPOSURE OF RODENTS IN VIVO.** A. Bitz<sup>1</sup>, S. Bloch<sup>1</sup>, V. Hansen<sup>1</sup>, D. Krause-Finkeldey<sup>2</sup>, K. Ladage<sup>2</sup>, T. Reinhardt<sup>1</sup>, J. Streckert<sup>1</sup>. <sup>1</sup>Chair of Electromagnetic Theory, Univ of Wuppertal, Germany, <sup>2</sup>Institute of Anatomy, Ruhr-Univ Bochum, Germany.

**INTRODUCTION:** One of the biological systems that is often suspected to be sensitive to electromagnetic exposure is the blood-brain barrier. There are controversially discussed results from several in vitro and in vivo investigations. In this project effects of microwave exposure (UMTS modulation) on the pattern of mRNA / protein expression in rats is studied. To do so partial brain exposure in vivo is necessary, since the blood compartment and the components of the BBB vessel wall are a functional entity and should be maintained during experiments, whereas none of the in vitro models used so far acquires the complex interaction of structural BBB components. The contribution describes the exposure concept for the running experiments.

**OBJECTIVES:** Several restrained rats shall be exposed simultaneously for at least 2 hours, whereby in sequentially performed tests a blinded scrambling of different applied specific absorption rates (0 W/kg, 0.1 SAR<sub>max</sub>, and SAR<sub>max</sub>) shall be provided by the computerized experimental protocol. The exposure of the rats' brains shall be as localized and as uniform as possible, but with SAR<sub>max</sub> not exceeding the thermal limit which is acquired in a pilot study. The stability of the exposure field and therefore also the rf shielding of the set-up is another point of importance.

**METHODS AND RESULTS:** For the rf exposure of a number of animals an approved concept is to arrange the subjects on a circle around a common source, e.g. to use a carousel [1] or a radial waveguide [2] arrangement, and to align the snouts towards the feed. For the case of investigations of BBB, however, such a concept has been criticized by experts [3], arguing that the sensitive sensors around the rodents' snouts could be overexposed thus masking the expected small effects from the brain. Another concept which avoids the latter is to place a loop antenna directly onto the head of a restrained rat [4]. The use of such an open structure, yet, is disadvantageous if multiple animals must be exposed, because of electromagnetic coupling between adjacent antennas and due to the rising complexity of the feeding network. In order to overcome these problems we modified the concept of the flat radial waveguide and constructed a spherical TEM waveguide [5] with a coaxial feed at the tip and the exposure field leaking from the rim. Immediately below the rim the restrainers with the animals are located. A specific inner ridge structure of the waveguide assures the lateral concentration of the field to the brain region and a decoupling of the exposure field of neighbouring animals. For a diameter of the ground plane of 1m a number of c. 20 rats could be exposed at a time. In this contribution results for a smaller set-up with 6 restrainers are shown. The detailed construction of the set-up, distribution of electromagnetic fields in the waveguide, SAR values in the rat's head, stability of the exposure and needed power will be discussed in the talk.

The authors thank Drs. G. Friedrich and F. Gollnick from Forschungsgemeinschaft Funk, Germany, for initialising and scientifically supporting this project.

#### REFERENCES:

- [1] Burkhardt, M., Spinelli, Y., Kuster, N.: Exposure setup to test effects of wireless communications systems on the CNS. *Health Physics*, vol. 73, pp. 770-778, 1997.
- [2] Hansen, V. W., Bitz, A. K., Streckert, J. R.: RF exposure of biological systems in radial waveguides. *IEEE Trans. EMC*, vol. 41, no. 4, pp. 487-493, 1999.
- [3] Workshop "The Blood-Brain-Barrier - Can it be influenced by RF field interactions?", Forschungsgemeinschaft Funk/COST 281, Reisingburg, Gemany, November 2003.
- [4] Leveque, P., Dale, C., Veyret, B., Wiart, J.: Dosimetric analysis of a 900-MHz rat head exposure system. *IEEE Trans. MTT*, vol. 52, no. 8, pp. 2076-2083, 2004.
- [5] Hansen, V., Streckert, J.: Waves in GTEM cells - A combined analytical - numerical approach. 17th Int. Wroclaw Symp. and Exhibition on Electromagnetic Compatibility, Wroclaw, 29.6. - 1.7.2004, 435-439.

P-B-17 STUDENT
----------------

**COMPARISON STUDY OF WHEEL-LIKE MOUSE EXPOSURE SYSTEMS AT 900MHZ.** S. Ebert, V. Berdiñas Torres, J. Fröhlich, N. Kuster. IT'IS Foundation, Swiss Federal Institute of Technology (ETH), Zurich, Switzerland.

**INTRODUCTION:** The so-called Ferris-Wheel exposure setup for mice has been used in several in vivo

risk assessment studies at the mobile communication frequency bands 900MHz and 1800MHz. This setup is a cylindrical cavity consisting of parallel circular plates shorted around the perimeter and fed at the center by a monopole or dipole antenna emitting a cylindrical TEM wave. Plastic restrainer tubes allow the insertion and equidistant positioning from the antenna of the mice, with the electric field parallel to the body axis.

**OBJECTIVE:** The objective of this study is the dosimetric comparison of three 900MHz Ferris-Wheel exposure setups used in different studies:

(A) Motorola M-40 wheel enables the exposure of up to 40 mice and was developed in 1999. This exposure setup was used in Adelaide, South Australia, as part of the National Health and Medical Research Council (NHMRC) Electromagnetic Energy (EME) Program [1].

(B) PERFORM A M-65 wheel enables the exposure of up to 65 mice and was developed by IT'IS in 2001. The setup was used at Fraunhofer ITEM (Germany) and RBM (Italy) as part of the PERFORM A program of the Fifth Framework European Union Program.

(C) Mini Wheel M-8 developed by IT'IS in 2003 enables the exposure of up to 8 mice and is still in use at the NRPB (Great Britain) within the PERFROM B project of the Fifth Framework European Union Program.

**METHOD AND RESULTS:** The setups were thoroughly examined using numerical and experimental dosimetric methods. The following performance parameters were examined:

- uniformity: simulations with high resolution numerical models.
- SAR efficiency: Due to the cavity design the exposure systems efficiently dissipate up to 80% of the incident power into the mice. RF power leakages from the cavity are very low.
- SAR uncertainty: four different mouse dummy sizes (17ml, 31ml, 37ml, 46ml) were used to characterize the behavior under various loading scenarios to simulated lifetime changes in long-term studies.
- loading efficiency: space requirements for amount of animals exposed.
- provision of exposure and environmental control: field/power controlled, monitoring parameters, handling.

The Ferris-Wheel setup is simple and can be easily reproduced and manufactured. However, it has the disadvantage of any multi-mode setup. Higher modes can be excited by the smallest asymmetries. This is particularly true for these Ferris-Wheels, since the Q of the cavity is high (small absorbing cross-section). Instant SAR variations of larger than 10dB have been measured. Measures such as lowering the Q value or reducing the interaction between animals or higher-mode stirrers can considerably improve the performance of this kind of setup. It must also be noted that the inter-animal variation of the averaged exposure over lifetime can be kept low by following a strict rotational schema in the exposure protocol.

#### ACKNOWLEDGEMENTS:

This study was supported by the Mobile Manufacturers Forum (MMF), Bruxelles.

#### REFERENCES:

- [1] Utteridge TD, et. al. 2002, "Long-Term Exposure of Em- Pim1 Transgenic Mice to 898.4 MHz Microwaves does not Increase Lymphoma Incidence", *Radiation Research*, 158, 357–364.
- [2] Q. Balzano, C. K., et al. 2000, "An efficient RF exposure system with precise whole-body average SAR determination for in vivo animal studies at 900 MHz," *IEEE Transactions on Microwave Theory and Techniques*, vol. 48, pp. 2040-2049.

**EXPOSURE SYSTEM FOR STUDYING OF EEG CHANGES EVOKED BY 900 MHZ GSM-MODULATED EMF IN ANESTHESIZED PIGS.** K. Jokela<sup>1</sup>, T. Toivonen<sup>1</sup>, T. Toivo<sup>1</sup>, L. Puranen<sup>1</sup>, L. Korpinen<sup>2</sup>, T. Lipping<sup>2</sup>, M. Rorarius<sup>3</sup>. <sup>1</sup>STUK, Radiation and Nuclear Safety Authority, <sup>2</sup>Tampere Univ of Technology, <sup>3</sup>Tampere Univ.

## INTRODUCTION

The effect of radiofrequency radiation on EEG has been widely studied in animals and human subjects. Changes in vigilance and other external stimuli, however, cause variability which is sometimes difficult to control. These problems can be avoided by using general anesthesia where the brain is in a very stable state, reflected in EEG [1]. In this study we anesthetize a pig to different stable levels of anesthesia and then analyzed the reactions to different levels of radio-frequency electromagnetic stimulation. We compare these effects with the effects of auditory and somatosensory stimulation. This model enables the use of a wide range of stimuli, as the animals are sacrificed after the experiment. Due to surgical anesthesia even neurosurgical procedures such as insertion of probes in the brain can be done without ethical problems.

In order to increase the likelihood of the detection of the response, the exposure level should be relatively high, close to or slightly exceeding 10 W/kg (average of 10 g tissue )which is the basic restriction recommended by ICNIRP for the occupational exposure.

In this stage of the study we report the development of the system to be used for the exposure of anesthetized pigs to GSM-modulated RF-EMF in the 900 MHz range. During the exposure the EEG of the animals will be recorded with particular focus on the bursts evoked with the RF-stimulus.

## EXPOSURE SYSTEM

The exposure system consists of a dipole antenna, power meter, power amplifier and signal source (Fig. 1). For well controlled dosimetry a simple dipole is preferred to a true mobile phone where the power is limited and radiation properties vary greatly depending on the model. Additionally it is important that the dipole is positioned so that the set-up is repeatable and insensitive to small variations of the anatomy of the pig and distance of the antenna [2]. During the exposures the experimental animal is lying on a table made of non-conducting material and the dipole is placed symmetrically at the top of the head perpendicular to the axis of the head. The temperature increase of the exposure site is continually monitored with a fluoro-optic sensor with a thickness of 1 mm (Luxtron 750).

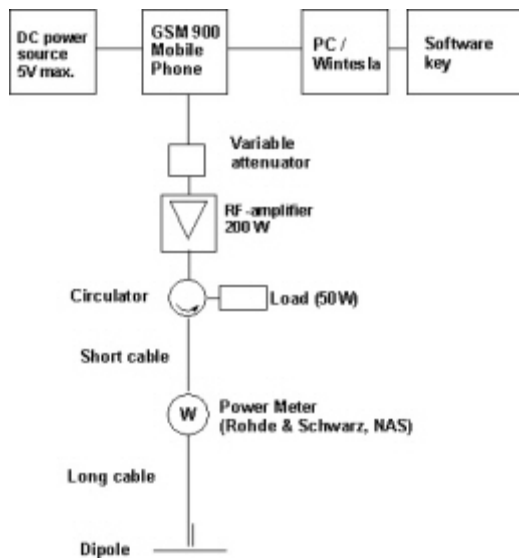


Figure 1. Block diagram of the exposure system.

The antenna is a half-wave dipole designed according to the specifications for SAR test validation dipoles. During exposures it is attached to a non-conducting table mounted jig. The dipole was equipped with the quarter-wavelength balun transformer and N-connector. RF-power transmitted to and reflected from the antenna is continuously monitored. The dipole is tuned so that the minimum return loss is 20 dB. The exact frequency in the 900 MHz mobile phone frequency band is allocated by the Finnish Communications Regulatory Authority for this experiment. The power source comprises of a 200 W amplifier and computer- controlled GSM-phone functioning at a constant power level in basic GSM-mode. The phone transmits phase modulated pulses of 0.577 ms duration and repetition rate of 4.615 ms. Therefore, the average power is approximately 1/8 of the pulse power.

The functioning of EEG and other sensitive measuring systems in strong electromagnetic field was tested by using a watermelon as a load of the antenna. The tests showed that no electromagnetic interference arose with maximum available power. The safety distance, where the occupational limit 22 W/m<sup>2</sup> is exceeded was 0.5 m based on microwave hazard measurements (Narda 8712 with 8721 probe).

#### DOSIMETRY

Preliminary SAR assessment was carried out by irradiating a standard SAR flat test phantom (SAM) provided by SPEAG. When the antenna was at the distance of 15 mm from the brain tissue simulating liquid, the normalized SAR (10 g average) was 7 W/kg/W. Due to the curvature of the pig head the true SAR is probably lower. Additionally, too short distances must be avoided to avoid excessive skin heating. The minimum distance to the skin is 10 mm. The best estimate for the 10 g average SAR is 2 to 4 W/kg/W. The more precise SAR assessment will be based on SAR measurements in an homogeneous liquid phantom simulating the pig head. Additionally, SAR will be computed in a heterogeneous model of pig head.

#### CONCLUSIONS

Low-cost, simple and reliable high SAR exposure system was developed for in vivo exposures of anesthetized pigs at 900 MHz.

This work is part of Finnish research programme HERMO (Health Risk Assessment of Mobile Communications) supported by TEKES-National Technology Agency, mobile phone manufacturers (Nokia) and Finnish network operators.

## REFERENCES

- [1] Jäntti V, Yli-Hankala A. Neurophysiology of anesthesia. *Suppl Clin Neurophysiol.* 53:84-8, 2000.
- [2] Kuster N, Schuderer J, Christ A, Futter P, Ebert S. Guidance for exposure design of human studies addressing health risk evaluations of mobile phones. *Bioelectromagnetics* 25:524-529, 2004.

P-B-23 STUDENT

**GENERAL CORRECTION FACTOR TO BE APPLIED TO THE SAR FOR OCCUPATIONAL ELECTROMAGNETIC EXPOSURE IN PHANTOM MODELS.** W. Joseph, L. Martens. Dept of Information Technology, Ghent Univ, Sint-Pietersnieuwstraat 41, Ghent, Belgium.

**Objective:** If one determines the safety distances for occupational electromagnetic exposure of e.g., base station antennas, the Specific Absorption Rate (SAR [W/kg]) has to be determined and be compared to the basic restrictions [1]. The SAR is experimentally determined in homogeneous phantoms, which may result in lower SAR values than the SAR in a heterogeneous and anatomically realistic model. Therefore the measured SAR must be multiplied by a correction factor [2]. We will show in this paper that if one wants to obtain a fully conservative approach (i.e., producing a higher SAR), a correction factor which depends on the type of polarization, frequency, and phantom has to be defined. By considering the highest correction factor of the investigated polarizations a conservative approach is assured.

**Methods:** We investigate electromagnetic plane-wave excitation with different polarizations incident on a homogeneous rectangular box phantom (corresponds to the average trunk of an adult man, CENELEC [2]), a homogeneous prolate spheroid phantom (average man [3], widely used simplified model of a human) and a realistic heterogeneous model of a man (Visible Human, developed at Brooks Air Force Base Laboratories). For the box and spheroid phantom the dielectric parameters are those of muscle tissues at the investigated frequencies. Three different polarizations, E-polarization (electric field parallel to the major axis of the spheroid or to the longest dimension of other phantoms), H-polarization (magnetic field parallel to major axis), and K-polarization (direction of incidence along the major axis) have been considered and for each polarization, the whole-body SAR for the three phantoms has been calculated using Finite-Difference Time-Domain (FDTD) simulations and theoretical calculations. We investigate a frequency range of 10 MHz up to 2000 MHz. We define the correction factor  $\Sigma$  for the three different polarizations as the ratio of the whole-body SAR in the human model and the whole-body SAR in the different phantoms:

$$\Sigma|_{\text{phantom}} = \frac{\text{whole-body SAR}_{\text{human}}}{\text{whole-body SAR}_{\text{phantom}}}|_{\text{u-polarisation}}$$

with  $u = E, H$  or  $K$ . To assure a fully conservative approach the maximum value of  $\Sigma$  for the three considered polarizations has to be used. If one combines these three polarizations, every possible incident field polarization can be obtained and thus using the maximum value avoids underestimation of the SAR.  $\Sigma$  is based on the whole-body SAR, which is the best and most restrictive parameter to take the influence of a phantom

into account using plane-wave excitation. The advantage of using the correction factor  $\Sigma$  is that for measurements and simulations of the SAR a simple and homogeneous phantom can be used and by applying  $\Sigma$  realistic worst-case SAR values can be obtained.

**Results:** Fig. 1 and 2 show  $\Sigma$  for the three polarizations for the rectangular box phantom and the spheroid phantom, respectively. We can clearly see that  $\Sigma$  is frequency- and polarization-dependent. These figures show that  $\Sigma$  for E-polarization has mostly the largest values. For frequencies higher than 500 MHz,  $\Sigma$  varies much less than at lower frequencies.  $\Sigma$  reaches a minimum for the different phantoms and polarizations due to resonance. For E-polarization for example, 73 MHz is the resonance frequency of the spheroid phantom in free space. For the rectangular box phantom  $\Sigma$  is of the same order for the three polarizations for frequencies higher than 500 MHz but E-polarization delivers for almost all frequencies the highest correction factor. For the spheroid phantom  $\Sigma$  is higher for H- and K-polarization than for E-polarization for frequencies lower than 400 and 280 MHz, respectively. Fig. 1 shows that for frequencies higher than 500 MHz,  $\Sigma$  is larger than 2 for the box phantom. This shows that the arbitrary factor 2 of CENELEC standard 50383 is not a good choice for the rectangular box phantom. We advise to use for each type of phantom the highest value of  $\Sigma$  of the three polarizations at the considered frequency to obtain a conservative approach.

**Conclusions:** A correction factor for the determination of the SAR in a homogeneous phantom exposed in occupational conditions is presented. The correction factor is frequency, phantom, and polarization dependent. To assure a conservative approach, the highest correction factor of the investigated polarizations (E, H and K) has to be used.

#### References.

1. International Commission on Non-ionizing Radiation Protection, "Guidelines for limiting exposure to time-varying electric, magnetic, and electromagnetic fields (up 300 GHz)," Health Physics, Vol. 74, No. 4, pp. 494-522, 1998.
2. CENELEC EN50383, "Basic standard for the calculation and measurement of electromagnetic field strength and SAR related to human exposure from radio base stations and fixed terminal stations for wireless telecommunication systems (110 MHz - 40 GHz)", Sept. 2002.
3. C. H. Durney, M. F. Iskander, H. Massoudi and C. C. Johnson, "An Empirical formula for Broad-Band SAR Calculations of Prolate Spheroidal Models of Humans and Animals," IEEE Trans. Microwave Theory Tech., vol. MTT-27, No. 8, pp. 758 – 763, Aug. 1979.

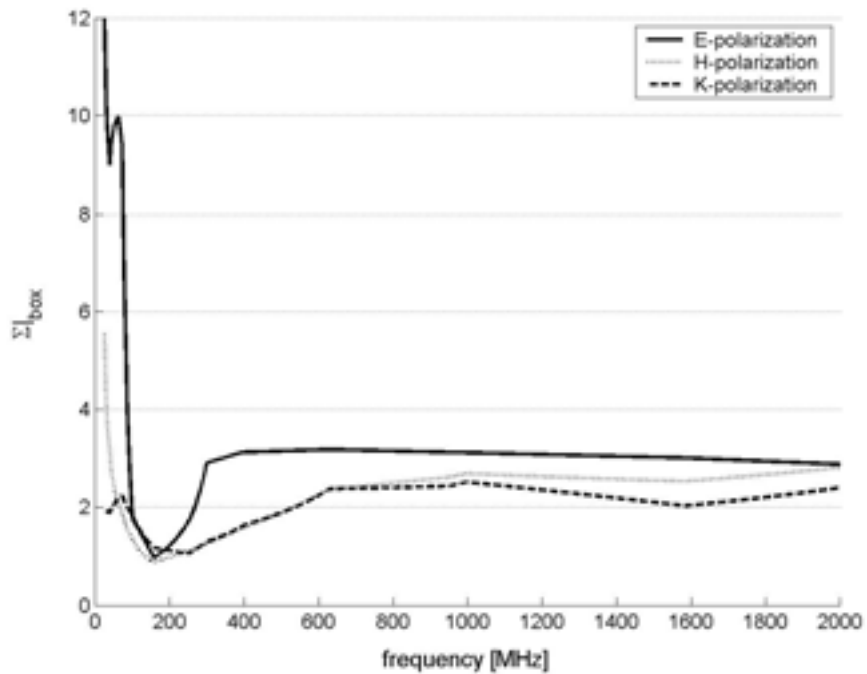


Figure 1:  $\Sigma$  for the rectangular box phantom as a function of the frequency from 10 MHz to 2000 MHz for the three polarizations under study.

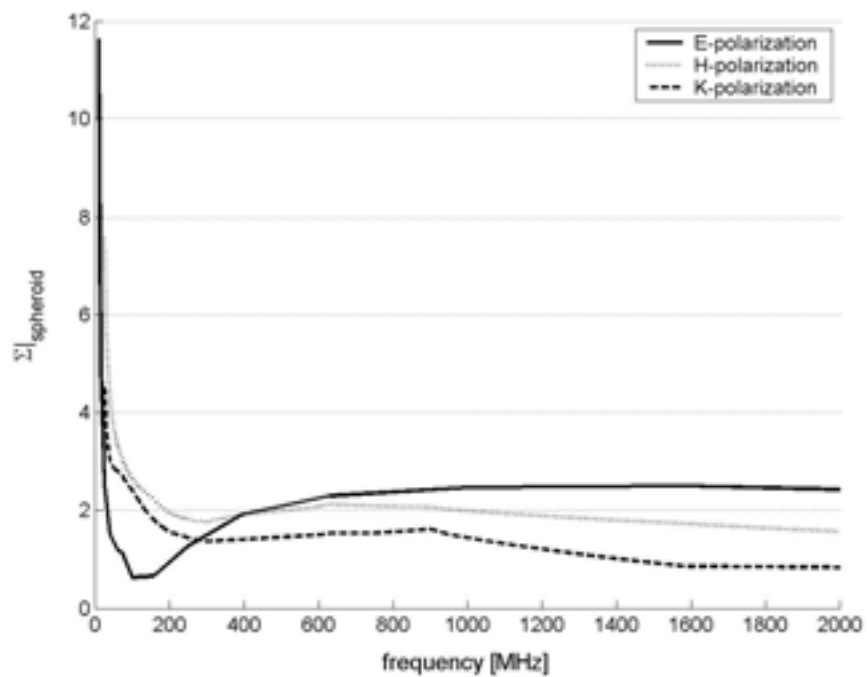


Figure 2:  $\Sigma$  for the spheroid phantom as a function of the frequency from 10 MHz to 2000 MHz for the three polarizations under study.

**FINITE-DIFFERENCE TIME-DOMAIN COMPUTATIONS OF SAR DISTRIBUTION WITHIN AN EXPOSURE SYSTEM FOR STUDYING THE EFFECTS OF RADIOFREQUENCY/MICROWAVE FIELDS ON SKELETAL MUSCLE CONTRACTION.** M. Lambrecht<sup>1</sup>, I. Chatterjee<sup>1</sup>, D. McPherson<sup>1</sup>, J. Quinn<sup>2</sup>, G. L. Craviso<sup>2</sup>. <sup>1</sup>Dept of Electrical Engineering, Univ of Nevada, Reno, Nevada, USA, <sup>2</sup>Dept of Pharmacology, Univ of Nevada, Reno, Nevada, USA.

**OBJECTIVE:** In order to assess whether skeletal muscle contraction is affected by non-thermal levels of radiofrequency (RF)/microwave (MW) fields in the frequency range 0.75 to 1 GHz, it is important to have a well-characterized exposure system, with an acceptable degree of field and SAR homogeneity in the region where the muscle is placed. The work described here addresses this issue with respect to a waveguide-based exposure system within which is placed a semi-custom designed organ bath chamber containing the muscle being tested. Since in the experimental study, both the RF/MW fields and the stimulating electric field are applied simultaneously, the RF/MW fields and SAR in a muscle sample are computed in the presence of the stimulating electrodes.

**METHODS:** The Finite-Difference Time-Domain (FDTD) method is used to numerically compute the detailed SAR distribution in the organ bath chamber containing the muscle. The organ bath chamber is one that is available from Radnoti Glass Technology, Inc. with some design modifications incorporated into it as a result of FDTD modeling that showed that only a certain stimulating electrode configuration was compatible with the standard WR-975 rectangular waveguide-based exposure system [1]. A detailed geometry of the organ bath chamber was created using Solidworks 2003 (Solidworks Corp.) and included the following: 1. An inside compartment containing oxygenated Krebs solution super fused through an inlet and outlet port; 2. An outer jacket containing heated water for maintaining the Krebs solution at 37 degrees C super fused through an inlet and outlet port; 3. The muscle sample; 4. The suture attaching one end of the muscle tendon to a force transducer outside the waveguide; 5. The suture attaching the other end of the muscle to a glass hook at the bottom of the chamber; 6. A pair of platinum ring electrodes that were shown to cause very little field distortion of the RF/MW field as compared to conventional parallel electrodes [1]. The suture connected to the force transducer, which is in turn connected to a bridge amplifier and recorder exits the waveguide through one of several non-radiating slots in the waveguide walls. All tubing that attaches to the organ bath chamber and the fluoroptic temperature probes that measure the temperature in the chamber also pass through non-radiating slots. The Solidworks model was imported into a commercially available FDTD software package XFDTD (Remcom, Inc., BioPro version 6.1) and computations of detailed distribution of SAR in the organ bath chamber were performed. The adaptive meshing capability of XFDTD is used to create a fine mesh in the vicinity of the muscle sample as well as near the ring electrodes.

**RESULTS:** It was shown that the SAR in the region containing the muscle was homogeneous to within 5%, which is well within acceptable limits for performing well-characterized experiments to assess the effects of RF/MW fields on muscle contraction [2]. Computed SAR results for muscle strips obtained from the hind foot of mice (flexor digitorum brevis) will be presented for the range of frequencies between 0.75 and 1 GHz.

**CONCLUSIONS:** It is possible to expose skeletal muscle tissue samples placed in a semi-custom designed organ bath chamber within a rectangular waveguide to RF/MW fields that are almost constant in the region containing the muscle, while simultaneously stimulating the muscle with 1- 200 Hz electric field to study effects on muscle contraction.

1. M. Lambrecht, I. Chatterjee, D. McPherson, J. Quinn and G.L. Craviso, "Design and optimization of a radiofrequency/microwave exposure system for assessing bioeffects on skeletal muscle contraction", to be presented at Electromed2005, Portland, OR, May 15-18, 2005.

2. N. Kuster and F. Schoenborn, "Recommended minimal requirements and development guidelines for exposure setups of bio-experiments addressing the health risk concerns of wireless communications", *Bioelectromagnetics*, Vol. 21, pp.508-514, 2000.

Supported by the Air Force Office of Scientific Research, grants F49620-03-1-0262 and FA9550-04-1-0194

P-B-29

**ASSESSMENT OF USERS' EXPOSURE TO GSM MOBILE PHONE EMISSIONS USING A SARMETER.** P. Le Duigou<sup>1</sup>, S. Chauvin<sup>2</sup>, D. Picard<sup>1</sup>, R. Veysset<sup>2</sup>. <sup>1</sup>Supelec, Plateau du Moulon, Cedex, France, <sup>2</sup>Bouygues Telecom, Boulogne-Billancourt Cedex, France.

#### INTRODUCTION:

The electromagnetic power absorbed by a person using a GSM phone is quantified by the Specific Absorption Rate (SAR in W/kg). ICNIRP's Guidelines specify that the localized SAR absorbed by the head has to be less than 2W/kg. To comply with this limit, phones are tested in laboratory at their maximum power, according to the CENELEC Standard EN50361. During an actual telephone call, the power emitted by a cell phone is variable and the phone rarely emits at its maximum power. This is due to Power Control (PWC), Discontinuous Transmission (DTX), Handovers and many other parameters. In January 2001, the French Health General Directorate (DGS) published a report on mobile telephony and health which gave recommendation on handsets use. One recommendation was that users should have an indication of their exposure during their telephones calls expressed in a simple way (e.g. % of maximum power, averaged over the duration of the last call). This would have an educational effect, telling the users that for example making calls under poor reception conditions increases quite significantly the radiation they receive.

#### OBJECTIVE:

We have developed a portable measurement device, called SARMeter, which was used to measure the power emitted by a cell phone during a mobile phone call. The aim of our study was to use this device to assess the typical user's exposure to cell phone emission on a GSM network. We also have made comparisons of measurements performed in different environments and different phone uses to assess the influence of the GSM networks .

#### METHODS:

The SARMeter is made of three different parts. A probe placed close to the cell phone antenna, an electronic box to filter and amplify the signal, a personal computer connected to the case to save and process the data.

The SARMeter operates at a sampling period of 4.615ms, corresponding to the frame period of the GSM signal. For each frame, the SARMeter gives a Boolean, representing the presence or absence of a pulse in the frame, due to DTX, and the value of the relative power in comparison to the maximum power of the handset in the operating frequency band.

Measurement scenarios have been chosen from a market study to represent the common users' habits. We have then defined eight categories corresponding to common usage of a mobile phone: at home, at work, during transportation, in cars, restaurants, shops, in the street and other public places.

With the measurements performed under all these scenarios, we have calculated an exposure reduction factor, corresponding to the average relative power in comparison to the maximum power, and the emitted frames density.

Other comparisons have been made to analyze the influence of the coverage density of the network, the distance to the base station, and the mobility of the user. We have compared outdoor and indoor measurements, rural and urban measurements, in-car and by-foot measurements

#### RESULTS:

We have checked that the power given by the SARmeter, the pulse detection and the time response was good using a spectrum analyzer and a TEMS. The accuracy of the SARmeter was found to be very good. The actual measurements have shown that the exposure reduction factor of a typical customer is 38% compared to the maximum power that a mobile phone can emit.

As we could expect, the measurements we have done indoor have shown higher exposure levels than measurements done outdoor because of a poorer network coverage. The relative difference between indoor and outdoor levels is about 40%. Comparisons between rural and urban areas have shown that the power emitted by a cell phone is higher in rural areas, because of the distance to the base stations. The relative difference between mean reduction factors is 41%. Finally, the measurements done by foot and in car have shown that the mean user's exposure was higher in cars. The relative difference varies between 30 and 55%.

#### CONCLUSION AND DISCUSSION:

These measurements allowed us to characterize efficiently the user's exposure during a real mobile phone call. The results have been obtained on one network with one type of phone. It's planned to extend this study to several networks and several phones to analyze the dependence on networks and phones.

P-B-32

**AN IN VITRO EXPOSURE DEVICE FOR EXPERIMENTAL STUDIES ON THE EFFECTS OF UMTS MOBILE COMMUNICATION SYSTEM.** V. Lopresto, L. Ardoino, S. Mancini, R. Pinto, G. A. Lovisolo. Section of Toxicology and Biomedical Sciences, ENEA Casaccia Research Centre.

**INTRODUCTION:** In the last year, due to the beginning of third generation universal mobile telecommunications system (UMTS) service, there has been a remarkable increase in the number of radio-base stations and UMTS mobile phones, particularly in urban areas. This has revived the discussion about possible health effects of weak electromagnetic fields, like those produced by UMTS mobile phones. Investigation in such a field requires appropriate exposure systems. In 1996, the World Health Organization (WHO) established guidelines for quality EMF experiments, emphasizing the importance of well-defined and characterized exposure conditions. The radio-frequency (RF) exposure is defined in terms of specific absorption rate (SAR), i.e. the time rate of electromagnetic energy deposition per unit mass. The choice of the exposure system is related to the typology of experiment (in vitro or in vivo) and to the samples used. Additionally, it has to ensure the required SAR levels and sufficient homogeneity of dose distribution. Appropriate dosimetric techniques enable the required information to be obtained with suitable accuracy [1], [2].

**OBJECTIVES:** In this work, an in vitro exposure device, named UMTS wire patch cell (WPC) and derived from the original 900 MHz model [3], is presented and discussed. The UMTS WPC is designed to operate at the up-link frequencies (1920-1980 MHz) of the UMTS system, it can be easily placed into

a standard incubator, and allows the simultaneous exposure of four 3.5 or 5 cm Petri dishes with a high efficiency of irradiation.

**METHODS AND MODELS:** The UMTS WPC has been designed by scaling, with respect to the signal wavelength  $\lambda$ ; the dimensions of the 1800 MHz WPC device [4]. A further optimization of the cell model has been done by means of numerical simulations, performed with a commercial code based on the finite integral technique (CST Microwave Studio 5.0). In numerical analysis, the complete system (the cell containing four 3.5 cm Petri dishes, symmetrically positioned and filled with different levels of culture medium) has been studied, to achieve best match in the UMTS up-link frequency band and homogeneous SAR distribution in the biological samples. The outcome of this study has been a cell consisting of two  $18.2 \times 18.2$  cm<sup>2</sup> conducting plates (the ground plane and the roof), placed at a distance of 1.8 cm by means of four cylindrical grounding contacts (props) with a diameter of 1 cm, and one coaxial probe with an inner diameter of 3.8 mm (located at the center of the cell, passing through the roof and connected to the ground). This symmetric structure (Fig. 1) allows easy insertion of four 3.5 or 5 cm Petri dishes, and fits adequately into an incubator. Homogeneity of exposure and efficiency of irradiation have been investigated by means of both numerical simulations (Fig.2,3) and experimental measurements on a prototype of the device. The SAR dose induced in the biological samples has been experimentally assessed by means of thermal measurements, using a non-perturbative thermistor thermometer.

**RESULTS:** Computed average SAR for 1 W input power (power efficiency) have provided high values (2.3 W/kg/Win in one 3.5 cm Petri dishes filled with 3.5 ml of culture medium), with good agreement with experimental measurements. Even higher power efficiency (3.4 W/kg/Win) has been computed in the bottom layer of the Petri dish, this result is of particular interest for the exposure of plated-cell cultivations, as for instance nerve cells.

**CONCLUSIONS:** A model of wire patch cell, designed to operate at the up-link band of UMTS system has been presented and discussed. This device is easy to build at an affordable cost, and allows simultaneous irradiation of four Petri dishes. Thanks to its small size, it easily fits into a standard incubator. Hence, the UMTS WPC is particularly suitable for use in in vitro experiments, aimed at investigating possible biological effects of electromagnetic radiation associated with UMTS mobile phones. Direct experimental measurements and numerical simulations have shown that the device allows obtaining good homogeneity of exposure and high efficiency of irradiation of the biological target.

#### CAPTION

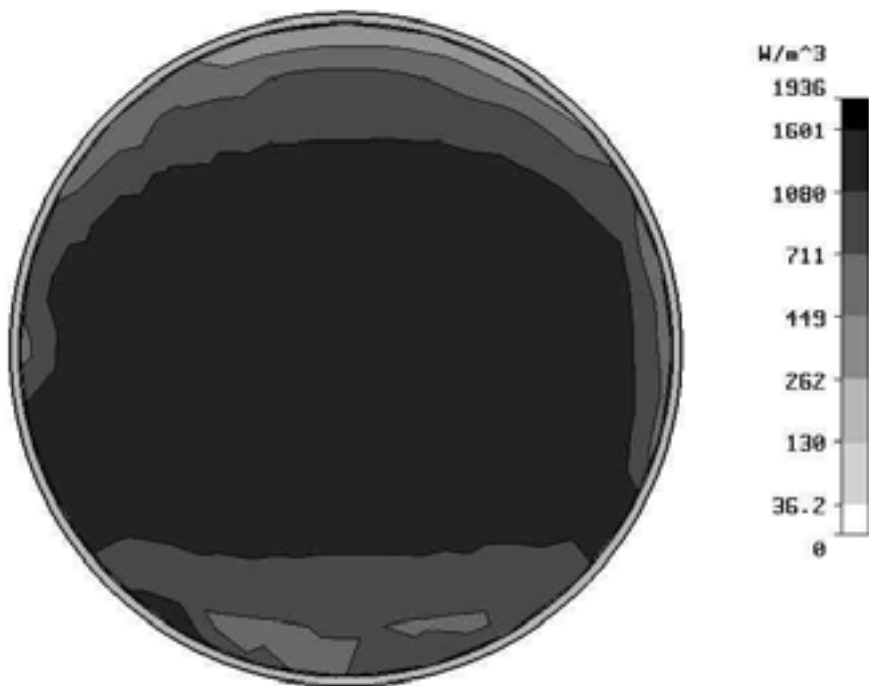
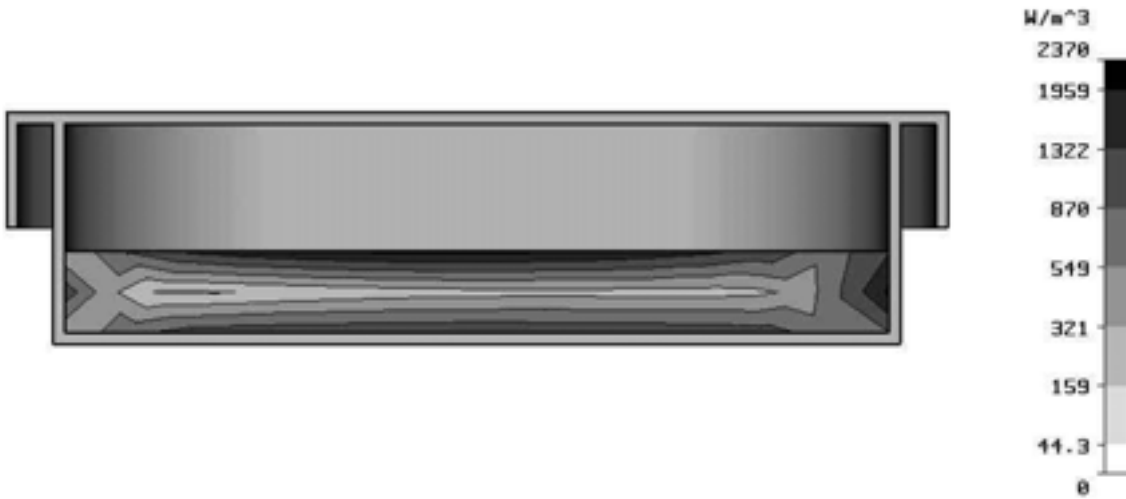
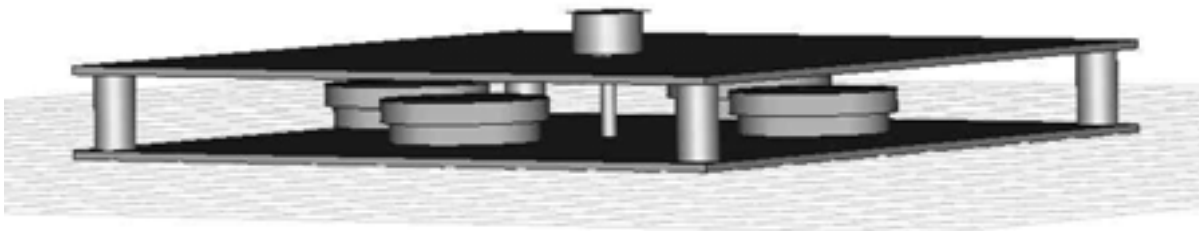
Fig.1: Numerical model of the UMTS WPC containing four Petri dishes ( $\Phi$ ; = 3.5 cm).

Fig.2: Power loss density distribution, calculated at 1975 MHz for 1 W peak input power, inside one Petri dish in a vertical layer at the centre of the dish.

Fig.3: Power loss density distribution, calculated at 1975 MHz for 1 W peak input power, inside one Petri dish in a horizontal layer at 0.5 mm from the bottom of the dish.

#### References.

- [1] A. W. Guy, C. K. Chou, and J. A. McDougall, 'A quarter century of in vitro research: a new look at exposure methods', *Bioelectromagnetics*, vol. 20, pp. 21-39, 1999.
- [2] F. Schonborn, K. Poković;, M Burkhardt, and N. Kuster, 'Basis for optimization of in vitro exposure apparatus for health hazard evaluations of mobile communications', *Bioelectromagnetics*, vol. 22, pp. 547-559, 2001.
- [3] L. Laval, Ph. Leveque, and B. Jecko, 'A new in vitro exposure device for the mobile frequency of 900 MHz', *Bioelectromagnetics*, vol. 21, pp. 255-263, 2000.
- [4] L. Ardoino, V. Lopresto, S. Mancini, R. Pinto, and G. A. Lovisolo, 'A 1800 MHz in vitro exposure device for experimental studies on the effects of mobile communications devices', *Radiat. Prot. Dosimetry*, vol. 112, pp. 419-428, 2004.



P-B-35

**TRANSMEMBRANE VOLTAGE INDUCED ON MORPHOLOGICALLY ALTERED HUMAN ERYTHROCYTES EXPOSED TO RF FIELDS.** S. Muñoz, J. L. Sebastián, M. Sancho, J. M. Miranda. Dpto. Física Aplicada III. Facultad de Ciencias Físicas. UCM. Spain.

Macrocyte and microcyte are morphological alterations of human erythrocytes, and a better understanding of these alterations has always been a classic problem in cell biology. Also, it is well known that transmembrane voltage plays an important role in all cell activity. Therefore, it is important to know how an external RF radiation could modify this voltage. In this paper, the transmembrane voltage induced in macrocyte and microcyte cell models exposed to a linearly polarized electromagnetic plane wave of frequency 1800 MHz is calculated. The results show that the value of the induced voltage on the macrocyte shape is always higher than the one observed on the microcyte cell geometry for all polarizations considered in this study.

A variety of morphological changes have been observed in erythrocytes by examination of cells prepared for scanning electron microscopy. These changes in erythrocyte morphology are associated with various medical disorders. The morphological alterations of erythrocytes are mainly due to variations in size, anisocytosis, or in shape, pokilocytosis. In this paper the authors have focused their attention on the effect of an RF electromagnetic field on anisocytosis, as effects over the pokilocytosis have already been studied and information can be found in the literature. Anisocytosis describes an abnormal variation in size of red blood cells, and it is mainly associated to two conditions: the presence of young red blood cells such as polychromatophils which are larger than mature erythrocytes, macrocytes, and the presence of smaller red blood cells, microcytes.

In this study, the basic erythrocyte cell model has a biconcave shape with a diameter of 7.8 microns. This value has been found to be less than 5  $\mu\text{m}$  for microcytes and higher than 9  $\mu\text{m}$  for macrocytes. The minor semi-axis of the erythrocyte varies from 1  $\mu\text{m}$  to 1.7  $\mu\text{m}$ . The cytoplasm is in all cases a physiological saline solution with a protein volume fraction of 0.26 and the membrane is formed by a shell of constant thickness  $d = 8\text{nm}$ . In all analysis, the cell is considered to be immersed in an external continuous medium formed by electrolytes in free water. The electric permittivity and conductivity of the external medium are those of the physiological saline,  $\epsilon_r = 80$  and  $\sigma = 0.12\text{ Sm}^{-1}$  respectively. The values used for the permittivity and conductivity of the membrane and cytoplasm were be  $\epsilon_r = 9.04$ ,  $\sigma = 10^{-6}\text{ Sm}^{-1}$  and  $\epsilon_r = 50$ ,  $\sigma = 0.53\text{ Sm}^{-1}$  respectively. The frequency of the RF signal used in this study is 1800 MHz, typically used in cellular phones and in wireless surveillance systems.

As the cell dimensions are much smaller than the wavelength at the working frequency, it is reasonable to assume that the cell is exposed to a uniform field. Therefore, for this analysis, the cells have been considered exposed to an electromagnetic plane wave linearly polarized along the minor axis of the cell. For normalizing purposes, the electric field intensity has been considered to be 1 V/m. To determine the induced transmembrane voltage, a finite element (FE) numerical technique has been used. The full Maxwell equations are solved considering a discretization of the cell model geometry into tetrahedral elements. An adaptive mesh is used so that the size of the basic tetrahedron is different in the cytoplasm and membrane regions to improve accuracy. In order to keep the computational resource requirements reasonable, the computational domain is truncated to a radiation region (external medium) in which the cell is immersed and surrounded by finite thickness absorbing layers, called perfectly matched layers (PML). The dimensions of the radiation region are adjusted so that a good compromise between accuracy and reasonable computing times is obtained. The electric field values are found by an iterative method and a solution is found when a convergence criterion limit is accomplished. This technique has already been satisfactorily tested with analytical solutions found for other basic geometrical cell shapes such as spheres and confocal ellipsoids.

Due to the influence of the polarization of the electric field on the induced transmembrane voltage, an analysis of the sensitivity of the results to changes in polarization of the electric field is of primary importance. Figure 1 shows the transmembrane potential value as a function of the angle  $\alpha$  formed by the direction of the applied electric field and the minor axis of the cell. As it can be observed, the value of the induced transmembrane voltage varies with the orientation of the cell and therefore it is not uniform over the whole membrane surface. It is observed that for both geometries, the value of the transmembrane potential is significantly reduced as the value of  $\alpha$  increases. Also, for all values of  $\alpha$ , the induced transmembrane voltage in the macrocyte shape cell is higher than the voltage induced in the microcyte. When the incident electric field is parallel to the minor axis of the cell, the voltage induced is higher than the value obtained when the electric field is parallel to the major axis.

The maximum induced transmembrane voltage is always found along the minor axis and in the centre of the cell. This is mainly due to the mutual polarization effects of the neighbouring regions of the membrane along the minor cell axis. For an external field of 1 V/m, the maxima transmembrane voltages induced in the macrocyte and microcyte were found to be 76.9 and 52 nV respectively.

The results of the analysis show the significant role of the polarization of the applied RF field and that under the same RF exposure conditions, the macrocyte and microcyte have higher and lower induced transmembrane voltages than the basic erythrocyte.

Support of Dr. Jocelyne Leal

#### Acknowledgments

This work was supported by the Fondo de Investigaciones Sanitarias under grant PI03/0295.

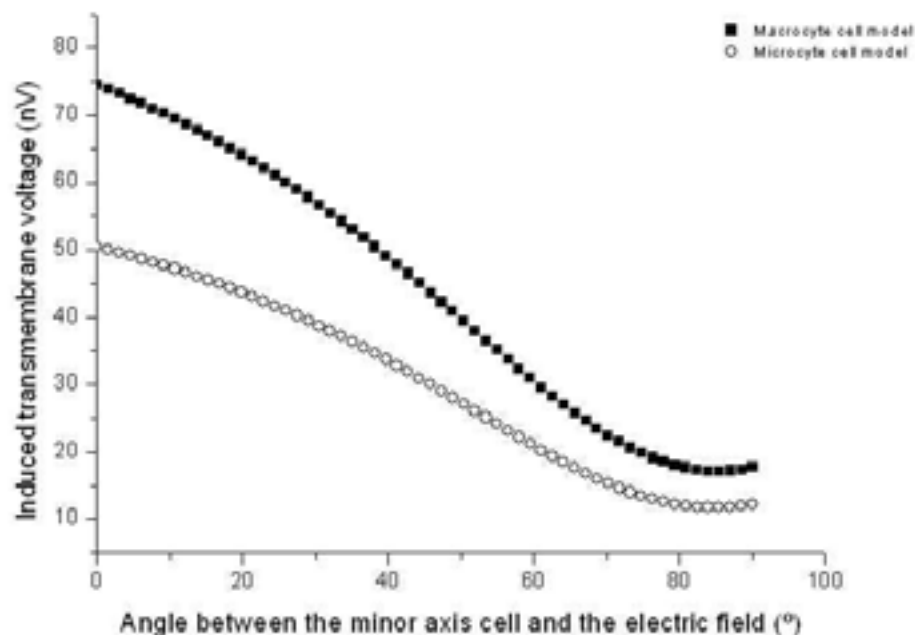


FIGURE 1

**DETAILS OF VOXEL-BASED NUMERICAL MODELS OF THE AVERAGE JAPANESE FIGURE AND DISTRIBUTION OF THESE MODELS DATABASE.** T. Nagaoka<sup>1</sup>, S. Watanabe<sup>1</sup>, E. Kunieda<sup>2</sup>, M. Taki<sup>3</sup>, Y. Yamanaka<sup>1</sup>. <sup>1</sup>National Institute of Information and Communications Technology, Tokyo, Japan, <sup>2</sup>Keio Univ, Tokyo, Japan, <sup>3</sup>Tokyo Metropolitan Univ, Tokyo, Japan.

With advancement of computer performance, numerical simulation is indispensable to human dosimetry. Therefore, it is very important for the numerical dosimetry to use voxel-based computational human models of real human anatomy. In recent years, several high-resolution whole-body voxel models have been developed with the progress medical imaging technology [1- 4]. However, the voxel model that is available to the public is only Brooks AFB model developed based on male data of the Visible Human Projects [1]. We have previously developed realistic high-resolution whole-body voxel models that are 2mm spatial resolution and are identified with 51 tissues and organs, using magnetic resonance imaging data of adult male and female of average Japanese figure [5]. The adult female model is the first of its kind in the world and both are the first Asian voxel models that enable the numerical evaluation of electromagnetic dosimetry at frequencies of up to about 3 GHz. We also revealed that Most of the tissue and organ masses of these models are close to those of the average Japanese. Quite a few researchers from all over the world have inquired about distribution of these models dataset, because these models have excellent property. Therefore, we decided to make these models database available to the public for various researches. These models are compared with other models as to identified tissues and organs, body dimension, and tissue and organ masses prior to the public release, because understanding in detail the features of these models is great help for numerical dosimetry. In this presentation, we show that the features of these models were different from the others, and also explain the full background to the public release of the database, and terms and conditions for the use of the database.

- [1] P. Gajsek, et.al., (2001) Parametric dependence of SAR on permittivity values in a man model. IEEE Trans Biomed Eng, 48(10):1169-1177
- [2] T. W. Dawson, et.al., (1997) A comparison of 60 Hz uniform magnetic and electric induction in the human body. Phys Med Biol, 42:2319-2329
- [3] O. P. Gandhi (1995) Some numerical methods for dosimetry: Extremely low frequencies to microwave frequency. Radio Sci, 30(1):161-177
- [4] P. J. Dimbylow (1997) FDTD calculation of the whole-body averaged SAR in an anatomically realistic voxel model of the human body from 1 MHz to 1 GHz. Phys Med Biol, 42:479-490
- [5] T. Nagaoka, et.al., (2004) Development of realistic high-resolution whole-body voxel models of Japanese adult male and female of average height and weight, and application of models to radio-frequency electromagnetic-field dosimetry. Phys Med Biol, 49:1-15

P-B-41 STUDENT

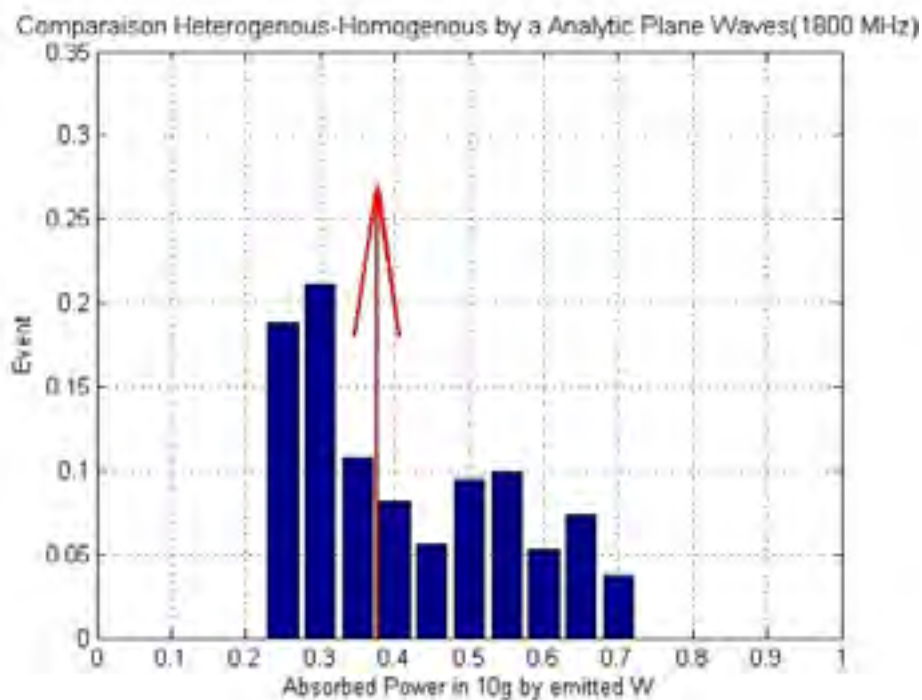
**NUMERICAL ANALYSIS OF ELECTROMAGNETIC FIELDS INDUCED IN A MULTILAYER BIOLOGICAL STRUCTURE.** A. Pradier<sup>1</sup>, D. Lautru<sup>2</sup>, M. F. Wong<sup>1</sup>, V. F. Hanna<sup>2</sup>, J. Wiart<sup>1</sup>. <sup>1</sup>France Telecom RD Issy les Moulineaux, <sup>2</sup>Universite de Paris VI.

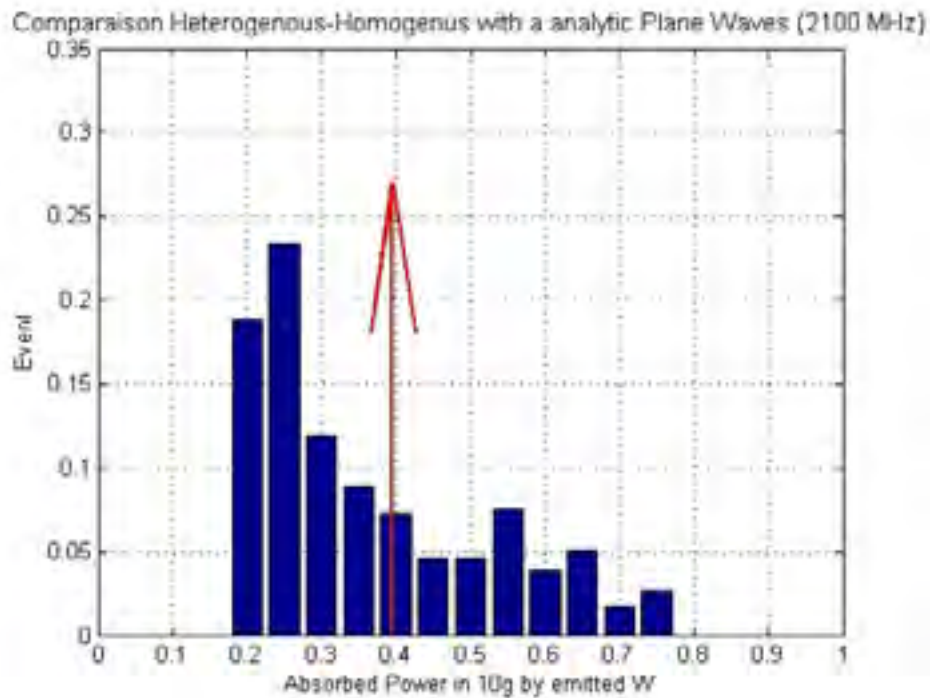
Introduction: Nowadays, more and more technologies in telecommunications used in wireless systems are based on the transmission and reception of electromagnetic waves. To protect the general public from possible undesirable effects, international limits have been established by international

organizations such as the International Commission on Non Ionising Radio Protection (ICNIRP). To check the compliance to these limits, standards have been established for the case of a handset close to a human head. In a new current trend when using mobile phones, the handset is often close to the body. It is fundamental to check if a flat phantom with the equivalent head liquid can be used with an adequate factor.

Objectives: Since the thickness of organs like skin of hypoderm depends on the person and on the location, it is of interest to analyze in a statistical way, the influence of these variations and to compare the SAR induced in such structures with that induced in the uniform liquid used in standards.

Methods and Results: Firstly, from the Visible Man model, the thickness layers distribution has been determined. Using this statistical distribution, multilayer planar structures have been built in order to analyse the SAR in 10 grams of tissue. Then, two cases of illumination are considered for the different tissues distributions. The case of a plane wave and thereafter, the case of a Hertz dipole have been studied. These different models of multi-layer are then compared with the model of equivalent liquid. Examples of the result are given in Figures A and B





P-B-44

**RADIATION EFFECTIVENESS OF GSM CELLULAR PHONES HAS LITTLE EFFECT ON CUMULATIVE EXPOSURE.** D. Spat<sup>1</sup>, C. Sulser<sup>2</sup>, S. Kuhn<sup>1</sup>, M. Kelsh<sup>3</sup>, A. R. Sheppard<sup>4</sup>, N. Kuster<sup>1</sup>.  
<sup>1</sup>IT'IS Foundation, Swiss Federal Institute of Technology (ETH), Zurich, Switzerland, <sup>2</sup>SPEAG, Zurich, Switzerland, <sup>3</sup>Exponent, Inc., Menlo Park, California, USA, <sup>4</sup>Asher Sheppard Consulting, Redlands, California, USA.

**INTRODUCTION:** Cumulative exposure from cellular phones during use on a network is a function of the magnitude and anatomical distribution of SAR (SARdistr), which are determined for the maximum power level (PWCmax), average power control level (PWCavg), which depends on network properties and transmission mode, and the duration of exposure (t). We assume that for a phone always operated at the same position on the head, cumulative exposure represents a dose that can be expressed as

$$\text{Dose} = \text{SARdistr} * \text{PWC}(\text{avg}) / \text{PWC}(\text{max}) * t .$$

SAR magnitudes and their distribution in tissue are strongly dependent on the phone design. Radiation effectiveness, a measure of efficiency in converting RF power into useful radiated power, is also greatly affected by phone design. Since power control is a function of the received signal strength at the base station, radiation effectiveness is expected to be a parameter that indirectly determines dose through an effect on PWC(avg).

**OBJECTIVE:** The objective of this study was to evaluate the significance of radiation effectiveness on cumulative exposure from GSM phones.

**METHODS:** Several GSM phones were evaluated with different environments and networks using the SYstem NETwork and HAndset (SYNEHA) Analyzer that can compare the power control of four

handsets simultaneously. The phones were mounted on the SAM phantom, and the relative PWC was measured locally with an SAR sensor behind the ear position. The system specifications for SAR measurements were:

- \* sampling rate: > 3000 samples/s per channel (rise/fall time < 0.3ms)
- \* dynamic range: > 33dB (> 48dB for whole system with different sensor lengths)
- \* cross talk attenuation: > 34dB
- \* linearity: < 0.2dB deviation
- \* noise: < 1mW/kg
- \* temperature range: 10 - 40 °C (<< 1dB)
- \* humidity: 0 - 90%
- \* relative position accuracy (head/phone/probe): < 1mm
- \* battery and DC operated

**RESULTS:** During measurements made in urban and remote environments in Zurich and surroundings as well as near San Francisco, we found that radiation effectiveness had little effect on the cumulative dose by GSM phones, since exposure was dominated by handovers (transfers from one base station to another) during which the base station set PWC to PWC(max). Therefore, phone exposure closely reflected SAR at the maximum power level. Consequently, the spatial peak SAR determined during compliance testing is an accurate indicator of relative average exposure by a particular phone compared to other phones.

#### ACKNOWLEDGEMENTS:

Support from SPEAG and the Cellular Telephone and Internet Association (CTIA).

P-B-47

**IN VIVO TEMPERATURE MONITORING IN RF EXPERIMENTS USING WIRELESS TRANSPONDERS.** C. Sulser<sup>2</sup>, V. B. Torres<sup>1</sup>, J. Frohlich<sup>1</sup>, U. Lott<sup>1</sup>, N. Kuster<sup>1</sup>. <sup>1</sup>IT'IS Foundation, Swiss Federal Institute of Technology (ETH), Zurich, Switzerland, <sup>2</sup>SPEAG, Zurich, Switzerland.

**INTRODUCTION:** The highest SAR exposure value in RF bioassay studies following NTP protocols is just below the thermal threshold. Since an exposure value resulting in thermal stress and breakdown is a function of weight, stress, health condition and environment [1], continuous monitoring of the temperature is desired. Rectal measurements using optical based sensors or thermistors with RF transparent leads have been used in the past but are only applicable for short term monitoring in anesthetized or restrained animals. Although wireless implantable thermal transponders have been developed for long-term surveillance and are commercially available, they have not been tested for usage in electromagnetic harsh environments.

**OBJECTIVE:** The objective of this study was to evaluate the suitability of commercially available wireless implantable thermal transponders for in vivo thermal monitoring of mice and rats in RF experiments using GSM and CDMA exposure signals.

**METHOD:** Wireless transponders are suitable if (1) the presence of the transponder does not significantly alter the global and local absorption strength and pattern, (2) the transponder does not result in any local temperature hotspot when exposed, (3) the response of the transponder is not disturbed by the EMF after and/or during the exposure by EMI. The evaluations were conducted using the FDTD simulation platform SEMCAD X and the dosimetric scanner DASY4 with the latest dosimetric and

temperature probe technology. In the experimental setup, a flat phantom configuration filled with tissue simulating liquids (900MHz: relative permittivity of 40.8 and sigma of 0.96 S/m; 1900 MHz: relative permittivity of 40.8 and sigma of 0.96 S/m) was used and exposed by the dipole at 15mm distance from the liquid-shell interface at 900 MHz and 10mm at 1900 MHz. The peak SAR values at the location of the transponder were 60/500W/kg and 75/500 W/kg respectively.

RESULTS: Four different systems for temperature measurements were considered: CFM-6 of Bioelemetrics, IPTT-300 of Biomedic Data Systems, VVS4000 of Mini Mitter and TA-F20 of Transoma Medical. Only the IPTT-300 of Biomedic Data Systems met all the requirements: sufficiently small, passive operation, i.e., not limited by battery life, no significant effect on the absorption pattern, no thermal hotspots under RF exposure, and immune against interference of induced pulsed RF fields (1 Hz to 1500 Hz).

#### ACKNOWLEDGEMENTS:

This study was supported by NIEHS (USA).

#### REFERENCE:

[1] S. Ebert S, C. Dasenbrock, T. Tillmann, N. Kuster, "Thermal Response and Threshold Measurements in Mice Exposed to 905MHz", Proceedings of 27th Annual Meeting of BEMS, Dublin, 2005.

P-B-50

**A NEW ANATOMICAL VOXEL MODEL: THE DOMESTIC SWINE (SUS SCROFA).** J. M. Zirias<sup>1</sup>, J. D. Duncan<sup>1</sup>, R. Garay<sup>1</sup>, A. D'Andrea<sup>1</sup>, J. H. Gao<sup>2</sup>, J. L. Li<sup>2</sup>. <sup>1</sup>Naval Health Research Center Detachment, Brooks City-Base, TX, USA, <sup>2</sup>Research Imaging Center, Univ of Texas Health Science Center, San Antonio, TX, USA.

BACKGROUND: The Brooks Anatomical Models are a collection of high-resolution realistic anatomical models for calculating specific absorption rate (SAR) using the finite difference time domain (FDTD) algorithm. To date, the Brooks models include a human model based on the National Library of Medicine's Visible Human Project, a rat, a goat, a rhesus monkey, and a baboon eye. Each model is based on a series of equally-spaced images collected as magnetic resonance images (MRI) or, in the case of the man model, photographs. To define the tissue type and the associated electrical properties, each of the original images was color coded. In the resulting stack of colored images, the color of each pixel represents the tissue located in a 3-dimensional volume or voxel.

OBJECTIVE: As research requirements change, new laboratory animals are required as well as the corresponding anatomical model. The goal of this project is to create an anatomical model of the domestic swine (*Sus scrofa*).

METHODOLOGY: A 70 kg female domestic swine was transported to the Research Imaging Center, Univ of Texas San Antonio Health Sciences Center where it was euthanized. In order to minimize movement artifacts, the carcass was positioned on its back in a foam restrainer and its legs were held in position with foam blocks and plastic tape. MRI scans of the entire swine carcass were used to create the model. Figure 1 shows a 3-D visualization of the unaligned MRI images. A sample gray-scale MRI image is shown to the lower left in Figure 2 with a preliminary color-coded image from the same

anatomical area shown on the right. In order to achieve maximum resolution and due to the size of the swine, the MRI images were collected in four sections, with each section slightly offset in order to center the mass of that section in the MRI coil allowing for maximum image resolution. The four sections were realigned and converted from a 2mm x 2mm x 3mm resolution to a cubic voxel size of 2mm x 2mm x 2mm. Initial color-coding was started on the torso sections to make the torso available as soon as possible. Coding of other sections and finer structures in all sections will be added later.

**RESULTS:** The color-coding associates the coded location (voxels) with a tissue type and defined electrical properties. The resulting 3-D matrix of color-coded electrical properties is the input to the FDTD algorithm.

**CONCLUSION:** High-resolution anatomical models allow calculation of SAR distributions as part of the planning phase of an empirical effort. This process not only validates the computational model, but also allows the empirical effort to focus on likely target organs.

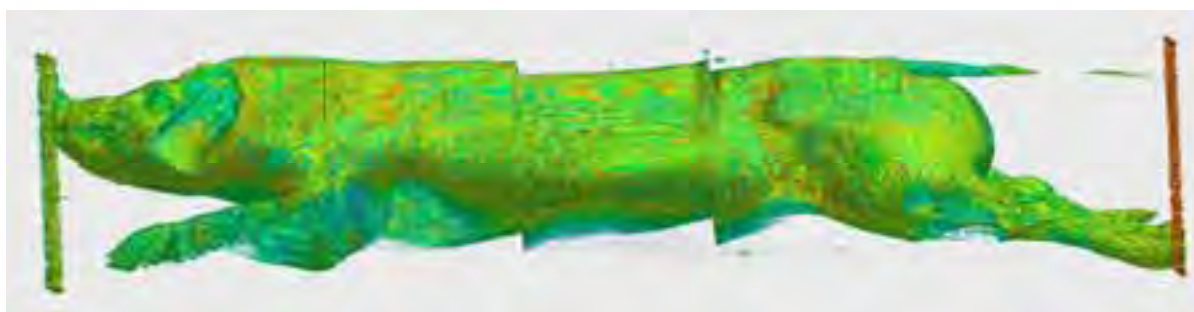


Figure 1. A 3-D visualization of the raw MRI images.

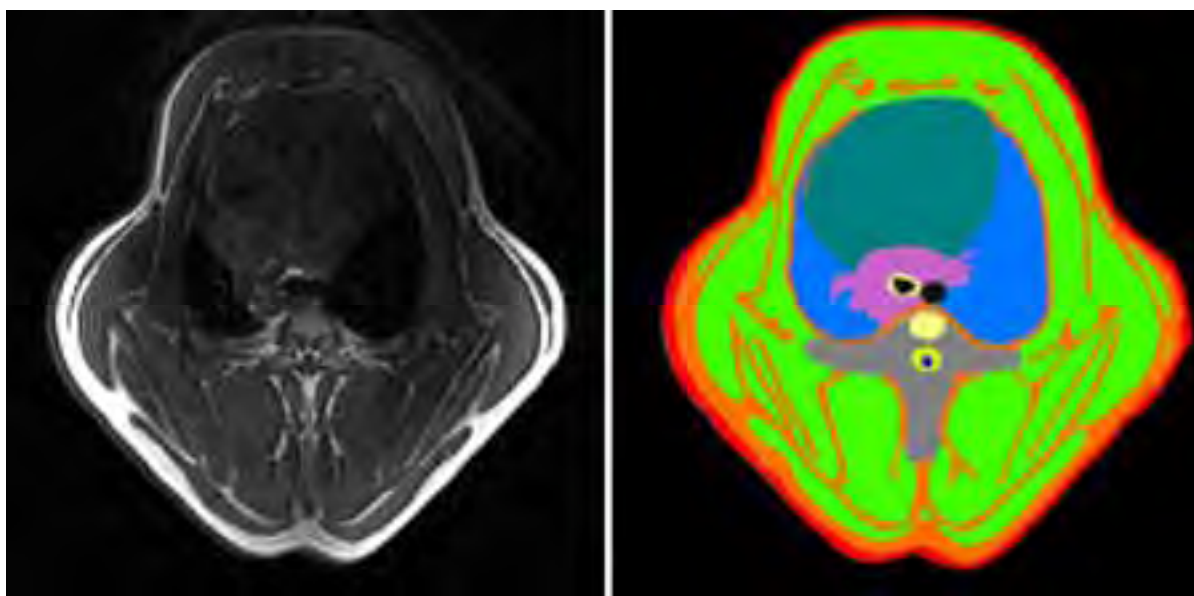


Figure 2. To the left, an unprocessed MRI image from the torso of the swine carcass. An image from approximately the same area after rescaling and initial color-coding.

This work was funded by the U.S. Air Force and U.S. Navy (Project Numbers: 0602236N/M04426.w6, 0601153N/M4023/60182). This research was in compliance with the Animal Welfare Act and adhered to the principles enunciated in the Guide for the Care and Use of Laboratory Animals per SECNAVINST 3800.38B. The views, opinions, and/or findings contained in this report are those of the authors and should not be construed as official Dept of the Air Force, Dept of the Navy, Dept of

Defense, or U.S. government position, policy, or decision unless so designated by other documentation. Trade names of materials and/or products of commercial or nongovernment organizations are cited as needed for precision. These citations do not constitute official endorsement or approval of the use of such commercial materials and/or products. Approved for public release; distribution unlimited.

## Epidemiology

P-B-53

**ASSESSING THE RELATIVE IMPACT OF FACTORS THAT INFLUENCE RF EXPOSURE FOR MOBILE PHONES.** L. S. Erdreich<sup>1</sup>, M. D. Van Kerkhove<sup>1</sup>, C. Scrafford<sup>2</sup>, M. Shum<sup>3</sup>, M. A. Kelsh<sup>3</sup>. <sup>1</sup>Exponent, Inc., New York, NY, <sup>2</sup>Exponent, Inc., Washington, DC, <sup>3</sup>Exponent, Inc., Menlo Park, CA.

**Purpose:** Our study was designed to measure how environmental factors and characteristics of cell phone use affect radiofrequency (RF) power output, a surrogate measure of individual exposure from mobile phone use. Variability in power output is known to occur based on engineering principles, but the parameters that affect the required RF output power have not been characterized quantitatively under typical usage patterns. We assess variability among calls as part of an exposure assessment study designed to develop exposure metrics for future epidemiologic studies. While subscriber records can minimize recall bias in self-reported years or minutes of use, these methods are unlikely to be available for long term information, and do not capture potential significant variations in the level of RF power. Using software-modified phones (SMPs), we examine power control levels (PWC) among individuals, to determine the effect on exposure of different geographic areas and characteristics of phone use such as location and mode of travel.

**Methods:** Data were gathered on call time, date, duration, and the RF power control by SMPs that use GSM (Global System for Mobile) technology. The SMPs record the RF PWC of mobile phones to monitor variations in RF power output. To obtain sample cellular telephone data for each subject, subjects were instructed to use the SMP over a period of five days, including weekdays and weekend days.

The SMP can collect data for 3.0 hours of talk time, collecting power output data every 2.5 seconds. Data on where and when the individual used the SMP were collected by means of a logbook during the five-day study period in which the individual noted situational factors such as urban/suburban; indoor/outdoor; clear/rainy; and use of hands-free device for each call made during the study period. Because all the modified phones are the same model, the effect of phone design and antenna geometry is constant. Demographic information was collected from the study subjects via a self-administered online questionnaire at the time of study enrollment. The questionnaire collected data such as birth date, gender, occupation, as well as typical phone use patterns.

**Results:** Subjects were recruited from three study areas (SA): Southern New Jersey representing a young adult population; New York City representing an adult population; and an adult population from the San Francisco Bay area; for a total of 53 subjects. Compliance increased as the study progressed (SA 1=77.7%, SA2= 82.8%, SA3=89.0%). Reasons for dropping the study included difficulties with the SMP and inconvenience of using the logbook.

Our findings suggested significant differences in per call average output level for several behavioral and situational factors. Average energy output per call differed by urbanicity, however this varied by geographic location. The PWC was higher for calls made while stationary vs. moving in all three study

areas. As expected, the relationship between length of call and RF energy output per call was strong, and calls made indoors had higher average energy output per call compared to calls made outdoors. There was little variation across weekday versus weekend calls in all study areas. Data were combined in a multivariate stepwise regression. The highest predictors of power output were study area and movement, with modest contributions from location (indoor/outdoor.)

Discussion and Conclusions: Other studies have assessed factors that influence power output in general, such as geographic areas with different base station densities, or driving versus walking in urban areas (Wuart et al, 2000l; Lonn et al, 2004). These results suggest that cell phone power output, and therefore potential human exposure, differs among calls made from different locations within the same geographic region, as well as among calls made from different geographic regions. These data provide guidance for making preliminary estimates of the range of exposure variability determining sample size for surveys of actual users, and for incorporating use patterns in exposure metrics for epidemiologic studies.

This research is sponsored by the Cellular Telecommunications & Internet Association (CTIA) under a Collaborative Research and Development Agreement (CRADA) with the US Food and Drug Administration (FDA). This study was reviewed by the Western Institutional Review Board (WIRB).

	Study Area 1	Study Area 2	Study Area 3
Subjects (n)	11	22	20
Geographic region	Southern New Jersey (Suburban)	New York City (Urban)	San Francisco Bay Area (Urban/Suburban)
Mean age (range)	19.8 (18-22)	31.7 (18-45)	35.1 (23-50)
# Calls during study period	580	1193	573
Average duration of calls (range)	1.9 (0.08 - 58.2)	2.0 (0.08 - 70.0)	2.65 (0.04 - 51.63)

Table 2. Bivariate Analysis of Behavioral and Situation Variables

Predictor		SA1		SA2		SA3	
		Energy Output Per Min <sup>1</sup>	P-value <sup>2</sup>	Energy Output Per Min <sup>1</sup>	P-value <sup>2</sup>	Energy Output Per Min <sup>1</sup>	P-value <sup>2</sup>
		Mean		Mean		Mean	
Location	Inside	40.8	NS	33.9	<0.001	27.1	0.006
	Outside	35.7		22.6		20.4	
Urbanicity	Suburban	39.7	NS			24.6	NS <sup>3</sup>
	Rural	—				29.9	
	Urban	51.9				23.5	
Movement	Moving	34.2	0.001	19.7	0.001	19.6	<0.001
	Not moving	42.0		30.6		27.7	
Day of Week	Weekend	38.8	NS	27.3	NS	28.6	0.036
	Weekday	40.7		29.5		23.2	
Mode	Hands-Free	19.9	<0.001	28.0	NS	23.5	NS
	No Hands-Free	42.9		29.1		24.2	

<sup>1</sup>Because energy output per minute was not normally distributed, non-parametric tests were performed.

Parametric and non-parametric results were similar.

<sup>2</sup>Mann-Whitney Test unless otherwise noted

<sup>3</sup>Kruskal-Wallis Test

**RELATIONSHIP BETWEEN URINARY MELATONIN LEVELS AND EXTREMELY LOW FREQUENCY MAGNETIC FIELDS FOR THE SELECTED PRIMARY SCHOOLCHILDREN LIVING NEARBY AND AWAY FROM OVERHEAD TRANSMISSION POWER LINE.** S. C. Hong<sup>1</sup>, Y. S. Cho<sup>2</sup>, Y. Shin Kim<sup>3</sup>.

<sup>1</sup>Dept. of Occupational Health & Safety Engineering, College of Biomedical Science & Engineering, Inje Univ, Korea, <sup>2</sup>Indoor Air Quality Research Laboratory, National Institute of Environmental Research, <sup>3</sup>Institute of Environmental and Industrial Medicine, College of Medicine, Hanyang Univ, Seoul, Korea.

**Objectives:** The present study investigated the hypothesis that a extremely low frequency magnetic field partially suppresses the synthesis of melatonin in a group of 28 primary schoolchildren living nearby and 60 primary schoolchildren aged 12 years living far away from overhead transmission power lines from December 2003 to April 2004 in Seoul, Korea.

**Methods:** All subjects were measured for personal 24hr continuous exposure, using EMDEX 2 and EMDEX Lite, recorded total urine volume, the clock time of urination before sleeping necessarily, and the clock time of urine sampling. At the same time, the submitted a logbook for identification of their daily activity pattern, for example, time to go to school/home and the dietary habits that were taken in their 1 week before sampling days. Nocturnal melatonin and growth hormone were analyzed by radioimmunoassay and enzymeimmunoassay, respectively.

**Results:** The mean personal exposure levels of the primary schoolchildren living nearby overhead transmission power line were 0.37 uT, whereas the value for the primary schoolchildren living away from overhead transmission power line 0.05 uT. From simple analysis, the mean melatonin levels in the primary schoolchildren living nearby were lower than those levels away from overhead transmission power line, but not statistically significant differences in the levels of the melatonin ( $p=0.2421$ ), whereas the statistically significant differences in the levels of the melatonin related to the distance from residence to power line less and more than 100 m by cut-off point ( $p=0.0139$ ). In multiple linear regression analysis, a distance from residence to power line ( $p=0.0146$ ) and dietary habit about burned meat ( $p=0.0170$ ) seemed to be significant risk factors in the mean nocturnal melatonin levels in the primary schoolchildren.

**Conclusions:** In conclusion, these results demonstrate that urinary levels of nocturnal melatonin are not altered in primary schoolchildren exposed to extremely low frequency magnetic field (ELF-MF) at overhead transmission power line.

Urinary Melatonin log-transmitted levels (ng/g creatinine) in relation to exposure, distance from residence to powerline, dietary habit about burned meat, dietary habit about fast-food, and status of electric sheet usage

Variables	Na (%)	AMb	SDc	Range	P-value
Exposure group					
Nearby powerlines	28 (31.8)	2.06	0.24	1.55-2.43	0.2421
Away from powerlines	60 (68.2)	2.11	0.21	1.55-2.55	

Distance from residence to powerline					
Less than 100m	22 (25.0)	2.00	0.25	1.55-2.35	0.0139
More than 100m	66 (75.0)	2.13	0.20	1.55-2.55	
Dietary habit(burned meat)					
1 time less than per week	13 (14.9)	1.96	0.23	1.65-2.38	0.0471
2 to 5 times per week	53 (60.9)	2.12	0.21	1.55-2.55	
5 times more than per week	21 (24.2)	2.12	0.21	1.55-2.45	
Dietary habit(fast-food)					
1 time less than per week	53 (61.6)	2.11	0.22	1.55-2.55	0.2443
2 to 5 times per week	31 (36.1)	2.07	0.22	1.55-2.41	
5 times more than per week	2 (2.3)	2.32	0.03	2.30-2.34	
Status of electric sheet usage					
Yes	6 (6.8)	2.02	0.27	1.74-2.43	0.3699
No	82 (93.2)	2.10	0.22	1.55-2.55	

## P-B-59 STUDENT

**A COMPARISON OF PERSONALITY AND OTHER INDIVIDUAL-RELATED FACTORS IN SUBJECTS WITH MOBILE PHONE RELATED SYMPTOMS AND SUBJECTS WITH ELECTRICAL HYPERSENSITIVITY - A QUESTIONNAIRE STUDY.** A. Johansson<sup>1</sup>, M. Sandström<sup>1</sup>, S. Nordin<sup>2</sup>. <sup>1</sup>National Institute for Working Life, <sup>2</sup>Dept of Psychology, Umeå Univ.

**INTRODUCTION:** Among researchers in the field of “idiopathic environmental intolerance” it is a common view that the development of intolerance of this kind is determined by interplay between sensitivity to physical/chemical exposure and psychological factors. However, there is not enough data to determine the importance of the possible external and internal causes. To what extent do individuals with different types of “environmental illness” differ from the general population in terms of personality traits etc.? It is also not clear whether the different subtypes of environmental illness (e.g. perceived electromagnetic hypersensitivity, subjective symptoms associated with mobile phone-use, building-related illness, multiple chemical sensitivity) differ from each other concerning individual-related parameters.

Previous, neurophysiological studies have indicated a relationship between subjective symptoms related to various environmental factors and an elevated autonomic stress response. This indicates that not only physical stressors may be of importance in the development of environmental intolerance, but also individual factors such as personality, stress, anxiety etc. Results from our previous studies, where we have focused on persons with perceived electromagnetic hypersensitivity and persons with subjective symptoms related to the use of mobile phones, support this idea. However, our earlier studies also indicate that these two groups may differ with respect to personality and other individual-related factors.

**OBJECTIVES:** The overall aim of the study is to investigate possible differences between people with perceived electromagnetic hypersensitivity, people with subjective mobile phone-related symptoms and healthy control subjects with respect to individual-related factors such as personality traits, anxiety, depression, perceived stress, cognitions about body and health, quality of life, somatic manifestations and general environmental sensitivity.

**METHODS:** Fifty subjects reporting general electromagnetic hypersensitivity, 50 subjects reporting mobile phone related symptoms and 100 controls, matched with respect to age and gender, will be recruited. Personal characteristics of the subjects, the nature of their symptoms and the individual-related factors mentioned above will be registered by means of validated questionnaires distributed by mail. Processing and interpretation of the questionnaire data will be performed according to established manuals.

**RESULTS:** The presentation will include a description of the measured variables, the questionnaires used, the study protocol and the time schedule.

P-B-62

**ASSESSMENT OF PERSONAL EXPOSURE TO EXTREMELY LOW FREQUENCY MAGNETIC FIELDS FOR THE SELECTED PRIMARY SCHOOLCHILDREN LIVING NEARBY AND AWAY FROM A OVERHEAD TRANSMISSION POWER LINE.** Y. S. Kim<sup>1</sup>, Y. J. Hyun<sup>1</sup>, S. C. Hong<sup>2</sup>. <sup>1</sup>Institute of Environmental and Industrial Medicine, College of Medicine, Hanyang Univ, Seoul, Korea, <sup>2</sup>Dept. of Occupational Health & Safety Engineering, College of Biomedical Science & Engineering, Inje Univ, Korea.

**Objectives:** The objectives of this study were to analyze and compare 24 h personal exposure levels of MF at microenvironments such as home, school, educational institute, internet personal computer game room, transportation, and other places according to time activity patterns using various metrics for children attending the primary schools located near and away from the power lines. And we characterize the major microenvironments and impact factors attributed personal exposure level. Also, it was to evaluate personal exposure estimated using a time activity pattern and microenvironmental model.

**Methods:** The study was carried out for 44 school children attending a primary school away from the lines(school A) and 125 children attending a school away from 154 kV power lines(school B), all who aged 12 years and were 6 grade, from July 2003 to December 2003. All participants filled in a questionnaire about general characteristics, residence, use of electrical appliances and others. Children wore a small satchel in which EMDEX II and Lite (Enertech, Co. Ltd) and a diary of activity list for period of registration in 20 minutes blocks. All statistical calculations were made with the SAS System, Release 6.12.

**Results:** For the children attending school A, the results indicated that average 24 h personal exposures was well represented by exposure level at home because of high correlations and high time spent at home. The other hands, for children attending school B, the more residence close to the power line, the higher the personal exposure level, and the exposure level at school was more correlated with personal exposure level than these at home. Significant major variable was the distance from the power line to home, in which personal exposure for children living near the line(150m).

The various type of microenvironmental model (TWA model) and time activity were used to estimate the personal exposure level. For children attending school A, the estimated personal level was a little weak correlated with the measured level (Pearson  $r = 0.34 \sim 0.35$ ). This difference between the measured level and estimated level was caused by the activity at other place in school. For children attending school B, the correlation was very low (Pearson  $r = 0.09 \sim 0.16$ ) using the TWA Model II, otherwise, TWA Model II-1 which considered the average residential MF level according to the distance from the power line and home explained 39 ~ 53 % of the correlation in MF personal exposures. The estimated personal exposure level was very well represented the measured exposure level using TWA Model II-2 which consisted on spot and 24 h stationary measurements at subject's home (Pearson  $r = 0.65 \sim 0.85$ ).

Conclusions: In conclusion, the significant major determinants of personal exposure level is the distance from the power line to residence, and exposure from power lines might totally overshadow exposure from local sources in the home. Spot and stationary measurements are not assess totally the personal exposure level, but when we used the TWA Model II-2 which considered these measurements at home and other microenvironments, the association between estimated personal exposure and measured level are very higher than the results of TWA Model II. Therefore, personal magnetic field exposure estimated using a TWA Model II-2 provided a reasonable estimate of measured exposure for schoolchildren living near the power line.

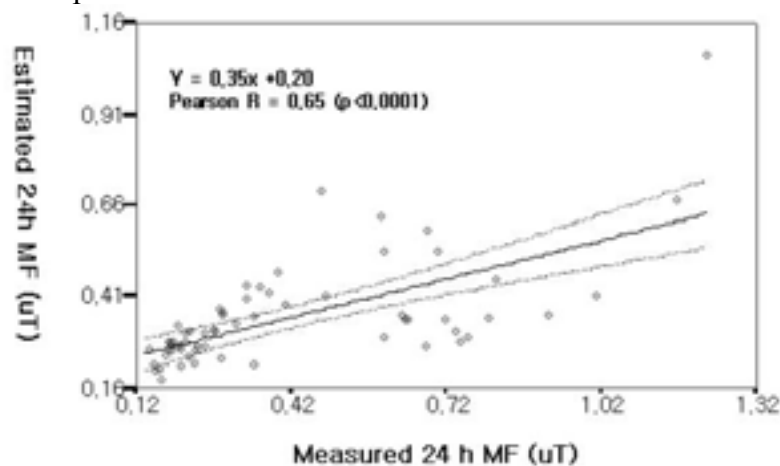


Figure 1. Association between arithmetic means of 24 h measured personal magnetic field exposure and estimated magnetic field exposure, showing regression line with 95% confidence limites by time weighted average model (TWA Model II-2 for children attending a school near the line.

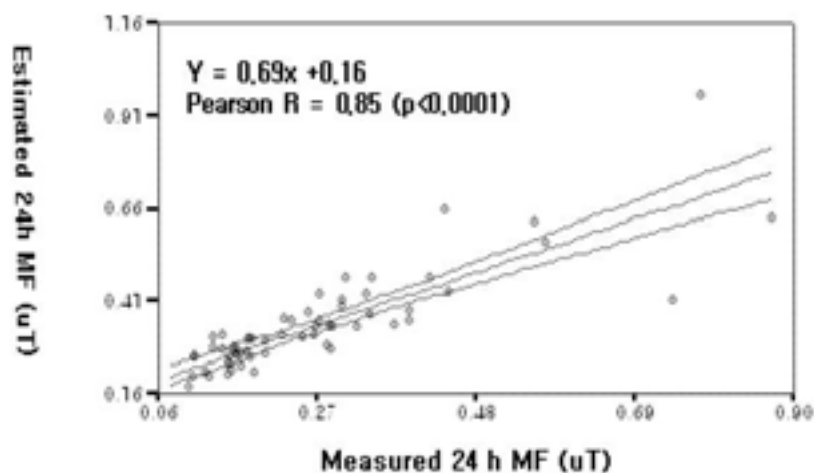


Figure 2. Association between geometric means of 24 h measured personal magnetic field exposure and estimated magnetic field exposure, showing regression line with 95% confidence limits by time weighted average model (*TWA Model II-2* for children attending a school near the line).

P-B-65 STUDENT

**PATTERNS OF USE OF THE TETRA COMMUNICATION SYSTEM AMONGST TWO POLICE FORCES IN THE UK.** I. Litchfield, T. Sorahan. The Institute of Occupational and Environmental Medicine, The Univ of Birmingham, Edgbaston, Birmingham, UK.

The study was undertaken to investigate the patterns of use of the Airwave communication system amongst police officers and police staff in the United Kingdom as part of a larger study funded by the Home Office. The Airwave system was designed to be used by the Emergency Services in the UK and is built to the TETRA standard. When completed it will be the largest TETRA network in the world.

The study used a questionnaire to collect information on Airwave use amongst police officers and police staff co-workers. The first section of the questionnaire collected information on force, rank, division or Local Policing Unit (LPU), Airwave terminal number and duty start and end time. The second section allowed for the participant to record the number of calls made from several locations and whether the radio used was a handheld or vehicle set. The number of minutes during the shift that were spent using non-Airwave mobile telephony was also recorded.

This questionnaire was distributed amongst two police forces, one rural and the other primarily urban to record any potential difference between geographical locations. Each force selected five police stations or LPUs to partake in the study. In order to ensure that a full range of job types and titles were incorporated in the study, all staff that use Airwave at each location were invited to participate. At each location this meant that a minimum of 75 staff were invited to join the study. The questionnaires were distributed in Summer 2003 (phase I) and Winter 2004 (phase II) so that any seasonal variation could be

observed. In addition, data from the Call Detail Records (CDR) were used to determine the percentage of each type of call made during the months surveyed.

Over the course of the study, the urban force completed nearly 400 questionnaires and the rural force 1375. The questionnaires were analysed according to rank, day and shift. Each phase of the study was analysed independently and together. Finally the median number of calls was calculated for both phases and both forces and was 2.2 calls per hour. Each shift (each completed questionnaire) was then categorised as “high usage” ( $\geq 2.2$  calls per hour) or “low usage” (< 2.2 calls per hour). The simultaneous investigation of rank and season (summer = April-September; winter = October-March) as determinants of heavy use of Airwave was undertaken and demonstrated that the odds of being a heavy user were significantly lower in the winter months.

Finally the simultaneous investigation of rank, season, phase of the study, shift, force (urban/rural) and day (weekday/weekend) as determinants of heavy use of Airwave was conducted. The figures showed that PC is the rank with the highest usage, and that this effect is independent of all the other variables considered. The odds of being a heavy user were significantly lower in phase II of the study, in later shifts (particularly the night shift), and the rural force. The figures for non-Airwave mobile telephony showed that the rural force used it more than the urban force with the highest figures recorded by Community Support Officers in the rural force who used it on average 1.26 minutes a day.

The Call Detail Records were analysed for each phase of the study to determine the percentage of calls that were emergency, group or private. In the urban force private calls accounted for 7.8% and 8.1% for August 2003 and February 2004 respectively, group calls 91.8% in August 2003 and 92.1% in February 2004. Emergency calls were 0.1% for both phases. In the rural force private calls account for 4.2% in August 2003 and 4.4% in February 2004, group calls 95.8% August 2003 and 95.6% February 2004 and emergency calls were less than 0.1% for both phases.

It will be possible for later studies of health effects to make use of this information in order to estimate occupational RF exposures of Police staff. In addition, a number of variables were found to be independent predictors of high/low usage. The odds of being a high user were significantly increased in PCs, later shifts and the rural force, and significantly reduced in phase II of the study. The latter finding is likely to be an artefact of data collection such that staff may have recorded calls less enthusiastically in phase II and we do not propose that much attention be given to this particular finding.

RF exposures to current Airwave users are well below the currently recommended maximum occupational exposure levels. If such exposure levels were to be dramatically reduced in the future, then it follows that the exposures received by PCs working the night shift in a rural setting should be given special attention, because as long as RF safety precautions are in place for this group then all other groups will also be protected.

Rank	Low user (n)	High user (n)	Odds Ratio (95% C.I.)
PC	652	792	1.0
Sgt	140	79	0.50*** (0.37 to 0.68)

C.S.O.	17	6	0.31* (0.12 to 0.82)
SOCO	10	7	0.60 (0.23 to 1.61)
Inspector	33	6	0.15*** (0.06 to 0.37)
Traffic Warden	12	5	0.57 (0.20 to 1.66)
Season			
Summer	654	721	1.0
Winter	210	174	1.09 (0.81 to 1.50)
Phase			
I	398	451	1.0
II	407	444	0.77* (0.61 to 0.98)
Shift beginning			
0600 to 1100	502	364	1.0
1200 to 1700	237	313	1.76* (1.40 to 2.20)
1800 onwards	116	213	2.49* (1.90 to 3.27)
Force			
Leicestershire	204	141	1.0
West Mercia	660	754	1.81* (1.38 to 2.37)
Weekday/weekend			
Weekday	628	647	1.0
Weekend	236	248	.95 (0.76 to 1.18)
* P <0.001			

## Human studies

P-B-68

**GEOMAGNETIC FIELD EFFECT ON AFFECTIVE AND COGNITIVE COMPETENCE IN CHILDREN.** J. Gmitrov<sup>1</sup>, V. Gmitrova<sup>2</sup>. <sup>1</sup>Internal Specialist Polyclinic, Presov, Slovak Republic, <sup>2</sup>Dept of Education of City Council in Presov, Slovak Republic.

OBJECTIVE: The goal of our research was to study the effect of geomagnetic field (GMF) disturbances,

in terms of K, Kp, Ak, Ap, and SK indices, on children's affective (emotional) and cognitive competence during different forms of organization of pretend play.

**METHODS:** We studied two forms of management of the playing process: 1) teacher-directed frontal play with simultaneous involvement of all children in the classroom and 2) child-directed play in various small groups. Twenty-six lessons were performed on 51 children (one lesson daily) in mixed-age classrooms. The mean age of the children was 4.6 years, with age span from 3 to 6 years. The duration of the lessons was 20-25 min. Data were collected regarding children's affective and cognitive behaviors according to generally accepted taxonomies from Bloom for the cognitive domain and Krathwohl for affective domain. A frequency count of every behavior was calculated during each particular lesson, comprising the unit of the analysis. Similarly, teacher's educational performance was measured by the sum of educational stimuli used to direct the playing process during the lesson. The values of geomagnetic indices were kindly supplied by the nearby Magnetic Observatory in Hurbanovo (Slovakia).

**RESULTS:** GMF effect depended of the on the type of the organization of the educational process. During child-directed play children's behavior was negatively correlated with geomagnetic disturbance in both affective and cognitive domains as compared with teacher-directed play where there was no significant interaction. Similar to children, teacher's educational performance negatively correlated with GMF disturbance only during child-directed play.

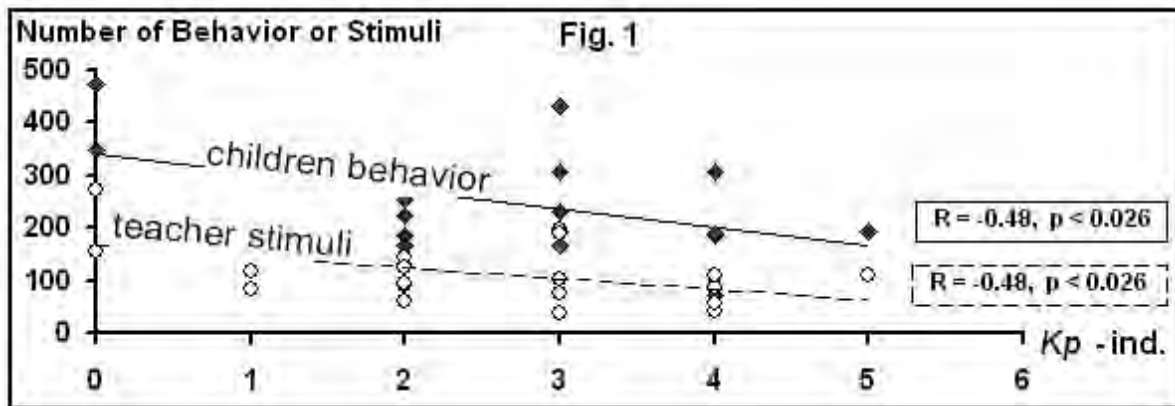


Fig. 1. The analysis of the relationship between GMF disturbance (reflected by Kp-index) and children's behavior (filled squares, solid line) or between GMF disturbance and teacher's behavioral stimuli (open rings, dashed line) during child-directed pretend play. Each square represents the sum of all children behaviors (affective + cognitive), rings - the sum of teacher's stimuli, which occurred during 1 lesson [1].

**CONCLUSIONS:** We believe the dependence of the GMF effect on the type of the organization of the educational process is explained by the less-stressful environment of the child-directed playing conditions compared with teacher-directed in which the directive role of the teacher can mask GMF effect. Similar to children, GMF impact on teacher's educational performance only during child-directed playing conditions is probably linked with free-flow character of the playing process demanding creative improvisations with larger involvement of teacher's emotional and cognitive potential. This may result in a larger sensitivity to external disturbing factors compared with strict organization of the teacher-directed frontal play that suppress spontaneous behavior - the key condition to display GMF effect both in children or adults. The worsening of the cognitive and affective performance during GMF disturbance may be the result of facilitation of the inhibitory processes in CNS and probably is linked with increased

incidence of nervous and psychical disorders including depression, suicidal peaks, and traffic accidents, which have been observed during geomagnetic storms [2].

#### References

- [1] J. Gmitrov, V. Gmitrova (2003) *Electromagnetic Biology and Medicine* 22:203-215  
[2] E. Stoupe (1995) *Int J Biometeorol* 38:199-204

P-B-71

**THE EFFECTS OF 900 MHZ GSM WIRELESS COMMUNICATION SIGNAL ON SUBJECTIVE SYMPTOMS, PHYSIOLOGICAL REACTIONS, ALERTNESS, PERFORMANCE AND SLEEP, AN EXPERIMENTAL PROVOCATION STUDY.** L. Hillert<sup>1</sup>, T. Åkerstedt<sup>2</sup>, N. Kuster<sup>3</sup>, A. Lowden<sup>2</sup>, M. Berg<sup>4</sup>, C. Wiholm<sup>5</sup>, S. Ebert<sup>3</sup>, S. D. Moffat<sup>6</sup>, B. B. Arnetz<sup>5</sup>. <sup>1</sup>Dept of Public Health Sciences, Div of Occup Med, Karolinska Institutet and Occup and Environ Health, Stockholm, Sweden, <sup>2</sup>IPM, Karolinska Institutet, Stockholm, Sweden, <sup>3</sup>IT'IS Foundation, Swiss Federal Inst of Technology, Zurich, Switzerland, <sup>4</sup>Dept of Medical Sciences, Div of Dermatol, Uppsala Univ Hospital, Uppsala, Sweden, <sup>5</sup>Dept of Public Health and Caring Sciences, Uppsala Univ, Uppsala, Sweden, <sup>6</sup>Inst of Gerontology and Dept of Psychology, Wayne State Univ, Detroit, MI, USA.

**INTRODUCTION:** Health complaints as heat sensation, headache, difficulties concentrating and fatigue have been reported to be triggered by the use of mobile phones. Some studies have indicated effects of radio frequency fields (RF) on symptoms, cognitive functions, blood pressure and sleep while other studies did not show any effects. Further investigations of these possible biological effects are motivated. The present provocation study focuses on acute effects of radio frequency fields relevant to the exposure situation of mobile phone users. A multidisciplinary team will investigate interactions of environmental (RF, heat), physiological (individual physiological response patterns), and social (stress induced through test during the exposures) factors. Data collection has started during 2004 and will continue during 2005.

**OBJECTIVE:** To establish whether exposure to radio frequency fields (RF) caused by mobile phone use during the day has any acute effect on:

1. Self-reported symptoms such as headache, skin irritation, and sensations of heat
2. Biological correlates to subjective symptoms (e.g. skin temperature, serum levels of stress-related hormones, breath rate)
3. Cardiovascular system with regard to blood pressure, heart rate, heart rate variability
4. Sleepiness and performance
5. Subsequent night sleep

Specific hypotheses tested:

1. Exposure to radio frequency fields (RF) caused by mobile phone use leads to a significant increase in systolic blood pressure and heart rate.
2. Exposure to radio frequency fields (RF) caused by mobile phone use leads to a decrease in response time in simple serial reaction test and vigilance test.
3. Exposure to radio frequency fields (RF) caused by mobile phone use leads to a change in cerebral electric oscillations, particularly in cognitive processes.
4. Exposure to radio frequency fields (RF) caused by mobile phone use leads to a change in cerebral electric oscillations during subsequent sleep.

**METHODS:** The study is designed to study effects of electromagnetic fields consistent with the exposure during mobile phone use. The exposure setup was developed and installed by the Foundation ITIS (Zurich, Switzerland). The setup enables the exposure of the left head hemisphere and is designed to maximize the exposure of brain tissue as may occur during actual usage of GSM phones. The system is based on a low-weight, stacked micro patch antenna fixed on a headset and allows the subject to move/rotate within a limited area without changing the exposure distribution, this allows flexible and comfortable exposure situations and also simultaneous recording of an EEG. A fully computer-controlled signal unit allows the application of GSM modulated RF exposures for two different subjects. The RF exposure is monitored, controlled and recorded in an encoded file at all times and is in compliance to double blind exposure protocols. The exposure signal was chosen with respect to exposure strength (SAR), GSM modulation (DTX, power control), time course of exposure and consist of a GSM signal at an average SAR of 1.4 W/kg simulating a conversation, i.e., including periods of DTX (active during talking) and Non-DTX (active during listening). A 2 degree increase in skin temperature of the ear lobe is induced during all sessions by laser heating of a small ceramic plate. The chosen exposure will ensure that the study meets the ethical standards for human studies, as the RF exposure is equivalent to that of frequent users and will not exceed the ICNIRP guidelines. Each exposure session is three hours. The study group will consist of 80 subjects, age 20 to 45. Forty subjects in the study group are chosen based on self-reported symptoms in relations to mobile phone use. Exclusion criteria are medical or psychological illness where current symptoms can not be excluded, present medication, sleep disorders, hypertension and ongoing pregnancy. EEG, heart rate, and skin temperature are continuously monitored from two hours before the start of exposure at 7.30 PM. EEG and heart rate monitoring will be continued throughout the night. Symptoms are reported, blood pressure taken and blood samples drawn before, after 1 ½ hour as well as at the end of the exposure sessions. Blood analyzes include serum levels of e.g. Prolactine, Thyroxine, Growth Hormone, DHEAS. Cognitive tests before and during exposure include tests for vigilance, simple reaction time and spatial memory.

**RESULTS AND DISCUSSIONS:** The study will provide new knowledge on possible safety or health risks of mobile phone use with special focus on sleep, sleepiness and performance, cardiovascular effects, headache, and skin irritation. We will report the specific study design and preliminary results of comparisons between the group of subjects reporting complaints in relation to mobile phone use and the symptom free group regarding base line data and reactions during test sessions (regardless of exposure).  
Research Funding: Mobile Manufacturers Forum (MMF)

P-B-74

**A SURVEY ON ELF MAGNETIC FIELDS AROUND STUDENTS DURING THEIR LAB HOURS IN ELECTRICAL AND ELECTRONIC ENGINEERING DEPT AND MECHANICAL ENGINEERING DEPT.** K. Isaka, N. Matsuuchi, M. Kawada, K. Yamaji, M. Masuda. Faculty of Engineering, The Univ of Tokushima, Japan.

Experimental efforts have been paid to clarify the characteristics of ELF magnetic fields around people who stay in residential and occupational environments. Much data has been collected using magnetic field meters and/or dosimeters in a number of epidemiological studies. Its ample data is now available. The minimum requirements for the protection of workers from risks to their health and safety arising or likely to arise from exposure to electromagnetic fields during their work were laid down in the EU community in April 2004 for the electromagnetic environments in the work places. The Univ

engineering students are not workers, but may interact with high magnetic fields in labs in the same manner as workers. It is also important to protect students from the exposure to electromagnetic fields in universities. However no attentions have been paid to this situation. They may stay in the labs for their experimental training in their undergraduate days and/or experimental researches in their graduate days. The ELF magnetic field exposure data has been so scanty for Univ engineering students that we started the measurements of magnetic fields around junior students who were involved in experiments in the labs.

We explained the aim of our research project to the junior students in Electrical and Electronic Engineering Dept and Mechanical Engineering Dept of The Univ of Tokushima, and asked them to carry the dosimeters (EMDEXII, frequency: 40Hz to 800Hz) at their waists during the lab hours. They performed experiments usually for about three hours once a week. About seven students of the Dept of Electrical and Electronic Engineering joined an experiment each week, and continued the eleven kinds of experiments. About seven students of the Dept of Mechanical Engineering performed the three kinds of experiments in the same way. The measurement data was collected for the following fourteen kinds of experiments:

1. Lighting ( characteristics of fluorescent lamp and incandescent electric lamp }
2. relay (application of relay circuit to power circuit)
3. transmission and distribution line simulators
4. Control of DC shunt motor
5. Control of DC shunt generator
6. Control of DC series motor
7. Operation of transformers
8. Control of currents using thyristor
9. Control of separately excited motor
10. Control of three-phase induction motor
11. Single phase three-wire type power line
12. Processing using milling machine
13. Electric welding
14. Processing using NC lathe

It was found from the measurement results that the average of the time-weighted average of magnetic fields of each student is the highest for the experiment on electric welding, and the second highest for the experiment on relay for an electric power circuit. In the experiment using thyristor elements, the harmonic component between 100 and 800 Hz is predominant compared with the 60Hz one. We took out the highest magnetic field from the individual data and it was compared with each other. The highest magnetic field over 200 $\mu$ T was recorded in electric welding experiment. Since the dosimeter was held at a position of one's waist, this meter might collect the magnetic fields from the nearby current- carrying conductor. If the meter had been held at the other side of the waist, the recorded magnetic fields would have been much lower than the data obtained. In fact, it is important to use a number of dosimeters to measure personal exposure values in case the distribution of magnetic fields is non-uniform and localized in some places.

In order to protect the students from the excess amount of exposure to magnetic fields, we employed the method for suppressing the ELF magnetic fields to which the students were exposed during those two experiments. The basic principles for this method are to make the conductors, in opposite current directions, closer to each other so that the cancellation of magnetic fields is anticipated, and/or to make the current loop smaller so that the induced magnetic fields decrease predominantly with distance. With these principles in mind, the electric circuits for the two experiments were modified, resulting that the

magnetic fields were found to be smaller enough on relay experiment, and moderately on welding experiments.

P-B-77

**DOES THE IMPLANTATION OF AN ICD LEAD TO A WORK INAPTITUDE IN AN ELECTRICAL COMPANY?** I. Magne<sup>1</sup>, M. Souques<sup>2</sup>, M. Héro<sup>3</sup>. <sup>1</sup>EDF R&D, Les Renardi&egraveres, Moret sur Loing, France, <sup>2</sup>SERVICE DES ETUDES MEDICALES, EDF Gaz de France, Paris, France, <sup>3</sup>MEDTRONIC FRANCE, Boulogne Billancourt, France.

#### Objective

An EDF worker had been implanted with a ICD. His occupational doctor had to define his work aptitude. This person was working in hydroelectric plants, so was exposed to 50Hz magnetic field. The ICD may be perturbed by magnetic field, and the risk had to be evaluated. From this case study, we present in this paper our approach to define the work aptitude or inaptitude.

#### Method

The protocol consists in measuring magnetic field in the presence of implanted worker. A pluridisciplinary team performed the study: the cardiologist was there with cardiac reanimation material; the ICD constructor questioned the ICD with the telemetry material and the engineer performed magnetic field measurements. All areas of the hydroelectric plants where the worker could go were visited (substations, alternators, turbines, control rooms, proximity of cables), beginning with the areas of lowest magnetic field, and questioning the ICD in all situations.

#### Results

The ICD was Medtronic, bipolar and a 0.3mV sensitivity setting. In the different areas, 50Hz magnetic field has been measured from 0 to 650<sup>3</sup>/<sub>4</sub>T at the ICD location. No dysfunction of the ICD has been seen with the bipolar mode.

#### Conclusion

Following these measurements, this person has been declared apt to work and has worked again in hydroelectric plants. Six months after, no incident has been reported. This example shows the interest of measuring magnetic field and questioning the implant in the same time, at the different working places, in order to evaluate risks of ELF interference and to help the occupational doctor to define the work aptitude or inaptitude.

P-B-80

**HEARING LOSS EVALUATION IN CHILDREN EXPOSED BY ANTENNA OF 1062 KHZ MEDIUM WAVE RADIOBROADCASTING STATION.** F. Meric<sup>1</sup>, S. Dasdag<sup>2</sup>. <sup>1</sup>ENT Dept of Dicle Univ Medical Faculty, Diyarbakir, Turkey, <sup>2</sup>Biophysics Dept of Dicle Univ Medical Faculty, Diyarbakir, Turkey.

The affects of RF and microwave radiation on human have been a subject of continuing investigations. Since one of the major exposed children is that who has been living in houses provided to employees of

radio broadcasting and TV transmitter stations the present study intended to investigate whether radio-frequency (RF) affects auditory system of children exposed to RF by means of antenna of 1062 kHz medium wave radio-broadcasting station.

The study was carried out on 25 voluntary children (Boy: 13, Girl: 12) living in house provided to workers of radio-broadcasting station mentioned above because of their parent's job. A portable pure tone audiometer (Mercury, M.158 Audiometer) used to evaluate hearing of all the children under investigation. Ten of the children (Boy: 6, Girl: 4) have been living in these houses since they born while living duration of 15 children in this area have been changing from 2 years to 11 years. Sensory neural and conductive hearing loss was observed 5 of children (Boy: 3, Girl: 2). Typically, SNHL was observed in boys while the conductive hearing loss observed. Hearing losses were observed on right ears of the experimental subjects except one of the children has hearing loss problem. However, two types of the hearing loss observed in these 5 children in experimental group were at minimal level. On the other hand, comparison of the control and the exposed subjects shown that right ears of the exposed children affected by radiofrequencies at 500Hz ( $p < 0.05$ ).

Additionally, hearing levels of the ten of children in experimental group who have been living in these houses since they born were compared with control children. No differences observed in these children of the experimental group ( $p > 0.05$ ).

Power density and E field in houses and playing area of the children was measured by means of EMR300 (NARDA, Pfullingen, Germany). The distance of the antennas to the employee residential houses was between 300 and 350 meters. E field and power density inside houses provided to employees measured between 0.48 V/m - 2.86 V/m and 0.0001 mW/cm<sup>2</sup> - 0.0023 mW/cm<sup>2</sup>, respectively, depending on the distance from the antenna. However, average E field and power density in children's playgrounds were measured as 12.75 V/m and 0.0436 mW/cm<sup>2</sup>, respectively. Average E field and power density outside the playgrounds and employee residential houses were measured as 18.64 V/m and 0.0971 mW/cm<sup>2</sup>.

P-B-83 STUDENT

**GUARD PROJECT: EFFECT OF GSM MOBILE PHONE IRRADIATION ON AUDITORY BRAINSTEM RESPONSE (ABR) AND COCHLEAR MICROPHONY (CM).** F. Molnár<sup>1</sup>, G. Kubinyi<sup>1</sup>, L. Kellényi<sup>2</sup>, G. Thuróczy<sup>1</sup>. <sup>1</sup>National Research Institute for Radiobiology and Radiohygiene, Dept of Non-Ionizing Radiation, Budapest, Hungary, <sup>2</sup>Univ of Pécs, Dept of General Zoology and Neurobiology, Pécs, Hungary.

#### Objectives

The aim of GUARD project was to assess potential changes of the hearing function of animals and humans after exposure to low-intensity electromagnetic fields produced by cellular mobile phones at frequencies of 900 and 1800 MHz.

Highly sensitive methodology is necessary to study the effects of short term RF exposure generated by mobile phones since the energy radiated by cell phones is mostly absorbed in the area of the cochlea and 8th nerve according to liquid phantom dosimetry results. The non-invasive Cochlear Microphony (CM) potential together with the Auditory Brainstem Response (ABR) seems to be localized and sensitive method for human studies.

## Methods

The study was carried out on 20 volunteers (5 men, 15 women) aged  $27 \pm 3$  years. Participants were healthy young adults without any clinical history of hearing disorder. ABR potentials were recorded with three polarized Ag – AgCl electrodes. The active electrode was placed on the left mastoid and the reference electrode over the vertex (Cz of international 10-20 system). The ground electrode was placed on the forehead and connected to the active ground of the biological preamplifier. The preamplifier was set for gain of 100 dB. The upper and lower cut-off frequencies of amplifier were set at 10,000 Hz and 100 Hz, respectively. Three kind of acoustic stimuli were delivered to the subjects. Condensation, rarefaction and alternating click sound stimuli at 80 dB were applied at rate of 20 Hz and 80 Hz. For measuring ABR evoked potentials the acoustic stimuli were generated by a loudspeaker embedded in a 34 cm long sound tube causing an acoustic delay of 1 ms to separate the electrical artefact impulses from the CM recordings.

The exposure was applied before and after the ABR recording by NOKIA 6310 commercial mobile phone. According to the GUARD protocol the subjects were exposed to 10 min GSM cellular phone irradiation at 900/1800 MHz by a double blind protocol. The SARs on 900 MHz and 1800 MHz at the area of cochlea were 0,41 W/kg and 0,19 W/kg respectively (1).

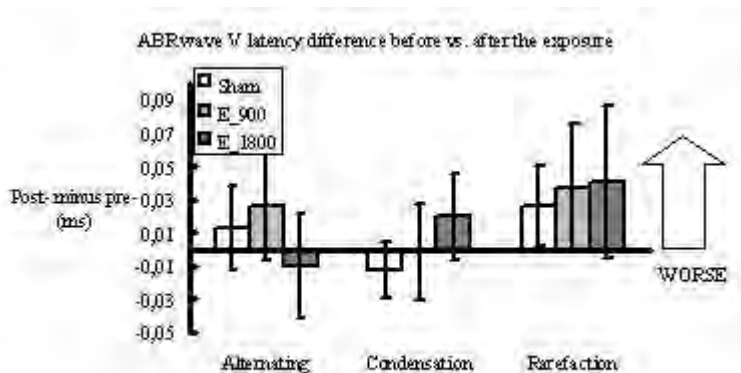
## Results

No significant effects have been found in the latency of V. potential in ABR response (see Fig.) nor in the latency of CM potentials before and after the exposure.

## Reference

(1) Thuróczy et al, BEMS 2004 Annual meeting, P-C-135, p.281

\* This study was partially financed by the European Project GUARD "Potential adverse effect of GSM cellular phones on hearing" (European Commission, 5th Framework Programme, QLK4-CT-2001-00150, 2002-2004)



P-B-86

**MAY THE RF FIELDS EMITTED BY MOBILE PHONES CAUSE HEADACHES? A PROVOCATION STUDY.** G. Oftedal<sup>1,2</sup>, A. Straume<sup>1</sup>, L. Jacob Stovner<sup>3</sup>, A. Johnsson<sup>1</sup>. <sup>1</sup>Norwegian Univ of Science and Technology, Dept of Physics, Trondheim, Norway, <sup>2</sup>Sør-Trøndelag Univ College,

Trondheim, Norway, <sup>3</sup>Norwegian National Headache Center, Dept. of Neurology and Clinical Neurophysiology, St. Olavs Hospital, Trondheim, Norway.

**BACKGROUND:** In a Norwegian-Swedish epidemiological investigation (Ofstedal et al, 2000), we found that headache was the most frequently occurring symptom attributed to the use of the mobile phone. (Then warmth sensations are not regarded as symptoms.) The majority of people reporting about symptoms in connection with the use of mobile phone did not have symptoms when using VDTs. This suggests that many of those attributing headaches to mobile phone use are not “hypersensitive to electricity” in general.

**OBJECTIVE:** The study is designed to investigate whether the radio frequency (RF) fields from mobile phones may cause headaches, changes in the blood pressure and/or changes in heart rate. Subjects to be included should experience headaches in connection with mobile phone calls, but not in connection with electricity in general. We will also describe and classify the headaches experienced by the persons selected to take part in the double blind provocation study.

**METHODS:** We intend to select 30 subjects to take part in the study. The selection criteria and procedure should result in a group with a high probability of having symptoms caused by the RF exposure, if such a connection exists. By using a questionnaire and telephone interviews, people having symptoms in close connection with the use of mobile phones and no indication of being “electrical hypersensitive” in general will be identified. An open test will be performed as the last step. Only subjects getting headaches during or after the exposure will be selected for the double blind provocation study. For each of the finally selected subjects there will be up to four pairs of trials, each consisting of a real exposure and a dummy exposure (in random order). Each exposure will last for 30 min, and there will be at least two days between each trial to allow for complete recovery. The RF signal from a GSM 900 mobile phone (902.4 MHz in pulses with a rate of 217 Hz and with a duty factor of 1/8) will be amplified by an RF amplifier, and the field will be emitted by a dipole antenna (Indoor Multiband Omni Antenna, Allgon, 800-2100 MHz).

The antenna will be fixed at a specified position close the head of the subject. With the antenna in this position the spatial peak SAR(1g) is measured to be 1.0 W/kg. Two dipole antennas are symmetrically mounted, however, only one of them will be used in each exposure trial. The subject will not be informed which one of the two antennas that will be active. During dummy exposures, the signal from the amplifier is absorbed by a load. The exposure system is the same as was used by Wilén et al. (2004). The seriousness of symptoms will be registered in a questionnaire before and at various times after the exposure. The diastolic and systolic blood pressure and the pulse rate will be continuously registered before, during and after the exposure. Various factors that may influence the responses will be controlled and/or registered. The classification of headaches will be done by a neurologist in accordance with the criteria of the “international classification of Headache Disorder”. At the meeting, more methodological details, including photos, and probably also preliminary results, will be presented.

**REFERENCES:**

Ofstedal G, Wilén J, Sandström M, Mild KH. Symptoms experienced in connection with mobile phone use. *Occup. Med.* 2000;50(4):237-245.

Wilén J, Sandström M, Johansson A, Stensson O, Hansson Mild K. Description of an exposure system in a provocation study to mobile phone like signals. In *Abstract book of Bioelectromagnetics Society Twenty sixth Annual Meeting, Washington DC, June 20-24, 2004*:105.

**CHANGES IN THE ELECTROENCEPHALOGRAPHIC SPECTRUM OF EPILEPTIC PATIENTS INDUCED BY MOBILE PHONES.** J. Luis Relova<sup>1,2</sup>, M. Peleteiro<sup>1,2</sup>, S. Pértega<sup>5</sup>, J. Antonio Vilar<sup>6</sup>, E. López-Martín<sup>3</sup>, F. José Ares-Pena<sup>4</sup>. <sup>1</sup>Servicio Neurofisiología Clínica, Hospital Clínico Universitario Santiago de Compostela, Spain, <sup>2</sup>Departamento de Fisiología, Universidad de Santiago de Compostela, Spain, <sup>3</sup>Departamento de Ciencias Morfológicas, Universidad de Santiago de Compostela, Spain, <sup>4</sup>Departamento de Física Aplicada, Universidad de Santiago de Compostela, Spain, <sup>5</sup>Unidad de Epidemiología Clínica y Bioestadística, Complejo Hospitalario Juan Canalejo, A Coruña, Spain, <sup>6</sup>Departamento de Matemáticas, Facultad de Informática, Universidad de A Coruña, Spain.

Radiofrequency irradiation studies in human being with epileptic disorders have not been, in our knowledge, reported. The aim of the present work is to determine the effects of the mobile phone radiation on the neural function of epileptic patients.

The study was designed as a single-blind trial with nine epileptic patients that were under the routinely procedure of some days duration of continuous electroencephalographic (EEG) and video tape recording for diagnostic purposes of their illness. The patients give their informed consent in order to participate in the study. One mobile phone, the emitter, was placed over the head and other mobile phone, the receiver, was placed in a different room with all the recording equipment.

The experiment lasted two hours. Within this time the mobile phone (MP) placed over the head started to emit during twenty minutes taking care that the patient has not knowledge when the mobile was emitting. The analysis was made over EEG segments of ninety seconds within the following periods: 1) at the start of the experiment without phone emitting (IN-OFF), 2) at the start of the emitting period (IN-ON), 3) at the end of the emitting period (FIN-ON) and 4) at the end of the experiment without phone emitting (FIN-OFF). These experimental conditions will be thought as four ordered levels of a treatment-factor named PHASE.

The corresponding spectra were derived under each experimental condition and for each subject by using fast Fourier analysis, on the basis of stored time domain EEG data. To approximate normality and reduce heterocedasticity, natural logarithm of each spectrum was considered. An example is shown in Fig.1.

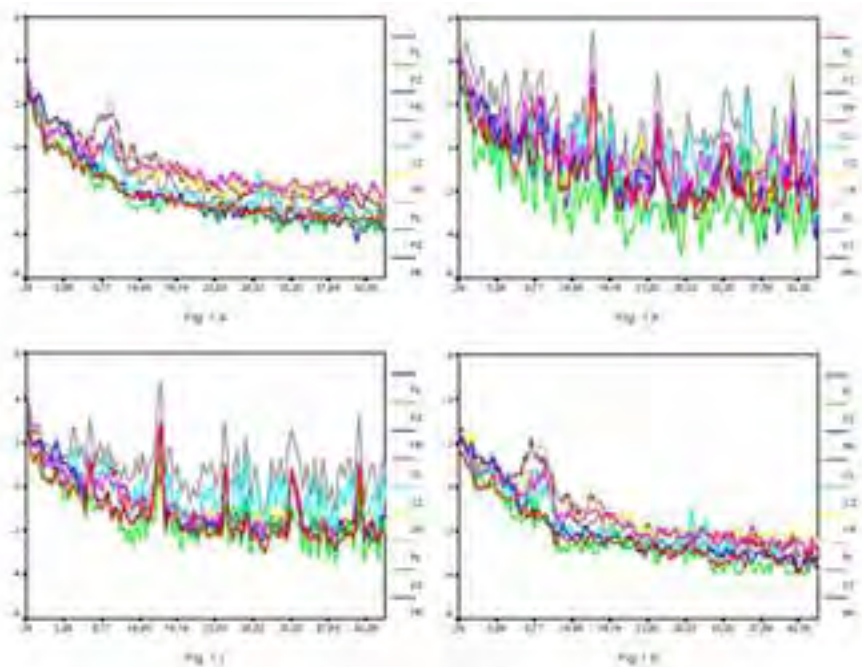


Fig. 1. Log-spectra for one of the subjects under IN-OFF (1.a), IN-ON (1.b), FIN-ON (1.c) and FIN-OFF (1.d) conditions.

Also, in order to gain some intuition on MP-related EEG changes, log-spectra obtained with MP emitting-off and with MP emitting-on were averaged separately as shown in fig.2.

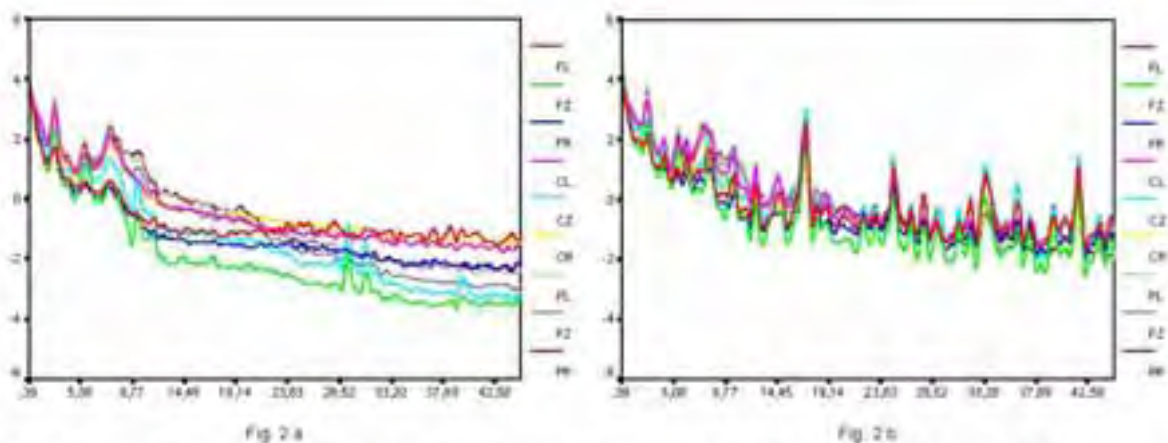


Fig. 2. Average log-spectrum with MP emitting-off (2.a) and with MP emitting-on (2.b) plotted in the 0.39 Hz to 44.92 Hz range.

Interesting features for the two resulting EEG patterns are highlighted from Fig. 2. No substantial differences appear to exist in the 0.39 Hz to 12 Hz range, where the most part of the frequency content is concentrated. However, waveforms in Fig. 2.a and in Fig. 2.b appear to differ above 12 Hz. In fact, regardless of the particular scalp location, the log-spectrum generated when MP was active (Fig. 2.b) presents a high variability, with a rough profile and the presence of some important peaks. In the opposite, the log-spectrum generated when MP was emitting-off (Fig. 2.a) is less variable without significant peaks. On the other hand, it is not clear from a simple visual inspection of Fig. 2 that the mean functions of the two EEG spectral patterns are significantly different. However, Fig. 2 suggests much reason exist to suspect that a statistical test for equality of spectra would be likely rejected. In other words, the possible EEG changes related to the MP usage could be statistically determined by

comparing the auto-covariance functions of time domain data or analogously by testing the equal spectra hypothesis in the frequency domain.

Several spectral analysis measurements were extracted from the log-spectra in hand and used as dependent variables. In particular, the area enclosed in the log-spectrum, the area enclosed in the log-spectrum once this was smoothed by local polynomial regression techniques, the average amplitude and the maximum amplitude were some of the spectral features used as dependent variables. These indexes were computed globally as well as separately for five different frequency bands: 0-4 Hz, 4-8 Hz, 8-12 Hz, 12-30 Hz and 30-45 Hz. According with intuition from Fig. 2, analysis for different frequency bands led to especially interesting conclusions.

In this work, the results obtained when AREA= area enclosed in the log-spectrum within a specific frequency band was selected as dependent variable are presented. The aforementioned variables provided analogous results and their analysis is not included here.

A repeated measures model was considered to test for differences among the mean responses of AREA for the four experimental conditions or levels of PHASE. Orthogonal polynomial contrasts were also used to test for relations between AREA and PHASE. Both the equality of means test and the orthogonal polynomial tests were performed by evaluating AREA within each of five different frequency bands (0-4 Hz, 4-8 Hz, 8-12 Hz, 12-30 Hz and 30-45 Hz) and at each of the nine scalp locations separately. A significance value  $p < 0.05$  was considered to be statistically significant.

The means of AREA estimated from the repeated measures model and grouped into frequency bands and scalp locations are plotted against the levels of PHASE in Fig. 3.

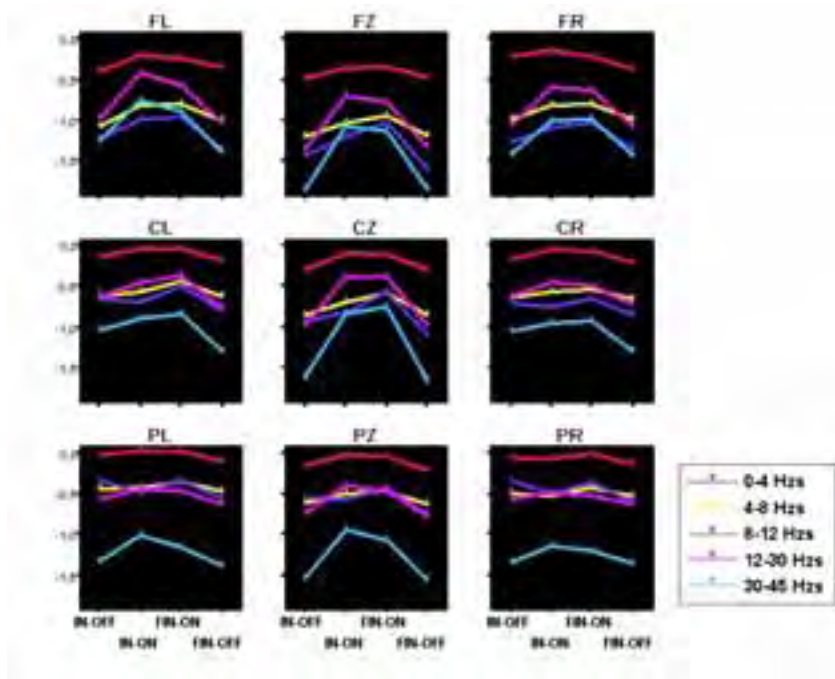


Fig. 3. Sample means for AREA against experimental conditions grouped into frequency bands and scalp locations

Since Mauchly sphericity tests were not rejected, univariate F-tests with 3 and 8 degrees of freedom were computed to assess the assumption that the means of AREA are equal at the four levels of PHASE. Table in Fig. 4 shows the significance values (P) obtained from F-tests as well as the partial  $\eta^2$  values.

		Frequency bands (Hz)				
		0-4	4-8	8-12	12-30	30-45
Scalp location	FL	P = 0.487 $\eta^2 = 0.095$	P = 0.085 $\eta^2 = 0.237$	P = 0.009 $\eta^2 = 0.380$	P = 0.000 $\eta^2 = 0.557$	P = 0.009 $\eta^2 = 0.376$
	FZ	P = 0.674 $\eta^2 = 0.061$	P = 0.139 $\eta^2 = 0.201$	P = 0.001 $\eta^2 = 0.514$	P = 0.000 $\eta^2 = 0.724$	P = 0.000 $\eta^2 = 0.674$
	FR	P = 0.423 $\eta^2 = 0.108$	P = 0.242 $\eta^2 = 0.157$	P = 0.097 $\eta^2 = 0.227$	P = 0.009 $\eta^2 = 0.376$	P = 0.055 $\eta^2 = 0.267$
	CL	P = 0.732 $\eta^2 = 0.051$	P = 0.255 $\eta^2 = 0.153$	P = 0.115 $\eta^2 = 0.215$	P = 0.003 $\eta^2 = 0.430$	P = 0.062 $\eta^2 = 0.259$
	CZ	P = 0.407 $\eta^2 = 0.112$	P = 0.182 $\eta^2 = 0.180$	P = 0.006 $\eta^2 = 0.396$	P = 0.000 $\eta^2 = 0.568$	P = 0.000 $\eta^2 = 0.610$
	CR	P = 0.568 $\eta^2 = 0.079$	P = 0.525 $\eta^2 = 0.087$	P = 0.293 $\eta^2 = 0.141$	P = 0.050 $\eta^2 = 0.273$	P = 0.153 $\eta^2 = 0.194$
	PL	P = 0.814 $\eta^2 = 0.038$	P = 0.708 $\eta^2 = 0.055$	P = 0.338 $\eta^2 = 0.128$	P = 0.043 $\eta^2 = 0.283$	P = 0.025 $\eta^2 = 0.318$
	PZ	P = 0.607 $\eta^2 = 0.072$	P = 0.389 $\eta^2 = 0.116$	P = 0.201 $\eta^2 = 0.172$	P = 0.022 $\eta^2 = 0.326$	P = 0.006 $\eta^2 = 0.403$
	PR	P = 0.830 $\eta^2 = 0.035$	P = 0.774 $\eta^2 = 0.044$	P = 0.302 $\eta^2 = 0.138$	P = 0.141 $\eta^2 = 0.200$	P = 0.285 $\eta^2 = 0.143$

Fig. 4. Significance and partial  $\eta^2$  values of the univariate F-test for equality of AREA means at the four experimental conditions. The F-tests were performed at each frequency band and each scalp location.

Where analysis of variance led to significant results, the treatment sum of squares was split into sums of squares for orthogonal polynomial contrasts. As the number of degrees of freedom for treatments is 3, the existence of lineal, quadratic or cubic trends could be tested, resulting that a quadratic fit was strongly significant in all cases.

On the basis of the studied epileptic patients, statistical tests shown that the EEG recordings are affected by exposure to an active MP since significant differences between the EEG spectra with MP turned-off and with MP turned-on were found.

P-B-92

**EFFECTS OF 50 HZ MAGNETIC FIELD INTERFERENCES ON RECENT GENERATIONS OF IMPLANTED PACEMAKERS.** M. Souques<sup>1</sup>, J. Alexandre Trigano<sup>2</sup>, R. Frank<sup>3</sup>, I. Magne<sup>4</sup>, O. Blandeau<sup>2</sup>, J. P. Gernez<sup>4</sup>. <sup>1</sup>SERVICE DES ETUDES MEDICALES, EDF-Gaz de France, Paris, France, <sup>2</sup>SERVICE DE CARDIOLOGIE, Hôpital Nord, CHU de Marseille, Marseille, France, <sup>3</sup>SERVICE DE RYTHMOLOGIE, Institut de Cardiologie, Hôpital Pitié-Salpêtrière, Paris, France, <sup>4</sup>EDF R&D, Avenue des Renardières, Moret sur Loing, France.

Objective: The objective of these study is to evaluate the behavior of implanted pacemakers in the presence of a magnetic field of 50 Hz 100  $\frac{3}{4}$ T, the value retained in the European recommendation 1999/519/EC, concerning public exposure to electromagnetic fields. Materials and Methods: More than 250 patients recently implanted with pacemakers from different manufacturers were monitored while passing through, and standing between a system of two coils generating a 50 Hz 100  $\frac{3}{4}$ T magnetic field. The tests were performed with clinically used sensing setting. Recordings were made with the field on

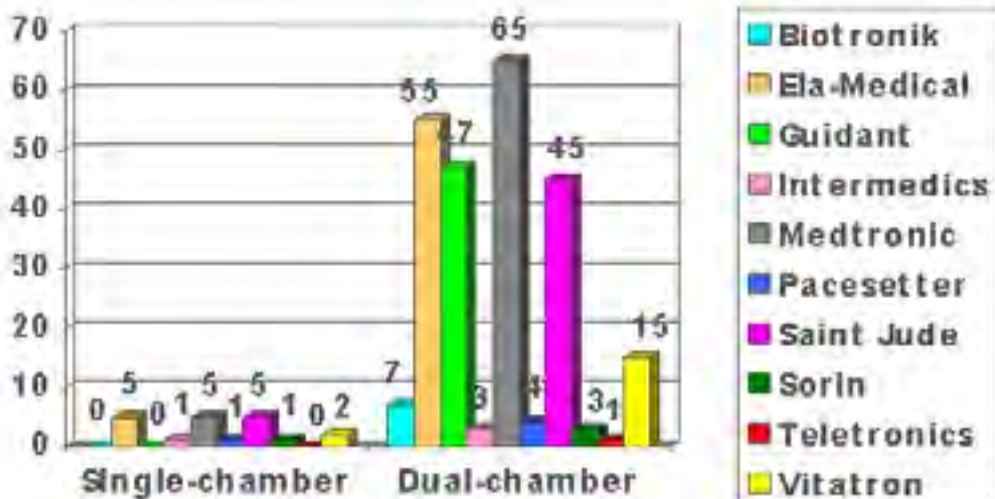
and off for each patient position. The tracings were analyzed in real time, with the physician blinded to the intensity of the patient's exposure. At the end of the tests, the pacemaker programming was controlled and reprogrammed if necessary.

Results: The population included 265 patients, aged from 18 to 87 years. Half of them had a recent implantation, between 2001 and 2004. Pacemakers from 10 manufacturers were included in the study, with 1 to 23 different models per manufacturer and 1 to 23 patients with the same model (Figure 1). Pacemaker dependency was found before testing in 145 cases. The sensing configuration was bipolar in 165 cases and unipolar in 53. Bipolar was combined with unipolar sensing in 47 patients.

Mode reversion to asynchronous mode pacing during the test was recorded in 3 patients with atrial and or ventricular unipolar programming (Table 1). In 2 of these cases, this interference was asymptomatic. In a third case, persistent asynchronous mode reversion was followed by pacing inhibition, resulting in complete atrioventricular block with severe bradycardia and dizziness. Only one mode reversion was recorded in 145 tests with bipolar sensing, transient ventricular pacing in safety mode with shorter than programmed atrioventricular delay. No change in programming was observed at the end of the tests. Conclusion: High magnetic field at industrial frequency (50 Hz) can cause intermittent mode reversion or pacing inhibition in patients with unipolar sensing programming. The overall incidence of this interference is low with usual pacemaker settings.

In Practice: The advice to give to pacemaker patients must be cautious and in fact depends on each situation. The absence of any serious events in our series, which corresponds to the extreme rarity of reported incidents, suggests that patients can be reassured. Only pacemaker-dependent subjects with unipolar ventricular sensing, exposed to high magnetic field, should have their pacemaker tested in exposure situations.

Positive tests				
	Positive test n°1	Positive test n°2	Positive test n°3	Positive test n°4
Sex and age	F - 53 years	M – 78 years	M – 80 yeras	M – 61 years
Implantation site	Right	Left	Left	Left
Manufacturer and model	Medtronic 7960	St Jude 5376	Guidant 1280	Medtronic 731
Year of implantation	1997	2003	2001	2000
Dependency	Yes	No	Yes	Yes
Atrial polarity mV	Unipolar 0.50	Bipolar 0.75	Unipolar 0.50	Unipolar 0.50
Ventricular polarity mV	Unipolar 2.80	Bipolar 2.00	Bipolar 2.50	Unipolar 2.80
Interference	Asynchronous mode reversion	modification of the autcapture program	Asynchronous mode reversion	Asynchronous mode reversion



## In vivo studies

P-B-95

**EFFECTS OF LONG-TERM RADIOFREQUENCY ELECTROMAGNETIC FIELDS EXPOSURE ON TUMORIGENESIS IN P53-DEFICIENT (+/-) MICE.** T.-Q. Huang<sup>1</sup>, J.-S. Lee<sup>1,2</sup>, J.-K. Park<sup>4</sup>, J.-J. Jang<sup>3</sup>, J.-S. Seo<sup>1</sup>. <sup>1</sup>ILCHUN Molecular Medicine Institute MRC, and Dept of Biochemistry and Molecular Biology, Seoul National Univ College of Medicine, Seoul, KOREA, <sup>2</sup>BK21 Human Life Science, Seoul National Univ College of Medicine, Seoul, KOREA, <sup>3</sup>Dept of Pathology, Seoul National Univ College of Medicine, Seoul, KOREA, <sup>4</sup>Dept of Radio Sciences & Engineering, Chungnam National Univ, Daejeon, KOREA.

The p53 tumor suppressor gene is the most widely mutated gene in human tumorigenesis. Thus, the p53-deficient mice are useful model system to study effect of radiofrequency electromagnetic fields (RF EMFs) radiation exposure on tumorigenesis. In present study, the p53-deficient (+/-) mice (C57BL/6 strain) were exposed at whole body average SAR 0.4 W/kg of 849 MHz or 1,763 MHz RF EMFs, to elucidate effect of RF EMFs from mobile phones on tumorigenesis and survival. Exposure conditions were twice daily for 45 min exposure, with a 15 min interval between exposures, 5 days a week. After 1 year exposure, sham-exposed, 849 MHz RF EMFs-exposed, and 1,763 MHz RF EMFs-exposed mice (each group, n=34) were biopsied and macroscopically examined. Major tissues, i.e., brain, liver, adrenal gland, kidney, spleen, stomach, bladder, lung, heart, thymus, and testis or ovary were isolated for the histopathological and immunohistochemical examinations. No discernible change in any major tissue was attributable to RF EMFs exposure in macroscopical and microscopical examination. No alteration was observed by histopathological and immunohistochemical analysis using anti-PCNA antibody between the sham- and RF-exposed groups. The mean overall survival time and survival rate was not influenced by the RF EMFs exposure. Therefore, we suggests that the risk of development of particular type of tumor in p53-deficient mice is not increased by the exposure of RF-EMFs

**EFFECTS OF RADIOFREQUENCY ELECTROMAGNETIC FIELDS ON YOUNG RATS – A STUDY RELEVANT TO CHILDREN'S USE OF MOBILE PHONES.** T. Kumlin<sup>1</sup>, H. Iivonen<sup>2</sup>, H. Tanila<sup>2</sup>, T. van Groen<sup>2</sup>, J. Juutilainen<sup>1</sup>. <sup>1</sup>Univ of Kuopio, Dept of Environmental Sciences, KUOPIO, <sup>2</sup>Univ of Kuopio, Dept of Neuroscience and Neurology, KUOPIO.

Although radio frequency (RF) electromagnetic fields from mobile phones are below exposure limits (which are based on well-documented health effects and additional safety factors), concerns have been expressed about the safety of long-term exposure to mobile phone fields. Children are generally considered more vulnerable to chemical and physical exposures, and it has been suggested that a precautionary approach should be used to limit children's exposure to fields from mobile phones. For example, the Independent Expert Group on Mobile Phones (IEGMP, 2000), established by the UK Government stated: *“If there are currently unrecognised adverse health effects from the use of mobile phones, children may be more vulnerable because of their developing nervous system, their greater absorption of energy in the tissues of the head, and longer lifetime of exposure. In line with our precautionary approach, we believe that the widespread use of mobile phones by children for non-essential calls should be discouraged.”*

Various effects of *short-term* RF exposure on the central nervous system have been reported both in humans and in animals. Salford et al. (2003) reported neuronal damage in young rat brains examined 50 days after a single 2-hour exposure to GSM-type RF fields at low SAR levels from 2 to 200 mW/kg, and linked in the discussion their findings to teenagers' use of mobile phones. The result is based on only 8 rats per group.

There are no data directly relevant for assessing possible effects of *long-term* childhood use of mobile phones on the developing nervous system. This study directly addresses the concern of possible adverse effects of mobile phone-type RF exposure during young age on the developing nervous system.

## OBJECTIVES

1. To study whether exposure to RF exposure similar to that emitted by mobile phones affects the developing nervous system in young rats, as assessed by behavioral tests.
2. To further investigate the surprising finding of neuronal damage after a single 2-hour exposure (Salford et al. 2003). In this study, possible neuronal damage are investigated using the same histopathological method, but after chronic exposure of young rats.

## METHODS

### **Animals and exposure to RF fields:**

Male Wistar rats are weaned at the age of three weeks and randomly assigned to one of the following groups: high exposure, low exposure or sham-exposure, 24 animals per group. The animals are kept in the radial transmission line exposure chamber developed during a previous Finnish national research programme by the Non-Ionizing Radiation Laboratory of the STUK-Finnish Radiation and Nuclear Safety Authority, and later used for carcinogenicity studies on rats in the EU-funded CEMFEC project ([www.uku.fi/cemfec](http://www.uku.fi/cemfec)). The exposure system has been designed so that the animals can be kept continuously in the exposure chamber in individual cages. The dosimetry of the exposure chamber has been characterized by FDTD modelling (Laukkanen and Pitkääho, 2003), which shows moderate variation of the SAR with posture of the animals. Exposure of GSM-type RF radiation is 2 h/d at a

whole-body SAR of 1.5 or 0.15 W/kg (high dose vs. low dose), and lasts until the rats reach sexual maturity (8 weeks of age).

### **Behavioural testing:**

The behavioural effects of RF exposure are assessed during 2 weeks after the end of the exposure. The behavioural assessment include the open field test for locomotor and exploratory activity, plus maze test for anxiety, pre-pulse inhibition of the startle reflex to test general reactivity and attention and Morris water maze test for spatial learning and memory.

### **Evaluation of neuronal damage:**

Histopathological examination is focused on the hippocampus and is done at two stages. First, 6 animals in each group are taken for histology right after the exposure period to see possible acute effects of the exposure (general morphology, detection of dying cells and possible leakage of the dye through blood-brain barrier). The remaining 18 animals/group are prepared for histology at the end of the test period.

### **REFERENCES**

Laukkanen K, Pitkäaho R: Computational dosimetry of exposure systems. In: Juutilainen J, Kumlin T. (eds): Mobile Telephones and Health. Proceedings, Final Seminar of the Finnish National Research Programme 1998-2003. Helsinki, October 17, 2003. pp 28-32.

Salford LG, Brun AE, Eberhardt JL, Malmgren L, Persson BRR: Nerve cell damage in mammalian brain after exposure to microwaves from GSM mobile phones. *Environ Health Perspect* 111:(7)881-883, 2003.

*This study is sponsored by Tekes- National Technology Agency of Finland, Nokia Research Center, Sonera Mobile Networks, Elisa Corporation and Finnet Networks.*

P-B-101

**EVALUATING DNA DAMAGE IN RODENT BRAIN FOLLOWING ACUTE 60 HZ MAGNETIC FIELD EXPOSURE.** J. McNamee, P. Bellier, E. Lemay, G. Gajda, A. Thansandote. Consumer and Clinical Radiation Protection Bureau, Health Canada, Ottawa, Ontario, Canada.

In recent years, numerous studies have reported a weak association between 60 Hz magnetic field (MF) exposure and the incidence of childhood leukemia. To date, no mechanism to explain these findings has been identified. Several studies conducted have reported that exposure of rodents to MF can result in DNA strand breaks in the brains of adult rats and mice (Lai and Singh, 1997a,b, 1998, 2004; Svedenstal et al. 1999a,b). Our lab found no such evidence of either MF-induced DNA damage or apoptosis in a sensitive cell region of the immature mouse cerebellum (McNamee et al., 2002). However, the possibility remained that MF may damage the adult rodent brain preferentially or may affect regions other than the cerebellum. Furthermore, due to ongoing development and proliferation in the immature rodent brain our previous study may have failed to detect MF-induced DNA damage due to a higher background of alkali-labile sites. Therefore, the objective of the current study was to investigate whether acute MF exposure could elicit a DNA damage within brain cells from both whole brain and cerebellar homogenates from adult rats, adult mice and immature mice.

**METHODS:** Rodents were exposed to a 60 Hz MF (0, 0.1, 1.0 or 2.0 mT) for 2 h. Then, at 0, 2 and 4 h after exposure, animals were sacrificed and their brains rapidly removed, homogenized and cells cast into agarose gels for processing via the alkaline comet assay, as previously described (McNamee et al.,

2002). Rats were euthanised by CO<sub>2</sub> inhalation, while mice were sacrificed by decapitation. Four parameters (Tail Ratio, Tail Moment, Comet Length and Tail Length) were used to assess DNA damage for each comet. A minimum of 50 cells were scored for each brain region/animal with a total of 6 animals per group. Concurrent negative (cage) and positive (2 Gy X-ray) control samples were conducted for each experiment.

**RESULTS:** For each species, a significant increase in DNA damage was detected by each of the four parameters in the positive control (2 Gy X-ray), relative to the non-irradiated negative and sham controls. However, none of the four parameters detected a significant increase in DNA damage from any dose of magnetic field exposure (0-2 mT), at any time period after exposure in any species, within either brain cell homogenate.

**CONCLUSIONS:** The dose-response and time course data from the multiple species tested in this study provide no evidence of MF induced DNA damage, as previously reported by other studies (Lai and Singh, 1997a,b, 1998, 2004; Svedenstal et al. 1999a,b). It is unclear why our group has repeatedly failed to reproduce the findings of Lai and Singh. One obvious difference between these studies is the method of DNA damage quantification for the comet assay. Our group has used an image analysis system to calculate the DNA damage parameters in an automated fashion, while the studies of Lai and Singh et al. have employed user derived (micrometer based) measurements of Tail migration. In conclusion, the current study and our previous study (McNamee et al., 2002) have found no evidence of DNA damage to the brains of adult rats, adult mice or immature mice following acute exposure to 60 Hz MF (0-2 mT).

P-B-104

**BEHAVIOURAL EFFECTS OF CHRONIC, SIMULTANEOUS EXPOSURE TO WEAK VARIABLE MAGNETIC FIELD AND RED LIGHT IN RATS.** J. Mrowiec<sup>1</sup>, G. Cieslar<sup>1</sup>, K. Sieron-Stoltny<sup>1</sup>, A. Plech<sup>2</sup>, S. Kasperczyk<sup>3</sup>, A. Sieron<sup>1</sup>. <sup>1</sup>Chair and Clinic of Internal Diseases, Angiology and Physical Medicine, Silesian Medical Univ, Poland, <sup>2</sup>Chair and Dept of Pharmacology, Silesian Medical Univ, Poland, <sup>3</sup>Chair and Dept of Biochemistry, Silesian Medical Univ, Poland.

**Objectives.** The aim of the study was to estimate the influence of chronic whole body simultaneous exposure to weak variable magnetic field used in magnetostimulation and red light radiation on such behavioural reactions as locomotor activity, exploratory activity, space memory and irritability in rats. **Methods:** Experimental material consisted of 16 male Wistar rats weighting 180-200 g. Weak variable magnetic field of saw-like shape of impulse, at a frequency of basic impulse 180-195 Hz and induction of 336-672  $\mu$ T (depending on the position of magnetic field induction measuring points) and light radiation (wavelength – 630 nm, mean power – 0,35 W, energy density – 0,48 J/cm<sup>2</sup>) generated by magnetic-light applicator of device for magnetostimulation Viofor JPS (Poland) were used. All animals were randomly divided into 2 groups (8 animals each). In first group whole body simultaneous exposure to variable magnetic field and light radiation lasting 12 minutes daily for 2 periods of 5 consecutive days with 2 days-lasting break between them, was made. In second, control group sham-exposure without generating magnetic field and light radiation inside of applicator was made. During whole-body exposure animals were placed individually in a specially designed plastic chamber with cover made up by square magnetic-light applicator. A locomotor activity was determined in the open field test by recording a number of episodes of crossings, peepings, rearings, washing and defecation per 3 minutes. Simultaneously an exploratory activity was examined in the hole test by recording a number of head dips into a board hole per 3 minutes. Space memory was determined by means of water maze test on the

basis of measurement of time required for crossing of a specially constructed water maze. Afterwards an irritability was investigated by means of Nakamura and Thoenen score test. The evaluation of behaviour was made at 24 hours before first exposure, immediately after first exposure, at 24 hours after first exposure, at 2nd, 5th and 12th day of exposure cycle and at 7th and 14th day after the end of a cycle of exposures. The results in particular days of observation were presented as percentage of initial values before exposure. In the statistical evaluation ANOVA analysis with subsequent post-hoc Mann-Whitney's U test were used. Summary of results: The results of estimation of behavioural reactions in particular days of observation in both groups of rats with statistical evaluation are presented in table 1. As a result of repeated exposures a significant increase in number of episodes of peepings and rearings, a significant decrease in number of episodes of defecation, as well as significantly smaller decrease in water maze crossing time was observed at 14th day after the end of exposure cycle, as compared with control group. No significant changes of any behavioural reaction during exposure cycle were observed in magnetic field and light-exposed group comparing to control group. Conclusion: Chronic simultaneous exposure of rats to weak variable magnetic field and red light does not affect significantly behaviour of these animals during exposure cycle. On the other hand this exposure causes a slight stimulation of locomotor activity and slight worsening of space memory in rats after the end of exposure cycle.

Table 1 The mean values of behavioural tests presented as percentage of initial values before exposure cycle in exposed rats and control group in particular days of exposure cycle with statistical evaluation

Behavioural reaction calculation comparison initial values	Group < /td>	1 day of exposure cycle	2 day of exposure cycle	7 day of exposure cycle	14 day of exposure cycle	7 day after the end of exposure cycle	14 day after the end of exposure cycle
		Mean $\pm$ SEM [%]	Mean $\pm$ SEM [%]	Mean $\pm$ SEM [%]			
Water maze crossing time	Exposed	60 $\pm$ 20	70 $\pm$ 20	40 $\pm$ 10	30 $\pm$ 10	80 $\pm$ 40	30 $\pm$ 10*
	Control	70 $\pm$ 20	70 $\pm$ 30	70 $\pm$ 20	50 $\pm$ 20	80 $\pm$ 40	50 $\pm$ 20
Number of crossing	Exposed	127 $\pm$ 19	72 $\pm$ 5	41 $\pm$ 8	42 $\pm$ 8	46 $\pm$ 11	53 $\pm$ 14
	Control	150 $\pm$ 13	77 $\pm$ 13	58 $\pm$ 17	53 $\pm$ 16	50 $\pm$ 19	34 $\pm$ 11
Number of peepings	Exposed	143 $\pm$ 25	92 $\pm$ 19	51 $\pm$ 6	50 $\pm$ 10	93 $\pm$ 22	96 $\pm$ 16*
	Control	149 $\pm$ 33	76 $\pm$ 22	84 $\pm$ 14	68 $\pm$ 17	95 $\pm$ 28	54 $\pm$ 13
Number of rearings	Exposed	267 $\pm$ 118	0 $\pm$ 0	33 $\pm$ 22	83 $\pm$ 56	17 $\pm$ 17	200 $\pm$ 84*
	Control	50 $\pm$ 30	10 $\pm$ 10	10 $\pm$ 10	0 $\pm$ 0	0 $\pm$ 0	0 $\pm$ 0
Number of washing	Exposed	200 $\pm$ 46	188 $\pm$ 58	106 $\pm$ 37	94 $\pm$ 24	119 $\pm$ 52	31 $\pm$ 13
	Control	218 $\pm$ 36	96 $\pm$ 14	191 $\pm$ 75	118 $\pm$ 49	182 $\pm$ 57	91 $\pm$ 41
Number of defecations	Exposed	111 $\pm$ 19	153 $\pm$ 19	89 $\pm$ 31	137 $\pm$ 30	137 $\pm$ 26	74 $\pm$ 11*
	Control	100 $\pm$ 41	143 $\pm$ 46	221 $\pm$ 52	293 $\pm$ 25	264 $\pm$ 44	257 $\pm$ 39
Number of head dips	Exposed	85 $\pm$ 14	81 $\pm$ 26	20 $\pm$ 6	31 $\pm$ 7	66 $\pm$ 22	50 $\pm$ 10
	Control	60 $\pm$ 11	20 $\pm$ 9	40 $\pm$ 8	21 $\pm$ 13	49 $\pm$ 10	63 $\pm$ 10
Irritability	Exposed	27 $\pm$ 13	55 $\pm$ 27	55 $\pm$ 12	73 $\pm$ 24	191 $\pm$ 47	164 $\pm$ 36
	Control	46 $\pm$ 23	85 $\pm$ 31	77 $\pm$ 32	77 $\pm$ 32	138 $\pm$ 54	154 $\pm$ 51

\*p less 0,05, \*\*p less 0,01, \*\*\*p less 0,001

**A DEVELOPMENTAL TOXICITY STUDY OF 20 KHZ MAGNETIC FIELD EXPOSURE ON CHICK EMBRYOS - A TWO-DAY EXPOSURE STUDY.** I. Nishimura, S. Imai, T. Negishi. Environmental Science Research Laboratory, Central Research Institute of Electric Power Industry, Japan.

Background: Intermediate frequency electromagnetic field was widely used for anti-theft devices and security systems, medical devices, broadcasting and transmitting equipments, and induction heaters. WHO indicated a need for biological studies to evaluate the effects of intermediate field exposure because of the lack of such studies for the assessment on potential health risks.

Objective: This study aims at determining whether or not the intermediate frequency of 20 kHz, sinusoidal magnetic field (MF) exposure has effects on the chick embryo development, particularly at the most sensitive stage to exogenous stimuli.

Methods: Exposure was conducted at 1.1 mTrms at 20 kHz that is 176 times greater than the reference level advised by the ICNIRP guidelines (1998) for the public, 6.25 micro-T. A Helmholtz-type exposure coil and an associated cellular incubator were employed. A set of two square coils, 60 x 60 cm, was capable of producing a vertical MF in the middle of the coils ranging from 2 kHz up to 60 kHz. Field linearity was well preserved. Sinusoidal-wave field contained very few harmonics. A magnetic permeable incubator was placed in the designated exposure area. The generated field inside the incubator, 20 x 20 x 20 cm, varied less than 5 % to its average intensity. Forty ampere was required to provide 1.1 mTrms in 20 kHz. Vibration of the coils was negligible. Although heat elevation was detectable, it did not affect incubation temperature.

The incubator made of polyvinylchloride had water-jacketed structure. Hot water was supplied from a remotely located circulator to maintain the incubator at 38 C +/- 0.4 C. In the incubator 3 shelves could hold 60 eggs in total. The exposure facility was duplicated for simultaneous runs of control (sham-exposure) and exposure experiments. Control facility located 20 m apart from the exposure one. Background plus stray field in 20 kHz and 50 Hz in the control incubator were less than 0.001 and 0.03 micro-Trms, respectively, when the exposure coil was energized.

Freshly harvested White Leghorn, fertile eggs were purchased from Saitama Experimental Animals Supply Co., LTD. Eggs were maintained in a temperature controlled, 10 to 20 C, storage box for a maximum of 3 days before incubation. Eggs were weighed and randomly assigned to each group. They were preincubated for 2 hours prior to field exposure. Exposure condition was blinded to an experimental technician. After 48 hours incubation, embryos were fixed in 10 % formalin neutral buffer solution. They were observed under stereoscopic microscope for abnormalities such as opened neural tube, delayed development or death. Number of somites, developmental stage under H&H definition, and body length were recorded. Morphologically abnormal embryos were recorded and all photographed. Our historical data indicated that egg fertility was over 90 %, and the proportion of spontaneously abnormal embryo was 12 % in average throughout a year. Such low and constant incidence of abnormality indicated that our embryo is suitable for teratological evaluation.

Results: Exploratory studies were performed to find an appropriate positive-control dosing and to estimate minimum sample sizes required for statistical evaluations (Nishimura and Imai, J Toxicol Sci. 2004 Oct; 29(4):421). All-trans retinoic acid (RA) at doses of 0.01, 0.1, 1, 10 and 100 micro-g/egg, or 10 micro-L of saline as vehicle alone were injected into yolk sac at day-0; and they were incubated for 2, 7, or 11 days. RA teratogenicity displayed both dose- and time-dependency. Doses of RA treatment resulted in total abnormality rate from 40 to 90 %. Proportion of dead embryos in the total abnormality

also tended to increase as the RA dose increased. Consequently, a suitable, i.e., 40 to 60%, abnormality range was yielded when 1 micro-g RA/egg was given for 2 days development. The minimum sample sizes to detect a biologically significant change over 20 % were calculated at significance level alpha as 0.05 and statistical power 1-beta as 0.8. They were estimated to be 14 embryos per group for numerical indices such as number of somites, and to be 52 for proportional indices such as proportion of abnormal embryos. MF exposure experiments were therefore conducted with 60 eggs in each group.

Sham-sham experiment was conducted to confirm the baseline in our two facilities. Two identical facilities of exposure and control gave no statistical differences in the developmental indices of chick embryos when no current was loaded in the exposure coil. Measured endpoints were embryonic stage, number of somites, body length, and the proportions of dead and morphologically abnormal embryos. These results validate our experimental regime.

Finally, a group of 60 eggs was exposed to sinusoidal 20 kHz, 1.1 mTrms vertical MF for 48 hours. The same number of eggs was served as a control. Additionally, 120 eggs given 1 micro-g RA were divided into two groups; one was exposed and the other was sham-exposed to investigate if any accelerative effects occur in teratogenicity by the field exposure. Statistical evaluation revealed that there has been no adverse effect of the MF exposure alone in every endpoint measured or observed when the non-treated, MF exposed group was compared to the negative-control. RA injection produced medium degree of teratogenic responses as expected, however the field exposure did not change the proportion of abnormal embryo significantly in comparison with the positive-control group. Both sets of experiments were repeated three times, and all gave the same results.

Conclusion: Under the experimental conditions tested, a 20 kHz sinusoidal wave form, 1.1 mTrms vertical MF exposure for the first 48 hours of embryogenesis did not exhibit any adverse effects on the development of White Leghorn, chick embryos. Lack of modification by the field on the teratogenicity of a known teratogen was also demonstrated. We plan to extend exposure period to evaluate whether the intermediate frequency MF affect embryos of later stages.

P-B-110

**NO EFFECT OF 50 HZ, CIRCULARLY POLARIZED MAGNETIC FIELD EXPOSURES UP TO 700 MICRO-TRMS FOR 12 WEEKS ON CYTOKINE PRODUCTIONS IN LPS-STIMULATED MOUSE.** I. Nishimura. Environmental Science Research Laboratory, Central Research Institute of Electric Power Industry, Japan.

Background: We have been studied the effects of 50 Hz, circularly polarized magnetic field exposure on cytokine production in mice. Cytokine is a polypeptide hormones secreted mainly from immune cells regulating a variety of immunological processes. Previous study revealed that T-cell originated cytokine productions, induced by anti-CD3 antibody treatment, in the mouse have not been affected by the MF exposures. In the present study, we employed an experimental model of enhanced immune functions in vivo that is a systemic production of cytokines induced by lipopolysaccharide (LPS) treatment. Induced cytokines include interleukin (IL) 1-beta, IL-6, IL-10, IL-12, and tumor necrosis factor (TNF)-alpha. Because the immune system does not respond to immunologically inert events but it shows clear and dynamic responses once the first immunological step is triggered, certain stimulation is needed to initiate the immunological processes. From this view point, the LPS-induced cytokine production is an excellent model to detect possibly subtle, immunological effect of MF exposure.

Objective: Specific objective of this study is to reveal whether or not the MF exposures, that are 50 Hz,

circularly polarized, up to 700 micro-Trms for 12 weeks, could change the ability of the mouse to produce cytokines that is induced by an injection of LPS.

Methods: Groups of 10 male BALB/c mice, 6 weeks of age and specific pathogen free, were assigned either control or exposed. They were quarantined and sham-exposed or exposed to MF in our four identical, animal exposure facilities that were barrier system. Multiple-square coils consisted of two orthogonal sets of four bobbins, one set for vertical MF and the other for horizontal. Equal amount of flux density in each direction with 90 degrees out of phase resulted in circularly polarized MF in the middle of coils, 1 m x 1m x 1 m of animal housing space. The produced field intensity was as uniform as less than 5 % in the variance. Each facility was located over 15 m apart to keep stray field as low as reasonable. Background 50 Hz MF in a control facility was less than 0.02 micro-Trms, when all coils and equipments were powered.

Exposures were conducted at 1.4, 70, 350 or 700 micro-Trms with circularly polarized, 50 Hz MF, over 22 hours a day, 7 days a week for 3, 6, or 12 weeks. Immediately after the exposure, mice were treated with an intraperitoneal injection of 10 micro-g of LPS. They were sacrificed 90 min after the injection, and produced amounts of IL-1beta, IL-6, IL-10, IL-12 and TNF-alpha in sera, spleens and lungs were measured with enzyme-linked immunosorbent assay. Mean cytokine values of MF-exposed and control groups were statistically evaluated if the group differences were significant. Exposure and matched control experiments were conducted simultaneously with a batch of animals in a blind fashion. The experiment under the same exposure condition was repeated three times to confirm the reproducibility.

Results: Bases of all cytokine productions in the organs of the LPS-treated mice housed in the four facilities were first determined without MF exposure. No difference among the four facilities in either cytokine level in the organs was evident. Obtained results from MF exposure experiments, overall, indicate the lack of MF effect on the cytokine productions. Exceptional experiments, i.e., 2 out of 372 cytokine measurements, showed statistically significant difference between MF-exposed and matched control group values. These changes were a decrease in serum IL-6 of the mice exposed to 1.4 micro-Trms MF for 6 weeks and an increase in spleen IL-12 of the mice exposed to 70 micro-Trms MF for 12 weeks. All the rest of cytokine productions did not show any significant effect of MF exposure. These two changes were considered to be biologically insignificant, because the changes were not dose-related nor exposure time-dependent, directions of the changes were not biologically explainable, organ or cytokine specificity is not clear, and further, the reproducibility was not preserved.

Conclusion: Obtained results therefore suggest that the MF exposure did not affect the LPS-induced cytokine productions in the mice under experimental conditions we employed.

## **In vitro - cellular**

P-B-113

**NO DNA STRAND BREAKS INDUCTION IN HUMAN CELL LINES EXPOSED TO 2-GHZ BAND CW OR W-CDMA MODULATED RADIOFREQUENCY FIELDS.** H. Hirose<sup>1</sup>, N. Sakuma<sup>1</sup>, Y. Komatsubara<sup>1</sup>, H. Takeda<sup>1</sup>, M. Sekijima<sup>1</sup>, T. Nojima<sup>2</sup>, J. Miyakoshi<sup>3</sup>. <sup>1</sup>Mitsubishi Chemical Safety Institute Ltd., Japan, <sup>2</sup>Hokkaido Univ, Sapporo, Japan, <sup>3</sup>Hirosaki Univ, Hirosaki, Japan.

OBJECTIVE: We tested the hypothesis that modulated radiofrequency (RF) fields may act as a DNA

damaging agent. Firstly, to confirm the response of the human cell lines exposed to microwaves at specific absorption rate (SAR) of 80 mW/kg, which corresponds to the limit of the whole-body average SAR for general public exposure defined as the basic restriction in the International Commission on Non-Ionizing Radiation Protection (ICNIRP) guidelines [1]. Secondly, to investigate if continuous wave (CW) and Wide band Code Division Multiple Access (W-CDMA) modulated signal RF fields at 2.1425 GHz affect genotoxicity to different extents.

**MATERIALS AND METHODS:** We used the in vitro exposure system with a horn antenna and dielectric lens in an anechoic chamber, which was developed by NTT DoCoMo [2, 3]. Human glioblastoma A172 and normal human fibroblasts IMR-90 from fetal lung were used, and the cells were exposed in plastic 35 mm culture dishes at 15 dishes (five replicate culture each; sham, expose and positive control) per cell line. The alkaline single cell gel electrophoresis (SCG) assay was performed on log-phase cultures for period 2 or 24 h exposure at average SAR of 80, 250, and 800 mW/kg. Concurrent negative (sham) and positive (methyl methane sulfonate; 20 µg/mL MMS) control cultures were run for each experiment. Comets were visualized by ethidium bromide staining (10 µg/mL) and were analyzed by Komet5 imaging system (Kinetic Imaging LTD.) at least 100 comets from each of five replicate cultures. DNA damage was quantified immediately after RF-field exposures using three parameters (tail moment, comet length and tail length) for each comet.

**RESULTS AND DISCUSSION:** A172 cells were exposed at average SAR of 80, 250, and 800 mW/kg with W-CDMA, and 80 mW/kg with CW radiations for 2 and 24 hours. IMR-90 cells were exposed in vitro at 80 mW/kg with both W-CDMA and CW radiation for the two periods. No differences in either cell morphological phenomenon or in cell cycle profile were detected when the exposure took place during the period of incubation. In the same RF field exposure conditions, no significant differences in DNA strand breaks were observed between the test group exposed to W-CDMA or CW radiation and the sham-exposed negative controls when processed immediately after the exposure periods by the alkaline comet assay. In contrast, the response of human cells exposed to MMS was significantly different from RF-radiation- and sham-exposed cells. Thus, under the experimental conditions tested, there is no evidence for induction of DNA single-strand breaks and alkali-labile lesions in human cultured cell lines exposed to W-CDMA and CW 2.1425 GHz microwave radiation. Our results confirm that low-level exposures did not act as a genotoxicant at up to 800 mW/kg SAR. In a future plan, we will evaluate whether or not there are biological effects of exposure to microwave radiations on the gene expression profile using DNA microarray in human cell lines. This work was supported by NTT DoCoMo Inc.

References:

- [1] ICNIPR, 1998. Guidelines for limiting exposure to time-varying electric, magnetic, and electromagnetic fields (up to 300GHz). *Health Phys* 74, 494-522.
- [2] Uebayashi et al., 2003. Large-scale in vitro experiment system for low-level long-term irradiation by 2-GHz mobile radio base-stations: System design and its performance. 25th BEMS annual meeting, Maui, Hawaii, p19.
- [3] Iyama et al., 2004. Large-Scale In Vitro Experiment System for 2 GHz-Exposure. *Bioelectromagnetics* 25, 599-606.

P-B-116

**EFFECTS OF A TIME-VARYING MAGNETIC FIELD ON INTRACELLULAR  $Ca^{2+}$  MOVEMENTS OF CULTURED BOVINE ADRENAL CHROMAFFIN CELLS.** T. Ikehara<sup>1</sup>, H. Sasaki<sup>2</sup>, T. Teramoto<sup>2</sup>, H. Houchi<sup>2</sup>, K. Hosokawa<sup>1</sup>, H. Yamaguchi<sup>3</sup>, M. Kitamura<sup>1</sup>, M.i Shono<sup>1</sup>, K. Yoshizaki<sup>1</sup>, Y. Kinouchi<sup>4</sup>, H. Miyamoto<sup>1</sup>. <sup>1</sup>Dept of Physiology, Institute of Health BioSciences, The

Univ of Tokushima Graduate School, Tokushima, Japan, <sup>2</sup>Dept of Pharmacy, Tokushima Univ Hospital, Tokushima, Japan, <sup>3</sup>Dept of Environmental Physiology, Faculty of Human Life Sciences, Tokushima Bunri Univ, Tokushima, Japan, <sup>4</sup>Dept of Electrical and Electronic Engineering, Faculty of Engineering, The Univ of Tokushima, Tokushima, Japan.

**OBJECTIVE:** We have recently found that the time-varying magnetic field inhibited the  $\text{Ca}^{2+}$  release from intracellular stores of adrenal chromaffin cells. In this study, we examined to find out the mechanisms that exposure to the magnetic field affected  $\text{Ca}^{2+}$  movements in the cells.

**MATERIALS AND METHODS:** Bovine adrenal chromaffin cells were plated on 35-mm culture dishes or cover glasses placed in the same culture dishes. After the cells were attached to the dishes or cover glasses, they were maintained for 2-5 days. Magnetic field is produced by an electromagnet designed and set up by Hitachi Metal Indust. Co. (Tokyo, Japan). Magnetic flux density was varied intermittently from 0.07 to 1.5 T at an interval of 3 sec. The concentration of intracellular  $\text{Ca}^{2+}$  ( $[\text{Ca}^{2+}]_i$ ) was measured with Fura 2 by ARGUS 50/CA (Hamamatsu Photonics, Hamamatsu, Japan). Cells were also observed with a laser scanning confocal microscope (Leica TCS-NT, Heidelberg, Germany). Oxygen consumption and ATP were measured by using oxygen electrode and the luciferin-luciferase reaction, respectively.

**RESULTS AND DISCUSSION:**  $[\text{Ca}^{2+}]_i$  was increased by addition of acetylcholine (ACh). The exposure to the magnetic field for 2 hr inhibited these activators-stimulated increase in  $[\text{Ca}^{2+}]_i$  in  $\text{Ca}^{2+}$ -free medium, but slowed only the decay phase of  $[\text{Ca}^{2+}]_i$  after peak in  $\text{Ca}^{2+}$  containing medium. In the presence of ACh delay of the decay phase was also caused by addition of NaCN. Measurement of mitochondrial membrane potential by using fluorescent probe, JC-1 (Molecular Probe), showed depolarization of the membrane in both cells exposed the magnetic field and added NaCN. The intracellular ATP content and oxygen consumption were influenced by the exposure in glucose-free medium. Fluorescent intensity of actin stained by phalloidin was decreased by the exposure. These results suggests that the former influences by exposure to the magnetic field were related to depolarization of mitochondrial membrane. These effects of magnetic field would be related to the eddy current.

P-B-119

#### **EVALUATION OF MUTAGENICITY BY EXPOSURE TO A EXTREMELY LOW FREQUENCY INTERMITTENT PULSED MAGNETIC FIELD.** M. Ikehata<sup>1</sup>, T. Koana<sup>2</sup>.

<sup>1</sup>Biotechnology laboratory, Environmental Engineering Division, Railway Technical Research Institute, <sup>2</sup>Low Dose Radiation Research Center, Nuclear Technology Research Laboratory, Central Research Institute of Electric Power Industry.

**OBJECTIVE:** There are many studies that investigate the effects of electric and magnetic fields (EMFs) on biological systems. These findings provide us the important knowledge of the biological effects of ideal EMFs. However, besides these scientific data, it is necessary to estimate the effect of environmental complex EMFs to guarantee the safety. In this study, we have views upon an extremely low frequency intermittent pulsed magnetic field and investigate its mutagenicity using two independent mutation assay systems.

**METHODS:** For intermittent pulsed magnetic field (IPMF) exposure, we developed a pair of exposure coil. An exposure coil was constructed using two Merritt coils assembled quadrature. The exposure coil was energized by bi-polar amplifier with artificial waveform that generated by Personal Computer. Each exposure coil was located in the conventional  $\text{CO}_2$  incubator, respectively. The setup of this exposure

apparatus was shown in figure 1. In this study, the condition of IPMF is 17 train pulses of 6Hz, 2.7mT magnetic field. Duration of this IPMF was approximately 3 seconds and the field was generated every 30 seconds. Exposure space was maintained at 37±1 or 34±1 °C. To evaluate the mutagenicity, we employed two mutation assays. One is the bacterial mutation assay (Ames test) and *Salmonella typhimurium* TA98, TA100, TA102 and *Escherichia coli* WP2 *uvrA* was used in this study. These bacterial cells were exposed to complex EMFs for 48 hours after plating onto glucose minimal media with trace of required amino acid (histidine and biotin for *S. typhimurium* strains and tryptophan for *E. coli* strain) at 37±1°C. Control cells were incubated in conventional incubator. After 48 hours of incubation, number of prototroph mutant colony appearing on each plate was scored. The other mutation assay is yeast mutation assay using *Saccharomyces cerevisiae* XD83 (*MAT a/MAT $\alpha$* , *lys1-1/lys1-1*, *arg4-4/+*, *+/arg4-17*). For detecting point mutation frequency on *lys 1-1*, harvested cells were mixed with molten soft agar (0.6 % Bacto-agar, 0.5 % NaCl) and were poured onto low lysine synthetic complete plate. For detecting gene conversion frequency on *ARG4* allele (between *arg 4-4* and *arg 4-17*), cell suspension was poured on to low arginine synthetic complete plate. At least 6 plates were made for both condition and randomly divided into two groups. One group was exposed to complex EMFs for 5 days at The other group was incubated in other exposure coil which was not energized at 34 ± 0.5 °C as control. Number of colonies on each plate was scored as reverse mutant and the mutation frequency was calculated.

**RESULTS:** No significant difference in either point mutation on *LYS1* allele or gene conversion/recombination frequency on *ARG4* was observed in *S. cerevisiae* XD83. And also in bacteria, we observed no difference between exposed and control group on each point mutation in four tester strains of *S. typhimurium* and *E. coli*. These results suggest that exposure to the IPMF used in this study did not have a potential to affect the mutation induction. Our previous studies [1-3] showed that strong magnetic fields such as 5T static magnetic field or 20mT, 50Hz magnetic field have weak mutagenicity or co-mutagenicity. Comparing with those conditions, the IPMF (6Hz, 2.7mT) used in this study is much lower than the previous studies in field density and also in frequency. Therefore, these results reasonably suggest the IPMF used in this study does not have significant biological effects, especially related to initiate cancer. This work was financially supported in part by the Ministry of Land, Infrastructure and Transport, Japan.

#### REFERENCES

- [1] T. Koana, M. O. Okada, M. Ikehata and M. Nakagawa, *Mut. Res.*, vol. 373, pp. 55-60, 1997.
- [2] M. Ikehata, Y. Suzuki, H. Shimizu, T. Koana and M. Nakagawa, *Mut. Res.*, vol. 427, pp. 147-156, 1999.
- [3] T. Koana, M. O. Okada, Y. Takashima, M. Ikehata and J. Miyakoshi, *Mut. Res.* Vol. 476, pp. 55-62, 2001.



Fig. 1 Exposure apparatus for IPMF experiments

P-B-122 STUDENT

**MICROWAVES EFFECTS ON NEURONAL CELLS: STUDY OF APOPTOSIS.** V. Joubert<sup>1</sup>, P. Lévêque<sup>2</sup>, A. Rametti<sup>1</sup>, A. Collin<sup>2</sup>, S. Bourthoumieu<sup>1</sup>, F. Terro<sup>1</sup>, C. Yardin<sup>1</sup>. <sup>1</sup>Laboratory of Neurobiology, 2 rue Dr Marcland, Limoges, France, <sup>2</sup>Institut de Recherche en Communications Optiques et Micro-ondes, Limoges, France.

**INTRODUCTION:** At high level, microwaves (MW) may induce neuronal injury, and MW effects on the blood-brain barrier, on neurochemistry of the brain, on electroencephalography, as well as cognitive effects have been studied during the last years. However, few papers have been published on the apoptosis of neuronal cells.

**OBJECTIVE:** The aim of our work was to study MW effects on neuronal apoptosis in vitro.

**METHODS:** Human neuroblastoma cells SH-SY5Y were used. Cells were exposed in wire-patch cell in an incubator (37°C, 5 % CO<sub>2</sub>) at 900 MHz, continuous waves (CW) for 8, 24 or 48 hours, at a specific absorption rate (SAR) of 2 W/kg. Cells were fixed at 0, 24 or 48 hours after exposure. During exposure, the temperature inside the Petri dishes was measured using a fiber optic probe (Luxtron). This control showing an increase of 2°C, cells were also exposed at 39°C.

A positive control was performed using staurosporine (a protein kinase inhibitor, 1µM for 2 hours).

Apoptosis rate was assessed using three methods:

- DAPI staining: the rate of stained nuclei with apoptotic morphology was evaluated using a fluorescence microscope (Nikon),
- Flow cytometry using double staining with TdT-mediated dUTP nick-end labeling (TUNEL) and propidium iodide (PI),
- Measurement of caspase 3 activity by fluorimetry.

Three independent experiments were conducted, and the data were expressed as means ± SD.

Statistical comparison was performed using the CHI<sup>2</sup> test, with a significance level of 0.05.

RESULTS:

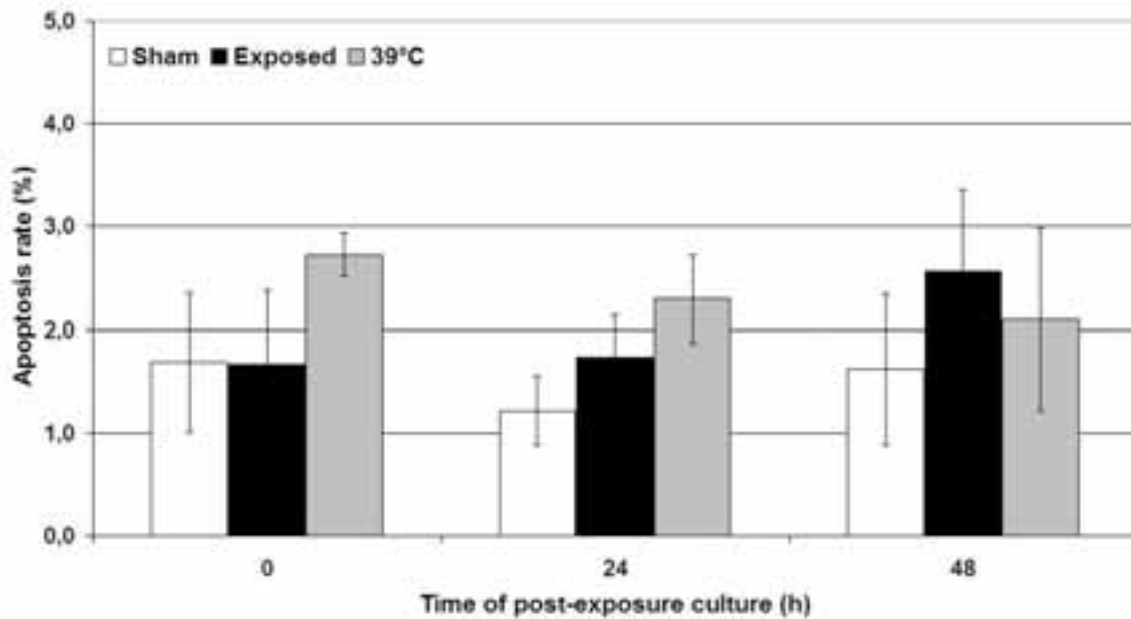


Figure 1: SH-SY5Y exposed at 900 MHz (CW) for 24 hours at a SAR of 2 W/kg or exposed at 39°C for 24 hours.

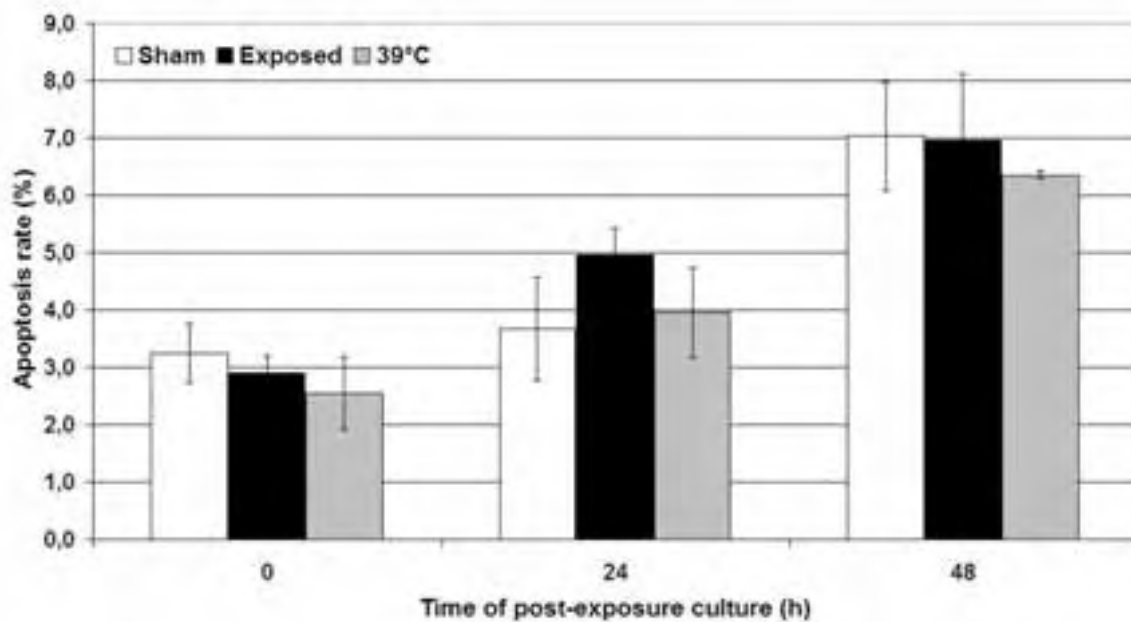


Figure 2: Caspase3 activity.

The positive control (staurosporine) showed 36% apoptosis rate. No significant difference in apoptosis was observed with DAPI staining method nor with TUNEL/PI staining between sham- and radiofrequency-exposed cells(Fig 1). Furthermore, the evaluation of caspase 3 activity showed no significant difference in sham compared to MW-exposed SH-SY5Y cells. The measurement of temperature during exposure showed an increase of 2°C in exposed dishes. However,

apoptosis assessment showed no significant difference between control (37°C) and heat-exposed (39°C) cells, neither between heat- and microwave-exposed cells.

**CONCLUSION:** These results indicate that MW exposure of 900 MHz, CW at a SAR of 2 W/kg during 8, 24 or 48 hours causes no significant effect on neuronal apoptosis in vitro under our exposure conditions in SH-SY5Y cells.

**PERSPECTIVES:** (i) The expression of TRAIL, FAS, Bad, Bax, HSP72 will be studied using immunohistochemical staining under the same exposure conditions (900 MHz, CW, 2 W/kg). (ii) A cytogenetic study will be carried out in the laboratory on another cell type. The karyotype of MW exposed amniotic human cells will be compared to the karyotype of sham-exposed cells. Sister chromatid exchanges and formation of micronuclei will also be studied.

**Acknowledgments:** We wish to thank I. Lagroye and B. Veyret for critical reading of the abstract and for their support.

P-B-125

**EFFECT OF EXTREMELY LOW FREQUENCY ELECTROMAGNETIC FIELD (ELFMF) ON OSTEOBLAST CELL DIFFERENTIATION IN MC3T3-E1 CELLS.** Y. Komatsubara<sup>1,2</sup>, T. Sakurai<sup>1</sup>, S. Koyama<sup>1,3</sup>, W. Jing<sup>1</sup>, J. Miyakoshi<sup>1</sup>. <sup>1</sup>Faculty of Medicine, Hirosaki Univ, Hirosaki, Aomori, Japan., <sup>2</sup>Kashima Laboratory, Mitsubishi Chemical Safety Institute Ltd., Kashima-gun, Ibaraki, Japan., <sup>3</sup>Graduate School of Human and Environmental Studies, Kyoto Univ, Yoshida-Konoe-cho, Sakyo, Kyoto, Japan.

**INTRODUCTION:** Electromagnetic stimulation has been used successfully to treat a wide range of bone healing. On the other side, negative reports on the in vitro effect of electromagnetic stimulation were reported. The mechanism by which the electromagnetic fields can influence the behavior of bone cells remains poorly understood. The elucidation considered that the mechanism of an electromagnetic field to the osteoblast was helpful to fracture treatment.

**OBJECTIVE:** The purposes of this research were to assess the stimulatory effect of electromagnetic fields on bone cells and to assess the possible mechanism from differentiation inducing.

**METHODS:** The exposure system a sinusoidal magnetic field at a frequency of 60Hz, 5mT, was performed previously described [1]. Mouse osteoblast-like cell line of MC3T3-E1 was seeded onto 6-well multi well plate at a density of  $1 \times 10^5$  cells/cm<sup>2</sup> and was grown for 3 days before ELFMF exposure. The temporal effect of ELF on the osteoblasts were evaluated 1, 2, 3 days after starting ELFMF exposure. We examined about cell number, alkaline phosphatase activity and calcium assay.

**RESULTS:** No significant difference was detected to cell number, alkaline phosphatase activity between sham and expose of ELFMF treatment for 3 days (Fig. 1). Moreover, in this calcium assay, the difference was not seen between sham and exposure (Fig. 2).

**CONCLUSION:** The effect of an electromagnetic field was not observed in this experiment. As a future plan, we will evaluate the gene expression mechanism which it exerts on the osteoblast of an electromagnetic field using RT-PCR method whether ELF stimulation affect to osteoblast differentiation or not.

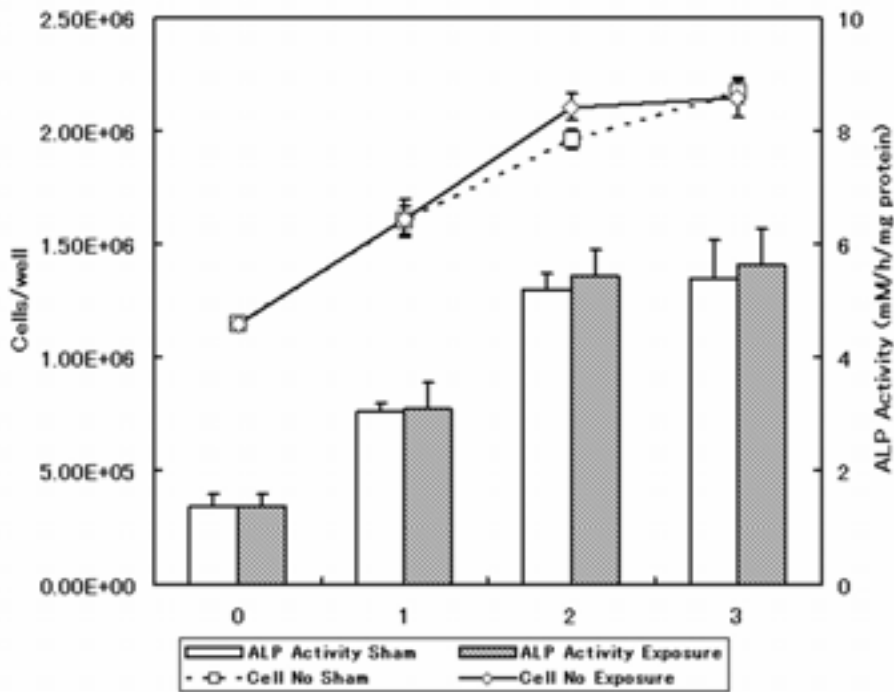


**Figure.1** Effect of EMF exposure on the cell number and alkaline phosphatase activity at a sinusoidal magnetic field at a frequency of 60Hz, 5mT.

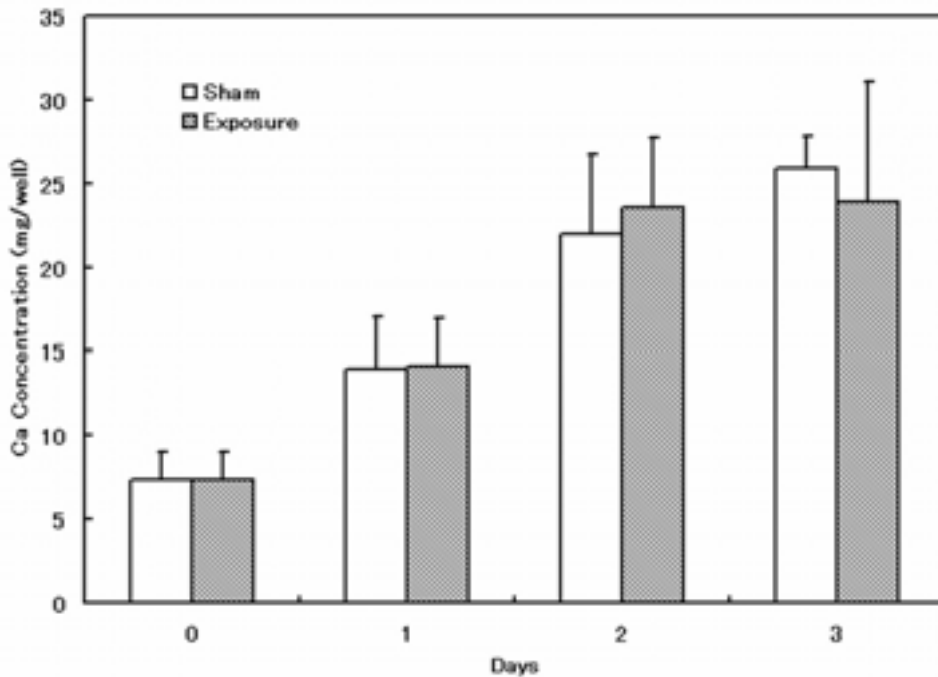


**Figure.2** Effect of EMF exposure on calcium concentration at a sinusoidal magnetic field at a frequency of 60Hz, 5mT.

**REFERENCE:**

[1] Miyakoshi J, et al. 1996. Exposure to magnetic field (5mT at 60Hz) does not affect cell growth and c-myc gene expression. J Radiat Res. 37:185-191.

**EFFECT OF HIGH FREQUENCY ELECTROMAGNETIC FIELDS (HFEMFS) WITH A WIDE RANGE OF SARs ON DNA DAMAGE IN MO54 CELLS.** Y. Komatsubara<sup>1,2</sup>, H. Hirose<sup>3</sup>, T. Sakurai<sup>1</sup>, S. Koyama<sup>1,4</sup>, Y. Suzuki<sup>5</sup>, M. Taki<sup>5</sup>, J. Miyakoshi<sup>1</sup>. <sup>1</sup>Faculty of Medicine, Hirosaki Univ, Hirosaki, Aomori, Japan., <sup>2</sup>Kashima Laboratory, Mitsubishi Chemical Safety Institute Ltd., Kashima-gun, Ibaraki, Japan., <sup>3</sup>Graduate School of Science, Kyoto Univ, Kitashirakawa-Oiwake, Sakyo, Kyoto, Japan., <sup>4</sup>Graduate School of Human and Environmental Studies, Kyoto Univ, Yoshida-Konoe-cho, Sakyo, Kyoto, Japan., <sup>5</sup>Graduate School of Engineering, Tokyo Metropolitan Univ, Hachioji, Tokyo, Japan.

**INTRODUCTION:** Exposure to HFEMFs in the microwave range (300MHz to 300GHz) has become unavoidable in modern society, because of the multitude of uses of HFEMFs in consumer products, communications and broadcasting, medicine, industry, defenses, etc. There is general public concern regarding the potential for adverse human health effects due to HFEMFs exposure [1]. In the present study, we examined the presence or absence of DNA strand breaks in mammalian cells exposed to 2.45GHz HFEMFs with a wide range of SARs in human glioma MO54 cells.

**OBJECTIVE:** We considered that if exposure to HFEMFs could cause a positive cellular effect, it would be worthwhile to assess the dose-response relationship, especially seeking a threshold level. In the present study, we examined the presence or absence of single-strand DNA breaks in mammalian cells exposed to 2.45GHz HFEMFs with a wide range of SARs in human glioma MO54 cells. Temperature elevation is an important factor in the evaluation of the biological effects of HFEMFs.

**METHOD:** MO54 cells were seeded onto Quadri PERM plates, and then cultured for about 24h. The cells were exposed to HFEMFs at SARs of 5, 10, 20, 50, 100, or 200W/kg for 2h. Therefore, we also examined the effects of high temperatures at 39 to 44 °C on DNA strand breaks. To detect DNA damage at an alkaline comet assay was performed. The method of the comet assay has been described previously [2].

**RESULTS:** The effects of exposure to HFEMFs on tail moment are shown in Figure 1. No significant differences in tail moment were seen for each exposure condition at SAR levels from 5 W/kg to 200 W/kg. The effects of exposure to heat treatment on tail moment are shown in Figure 2. No significant differences were observed in tail moment for each of the treatment conditions with sham and heating at 39-44 °C.

**CONCLUSION:** We could not detect a significant increase in DNA strand breaks using the comet assay, when HFEMF at very wide range of SARs (5 to 200 W/kg) was applied. We considered that HFEMF exposure at 2.45GHz for 2 h did not cause DNA strand breaks even at a SAR of 200W/kg.

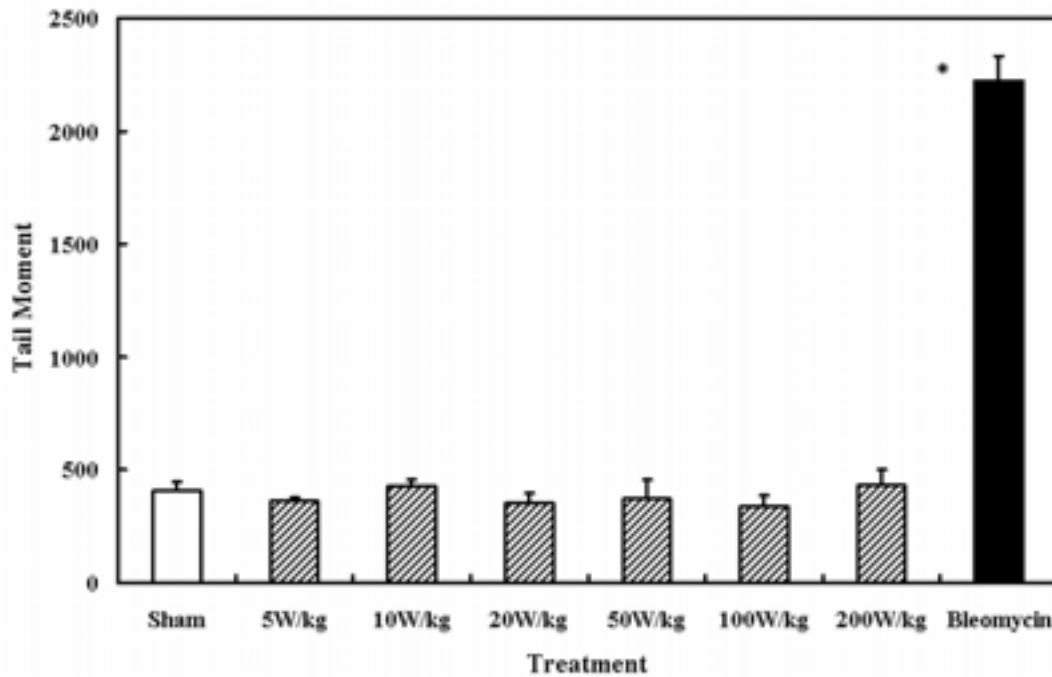


**Figure.1** The effect of HFEMF exposure on tail moment. MO54 cells were exposed to HFEMFs at a SAR of 5 W/kg to 200 W/kg for 2 h. Data are presented as the mean ± standard deviation, based on three experiments. (\*,  $p < 0.001$ )

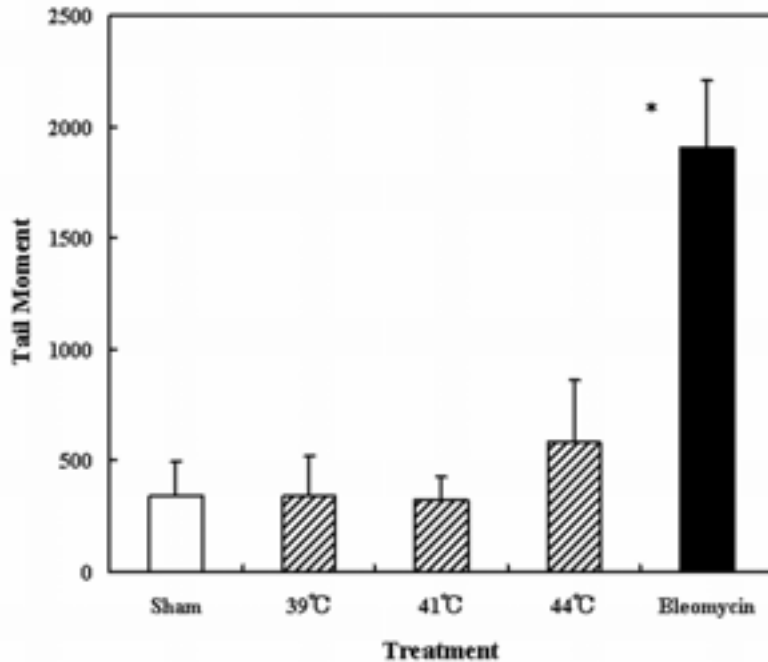


**Figure.2** The effect of heat treatment on tail moment. MO54 cells were exposed to heat treatment at 39, 41 and 44°C for 2 h. Data are presented as the mean ± standard deviation, based on three experiments. (\*,  $p < 0.001$ )

**REFERENCES**

[1] ICNIRP. 1998. Guidelines for limiting exposure to time-varying electric, magnetic, and electromagnetic fields (up to 300GHz). Health Phys. 74:494-522.

[2] Miyakoshi J, et al. 2000. Exposure to strong magnetic fields at power frequency potentiates X-ray-induced DNA strand breaks. *J Radiat Res.* 41:293-302.

\* This work was supported in part by the committee to Promote Research on the Possible Biological Effects of Electromagnetic Fields, Ministry of Public Management, Ministry of Internal Affairs and Communications, Japan.

P-B-131 STUDENT

**EFFECTS OF EXPOSURE TO A 1950 MHZ RADIO-FREQUENCY (RF) FIELD ON MICRONUCLEUS FORMATION IN A172 CELLS.** S. Koyama<sup>1,2</sup>, Y. Komatsubara<sup>1</sup>, T. Sakurai<sup>1</sup>, Y. Isozumi<sup>2</sup>, J. Miyakoshi<sup>1</sup>. <sup>1</sup>Dept of Radiological Technology, School of Health Sciences, Faculty of Medicine, Hirosaki Univ, Hirosaki, Japan, <sup>2</sup>Dept of Interdisciplinary Environment, Graduate School of Human and Environmental Studies, Kyoto Univ, Kyoto, Japan.

**OBJECTIVE:** There has been considerable discussion about the influence of radio-frequency (RF) fields on the human body. In particular, RF from mobile phones may be of great concern for human health. In order to investigate the properties of RF, we have examined the effects of 1950 MHz electromagnetic fields on micronucleus (MN) formation in human glioblastoma A172 cells.

**METHODOLOGY:** RF fields were generated by REFLEX 1950 (Switzerland). The frequency (1950 MHz) corresponds to the middle frequency allocated to the uplink band of IMT-2000 from mobile phone terminals. The apparatus consisted of two single-mode resonator cavities for 1.8 GHz, which were based on the R18 waveguide placed in an ordinary incubator. Cells in the exponential growth phase, were cultured in 35 mm dishes ( $3 \times 10^5$  cells/dish) and were moved to dish holders in two waveguides (one for sham, the other for exposure). Cells were exposed to sham conditions or 1950 MHz continuous-wave in the presence or absence of bleomycin for 5, 10, 30, 60 and 120 min. The specific absorption rates (SARs) were 2, 5 and 10 W/kg. According to the records of exposure apparatus, none of the exposure conditions resulted in an increase in temperature greater than 0.1 degree C. A total of 1000 binucleate cells were scored for evaluation of the frequency of induction of MN, using fluorescence microscopy. Cells were counted as exhibiting MN formation when they contained at least one micronucleus. Statistical analysis was conducted using ANOVA followed by Fisher's PLSD test.

**RESULTS:** There was no increase in MN formation in cells exposed to RF at SARs from 2 to 10 W/kg at exposure time points from 5 to 120 min compared with sham-exposure. Bleomycin induced MN formation significantly ( $P < 0.05$ ). However, there was no enhancement of this effect in the combined treatment of bleomycin and RF-exposure compared with bleomycin-treatment alone.

**CONCLUSIONS:** The MN frequency in cells exposed to a 1950 MHz RF at a SAR  $< 10$  W/kg did not differ from the sham-exposed controls. Exposure to 1950 MHz RF at a SAR  $< 10$  W/kg did not enhance the formation of MN induced by bleomycin. It is well known that temperature increases can induce MN formation. The temperature increase by the RF-exposure at a SAR  $< 10$  W/kg was negligible. This indicates that 1950 MHz RF-exposure does not induce MN nor does it exhibit any thermal effects.

This work was supported in part by NTT docomo.

P-B-134 STUDENT

**EFFECTS OF 2.45 GHZ ELECTROMAGNETIC FIELDS WITH A WIDE RANGE OF SARs ON MICRONUCLEUS FORMATION IN CHO-K1 CELLS.** S. Koyama<sup>1,2</sup>, T. Sakurai<sup>1</sup>, Y. Suzuki<sup>3</sup>,

M. Taki<sup>3</sup>, Y. Isozumi<sup>2</sup>, J. Miyakoshi<sup>1</sup>. <sup>1</sup>Dept of Radiological Technology, School of Health Sciences, Faculty of Medicine, Hirosaki Univ, Hirosaki, Japan, <sup>2</sup>Dept of Interdisciplinary Environment, Graduate School of Human and Environmental Studies, Kyoto Univ, Kyoto, Japan, <sup>3</sup>Dept of Electrical Engineering, Graduate School of Engineering, Tokyo Metropolitan Univ, Tokyo, Japan.

**OBJECTIVE:** There has been considerable discussion about the influence of high frequency electromagnetic fields (HFEMFs) on the human body. In particular, HFEMFs from mobile phones may be of great concern for human health. In order to investigate the properties of HFEMFs, we have examined the effects of 2.45 GHz electromagnetic fields on micronucleus (MN) formation in Chinese hamster ovary (CHO)-K1 cells. MN formation is induced by chromosomal breakage or inhibition of spindles during cell division and leads to cell damage. We also examined the influence of heat on MN formation, since HFEMF exposure causes an increase in temperature.

**METHODOLOGY:** Cells were exposed to HFEMF of 2.45 GHz sinusoidal continuous waves (CW). The applicator is based on a rectangular waveguide. The electromagnetic waves are propagated along the waveguide in TE<sub>10</sub> mode. After 23 h of preincubation, the medium was exchanged for fresh medium or a new medium containing bleomycin (final concentration: 10 µg/ml). An additional 1-hour incubation was then performed. Cells treated with or without bleomycin were washed three times with PBS, cultured in fresh medium, and then exposed to a HFEMF (SAR 5, 10, 20, 50, 100 or 200 W/kg) for 2 h. In the heat treatment, after treatment with or without bleomycin, the cells were washed three times with PBS, cultured in fresh medium, and then incubated at 38, 39, 40, 41 or 42°C for 2 h. A sham-exposure experiment was performed as a negative control, and as a positive control, cells were treated with bleomycin alone. A total of 1000 binucleated cells were scored to evaluate the frequency of induction of MN, using fluorescence microscopy. Cells were counted as having MN formation when they contained at least one micronucleus. Statistical analysis of the data in the control and experimental groups was performed using ANOVA followed by Fisher's PLSD test.

**RESULTS:** MN formation did not increase in cells exposed to HFEMFs at SARs from 5 to 50 W/kg. However, the frequencies of MN formation in cells exposed to HFEMFs at SARs of 100 and 200 W/kg were significantly different compared to that observed following sham exposure. The frequency of MN formation following treatment with bleomycin alone was statistically higher than sham-exposed controls. Although MN formation did not increase in cells treated with a combination of bleomycin and HFEMF exposure, at SARs from 5 to 100 W/kg, there was a statistically significant difference in MN formation between cells treated with bleomycin alone and those treated with both bleomycin and HFEMF exposure at a SAR of 200 W/kg. The frequency of MN formation with heat treatment increased in a temperature-dependent manner. However, no differences were observed between bleomycin-treated cells and cells treated with a combination of heat and bleomycin at temperatures from 38 to 41°C. MN formation in cells that underwent combined treatment with heat (42°C) and bleomycin was statistically different compared to that in cells treated with bleomycin alone, but there was no difference compared to cells treated with heat alone (42°C).

Fig. 1 presents the relationship between the effects of exposure to HFEMFs and temperature. Bars indicate the mean MN frequency, and the line graph indicates the changes in temperature generated by exposure to HFEMFs in Fig. 1.

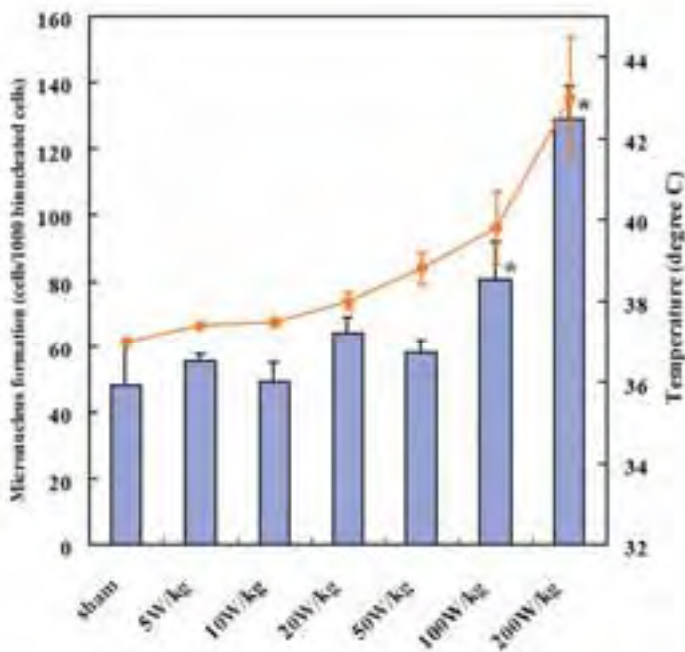


Fig. 1

The frequency of MN formation increased in a temperature-dependent manner ( $r^2 = 0.978239$ ).

**CONCLUSIONS:** The MN frequency in cells exposed to a HFEMF at SAR < 50 W/kg did not differ from sham-exposed controls, while those at SARs of 100 and 200 W/kg were increased significantly compared with sham-exposed controls. There was no apparent combined effect of HFEMF exposure and bleomycin treatment. Upon heat treatment at temperatures from 38 to 42 °C, MN frequency increased in a temperature-dependent manner. We also demonstrated that increases in SAR results in a rise in temperature, and that this may be connected to the increase in MN formation generated by exposure to a HFEMF.

This work was supported in part by Ministry of Internal Affairs and Communications, Japan.

P-B-137

**PROLIFERATION, DIFFERENTIATION AND APOPTOSIS IN A NEUROBLASTOMA CELL LINE EXPOSED TO 900 MHZ MODULATED RADIOFREQUENCY FIELD.** P. Merola, C. Marino, G. Alfonso Lovisololo, R. Pinto, C. Laconi, A. Negroni. Italian National Agency for New Technologies, Energy and the Environment, Section of Toxicology and Biomedical Sciences, Rome, Italy.

A widespread use of mobile phones evokes a growing concern for their possible adverse effects on the human central nervous system. The aim of this study was to explore the possible influence of a modulated radiofrequency (RF) radiation exposure generated by mobile phones on proliferation, differentiation and apoptosis processes in a neuroblastoma cell line (LAN-5).

The field was generated by signal simulation of the Global System for Mobile communications GSM of 900 MHz and at a specific absorption rate (SAR) of 1 W/kg. The exposures were performed until 72 hours in a Wire Patch Cell (WPC) RF source and in blind procedure (incubator control, sham and

exposure samples were adopted). In order to evaluate the possible effect of RF fields on cell proliferation, we first performed a WST-1 assay in cells under standard culture conditions after 24, 48 and 72 hours of exposure. Later, to increase the number of cells that would be initiating cell cycle progression, during radiofrequency exposure, we examined serum stimulated cultures after synchronization. No significant change in proliferation rate was found in the sham and exposed cells. Furthermore, we carried out combined exposures to radiofrequency and the differentiative agent retinoic acid to test possible interference between electromagnetic field and differentiation process. For this purpose, we tested two specific markers as oncogenes B-Myb and N-Myc and a cytoskeleton protein by a molecular analysis. We observed no substantial difference in exposed cells compared to sham ones. To assess if RF could interfere with an apoptosis process, we treated cells in the presence or absence of the apoptosis-inducing agent camptothecin and immediately we exposed cells at the radiofrequency. To detect an apoptotic process induced by RF we used a caspase activation assay, moreover apoptosis was also evaluated by molecular detection of Poly (ADP-ribose) polymerase cleavage. In all conditions and for all endpoints tested, there was no significant difference between RF- and sham-exposed cells. So that, 900 MHz RF could not induce apoptosis by itself or affect the apoptotic phenomenon when induced by an apoptotic agent.

The findings of our study suggest that a 900 MHz radiofrequency exposure until 72 hours emitted by cellular phones has no abnormal effects in the three principal cell activities in a neuroblastoma cell line.

These activities were partially supported by RAMP 2001, QLK4-CT-2001-00463; the national research project "Protection of humans and environment from electromagnetic emissions" MIUR

P-B-140

**EXPOSURE TO INTERMEDIATE FREQUENCY MAGNETIC FIELDS DID NOT HAVE MUTAGENIC POTENTIAL IN BACTERIAL MUTATION TEST.** S. Nakasono<sup>1</sup>, M. Ikehata<sup>2</sup>, I. Nishimura<sup>1</sup>, T. Negishi<sup>1</sup>, T. Shigemitsu<sup>1</sup>. <sup>1</sup>Biological Environment Sector, Environmental Science Research Laboratory, CRIEPI, Abiko, Abiko-city, Japan., <sup>2</sup>Biotechnology Laboratory, Environmental Engineering Division, RTRI, Kokubunji, Tokyo, Japan.

**OBJECTIVES:** In contrast of extremely low frequency and radio frequency electromagnetic fields (EMF), the biological effects of the intermediate frequency (IF: 300Hz to 10MHz) EMF has not been studied very well. In this research, to provide scientific knowledge about toxicological information of the IF fields, we have investigated the mutagenic potential of the IF magnetic field (MF) by using bacterial mutation test.

**METHODS:** We constructed a Helmholtz type exposure system for the in vitro research, which can generate a vertical and sinusoidal MF in the frequency range from 2 to 60 kHz. The maximum field strength depends on the MF frequency, and 0.91mTrms (146 times greater than the strength of ICNIRP guideline), 1.1mTrms (176 times) and 0.11mTrms (18 times) of MF was generated at 2 kHz, 20 kHz and 60 kHz, respectively. This system provides a large uniform MF environment (20cm-cube, field variation below 5%), for the bacterial mutation test. Incubator with water jacket was located in the center of the system, and the incubation temperature was controlled at  $37 \pm 0.3^{\circ}\text{C}$ . Four strains of *Salmonella typhimurium* (TA98, TA100, TA1535, TA1537) and two strains of *Escherichia coli* (WP2 uvrA, WP2 uvrA/pKM101) were chosen to examine a wide spectrum of point mutation, including AT base substitution, GC base substitution, suppressor mutation, and frame shift. Twelve plates were randomly divided into two groups: six plates were placed at the center of the MF exposure system while the other six were placed in a control incubator. Revertant colonies were scored after 48 hr of incubation at 37C.

Each experiment was repeated at least four times. Student's t-test was used for the statistical analysis of the results.

**RESULTS:** In all test set, all of the test strain were responsive against corresponding positive controls, such as 2-(2-furyl)-3-(5-nitro-2-furyl) acrylamide, sodium azide (DNA reactive reagents), 2-amino anthracene (frame shift), 9-amino acridine and benzo[a]pyrene (DNA reactive promutagen which activated metabolically by rat S9mix). Mutagenicity tests of four MF exposure conditions, such as 0.91mT at 2kHz, 0.27mT or 1.1mT at 20kHz and 0.11mT at 60kHz, were carried out. The ratio of the colony number between exposed and unexposed control groups were mostly in the range of 0.7 to 1.4. Most of large differences were found in low colony number strains. In statistically analysis, neither significant nor reproducible difference was found between exposed and unexposed control groups in all exposure condition with six test strains. The shape and size of revertant colony were almost same between the exposed and unexposed control groups.

**CONCLUSIONS:** These results suggest that the IF MF exposure that ranged 20-180 times high as ICNIRP guideline could not affect the mutation frequency, such as AT base substitution, GC base substitution, suppressor mutation, and frame shift, in the bacterial mutation test.

Bacterial mutation test for Intermediate frequency magnetic fields							
		Exposure Condition					
		Control	20kHz		60kHz	2kHz	
Exposure Condition		Type of Mutation		0.27mT	1.1mT	0.11mT	0.91mT
<i>S. typhimurium</i>	TA98	Frame shift	1/10	0/4	0/5	1/6	0/5
	TA100	GC base substitution	1/10	0/4	2/11	0/6	0/6
	TA1535	GC base substitution	0/10	0/4	2/11	0/6	0/5
	TA1537	Frame shift	0/10	0/4	1/11	0/6	1/6
<i>E. coli</i>	WP2 uvrA	AT base substitution, suppressor mutation	1/10	0/4	0/11	0/6	1/6
	WP2 uvrA/pKM101	AT base substitution, suppressor mutation	3/10	0/4	0/10	0/6	0/6

Denominator shows the number of tests. Numerator shows the number of positive results with  $P < 0.05$  in Student's t-test.

P-B-143

**EFFECT OF RFR ON HUMAN LYMPHOCYTE DERIVED CELL LINES.** S.D. Naughton, C. D. Lindsay, R. Simpson, J. Gibson, R. I. Grose, S. J. Holden, A. Wright, J. N. Hughes, S. A. Smith, C. Taylor, R. H. Inns. Dstl Biomedical Sciences Porton Down, Salisbury, Wiltshire, UK.

ICNIRP safety guidelines recommend two-tier occupational and public exposure levels to radiofrequency radiation (RFR). The basis for this is that some individuals in the human population may be potentially vulnerable to RF field effects for various reasons e.g. ill health. A potential model for examining susceptible individuals is that of lymphoid cell lines from human subjects with the condition

ataxia telangiectasia (AT), which have been demonstrated to be responsive to ionising radiation. AT is an autosomal recessive multisystem disorder associated with a high incidence of chromosome breaks and malignancies such as brain tumours, leukaemia and gastric cancer. The genetic lesion underlying AT is a mutation in the AT gene (ATM) which codes for a kinase activity associated with nibrin phosphorylation. This leads to downstream G1 cell-cycle arrest-related defects and in DNA mismatch repair. Many of the various aspects of the phenotype associated with AT are attributable to defective DNA damage responses. AT-derived cells are consequently hypersensitive to ionising radiation because they are unable to down-regulate replication of DNA in S-phase of the cell cycle after exposure to genotoxic insult. This leads to the accumulation of genetic damage and subsequent DNA mutations and chromosome breaks. Cells from AT subjects were used on the hypothesis that sensitivity to ionising and other radiation may be related to sensitivity to RFR. Cell cycle, cell viability/death (by apoptosis/necrosis), light microscopy and electron microscopy parameters were studied in AT and control cell cultures following exposure to ultra-wideband (UWB) RFR.

Five cell lines were used in this study: BD2624 and BD2630 (diagnosed AT subjects), BD2505 (an affected AT carrier), BD2510 (an unaffected AT carrier) and GG0257 (an unaffected family member). Using a Bournelea 3153A source, cells were exposed in 25 cm<sup>2</sup> flasks for 3 hours (h) at 37°C to sub-thermal doses of UWB RFR (5.4 kV/m), at a pulsed repetition frequency of 2.17 kHz (rise time 10 ns). This work was funded by the Electronics Systems Domain of the UK Ministry of Defence Scientific Research Programme.

Crown Copyright 2005, Dstl

P-B-146

**EFFECTS OF 900 MHZ MOBILE PHONE RADIATIONS ON NEUROTRANSMITTERS SYSTEM OF RAT.** A. Piotrowski, E. Brillaud, R. de Seze. INERIS, Parc technologique ALATA, BP2, Verneuil-en-Halatte, France.

Objectives:

Low power electromagnetic fields (EMF) are suspected to produce biological effects. In the framework of RAMP 2001 project, we try to evaluate possible effects of GSM exposure on the central nervous system, and to determine the Specific Absorption Rate (SAR) and the duration limits that produce them. A previous study (A.L. Mausset et al., December 2004) showed that binding properties of dopamine transporters (DAT) are modified after 15 min exposure to GSM-type radiation at a local SAR of 6 W/kg (head). Binding of the [3H]BTCP-ligand was used as a tracer of dopamine transporters (DAT). Autoradiography experiments revealed binding in the cortex and an increase (30%,  $P < 0.001$ ) in the striatum of exposed rats. Determination of the binding parameters,  $K_d$  and  $B_{max}$ , indicated that the decreased binding in the cortex is due to a decrease of the ligand–transporter complex affinity, as attested by the increased  $K_d$  value ( $7.1 \pm 1.6$  vs.  $3.9 \pm 0.2$  nM). In contrast, the increased [3H]BTCP radiolabeling in the exposed striatum is rather a consequence of a slight increase of the  $B_{max}$  value ( $3.3 \pm 1.3$  vs.  $2.9 \pm 0.8$  pmol/mg protein).

The goal of this study was to reproduce and complete the A.L. Mausset's study using autoradiographic and saturation binding experiments, which allow investigating the modifications of the binding properties of DAT following an exposure at 900MHz signal.

#### Materials and methods:

96 Rats were exposed using a head only set up (loop antenna) to a GSM 900 MHz signal to various SAR and duration. They were randomly assigned to sixteen groups (n=6):

- 1 control group,
- 5 sham groups: SAR 0 W/kg,
- 10 exposed groups: SAR 6 W/kg.

#### SAR and duration tested are:

- 15, 30, 45, 60 or 120 min,
- - and for each duration, three SAR were used : 0; 1.5 and 6 W /kg.

- The rats were sacrificed immediately after exposure. Brains were removed for binding (dissection of cortex and striatum) and autoradiography (sagittal section).
- To study the dopamine transporter we used the [3H]GBR as specific radioligand.
- The binding parameters, Kd and Bmax, are determined by saturation of DAT with an increasing concentration of [3H]GBR.
- The quantity of DAT is estimated by the measurement of :
  - the radioactivity emitted by DAT-[3H]GBR complex (binding parameters were determined by Scatchard plot using linear regression analysis).
  - the optical density on autoradiographic film exposed to tritium labeled brain slices (using the imaging analysis software Visilog®, NOESIS).
- Three cerebral areas are studying (on the basis of Mausset's work) including cortex, striatum and the hippocampus.
- The data are assessed using parametric statistical analysis.

#### Results:

The data analysis is in progress. Furthermore, the first results will be released at the congress.

Support: European project RAMP (CE) contract no. QLK4-CT-2001-00463, Ministry of Ecology and Durable Development and Research Ministry BCRD no. 12-02

### **In vitro – sub cellular**

P-B-149 STUDENT

**50 HZ ELECTROMAGNETIC FIELDS INDUCE ACTIVATION OF UMBILICAL CORD BLOOD-DERIVED MONOCYTES.** M. Lupke<sup>1</sup>, J. Rollwitz<sup>1</sup>, M. Lantow<sup>1</sup>, C. Maercker<sup>2</sup>, M. Simko<sup>1</sup>. <sup>1</sup>Univ of Rostock, Institute of Cell Biology and Biosystems Technology, Division of Environmental Physiology, Rostock, Germany, <sup>2</sup>German Resource Center for Genome Research (RZPD), Heidelberg, Germany.

**INTRODUCTION:** In previous studies we investigated the activating capacity of murine macrophages (Rollwitz et al. 2004) and human umbilical cord blood-derived monocytes (Lupke et al. 2004) after exposure to extremely low frequency magnetic fields (ELF-MF; 1 mT, 45 min). Both murine

macrophages and freshly isolated human monocytes exposed to ELF-EMF showed significant increases in superoxide production and reactive oxygen species release.

**OBJECTIVES:** The aim of this study is to examine which genes that are involved in the cell activation process in human monocytes after 0, 5, 15, 30 and 45 min of ELF-MF exposure. Furthermore, protein profiling is performed to confirm the data at the RNA level.

**METHODS:** Umbilical cord blood-derived monocytes were isolated as previously described (Lupke et al. 2004). Gene expression analysis on a whole-genome cDNA array (Human Unigene RZPD-2) was performed with total RNA isolated from cells after 45 min ELF-MF exposure (50 Hz, 1 mT). Additionally, real time PCR was used with RNA samples from ELF-MF exposed monocytes after 0, 5, 15, 30 and 45 min of exposure. Furthermore, a protein expression array of lysates from human monocytes exposed 45 min to ELF-MF was carried out with 512 human antibodies (Becton Dickinson).

**SUMMARY:** The gene expression analysis of 5637 fully annotated genes showed a dys-regulation of 999 genes, of which 668 genes were up-regulated and 331 genes were down-regulated. The data show that interleukin receptors (IL20RA, IL15RA) are involved in the cell activation process as well as the early response gene FOS. Real time PCR verified the up-regulation of the interleukin receptor IL15RA and FOS. Further analysis showed an up-regulation of related genes encoding the interleukin receptors IL2RA and IL10RA and two other early response genes, MYC and JUN. Time-course studies revealed that IL10RA and FOS are expressed at a higher magnitude after 15 min, whereas IL2RA and JUN are up-regulated after 30 min. This work is supported by the Verum Foundation, Germany.

#### P-B-152 STUDENT

**EXPOSURE TO A 50 HZ MAGNETIC FIELD INFLUENCES HSP EXPRESSION IN HUMAN LEUKEMIA CELL LINES.** A.-C. Mannerling<sup>1</sup>, S. Hannemann<sup>2</sup>, M. Simkó<sup>2</sup>, K. Hansson Mild<sup>1,3</sup>, M.-O. Mattsson<sup>1</sup>. <sup>1</sup>Cell Biology Laboratory, Dept of Natural Sciences, Örebro Univ, Örebro, Sweden., <sup>2</sup>Division for Environmental Physiology, Institute for Cell Biology and Biosystems Technology, Univ of Rostock, D-18059 Rostock, Germany, <sup>3</sup>National Institute for Working Life, Umeå, Sweden.

**OBJECTIVE:** The objective of this study is to investigate possible stress induced responses in human cells by 50 Hz magnetic fields monitored as heat shock protein expression.

**INTRODUCTION:** The stress response genes collectively known as heat shock protein genes (Hsp genes) can be induced by many different external factors, including temperature stress, various chemicals, oxidative stress, heavy metals, ionizing radiation etc. It has further been suggested that ELF MF exposure can act as a stressor which promotes e.g. Hsp70 expression. The biological relevance of any induction of Hsp70 or any other Hsp gene is difficult to forecast. However, an increased HSP70 protein level is often associated with stress protection on the cellular level, which could indicate a general stress effect by ELF MF if the exposure causes induction of the gene. To test this assumption, ELF exposure was performed on several human cell lines.

**METHODS:** Several human leukemia cell lines were used in this study and cultured according to standard procedures. Exposure to 50 Hz sinusoidal MF (various flux densities, horizontal or vertical polarization) was performed in cell culture incubators equipped with Helmholtz coils for one hour followed by different post-exposure incubation times (0-24 hours). As a positive control, heat shock was employed (42°C). The possible induction of HSP proteins was semi-quantitatively investigated by immunoblotting. Furthermore, a quantitative determination of HSP70 was done by flow cytometric analysis. All experiments were performed in the presence of the local geomagnetic field and under controlled temperature conditions.

**SUMMARY AND CONCLUSION:** Induction of HSP70 expression on the protein level is obtained after exposure to both vertical and horizontal 50 Hz MF, 0.025-0.1 mT. The response increases in amplitude up to 24 h post-exposure. Experiments to investigate possible dose-response relationships, threshold levels, and effects on additional hsp genes are under way.

P-B-155

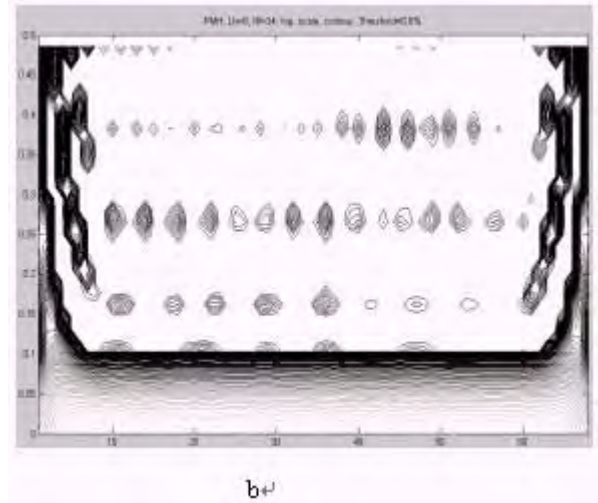
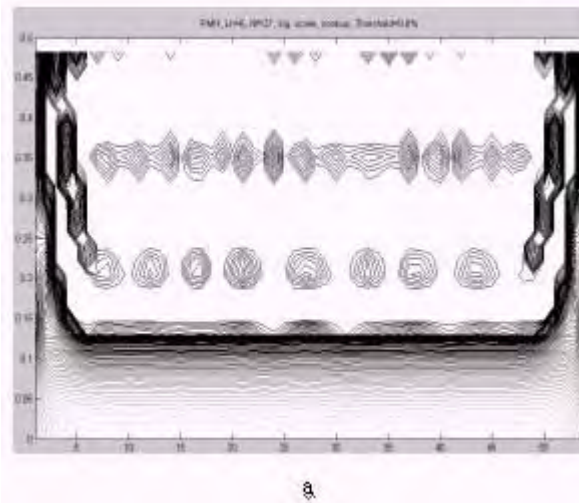
**TIME-FREQUENCY ANALYSIS OF  $Ca^{2+}$  CONCENTRATION IN CYTOPLASM OF CANCER CELL AND EFFECT OF ELF WAVE.** Z. Qi Niu<sup>1</sup>, J. Qiang Hou<sup>1</sup>, H. B. Wang<sup>1</sup>, Z. Yuan Lu<sup>1</sup>, G. Kang<sup>2</sup>. <sup>1</sup>School of Electronic Engineering, Xidian Univ, Xi'an,China, <sup>2</sup>Dept of Electrical and Computer Engineering, Duke Univ, Durham, NC, USA.

**INTRODUCTION:** Calcium ions ( $Ca^{2+}$ ) are widely concerned with life action, which control cells metabolism and have relation with duplication of DNA, etc. Therefore,  $Ca^{2+}$  in cytoplasm are frequently used in researches on bio-effects of electromagnetic waves (EMW). It is well known that cancer is the formidable enemy of human health, so the researches on cancer cells are of significance for the clinical application of the EMW.

**OBJECTIVES:** The objective of this study is to research the window effect of EMW on  $Ca^{2+}$  concentration in cytoplasm by the method of the time-frequency analysis.

**METHODS:** The body's liver cancer cell was made into suspension and loaded by fluorescent reagent Fluo-3, which became into biological samples. The samples were put in laser scanning confocal microscope to measure the fluorescent intensity in cytoplasm and in the background of the sample (i.e. in the sample and outside cell), thus the data of the fluorescent intensities both in the cytoplasm and in the background were obtained, which are the data of a control group. Then the control data were obtained, these samples were put in TEM cell at once to be exposed by EMW at the given frequency and intensity. The fluorescent intensity in the cytoplasm and in the background were measured once more again, so that, the data of the exposed group were obtained. The exposure parameters are divided 7 groups. It should be emphasized that the  $Ca^{2+}$  concentration in the cytoplasm and in the background is expressed by the fluorescent intensity, and all the data are one expressed in time domain. In fact, research on any change law can be made by analysis method of time-frequency. The time-frequency analysis is mapping the function of the time i.e.  $X(t)$  to the function of time-frequency i.e.  $C_x(t, f)$ , which can display the spectrum characters, i.e. what is the distribution of the spectrum and when dose each spectrum component produce in the change process. In this paper Pseudo-Margenau-Hill analysis was used, and the  $C_x(t, f)$  is expressed by  $PHM_x(t, f)$ , the  $f$  is frequency.

**RESULTS:** Fig.1 shows an example of the results in time-frequency domain, which is obtained from the sample exposed by pulse EMW at  $f=16\text{Hz}$  and  $E_{pp}=53\text{v/m}$ . In Fig.1, abscissa is time axes and the ordinate is frequency axe. The graph expresses the contours of the function  $PHM_x(t, f)$  of the  $Ca^{2+}$  concentration cytoplasm. The Fig.1 (a) is the contours of control group, Fig.1 (b) is the contours of exposed group. In the Fig1 (a) and (b), the continuous curves in the bottom are continuous spectrum components, the dispersive and sealed curves in the top are dispersive spectrum components. After the sample exposed by the pulse EMW at  $f=16\text{Hz}$  and  $E_{pp}=53\text{v/m}$ , it is can be seen that the frequency range of continuous spectrums is narrowed and the frequencies of dispersive spectrum is changed. It indicate the pulse EMW at  $f=16\text{Hz}$  and  $E_{pp}=53\text{v/m}$  produce the remarkable change of cytoplasm  $Ca^{2+}$  in time-frequency domain i.e. produce bio-effects. The result indicate that too, the pulse EMW at  $f=45\text{Hz}$  and  $E_{pp}=53\text{v/m}$ ,  $f=16\text{Hz}$  and  $E_{pp}=80\text{v/m}$  produce bio-effects, and the pulse EMW at  $f=16\text{Hz}$  and  $E_{pp}=26\text{v/m}$ ,  $f=32\text{Hz}$  and  $E_{pp}=53\text{v/m}$ ,  $f=60\text{Hz}$  and  $E_{pp}=53\text{v/m}$  do not produce bio-effect. Therefore,  $f=16\text{Hz}$  and  $f=45\text{Hz}$  are two frequency windows,  $E_{pp}=53\text{v/m}$  is a intensity windows.



(\*\*The project supported by National Natural Science Foundation of China)

P-B-158 WITHDRAWN

### In vitro – tissue and organ

P-B-161

**EXPERIMENTAL STUDY ON THE BIOLOGICAL FREE RADICAL PRODUCTION DUE TO MICROWAVE EXPOSURE.** T. Hikage, T. Manabe, T. Nojima. Hokkaido Univ, Sapporo, Hokkaido, JAPAN.

**OBJECTIVE:**

The purpose of this study is to investigate the effects of microwave exposure on biological free-radical production, especially focusing on mobile radio frequencies.

**MATERIALS AND METHODS:**

We developed an experimental system shown in Fig.1, consisting of open type 2.45 GHz high power microwave exposure equipment and an Electron Spin Resonance (ESR) Spectrometer. Free-radical production was assessed from an analysis of the ESR spectra of the tissues. To observe the influence of microwave exposure on biological free radicals generation, the excised tissues (muscle and liver of animal) were used as the first fundamental experiments for radical generation. Fig.2 shows the developed high intensity 2.45GHz exposure system, which consists of a high power magnetron tube, dielectric lenses and a horn antenna [1]. This system enables an efficient beam-forming exposure and effective EMF irradiation concentration on the target tissues. A high intensity and a uniform exposure on the sample tissues are available at the same time without special degradation of the impedance matching caused by the scattering waves from the sample tissues.

Furthermore, in order to estimate the SAR of irradiated tissues, the FDTD based commercial software, SEMCAD is used for the calculation of the field distributions in the whole area including the antenna, lenses and sample tissues.

**SUMMARY OF RESULTS:**

Fig.3 shows an example of the FDTD analysis result of electric field strength pattern from horn antenna to the target tissue used in the experiments. Thus, the calculated peak SAR of muscle tissue was 1.7 kW/kg when the output power of the exposure equipment was set at 3 kW. Table1 denotes the experimental result of relation between exposure time and radical excitations on extracted muscle tissue when the output power was set at 3 kW, the same as above. The tissue irradiated for 240 seconds has an absorbing spectrum that indicates the existence of radical production. As a result, free radicals were clearly produced once the microwave exposure exceeded a certain level of absorbed microwave energy. Moreover, the temperatures of tissues were estimated using the infrared thermal imaging camera. The temperature of tissues becomes high with increasing exposure time, and in the case of temperature above 170 degree Celsius, radical spectra were clearly seen.

**CONCLUSIONS:**

Some of free radicals are produced in biological tissue by microwave exposure if the power level of the microwaves exceeds a certain level. There is a strong relation between radical production and tissue temperature. The measured temperatures of the samples rose to about 170 degrees Celsius with heavy microwave exposure. So far, some experimental investigations about relatively long life radicals were carried out. Currently, we are performing the further experiments for the hydroxyl radicals that treat cultured human fibroblast cells and mobile radio frequency of 900MHz. These results will be presented soon.

This work is supported by Grant-in-Aid from the Ministry of Internal Affairs and Communications (MIC) of Japan.

[1] Hikage et al., (2004) " Microwave Exposure Effects on the Biological Free Radical Production - 2.45GHz exposure system design and estimation with ESR -", BIOLOGICAL EFFECTS of EMFs 3rd International Workshop, pp. 82-86,Greece.

Table1. Exposure time and Radical excitation								
Exposure time (sec)	0	180	200	220	240	260	280	300
Radical detection	No	No	No	No	Yes	Yes	Yes	Yes
The sample tissue is an extracted muscle. The output power of Exposure equipment is set at 3 kW.								

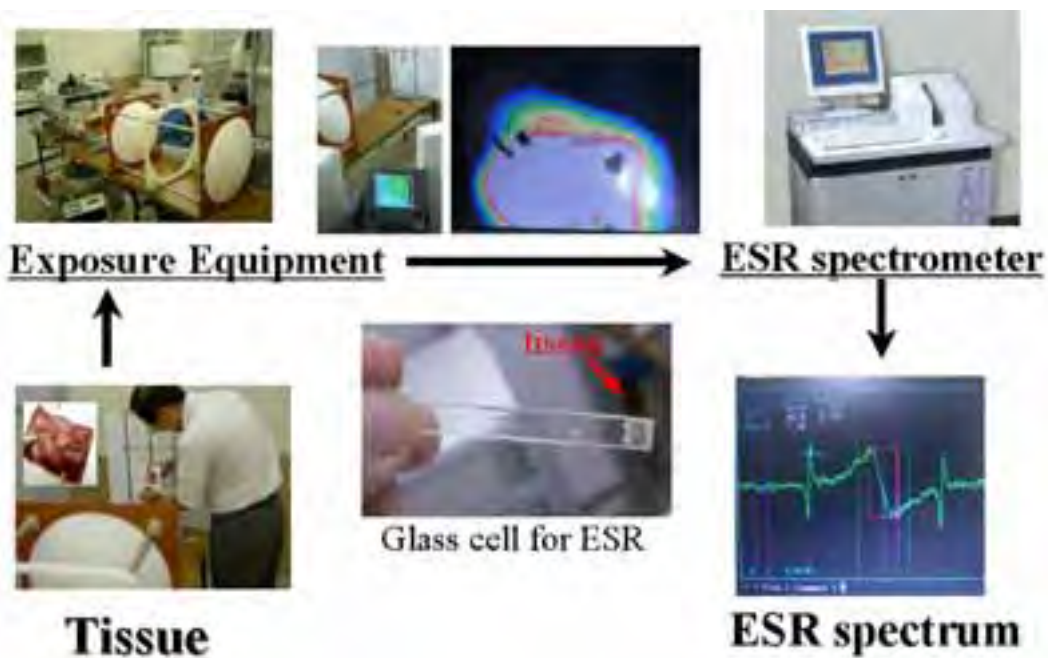


Fig.1 Experimental system.

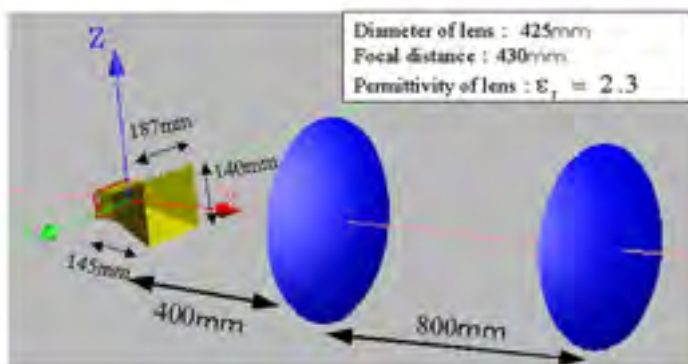
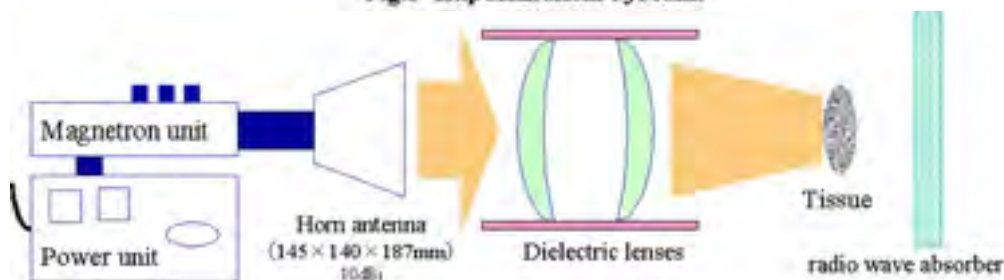


Fig.2 Exposure equipment.

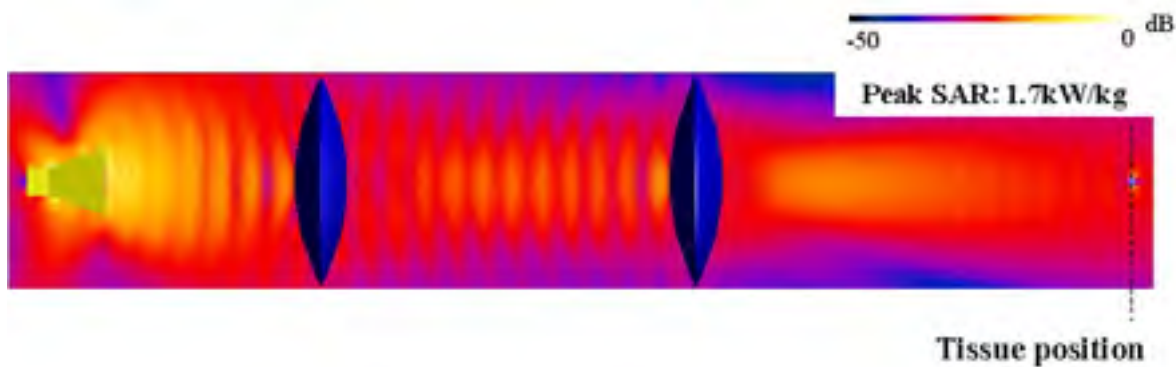


Fig.3 Example of FDTD analysis.

## Mechanisms of interaction - biological

P-B-164

**AN INNOVATIVE MICROWAVE SYSTEM FOR WOOD ART OBJECT DISINFESTATIONS. EXPERIMENTAL RESULTS.** B. Bisceglia, sj.<sup>1</sup>, V. Cimino<sup>2</sup>, R. De Leo<sup>3</sup>, N. Diaferia<sup>4</sup>, K. Mlynarska<sup>2</sup>, S. Pandozy<sup>2</sup>, A. Pompili<sup>2</sup>, Ulderico Santamaria<sup>2</sup>. <sup>1</sup>Engineering Faculty, Università del Sannio at Benevento, Benevento, Italy, <sup>2</sup>Laboratory†of Scientific Research of† Vatican† Museum. Vatican City, <sup>3</sup>Dipartimento di Elettromagnetismo e Bioingegneria, Università Politecnica delle Marche, Ancona, Italy, <sup>4</sup>EMITECH, CORATO (BA), Italy.

### Introduction

Many objects made up of wood as well as paper and cloth with artistic or cultural value are seriously damaged by a variety of pests and often such damages are irreversible. Therefore the need to intervene with effective disinfestation treatments is every day more and more imperative.

The current technologies employed in disinfestation of works of art present big limits as regards very long treatment times, risks of pollution both for the operator and for the environment and possible damages for the treated objects.

In most cases fumigation is employed, that is the use of extremely toxic and polluting gases, such as Methyl Bromide, Ethylene Oxide and Formaldehyde.

Besides fumigation, also anoxic treatments in controlled atmosphere are being used for disinfestation. They are based on the use of inert gases as nitrogen, argon and helium and of mixtures of CO<sub>2</sub> that, though not highly toxic, can interact with the treated materials (as in the case of or CO<sub>2</sub>); such treatments require very long times of exposure (from 7 to 30 days).

Further technologies alternative to the chemical and anoxic methods are those employing physical means (g rays, UV rays, high and low temperatures), whose applications are still experimental, proving scarcely practical and valid.

### Objectives

In the disinfestations field it is essential to use innovative technologies that are

- safer for the work of art
- less expensive

- less dangerous for the environment and the operator .

Our idea is based on the evidence that a lot of biological forms don't survive over a certain temperature, called *lethal temperature* which, for most xylophages is about 53-55°C, while for moulds and fungus is between 65 and 70 °C.

From a technical-scientific point of view, an equipment has been realized which is able to provoke inside the objects under treatment, of any shape, and in particular in pests, a uniform temperature distribution in order to guarantee that:

- organisms or microorganisms are heated up over their lethal temperature.
- the temperature reached by the object and its spatial variations don't provoke deformations.

This technology could be applied to objects of historical-artistic interest made up of:

- wood (furniture, frames, musical instruments, etc.),
- paper (books, documents, etc.),
- cloth (carpets, tapestries, canvas, etc.).

Which are generally subjected to the attack of:

- bugs (woodworms)
- moulds
- fungus

Experimental evaluation

Some samples were prepared in the Vatican Museums to test the use of MISYA on wooden works of art. The samples were very similar to real artistic objects, both painted and not.



## Apparatus, samples and methodology

### Apparatus

The disinfestations system MISYA consists in a metallic shielded treatment chamber. Here, through appropriate openings in the walls, electromagnetic energy at the frequency of the microwaves is introduced. Its propagation inside the chamber is controlled as to obtain a uniform power distribution in the area where the objects are placed.

After the treatment the temperature of the object is measured with infrared thermal sensors, as to control the selective action of the heating, but at the moment a real time monitoring is not available.

The level of electromagnetic field recorded outside the system is well below the threshold of 6 V/m set by the Italian standards. Therefore the complete safety of the operators and the absence of any risk of electromagnetic pollution are fully guaranteed. For the experimental evaluation of effects EMITECH realized a stirred room having dimensions of about 2x2x3 m and fed by a 6 KW magnetron working at 2.45 GHz. Stirring permits to obtain a nearly uniform distribution of density of power in the treatment area.



### Samples

We exposed five groups of samples:

- I. seasoned and green wood
- II. wooden frames with different surface treatments
- III. glued wood (adhesive)
- IV. wood with natural and synthetic adhesives on surface
- V. painted wood with different pigments and varnishes

### Results

We tested the Misya system in order to evaluate the management of disinfestations of wooden works, monitoring

- *incident power*
- *temperature*
- *exposure time*.

We did not observe any chromatic modifications in the samples. The treatment can induce an increase of deformations in presence of breaks, cracks or lacks of homogeneity in the woods. Some changes of water percentage were observed in the samples of the 1st and 2nd groups without relevant modifications in size. In the 3rd group a glue loss took place for temperature  $T > 105^{\circ}\text{C}$ . Some changes in shape were observed in the *Arabic gum* and in *animal glues*. Preliminary results showed that the treatment is optimized for wood samples in the temperature range  $T \leq 50\text{--}60^{\circ}\text{C}$ . Some pigments, such as *Ultramarine blue*, *Geranium Lake Red* and a few natural glues showed some susceptibility to the MW treatment. The tests carried out demonstrate the potential application of the system MISYA to works of art. It is nevertheless necessary to develop a real time monitoring of temperature in order to avoid negative heating effects and it is essential to create a database including information about kinds of wood, conservation state, pigments, bindings, etc versus operating parameters - *incident power*, *exposure time*. These data are useful in order to obtain treatments protocols.

#### References

- R. DE LEO, *A microwave stirred room for woodworm disinfestation of artistic painted boards*, PIERS 2002, Boston.
- C. CASIERI, L. SENNI, M. ROMAGNOLI, U. SANTAMARIA, F. DE LUCA, *Determination of moisture fraction in wood by mobile NMR device*, *Journal of Magnetic Resonance*, n. 171, 2004.

P-B-167 STUDENT

**EFFECTS OF 50HZ MAGNETIC FIELD EXPOSURE ON SECRETION OF PTERIDINE IN MICE IS DEPENDENT ON FIELD POLARIZATION.** E. Kezuka<sup>1</sup>, M. Masada<sup>1</sup>, Y. Nagata<sup>1</sup>, T. Shigemitsu<sup>2</sup>, M. Kato<sup>3</sup>. <sup>1</sup>Faculty of Horticulture, Chiba Univ, <sup>2</sup>Biological Environment Sector, Environmental Science Research Lab, CRIEPI, <sup>3</sup>School of Medicine, Hokkaido Univ.

**OBJECTIVES:** Our previous study suggested that circularly polarized magnetic fields are more effective than horizontally and vertically polarized fields in suppressing melatonin production(1). The effect of magnetic field polarity on the secretion of pteridine in mice was investigated in this study.

**METHODS:** Five week-old male mice (JcL:ICR) were obtained from CLEA, Inc, Japan. Five mice per group were used in this study. Each group of five mice was kept in commercial cages. Due to limitations on space, exposure and sham-exposure systems were located in the same room. Therefore, the sham-exposed mice were exposed to stray magnetic fields from the exposure system. Mice were adapted to a 12:12h light-dark cycle with light off at 19:00h under controlled room conditions. Water and food were given ad libitum. Mice were exposed to 50Hz, circularly, vertically and horizontally polarized magnetic fields ( $B_h=B_v=0.35\text{mTrms}$ ) for periods of one, three and six weeks. The sham-exposed animals were exposed to stray fields of less than  $0.14\mu\text{Trms}$ . After each exposure period, mice were sacrificed to analyze the pteridines in tissues (liver, kidney, cerebrum, cerebellum and blood). These tissues were stored at  $-80$  degree until assayed. The same exposure experiment was repeated three times for each magnetic field polarization. For each experiment, the concentration of pteridine; neopterin(NP),

biopterin(BP), tetrahydrobiopterin(BH4) and guanosine triphosphate cyclohydrolase I(GTP-CHI) activity were measured by the high performance liquid chromatography (HPLC) method. Statistical significance of difference was evaluated by the student't test. A value of  $p < 0.05$  was regarded as significant.

RESULTS: There were no differences in body weights and growth curves between exposed and sham-exposed groups. Among the pteridines, NP is postulated to correlate with cellular immune system and aging. BP can serve to estimate the state of cellular immunity. BH4 is a putative co-factor required for the neurotransmitters, dopamine and serotonin, a precursor of melatonin. Here, the data for liver is shown. Similar results were obtained for other tissues. In circularly polarized magnetic field exposure groups, the level of NP increased significantly compared to sham-exposed groups for all exposure periods, and the level of BH4 decreased significantly compared to sham-exposed groups for the one and three week exposures. On the other hand, for the vertically and horizontally polarized magnetic fields, levels of NP and BH4 in exposed groups were not significantly different from sham-exposed groups. However, the ratio of BH4/BP for circularly polarized magnetic field exposures was significantly lowered compared to the two linearly polarized magnetic fields exposures. The level of BP in exposed groups did not differ from sham-exposed groups in linearly and circularly polarized magnetic fields. The activity of GTP-CHI was not different between the two groups for all magnetic field polarization.

CONCLUSIONS: In this study, the levels of NP, BP and BH4 in mice were measured after the exposure to magnetic fields with three types of polarization for periods up to six weeks. Circularly polarized magnetic fields may affect the activity of cellular immune systems and the biosynthesis pathway from q-BH2 to BH4 due to both changes in NP level and BH4/BP ratio. However, NP levels and BH4 biosynthesis were not affected by the exposures to linearly polarized magnetic fields. Thus there was no evidence for effects on cellular immune systems of exposure to linearly polarized magnetic fields. From these results, only circularly polarized magnetic field exposures may affect the pteridine levels in mice that provide an indirect estimate of the degree of stress emerging during immune response. The results indicated that the degree of polarization may affect the pteridine levels in mice.

This work was supported by the Research Grand-in-Aid from Magnetic Health Science Foundation.

#### Reference

(1) Kato.M and T.Shigemitsu. "Effects of 50-Hz magnetic fields on pineal function in the rat." In the Melatonin Hypothesis-breast cancer and use of electric power. R.G.Stevens et al(eds) Battelle Press pp.337-376 (1997)

P-B-170

**EFFECTS OF 900 MHZ RF EXPOSURE ON BRAIN ACTIVITY IN PICROTOXIN-MODEL OF EPILEPTIC RATS.** E. Lopez-Martin<sup>1</sup>, A. Trastoy<sup>2</sup>, J. L. Relova-Quinteiro<sup>3</sup>, M. Peleteiro<sup>3</sup>, R. Gallego<sup>1</sup>, F. Javier Jorge-Barreiro<sup>1</sup>, E. Moreno<sup>2</sup>, F. J. Ares-Pena<sup>2</sup>. <sup>1</sup>Morphological Sciences Dept, Univ of Santiago de Compostela, Spain, <sup>2</sup>Applied Physics Dept, Univ of Santiago de Compostela, Spain, <sup>3</sup>Physiology Dept, Univ of Santiago de Compostela, Spain.

Because of their biological sensitivity, people suffering from epilepsy may be especially susceptible to radiofrequency radiation emitted by mobile phones. A study of this influence in an animal model of epilepsy consisting of rats to which subconvulsive doses of picrotoxin had been administered was conducted with the animals exposed to controlled radiation during two hours. An appropriate experimental setup was designed trying to avoid, as far as possible, additional neural disturbances that may affect to the study conclusion.

With this aim, a metallic chamber was designed to avoid all spurious signals and also the laboratory staff exposure while radiating animals without additional stress. Inside, two commercial antennas –for transmission and reception, respectively- were located and the field distribution inside the chamber was studied so that the rats were placed in a local maximum. The chamber with and without the animal was electromagnetically characterized using a network analyzer and the measured S-parameters were used to calculate the percentage of power absorbed by the animal. During the experiment the transmission antenna was fed with a 210 mW power and was continuously radiating a 900 MHz GSM modulated signal. The receiving antenna was connected to a spectrum analyzer to assure that there was no spurious radiation within. The S-parameters were measured for each animal and absorption power ratios of 15.5% to 23.4% were obtained (i.e. from 32.5 to 49.1 mW) depending on its size and exact location. During irradiation the animals were videotaped to record clinical signs of seizures and their EEGs were recorded. Four groups of seven rats were given the following treatments: group one and two were injected of picrotoxin, besides the first and third group (without drug) were exposure to radiation, the fourth group exposure to neither radiation nor picrotoxin. After two hours in the radiation cage the animals were removed from it and sedated and one hour later were prefixed by transcardial perfusion. The immunohistochemistry studies were assayed in the free-floating sections: genomic response marker of neuronal activity in the rat brains (c-Fos). The c-Fos positive expression was examined and the nucleus were counted in cortical areas, hippocampal structures and thalamic structures. The significance of between-group differences was estimated taking into account two way: radiation and treatment with picrotoxin. In the rats not treated with picrotoxin, regardless of whether the rats had been irradiated or not, clinical or EEG signs of seizures during radiation were not showed and immunoreactivity was observed in only a few scattered cells in cortical areas. C-Fos-positive neuron counts in irradiated picrotoxin-treated rats about double those found in non-irradiated picrotoxin-treated in cortical areas. In hippocampal and thalamic structures the c-Fos expression was more marked in some areas so dentate gyrus, showed significance differences in centrolateral nuclei and not significance differences in the rest of the areas. The picrotoxin-exposed rat group was coincident with the more seizure clinical and the electroencephalography manifestations. On the other hand, minimal clinical signs of seizure and single spikes in epileptic and non-exposed rats. According to these results, GSM radiation may be able to cause alteration of the activity of cerebral tissue in experimental animal model with subconvulsive doses of picrotoxin.

P-B-173

**IN AN ELECTROMAGNETICALLY SHIELDING ENVIRONMENT A 125 NANOTESLA PULSED MAGNETIC FIELD INDUCES CHANGES IN NOCICEPTION IN MICE.** F. S. Prato<sup>1,2,3</sup>, D. Desjardins<sup>1</sup>, L. Keenlside<sup>1</sup>, J. Robertson<sup>1,2</sup>, A. W. Thomas<sup>1,2,3</sup>. <sup>1</sup>Bioelectromagnetics, Imaging Program, Lawson Health Research Institute, <sup>2</sup>Dept of Medical Biophysics, Faculty of Medicine and Dentistry, Univ of Western Ontario, <sup>3</sup>Dept of Nuclear Medicine, St. Joseph's Health Care.

**INTRODUCTION:** It has been recently shown that if mice are placed in an electromagnetically shielded environment for one hour per day, for consecutive days that analgesia is induced between days 3 to 7, peaking at day 5 (Prato *et al.* 2005). This decreased nociception seems to be opioid mediated as it is eliminated by the opioid antagonist naloxone. There is also evidence that this effect is not caused by the shielding of either the ambient electric field or the static component of the geomagnetic field. This suggests that it may be caused by the shielding of the very weak ambient time changing magnetic fields primarily in the ELF (<300 Hz) range. An examination of the effects of exposure to a reproduced geomagnetic storm within this same paradigm is presented elsewhere (see Robertson *et al.*)

**OBJECTIVE:** To observe the effects of exposure to an extremely weak (50 nT to 25  $\mu$ T) specific pulsed magnetic field on magnetic field shielding induced nociception in CD-1 mice.

**METHOD:** Mice (CD-1) were placed singly in: a) sham/control box made of opaque acrylic, or b) a  $\mu$ -metal box of the same dimension as the sham box and lined with the same opaque acrylic. The  $\mu$ -metal box was fitted with 4 single-wound coils in a Merritt configuration which when electrically energized produced a horizontal magnetic field along the long axis of the mouse transparent acrylic cage which had been inserted into the boxes within the coils. All mice were exposed each of 5 consecutive days, and pre- and post-exposure tested for nociceptive latency. Each experiment was completely randomized over 4 continuous 5 days of testing with the results of the 4 5-day runs combined for analysis. Two separate experiments were performed. In experiment one, 5 groups of animals (N=60, sham = 20, other groups = 10) were studied in which a sham group and a  $\mu$ -metal box group without internal fields was compared to 3 groups in the  $\mu$ -metal box with peak fields of 125 nT, 250 nT, and 500 nT. In the second experiment (data not shown here), the 5 groups were identical except the peak fields were 1.25  $\mu$ T, 2.5  $\mu$ T, and 25  $\mu$ T. Animals were randomly exposed to their respective conditions for 1 hour per day during the light cycle for 5 consecutive days. Hotplate latency (level of nociception, the longer a mouse stays on the hotplate, the greater the induced antinociception) was tested before and immediately after each exposure and was measured as the time delay (or latency time) to an aversive surface at 50 degree C. The pulsed magnetic field parameters (except for peak amplitude) were identical to those known to induce analgesia in mice when the peak amplitude is 200  $\mu$ T (Shupak *et al.* 2004).

**RESULTS:** In all cases, the pulsed magnetic field exposure significantly reduced or completely attenuated the magnetic field shielding induced antinociception seen in the 'no mf' condition. Figure 1 details the data from experiment one. The data from experiment two (not shown here) continues the trend of attenuating the typical magnetic field shielding induced antinociception (analgesia).

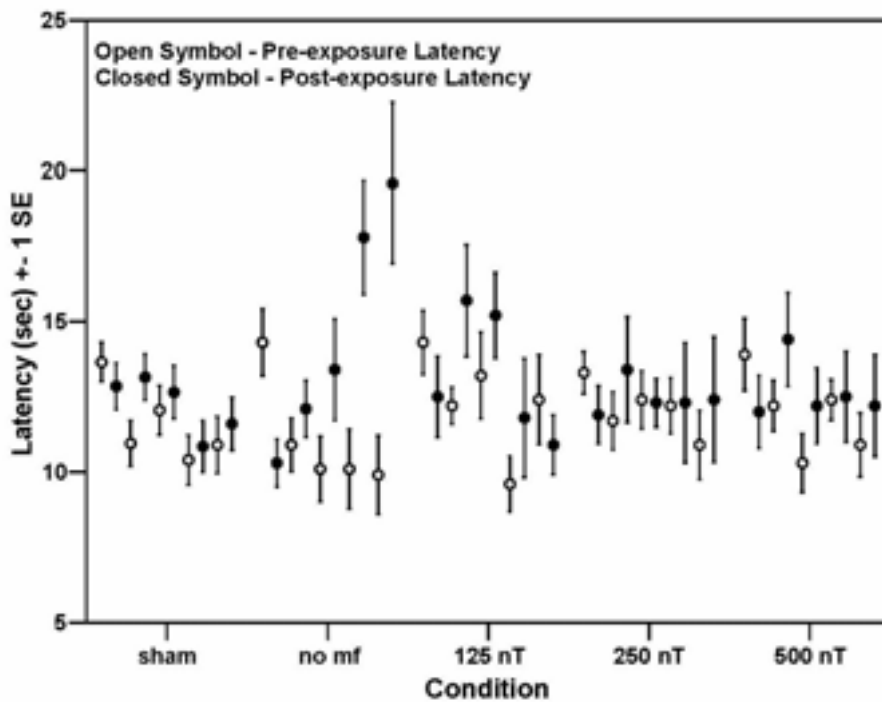


Figure 1: Mice (N=60, sham = 20, other groups = 10) were exposed for 1 hour during the day cycle to either an enclosed acrylic box (sham), mu-metal mf-shielded enclosure (ambient mf attenuated by a factor of 125) with no added magnetic field (no mf), or a specific pulsed magnetic field at 125, 250, or

500 nT (nanoTesla) peak while inside the mf-shielded. In the 'no mf' condition, we see a typical increase of latency (sec spent on a 50 degree C hotplate before an aversive behavior, pre-exposure (open symbol) versus post-exposure (closed symbol)). Error bars represent the standard error of the mean

**DISCUSSION:** Under shielded conditions, a 125 nT peak field produces a significant attenuation of analgesia equivalent to that achieved with naloxone. We estimate from measurements made, that the maximum time changing field from the 125 nT peak field is  $2.5 \times 10^{-4}$  Tesla/sec. This is comparable to the Tesla per second produced by a 0.7  $\mu$ T peak 60 Hz magnetic field.

**SUMMARY:** While shielded (attenuated by a factor of  $\sim 125$ ) from the ambient magnetic field, a weak specific pulsed field of 125 nT or more can affect mf-shielding induced antinociception in mice.

## Medical applications

P-B-176

**CASE STUDY PART B: THE EFFECTS OF ACOUSTIC THERAPY ON CORE TENDON LESIONS OF THE THOROUGHBRED RACEHORSE.** E.B. Bauer, K. Cooper, P. Jenks, A.H.J. Fleming. Biophotonics Research Institute, Malden, MA.

The case study aimed to assess the effectiveness of an acoustic device on core tendon lesions of the thoroughbred race horse. The therapeutic method involved the application of an acoustic device (Cyma 1000), which delivered specific frequencies, within the audible sound range, to acupuncture points and meridians as well as the areas of injury. These audible frequencies ranged from 100 to 1600 Hz. In our case studies, we have found a rapid rate of tendon healing; as evidenced by tendon healing with ultrasonographic imaging that clearly showed the return to normal and homogeneous tendon cell integrity as proven by the uniform and normal echogenicity. A complete reduction of the core lesions to a well defined tendon cell regeneration area with no evidence of a prior tendon lesions was evident. The mean duration of healing time, per follow-up ultrasonography, as well as the clinical signs of healing and rapid return to function was 40 days; from the first diagnostic ultrasound scan to the last follow-up ultrasound scan. The case studies demonstrated a significant improvement in pain and swelling, as well as objectively measurable functional improvements. Objective markers such as clinical improvement in ROM, function and return to work with no signs of lameness at the jog or the gallop. With the encouraging results of these case studies, further investigation of the efficacy of this acoustic device is warranted. The high quality of the homogeneous, healed, tendon tissue, per ultrasonographic evidence, translated into a low to null continued morbidity or threat of reinjury. The cost savings in veterinary diagnostics, care, treatment and maintenance over time, as well as the preservation in value of this athletic horse will further insure this horse owner a gainful return on their substantial financial investment.

P-B-179

**EXPERIMENTAL SETUP TO INVESTIGATE OCULAR CHANGES INDUCED BY MILLIMETER-WAVE EXPOSURE.** M. Kojima<sup>1</sup>, I. Hata<sup>1</sup>, M. Hanazawa<sup>2</sup>, K. Wake<sup>2</sup>, S. Watanabe<sup>2</sup>, M. Taki<sup>3</sup>, Y. Kamimura<sup>4</sup>, K. Sasaki<sup>5</sup>. <sup>1</sup>Dept of Ophthalmology, Kanazawa Medical Univ, Ishikawa, *Bioelectromagnetics 2005, Dublin, Ireland*

JAPAN, <sup>2</sup>Wireless Communications Dept, EMC Center, Biomedical EMC Group, Information and Communications Technology, Tokyo, JAPAN, <sup>3</sup>Dept of Electrical Engineering Graduate School of Engineering, Tokyo Metropolitan Univ, Tokyo, JAPAN, <sup>4</sup>Dept of Information Science, Faculty of Engineering, Utsunomiya Univ, Utsunomiya, JAPAN, <sup>5</sup>Division of Vision Research for Environmental Health, Kanazawa Medical University, Ishikawa, JAPAN.

**Purpose:** Millimeter-wave (MMW) band have just started to use various wireless applications in our daily life. The safety guidelines such as ICNIRP have been decided one value between relatively wide ranges between 1.5 to 300 GHz. This study developed experimental system which examined the effect for 60GHz to the eye. **Methods:** The eyes of pigmented rabbit were exposed unilaterally to a 60 GHz MMW (3W) with either horn (-3 dB beam width:19.5mm) or lens (-3 dB beam width:6.02mm) antenna. Ocular changes were evaluated by slit lamp, laser flare cell meter, and specular microscope. To adjust the exposure area, XY laser indicators and thermography were used. **Results:** In eye vicinity exposure by the horn antenna, rabbit eyes were closed due to blepharidema within 5 minutes MMW exposure. This blepharidema inhibited the penetration of MMW into the eye, and then no ocular injury was developed. In the exposure by the lens antenna, corneal epithelial and endothelial injuries, iris hemorrhage, miosis, and ocular inflammations were induced. Even when the eye was exposed by lens antenna, the avoidance response of the rabbit and blepharidema was generated if exposure area included eye lid. **Conclusions:** In ICNIRP, biological effect position is skin and eyeball surface by MMW exposure. This system is useful to investigate the ocular injury by MMW or to get clear evidences of defense guideline data for eye injury generation by MMW.

P-B-182 WITHDRAWN

P-B-185

**USE OF A QUALIFIED PULSED MAGNETISM DEVICE FOR TREATING PAIN.** B. Matta, J. M. P. Chapellier. Consultation Anti-Douleur, Centre Hospitalier Général de Soissons, Soissons, France.

**Introduction and context:** Pulsed magnetic signal had been tested for treating pain and cause of pain, for more than twenty years, in different countries. It appears as a non-invasive therapy. The previous evaluations indicate good to complete subsidence of pain for: chronic pelvic pain, headache, migraine, neck and low back pain, persistent neck pain, painful osteoarthritis of the knee or cervical spine, osteoarthritis, pseudo-arthrosis, rotator cuff tendonitis, tennis elbow, etc. But the previous evaluations indicate nothing for subsidence of arthrosis'pain.

The "Anti-Pain Dept" in our hospital try to offer experimental non-invasive therapies to the patients whose pain is becoming resistant to drugs. We got the opportuneness to test during several years a new patented device, offering a  $\diamond$  magnetic signal. This signal qualification concerns the sophisticated use of a solar source of energy; and it concerns also the specific quality of the signal form, (close to natural pulsations,) - in order to improve general efficiency. The clinical name of this therapy is "Helio-Magneto-Therapy".

**Objectives:** 1/ To offer a subsidence of pain to clinical patients suffering with degenerative diseases as

arthrosis. 2/ Then, to confirm or to enhance, the effectiveness of an extremely low frequency qualified magnetic field, applied on patients with pain becoming resistant to drugs.

Methods: The clinical context impose a transversal descriptive study based on long term experimentation. We have registered clinical signs for 24 patients, followed during around one year or more. Among them, 4 "psychiatric followed" patients get never any results of any way and are results'excluded. The fact is they cannot deal with the evaluation: The method to evaluate the release of pain is to use the medical consensus about the global scales, namely Digital Scale, DS, coupled with Visual Analogic Scale, VAS. These evaluations are associated to a simplified Mac Gill questionnaire, about different objective factors, as decreasing or cessation of taking therapeutics, points of best day life, back to daily work, etc.

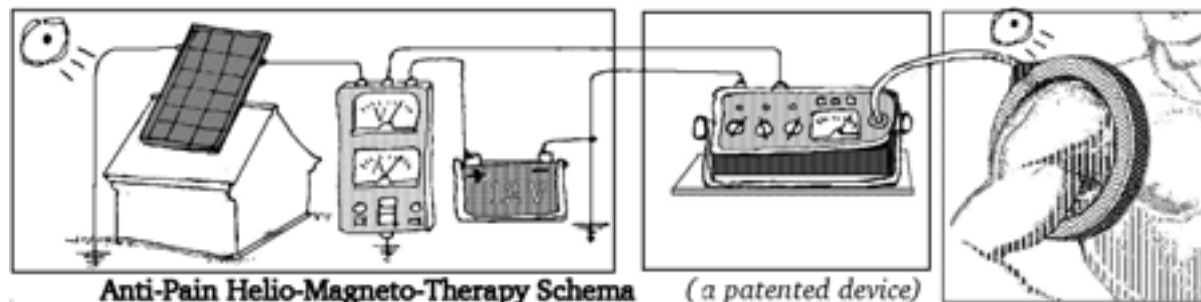
The magnetic field, 50 to 250 Gauss, is pulsed in the organic space of pain location, during 20 to 30 minutes, 2 to 3 sessions a week, with the help of a wood ring coil, threaded on, or put around it. Photoelectric solar energy supplies directly the full device, through a 12 Volt battery. If it is possible, the patient is then sitting calmly in the sunny part of the room.

Results: By progressive sophistication, a two main frequencies pulses sytem has been used. First frequency, called "neural frequency" is mainly used between 8 and 10 Hertz. Second one, called "cat frequency" is a second harmonic of the first one, mainly setted between 32 and 40 Hertz. The absorbed pulse duration is about 10 ms, 1 period. Treated pathologies include mainly arthrosis at different locations, and also some other painful diseases as these previously evaluated. After an average number of 25 pulsed magnetism sessions, the medium evaluation pain scale value pass steadily from 7,0 to 1,4 in more than 80 % of the cases.

Conclusion is that "HelioMagnetoTherapy", with its qualified magnetic signal associated to sunlight, can transcend prior art, by newly offering a steadily subsidence of pain for arthrosis pathologies. Of course this result is only a first descriptive study. A real double-blind evaluation study has to be driven.

Then, according to the clinic treatment room, two technical difficulties are to master for setting properly the device. First one is to be able to fit a photovoltaic panel on a South exposed roof, not too far of the treatment room. Second one is to have enough well-exposed windows, allowing to place the patient in the natural sunlight during the magnetic treatment. Nevertheless, the results remain good when the patient is comfortably lying on a hospital bed, prior to any possible sunbath.

At writing time, our descriptive study has got not any source of financial support, otherly than good will of the hospital direction and members. The french patent publication number, from November 2004, is 2 855 060.



P-B-188 STUDENT

**THE EFFECT OF A SPECIFIC PULSED MAGNETIC FIELD ON MICROVASCULAR RESPONSIVENESS TO A VASODILATOR.** J. C. McKay<sup>1,2</sup>, K. Tymi<sup>2</sup>, F. S. Prato<sup>1,2,3</sup>, A. W. Thomas<sup>1,2,3</sup>. <sup>1</sup>Bioelectromagnetics, Imaging Program, Lawson Health Research Institute, London, Ontario, Canada. <sup>2</sup>Dept of Medical Biophysics, Faculty of Medicine and Dentistry, The Univ of Western Ontario, London, Ontario, Canada. <sup>3</sup>Dept of Nuclear Medicine, St. Joseph's Health Care, London, Ontario, Canada.

#### INTRODUCTION:

A small body of research has investigated the effects of magnetic field (MF) exposure on microcirculation. The bulk of this research has focused on static fields (SMF) and has yielded mixed results. Some studies report that MF exposure leads to vasodilation and increased perfusion, while others report otherwise.

Exposure to a SMF (0.25 T) has been shown to increase microcirculation within the cutaneous tissue of the rabbit ear lobe by 20-40% [Gmitrov et al., 2002]. Likewise, Xu et al. (2000) found that peak blood velocity in the tibialis anterior muscle of mice was increased by 20-45% when exposed to a 1 and 10 mT SMF. In contrast to the previous two studies, Okano et al. (1999) reported biphasic effects of a 1 mT SMF on the cutaneous microcirculation of rabbits. When vascular tone was high, SMF exposure led to increased vasomotion and vasodilation, and when vascular tone was low, SMF exposure led to decreased vasomotion and vasoconstriction. Little is known about the effects of pulsed fields on microvascular perfusion. The ability to increase perfusion to a localized area of the body has much clinical relevance. Such research could lead to more site-specific drug absorption, increased effectiveness of radiotherapy by increasing oxygen levels to the site of tumor, and faster tissue regeneration.

#### OBJECTIVE:

The objective of the current research is to determine whether exposure to a particular pulsed electromagnetic field will enhance the vasodilatory effect of acetylcholine on microvascular perfusion.

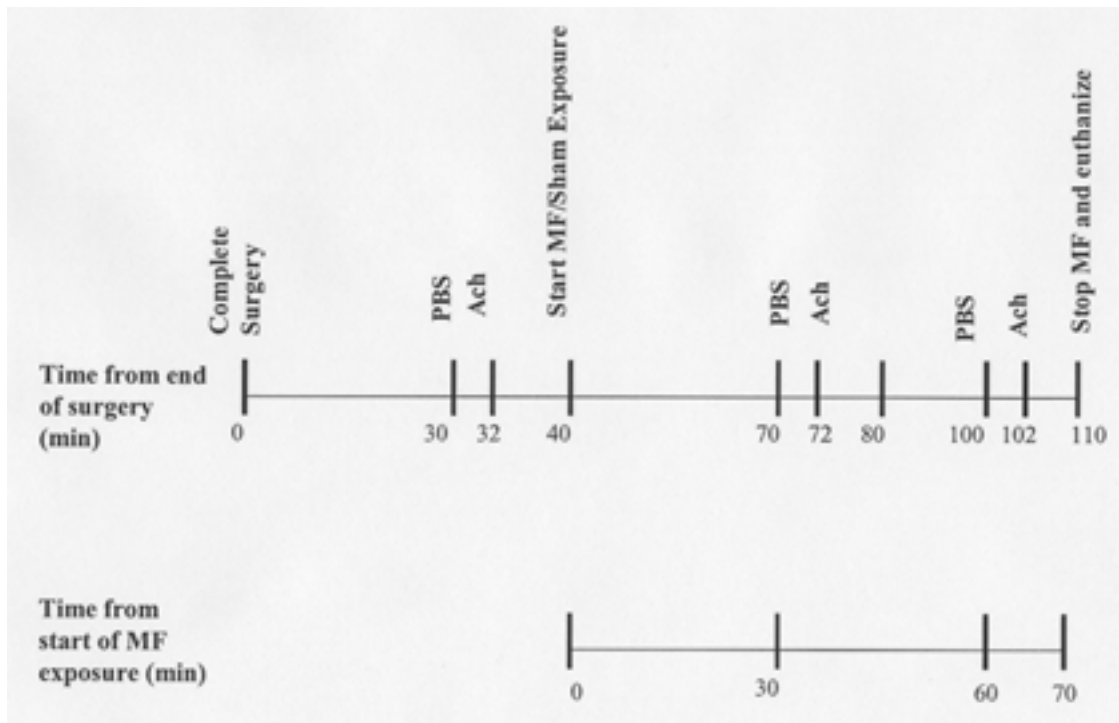
#### METHODS:

Male Sprague-Dawley rats are anesthetized using sodium pentobarbital and surgery is performed on the hind-limb to expose the extensor digitorum longus (EDL) muscle. The rats are allowed to stabilize for half an hour, at which point a Doppler probe is placed directly on top of the EDL and a baseline perfusion measurement is taken using Doppler flowmetry. Next, a 0.1mL bolus of phosphate-buffered solution (PBS) (used as a control) is injected on top of the EDL muscle. Data is recorded for 2 minutes. Acetylcholine (Ach) (either 0.1mM, 1mM, or 10mM) is then injected on top of the EDL and data is recorded for 8 minutes. Magnetic field exposure then begins (200 $\mu$ T peak, 400mT/sec, see Thomas et al., 1997). At 30 and 60 minutes from the start of exposure, the same procedure of injecting PBS and Ach occurs. The rat is then euthanized using a lethal dose of sodium pentobarbital. Please refer to Figure 1.

Six groups are tested. Group 1 receives 0.1 mM Ach + MF, Group 2 receives 1mM Ach + MF, Group 3 receives 10mM Ach + MF, Group 4 receives 0.1mM Ach + Sham, Group 5 receives 1mM Ach + Sham, Group 6 receives 10mM Ach + Sham.

Data is analyzed using SPSS 10.0. All data is normalized to the individual perfusion baselines of the rat. A split-plot analysis of variance is performed.

FIGURE 1: Timeline for experimental protocol



#### RESULTS:

Initial data suggests that exposure to this field can lead to a 50-60% increase in perfusion using a 1mM solution of Ach. Additional data from 50-150 rats is pending. The data currently under analysis tests both the time-dependency of the MF and the dose-dependency of the Ach.

#### CONCLUSIONS:

This research may provide a gateway into the search for the mechanisms responsible for the biological effects of MF on perfusion. If this MF increases the vasodilatory potential of Ach, this may lend support to the theory that nitric oxide synthase (a post-cursor to Ach) is implicated in the MF effect. Alternatively, guanylyl cyclase (a post-cursor to NO) could be the target of the MFs. Much follow-up work could be done based on this experiment.

#### SOURCES OF FUNDING:

FrAlex Therapeutics Inc., St. Joseph's Health Care (London) Foundation, the Lawson Health Research Institute Internal Research Fund, the Dept of Diagnostic Imaging SJHC, Canadian Institutes of Health Research (CIHR), National Research Council (NRC), the Ontario Research and Development Challenge Fund (ORDCF), Canada Foundation for Innovation (CFI), and the Ontario Innovation Trust (OIT).

#### REFERENCES

- Gmitrov J, Ohkubo C, Okano H. *Bioelectromagnetics* 23: 224-9, 2002.
- Okano H, Ohkubo C. *Bioelectromagnetics* 22: 408-18, 2001.
- Thomas AW, Kavaliers M, Prato FS, Ossenkopp KP. *Neurosci Lett* 222: 107-10, 1997.
- Xu S, Okano H, Ohkubo C. *Bioelectrochemistry* 53: 127-35. 2000.

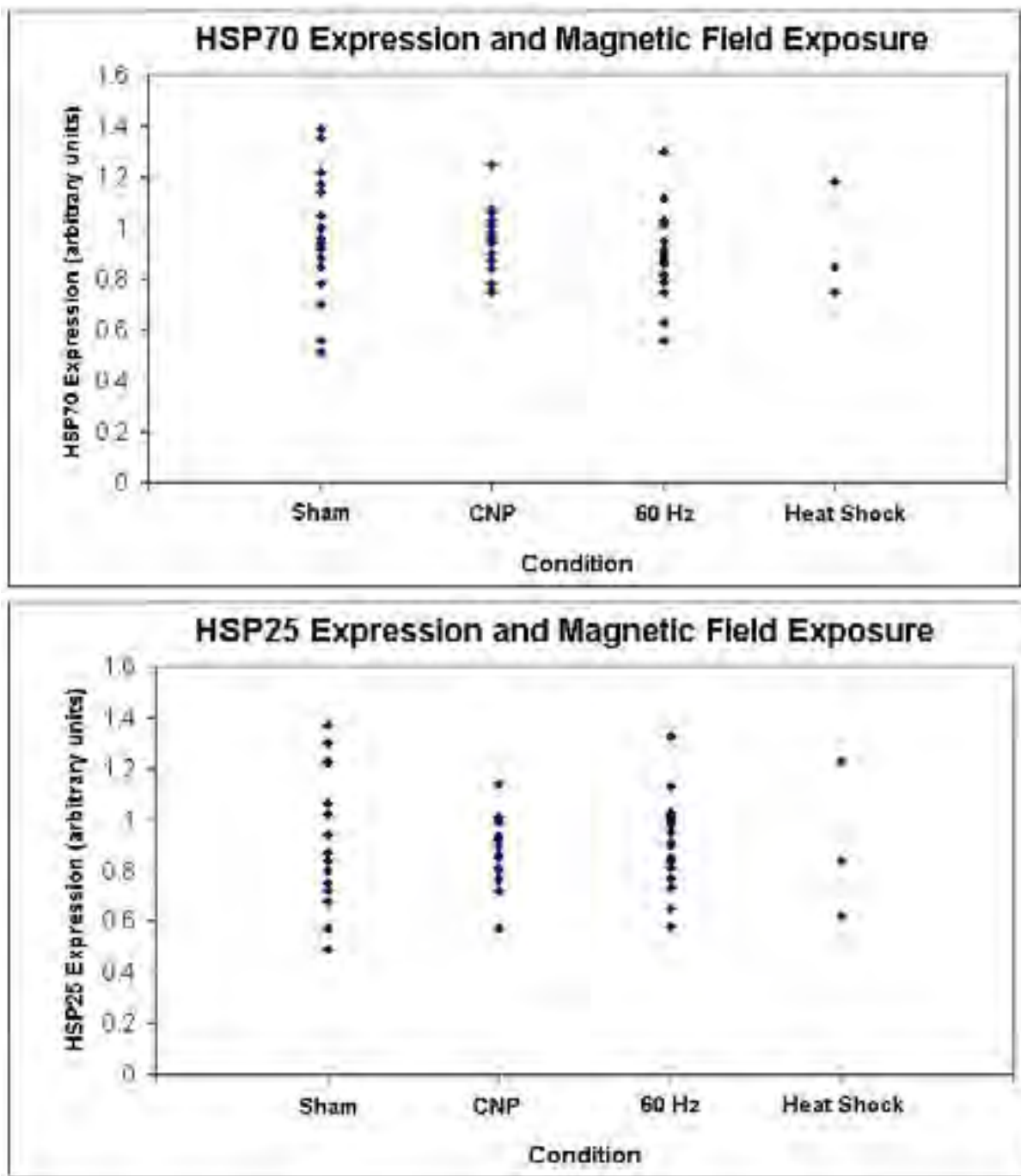
**MAGNETIC FIELDS AND HEAT SHOCK PROTEIN EXPRESSION.** J. A. Robertson<sup>1,2</sup>, Y. Bureau<sup>1</sup>, F. S. Prato<sup>1,2,3</sup>, A. W. Thomas<sup>1,2,3</sup>. <sup>1</sup>Bioelectromagnetics, Lawson Health Research Institute, St. Joseph's Health Care, ON, Canada. <sup>2</sup>Dept. of Medical Biophysics, Univ of Western Ontario, London, ON, Canada, <sup>3</sup>Imaging & Nuclear Medicine, St. Joseph's Health Care, London, ON, Canada.

**INTRODUCTION:** Heat shock proteins (HSPs), in particular the 70 kDa family, have been shown to protect tissue from damage following ischemia-reperfusion injuries, such as those suffered during a heart attack. These treatments are most effective when the HSPs can be induced prior to reperfusion and the influx of free radicals that entails. The use of HSPs as a treatment avenue is in part limited by the ability to induce their production, as traditional methods such as hyperthermia and ischemic preconditioning themselves damage the tissue they are meant to protect, and pharmacological treatments typically rely on blood delivery, which is by definition impaired. Magnetic fields have been shown to induce HSPs in cell cultures and chick embryos, which is highly promising for treatment as magnetic fields do not produce gross damage, and the protection in these studies was induced suitably quickly (hours). However, reports of difficulty replicating these results abound.

**OBJECTIVE:** To determine whether HSP production can be induced by ELF magnetic fields in a mouse model, and whether the induction is pulse-form or tissue dependent.

**METHODS:** Swiss CD-1 mice approx. 45 days old are exposed to a  $\pm 200$   $\mu$ T magnetic field with either a 60 Hz sinusoidal or a complex pulsed waveform delivered by a set of square Helmholtz coils (1.2 m); or to a sham (coils deactivated) condition. The ambient geomagnetic field of approx. 55  $\mu$ T was not shielded or canceled. Mice were exposed for 30 or 60 minutes, with a rest time of 0, 30 or 90 minutes prior to sacrifice and tissue extraction. Heat stress produced via a heat lamp while under anesthesia was used as a positive control (40°C for 30 or 60 minutes). Tissues (hearts, livers, and brains) were frozen in liquid nitrogen and stored at  $-80^{\circ}\text{C}$  until Western blots were performed. Blots were stained with HSP25 and HSP70 antibodies (SPA-801 and SPA-812, respectively, from Stressgen, Victoria, BC) for the proteins of interest, and actin was used as a control protein.

**RESULTS:** To date, 61 mouse hearts have been analyzed. No significant effect of either a 60 Hz sinusoidal field or the complex pulsed magnetic field was seen on the expression of either heat shock protein ( $p > 0.5$ ). See figure 1 and 2 for a depiction of the HSP70 and HSP25 (respectively) data collected to date. Each figure displays the HSP band intensity relative to that of actin for each exposure condition. Each point represents the average of two repetitions of a western blot for a single mouse.



CONCLUSION: While the sample size is still small and further work needs to be done, it does not appear as though 200 mT magnetic fields induce the expression of either HSP70 or HSP25 in normal unstressed mouse hearts.

ACKNOWLEDGEMENTS: This study was funded (in part) by St. Joseph's Health Care (London) Foundation; the Lawson Health Research Institute Internal Research Fund; the Dept of Nuclear Medicine, SJHC; Canadian Institutes of Health Research (CIHR); the Ontario Research and Development Challenge Fund (ORDCF), Canada Foundation for Innovation (CFI); and the Ontario Innovation Trust (OIT).

**GEOMAGNETIC STORMING AND HEAT SHOCK PROTEIN 25 EXPRESSION IN MICE.** J. A. Robertson<sup>1,2</sup>, Y. Bureau<sup>1</sup>, D. Desjardins<sup>1</sup>, F. S. Prato<sup>1,2,3</sup>, A. W. Thomas<sup>1,2,3</sup>. <sup>1</sup>Bioelectromagnetics, Lawson Health Research Institute, St. Joseph's Health Care, ON, Canada. <sup>2</sup>Dept. of Medical Biophysics, Univ of Western Ontario, London, ON, Canada, <sup>3</sup>Imaging & Nuclear Medicine, St. Joseph's Health Care, London, ON, Canada.

**INTRODUCTION:** Heat shock proteins (HSPs) have great potential to protect cells from numerous types of damage, and as a result, research into exploiting this natural defense mechanism for therapeutic benefit is ongoing. Magnetic fields have been shown to induce HSP expression in vitro, although replication of these studies has not always been successful. The geomagnetic field should also be considered with respect to HSPs. While the magnitude of the field fluctuations during a geomagnetic storm are considerably weaker than applied fields typically tested (100s of nT vs mT-mT), they may be more ethologically relevant, as disturbances in the geomagnetic field may signal catastrophic events such as earthquakes.

**OBJECTIVE:** To determine whether geomagnetic storms influence heat shock protein expression in a mouse heart.

**METHODS:** Hearts from several swiss CD-1 mice were obtained from related studies and HSP25 expression was determined relative to actin with western blot analysis. A correlation between geomagnetic activity and HSP25 expression was first noted in a study investigating the influence of a single exposure of weak (200 mT) extremely low frequency magnetic fields on HSP expression (n = 16). 8 mice were then obtained following a study involving repeated exposure (1 hour per day for 5 days) to a simulated geomagnetic field, which was produced with a set of 4 small rectangular coils inside a shielded mu metal box. The standard deviation of the delivered waveform was set at 50, 100, or 200 nT – corresponding to unsettled, stormy, and severely stormy levels of geomagnetic activity. It should also be noted that as part of this study the mice were also tested twice daily for nociceptive responses (foot lift/lick) on a hotplate analgesiometer. A further 8 mice were obtained from the sham condition of this same nociception study (that is, mice that were tested for nociceptive responses twice daily for 5 days, but which had not been exposed to an altered magnetic field). These were obtained 2-3 at a time over different days in order to obtain mice that had been exposed to different levels of natural geomagnetic activity.

**RESULTS:** A significant correlation ( $p < 0.01$ , Spearman's rho = 0.7) between HSP25 expression and geomagnetic activity (as measured by the Ap index, in nanoTesla) was seen in mice following a severe geomagnetic storm. Another 8 specimens were obtained from a study that repeatedly applied geomagnetic-mimicking fields. While there was no significant correlation in this data ( $p > 0.3$ ), there was a general tendency for higher levels of simulated geomagnetic activity (that is, larger field strengths) to have higher HSP25 expression levels. Finally, sham mice obtained from this study after periods of geomagnetic storming did not have higher HSP25 levels than sham mice obtained after periods of low geomagnetic activity.

**CONCLUSION:** The different experimental procedures for the different groups of mice prevent pooling the data, and each set suffers from a small sample size. However, despite the contradictory nature of the final group of mice, the influence of geomagnetic activity on heat shock protein expression is interesting and promising. As a subterranean species, mice may be particularly sensitive to signals of impending earthquakes, such as disturbances in the geomagnetic field, and respond by producing protective proteins such as HSP25.

**ACKNOWLEDGEMENTS:** This study was funded (in part) by St. Joseph's Health Care (London) Foundation; the Lawson Health Research Institute Internal Research Fund; the Dept of Nuclear Medicine, SJHC; Canadian Institutes of Health Research (CIHR); the Ontario Research and

Development Challenge Fund (ORDCF), Canada Foundation for Innovation (CFI); and the Ontario Innovation Trust (OIT).

P-B-197 STUDENT

**REINTRODUCED TIME-VARYING GEOMAGNETIC FIELD ATTENUATES ANALGESIA DUE TO REPEATED MAGNETIC FIELD SHIELDING.** J. A. Robertson<sup>1,2</sup>, F. S. Prato<sup>1,2,3</sup>, D. Desjardins<sup>1</sup>, L. Keenlside<sup>1</sup>, A. W. Thomas<sup>1,2,3</sup>. <sup>1</sup>Bioelectromagnetics, Lawson Health Research Institute, St. Joseph's Health Care, London, ON, Canada. <sup>2</sup>Dept. of Medical Biophysics, Univ of Western Ontario, London, ON, Canada, <sup>3</sup>Imaging & Nuclear Medicine, St. Joseph's Health Care, London, ON, Canada.

**INTRODUCTION:** Previously, we have reported that repetitive shielding of the geomagnetic field with a mu metal enclosure lead to an analgesic effect in mice. After 5 days at 1 hour per day of magnetic field shielding, a peak delay in foot-lift/lick response is seen when mice are tested on a hotplate analgesiometer, equivalent to that seen from a low dose of morphine (~5 mg/kg). Simply zeroing the static component of the field with a set of Helmholtz coils is not sufficient to induce the analgesic effect, nor is confining the mice to copper boxes which shield the ambient electric -- but not magnetic -- fields. Based on this observation, we hypothesize that it is the removal of the time-varying component of the geomagnetic field that is responsible for the effect, despite the fact that the magnitude of the fluctuations in the earth's field are on the order of nanoTesla.

**OBJECTIVE:** To investigate whether reintroducing a simulated geomagnetic field will influence the analgesic effect of a 5-day course of repetitive mu metal shielding.

**METHODS:** Swiss CD-1 mice were held in specially designed mu metal boxes or equivalent Plexiglas boxes (sham condition) for 1 hour per day for 5 consecutive days. Analgesia was measured before and after each exposure by placing the mice on a 50°C hotplate analgesiometer and measuring the time for a foot lift/lick response. Within each mu metal box (but not the sham box) 4 rectangular coils were inserted to produce a simulated geomagnetic field. A recording was made of the extremely low frequency components (0.1 Hz – 2500 Hz) of the geomagnetic field with a computerized fluxgate magnetometer on a day with normal geomagnetic activity (that is, no solar flares or other activity reported by the National Oceanic and Atmospheric Administration's Space Environment Center). This recording was manipulated slightly so that it could be looped continuously with a smooth transition between the end of one loop and the beginning of the next. Each cycle was approx. 8 seconds long. The recording was amplified to three different levels to give different conditions: 50, 100, and 200 nT, where the magnetic field magnitude here refers to the standard deviation of the changing field; used due to the chaotic nature of the waveform. Thus 5 conditions in all were used: sham (n=40), mu metal shielding without active coil inserts, and mu metal shielding with coil inserts activated to give geomagnetic mimicking fields of 50, 100, and 200 nT standard deviation (n=20 for each shielding condition). For data analysis, an ANOVA was performed with Tukey post-hoc tests using SPSS 10.0.

**RESULTS:** As in previous experiments, mice that were repetitively shielded for 5 days developed a significant increase in the latency time to a foot lick as compared to sham animals ( $p < 0.001$ ), that is, a reduced response to a noxious stimulus. This analgesic effect was significantly attenuated in the mice that had the 50 nT reintroduced field ( $p < 0.001$ ), and slightly attenuated in the 100 nT ( $p < 0.01$ ) and 200 nT (no significant difference with respect to the shielded condition) reintroduced fields.

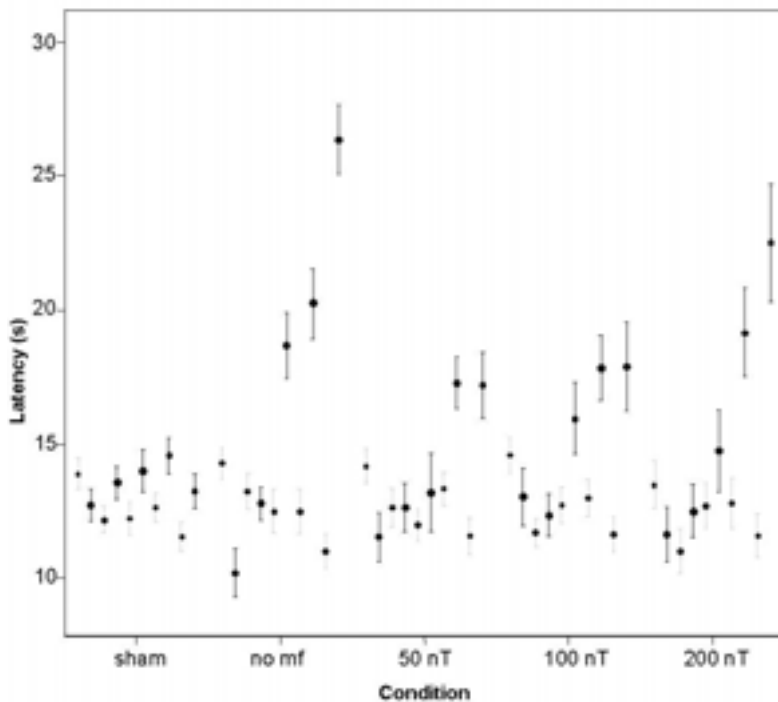


Figure 1: The average latency to foot lift/lick is shown prior to (grey bars) and following (dark bars) the hour long exposure for each day from left (1) to right (5), for each exposure condition. Error bars represent S.E.M.

**CONCLUSION:** Repetitive magnetic field shielding induces an analgesic effect. This appears to be due to the shielding of the time-varying component of the geomagnetic field, as introducing a time varying magnetic field that mimics the natural field attenuated the analgesic response. Interestingly, the reintroduced field that was closest to the natural field on a quiet day (50 nT) was the most effective at attenuating the analgesia; variations of 100 or 200 nT in the field would represent geomagnetic storm conditions.

**ACKNOWLEDGEMENTS:** This study was funded (in part) by St. Joseph's Health Care (London) Foundation; the Lawson Health Research Institute Internal Research Fund; the Dept of Nuclear Medicine, SJHC; Canadian Institutes of Health Research (CIHR); the Ontario Research and Development Challenge Fund (ORDCF), Canada Foundation for Innovation (CFI); and the Ontario Innovation Trust (OIT).

P-B-200

**MODELING OF ELECTRIC POTENTIAL GENERATED IN PHYSIOLOGICAL TISSUES BY COCHLEAR IMPLANTS.** G. Tognola<sup>1</sup>, A. Pesatori<sup>1,3</sup>, M. Parazzini<sup>1</sup>, L. Di Rienzo<sup>2</sup>, F. Grandori<sup>1</sup>, P. Ravazzani<sup>1</sup>. <sup>1</sup>Inst. Biomedical Engineering CNR, Milan, Italy, <sup>2</sup>Dip. Electrotechnics, Polytechnic of Milan, Italy, <sup>3</sup>Dip. Electronics and Information, Polytechnic of Milan, Italy.

A cochlear implant is a prosthetic device implanted into the inner ear -the cochlea- and is used to stimulate through bipolar electrical pulses the acoustic nerve. The neural discharges resulting from such stimulation induce auditory sensations and can restore partial hearing to deaf people. The stimulation parameters, such as the stimulus intensity, the electrode configuration, material, and

shape affect, through the generated electric potential, the number of fibers excited and the patient perception.

Aim of this study is a systematic investigation of the relationship between stimulation parameters and electric potential generated in cochlear tissues around the electrode array. This is crucial to develop more efficient and spatially focused excitations of cochlear tissues and to investigate possible interactions of the electric potentials generated by the cochlear implant with neural tissues surrounding the cochlea.

## Methods

A finite element method (FEM) was used to calculate the 3D electric potential induced by the bipolar electric pulses inside the cochlea. Simulations were implemented through the software package 'Maxwell 3D field simulator v.3.0.21' (by Ansoft). In the frequency range of the electrical signal used to stimulate cochlear tissues (i.e., up to 20 kHz), the cochlea can be considered purely resistive, so that a quasi-static approximation is justified. In practice, the FEM is used to solve the Poisson equation, which describes the relationship between the electrical potential  $\phi$  produced inside the cochlea and the current source  $i$  injected by the cochlear implant inside the cochlea.

Differently from previous studies, the modeling here developed was extremely accurate in describing: i) the shape of the cochlea, ii) the electromagnetic properties of cochlear tissues, iii) the shape of the electrode array, iv) the position of the electrode array inside the cochlea.

Four different geometries of the conducting volume were considered, starting from the easiest ones (toroidal models) to the most difficult ones, i.e., two synthetic shapes resembling the true anatomy of human cochlea, which were derived by a microphotograph of a section of a human cochlea and from the volumetric reconstruction of CT scans of the petrous bone.

On average, the cochlear volume conduction of  $4.3 \times 4.3 \times 8 \text{ mm}^3$  was divided into a minimum of 60,000 tetrahedra (for the simplest models) to a maximum of 125,000 tetrahedra (for the human-like cochlear models).

The electrode array was modeled according to the size, shape, and materials of a real cochlear implant array (Nucleus® CI24R), which consisted of 22 equally-spaced platinum electrode bands on a flexible silicone carrier. The length of the electrode array is 17 mm, each electrode has diameter of 0.4-0.6 mm and width of  $\sim 0.4$  mm.

For all the four cochlear models, three different electrode configurations were considered: the monopolar (MP) mode (a single electrode inside the cochlea is active, the ground being located outside the cochlea), ii) the bipolar (BP) mode (the active and the ground electrodes are a pair of electrodes in the array), and iii) the common ground (CG) mode (the active electrode is one of the 22 electrodes of the array, the ground being obtained by shorting all the remaining electrodes).

For all configurations, the current source was set equal to 1 mA.

## Results

For all simulations, the energy error obtained with the FEM package was lower than 1.3%.

For a given geometric model of the cochlea, the distribution of the electric potential was deeply influenced by the electrode configuration. Namely, the MP mode generated the highest values of the electric potential with respect to the other two modes, the BP mode generated the lowest values of the potential and the CG mode gave rise to potentials of moderate intensity. Differences were observed also for the shape of the potential distribution. The BP mode produced the most focused stimulation: the

potential was maximally focalized around the active electrode and had a steep decrease with the distance from the active electrode. Viceversa both the CG and the MP modes produced less focused potentials. The electrode array stimulates different auditory nerve fibers at different locations inside the inner ear, thus mimicking the place mechanism for coding acoustic frequencies. This means that highly focused stimulations are able to excite a single (isolated) site of auditory neurons, just those who are tuned to the frequency of the incoming sound.

This trend of highest potential values and lesser focusing for the MP mode are in agreement with clinical data where implanted patients stimulated with the MP mode generally required the lowest values of the stimulating current to obtain cochlear neural stimulation.

For a given electrode configuration, great differences were observed both in the amplitude and the shape of the electric potential by considering different geometric models of the volume conduction. In particular, the two most approximated models (i.e., the toroidal models) were able to give only a rough description of the true potential distribution inside the cochlea. For example, the two approximated models do not show the phenomenon of cross-turn stimulation, which is actually present in the human like cochlea for high level stimulations.

### Conclusions

The modeling here described estimates with good accuracy the effects of various stimulation parameters on the electric potential generated by a cochlear implant electrode array. Results showed a significant influence of stimulus parameters and the geometric model used to describe the volume conduction on the induced potential, both for what concerns its magnitude and its spatial distribution. This approach give some help to study how different material of the stimulating electrode or different electrode shapes may influence the resulting electric field and its focusing inside the cochlea. Also, this approach can be valuable to predict the best type of stimulation able to produce the most focused excitation for a given patient.

The authors thank Dr. F. Baruzzi of Ospedale di Circolo di Varese for the CT scans and assistance.

## **Risk, safety standards and public policy**

P-B-203

**A FLAT PHANTOM SETUP FOR THE COMPLIANCE TESTING OF WIRELESS TRANSMITTERS OPERATING IN THE CLOSE ENVIRONMENT OF THE HUMAN BODY FOR A FREQUENCY RANGE FROM 30 MHZ TO 5800 MHZ.** A. Christ<sup>1</sup>, A. Klingenböck<sup>1</sup>, T. Samaras<sup>2</sup>, M. Zankl<sup>3</sup>, N. Kuster<sup>1</sup>. <sup>1</sup>Foundation for Research on Information Technologies in Society, Zurich, Switzerland, <sup>2</sup> Radiocommunications Laboratory, Aristotle Univ of Thessaloniki, Greece, <sup>3</sup>GSF - National Research Center for Environment and Health Institute of Radiation Protection, Neuherberg, Germany.

INTRODUCTION: With the increasing number of wireless devices which work in close proximity to the human body, the current safety standards are being extended to provide methods and procedures for the compliance testing at positions covering the whole body. A body phantom which enables the reproducible and conservative assessment of the SAR represents the cornerstone of the novel

procedures. For this purpose, IEC 62209 suggests a liquid filled flat phantom of the dimensions 600mm times 400mm whereas the dimensions shall not be smaller than the ellipse of this dimension [1].

**OBJECTIVE:** The goal of this study is to evaluate the conditions under which the shape and the size of a flat phantom can be neglected for conservative exposure estimate and to evaluate if the proposed phantom is applicable for the compliance testing of body-worn wireless devices.

**METHODS:** 1g and 10g average SAR values were evaluated with flat phantoms of different shapes and sizes and compared to the values obtained using homogeneous human body phantoms (different ages, sizes, sexes) at different locations of the body and distances (5 mm – 200 mm) from it. Further, resonance effect depending on antenna distance and phantom or body size were evaluated. Different antenna (e. g. dipole, helix, patch) and device types operating in the frequency range from 30 MHz to 5800 MHz are considered. The SAR was calculated using the FDTD method and the integrated simulation platform SEMCAD.

**RESULTS and DISCUSSION:** Shape and size of the body or the phantom have a minor impact at close distances as well as at higher frequencies, which lie significantly above the resonances of the respective phantom or human model (length of phantom  $\gg \lambda/2$ ). Strong resonance effects ( $> 10\text{dB}$ ) could only be observed at distances above 200 mm both in flat phantom and the human models.

Nevertheless, the shape of the phantom can have a significant effect on the results ( $>1 \text{ dB}$ ) for the same dimensions but different shapes if phantom dimensions are smaller than  $\lambda/2$ . In conclusion, reproducible results can only be obtained if the phantom size and shape is well defined. In order to minimize the amount of liquid to be used and to ensure minimum sagging, the elliptical phantom with the dimensions 600 mm (major axis) and 400 mm (minor axis) is the most suitable phantom applicable for the entire frequency range from 30 MHz to 6 GHz.

**REFERENCES:**

[1] IEC 62209 Part 2, Draft Version 0.10, "Human Exposure to Radio Frequency Fields from Handheld and Body-Mounted Wireless Communication Devices, Human Models, Instrumentation and Procedures, Part 2: Procedure to determine the Specific Absorption Rate (SAR) in the head and body for 30MHz to 6GHz Handheld and Body-Mounted Devices used in close proximity to the Body", IEC TC 106, Brussels, December 2004.

P-B-206

**PEOPLE CONCERNED WITH HEALTH EFFECTS OF THE ELECTRIC AND MAGNETIC FIELDS.** T. Karjanlahti, N. Laakkonen, R. Koskinen, J. Kurikka-Oja, L. Korpinen. Laboratory of Electrical Engineering and Health, Tampere Univ of Technology, Tampere, Finland.

During several years many studies about the exposure to electric and magnetic fields, measuring the fields and the techniques about minimizing the fields have been made at Tampere Univ of Technology. At the beginning of 2001 the Laboratory of Electrical Engineering and Health was founded to further research the health issues of the electric and magnetic fields.

People are very interested in the health effects of the electric and magnetic fields. There have been 82 inquiries about the topic since 2001, excluding inquiries by the media. That is roughly one inquiry every two weeks. The content of the inquiries can be divided into two main categories. Technical inquiries about the health effects of commercial products form the biggest category. The reason for these inquiries is the growing awareness and concern about health issues among consumers. That is the reason why developers want to incorporate health issues into design processes.

People who are concerned about their own or their children's health form the other main category. Some questions are related to safety of electrical home equipment such as coffee maker, radio, etc. One of the most typical questions is related to the safety of buying a house near power lines. People are concerned about the health effect of the electric and magnetic fields the power lines produce in their immediate surroundings.

Inquiries about the safety of living next to power lines usually get the answer that it is safe. According to EU's recommendations for public exposure to low frequency electric and magnetic fields, the Finnish Ministry of Social Affairs and Health has published a degree (294/2002) in which the maximum field values are 100  $\mu$ T and 5 kV/m [1, 2]. Furthermore, a handbook about public exposure to low frequency electric and magnetic fields has been issued [3]. The maximum values are not usually exceeded in places where the public have access. F 1 shows that the electric field strength dampens down a lot when moving away from the power lines. The buildings are usually constructed some dozens of meters away from the power lines and therefore the electric and magnetic fields at the residence are only the size of the background field. However, people are concerned about living next to power lines. Due to public concern it is recommended not to locate nursery schools etc. near power lines.

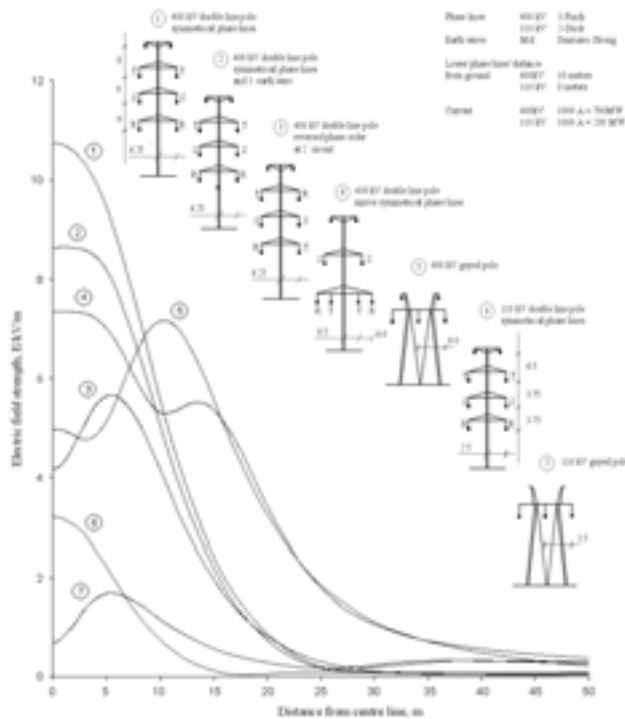


Figure 1. Electric field strengths at 1 m height from the ground under 400 kV and 110 kV power lines. The characteristics are calculated according to reference Valjus 1987. [4]

As a conclusion, it can be stated that electric and magnetic fields produced by electrical home equipment remain under maximum values in most cases. At the residence near power lines the electric and magnetic fields are usually the size of the background field.

#### References

1. Council of the European Union, Council Recommendation of 12 July 1999 on the limitation of exposure of the general public to electromagnetic fields (0 Hz to 300 GHz), "Official Journal of the EC: L" 199 on 30 July 1999, pp.59-70.

2. ICNIRP, Guidelines for Limiting Exposure to Time-varying Electric, Magnetic and Electromagnetic Fields (up to 300 GHz), "Health Physics", 74(4), 1998, pp. 494-522.
3. Leena Korpinen, 2003. Public exposure to low frequency electric and magnetic fields in Finland. Helsinki, Handbook of the Ministry of Social Affairs and Health. 87 pp. (in Finnish)
4. Valjus J. 1987. Pientaajuisten sähkö- ja magneettikenttien fysiologiset vaikutukset. Helsinki, Imatran Voima Oy, Tutkimusraportti IVO-A-04/87. 154 s. (in Finnish)

P-B-209

**GUIDELINES COMPLIANCE AT DIFFERENT FREQUENCIES NEAR BASE-STATION ANTENNAS.** A. Martín, R. Villar, M. Martínez-Búrdalo. Consejo Superior de Investigaciones Científicas, Instituto de Física Aplicada, Madrid, SPAIN.

**OBJECTIVE:** To point out that the assessment of guidelines compliance [1] in the near-field of base-station antennas by using the comparison of the spatially averaged field (over the region occupied by an individual potentially exposed to the antenna radiation), with the corresponding reference levels, can not be adequate at certain frequencies because, as frequency increases, the distance at which reference levels are fulfilled can be shorter than the safety distance obtained by using local peak specific absorption rate (SAR) as basic restriction.

**METHOD AND MODELS:** The finite-difference time-domain method (FDTD) [2] has been used to simulate the radiation of actual models of base-station antennas up to a distance of  $20\lambda$ , assuming free space conditions. Cubic FDTD cells with a side length of 0.5 cm are used and a problem space is generated to include the source of radiation and a human body model close to it. We have modeled nine typical models of base-station antennas, consisting in three kinds of dipole arrays -4x1, 4x2 and 6x2- operating at 900, 1800 and 2170 MHz, with a radiated power of 30 W in all cases, for comparison. They are half-wavelength dipoles with reflecting plates above and below each one, at a distance of  $\lambda/8$ , and also at both sides and behind, at a distance of  $\lambda/4$ . The distance between parallel dipoles is also  $\lambda/8$ . For SAR calculations, a realistic high-fidelity 3D body mesh from REMCOM Inc., which simulates an adult man and contains 23 different tissues -with dielectric characteristics, at the desired frequency, obtained from [3]-, have been used.

**RESULTS:** For each antenna model and each frequency, E and B fields have been computed in all cells, and spatially averaged values of electric ( $E_{avg}$ ) and magnetic ( $B_{avg}$ ) field strength in the maximum radiation direction, as a worse case, have been calculated at different distances from the antennas. SAR calculations as a function of the distance to the antennas have also been made to be compared with basic restriction limits from the guidelines. Results show that, at 900 MHz, for an antenna-body distance over the near zone limit, in a worst case, localized SAR is under the basic restriction limit (at such a distance spatially averaged E or B fields are always above reference levels). Nevertheless, for higher frequencies, the distance of accomplishment of reference levels can be almost the same or even greater than the distance at which basic restrictions are fulfilled. As an example, the variations with the distance to the antenna of  $E_{avg}$  and maximum 10-g averaged SAR ( $SAR_{10g}$ ) are shown in figures 1 and 2, respectively, for a frequency of 2170 MHz. The continuous horizontal line in each plot indicates the value of the guidelines limit (reference level or basic restriction).

**CONCLUSIONS:** It has been observed that, in the lower near-field of base-station antennas, where the spatial field distribution is not that of a plane wave, distances to the antenna considered as safe

according to reference levels could be above the safety distance according to basic restrictions, specially for the higher considered frequencies. That is, in those conditions, reference level would not be always conservative, and the presence of possible obstacles in the surroundings need to be considered because small variations in field levels in a certain region could produce the SAR be above basic restrictions limit.

ACKNOWLEDGMENTS: This work has been supported by the National Programme of I+D+I of the Spanish Ministry of Science and Technology, project TIC 2003-00130.

## REFERENCES

- [1] ANSI/IEEE C.95.1-1992: IEEE Standard for Safety Levels with Respect to Human Exposure to Radiofrequency Electromagnetic Fields 3 KHz to 300 GHz. New York: IEEE Press, 1992.
- [2] A. Taflove, Computational Electrodynamics: The Finite-Difference Time-Domain Method in Electromagnetics, 2nd edition, Artech House, Norwood, MA, 2000.
- [3] C. Gabriel and S. Gabriel, Compilation of the dielectric properties of body tissues at RF and microwave frequencies, Physics Dept, King's College London, London, England, 1996.

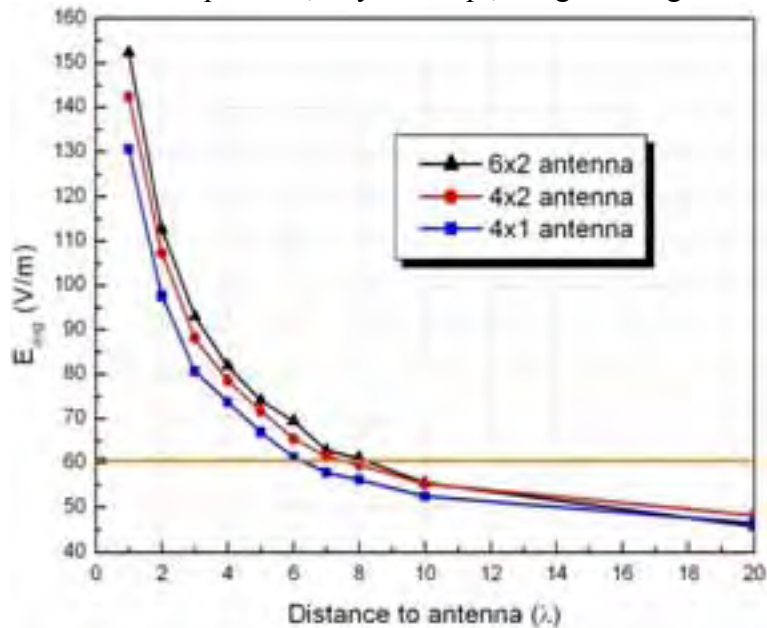


Figure 1 - Spatially averaged electric field as a function of the antenna-body distance. Frequency: 2170 MHz. Radiated power: 30 W.

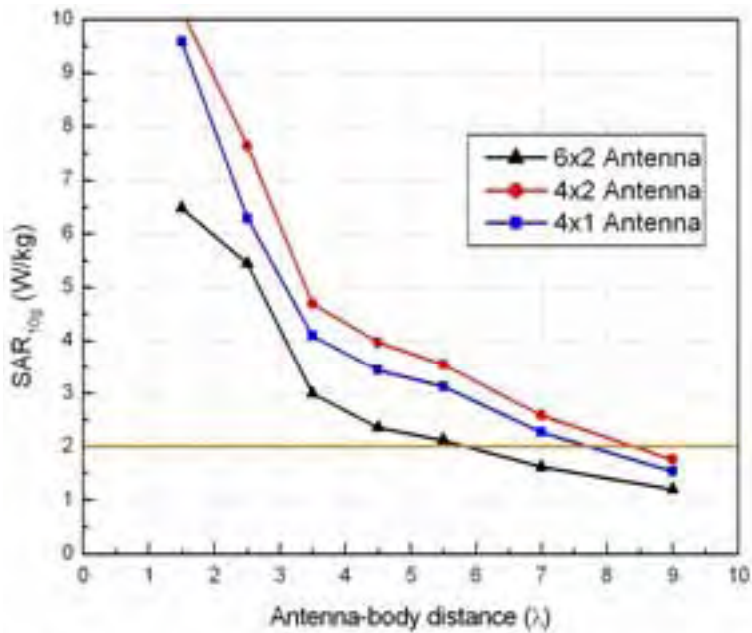


Figure 2 - Maximum SAR averaged over 10 g of tissue as a function of the antenna-body distance. Frequency: 2170 MHz. Radiated power: 30 W.

P-B-212

**PHYSIOLOGICAL EFFECTS OF CDMA CELLULAR PHONE EXPOSURE ON HUMAN.** K.-C. Nam<sup>1</sup>, S.-W. Kim<sup>1</sup>, S.-C. Kim<sup>2</sup>, D.-W. Kim<sup>1</sup>. <sup>1</sup>Dept of Medical Engineering, Yonsei Univ College of Medicine, Seoul, Korea (120-752), <sup>2</sup>Graduate School of Bio & Information Technology, Hankyong National Univ, Ansong, Kyonggi-do, Korea.

**Objective :**

The wide and growing use of cellular phones has raised the question about the possible health risks associated with radio-frequency electromagnetic fields. Recently, some researches reported on the effects of GSM cellular phone exposure on human, but the study on the effects of CDMA cellular phone exposure was a few. This study was to investigate RF effects of a CDMA cellular phone on heart rate, blood pressure, respiration rate, and sympathetic nervous system activation.

**Methods :**

The study group consisted of 21 adult and 21 teenager volunteer subjects. The mean ages were 25.9 year for the adults and 15.9 years for the teenagers. The volunteers were informed in detail about the purpose and procedure of the study, and a written consent was obtained from the subjects.

A CDMA cellular phone was used to transmit signal at a frequency of 835 MHz. The power of CDMA phone was set at 300 mW all the time. The antenna was not extended, and the microphone and the speaker were disabled not to be heard any sound by the subjects during the test. The phone was insulated from the headset, so that the subjects could not recognize if it operated or not.

The subjects'; heart rate (HR), systolic (SP) and diastolic blood pressure (DP), respiration rate (RR), and galvanic skin resistance (GSR) were measured during the real and sham exposures with double blind test procedure. The heart rate was measured by infrared photoplethysmography (PPG) using optical finger probe. The blood pressure was measured with automatic blood pressure monitor (Omron T4, Japan). The respiration rate was measured by respiratory inductive plethysmography (RIP) using an inductance

coil band. The sympathetic nervous system is subconsciously activated when the body is under stress. The constructed GSR meter was used to measure skin resistance change. These data were measured using data acquisition board (DAQPad-6020E, National Instrument, USA) and recorded using a notebook PC.

The test room had no working electric facilities. The subject was lying comfortably in a bed, and the cellular phone was positioned on the left side of the head. Each session consisted of resting for 15 minute (rest), exposure for 30 minutes (15 min and 30 min), and resting after exposure for 15 min (finish). PPG, RIP, GSR were simultaneously measured for one minute, and the blood pressure was measured for three times at every 15 minutes. From the measured data, PPG and RIP were calculated as beats/min, GSR was calculated as a mean and converted to percentage of resting value, and the systolic and diastolic blood pressure were averaged at each stage. All the subjects were asked to describe any symptoms or sensations after tests.

**Results :**

The associations of real and sham exposure results with exposure stages were analyzed by two-way ANOVA (SPSS 8.0, USA) for each physiological response. No subjects perceived the real or the sham exposure nor felt any warming or discomfort. There were no statistically significant differences in HR, RR, GSR and blood pressure by CDMA cellular phone exposure for 21 volunteer teenagers and 21 adults, except teenagers'; skin resistance change ( $p < 0.01$ ).

Skin resistance of teenager group decreased while real exposed. There were significantly differences between real and sham group ( $p=0.000$ ), and between the exposure stages ( $p=0.000$ ) by two-way ANOVA. By one-way ANOVA test for real exposure of teenager, the significant differences between rest and 15 min ( $p=0.004$ ), between rest and 30 min ( $p=0.000$ ), between 30 min and finish ( $p=0.001$ ), with a Tukey post-hoc comparison. And there was no significant difference by one-way ANOVA test for sham exposure of teenager. The effect on teenagers'; group showed reversible response as there was no difference between rest and finish.

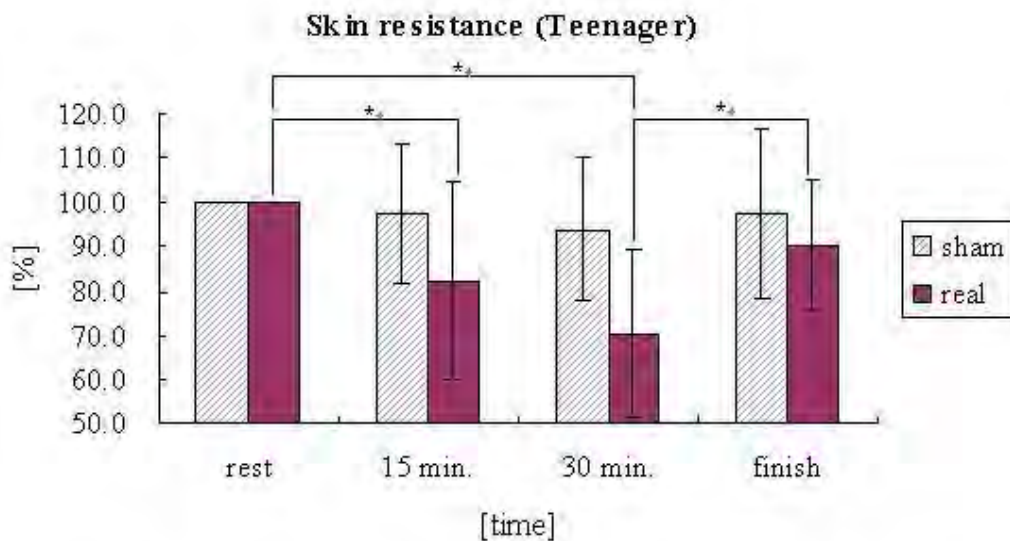


Figure 1. The skin resistance changes of the teenager group for real and sham CDMA exposures (n = 21) (\*:  $p < 0.01$ )

**THE GERMAN MOBILE TELECOMMUNICATION RESEARCH PROGRAMME.** G. Ziegelberger. Federal Office for Radiation Protection (Bundesamt für Strahlenschutz), Neuherberg/Oberschleissheim, Germany.

The German Ministry for the Environment, Nature Conservation and Nuclear Safety (BMU) and the Federal Office for Radiation Protection (BfS) initiated a Mobile Telecommunication Research Programme based on recommendations of national and international expert groups, several workshops and a public consultation process. The total costs of 17 million € are equally shared between the BMU and the German mobile network providers. The programme aims at a reduction of scientific uncertainty for health risk assessment in this field.

The priorities of the research programme were fixed in autumn 2003:

**Biology** - Appr. half of the budget is spent on biological projects carried out in vivo on humans and animal models and in vitro on cell cultures. The main end points include possible RF-influences on brain function (in humans: EEG, sleep and cognition), sensory physiology of hearing and vision (in vitro), the blood brain barrier (in vivo and in vitro), genotoxicity (in vitro on isolated human blood lymphocytes), possible long-term effects on cancerogenesis and behaviour (in rats), fertility and development (in mice), electromagnetic hypersensitivity and a verification of the often postulated age dependency of RF-effects.

**Dosimetry** - In more than ten different projects, the actual RF-exposure caused by different emitting sources (GSM, UMTS, WLAN etc.) at home and at work is examined. While some projects deal with base stations, others address near field exposure caused by transmitters operating near the human body. For typical exposure scenarios, detailed SAR-distribution will be simulated and thermophysiological Dosimetry also provides essential support to the other projects of the programme.

**Epidemiology** - The projects focus on:

- (i) mobile phones in a prospective cohort study and in case control studies on different brain tumours and on uveal melanoma,
- (ii) other RF-sources, i.e. powerful transmitters in association to childhood leukemia, and base stations and their possible influence on human well-being.
- (iii) Risk communication - Projects will analyse and improve the communication with different public groups. A better transfer of scientific data allows a knowledge-based handling of telecommunication concerns by the general public.
- (iv) The study design of single projects, relevant literature reviews and progress reports are available at the web site of the research programme (see [www.emf-forschungsprogramm.de](http://www.emf-forschungsprogramm.de)). In addition, the protocols of the programme-accompanying workshops as well as national and international research results including a discussion on their relevance for human health are published here.
- (v) Round Table An independent group of stakeholders will accompany the research programme to ensure the transparency of the programme and the optimal communication of the research aims and results to the public. It will also assist the publication of the overall research results.

## Theoretical and practical modelling

P-B-218

**POSSIBLE DIFFERENCES IN THE RF EXPOSURE OF CELLS IN TEST TUBES VERSUS FLASKS OR PETRI DISHES.** Q. Balzano<sup>1</sup>, A. R. Sheppard<sup>2</sup>. <sup>1</sup>Univ of Maryland, College Park, MD, USA, <sup>2</sup>Asher Sheppard Consulting, Redlands, CA, USA.

**INTRODUCTION:** The RF exposure of cell preparations always entails the disposal of the heat imparted to the biological system by the incident electromagnetic energy. It is the goal of many experiments to expose the cell system under isothermal conditions to match the thermodynamic state of the sham-exposed cell sample, which is kept at a constant temperature. The engineering task of heat removal while keeping the preparation at a constant temperature grows in difficulty as the exposure level increases. This is because the RF heating of the cell system is a bulk effect while the heat dispersal into the environment occurs via energy flow at the boundary of the container or the surface of the medium.

**METHODS:** This paper analyzes the temperature distribution and the thermodynamic events in cell preparations exposed in test tubes, flasks, and Petri dishes. The uncertainty of the thermal state of exposure in the various containers is discussed in detail in an effort to clarify physical differences in the cell environment during RF exposure.

**RESULTS:** The analysis shows that achieving temperature uniformity is increasingly more difficult as the level of RF exposure increases and that there are substantial differences in the temperature distribution depending on the cooling system adopted for heat removal. In some exposure conditions, convective heat transport, quantified by a large value of the Grashof number<sup>[1, p 423]</sup>, may be present in the exposure vessel. The Grashof number, which indicates the ratio of the buoyancy force to the viscous force (drag) acting on the fluid mass, is very large for test tubes with a deep column of medium above the cell layer. Convection, a non-random motion in the medium, presents a radical difference in the thermodynamic environment of the exposed vs. sham-exposed cell cultures. This phenomenon can alter the availability of nutrients to cells layered at the bottom of the vessel. The presence of convection may help explain the difference in the results of biological experiments exposing cells to high level of RF energy in different vessels and different cooling systems. Convective motion in liquids can be directly observed in the laboratory using existing techniques.

**CONCLUSIONS:** So-called isothermal experimental studies may need to be evaluated for effects of convection, which may cause biologically significant differences in exposure conditions even when sham and exposed samples are held at the same overall temperature. Exposure vessel shape and the volume of medium are important factors possibly influencing experimental outcome, particularly for test tube-like vessels filled to considerable depth.

### REFERENCE:

[1] Incropera F and DeWitt DP, 1985. Fundamentals of Heat and Mass Transfer, Chapter 9. New York: John Wiley & Sons.

### ACKNOWLEDGEMENT:

Research support (QB) through a CRADA between the US FDA, CDRH and the CTIA.

**DEVELOPMENT OF FORMULAS FOR PREDICTING PERSONAL EXPOSURES TO ELF MAGNETIC FIELD IN LIVING ENVIRONMENTS.** M. Ju<sup>1</sup>, K. Yang<sup>1</sup>, S. Myung<sup>1</sup>, G. Hwang<sup>2</sup>, J. Kim<sup>3</sup>. <sup>1</sup>Korea Electrotechnology Research Institute(KERI), <sup>2</sup>Ubiquitous Computer Center, Dongseo Univ, <sup>3</sup>Korea Electric Power Corporation.

**BACKGROUND:** Although scientific research is currently conducted on potential health hazard of electric and magnetic field, there is a nonobjective and psychological belief that it is harmful without scientific and objective proof. The ELF magnetic field has become one of Korea's social issues. Therefore, in order to evaluate the magnetic field(MF) exposure levels of Korean people in general living environment, 500 subjects were randomly selected from nine occupations and personal MF exposures of 466 people were measured from 2001 to 2004 under government fund. This study developed three types of formulas using the above data to predict personal MF exposure during the period in bed, at work place and entire 24-hour. These formulas can serve as a valuable tool in predicting 24-hour personal MF exposure without directly measuring the exposure.

**OBJECTIVE:** To predict and characterize personal MF exposure in general living environments

**METHODOLOGY:** Three types of personal MF exposure prediction formulas, day(24-hour) formula, work place formula, and bedroom formula, were developed by applying evolutionary computation method to personal MF exposure database of 466 subjects. Genetic algorithm and genetic programming were used among the evolutionary computations. After tuning database with the above methods, final three formulas with small estimation error were selected and proposed. The parameters of each formula include gender, age, residence type, residence size, occupation, distance between residence and power line, and the usage and condition of electric appliances.

**RESULTS:** For example, the following formula, developed using genetic programming method, calculates 24-hour average MF exposure.

$$MF = \log\left\{\frac{TL+19}{\log(O)+0.7O}\right\} - (1/H)(\log(HS)) - \log(O-93) - \log(S+A-O) + 1.58 + k$$

Where S is the gender, A is the age, H is the residence type, O is the occupation, TL is the distance between residence and power line, HS is the residence size and k is a calibrating constant that represents key factor which influence MF exposure such as the usage of electric appliances in work and home. The calibrating constant significantly increases reliability of the estimation. In this study, average MF exposure of all participants was 1.3mG and absolute average estimation error calculated by prediction formula was 0.26mG. This result shows that the 24-hour average MF exposure of an individual can be predicted with estimation error below 0.3mG using the above 24-hour formula. In the bedroom formula, occupation was not included as the parameter. The absolute average estimation error for the work place formula and bedroom formula were 0.37mG and 0.36mG, respectively. The above formulas will be further developed into a prediction formula that can calculate MF exposure in case and control groups for subjects below Korean middle school students. The future formulas will be used in epidemiological study on correlation between magnetic field and tumors found in children.

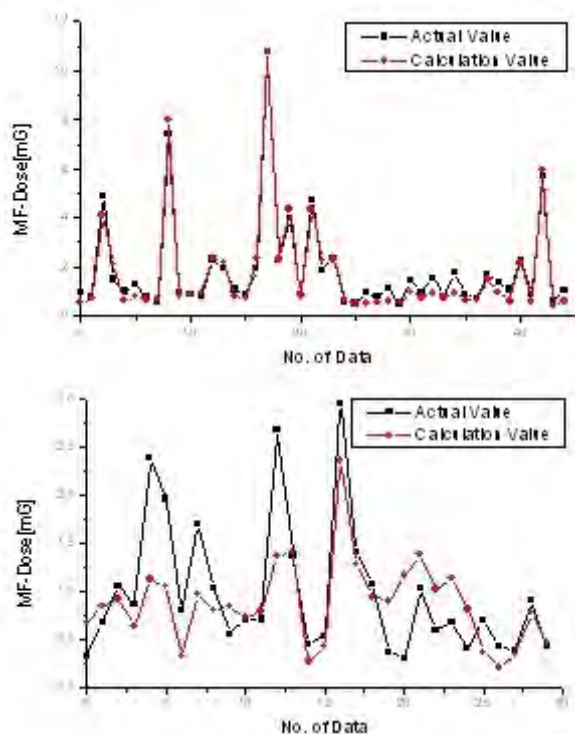


Fig.1. 24-hour personal MF exposure estimation curve Fig.2. MF exposure estimation curve at work place

P-B-224

**SIMULATION OF ENVIRONMENTAL MEASUREMENT ERROR DUE TO RF FIELD INTERACTION WITH THE INSTRUMENT OPERATOR.** E. D. Mantipty, R. F. Cleveland. Office of Engineering and Technology, Federal Communications Commission, Washington, DC, USA.

For transmitters regulated by the Federal Communications Commission (FCC), most problems related to compliance with radiofrequency (RF) environmental exposure limits occur near high power FM radio stations where broadcast antennas may be mounted relatively close to ground level. Since broadcast antennas are usually circularly polarized, and the ground is reflective, exposure typically occurs with mixed electromagnetic polarization in a standing wave field. Compliance with exposure limits is determined by spatial averaging using an isotropic broadband survey meter with a shaped electric field probe calibrated at 100 MHz. For a single, dominant transmitter, or multiple transmitters propagating in the same direction, the operator typically makes a single, spatially-averaged measurement facing a direction transverse or to the side of the direction of propagation, neither blocking nor facing the transmitting antenna(s). The spatial average is made by sweeping the probe vertically from ground to 180 cm (6 feet) while facing the measurement location. For the case where significant transmissions come from different directions, four spatial averages are made at the same location while facing the four cardinal points (true north, south, east, and west). A calibration factor is applied to the single measurement or average of the four measurements and the resultant is compared to exposure limits to determine compliance.

The body of the individual performing the measurement is normally relatively close to the region where the field is to be determined and can interfere significantly with measured values. Spatial averages taken from different directions have been observed to vary as much as 5 to 7 dB. While standing during spatial averaging, using a Wandel and Golterman EMR-30 meter, the center of the torso is about 110 cm from the field probe and the arm is extended to hold the readout instrument such that the hand is about 40 cm from the probe.

Initial studies have been performed using SEMCADlight FDTD code at 100 MHz with a simple cylindrical human phantom model having a height of 175 cm, radius of 12 cm, conductivity of 1 S/m, and relative dielectric constant of 50. Ground was simulated as a perfect conductor. The transmitting antenna was modeled as either a vertical dipole 3 m above ground or a vertical monopole at ground and the phantom was placed at a horizontal distance of 3.5 m from the antenna. The spatial RMS electric field (spatial average equivalent power density) was calculated 1 m from the phantom location with and without the phantom present in directions such that the phantom is either facing the source (facing), facing away from the source (blocking), or facing perpendicular to the direction of propagation (side). The table below shows ratios, both unitless and in dB, of the electric field squared measured with and without the phantom present for various measurement directions.

These preliminary results support the necessity of making measurements transverse to the direction of propagation. A single measurement made when blocking the source may cause significant negative error. However, a set of four measurements made perpendicular to each other will tend to cancel this error. Errors are less for the case of a single dipole than for a monopole, probably because the field is more horizontally polarized and less aligned with the vertical phantom for the dipole case.

Note: Views expressed in this abstract are those of the authors. They do not necessarily reflect the views of the Federal Communications Commission (FCC). Mention of commercial products does not constitute endorsement by the FCC.

Source	Transverse	Facing Antenna	Blocking Antenna
Vertical Dipole	0.96 or -0.2 dB	1.12 or +0.5 dB	0.75 or -1.2 dB
Vertical Monopole	1.04 or +0.2 dB	1.30 or +1.2 dB	0.42 or -3.8 dB

P-B-227

**CONSTRUCTION OF A LARGE-SCALE 3D MODEL OF ELECTRIC FIELD STRENGTHS FOR A HIGH VOLTAGE TRANSMISSION SYSTEM.** H. Tripp<sup>1</sup>, I. Glover<sup>1</sup>, K. Jacobs<sup>2</sup>, S. Redhead<sup>2</sup>, J. Swanson<sup>1</sup>. <sup>1</sup>National Grid Transco, NGT House, Warwick, UK, <sup>2</sup>Network Mapping Ltd, Thorpe Park, Leeds, UK.

Introduction:

Electric and magnetic fields (EMF) are produced under high voltage transmission lines as a consequence of electricity transmission. These EMF can be modelled using software packages, if the physical characteristics of the transmission line are known. The strength of the electric field produced under the

transmission line will depend on the voltage, the distance of the conductors to ground, conductor and sub-conductor geometries. EMF calculations are usually carried out on isolated line cross sections or on short sections consisting of one span in 2D, which in many cases do not allow for sagging conductor geometries making assessment of field strengths for extended parts of a network slow and painstaking. We have combined extensive, accurate helicopter surveys of the National Grid system in England and Wales with 3D field calculation software to produce a detailed three-dimensional electric field map of over 5000 route-km of the electricity transmission system.

#### Objectives:

The aim was to construct a large-scale map of calculated electric field strength, 1m above the ground, which incorporated use of actual ground profile details across the whole of the UK transmission system. This may be used to assess electric field exposure with respect to a number of features including land use. To achieve this an automated system was developed to calculate three-dimensional electric field strengths coupled with detailed and accurate aerial laser survey data of the transmission system provided by Network Mapping Ltd.

#### Methods:

The transmission lines in the UK were surveyed using Aerial Laser Survey technology, which captures accurate line survey data including tower type and conductor and sub-conductor information along with topographic information for the surrounding land and its usage. Briefly, the aerial laser survey, records laser reflections from the transmission line and surrounding features and positioning of the recorded objects are accurate within 20 cm. Within the UK, aerial laser data is available for over 5000 route-km of transmission line. A specific software programme has been developed to enable the automatic import of tower position, conductor catenaries, system operational information, ground profiles and minimum clearance from the laser survey directly into a 3-dimensional electric and magnetic field calculation software package (EFC-400). Unlike many other EMF calculation packages EFC-400 allows the calculation of conductor geometries (i.e. sagging conductors) in 3D space. Both electric and magnetic field strengths can be calculated using EFC-400 and exported as coloured strength contours in both 2D and 3D (Fig. 1). Entire line routes can be modelled within EFC-400 using this system and stored, with rapid recalculation of field strengths if modifications to the line occur.

Further capabilities have been added; the exported field exposures can be incorporated into aerial photography (collected at time of aerial laser survey) and coupled with searchable land use databases (Fig. 2). These land-use databases include precise geographical location of features such as homes, schools, roads and leisure facilities such as golf courses. The combination of information from a number of different sources within the same overall model allows the rapid search and identification of field exposures and correlations with land usage particularly in proximity to schools and homes. This information can also be viewed in three-dimensional perspectives, using PLS-CADD software which models the exact features of the transmission as surveyed (Fig. 3) and allows the user to 'fly' a transmission route and view the overhead line and the field it produces in relation to all the topographic or land use features.

#### Conclusions:

This, we believe, is the most extensive and detailed model of electric field strengths from high voltage power lines in the world. Using the aerial photography with land use database and 3D PLS CADD model and incorporating EMF exposure data from EFC-400, we can create a large-scale map of the EMF produced by the UK transmission system based on accurate line survey data and rapidly search for exposure strengths and areas of potential interest. This will add to our knowledge of EMF exposure in

the UK and help understand the land use types near transmission systems and the range of field exposure produced by electricity transmission.

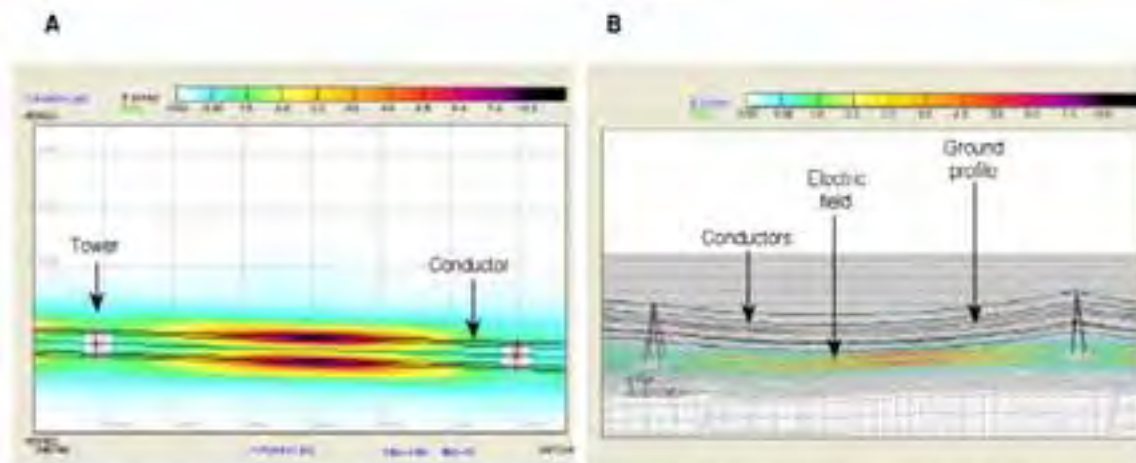


**Fig.1 A.** 2D graphical representation of electric field contours produced under an overhead line span modelled in EPC 400. **B.** 3D representation of electric field strength produced under overhead line span. The electric field is shown calculated with respect to the illustrated ground profile.

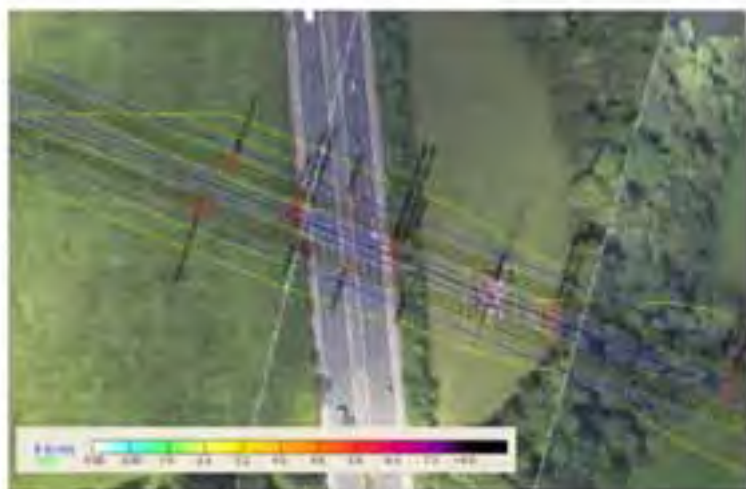


**Fig.2.** Aerial photograph of an overhead line span with electric field strengths superimposed. Electric field strength contours determine the extent to which the electric field falls above or below particular values within the topography.

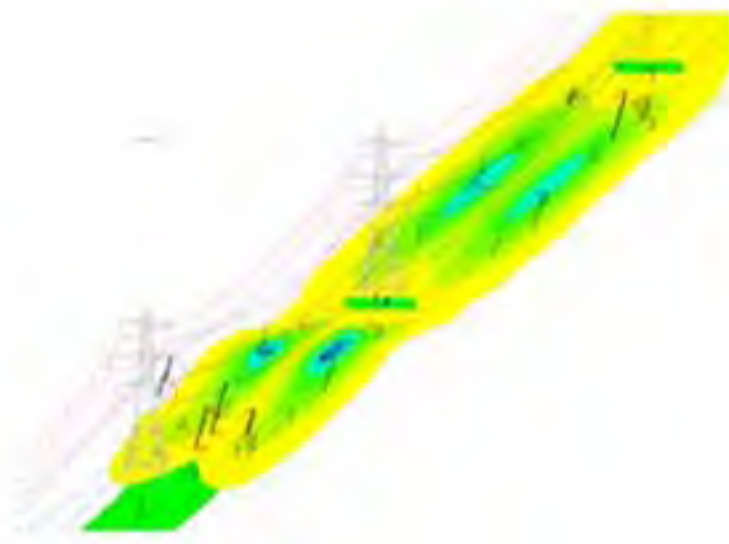


**Fig.3.** Three dimensional representation of a transmission line, the ground profile under the line and the electric field produced. The electric field was calculated in respect to the undulating ground profile, shown in the figure.

MYOELECTRICAL ACTIVITY OF THE SMALL INTESTINE INDUCES HEAT SHOCK PROTEINS. D. Laubitz<sup>1</sup>, A. Sikora<sup>2</sup>, A. Lubańska<sup>1</sup>, J. Woliński<sup>1</sup>, R. Zabielski<sup>1</sup>, E Grzesiuk<sup>2</sup>. <sup>1</sup>The Kielanowski Institute of Animal Physiology and Nutrition, Polish Academy of Sciences, Jablonna, Poland. <sup>2</sup>Institute of Biochemistry and Biophysics, Polish Academy of Sciences, Pawinskiego Warsaw, Poland.

One of the mechanisms protecting cells against stress is heat shock response, the phenomenon observed from bacteria to man. There are many stress factors inducing heat shock response in cells: high temperature, oxidative stress, chemicals, UV radiation, nutritional deficiencies, diseases. In all organisms HSPs expression under stress conditions is regulated at transcriptional level, in *Escherichia coli* by replacement of RNA polymerase sigma factor  $\sigma^{70}$  for sigma factor  $\sigma^{32}$ . Here we have found that electrical current generated during physiological activity of the small intestine induces heat shock response.

The myoelectrical activity of the gut displays a regular three-phased pattern known as the myoelectrical migrating complex, MMC (Fig.1).

Previously we have shown that *E.coli* cells treated with MMC-related electromagnetic field (EF) are resistance to UVC irradiation as a result of heat shock proteins induction by the EF. In this study we have revealed expression of the sigma factor  $\sigma^{32}$  in the cell extracts obtained from bacteria treated with MMC-related EF as well as induction of Hsp70 in the enterocyte-like CaCo-2 cells under confocal microscope.

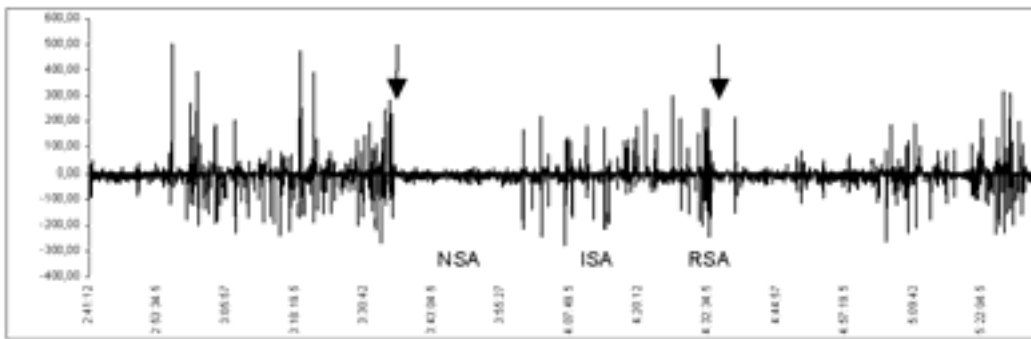


**Figure 1.** Electromyography trace of the interdigestive duodenal myoelectrical migrating complex (MMC) registered by bipolar electrode in the calf. RSA - regular spiking activity; NSA - non-spiking activity; ISA - irregular spike activity. Arrows indicate one MMC cycle which was extracted and saved as a text file for an electromagnetic field generator.

Materials and methods. The digital recording of one MMC cycle was transmitted into the flash-memory of an electrical field generating device (SGP-generator, ESCO, Warsaw, Poland). The cultured cells were exposed to EF via platinum electrodes fixed in culture plates; characteristic of the “MMC” current:  $E_{\min} = -251$  mV/cm,  $E_{\max} = 177$  mV/cm; average conductivity of medium  $s = 20$  mS/cm; current density in the medium was from  $j_{\min} = -3,5 \times 10^{-9}$  A/cm to  $j_{\max} = 5 \times 10^{-9}$  A/cm.

For the experiments *E.coli* AB1157 and human colon carcinoma cell line Caco-2 were used. Overnight bacterial cultures in C medium were diluted 1:20 and grown in the same medium for 120 min with shaking at 37°C in the presence of the EF (bacteria grown without EF served as a control). Bacterial cell

lysates were prepared for western-blot analysis according to standard method. Samples were separated on the three layers SDS-PAGE gel electrophoresis. Protein bands were transferred on the 0,45  $\mu\text{m}$  membrane in electrotransfer tank at 25 mA for 12 hours. The level of  $\sigma^{32}$  was determined on the membrane using primary antibodies (rabbit anti- $\sigma^{32}$ ) and a visualization was done by ProtoBlot II AP System (Fig. 2).

**Detection of Hsp70.** For EF study, cells at the density of  $1 \times 10^6$  cells/ml, were grown on micro cover glasses in 6-well plastic plates for 2-3 days, then glasses were transferred to Petri dish with fresh medium and located between two electrodes connected to the SGP generator for 18-24 hours. Caco-2 cells were fixed to glass by incubation in 4% formalin. The slides were stained using monoclonal, mouse anti-humanHsp70 antibodies conjugated with Alexa Fluor 488. The level of expression of Hsp70 in the CaCo-2 cells were measured with confocal microscope.

**Results.** In this study, the expression of  $\sigma^{32}$  - transcription factor in the extracts of EF treated *E.coli* cells was examined. We observed an increased amount of  $\sigma^{32}$  factor in the extracts from cells growing at 37° C and treated for 2 hrs with the MMC-related EF (Fig. 2 lane 5) but not in those untreated (Fig. 2 lane 4). The level of  $\sigma^{32}$  factor in EF-treated samples was even higher than observed in bacteria grown at 45° C (Fig. 2 lane 2).

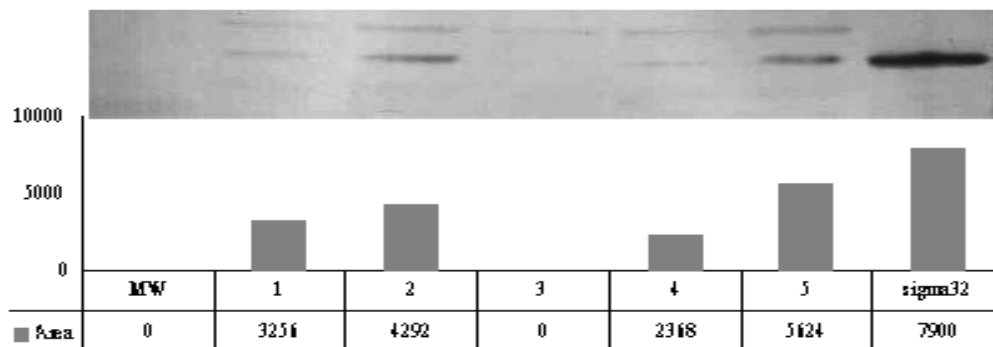


**Figure 2.** Immunodetection of sigma<sup>32</sup> in *E. coli* AB1157 lysates. The test was done in a presence of pure sigma<sup>32</sup> protein (last line). 1 - 45°C, 15 min.; 2 - 45°C, 40 min.; 3 – 28°C, 40 min.; 4 - 37°C, 40 min.; 5 - 37°C, 40 min + MMC-related EF.

Similar effect of MMC-related EF we have observed in eucaryotic cells. Higher expression of hsp70 was detected under confocal microscope in the cell cytoplasm after electrical stimulation compared to the cells incubated under standard conditions (negative control). As a positive control CaCo-2 cells were used incubated at 56°C for 20 minute. The level of hsp70 in the tested cells was similar to the positive control.

**Conclusion.** We have shown that the MMC related EF induces heat shock proteins both, in prokaryotic and eukaryotic cells. It is widely accepted that gastrointestinal tract epithelium is exposed to various stress agents such as pathogens, xenobiotics, and chemicals but it is also a barrier preventing passage of potentially harmful substances to the sterile host environment. The role of gastrointestinal motility in gut cytoprotection has been discussed until now in terms of motility that expel the digesta remnants and desquamated epithelia as well as controls the number of gastrointestinal microorganisms. We propos a novel role for gut motility that is solely associated with the electrical activity of the gut smooth muscles, i.e. the protection of the epithelial cells against toxins and harmful substances in food by inducing heat shock proteins.

**Poster Session C**  
**1:45 - 3:45 pm, O'Reilly Hall**  
**Highlights 1:30 – 1:45 by Asher Sheppard**

**Clinical devices**

P-C-3

**ENHANCEMENT OF NITRIC OXIDE PRODUCTION IN MEN FOLLOWING 1.5 T STATIC MAGNETIC FIELD EXPOSURE.** O. Sirmatel<sup>1</sup>, C. Sert<sup>2</sup>, C. Tumer<sup>3</sup>, A. Ozturk<sup>1</sup>, S. Dasdag<sup>4</sup>, M. Bilgin<sup>3</sup>. <sup>1</sup>Radiology Dept of Harran Univ Medical Faculty, Sanli Urfa, Turkey, <sup>2</sup>Biophysics Dept of Harran Univ Medical Faculty, Sanli Urfa, Turkey, <sup>3</sup>Physiology Dept of Dicle Univ Medical Faculty, Diyarbakir, Turkey, <sup>4</sup>Biophysics Dept of Dicle Univ Medical Faculty, Diyarbakir, Turkey.

This study was carried out on 33 voluntary and healthy young men from 20 to 25 years old to determine nitric oxide production immediately after 1.5 Tesla magnetic field exposure. The subjects were exposed to 1.5 T static magnetic field by using Magnetic Resonance Imaging apparatus for 30 minutes. 5 ml blood was taken intravenously from all the subjects one minute before and after exposure immediately.

Nitrite and nitrate concentration was determined by UV- VIS spectrophotometer. The obtained results related to the parameters under investigation were compared between Pre and post exposure groups. The results related to the parameters measured in this study were analyzed by paired Student t-test.

Finally, total nitric oxide concentration in post exposure samples was found higher than pre-exposure samples.

In conclusion, 30 minutes of 1.5 T static magnetic field affected nitric oxide concentration.

**Dosimetry**

P-C-6

**DIRECT MEASUREMENT OF RADIO-FREQUENCY FIELD EXPOSURE FROM A SHORTWAVE AMATEUR RADIO STATION.** E. M. Barnes<sup>1</sup>, E. Hare<sup>1,2</sup>. <sup>1</sup>Aerodyne Laboratories, Austin, TX, USA, <sup>2</sup>American Radio Relay League, Newington, CT, USA.

**INTRODUCTION:** Although it seems that most typical amateur radio equipment and antenna systems are likely to cause indoor and outdoor RF exposure levels within compliance with the U.S. Federal Communications Commission (FCC) RF exposure guidelines [1,2] (based on various estimating techniques), only direct RF field measurements can resolve any such questions with certainty. **OBJECTIVE:** Investigate, with accurate and reliable RF field measuring equipment, exposure intensity

from two independent antenna systems of a 100-watt amateur radio station, and extrapolate readings (10db increase) to what these RF exposure levels would be with the maximum legal CW power of 1.0 kilowatt (unmodulated).

**METHODS:** For this study, a Holaday Industries HI-4433 Broadband Isotropic Field Probe and an HI-4416 Readout System were used. With the RF probe at one meter above ground, all measurements were directly logged in "E-field volts per meter" (V/m) units. From these data were calculated field strengths (both V/m and mW/cm<sup>2</sup>) to be had if the transmitter output were the maximum legal limit of 1.0 kW CW. The two antenna systems under investigation are a 180-foot long (55m) twin-cage doublet, 80 feet (55m) high at the center, energized at 7 mHz (40-meter band), and a 12-element log-periodic rotary beam atop a 62-foot (19m) tower, energized at 14 and 28 mHz (20 and 10 meter bands). With both antennas on the same general premises, and fed with 100 watts CW, measurements were taken at the tower base and along the maximum radiation lobe's axis, as well as at other locations of interest.

**SUMMARY OF RESULTS:** The highest near-field measured anywhere on the premises was directly under the 10-ft. (3m) high open-wire, 400-ft. (122m) transmission line to the twin-cage doublet antenna, where 6.12 V/m was read at a voltage node. Extrapolated to 1.0 kW, this 7-mHz field would be 9.957 V/m. The maximum far-field measured was along the log-periodic rotary-beam antenna's main radiation lobe. At one wavelength--ten meters--from the tower base, 2.404V/m was read, which at 1.0 kW would be 7.6 V/m. Supplementary to these data, the full poster presentation includes additional field data covering a broader premises area and indoor measurements at the radio operating position.

**CONCLUSIONS:** At this particular amateur radio facility, all near-field and far-field levels measured at 1 meter above ground--and even when extrapolated to 1.0 KW--are below the maximum permissible exposure (MPE) strengths specified by the U.S. FCC [1,2].

#### REFERENCES:

1. FCC Staff. Evaluating Compliance with FCC Guidelines for Human Exposure to Radiofrequency Electromagnetic Fields-Additional Information for Amateur Radio Stations-Supplement B (Edition 97-01) to OET Bulletin 65.
2. Hare,E.RF Exposure and You, American Radio Relay League, Newington CT, 1998.

The author gratefully acknowledges the support and review of this project provided by the American Radio Relay League.



P-C-9 STUDENT

**DOSIMETRY BASED ON ELECTROMAGNETIC, THERMAL AND CONVECTION SIMULATIONS FOR IN VITRO MICROWAVE EXPOSURE SYSTEM.** M. Cueille<sup>1</sup>, A. Collin<sup>1</sup>, R. O'Connor<sup>2</sup>, P. Leveque<sup>1</sup>. <sup>1</sup>IRCOM CNRS, Limoges, France, <sup>2</sup>Laboratory of molecular signalling, Babraham Institute, Babraham, UK.

#### OBJECTIVE :

This paper describes the results of the dosimetry of in vitro microwave exposure systems. This dosimetry is based on electromagnetic, thermal and convection.

#### INTRODUCTION :

When the attention of bioelectromagnetics researchers was directed to the safety of the rapidly proliferation use of personal wireless devices, it became clear that in vitro biological studies would play a role in addressing questions of interactions between electromagnetic wave and biological tissues. In vitro exposure systems must be well-controlled, and that's the reason why the specific absorption rate (SAR, W/kg) distribution is determined in radio-frequency exposed biological solutions containing suspended or plated cells.

#### METHOD :

A three-dimensional numerical model was developed to predict the distribution of electromagnetic fields, power distribution, temperatures, and velocities within the different containers (Petri dish, flask, test tube). The instantaneous dissipated electromagnetic power distributions were calculated by the finite difference time domain method applied to the Maxwell's equations, and a time-scaled form of the heat transfer equation allowed to calculate the temperature distribution in the heated media. If necessary, temperature dependence of liquid dielectric properties is simulated through an iterative process. Finally, the governing equations for the flow, Navier-Stokes equations, was used to take into account the natural convection.

Exposure sources include opened transverse electromagnetic (TEM) cell for microscope, a cylindrical cavity and a plane wave exposure.

#### RESULTS :

In order to illustrate aspects of microwave heating and natural convection, a cylindrical cavity containing a test tube is used. Sequences for microwave exposure were defined according to the initial temperature (20 degreeC), the microwave power (between 200-2000 W) and the final temperature desired (37 degreeC). It is clear that rapid variations occurred in the temperature during the microwave exposure and a significant gradient in temperature existed in the test tube. The convection phenomena were included in the numerical simulations and thermal characterization of the biological solution was performed with a fluoroptic thermometer.

Then the dosimetry was calculated for an opened TEM developed to observe samples under a microscope during the irradiation.

P-C-12

**TECHNIQUE FOR CONSTRUCTING A REALISTIC PHANTOM OF A HUMAN FACE.** D. Hatcher, J. Ziriak, M. J. D'Andrea. Naval Health Research Center Detachment Directed Energy Bioeffects Laboratory, Brooks City-Base, TX, USA.

**BACKGROUND:** Homogeneous tissue equivalent phantoms (Figure 1) are frequently used as surrogates for a biological system. Typically these phantoms only model gross anatomical structures and never attempt to model a specific individual's anatomical geometry.

**OBJECTIVE:** Develop a technique for constructing tissue equivalent phantoms of the faces of particular individuals.

**METHOD:** Positive plaster molds created from the faces of movie actors (Haunted Studios, Inc., Birch Row, MN) were used to create a negative plastic mold from which the phantom equivalent faces were created (Figure 2). To accomplish this, a vacuum forming machine (Kingston Vacuum Works, Kingston, NY) and two types of plastic sheets (White Styrene, Clear Acetate Butyrate) that are moldable when heated were used. The plaster molds were centered on the table of the vacuum forming machine and any holes on the vacuum table that were visible were covered with tape to focus the vacuum around the plaster mold. The plastic sheet was clamped between two metal frames and placed on blocks inside an oven heated to 350°F for 1-min. A shop-vacuum (Clark STV10) was connected to the vacuum table and turned on, then the plastic sheet was quickly placed over the positive face mold and pressed downward until the metal frame holding the heated plastic made contact with the vacuum forming box of the vacuum table. Once the plastic had been shaped the shop-vacuum was turned off and the negative mold was ready to use. A custom holder was constructed to support the plastic negative while it was filled with the tissue equivalent material. Once the phantom was poured it was allowed to equilibrate to the ambient temperature for a minimum of 24-hr. The phantom face was then removed from the plastic negative placed in a tri-pod holder that allowed exposure varying angles. The plastic negative is reusable. The effects of physical obstructions (e.g., eye glasses, binoculars, night-vision goggles, and even string) and natural facial features on the distribution of energy on the phantom face were examined using an infrared camera (FLIR S-60, North Billerica, MA). The results were compared to an IR image taken before exposure to the energy source.

**RESULTS:** This technique proved effective in creating a life-like homogeneous tissue equivalent model that can be used to examine the distribution of energy on a particular face and the effects of physical obstructions on the energy distribution. Each of the items we placed on or in front of the phantom face, as well as the shapes of the faces, changed the distribution of energy.

**CONCLUSIONS:** The ability to create phantoms of individuals' faces can reduce the need for human exposures and increase the ability to systematically investigate the facial geometry and likely obstructions. Even small obstructions (e.g. string) can dramatically effect the distribution of energy on the face.

**REFERENCES:**

Chou, C.K., et al. Formulas for preparing phantom muscle tissue at various radiofrequencies. *Bioelectromagnetics* 5:435-441 (1984).

This work was funded by the U.S. Air Force and U.S. Navy (Project Numbers: 0602236N/M04426.w6, 0601153N/M4023/60182). The views, opinions, and/or findings contained in this report are those of the authors and should not be construed as official Dept of the Air Force, Dept of the Navy, Dept of Defense, or U.S. government position, policy, or decision unless so designated by other documentation. Trade names of materials and/or products of commercial or non-government organizations are cited as needed for precision. These citations do not constitute official endorsement or approval of the use of such commercial materials and/or products. Approved for public release; distribution unlimited



Figure

1.



Figure 2. Mr. John Neville.

P-C-15

**COMPLIANCE ZONE PROFILING OF A COMMERCIAL GSM BASE STATION ANTENNA BASED ON NUMERICAL SAR CALCULATIONS.** F. J. C. Meyer, M. J. van Wyk, R. A. Kellerman. EM Software and Systems-S.A., EMSS Building, Technopark, Stellenbosch, South Africa.

OBJECTIVES AND METHOD: SAR calculations in the human body in close proximity to base station antennas are of importance for the assessment of occupational compliance to international exposure

guidelines and standards [1]. We have implemented a hybrid Finite Element Method (FEM) / Method of Moments (MoM) technique for the efficient and accurate calculation of the spatial-peak and whole-body-averaged SAR in a human phantom close to a base station antenna [2]. The main advantage of the hybrid FEM/MoM compared to the popular FDTD technique is the efficiency with which the large free-space region around the base station antenna can be modeled. In previous work, we investigated the level of detail that needs to be included in the numerical models, and in particular, the base station antenna [3]. This demonstrated another important advantage of the FEM/MoM and that is the accuracy with which the antenna elements can be modeled, which turned out to be critical for accurate exposure assessment of humans within a few hundred millimeters of such an antenna. We also applied the technique to the calculation of a three-dimensional (3D) SAR compliance zone around a generic base station antenna in [3]. In the work presented in this paper the technology has been applied to a real commercial base station antenna used in GSM networks. We have validated the antenna model by comparing measured and simulated results. As shown before [3], this validation is of critical importance due to the significant influence the phantom can have on the feed network, and thus on the active power of the antenna elements. Numerical experiments have been performed to quantify the effect of the shape and size of different phantoms on SAR and investigations were done on a homogeneous vs heterogeneous phantom to ensure conservative but realistic SAR profiling. The phantoms were rotated and translated to obtain a complete 3D SAR profile. The efficiency of the FEM/MoM technique [2] together with the automated SAR extraction routines implemented [4], enable SAR calculations within realistic solution time and computer memory requirements.

**RESULTS AND CONCLUSIONS:** The results obtained yields a three-dimensional (3D) SAR profile around the commercial base station antennas. This profiles is compared to the 10g spatial-peak and whole-body-averaged basic restriction [1] of the exposure guidelines. This, in turn, yields an occupational exposure compliance zone around such an antenna which is more realistic and accurate and less restrictive than the compliance zone based on reference levels [1].

#### REFERENCES:

- [1] "ICNIRP Guidelines for limiting exposure to time-varying electric, magnetic, and electromagnetic fields (up to 300GHz)," *Health Physics*, vol. 74, no. 4, pp. 494-522, April 1998.
- [2] F.J.C Meyer, D.B Davidson, U Jakobus and M.A Stuchly, "Human Exposure Assessment in the Near Field of GSM Base-Station Antennas Using a Hybrid Finite Element / Method of Moments Technique," *IEEE Transactions on Biomedical Engineering*, Vol. 50 No. 2, page 224-233, February 2003.
- [3] FJC Meyer, MJ van Wyk and M Bingle, "Accurate Compliance Zone Calculations around Base Station Antennas using Full Body SAR Profiling," in *Proceedings of the Twenty-Sixth Annual Meeting of the Bioelectromagnetic Society*, (Washington D.C., USA), June 2004.
- [4] M Bingle and F.J.C Meyer, "Determination of the Spatial-Peak SAR in Human Models from a Hybrid FEM/MoM Solution," in *Proceedings of the Twenty-Sixth Annual Meeting of the Bioelectromagnetic Society*, (Washington D.C., USA), June 2004.

P-C-18

**OPTIMAL SETTINGS FOR FREQUENCY-SELECTIVE ELECTROMAGNETIC FIELD MEASUREMENTS FOR EXPOSURE ASSESSMENT AROUND BASE STATIONS.** C. Olivier, L. Martens. Ghent Univ, Dept. of Information Technology, Ghent, Belgium.

**Objective:** To derive the optimal configuration of the spectrum analyzer when used for the exposure

assessment around base stations, together with the associated uncertainty and the underlying rationale for the chosen settings.

**Method:** A base-band simulation model for both the spectrum analyzer and the GSM and UMTS communication signals have been developed to investigate the behavior of the spectrum analyzer when used for exposure assessment. Simulations enable to determine the theoretical bounds on the achievable accuracy for the measurement of a mobile communications signal and to examine the impact on the measurement result of one individual setting of the spectrum analyzer. The simulation models have been validated with measurements on realistic mobile communication signals.

**Results:** (a) *GSM*: The resolution filter should on the one hand be wide enough to measure the actual power of the GSM signal, but on the other hand, the contribution of the neighboring GSM channel to the channel under investigation should be minimized. Since for the exposure assessment, the worst-case situation where the GSM channel is continuously emitting at maximum power has to be considered, the positive-peak detector is preferred, since it will deliver an accurate power level, even if the GSM signal is time-intermittent (e.g., because of low traffic). Moreover, because the GSM signal has a constant envelope, the use of the positive-peak detector with a resolution bandwidth of 30 kHz enables to estimate the actual RMS power of the signal, which is illustrated in Fig. 1. For the sweep time, an increased accuracy has to be weighed up against a longer measurement time. Repeating the scan several times over a certain frequency range, instead of executing one slow measurement, delivers a measurement result that is less dependent on the instantaneous traffic. The resulting optimum settings (see also [1]) are given in Table 1.

(b) *UMTS*: Although for UMTS, a channel decoder will provide more information (e.g., the power of the pilot channel) to estimate the maximum possible exposure, the use of a spectrum analyzer remains an attractive alternative because of its general applicability. Due to the noise-like behavior of the UMTS signal, the RMS-detector of the spectrum analyzer is preferred. However, it is possible to estimate the RMS level from a measurement with the positive-peak detector by taking into account a correction factor. This factor depends on the - a priori unknown - number of channels that are transmitted simultaneously. This is illustrated in Fig. 2, where also the worst-case correction factor that should be applied, is indicated. If a resolution filter smaller than the UMTS bandwidth is chosen, the measured level (both for the RMS as for the positive-peak detector) have to be corrected, since only a portion of the signal is measured. But on the other hand, the resolution bandwidth cannot be too wide because otherwise neighboring channels would contribute significantly to the measured power of the UMTS channel under consideration. Although the standard deviation on the measured power level decreases for larger sweep times, the sweep time by itself, is constrained because the power of the UMTS signal only remains constant during a limited period. Indeed, because of the fast power control (at a rate of 1500 times per second) of the UMTS signal, every 0.67 ms the power of the UMTS signal is augmented or diminished by a certain power step. Moreover, it is recommended to fix the sweep time over one measurement point to two times the power control period, to ensure that the maximum measured power level is caused by only one power control period where the UMTS signal was transmitted at its maximum power level. The resulting settings for the spectrum analyzer are also summarized in Table 1 for the measurement of a UMTS signal.

**Conclusions:** By using simple simulation models for the spectrum analyzer and the signals under investigation, the optimal settings of the spectrum analyzer for assessing the exposure around a base station have been derived, together with the uncertainty associated with the stochastic characteristics of a certain modulation signal.

**Acknowledgment:** Christof Olivier was research assistant of the Fund for Scientific Research (F.W.O.-Vlaanderen) during this work.

## References

[1] C. Olivier and L. Martens, "Optimal settings for narrow band signal measurements used for exposure assessment around GSM base stations," *to appear in Trans. Instr. and Meas.*, Vol. 54, No. 1, Feb. 2005.

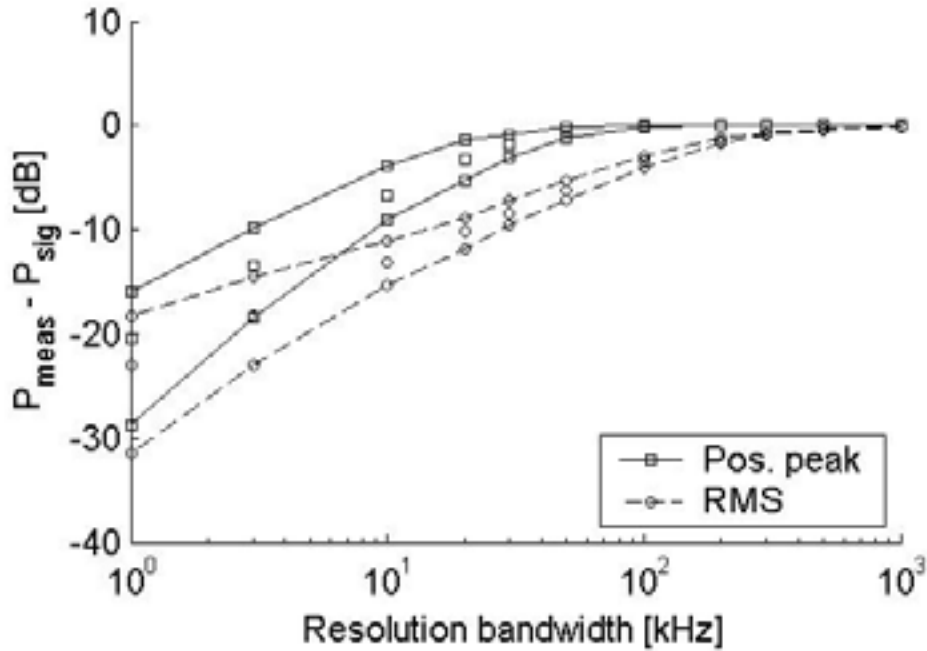


**Fig. 1.** Mean level of a GSM channel measured by the RMS and positive-peak detector for different resolution bandwidths, together with its 95% confidence interval.

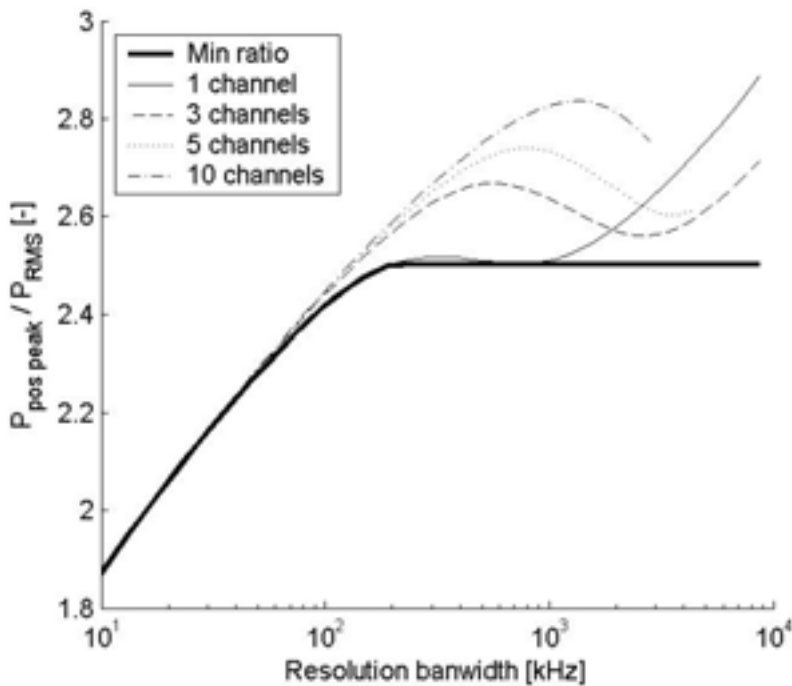


**Fig. 2.** Relation between the power level of a UMTS signal measured with the positive-peak detector and with the RMS detector for different configurations of the UMTS signal.

<b>Table 1: Proposed spectrum analyzer settings</b>		
	<b>GSM</b>	<b>UMTS</b>

Detector	Positive peak	RMS <sup>[1]</sup>
Resolution bandwidth	30 kHz	500 kHz
Sweep time	$F_{\text{span}} \text{ [MHz]} / (20 \text{ MHz/s})$ <sup>[2]</sup>	$N_{\text{bin}} \times 1.33 \text{ ms}$

$F_{\text{span}}$ : frequency span.  $N_{\text{bin}}$ : number of measuring points in one frequency span.  
<sup>[1]</sup>For the positive-peak detector a correction factor of 2.5 should be applied.  
<sup>[2]</sup>Preferrably 10 subsequent sweeps are taken.

P-C-21

**SAR MEASUREMENT EMPLOYING ELECTRO-OPTIC (EO) PROBE WITHOUT USING METAL.** T. Onishi<sup>1</sup>, H. Togo<sup>2</sup>, N. Shimizu<sup>2</sup>, K. Kiminami<sup>1</sup>, S. Uebayashi<sup>1</sup>, T. Nagatsuma<sup>2</sup>. <sup>1</sup>Wireless Labs., NTT DoCoMo, Inc., Kanagawa, Japan, <sup>2</sup>NTT Microsystem Integration Labs., NTT Corp., Kanagawa, Japan.

**BACKGROUND:** Using an optical electric field probe to measure the Specific Absorption Rate (SAR) is expected to be superior to using conventional probes with respect to RF exposure from a mobile radio terminal and in-vitro or in-vivo exposure systems. This is because the optical probe can measure the field distribution at a low level of invasiveness and is capable of measuring both the frequency spectrum and phase. A previously proposed optical probe [1] uses metal dipole antennas to enhance the sensitivity. However, this approach still causes a disturbance in the field and has a limited bandwidth due to the use of the metal dipole antennas. Furthermore it is difficult to miniaturize the probe.

**OBJECTIVE:** The objective of this study is to develop a noninvasive SAR measurement probe, which can measure the SARs at multiple frequencies simultaneously and has high spatial resolution, employing a small Electro-Optic (EO) crystal without using metal [2].

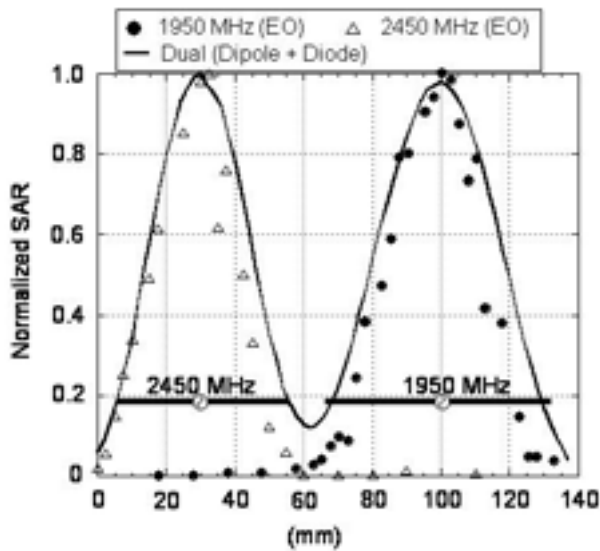
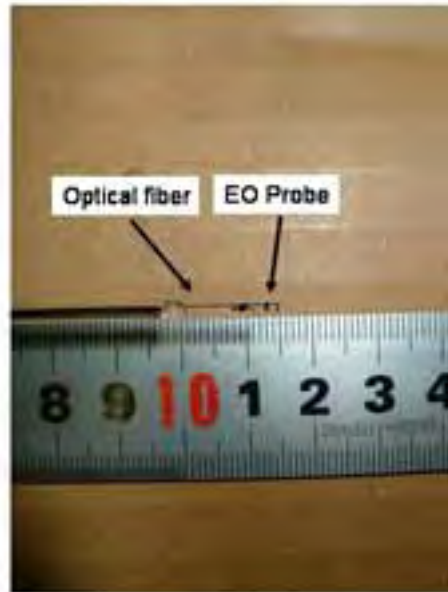
**METHODS:** Figure 1 is a picture of the prototype Electro-Optic (EO) probe, which comprises an EO crystal, dielectric mirror, and optical fiber in glass. CdTe is selected as the EO crystal and its scale is 1 mm x 1 mm x 1 mm. The EO crystal is directly connected to the optical fiber and can detect an electric field parallel to the EO surface. A main feature of this construction is that there is no metal in the probe. In this study, 1950 and 2450 MHz are selected as the frequencies because they correspond to the frequencies used in IMT-2000 and W-LAN systems, respectively. The tissue-equivalent liquid for 1950 MHz is filled in a cubic container (200 mm x 200 mm x 200 mm) and a 1950 MHz half-wave dipole is located at 10 mm below the container. The degree of the probe sensitivity is evaluated using this configuration. In order to verify the frequency discrimination, a 2450 MHz half-wave dipole antenna is arranged at the interval of 10 mm along the antenna axis.

**RESULTS:** The SAR sensitivity of this prototype is approximately 0.015 W/kg at 1950 MHz. The results nearly satisfy the minimum detection limit defined in [3]. Figure 2 shows the measured SAR distributions at 1950 and 2450 MHz, respectively, when both dipole antennas are active. For comparison, distributions measured using the conventional probe, which comprises the small dipole and the diode, are also plotted. It is clear that the EO probe can discriminate between 1950 and 2450 MHz even though both antennas were active. The SAR at 1950 MHz is almost zero in the area of the 2450 MHz dipole and vice versa. On the other hand, the conventional probe detected both frequencies as anticipated.

**CONCLUSION:** SAR measurement was performed employing the small EO probe that does not use any metal. The results show that the EO probe measured the SARs at both frequencies simultaneously.

References.

- [1] B. G. Loader, et al., "An optical electric field probe for Specific Absorption Rate measurements," The 15th International Zurich Symposium, pp. 57 – 60, 2003.
- [2] H. Togo, A. Sasaki, A. Hirata, and T. Nagatsuma, "Characterization of Millimeter Wave Antenna Using Photonic Measurement Techniques," Int J RF and Microwave CAD, vol.14, No.3, pp. 290 – 297, 2004.
- [3] IEEE Std. P1528, 2003.



**DEVELOPMENT OF ELECTROMAGNETIC EXPOSURE SYSTEMS FOR *IN VITRO* EXPERIMENTS IN MOBILE FREQUENCY BANDS.** M.Y. Park, C.O. Ko, J. K. Pack. Dept. of Radio Science & Engineering, Chungnam National Univ, Yuseong-gu, Daejeon, KOREA.

**OBJECTIVE:** In this study, a rectangular-cavity-type exposure system for *in vitro* experiments have been developed for biological studies on the possible effects of mobile phone EMFs (PCS: 1762.5 MHz, Cellular: 848.5 MHz). The exposure systems were designed to allow proper environmental conditions and a computer-controlled exposure level. Key results are presented in this paper.

**METHODS:** The exposure system specifically designed in this study is a rectangular-cavity type. A real CDMA signal is generated and applied to the cavity after amplification as shown in Fig. 1. Exposure level and time schedule can be controlled by a computer. The cavity is fed with a  $f_g/8$  monopole antenna at the  $f_g/4$  position along the center line of the top plate in order to excite only the fundamental TE<sub>102</sub> mode. The external dimension of the cavity for exposure at PCS frequency is 115 mm x 80 mm x 240 mm. The length of the monopole antenna is 22 mm and the diameter is 0.8 mm. The cavity is made of aluminium. The system allows a uniform exposure for one 8.5 cm (inner diameter) petri dish. Particularly, the exposure system is designed to meet the required environmental conditions like ventilation, temperature and humidity. To maintain the CO<sub>2</sub> density and the humidity inside the cavity, gas from an incubator is circulated through the cavity. Also a cooling device for circulating cooling water through the bottom of the cavity is used to prevent the temperature rise of the culture medium. The SAR distribution inside the exposed medium has been characterized by numerical simulations, using the FDTD(Finite Difference Time Domain) method (XFDTD, Remcom Inc.), and it has been verified by measurement. In the measurement, the temperature rise for 60 sec was measured using fluoroptic temperature probes (Luxtron Corp.) at the 9 points in petri dish as shown in Fig. 2. Similar system has also been developed for exposure at Cellular frequency. The external dimension of the cavity is 317 mm x 100 mm x 420 mm and monopole antenna length is 33 mm.

**RESULTS AND DISCUSSIONS:** The results of measurement and simulation are compared in Table.1. The measurement results show an excellent agreement with the simulation data. The exposure system is currently used for *in vitro* experiments.

#### References

- [1] D. M. Pozar, "Microwave Engineering", Wiley, 1998.
- [2] K. YEE, "Numerical Solution of Initial Boundary Value Problems Involving Maxwell's Equation in Isotropic Media", IEEE Transactions on Antennas and Propagation, pp. 302-307, May 1966.
- [3] K. S. Kunz, and R. J. Luebbers, "The Finite Difference Time Domain Method for Electromagnetics", CRC Press, 1993.
- [4] C. K. Chou, H. Bassen and Q. Balzano, "Radio Frequency Electromagnetic Exposure : Tutorial Review on Experimental Dosimetry", Bioelectromagnetics, vol. 17, pp. 195-208, 1996
- [5] T. Toivo, "Water Cooled Waveguide Exposure Chamber For In Vitro Studies at 900 MHz", Proceeding of BEMS Meeting, pp. 124-127, 2000.

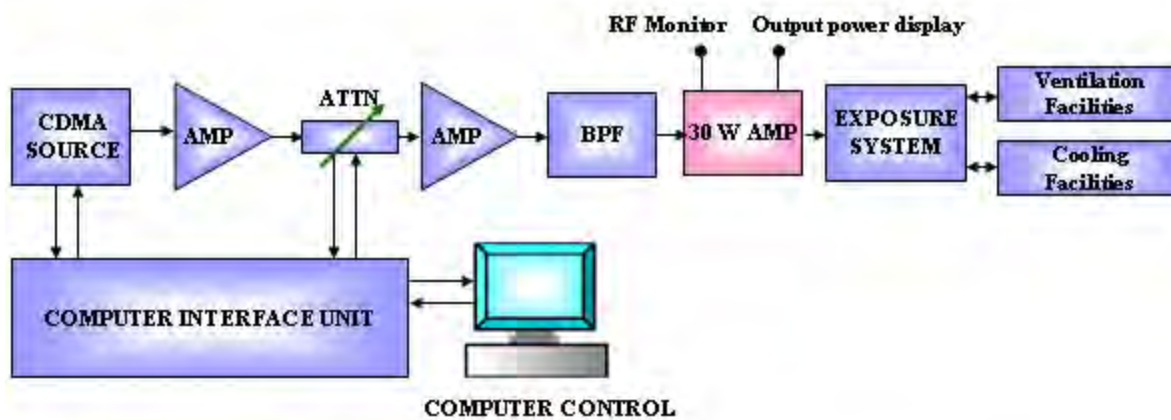


Fig. 1 Block diagram of the exposure system

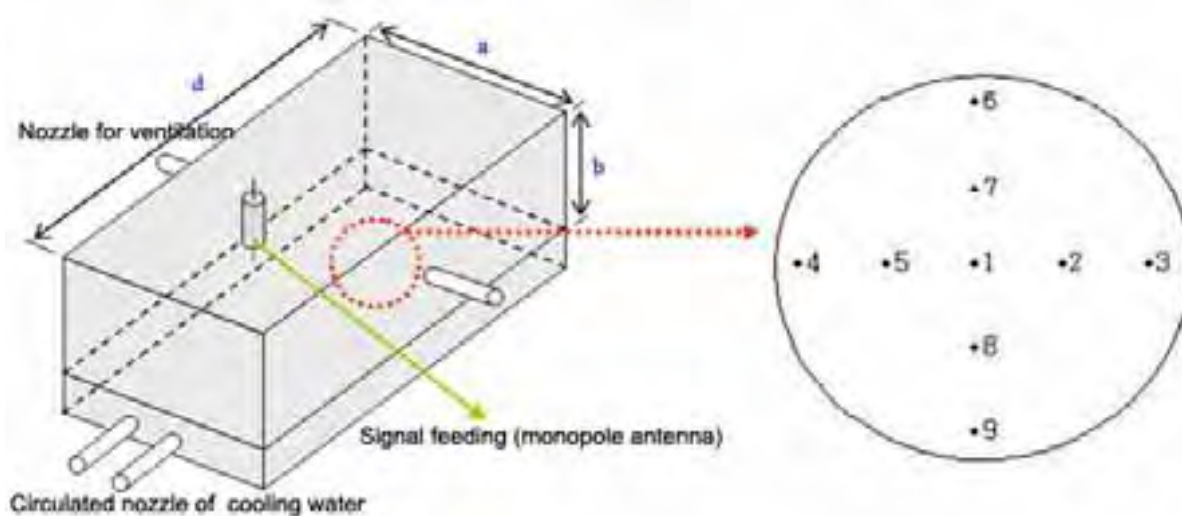


Fig. 2 Cavity structure and measurement points in petri dish

Table. 1 Comparison of the simulated and the measured SAR values at PCS frequency

Position	SAR [W/kg/W]		
	Center (point 1)	Middle (point 2,5,7,8)	Edge (point 3,4,6,9)
Simulation	7.9	10.4	5.2
Measurement	5.1	10.7	5.5
Diff. [M-S] (%)	-35.5	+2.8	+5.7

**MEASURED OUTPUT POWER DISTRIBUTION FOR 3G WCDMA MOBILE PHONES.** T. Persson<sup>1</sup>, L. Hamberg<sup>1</sup>, C. Törnevik<sup>1</sup>, L. E. Larsson<sup>2</sup>. <sup>1</sup>Ericsson Research, Ericsson AB, Stockholm, Sweden, <sup>2</sup>TeliaSonera Mobile Networks AB, Karlstad, Sweden.

**INTRODUCTION:** A third generation (3G) mobile phone using WCDMA (Wideband Code-Division Multiple-Access) technology adjusts the output power rapidly to keep the received power at the base station at approximately the same level as for other connected phones. In addition the power is kept at the lowest level needed for the required quality of service. The location of the user, fading conditions, other simultaneous users and required data rates are some of the factors that determine the required mobile phone output power. In the WCDMA system the peak output power for mobile phones ranges from 250 mW down to below 0.01  $\mu$ W (24 dBm to below -50 dBm) and is adjusted in 1 dB steps 1500 times per second.

**OBJECTIVE:** To analyze the output power distribution and the corresponding average RF exposure for WCDMA mobile phones in various environments.

**METHODS:** It is possible to characterize the output power of a WCDMA mobile phone in use by utilizing a dedicated measuring system called TEMS™ Investigation WCDMA, which is made by Ericsson. This system is a powerful tool that is used extensively for initial tuning and network troubleshooting. The measuring system consists of a mobile phone provided with a special software, which can record a large number of network system parameters including the output power of the mobile phone, for transfer to a connected PC. A SonyEricsson Z1010 TEMS phone with a Telia subscription was used in various environments in Sweden, such as indoor, urban, suburban and rural areas enabling the output power of the phone to be logged. The indoor measurements were performed with the phone held in the hand while walking, and the outdoor measurements were conducted while driving a car with the phone mounted at the dashboard. Further measurements will be performed and if possible network statistics of the output power of a large number of WCDMA mobile phones will also be analyzed to increase the amount of data.

**RESULTS:** When using voice application (up to 12.2 kbit/s) the median output power of the WCDMA mobile phone was recorded to be below -20 dBm (0.01 mW) in indoor and urban areas. The output power was slightly higher in suburban and rural areas but in all environments the output power was less than 0 dBm (1 mW) for more than 90% of the measurement points. The maximum output power was almost never used. For video calls (64 kbit/s) the median output power was about 6 dB higher than for voice calls, and differences in output power were noted also depending on the speech activity due to the DTX (Discontinuous Transmission) function of the WCDMA technology. In figure 1 the output power distribution is shown for a voice call using a WCDMA phone in a rural area.

**CONCLUSIONS:** The average output power of a 3G WCDMA mobile phone is typically substantially below the maximum available output power. In initial measurements for Telia 3G voice calls, the output power was below 1 mW in more than 90% of the measurement points in different environments. Consequently, the typical RF exposure from the use of a 3G WCDMA phone is significantly below the maximum exposure and the relevant SAR limits.

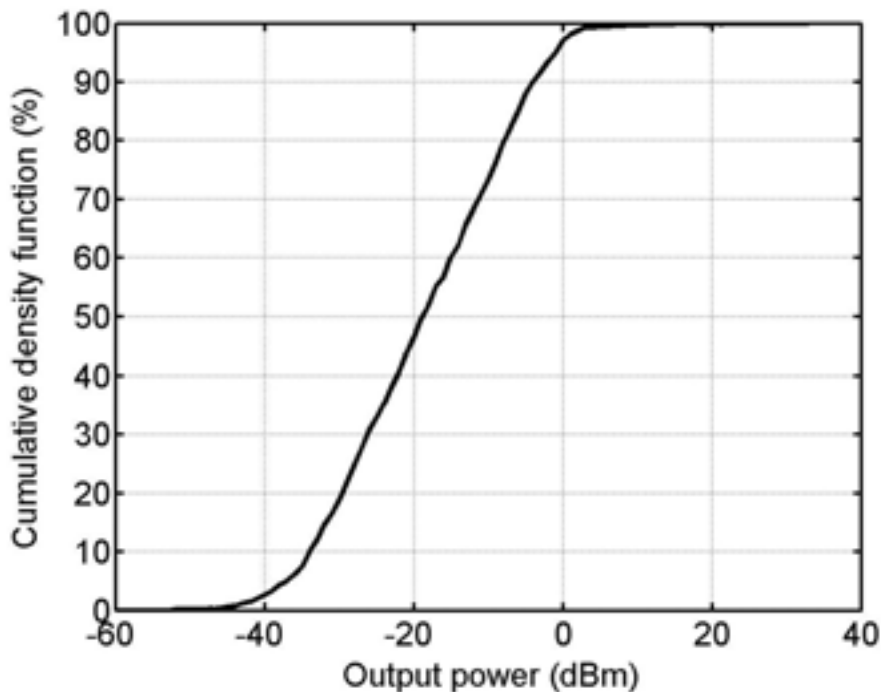


Fig 1. Example of output power distribution for a WCDMA phone during a voice call in a rural area.

P-C-30

**60 CAGES-EXPOSURE SYSTEM FOR LONG-TERM EXPERIMENTS WITH NON-RESTRAINED MICE.** T. Reinhardt<sup>1</sup>, A. Bitz<sup>1</sup>, J. Streckert<sup>1</sup>, V. Hansen<sup>1</sup>, C. Tillmann<sup>2</sup>, T. Dasenbrock<sup>2,3</sup>. <sup>1</sup>Chair of Electromagnetic Theory, Univ of Wuppertal, Germany, <sup>2</sup>Fraunhofer Institute of Toxicology and Experimental Medicine, Germany, <sup>3</sup>Present address: Boehringer-Ingelheim Pharma GmbH & Co. KG, Germany.

The launch of the wideband UMTS in Europe causes an enhancement of the number of base station antennas which reinforces the ongoing public discussion about health risks, even if the field intensities lie below the recommended thresholds.

The present project is designed to investigate a number of biological endpoints during the development of mice that will be exposed to electromagnetic fields around 2 GHz which are modulated by UMTS-typical signals.

The exposure of the mice must be chosen in such a way that thermal effects are avoided in any stage of the experiment. The animals' body temperature as a function of power density was determined in a pilot study.

This biological design implies that mice of different body masses are kept inside the same cage and that the mice are able to move freely within their cages. In order to minimize the variation of the absorption inside the mice to that amount which is introduced by the biological design, the exposure field shall be as uniform as possible. Therefore, 3 stacked radial waveguides of about 1.9 m in diameter, each loaded with 20 cages, are used. Because the prescribed cage dimensions are larger than half the wavelength a tapered transition area connects the flat inner waveguide region with the feeding system in its centre and the outer cage region in order to operate in the fundamental TEM-mode. Due to the free-moving mice

within their cages strong scattering fields would produce strong coupling between adjacent cages. For maintaining the propagation of the fundamental TEM mode adjacent cages are separated by special walls whose surface impedance tends to infinity.

In order to get reliable results of the whole body SAR variation and the value and location of the maximum local SAR respectively, extensive numerical computations were performed under consideration of differently sized animals and for a wide range of their positions and postures within the cages. Detailed models with a resolution of  $1.2\text{mm}^3$  for the mice were used. The actual dosimetric results are compared with the results of previous studies and with animals located in an ideal homogeneous electromagnetic field. Details of the construction of the setup, the optimization process for the high impedance walls, the field distribution in the waveguides, SAR values in the mice, SAR variations and needed RF power will be discussed. The large number of computations enables a reasonable statistical examination. From this data set can be judged which configuration is the most critical with respect to the exposure of an individual mice in order to determine the maximum admissible total input power.

The support of the project by Compagnia di San Paolo in Torino, Italy, is gratefully acknowledged.

P-C-33

#### **A PROCEDURE TO REDUCE THE QUALIFICATION TIME IN SAR COMPLIANCE TESTS.**

A. Schiavoni, M. Francavilla, D. Forigo, M. Deplano. Telecom Italia Lab, Torino, Italia.

**OBJECTIVE:** Last generation cellular phones implement different mode of operation such as GSM, PCS, UMTS, EDGE, GPRS etc and require a test time that could be very long following the compliance procedures described in the international standards [1-2]. The goal of this work is the research of an exclusion criterion that, if verified, avoids the cube scan measurement inside human head like phantom assuring in any case that the SAR limit is not exceeded, even considering the uncertainty associated to the procedure.

**METHOD:** The SAR qualification procedure for the compliance of cellular phones, in each frequency band and for each mode of operation, consists of six single tests to check both the right and left side of the head like phantom (SAM) and to take into account for the bandwidth, as described in the international standards [1-2]. Each test is made up of a surface scan to locate the maximum of the exposure and of a cube scan to get the sufficient number of points to evaluate the SAR averaged over a cubic mass, to be compared with basic limits. The second step takes about 40% of the measurement time per scan. The last models of cellular phones that are now on the market could implement a lot of mode of operation leading to also 70-80 single scans resulting to a too long qualification time. The question then is if it is possible to reduce the qualification time satisfying, in any case, the requirements established by the standards. The basic idea is to avoid performing the cube scan session in each single test if the measured peak SAR value is below a threshold assuring that the averaged SAR value is lower than the basic limit. In order to define the value of the threshold it was analyzed some of the test results performed in the TILAB SAR laboratory in the past few years and the averaged SAR (over 1.0 g and 10.0 g) has been correlated to the measured peak SAR value. It was observed that, as can be noted in figure 1 and figure 2, if the peak measured SAR value is lower than a threshold, and then the limit for the averaged SAR is never exceeded. When that happens the SAR averaged over cubic masses could be directly estimated from the surface scan with different methods, as an example in [3]. We have used a different approach, with respect to [3], based on neural networks to estimate the averaged SAR directly

from the area scan [4]. The use of a neural network approach for the averaged SAR evaluation avoids to estimate the SAR inside the phantom by the knowledge of the electromagnetic characteristics of the brain simulating liquid, reducing the uncertainty of the evaluation and avoiding the approximation in using the field penetration inside a lossy medium due to the evaluation of the fields in the very close proximity region of the source. The learning process of the neural network that was used has been based on previous measurements performed in TILAB SAR laboratory, resulting in evaluating the averaged SAR with an uncertainty lower than 10 % with respect to the measured value. Even if there is another term to be associated to the uncertainty budget, due to the uncertainty of the neural network, if the averaged SAR value is well below the basic limit, it could be accepted as compliance value, accepting also a greater level of uncertainty associated to the measurement process.

**CONCLUSION:** The qualification time for the evaluation of the exposure produced by mobile terminals equipments can be reduced by avoiding performing the cube scan measurement when the peak SAR measured in the areas scan does not exceed a threshold limit. The estimation of the averaged SAR over cubic masses can be performed by using an ad hoc tool starting from the areas scan data. The uncertainty of the estimation tool can be considered in the uncertainty budget of the compliance tests, but even if the uncertainty associated to the SAR value could be higher with respect to the one defined on the standards for complete compliance tests, the peak measured SAR lower than the threshold limit assures the averaged SAR never exceeds the basic limits of international standards. The proposed approach could be a base for discussion in standardization bodies.

**ACKNOWLEDGEMENT:** This work has been fully supported by TIM, Telecom Italia Mobile

#### **REFERENCES:**

- [1] IEC 106/84/DIS, "Human exposure to radio frequency fields from hand-held and body-mounted wireless communication devices – Human models, instrumentation, and procedures – Part 1: Procedure to determine the Specific Absorption Rate (SAR) for hand-held devices used in close proximity of the ear (frequency range of 300 MHz to 3 GHz)"
- [2] IEEE std P1528 "DRAFT Recommended Practice for Determining the Peak Spatial-Average Specific Absorption Rate (SAR) in the Human Body Due to Wireless Communications Devices: Experimental Techniques
- [3] M.Y. Kanda, M.G. Douglas, E. D. Mendivil, M. Ballen, A. V. Gassner, C. K. Chou, "Faster determination of mass-averaged SAR from 2-D area scans", IEEE Transactions on Microwave Theory and Techniques, vol. 52, no. 8, August 2004.
- [4] M. Francavilla, A. Schiavoni, "Averaged SAR computation: a neural network approach", to be presented in EMC Zurich 2005, February 2005.

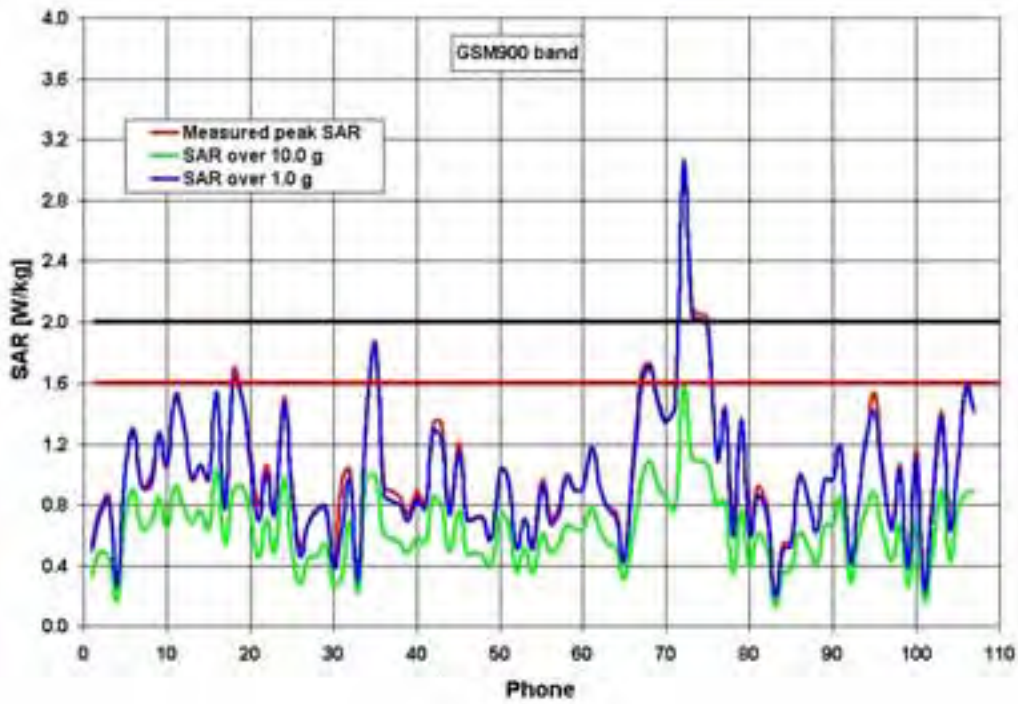


Figure 1: Correlation between peak measured SAR and averaged SAR at GSM900 band.

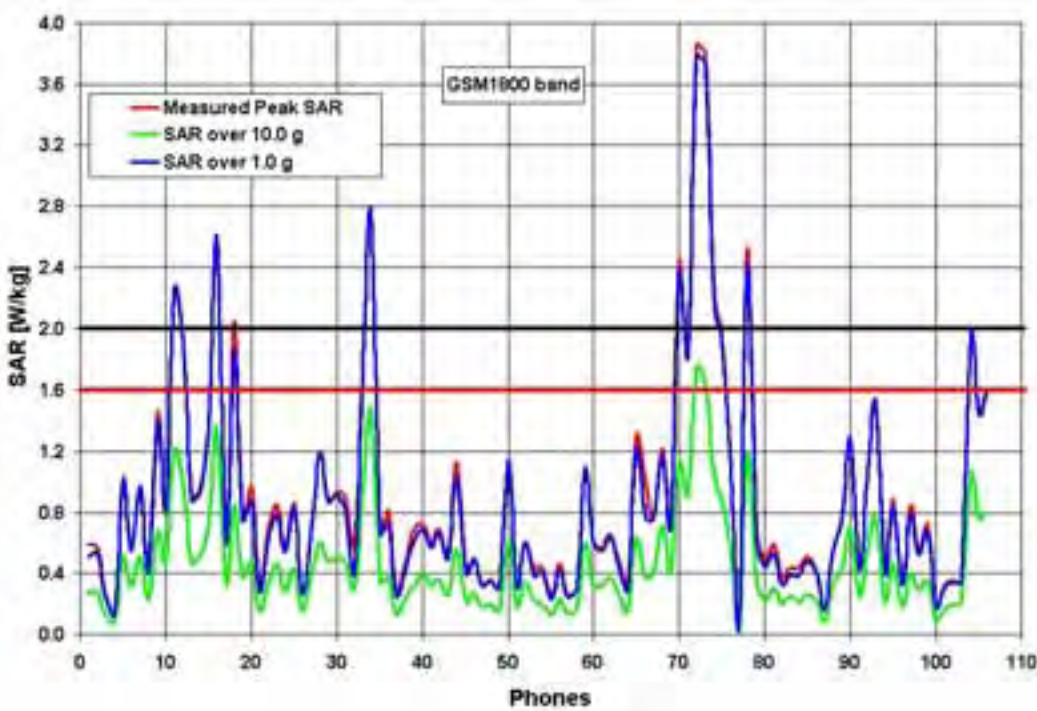


Figure 2: Correlation between peak measured SAR and averaged SAR at GSM1800 band.

**EXPOSURE ASSESSMENT IN THE ELECTROMAGNETIC FIELDS OF INDOOR-USED MODERN WIRELESS COMMUNICATION DEVICES.** G. Schmid, D. Lager, P. Preiner. ARC Seibersdorf research GmbH, Seibersdorf, Austria.

**INTRODUCTION:** In recent years several wireless communication technologies (e.g. WLAN, Bluetooth, ) and their applications in home as well as in office environments became very popular and widespread. Although the maximum transmit power of these devices is limited to a few hundred milliwatts or lower (depending on the technology, the used frequency band and local regulations), there is public concern about the personal RF exposure in the environment of the mentioned devices.

**OBJECTIVE:** The aim of this study was to assess typical magnitudes of public exposure from these technologies in household and office environments.

**MATERIALS AND METHODS:** Based on the technical specifications of the technologies under scope (e.g., WLAN IEEE 802.11a,b,g,h, Bluetooth and DECT) different measurement procedures were evaluated and the corresponding uncertainties with respect to the assessment of the time averaged exposure (as required by the current safety standards) were derived. Furthermore the capabilities of the simulation software Wireless Insite (Remcom, Inc., USA) [1], when used for exposure assessment in the considered indoor environments was evaluated.

**RESULTS:** Due to the partially complex modulation-, duplex-, access- and frequency allocation schemes used in the considered technologies, accurate measurements of the corresponding RF emissions require sophisticated (and expensive) measurement equipment (e.g., spectrum analyzers providing rms-detectors, channel power and averaging functionality) and detailed knowledge about the characteristics of the RF signal to be measured. Without these capabilities it is only possible to assess instantaneous peak emissions, which are often reported as 'worst case' emissions (e.g., in 'maxhold' mode of the spectrum analyzer). However, taking into account real scenarios with respect to data traffic, the implemented media-access-schemes and 6 minutes time averaging of exposure (as required by the current safety standards), it could be shown that such 'worst case'-exposure numbers might overestimate the actual exposure by up to several orders of magnitude.

Numerical exposure assessment using a ray-tracing software tool [1] was found to be principally feasible, provided a sufficiently detailed modeling of the considered scenario (especially regarding the properties of the radiation sources) and appropriate scaling of the simulation results. The mentioned scaling of the numerical results (which correspond to continuous wave emissions) is needed, because as a ray tracing tool the software is not able to take into account the implemented time division access- and duplex schemes. Although, the numerical results can selectively deviate considerably from corresponding measurements (even in case of appropriate source modeling), the remaining deviations become much less and acceptable when spatially averaged field strengths are considered (as required by most of the current safety standards). Finally, in order to provide estimations of 'worst case' as well as time averaged exposure for different scenarios, a numerical exposure model was implemented using the programming environment. Based on results from 'worst case' measurements or from ray tracing simulations, this model allows the prediction of instantaneous as well as time averaged exposure using the features of the access- and duplex schemes of the considered technologies and definable statistical models for the data traffic in the networks.

**CONCLUSIONS:** The results of this study showed that accurate (i.e., not only 'worst case') assessment of actual exposure from the considered wireless technologies as WLAN, Bluetooth and requires sophisticated measurement equipment, detailed knowledge of the signal characteristics and well educated personal. Performing only 'worst case' exposure assessment in the electromagnetic fields of the considered devices might lead to substantial overestimation of the actual exposure. In view of aspects as risk communication and risk perception we recommend to not only publish such 'worst case' numbers,

but also providing figures about the actual time averaged exposure which can be expected and which is mainly depending on the data traffic in the network.

ACKNOWLEDGEMENTS: This project was funded by the Federal Office for Radiation Protection (BfS), Germany.

REFERENCES:

[1] <http://www.remcom.com/WirelessInSite/>

P-C-39

**INTERNAL ANTENNA MOUNTED ON FOLDER-TYPE MOBILE PHONE WITH LOW SAR.**  
C.-S. Shin<sup>1</sup>, N. Kim<sup>1</sup>, J.-I. Choi<sup>2</sup>, J.-D. Park<sup>2</sup>. <sup>1</sup>Engineering of Information and Communication, Chungbuk National Univ, <sup>2</sup>Electronics and Telecommunications Research Institute.

OBJECTIVE: The increasing use of mobile phone has caused public concern about possible radiation hazard. In this research, folder-type mobile phone with the has internal planar antenna (shown Fig. 1(a)) was designed to reduce the SAR on the human head. In addition, 1g peak average SAR is calculated.

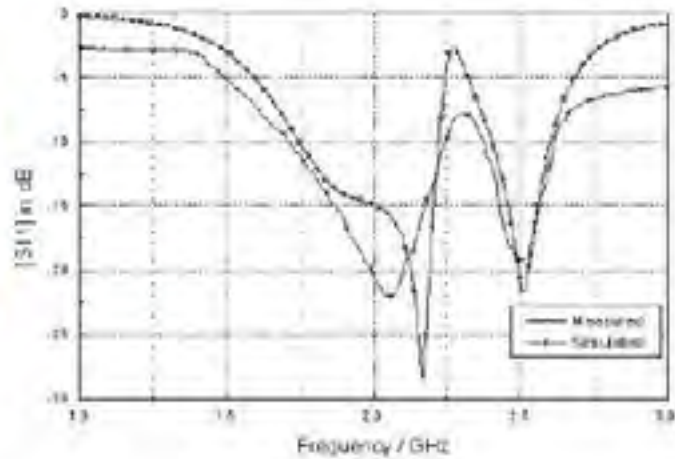
METHODS: In order to design the antenna and the mobile phone, SAMCAD (SPEAG Co., based upon FDTD) was used. The resonance frequency was tuned for PCSs, IMT-2000, and WLAN. Internal planar antenna was adopted in order to improve the narrow band and to minimize the size. The dimensions of the antenna are 23.5 mm  $\times$  60 mm. In this simulation, the bandwidth, the resonant frequencies, and the radiation patterns were calculated. 1g peak averaged SAR values were also calculated and compared with those of conventional folder-type mobile phone. In addition, 1g peak averaged SAR values were compared with variation of antenna mounted position.

RESULTS: The simulated and measured return losses of an antenna are as follows. The measured bandwidths are 1.75~2.25 GHz and 2.3~2.6 GHz (as shown in Fig.1(b)). And internal planar antenna and external monopole antenna attached on the handset are tested. As a result, internal planar antenna's 1 g peak average SAR is 0.686 [W/kg]. And external monopole antenna's result is 1.33 [W/kg] (as shown in Fig.2). So internal planar antenna has a about 50 % SAR reduction in comparison with external monopole antenna (as shown in Fig.2). Also, internal planar antenna is compared mounted on up-case of phone with mounted on down-case of phone. Mounted on up-case phone's 1 g peak average SAR is 1.125 [W/kg]. Another case is 0.656 [W/kg].

DISCUSSION: In this study, we have applied the internal planar antenna to folder-type mobile phone. Comparing monopole antenna, the performances of the planar antenna mounted on down-case of phone show the possibility of application to mobile phone to reduce SAR.



(a) Structure of proposed antenna

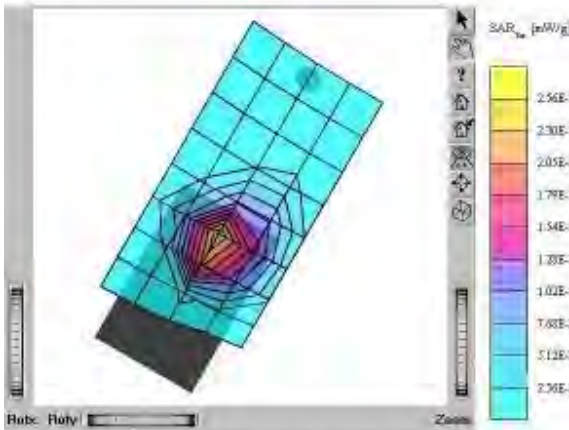


(b) Return loss

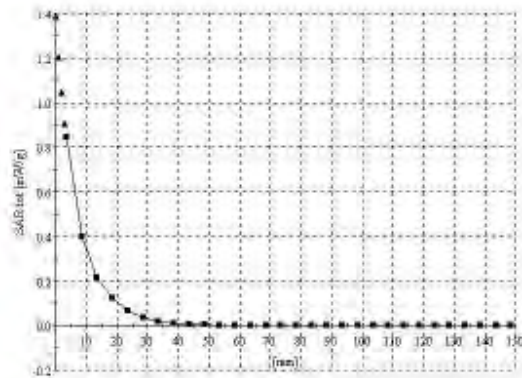
Fig. 1. The structure and return loss of internal planar antenna

SAM II Phantom: Left Hand [ICRP] Section: Position: (30,180) Frequency: 1900 MHz  
 Probe: ET30V6 - SN1609 Conv(15.34,5.34,5.34) Crest factor: 1.0 Brain 1900 MHz  $\epsilon = 1.39$   
 $\rho_{\text{brain}} = 40.3 \text{ g/cm}^3$   
 Cube Size: SAR (1g): 0.686 mW/g, SAR (10g): 0.356 mW/g  
 Course: Dx = 15.0, Dy = 15.0, Dz = 10.0  
 PowerIntr: -0.08 dB  
 Comment:

SAM II Phantom: Section: Position: Frequency: 1900 MHz  
 Probe: ET30V6 - SN1609 Conv(15.34,5.34,5.34) Crest factor: 1.0 Brain 1900 MHz  $\epsilon = 1.39$   
 $\rho_{\text{brain}} = 40.3 \text{ g/cm}^3$   
 Z-Axis: Dx = 0.0, Dy = 0.0, Dz = 5.0  
 Comment:



(a) SAR distribution profile



(b) SAR value variation due to the depth of human head

Fig. 2. Test results of the mounted internal planar antenna on mobile

P-C-42

**RF EXPOSURE FROM BODY-WORN MOBILE PHONES: COMPARISON OF SAR LEVELS IN HUMAN BODY MODEL AND IN FLAT PHANTOM.** M. Siegbahn, C. Törnevik. Ericsson Research, Ericsson AB, Stockholm, Sweden.

**INTRODUCTION:** The International Electrotechnical Commission (IEC) has established a project team (PT62209 of TC106) that is developing a standard for SAR testing of wireless devices used both at the ear (part I), and at other places of the body, for instance at the waist (part II). Part I is expected to be published as an International Standard during 2005 while work on part II is still ongoing. It has been suggested that a flat phantom filled with the same tissue simulating liquid as specified for head SAR

measurements should be used for body SAR measurements. Additional research is however needed to verify that this phantom will give SAR results that corresponds to SAR levels in a real human body or if correction factors might be needed for adjusting the flat phantom SAR values.

**OBJECTIVE:** To investigate the feasibility of using a flat phantom filled with head tissue simulating liquid for assessing SAR for body positions of wireless terminals.

**METHODS:** Calculations of SAR were conducted with the FDTD software SEMCAD 1.8 from SPEAG on CAD-based models of two Sony Ericsson mobile telephones positioned close to both a male body model based on data from the Visual Human Project® and a flat phantom model. The phone models were computed for 5, 10, 25 and 50 mm distance to the body model/flat phantom with the phone backside, incorporating the antenna, facing the tissue material. The phone models were positioned in front of the waist of the body model as shown in Figure 1(a). All calculations were carried out for a carrier frequency of 1880 MHz, corresponding to the center channel of the GSM1900 band. The minimum and maximum FDTD grid resolutions were 0.2 and 0.5 mm respectively for the CAD-based phone models and 0.4 and 1 mm for the human body model and the flat phantom. The dielectric parameters of the tissue of the human body model were those given by [1] and the parameters of the flat phantom were those specified in international standards for head tissue simulating liquid at 1900 MHz, i.e.  $\epsilon_r=40$ ,  $\sigma=1.40$  S/m [2-4]. The dimension of the flat phantom along the length of the phone was 280 mm and the width 200 mm. The depth of the phantom was 150 mm with a 2 mm plastic shell facing the phone.

**RESULTS:** The FDTD computed SAR results were normalized to an equivalent output power that takes into account the change in antenna impedance when the phone is placed close to the lossy material as compared to when it is in free-space. The 1g and 10g average SAR in the flat phantom was for all investigated distances higher than the SAR in the human body model. The overestimation by the flat phantom was found to be in the range 5% to 50%.

**CONCLUSIONS:** At 1900 MHz, a flat phantom with head tissue simulating liquid overestimates the 1g and 10g average SAR for body-worn usage of a mobile telephone. The results indicate that it is feasible to use a flat phantom for SAR testing of body-worn wireless devices and that no correction factor is needed.[1] S. Gabriel, R.W. Lau and C. Gabriel, “;The dielectric properties of biological tissues: III parametric models for the dielectric spectrum of tissues”;, *Physics in Medicine and Biology*, vol. 41, pp. 2271-2293, 1996.

[2] IEC 62209 Part I FDIS, 2004

[3] IEEE Standard 1528, June 2003.

[4] CENELEC European Standard EN 50361, July 2001.



(a)



(b)

Figure 1: (a) The Visual Human body model with one of the computed Sony Ericsson telephone models. (b) The other telephone model close to the flat phantom.

P-C-45

**NUMERICAL DOSIMETRY OF INDUCED CURRENT DENSITIES WITH JAPANESE ADULT MALE AND FEMALE MODELS IN THE PROXIMATELY OF INDUCTION HEAT HOB.** Y. Suzuki<sup>1</sup>, K. Wake<sup>2</sup>, M. Taki<sup>1</sup>, S. Watanabe<sup>2</sup>. <sup>1</sup>Tokyo Metropolitan Univ, Japan, <sup>2</sup>National Institute of Information and Communications Technology, Tokyo, Japan.

**INTRODUCTION:** Induced heat (IH) hobs, which use 20 kHz magnetic fields for heating frequency, increase in its number for general use because of their convenience for cooking. IH hobs are used in the proximately of a human body and the time varying magnetic field around IH hob induces electric current in the human body. Since basic restrictions are provided on electric current density to prevent effects on nervous system functions [1], it warrants estimating induced current in the human body to compare basic restrictions.

**OBJECTIVE:** The objective of this study is to examine numerical dosimetry for induced current densities within the human body caused by magnetic field in the proximately of IH hobs with the impedance method (IM)[2], and to compare results of induced current density calculation with the current density values given in basic restrictions.

**METHODS:** We have attempted to calculate induced current density distribution with IM. Distribution of magnetic flux density was measured by the magnetic field probe in the vicinity of IH hob to prepare for IM. Two voxel models[3] of whole human-bodies based on the average Japanese adult male and female data are used to construct realistic cooking condition. These detailed human models have 2 mm resolutions, and are composed of over 50 tissues and organs. In this case, electric conductivities at 20 kHz are provided for each tissue by use of parameter model[4]. The calculation condition is as follows. The top of the IH cooker is located at 800 mm position from the floor, and the front edge of IH cooker is placed 50 mm away from the nearest surface of the human model. That is the nearest position where human can approach to an IH hob.

**RESULTS:** The detailed distribution of induced current density is shown in Fig.1. These figures indicate that hot spots of induced current density are observed at a few cm inside from the surface of two models because of inhomogeneous conductivity. The maximum values of current density for trunk are 21 mA/m<sup>2</sup> in the male model and 11 mA/m<sup>2</sup> in the female model, respectively. The basic restriction of induced current for general public exposure given by ICNIRP is 40 mA/m<sup>2</sup> at 20 kHz, and induced current values are smaller than the basic restriction in this case.

**CONCLUSIONS:** Magnetic flux density distribution in the proximately of an IH hob is measured by the magnetic probe. Numerical dosimetry on induced current density is performed by the impedance method with measurement data. Two voxel models of the average Japanese adult male and female are applied to these analyses. It is found that hot spots of induced current density are observed at a few cm inside from human skin. In this case study, induced current densities estimated by numerical method do not exceed basic restrictions for general public exposure given by ICNIRP.

Figure 1. Results of induced current analysis for the male (left figure) and the female (right figure)

model.

References:

- [1] International Commission on Non-Ionizing Radiation Protection, "Guidelines for Limiting Exposure to Time Varying Electric, Magnetic, and Electromagnetic Fields (up to 300GHz)", Health Phys., 74, pp. 494-522, (1998).
- [2] N. Orcutt and O. P. Gandhi, "A 3-D Impedance Method to Calculate Power Deposition in Biological Bodies Subjected to Time Varying Magnetic Field", IEEE Trans. Biomed. Eng., Vol.35, pp.577-583, 1988.
- [3] T. Nagaoka, S. Watanabe, K. Sakurai, E. Kunieda, S. Watanabe, M. Taki and Y. Yamanaka, "Development of realistic high-resolution whole body voxel models of Japanese adult and females of average height and weight, and application of models to radio-frequency electromagnetic-field dosimetry", Phys. Med. Biol., 49, pp. 1-15 (2004).
- [4] S. Gabriel, R. W. Lau and C. Gabriel, "The dielectric properties of biological tissues: III. Parametric models for the dielectric spectrum of tissues", Phys, Med, Biol., pp.41, 2271-2293, (1996).

P-C-48 STUDENT

**SETUP FOR THE CONTROLLED PLANE WAVE EXPOSURE AT GSM AND UMTS BANDS FOR *IN VIVO* EXPERIMENTS USING A PARABOLIC REFLECTOR.** S. Tejero<sup>1</sup>, S. Schelkshorn<sup>1</sup>, J. Detlefsen<sup>1</sup>, S. Okorn<sup>2</sup>, M. Bornhausen<sup>2</sup>, O.Petrovicz<sup>3</sup>. <sup>1</sup>Institute for Highfrequency Engineering, Dept of Electrical Engineering and Information Technology, Technische Universität München, Germany, <sup>2</sup>Institute of Animal Physiology, Faculty of Veterinary Medicine, Ludwig-Maximilians-Universität München, Germany, <sup>3</sup>EMF Research Coordinator, Technische Universität München, Germany.

As in any other biological investigation, controlled, well defined, standard and repeatable conditions are of capital importance in RF exposure experiments. These conditions are fulfilled by the exposure system presented here, which is based on a mass-production parabolic reflector. Although the setup is designed for GSM and UMTS bands, the concept can be applied to any other frequencies as well.

The setup is intended for a long-term, continuous and controlled exposure of living rats. Three chambers are built: for GSM-, UMTS- and sham-exposure, with high isolation between them. A minimum of 100 rats per setup should be exposed simultaneously to provide sufficient statistic support for different experiments. Other requirements are imposed by the *in vivo* characteristic of the exposure: the chamber must be air-conditioned and the access to the cages must be assured for the daily animal care. The animals will be exposed by a linear polarized plane wave. Of course, the local variations of the exposure dose must be kept as small as possible.

To achieve the plane wave condition in a radiated field a long distance from the antenna to the observation point is usually required. That allows to approximately consider the spherical wavefront radiated from the source as a plane or quasi plane wave, i.e. a wave with small deviations from the pure plane wave. This approach requires an extended exposure facility, which is also very energy inefficient, as the signal power density decreases with the square of the distance. Other energy efficient approaches found in the literature are not suitable for long-term continuous exposure (e.g. Schönborn et al., 2004) or are based on the propagation of guided transversal electromagnetic waves and may run into problems when frequency increases (e.g. Hansen et al., 1999; Balzano et al., 2000).

The setup presented here is in analogy to the "compact range" concept, which is used in antenna measurement facilities to obtain a plane wave at relative short ranges. The idea behind is to use a parabolic reflector to convert a spherical wavefront emanating from the focus into a plane wave. The less strict error requirements for exposition in comparison to antenna measurements, allows us to use a common reflector instead of a high-precision one. The selected reflector has a diameter of 320cm and a focal distance of 112cm and is a mass-product, which reduces its cost drastically. Assuming a prime focus paraboloid illuminated from the focal point by an ideal source, i.e. a point source radiating only towards the reflector and illuminating it uniformly, the reflected wave would be plane and with a rather constant electric field at the focal plane. The main problems of this focussed approach are those created by the non-ideal feed. The near fields of the primary source are not negligible at the focal plane and to achieve a uniform illumination of the reflector's surface is rather difficult. In our approach, these problems are overcome by moving the exposure zone away from the focal plane and by axially defocussing the feed. If the exposure zone is moved away from the primary feed, the influence of its backradiated/near field becomes negligible as it decreases with the square of the distance. By axially defocussing the feed, moving it towards the reflector, the reflected wave will not be plane but will show spherical phasefronts with a large curvature. This resulting wave can be considered as quasi plane in the zone of interest. In addition, the solid angle which must be uniformly illuminated by the feed decreases by this approach, resulting in a simplification of its design. This benefits also the minimization of the diffraction effects caused by the reflector rims, which are illuminated with low intensity.

Figure 1 shows the final exposure setup which is placed in a metallicly shielded chamber. The drawing shows the paraboloid, the defocussed feed, the cages for the animals and the absorber material on the walls, placed to avoid uncontrolled reflection of the waves propagating in the chamber. The animals are inside polysulfan cages with size (HxWxL) 24x28.5x42.5cm<sup>3</sup>. The cages are placed on wood slats with the cage frontal looking towards the reflector and with an horizontal spacing of 30cm. The distance between the slats is 34cm.

Simulation results for the field distribution (without cages and animals) show that a total of 40 cages can be homogeneously exposed. The maximum phase error is  $\pm 12^\circ$  in the volume of a cage and the standard deviation of the absolute value is approximately 11%. The power efficiency is approximately 34%.

The advantages of this setup suitable for a large number of animals are its good power efficiency and its relatively small size and low cost.

Measurements results for the field in the finished setup are expected to confirm the chamber design, fulfilling the requirements recommended in the literature (Kuster and Schönborn, 2000), and will be presented.

## References

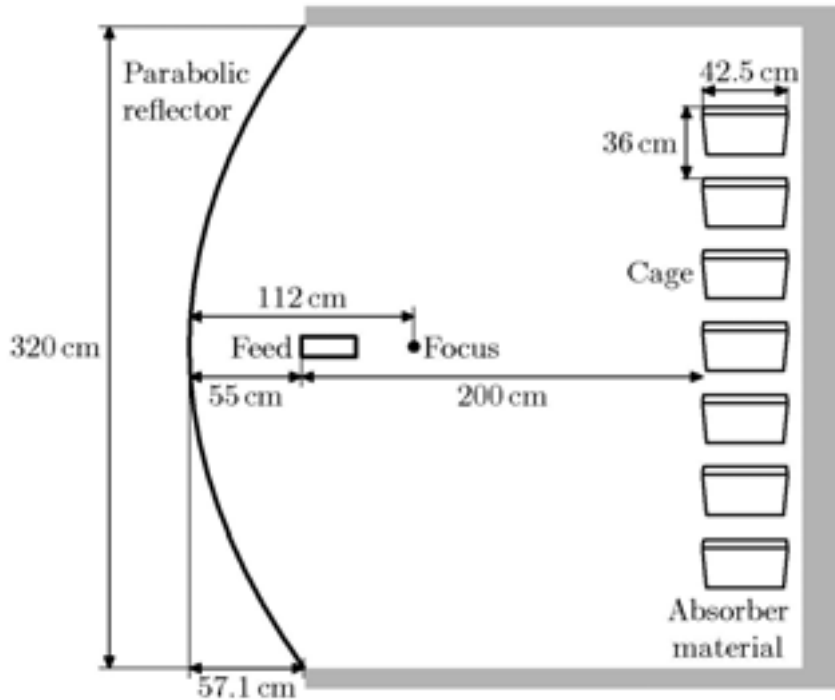
Balzano, Q., Chou, C.-K., Cicchetti, R., Faraone, A., and Tay, R.Y.-S.: An Efficient RF Exposure System with Precise Whole-Body Average SAR Determination for in vivo Animal Studies at 900MHz, *IEEE Transactions on Microwave Theory and Techniques*, 48, 2040-2049, 2000.

Hansen, V. W., Bitz, A. K., and Streckert, J. R.: RF Exposure of Biological Systems in Radial Waveguides, *IEEE Transactions on Electromagnetic Compatibility*, 41, 487-493, 1999.

Kuster, N. and Schönborn, F.: Recommended Minimal Requirements and Development Guidelines for

Exposure Setups of Bio-Experiments Addressing the Health Risk Concern of Wireless Communications, *Bioelectromagnetics*, 21, 508-514, 2000.

Schönborn, F., Pokovic, K., and Kuster, N.: Dosimetric Analysis of the Carousel Setup for the Exposure of Rats at 1.62GHz, *Bioelectromagnetics*, 25, 16-26, 2004.



P-C-51

**A FILTERING-BASED FDTD SUBGRIDDING ALGORITHM FOR RADIOPROTECTION PURPOSES.** A. Vaccari<sup>1</sup>, L. Cristoforetti<sup>1</sup>, C. Malacarne<sup>1</sup>, L. Sandrini<sup>1</sup>, E. Bort<sup>2</sup>, R. Pontalti<sup>1</sup>. <sup>1</sup>Istituto Trentino di Cultura – Centro per la Ricerca Scientifica e Tecnologica, Trento, Italy, <sup>2</sup>Inter-university Consortium for Bioelectromagnetic Interactions (ICeMB), Genova, ITALY.

Objective: The FDTD (Finite Difference Time Domain) method, apart from its physical interest and its potential extension to electrodynamics, has become a milestone in the assessment of the human exposure to em fields. Compared with other approaches to the same problem, the FDTD method is attractive for its low cost in terms of computational burden, regarding both machine memory allocation and computational times. However, in some cases, particularly with media having high dielectric contrast, mesh refinement is desirable: higher spatial resolutions, i.e. increased mesh densities, are introduced only in subregions where they are really needed, thus achieving, outside those subregions, computer resource savings of the order of  $n^3$  where  $n$  is the refinement factor. Nevertheless, the introduction of high density meshes in the FDTD method is recognized as a source of inaccuracies and, even more important, of instabilities. In this work we propose a nonrecursive three-dimensional (3-D) algorithm that allows straight embedding of fine meshes into coarse ones which have larger space steps, in each direction, by a factor of 5 or more, while maintaining a satisfactory stability and accuracy. A typical application to a radioprotection study where both the source and the exposed subject are embedded each in its own subgrid, is here presented.

Method: When grids with different space-time resolutions interact, fulfilling the CFL (Courant Friedrich Levy) condition inside each single grid is not enough for the overall stability of the FDTD algorithm. In such a case one has to deal, from a numerical point of view, with extra BCs at the grids interface which must obey, more or less implicitly, to further stability criteria. Since grids have different dispersion properties, negative slope parts of the dispersion relationship of the coarse grid may correspond to positive slopes on the refined grid. We recognized it as the source of subgridding instability [1], because positive slope means forward waves, while negative slope means backward waves, i.e., the two grids have conflicting behaviours. Frequencies which correspond to the maxima of the coarse grid dispersion curve constitute a set of critical values at which total reflection occurs. This happens because the group velocity of the coarse medium vanishes there, but not that of the refined one. Even worse, there are frequencies beyond those critical values at which the reflection coefficient becomes infinity for wave packets, suggesting the onset of reflected waves even without stimulus.

The previous discussion suggests that if we were able to impose a low-pass filtering action at the grids coupling level, such as to confine signals bandwidth well below the critical frequencies, the unstable behavior of the subgridding algorithm could be mitigated.

In designing the low-pass filter time derivatives must be avoided, because they require values ahead in time, which have not been calculated yet at the current FDTD time step. So a formulation involving space derivatives only is proposed:

$$\mathcal{U}_{\mathcal{F}}(x, y, z, t) = \mathcal{U}(x, y, z, t) + \sum_{n=1}^{\infty} (-1)^n \mathcal{F}_{2n} (c_0^2 \vec{\nabla}^2)^n \mathcal{U}(x, y, z, t)$$

where  $\mathcal{U}_{\mathcal{F}}$  is the low-pass filtered component obtained by the corresponding unfiltered value  $\mathcal{U}$ , by a  $n$ -fold repeated application of the Laplacian operator to  $\mathcal{U}$ , and by  $\mathcal{F}_{2n}$  which are the Taylor coefficient of the filter response  $\mathcal{F}(x)$ , taken to be a non-negative real valued even function of  $x$ , in order to have a filter without phase shift [1]. All the involved spatial partial derivatives are of even order, the maximum order depending on the number of terms retained in the summation. They are numerically implemented by second-order accurate centered difference expressions. Due to their stencil, a mesh refinement factor of  $2n+1$  permits to retain terms up to  $\mathcal{F}_{2n}$  included only: higher order terms, if desired, require higher mesh refinement factors.

## Results

To assess the stability and accuracy of the proposed subgridding algorithm, a group of tests has been performed. They concern with the comparison, in the case of a plane TEM wave impinging a dielectric sphere, between the numerical FDTD solution and the analytical one. The refinement factors we used are 5 to 15. To analyze the grids behavior during the FDTD runs, we introduce two quantities. The first, denoted by  $S$ , characterizes what one would qualitatively call the "mean electric field" in the discrete computational domain at a given FDTD time iteration. Due to the transitory character of the excitation,  $S$  rises to a maximum value after the start of a run, then it should decrease and reach a stationary value which represents the residual numerical noise on the grid.

However, if instability occurs,  $S$  starts to grow uncontrollably until a numerical overflow condition is reached. The second quantity we introduce, denoted by  $A$ , monitors the accuracy during the FDTD runs being defined as the average of the difference between the FDTD and the analytical values, both in the frequency domain and normalized to the incident field.  $A$  measures the mean normalized error on the grid.

Results show that, without the filter,  $S$  starts to exponentially increase already before 1000 FDTD time iterations of the coarse grid are completed. Instead, by using a simple second-order filter there is a net gain of more than 3 in the overall duration of the FDTD run, with  $S$  remaining flat on its residual value.

On the other hand, having so stabilized the algorithm,  $A$  tends to become lower and lower as refinement factor increases.

Having verified the feasibility of the method for a spherical canonical target, a study of practical interest such as that of a subject exposed in the near field of a base-transceiver antenna, was conducted. Two refined domains were used both embedded into a coarser one. The first allows an accurate description of the antenna electrical structure while the second one, containing the body model, permits to fulfill the FDTD accuracy constraints for high permittivity media.

Results show the suitability of this new subgridding algorithm for dosimetric problems.

#### References

[1] A. Vaccari, R. Pontalti, C. Malacarne, L. Cristoforetti, A Robust and Efficient Subgridding Algorithm for the Finite-Difference Time-Domain Simulation of Maxwell's Equations, Journal of Computational Physics, Vol. 194/1, 117-139, 2004.

P-C-54 STUDENT
----------------

**ASSESSMENT OF THE SAR FOR A WALKIE-TALKIE SETUP.** G. Vermeeren, L. Martens. Dept of Information Technology, Ghent Univ.

**INTRODUCTION:** The successful reintroduction of the walkie-talkie demands an evaluation of the SAR in front of the face. The digital walkie-talkie standard is known as PMR446. PMR446 stands for Private Mobile Radio operating at a frequency of 446 MHz and radiating at maximum 500 mW ERP.

**OBJECTIVE:** Assessment of the local averaged SAR in 1 g and 10 g of human body tissue produced by a generic walkie-talkie. The SAR in three homogenous and one heterogeneous phantom will be examined for a typical operating position of the walkie-talkie.

**METHOD:** A simulation model has been developed for the walkie-talkie: a helical antenna mounted on a ground plane. The model has been simulated in free space using SEMCAD as well as FEKO. Free-space measurements in an anechoic chamber have been carried out to validate the free-space model. The validated model has been placed in the proximity of several human body phantoms. *Table 1* tabulates the investigated setups. Where possible, the simulation setups have been verified with measurements. The influence of the distance  $d$  between phantom and device has been examined. The flat phantom setup has the advantage of an easy positioning of a portable device in front of it and, thus, an easy to reproduce SAR measurement. Therefore, it is interesting to investigate how the flat phantom setup behaves in comparison with the more realistic setups.

**RESULTS:** *Figure 1* shows the simulation results of the walkie-talkie in front of three different phantoms. We see that the 10 g averaged SAR: (1) decreases with distance  $d$  between phantom and device, (2) achieves its highest value in the flat phantom setup, (3) is conservative in the homogenous phantoms compared with the heterogeneous Visible Human. The SAR distribution in a vertical cut of the homogenous and heterogeneous Visible Human phantom is drawn in *Figure 2*. The measurement results for this walkie-talkie case will be reported at the conference.

**CONCLUSION:** A popular portable device, i.e. a generic walkie-talkie, has been examined in terms of the local averaged SAR it originates in a human body. The model of the device as well as the setups to assess the SAR have been validated with measurements. The homogeneous phantoms showed a conservative local averaged SAR compared with the heterogeneous Visible Human.

**ACKNOWLEDGMENT:** This research within the framework of the European Eureka project SARSYS-BWP is supported by the *Belgian Federal Science Policy Office*.

**REFERENCES:**

- [1] CENELEC EN50361, "Basic Standard for the measurement of Specific Absorption Rate related to human exposure to electromagnetic fields from mobile phones (300 MHz –; 3 GHz)", 2001.
- [2] IEC TC106/61/CDV,"Procedure to measure the Specific Absorption Rate (SAR) in the frequency range of 300 MHz to 3 GHz –; Part 1: hand-held mobile wireless communication devices, 2004.

Device	Simulation setup
Walkie-talkie	Free space
	Flat phantom
	SAM head phantom
	Homogenous Visible Human
	Heterogeneous Visible Human

Table 1: Overview of the examined setups for SAR assessment.

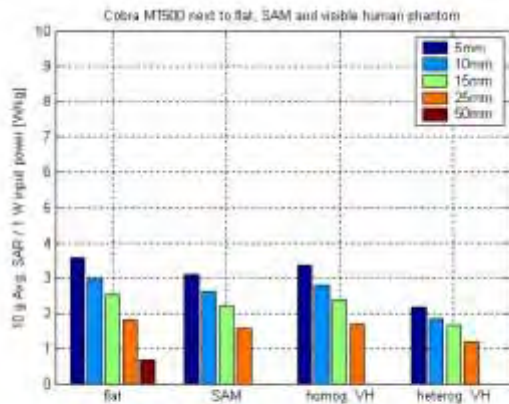


Figure 1: Assessment of the 10 g Averaged SAR caused by a walkie-talkie radiating in the proximity of a flat, the SAM head and the Visible human head phantom.

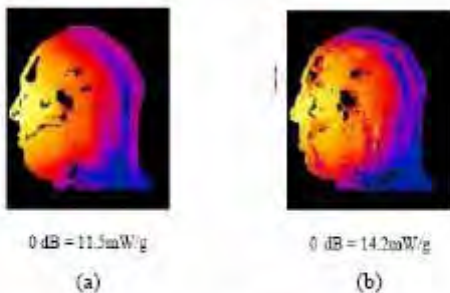


Figure 2: The SAR distribution in a vertical cut of the (a) homogenous and (b) heterogeneous Visible Human head caused by a walkie-talkie.

**DEVELOPMENT OF A SAR-PROBE CALIBRATION SYSTEM BASED ON TEMPERATURE MEASUREMENT.** S. Watanabe<sup>1</sup>, H. Asou<sup>2</sup>, K. Sato<sup>2</sup>, L. Hamada<sup>3</sup>, T. Iwasaki<sup>3</sup>. <sup>1</sup>National Institute of Information and Communications Technology, Tokyo, Japan, <sup>2</sup>NTT Advanced Technology Co., Tokyo, Japan, <sup>3</sup>The Univ of Electro-Communications, Tokyo, Japan.

**Introduction:** SAR probe is usually calibrated with waveguide systems[1] [2] [3] with quarter-wavelength matching slab at frequencies used for cellular telephones. This calibration method is however difficult to apply at lower frequencies due to the size of the waveguide although there are needs for SAR-probe calibration at lower frequencies because many professional and amateur portable radios are used at VHF band.

**Objective:** We have therefore developed a SAR-probe calibration system based on temperature measurement, which does not need the waveguide. As a preliminary study, we have calibrated a SAR probe at 900 MHz and compared the calibration factors with those evaluated by the waveguide method.

**Method and Models:** We have developed the new calibration system with a commercial SAR measurement system (SPEAG Inc., DASY3). The schematics of the calibration system is shown in Fig.1. The calibration factors are evaluated as following:

$$\text{SAR} = \sigma |E|^2 / \rho = \sigma (V_x / CF_x + V_y / CF_y + V_z / CF_z) / \rho = c \Delta E dT / dt$$

The temperature increase (dT) in a flat phantom filled with tissue-equivalent liquid was measured during exposure from 900 MHz resonant dipole antenna. In order to increase S/N ratio, the temperature measurement was performed close to the phantom bottom, i.e., within 10 mm from the bottom. The SAR probe under calibration was then inserted in the phantom and scanned along with the vertical axis through the center of the dipole antenna. Finally we evaluated the calibration factors by comparing the reference SAR value, which evaluated by the temperature measurement, with the SAR distribution obtained by the vertical scan of the SAR probe.

**Results and Discussion:** The calibration factors evaluated by the temperature measurement were within 6% of those evaluated by the waveguide method. The deviation could be improved to less 1% if the boundary effects were appropriately compensated. In the conference, we will present the detail of development of the new calibration system.

**Reference:**[1] IEC 106/84/FDIS, [2] ARIB STD-T56, [3] IEEE Std. 1528-2004

**VARIATION OF MEASURED MAXIMUM LOCAL SARs BETWEEN STANDARD-COMPATIBLE COMMERCIAL MEASUREMENT SYSTEMS (PART 2).** S. Watanabe<sup>1</sup>, Y. Miyota<sup>2</sup>, K. Sato<sup>2</sup>, L. Hamada<sup>3</sup>, T. Iwasaki<sup>3</sup>. <sup>1</sup>National Institute of Information and Communications Technology, Tokyo, Japan, <sup>2</sup>NTT Advanced Technology Corporation, Tokyo, Japan, <sup>3</sup>The Univ of Electro-Communications, Tokyo, Japan.

**Introduction:**

The maximum local SARs in human heads during use of cellular phones must be checked by SAR measurement systems. The procedure of the SAR measurement and the specification of the

measurement system are described in internationally-harmonized standards (IEC, IEEE, CENELEC, ARIB, and so on). We have previously presented the comparison of the measured maximum local SARs between three standard-compatible SAR measurement systems[1]. We have found that the maximum variation is about 30% which coincides with the typical expanded uncertainty described in IEEE Std.1528. After the presentation we have continued to investigate sources of these variations with manufacturers of the measurement systems.

**Objective:**

We have re-examined SAR measurement with following the indications of the manufacturers. We have also performed some additional measurement in order to investigate dominant sources of the variation of the measured SAR among the measurement systems.

**Method and Material:**

We have used the same SAR measurement systems as those used in our previous study, i.e., SPEAG DASY3, DASY4 and IndexSAR SARA2. We have also used the same five cellular phones as those used in our previous study. In this study, we have improved the surface detecting function of DASY3, which has been pointed out by the manufacturer.

**RESULTS AND DISCUSSIONS:**

The comparison of the SAR measurement with DASY3 between before and after the improvement of the surface detection is shown in Fig. 1. The new results of the measured maximum local SARs are lower than the previous ones. The comparisons of the SAR measurement between the three measurement systems are shown in Fig.2. It is found that the improvement of the DASY3 surface detection decreases the variation about 30% to 20%. We have also found that large variation occurs when the maximum local SAR appears upper or lower parts of the head. In those cases, the angle of the SAR probe against the surface of the head phantom bottom is significantly different between the measurement system. We will present additional measurement to demonstrate the effect of the incident angle of the SAR probe.

**Acknowledgement:**

We'd like to acknowledge Dr. Niels Kuster and his colleagues with SPEAG Inc., for their helpful suggestions.

**Reference:**

[1] S.Watanabe et al, 2004 BEMS "Variation of SAR values measured by commercial measurement systems compatible to international standards "

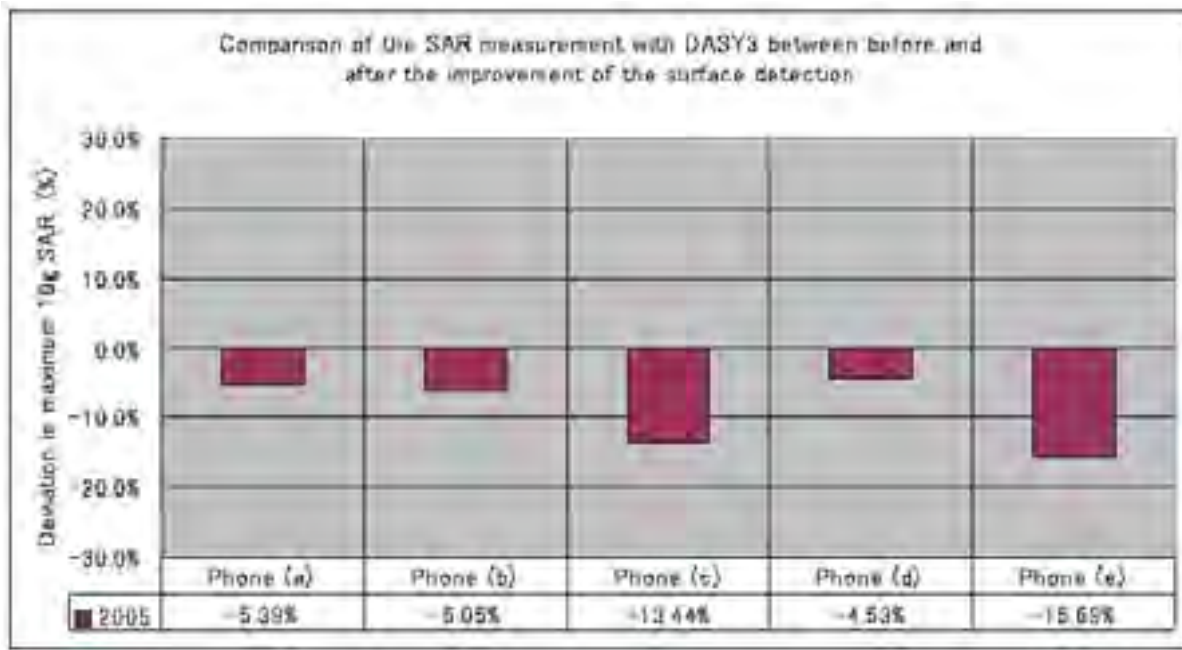
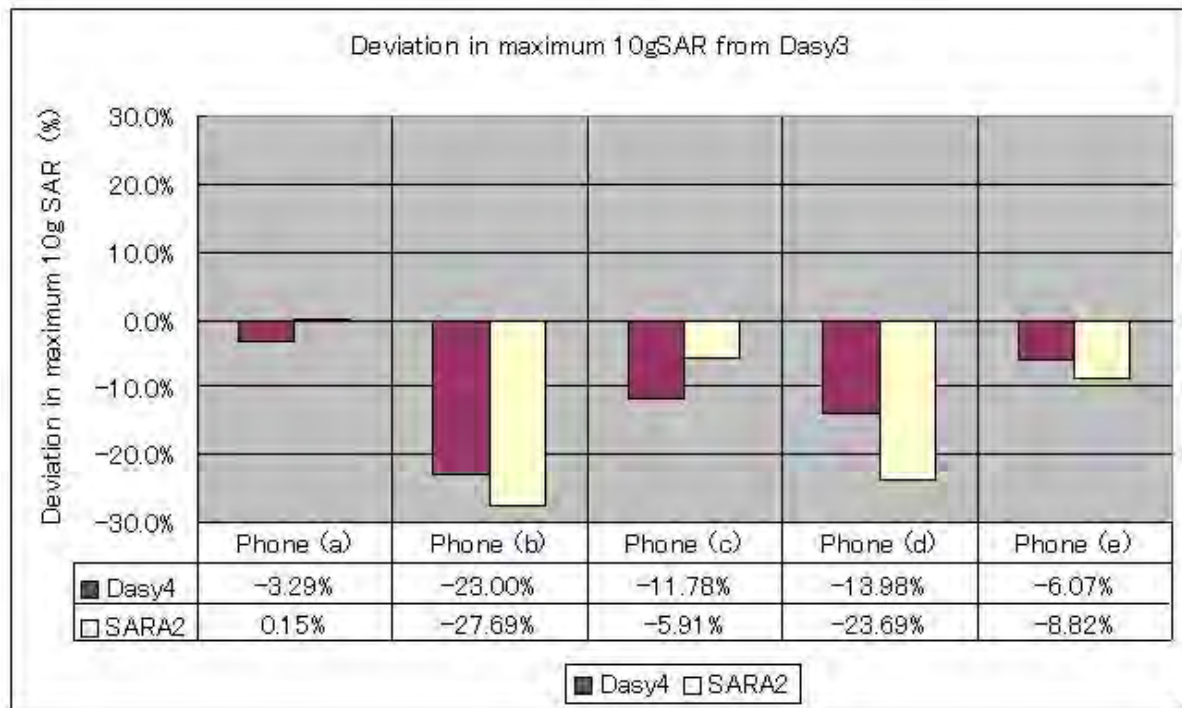
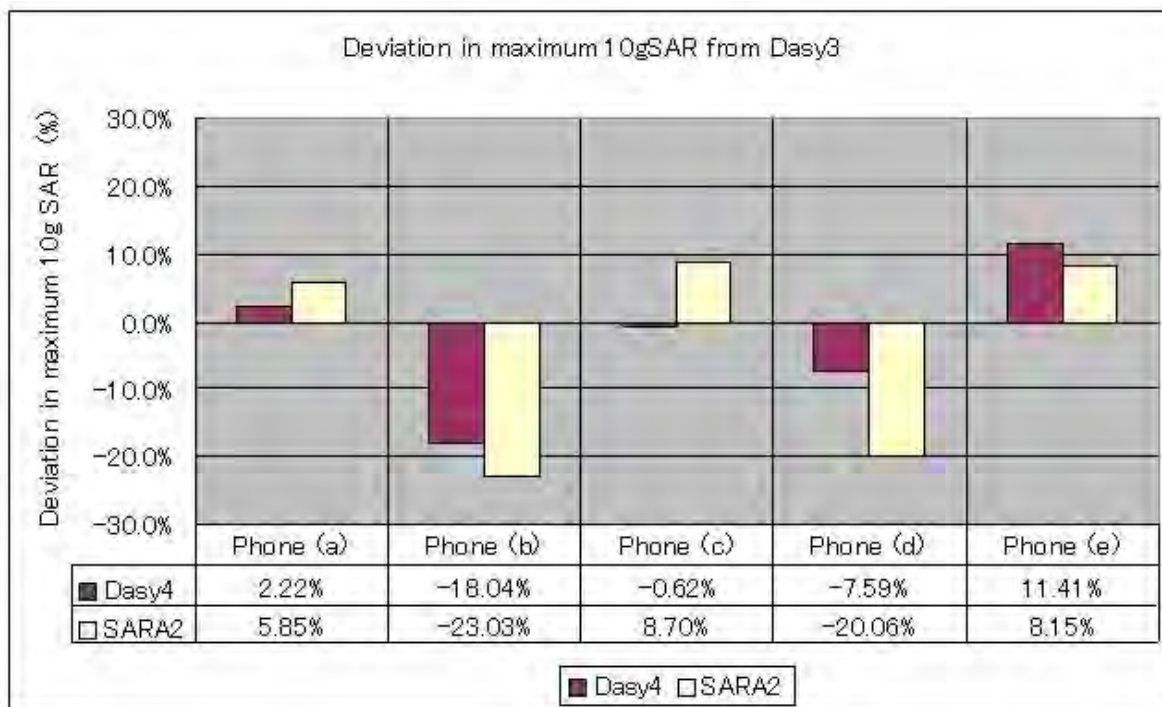


Figure.1

Comparison of the SAR measurement with DASY3 between before and after the improvement of the surface detection.



(a)



(b)

Figure.2 Comparisons of the SAR measurement between DASY3, DASY4 and SARA2. DASY3 data are obtained from old setting (a) and from new setting where its surface-detection function is improved (b).

P-C-63

**INFLUENCE OF HUMAN BODY SHAPE ON EMF EXPOSURE AT 100 MHZ.** M. F. Wong<sup>1</sup>, V. Dronne<sup>1</sup>, E. Nicolas<sup>2</sup>, F. Jacquin<sup>2</sup>, J. Wiart. <sup>1</sup>France Telecom RD, <sup>2</sup>Télédiffusion de France.

introduction : ICNIRP guidelines have defined basic restrictions in terms of SAR (Specific Absorption Rate) and reference levels in terms of field strength to protect public and workers from the exposure to electromagnetic fields (EMF). The compliance to the field limit implies the compliance to the SAR limit. However the non-compliance to the field limit does not mean necessarily non compliance to the basic restrictions. The reference limits offer a simpler way for assessing compliance and generally the limits are more stringent, i.e. some margins on the field strength may exist before the fundamental SAR limit is reached. However a margin assessed for a given human body shape may be different another one. The absorption of electromagnetic waves depends on the morphology.

Objectives : The aim of this study is to analyze the influence of human body shape on the local and whole body SAR. The analysis is carried out through FDTD (Finite Difference Time Domain) simulations using different scaled models of human body and sources at 100 MHz.

Methods : The human body model is the Zubal phantom from Yale Univ. From this reference model, 9 models have been derived with different heights and weights by using statistical data available on human height and weight and the body mass index. The 9 models have then exposed to plane waves and dipoles at 100 MHz.

Results : The SAR for the different configurations have calculated and normalized to the incident field. Thus, for each configuration a maximum field strength can be deduced in order to comply with the SAR

limit. A relative variation of 50 % has been observed between the configurations for both the whole body SAR as well as the local SAR.

## Epidemiology

P-C-66

**EXAMINATION OF MAGNETIC-FIELD PEAK-EXPOSURE MEASURES.** G. Mezei<sup>1</sup>, D. Bracken<sup>2</sup>, R. Senior<sup>2</sup>, R. Kavet<sup>1</sup>. <sup>1</sup>Electric Power Research Institute, Palo Alto, California, USA, <sup>2</sup>T. Dan Bracken Inc., Portland, Oregon , USA.

### Introduction

Past emphasis on exposure characterization and analyses for magnetic fields has been on measures of central tendency, such as long-term time-weighted average. Recent epidemiologic findings reporting an association between maximum magnetic-field exposure during a day and spontaneous abortion precipitated interest in magnetic-field peak-exposure measures. It has been hypothesized that the observed association between maximum magnetic-field exposure and spontaneous abortion is the result of behavioral differences between women with healthy pregnancies (less physically active) and women who were to miscarry, and not the result of a cause-effect relationship involving the peak magnetic field. Our objectives were to investigate characteristics of power-frequency magnetic-field peak-exposure measures.

### Methods

We analyzed four existing data sets: three of the data sets had 24-hour personal exposure measurements and one data set had at-home measurements only. Statistical analyses within and between data sets examined the consistency of peak-exposure measures across data sets; factors affecting peak exposure measures; and temporal stability of peak-exposure measures. The peak-exposure measures examined included the maximum, the 99th and 95th percentiles, and exposures above various threshold values from a time period. Analyses were performed for the full 24-hour period and for time spent in various activity categories, such as home, work and travel.

### Results

The value of the measured maximum magnetic-field exposure from a 24-hour time-series of measurements varied inversely with the sampling interval between measurements. This variation indicates that the 24-hour measured maximum for a subject and the average maximum for a group of subjects depend on the sampling interval. Based on multiple and pair-wise comparisons, the distribution of 24-hour peak-exposures was different for each of the four data sets. These differences could be attributed to the different sampling intervals used in the studies, or to the different measurement protocols, geographical locations and sampling frames of the studies.

We also found that the number of activity categories entered by study subjects determined the proportion of subjects with exposure above various threshold values. Exposure metrics based on maximum values exceeding thresholds tend to classify active people (those who register exposure in greater numbers of activity categories) into higher exposure categories.

Compared to the median and 95th and 99th percentile values, maximum values demonstrated less

stability over time in repeated measurements suggesting that the maximum measured on one day may not be representative of the maximum for another day and that it would require many visits to a house to reduce variability in the estimate of the maximum for an individual.

#### Conclusions

Our findings are consistent with the hypothesis suggesting that the association between maximum magnetic fields and spontaneous abortion is plausibly the result of behavioral differences between women with healthy pregnancies and women who experience miscarriages. The validity and robustness of magnetic-field peak-exposure measures are compromised by their dependence on measurement protocols and subject activities. Thus, generalization from a given study to more global exposure characterization should be made with particular caution and with due consideration to sampling interval and other characteristics of the measurement protocol potentially influencing the measured maximum.

P-C-69

**SURVEY OF RESIDENTIAL MAGNETIC FIELD ABOVE RECONSTRUCTED TRANSFORMER STATIONS.** J. Szabó, G. Thuróczy. Dept of Non-ionizing Radiations, National "Frédéric Joliot-Curie" Research Institute for Radiobiology and Radiohygiene, Budapest, Hungary.

#### Introduction

In our previous study we reported that residential extremely low frequency (ELF) magnetic (MF) field above 21 transformer stations represented higher than usual exposure in residences near high-voltage power-lines (BEMS 2003). Objectives of the present survey was to measure the magnetic field above transformer stations reconstructed by the electricity supplier company, in accordance with the precautionary framework of the EU/WHO.

#### Methods

Present study deals with 10/04 kV transformers reconstructed by the electricity supplier company (ELMU) in the years 2003-2004. Reconstruction of transformers focused mainly 1) on the expansion of the distance of the 0,4 kV connection of the transformer and the floor of the residence and 2) on more favorable geometric design of cable connections mainly responsible for the magnetic field. The average height of transformer stations was 3,2 m. Measurements of 50 Hz magnetic field above 10/04 kV transformers and measurements of electric current on the bus-bars were performed. Spot measurements were made by EMDEX II (ENERTECH, California) magnetic field loggers at 1 m height according to 1m square. Also the maximum value was measured at 1 m height and at floor level. Current was measured by a lock-holder type current meter according to the three phases (R,S,T), and the average was used in further analysis.

Correlation of current and MF was analyzed (n=14). Magnetic fields of reconstructed transformers were compared to magnetic fields of non-reconstructed transformers of the previous survey.

#### Results

The average magnetic field measured at 1m height, and the maximum value measured at floor level showed significant correlation with the average current measured in the bus-bars. (Diagram 1 & 2)

Diagram 1. Correlation of average magnetic induction ( $\mu\text{T}$ ) measured at 1 m height in the residence

above 10/04 kV transformer and average amperage of the three phases of reconstructed and non-reconstructed transformers. (Reconstructed=pink, non-reconstructed=blue)

Diagram 2. Correlation of maximum magnetic induction ( $\mu\text{T}$ ) at floor level above 10/04 kV transformer and average amperage of the three phases of reconstructed and non-reconstructed transformers. (Reconstructed = pink, non-reconstructed=blue)

The average amperage of the three phases of reconstructed transformers were much higher compared to non-reconstructed transformers (195 A (66 A – 462 A) v. 98 A (41 A - 179 A)). Because of this, the average magnetic fields in the residences above the transformers were about the same, in spite of the enhanced distance from the EMF source. By contrast, the measured MMF values at floor level were significantly lower, in spite of the twice as high amperage compared to the non-reconstructed transformers in the previous study.

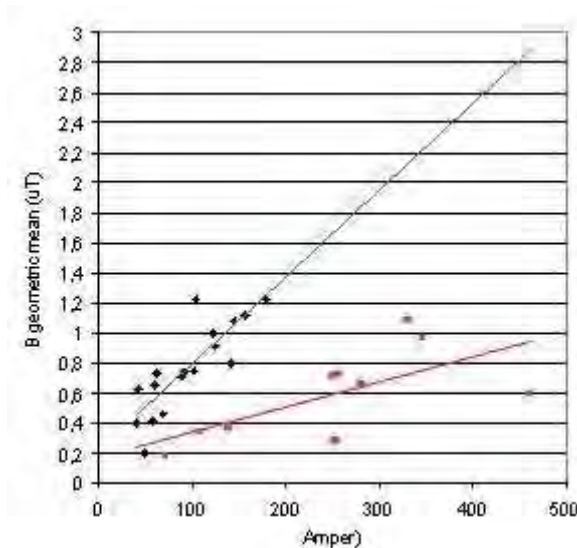
### Conclusions

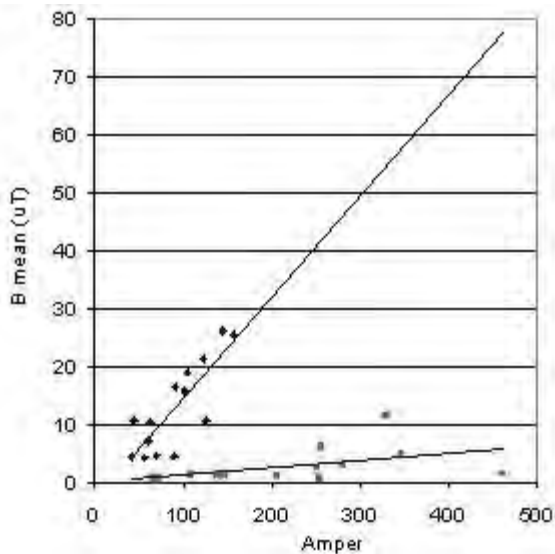
Correlation of magnetic field and current shows, that magnetic field of reconstructed 10/04 kV transformers are much lower, compared to the magnetic field of the non-reconstructed transformers with the same load. Enhancement of the distance from the EMF source reduced the magnetic field by an order in general, and reduction of the MMF was most pronounced.

Ref:

COM(2000) 1, COMMUNICATION FROM THE COMMISSION on the precautionary principle, Brussels, 02.02.2000

Szabó J., Jánossy G., Thuróczy Gy. (2003): EMF Exposure survey in residences above transformer stations. 25th Annual Meeting of the Bioelectromagnetics Society (BEMS) Maui, Hawaii, June 22-27, 2003. Abstract No. P-83-B, p.259.





P-C-72

**CORRELATION OF 24 H ELF MAGNETIC FIELD PERSONAL EXPOSURE MEASURED IN BUDAPEST.** J. Szabó, G. Thuróczy. Dept of Non-ionizing Radiations, National "Frédéric Joliot-Curie" Research Institute for Radiobiology and Radiohygiene, Budapest, Hungary Anna u.5. Budapest, Hungary.

#### Introduction

Objectives of the study were to measure the 24-hour extremely low frequency (ELF) personal magnetic field exposure on two different occasions

- 1) to reveal the main components of overexposure and to find out the correlation of repeatedly measured exposures and
- 2) to look beyond TWA as a biologically relevant EMF exposure metric because MMF was found to be a strong miscarriage risk.

#### Methods

40 personal magnetic field exposure measurements of 20 participants were performed between January-December 2003. Participants were recruited from the Institute. 24-hour measurements were performed by ELF magnetic field loggers (EMDEX PAL, Enertech) on two different occasions. Loggers were attached to the belt of the participants and were put near the bed for the night. Participants filled out a time-activity diary (home, bed, work, and travel). Overexposure was defined as: TWA (Time Weighted Average) exposure  $\geq 0,2 \mu\text{T}$  and/or MMF (Maximum Magnetic Field) exposure  $\geq 100 \mu\text{T}$ . Loggers' data transferred to computer were analyzed by Microsoft Excel 97.

#### Results

The mean personal exposure was  $0,158 \mu\text{T}$  ( $0,049 \mu\text{T} - 0,622 \mu\text{T}$ ). Average BED exposure was  $0,112 \mu\text{T}$  ( $0,009-0,843 \mu\text{T}$ ). Average HOME exposure was  $0,125 \mu\text{T}$  ( $0,021 \mu\text{T} - 0,649 \mu\text{T}$ ). Average WORK exposure was  $0,201 \mu\text{T}$  ( $0,036 \mu\text{T} - 1,895 \mu\text{T}$ ). Average TRAVEL exposure was  $0,181 \mu\text{T}$  ( $0,052 \mu\text{T} - 0,753 \mu\text{T}$ ). Four participants had TWA all day exposures higher than  $0,2 \mu\text{T}$  (two persons on both occasions., and two of them had  $>100 \mu\text{T}$  MMF exposures. Their TWA overexposures occurred from electric appliance use at home (kitchen electric appliances) or at work (sewing machine, densitometer)

and from travel (travelling by train). The other two persons (without MMF overexposure) acquired TWA overexposure at home from electric radiator below the bed and from 120kV power line within 25 meters.

Three persons had higher than 100  $\mu\text{T}$  MMF exposure. MMF raised the all day TWA exposure above 0,2  $\mu\text{T}$  by two of them, and only the work exposure of one person. TWA exposures correlated significantly with repeated exposures, except for travel exposure. TWA WORK exposure correlated the best ( $P < 0,001$ ). WORK and TRAVEL repeated maximum (MMF) exposures correlated significantly. MMF correlated with TWA significantly, except for bed exposure.

### Conclusions

Results suggest, that measurement of all day personal TWA exposure and the MMF work and travel exposures on one occasion represents the usual exposure of the person satisfactorily and thus it is suitable for exposure assessment needed in epidemiological research. High MMF ( $> 100 \mu\text{T}$ ) peak exposures may represent above average ( $> 0,2 \mu\text{T}$ ) 24 h TWA exposures.

P-C-75

**OPERATORS OF RADIOFREQUENCY PLASTIC SEALERS HAVE A DISTURBED HEART RATE VARIABILITY COMPARED TO A CONTROL GROUP.** U. Wiklund<sup>1,2</sup>, J. Wilén<sup>3</sup>, R. Hörnsten<sup>2</sup>, M. Sandström<sup>3</sup>, K. Hansson Mild<sup>3,4</sup>. <sup>1</sup>Dept of Biomedical Engineering & Informatics, Univ Hospital, Umeå, Sweden, <sup>2</sup>Dept of Clinical Physiology, Univ Hospital, Umeå, Sweden, <sup>3</sup>National Institute for Working Life, Umeå, Sweden, <sup>4</sup>Dept of Natural Science, Örebro Univ, Örebro, Sweden.

**INTRODUCTION:** Previously we have found that operators of radiofrequency plastic sealers normally operating at 27 MHz (RF operators) have significantly lower heart rate during both working-hours and nighttime compared to a control group. (Wilén et al 2004). In this work we carry on the analyses of the heart rate variability (HRV) to better understand possible underlying rhythm disturbances.

**OBJECTIVES:** To test the hypothesis that the decreased heart rate together with more episodes of bradycardia and arrhythmia is due to a dysfunction in the cardiac autonomic modulation caused by the radiofrequency exposure.

**METHOD:** Thirty five RF operators exposed to radiofrequency electromagnetic fields and 37 control subjects with similar work task, except from the RF exposure were included in the analyses. The mean electric and magnetic field strengths for the RF operators were 88 V/m and 0.19 A/m respectively. A continuous Electrocardiogram (ECG) was recorded during a 24-hour period, using a two-channel 24 hours ambulatory Holter recorder (Braemar DL700, Braemar inc.). For each individual, the Holter analysis started in the morning and ended approximately the same time the day after. Total power in the frequency range 0.003-0.4 Hz, as well as the power of the very low-frequency (VLF; 0.003-0.05 Hz), low-frequency (LF; 0.05-0.15 Hz), and high-frequency (HF; 0.15-0.40 Hz) components were calculated as average data for each hour (e.g. from 08:00-09:00).

**RESULTS AND DISCUSSION:** No statistically significant overall group differences were found in the analysis of HRV data on an hour-by-hour basis. However, the preliminary analyses showed that the interaction between the group and the time factors was statistically significant for the log-transformed total power ( $P=0.02$ ) as wells as for the VLF ( $P=0.03$ ) and LF ( $P=0.05$ ) components, but not for the HF ( $P=0.07$ ) component. The differences were most pronounced during nighttime where RF operators had

higher HRV as compared to controls. This finding, in combination with the overall difference in heart rate, might indicate a relative increase in parasympathetic cardiac modulation in RF operators as compared to the control subjects.

REFERENCES: Wilén J, Hörnsten R, Sandström M, Bjerle P, Wiklund U, Stensson O, Lyskov E, Hansson Mild K. 2004. Electromagnetic field exposure and health among RF plastic sealer operators. *Bioelectromagnetics* 25(1):5-15

## High-throughput screening

P-C-78

**EFFECTS OF CW OR W-CDMA MODULATED SIGNALS AT 2-GHZ BAND MICROWAVES ON GENE EXPRESSION PROFILE IN HUMAN CELL LINES OF THE DIFFERENT NATURE IN RESPONSE TO A HEAT SHOCK.** M. Sekijima<sup>1</sup>, H. Hirose<sup>1</sup>, N. Kaji<sup>1</sup>, T. Nojima<sup>2</sup>, J. Miyakoshi<sup>3</sup>. <sup>1</sup>Mitsubishi Chemical Safety Institute, <sup>2</sup>Hokkaido Univ, <sup>3</sup>Hirosaki Univ.

**OBJECTIVE:** The aim of this work was to examine if any radio frequency (RF) fields exert their inherent mechanisms, although some of which are poorly understood. To investigate the changes in the gene expression profile of four human cell lines following exposure to 2.1425GHz continuous wave (CW) and Wideband-Code Division Multiple Access (W-CDMA) RF fields.

**MATERIALS AND METHODS:** We used the in vitro exposure system with a horn antenna and dielectric lens in an anechoic chamber; two anechoic chambers (exposure area was 30x30cm<sup>2</sup>) with one for the group exposed to the electromagnetic field and the other for the sham exposure, which was developed by NTT DoCoMo [1]. Two tumor cell lines, A172 (glioblastoma) and H4 (neuroglioma), and/or two normal cell lines, IMR-90 (normal fibroblasts from fetal lung) and CCD25SK (normal fibroblasts from skin), were seeded separately at 20% - 50% confluence per 3 ml culture medium in plastic 35 mm petri dishes. Each human cell was exposed to 2.1425GHz CW and W-CDMA radio frequency fields at three field levels at the limit of whole-body average SAR levels on the basis of ICNIRP guidelines [2]. Microarray hybridization was performed using the Affymetrix GeneChip® Human Genome U133 Plus 2.0 Array using protocols described by Affymetrix, Inc. Data was analyzed using SiliconGenetics GeneSpring® 7.0 software.

**RESULTS AND CONCLUSIONS:** No cytostatic effect of CW and/or W-CDMA exposure was observed either of the cell lines. Each cell was immediately harvested after exposure with RF at SAR of 80, 250 and 800 mW/kg with both CW and W-CDMA electromagnetic fields at 2.1425GHz for 24 to 96 hrs and/or heat treatments in both 39 and 41 °C for 2 and 24hr. No marked difference between sham and RF exposed cells was observed in the gene expression profiles of individual tested conditions. Only a very small (

[1] Iyama et al., 2004. Large-Scale In Vitro Experiment System for 2 GHz-Exposure. *Bioelectromagnetics* 25, 599-606. [2] ICNIRP, 1998. Guidelines for limiting exposure to time-varying electric, magnetic, and electromagnetic fields (up to 300GHz). *Health Phys* 74, 494-522.

## Human studies

P-C-81

**EXPOSURE AT UMTS ELECTROMAGNETIC FIELDS: STUDY ON POTENTIAL ADVERSE EFFECTS ON HEARING. THE EUROPEAN COMMISSION EMFNEAR PROJECT.** P. Ravazzani. Biomedical Engineering Institute, National Research Council, Milano, Italy.

**INTRODUCTION:** Although in the last decade the European public concern was growing on the potential adverse health effects due to the use of mobile phones, among the studies addressing their potential health effects, only in 2002 a systematic multicenter research project was established by the European Commission (GUARD “Potential adverse effects of GSM cellular phones on hearing” FP5, QLK4-CT-2001-00150, 2002-2004) investigating the effects of GSM phones at 900 and 1800 MHz on hearing, actually a highly sensitive biological system to exogenous and endogenous agents and the first one to be affected by the microwaves (results of GUARD on animals and humans are presented in other abstracts during this Conference) .

Considering the crucial importance of the study of the effects at other frequencies and modulations and the diffusion of 3G technologies for mobile communications, specifically UMTS, the EMFNEAR Project “Exposure at UMTS Electromagnetic Fields: Study on Potential Adverse Effects on Hearing” (DG Health & Consumer Protection, Agreement Number: 2004127, 2004–2007) aims to study the effects on the hearing of animals (Sprague-Dawley rats) and humans of UMTS cellular phones, assessing potential changes of audiological measures (otoacoustic emissions and auditory evoked potentials) of hearing functionality due to exposure.

**PARTICIPANTS:** Eight European partners are envisaged: P. Ravazzani, Scientific Coordinator, L. Collet, Université Claude Bernard Lyon1/ CNRS, Lyon, F, M. Lutman, ISVR, Univ of Southampton, UK, C. Marino, Section of Toxicology and Biomedical Sciences, ENEA, Rome, I, M. Sliwinska-Kowalska, Nofer Institute of Occupational Medicine, Lodz, Pl, G. Tavartkiladze, Dept of Experimental and Clinical Audiology, Moscow, Ru, G. Thuroczy, National Research Institute for Radiobiology and Radiohygiene NIRR, Budapest, H, I. Uloziene, Kaunas Univ of Medicine, Kaunas, Lt.

**SCIENTIFIC APPROACH:** The EMFNEAR project workplan is broken down in workpackages, that can be summarized as:

- Exposure and positioning systems. Localized exposure and positioning systems are used, allowing the setting of the level of SAR and exposure time.
- Exposure and measuring protocols. The effects of UMTS exposure on the auditory function of animals and humans are investigated by subjective and objective classical audiological tests.
- Data processing: All data obtained from the experiments are processed by the Central Data Processing Unit (CDPU), which will be in charge of data processing and analysis.
- Expected results of project EMFNEAR are: information on the adverse effects of UMTS phones on hearing, data on the minimum level of SAR and minimum exposure times for measuring changes or potential adverse effects, feedbacks to producers in order to reduce the potential hazards for hearing.

**ACKNOWLEDGEMENTS:** This work is supported by the European Project EMFNEAR “Exposure at UMTS Electromagnetic Fields: Study on Potential Adverse Effects on Hearing” (DG Health & Consumer Protection”, Agreement Number: 2004127, 2004–2007).

**NOVEL INSIGHTS INTO THE COMPLEXITY OF ELECTROMAGNETIC HYPERSENSITIVITY FOR GENERAL PRACTITIONERS.** J. Reissenweber, A. Wojtysiak, E. David. Electropathological Research Center, Witten/Herdecke Univ, Witten, Germany.

**OBJECTIVES:** Electromagnetic hypersensitivity represents a not-to-be-underestimated problem within the medical profession, especially for general practitioners and family doctors. Novel concepts and views of self-reported electromagnetic hypersensitivity based on a historical summary and the clinical picture of this subjective phenomenon shall be presented. Meanwhile, various groups in society including self-help groups for persons suffering from environment-related illnesses and citizens' action groups have shown an increasing interest in this subject. That is why electrical engineers and physicians as well as biologists, psychologists and social scientists are becoming increasingly involved in the research into this subject.

**CLINICAL PICTURE:** To date, attempts at determining a typical clinical picture of electromagnetic hypersensitivity have not been successful. The range of symptoms in those individuals affected is so diverse, that although the most-frequently cited symptom, that of headache, can be determined statistically, the second and third-most frequent symptom is different in everyone affected. The range of symptoms correlates more closely with other types of illness, for instance those from the allergic, rheumatic and haemodynamic type groups. Until now, scientists have not mostly struck upon the idea of correlating mathematically the individual pathological patterns with others. The situation could be interpreted theoretically as if everyone affected developed a personal, conditioned response – individually different – in the presence of electromagnetic fields.

**SOCIO-POLITICAL PROBLEMS:** Persons with alleged electromagnetic hypersensitivity are increasingly seeking out general practices where the general practitioner is fairly powerless when confronted with the phenomenon. He is unable to assess the environmental situation of those affected, let alone measure the field strength around the home. Patients often give curious descriptions of the influences they are subjected to. Persons claiming to suffer from electromagnetic hypersensitivity are only defined as such by virtue of self diagnosis. The specialist expression "self-reported" electromagnetic hypersensitivity expresses this succinctly. Colleagues in general practice currently still have insufficient knowledge about electromagnetic hypersensitivity, because they learn too little about this topic, both before as well as after their state medical examination.

**METHODS:** A comparison of hormone concentrations in the blood as well as other blood values in persons claiming to suffer from electromagnetic hypersensitivity and healthy control subjects has, to date, found no important differences between these two groups. During the Witten test for electromagnetic hypersensitivity which will be described in detail the test subjects with electromagnetic hypersensitivity were apparently unable to sense objectively the presence of the electromagnetic fields which they are convinced causes their suffering, in other words: the perceived burden of suffering by test subjects with self-reported electromagnetic hypersensitivity appears to be unconnected to an ability to sense the presence of such fields.

**HISTORICAL SUMMARY:** The problem of self-reported electromagnetic hypersensitivity became relevant in the nineteen eighties in Scandinavia as attempts there were being made to gain new insights into the origination of the putative syndrome of electromagnetic hypersensitivity as part of studies into the provision of occupational health programmes and care measures for employees. The phenomenon still remains unsolved in modern, industrial societies. There continues to be a lack of medical and

biological indicators, as well as examination processes, which would allow this feeling of ill-health to be proven. What is being sought is a way to objectivate the existence of electromagnetic hypersensitivity, if it exists at all, as an own clinical syndrome. Electromagnetic hypersensitivity can also be regarded as the hypothetical ability to sense fields far beneath statutory threshold values. This can additionally involve the association of rather negative sensations as well as tingling and other dysaesthesias, through to neurological disorders. Those affected also suffer from the shortcomings in knowledge of relatives and acquaintances. Briefly, the phenomenon has not yet been researched sufficiently.

**CONCLUSIONS:** Our increasingly mechanised environment has resulted in a large variety of physical phenomena and chemical substances whose illness-inducing characteristics we are unaware of. Electromagnetic hypersensitivity can be regarded as a response of sensitive persons to a situation in this environment. As part of the duty of care and duty of preventative health care exercised by the state, the latter is forced to grapple with this subject. It presumably depends on how one wishes to define preventative health care. It is normally understood to mean the protection against known risks. Opinion contrary to this states that preventative health care provides protection against foremost unknown effects. Though, all of the research approaches to date, such as viewing electromagnetic hypersensitivity as a neurocirculatory disease or as a heightened irritability of the central nervous system, have still been unable to completely solve this puzzle. The physician in general medical practice must be advised to take his patients seriously, to also take their social and physical environment into consideration and not to rule out alternative medical treatments. Seen realistically, one comes to the conclusion that, within the spectrum of potentially harmful accompanying factors in our daily life, electromagnetic fields should be classified as playing a lesser aggressive role.

P-C-87 WITHDRAWN

P-C-90 WITHDRAWN

P-C-93

**INVESTIGATION INTO THE EFFECTS OF MILITARILY RELEVANT RADIO FREQUENCY RADIATION (RFR) ON COGNITION.** S. J. Smith<sup>1</sup>, S. C. Bowditch<sup>1</sup>, L. O. Evans<sup>1</sup>, J. A. Groeger<sup>2</sup>, R. I. Grose<sup>1</sup>, R. H. Inns<sup>1</sup>. <sup>1</sup>Dstl Biomedical Sciences, Porton Down, Salisbury, Wiltshire, UK, <sup>2</sup>Surrey Univ, Guildford, Surrey, UK.

**BACKGROUND:** Current radiofrequency radiation (RFR) exposure guidelines are based upon well-established thermal effects. However, recent research into digital (pulsed carrier wave) and analogue (continuous wave) transmission fields at levels within the exposure guidelines, have indicated potential effects on human cognitive performance. Military communication systems operate on frequencies which differ considerably from those used by mobile phones. The effects such electromagnetic sources may have on human cognition and performance in the military operational context are unknown

**OBJECTIVE:** The aim of this study was to determine whether realistic exposure to RFR present in current army communication systems affected human cognitive performance.

DESIGN: The study design incorporated a two-week period during which the effects of a High Frequency (HF) and Very High Frequency (VHF) RFR signal (29.725MHz and 75.9MHz) on the performance of computer based cognitive tasks was assessed. Performance was compared to a sham exposure control condition. The exposures were designed to give 50V/m at the volunteer position; local SAR in the head of a phantom being measured as 1.7W/kg and 1.5W/kg for HF and VHF exposures respectively. Forty-eight male volunteers were trained on a battery of cognitive tasks, which were performed on three test days, each of which were separated by a period of 72 hours. Subjective self-assessments of mood-state, perceived workload and symptoms were also recorded.

RESULTS: Statistically significant results were observed on only two of the twenty-two cognitive tasks. The tasks were the Sustained Attention Response Task (SART) and the Visual Recognition Task. On both of the tasks there was a significant decrease in response latency when participants were exposed to the HF RFR (29.725MHz) condition, on only one of the tasks, the SART, was this accompanied by a corresponding decrease in response accuracy. There was no significant effect of condition on the subjective self-assessments of mood-state, perceived workload or symptoms.

CONCLUSIONS: The results from this study indicate that, on the whole, exposure to two types of RFR (29.725 and 75.9MHz) within ICNIRP safety guidelines did not significantly affect the aspects of cognitive and psychomotor performance measured.

These findings are of note but should not be interpreted as evidence of a robust effect on overall cognitive performance.

This work was funded by the Human Sciences Domain of the UK Ministry of Defence Scientific Research Programme

Crown Copyright 2005, Dstl

P-C-96

**EMF FROM LOW ENERGY, SUB LUMINOUS, LIGHTNING MAY PRODUCE FATAL CARDIAC ARRHYTHMIAS.** H. Wachtel<sup>1,2</sup>, M. Cherington<sup>2</sup>, P. Yarnell<sup>2</sup>. <sup>1</sup>Depts of ECE and of Neuroscience, Univ of Colorado, Boulder, CO, USA, <sup>2</sup>Lightning data center, Saint Anthony Hospital, Denver, CO, USA.

OBJECTIVE: To explore the hypothesis that electromagnetic fields from “low energy” (sub-luminous) forms of lightning may still be strong enough to produce current pulses in the heart sufficient to induce ventricular fibrillation and lead to “sudden cardiac' death in some instances

BACKGROUND: Overt instances of death due to a lightning “strike” are fairly rare (about 100 a year for the entire USA)—but "sudden cardiac deaths" are far more numerous and some of these may be due to a more subtle form of lightning. A diagnosis of death by lightning is usually made on the basis of observable tissue damage (burns, etc.) and reports of incident lightning flashes (and thunder). It seems to us, however, that certain lethal effects of atmospheric electrical discharges need not be accompanied by luminous flashes or result in burns or other visible tissue damage to the victim.

METHOD AND RESULTS: We explored this hypothesis by modeling the response of electrically

excitable cells (nerve and muscle) to brief pulses typical of lightning current durations (on the order of a microsecond). The model predicts that a trans-torso current of less than 100 amperes could depolarize cardiac cells by about 10 to 50 millivolts while producing no discernable aqueous (muscle etc) tissue heating (less than 0.001 degrees). Heating of cutaneous tissue would be somewhat higher—depending on its particular electrical resistivity---but would still be orders of magnitude below burn thresholds.

CONCLUSION: A brief (several millisecond) 10 to 50 millivolt depolarization would, in most cases, have only a transitory cardiac (or neural) effect (such as a PVC) However, if it were to occur during the most vulnerable portion of the cardiac cycle (the T wave of the ECG,) it could lead to ventricular fibrillation which is often fatal. Low energy lightning “strokes” of less than 1000 amperes are likely to be "sub-luminous" -- especially during daylight hours -- and would not produce a sonic effect either (no thunder). Thus it is possible that many cases of sudden cardiac death might be attributable to "low energy lightning" discharges even though the usual indicators of a lightning strike to the victim are entirely absent. If this theory is correct, it could turn out that many more victims (thousands per year) succumb to this form of lightning than to its more overt forms. The design of an epidemiological study that could test the validity of this implication will also be discussed in our presentation.

P-C-99

**EXPERIMENTAL SYSTEM FOR STUDIES ON PRENATAL AND POSTNATAL EXPOSURE OF RATS TO RADIO-FREQUENCY FIELDS OF CELLULAR TELECOMMUNICATIONS.** K. Wake<sup>1</sup>, S. Watanabe<sup>1</sup>, M. Taki<sup>2</sup>, Y. Ugawa<sup>3</sup>, Y. Terao<sup>3</sup>, M. Nishikawa<sup>3</sup>, T. Okano<sup>3</sup>, S. Shirasawa<sup>3</sup>, T. Furubayashi<sup>3</sup>, C. Ohkubo<sup>4</sup>, A. Ushiyama<sup>4</sup>, H. Masuda<sup>4</sup>, S. Soukejima<sup>4</sup>. <sup>1</sup>National Institute of Information and Communications Technology, Tokyo, Japan., <sup>2</sup>Graduate School of Engineering, Tokyo Metropolitan Univ, Tokyo, Japan., <sup>3</sup>Univ of Tokyo, Tokyo, Japan., <sup>4</sup>National Institute of Public Health, Saitama, Japan.

OBJECTIVE: The concerns about possible health effects by electromagnetic field of cellular telecommunications are growing among general public. There are several reports that investigate the relation between subjective symptoms of electromagnetic hypersensitivity (EHS) and radio frequency electromagnetic field (RF-EMF) exposure of non-thermal level. The purpose of this study is to develop the exposure system in order to put into practice the study on EHS in Japan[1].

EXPOSURE SYSTEM: Subjects are exposed to EMF of W-CDMA signal at 2 GHz region. Each subject is experienced continuous, intermittent, sham and noise exposures. The period of each exposure is 30 minutes. The orders of these 4 exposures are randomized. The W-CDMA signal generated by signal generator is amplified and applied to a horn antenna in a special shielded chamber. The antenna input power is controlled and monitored by a personal computer. The subjects are exposed at the distance of 2-3 m from the aperture of the horn antenna with the electric field of 10.0 V/m. We also monitor the level of electric field inside the chamber. Exposures can be stopped automatically when the electric field value exceed a limit for safety. We will also show the results of numerical analysis of the specific absorption rate (SAR) inside the human exposed with this system at the meeting. [1] Y. Ugawa et al., "Studies on hypersensitivity to non-thermal radiofrequency electromagnetic field in Japan", 27th Annual meeting of Bioelectromagnetics, 2005.

## In vivo studies

P-C-102

**GENE EXPRESSION CHANGES IN SKIN OF RATS EXPOSED TO SUSTAINED 35-GHZ RADIO FREQUENCY RADIATION.** N. J. Millenbaugh<sup>1,2</sup>, R. Sypniewska<sup>1,2</sup>, C. C. Roth<sup>1,2</sup>, J. L. Kiel<sup>3</sup>, R. V Blystone<sup>4</sup>, P. A. Mason<sup>1</sup>. <sup>1</sup>Directed Energy Bioeffects Division, Air Force Research Laboratory, Brooks City-Base, TX, <sup>2</sup>Advanced Information Engineering Services, San Antonio, TX, <sup>3</sup>Biosciences and Protection Division, Air Force Research Laboratory, Brooks City-Base, TX, <sup>4</sup>Dept of Biology, Trinity Univ, San Antonio, TX.

**INTRODUCTION:** Communication, military radar, and weapon detection technologies are being developed that make use of the millimeter wave (MMW) range of the electromagnetic spectrum. Some of these emerging technologies will require increasingly higher power outputs which may be capable of causing temperature rises in the body. As these systems are fielded, there will be an increased possibility of brief or prolonged overexposures leading to acute or chronic effects, especially of the maintenance technicians or operators. Laboratory and clinical case reports indicate that exposure to radio frequency radiation beyond permissible exposure limits may result in biological effects; however it is unclear whether these effects result in significant health consequences. It has been estimated that frequencies at or greater than 35-GHz will be primarily absorbed within the first 0.9 mm of tissue, and thus skin is a primary target for investigating potential effects. The goal of this study is to characterize gene expression changes in skin in response to MMW overexposure.

**METHODS:** Male Sprague-Dawley rats were anesthetized with isoflurane and either sham-exposed or exposed to 35-GHz MMW at 75 mW/cm<sup>2</sup> or environmental heat (EH) at 42 degreeC (n=3 per group). Colonic and skin surface temperatures were measured using a thermistor probe and infrared camera, respectively. The endpoint of these prolonged (approximately 40-50 minutes) exposures was a colonic temperature of 42 degreeC. Following exposure, rats were allowed to recover and skin was collected at 6 or 24 hr post-exposure. RNA was extracted and analyzed using Affymetrix GeneChips,  $\mu$  to determine gene expression changes in MMW-exposed skin compared to changes in skin from sham and EH-exposed rats. Differential gene expression in skin after MMW treatment was identified by applying Affymetrix Comparison Analysis and two-sample t-tests ( $p < 0.05$ ).

**RESULTS:** Changes were detected in 57 genes at 6 hr and in 61 genes at 24 hr in the MMW-exposed rats. Only 8 of these genes were the same at the two time points indicating that early and late responses to MMW exposure in the skin involve two distinct phases of response involving different sets of genes. MMW exposure caused greater up-regulation of some genes compared to EH exposure suggesting that the response of skin to MMW overexposure may be different than response to conventional methods of heating. At both 6 and 24 hr, heat and oxidative stress response genes were up-regulated including several members of the heat shock protein family, heme oxygenase and superoxide dismutase. Comparison of 6 and 24 hr genes showed that fewer HSPs remained up-regulated at 24hr indicating the HSP response is an early phase response to MMW exposure. At 24 hr, genes involved in extracellular matrix turnover and angiogenesis were up-regulated indicating a separate phase of response involving tissue matrix recovery and repair.

**CONCLUSIONS:** MMW-inducible genes in skin have been identified and the data suggest that different phases of response involving different groups of genes occur after MMW overexposure. Experiments are in progress to validate the GeneChip results and to identify specific responder cells within skin as

targets for further study of mechanisms of response. Research was funded, in part, by the Air Force Office of Scientific Research.

P-C-105 STUDENT

**AN IMMUNOHISTOCHEMICAL AND MORPHOMETRICAL STUDY OF THE POWER-FREQUENCY ELECTROMAGNETIC FIELD INFLUENCE ON SKIN AND THYROID AMINE- AND PEPTIDE-CONTAINING CELLS IN RATS.** V. Rajkovic<sup>1,2</sup>, M. Matavulj<sup>1</sup>, O. Johansson<sup>2</sup>. <sup>1</sup>Dept of Biology, Faculty of Science, Univ of Novi Sad, 21000 Novi Sad, Serbia and Montenegro, <sup>2</sup>Experimental Dermatology Unit, Dept of Neuroscience, Karolinska Institute, Stockholm, Sweden.

**INTRODUCTION:** Substance P (SP) and calcitonin gene-related peptide (CGRP) are two neuropeptides stored in cutaneous sensory nerves that affect blood vessels exerting vasodilatation and/or protein extravasation upon release. Increased vascular permeability in the skin is also attributed to serotonin, a biogenic amine harbored by cutaneous mast cells (MC). Mediators known to express vasoactive effect on thyroid microcirculation leading to increase in thyroid blood flow and/or capillary permeability are, among others, mast cell-derived histamine and neuropeptide Y (NPY) stored in adrenergic nerve fibers. Parafollicular (PF) cells of the thyroid contain several peptides, including CGRP, that is also found in nerve fibers around blood vessels, follicles and PF cells. Since the physiological role of above-mentioned peptides and amines in their respective organs is indisputable, it is of interest to investigate whether the fibers/cells containing these mediators are affected by electromagnetic field (EMF) exposure. **OBJECTIVES:** The objective in this study was to: 1) investigate the influence of power-frequency electromagnetic fields (EMF) on cutaneous mast cells (MC) and nerve fibers in rats, 2) determine the EMF influence on thyroid gland mast cells, nerve fibers and parafollicular cells in rats and 3) to quantitatively analyze cells and nerve fibers in control rats and rats exposed to EMF during one month. **METHODS:** Experiment was performed on two months old 24 white male rats of Wistar strain. Animals were housed under laboratory conditions with  $20 \pm 2^{\circ}$  C and subjected to a controlled photoperiod (14 h light, 10 h dark). Twelve animals were exposed four hours a day, seven days a week during one month to 50 Hz EMF of decaying intensity along the animal cages from 300  $\mu$ T (at the side of the cage near the coil which produced EMF) to 100  $\mu$ T (at the opposite side of the cage) while the intensity of electric field was 160 V/m and 54 V/m respectively. Twelve animals served as controls and were maintained in a similar environment, but without the presence of artificially produced EMF. Immediately after the last hour at the last day of exposure, animals were sacrificed and the samples of skin from interscapular region and the thyroid were taken. After fixation, samples were cut on cryostat into 14  $\mu$ m thick sections and further processed for indirect immunohistochemistry to histamine, serotonin, protein gene product 9.5 (PGP), SP, CGRP and NPY. The number of immunoreactive cells or nerve fibers per projected  $\text{mm}^2$  were counted using a special microscopic frame under the 20x objective on 2 skin sections per sample and 2 test fields per section and 2 thyroid sections per sample and 4 test fields per section according to the principles of design-based stereology. A non-parametric Mann-Whitney U-test was used for statistical analysis. **RESULTS: Skin.** After one month of exposure to 50 Hz EMF the papillary dermis was characterized by degranulated serotonin-positive MCs as indicated by a variable cell morphology and a prominent reduction of cell size. SP-immunoreactive (IR) nerve fibers were of very low distribution density in dermis of both experimental groups. The only noticeable difference between groups was the pale fluorescence of SP-IR fibers in the exposed rats. Cutaneous nerve fibers containing CGRP had a higher distribution density compared to the SP, they were frequently observed terminating in the epidermis of exposed rats. The fluorescence signal of

CGRP-IR fibers populating both epidermis and dermis was weaker than in controls. Stereological analysis demonstrated the statistically significant increase of serotonin-IR MC number in the exposed group compared to the control ( $p < 0.05$ ). The lowered number of SP-IR fibers and the higher number of CGRP-IR fibers in the EMF exposed rats were not significant when compared to the controls ( $p=0.95$  and  $p=0.64$ , respectively). **Thyroid.** A number of degranulated histamine-IR MCs with free MC granules in the connective tissue surroundings were observed in the thyroid interfollicular space after EMF exposure. The NPY-IR nerve fibers were appearing as thin fibers with pale fluorescence in both experimental groups. EMF exposure demonstrated no apparent differences in distribution, fluorescence intensity or morphology of PGP 9.5-IR and CGRP-IR nerve fibers and PF cells between the exposed and the control group. According to the Mann-Whitney test, the increased number of NPY-IR nerve fibers in the exposed group was statistically significant compared to the control ( $p < 0.01$ ). The increased number of histamine-IR MCs ( $p=0.06$ ), CGRP-IR nerve fibers ( $p=0.07$ ) and PGP-IR PF cells ( $p=0.54$ ) in EMF exposed rats and the decreased number of PGP-IR nerve fibers ( $p=0.50$ ) and CGRP-IR PF cells ( $p=0.45$ ) were not found significant compared to calculated control values. **CONCLUSION:** Our results clearly demonstrate the significantly increased number of serotonin-IR mast cells in skin and NPY-IR nerve fibers in the thyroid gland as well as the elevated number of degranulated intrathyroid MCs containing histamine in rats exposed to EMF during one month. According to our findings, the effect on other investigated mediators is moderate. Since the physiological role of serotonin, histamine and NPY is connected to their vascular effect, it could be presumed that 50 Hz EMF affects blood vessels in skin and thyroid gland through mast cell-derived amines and mediators released from peptidergic neurons. Supported by the Cancer- och Allergifonden, Karolinska Institute and the Serbian Ministry of Science and Technology grant No 1334.

P-C-108

**EFFECTS OF EXPOSURE OF PATCHED1 HETEROZYGOUS KNOCKOUT MICE TO GSM, 900 MHZ.** A. Saran, M. Teresa Mancuso, S. Pazzaglia, G. Alfonso Lovisolo, C. Marino. Section of Toxicology and Biomedical Sciences, Enea Casaccia, Rome, Italy.

Introduction: individuals affected with the Gorlin syndrome inherit a germ-line mutation of the patched (Ptch1) developmental gene and, analogously to Ptch1 heterozygous mice, show an increased susceptibility to spontaneous tumor development. Human and mouse Ptch1 heterozygous are also hypersensitive to ionizing radiation (IR)-induced tumorigenesis in terms of basal cell carcinoma (BCC) induction. We have previously reported that irradiation dramatically increases the incidence of medulloblastoma development (81%) over the spontaneous rate (7%) in neonatal Ptch1 heterozygotes. Thus newborn Ptch1 $\pm$  heterozygous mice constitute an extremely sensitive mouse model of medulloblastoma, and represent a useful tool to evaluate the detrimental effects of exposure to potentially harmful agents.

Materials and Methods: this mouse model has been utilized to study the effects of whole body exposure to GSM Basic 900 MHz, at 0.4 W/kg average, in two special length (4f $\ddot{U}$ ) TEM cells, for 5 days, 30i twice a day. Newborn Ptch1 heterozygous and wild type mice (about 100 per genotype) were divided in sham and exposed groups in blind. Room and superficial body temperature has been monitored during exposure.

Results: the experiments and the statistical evaluation are performed in blind mode with respect to the exposure conditions (sham or exposed). Mortality of Ptch1 heterozygous and wild type mice, obtained until now, show a similar trend in the two groups (the experiment code is still closed). Preliminary results on tumour development will be presented and discussed.

**REVIEW OF JAPANESE IN VIVO STUDIES ON BRAIN TUMOR CARCINOGENESIS OF CELLULAR PHONES.** T. Shirai<sup>1</sup>, M. Kawabe<sup>2</sup>, T. Ichihara<sup>2</sup>, J. Wang<sup>3</sup>, O. Fujiwara<sup>3</sup>, M. Taki<sup>4</sup>, K. Wake<sup>5</sup>, S. Watanabe, Y. Yamanaka<sup>5</sup>, K. Imaida<sup>6</sup>, S. Tamano<sup>2</sup>. <sup>1</sup>Nagoya City Univ, <sup>2</sup>DIMS Laboratory, <sup>3</sup>Nagoya Institute of Technology, <sup>4</sup>Tokyo Metropolitan Univ, <sup>5</sup>National Institute of Information of Communications Technology, Tokyo, Japan, <sup>6</sup>Kagawa Univ, Kagawa, Japan.

Introduction: Ministry of Internal Affairs and Communications has started a research consortium to investigate non-thermal adverse effects on RF fields. One of the main topics of the consortium is effects on brain tumor. We, the member of the consortium, have started the large-scale long-term in vivo studies on brain tumorigenesis since 2000.

Objective: In this presentation, we summarize the Japanese studies on the brain tumor carcinogen.

Results and discussion: First study was designed for exposure to digital signal of Japanese cellular system in 1.5-GHz band [1]. F344 rats were exposed to ENU transplacentally to initiate brain tumorigenesis. 500 F1 rats were categorized into high (brain-average SAR 2 W/kg), low (brain-average SAR 0.67 W/kg), and sham exposure, ENU-control, and cage-control groups. The heads of the rats in the exposure groups were locally exposed to electromagnetic waves for 1.5 hr/day, 5 day/week, and 2 years. The results obtained were (1) There were no effects of EMF on the survival rates; (2) No enhancement of tumor development by EMF was evident either in the brain or spinal cord; (3) Pituitary tumor development was reduced by EMF exposure. From these data, it was concluded that under the present experimental conditions, 1.5 GHz EMF exposure to the heads of rats for 2-year period did not accelerate ENU-initiated brain tumorigenesis. The 2nd study using IMT-2000 signal (W-CDMA) is now in progress. Preliminary results will be presented in the conference.

[1] Shirai, et al., Bioelectromagnetics, Vol.26, pp.59-68, 2005

**ELECTROPHYSIOLOGICAL PROPERTIES OF HIPPOCAMPAL SLICES FROM MICE EXPOSED TO ELECTROMAGNETIC FIELDS.** A. J. Smith, P. K. Harrison, G. Underwood, N. C. D. Mifsud, J. E. H. Tattersall. Biomedical Sciences Dept, Dstl Porton Down, Salisbury, Wiltshire, UK.

OBJECTIVE: Previous studies have suggested that *in vitro* exposure to 700MHz radiofrequency (RF) fields can affect both evoked and spontaneous electrical activity in rat hippocampal slices, an effect which lasted beyond the end of the exposure period (Tattersall et al, 2001). The aim of the present study was to determine whether *in vivo* exposure of mice to RF fields results in electrophysiological changes in brain tissue, using sensitive *in vitro* techniques. This work forms part of a larger study in which effects of the exposure on behaviour and gene expression are also being studied.

METHODS: Adult male C57BL mice (30-45g) were restrained in Perspex "rockets" and exposed to 400MHz TETRA, 900MHz GSM or 2200MHz UMTS signals or to equivalent unmodulated fields for 1 hour using a head-only loop antenna system. Sham-exposed control mice were treated in the same way,

but the RF signal was not switched on. Immediately following exposure, the mice were anaesthetised with halothane and decapitated, and parasagittal slices of brain tissue (300µm thick) containing the hippocampus were prepared. The slices were maintained at  $31.0 \pm 0.1^\circ\text{C}$  and perfused with oxygenated artificial cerebrospinal fluid. Extracellular field potentials were recorded in CA1 stratum pyramidale using glass microelectrodes filled with 2M NaCl. Responses were evoked every 30s by a concentric bipolar stainless steel stimulating electrode placed in stratum radiatum. Constant current pulses (100µs duration) were delivered at increasing intensities to characterise stimulus-response relationships for the field excitatory postsynaptic potential (fEPSP) and population spike (PS). These were also used to derive the E-S relationship between the fEPSP and PS. A paired-pulse protocol (two stimuli separated by 15, 25, 35, 50, 75 and 100ms) was used to characterise facilitation and inhibition of field potentials. Finally, the ability of the slice to express long term potentiation (LTP) was determined using theta burst stimulation: 5 trains of 4 pulses at 100Hz separated by 200ms, repeated twice with an interburst interval of 10s (Morgan and Teyler, 2001). LTP was evaluated by the change in fEPSP and PS 1 hour after theta burst stimulation and by the change in the E-S relationship. The investigators recording and analysing the slice data were blind to the exposure conditions for each animal.

RESULTS: No significant differences in any of the parameters measured were found between slices from sham exposed animals and those from animals exposed to 400MHz (20W.kg<sup>-1</sup>), 900MHz (36 W.kg<sup>-1</sup>) or 2200MHz (20W.kg<sup>-1</sup>) fields. DISCUSSION: The lack of any significant changes in hippocampal electrophysiology following exposure to radiofrequency fields is consistent with the absence of behavioural effects in mice exposed to the same fields in an identical system (Bottomley et al, 2004).

The work was supported by the Mobile Telecommunications and Health Research Programme but the views expressed are those of the authors. © Crown Copyright 2005, Dstl

#### REFERENCES

- Bottomley, A.L., Bartram, R., Blackwell, R.P., Haylock, R.G.E. and Sienkiewicz, Z.J. Effects of head-only exposure to radiofrequency fields on learned behaviour in mice. *Bioelectromagnetics Society Abstracts* 26: 260, 2004.
- Morgan, S. L. and Teyler T. J. Electrical stimuli patterned after the theta-rhythm induce multiple forms of LTP. *J. Neurophysiol.* 86: 1289–1296, 2001.
- Tattersall J. E. H., Scott I. R., Wood S. J., Nettell J. J., Bevir M. K., Wang Z., Somasiri N. P., and Chen X. Effects of low intensity radiofrequency electromagnetic fields on electrical activity in rat hippocampal slices. *Brain Res.* 904: 43-53, 2001

P-C-117

**50-HZ SINUSOIDAL MAGNETIC FIELDS (1 MT) DO NOT PROMOTE LYMPHOMA DEVELOPMENT IN AKR/J MICE.** A. M. Sommer, A. Lerchl. School of Engineering and Science, International Univ Bremen, Bremen, Germany.

BACKGROUND: Some epidemiological studies suggest that exposure to 50 or 60 Hz magnetic fields might increase the risk of leukemia, especially in children with a high residential exposure. In contrast, most animal studies could not find a correlation between magnetic field exposure and hematopoietic diseases. The presented study was performed to investigate if chronic, high (1 mT, 12 or 24 hours per day) magnetic field exposure had an influence on lymphoma development in a mouse strain that is genetically predisposed to thymic lymphoblastic lymphoma.

**OBJECTIVE:** To investigate experimentally whether 50 Hz magnetic field exposure (1 mT) influences lymphoma development in a mouse strain that is genetically predisposed to this disease.

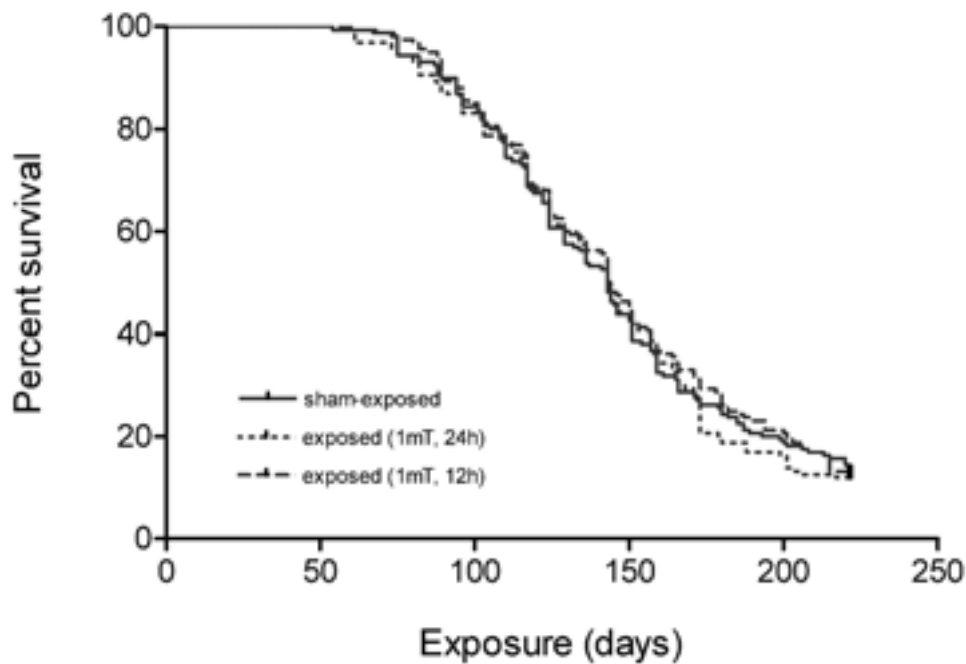
**METHODS:** Groups of 160 unrestrained female AKR/J mice were sham-exposed or exposed to sinusoidal 50 Hz magnetic fields at 1 mT for 12 or 24 hours per day, 7 days per week. Animals were visually checked daily for signs of developing disease and were weighed and palpated weekly to detect swollen lymph nodes. Starting at the age of 6 months, blood samples were taken twice monthly from the tail to perform differential leukocyte counts. Animals with signs of disease or with an age of about 44 weeks were sacrificed and a gross necropsy was performed.

The presence or absence of the magnetic fields was not known to the persons actually involved in the experiment (blinded design). This code was broken only at the end of the study.

**RESULTS:** Magnetic field exposure did not affect body weight, hematological parameters or lymphoma development in exposed versus sham-exposed animals.

**CONCLUSION:** These data do not support the hypothesis that exposure to sinusoidal 50 Hz magnetic fields is a significant risk factor for hematopoietic diseases, even at this relatively high exposure value.

This study was part of a project supported by the Bundesamt für Strahlenschutz, St. Sch 4323: "Beeinflussung der spontanen Leukämierate bei AKR-Mäusen durch niederfrequente Magnetfelder".



P-C-120

**EFFECT OF STRONG MAGNETIC FIELDS ON NERVE EXCITATION.** H. Tatsuoka<sup>1</sup>, Y. Eguchi<sup>2</sup>, S. Ueno<sup>2</sup>. <sup>1</sup>Research Center for Frontier Medical Engineering, Chiba Univ, <sup>2</sup>Dept of Biomedical Engineering, Graduate School of Medicine, Univ of Tokyo.

**Objective:** Recent technological developments in medicine, such as magnetic resonance (MR) imaging have increased human exposure to strong magnetic fields. This study investigated nerve excitation such as conduction velocity and refractory period and nerve fatigue of bullfrog sciatic nerve fibers exposed to 8T static magnetic fields (SMF).

Methods: The dissected sciatic nerve bundle of a bullfrog, *Rana catesbeiana*, was placed on platinum electrodes in an acrylic moist nerve chamber to measure compound action potentials (CAPs). The chamber was positioned at the center of a superconducting magnet (Oxford, U.K.), 100 mm in diameter and 700 mm long, which produced magnetic fields of up to 8T at its center. The ambient temperature in the magnet was maintained at  $24 \pm 0.2$  °C by circulating temperature-regulated water in a coiled tube. The nerve bundle was then selectively stimulated under a stimulus intensity of 4.0 mA-16.0 mA for a duration of 1.0 ms and exposed to 8 T SMF for the long axis of the nerve bundle parallel to magnetic field and the CAPs such as  $A_{\beta}$ -fiber (37 m/s),  $A_{\delta}$ -fiber (3.3 m/s) and C-fiber (0.5 m/s) were measured during 8T SMF exposure. The CAPs were measured for two groups, the control group (without SMF) and the exposed group (with SMF for 3 hours)

Results and Discussion: The experimental results show that 8T SMF enhanced the CAP of  $A_{\beta}$ -fiber in the relative refractory period by 10% but did not affect conduction velocity of  $A_{\beta}$ -fiber,  $A_{\delta}$ -fiber and C-fiber, and nerve fatigue of  $A_{\beta}$  fiber. These results indicate that SMF affect the threshold of excitatory membrane during refractory period, hypothesizing that channels associated with nerve fibers are affected by SMF. We need more experiments using rats to investigate the effects of SMF on the nerve function of human.

P-C-123

**DEVELOPMENT OF REAL-TIME MEASURING SYSTEM FOR BLOOD-BRAIN BARRIER FUNCTION AND ACUTE EFFECTS ON BBB FUNCTION BY RF EXPOSURE TO RAT BRAIN.** A. Ushiyama<sup>1</sup>, H. Masuda<sup>1</sup>, S. Hirota<sup>1</sup>, H. Watanabe<sup>2</sup>, K. Wake<sup>2</sup>, S. Watanabe<sup>2</sup>, M. Taki<sup>3</sup>, C. Ohkubo<sup>1</sup>. <sup>1</sup>Dept of Environmental Health, National Institute of Public Health, Saitama, Japan, <sup>2</sup>Biomedical EMC group, EMC center, Wireless Communications Dept, National Institute of Information and Communication Technology, Tokyo, Japan, <sup>3</sup>Dept of Electrical Engineering, Graduate School of Engineering, Tokyo Metropolitan Univ, Tokyo, Japan.

**OBJECTIVE:** Use of cellular phones is increasing dramatically. Concerns about possible biological and health effects of radio-frequency (RF) signals have been raised, although they are based on limited scientific evidence. Particularly, effect(s) on the blood-brain barrier (BBB) is a controversial issue. BBB prevents high molecular weight substances in the blood from getting into the brain, while nutrients and metabolites are allowed to pass the barrier. A few positive effects of RF exposure are reported, however, most results appear to be due to thermal effects and attempts to replicate studies have been unsuccessful. In these reports, histological approaches were examined, however, the time delay after RF exposure to specimen fixation may produce artifacts. Therefore, we set about to develop a real-time measuring system for blood-brain barrier function using a micro-perfusion method, which enables us to collect cerebrospinal fluid (CSF) continuously. Moreover, we examined high intensity RF exposure to rat brains and monitored albumin concentration in CSF during exposure.

**METHODS:** *Animals and surgical procedure* Experiments were performed on male Sprague-Dawley rats (8-12 weeks old). All surgical procedures were performed under sterile conditions. Anesthesia was initiated with a mixture of ketamine and xylazine (9:1). Rats were set on a stereotaxic instrument, and an incision was made in the rat's scalp to expose coronal sutures. A hole was made at 0.8 mm caudal and 1.3 mm lateral to the sagittal suture. A guide cannula (NG-8FS, Eicom Co., Kyoto) was introduced to the hole to reach one of the lateral ventricles and secured to the skull with acrylic dental cement. A dummy cannula (ND-8, Eicom Co.) was inserted into the guide cannula until experiment. At the end of experiment, Evans blue dye was injected into the lateral ventricle to confirm the placement of the cannula.

Experimental protocol After a 48hrs recovery period, rats were anesthetized, and a push pull cannula (NDP-I-8-01FEP, Eicom Co.) inserted into the guide cannula. The in-line and the out-line of cannula were connected to the push-pull pump unit (EP-70, Eicom Co.). At the beginning of RF exposure, FITC-labeled albumin was injected into caudal vein and CSF perfusion was started at a rate of 1  $\mu$ l/min. Fluorescence intensity of FITC-albumin in perfusate was monitored by spectrofluorometry (FP-6500, Jasco Co., Tokyo).

**RESULTS:** The sensitivity for FITC-albumin of this system was less than 1 ng/ml in CSF and sufficient to detect albumin leaked from blood into CSF. After 1,439 MHz RF exposure for 30 minutes at 35W/kg (average local SAR for brain) using a loop antenna, the fluorescence intensity increased indicating BBB function affected by RF exposure.

**CONCLUSION:** In this study, we developed a new system, which enables us to quantify BBB function in vivo with high sensitivity, and can be applied during exposure. Using this system, we detected leakage of albumin from blood under high dosage conditions. More detailed study is currently in progress.

## In vitro – cellular

P-C-126

### **CHARACTERIZATION OF CONNEXINS IN NEURONES SUBMITTED TO APPLIED EMF.**

M. J. Azanza<sup>1</sup>, M. Raso<sup>1</sup>, N. Pes<sup>1</sup>, R. N. Perez Bruzon<sup>1</sup>, C. Junquera<sup>1</sup>, C. Maeztu<sup>1</sup>, J. Aisa<sup>1</sup>, M. Lahoz<sup>1</sup>, C. Perez-Castejon<sup>1</sup>, C. Martinez Ciriano<sup>1</sup>, A. Vera Gil<sup>1</sup>, A. del Moral<sup>2</sup>. <sup>1</sup>Laboratorio de Magnetobiologia. Departamento de Anatomia e Histologia Humanas. Facultad de Medicina. Universidad de Zaragoza, Spain, <sup>2</sup>Laboratorio de Magnetismo. Departamento de Física de Materia Condensada. Facultad de Ciencias e ICMA. Universidad de Zaragoza, Spain.

**INTRODUCTION:** We have developed elsewhere a physical model which explains the ability of a sinusoidal magnetic field (AMF) to induce oscillatory, recruitment and eventual synchronizing activity in molluscan pacemaker neurones (1,2,3). Nonetheless we should take into account that the so called electric synapses could also be mediators of such an effect. We are trying to evaluate the relative contribution, of both parameters: magnetic field and gap-junctions in the synchronizing process.

**OBJECTIVES:** The objectives of this work were: 1) to characterize the expression of connexins and glial fibrillary acidic protein (GFAP) in control and exposed samples to ELF-AMF of *Helix aspersa* brain ganglia by immunostaining; 2) to study the ultrastructural interconnections with electron microscopy.

**METHODS:** The brain ganglia were placed between a pair of Helmholtz coils immersed in molluscs Ringer solution. The AMF exposure conditions were coincident with the ones applied to test the bioelectric activity (3) with exposure times of 30 min. The control samples were maintained in Ringer solution for times of 15min (Ha 104), 30min (Ha 114, Ha 12) and 60 min (Ha 109). The exposed samples were: Ha 16, 1mT, 4 Hz; Ha 24, 10  $\mu$ T, 8.3 Hz; Ha 30, 10  $\mu$ T, 217 Hz; Ha 54, 1 mT, 8 Hz. The immunocytochemistry (IC) EnVision® (DAKO) method was applied. Being the antisera specific for mammals there exists the possibility of a certain non-specific reaction, so that we are studying the expression of connexin 26 (Chemicon) (specific of neurons), enolase (Dako) (specific of neurons) and connexin 43 (Chemicon) and glial fibrillary acidic protein (GFAP, Dako), both specific for astrocytes.

Standard methods for electron microscopy (EM) have been used to study the the ultrastructural characteristics of the molluscs brain ganglia.

RESULTS: On Figure 1 (EM 3.500X) are shown two neurones surrounded by membrane expansions from glia cells. Figure 2 (EM 30.000X) is an amplified detail of Fig. 1, the arrows show gap-like junctions: neuron-glia and glia-glia. Figures 3 (Ha 54, 10x) and 4 (Ha 109, 60x) show the results for connexin 26 (IC). Fig. 3 shows the relative number of positive versus negative neurons for immunostaining in a section of 3  $\mu$ m. Two kind of positive cells have been observed: small size cells disposed near the neuropile (Figs 3 and 4) and typical neurones (3). We are trying to characterize the nature of the small cells with additional immunostaining reactions. As we compare the number of positive cells versus negative cells for connexin 26, from a total of 2500 cells it has been shown that for control samples the positive cells are the 4.9 % and for the exposed ones is the 3.4 %. A more detailed statistics study is in progress.

DISCUSSION. The oscillatory, recruitment and synchronizing activity has been observed from a 27 % of the experiments made (1,2,3). The number of neurons from which we have made the electrophysiological studies can be estimated to be around 120 neurones, being the studied neurons those which are placed at the surface of the ganglia. But the IC method has allowed us to explore and make the quantification from the whole brain ganglia. From the control samples it can be considered that during 60 min in Ringer solution, the neuron metabolic activity is maintained in good conditions since it is observed an increase of

connexin 26 expression (for 15 min, 4.15%; for 30 min, 5.02%; for 60 min, 5.4 %). In exposed cells, the number of positive cells drops to 3.4%. By comparing these data with the 27% out of 120 neurones showing oscillatory and recruitment activity, we could get to the conclusion that gap junctions have to been considered to participate to a minor extension, but can not explain by themselves the synchronizing process, which appears to be produced by the applied ELF-magnetic field.

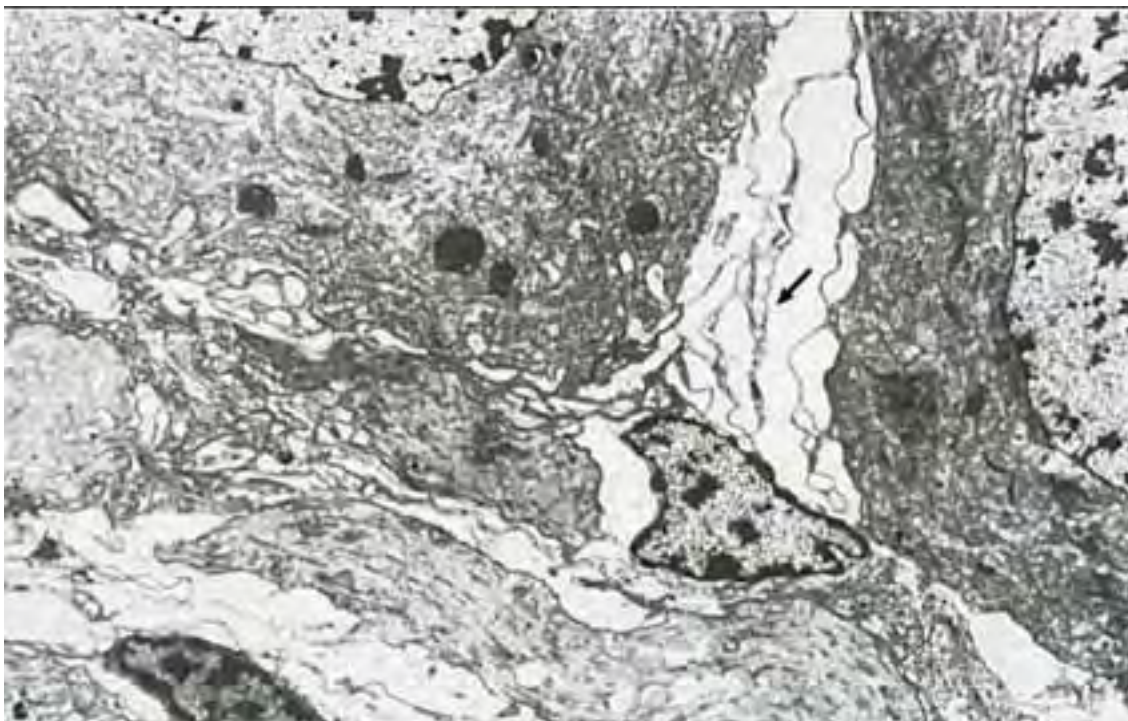


Figure 1

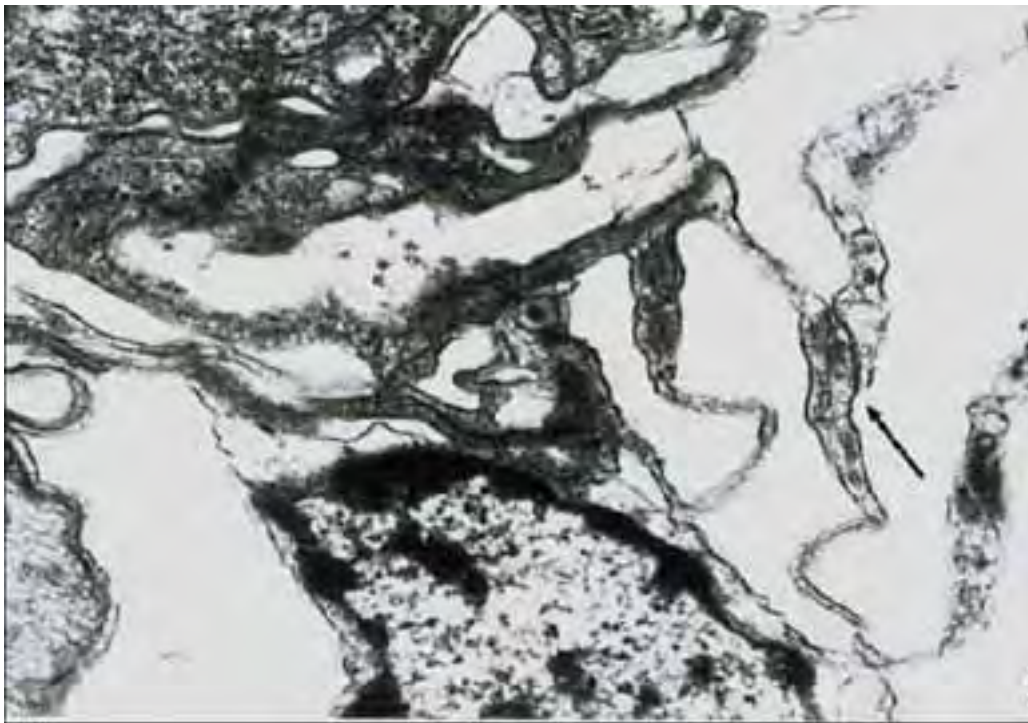


Figure 2

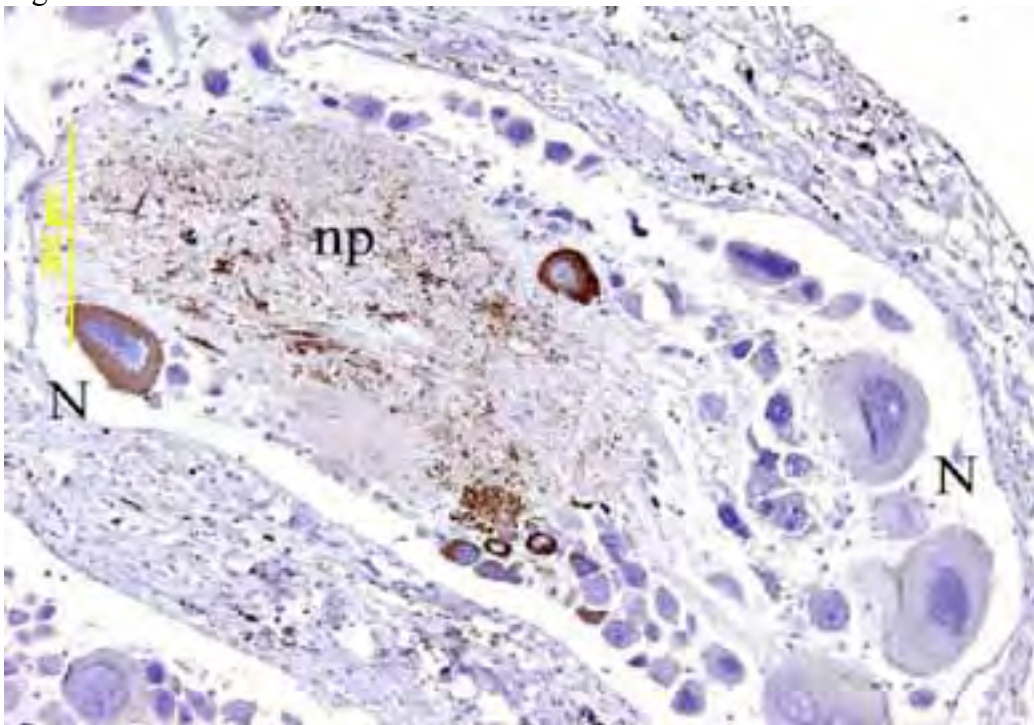


Figure 3

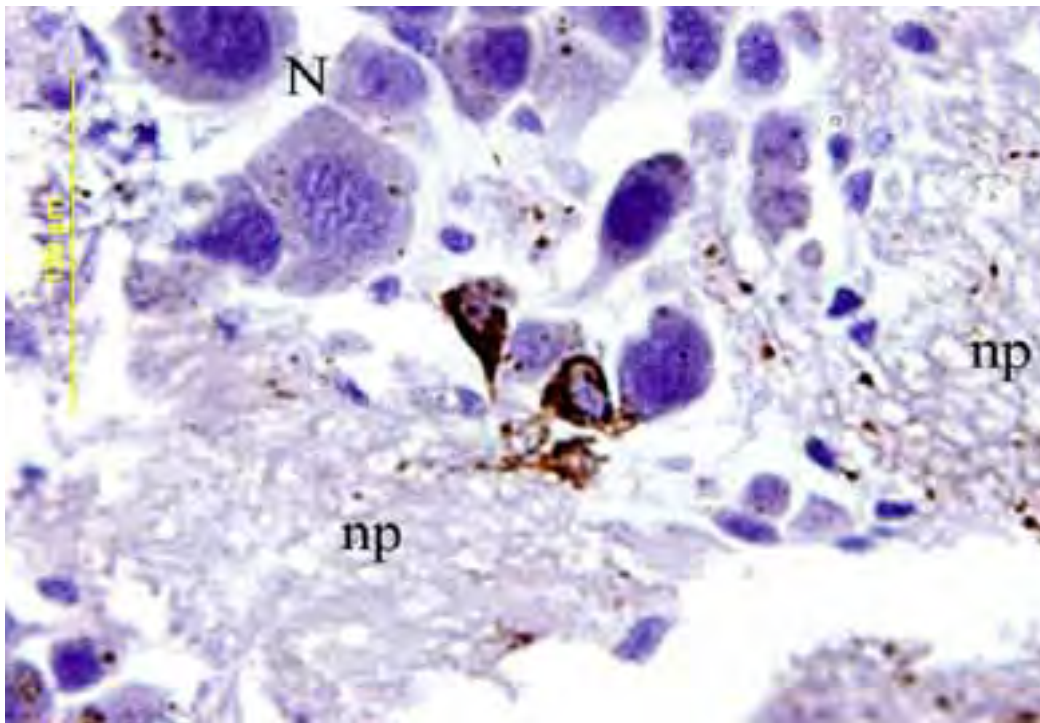


Figure 4

#### REFERENCES

- 1.- MJ Azanza, A del Moral. ELF-magnetic field induced effects on the bioelectric activity of single neurone cells. *J.Magn.Magn.Mat.* 177-181:1451-1452, 1998.
- 2.- M.J Azanza, AC Calvo, A.del Moral. Evidence of synchronization of neuronal activity of molluscan brain ganglia induced by alternating 50 Hz applied magnetic field. *Electromagn. Biol.Med.* 209-220, 2002.
- 3.- RN Pérez Bruzón, MJ Azanza, A.C.Calvo, A del Moral. Neurone bioelectric activity under magnetic fields of variable frequency in the range of 0.1-80 Hz. *J. Magn.Magn.Mat.* 272-276, 2424-2425,2004.

#### ACKNOWLEDGEMENTS

The authors are indebted to the PROFIT Project FIT 070000-2003-658 (Spanish Ministry of Science & Tecnology Spain), Project B-17-DGA (Diputación General de Aragon, Spain) and to the Project of the "Fundacion Humanismo y Ciencia" (Madrid, Spain)

P-C-132

**GENOME-WIDE ANALYZING OF THE RESPONSE TO 2-GHZ BAND W-CDMA MODULATED SIGNALS ALLOCATED TO MOBILE RADIO BASE STATIONS.** M. Sekijima<sup>1</sup>, H. Takeda<sup>1</sup>, H. Hirose<sup>1</sup>, N. Sakuma<sup>1</sup>, T. Nijima<sup>2</sup>, J. Miyakoshi<sup>3</sup>. <sup>1</sup>Mitsubishi Chemical Safety Institute, Ibaraki, Japan, <sup>2</sup>Hokkaido Univ, Japan, <sup>3</sup>Hirosaki Univ, Hirosaki, Japan.

**OBJECTIVE:** The aim of the present study was to see if any radio frequency (RF) fields exert their activity a variety of mechanisms, some of which are poorly understood, and to investigate the changes in the gene expression profile of four human cell lines following exposure to continuous wave (CW) and Wideband-Code Division Multiple Access (W-CDMA) RF fields at three field levels to assess the biological effects of low-level and long-term irradiation from a 2-GHz mobile radio base station.

**MATERIALS AND METHODS:** We used the in vitro exposure system with a horn antenna and dielectric lens in an anechoic chamber, which was developed by NTT DoCoMo [1]. Four human cell lines, A172 (glioblastoma, CRL-1620), H4 (neuroglioma, HTB-148), IMR-90 (normal fibroblasts from fetal lung, CCL-186), and CCD-25SK (normal fibroblasts from skin, CRL-1474), were obtained from American Type Culture Collection (ATCC, Rockville, MD). In all experiment reported here, cells were exposed for 24 hr period up to 96 hr to Specific Absorption Rate (SAR) of 80, 250 and 800 mW/kg with both CW and W-CDMA modulated signal RF fields, respectively. Microarray hybridization was performed using the Affymetrix GeneChip® Human Genome U133 Array using protocols described by Affymetrix, Inc. Data was analyzed using SiliconGenetics GeneSpring® 6.1 software.

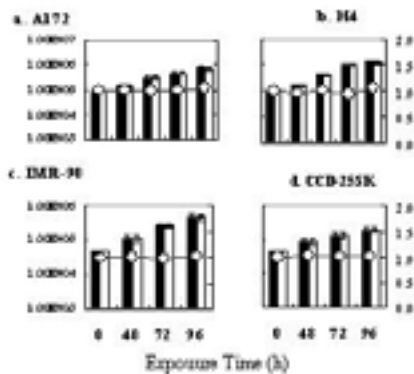
**RESULTS:** The temperatures were at  $37.0 \pm 0.5^{\circ}\text{C}$  in both the CW and W-CDMA experiments. No difference of cell morphological phenomenon was detected when the exposure took place during the period of incubation. No significant effects were detected between the sham and exposed cell growth ratio, viability and cell cycle profile after exposure in both the CW and W-CDMA of SAR up to 800mW/kg. Using the Affymetrix GeneChip® system, the inherent gene expression profile was observed in each cell lines. Two tumor cell lines and/or two normal cell lines were classified as family of cells closely related to gene expression profile. No marked difference between sham and RF exposed cells was observed in the gene expression profiles of individual tested conditions. Only a very small (

**CONCLUSIONS:** Our results confirm that long-term and low-level exposures to CW and W-CDMA 2.1425 GHz microwave did not affect the gene expression profile at the limit of whole-body average SAR levels on the basis of ICNIRP guidelines [2]. In conclusion, the long-term exposure for up to 96 hr to a mobile radio base station does not effect cell proliferation or the gene expression profile in human cells.

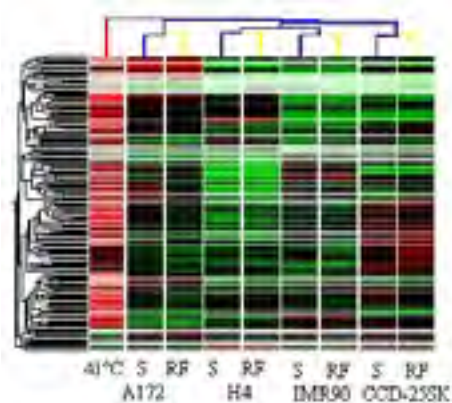
This work was supported by NTT DoCoMo Inc.

[1] Iyama et al., 2004. Large-Scale In Vitro Experiment System for 2 GHz-Exposure. *Bioelectromagnetics* 25, 599-606.

[2] ICNIPR, 1998. Guidelines for limiting exposure to time-varying electric, magnetic, and electromagnetic fields (up to 300GHz). *Health Phys* 74, 494-522.



Cell growth and proliferation ratio of a human cell lines exposed to 80 mW/kg W-CDMA modulated RF fields.



Comparison of gene expression results for the intersection of thermal stress regulated genes from A172 cells on the Affymetrix U133 platform.

P-C-135

**EFFECT ON DNA REPAIR GENES TRANSCRIPTION IN CULTURED CELLS OF 2.45 GHZ MICROWAVE EXPOSURE.** A. Perrin<sup>1</sup>, C. Bachelet<sup>1</sup>, C Fournier<sup>2</sup>, P. Leveque<sup>3</sup>, A. Collin<sup>3</sup>, A. Peinnequin<sup>3</sup>. <sup>1</sup>Molecular and Cellular Biophysics Unit of the Health Service Research Center for Defense (CRSSA), La Tronche, France, <sup>2</sup>Radiobiology and Inflammation Unit of the Health Service

Research Center for Defense (CRSSA), La Tronche, France, <sup>3</sup>Research Institut in Optic Communication and UMR, Limoges, France.

**OBJECTIVE :** The aim of the study is to investigate, in vitro, the effect of 2.45 GHz continuous (CW) and pulsed (PW) electromagnetic field exposure combined with a known mutagen agent on the induction of enzymes implicated in the DNA repair. Microwaves do not create bonds breaks within molecules and there is no clear hypothesis for a possible mechanism supporting a biological action. An indirect influence of microwaves during an intermediary step of the complex sequence of events involved in mutagenesis cannot yet be excluded.

Highly sensitive real-time RTqPCR was used to monitor transcriptional variations of DNA repair genes. The experiments were carried out using the monocyte human cell line THP1 with the mutagenic agent 4-nitroquinoline-N-oxide (4-NQO).

**METHOD :** The carrier frequency was 2.45 GHz CW and PW (1 kHz repetition time, 10 % duty cycle) with the same average power density. The power density allowed a SAR compatible with the ICNIRP exposure limits in the biological samples. Non exposed (sham) and exposed (PW and CW) cell culture plates (N=6 for each condition) were incubated simultaneously in three identical incubators in the presence of 4-NQO, under shaking, at 37°C. The incubators were integrated in three identical anechoic chambers equipped with waveguide antennas. The temperature inside the cell plates was measured with an optic fiber probe (Luxtron) and numerical dosimetry was calculated using the Finite Difference Time Domain method. Care was taken to increase the reproducibility of the experiments and to avoid false positive or misinterpretation of the results. The presence or the absence of the electromagnetic field was the only difference between the sham and exposed assays.

First, the genes implicated in DNA repair after 4-NQO treatment were screened using thematic human DNA repair GEMArray™ (SuperArray). Four targets dramatically modified at the transcriptional level were chosen : APEX, RAD 54, RAD52, MSH6. The expression of these genes normalised using geometric average of two internal control genes (PPIA and HPRT) was assessed using a LightCycler real-time PCR device (Roche).

Each experiment was reproducibly repeated 3 times. The electromagnetic field was applied alternatively in the three anechoic chambers in order to avoid cage effects.

The exposure power level was controlled and didn't induced temperature increases in the cell culture medium.

**RESULTS :** The RT-PCR quantification of target genes expression is currently in progress. The precise SAR value and final analysis of the results will be available at the time of the congress.

Research supported by the DGA (Delegation Generale pour l'Armement)

P-C-138 STUDENT WITHDRAWN

P-C-141

**EFFECTS ON APOPTOSIS AND OXIDATIVE STRESS ON JURKAT CELLS EXPOSED TO 50 HZ ELECTROMAGNETIC FIELDS.** R.Palumbo <sup>1</sup>, D.Capasso <sup>1</sup>, F. Brescia <sup>2</sup>, P. Mita <sup>2</sup>, M. Sarti <sup>2</sup>, F. Bersani <sup>3</sup>, M. Rosaria Scarfi' <sup>2</sup>. <sup>1</sup>CNR-Institute of Biostructure and Bioimaging, Naples, Italy, <sup>2</sup>CNR-

Institute for Electromagnetic Sensing of Environment, Naples, Italy, <sup>3</sup>Department of Physics, Univ of Bologna, Italy.

**OBJECTIVE:** To investigate the effect of 1 hour intermittent (5 min field on/10 min field off) exposure to 50 Hz electromagnetic field (powerline signal) on human T leukemia cells (Jurkat) by evaluating its influence on Reactive Oxygen Species (ROS) production and on apoptosis, either spontaneous and induced by anti Fas specific antibody (anti-Fas).

**METHODS:** Cells were cultured in complete RPMI-1640 medium and were subcultured every two days.  $2-3 \times 10^5$  cells/ml were seeded for ROS and apoptosis evaluation, respectively. The exposure system was kindly provided by the IT'IS-foundation (Zurich, Switzerland) and its characteristics have been described in details in Ivancsits et al (2002). All the parameters were continuously monitored by a computer, including magnetic flux density (1 mT) and temperature ( $37 \pm 0,5$  °C). In order to have blind exposures, the function generator was controlled by a computer to fix randomly the exposure/sham exposure condition. The experiments were carried out at frequency of 50 Hz, by applying a powerline signal which consists of 50Hz-components and their harmonics. The exposure was intermittent (5 min field on followed by 10 min field off) for 1 h (4 on/off cycles). Results were decoded following the analysis of the parameters investigated.

ROS formation was evaluated in exposed, sham exposed samples and positive controls (1h treatment with 500  $\mu$ M H<sub>2</sub>O<sub>2</sub>). The method that measures the conversion of 2'7'-dichlorofluoresceine diacetate (DCFH-DA) to dichlorofluoresceine (DCF) by ROS mediated oxidation was employed, as previously described (Zeni et al., 2004). Cell suspensions were analysed spectrofluorimetrically (Perkin-Elmer, LS50B) at an excitation wavelenght of 495 nm and an emission wavelenght of 530 nm. ROS concentration was expressed in arbitrary units (DCF/mg total proteins). To evaluate apoptosis, caspase-3 activity was measured. EMF-exposed and sham exposed samples were incubated for 6h with or without anti-Fas (50 ng/ml) and the activity was evaluated spectrofluorimetrically as previously reported (Russo et al., 2003) and specific activity was calculated as nanomoles of amino-4-trifluorometyl coumarin (AFC) produced/min/ $\mu$ g proteins at 37°C.

**RESULTS:** Our results suggest that one hour intermittent (5 min field on/10 min field off) exposure does not affect ROS formation, while a 63% increase over sham exposed cultures was detected in positive controls (two tailed paired Student's t test:  $P < 0.01$ ), as expected. Concerning Caspase-3 activity, a slight but statistically significant decrease (16%) of spontaneous apoptosis was observed ( $P > 0,05$ ). In addition, a reduction of anti-Fas induced apoptosis was also detected (22%).

**CONCLUSION:** Our findings are in agreement with data reported in literature on the decrease in spontaneous apoptosis when transformed cells are exposed to 50 Hz ELF EMFs (Simko et al., 1998; Tofani et al, 2001).

#### REFERENCES

- Zeni O et al. (2004). Toxicology Letters, 147, 79-85  
Ivancsits S et al. (2002). Mutation Res., 519, 1-13  
Simkó M et al. (1998). Bioelectromagnetics, 19, 85-91.  
Tofani S et al. (2001). Bioelectromagnetics, 22, 419-428.

P-C-144

**THE EFFECTS OF LONG-TERM EXPOSURE TO EXTREMELY LOW FREQUENCY MAGNETIC FIELDS ON INSULIN SECRETION.** T. Sakurai<sup>1</sup>, S. Koyama<sup>1,2</sup>, Y. Komatsubara<sup>1,3</sup>, J. Wang<sup>1</sup>, J. Miyakoshi<sup>1</sup>. <sup>1</sup>Dept of Radiological Technology, School of Health Sciences, Faculty of Medicine, Hirosaki Univ, Hirosaki, 035-8564, Japan, <sup>2</sup>Dept of Interdisciplinary Environment, Graduate

**INTRODUCTION:** Recently, we have demonstrated that exposure to ELFMF for 1 h decreased insulin secretion from the rat insulinoma cell line, RIN-m. In insulin secreting cells, it is known that there are differences between proteins related to insulin secretion with short-term versus long-term glucose stimulation. Therefore, the effects of long-term ELFMF exposure on insulin secretion are thought to be different from those of short-term exposure.

**OBJECTIVE:** The objective of this study was to evaluate the effects of long-term (1-5 days) exposure to ELFMF on glucose-stimulated insulin secretion. **METHODS:** We stimulated the hamster-derived insulin secreting cell line, HIT-T15, with glucose under exposure to ELFMF or sham-exposure conditions for 1 or 5 days, using our established system for the exposure of cultured cells to the ELFMF (a sinusoidal vertical magnetic field at a frequency of 60 Hz and a magnetic density of 5 mT). The effects of ELFMF were assessed by the amount of insulin secreted during exposure.

**RESULTS:** The effects of long-term exposure to ELFMF on insulin secretion were variable, depending on the culture period, and the concentration of glucose in the culture medium. In the absence of glucose stimulation, insulin secretion increased following exposure to ELFMF for 1 day (Figure 1A). Under glucose-stimulation (100 mg/dL glucose), the exposure to ELFMF for 5 days enhanced insulin secretion (Figure 1B).

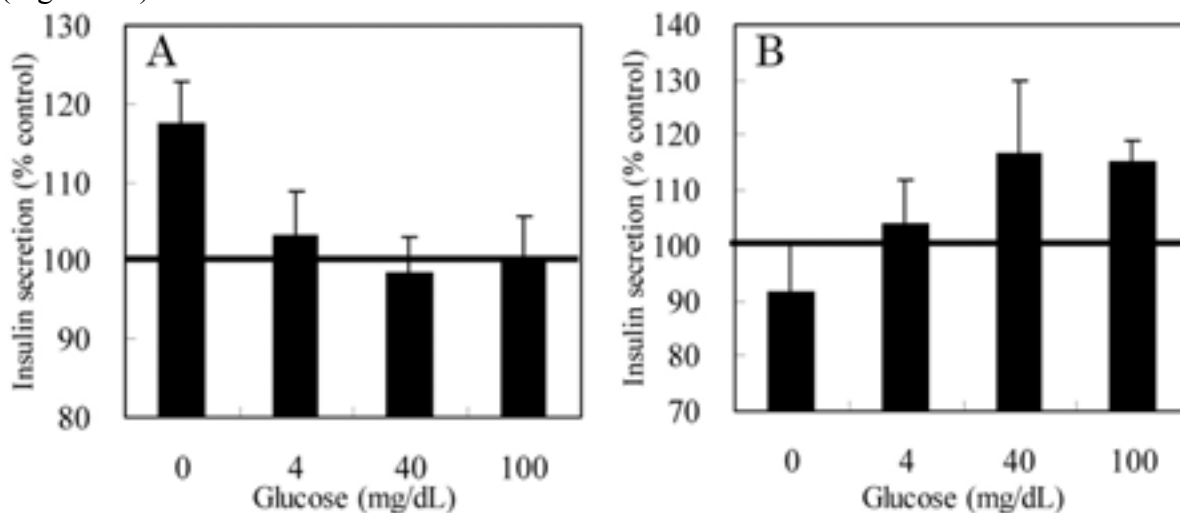


Figure 1. The effects of long-term exposure (A; for 1 day, B; for 5 days) to ELFMF on insulin secretion from HIT-T15 cells in the presence of various concentrations of glucose. Data are presented as the ratio of insulin secretion under ELFMF conditions to that under sham exposure conditions.

**CONCLUSION:** Long-term exposure to ELFMF enhanced insulin secretion differently according to the duration of exposure and the concentration of glucose in culture medium.

P-C-147

**DIELECTRIC CHARACTERIZATION OF BACTERIAL CELLS USING DIELECTROPHORESIS.** A. Sanchis<sup>1</sup>, M. Sancho<sup>1</sup>, J. L. Sebastian<sup>1</sup>, S Munoz<sup>1</sup>, J. M. Miranda<sup>1</sup>, A. Brown<sup>2</sup>. <sup>1</sup>Departamento de Física Aplicada III. Universidad Complutense. Madrid. Spain, <sup>2</sup>Cell Analysis Ltd., York, Berkshire, U.K.

Introduction: Dielectrophoresis (DEP) is the movement of particles in nonuniform electric fields caused by polarization effects. DEP has been exploited at increasing rate for a variety of applications including manipulation, separation and concentration of biological cells. Less attention has been paid to the potential of DEP as an analytical technique capable of providing measurement of the electrical parameters of cell compartments. These parameters, permittivity and conductivity, are related to important physiological characteristics. In this work we show the usefulness of simple dielectrophoresis measurements combined with realistic numerical modelling, to extract significant information about the electrical properties of Gram-negative and -positive bacteria.

## Methods

Experimental. The experiments were performed on *E. coli* ATCC 25922 and *Staph. aureus* ATCC 29213 strains. Bacteria from isolates cultures were centrifugated and re-suspended in deionised water to reduce the conductivity of samples. The bacterial suspension was re-circulated through a small chamber with a set of parallel microelectrodes. A signal generator was triggered to produce a sine wave of 12 V for 5 s. Positive DEP action caused aggregation of cells upon electrodes. Upon cessation of the field, the cells were released and immediately enumerated by image analysis. The procedure was repeated from 10 kHz to 50 MHz, producing a dielectrophoretic spectrum.

Numerical modelling. In order to deduce values for the parameters of cell compartments, a physical model of the bacterial cell is needed. Gram-negative and -positive bacteria differ in their structural organization. Gram-positive bacteria have a thick cell wall, composed of peptidoglycan with some polymers covalently attached. In contrast, Gram-negative bacteria have a more complex cell envelope with an outer membrane, a thin peptidoglycan wall and a periplasmic space. Our modelling takes into account the shape – rod like for *E. coli* and spherical for *Staph. aureus* – and different compartments of the cell and uses a modified BEM approach to obtain its polarization properties. This numerical technique is based on the solution of an integral equation for the induced charge density at each dielectric interface and provides an accurate prediction for the overall polarizability of the cell.

A theory relating cell collection and dielectric polarizability of each cell is also needed. We have extended early models developed by Pohl for cylindrical and spherical electrode geometry to the case of parallel bar electrodes and shown that yield collection is proportional to the 1/2 power of the effective polarizability of cells for this type of electrodes.

Results DEP collection spectra obtained for *E. coli* and *Staph. aureus* bacteria in buffered suspending media are shown in Fig. 1. Curve fittings of these spectra are also shown and give dielectric permittivity and conductivity for each of the different cell compartments. These results, together with those obtained for these micro-organisms by other authors, using different methods, are shown in Table I.

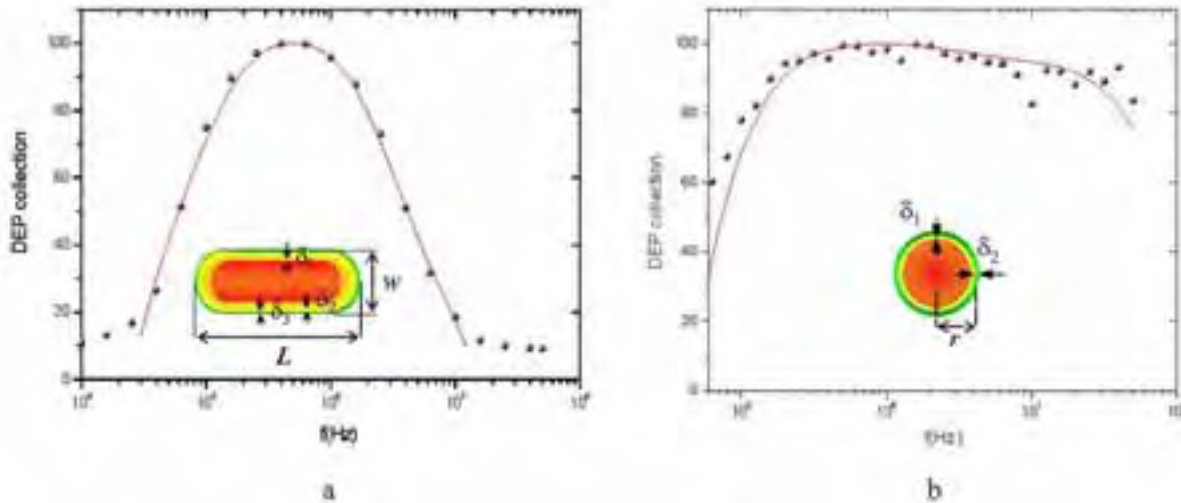


Figure 1. Fitting of experimental data of DEP collection of E. Coli and S. Aureus bacteria. Dielectric models of such particles in each case are shown. (a) E. Coli is modelled as a three shelled rod-like particle, with  $L = 3.35 \mu\text{m}$  and  $w = 0.82 \mu\text{m}$ , composed of cytoplasm, plasma membrane with thickness  $\delta_1 = 8 \text{ nm}$ , wall with  $\delta_2 = 15 \text{ nm}$ , and capsule with  $\delta_3 = 8 \text{ nm}$ . (b) S. Aureus is modelled as a spherical particle of radius  $r = 0.6 \mu\text{m}$  with two shells: plasma membrane, of thickness  $\delta_1 = 8 \text{ nm}$  and wall with  $\delta_2 = 20 \text{ nm}$ .

	<i>Escherichia Coli</i>						<i>Staphylococcus Aureus</i>			
	Asami [1]		Suehiro [2]		Fit values		Johari [3]		Fit values	
	$\epsilon / \epsilon_0$	$\sigma(\text{S/m})$	$\epsilon / \epsilon_0$	$\sigma(\text{S/m})$	$\epsilon / \epsilon_0$	$\sigma(\text{S/m})$	$\epsilon / \epsilon_0$	$\sigma(\text{S/m})$	$\epsilon / \epsilon_0$	$\sigma(\text{S/m})$
cytoplasm	61	0.19	60	0.1	60	0.07	Insens.	0.2	60	0.8
plasma membrane	10.8	5E-8	10	5E-8	10.8	5E-8	4.5	5E-8	16	5E-8
wall	60	0.68	60	0.5	60	0.5	Insens.	0.3	60	0.01
capsule	-	-	-	-	10	1E-6	-	-	-	-
external medium	80	0.121	80	2E-4	80	2.7E-3	80	1E-3	80	2.5E-3

Table 1. Electrical parameters of E. Coli and S. Aureus, obtaining by fitting DEP collection spectra, compared with values reported in the literature for the same or similar bacteria.

As shown, our fit is better for Escherichia than for Staphylococcus, especially in the low frequency region, probably due to electrode polarization influence or to the presence of a dielectric dispersion effect not included in the present model. Values for conductivity and permittivity of the different cell compartments deduced by our method are in broad agreement with those found in literature. Our model for Escherichia, considering three shells and a rod-like shape, is more realistic than those previously used, based on spherical or ellipsoidal particles with a confocal layer. Our model for Staph. Aureus, a two-shelled sphere, is similar to that used by Johari for Staph. Epidermis, another Gram positive bacteria closely related with the first one. However, we obtained fits sensitive to the parameter values in all cases and considerable differences for the cytoplasm and wall conductivity values. These differences may be due to different values of electrical properties between the two species (Staph. Aureus is known to be more pathogenic than Staph. Epidermis, what may be reflected in their respective electrical properties)

or to error sources in the experimental method, to be investigated. Conclusion As described here, combination of measurement of dielectrophoretic collection spectra and realistic cell modelling can be used to obtain values of the electrical properties of bacteria. This characterization is fast and non-invasive and open a wide range of applications, for example, the selective identification of species or the analysis of the action of specific chemical or physical agents on bacterial samples. Acknowledgement Financial support from a EU grant (QLK2-CT-2001-70561 RASTUD) is gratefully acknowledged.

Bibliography [1] K. Asami et al., *Biophys. J.*, 31 (1980) 215-228. [2] J. Suehiro et al., *J. Electrostatics*, 57 (2003) 157-168. [3] J. Johari et al., *Phys. Med. Biol.* 48 (2003) N193-N198.

P-C-150

**EFFECTS OF DAMPS 835 MHZ SIGNALS ON ORNITHINE DECARBOXYLASE ACTIVITY IN LIVE L-929 MOUSE FIBROBLASTS.** M. Taxile<sup>1</sup>, B. Billaudel<sup>1</sup>, G. Ruffie<sup>1</sup>, N. Nikoloski<sup>2</sup>, J. Schuderer<sup>2</sup>, N. Kuster<sup>2</sup>, I. Lagroye<sup>1</sup>, B. Veyret<sup>1</sup>. <sup>1</sup>Bioelectromagnetics Laboratory / UMR 5501, EPHE / PIOM-ENSCPB, Pessac, France., <sup>2</sup>IT'IS Laboratories, Zurich, Switzerland.

**OBJECTIVES:** The ornithine decarboxylase (ODC) enzyme plays a pivotal role in the synthesis of polyamines that are essential for cell growth. The Litovitz group had reported a temporary increase in ODC activity in L929 fibroblasts after exposure to modulated RF microwaves emitted by mobile phones(1) in contrast to continuous wave (CW) signals. Such an increase in ODC activity might indicate that RF act as a non-genotoxic carcinogen. As part of the Perform-B programme, the investigation of ODC in live cells, instead of a strict replication of the Litovitz experiments as first planned, was intended as a more physiological approach of ODC enzyme activity

**METHODS:** L-929 cells, cultured in EMEM medium, were plated in 5 ml DMEM medium at a density of  $3 \times 10^6$  cells in 25 cm<sup>2</sup> flasks. Following a 20-h incubation, the cells were blindly sham exposed or exposed for 7 hours inside TEM Crawford cells (IT'IS, Zurich, Switzerland) to 50 Hz modulated DAMPS-835. Immediately after exposure, cells were maintained in 25 cm<sup>2</sup> flasks, and kept in 1.5 ml DMEM medium. Then, DMEM medium (100  $\mu$ l), supplemented with  $2.22 \times 10^5$  d.p.m. <sup>14</sup>C-labeled L-ornithine and 0.04 mM unlabeled L-ornithine was added and flasks were closed and incubated for 2 hours. Thereafter, the <sup>14</sup>CO<sub>2</sub> generation by ODC was terminated by addition of 20% aqueous trichloroacetic acid through a needle inserted through the rubber septum and <sup>14</sup>CO<sub>2</sub> trapping pursuit for an additional 1 h. The center well was then transferred to a scintillation vial containing Pico-Fluor (Packard) and counted by liquid scintillation. The amount of protein of cell lysate was determined by the Bradford method in matched experiments run in parallel. Total ODC activity was calculated as generated dpm <sup>14</sup>CO<sub>2</sub>/h/mg and expressed as exposed/sham ODC ratios. The Wilcoxon matched-pairs test was used when looking at differences between sham and exposed cells in the same exposure run.

**RESULTS:** Using live L-929 fibroblast cells, no significant modification of ODC activity was observed for all tested exposures to DAMPS-835 at a SAR 2.5 W/kg. Under the experimental conditions used by the Litovitz group (L-929 cells, 8 hours DAMPS-835 exposure at 2.5 W/kg) there was a 40% increase in ODC activity, but according to the dosimetry performed by Kuster and co-workers(2), the real exposure conditions used by Litovitz and colleagues corresponded to 5.7 W/kg and resulted in a temperature increase of 0.78°C. Using this SAR value on L-929 cells with active fans in the setup, no significant modification of ODC activity was observed.

**CONCLUSION:** Exposure of live L-929 cells to DAMPS-835 had no influence on ODC activity. These data are in good agreement with those recently published by Owen and co-workers at FDA(3) and our Perform-B Finish partner(4) using lysed cells. All together, these results do not agree with the previous

observations of the Litovitz group using a Crawford cell exposure system and measuring ODC activity after cell lysis(1). The present data do not support the possibility of neoplastic transformation via an effect of ODC activity induced by RFR.

#### REFERENCES:

- (1) Penafiel et al., 1997, *Bioelectromagnetics*, 18, 132-141.
- (2) Nikoloski et al., 25th Annual Meeting of the Bioelectromagnetics Society, June 2003, Maui, USA, p. 52.
- (3) Desta et al., 2003, *Radiation Research*, 160, 488-491.
- (4) Höytö et al., Biological effects of electromagnetic fields-Workshop 2004, Kos, Greece.

This work was supported by the MMF and the GSM Association, the Aquitaine Council for Research and the CNRS.

P-C-153

**INFLUENCE OF DIFFERENT INCUBATOR MODELS ON MAGNETIC FIELD –INDUCED CHANGES IN NEURITE OUTGROWTH IN PC-12 CELLS.** M. A. Trillo<sup>1</sup>, A. Ubeda<sup>1</sup>, S. G. Benane<sup>2</sup>, D. E. House<sup>3</sup>, C. F. Blackman<sup>4</sup>. <sup>1</sup>Dept. Investigacion, Hospital Ramon y Cajal, Spain, <sup>2</sup>Wendell, NC, USA, <sup>3</sup>Durham, NC, USA, <sup>4</sup>National Health & Environmental Effects Research Lab, EPA, Res. Tri. Park, NC, USA.

**OBJECTIVE:** Devise a method to standardize responses of cells to magnetic field (MF)-exposure in different incubator environments.

**METHODS:** We compared the cell responses to generated MF in a standard cell-culture incubator (Forma, model #3158) with cell responses to the same exposure when a mu-metal box is in the incubator to shield the cells from EMF generated outside the box. A standard assay of neurite outgrowth (NO) from NGF-stimulated, primed PC-12 cells was used to explore the effects of 23 hours of exposure to magnetic fields (e.g., Blackman et al., 1994). The cells were exposed to a 45-Hz, ac, vertical magnetic field (Bac) over the flux density range of 12.0-31.0 mGrms [1.20-3.10 microTrms]. The Bac was parallel to a dc MF (Bdc) of 29.7 mG [2.97 microT], with a perpendicular Bdc < 2.0 mG [0.20 microT]. These MF exposure conditions are predicted by the IPR model (Blanchard and Blackman, 1994) to produce the maximal reduction in NO under resonance conditions for hydrogen ions. Exposures of the cells to MF were performed under two conditions: with and without a mu-metal box in the incubator. These results were compared to those reported for similar exposures (Trillo et al., 1996; Blackman et al., 1999) using an older incubator (Forma, model #3156).

#### RESULTS:

The experimental results using the model #3158 incubator showed the expected U-shaped inhibitory response function with a peak of no inhibition at the general center of the response (Trillo et al., 1996). However, the ac MF flux density for the center of the response was shifted from a 2Bacpk/(Bdc) value of 1.70 (seen using the model #3156 incubator) to 2.12, and the response shape was distorted at higher values. When the mu-metal box was in the model #3158 incubator, the cell response returned to the original values observed using the older incubator (model #3156).

#### DISCUSSION:

We report that different models of a manufacturer's incubators can alter some cell responses to MF. One major distinction between the two incubator models we tested is the circuitry used to maintain a given temperature. In the older incubator, Forma model #3156, the heater current was either on or off to maintain temperature. In the newer incubator, Forma model #3158, a proportional heater circuit clips the

60-Hz sine wave into on-off segments that change as the temperature approaches the set point. A clipped sine wave could introduce higher frequency fields to the incubator chamber. Although the cause and implications of this result were not pursued further, a likely explanation for our results is that the additional EMF introduced by the proportional heating circuit interfered with the cell responses to the low-intensity ac MF we used. It should be noted that there was no detectable difference in cell response between the two incubator types when approximately 10-fold higher-intensity ac MF were used (e.g., Blackman et al., 1994, 1996). Our results show the mu-metal box provided satisfactory shielding from the causative agent, presumably the proportional heater circuit. This report is a warning for scientists to avoid additional sources of EMF in exposure systems because any results could be hard to interpret and to be duplicated elsewhere.

Authors received Spanish support (AU, MAT) by Fondo de Investigacion Sanitaria (BAE 92/5044 and BAE 92/5045), EPA support (CFB, SGB, DEH), and DOE support (CFB, SGB), IAG# DE-AI01-89CE34024 and DE-AI01-94CE34007. This abstract does not necessarily reflect the policy of EPA or other support organizations. Mention of specific vendors and equipment does not constitute endorsement for use.

P-C-156

**DNA DAMAGE IN CULTURED HUMAN LEUKOCYTES FOLLOWING 24 H INTERMITTENT RADIOFREQUENCY EXPOSURE AT 1950 MHZ UMTS SIGNAL.** O. Zeni<sup>1</sup>, A. Schiavoni<sup>2</sup>, A. Perrotta<sup>1</sup>, D. Forigo<sup>2</sup>, M. Rosaria Scarfi<sup>1</sup>. <sup>1</sup>CNR- Institute for Electromagnetic Sensing of Environment (IREA), Napoli, Italy, <sup>2</sup>Telecom Italia, Torino, Italy.

**OBJECTIVE:** The objective of this study is to evaluate the ability of 1950 MHz universal mobile telecommunication system (UMTS) signal to induce DNA damage in cultured human blood leukocytes, using the alkaline single-cell gel electrophoresis (SCGE) / Comet assay.

**METHODS:** We used blood from healthy adult donors, and unstimulated (Go phase) whole blood cultures were established, in order to expose synchronized cell population, to prevent interferences due to the different phases of cell cycle. For each donor, four conditions were considered: negative control (incubator), positive control (2 h treatment with Methylmethanesulfonate, MMS, at 150  $\mu$ M final concentration), radiofrequency (RF) exposure and sham exposure. To obtain duplicate samples for each condition, 8 cultures were set up in 25 ml pyrex flasks. Exposures were performed in a TEM cell IFI CC110SEX hosted in an incubator, opportunely equipped to maintain constant the temperature, supplied by a feeding and controlling line to get well defined exposure condition. Sham exposures were performed in a completely equivalent exposure set-up, except for the presence of the radiofrequency power, and hosted inside the same incubator. Computational dosimetry was used to establish the exposure conditions of the cell cultures. 24 h exposures were conducted in intermittent modality with 6 min. RF on and 2 h RF off at Specific Absorption Rate (SAR) of 2.2 W/kg. DNA damage was quantified immediately after RF exposure using the alkaline comet assay. For each culture, 2 slides were prepared as previously described [1], and three parameters (percentage DNA in tail, Comet Moment and Tail Moment) were analyzed to assess DNA damage for each nucleus, by means of a computerized image analysis system (Delta Sistemi, Rome, Italy), fitted with a Leica DM BL fluorescence microscope at 250 X magnification. A total of 300, randomly selected, nuclei were scored for each culture (150 from each of two replicate slides) and, for each parameter, the results were reported as mean values of the replicate cultures for each donor.

**RESULTS AND CONCLUSIONS:** To date we present only preliminary results obtained on samples, from 2 healthy donors, intermittently exposed for 24 h to 1950 MHz UMTS signal. As shown in table 1, each of the parameters studied does not exhibit significant difference in RF exposed samples with respect to sham exposed ones, even if statistical analysis has not been performed due to the esiguous number of donors employed. On the contrary, as expected, MMS treatment induces a consistent DNA damage. In conclusion, these very preliminary findings, if validated on a larger number of donors, extend and confirm our previous results showing, in the same experimental conditions, absence of micronucleus formation in human lymphocytes stimulated to divide post exposure (manuscript submitted). It is interesting to note that, at our knoweledge, there are no data, published in peer reviewed journals, on the induction of genotoxic effects following RF exposure to the forthcoming third generation UMTS signal.

## References

[1] Zeni O, Romanò M, Perrotta A, Lioi MB, Barbieri R, d'Ambrosio G, Massa R, Scarfi MR. Evaluation of genotoxic effects in human peripheral blood lymphocytes following an acute in vitro exposure to 900 MHz radiofrequency fields. *Bioelectromagnetics*, in press.

## Acknowledgements

This work was fully funded by TIM – Telecom Italia Mobile.

**Table 1-** DNA damage in cultured human leukocytes following 24 h intermittent exposures to 1950 MHz UMTS signal (2.2 W/kg). Data related to negative (incubator) and positive (MMS, 150 µM) controls are also reported.

	<b>RF Exposed</b>	<b>Sham-exposed</b>	<b>Incubator</b>	<b>MMS</b>
<b>Tail DNA %</b>	0.64 ± 0.16	0.67 ± 0.18	0.53 ± 0.24	19.60 ± 3.90
<b>Comet Moment</b>	0.56 ± 0.13	0.52 ± 0.07	0.51 ± 0.11	10.38 ± 1.89
<b>Tail Moment</b>	0.15 ± 0.07	0.14 ± 0.04	0.12 ± 0.05	7.75 ± 1.91

Each data point represents the mean ± SE for 2 healthy donors.

## In vitro – tissue and organ

P-C-159 STUDENT

**A REAL-TIME EXPOSURE SYSTEM FOR ELECTROPHYSIOLOGICAL RECORDINGS FROM BRAIN SLICES: DESIGN AND REALIZATION.** M. Pellegrino<sup>1</sup>, A. Paffi<sup>1</sup>, R. Beccherelli<sup>2</sup>, M. Liberti<sup>1</sup>, F. Apollonio<sup>1</sup>, G. D'Inzeo<sup>1</sup>. <sup>1</sup>ICEmB @ Dept of Electronic Engineering, “La Sapienza”, Univ of Rome, Rome, Italy, <sup>2</sup>Consiglio Nazionale delle Ricerche, Istituto per la Microelettronica e Microsistemi, Sezione di Roma, Rome, Italy.

**OBJECTIVES:** Brain slices are considered as appropriate structures for evidencing of possible changes induced by electromagnetic (EM) fields in the coordinate activity of neuronal networks related to high cognitive functions, such as memory and learning [1]. As a consequence, experimental investigations on

hippocampal slices have been widely increased [2, 3]. Purpose of this work is to make possible real-time electrophysiological recordings from brain slices in the whole frequency band used in telecommunication standards. Moving from the structure for patch-clamp experiments described in [4], a suitable exposure system has been designed and fabricated.

**METHODS:** The referred EM structure is the same described in [4]: a coplanar waveguide (CPW), with a glass substrate and three metalizations. Compared with other exposure systems already existent for electrophysiological recordings from brain slices [2, 3], the open structure and the transparent substrate permit reduced dimensions and guarantee an easy access to the sample. Furthermore, being the E field lines almost parallel to the CPW surface [5], the interferences between the field and the electrodes are minimized. Referring to Fig.1, the dimensions of the slice (cylinder of radius equal to 0.4 cm and height of 0.04 cm) forced to have the two openings (slots) between the central conductor and the lateral ones (where cells are monitored) at least 0.8 cm wide, in order to expose the whole sample to an almost uniform field. Since slots of such dimensions could have worsened the CPW performances, in terms of confinement of the fields on the openings [5, 6], an in-depth theoretical and numerical study has been conducted. The structure and its main dimensions are reported in Fig.1, with the biological samples on it. Two perfused chambers containing the slices, one for each slot, must be used in order to maintain the symmetry of field distribution. In summary, the global (experimental and EM) features for the system are:

- a transparent dielectric substrate for the lighting of the biological sample (chosen: glass),
- an easy access to the sample,
- a high efficiency value, in terms of induced SAR for 1 W of net incident power,
- a uniform distribution of the fields in the slice for the whole operating range of frequencies,
- low EM coupling of the structure with the laboratory equipment,
- minimum radiation losses,
- impedance matching with a feeding coaxial cable.

**RESULTS:** Numerical characterization has been conducted with the commercial software Ansoft HFSS 9.1. Results for the simulated scattering parameter  $S_{11}$  are reported in Fig.2, where the value of  $|S_{11}|$  is always less than - 11 dB. In order to evaluate the EM coupling of the CPW with the laboratory equipment, the E field decay has been evaluated in the whole frequency range, along a vertical line passing through the center of one of the exposure zones. In Fig.3 results are shown only for 900 MHz, which has been considered as worst case representative. As evident from the figure, the E field reaches the 10% of its maximum amplitude at the distances of 2.12 cm below and 1.9 cm above the structure, so a minimum interference occurs with objects distant more than 2 cm from the CPW surface. Results for E field homogeneity in the sample at 900 MHz and 1800 MHz are reported in Tab.I, showing good homogeneity for both frequencies. The worst values occur along the x axis due to losses in the sample that make the field to decay more rapidly along its own propagating direction. The worsening at 1800 MHz (Tab.I) was expected, because of a higher concentration of the fields close to the slots and a greater dissipation in the sample. The efficiency of the system has been numerically estimated at 900 and 1800 MHz. For both frequencies, the average value in the sample is quite high and homogeneous:  $49.86 \pm 1.04$  (W/kg)/W at 900 MHz, and  $71.08 \pm 1.16$  (W/kg)/W at 1800 MHz. Finally, the chosen CPW has been manufactured by photolithographic process. A carefully cleaned soda-lime glass plate is used as substrate. On this, a uniform stack of aluminum (500 nm approximately) and chromium (200 nm approximately) has been evaporated in vacuum. They provide high conductivity and mechanical ruggedness, respectively. Then a positive type photoresist layer has been spin-coated, baked, UV exposed through a photolithographic mask and developed. Unprotected chromium and aluminum have been sequentially wet etched in suitable chemical baths.

**CONCLUSIONS:** An exposure system for real-time electrophysiological recordings from brain slices has been designed, fabricated and characterized. The system is based on a CPW operating from 0.8 up to

2 GHz, and it presents low coupling with laboratory equipment, good homogeneity of the E field in the sample, and high efficiency.

References

- [1] R.D. Traub and R. Miles, (1991), *Neuronal networks of the Hippocampus*, Cambridge Univ Press.
- [2] J. E. H. Tattersall et al., (2001), *Brain Research*, vol. 904, pp. 43-53.
- [3] A. G. Pakhomov et al., (2003), *Bioelectromagnetics*, vol. 24, pp. 174-181.
- [4] M. Liberti et al., (2004), *IEEE Trans. on MTT*, vol. 52, pp. 2521- 2528.
- [5] K. C. Gupta et al., (1996), *Microstrip Lines and Slotlines*, 2nd ed. Boston, MA: Artech House.
- [6] M. Riaziat et al., (1990), *IEEE Trans. on MTT*, vol. 38, pp. 245-251.

This work has been supported by European Union, V framework under the RAMP2001 Project.

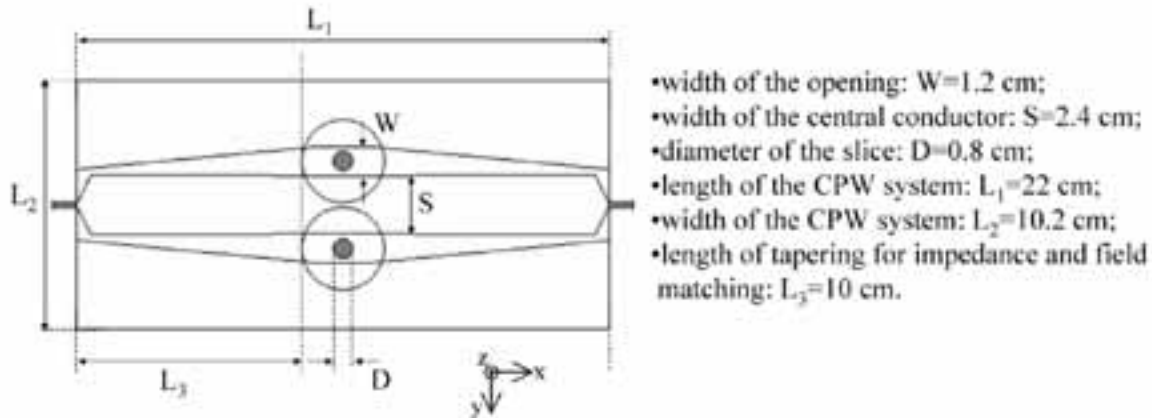


Figure 1: Top view of the system with the perfused chambers and the biological samples on it. The main design parameters are described with their own dimensions. It should be noticed that a linear tapering is necessary to obtain impedance and field matching.

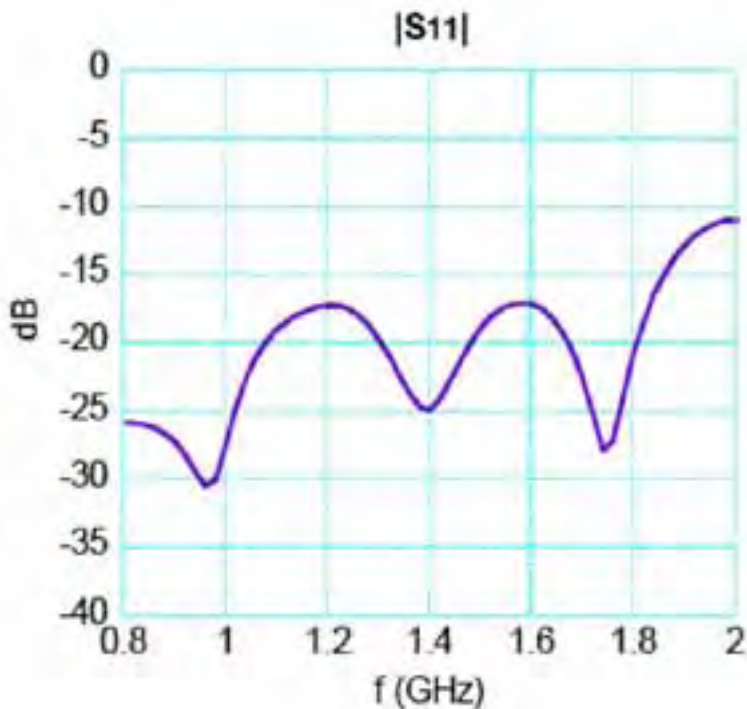


Figure 2:  $|S_{11}|$  versus frequency of the structure alone.

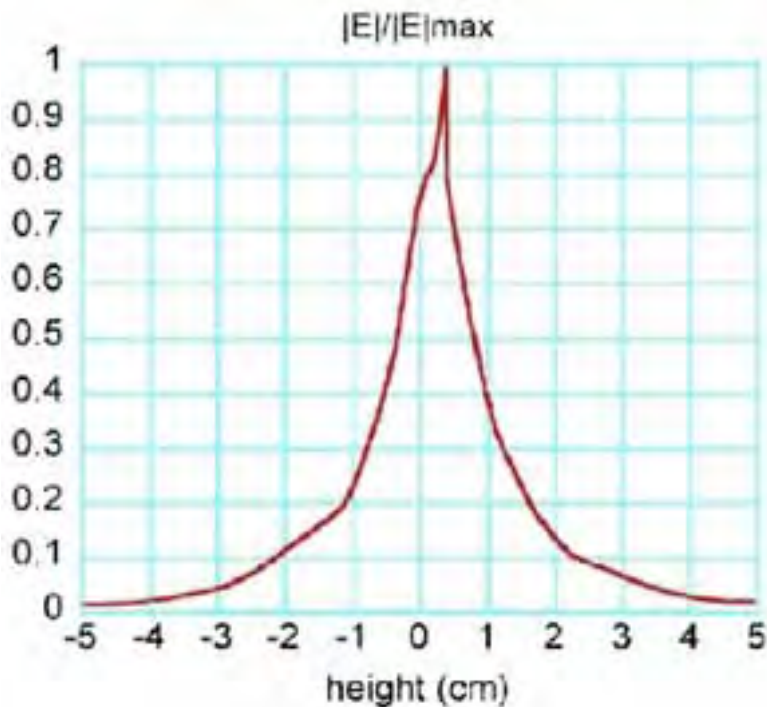


Figure 3: Normalized E field at 900 MHz along a vertical line passing through the centre of one of the slots of the CPW alone.

	900 MHz		1800 MHz	
	Max difference %	Std. deviation %	Max difference %	Std. deviation %
E  along x	7	3.5	20	9.8
E  along y	0.85	0.28	3	1
E  along z	0.28	0.14	2.8	1.4

Homogeneity of the E field in the sample at 900 and 1800 MHz, evaluated in terms of percentage difference between maximum and minimum values and standard deviation.

## Mechanisms of interaction - biological

P-C-162

**EFFECTS OF NECK EXPOSURE TO 12 MT STATIC MAGNETIC FIELD ON PHARMACOLOGICALLY INDUCED HYPERTENSION IN WISTAR RATS.** H. Okano<sup>1,2</sup>, C. Ohkubo<sup>1</sup>. <sup>1</sup>Dept of Environmental Health, National Institute of Public Health, Saitama, Japan., <sup>2</sup>Dept of Science, Pip Tokyo Co., Tokyo, Japan.

**OBJECTIVE:** Characterizing the physiological effects of static magnetic fields (SMF) on blood pressure (BP) remains an important area of research. Significant cardiovascular system responses to

SMF were recently reviewed in experimental animals [1]. Moreover, recently experimental approaches for neck exposure to moderate-intensity SMF are revealing a possible effect of SMF on arterial baroreceptors in the regulation of BP [2]. However, the effect of neck exposure to SMF on hypertension in  $\alpha_1$ -agonist, phenylephrine or  $\beta_1$ -agonist, dobutamine induced hypertension has not yet been investigated, and the mechanisms by which SMF might inhibit the hypertensive actions are still unknown. This study examines the hypothesis that SMF may influence sympathetic nerve activity in pharmacologically induced hypertension and suppress elevated BP.

**METHODS:** Five week-old male rats were exposed to SMF intensities, 12 mT ( $B_{max}$ ) with a peak spatial gradient of 3 mT/mm for 10 weeks. A loop-shaped flexible rubber magnet was adjusted to fit snugly around the neck region of a rat (diameter adjustable to an animal size). Sham exposure was performed using a sham magnet. Six experimental groups of 6 animals each were examined: 1) sham exposure with intraperitoneal (ip) saline injection (control); 2) SMF exposure with ip saline injection (SMF); 3) sham exposure with ip phenylephrine injection (PE); 4) SMF exposure with ip phenylephrine injection (SMF + PE); 5) sham exposure with ip dobutamine injection (DOB); 6) SMF exposure with ip dobutamine injection (SMF + DOB). phenylephrine (1.0  $\mu\text{g/g}$ ) or dobutamine (4.0  $\mu\text{g/g}$ ) was administered ip three times a week for 10 weeks, and then 15 min after each injection, arterial BP, heart rate (HR), skin blood flow (SBF), arterial baroreflex sensitivity (BRS), plasma catecholamine levels, the number of rearing (exploratory behavior) events and body weight were monitored.

**RESULTS AND DISCUSSION:** Neck exposure to SMF for at least 2 weeks significantly prevented the phenylephrine-induced BP increase, SBF decrease, dopamine reduction, and reduction in the rearing activity in the SMF + PE group compared with the respective PE group. On the other hand, the exposure to SMF for at least 2 weeks significantly suppressed the dobutamine-induced BP increase, BRS decrease, SBF increase, norepinephrine elevation, and increase in the rearing activity in the SMF + DOB group compared with the respective DOB group. However, the exposure to SMF alone for up to 10 weeks did not change any of the physiological parameters. These results suggest that the SMF may suppress pharmacologically induced hypertension by modulating sympathetic nerve activity. Theoretical considerations indicate that the magnetic forces applied to aortic smooth muscle cells should be in the nanonewton range and the applied SMF could be converted into a temporally changing magnetic field by means of the carotid artery pulsation. These magnetic forces and frequencies applied in this experiment could be within the range of mechanotransduction-based responses to external stimuli in vascular smooth muscle cells.

#### References

[1] Saunders R. 2005. *Prog Biophys Mol Biol* 87:225–239.

[2] Okano H, Masuda H, Hirota S, Ohkubo C. 2004. Abstract Book of the 26th Annual Meeting of the Bioelectromagnetics Society, Washington, DC. 265–266 p.

P-C-165

**LOW FREQUENCY-ELECTROMAGNETIC FIELD-INDUCED ALTERATIONS IN ARTERIOLAR VASOMOTION IN VIVO.** L. L. Traikov<sup>1,2</sup>, A. Ushiyama<sup>1</sup>, R. Sasaki<sup>1</sup>, G. F. Lawlor<sup>1</sup>, C. Ohkubo<sup>1</sup>. <sup>1</sup>Dept of Environmental Health National Institute of Public Health-NIPH Tokyo, Saitama, Japan, <sup>2</sup>Dept of Medical Physics and Biophysics, Faculty of Medicine, Medical Univ-Sofia, Sofia, Bulgaria.

**OBJECTIVE:** In this study, we investigated the possible modulating effects of extremely low-frequency (ELF) electromagnetic fields (EMF), which have potential physiotherapeutic uses, on the regulation of microcirculatory dynamics, by examining changes in blood vessel diameter. Dynamic changes in the

diameter of blood vessels, i.e., vasomotion, are regulated by many physiological and biochemical factors that play important roles in regulating homeostasis in living organisms. Vasomotion is related to the pathophysiological condition of the body, although generation of vasomotion frequency is a complex process involving numerous pathways for conductance and regulation. Elucidating the processes of modulating microcirculatory regulation by external physical factors, such as ELF-EMF, is essential to better understanding the mechanisms of ELF-EMF applied in various medical therapies.

**MATERIALS AND METHODS:** Male BALB/c mice (8-12 weeks old, 22-25 g; Tokyo Zikken Doubutsu, Japan) were used, and a dorsal skin-fold chamber made of polyacetal resin was surgically implanted 4 days before the experiment.

Mice were divided into four groups with different exposure frequencies: sham (n=14), 10 Hz (n=9), 16 Hz (n=9) and 50 Hz (n=10). Prior to ELF-EMF exposure, fluorescein isothiocyanate-labeled dextran 250 kDa (FITC-dextran-250, 2.5 % (w/v) in PBS, 50 $\mu$ l/25g body weight) was injected into the caudal vein to visualize vasculature. Mice were fixed on a plastic stage, under conscious conditions, and set inside a magnet for whole body ELF-EMF exposure (AMG-1500A, Takano Giken, Kanagawa, Japan) and intravital microscopy.

For every investigated animal, one small arteriole (45-80  $\mu$ m in diameter) was chosen under fluorescent microscopy and vasomotion was recorded on digital video tape throughout the experiment for off-line analysis. One recording process period (total 33 min) included: 3 min pre-exposure, 10 min of exposure, and 20 min post-exposure. For off-line analysis, noise in recorded video images was reduced with a signal amplifier (DVS-3000, Hamamatsu Photonics Inc., Hamamatsu, Japan), and diameters were measured automatically and recorded with a High-speed Digital Machine Vision System CV-2100 (KEYENCE Inc., Osaka, Japan), using an edge-gap detection algorithm.

To evaluate changes in mean diameters between different animals and different time intervals measured (pre-, exp/sham-, and post-exposure), we applied non-parametric statistical analysis using the Friedman-test, to distinguish tendencies in change exceeding natural variations between different individuals.

**RESULTS:** In this study, we examined 33 min non-stop measurements of arteriole diameters. No significant differences in vessel diameters throughout the whole measurement period were detected in the sham-exposure group, except for normal vasomotion. However, in the 16 Hz exposure group, significant vasodilation was observed in the post-exposure period compared with the pre-exposure and exposure periods. No significant effects on vascular diameter in the 10 Hz and 50 Hz exposure groups were determined according to chi-square ( $\chi^2$ ) analysis.

Arteriole diameters in the 16 Hz exposure group showed a stable tendency in change after 8 min ELF-EMF exposure, and vessel diameters continued to increase up to 15 min of exposure in some animals. However, significant changes with 16 Hz ELF-EMF exposure were not seen in all animals.

Differences in this effect between the 16 Hz exposure group and the 10 Hz and 50 Hz exposure groups, could be a result of frequency-specific interactions between externally applied ELF-EMF and existing biological signal transduction pathways involved in the process of vascular tone regulation.

**CONCLUSION:** 16 Hz EMF exposure induced vasodilation under these experimental conditions, but not in mice exposed to 10 Hz or 50 Hz EMF. However, exposure conditions in this study were limited to 10 minutes in duration and 28 mT in magnetic intensity, therefore broader ELF-EMF exposure studies are necessary.

**ACKNOWLEDGEMENT:** This work was supported by the Japanese Society for Promotion of Science (JSPS), 2002/04 ID#P02457 (Dr. Lubomir Traikov).

## Mechanisms of interaction - physical

P-C-171

**NUMERICAL EXAMINATION OF PHANTOM TYPES USED FOR DOSIMETRIC EVALUATION OF CELLULAR TELEPHONES.** S. Nicol, D. Brooks, J. Wojcik. APREL Laboratories Canada.

### Objectives

The objective was to compare data from a study conducted by IEEE into uncertainty resulting from the study titled “Protocol for the Computational Comparison of the SAM Phantom (figure 1) to Anatomically Correct Models of the Human Head” where the SAR values documented would be compared against the computational data resulting from a study of an alternative phantom.

### Methodology

This paper discusses the methods used during a comparison of two types of commercially available phantoms used for Dosimetric evaluation (Specific Absorption Rate) of cellular telephones for head exposure. The alternative phantom (figure 2) was modeled within a commercially available FDTD program. The IEEE protocol was observed for the generation of the cellular telephone used to generate the appropriate fields. Placement of the cellular device against the phantom followed as close to the method detailed in the IEEE study (as physically possible).



Figure 1. Alternative Phantom

The design of the phantom (figure 2) used within this study is such that the closest distance between the tissue boundary and the outer face of the cellular telephone is 6mm. This 6mm distance is equivalent to the Ear Reference Point (ERP) of the SAM phantom which has a dimension of 6mm.

Table 1.

Frequency (MHz)	Epsilon $\epsilon^r$	Sigma $\delta$
835	41.5	0.9
1900	40.0	1.4

By extruding the ERP along the NF line (for the pinna) it is expected that a worst case measurement can be determined without repeating the secondary measurement (left and right assessment of SAM) relating to the sagittally bisected SAM phantom.

### Process

A numerical mesh was then generated for the model which was excited with a Gaussian signal at 835MHz and 1900MHz. the phantom was filled with a simulation fluid which had dielectric properties as described in table 1. The feed power of the circuit was normalized to 1W for this study.

## Summary

Results showed that comparable data could be achieved when comparing the numerical values resulting from the SAM inter comparison study against those assessed using the alternative phantom. In some cases the SAR values calculated using the alternative phantom were more conservative than those from the SAM inter comparison exercise. More work shall be conducted over the coming months to investigate this and provide more data.



Figure 2.

## Conclusions

A method which allows faster analysis of SAR by reducing the number of activities needed to assess fully a wireless device has been identified. This method has now been validated against an internationally recognized program. By reducing the number of assessments needed to perform accurate assessments of a cellular telephone this alternative phantom may provide a means for industry to be more effective with time and resources in the assessment of wireless devices.

P-C-174

**COOPERATIVITY AS AN AMPLIFIER OF PHYSICAL EFFECTS AT RF IN BIOELECTROMAGNETICS.** A.R. Sheppard. Asher Sheppard Consulting, Redlands, California, USA.

**INTRODUCTION:** Cooperative interactions occur in a variety of physical, chemical, and biological contexts. Typically, cooperative interactions lead to increased sensitivity of the ensemble to a triggering event and an output that increases more steeply than the input signal (non-linear behavior). Well known examples are found in falling dominoes, where a small trigger energy topples an ensemble of dominoes arranged in a near-unstable configuration, magnetophysics, where interacting magnetic domains act cooperatively, and chemistry and biochemistry, where presence of a catalyst or enzyme accelerates a reaction rate by large factors, for example, as much  $10^{15}$  to  $10^{17}$ . Physiologically significant reactions exhibiting cooperativity include binding to hemoglobin, chemotaxis of microorganisms, ion channel function, and neurotransmitter release. Because the interaction energies of RF electric and magnetic fields with individual ions, molecules, and cells are much too weak compared with chemical energies,

physical noise processes, and EMFs in the visible and ionizing regions, a common conclusion is that typical environmental exposure are orders of magnitude too weak to produce observable effects. However, various authors have proposed that cooperative interactions in biological systems could bridge the energy gap. This paper explores some candidate cooperative interactions to evaluate quantitatively the prospect that cooperative interactions may underlie observed bioelectromagnetic effects.

**METHOD:** Proposed cooperative effects were analyzed using relevant quantitative models from biophysics, thermodynamics, and biochemistry.

**RESULTS and DISCUSSION:** The magnitude of amplification that might be needed from cooperative interactions is evident from these typical interaction energies: a) a weak chemical bond (H-H) energy is  $20 \text{ kJ mol}^{-1}$ ; b) a photon of green light,  $230 \text{ kJ mol}^{-1}$ ; c) thermal energy at 310K  $kTB = 2.6 \times 10^{-2} \text{ eV}$ , or  $RT = 2.6 \text{ kJ mol}^{-1}$ ; d) a RF photon ( $f = 1 \text{ GHz}$ ),  $4.0 \times 10^{-4} \text{ kJ mol}^{-1}$ . These energies suggest that a cooperative process would have to recruit roughly 50,000 RF photons in one location (a “multi-photon event”) to break one H-H bond, and several thousand RF photons would be needed locally to compete with thermal energy. For simple chemical reactions, where reaction rates are determined by the height of an energy barrier, reaction rate might be changed by, for example, a factor of 3 when temperature increases by 10K ( $Q_{10}=3$ ). Cooperativity in the binding of successive oxygen atoms to hemoglobin, involves at most a 50% reduction in the energy barrier and a change in binding affinity by successive oxygen atoms of similar magnitude. Enzymes, on the other hand, can change reaction rates by vastly greater factors, but require highly specific spatial arrangements of charge to fit the substrate molecule. Cooperative effects can alter neurotransmitter release in neurons by factors of hundreds and more for relatively small changes in a ligand concentration (e.g., a factor of 3 in  $[\text{Ca}^{2+}]$ ). Froehlich (Int. J. Quant Chem, 2:641, 1968) proposed cooperative behavior arising in dipole-dipole interactions for frequencies of the order of  $10^{11} \text{ Hz}$ . When summed over large number of dipoles of a cell membrane such interactions could represent a significant coupling at these frequencies, but Adair (Bioelectromagnetics 24:39, 2003) pointed out that the exceptionally narrow line widths of approximately  $10^{-8} \text{ Hz}$  would permit very little energy absorption and a signal that remains weaker than thermal noise levels.

**CONCLUSIONS:** Various cooperative mechanisms can achieve effective amplification factors ranging from factors less than two to several thousand-fold, but there does not appear to be a cooperative mechanism that overcomes the small energy content of RF quanta (relevant to events at a molecular site) or the weak magnitude of RF electric and magnetic fields (relevant for effects distributed over an ensemble of interacting elements), nor do proposed cooperative mechanisms appear to achieve signals comparable to background noise of thermal, chemical, and other origins.

P-C-177 STUDENT WITHDRAWN

## Medical applications

P-C-180

**PULSED RADIO FREQUENCY WAVEFORMS ACCELERATE ACHILLES TENDON REPAIR IN A RAT MODEL.** M. K. Patel, M. R. Berdichevsky, B. Strauch. Dept of Plastic and Reconstructive Surgery, Albert Einstein College of Medicine and Montefiore Medical Center, Bronx, New York, NY, USA.

**INTRODUCTION:** Generally, primary tendon healing progresses at a relatively slower rate than healing of other connective tissues because of the lower vascular and cellular components of tendon tissue. Efforts made to accelerate primary tendon healing to decrease restrictive adhesions and enhance tensile strength include improvement of suturing technique, early postoperative passive mobilization, therapeutic ultrasound, anti-inflammatory agents and administration of growth factors, all with varied results. Pulsed magnetic fields (PMF) have been shown to improve or accelerate angiogenesis in bone repair and arterial transplant models, with attendant acceleration of healing. This study examines the utility of radio frequency PMF on Achilles tendon repair in a rat model.

**METHODS:** Using a well established model for tendon repair, the Achilles tendon of male adult Sprague Dawley rats was transected and stabilized with a single suture. There was no additional mechanical stabilization. Upon recovery the animals were divided into sham exposed and active groups. Active animals were treated in individual plastic cages with a non-thermal pulsed radio frequency EMF signal consisting of a 65  $\mu$ sec burst of 27.12 MHz sinusoidal waves repeating at 600/sec. Average peak to peak magnetic field amplitude at the treatment site was 0.8G. Exposure time was 30 min twice daily. Sham exposed animals were treated identically. Animals were sacrificed at 21 days and the tensile strength of the isolated tendon was determined using a standard laboratory tensiometer. Pull rate was 25mm/min.

**RESULTS:** PMF exposed tendons exhibited approximately 25% greater tensile strength vs controls ( $p < 0.005$ ) at 21 days.

**CONCLUSIONS:** This preliminary study suggests a PMF signal, which has been reported to accelerate chronic and acute wound repair, could be a useful adjunct to tendon repair. The PMF signal was applied using the dose (amplitude) shown to be effective for tissue targets much larger than the rat tendon. No attempt was made to scale up the signal amplitude to account for the significantly lower induced electric field in the small tendon target. In addition, the signal was not specifically tuned to biochemical regulators of growth factor release such as the Ca/CaM pathway. The results remain very promising and suggest a simple non-invasive, non-pharmacological approach to tendon repair may be at hand. Further animal and human clinical trials will follow.

P-C-183

**ARCHEMIDIAN SPIRAL ANTENNA AND ANTENNA-ARRAY FOR MICROWAVE HYPERTHERMIA: INITIAL INVESTIGATION.** M. Popovic, L. Duong. McGill Univ, Dept of Electrical and Computer Engineering, Montreal, Quebec, Canada.

**OBJECTIVES:** In this work, we present numerical assessment of the Archemidian spiral antenna intended for use in microwave hyperthermia at 2450 MHz in an eight-element circular array configuration.

**METHODS:** A single Archimedian spiral antenna is first investigated numerically by two different simulation tools (SEMCAD, based on finite-difference time-domain method, and HFSS, based on finite-element method) for verification of its design and properties in the frequency range of interest (central frequency: 2450 MHz). Next, SEMCAD is used to simulate radiation of an eight-element circular array of spiral antennas placed in the immediate vicinity and around a cylindrical phantom with electrical properties similar to those of the muscle tissue. Antennas are sourced with a 100-V continuous-waveform (CW) signal. Specific absorption rate (SAR) distribution is calculated throughout the phantom volume as a measure of power deposition. Finally, the power deposition pattern and the location of the nulls and the maxima of the calculated SAR are observed for variable phase differences between signals that excite individual array elements.

**SUMMARY OF RESULTS:** Archimedian spiral antenna exhibits broadband properties and is chosen for the design with the intention to carry the investigation further towards the pulsed microwave imaging. The antenna design presented here is a 1.5-turn Archimedean spiral with a 4.5-cm diameter, as shown in Figure 1. The spiral is assumed to be made of a 0.5-mm thick perfect conductor with arm width of 1.5mm. The optimal operational bandwidth of the spiral antenna is obtained for a self-complimentary geometry; i.e. for the spiraling gap equal to the spiral arm width. To simulate the microwave hyperthermia environment encountered in practice, the reflection coefficient of the spiral antenna is calculated for the antenna immersed in water (relative\_permittivity = 80, conductivity = 0 S/m). Figure 2 shows the reflection coefficient parameter calculated with SEMCAD and HFSS, confirming minimal reflection coefficient value within a wide band of frequencies centered around 2450 MHz. The point-wise discrepancies between the results obtained with the two software tools can be attributed to the difference between the numerical mesh generation procedures present in the two very different numerical approaches upon which the tools are based. Next, point-wise SAR is calculated within a cylindrical muscle phantom (relative\_permittivity = 52.73, conductivity = 1.74 S/m, and mass\_density = 1040 kg/cubic\_meter) irradiated with a six-element Archimedian spiral circular array. The distance between adjacent array elements is kept constant and each element is placed 1mm away from the muscle phantom. The phantom and antenna array are immersed in deionized water, used in practice for improved signal coupling and superficial cooling. SAR distribution is observed in the muscle cylinder cross-section. When signals from antenna-elements are in phase, we see the expected symmetry of low and high power deposition regions, as shown in Figure 3. The "null" and the "hotspot" location can be changed with strategically assigned phase differences between individual element signals. For example, Figure 4 shows the how the SAR distribution changes from an all-in-phase scenario of Figure 3 to the case when antenna signals alternate between zero phase (odd-numbered antennas) and a 45-degree phase (even-numbered antenna-elements).

**CONCLUSIONS:** Archimedian spiral antenna is designed and numerically tested for the use in microwave hyperthermia in the frequency range around 2450 MHz. The reflection coefficient calculated for a single antenna when placed in deionized water confirms its broadband behavior, which is of interest to the authors of this work as the immediate future work involves pulsed microwave hyperthermia. The power deposition is calculated and observed in a cylindrical muscle phantom immersed in water and surrounded by an eight-element antenna array, demonstrating the manipulation of lower- and higher-level SAR locations by phase shifts introduced between antenna signals. Current work involves numerical testing of the Archimedian spiral antenna array placed around realistic anatomical geometry of a human arm.

**ACKNOWLEDGMENT:** This work was supported by Natural Sciences and Engineering Research Council of Canada through an Individual Research Grant.

**MAGNETIC RESONANCE ANGIOGRAPHY OF THE CEREBRAL ARTERIES IN A RAT MODEL OF SUBARACHNOID HEMORRHAGE.** M. Sekino<sup>1</sup>, K. Yamaguchi<sup>1</sup>, H. Wada<sup>2,3</sup>, T. Hamakubo<sup>3</sup>, T. Kodama<sup>3</sup>, S. Ueno<sup>1</sup>. <sup>1</sup>Dept of Biomedical Engineering, Graduate School of Medicine, Univ of Tokyo, <sup>2</sup>Dept of Molecular and Vascular Medicine, Beth Israel Deaconess Medical Center, <sup>3</sup>Dept of Molecular Biology and Medicine, Research Center for Advanced Science and Technology, Univ of Tokyo.

**INTRODUCTION:** A cerebral vasospasm following a subarachnoid hemorrhage (SAH) is a clinically important symptom because the vasospasm severely exacerbates the prognosis. Because the detailed mechanisms of the vasospasm have not yet been understood, it has been investigated in numerous studies using animals. In this study, we detected cerebral vasospasms in rats using high-resolution magnetic resonance (MR) angiography.

**MATERIALS AND METHODS:** The SAH was produced in six Sprague-Dawley rats (12 W) using the double hemorrhage injection method. At day 0 and day 2, the rats were anesthetized with ketamine (100 mg/kg) and xylazine (10 mg/kg). Autologous blood (0.35 ml) withdrawn from a femoral artery was injected into the cisterna magna. MR angiography was performed at day 0, day 4, day 7, and day 14 for seven rats in the SAH group and six rats in the control group (normal rats of 13 W). Measurements were performed using a 4.7 T MR spectrometer equipped with imaging gradient coils (maximum gradient strength 60 mT/m). Signals from the cerebral arteries were selectively measured using the 3D flow-compensated recalled gradient echo sequence. The angiogram was obtained by generating a maximum intensity projection (MIP) from a 3D data set.

**RESULTS AND DISCUSSION:** In the SAH model rat, a decrease in the signal intensity was observed in the middle cerebral artery (MCA), the posterior cerebral artery (PCA), the basilar artery (BA), and the internal carotid artery (ICA) because the SAH caused a cerebral vasospasm. The locations of the vasospasms were distributed among the ACA, the MCA, the PCA, the BA, and the ICA, and were different among animals. The signal intensities of the arteries were evaluated using the regions of interest (ROIs) selected on the ACA, the MCA, the PCA, and the BA. Each ROI had a dimension of 1x1x1 mm<sup>3</sup> and was located 5 mm away from the circle of Willis. The basilar artery (BA) showed a significant decrease in the signal intensity. The SAH group exhibited decreases in the signal intensity in all arteries, however, statistical significance was not found except for the BA because of relatively large error bars. The errors were attributable to the distribution in locations of vasospasm among animals, or variation in positioning the RF coil onto the brain. These results suggest that a vasospasm following an SAH causes a detectable decrease of the signal intensity in MR angiograms.

**COMPARISON OF STATIC AND PULSING MAGNETIC FIELD EFFECTS ON NEUROMUSCULAR JUNCTION DISORDERS.** F. Sivo<sup>1,2</sup>, A. A. Pilla<sup>1,2</sup>. <sup>1</sup>Dept of Biomedical Engineering, Columbia Univ, New York, NY, <sup>2</sup>Dept of Orthopaedics, Mount Sinai School of Medicine, New York, NY.

**INTRODUCTION:** We have reported that PMF can be configured to be remarkably successful when used to address neuromuscular disorders which involve abnormal skeletal muscle tonicity and motor function. This study compares the effect of a PMF signal with that of a static magnet on several patients presenting neuromuscular disorders of both upper and lower extremity musculature. These syndromes

are easily diagnosed and tested using the standard orthopedic grading assessment for muscle range of motion against gravity and manual resistance.

**METHODS:** The PMF waveform was configured assuming a Ca/CaM target and consisted of a 30msec burst of 10µsec bipolar pulses repeating at 1/sec and induced a peak electric field of 5mV/cm. PMF was applied with a 9 cm diameter coil. The static magnetic field (SMF) was applied with an axially magnetized 4 cm diameter ceramic magnet having a surface field of approximately 800G. Applied SMF was 20, 200 or 800G. Both PMF and SMF signals were applied to the belly of the treated muscle targeting the muscle motor end plate and its spindle apparatus. SMF was applied starting with 20G (which matches the peak magnetic field of the PMF device), with north or south pole randomly facing the skin for each amplitude. Exposure for both modalities was 15 seconds. In all cases SMF was applied first. Patients were selected by the demonstration of a grade 3 muscle contractile weakness upon standard orthopedic physical assessment and manual muscle testing (Grade 1 = weakest, Grade 5 = strongest). Patients were identically assessed pre, during and post treatment.

**RESULTS:** Seventeen individuals (8 male, 9 female) exhibiting muscle weakness in any of the four anatomical quadrants were evaluated. None of the patients responded to SMF at any of the intensities employed, in either polarity. In contrast, 14 of 17 subjects exhibited a positive response to the PMF signal. Patients presenting with Grade 3 functional assessment for motor strength in either flexor or extensor muscle groups demonstrated up to two levels of graded improvement within minutes of PMF treatment, along with measured increase in range of motion for the associated joint when tested under active physiologic muscle contraction.

**CONCLUSIONS:** There have been several in vitro and in vivo studies which suggest both static and pulsing magnetic fields could modulate Ca/CaM binding. We have previously suggested PMF and SMF signals may both function via Ca<sup>+</sup> binding/release at CaM, which, in the neuromuscular junction, is associated with neurotransmitter release in the synaptic cleft at the motor end plate. Interestingly, SMF did not correct the neuromuscular junction disorder, suggesting either that Ca/CaM is not the transduction pathway, or that SMF effect on the timing of Ca<sup>2+</sup> binding was incorrect. Indeed, if the timing of neurotransmitter release at the neuromuscular synaptic cleft, relative to the feedback component of the muscle spindle's reference signal, is a factor, the continuous presence of a Ca<sup>2+</sup> binding signal could not reset the junction. In fact, SMF may well jam the transduction pathway and could even exacerbate the problem if applied for hours, as is often the case with magnet use. Discovery of the differential effects of SMF and PMF for this pathology appears to suggest repetition rate is a more important dosimetric in PMF therapies than previously thought. These results further reinforce the importance of PMF therapy in the treatment of neuromuscular disorders.

## **Risk, safety standards and public policy**

P-C-192

**RFSCIENCEFAQS.COM – AN INTERNET SCIENCE HELPDESK ON EMF HEALTH ISSUES.** J. C. Male, S. A. Johnston. RFScienceFAQs.com, London, UK.

RFsciencefaqs.com is a non-profit UK company whose website is designed to help users understand,

summarise and keep up with ongoing international research and with scientific and regulatory issues related to possible health effects of electromagnetic fields, with a focus on telecommunications emissions. The library of key papers, conference reports and reviews has been compiled since 1996, with the sponsorship of many national and international groups. Operating costs of the website are met by annual subscription fees from users. The publishers Wiley, Harcourt, Elsevier, Kluwer, Nuclear Technology Publishing, IEEE Publications and others have generously allowed us to use their scientific abstracts in return for due acknowledgement. We also acknowledge the generosity of many international scientists who have made available their conference presentations and reports. The website has eight key features:

MEMBERS' DIALOGUE – including Bulletin Board (documents on EMF), Forum (for discussion) and Hot Issues (outlining the day's high-profile topics).

ABSTRACTS – original abstracts from over 1000 papers on EMF & health with reference to international research criteria

BIO-EFFECTS – a tutorial of the key RF human-health topics cancer, and genotoxic, nervous system and thermal effects, with recent experts' published reviews giving the weight of scientific evidence on each.

POSITION STATEMENTS – Government, WHO and Industry summary statements on EMF Health issues.

STANDARDS – providing up-to-date information on guidelines and exposure limits

WEBLINKS – connecting with key sites of health reports

EMF STUDIES DATABASE – including ongoing studies worldwide

EMF FUNDING AGENCIES – sources of funding for both ELF and RF research

The website is updated daily. Access is limited by subscription and password, but a free 24-hour trial is available on application to Sheila Johnston (sajohnston@btclick.com)

P-C-195
---------

**MOBILE TELEPHONY AND HEALTH – RECENT RISK COMMUNICATION ACTIVITIES IN SWEDEN.** L. H. Mjönes. Swedish Radiation Protection Authority.

The roll-out of the third generation system for mobile telephony has been fast in Sweden. The decision to build the UMTS system was taken in 1999. The licences for the operators were delivered in 2000. In spring 2005 the population coverage for the system is almost 90 percent in Sweden. The rapid launch has created considerable concern and opposition among certain parts of the general population. The media coverage of the 3G issue has been intensive. Interest groups are active in the resistance towards the launch of the new system and sabotage against UMTS masts has occurred. The Swedish Radiation Protection Authority, SSI, is the competent authority for radiation protection in Sweden, both for ionising and non- ionising radiation. During 2004 SSI has made special efforts to inform and educate

health officials and politicians in the municipalities, as well as the general public, about mobile telephony and health. Early in the year SSI took the initiative to a network of experts on mobile telephony and health in the five Nordic countries, Denmark, Finland, Iceland, Norway and Sweden. The work in this group resulted in a common position paper “Mobile Telephony and Health”. In short the Nordic authorities pointed out that there is no scientific evidence for adverse health effects from mobile telecommunication systems, but that some scientific uncertainty and knowledge gaps could justify a precautionary attitude regarding the use of handsets for mobile telephony. Later in 2004 a series of six regional one-day training courses, “Mobile telephony and health”, was arranged by SSI and the National Board of Health and Welfare. The training course was offered to all Swedish municipalities. Altogether more than 300 regional and municipal employees and politicians attended the courses. The response from the attendants has been very positive. In addition the National Institute for Working Life has held a series of three local information seminars for politicians and health officials in northern Sweden. A continuation of these seminars for other parts of the country is planned for 2005. During the autumn of 2004 SSI initiated “Transparency Forum”, TF, a series of four open seminars regarding the 3G roll-out where all stakeholders, authorities, industry and NGO:s, including interest groups, will be given the opportunity to express their opinions. The basis for TF is a risk communication model (RISCOM) for delicate situations, which has been tested earlier for the nuclear waste issue with good results. A key element in TF is that all stakeholders are involved on equal terms in the planning and realization of the project. The four seminars cover: Roles and responsibilities of the different organisations, The scientific basis for risk assessment, Risk management and precautionary principles and Risk communication and the role of media. The first seminar was held late in 2004, the second was arranged in March and the third in May 2005. The fourth seminar is planned for early autumn 2005.

P-C-198

**DEVELOPMENT OF TISSUES FOR USE IN NUMERICAL AND EXPERIMENTAL SAR ASSESSMENTS FROM 5-6GHZ.** S. Nicol, J. Wojcik, D. Brooks. APREL Laboratories Canada.

Objectives

This paper shall discuss the means in which numerical studies involving high resolution anatomical models, have helped derive tissues for use in experimental SAR activities in the frequency range of 5-6GHz. Research has been conducted utilizing multiple heterogeneous models based on an average male model (utilizing both thighs and torso). This study identified parameters which are anatomically correct with regards the dielectric composition of tissue layers (heterogeneous) which can yield comparable data within a homogenous platform which can be verified experimentally.

$$Cell\ Size \leq \frac{1}{20} \frac{c_0}{\sqrt{\epsilon_r} f} \leq 0.4mm$$

Figure 1.

Methodology

This study utilized the High Resolution Segmented Anatomical Model (HRSAM) developed for high frequency applications. The model observed the FDTD rule for spatial and temporal aspects of a defined problem (figure 1). The HRSAM was based on the Visible Man and up to date MRI models and was scaled to represent an average male body mass with a voxel size of 0.33mm in all directions (figure 2).



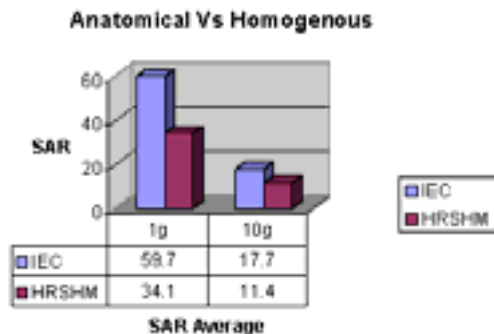
Figure 2.

### Alternatives

Experimental tissues were created and investigated for their dielectric values to establish the applicability within the study for frequencies of 5-6GHz. Tissues were based on internationally accepted methodologies (accepted by regulators) and the specific tissue layers (skin, fat and muscle) used in HRSAM. Numerical assessments were conducted using a numerically tuned broad band dipole (5.1-5.9GHz) at the frequency of 5.2GHz. This enabled the conservative SAR for the various numerically derived and experimentally available tissues to be established.

### Results

Comparisons were made against the HRSAM to establish a correlation between complex and simplified models. It was observed that when comparing a conservative homogeneous model against the worst case location of HRSAM conservative SAR was close to 43% higher (figure 3).



Figure

3.

### Further Studies

Physical experimental tissue compositions were assessed for values of epsilon (F/m) and sigma (S/m) using the open ended coaxial probe method. A broad band dipole was then experimentally evaluated for return loss, standing wave ratio, and impedance, while loaded with the tissue simulation fluid. Results from this showed extremely good correlation with numerically derived values. An E-Field probe was then calibrated using the experimental tissues so as to establish the sensitivity and isotropicity at the frequency of 5.2GHz. Calibration of the probe followed the open ended wave guide method. Experimental and numerical assessments following the IEEE 1528 validation methods were then executed. Experimental assessments were run to verify the numerically derived SAR values for peak, 1g and 10g SAR within the homogenous tissues which formed part of this study.

**LOW-FREQUENCY ELECTRIC AND MAGNETIC FIELD EXPOSURE AND GUIDELINES IN FINLAND.** R. Paakkonen<sup>1,2</sup>, T. Karjanlahti<sup>1</sup>, R. Koskinen<sup>1</sup>, J. Kurikka-Oja<sup>1</sup>, L. Korpinen<sup>1</sup>. <sup>1</sup>Tampere Univ of Technology, Lab. of Electrical Engineering and Health, <sup>2</sup>Finnish Institute of Occupational Health.

In the past years there has been much discussion about possible health effects due to exposure to EM-fields. New directives by European Union (2004) based on ICNIRP (International Commission on Non-Ionising Radiation Protection) (1998) for the exposure to electric and magnetic fields have been published. In the guidelines the exposure limit value for 50 Hz for occupational exposure is 10 mA/m<sup>2</sup> and maximum action values are 500  $\mu$ T and 10 kV/m.

At Tampere Univ of Technology and Finnish Institute of Occupational Health exposure to fields has been studied for a long time. The aim of this paper is to draw together electric and magnetic fields in work environment. Fields are caused for example by tools, machines, substations, cables, transmission lines and safety gates. Table presents a summary of the recent measurement results from these sources.

Generalization of situations is difficult because many technical detail solutions influence on the results. As a conclusion, it can be stated that exposure to the fields usually remains under the action values except in some special cases. Highest magnetic flux densities were measured at NDT and magnetic powder testing, generator condition monitoring and near arc furnaces. In those areas the magnetic flux density action value (500  $\mu$ T) was exceeded. Electric field strength action values (10 kV/m) were exceeded at 400 kV substations which have been constructed according to safety and other requirements valid at the time of the commissioning of the substations. However, the action values exceedings are local and many areas are only visited sometimes, and then the daily exposure values are significantly smaller both for magnetic and electric fields. The respective current densities for these field values have not been evaluated, calculated or measured. In other words, more studies are required before we know if the limit values of EU are exceeded.

#### References

1. ICNIRP (International Commission on Non-Ionising Radiation Protection). Guidelines for limiting exposure to time-varying electric, magnetic and electromagnetic fields (up to 300 GHz). Health Physics, 74(1998):4, 494-522.
2. Directive 2004/40/EC of the European Parliament and the Council of 29 April 2004 on the minimum health and safety requirement regarding the exposure of workers to the risks arising from physical agents (electromagnetic fields). Official Journal of the European Union on 30 April 2004, L159, 1-26.

Examples of measured fields (50 Hz) in different types of work areas and action values			
Work	Source of field	Magnetic flux density, $\mu$ T	Electric field strength, kV/m
Non-destructive (NDT) testing	magnetizing	300-1000	0.1
Magnetic powder testing	hand tool and bench	100-2000	-
Generator condition monitoring	cables/bushbars	100-600	0.05

Car service	tools	10-200	0.2
Wood working	tools	50-200	0.01-0.03
Power plant	generators	100-400	0.002-0.05
Steel factory	arc furnaces	500-4000	0.1-0.2
Railway lines	catenary line	2-10	over 2
400 kV, substation	switching yard	0.5-20	0.5-14
400 kV transmission lines	under the lines	1-12	1-9
Cash work at supermarket	cash register	0.3-3	
Library, old fashion type	safety gate	100-200	-
Action values according to EU		500	10

P-C-204

**EFFECTS OF THE EXPOSURE TO ELECTROMAGNETIC FIELDS: FROM SCIENCE TO PUBLIC HEALTH AND SAFER WORKPLACE: THE EUROPEAN COMMISSION COORDINATION ACTION EMF-NET.** P. Ravazzani. Biomedical Engineering Institute, National Research Council, Milano, Italy.

INTRODUCTION: The European Coordination Action EMF-NET “Effects of the Exposure to Electromagnetic Fields: from Science to Public Health and Safer Workplace” is financed by the 6th Framework Programme of the European Commission. The aim is not to produce new studies, but to ensure the best use of existing data on exposure to electromagnetic fields by identifying all relevant studies and analysing their findings: the EMF-NET efforts will be to scientifically inform political and health authorities, providing them with the tools and building blocks to take appropriate actions and decisions. The focus of the work is not only exposure associated with cell phones, but also exposure to many other sources such as power lines, broadcasting antennas, and electric household appliances, as well as various electromagnetic sources used in the work environment especially in the industry and health care.

The project, which will last four years (2004-2008) involves more than 40 partner organisations. It includes all the coordinators of previous projects supported by the EC on these topics, representatives of the main National research activities in the field, the coordinators of other European and International research projects, industrial partners from mobile phone operators and the electrical and electronic industries, and representatives from trade unions, regulatory bodies and other stakeholders. Several separate tasks will be undertaken in the EMF-NET coordination action. The results of current research will be brought together and analysed, with consideration of both general public and occupational exposure. The issues of risk perception and risk communication will be investigated, with an emphasis on how to communicate information about potential risks, so that that health hazards are properly addressed without introducing groundless fears. A particular emphasis will be on the monitoring of emerging technologies, including third and fourth generation mobile communications, to

identify future research priorities. The EMF-NET coordination and interpretation activities will include research (both completed and planned) from outside EU, particularly in Eastern Europe, but also activities in North America, Japan, Korea and Australia.

Approach: The EMF-NET approach will be based on the activities of Technical Working Groups of experts, in order to produce a series of EMF-NET Interpretation Reports, each based on the consolidation of all available evidence in a topic area. These reports will be disseminated first to policy and health authorities, and then adapted for release to the general public in Europe. EMF-NET will also provide the European Commission with the European Fast Response Team on EMF and Health, comprising nine European experts whose expertise covers all aspects of the relationship between electromagnetic fields and health. The Fast Response Team, who will give prompt and concise answers, will assist the European Commission Services with questions on these topics. EMF-NET will also organize public meetings, round-tables, workshops and conferences, targeted to the different needs of those concerned (scientists, political and health authorities, stakeholder associations, European citizens), and will contribute to education and information activities in the field. Contacts. Email: [emf-net@polimi.it](mailto:emf-net@polimi.it); EMF-NET website: <http://EMF-NET.isib.cnr.it>

ACKNOWLEDGEMENTS: This work is supported by the European Coordination Action EMF-NET "Effects of the Exposure to Electromagnetic Fields: from Science to Public Health and Safer Workplace", European Commission FP6 Coordination Action, Thematic Priority 8, Policy support and anticipating scientific and technological needs, Contract N° SSPE-CT-2004-502173 (2004-2008)

P-C-207

**FEASIBILITY AND REASONABLE ENDPOINTS OF INVESTIGATIONS REGARDING A POSSIBLY HIGHER RF-EXPOSURE-RISK FOR CHILDREN.** G. Schmid<sup>1</sup>, L. Pipal<sup>2</sup>, K. Widhalm<sup>2</sup>, M. Tschabitscher<sup>3</sup>. <sup>1</sup>ARC Seibersdorf research GmbH, AUSTRIA, <sup>2</sup>Dept of Pediatrics, Medical Univ of Vienna, Vienna, AUSTRIA, <sup>3</sup>Dept of Anatomy, Medical Univ of Vienna, Vienna, AUSTRIA.

INTRODUCTION: One of the conclusions in the report Mobile Phone and Health [1], released by the Independent Expert Group on Mobile Phones (IEGMP) in 2000, was that non-essential usage of mobile phones by children should be discouraged, because they might be at higher risk with respect to possible adverse health effects due to the RF-emissions from such devices. This statement caused worldwide increasing concern and several scientific initiatives were launched having their scope on this issue, e.g., in the frame of COST281 the Short Term Mission Mobile Phone and Children [2] was defined. OBJECTIVE: For a planned main study to be carried out within a time frame not longer than 2-3 years and dealing with the issue of possible age dependent effects of RF exposure, current knowledge gaps should be identified. Based on this, possible scopes and endpoints of a feasible main study should be proposed, which could lead to new insights into some aspects of this research area. MATERIALS AND METHODS: In order to identify current gaps of knowledge, a comprehensive literature survey was carried out, having the scope on the following (mainly head related) aspects: postnatal anatomical development and growth, variations in tissue distribution and tissue composition during postnatal development, age dependence of dielectric and thermal properties of tissues, sensitive developmental stages of tissues, thermoregulatory changes during development, close near field dosimetry capabilities (including availability of anatomical head models for different ages) and already documented biological as well as human studies with relevance to age dependent effects of RF exposure.

**RESULTS AND CONCLUSION:** The body of the reviewed literature clearly indicated the complexity and the manifoldness of biological, medical and dosimetric aspects to be taken into account with respect to the objective issue. Unfortunately in the relevant biological and medical areas there is partially very little knowledge on postnatal age dependence of human parameters which would be of importance in this context (e.g., tissue composition, tissue properties, sensitive postnatal developmental stages of tissue).

Regarding RF dosimetry, despite lacks due to still missing age related data of tissue parameters and hardly available head models, the question of age (and head size) dependent RF absorption is still not satisfactorily solved. Although contradictory results published in recent years can mainly be attributed to antenna -tuning effects not considered appropriately by some researchers, this does not help very much with respect to the practical situation, because these simulations were almost entirely based on generic antenna configurations. Due to the fact that the antenna current (mainly responsible for the SAR) is not only affected by antenna-de-tuning, but also by the matching between the antenna and the amplifier of the radiation source, it might strongly depend on the device type. Current procedures of compliance testing are assuming the SAM head phantom as a conservative representation of all heads (including children). Doing so, one does silently assume 'worst case' antenna de-tuning and matching (i.e., leading to maximum antenna current) when positioning the device at the SAM phantom. For giving scientific justification to this assumption for the (wide) practical range of devices, head sizes, head shapes and tissue properties, further dosimetric research must be strongly recommended.

From the current situation it seems that the question of possible age dependent effects of RF exposure can not be solved comprehensively on a short time view due to the mentioned complexity and manifoldness of this issue. However, there are several important aspects as e.g., age dependence of tissue properties, development of representative head models of children and identification of sensitive developmental stages of the most exposed tissues, which should be investigated urgently in order to close the most essential gaps of knowledge as soon as possible.

Biological (animal) investigations during postnatal development having their scope on currently heavy discussed topics as e.g., blood brain barrier and synaptogenesis in the brain might be also reasonable endpoints, provided the usage of practical relevant exposure situations, i.e. head only exposure without elevating body core temperature.

**ACKNOWLEDGEMENTS:** This project was funded by the Federal Office for Radiation Protection (BfS), Germany.

**REFERENCES:**

- [1] IEGMP 2000: Mobile Phones and Health ( "Stewart-Report"); Independent Expert Group on Mobile Phones, National Radiological Protection Board, Chilton, Oxon OX11 0RQ, UK; [www.iegmp.org](http://www.iegmp.org).
- [2] COST281 STM Mobile Phone and Children <http://www.intec.ugent.be/wica/group.html>

P-C-210 STUDENT
-----------------

**OUTDOOR ELF –MAGNETIC FIELDS IN A NORWEGIAN CITY (63 DEEGRES N).** A. Straume<sup>1</sup>, G. Oftedal<sup>2</sup>, A. Johnsson<sup>1</sup>. <sup>1</sup>Norwegian Univ of Science and Technology, Dept of Physics, Trondheim, Norway., <sup>2</sup>Sør-Trøndelag Univ College, Trondheim, Norway.

**OBJECTIVE:** Extremely low frequency (ELF) magnetic fields have not previously been mapped in the outdoor environment of Norwegian cities. The aim of this study was to assess the magnetic flux density

(MFD) downtown Trondheim both summer and winter, and to compare the results with ICNIRP limits and with similar measurements in other countries.

**METHODS:** The power frequency in Norway is 50 Hz. The three perpendicular components of the field vector was measured by an EMDEX II both using the broadband (40-800 Hz) and the harmonics (100 – 800 Hz) setting. The true r.m.s value of the MFD was calculated. A person carried the EMDEX II 0.8-1.0 m above the ground while walking along sidewalks. The sampling rate was 3 s for each of the two frequency ranges recorded, and the distance between each sampling was about 3 m. All together, 8.5km of sidewalks were mapped. The same distance was measured in summer time (temperature 15 - 20 gr.C) and in winter when snowing (-9 - 0 gr.C). In cold winter days (<-10 gr.C) approximately 40% of the distances have so far been measured. When it was snowing, electric cables in some parts of the sidewalks were switched on to melt the snow. The flux densities were plotted on a map to show the geographical distribution, and statistical distributions of flux densities were calculated. The measurement procedure and the analyses are based on the methods used to map the ELF magnetic fields downtown Göteborg, Sweden (Lindgren, 2001)

**RESULTS:** Figures 1 shows that the magnetic flux densities are relatively low for most of the distance along the side walks. For some small areas, however, the figures show that values were considerably higher. This is also reflected in results presented in Table 1A showing the percentage of values measured within different MFD intervals. In the summer period almost all registered values were below 0.2  $\mu\text{T}$ , while in the winter period about 30% of the recordings were above 1.0  $\mu\text{T}$ . In average, the MFD in winter was about 7 times higher than in summer, and slightly higher values were measured in cold winter days than when it was snowing. (See Table 1B for more details.) The geographical distributions indicated a slightly different distribution in cold winter days than in days when it was snowing. In the latter case, higher flux densities were measured along side walks where electrical cables were switched on to melt the snow. A greater percentage of the measured MFDs were below 0.2  $\mu\text{T}$  in Trondheim at summer time than in Göteborg (Sweden) with 49% and in the cities in Extremadura (Spain) with 67%. The maximum values, however, were higher than in the other cities (Göteborg: 9.7  $\mu\text{T}$ , Extremadura: 7.0  $\mu\text{T}$ ). Average values indicate that the harmonics were about 9% of the broadband values in summer and about 3% in winter.

**CONCLUSION:** In summer time, for most parts downtown in the Norwegian city the ELF magnetic fields appear to be lower than downtown in the Swedish city and in the Spanish cities. However, the maximal field strength that may occur seems to be higher in the Norwegian city than in the others. In winter time the magnetic fields are markedly stronger than in summer time. The broadband data suggest that at the ICNIRP limit for 50 Hz magnetic flux density (100  $\mu\text{T}$ ) was not exceeded neither in the summer nor in the winter period. However, frequency analyses of the fields have to be done to make an accurate assessment to compare with the ICNIRP limits.

**REFERENCE:** Lindgren M, Gustavsson M, Hamnerius Y, Galt S. 2001. ELF magnetic fields in a city environment. *Bioelectromagnetics* 22:87-90.

Paniagua JM, Jiménez A, Rufo M, Antolin A. 2004. Exposure Assessment of ELF Magnetic Fields in Urban Environments in Extremadura (Spain), *Bioelectromagnetics* 25:58-62

Figure 1: The magnetic flux density downtown Trondheim summer and winter (see the abstract online for figure in colour).

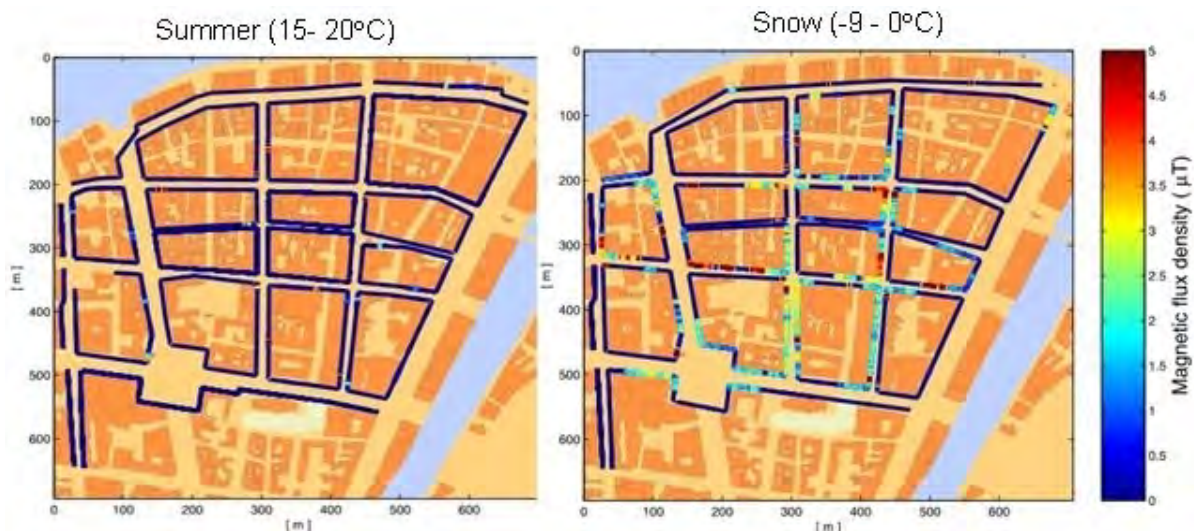


Table 1: Table 1 A and B.

A: Percentages of the measured values in each of three magnetic flux density intervals.				B: Minimum, mean, and maximum values of the magnetic flux densities (40-800 Hz).			
	Percentage				Magnetic flux density ( $\mu\text{T}$ )		
	Summer	Winter snow	Winter cold <sup>1)</sup>		Summer	Winter snow	Winter cold <sup>1)</sup>
< 0.2 $\mu\text{T}$	94	62	58	Minimum	0.00	0.00	0.00
0.2 – 1.0 $\mu\text{T}$	4	8	10	Mean	0.13	0.90	1.17
> 1.0 $\mu\text{T}$	2	30	32	Maximum	16.0	28.6	37.4

1: Preliminary results. Only 40% of the distances mapped.

P-C-213 STUDENT

**EMF-PORTAL: BENEFIT FOR INFORMATION RETRIEVAL ON THE BIOLOGICAL EFFECTS OF ELECTRO-MAGNETIC FIELDS.** R. Wienert, S. Driessen, M. Meyer, F. Klubertz, J. Silny. FEMU, Univ Hospital, Aachen Univ (RWTH), Aachen, Germany.

### Introduction:

The "EMF-Portal" is an Internet-based information platform in the research area of non-ionizing radiation effects. It is supplied by a variety of linked information sources and it provides scientific knowledge based on the results of more than 7.600 (mostly peer-reviewed) publications related to bioelectromagnetic interaction. Different help tools support the interested user in both finding and interpreting relevant data. The EMF-Portal is multi-lingual: English and German are currently supported, other languages can be added.

### Objectives:

To make possible for all users, regardless of their education or occupation, to ask complex questions

about EMF and their effects and to receive specific and comprehensive answers. Assisted by an interdisciplinary glossary and a database of every day's exposure sources, as well as an in-depth literature database, the user obtains a dynamically generated answer based on the results of all related publication data. The answer may consist of either a list of corresponding literature references or of different types of statistics e.g. regarding the described effects and/or the transferability of the investigation results to humans.

### **Methods:**

The EMF-Portal consists of four main modules which can be either used separately or linked together in order to support the user in phrasing questions and in interpreting the database results. The **knowledge based literature database** (a.k.a. WBLDB) contains most of the relevant scientific literature published so far. In addition to the publication data, the descriptors (exposure, methods, results etc.) of each study are extracted (cf. Driessen et AL.). With the help of this database the user has detailed insight into individual publications without having to read the full text, and he can produce statistical overviews over corresponding related studies as well as an objective comparison between different publications. The **interdisciplinary glossary** comprehensively explains related biological, medical, epidemiological, technical or dosimetric terms. The **database of every day's exposure sources** is a collection of important technical parameters of common EM fields. Finally, a so-called **inference machine** links the three databases to help the user in making a database query as well as to present the result set. Three different query options have been implemented into the inference machine to obtain a list of corresponding publications.

The **simple query** is able to translate and "understand" the entered keywords with help of the interdisciplinary glossary and the exposure database. The search engine determines synonyms, acronyms and words similar to the search term. When the user query concerns an exposure source, the field characteristics (e.g. frequency range) are also taken into account for the reply. This query option is targeted mainly towards occasional non-expert users.

The **detailed query** represents an ordinary database query. The user is able to phrase conjunctions and disjunctions, looking for publication data and keywords.

Precise information can be entered into the **expert query**. This option is the most powerful and flexible query tool, as the user can describe exactly what he wants to look for: exposure parameters (frequency range, modulation, SAR etc.) and medical/biological data (exposed system, endpoints) can be narrowed down.

All three queries initially return a list of publications that meet the entered criteria. These lists can be sorted and browsed; detailed data of every listed and extracted article can be accessed. Based on the publication information extensive statistical analysis can be generated automatically: bibliographical statistics (e.g. year of publication), text statistics (e.g. investigated endpoints) and results-oriented statistics (e.g. how many studies have found an effect, how many results are transferable to human health).

### **Results:**

Citizens, politicians, decision makers and experts are able to gain valuable, scientific based knowledge, answering their individual questions and information needs. All users are assisted in obtaining correct answers and in interpreting the results correctly.

Query example: The user asks for "blood cancer" and "mobile phones". The search engine looks for synonyms and acronyms of the medical term (result: leukemia, ALL etc.) and the most important exposure characteristics of the technical term (e.g. frequency range). Subsequently, a query collects all corresponding articles from the literature database.

Output example: To begin with, the user receives a list of all articles corresponding to his query. When he selects an individual article he obtains the detailed (extracted) information stored in the literature

database. Based on the publication list, the user additionally can get different statistics, e.g. how many publications describe an effect and whether those are transferable to human health.

The EMF-Portal is accessible free of charge at <http://www.emf-portal.org>

## Theoretical and practical modelling

P-C-216

### **PARAMETRIC ANALYSIS OF TISSUE TEMPERATURE SENSITIVITY TO THERMAL PROPERTY VALUES FOR WHOLE-BODY SIMULATIONS OF HUMAN EXPOSURE TO 915 MHZ.**

D. A. Nelson<sup>1</sup>, E. T. Ng<sup>1</sup>, A. R. Curran<sup>2</sup>, E. A. Marttila<sup>2</sup>, J. M. Ziriak<sup>3</sup>, P. A. Mason<sup>4</sup>, W. D. Hurt<sup>4</sup>.  
<sup>1</sup>Michigan Technological Univ, Houghton, MI, USA, <sup>2</sup>ThermoAnalytics, Inc., Calumet, MI, USA, <sup>3</sup>Naval Health Research Center Detachment, Brooks City-Base, TX, USA, <sup>4</sup>Air Force Research Laboratory, Directed Energy Bioeffects Division, Brooks City-Base, TX, USA.

**INTRODUCTION:** The use of numerical modeling techniques shows promise for predicting thermal effects of RF exposure in humans and animals. While the finite difference time domain (FDTD) method has gained acceptance as a tool for predicting local specific absorption rate (SAR) values, the development of corresponding computational tools to estimate tissue temperatures will require an accepted set of thermal property values for human tissues. As there may be a great deal of variability in thermal property data obtained from the open literature, it is important to know the extent to which tissue temperature calculations are sensitive to assumed values of tissue thermal properties.

**OBJECTIVES:** The objective of this study was to estimate tissue temperatures in selected organs, using a whole-body model simulation at an exposure frequency of 915 MHz, and determine the sensitivity of the tissue temperature increase to changes in four variables: thermal diffusivity, thermal conductivity, specific metabolic rate, and specific blood flow rate.

**METHODS:** Specific absorption rates were determined using the FDTD method and the voxelized 3D heterogeneous tissue model of the adult male ("Brooks Man") with a voxel size of 2 mm x 2 mm x 2 mm. The SAR values thus obtained were used in a Pennes-type model thermal model, which was also implemented on the 2 mm Brooks Man model. A uniform power density of 958 mW•cm<sup>-2</sup> (+EHK orientation) was used, corresponding to a whole-body SAR of 58.6 W•kg<sup>-1</sup>. A high SAR was necessary to produce observable temperature increases in most tissues and organ systems.

Tissue temperatures were calculated for a series of 10-minute exposure simulations, using property data extracted from the literature. Simulations were then repeated while varying the value of a given property by +20% from the baseline value. A third set of simulations was performed for each of the four properties studied, changing the property value by -20%.

**RESULTS:** Results show changes in rates of temperature increase are generally consistent with the magnitude of a given property variation, although some organs showed a higher sensitivity to changes in selected properties. Decreasing the blood flow to the kidney by 20% (Fig. 1a) increased the magnitude of temperature change at the end of a 10-minute exposure by 60%. In absolute terms, the temperature change was very slight, however. More substantial temperature increases were observed in the gray matter (Fig. 1b), in which changes in the magnitude of the temperature increase were approximately proportionate with changes in the blood flow rate per unit volume.

Tissue temperatures were generally less sensitive to changes in thermal diffusivity, thermal conductivity, and alterations in tissue metabolic rates than to imposed changes in blood flow rate, at least for the most highly-perfused tissues and organs.

**DISCUSSION:** There is considerable variability in published values for thermal properties for biological tissues. This is especially true for specific blood flow rates, where extrapolating animal data to humans is especially problematic. Care must be exercised in calculating temperature increases associated with RF exposure, particularly in the case of organs and tissues with relatively high blood flow rates.

**ACKNOWLEDGEMENT:** This work was supported by the Small Business Innovation Research (SBIR) Program and administered through the Office of Naval Research (ONR). The Program Officer was CDR Stephen Ahlers of ONR and the Technical Monitor was John Ziriaux of the Naval Health Research Center Detachment at Brooks City-Base, TX.

This work was funded by the U.S. Air Force and U.S. Navy (Project Numbers: 0602236N/M04426.w6, 0601153N/M4023/60182). The views, opinions, and/or findings contained in this report are those of the authors and should not be construed as official Dept of the Air Force, Dept of the Navy, Dept of Defense, or U.S. government position, policy, or decision.

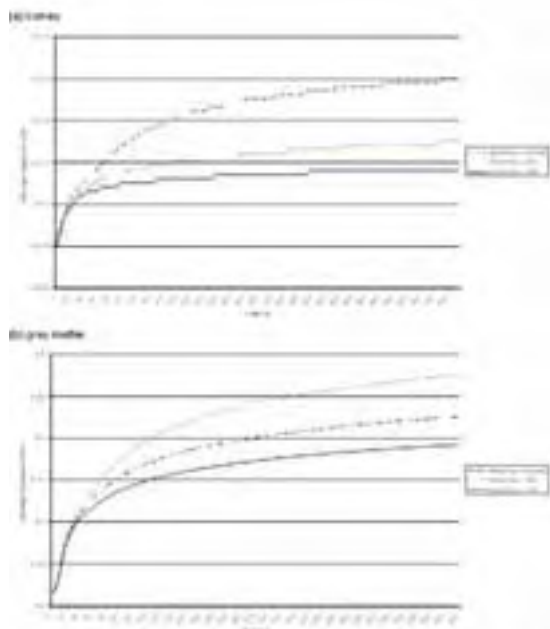


Fig. 1. Tissue average temperature response and change for 1000 MHz and 2000 MHz in the brain for various blood flow rates, 0.010, 0.020, 0.040, 0.080, 0.160, 0.320, 0.640, 1.280, 2.560, 5.120, 10.240, 20.480, 40.960, 81.920, 163.840, 327.680, 655.360, 1310.720, 2621.440, 5242.880, 10485.760, 20971.520, 41943.040, 83886.080, 167772.160, 335544.320, 671088.640, 1342177.280, 2684354.560, 5368709.120, 10737418.240, 21474836.480, 42949672.960, 85899345.920, 171798691.840, 343597383.680, 687194767.360, 1374389534.720, 2748779069.440, 5497558138.880, 10995116277.760, 21990232555.520, 43980465111.040, 87960930222.080, 175921860444.160, 351843720888.320, 703687441776.640, 1407374883553.280, 2814749767106.560, 5629499534213.120, 11258999068426.240, 22517998136852.480, 45035996273704.960, 90071992547409.920, 180143985094819.840, 360287970189639.680, 720575940379279.360, 1441151880758558.720, 2882303761517117.440, 5764607523034234.880, 11529215046068469.760, 23058430092136939.520, 46116860184273879.040, 92233720368547758.080, 184467440737095516.160, 368934881474191032.320, 737869762948382064.640, 1475739525896764129.280, 2951479051793528258.560, 5902958103587056517.120, 11805916207174113034.240, 23611832414348226068.480, 47223664828696452136.960, 94447329657392904273.920, 188894659314785808547.840, 377789318629571617095.680, 755578637259143234191.360, 1511157274518286468382.720, 3022314549036572936765.440, 6044629098073145873530.880, 12089258196146291747061.760, 24178516392292583494123.520, 48357032784585166988247.040, 96714065569170333976494.080, 193428131138340667952988.160, 386856262276681335905976.320, 773712524553362671811952.640, 1547425049106725343623905.280, 3094850098213450687247810.560, 6189700196426901374495621.120, 12379400392853802748991242.240, 24758800785707605497982484.480, 49517601571415210995964968.960, 99035203142830421991929937.920, 19807040628566084398385987.840, 39614081257132168796771975.680, 79228162514264337593543951.360, 158456325028528675187087902.720, 316912650057057350374175805.440, 633825300114114700748351610.880, 1267650600228229401496703221.760, 2535301200456458802993406443.520, 5070602400912917605986812887.040, 10141204801825835211973625774.080, 20282409603651670423947251548.160, 40564819207303340847894503096.320, 81129638414606681695789006192.640, 162259276829213363391578012385.280, 324518553658426726783156024770.560, 649037107316853453566312049541.120, 1298074214633706907132624099082.240, 2596148429267413814265248198164.480, 5192296858534827628530496396328.960, 10384593717069655257060992792657.920, 20769187434139310514121985585315.840, 41538374868278621028243971170631.680, 83076749736557242056487942341263.360, 166153499473114484112975884682526.720, 332306998946228968225951769365053.440, 664613997892457936451903538730106.880, 132922799578491587290380707746021.760, 265845599156983174580761415492043.520, 531691198313966349161522830984087.040, 1063382396627932698323045661968174.080, 2126764793255865396646091323936348.160, 4253529586511730793292182647872696.320, 8507059173023461586584365295745392.640, 17014118346046923173168730591490785.280, 34028236692093846346337461182981570.560, 68056473384187692692674922365963141.120, 136112946768375385385349844731926282.240, 272225893536750770770699689463852564.480, 544451787073501541541399378927705128.960, 1088903574147003083082798757855410257.920, 2177807148294006166165597515710820515.840, 4355614296588012332331195031421641031.680, 8711228593176024664662390062843282063.360, 17422457186352049329324780125686564126.720, 34844914372704098658649560251373128253.440, 69689828745408197317299120502746256506.880, 139379657490816394634598241005492513013.760, 278759314981632789269196482010985026027.520, 557518629963265578538392964021970052055.040, 1115037259926531157076785928043940104110.080, 2230074519853062314153571856087880208220.160, 4460149039706124628307143712175760416440.320, 8920298079412249256614287424351520832880.640, 17840596158824498513228574848703041665761.280, 35681192317648997026457149697406083331522.560, 7136238463529799405291429939481216666244.120, 14272476927059598810582859878962433332488.240, 28544953854119197621165719757924866664976.480, 57089907708238395242331439515849733329952.960, 114179815416476790484662879031699466559905.920, 228359630832953580969325758063398933119811.840, 45671926166590716193865151612679786623962.720, 91343852333181432387730303225359573247925.440, 182687704666362864775460606450719146495850.880, 36537540933272572955092121290143829299171.760, 73075081866545145910184242580287658598343.520, 146150163733090291820368485160575317196687.040, 292300327466180583640736970321150634393374.080, 58460065493236116728147394064230126878674.960, 116920130986472233456294788128460253757349.920, 233840261972944466912589576256920507514699.840, 467680523945888933825179152513841015029399.680, 935361047891777867650358305027682030058799.360, 1870722095783555735300716610055364060117598.720, 3741444191567111470601433220110728120235197.440, 7482888383134222941202866440221456240470394.880, 14965776766268445882405732880442912480940789.760, 29931553532536891764811465760885824961881579.520, 59863107065073783529622931521771649923763159.040, 119726214130147567059245863043543299847526318.080, 239452428260295134118491726087086599695052636.160, 478904856520590268236983452174173199390105272.320, 957809713041180536473966904348346398780210544.640, 1915619426082361072947933808696692797560421089.280, 3831238852164722145895867617393385595120842178.560, 7662477704329444291791735234786771190241684357.120, 15324955408658888583583470469573542380483368714.240, 30649910817317777167166940939147084760966737428.480, 61299821634635554334333881878294169521933474856.960, 122599643269271108668667763756588339043866949713.920, 245199286538542217337335527513176678087733899427.840, 490398573077084434674671055026353356175467798855.680, 980797146154168869349342110052706712350935597711.360, 1961594292308337738698684220105413424701871195422.720, 392318858461667547739736844021082684940374239084.480, 784637716923335095479473688042165369880748478168.960, 1569275433846670190958947376084330739761496956337.920, 3138550867693340381917894752168661479522993912675.840, 627710173538668076383578950433732295904598782535.680, 1255420347077336152767157900867464591809197565071.360, 2510840694154672305534315801734929183618395130142.720, 5021681388309344611068631603469858367236790260285.440, 10043362776618689222137263206939716734473580520570.880, 20086725553237378444274526413879433468947161041141.760, 40173451106474756888549052827758866937894322082283.520, 80346902212949513777098105655517733875788644164567.040, 16069380442589902755419621131103546775157728832913.920, 32138760885179805510839242262207093550315457665827.840, 64277521770359611021678484524414187100630915331655.680, 128555043540719222043356969048828374201261830663311.360, 257110087081438444086713938097656748402523661326622.720, 514220174162876888173427876195313496805047322653245.440, 102844034832575377634685575239062699361009465330649.880, 205688069665150755269371150478125398722018930661299.760, 41137613933030151053874230095625079744403786132259.520, 82275227866060302107748460191250159488807572264519.040, 164550455732120604215496920382500318977615145329038.080, 329100911464241208430993840765000637955230290658076.160, 658201822928482416861987681530001275910460581316152.320, 1316403645856964833723975363060002551820921162632304.640, 263280729171392966744795072612000510364184232526460.880, 526561458342785933489590145224001027328368465052921.760, 1053122916685571866979180290448002054656736930105843.520, 2106245833371143733958360580896004109313473860211686.720, 4212491666742287467916721161792008218626947720423373.440, 842498333348457493583344232358401637245389544084674.880, 1684996666696914987166688464716803274490779088169349.760, 336999333339382997433337692943360654898155817633869.520, 673998666678765994866675385886721309796311635267739.040, 134799733735753198973335077177344261959262327053549.880, 269599467471506397946670154354688523918524654107099.760, 539198934943012795893340308709377047837049308214199.520, 107839786988602559178668061741875409567409661642839.040, 215679573977205118357336123483750819134819323285678.080, 431359147954410236714672246967501638269638646571357.160, 862718295908820473429344493935003276539277293142714.320, 172543659181764094685868898787000655307855458628542.640, 345087318363528189371737797574001306615710917257085.280, 690174636727056378743475595148002613231421834514170.560, 1380349273454112757486951190296005226462843670028341.120, 2760698546908225514973902380592010528925687340056682.240, 5521397093816451029947804761184021057851374680113364.480, 1104279418763290205989560952236804211570274936022672.960, 2208558837526580411979121904473608423140549872045345.920, 4417117675053160823958243808947216846281097744090691.840, 8834235350106321647916487617894433692562195488181383.680, 1766847070021264329583297523578886738512439097636276.720, 353369414004252865916659504715777347702487819527255.440, 706738828008505731833319009431554695404975639054510.880, 141347765601701146366663801886310939080995127810902.160, 282695531203402292733327603772621881601990255621804.320, 565391062406804585466655207545243763203980511243608.640, 1130782124813609170933310415090487526407961022487217.280, 226156424962721834186662083018097505281592204497443.520, 452312849925443668373324166036195010563184408994887.040, 90462569985088733674664833207239002112636881798977.680, 180925139970177467349329666414478004225273763597955.360, 361850279940354934698659332828956008450547527195910.720, 723700559880709869397318665657912016901095054391821.440, 1447401119761419738794637331315824033802190108783642.880, 289480223952283947758927466263164806760438021756728.160, 578960447904567895517854932526329613520876043513456.320, 1157920895809135791035709865052659227041752070026912.640, 2315841791618271582071419730105318454083504140053825.280, 4631683583236543164142839460210636908167008280107650.560, 9263367166473086328285678920421273816334016560215301.120, 185267343329461726565713578408425476326680331204302.240, 370534686658923453131427156816850952653360662408604.480, 741069373317846906262854313633701905306721324817208.960, 1482138746635693812525708627267403810613442696334417.920, 296427749327138762505141725453480762122688539266883.840, 592855498654277525010283450906961524245377078533767.680, 1185710997308555050020566901813923048490754157067535.360, 2371421994617110100041133803627846096981508314135070.720, 4742843989234220200082267607255692193963016628270141.440, 9485687978468440400164535214511384387926033256540282.880, 18971375956936880800329070429022768775852066513080565.760, 37942751913873761600658140858045537551704133026161131.520, 7588550382774752320131628171609107510340826605232226.040, 15177100765549504640263256343218215020681653210464452.080, 3035420153109900928052651268643643004136330642092890.160, 6070840306219801856105302537287286008272661244185780.320, 12141680612439603712210605074574572016545322488371560.640, 24283361224879207424421210149149140331090644976743121.280, 4856672244975841484884242029829828066218128995348624.560, 9713344489951682969768484059659656132436257990697249.120, 19426688979903365939536968119319312248772515981394498.240, 38853377959806731879073936238638624497545031962788996.480, 777067559196134637581478724772772489950900639255779.360, 1554135118392269275162957449545544979901801278511558.720, 3108270236784538550325914899091089959803602557023117.440, 621654047356907710065182979818217991960720511404634.880, 1243308094713815420130365959636435983921441022809269.760, 2486616189427630840260731919272871967842882045618539.520, 4973232378855261680521463838545743935685764091237079.040, 9946464757710523361042927677091487871371528182474158.080, 198929295154210467220858553

presented for use in international standards has not been repeatable and as such guidelines need to be established. By creating a set of rules and an FDTD model (geometry guide) which can be used for SAR applications it is expected that users of the guide shall achieve repeatable data throughout FDTD numerical operations independent of the software platform.

#### Methodology

The model is based on parameters which have been defined through studies utilizing skin fold, MRI and ultrasonic methods. The heterogeneous model consists of three layers, and provides an anatomically traceable means for conducting numerical studies. The layers used within the model consist of skin, fat and muscle and the dielectric parameters for each layer can be changed to meet the radio frequency requirement for the study. The means for excitation of the model are determined by the user, but positioning, feed point, and distance have to be documented. The geometry for the model is also well defined, and has frequency dependent rules with respect to the cell size. Considerations for the time steps, along with pulse width are also described, and are frequency dependent. A simplified excitation model has been defined for users of the guideline to validate their FDTD platform, and methods prior to more complex studies (problems) being run for example cellular telephones.

#### Conclusions

Results from the study are repeatable across users of the same FDTD platform and could be used as a reference for international studies. Comparisons can be made by other numerical code users to gauge the effectiveness of both process and user. Wireless product manufacturers can assess products for efficiency and safety using the model and show traceability back to a known international reference.

#### Benefits

It is anticipated that by describing the process fully, users of the model shall be able to initiate inter comparisons for specific scenarios or methods of excitation. The model and methods can be used internationally when new initiatives are being developed for studies into the effects of SAR (Specific Absorption Rate) to users of new and advanced wireless equipment/technologies.

P-C-222

**INFLUENCE OF OSCILLATING MAGNETIC FIELDS ON BIOCHEMICAL REACTIONS.** J. Boiden Pedersen, N. N. Lukzen, A. B. Doktorov. Dept. of Physics, Univ of Southern Denmark.

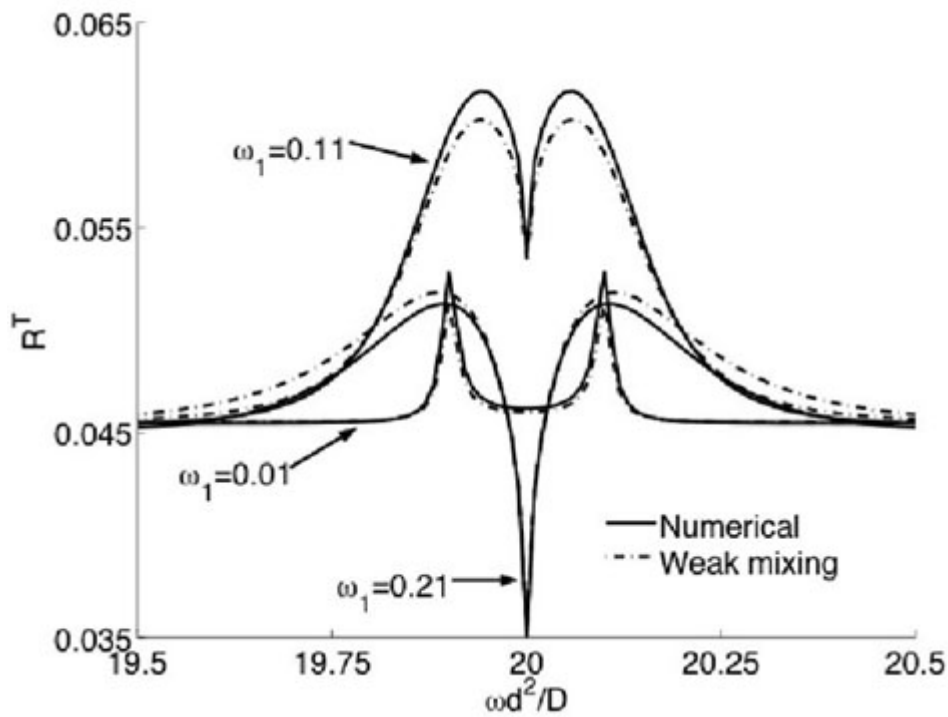
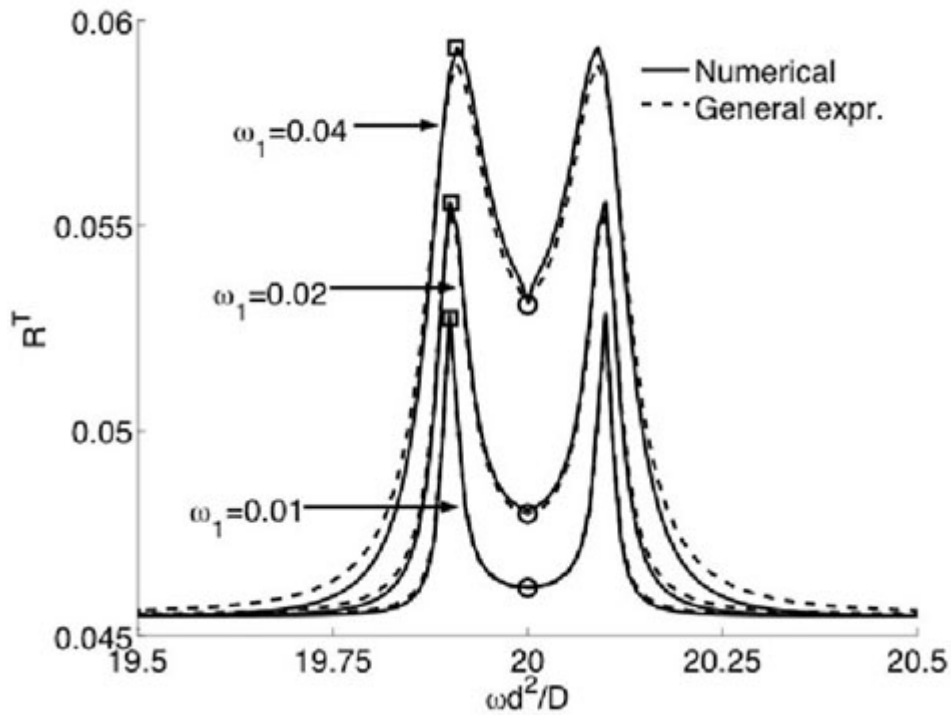
We study the influence of oscillating magnetic fields on the reaction yield of chemical reactions by accurate computer simulations. While the dielectric heating effect of a microwave-field is well known, much less attention has been given to the effect of the magnetic component. It has, however, been established that both static and oscillating magnetic fields can influence chemical reactions that include an intermediate radical pair step. The effect of strong static magnetic fields, of the order of 0.1 T, has been studied for several decades and it is well understood and can be accurately described theoretically. The mechanism is called the radical pair mechanism (RPM) and is currently the only established mechanism that explains how magnetic fields can influence chemical reactions. This mechanism is very different from the dielectric heating; it is a quantum mechanical effect caused by a magnetic interaction much smaller than the thermal energy. It is generally accepted that the theoretical description is correct. However, there are serious difficulties in solving the model equations in the presence of rf-fields under low static magnetic fields, as that of the earth. Experimental investigations are similarly complicated

and, at present, we believe that the most precise method of investigation of the effect is a numerical simulation, although accurate calculations are very demanding.

The project intends to study the effect under well-defined conditions by performing a series of accurate calculations; the aim is to produce a catalog of the effect under varying situations that might serve as a guideline for possible health hazards of mobile phones. The figures are the results of calculations at higher magnetic fields. They illustrate the dependence of the reaction yield  $RT$  versus on the frequency ( $\omega$ ) and amplitude ( $\omega_1$ ) of the radio frequency field. For weak rf-fields, the yield increases with the power but for stronger fields the most evident feature is that the range of frequencies affecting the yield is significantly broadened.

Preliminary, approximate calculations indicate that significant effects require that the rf-field contains frequencies of the order of the hyperfine constants and that the magnitude of the field creates an interaction of the order of the hyperfine interactions. Although such a situation can occur, the effect is expected to be small unless the effect is amplified by the reaction sequence. A possible reaction scheme with these properties will be shown.

+This project is supported by the Danish Council for Strategic Research under the program: Non-ionizing Radiation.



P-C-225

**BIOLOGICAL CELL MODELLING USING QUASI-LUMPED-ELEMENT FDTD METHOD.**  
 C. H. See, R. A. Abd-Alhameed, P. S. Excell. Mobile and Satellite Communications Research Centre,  
 Bradford Univ, Bradford, UK.

There is an increasing need for accurate models describing the electrical behaviour of individual biological cells exposed to electromagnetic fields. In this area, the most frequently used technique for computing the EM field is the Finite-difference Time-domain (FDTD) method. The standard FDTD method [1,2] requires extremely small time-step sizes when modelling electrically-small regions (much smaller than a wavelength): this will be especially severe when modelling biological cells with dimensions of the order of a few tens of micrometres. Thus, it can become impractical due to the unaffordable computation times required. This problem can be solved by implementing a quasi-static approximate version of FDTD, based on transferring the working frequency to a higher frequency, to reduce the number of time steps required. Then, the generated internal field at the higher frequency can be scaled back to the frequency of interest [3,4]. The method has also been extended to model complicated distributed electromagnetic systems with various active, passive, linear and nonlinear lumped electrical components, the so-called lumped-element finite difference time domain (LEFDTD) method [5-7].

This paper presents an approach to modelling and analysis of the HH (Hodgkin and Huxley) membrane model [8,9] that is represented as an electrical circuit on the surface of the biological equivalent spherical cell. Since the external medium of the biological cell is lossy material, a modified Berenger perfectly matched layer (PML) absorbing boundary condition (ABC) is used to truncate the computation grid [10-12], in order to reduce the reflections on the interface layers.

Modified Berenger Perfectly Matched Layer: Fig.1 shows the geometry of the FDTD computation domain, with the equivalent surface (Huygens surface) that replaces the incident plane wave. It also shows the PML surrounding the edge of the problem space, with Berenger matching impedance condition. In order to reduce the reflection on the interface layer, an optimum value of the geometric grading factor ( $g$ ) has been selected, by using an empirical expression as in Refs. [10-12].

Cell Model: The dimensions of a biological cell are around a few tens of micrometres and the thicknesses of the membranes are in the scale of a few nanometres, strongly depending on the type of the tissue. Depending on the type of the cell, voltages in the range of 20-200mV can be obtained across the membrane. When the cell is in a resting state, the current across the membrane averages zero, but more generally it depends on the variation on the membrane voltage [8,9].

Hodgkin and Huxley (HH) gave a general description of the time course of the current which flows through the membrane of a squid giant axon when the potential difference across the membrane suddenly changed from its steady state [8], suggesting that the behaviour of the membrane could be represented by the electrical circuit shown in Fig. 2. Current can be carried through the membrane either by charging the membrane capacitance or by movement of ions through the nonlinear conductance in parallel with the membrane capacitance. A set of equations governing the model are given in [3,8-9].

Simulated Example: A stack of 10 cells (spheres) along the z-axis was investigated, as shown in Fig. 3. The radius of the each cell was 15 micrometres. The dielectric properties inside and outside the cell are conductivity = 0.66 S/m and relative permittivity = 77.59. The membrane properties are conductivity =  $13e-9$  S/m and relative permittivity = 6.0. A plane wave of 100 V/m propagating in the z-direction and polarised in the x-direction was used as the excitation. The FDTD problem space was 325 x 50 x 50 FDTD cells for 1 micrometre FDTD cell size. The PML was 6 FDTD cells wide and the grading factor for optimal ABC was 7.957. The operating frequency was 1800MHz whereas the transformed intermediate frequency was 30GHz. The variations of the electric field in V/m at 1800MHz along the axis of the cells are shown in Fig. 4 and these variations were in agreement with expectations.

CONCLUSIONS: This work is still in progress, but the utility of the method has been demonstrated, in that the quasi-lumped element FDTD method applied to electrically very small cells and the HH model inside the cell membrane has been shown to give reasonable and stable results.

REFERENCES:

[1] A.Taflove, Computational Electrodynamics, Norwood, MA: Artech House, 1995.  
 [2] K.S.Yee, Numerical solution of initial boundary value problems involving Maxwell's equations in isotropic media, IEEE Trans. Antennas Propagation, vol.AP-14, 1966, pp.302-307  
 [3] G Emili, A Schiavoni, F L Roselli and R Sorrentino, Computation of electromagnetic field inside a tissue at mobile communications frequencies, IEEE Trans MTT, vol. 51, 1, 2003, pp. 178-186.  
 [4] O P Gandhi and J Chen, Numerical dosimetry at power- line frequencies using anatomically based models, Bioelectromagnetics, vol.1, 1992, pp. 43-60.  
 [5] M.Piket-May, A.Taflove and J.Baron, FDTD modeling of Digital Signal Propagation in 3D circuits with Passive and Active Loads, IEEE Trans. MTT, vol.MTT-42, Aug 1994, pp.1514-1523.  
 [6] W.Sui, D.A.Christensen and C.H.Durney, Extending the two-dimensional FDTD method to hybrid electromagnetic systems with active and passive lumped elements, IEEE Trans. MTT, vol.MTT.40, 1992, pp.724-730  
 [7] P.Ciampolini, P.Mezzanotte, L.Roselli, R.Sorrentino, Accurate and Efficient Circuit Simulation with Lumped-element FDTD technique, IEEE Trans. MTT, vol.44, No.12,1996, pp.2207-2214  
 [8] A.L.Hodgkin and A.F.Huxley, A quantitative description of membrane current and its application to conduction and excitation in nerve, J.Physiol., vol. 117, 1952, pp.500-544  
 [9] A.L.Hodgkin and A.F.Huxley, Current carried by sodium and potassium ions through the membrane of the giant axon of Loligo, J.Physiol., vol. 116, 1952 (a), pp.449-472  
 [10] J. Berenger, Perfectly Matched layer for the FDTD solution of wave-structure interaction problems, IEEE Trans. Ant. and Propag., Vol. 44:1, 1996, pp.110-117.  
 [11] J.Berenger, A perfectly matched layer for Absorption of Electromagnetic waves, J. Computational Physics, vol.114, no.2, 1994, pp.185-200.  
 [12] J.Berenger, Improved PML for the FDTD solution of wave-structure Interaction problem, IEEE Trans. Ant. and Prop., vol.45, No.3, 1997, pp.466-473

This work is supported by the European Union and a studentship from the Government of Malaysia.

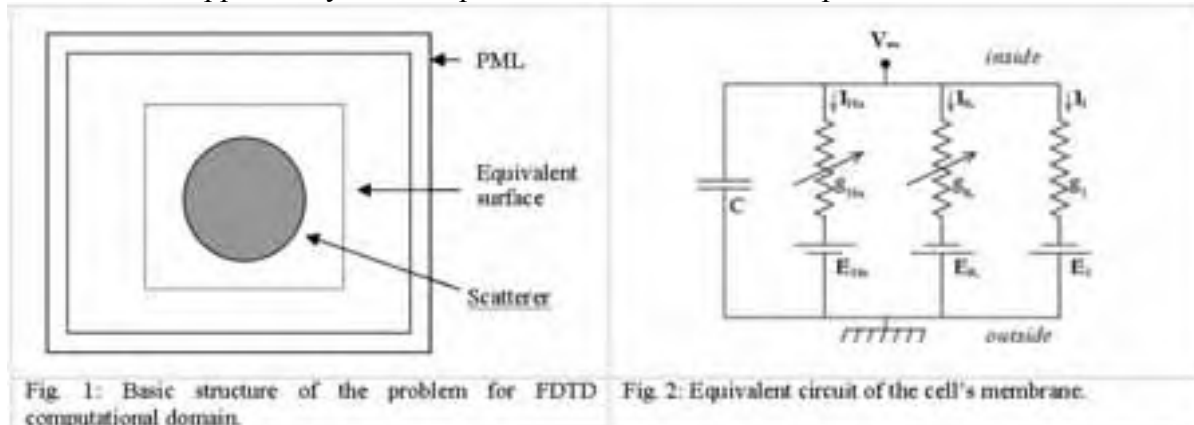


Fig. 1: Basic structure of the problem for FDTD computational domain.

Fig. 2: Equivalent circuit of the cell's membrane.

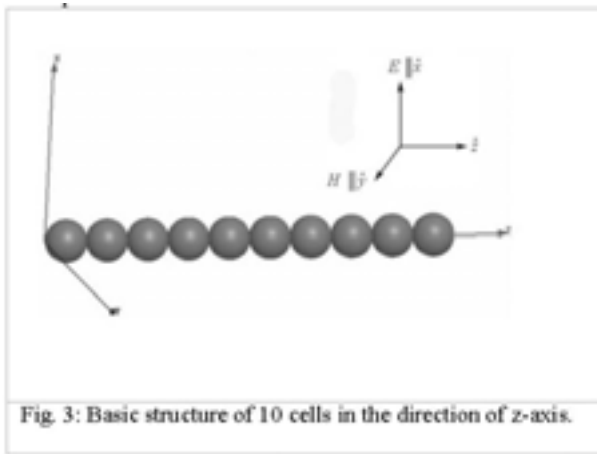


Fig. 3: Basic structure of 10 cells in the direction of z-axis.

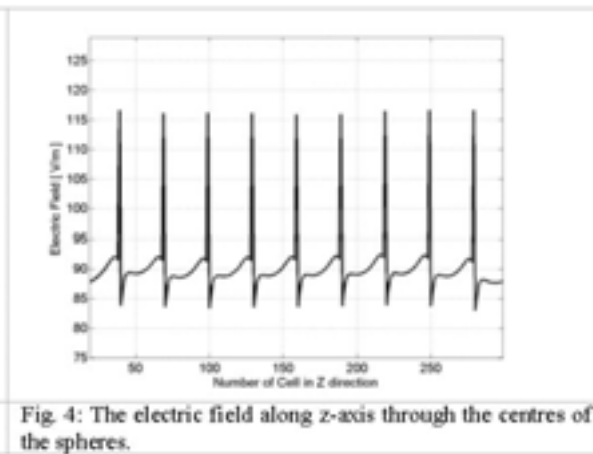


Fig. 4: The electric field along z-axis through the centres of the spheres.

P-C-228 STUDENT

**AN ELECTROCHEMICAL BIOSENSOR FOR GERMS DETECTION IN THE MILK.** Y. J. Zhou, Z. Yuan Lu, Z. Qi Niu, A. H. Liang, B. Feng Wei. School of Electronic Engineering, Xidian Univ, Xi'an City, Shaanxi Province, China.

**Abstract:** Biosensor is a sort of high-new technology composed of microelectronics, material science, biology technology, and is a system consisted of molecule identify components (sensor) and signal converted apparatus connecting with the former. The microbe sensor is a major branch of biosensor, which uses the live microbe as a sensitive material and utilizes all series of microbe and metabolism system to detect and recognize bottom material. Based on the application and characteristics of the microbe sensor, our work next will focus on how to use the microbe sensor to detect the number of bacteria in fresh milk in order to investigate a new method to detect fresh milk with good social and economic benefit.

**Principle:** The principle of the method of pigment reduction is that the oxidation-reduction potential can be reduced in foundation such as fresh milk because of the bacteria reproduction and the metabolism leading to consuming of oxygen. So if the color of a pigment changing with deoxidization added into foundation beforehand without impeding bacteria cultivation, we can determine the number of bacteria. The critical of the technology is to apply microbe battery into pigment reduction, that is to say, the number of bacteria can be detected by detecting electronics engendered during the process of bacteria oxidation-reduction. With oxygen consuming the bacteria in bio-cell box make foundation to metabolize substance and nutrient with H<sub>2</sub>O and CO<sub>2</sub> producing. Microbes just depend on the energy to survive. The process of bacteria metabolism and electrons engendered are showed as the following formula. Formula (1) describes that coenzyme FAD is oxidized by the cathode.:  $4\text{FADH} \rightarrow 4\text{FAD} + \text{H}^{++} + 4\text{e}^-$  (1) The reaction around the surface of anticathode is as formula (2):  $\text{Ag}_2\text{O}_2 + 4\text{H} \rightarrow 2\text{Ag} + 2\text{H}_2\text{O}$  (2) And the integrated formula is expressed as follows:  $4\text{FADH} + \text{Ag}_2\text{O}_2 \rightarrow 4\text{NAD} + 2\text{Ag} + 2\text{H}_2\text{O}$  (3) Besides offering and acceptance of H there exists acceptance of electron (e<sup>-</sup>) in the process of deoxidization and oxidization. With e<sup>-</sup> accepting in the processes of deoxidization and oxidization, one can realize the measure of bacteria by current.

**Results and Discussion:** It is to do logarithm operation on data of the experiment we can acquire two graphs. One shows the relationship between the number of bacteria and the voltage illustrated as figure 3a, and the other shows the relationship between the number of bacteria and the current illustrated as figure 3b.

According to the results of the experiment analyzed above, there is an initial voltage before adding the coenzyme to samples and there exists the linear proportion relationships between the outputted voltage and current and the number of microzymes. In fact, there are some deficiencies of the method such as ill linearity of output characteristic of the biosensor. There are two reasons :one is very little current formed by electrons engendered in the process of the oxidization and deoxidization of radical matter while it need very high precision and very strong anti-jamming ability to check magnifying circuit or else there exists output error, and the other is that there is output error engendered by the asymmetry of reagent, samples and reagent inspiring ion added to the liquor and temperature change. Although it is necessary to further improve the experiment, it is enough to supply some gap with simple and convenient operation and very fast checkup. It is important that there is appreciated social benefit and enormous economic profit.

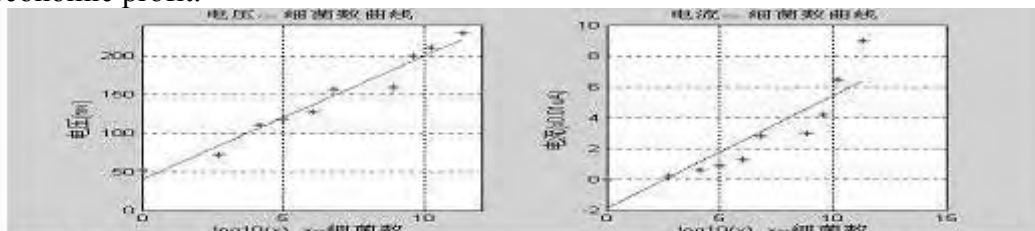


Fig.3a the graph of the relationship of the number of bacterium and voltage outputted by Biosensor

Fig.3b the graph of the relationship of the number of bacterium and current outputted by Biosensor

## Author Index

Abd-Alhameed, Raed A.....	289, 339, 552	Bauer, E.B.....	433
Abelin, T.....	106	Beard, Brian.....	269
Ackerman, Jerome L.....	328	Beccherelli, Romeo.....	525
Adair, Eleanor R.....	198	Beebe, Stephen J.....	123, 161, 164
Adams, Evan.....	295	Beers, G. Jerome.....	328
Agostini, Chiara.....	323	Bell, Steven.....	186
Ahlbom, A.....	105	Bellier, Pascale.....	398
Ahmed, Iftekhar.....	289	Belyaev, Igor.....	191
Aisa, J.....	511	Benane, S. G.....	523
Aizawa, K.....	348	Berdichevsky, M R.....	227, 534
Akdag, M. Zulkuf.....	291, 334	Berdiñas Torres, Verónica J.....	96, 354, 371
Åkerstedt, Torbjörn.....	384	Berg, Mats.....	384
Aksen, Feyzan.....	334	Bernardi, Paolo.....	131, 143
Alexandrov, Vladimir V.....	349	Bersani, Ferdinando.....	517
Alfadhli, Yasir.....	305, 319	Bersani, Ferdinando.....	81, 228, 318, 323
Ali, M.....	55	Bertichevsky, Max R.....	228
Alias, Rozlan.....	339	Beuter, A.....	14
Allen, Stewart J.....	69	Bhanushali, Ashok.....	190
Altpeter, E.....	106	Bianchi, Enrica.....	318
Aly, Ashraf.....	85	Bianco, B.....	330
Ambron, Richard T.....	239	Bickens, C.....	164
Apollonio, Francesca.....	210, 214, 324, 525	Bilgin, Murat.....	460
Appolloni, Massimo.....	196	Billaudel, Bernard.....	176, 181, 192, 296, 307, 522
Arai, Katsuaki.....	109	Birkner, Ewa.....	297, 299
Aran, Jean Marie.....	179	Bisceglia, Bruno.....	314, 330, 426
Ardoino, Lucia.....	175, 247, 363	Bit-Babik, Giorgi.....	251
Ares-Pena, Francisco José.....	391, 430	Bitz, A.....	31, 177, 261, 353, 474
Arnetz, Bengt B.....	384	Blackman, C. F.....	523
Asamoto, Makoto.....	173	Blackmore, P F.....	164
Asou, Hiroyuki.....	42, 264, 489	Blandeau, Olivier.....	394
Astumian, R.D.....	207, 209	Blank, Martin.....	233, 239
Azanza, M J.....	312, 511	Bloch, Isabelle.....	146
Baba, Madoka.....	250	Bloch, S.....	353
Bach Andersen, J.....	197	Blystone, R V.....	504
Bachelet, C.....	516	Bogodist, Olesja.....	349
Bahr, Achim.....	90	Boice, Jr, John D.....	103
Bailey, William H.....	287	Boiden Pedersen, J.....	197
Bakos, J.....	283	Bolomey, Jean Charles.....	272
Balcavage, W. X.....	66	Bolz, Thomas.....	90
Ball, A. D.....	92	Bonmassar, Giorgio.....	328
Balzano, Quirino.....	57, 207, 209, 352, 452	Borgens, Richard.....	8
Bao, Xiuqi.....	149, 320	Bornhausen, Michael.....	483
Barchanski, Andreas.....	218	Bort, E.....	485
Barnes, E M.....	460	Bottomley, Anna.....	184, 292
Barnes, F.S.....	85, 207, 209	Bourthoumieu, Sylvie.....	408
Barton, Julie J.....	121	Bowditch, S C.....	501

Bowman, Joseph D. ....	34, 233	Chou, C-K. ....	55, 198, 251
Bracken, T D. ....	35, 287, 493	Christ, Andreas. ....	58, 269, 444
Braunhut, Susan J. ....	9	Christensen, Helle C. ....	103
Brazzale, Alessandra. ....	179, 183, 186	Cid, M. Antonia. ....	316
Brescia, Francesca. ....	517	Cieslar, Grzegorz. ....	297, 299, 301, 399
Brillaud, Elsa. ....	111, 293, 419	Cimino, V. ....	426
Brooks, Daniel. ....	531, 539, 549	Cleveland, Robert F. ....	335, 454
Brouse, David. ....	317	Coey, J MD. ....	61
Brown, A. ....	519	Collet, Lionel. ....	186
Bruno, Maria Carmela. ....	314	Collier, Mitchel N. ....	199
Bucci, E M. ....	244	Collin, Alice. ....	351, 408, 462, 516
Bucci, O M. ....	244	Commerford, Kristy. ....	67
Bureau, Yves. ....	294, 295, 438, 440	Cook, Charles M. ....	10
Cadossi, Ruggero. ....	224, 330	Cook, M C. ....	171
Calabrese, M L. ....	188, 244	Cooper, K. ....	433
Calabrese, Marilu'. ....	311	Cordelli, Eugenia. ....	196
Caldwell, Jacques R. ....	225	Correa, Carlos. ....	280
Calvo, A C. ....	312	Cosquer, Brigitte. ....	182
Campbell, V. ....	61	Cotignola, G. ....	214
Capasso, Dominga. ....	517	Craviso, Gale L. ....	317, 361
Capri, Miriam. ....	318	Crawford, F. ....	158
Carrere, Nathalie. ....	179	Creasey, William A. ....	199
Carson, Jeffrey JL. ....	67	Cristoforetti, L. ....	485
Casper, Diana. ....	228	Croce, Rocco Paolo. ....	314
Cassel, Jean-Christophe. ....	182	Croft, Rodney J. ....	116, 121
Cavagnaro, Marta. ....	131, 143	Cueille, M. ....	462
Cech, Roman. ....	19	Curran, Allen R. ....	74, 548
Celik, M. Salih. ....	291	Daigle, Jeff P. ....	37
Chadwick, Phil. ....	28, 89	d'Ambrosio, G. ....	188, 244, 311
Chadwick, Philip. ....	336	D'Andrea, A. ....	372
Chapellier, J MP. ....	434	D'Andrea, John A. ....	198
Chari, Sesh. ....	147	D'Andrea, M J. ....	463
Charlet de Sauvage, Renaud. ....	296	Darrigo, Antonello. ....	318
Chatterjee, Indira. ....	317, 361	Dasdag, Suleyman. ....	291, 334, 387, 460
Chauvin, Sébastien. ....	362	Dasenbrock, Clemens. ....	173
Chavannes, Nik. ....	127	Dasenbrock, T. ....	474
Cheema, Muhammad. ....	85	David, E. ....	500
Chemeris, Nikolai K. ....	304	Davis, Christopher C. ....	57, 352
Chen, Ching-Jen. ....	86	De Leo, Roberto. ....	426
Chen, Ji. ....	137, 270	De Marco, Marco. ....	245
Chen, Wei. ....	238	de Seze, René. ....	111, 122, 146, 293, 419
Chen, Xiadong. ....	305, 319	DeFrank, John J. ....	198
Chen, Y. Iris. ....	328	del Moral, A. ....	312, 511
Cherington, Michael. ....	502	Del Re, Brunella. ....	323
Chiadini, Francesco. ....	314	Deplano, Monica. ....	318, 475
Cho, Yong Sung. ....	376	Desjardins, Dawn. ....	431, 440, 441
Choi, Dong-Geun. ....	252	Detlefsen, Jürgen. ....	483
Choi, Jae-Ic. ....	479	Di Rienzo, Luca. ....	442
Choi, Sung ho. ....	254	Diaferia, Nicola. ....	426

Diaz-Enriquez, Manuela	316	Fleming, A.H.J.	433
Dimbylow, Peter J	342	Forigo, Davide	318, 475, 524
d'Inzeo, Guglielmo	210, 214, 324, 345, 525	Foster, K.R.	207, 209
Dixon, S J	82	Fouad Hanna, Victor	146, 263, 368
Doi, Yuko	173	Fourie, Francois le R.	114
Doktorov, Alexander B	550	Fournier, C	516
Dominici, L	210	Fraher, L J	82
Donatiello, S	210	Francavilla, Mauro	475
Donsì, Giorgio	314	Franceschi, Claudio	318
Doria, Andrea	217	Frank, Robert	394
Dorn, Hans	90	Franken, Daniel	114
Douglas, M. G.	55	Frederiksen, Heidi B	204
Driessen, Sarah	337, 546	Freseigna, Anna Maria	196
Dronne, Vincent	492	Fröhlich, Jürg	96, 139, 182, 354, 371
Dubovoy, Leonid V	349	Fu, Jia	303
Duchesne, Luc	272	Fujimoto, Masaki	268
Duncan, J D	372	Fujiwara, Osamu	78, 109, 173, 268, 507
Dunlop, David	294	Fukunaga, Kaori	42, 250
Dunlop, David	294	Funamizu, Hirofumi	324
Duong, L	534	Furubayashi, Toshiaki	24, 308, 503
East, C J	256	Gabriel, Camelia	49, 276, 278
Ebara, Hidetoshi	258	Gadi, Nagib	146
Ebert, Sven	96, 125, 173, 354, 384	Gaillot, P	14
Edwards, Alan	196	Gajda, Greg	398
Efremov, Vitalii A	349	Galani, Rodrigue	182
Eguchi, Yawara	65, 509	Galindo, Cynthia	166, 167
El Ouardi, A.	31, 261	Gallego, Rosalía	430
Elabbassi, E B	122	Gallerano, Gian Piero	217
Elder, Joe A	302	Galloni, Paolo	179, 183
Engel, J	261	Ganey, Timothy M	225
Engstrom, Stefan	308	Gao, J H	372
Erdreich, Linda S	108, 374	Gapeyev, Andrew B	304
Ericsson, Arthur D	158	Garay, R	372
Espinosa, J. M.	124	Garreau, Philippe	272
Esser, Axel T	343	Gati, Azedine	262
Evans, L O	501	Gealt, Michael A	161, 165
Evans, N. E.	92	Geddis, Matthew S	239
Excell, Peter Stuart	289, 339, 552	Gernez, Jean Pierre	394
Falzone, Nadia	114	Gernez, Jp.	124
Faraone, Antonio	55, 251	Gialanella, G	188
Farrell, E	61	Gianni, Matteo	324
Fauntleroy, L I	164	Gibson, J	418
Fedrowitz, Maren	174	Giczi, Wolfram	274
Ferrari, Giovanna	314	Giichirou, Tsurita	178
Feychting, Maria	102, 105, 282	Giorgi, Gianfranco	323
Figuroa Karlström, Eduardo	33	Giovenale, Emilio	217
Findlay, Richard P	342	Giuliani, Livio	88
Fitzner, Rudolf G.	194	Gjedde, Albert	197
Fiumara, Vincenzo	314	Glaser, R.	207, 209

Glover, Ian .....	455	Hazlewood, Carlton F .....	158
Gminski, Richard .....	194	He, Sailing .....	220, 343
Gmitrov, J .....	169, 382	He, Y David .....	225
Gmitrova, V .....	382	Hernandez-Bule, M. Luisa .....	316, 332
Goldberg, Robert B. ....	199	Héro, Marc .....	387
Goodman, Reba .....	233, 239	Hietanen, Maila .....	17
Gordon, Steven L .....	225	Hikage, T .....	423
Goulet, D .....	14	Hillert, Lena .....	191, 384
Gowrishankar, Thiruvallur R .....	343	Hirata, Akimasa .....	97, 268
Graham, Karissa .....	229	Hirose, Hideki .....	404, 412, 498, 514
Grandori, Ferdinando .....	142, 442	Hirota, S. ....	170, 510
Green, A Chris .....	305, 319	Hocking, Bruce .....	201
Greenebaum, Ben .....	244	Hoffman, Kent C .....	225
Grimaldi, Settimio .....	88	Holden, Simon John .....	49, 278, 418
Groebl, J.C. ....	181	Hondarrague, Yannick .....	179
Groeger, J A .....	501	Hong, Seung Cheol .....	254, 376, 378
Grose, R I .....	418, 501	Hörnsten, Rolf .....	497
Grose, R Iain .....	319	Hosokawa, K .....	348
Grossi, G .....	188	Hosokawa, Keiko .....	405
Grzesiuk, E .....	458	Hou, Jian Qiang .....	422
Hadjem, Abdelhamid .....	146, 263	Houchi, Hitoshi .....	405
Hagan, Todd .....	317	House, D. E. ....	523
Haider, Harald .....	274	Hoyto, A .....	181
Haik, Yousef .....	86	Huang, Tai-Qin .....	286, 396
Hakala, Kevin .....	166	Hudes, Mark .....	285
Hall, E H .....	123, 164	Hughes, E. F .....	66
Hall, Henry .....	28, 89, 336	Hughes, J N .....	418
Hall, P .....	105	Hungerford, David S .....	225
Halonen, Pirjo .....	17	Hunziker, Ernst B .....	225
Hamada, Lira .....	42, 99, 264, 489	Huo, Xiaolin .....	149, 320
Hamakubo, Takao .....	536	Hurt, William D. ....	74, 280, 548
Hamberg, L. ....	70, 473	Huysen, Carin .....	114
Hamblin, Denise L .....	116	Hwang, Gihyun .....	453
Hamnerius, Yngve .....	102, 274	Hyun, Youn Joo .....	378
Hanazawa, Masahiro .....	59, 266, 433	Ichihara, Toshio .....	507
Hannemann, Sandra .....	421	Iivonen, Hennariikka .....	397
Hansen, V .....	31, 177, 261, 353, 474	Ikehara, T .....	348
Hansson Mild, Kjell .....	33, 106, 201, 421, 497	Ikehara, Toshitaka .....	405
Hardell, Lennart .....	106	Ikehata, Masateru .....	406, 417
Hare, E .....	460	Imai, Setsuo .....	402
Haro, Emmanuelle .....	176, 192, 307	Imaida, Katsumi .....	507
Harrison, Patrick K .....	507	Inns, R H .....	418, 501
Hart, F X .....	27	Isaka, Katsuo .....	385
Hartwig, Christiane .....	126	Ishii, Nozomu .....	99
Hashimoto, Osamu .....	258	Iskra, S .....	256
Hata, Ikuho .....	97, 433	Isozumi, Yasuhito .....	414, 415
Hata, Keisuke .....	178	Isseroff, Rivkah .....	27
Hatcher, D .....	463	Ito, H. ....	133
Haylock, Richard .....	184, 292	Ito, K. ....	47, 133

Ivancsits, Sabine .....	81	Kheifets, Leeka .....	102
Iwasaki, Takashi .....	99, 264, 489	Kiel, Johnathan L .....	189, 504
Jacobs, Kevin .....	455	Kiernan, Jim .....	152
Jacobsen, Rune .....	284	Kim, Deok Won .....	241, 449
Jacquin, Francois .....	492	Kim, Jaejoon .....	453
Jang, Ja-June .....	396	Kim, Nam .....	252, 254, 479
Jenks, P. ....	433	Kim, Soo Chan .....	241, 449
Jenrow, Kenneth A. ....	238	Kim, Sung-Woo .....	449
Jing, Wang .....	410	Kim, Tae-Hyung .....	286
Joe, Wiart .....	262	Kim, Yoon Shin .....	254, 376, 378
Johansen, Christoffer .....	103, 197, 204, 284	Kiminami, K. ....	469
Johansson, A. ....	377	Kinouchi, Y .....	348
Johansson, Olle .....	505	Kinouchi, Yohsuke .....	405
Johnson, Gary .....	287	Kitamura, M. ....	348
Johnsson, Anders .....	389, 544	Kitamura, Mitsuo .....	405
Johnston, S A .....	537	Kjaergaard, Soren .....	197
Jokela, Kari .....	75, 356	Kleinstejn, Bruce H. ....	199
Jones, Lynne C .....	225	Klingenböck, Anja .....	58, 96, 444
Jones, Nancy .....	184, 292	Klubertz, Frank .....	546
Joosten, Stephan .....	12	Ko, C.O .....	471
Jorge-Barreiro, Francisco Javier .....	430	Koana, Takao .....	406
Joseph, Wout .....	118, 358	Kodama, Tatsuhiko .....	536
Joshi, R P .....	163	Kodera, Sachiko .....	78
Joubert, Vanessa .....	408	Kojima, Masami .....	97, 433
Ju, Munno .....	453	Kolb, J F .....	164, 168
Junquera, C .....	511	Komatsubara, Yoshiki .....	84, 309, 404, 410, 412, 414, 518
Juutilainen, Jukka .....	185, 397	Konno, Takeshi .....	59, 266
Kainz, Wolfgang .....	137, 269, 270	Koreman, Kees .....	38
Kaji, Naoko .....	498	Korpinen, Leena .....	356, 445, 541
Kamimura, Yoshitsugu .....	433	Koskinen, Riku .....	445, 541
Kanda, Michael .....	352	Kosteljanetz, Michael .....	103
Kang, Gang .....	422	Koyama, Shin .....	84, 309, 410, 412, 414, 518
Kanj, H .....	151	Koyanagi, Y. ....	133
Karjanlahti, Tapani .....	445, 541	Kramer, A. ....	29
Kasperczyk, Slawomir .....	297, 299, 301, 399	Krause-Finkeldey, D. ....	353
Kato, Masamichi .....	429	Kristiansen, Ivar S .....	197, 204, 284
Kavet, Robert .....	34, 35, 37, 493	Kronberg, James W .....	225
Kawabe, Mayumi .....	507	Kubinyi, Györgyi .....	388
Kawada, Masatake .....	385	Kuchel, T .....	256
Kawai, H. ....	133	Kuehn, S .....	29
Kawato, Suguru .....	324	Kuhn, S .....	370
Kaya, Abdurrahman .....	334	Kumahara, Ryo .....	266
Keenlside, Lynn .....	229, 350, 431, 441	Kumlin, Timo .....	397
Kellényi, Lóránd .....	388	Kunieda, Etsuo .....	368
Kellerman, R A .....	465	Kuribayashi, Masanori .....	173
Kellom, Tocher R .....	137, 269	Kurikka-Oja, Jussi .....	445, 541
Kelsh, Michael A. ....	79, 108, 139, 370, 374	Kurokawa, Hideyuki .....	264
Ketani, Aydin .....	334		
Kezuka, Etsuko .....	429		

Kuster, Niels	29, 58, 79, 96, 102, 125, 127, 139, 173, 181, 182, 184, 269, 292, 354, 370, 371, 384, 444, 522
Kuusela, Tom	17
Kwong, Kenneth K.	328
Laakkonen, Noomi	445
Laclau, Muriel	307
Laconi, Cristiana	416
Ladage, K.	353
Lager, Daniel	478
Lagroye, Isabelle	124, 176, 181, 192, 296, 307, 522
Lahoz, M.	511
Lambrecht, Michael	361
Lambrozo, Jacques	347
Lang, Sakari	198
Lansimies, Esko	17
Lantow Margareta	420
Lantow, Margareta	126
Larkin, John	155
Larsson, L. E.	473
Laubitz, D.	458
Lautru, David	146, 263, 368
Lawlor, George F.	303, 529
Le Duigou, Pierre	362
Leal, Jocelyne	316, 332
Ledda, Mario	88
Lee, Jae-Seon	286, 396
Legoff, Marc	272
Legros, A.	14
Leitgeb, Norbert	19
Lemay, Eric	398
Leon, Alberta	318
Lerchl, Alexander	177, 508
Leszczynski, Dariusz	114
Lévêque, P.	307, 351, 408, 462, 516
Li, J L.	372
Li, Jie	152
Liang, An Hui	555
Liberti, Micaela	214, 324, 345, 525
Liboff, Abraham R.	238, 242
Lin, Chien Chi	152
Lin, James C.	112, 131, 141
Lindenblatt, Gunnar	220, 343
Lindholm, Harri	17
Lindsay, C D.	418
Lipping, Tarmo	356
Lisi, Antonella	88
Litchfield, Ian	380
Lloyd, David	196
Logani, Mahendra K.	190
Lonn, S.	105
López-Martín, Elena	391, 430
Lopresto, Vanni	143, 247, 363
Lörtscher, M.	41
Löscher, Wolfgang	174
Lott, U.	29, 371
Loughran, Sarah P.	121
Lovisolò, Giorgio A.	175, 247, 363, 416, 506
Lowden, Arne	384
Lu, Zhi Yuan	422, 555
Lubańska, A.	458
Luise, Diego	318
Lukzen, Nikita N.	550
Lundgren, Erik	54
Lundström, Ronnie	33
Lupke, Madeleine	420
Lushnikov, Konstantin V.	304
Lutman, Mark	186
Luukkonen, J.	181
MacKenzie, Robert A.	229
Maercker, Christian	81, 126, 420
Maeztu, C.	511
Maggi, Stefania	245
Magne, Isabelle	347, 387, 394
Makar, Vera R.	190
Malacarne, C.	485
Male, J C.	537
Malmgren, Lars	191
Man Fai, Wong	262
Manabe, T.	423
Mancini, Sergio	247, 363
Mancuso I, Maria Teresa	506
Mannerling, Ann-Christine	421
Manti, L.	188
Mantiply, Edwin D.	335, 454
Marinkovich, Peter	27
Marino, Carmela	175, 179, 183, 196, 416, 506
Markov, Marko S.	158, 159
Markova, Eva	191
Marquina, Nelson	152
Martens, Luc	118, 358, 466, 487
Martín, Agustín	447
Martinez Ciriano, C.	511
Martinez, M. Antonia	316
Martínez-Búrdalo, Mercedes	447
Marttila, Eric A.	74, 548
Marx, Kenneth A.	9

Masada, Masahiro.....	429	Mlynarska, K.....	426
Mason, Patrick A ..... 69, 74, 171, 189, 280, 504, 548		Moeller, Arne.....	197
Massa, Rita.....	188, 244, 311	Moffat, Scott D.....	384
Masuda, Hiroshi.....	170, 176, 303, 308, 503, 510	Molnár, Ferenc.....	388
Masuda, Masahiro.....	385	Monebhurrin, Vikass.....	45, 272
Matavulj, Milica.....	505	Mont, Michael A.....	225
Matsuuchi, Naohisa.....	385	Montague, Russell G.....	319
Matta, B.....	434	Moquet, Jean.....	196
Mattsson, Mats-Olof.....	239, 421	Moreno, Eduardo.....	430
Mazzanti, M.....	214	Morgan, Lloyd.....	285
McCaig, Colin.....	8	Morley Forster, Patricia.....	229
McCreary, C R.....	82	Morrissey, Anthony.....	155
McIntosh, Donna.....	9	Moulin, Annie.....	186
McIntosh, R L.....	256	Moulin, Dwight.....	229
McKay, Julia C.....	436	Mrowiec, Janina.....	299, 301, 399
McKenzie, R J.....	256	Msuda, Hiroshi.....	24
McLaughlin, Joseph K.....	103	Muehsam, D J.....	153, 223
McLean, Michael J.....	308	Münkner, S.....	261
McNamee, James.....	398	Munoz, S.....	519
McNeely, Mark.....	139	Muñoz, Sagrario.....	366
McPherson, Dana.....	317, 361	Murphy, Michael.....	168, 202
McQuade, Jill.....	69, 171	Musumeci, D.....	244
Meltz, Martin L.....	166, 167	Mylacraine, Kevin S.....	69
Meric, Faruk.....	387	Myung, Sungho.....	453
Merla, C.....	345	Naarala, J.....	181
Merola, Paola.....	416	Nabae, Kyoko.....	173
Merritt, J H.....	171	Naftel, James A.....	225
Mesirca, Pietro.....	318, 323	Nagaoka, Tomoaki.....	109, 368
Messere, A.....	244	Nagata, Yoshiho.....	429
Messina, Giovanni.....	217	Nagatsuma, T.....	469
Meyer, F JC.....	465	Nagawa, Hirokazu.....	178
Meyer, Michael.....	337, 546	Nakasono, Satoshi.....	417
Mezei, Gabor.....	23, 493	Nam, Ki Chang.....	241, 449
Mezei, Katalin.....	23	Nasta, Francesca.....	175
Mifsud, Nicola CD.....	305, 319, 507	Natarajan, Mohan.....	166, 167, 190
Miki, Daisuke.....	258	Naughton, S D.....	418
Milano, G.....	244	Navarro, A.....	227
Millenbaugh, N J.....	504	Nayak, Bijaya K.....	166, 167
Miller, Christian K.....	233	Negishi, Tadashi.....	402, 417
Miller, S A.....	171	Negrone, Anna.....	416
Miranda, Jose Miguel.....	366, 519	Nelson, David A.....	74, 548
Mita, Paolo.....	311, 517	Neubauer, Georg.....	102, 274
Miyakoshi, Junji..... 84, 309, 404, 410, 412, 414, 415, 498, 514, 518		Neufeld, Ezra Z.....	127
Miyamoto, H.....	348	Ng, Erwin T.....	548
Miyamoto, Hiroshi.....	405	Nguyen, D.....	14
Miyota, Yukihiro.....	264, 489	Nicol, Stuart.....	531, 539, 549
Mjõnes, Lars H.....	538	Nicolas, Emmanuel.....	492
		Nielsen, Jesper Bo.....	197, 204, 284
		Nijima, Toshio.....	514

Nikoloski, Neviana .....	181, 269, 522	Pereira de Vasconcel, Anne .....	182
Nindl, G.....	66	Perez-Bruzon, R N.....	312, 511
Nino, Juanita.....	17	Perez-Castejon, C.....	511
Niple, John C. ....	34	Perrin, A.....	351, 516
Nishikawa, Masami.....	24, 308, 503	Perrine, Martin L.....	335
Nishimura, Izumi .....	402, 403, 417	Perrone, Angela.....	318
Niu, Zhong Qi.....	422, 555	Perrott, Rose.....	278
Nojima, Toshio .....	404, 423, 498	Perrott, Rosemary .....	49
Nordin, S. ....	377	Perrotta, Alessandro.....	524
Nordström, E.....	70	Persson, Bertil.....	191
Nuccitelli, P.....	26	Persson, T.....	473
Nuccitelli, R.....	26	Pértega, Sonia .....	391
O'Connor, R.....	462	Pes, N.....	511
Oftedal, Gunnhild .....	389, 544	Pesatori, Alessandro.....	442
Ogawa, K. ....	133	Petersen, Ronald C.....	198, 202
Ogiso, Tadashi .....	173	Petraglia, G .....	244
Ogiue-Ikeda, Mari.....	129	Petrovicz, Otto .....	483
Ohkubo, Chiyoji.....	24, 170, 303, 308, 503, 510, 528, 529	Peyman, Azadeh .....	49, 276, 278
Okano, Hideyuki.....	528	Pflugger, D.....	41
Okano, Tomoko .....	24, 308, 503	Phillips, John B.....	160
Okorn, Sabine .....	483	Picard, Dominique .....	362
Olivier, Christof.....	466	Pidel, Ann .....	228
Olsen, Jørgen H.....	197, 204, 284	Piggott, John .....	155
Olsson, Martin.....	274	Pilla, Arthur A.....	153, 223, 227, 536
Onishi, Teruo .....	47, 258, 469	Pinto, Rosanna .....	175, 179, 183, 247, 363, 416
Osada, H.....	133	Pioli, Claudio .....	175
O'Sullivan, Gerald C.....	155	Piotrowski, Aleksandra.....	111, 293, 419
Ozturk, Adil .....	460	Pipal, Lorenz.....	543
Paakkonen, Rauno.....	541	Pisa, Stefano.....	131, 143
Pack, Jeong -Ki .....	286, 396, 471	Piscitelli, Marta.....	179, 183
Paffi, Alessandra.....	214, 324, 525	Piuzzi, Emanuele.....	131, 143
Pakhomov, Andrei .....	168	Plante, M.....	14
Palumbo, Rosanna.....	517	Plech, Andrzej.....	301, 399
Pammler, Katharina .....	12	Pompili, A. ....	426
Pande, Rajiv .....	9	Pongpaibool, P .....	308
Pandozy, S.....	426	Pontalti, R .....	485
Parazzini, Marta .....	142, 179, 183, 186, 442	Popovic, M.....	151, 534
Park, Ju-Derk .....	479	Poullietier de Gannes, Florence .....	176, 192, 307
Park, M.Y.....	471	Poulsen, Hans S .....	103
Pasi, Sara.....	318	Pradier, Aline .....	146, 368
Patel, Mitesh K.....	227, 228, 534	Prato, Frank S.....	10, 67, 82, 229, 294, 295, 350, 431, 436, 438, 440, 441
Patti, Annamaria .....	88	Preiner, Patrick.....	478
Pazzaglia, Simonetta.....	506	Prendergast, P J.....	61
Pedersen, Gert Frolund .....	197	Prina-Mello, A .....	61
Pedersen, Jørgen Boiden.....	550	Prisco, Maria Grazia .....	175
Peinnequin, A.....	516	Procyshen, Terry.....	152
Peleteiro, Manuel .....	391, 430	Prohofsky, E.W.....	207, 209
Pellegrino, Monica.....	525	Pugliese, M .....	188

Pullar, Christine E.....	27	Santamaria, Ulderico.....	426
Puranen, Lauri.....	75, 356	Saran, Anna.....	506
Qiang, Rui.....	137, 270	Sarimov, Ruslan.....	191
Quinn, Jeff.....	361	Sarti, Maurizio.....	311, 517
Ragland, Phillip S.....	225	Sasaki, Hiromi.....	405
Rahimi, O.....	171	Sasaki, Kazuyuki.....	97, 433
Rajkovic, Vesna.....	505	Sasaki, Ritsuko.....	529
Rametti, Armelle.....	408	Sato, Kenichi.....	42, 99, 264, 489
Ramundo-Orlando, Alfonsina.....	217	Saunders, Richard.....	184, 292
Raso, M.....	511	Scaglione, Antonio.....	314
Rathnabharathi, Kalani.....	85	Scampoli, P.....	188
Ravazzani, Paolo..	142, 179, 183, 186, 442, 499, 542	Scanlon, W. G.....	92
Redhead, Steve.....	455	Scarfi, Maria Rosaria.....	311, 517, 524
Reilly, J. Patrick.....	198	Schelkshorn, Simon.....	483
Reinhardt, T.....	261, 353, 474	Schiavoni, Andrea.....	318, 475, 524
Reissenweber, J.....	500	Schlatterer, Kathrin.....	194
Relova, José Luis.....	391, 430	Schmid, Gernot.....	52, 478, 543
Remkes, George.....	38	Schneiderman, Sue G.....	86
Remondini, Daniel.....	81, 318	Schoenbach, K H ..	123, 161, 164, 166, 167, 168
Richardson, Mary Ann.....	152	Scholin, T.....	171
Rienzo, A.....	188	Schreier, N.....	41
Roachefsky, Richard A.....	159	Schroettner, Joerg.....	19
Robertson, John A.....	431, 438, 440, 441	Schuderer, Jürgen.....	125, 181, 522
Rollwitz, Jana.....	420	Schüz, Joachim.....	102, 103, 282
Romanini, Paola.....	111	Scrafford, Carolyn.....	374
Rööslí, Martin.....	41, 102, 106	Sebastián, Jose Luis.....	366, 519
Rorarius, Michael.....	356	See, Chan Hwang.....	552
Roscigno, Angela.....	314	Seidman, Seth.....	269, 270
Rosola, Emanuela.....	88	Sekijima, Masaru.....	404, 498, 514
Roth, C C.....	504	Sekino, Masaki.....	129, 536
Roviello, G.....	244	Senior, Russell.....	35, 493
Roy, Colin.....	206	Seo, Jeong-Sun.....	286, 396
Rudiger, Hugo W.....	81	Sert, Cemil.....	460
Ruffié, Gilles.....	124, 176, 181, 192, 307, 522	Setti, S.....	330
Ruiz, Ignachio.....	102	Shen, Zheng.....	149
Saito, K.....	47, 133	Sheppard, Asher R. 79, 139, 207, 209, 370, 452, 532	
Saito, M.....	133	Shi, Yijun.....	149, 320
Sakuma, Noriko.....	404, 514	Shichijo, H.....	348
Sakurai, Tomonori ..	84, 309, 410, 412, 414, 518	Shigemitsu, Tsukasa.....	417, 429
Salazar, A L.....	171	Shimizu, N.....	469
Samaras, Theodoros.....	127, 444	Shin, Chan-Soo.....	479
Sanchez, Sandrine.....	176, 192	Shin, Ho-Sub.....	252
Sanchis, A.....	519	Shinozuka, Takashi.....	264
Sancho, Miguel.....	366, 519	Shiozawa, Toshiyuki.....	97, 268
Sandrini, L.....	485	Shirai, Hiroshi.....	59, 266
Sandström, Monica.....	377, 497	Shirai, Tomoyuki.....	173, 507
Sanger, R.....	26	Shirasawa, S.....	24, 308, 503
Sannino, Anna.....	311	Shono, Masayuki.....	405

Shum, Mona.....	79, 108, 139, 374
Shumilina, Julia V.....	304
Siegbahn, M.....	480
Sienkiewicz, Zenon.....	184, 292
Sieron, Aleksander.....	297, 299, 301, 399
Sieron-Stoltny, Karolina.....	301, 399
Sikora, A.....	458
Silny, Jiri.....	12, 337, 546
Silver, Deborah.....	280
Simkó, Myrtil.....	126, 239, 420, 421
Simpson, R.....	418
Singer, Sam.....	228
Sirmatel, Ocal.....	460
Sisken, B F.....	153
Sivo, Frank.....	536
Sloan, Mark A.....	189
Smith, Adam J.....	507
Smith, Kyle C.....	343
Smith, P J S.....	26
Smith, S A.....	418
Smith, S J.....	501
Soda, A.....	348
Soden, Declan M.....	155
Sokura, M.....	181
Sommer, A M.....	177, 508
Song, Chul Gyu.....	241
Song, Tao.....	149, 320
Sontag, Werner.....	242
Sorahan, Tom.....	380
Soukejima, Shigeru.....	24, 308, 503
Souques, Martine.....	347, 387, 394
Spaet, D.....	181
Spasovsky, Ivan.....	217
Spat, Denis.....	370
Spong, Jo-Lene.....	116
Stensson, Olle.....	33
Stetzer, Dave.....	285
Stevens, Paul.....	21
Stewart, Donald A.....	343
Stough, Con.....	116, 121
Stovner, Lars Jacob.....	389
Strauch, B.....	227, 228, 534
Straume, Aksel.....	389, 544
Streckert, J.....	31, 177, 261, 353, 474
Stronati, Laura.....	196
Stuck, Bruce.....	168
Sugiyama, Tsutomu.....	264
Sulser, Christof.....	139, 370, 371
Suzuki, Akira.....	264
Suzuki, Yukihisa.....	250, 309, 412, 414, 482
Swanson, John.....	455
Swicord, Mays L.....	198, 207, 209, 251
Sypniewska, R.....	504
Szabó, Judit.....	23, 283, 494, 496
Szasz, A.....	242
Tahvanainen, Kari.....	17
Takahashi, M.....	47, 133
Takeda, Hiroshi.....	404, 514
Taki, Masao.....	24, 59, 97, 109, 170, 178, 250, 266, 308, 309, 368, 412, 415, 433, 482, 503, 507, 510
Takimoto, T.....	47
Tamano, Seiko.....	173, 507
Tan, Puay.....	9
Tani, Kensuke.....	258
Tanila, Heikki.....	397
Tatsuoka, Hozumi.....	509
Tattersall, John EH.....	305, 319, 507
Tavartkiladze, George.....	186
Taxile, Murielle.....	176, 181, 307, 522
Taylor, C.....	418
Tejero, Simon.....	483
Tell, Richard.....	7, 198
Teramoto, Tadahiro.....	405
Terao, Yasuo.....	24, 308, 503
Terro, Faraj.....	408
Testa, Antonella.....	196
Testilier, G.....	351
Thansandote, Artnarong.....	398
Thomas, Alex W.....	10, 147, 229, 294, 295, 350, 431, 436, 438, 440, 441
Thomas, Nathan.....	186
Thompson, Bruce.....	121
Thuróczy, György.....	23, 186, 283, 388, 494, 496
Tijerina, Amanda J.....	189
Tillmann, C.....	474
Tillmann, Thomas.....	173
Timmel, C R.....	222
Tognola, Gabriella.....	142, 186, 442
Togo, H.....	469
Toivo, Tim.....	75, 356
Toivonen, Tommi.....	356
Törnevik, C.....	70, 473, 480
Traikov, Lubomir L.....	529
Trastoy, Ana.....	430
Trigano, J Alexandre.....	394
Trillo, M. Angeles.....	316, 332, 523
Tripp, Hayley.....	455

Tripp, Hayley .....	455	Wang, Jin .....	84, 309, 518
Troulis, S. E. ....	92	Wang, San M .....	161, 165
Truscott, Ben.....	305	Wang, Zhangwei .....	112, 141
Tsalighopoulos, Miltos .....	186	Watanabe, H.....	170, 510
Tschabitscher, Manfred.....	543	Watanabe, Soichi .....	24, 42, 59, 78, 97, 99, 109, 170, 178, 250, 264, 266, 308, 368, 433, 482, 489, 503, 507, 510
Tseng, Charles C.....	161, 165	Watts, Sarah .....	49, 278
Tumer, Cemil .....	460	Weaver, James C.....	163, 207, 209, 343
Tuor, Markus.....	125	Wei, Bao Feng .....	555
Tyml, Karel .....	436	Weiland, Thomas .....	218
Ubeda, Alejandro .....	316, 332, 523	Weingart, Michal .....	79
Überbacher, Richard .....	52	Weintraub, Michael I. ....	232
Uebayashi, Shinji .....	47, 258, 469	Weintraub, Susan .....	166, 167
Ueda, T.....	133	White, J A .....	164
Ueno, Shoogo.....	65, 129, 178, 324, 509, 536	wiart, joe .....	146
Ugawa, Yoshikazu .....	24, 308, 503	Wiar, Joe .....	102, 263, 368, 492
Uloza, Virgilijus.....	186	Widhalm, Kurt .....	543
Uloziene, Ingrida.....	186	Wienert, Roman .....	337, 546
Underwood, Georgina.....	507	Wiholm, Clairly .....	384
Uno, Toru.....	109	Wiklund, Urban.....	497
Ushiyama, Akira ....	24, 170, 303, 308, 503, 510, 529	Wilén, Jonna .....	497
Vaccari, A .....	485	Willis, L K .....	164
van Groen, Thomas.....	397	Wittorf, Sven.....	218
Van Kerkhove, Maria D.....	374	Wojcik, Jacek.....	531, 539, 549
van Wyk, M J.....	465	Wojtysiak, A .....	500
Vasilkoski, Zlatko .....	343	Woliński, J .....	458
Ventura, Carlo.....	228	Wong, Man Fai .....	146, 263, 368, 492
Vera Gil, A.....	511	Wood, Andrew W .....	116, 121, 206
Vermeeren, Gunter.....	487	Wright, A .....	418
Verrier, Agnes.....	347	Xiao, S.....	164
Veyret, Bernard....	124, 176, 181, 192, 296, 307, 522	Yamaguchi, H .....	348
Veysset, Rémy .....	362	Yamaguchi, Hironori .....	178
Vilar, José Antonio .....	391	Yamaguchi, Hisao.....	405
Villani, Paola.....	196	Yamaguchi, Kikuo .....	536
Villar, Raimundo.....	447	Yamaguchi, Sachiko .....	129
Vincze, C.....	242	Yamaji, Kenji.....	385
Vorotnikova, Ekaterina .....	9	Yamanaka, Yukio .....	170, 264, 368, 507
Vulcano, Antonella .....	88	Yamashita, Hiroharu .....	178
Wachtel, Howard .....	502	Yang, Kwangho .....	453
Wada, Hiromi.....	536	Yang, Wei .....	149
Waite, L. R. ....	66	Yardin, Catherine.....	408
Wake, Kanako....	24, 59, 97, 170, 178, 266, 308, 433, 482, 503, 507, 510	Yarnell, Philip.....	502
Walker III, Kerfoot .....	168	Yaws, Kalyn.....	280
Walker, J L.....	153	Yokus, Beran.....	334
Wang, Hai Bin .....	422	Yoshizaki, K .....	348
Wang, J. ....	109	Yoshizaki, Kazuo .....	405
Wang, Jianqing .....	78, 173, 268, 507	Yuan, Hang .....	86
		Zabielski, R.....	458

Zaffanella, Luciano E.....	37	Zhou, Tiean.....	9
Zalejska-Fiolka, Jolanta.....	297, 299	Zhou, Yong Jun.....	555
Zankl, Maria.....	444	Zhu, Hongyi.....	220, 343
Zeni, Olga.....	524	Ziegelberger, G.....	451
Zhang, Minhua.....	308	Zirix, John M.....	74, 280, 372, 463, 548
Zhao, Ke.....	108	Ziskin, Marvin C.....	190
Zhao, Min.....	9	Zizic, Tomas M.....	225
Zhou, Eileen.....	85		